MICROBIAL COMMUNITIES AND FUNCTIONS CONTRIBUTE TO PLANT PERFORMANCE UNDER VARIOUS STRESSES

EDITED BY: Hui Li, Diane Purchase, Xun Wen Chen and Hai-Ming Zhao

PUBLISHED IN: Frontiers in Microbiology

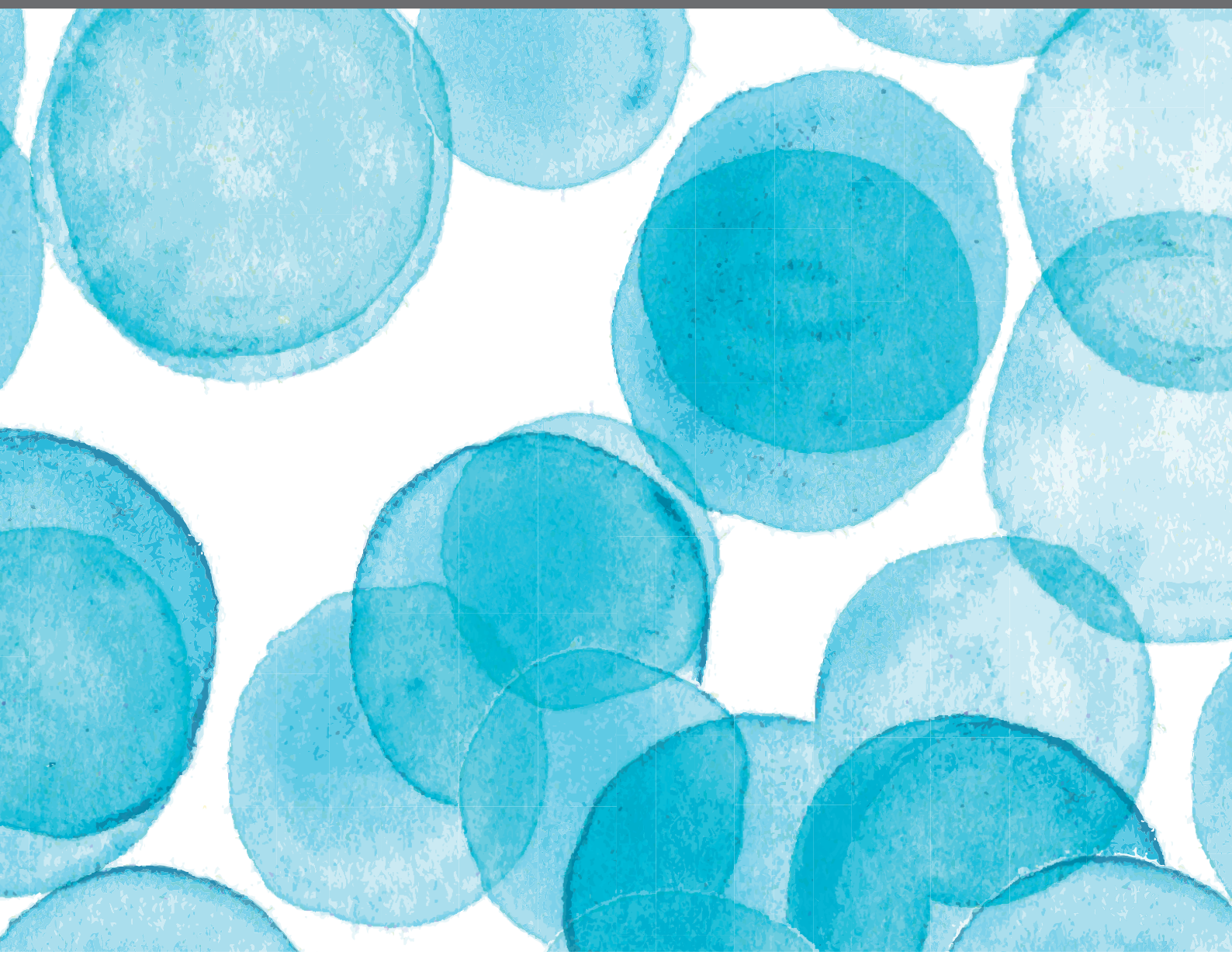

frontiers Research Topics

ISSN 1664-8714
ISBN 978-2-83250-827-5
DOI 10.3389/978-2-83250-827-5

About Frontiers

Frontiers is more than just an open-access publisher of scholarly articles: it is a pioneering approach to the world of academia, radically improving the way scholarly research is managed. The grand vision of Frontiers is a world where all people have an equal opportunity to seek, share and generate knowledge. Frontiers provides immediate and permanent online open access to all its publications, but this alone is not enough to realize our grand goals.

Frontiers Journal Series

The Frontiers Journal Series is a multi-tier and interdisciplinary set of open-access, online journals, promising a paradigm shift from the current review, selection and dissemination processes in academic publishing. All Frontiers journals are driven by researchers for researchers; therefore, they constitute a service to the scholarly community. At the same time, the Frontiers Journal Series operates on a revolutionary invention, the tiered publishing system, initially addressing specific communities of scholars, and gradually climbing up to broader public understanding, thus serving the interests of the lay society, too.

Dedication to Quality

Each Frontiers article is a landmark of the highest quality, thanks to genuinely collaborative interactions between authors and review editors, who include some of the world's best academicians. Research must be certified by peers before entering a stream of knowledge that may eventually reach the public - and shape society; therefore, Frontiers only applies the most rigorous and unbiased reviews.
Frontiers revolutionizes research publishing by freely delivering the most outstanding research, evaluated with no bias from both the academic and social point of view. By applying the most advanced information technologies, Frontiers is catapulting scholarly publishing into a new generation.

What are Frontiers Research Topics?

Frontiers Research Topics are very popular trademarks of the Frontiers Journals Series: they are collections of at least ten articles, all centered on a particular subject. With their unique mix of varied contributions from Original Research to Review Articles, Frontiers Research Topics unify the most influential researchers, the latest key findings and historical advances in a hot research area! Find out more on how to host your own Frontiers Research Topic or contribute to one as an author by contacting the Frontiers Editorial Office: frontiersin.org/about/contact

MICROBIAL COMMUNITIES AND FUNCTIONS CONTRIBUTE TO PLANT PERFORMANCE UNDER VARIOUS STRESSES

Topic Editors:
Hui Li, Jinan University, China
Diane Purchase, Middlesex University, United Kingdom
Xun Wen Chen, Southern University of Science and Technology, China
Hai-Ming Zhao, Jinan University, China

Citation: Li, H., Purchase, D., Chen, X. W., Zhao, H.-M., eds. (2022). Microbial Communities and Functions Contribute to Plant Performance Under Various Stresses. Lausanne: Frontiers Media SA. doi: 10.3389/978-2-83250-827-5

Table of Contents

frontiers | Frontiers in Microbiology

TYPE Editorial
PUBLISHED 07 November 2022
DOI 10.3389/fmicb.2022.992909

OPEN ACCESS

EDITED AND REVIEWED BY
Paola Grenni,
National Research Council, Italy

*CORRESPONDENCE
Xun Wen Chen
xchenat@connect.ust.hk

SPECIALTY SECTION
This article was submitted to Terrestrial Microbiology, a section of the journal Frontiers in Microbiology

RECEIVED 13 July 2022
ACCEPTED 25 October 2022
PUBLISHED 07 November 2022

CITATION
Li H, Zhao HM, Purchase D and Chen XW (2022) Editorial: Microbial communities and functions contribute to plant performance under various stresses. *Front. Microbiol.* 13:992909. doi: 10.3389/fmicb.2022.992909

Editorial: Microbial communities and functions contribute to plant performance under various stresses

Hui Li[1], Hai Ming Zhao[1], Diane Purchase[2] and Xun Wen Chen[1]*

[1]Department of Ecology, College of Life Science and Technology, Jinan University, Guangzhou, China, [2]Department of Natural Sciences, School of Science and Technology, Middlesex University, London, United Kingdom

KEYWORDS

microbiome, stress, function, crops, plant physiology

Editorial on the Research Topic
Microbial communities and functions contribute to plant performance under various stresses

Plant-microbe interactions in natural and agricultural ecosystems have attracted more attention than ever (Toju et al., 2018; Berg and Cernava, 2022). In fact, these interactions are important to ecological functions and essentially relevant to the ecological services that humans rely on Fester et al. (2014). Harnessing the benefits of the interactions is one of the most considered and sustainable opportunities for further crop improvements (Bailey-Serres et al., 2019). Nevertheless, additional stresses due to anthropogenic activities are uncertain driving factors of ecological functions and services (Crutzen, 2002; Rudgers et al., 2020; Berg and Cernava, 2022). Climate change, agriculture-related stress, chemical pollution, and ozone depletion are typical environmental stresses in the Anthropocene (McGill et al., 2015; Dietz, 2017; Cavicchioli et al., 2019). These factors profoundly change the mode of plant-microbe interactions (Berg and Cernava, 2022). A better understanding of the influencing mechanisms and the ecological consequences are critical to maintaining sustainable natural and agricultural ecosystems.

Due to the extremely complex processes within the tripartite system (i.e., plant-microbiome-environment), harnessing repeatable and applicable benefits of microbes is definitely still in its infancy. Repeatability and deterministic processes could be observed under well-controlled experimental conditions, such as using a synthetic community (SynCom) of microbes (Niu et al., 2017; Liu et al., 2019; Zhang J. et al., 2021) to identify essential microbial mechanisms in facilitating plant performance, e.g., regulating suitable levels of phytohormone (Finkel et al., 2020), adjusting root endodermal permeability for nutrient acquisition (Salas-González et al., 2020), and resisting fungal pathogen by establishing a stable bacterial community (Niu et al., 2017). When it comes to the complex field condition, the coupled deterministic (e.g., environmental filters that select species with certain traits) and stochastic processes

(chance events such as reproduction, death, and migration) (Zhou and Ning, 2017) and the influence of nonculturable microbial community (Lebeis, 2015) can often lead to difficulties in predicting the beneficial effects on plants.

Can plant microbiome really helps plants perform better in the way we desire, such as less disease and fertilizer with more yield? The question has been investigated from one-dimensional to multidimensional aspects: (1) symbiosis—symbionts of plants such as mycorrhizal fungi and rhizobia assist in nutrient acquisition and plant growth improvement (Smith and Read, 2008; Martin et al., 2017); (2) recruitment—protective microorganisms recruited by plants suppress the pathogen (Berendsen et al., 2012); (3) plant holobiont (an assemblage of species) and networking (i.e., microbe-microbe interactions)—assembly pattern determines plant health and fitness (Wei et al., 2015; van der Heijden and Hartmann, 2016; Niu et al., 2017; Finkel et al., 2020; Salas-González et al., 2020; Zhang L. et al., 2021). In the current Research Topic, Chen J. et al. further reviewed that harnessing the benefits of microbes is a promising approach to enhancing wheat performance under environmental stresses. Under such a backdrop, the present Research Topic collects studies investigating how microbes influence plant responses under typical stresses and their mechanisms, illustrating ongoing researches in this vivid and attractive field. The present Research Topic is categorized into sections considering different abiotic and biotic stress.

Agricultural activity-related stress

Agricultural activities such as continuous cropping, fertilization, grazing, application of pesticides, use of plastic products (leading to micro and nanoplastic pollution), breeding, etc., are challenges for sustainable agriculture. The current Research Topic collects 24 papers that consider, among others, fertilization, continuous cropping, and grazing.

To improve crop yield, applying nitrogen (N) fertilizer in soils is an efficient approach. However, N input and overuse create N emission/leaching problems (Zhang et al., 2011) and drastically alter soil microbial activities (Chen et al., 2019). Nitrogen deposition due to air pollution is also an additional source of N input (Adams et al., 2021). In the current Research Topic, Gu et al. found that N application indeed changed bacterial diversity and community structures of sugarcane cropping systems. Excessive application of N fertilizers had unexpectedly led to a lower yield. This also echoes Chen J. et al.'s view that an optimized level of chemical input is needed to keep useful microbe functioning.

Apart from fertilization, continuous cropping is common in agriculture. Continuously planting the same or similar cultivars in the same soils often leads to plant growth inhibition and serious soil-borne diseases, which is known as continuous cropping obstacle (CCO) (Shipton, 1977; Xiong et al., 2015). The imbalance of soil microbiota with a reduced abundance of beneficial microbes has been considered one of the major reasons for CCO (Hiddink et al., 2010). Yuan et al. found that the rhizosphere of soybean suffered from CCO, showing an unstable rhizosphere microbial community. Yu J. et al. also found that CCO of garlic was related to more potential plant pathogens, fewer plant growth promoters, and compromised microbial diversity of soils. Chen D. et al. also observed similar alterations in microbial functions in the tobacco fields. Taken together, these results show a generalized phenomenon that continuous cropping brings chemical stress and leads to the instability of the microbial community. It provides further evidence that a stable microbial network is critical to maintaining plant fitness (Wei et al., 2015; van der Heijden and Hartmann, 2016; Niu et al., 2017; Finkel et al., 2020; Salas-González et al., 2020; Zhang L. et al., 2021). But we should note that the CCO is plant species dependent (Yuan et al.). For instance, Yang et al. reported that long-term (up to 30 years) alfalfa cultivation in the field enhanced soil microbial diversity and bacterial networking, higher than those short-term cultivations of meadows.

Overgrazing could lead to soil degradation, greenhouse gas emission, water pollution, and loss of biodiversity (Springmann et al., 2018; Wang et al., 2020). Grazing exclusion by fencing is one of the simplest and most common practices to restore degraded grassland. In addition to plant productivity and diversity, researchers started to look at the effects of grazing exclusion on soil microbial response. In the current Research Topic, Wang et al. show that the 4-year grazing exclusion did not increase the complexity and connectivity of bacterial co-occurrence patterns indicating a longer term of grazing exclusion is needed for soil restoration in terms of microbial activities. The optimal duration of grazing exclusion seems essential for the restoration depending on the type of ecosystem (Li et al., 2018; Song et al., 2020).

Biotic stress

Plants can be infected by pathogens (i.e., bacteria, fungi, viruses, and nematodes) and attacked by herbivore pests (Atkinson and Urwin, 2012). The bacteria *Ralstonia solanacearum* can cause wilt disease in tobacco. Tan et al. investigated co-existence patterns of fungal communities in the rhizosphere and endosphere of tobacco infected by *R. solanacearum*. They found that the network structure was more complex under infection than under healthy conditions. The disease-resisting fungal genera may be suppressed due to the complex networking. It may let us re-think whether a complex microbial network is an indicator of a healthy plant holobiont.

The emission of volatile organic compounds (VOCs) triggered by plant growth-promoting rhizobacteria (PGPR) can resist herbivores. Herbivores can also induce plant volatile production. Understanding such chemical-mediated

plant-insect interactions is important to achieve sustainable agriculture. Raglin et al. compared six maize genotypes with or without PGPR and herbivores, and they found that plant genotype was the main factor driving the levels and composition of VOC. Inoculation of PGPR did not influence VOC emissions but improved maize growth. It implies that plant genotypic variation is the dominant factor controlling the bacteria-mediated benefits. Although PGPR can improve plant growth, it is also critical to know how such an "alien" species/community affects the indigenous soil microbiota. Renoud et al. measured plant performance and functional groups in soils grown with maize in the fields and noted that inoculation of PGPR enhanced maize growth, and the functional groups were field-dependent.

Drought and flooding

Plant-microbe interactions under drought stress are a popular research direction due to the widespread problem of the water crisis (de Vries et al., 2020). It is commonly reported that symbiotic fungi can alter soil water retention characteristics due to the production of glomalin (a glue-like substance) (Rillig and Mummey, 2006). In the current Research Topic, Cheng et al. review the roles of arbuscular mycorrhizal (AM) fungi (ancient and widespread symbiotic fungi of land plants) in helping their plant hosts to resist drought stress. Cheng et al. discuss the AM fungal diversity and activity, symbiotic relationship, morphological, physiological, and molecular mechanisms of AM fungi in assisting plant drought resistance. An outlook for future research is also provided. Not only fungi but also bacteria were considered to resist drought stress. Armanhi et al. study the impact of a synthetic community (SynCom) on the physiology and response of maize under drought stress. Results suggest SynCom inoculation reduced biomass loss and modulated vital physiological traits, such as lower leaf temperature, reduced turgor loss, and faster recovery upon rehydration. Gebauer et al. also determined the effect of water deficit history on soil microorganisms. They revealed interactive effects of soil type and water deficit condition. The approach allowed us to identify key microbial taxa promoting drought adaptation and improve the understanding of drought effects on plant-microbe interactions.

Different from the drought that leads to turgor pressure loss, embolism, and closure of stomata, precipitation and the subsequent flooding mostly increase the chance of leaf pathogen infection (Aung et al., 2018) and decrease rhizosphere oxygen levels hindering aerobic bacteria and mycorrhizal fungi (Unger et al., 2009). Francioli et al. found that flooding caused a significant reduction in wheat development and dramatic shifts in bacterial community composition at each plant growth stage, leading to detrimental effects on plant fitness and performance.

Metal stress

Soil heavy metal pollution is widespread (Shi et al., 2018). Heavy metals accumulated in crops pose significant ecological and health risks (Zeng et al., 2019; Hu et al., 2020). Cadmium (Cd) species in soils is an essential factor in determining the risks. In the current Research Topic, Hao et al. investigated the vertical profiles of Cd in rice fields and found that soil pH, organic elements, and soil microbes are important drivers of Cd speciation. To mitigate Cd accumulation in rice, Kuang et al. applied lime and calcium-magnesium phosphate (CMP) amendments to paddy soils to reduce Cd bioavailability. The increased pH and phosphorus (P) in soils contributed to the decreased bioavailability of Cd and increased bacterial biodiversity. Also, Yu X. et al. found that using a Cd-immobilizing bacterial agent together with fermented organic matters in Cd-polluted soils could reduce plant (*Houttuynia cordata*) Cd uptake. Such amendments increased soil bacterial diversity.

Arsenic (As) pollution is also another classic and severe environmental problem (Huang et al., 2019; Li et al., 2021). Iron-oxidizing bacteria (FeOB) show the potential to mitigate As pollution, because FeOB could oxidize Fe(II) and provide As binding sites, which reduce As bioavailability (Emerson et al., 2010). In the current Research Topic, Qian et al. investigated the effect of FeOB inoculation on the As migration and transformation in paddy soils. They found that inoculation of *Ochrobactrum* sp. increased As proportion in the binding fraction. The reduced As bioavailability in soils led to less As uptake in rice tissues.

Copper (Cu) is another heavy metal of concern (Tani and Barrington, 2005a,b; de Vries et al., 2013). The alfalfa-rhizobium symbiosis can resist Cu stress, but the regulatory mechanism is unclear. In the current Research Topic, Duan et al. assessed the effects of rhizobium inoculation on the growth of alfalfa and soil microbial characteristics under Cu stress. They found that rhizobium inoculation markedly alleviated Cu-induced growth inhibition in alfalfa by increasing the chlorophyll content, height, and biomass, in addition to N and P contents. This study provides insights into the mechanism of action of the legume-rhizobium symbiotic system to mitigate Cu stress.

The stress of multiple metals presents a complex influence on the plant holobiont. Metal stress is commonly the critical factor inhibiting revegetation of mine tailings (Wong, 2003; Li, 2006). The tailing soil could be seriously poor in nutrients, which complicates the revegetation process. Liu et al. investigated the direct planting of *Pennisetum giganteum* into tailing sand with the designed bio-matrix pots, which were made by mixing corn cob powder and stalk powder. The *P. giganteum* could grow well,

especially those in the bio-matrix pots, which had more nutrients and suitable microbial communities. However, in terms of ecological restoration, the key factors driving the recovery of ecological functions are not still clear. By integrating the factors of plant species, soil communities, and abiotic conditions, Zhu et al. provide a conceptual framework considering the plant-soil feedbacks (PSFs) (Bever, 1994; Rinella and Reinhart, 2018) to guide a better understanding of the mechanisms of the restoration process. Through this framework, we could enhance our ability to predict and optimize above- and below-ground communities for better restoring ecosystem functions.

Salinity and habitats or cultivation type

Soil salinity is one of the most important abiotic factors limiting plant productivity (Bernstein, 1975; Zhao et al., 2020). Exposure to salts leads to osmotic and ionic stresses. Salt-tolerant endophytes could assist plants in salt tolerance through accumulating osmolytes, improving ion homeostasis and nutrient uptake, and providing phytohormones (Otlewska et al., 2020). In the current Research Topic, Szymańska et al. found that the isolated salt-tolerant endophytes could promote the growth of all tested plant species, suggesting a universal ability of endophytes to assist plant salt tolerance.

Since the soil microbial community affects the growth, quality, and yield of plants, understanding the microbial ecology of the agroecosystem could provide hints for sustainable agriculture. Kui et al. characterized the microbiome of tea plantation soils (448 soil samples from 101 ancient tea plantations). The authors revealed that the bacterial community was sensitive to environmental factors while the fungal community was more responsive to farmer intervention.

Among natural ecosystems, the mangrove ecosystems represent unique and essential habitats serving as sensitive areas for shoreline ecological functions (Lugo and Snedaker, 1974). Mai et al. found that different mangrove species harbor distinct microbial taxa in the sediments. Specific microbial taxa associated with the species *R. apiculata* contributed the highest functional activities related to carbon metabolism, carbon fixation, and methane metabolism. It indicates that mangrove-microbe interaction is species-dependent regarding the carbon cycle.

Summary and prospects

The Research Topic themed on *Microbial communities and functions contribute to plant performance under various stresses* brings a diverse research collection to this key framework. The collection is not only targeting agricultural production but also involves ecological restoration and functions. The effects of microbes on plant performance and their mechanisms are complex, and they mostly seem site- and species-dependent, and comparability among studies could be improved. Combined stresses, rather than single stress, could be more typical in reality. Future studies shall focus on theories with more fundamental biological and ecological mechanisms for better generality leading to possible application.

Author contributions

XWC and HMZ drafted and revised the manuscript. HL and DP commented on and edited the manuscript. All authors contributed substantially to the final version and approved it for publication.

Funding

Supports from the National Key Technology R&D Program of China (2020YFC1807604), Guangdong Natural Science Fund for Distinguished Young Scholar (2021B1515020014), and the National Natural Science Foundation of China (42277211, 41877350, and 42077298) are gratefully acknowledged.

Acknowledgments

We thank all authors and reviewers that contributed to this Research Topic. The comments and suggestions from the editors and reviewer on the present editorial are highly appreciated.

Conflict of interest

The authors declare that the research was conducted in the absence of any commercial or financial relationships that could be construed as a potential conflict of interest.

Publisher's note

References

Adams, M. A., Buckley, T. N., Binkley, D., Neumann, M., and Turnbull, T. L. (2021). CO_2, nitrogen deposition and a discontinuous climate response drive water use efficiency in global forests. *Nat. Commun.* 12, 5194. doi: 10.1038/s41467-021-25365-1

Atkinson, N. J., and Urwin, P. E. (2012). The interaction of plant biotic and abiotic stresses: from genes to the field. *J. Exp. Bot.* 63, 3523–3543. doi: 10.1093/jxb/ers100

Aung, K., Jiang, Y., and He, S. Y. (2018). The role of water in plant–microbe interactions. *Plant J.* 93, 771–780. doi: 10.1111/tpj.13795

Bailey-Serres, J., Parker, J. E., Ainsworth, E. A., Oldroyd, G. E. D., and Schroeder, J. I. (2019). Genetic strategies for improving crop yields. *Nature* 575, 109–118. doi: 10.1038/s41586-019-1679-0

Berendsen, R. L., Pieterse, C. M. J., and Bakker, P. A. H. M. (2012). The rhizosphere microbiome and plant health. *Trends Plant Sci.* 17, 478–486. doi: 10.1016/j.tplants.2012.04.001

Berg, G., and Cernava, T. (2022). The plant microbiota signature of the Anthropocene as a challenge for microbiome research. *Microbiome* 10, 54. doi: 10.1186/s40168-021-01224-5

Bernstein, L. (1975). Effects of salinity and sodicity on plant growth. *Annu. Rev. Phytopathol.* 13, 295–312. doi: 10.1146/annurev.py.13.090175.001455

Bever, J. D. (1994). Feeback between plants and their soil communities in an old field community. *Ecology* 75, 1965–1977. doi: 10.2307/1941601

Cavicchioli, R., Ripple, W. J., Timmis, K. N., Azam, F., Bakken, L. R., Baylis, M., et al. (2019). Scientists' warning to humanity: microorganisms and climate change. *Nat. Rev. Microbiol.* 17, 569–586. doi: 10.1038/s41579-019-0222-5

Chen, S., Waghmode, T. R., Sun, R., Kuramae, E. E., Hu, C., and Liu, B. (2019). Root-associated microbiomes of wheat under the combined effect of plant development and nitrogen fertilization. *Microbiome* 7, 136. doi: 10.1186/s40168-019-0750-2

Crutzen, P. J. (2002). Geology of mankind. *Nature* 415, 23–23. doi: 10.1038/415023a

de Vries, F. T., Griffiths, R. I., Knight, C. G., Nicolitch, O., and Williams, A. (2020). Harnessing rhizosphere microbiomes for drought-resilient crop production. *Science* 368, 270–274. doi: 10.1126/science.aaz5192

de Vries, W., Groenenberg, J. E., Lofts, S., Tipping, E., and Posch, M. (2013). "Critical loads of heavy metals for soils," in *Heavy Metals in Soils Environmental Pollution*, ed B. J. Alloway (Dordrecht: Springer), 211–237.

Dietz, T. (2017). Drivers of human stress on the environment in the twenty-first century. *Annu. Rev. Environ. Resour.* 42, 189–213. doi: 10.1146/annurev-environ-110615-085440

Emerson, D., Fleming, E. J., and McBeth, J. M. (2010). Iron-oxidizing bacteria: an environmental and genomic perspective. *Annu. Rev. Microbiol.* 64, 561–583. doi: 10.1146/annurev.micro.112408.134208

Fester, T., Giebler, J., Wick, L. Y., Schlosser, D., and Kästner, M. (2014). Plant–microbe interactions as drivers of ecosystem functions relevant for the biodegradation of organic contaminants. *Curr. Opin. Biotechnol.* 27, 168–175. doi: 10.1016/j.copbio.2014.01.017

Finkel, O. M., Salas-González, I., Castrillo, G., Conway, J. M., Law, T. F., Teixeira, P. J. P. L., et al. (2020). A single bacterial genus maintains root growth in a complex microbiome. *Nature* 587, 103–108. doi: 10.1038/s41586-020-2778-7

Hiddink, G. A., Termorshuizen, A. J., and van Bruggen, A. H. C. (2010). "Mixed cropping and suppression of soilborne diseases," in *Genetic Engineering, Biofertilisation, Soil Quality and Organic Farming Sustainable Agriculture Reviews*, ed. E. Lichtfouse (Dordrecht: Springer Netherlands), 119–146.

Hu, B., Shao, S., Ni, H., Fu, Z., Hu, L., Zhou, Y., et al. (2020). Current status, spatial features, health risks, and potential driving factors of soil heavy metal pollution in China at province level. *Environ. Pollut.* 266, 114961. doi: 10.1016/j.envpol.2020.114961

Huang, Y., Wang, L., Wang, W., Li, T., He, Z., and Yang, X. (2019). Current status of agricultural soil pollution by heavy metals in China: a meta-analysis. *Sci. Total Environ.* 651, 3034–3042. doi: 10.1016/j.scitotenv.2018.10.185

Lebeis, S. L. (2015). Greater than the sum of their parts: characterizing plant microbiomes at the community-level. *Curr. Opin. Plant Biol.* 24, 82–86. doi: 10.1016/j.pbi.2015.02.004

Li, M. S. (2006). Ecological restoration of mineland with particular reference to the metalliferous mine wasteland in China: a review of research and practice. *Sci. Total Environ.* 357, 38–53. doi: 10.1016/j.scitotenv.2005.05.003

Li, W., Liu, Y., Wang, J., Shi, S., and Cao, W. (2018). Six years of grazing exclusion is the optimum duration in the alpine meadow-steppe of the north-eastern Qinghai-Tibetan Plateau. *Sci. Rep.* 8, 17269. doi: 10.1038/s41598-018-35273-y

Li, Y., Zhang, M., Xu, R., Lin, H., Sun, X., Xu, F., et al. (2021). Arsenic and antimony co-contamination influences on soil microbial community composition and functions: relevance to arsenic resistance and carbon, nitrogen, and sulfur cycling. *Environ. Int.* 153, 106522. doi: 10.1016/j.envint.2021.106522

Liu, Y.-X., Qin, Y., and Bai, Y. (2019). Reductionist synthetic community approaches in root microbiome research. *Curr. Opin. Microbiol.* 49, 97–102. doi: 10.1016/j.mib.2019.10.010

Lugo, A. E., and Snedaker, S. C. (1974). The ecology of mangroves. *Annu. Rev. Ecol. Syst.* 5, 39–64.

Martin, F. M., Uroz, S., and Barker, D. G. (2017). Ancestral alliances: plant mutualistic symbioses with fungi and bacteria. *Science* 356, eaad4501. doi: 10.1126/science.aad4501

McGill, B. J., Dornelas, M., Gotelli, N. J., and Magurran, A. E. (2015). Fifteen forms of biodiversity trend in the Anthropocene. *Trends Ecol. Evol.* 30, 104–113. doi: 10.1016/j.tree.2014.11.006

Niu, B., Paulson, J. N., Zheng, X., and Kolter, R. (2017). Simplified and representative bacterial community of maize roots. *Proc. Natl. Acad. Sci. U. S. A.* 114, E2450–E2459. doi: 10.1073/pnas.1616148114

Otlewska, A., Migliore, M., Dybka-Stepie,ń, K., Manfredini, A., Struszczyk-Swita, K., Napoli, R., et al. (2020). When salt meddles between plant, soil, and microorganisms. *Front. Plant Sci.* 11, 553087. doi: 10.3389/fpls.2020.553087

Rillig, M. C., and Mummey, D. L. (2006). Mycorrhizas and soil structure. *New Phytol.* 171, 41–53. doi: 10.1111/j.1469-8137.2006.01750.x

Rinella, M. J., and Reinhart, K. O. (2018). Toward more robust plant-soil feedback research. *Ecology* 99, 550–556. doi: 10.1002/ecy.2146

Rudgers, J. A., Afkhami, M. E., Bell-Dereske, L., Chung, Y. A., Crawford, K. M., Kivlin, S. N., et al. (2020). Climate disruption of plant-microbe interactions. *Annu. Rev. Ecol. Evol. Syst.* 51, 561–586. doi: 10.1146/annurev-ecolsys-011720-090819

Salas-González, I., Reyt, G., Flis, P., Custódio, V., Gopaulchan, D., Bakhoum, N., et al. (2020). Coordination between microbiota and root endodermis supports plant mineral nutrient homeostasis. *Science* 371, eabd0695. doi: 10.1126/science.abd0695

Shi, T., Ma, J., Wu, X., Ju, T., Lin, X., Zhang, Y., et al. (2018). Inventories of heavy metal inputs and outputs to and from agricultural soils: a review. *Ecotoxicol. Environ. Saf.* 164, 118–124. doi: 10.1016/j.ecoenv.2018.08.016

Shipton, P. J. (1977). Monoculture and soilborne plant pathogens. *Annu. Rev. Phytopathol.* 15, 387–407. doi: 10.1146/annurev.py.15.090177.002131

Smith, S. E., and Read, D. J. (2008). *Mycorrhizal Symbiosis*. 3rd ed. London: Academic Press.

Song, S., Zhu, J., Zheng, T., Tang, Z., Zhang, F., Ji, C., et al. (2020). Long-term grazing exclusion reduces species diversity but increases community heterogeneity in an alpine grassland. *Front. Ecol. Evol.* 8, 66. doi: 10.3389/fevo.2020.00066

Springmann, M., Clark, M., Mason-D'Croz, D., Wiebe, K., Bodirsky, B. L., Lassaletta, L., et al. (2018). Options for keeping the food system within environmental limits. *Nature* 562, 519–525. doi: 10.1038/s41586-018-0594-0

Tani, F. H., and Barrington, S. (2005a). Zinc and copper uptake by plants under two transpiration rates. Part I. Wheat (*Triticum aestivum* L.). *Environ. Pollut.* 138, 538–547. doi: 10.1016/j.envpol.2004.06.005

Tani, F. H., and Barrington, S. (2005b). Zinc and copper uptake by plants under two transpiration rates. Part II. Buckwheat (*Fagopyrum esculentum* L.). *Environ. Pollut.* 138, 548–558. doi: 10.1016/j.envpol.2004.06.004

Toju, H., Peay, K. G., Yamamichi, M., Narisawa, K., Hiruma, K., Naito, K., et al. (2018). Core microbiomes for sustainable agroecosystems. *Nat. Plants* 4, 247–257. doi: 10.1038/s41477-018-0139-4

Unger, I. M., Kennedy, A. C., and Muzika, R.-M. (2009). Flooding effects on soil microbial communities. *Appl. Soil Ecol.* 42, 1–8. doi: 10.1016/j.apsoil.2009.01.007

van der Heijden, M. G. A., and Hartmann, M. (2016). Networking in the plant microbiome. *PLoS Biol.* 14, e1002378. doi: 10.1371/journal.pbio.1002378

Wang, J., Li, Y., Bork, E. W., Richter, G. M., Eum, H.-I., Chen, C., et al. (2020). Modelling spatio-temporal patterns of soil carbon and greenhouse gas emissions in grazing lands: current status and prospects. *Sci. Total Environ.* 739, 139092. doi: 10.1016/j.scitotenv.2020.139092

Wei, Z., Yang, T., Friman, V.-P., Xu, Y., Shen, Q., and Jousset, A. (2015). Trophic network architecture of root-associated bacterial communities determines pathogen invasion and plant health. *Nat. Commun.* 6, 8413. doi: 10.1038/ncomms9413

Wong, M. H. (2003). Ecological restoration of mine degraded soils, with emphasis on metal contaminated soils. *Chemosphere* 50, 775–780. doi: 10.1016/S0045-6535(02)00232-1

Xiong, W., Li, Z., Liu, H., Xue, C., Zhang, R., Wu, H., et al. (2015). The effect of long-term continuous cropping of black pepper on soil bacterial communities as determined by 454 pyrosequencing. *PLoS ONE* 10, e0136946. doi: 10.1371/journal.pone.0136946

Zeng, S., Ma, J., Yang, Y., Zhang, S., Liu, G.-J., and Chen, F. (2019). Spatial assessment of farmland soil pollution and its potential human health risks in China. *Sci. Total Environ.* 687, 642–653. doi: 10.1016/j.scitotenv.2019.05.291

Zhang, J., Liu, Y.-X., Guo, X., Qin, Y., Garrido-Oter, R., Schulze-Lefert, P., et al. (2021). High-throughput cultivation and identification of bacteria from the plant root microbiota. *Nat. Protoc.* 16, 988–1012. doi: 10.1038/s41596-020-00444-7

Zhang, J.-S., Zhang, F.-P., Yang, J.-H., Wang, J.-P., Cai, M.-L., Li, C.-F., et al. (2011). Emissions of N_2O and NH_3, and nitrogen leaching from direct seeded rice under different tillage practices in central China. *Agric. Ecosyst. Environ.* 140, 164–173. doi: 10.1016/j.agee.2010.11.023

Zhang, L., Zhou, J., George, T. S., Limpens, E., and Feng, G. (2021). Arbuscular mycorrhizal fungi conducting the hyphosphere bacterial orchestra. *Trends Plant Sci.* 27, 402–411. doi: 10.1016/j.tplants.2021.10.008

Zhao, C., Zhang, H., Song, C., Zhu, J.-K., and Shabala, S. (2020). Mechanisms of plant responses and adaptation to soil salinity. *Innovation* 1, 100017. doi: 10.1016/j.xinn.2020.100017

Zhou, J., and Ning, D. (2017). Stochastic community assembly: does it matter in microbial ecology? *Microbiol. Mol. Biol. Rev.* 81, e00002–17. doi: 10.1128/MMBR.00002-17

frontiers in Microbiology

ORIGINAL RESEARCH
published: 06 September 2021
doi: 10.3389/fmicb.2021.722626

Fungi-Bacteria Associations in Wilt Diseased Rhizosphere and Endosphere by Interdomain Ecological Network Analysis

Lin Tan[1], Wei-ai Zeng[2], Yansong Xiao[3], Pengfei Li[4], Songsong Gu[5,6], Shaolong Wu[7], Zhengguang Zhai[2], Kai Feng[5,8], Ye Deng[5,6,8] and Qiulong Hu[1]**

[1] Hunan Agricultural University, Changsha, China, [2] Changsha Tobacco Company of Hunan Province, Changsha, China, [3] Chenzhou Tobacco Company of Hunan Province, Chenzhou, China, [4] Wenshan Tobacco Company of Yunnan Province, Wenshan, China, [5] CAS Key Laboratory for Environmental Biotechnology, Research Center for Eco-Environmental Sciences, Chinese Academy of Sciences, Beijing, China, [6] Institute for Marine Science and Technology, Shandong University, Qingdao, China, [7] Tobacco Company of Hunan Province, Changsha, China, [8] College of Resources and Environment, University of Chinese Academy of Sciences, Beijing, China

OPEN ACCESS

Edited by:
Hai-Ming Zhao, Jinan University, China

Reviewed by:
Tengxiang Lian, South China Agricultural University, China
Bing Yang, Sichuan Academy of Giant Panda, Chengdu, China
Biying Zhao, Jiangsu University, China
Juntao Wang, Western Sydney University, Australia
Wensheng Qin, Lakehead University, Canada

***Correspondence:**
Ye Deng
yedeng@rcees.ac.cn
Qiulong Hu
huqiulongnet@126.com

Specialty section:
This article was submitted to Terrestrial Microbiology, a section of the journal Frontiers in Microbiology

Received: *09 June 2021*
Accepted: *11 August 2021*
Published: *06 September 2021*

Citation:
Tan L, Zeng W, Xiao Y, Li P, Gu S, Wu S, Zhai Z, Feng K, Deng Y and Hu Q (2021) Fungi-Bacteria Associations in Wilt Diseased Rhizosphere and Endosphere by Interdomain Ecological Network Analysis. Front. Microbiol. 12:722626. doi: 10.3389/fmicb.2021.722626

In the plant rhizosphere and endosphere, some fungal and bacterial species regularly co-exist, however, our knowledge about their co-existence patterns is quite limited, especially during invasion by bacterial wilt pathogens. In this study, the fungal communities from soil to endophytic compartments were surveyed during an outbreak of tobacco wilt disease caused by *Ralstonia solanacearum*. It was found that the stem endophytic fungal community was significantly altered by pathogen invasion in terms of community diversity, structure, and composition. The associations among fungal species in the rhizosphere and endosphere infected by *R. solanacearum* showed more complex network structures than those of healthy plants. By integrating the bacterial dataset, associations between fungi and bacteria were inferred by Inter-Domain Ecological Network (IDEN) approach. It also revealed that infected samples, including both the rhizosphere and endosphere, had more complex interdomain networks than the corresponding healthy samples. Additionally, the bacterial wilt pathogenic *Ralstonia* members were identified as the keystone genus within the IDENs of both root and stem endophytic compartments. *Ralstonia* members was negatively correlated with the fungal genera *Phoma, Gibberella,* and *Alternaria* in infected roots, as well as *Phoma, Gibberella,* and *Diaporthe* in infected stems. This suggested that those endophytic fungi may play an important role in resisting the invasion of *R. solanacearum.*

Keywords: bacterial wilt invasion, soil microbiota, endophytic microbiota, molecular ecological network, biocontrol fungal resources

INTRODUCTION

Ralstonia solanacearum, the causative agent of soil-borne bacterial wilt disease in plants, is often found in agricultural land used for tobacco cultivation. Once the pathogen invades the plant root system, it rapidly spreads to the stem, causing an internal system imbalance of the entire tobacco plant, accelerating senescence and death (Li et al., 2017; Wei et al., 2018). As important

members of the plant microecosystem (Nilsson et al., 2019), fungi play a vital role in promoting the material cycle of agro-ecosystem and affecting plant growth and health (Lilleskov et al., 2011; Zhang et al., 2021). Therefore, dynamic changes in the structure and composition of the plant soil fungal community can indicate the alterations of soil micro-ecological environment (Shi et al., 2020). Plant endophytic fungi exist within the host plant and interact closely with other microorganisms to promote plant growth, resist the invasion of plant pathogens, and improve the disease resistance of host plant through their own metabolites or induction of the host's metabolites (Arnold, 2007; Mousa et al., 2016; Bastias et al., 2017). However, our knowledge about how the soil and endophytic fungal communities change under the invasion of *R. solanacearum* is quite limited.

With the surge of research on microbial communities in various ecological environments, the interdomain relationships between different types of microbial communities has attracted great attention (Kapitan et al., 2019; Wang et al., 2020). The association of plant bacterial and fungal communities is critical to overall microbial community structure and plant health (Hassani et al., 2018), and intrigues numerous botanists and microbiologists. Plant microbial communities live and colonize several zones including the bulk soil, rhizosphere soil, phyllosphere, and endosphere (Bulgarelli et al., 2013; Kumar et al., 2017). They play a vital role in the acquisition of nutrients by plants, mutual defense, and co-evolution (Martin et al., 2017; Fitzpatrick et al., 2018). Understanding the relationship between related microorganisms in natural ecosystems may help us better explore and learn about the assembly, diversity, and stability of plant-related communities (Haq et al., 2014; van der Putten, 2017). Recently, researchers have attempted to identify plant-related microbial communities from bacteria to fungi, as well as their associations, by means of microbiome annotation database or molecular-based experimental methods, broadening our basic knowledge of these types of microbial communities (Jackrel et al., 2017; Bamisile et al., 2018; Levy et al., 2018). Endophytic fungi are often considered to be beneficial to their host plants (Qian et al., 2019), because they may play various ecological roles such as promoting plant growth, enhancing the absorption of nutrient, resistance against various plant pathogens, as well as tolerance against various biotic and abiotic stresses (Waqas et al., 2012; Jia et al., 2016; Terhonen et al., 2016; Ripa et al., 2019). Current studies on tobacco wilt, a bacterial disease, mainly focus on the diversity and structural composition of the tobacco soil microbial community and its correlation with soil physicochemical properties, as well as the associations between the pathogen and bacterial species (Jiang et al., 2017; Li et al., 2017). However, the associations between the closely related bacterial and fungal communities in various zones of the plant-soil microecosystem under the invasion of *R. solanacearum* and the roles of endophytic fungi remains unclear.

The purposes of the current study are to: (i) Illuminate the characteristics of fungal communities in the bulk and rhizosphere soils and the root and stem endophytic compartments of healthy tobacco plants and those infected by *R. solanacearum*; (ii) Reveal the associations among species of fungal communities from various zones of the plant-soil microecosystem via molecular ecological network analysis; (iii) Explore the associations between fungi and bacteria through interdomain ecological network (IDEN) analysis; (iv) Study the associations between pathogenic *Ralstonia* members and fungi through sub-network analysis, and to explore fungal biocontrol resources that may antagonize the bacterial wilt pathogen. From the obtained results, we will provide a new strategy and theoretical support for enriching the study of tobacco endophytic fungal resources and for exploring the antagonistic fungal resources targeting *R. solanacearum*.

MATERIALS AND METHODS

Sample Collection and Processing

The general collecting locations and methods of collecting and processing for soil and endophytic samples have been described previously in detail (Hu Q.L. et al., 2020), and will only be summarized here. Detailed location and other information were list in **Supplementary Table 1**. Eighty samples of bulk soil, rhizosphere soil, roots, and stems for tobacco cultivar Yunyan 87, including healthy and severely infected by *R. solanacearum* (grade 5–9 infection) (Chinese Standards, 2008), were collected from 5 different tobacco field sites located in the Chenzhou tobacco-growing region of Hunan province of China on June 2016 (mature stage of tobacco). The samples included 10 bulk soils samples of healthy tobacco (HBS), 10 bulk soil samples of wilt-infected tobacco (IBS), 10 rhizosphere samples of healthy tobacco (HRS), 10 rhizosphere samples of wilt-infected tobacco (IRS), 10 root samples of healthy tobacco (HR), 10 root samples of wilt-infected tobacco (IR), 10 stem samples of healthy tobacco (HS), 10 stem samples of wilt-infected tobacco (IS). Bulk soil samples were collected by shaking soil off tobacco roots. After shaking off bulk soils, the rhizosphere soils adhering to plant roots were collected in 50 mL tubes containing PBS (0.1% Tween 80) with a brush. After stirring for 5 min, the resulting suspension was then poured into a sterile centrifuge tube, this process was repeated a further two times. The suspensions were mixed and centrifuged for 5 min at 2,000 × *g*. The resulting sediment pellets were collected as the rhizosphere soils, which were stored at –80°C until DNA extraction. The roots and stems were processed immediately by washing consecutively with 75% ethanol, 2.5% sodium hypochlorite, and sterile water. They were then cut into small pieces and homogenized using a mortar and pestle with PBS, then transferred into a centrifuge tube for further treatment. Ultimately, the resulting sediment pellets from soil samples and resulting cell pellet from endophytic samples were stored in a freezer at –80°C until DNA extraction.

DNA Extraction and High-Throughput Sequencing

Total DNA was extracted in duplicate using the FastDNATM SPIN kit (MP Biomedicals) following the manufacturer's instructions. Methods of PCR amplification and high-throughput sequencing for 16S rRNA genes followed those of Zhang et al. (2017). The V5-V6 region of 16S rRNA gene was amplied by the 799F (5′-AACMGGATTAGATACC CKG-3′)/1115R (5′-AGGGTTGCGCTCGTTG-3′)

primers, and ITS2 fragment was amplified using the primer pair 5.8F (5′-AACTTTYRRCAAYGGAT CWCT-3′)/4R (5′-AGCCTCCGCTTATTGATATGCTTAART-3′) (Taylor et al., 2016). PCR amplification was performed in a 50 μL reaction system including 5 μL DNA template, 2.5 U of Taq DNA Polymerase (TaKaRa), 1 × Taq buffer, 75 μM dNTP and 0.3 μM of each primer. The thermal cycle operations for ITS2 fragment was performed as follows: 94°C for 1 min; following 35 cycles of 94°C for 20 s, 57°C for 25 s, and 68°C for 45 s, with a final elongation step at 68°C for 10 min, and finally stored at 4°C. The recovered products were qualified and quantified by a NanoDrop Spectrophotometer (Nano-100, Aosheng Instrument Co., Ltd.). Subsequently, the purified amplicons were pooled together and sequenced on Miseq sequencing machine (Illumina) at Central South University, Changsha, China.

Sequence Processing and Analysis

Preprocessing of raw reads of 16S rRNA genes and ITS2 fragment were submitted to an in-house pipeline[1] integrated with various bioinformatics tools (Feng et al., 2017). All reads were assigned to individual sample according to their barcodes, allowing for a single mismatch. After trimming off the barcode and primer sequences, the pair-ended sequences for 16S rRNA genes were merged and their quality was checked by Flash program (Kong, 2011). The pair-ended sequences for ITS2 fragment with forward and reverse primers combinations were trimmed off. Subsequently, the sequences were passed through the ITSx program to remove the ITS flanking regions and non-fungal sequences (Bengtsson-Palme et al., 2013). Next, sequences were clustered into operational taxonomic units (OTUs) using UPARSE (SRP101823 for 16S rRNA gene sequences, and SRP123067 for ITS sequences) with a 97% sequence similarity threshold (Edgar, 2013). Ultimately, an OTU table was created and the total read counts were resampled before use in downstream analyses.

Statistical Analysis

The statistical significance of differences between two groups were tested by Wilcoxon test. Two measurements of alpha-diversity, Richness and Chao1, were calculated to assess the diversity of fungal communities. Richness was obtained by counting the number of species displayed in the OTU table. The Chao1 value was calculated using Mothur software (Chao, 1984; Schloss et al., 2009). Principal coordinate analysis (PCoA) was used to analyze the β-diversity of fungal communities in the bulk soil, rhizosphere soil, and root and stem endophytic compartments for both healthy and infected plants. Dissimilarity tests for soil and endophytic microbial community structures between healthy and infected samples were performed by using PERMANOVA based on Jaccard distance. Differences in soil and plant endophytic community compositions from healthy and infected samples were determined using an analysis of variance (ANOVA).

[1]http://mem.rcees.ac.cn:8080

Random Matrix Theory Based Molecular Ecology Networks

To reveal the associations among fungal species in soil and endophytic fungal communities, from both healthy and infected samples, we constructed phylogenetic molecular ecological networks (MEN) via a Random Matrix Theory (RMT)-based approach (Deng et al., 2012) in molecular ecological network analysis pipeline (MENA)[2] (Deng et al., 2016).

Interdomain Ecological Network Construction

The topology of ecological networks can represent the assembly process of microbial communities (Layeghifard et al., 2017), and the connections between interacting species can be used to predict ecosystem stability (Thebault and Fontaine, 2010). Recently, Feng et al. (2019) set up a workflow to construct IDEN, to find the association between two taxonomic groups (i.e., aboveground plants and underground bacteria) in ecological surveys. This method provided technical support for our analysis of the interdomain microbial associations between fungal and bacterial communities of soil and endophytes.

To elucidate associations between fungi and bacteria in soil and endophytic communities, by integrating the bacterial dataset (NCBI SRA database, accession PRJNA540089), interdomain ecological networks via SparCC approaches based on the inter-domain ecological network analysis pipeline[3] workflow (Feng et al., 2019) were constructed. The threshold value for generating regional IDEN was 0.30, with 0.05 significance, to filter the non-correlated associations. The obtained adjacent matrix associated with the bipartite graph consisted of 1 or 0, showing presence/absence of corresponding fungi-bacteria association. The topological properties (connectance, links per species, specialization asymmetry, and web asymmetry) were calculated to explore alterations in associations between fungi and bacteria in the soil and endophytic communities under the invasion of *R. solanacearum*. The SparCC method with default parameters (Feng et al., 2019) was used for correlation analysis of specific associations between the pathogen and fugal members. The constructed networks were visualized using Gephi 0.9.2 software (Bastian et al., 2009). The keystone microorganisms were identified by the Zi-Pi plot based on the nodes' roles within their own network (Deng et al., 2012).

RESULTS

Effects of Wilt Pathogen Invasion on the Fungal Community Diversity and Structure of Soil and Tobacco Endophyte

Using high-throughput sequencing, a total of 8, 317 operational taxonomic units (OTUs) were obtained from 80 samples, 7, 216 OTUs among the soil samples and 2, 786 OTUs among the endophytic samples. Both observed Chao1 (**Figure 1A**)

[2]http://ieg4.rccc.ou.edu/mena

[3]http://mem.rcees.ac.cn:8081

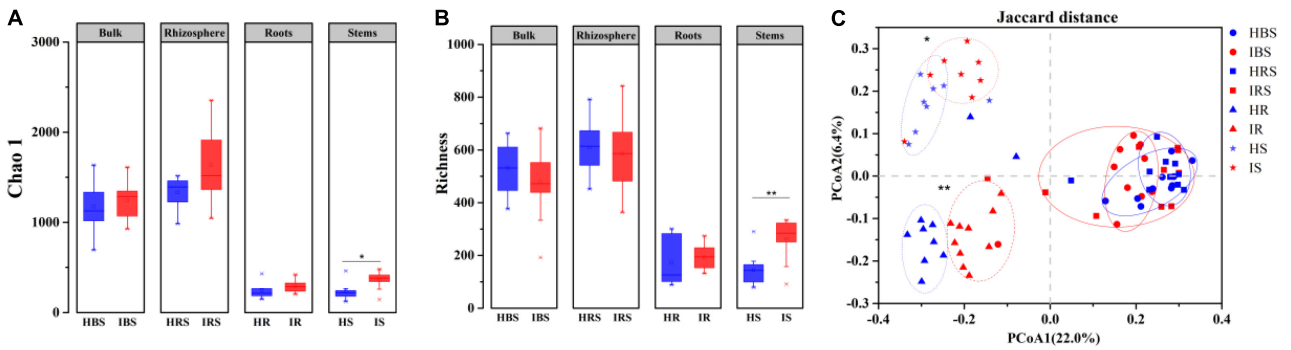

FIGURE 1 | Diversity and structure of fungal communities in the healthy and infected bulk soil, rhizosphere soil, and root and stem endophytic compartments based on internal transcribed spacer (ITS) sequencing. **(A)** Richness. **(B)** Chao 1 index. **(C)** PCoA plot of fungal communities in healthy and infected plants. Note: blue and red indicate healthy and infected samples, respectively. HBS: bulk soils samples of healthy tobacco, IBS: bulk soil samples of wilt-infected tobacco, HRS: rhizosphere samples of healthy tobacco, IRS: rhizosphere samples of wilt-infected tobacco, HR: root samples of healthy tobacco, IR: root samples of wilt-infected tobacco, HS: stem samples of healthy tobacco, IS: stem samples of wilt-infected tobacco. Wilcoxon test and PERMANOVA were used to examine the statistical significance of differences for alpha and beta diversity, respectively. Difference was significant at *, 0.05; **, 0.01.

and estimated richness (**Figure 1B**) demonstrated no significant difference in fungal community diversity between healthy and infected tobacco plants regarding the bulk soil, rhizosphere soil, and root endophytes. However, the fungal richness of infected stems was significantly higher than that of healthy counterparts (Wilcoxon test, $P < 0.05$). As shown in **Figure 1C**, the endophytic fungal communities for healthy and infected plants were clearly separated in the PCoA plot, while the bulk, and rhizosphere soil communities of healthy and infected plants partially overlapped, indicating significant differences in fungal community structure between the healthy and infected endophytic compartments (PERMANOVA, $P < 0.05$).

Effects of Wilt Pathogen Invasion on the Fungal Community Composition of Soil and Tobacco Endophyte

The composition of tobacco soils and endophytic fungal communities at the phylum level is shown in **Figure 2A** (with relative abundance > 1%). In the soil communities, the most abundant fungal phyla were *Ascomycota*, *Basidiomycota*, and *Zygomycota*, followed by *Chytridiomycota* and *Glomeromycota*. In the tobacco endophytic fungal communities, the most abundant fungal phyla were *Ascomycota* and *Basidiomycota*, followed by *Zygomycota*, *Chytridiomycota*, and *Glomeromycota*. The composition of tobacco soil and endophytic fungal communities at the genus level is shown in **Figure 2B** (with relative abundance > 1%). In the soil communities, the fungal genera with higher relative abundance included *Mortierella, Aleuria, Cyberlindnera, Cryptococcus, Plectosphaerella, Gibberella, Mucor, Debaryomyces, Podospora, Entoloma, Paraphoma, Rhodotorula, Fusarium, Conocybe,* and *Guehomyces*. In the tobacco endophytic fungal communities, the fungal genera with higher relative abundance included *Plectosphaerella, Paraphoma, Gibberella, Rhodotorula, Alternaria, Ceratobasidium, Nectria, Davidiella, Haematonectria, Bionectria,* and *Thanatephorus*. The genera whose abundance increased significantly in the infected soil samples as compared to healthy soil samples were *Gibberella, Cryptococcus, Mucor, Nectria, Debaryomyces,* and *Haematonectria*, and the genera that displayed significantly deceased abundance were *Rhodotorula, Ceratobasidium, Cyberlindnera, Podospora, Conocybe, Monoblepharis, Paraconiothyrium,* and *Phoma*. The genera whose abundance increased significantly in the endophytic communities of infected samples compared to those of healthy samples were *Haematonectria, Gibberella, Ceratobasidium, Nectria, Bionectria*, and *Didymella,* and the genera with significantly deceased abundance were *Cryptococcus, Didymella, Mortierella, Paraphoma, Davidiealla, Phoma,* and *Mucor*. In summary, the fungal community compositions and relative abundance were different between the healthy and infected soil communities, between the healthy and infected endophytic communities, and between the soil and endophytic communities (**Supplementary Table 2**, $P < 0.05$).

The Species Associations Among Fungal Communities

In the network structures of rhizosphere soil, root endophytes, and stem endophytes, the fungal network structures of the infected samples showed a higher complexity and more links than those of healthy samples (**Table 1**). For example, the number of network nodes and links of the infected rhizosphere soil were 187 and 518, respectively, and those of the healthy rhizosphere soil were 179 and 367, respectively. In addition, the average clustering coefficients (avgCCs) of the empirical networks of all tested samples (0.02–0.67) were higher than those of the corresponding random networks (0.01–0.228), suggesting that the eight constructed networks all had typical small-world network characteristics (Watts and Strogatz, 1998). The modularity (M) values of all empirical networks (0.534–0.91) were significantly higher than the M-values of the corresponding random networks (0.339–0.860), indicating modular topological features of constructed networks (Newman, 2016). The visualized networks were constructed to intuitively display the associations

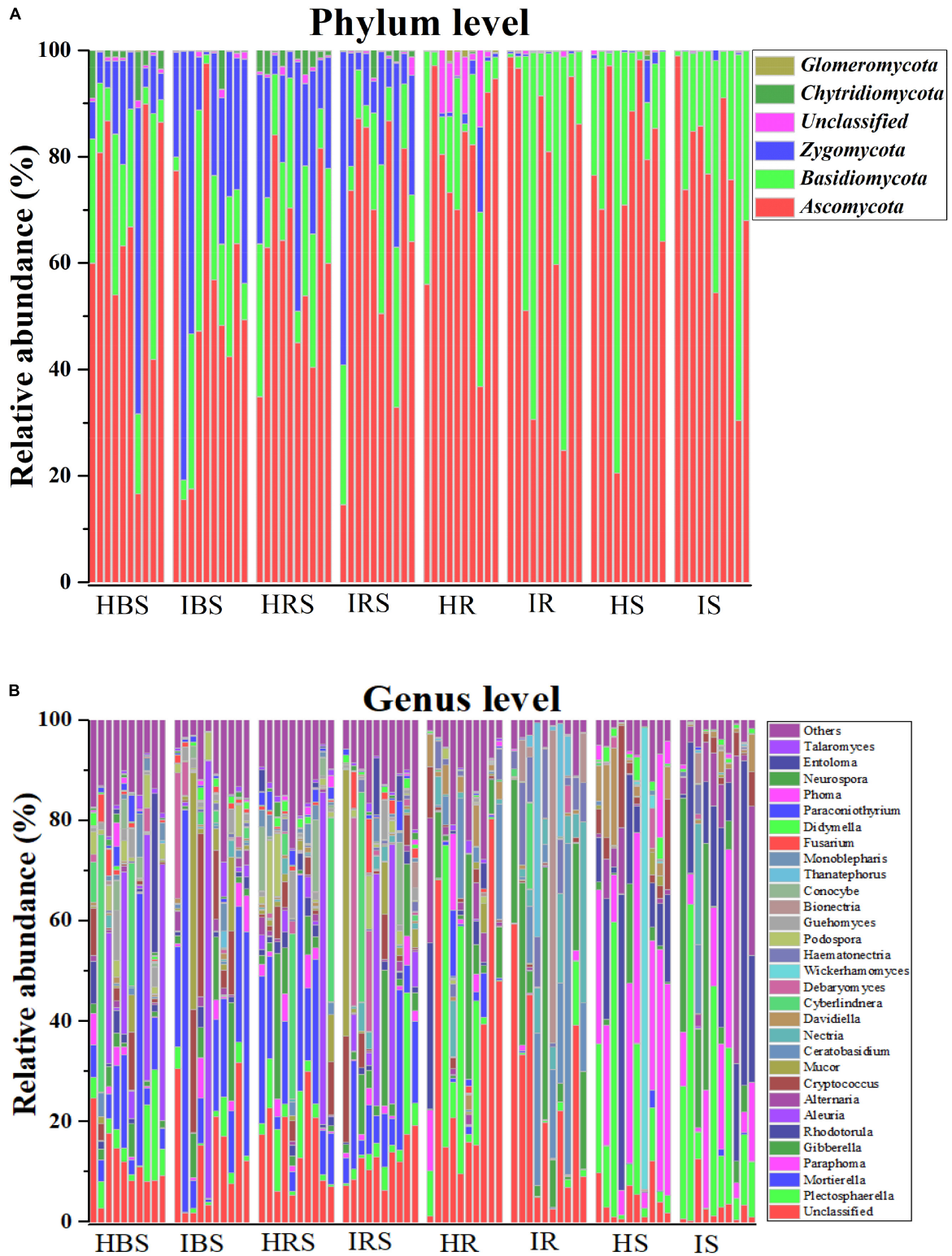

FIGURE 2 | Comparison of the community compositions of soil and plant endophytic fungi from healthy and infected samples. **(A)** Comparison of the community compositions of the healthy and infected bulk soil, rhizosphere soil, and root and stem endophytic compartments with relative abundance > 1% OTUs at the phylum level. **(B)** Comparison of the community compositions of the healthy and infected bulk soil, rhizosphere soil, and root and stem endophytic compartments with relative abundance > 1% OTUs at the genus level.

among microorganisms in the fungal communities of healthy and infected samples, as shown in **Figure 3**. In general, there were obvious differences in the network topological structure between infected and healthy samples from all four of the investigated microecosystem zones.

IDEN Between Fungal and Bacterial Communities

The eight constructed networks of fungi-bacteria associations in healthy and infected samples from the surrounding bulk soil, rhizosphere soil, and root and stem endophytic compartments showed some basic bipartite topological structures, e.g., the modular structure and high web asymmetry of two species groups (**Table 2**), and all showed significant topological differences (**Figure 4**). According to the topological indices of the networks (**Table 2**), the total numbers of network nodes and links of the infected samples were all higher than the corresponding healthy samples, indicating more complex and compact bacterial-fungal associations in the infected samples. The higher value of web asymmetry for networks of infected root and stems endophytes showed that more fungi were involved in the interdomain associations. Instead of higher positive and negative associations for soil samples, the IDENs contained large proportions of negative associations in infected root and stem endophytic compartments compared to healthy samples, with more fungal nodes involved (1,298 vs. 266 for roots, and 493 vs. 131 for stems), suggesting resistance relationships between bacteria and fungi. Module detection analysis further demonstrated smaller modularity and fewer modules for IDENs of the endophytic compartments, implying closer fungi-bacteria associations. In addition, we found the greatest number of network links and the highest number of links per species in the IDEN of infected root endophytic compartment, indicating larger proportions of bacterial-fungal associations among the infected root endophytes.

Mining of Keystone Fungal Genus With Biocontrol Potential Against Bacterial Wilt Pathogen

The Zi-Pi plots were drawn to exhibit the distribution of network nodes OTUs based on the modular topology (**Figure 5**). The topology of each node (genus) could be measured by its within-module connectivity ($Zi = 2.5$) and among-module connectivity ($Pi = 0.62$). According to the simplified categorization, all nodes in the networks were distributed among four subcategories: Peripherals, Connectors, Module hubs and Network hubs. Nodes that belonged to the latter three subcategories were considered to be keystone microbial microorganisms playing a critical role in the network (Zhou et al., 2011; Jiang et al., 2015) and were marked in the corresponding networks. Interestingly, the bacterial wilt pathogenic *Ralstonia* members were found to be the keystone genus in the IDENs of the infected root and stem endophytic compartments.

To find the fungal genus closely associated with *Ralstonia* members, we further analyzed the associations between *Ralstonia* members and fungal genus in IDENs for the infected root and stem endophytic compartments. The results showed that the fungal genera *Phoma, Gibberella, Alternaria, Haematonectria, Cryptococcus, Podospora, Spodiobolus, Malassezia, Aleuria, Dioszgia, Davidiealla,* and unclassified genera were negatively correlated with the pathogenic *Ralstonia* members in the root endophytic communities (**Figure 6**), and the fungal genera *Phoma*, *Gibberella, Diaporthe, Didymella,* and unclassified genera were negatively correlated with *Ralstonia* members in the stem endophytic communities (**Figure 6**). No positive correlations between fungal genus and the pathogen were found in the root and stem endophytic communities.

DISCUSSION

The occurrence of plant diseases is closely related to the microbial diversity in the soil and endophytic compartments

TABLE 1 | Topological features of the soil and endophytic fungal community networks in healthy and infected samples.

			Empirical networks						Random networks		
Samples	**Similarity threshold**	**Total nodes**	**Total links**	R^2	**Average degree (avgK)**	**Average path distance (GD)**	**Average clustering coefficient (avgCC)**	**Modularity: (module·no)**	**Average clustering coefficient (avgCC)**	**Modularity: (module·no)**	**Average path distance (GD)**
HBS	0.85	174	232	0.76	2.67	7.42	0.28	0.81 (21)	0.034 ± 0.01	0.67 ± 0.01	5.22 ± 0.16
IBS	0.85	133	368	0.74	5.53	4.14	0.42	0.91 (24)	0.01 ± 0.02	0.82 ± 0.01	6.57 ± 1.06
HRS	0.85	179	367	0.87	4.10	6.33	0.32	0.67 (15)	0.06 ± 0.02	0.52 ± 0.01	4.08 ± 0.12
IRS	0.85	187	518	0.80	5.54	4.26	0.29	0.54 (16)	0.11 ± 0.02	0.44 ± 0.01	3.58 ± 0.08
HR	0.90	27	49	0.79	3.63	1.90	0.50	0.534 (4)	0.228 ± 0.058	0.339 ± 0.018	2.56 ± 0.11
IR	0.90	66	138	0.69	4.18	2.07	0.67	0.653 (12)	0.188 ± 0.0278	0.383 ± 0.014	3.04 ± 0.12
HS	0.90	30	20	0.99	1.33	1.62	0.02	0.865 (10)	0.01 ± 0.002	0.860 ± 0.016	1.67 ± 0.18
IS	0.90	119	200	0.76	3.36	3.48	0.45	0.750 (19)	0.08 ± 0.02	0.522 ± 0.015	3.70 ± 0.11

HBS, bulk soils samples of healthy tobacco; IBS, bulk soil samples of wilt-infected tobacco; HRS, rhizosphere samples of healthy tobacco; IRS, rhizosphere samples of wilt-infected tobacco; HR, root samples of healthy tobacco; IR, root samples of wilt-infected tobacco; HS, stem samples of healthy tobacco; IS, stem samples of wilt-infected tobacco.

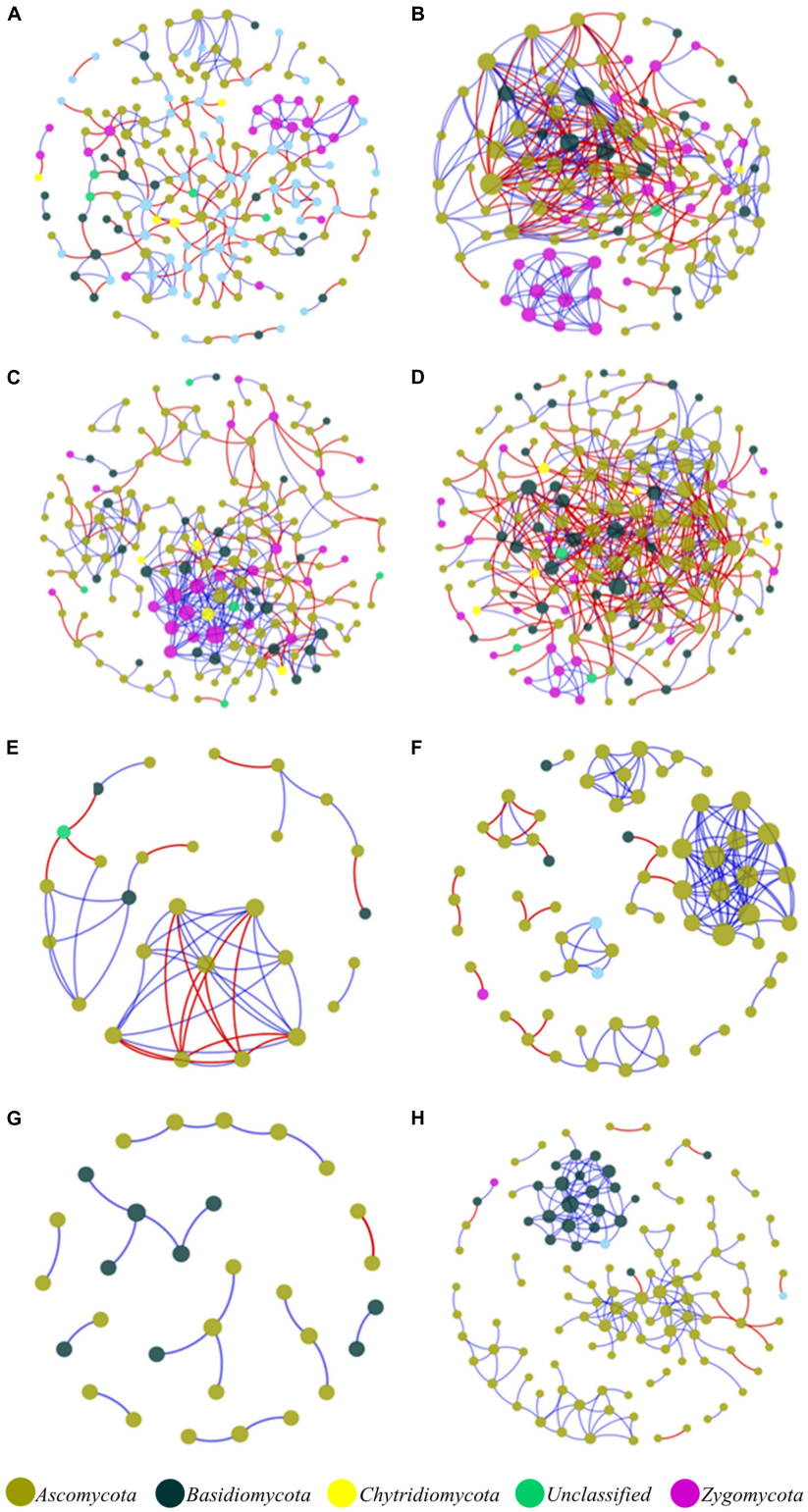

FIGURE 3 | Molecular ecological networks of microorganism associations in the fungal communities of healthy and infected samples. **(A)** Healthy bulk soil. **(B)** Infected bulk soil. **(C)** Healthy rhizosphere soil. **(D)** Infected rhizosphere soil. **(E)** Healthy root endophytic compartment. **(F)** Infected root endophytic compartment. **(G)** Healthy stem endophytic compartment. **(H)** Infected stem endophytic compartment. Node color represents phylum-level taxonomy. Blue links indicate positive correlations between nodes, and red links indicate negative correlations.

(Shi et al., 2019; Ulloa-Munoz et al., 2020). Our previous studies have shown that the diversity of endophytic bacterial communities in the roots and stems of plants with bacterial wilt infected was significantly higher than that of healthy samples (Hu Q.L. et al., 2020). In this study, there was no significant difference in the diversity of the root endophytic fungal community between infected and healthy samples. Endophytic fungal community diversity of the infected stem samples was significantly higher than that of the healthy samples. This may be explained by that the bacterial wilt pathogen invasion success within root endophyte could result in the destruction of plant's defense system. The bacterial wilt pathogen and fungal members interacted closely in the roots, inducing more fungal communities to migrate into the stem, and therefore resulted in an increased diversity of the stem endophytic fungal community compared to the healthy samples (Tan and Zou, 2001; Thebault and Fontaine, 2010; Kefi et al., 2012). Moreover, high diversity and close associations among various microorganism are beneficial to the stability of microbial communities, thereby boosting the microbial community's resistance to pathogen invasion (McCann, 2000; Wehner et al., 2010; van Elsas et al., 2012; Mallon et al., 2015). The increased diversity of fungal communities in stem endophytes may be a middle-late-stage immune response of the plant to the bacterial wilt pathogen invasion.

The invasion of bacterial wilt pathogen may cause changes in the fungal community composition of the various zones of the tobacco microecosystem. From the perspective of relative abundance, fungal composition displayed significant changes at the genus level between infected and healthy samples in the bulk soil, rhizosphere soil, and root and stem endophytic compartments. In the infected bulk soil and rhizosphere soil, the relative abundances of *Rhodotorula, Ceratobasidium, Cyberlindnera, Podospora, Conocybe, Monoblepharis, Paraconiothyrium*, and *Phoma* were significantly decreased, whereas the relative abundances of *Gibberella*, *Cryptococcus, Mucor, Nectria, Debaryomyces*, and *Haematonectria* were significantly increased, compared to the corresponding healthy samples. Such changes in composition might be because the invasion of bacterial wilt disease made pathogenic *Ralstonia* members the dominant species in soil and thus altered the composition of the soil fungal community. In the infected endophytic samples, the genera that significantly declined were *Cryptococcus, Didymella, Mortierella, Paraphoma, Davidiealla, Phoma,* and *Mucor*. Many of the secondary metabolites produced by these endophytic fungi have been reported to have inhibiting or antibacterial abilities (Melo et al., 2014; Xia et al., 2015; Li et al., 2018). These results indicated that the beneficial endophytes were either actively repelled by the host immune system or defeated by the more dominant migrating microbial community (Lundberg et al., 2012; Velásquez et al., 2017). The relative abundances of *Haematonectria, Gibberella, Ceratobasidium, Nectria, Bionectria*, and *Didymella* were significantly enhanced in the infected endophytic samples, indicating that they may benefit during the pathogen invasion process. It is possible they are opportunists that took advantage of the potential niche opened by pathogen invasion and entered the plant endophytic compartment (Lundberg et al., 2012). The compositional changes of these fungal communities may be caused by changes in root exudates or complex changes in the plant immune system during pathogen invasion (Martinoia and Baetz, 2014; dos Santos et al., 2020), and this promoted the differential recruitment and/or differential rejection of microorganisms to resist the invasion of bacterial wilt pathogen in plant roots and stems (Kwak et al., 2018).

Microbe-microbe associations are essential for the function of microecosystems in soil and endophytic compartments (Barberán et al., 2012). Molecular ecological network (MEN) analysis has been increasingly employed to explore potential microbial associations in various ecosystems (de Menezes et al., 2015). However, there are few reports on microbial associations in the fungal community of plants under invasion by bacterial wilt pathogen. In this study, we applied network analysis to quantify and visualize the associations among microorganisms of the fungal community under the invasion of *R. solanacearum*. The results showed that the fungal networks of infected samples had higher complexity and more links than the healthy samples in the rhizosphere soil and root and stem endophytic compartments. Furthermore, the corresponding topological structures demonstrated significant differences as well. Together this indicated that the invasion of bacterial wilt pathogen changed the composition of the soil fungal community and further strengthened the associations among species in the fungal community. The highly connected and modularized fungal community associations were conducive to regulating the stability of the community (Eisenhauer et al., 2013; Downing et al., 2014; Tardy et al., 2014), thereby controlling the propagation and colonization of the pathogen. Hence, it is necessary to study the associations of microorganisms in soil and endophytic fungal communities for more effective prevention and control of diseases.

TABLE 2 | Interdomain network topology features of healthy and infected soil and endophytic microbial communities.

	HBS	IBS	HRS	IRS	HR	IR	HS	IS
No. of bacteria	157	142	86	185	82	91	32	59
No. of fungi	55	72	78	114	23	96	28	139
Total link	301	532	281	357	385	1,336	137	622
Positive link	88	183	51	117	119	38	6	129
Negative link	213	349	230	240	266	1,298	131	493
Connectance	0.035	0.052	0.042	0.017	0.204	0.153	0.153	0.081
Web asymmetry	–0.481	–0.327	–0.049	–0.237	–0.562	0.027	–0.067	0.376
Links per species	1.42	2.49	1.713	1.194	3.667	7.144	2.283	0.291
No. of compartments	13	8	20	26	3	1	2	1
Specialization asymmetry	0.16	0.079	0.028	0.095	0.107	0.079	–0.026	–0.131
Modularity	0.593	0.46	0.533	0.787	0.276	0.269	0.423	0.527
No. of modules	23	17	28	36	6	5	4	5

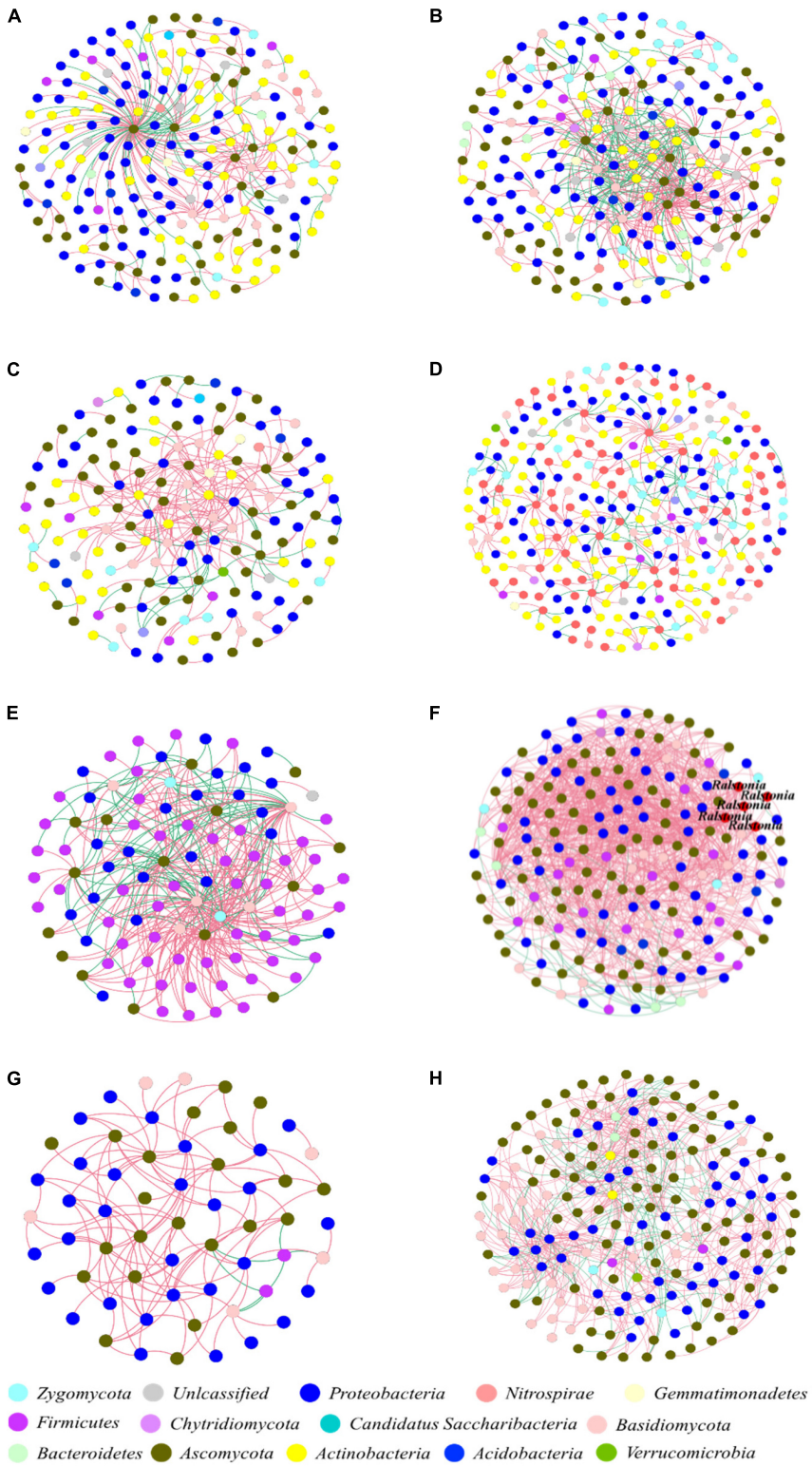

FIGURE 4 | Interdomain ecological networks of the bacterial-fungal associations of healthy and infected samples. **(A)** Healthy bulk soil. **(B)** Infected bulk soil. **(C)** Healthy rhizosphere soil. **(D)** Infected rhizosphere soil. **(E)** Healthy root endophytic compartment. **(F)** Infected root endophytic compartment. **(G)** Healthy stem endophytic compartment. **(H)** Infected stem endophytic compartment. Node color indicates phylum-level taxonomy, and the pathogen *Ralstonia* was labeled at the genus level. Blue links indicate positive correlations between nodes, and red links indicate negative correlations.

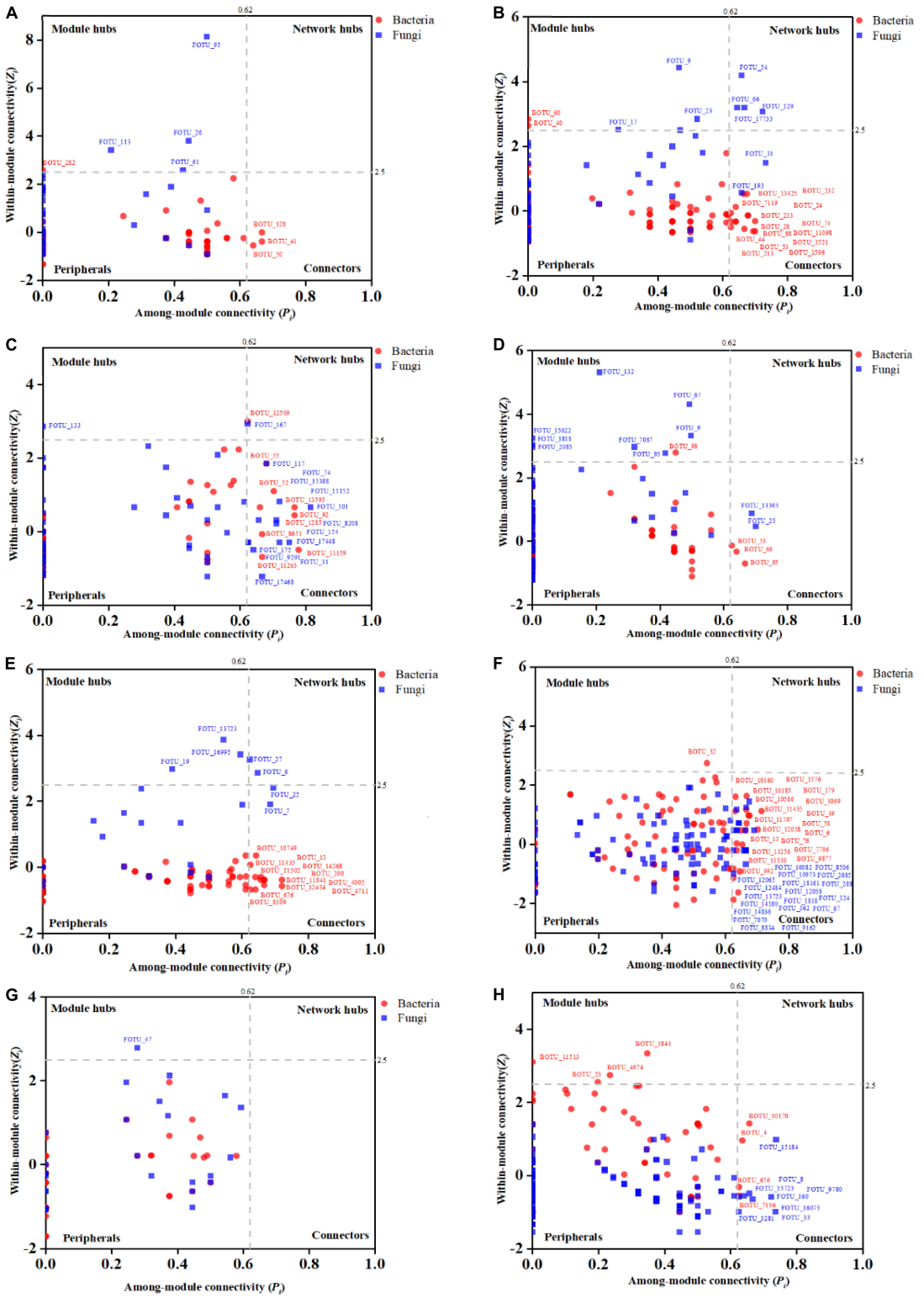

FIGURE 5 | The Zi-Pi plots exhibit the distributions of OTUs based on their topology. The symbols represent OTUs in the bacterial (red dots) and fungal (blue squares) networks. The threshold values of Zi and Pi for categorizing OTUs are 2.5 and 0.62, respectively. **(A)** Healthy bulk soil. **(B)** Infected bulk soil. **(C)** Healthy rhizosphere soil. **(D)** Infected rhizosphere soil. **(E)** Healthy root endophytic compartment. **(F)** Infected root endophytic compartment. **(G)** Healthy stem endophytic compartment; **(H)** Infected stem endophytic compartment.

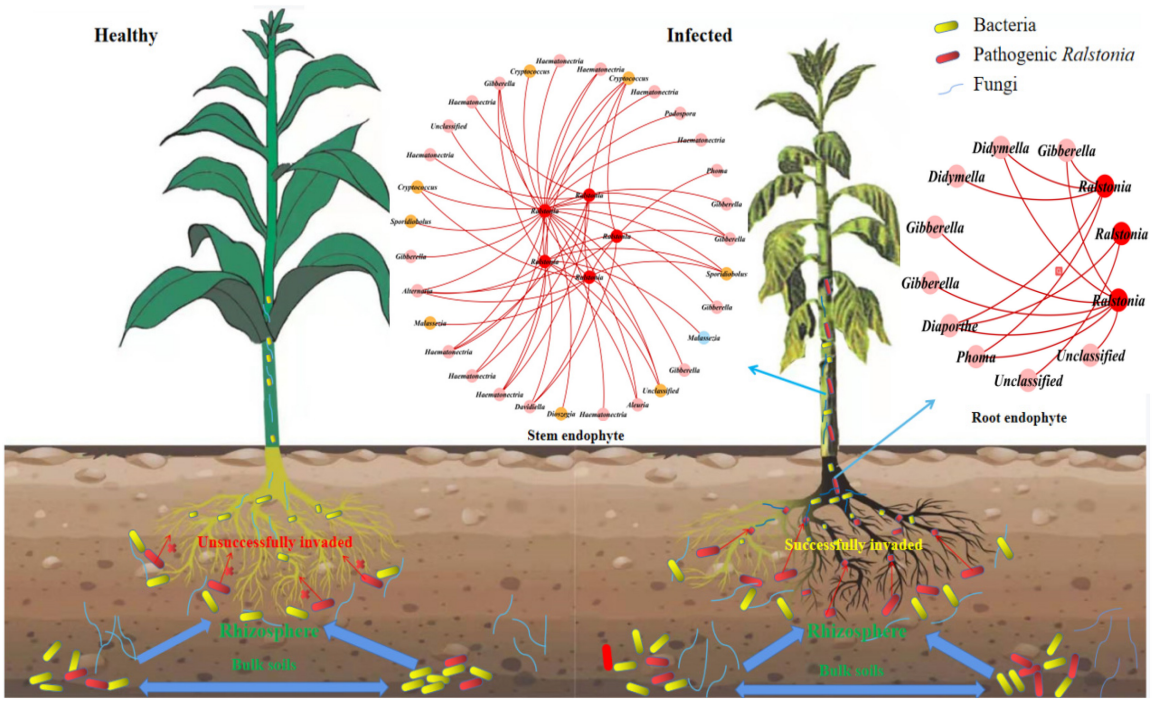

FIGURE 6 | Entangled webs of fungi-bacteria and fungi-pathogen associations in the microbial communities of the surrounding soil, rhizosphere, and root and stem endophytic compartments. The healthy plant **(left)** successfully suppressed invasion of pathogenic *Ralstonia*. The infected **(right)** plant was successfully invaded by the pathogen. The Interdomain ecological networks of the associations between pathogenic bacteria (red) and other fungal species in the root and stem endophytic compartments of the infected samples. Each node is marked at the genus level. Red links indicate negative correlations.

Soil is one of the main habitats for bacteria and fungi (Effmert et al., 2012). Endophytic microorganisms, including fungi and bacteria, live in the intercellular or intracellular spaces of plant tissues. The associations between fungi and bacteria are part of the communication network maintaining the balance of this microhabitat (Bamisile et al., 2018). We adopted IDENs to analyze the association network between fungi and bacteria in each zone of the plant-soil microecosystem, and found more complex and tighter fungal-bacterial associations in the infected samples than the corresponding healthy samples for all tested zones. In addition, the IDEN of the infected root endophytic compartment presented the most network links and the highest number of links per microorganism, suggesting a closer bacterial-fungal associations in this network. Interestingly, the Zi-Pi plots demonstrated that the pathogenic *Ralstonia* members were the keystone genus in the root and stem endophytic bacterial-fungal association networks. The reason for these results may be that with the invasion of the bacterial wilt pathogen, more soil fungi and bacteria developed a mutually beneficial relationship and entered the plant root endophytic community together, resulting in more complex associations among microorganisms (Hu Q.L. et al., 2020). It may also be that the competition of nutrient resources or niche space caused more diversified associations between fungi and bacterial microorganisms (Ghoul and Mitri, 2016). A third possibility is that because the microecological balance was broken by the pathogen invasion, leading to more intense antagonistic relationships between fungal, other bacterial members, and the pathogen (García-Bayona and Comstock, 2018; Hu J. et al., 2020). These phenomena were more prominent in infected root and stem endophytic compartments.

To further clarify which fungi interacted closely with the pathogenic *Ralstonia* members in the endophytic roots and stems, we built sub-networks centered on the pathogen, *Ralstonia* members, and included its associations with fungi. The results showed that the root endophytic fungal genera *Phoma, Gibberella, Alternaria, Haematonectria, Cryptococcus, Podospora, Spodiobolus, Malassezia, Aleuria, Dioszgia,* and *Davidiealla,* and the stem endophytic fungal genera *Phoma, Gibberella, Diaporthe,* and *Didymella* were all negatively correlated with *Ralstonia* members. Plant-associated endophytic fungi are rich sources of novel bioactive and structurally diverse secondary metabolites and other natural products, which were generally considered to protect their host plants by blocking or inhibiting the appropriate pathogenic microorganisms (Rustamova et al., 2020). According to previous research, the active compound named as barceloneic acid C isolated and purified from the secondary metabolites of the endophytic fungus *Phoma* sp. JS752, isolated from *Phragmites communis* Trinius, demonstrated an antibacterial activity against pathogenic gram-positive bacteria *Listeria monocytogenes and Staphylococcus pseuditermedius*, and gram-negative bacteria such as *Escherichia coli and Salmonella typhimurium* (Xia et al., 2015). The purified secondary metabolites [(3S)-3,6,7-trihydroxy-α-tetralone, Cercosporamide, β-Sitosterol and trichodermin] of *Phoma* sp. ZJWCF006, which was screened and isolated

from the *Arisaema erubescens* endophytes, showed remarkable antibacterial activity against four plant fungal pathogens (*Fusarium oxysporium, Rhizoctonia solani, Colletotrichum gloeosporioides, and Magnaporthe oryzae*) and two plant bacterial pathogens (*Xanthomonas campestris* and *Xanthomonas oryzae*) (Wang et al., 2012). The secondary metability compound ergosterol peroxide from the endophytic fungus *Gibberella moniliformis* JS1055, isolated from a halophyte *Vitex rotundifolia* (Kim et al., 2018), exhibited moderate inhibitory activity against bacteria *Staphylococcus aureus* and *Escherichia coli* (Zhu et al., 2017). The endophytic fungus *Alternaria alternata* AE1, isolated from *Azadirachta indica* A. Juss, could produce highly effective bioactive metabolites that showed a strong inhibitory effect on pathogenic bacteria *Listeria monocytogenes* and *Escherichia coli* (Chatterjee et al., 2019). The antibacterial activities of compounds phomosines A and C produced by endophytic fungus *Diaporthe* sp. F2934, isolated from the tropical plant *Aegle marmelos*, showed an antibacterial activity against a variety of gram-negative and gram-positive bacteria, and its inhibitory zone diameter (IZD) against *Staphylococcus aureus* was 20% larger than the standard antibiotic vancomycin (Sousa et al., 2016). It can be seen that these fungi revealed by our study and their secondary metabolites have been reported with antibacterial ability or activity against some bacteria, and they may have potential resistance to bacterial wilt pathogen invasion.

CONCLUSION

The bacteria wilt pathogen *Ralstonia* members and the infected root endophytic fungal genera *Phoma, Gibberella, Alternaria, Haematonectria, Cryptococcus, Podospora, Spodiobolus, Malassezia, Aleuria, Dioszgia,* and *Davidiealla,* as well as the infected stem endophytic fungal genera *Phoma, Gibberella, Didymella,* and *Diaporthe,* were negatively correlated, and these fungi may be potential biocontrol resources in dealing with tobacco bacterial wilt disease. At present, there are few reports on the exploration and application of tobacco endophytic fungal resources. This study will provide potential ideas and theoretical support for enriching the study of tobacco endophytic fungal resources and controlling tobacco bacterial wilt disease. Further experiment with species isolation and verification is needed to confirm these findings.

DATA AVAILABILITY STATEMENT

16S rRNA and ITS gene sequencing data of all samples were submitted to the NCBI SRA database (https://www.ncbi.nlm.nih.gov/) under accession numbers PRJNA540089 and PRJNA735450, respectively.

AUTHOR CONTRIBUTIONS

LT, WZ, YX, and SG performed the main experiments and analyzed data. LT, YD, and QH planned and designed the research, wrote the manuscript with substantial input from PL, SW, ZZ, and KF. All authors have read and agreed to the published version of the manuscript.

FUNDING

This research was supported by the Foundation for Tobacco Science of Changsha Tobacco Company of Hunan Province (Nos 19-21A01 and 19-21A02) and the Wenshan Tobacco Company of Yunnan Province of China (No. 2021530000241033).

ACKNOWLEDGMENTS

We thank James Walter Voordeckers for carefully editing the grammar of the manuscript and for some valuable suggestions for this manuscript.

SUPPLEMENTARY MATERIAL

The Supplementary Material for this article can be found online at: https://www.frontiersin.org/articles/10.3389/fmicb.2021.722626/full#supplementary-material

REFERENCES

Arnold, A. E. (2007). Understanding the diversity of foliar endophytic fungi: progress, challenges, and frontiers. *Fungal Biol. Rev.* 21, 51–66. doi: 10.1016/j.fbr.2007.05.003

Bamisile, B. S., Dash, C. K., Akutse, K. S., Keppanan, R., and Wang, L. (2018). Fungal endophytes: beyond herbivore management. *Front. Microbiol.* 9:544. doi: 10.3389/fmicb.2018.00544

Barberán, A., Bates, S. T., Casamayor, E. O., and Fierer, N. (2012). Using network analysis to explore co-occurrence patterns in soil microbial communities. *ISME J.* 6, 343–351. doi: 10.1038/ismej.2011.119

Bastian, M., Heymann, S., and Jacomy, M. (2009). "Gephi: an open source software for exploring and manipulating networks," in *Proceedings of the International AAAI Conference on Web and Social Media*, Palo Alto, CA.

Bastias, D. A., Martínez- Ghersa, M. A., Ballaré, C. L., and Gundel, P. E. (2017). Epichloë fungal endophytes and plant defenses: not just alkaloids. *Trends Plant Sci.* 22, 939–948. doi: 10.1016/j.fbr.2020.06.001

Bengtsson-Palme, J., Ryberg, M., Hartmann, M., Branco, S., Wang, Z., Godhe, A., et al. (2013). Improved software detection and extraction of ITS1 and ITS2 from ribosomal ITS sequences of fungi and other eukaryotes for use in environmental sequencing. *Methods Ecol. Evol.* 4, 914–919. doi: 10.1111/2041-210X.12073

Bulgarelli, D., Schlaeppi, K., Spaepen, S., van Themaat, E. V. L., and Schulze-Lefert, P. (2013). Structure and functions of the bacterial microbiota of plants. *Annu. Rev. Plant Biol.* 64, 807–838. doi: 10.1146/annurev-arplant-050312-120106

Chao, A. (1984). Nonparametric estimation of the number of classes in a population. *Scand. J. Stat.* 11, 265–270.

Chatterjee, S., Ghosh, R., and Mandal, N. C. (2019). Production of bioactive compounds with bactericidal and antioxidant potential by endophytic fungus Alternaria alternata AE1 isolated from *Azadirachta indica* A. Juss. *PLoS One* 14:e0214744. doi: 10.1371/journal.pone.0214744

Chinese Standards (2008). *Grade and Investigation Method of Tobacco Diseases and Insect Pests, GB/T 23222–22008*. Washington, DC: Chinese Standards.

de Menezes, A. B., Prendergast-Miller, M. T., Richardson, A. E., Toscas, P., Farrell, M., Macdonald, L. M., et al. (2015). Network analysis reveals that bacteria and

fungi form modules that correlate independently with soil parameters. *Environ. Microbiol.* 17, 2677–2689. doi: 10.1111/1462-2920.12559

Deng, Y., Jiang, Y. H., Yang, Y., He, Z. L., Luo, F., and Zhou, J. Z. (2012). Molecular ecological network analyses. *BMC Bioinform.* 13:e113. doi: 10.1186/1471-2105-13-113

Deng, Y., Zhang, P., Qin, Y. J., Tu, Q. C., Yang, Y. F., He, Z. L., et al. (2016). Network succession reveals the importance of competition in response to emulsified vegetable oil amendment for uranium bioremediation. *Environ. Microbiol.* 18, 205–218. doi: 10.1111/1462-2920.12981

dos Santos, T. C., Leandro, M. R., Maia, C. Y., Rangel, P., Soares, F. S., Reis, R., et al. (2020). Arabidopsis thaliana exudates induce growth and proteomic changes in *Gluconacetobacter diazotrophicus*. *Peerj* 8:e9600. doi: 10.7717/peerj.9600

Downing, A. L., Brown, B. L., and Leibold, M. A. (2014). Multiple diversity-stability mechanisms enhance population and community stability in aquatic food webs. *Ecology* 95, 173–184. doi: 10.1890/12-1406.1

Edgar, R. C. (2013). UPARSE: highly accurate OTU sequences from microbial amplicon reads. *Nat. Methods* 10, 996–998. doi: 10.1038/NMETH.2604

Effmert, U., Kalderas, J., Warnke, R., and Piechulla, B. (2012). Volatile mediated interactions between bacteria and fungi in the soil. *J. Chem. Ecol.* 38, 665–703. doi: 10.1007/s10886-012-0135-5

Eisenhauer, N., Schulz, W., Scheu, S., and Jousset, A. (2013). Niche dimensionality links biodiversity and invasibility of microbial communities. *Funct. Ecol.* 27, 282–288. doi: 10.1111/j.1365-2435.2012.02060.x

Feng, K., Zhang, Y. G., He, Z. L., Ning, D. L., and Deng, Y. (2019). Interdomain ecological networks between plants and microbes. *Mol. Ecol. Resour.* 19, 1565–1577. doi: 10.1111/1755-0998.13081

Feng, K., Zhang, Z. J., Cai, W. W., Liu, W. Z., Xu, M. Y., Yin, H. Q., et al. (2017). Biodiversity and species competition regulate the resilience of microbial biofilm community. *Mol. Ecol.* 26, 6170–6182. doi: 10.1111/mec.14356

Fitzpatrick, C. R., Copeland, J., Wang, P. W., Guttman, D. S., Kotanen, P. M., and Johnson, M. T. J. (2018). Assembly and ecological function of the root microbiome across angiosperm plant species. *Proc. Natl. Acad. Sci. U.S.A.* 115, E1157–E1165. doi: 10.1073/pnas.1717617115

García-Bayona, L., and Comstock, L. E. (2018). Bacterial antagonism in host-associated microbial communities. *Science* 361:eaat2456. doi: 10.1126/science.aat2456

Ghoul, M., and Mitri, S. (2016). The ecology and evolution of microbial competition. *Trends Microbiol.* 24, 833–845. doi: 10.1016/j.tim.2016.06.011

Haq, I. U., Zhang, M. Z., Yang, P., and van Elsas, J. D. (2014). The interactions of bacteria with fungi in soil: emerging concepts. *Adv. Appl. Microbiol.* 89, 185–215. doi: 10.1016/B978-0-12-800259-9.00005-6

Hassani, M. A., Duran, P., and Hacquard, S. (2018). Microbial interactions within the plant holobiont. *Microbiome* 6:e58. doi: 10.1186/s40168-018-0445-0

Hu, J., Wei, Z., Kowalchuk, G. A., Xu, Y. C., Shen, Q. R., and Jousset, A. (2020). Rhizosphere microbiome functional diversity and pathogen invasion resistance build up during plant development. *Environ. Microbiol.* 22, 5005–5018. doi: 10.1111/1462-2920.15097

Hu, Q. L., Tan, L., Gu, S. S., Xiao, Y. S., Xiong, X. Y., Zeng, W. A., et al. (2020). Network analysis infers the wilt pathogen invasion associated with non-detrimental bacteria. *NPJ Biofilms Microbiol.* 6:e8. doi: 10.1038/s41522-020-0117-2

Jackrel, S. L., Owens, S. M., Gilbert, J. A., and Pfister, C. A. (2017). Identifying the plant-associated microbiome across aquatic and terrestrial environments: the effects of amplification method on taxa discovery. *Mol. Ecol. Resour.* 17, 931–942. doi: 10.1111/1755-0998.12645

Jia, M., Chen, L., Xin, H. L., Zheng, C. J., Rahman, K., and Qin, L. P. (2016). A friendly relationship between endophytic fungi and medicinal plants: a systematic review. *Front. Microbiol.* 7:e906. doi: 10.3389/fmicb.2016.00906

Jiang, G., Wei, Z., Xu, J., Chen, H. L., Zhang, Y., She, X. M., et al. (2017). Bacterial wilt in China: history, current status, and future perspectives. *Front. Plant Sci.* 8:1549. doi: 10.3389/fpls.2017.01549

Jiang, Y. J., Sun, B., Li, H. X., Liu, M. Q., Chen, L. J., and Zhou, S. (2015). Aggregate-related changes in network patterns of nematodes and ammonia oxidizers in an acidic soil. *Soil Biol. Biochem.* 88, 101–109. doi: 10.1016/j.soilbio.2015.05.013

Kapitan, M., Niemiec, M. J., Steimle, A., Frick, J. S., and Jacobsen, I. D. (2019). Fungi as part of the microbiota and interactions with intestinal bacteria. *Curr. Top. Microbiol. Immunol.* 422, 265–301. doi: 10.1007/82_2018_117

Kefi, S., Berlow, E. L., Wieters, E. A., Navarrete, S. A., Petchey, O. L., Wood, S. A., et al. (2012). More than a meal. Integrating non-feeding interactions into food webs. *Ecol. Lett.* 15, 291–300. doi: 10.1111/j.1461-0248.2011.01732.x

Kim, J. W., Ryu, J., and Shim, S. H. (2018). Chemical investigation on an endophytic fungus *Gibberella moniliformis* JS1055 derived from a halophyte *Vitex rotundifolia*. *Nat. Prod. Sci.* 24, 189–193. doi: 10.20307/nps.2018.24.3.189

Kong, Y. (2011). Btrim: a fast, lightweight adapter and quality trimming program for next-generation sequencing technologies. *Genomics* 98, 152–153. doi: 10.1016/j.ygeno.2011.05.009

Kumar, J., Singh, D., Ghosh, P., and Kumar, A. (2017). "Endophytic and epiphytic modes of microbial interactions and benefits," in *Plant-Microbe Interactions in Agro-Ecological Perspectives*, eds D. Pratap Singh, H. Bahadur Singh, and R. Prabha (Berlin: Springer), 227–253.

Kwak, M. J., Kong, H. G., Choi, K., Kwon, S. K., Song, J. Y., Lee, J., et al. (2018). Rhizosphere microbiome structure alters to enable wilt resistance in tomato. *Nat. Biotechnol.* 36, 1100–1109. doi: 10.1038/nbt.4232

Layeghifard, M., Hwang, D. M., and Guttman, D. S. (2017). Disentangling interactions in the microbiome: a network perspective. *Trends Microbiol.* 25, 217–228. doi: 10.1016/j.tim.2016.11.008

Levy, A., Gonzalez, I. S., Mittelviefhaus, M., Clingenpeel, S., Paredes, S. H., Miao, J. M., et al. (2018). Genomic features of bacterial adaptation to plants. *Nat. Genet.* 50, 138–150. doi: 10.1038/s41588-017-0012-9

Li, C. S., Hu, Z. Q., Liu, Q. S., Wu, X. H., and Cao, S. G. (2018). Two new tricycloalternarenes from *Hawaiian endophytic* fungus *Didymella* sp FT433. *Tetrahedron. Lett.* 9, 3381–3383. doi: 10.1016/j.tetlet.2018.07.061

Li, X., Liu, Y., Cai, L., Zhang, H., Shi, J., and Yuan, Y. (2017). Factors affecting the virulence of *Ralstonia solanacearum* and its colonization on tobacco roots. *Plant Pathol.* 66, 1345–1356. doi: 10.1111/ppa.12675

Lilleskov, E. A., Hobbie, E. A., and Horton, T. R. (2011). Conservation of ectomycorrhizal fungi: exploring the linkages between functional and taxonomic responses to anthropogenic N deposition. *Fungal Ecol.* 4, 174–183. doi: 10.1016/j.funeco.2010.09.008

Lundberg, D. S., Lebeis, S. L., Paredes, S. H., Yourstone, S., Gehring, J., Malfatti, S., et al. (2012). Defining the core *Arabidopsis thaliana* root microbiome. *Nature* 488, 86–90. doi: 10.1038/nature11237

Mallon, C. A., Elsas, J. D. V., and Salles, J. F. (2015). Microbial invasions: the process, patterns, and mechanisms. *Trends Microbiol.* 23, 719–729. doi: 10.1016/j.tim.2015.07.013

Martin, F. M., Uroz, S., and Barker, D. G. (2017). Ancestral alliances: plant mutualistic symbioses with fungi and bacteria. *Science* 356:eaad4501. doi: 10.1126/science.aad4501

Martinoia, E., and Baetz, U. (2014). Root exudates: the hidden part of plant defense. *Trends Plant Sci.* 19, 90–98. doi: 10.1016/j.tplants.2013.11.006

McCann, K. S. (2000). The diversity-stability debate. *Nature* 405, 228–233. doi: 10.1038/35012234

Melo, I. S., Santos, S. N., Rosa, L. H., Parma, M. M., Silva, L. J., Queiroz, S. C. N., et al. (2014). Isolation and biological activities of an endophytic *Mortierella alpina* strain from the Antarctic moss *Schistidium antarctici*. *Extremophiles* 18, 15–23. doi: 10.1007/s00792-013-0588-7

Mousa, W. K., Shearer, C. R., Limay-Rios, V., Ettinger, C. L., Eisen, J. A., and Raizada, M. N. (2016). Root-hair endophyte stacking in finger millet creates a physicochemical barrier to trap the fungal pathogen *Fusarium graminearum*. *Nat. Microbiol.* 1:e16167. doi: 10.1038/NMICROBIOL.2016.167

Newman, M. E. J. (2016). Modularity and community structure in networks. *Proc. Natl. Acad. Sci. U.S.A.* 103, 8577–8582. doi: 10.1073/pnas.0601602103

Nilsson, R. H., Anslan, S., Bahram, M., Wurzbacher, C., Baldrian, P., and Tedersoo, L. (2019). Mycobiome diversity: high-throughput sequencing and identification of fungi. *Nat. Rev. Microbiol.* 17, 95–109. doi: 10.1038/s41579-018-0116-y

Qian, X., Li, H. Z., Wang, Y. L., Wu, B. W., Wu, M. S., Chen, L., et al. (2019). Leaf and root endospheres harbor lower fungal diversity and less complex fungal co-occurrence patterns than rhizosphere. *Front. Microbiol.* 10:e1015. doi: 10.3389/fmicb.2019.01015

Ripa, F. A., Cao, W., Tong, S., and Sun, J. (2019). Assessment of plant growth promoting and abiotic stress tolerance properties of wheat endophytic fungi. *BioMed Res. Int.* 2019, 1–12. doi: 10.1155/2019/6105865

Rustamova, N., Bozorov, K., Efferth, T., and Yili, A. (2020). Novel secondary metabolites from endophytic fungi: synthesis and biological properties. *Phytochem. Rev.* 19, 425–448. doi: 10.1007/s11101-020-09672-x

Schloss, P. D., Westcott, S. L., Ryabin, T., Hall, J. R., Hartmann, M., Hollister, E. B., et al. (2009). Introducing mothur: open-source, platform-independent, community-supported software for describing and comparing microbial communities. *Appl. Environ. Microbiol.* 75, 7537–7541. doi: 10.1128/AEM.01541-09

Shi, W., Li, M., Wei, G., Tian, R. M., Li, C. P., Wang, B., et al. (2019). The occurrence of potato common scab correlates with the community composition and function of the geocaulosphere soil microbiome. *Microbiome* 7:e14. doi: 10.1186/s40168-019-0629-2

Shi, Y., Delgado-Baquerizo, M., Li, Y., Yang, Y., Zhu, Y. G., Peñuelas, J., et al. (2020). Abundance of kinless hubs within soil microbial networks are associated with high functional potential in agricultural ecosystems. *Environ. Int.* 142:e105869. doi: 10.1016/j.envint.2020.105869

Sousa, J. P. B., Aguilar-Perez, M. M., Arnold, A. E., Rios, N., Coley, P. D., Kursar, T. A., et al. (2016). Chemical constituents and their antibacterial activity from the tropical endophytic fungus *Diaporthe* sp F2934. *J. Appl. Microbiol.* 120, 1501–1508. doi: 10.1111/jam.13132

Tan, R. X., and Zou, W. X. (2001). Endophytes: a rich source of functional metabolites. *Nat. Prod. Rep.* 18, 448–459. doi: 10.1039/b100918o

Tardy, V., Mathieu, O., Lévêque, J., Terrat, S., Chabbi, A., Lemanceau, P., et al. (2014). Stability of soil microbial structure and activity depends on microbial diversity. *Environ. Microbiol. Rep.* 6, 173–183. doi: 10.1111/1758-2229.12126

Taylor, D. L., Walters, W. A., Lennon, N. J., Bochicchio, J., Krohn, A., Caporaso, J. G., et al. (2016). Accurate estimation of fungal diversity and abundance through improved lineage-specific primers optimized for illumina amplicon sequencing. *Appl. Environ. Microbiol.* 82, 7217–7226. doi: 10.1128/AEM.02576-16

Terhonen, E., Sipari, N., and Asiegbu, F. O. (2016). Inhibition of phytopathogens by fungal root endophytes of Norway spruce. *Biol. Control* 99, 53–63. doi: 10.1016/j.biocontrol.2016.04.006

Thebault, E., and Fontaine, C. (2010). Stability of ecological communities and the architecture of mutualistic and trophic networks. *Science* 329, 853–856. doi: 10.1126/science.1188321

Ulloa-Munoz, R., Olivera-Gonzales, P., Castaneda-Barreto, A., Villena, G. K., and Tamariz-Angeles, C. (2020). Diversity of endophytic plant-growth microorganisms from Gentianella weberbaueri and Valeriana pycnantha, highland Peruvian medicinal plants. *Microbiol. Res.* 223:e126413. doi: 10.1016/j.micres.2020.126413

van der Putten, W. H. (2017). Belowground drivers of plant diversity. *Science* 355, 134–135. doi: 10.1126/science.aal4549

van Elsas, J. D., Chiurazzi, M., Mallon, C. A., Elhottova, D., Kristufek, V., and Salles, J. F. (2012). Microbial diversity determines the invasion of soil by a bacterial pathogen. *Proc. Natl. Acad. Sci. U.S.A.* 109, 1159–1164. doi: 10.1073/pnas.1109326109

Velásquez, A. C., Oney, M., Huot, B., Xu, S., and He, S. Y. (2017). Diverse mechanisms of resistance to *Pseudomonas* syringae in a thousand natural accessions of *Arabidopsis thaliana*. *New Phytol.* 214, 1673–1687. doi: 10.1111/nph.14517

Wang, F., Xin, C. Y., Liu, J. X., Ran, Z. N., Zhao, C. L., and Song, Z. Y. (2020). Interactions between invasive fungi and symbiotic bacteria. *World J. Microbiol. Biotechnol.* 36:e137. doi: 10.1007/s11274-020-02913-3

Wang, L. W., Xu, B. G., Wang, J. Y., Su, Z. Z., Lin, F. C., Zhang, C. L., et al. (2012). Bioactive metabolites from Phoma species, an endophytic fungus from the Chinese medicinal plant *Arisaema erubescens*. *Appl. Microbiol. Biot.* 93, 1231–1239. doi: 10.1007/s00253-011-3472-3

Waqas, M., Khan, A. L., Kamran, M., Hamayun, M., Kang, S. M., Kim, Y. H., et al. (2012). Endophytic fungi produce gibberellins and indoleacetic acid and promotes host-plant growth during stress. *Molecules* 17, 10754–10773. doi: 10.3390/molecules170910754

Watts, D. J., and Strogatz, S. H. (1998). Collective dynamics of 'small-world' networks. *Nature* 393, 440–442. doi: 10.1038/30918

Wehner, J., Antunes, P. M., Powel, J. R., Mazukatow, J., and Rillig, M. C. (2010). Plant pathogen protection by arbuscular mycorrhizas: a role for fungal diversity? *Pedobiologia* 53, 197–201. doi: 10.1016/j.pedobi.2009.10.002

Wei, Z., Hu, J., Gu, Y., Yin, S. X., Xu, Y. C., Jousset, A., et al. (2018). *Ralstonia solanacearum* pathogen disrupts bacterial rhizosphere microbiome during an invasion. *Soil Biol. Bioch.* 118, 8–17. doi: 10.1016/j.soilbio.2017.11.012

Xia, X., Kim, S., Bang, S., Lee, H. J., Liu, C., Park, C. I., et al. (2015). Barceloneic acid C, a new polyketide from an endophytic fungus *Phoma* sp JS752 and its antibacterial activities. *J. Antibiot.* 68, 139–141. doi: 10.1038/ja.2014.116

Zhang, X. X., Zhang, R. J., Gao, J. S., Wang, X. C., Fan, F. L., Ma, X. T., et al. (2017). Thirty-one years of rice-rice-green manure rotations shape the rhizosphere microbial community and enrich beneficial bacteria. *Soil Biol. Biochem.* 104, 208–217. doi: 10.1016/j.soilbio.2016.10.023

Zhang, Z. Q., Zhang, J., and Jiao, S. (2021). Fungi show broader environmental thresholds in wet than dry agricultural soils with distinct biogeographic patterns. *Sci. Total Environ.* 750:e141761. doi: 10.1016/j.scitotenv.2020.141761

Zhou, J. Z., Deng, Y., Luo, F., He, Z. L., and Yang, Y. F. (2011). Phylogenetic molecular ecological network of soil microbial communities in response to elevated CO2. *mBio* 2:e00122-11. doi: 10.1128/mBio.00122-11

Zhu, F., Li, J. S., Xie, W. C., Wang, C. Y., and Liu, Y. L. (2017). Identification and antibacterial activity of two steroids secreted by the fungus beetle xylographus bostrichoides (dufour, 1843). *Bangl. J. Bot.* 46, 1171–1176.

Conflict of Interest: The authors declare that the research was conducted in the absence of any commercial or financial relationships that could be construed as a potential conflict of interest.

Publisher's Note: All claims expressed in this article are solely those of the authors and do not necessarily represent those of their affiliated organizations, or those of the publisher, the editors and the reviewers. Any product that may be evaluated in this article, or claim that may be made by its manufacturer, is not guaranteed or endorsed by the publisher.

frontiers in Microbiology

ORIGINAL RESEARCH
published: 10 September 2021
doi: 10.3389/fmicb.2021.721441

Different Amounts of Nitrogen Fertilizer Applications Alter the Bacterial Diversity and Community Structure in the Rhizosphere Soil of Sugarcane

Yan Gu[1†], Jihua Wang[1†], Weijun Cai[2], Guoliang Li[3], Yu Mei[1] and Shaohai Yang[1]*

[1] Guangdong Provincial Key Laboratory of Crops Genetics and Improvement, Crop Research Institute, Guangdong Academy of Agricultural Sciences, Guangzhou, China, [2] Zhanjiang Academy of Agricultural Sciences, Zhanjiang, China, [3] Institute of Agricultural Resources and Environment, Guangdong Academy of Agricultural Sciences, Guangzhou, China

OPEN ACCESS

Edited by:
Hai-Ming Zhao, Jinan University, China

Reviewed by:
Lianghuan Wu, Zhejiang University, China
Decai Jin, Research Center for Eco-environmental Sciences (CAS), China

***Correspondence:**
Shaohai Yang
yangshaohai@gdaas.cn

[†]These authors have contributed equally to this work and share first authorship

Specialty section:
This article was submitted to Terrestrial Microbiology, a section of the journal Frontiers in Microbiology

Received: *07 June 2021*
Accepted: *06 August 2021*
Published: *10 September 2021*

Citation:
Gu Y, Wang J, Cai W, Li G, Mei Y and Yang S (2021) Different Amounts of Nitrogen Fertilizer Applications Alter the Bacterial Diversity and Community Structure in the Rhizosphere Soil of Sugarcane. Front. Microbiol. 12:721441. doi: 10.3389/fmicb.2021.721441

Sugarcane cropping systems receive elevated application of nitrogen (N) fertilizer for higher production, which may affect production costs and cause environmental pollution. Therefore, it is critical to elucidate the response of soil microbial to N fertilizer inputs in sugarcane soil. A field experiment was carried out to investigate the effects of optimum (N375, 375 kg N/ha) and excessive (N563, 563 kg N/ha) amounts of N fertilizer on soil bacterial diversity and community structure in a sugarcane cropping system by MiSeq high-throughput sequencing; 50,007 operational taxonomic units (OTUs) were obtained by sequencing the 16S rRNA gene amplicons. Results showed that the most abundant phyla in the sugarcane rhizosphere soil were *Proteobacteria*, *Actinobacteria*, *Acidobacteria*, and *Planctomycetes*, whose ensemble mean accounted for 74.29%. Different amounts of N application indeed change the bacterial diversity and community structures. Excessive application of N fertilizers significantly decreased the pH and increased the available N in soils and unexpectedly obtained a lower yield. Excessive N resulted in a relatively lower bacterial species richness and significantly increased the relative abundance of phyla *Proteobacteria*, *Acidobacteria*, and *Bacteroidetes* and the genera *Sphingomonas* and *Gemmatimonas*, while optimum N treatment significantly increased the phylum *Actinobacteria* and the genera *Bacillus* and *Nitrospira* ($P < 0.05$). N application shifted the N cycle in nitrification, mainly on the *Nitrospira*, but showed no significant effect on the genera related to nitrogen fixation, methane oxidation, sulfate reduction, and sulfur oxidation ($P > 0.05$). Overall, the optimum amount of N application might be conducive to beneficial microorganisms, such as *Actinobacteria*, *Nitrospira*, and *Bacillus* and, thus, result in a healthier ecosystem and higher sustainable crop production.

Keywords: 16S rRNA, bacterial community, rhizosphere microbe, nitrogen fertilizer, sugarcane

INTRODUCTION

Sugarcane (*Saccharum* L. spp.) is an important agroeconomic sugar crop which is planted in over 20 million hectares worldwide (Val-Moraes et al., 2016). Sugarcane contributed into more than 90% of the total sugar production and has been considered one of the most promising crops for generating renewable bioenergy, which is expected to become the second largest energy source in the world by 2030 (Li Y. R. et al., 2016). China is one of the major sugar-producing countries in the world, producing more than 10 million tons of sugar annually (Li and Yang, 2015). Due to continuously increasing consumption, there is a need to increase sugarcane production to meet the growing demand.

Sugarcane is a fast-growing large biomass crop which requires large amounts of nutrients and water. Nitrogen (N) is the essential macronutrient required for sugarcane growth and development (Yang et al., 2013). In order to obtain higher crop yield, large amounts of N fertilizers were applied to provide nutrients for growing sugarcane, and N fertilizer application rate has increased several times in the past decades worldwide (Robertson and Vitousek, 2009; Zhang et al., 2013; Li and Yang, 2015). N fertilizer application for sugarcane production varies largely between countries, ranging from 60 kg/ha in some regions of Brazil to 755 kg/ha in some parts of China (Robinson et al., 2011). In China, N fertilization varies from 300 to 800 kg/ha N in sugarcane production, which is 3–10 times higher than in other countries (Li and Yang, 2015). However, excessive application of N fertilizer not only causes waste of resources and higher production cost but also results in serious environmental pollution and ecological environment degeneration (Waclawovsky et al., 2010; Belén et al., 2016). Furthermore, superfluous N fertilizer has adverse effect on sugar quality and often leads to a substantial decrease of beneficial microflora related to N mineralization (Singh et al., 2020).

Microbes in the rhizosphere play important roles in nutrient cycling and acquisition. Soil microorganisms form complicated microbial communities that regulate the nutrient cycles and influence soil characteristics, plant growth, and ecosystem sustainability (Singh et al., 2017). In turn, agronomic practices, such as fertilization can alter soil physical and chemical properties and, consequently, soil microbiomes. The effect of N fertilizer application on soil microbial community composition may be caused by direct effects of N nutrient or by indirect changes in soil and plant properties (Klironomos et al., 2011). Many studies have been undertaken to explore the effects of N fertilizer on microbes in agriculture ecosystems. Du et al. (2019) found that application of inorganic N fertilizer resulted in distinctive changes on N-cycle microorganism. Moreover, applying N fertilizer influenced soil microbial composition, particularly fungal community (Guo et al., 2018). A recent meta-analysis demonstrated that N fertilizers decreased both soil microbial diversity and the relative abundances of *Actinobacteria* and *Nitrospirae* but did not significantly change the primary fungal groups (Wang et al., 2018).

During the sugarcane life cycle, the plants and its roots establish associations with various diversities of microorganisms, including beneficial, detrimental, or neutral microbes. Several studies expectedly have been conducted to reveal the microbial diversity and community in sugarcane rhizosphere soil. Savario and Hoy (2011) have demonstrated that sugarcane monoculture can affect the composition of the microbial community in field soil by evaluating the culturable microorganisms using community level physiological profiles (CLPP). A culture-independent approach using the 16S rRNA gene library sequencing also has been used to assess the bacterial community in the rhizosphere soil of sugarcane under different nitrogen fertilization conditions. Pisa et al. (2011) found that *Proteobacteria*, *Acidobacteria*, *Bacteroidetes*, *Firmicutes*, and *Actinobacteria* were the predominant phyla in the rhizosphere soil of sugarcane. However, previous studies did not reveal the microbial community structure very well due to poor sequencing technologies. Recent studies on microbials in sugarcane soils mainly focused on plant growth-promoting bacteria, endophytic bacteria, and fungi or functional bacteria associated with sugarcane, such as nitrogen-fixing bacteria, aiming at exploring the massive potential of biofertilizer to replace the chemical N fertilizer (de Souza et al., 2016; dos Santos et al., 2019; Pereira et al., 2019; Singh et al., 2020). Yeoh et al. (2016) found that regulating N fertilizer rates does not improve sugarcane yields by enriching diazotrophic populations and optimal N fertilizer crops had higher biomass and higher abundances of nitrification and denitrification genes. The above studies highlighted that a deep understanding of how N fertilizer application affects microbial communities is important for achieving a balance in maximizing crop yields and minimizing nutrient pollution associated with N fertilizer application.

Despite the wide plantation and economic importance of sugarcane, knowledge regarding the microbial diversity and community of sugarcane rhizosphere soils is limited. Meanwhile, there still lacks a deep understanding of how N fertilization regimes affect the sugarcane yields and rhizosphere soil microbiome. Therefore, in our work, a field experiment was conducted to evaluate the impacts of different amounts of N fertilizers on the diversity and community structure in the sugarcane rhizosphere soil. The main objectives were to (i) reveal the bacterial diversity and community structure in the rhizosphere soil of sugarcane and (ii) evaluate the effect of N application amount on the soil physicochemical characteristics and crop yields and on the rhizosphere bacterial diversity and community structure. Moreover, we hypothesized that (iii) N fertilizer impact on sugarcane yield may be through the regulation of rhizosphere bacterial community and functions. The results of our work may provide guidance for the reasonable fertilization management of sugarcane fields, so as to promote sustainable development of the sugarcane industry.

MATERIALS AND METHODS

Site Description and Experiment Design

The field trial was located in Mazhang district (21°15′36″N, 110°16′48″E) of Zhanjiang, Guangdong Province, China. The area has a south subtropical monsoon climate, with an annual mean precipitation and temperature of 1,800 mm and 23.5°C,

respectively. Land use was peanut and sweet potato rotation before and has been transformed to cultivate sugarcane since 2016. The experiments were conducted from 2016 with three different N fertilization rates in new planted sugarcane for 2 years. The experimental field was divided into plots of 30 m^2 (5 m × 6 m), and each treatment was performed in triplicate with a randomized block design from February to December. Four treatments were included in this study. The CK treatment was without fertilizers and the other three annual N fertilization regimens were applied with urea (46% N) as follows: N0 (0 kg N/ha), N375 (375 kg N/ha), and N563 (563 kg N/ha); 375 kg N/ha was the appropriate N fertilizer amount and 563 kg N/ha was the average N application of farmers after preliminary investigation and research. Phosphorus (P) and potassium (K) were supplied with equal amounts of 112.5 and 375 kg/hm^2 in the form of calcium superphosphate (12% P_2O_5) and potassium chloride (60% K_2O). N, P, and K were applied in three split doses in basal, tillering stage, and elongation stage at ratios of 5:8:7, 1:1:1, and 1:15:6, respectively. Field management was carried out by local cultivars and conventional crop practices.

Soil Sampling and Analysis of Physicochemical Properties

On February 20, 2018, rhizosphere soil samples were obtained by manually shaking the loosely attached soil from the roots, 1 week after sugarcane was harvested. The replicated samples were pooled in polyethylene self-sealing bags and then immediately transported to the laboratory in a container with enough dry ice. Each sample was a composite formed by mixing together the eight subsamples and then divided into two aliquots. One aliquot was stored at −4°C for subsequent biochemical analyses as soon as possible within 1 week. Another aliquot was stored at −80°C for DNA extraction and sequencing.

Several soil physicochemical properties were determined. Soil pH was determined with a suspension of soil/water (w/v) ratio at 1:2.5 by a glass electrode pH meter. Soil organic carbon (SOC) was determined using $K_2Cr_2O_7$ wet oxidation and titration by $FeSO_4$, and organic matter (OM) was converted from SOC (Bao, 2000). Alkali-hydrolyzable N (AN) was determined by alkali hydrolysis diffusion method. Available phosphorus (AP) measurement was extracted with HCl-NH_4F and determined using the phosphomolybdate blue colorimetric method. Available potassium (AK) was measured by flame photometry after ammonium acetate extraction.

Soil DNA Extraction, PCR Amplification, and Illumina Sequencing

Soil DNA was extracted from 0.50 g sample soil with E.Z.N.A. stool DNA Kit (Omega Bio-Tek, Norcross, GA, United States) according to the protocols of the manufacturer. A NanoDrop 2000c UV–Vis spectrophotometer (Thermo Fisher Scientific, Waltham, MA, United States) was used to check the DNA quality and quantity. DNA extracts were stored at −20°C until analysis.

The purified DNA was used as a template for amplifying the V3–V4 region of the 16S rRNA gene with the barcode primer set 341F (5′-CCTACGGGNGGCWGCAG-3′)/806R (5′-GGACTACHVGGGTATCTAAT-3′). The thermal cycle conditions were as follows: initial denaturation at 95°C for 2 min, followed by 27 cycles of 98°C for 10 s, 62°C for 30 s, and 68°C for 30 s, and a final extension at 68°C for 10 min. PCR amplification was carried out in a total of 50 μl reaction system containing 100 ng of template DNA, 1.5 μl of 5 μM forward and reverse primers, 1 μl KOD DNA polymerase, 5 μl of 10 × KOD buffer, and 5 μl of 2.5 mM dNTP mixture. Amplicons were extracted from 2% agarose gels and purified using the AxyPrep DNA Gel Extraction Kit (Axygen Biosciences, Union City, CA, United States) and quantified using a QuantiFluor fluorimeter-ST (Promega, Madison, WI, United States). Purified amplicons were pooled in equimolar concentrations and paired-end sequenced (2 × 250) on an Illumina HiSeq platform by Illumina NovaSeq 6000 according to standard protocols (Chen et al., 2019). Sequencing of the 16S rRNA gene was performed in Gene *Denovo* Biotechnology Co., Ltd. (Guangzhou, China).

Data Processing and Bioinformatics Approaches

Raw data containing adapters or low-quality reads [containing more than 10% of unknown nucleotides (N) or less than 80% of bases with quality (*Q*-value) > 20] were trimmed, after which pair-ended reads were merged into one sequence as raw tags using FLASH (version 1.2.11) with a minimum overlap of 10 bp and mismatch error rates of 2%. Raw tags were quality-filtered and processed using the Quantitative Insights into Microbial Ecology (QIIME) (version 1.9.1) according to the following three criterions (Caporaso et al., 2010). The clean tags were aligned in the Gold database and reference-based chimera checking was performed using the UCHIME algorithm to identity and eliminate putative chimeric sequences. The obtained effective tags were clustered into operational taxonomic units (OTUs) of ≥97% sequence similarity using UPARSE (Edgar, 2013). The representative sequences classified into organisms by a naive Bayesian model using the RDP classifier (version 2.2) based on the SILVA database in the main OTUs were analyzed using BLAST with the NCBI database to obtain the most similar published sequences (Gu et al., 2019). Finally, the complete dataset was deposited into the NCBI Sequence Read Archive (SRA) database under accession number SRP269446.

Statistical Analysis

A Venn diagram was conducted to compare the OTUs among the soil samples. The richness and evenness analysis based on OTU was performed to assess the biodiversity of microbial communities in different N fertilizer-applied soils. Duncan's multiple range test was employed to compare statistically significantly differences ($P < 0.05$) of the alpha-diversity indices and among different treatments. Principal coordinate analysis (PCoA) and the unweighted pair group method with arithmetic mean (UPGMA) clustering analysis based on Bray–Curtis were used to assess similarities and discrepancies of the bacterial community structure among all treatments. Differences in functional groups between fertilizer treatments were determined using one-way analysis of variance (ANOVA). The linear

discriminant analysis effect size (LEfSe) method was used to identify the biomarkers of soil bacteria among the treatments (Segata et al., 2011). Permutational multivariate analysis of variance (PERMANOVA) was performed using R software (version 3.6.3) to test the differences in community composition based on the Bray–Curtis distance.

RESULTS

Soil Physicochemical Characteristics and Crop Yield

The selected physiochemical characteristics of the soil samples are presented in **Table 1**. The yield of sugarcane was 107.75 t/ha in the N375 treatment, significantly higher than 102.11 t/ha in the N563 treatment and 96.24 t/ha in the N0 treatment ($P < 0.05$). The N563 treatment has the lowest pH and the highest organic matter and AN among all the treatments. There were no significant differences on available P and K between the N375 and N563 treatment ($P > 0.05$).

Soil Bacterial Community Diversity

A total of 620,112 reads with an average valid sequence length of 420 bp and 50,007 OTUs were obtained from the four treatments (including 12 soil samples) (**Table 2**). The similarities and differences among OTUs of the four treatments are shown in a four-set Venn diagram (**Figure 1**). The unique OTUs were 833, 583, 874, and 544 for the CK, N0, N375, and N563 treatments, respectively, and the four treatments shared 1,802 OTUs.

Good's coverage indices for all samples were above 0.96, indicating that the sequencing depth was large enough to capture the complete diversity of each sample. The Shannon indexes used to describe the community diversity showed no significant differences among the four treatments ($P > 0.05$). However, the indices including observed species, Chao1, and ACE of the N563 treatment were significantly lower than the N375 treatment ($P < 0.05$), indicating that excessive application of N fertilizer resulted in a relatively lower bacterial species richness.

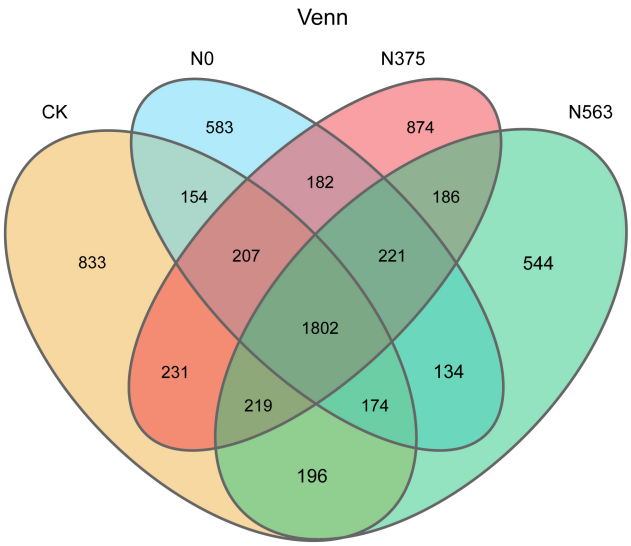

FIGURE 1 | A Venn diagram demonstrating the unique and common bacterial OTUs among the four treatments. CK, without fertilization; N0, without N fertilization; N375, application of 375 kg/ha N; N563, application of 563 kg/ha N.

TABLE 1 | Physiochemical properties and crop yields in all the treatments.

Treatments	pH	Organic matter (g/kg)	Alkali-hydrolyzable N (mg/kg)	Available P (mg/kg)	Available K (mg/kg)	Yield (t/ha)
CK	4.56 ± 0.06 a	13.77 ± 0.25 c	82.47 ± 5.90 b	47.45 ± 30.50 b	80.50 ± 12.50 b	84.13 ± 3.15 d
N0	4.38 ± 0.24 ab	14.29 ± 0.44 bc	80.53 ± 4.80 b	231.09 ± 14.30 a	117.67 ± 11.10 a	96.24 ± 2.06 c
N375	4.28 ± 0.02 b	14.70 ± 0.47 ab	89.02 ± 1.10 b	240.56 ± 26.00 a	116.50 ± 20.10 a	107.75 ± 0.21 a
N563	4.03 ± 0.04 c	15.27 ± 0.61 a	117.64 ± 4.80 a	251.99 ± 19.30 a	127.83 ± 9.90 a	102.11 ± 1.29 b

Values represent mean ± standard deviation of triplicate measurements.
Different lowercase letters in the same column indicate significant differences ($P < 0.05$) among the four treatments.
Yields were the average of 2 years.
CK, without fertilizers; N0, without N fertilization; N375, application of 375 kg/ha N; N563, application of 563 kg/ha N.

TABLE 2 | Species richness and diversity indices of the four treatments at a 97% identity threshold.

Treatments	Total tags	OTU numbers	Good's coverage	Observed species	Shannon index	Chao1	ACE
CK	45, 375 ± 4, 389	4, 190 ± 393	0.963 ± 0.003	4, 088 ± 298 ab	9.7261 ± 0.2646 a	5, 583.98 ± 424.41 ab	5, 558.58 ± 451.11 ab
N0	46, 772 ± 3, 071	3, 937 ± 194	0.964 ± 0.002	3, 803 ± 123 ab	9.4248 ± 0.1754 a	5, 394.90 ± 184.26 ab	5, 308.22 ± 276.03 ab
N375	55, 304 ± 3, 117	4, 646 ± 413	0.960 ± 0.003	4, 223 ± 299 a	9.6986 ± 0.2549 a	5, 932.30 ± 420.95 a	5, 974.41 ± 420.58 a
N563	48, 859 ± 3, 547	3, 896 ± 313	0.967 ± 0.004	3, 706 ± 259 b	9.5714 ± 0.0979 a	5, 100.39 ± 451.63 b	5, 070.81 ± 489.81 b

Values represent mean ± standard deviation of triplicate measurements.
Different lowercase letters in the same column indicate significant differences ($P < 0.05$) among the four treatments.
CK, without fertilization; N0, without N fertilization; N375, application of 375kg/ha N; N563, application of 563 kg/ha N.

Soil Bacterial Community Dissimilarity

An UPGMA cluster dendrogram of bacterial communities was constructed based on the Bray–Curtis distance indices calculated using OTUs to examine the similarity among different treatments (**Figure 2A**). Grouped together indicated that the HiSeq sequencing technique applied here was robust. Two major clusters could be classified for these 12 soil samples. Cluster 1 consisted of three samples of the CK treatment and was significantly different from the other treatments. Cluster 2 could be grouped into two subclusters. N0 and N375 treatments were clustered into one subcluster and N563 treatments belonged to another subcluster.

Consistent with the hierarchical cluster tree, a two-dimensional PCoA plot based on OTU composition also showed the variations among the four treatments clearly (**Figure 2B**). The PCoA1 and PCoA2 explained 45.11% of the total bacterial community. The samples treated with different N fertilization regimes separated well, suggesting that different N applications indeed change the soil bacterial community structures. PERMANOVA showed the significant differences in soil bacterial communities among the four treatments (Adonis: $P = 0.007 < 0.05$).

Soil Bacterial Community Composition

Based on species annotation and statistical analysis, the sequences were classified into a total of 38 different phyla (1.42% were unclassified at phylum). There were 10 phyla whose relative abundances were more than 1%, as shown in **Figure 3**.

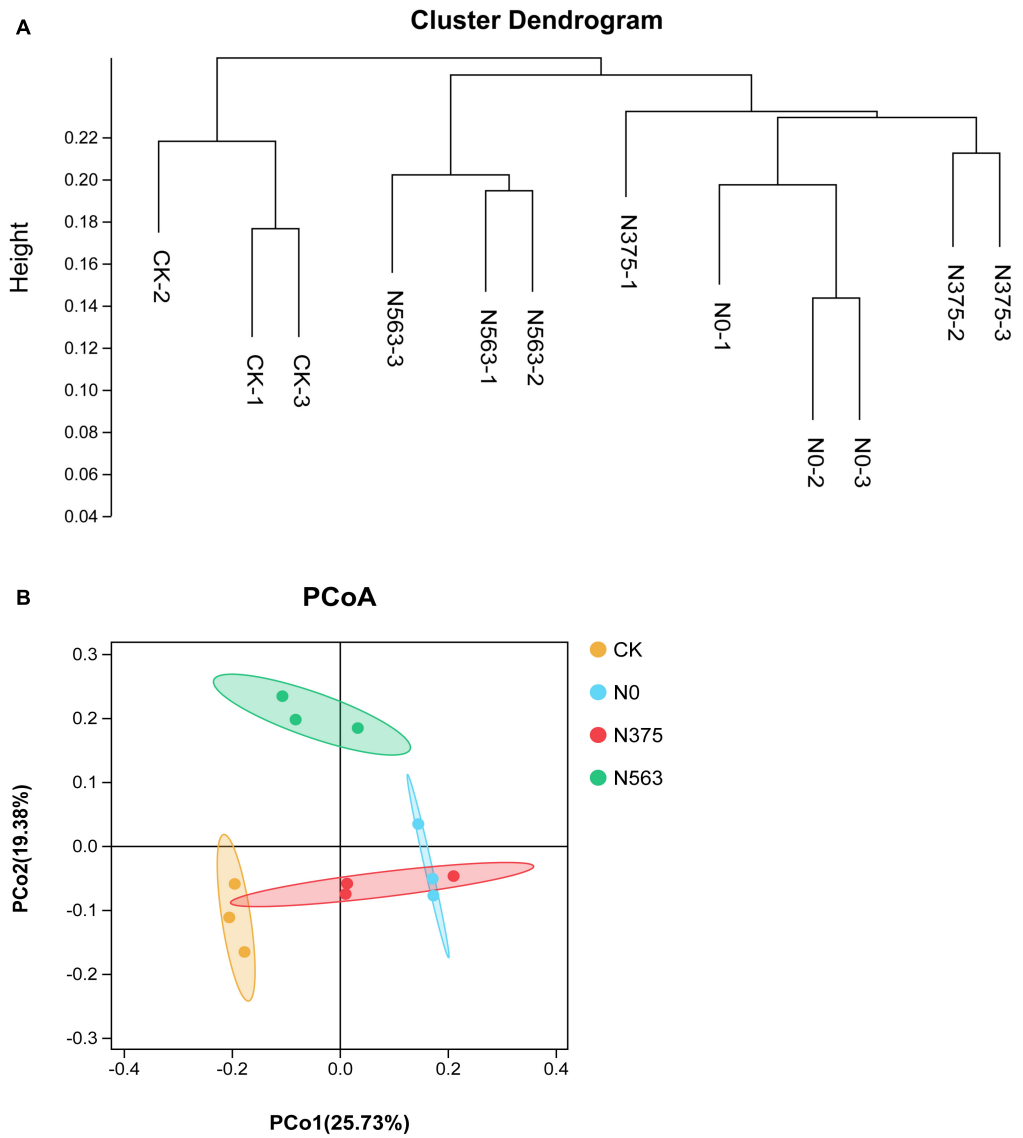

FIGURE 2 | The **(A)** unweighted pair group method with arithmetical averages (UPGMA) cluster analysis and **(B)** principal coordinate analysis of bacterial communities based on OTUs.

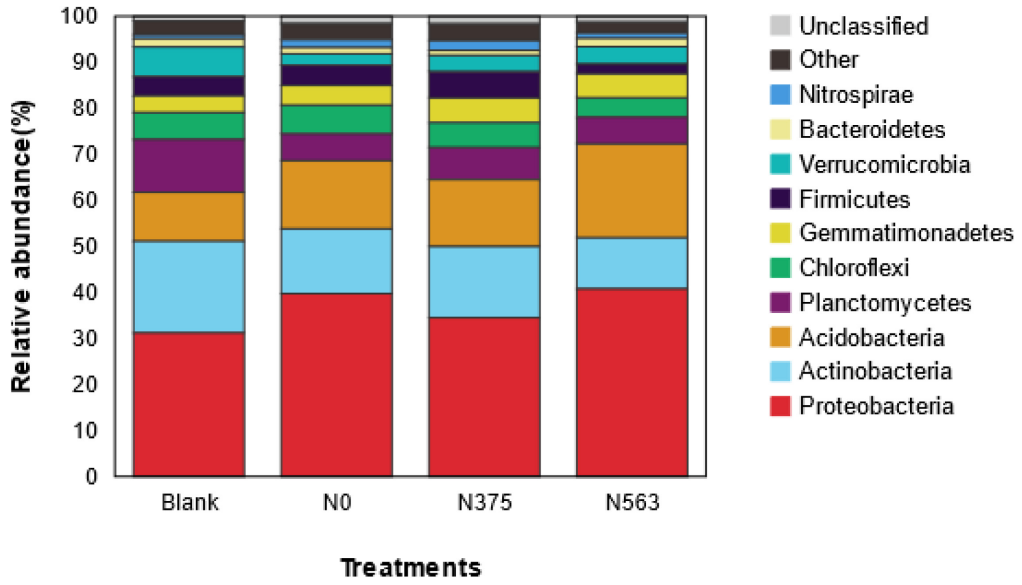

FIGURE 3 | Average relative abundance of the dominant bacteria phyla (relative abundance > 1%) in all treatments. Relative abundances are based on the proportional frequencies of those DNA sequences that could be classified at the phylum.

All samples were dominated by the phylum *Proteobacteria*, which accounted for 31.23–40.68% of the total sequences, followed by *Actinobacteria* (11.03–19.93%), *Acidobacteria* (10.67–20.40%), and *Planctomycetes* (5.82–11.45%); *Chloroflexi*, *Gemmatimonadetes*, *Firmicutes*, *Verrucomicrobia*, *Bacteroidetes*, and *Nitrospirae* were abundant (1–10%); and *Chlamydiae*, *Latescibacteria*. *Parcubacteria*, *Saccharibacteria*, *Armatimonadetes*, *Cyanobacteria*, *Elusimicrobia*, *TM6*, and *GAL15* were rare (<1%) (**Supplementary Table 1**). Obviously, there were some changes in the distribution of phylum as a result of different N application treatments. Compared with CK, N fertilizer application was combined to increase the relative abundance of *Proteobacteria* and *Gemmatimonadetes* and to decrease *Actinobacteria* and *Planctomycetes* ($P < 0.05$), and no statistical changes were found for *Chloroflexi*, *Verrucomicrobia*, and other rare phyla. There was no significant difference on the phyla except for *Elusimicrobia* between the N0 and N375 treatment. Compared with the N375 treatment, the N563 treatment significantly increased the relative abundances of *Proteobacteria*, *Acidobacteria*, and *Bacteroidetes* ($P < 0.05$) and decreased *Firmicutes* (*Bacilli*), *Latescibacteria*, and *Planctomycetes* ($P < 0.05$) (**Supplementary Table 1**).

The distribution of each class among the different treatments is shown in **Table 3** and evaluated by Duncan's multiple comparison test. The relative abundances of some classes showed no differences, such as Acidi*microbiia*, *Blastocatellia*, *Ktedonobacteria*, and *Spartobacteria*. We can conclude that N375 and N563 treatments significantly decreased the relative abundance of *Betaproteobacteria* but increased *Thermoleophilia* compared with the N0 treatment. Moreover, compared with the N375 treatment, the N563 treatment mainly significantly increased the relative abundance of *Alphaproteobacteria*, *Gammaproteobacteria*, *Acidobacteria*, and *Sphingobacteriia* and decreased *Bacilli*.

At the genus level, the reads represented 483 identifiable genera (59.6% of reads). The relative abundances of the 40 most relatively abundant bacterial genera in all treatments are listed in **Supplementary Table 2**. The results showed that *Sphingomonas* and *Gemmatimonas* were increased in the N563 treatment, while *Bacillus*, *Nitrospira*, and *Rhizobium*, which are beneficial bacteria, were more abundant in the N375 treatment. We found that N application shifts the N cycle in nitrification, mainly on the *Nitrospira* (**Supplementary Table 3**), but shows no significant effect on the genera related to nitrogen fixation, methane oxidation, sulfate reduction, and sulfur oxidation (**Table 4**).

LEfSe analysis showed that significant associations were found among predominant bacterial taxa in the four treatments (**Figure 4**). LEfSe analysis was conducted to explore which taxa (phylum to genus) were affected by different N applications (**Figure 4**). Those with an LDA score >2.0 were selected to identify bacterial taxa with statistically significant differences in abundance among treatments. The predominant bacterial taxa were the genera (the relative abundance > 0.1%) *Terrabacter*, *Oryzihumus*, and *Nocardioides* in the CK treatment; *Gluconacetobacter* in the N0 treatment; *Paenibacillus* in the N375 treatment; and *Candidatus_Koribacter*, *Haliangium*, and *Bryobacter* in the N563 treatment.

DISCUSSION

Soil microorganisms are vital in the agroecosystem environment on account of their important role in cycling mineral compounds, decomposing organic materials, and soil biochemical processes (Li J. G. et al., 2016). In turn, soil microbial biodiversity and

TABLE 3 | Relative abundances (%) of bacterial classes in all treatments.

Phylum	Class	CK	N0	N375	N563
Proteobacteria	*Betaproteobacteria*	10.13 ± 2.29 b	22.53 ± 3.57 a	14.55 ± 4.69 b	14.45 ± 2.34 b
	Alphaproteobacteria	14.3 ± 0.52 a	9.12 ± 0.32 b	10.42 ± 1.08 b	14.81 ± 1.43 a
	Deltaproteobacteria	4.23 ± 0.70 b	5.64 ± 0.29 ab	6.70 ± 1.71 a	5.98 ± 0.87 ab
	Gammaproteobacteria	2.53 ± 0.56 b	2.41 ± 0.06 b	2.83 ± 1.01 b	5.50 ± 1.34 a
Actinobacteria	*Thermoleophilia*	2.52 ± 0.32 a	1.80 ± 0.05 b	2.22 ± 0.22 a	2.38 ± 0.04 a
	Actinobacteria	15.98 ± 3.86 a	10.61 ± 2.62 ab	11.24 ± 2.38 ab	7.26 ± 1.95 b
	Acidimicrobiia	0.96 ± 0.21 a	1.23 ± 0.20 a	1.31 ± 0.54 a	1.11 ± 0.20 a
Acidobacteria	*Acidobacteria*	4.04 ± 0.32 c	6.87 ± 2.42 b	5.73 ± 0.94 bc	11.25 ± 0.14 a
	Solibacteres	1.81 ± 0.18 b	2.28 ± 0.61 ab	2.25 ± 0.44 ab	2.98 ± 0.10 a
	Blastocatellia	1.30 ± 0.47 a	1.25 ± 0.08 a	1.56 ± 0.59 a	1.42 ± 0.08 a
	Holophagae	0.55 ± 0.1 b	1.05 ± 0.18 a	1.26 ± 0.34 a	1.24 ± 0.18 a
Planctomycetes	*Phycisphaerae*	3.78 ± 0.76 a	1.99 ± 0.07 b	2.25 ± 0.68 b	1.91 ± 0.19 b
	Planctomycetacia	6.94 ± 2.30 a	3.29 ± 1.00 b	4.09 ± 2.41 ab	3.41 ± 0.18 b
Chloroflexi	*Ktedonobacteria*	3.97 ± 2.08 a	3.65 ± 1.07 a	2.61 ± 1.09 a	2.31 ± 0.37 a
Gemmatimonadetes	*Gemmatimonadetes*	3.54 ± 0.48 b	4.23 ± 0.54 ab	5.28 ± 0.78 a	5.18 ± 0.86 a
Firmicutes	*Bacilli*	3.74 ± 0.76 a	4.00 ± 0.22 a	5.31 ± 1.5 a	1.73 ± 0.17 b
Verrucomicrobia	*Spartobacteria*	2.10 ± 1.00 a	0.75 ± 0.44 a	1.64 ± 1.87 a	1.43 ± 0.53 a
Bacteroidetes	*Sphingobacteriia*	1.33 ± 0.23 ab	1.07 ± 0.45 b	0.95 ± 0.02 b	1.67 ± 0.20 a
Nitrospirae	*Nitrospira*	0.85 ± 0.22 b	1.71 ± 0.87 ab	2.13 ± 0.59 a	1.16 ± 0.20 ab

Values represent mean ± standard deviation of triplicate measurements.
Values within the same row followed by different lowercase letters indicated significant differences ($P < 0.05$) according to Duncan's multiple comparison tests.
CK, without fertilization; N0, without N fertilization; N375, application of 375 kg/ha N; N563, application of 563 kg/ha N.

TABLE 4 | Relative abundance (%) of the functional genera groups in all treatments.

Function	Genera	CK	N0	N375	N563
Nitrogen fixation	*Bradyrhizobium*, *Mesorhizobium*, *Rhizobium*, *Rhizocola*, *Rhizorhapis*	1.19 ± 0.10 a	0.99 ± 0.14 a	1.16 ± 0.08 a	1.06 ± 0.10 a
Nitrification	*Nitrosospira*, *Nitrospira*	0.41 ± 0.05 b	0.44 ± 0.18 b	0.78 ± 0.18 a	0.49 ± 0.04 b
Methane oxidation	*Methylobacterium*, *Methylocaldum*	0.14 ± 0.01 a	0.04 ± 0.02 b	0.07 ± 0.06 b	0.01 ± 0.00 b
Sulfate reduction	*Desulfitibacter*, *Desulfitobacterium*, *Desulfobulbus*, *Desulfosporosinus*, *Desulfovibrio*, *Desulfovirga*	0.03 ± 0.00 a	0.03 ± 0.00 a	0.03 ± 0.00 a	0.03 ± 0.01 a
Sulfur oxidation	*Sulfurifustis*, *Thiobacillus*	0.01 ± 0.00 a	0.03 ± 0.03 a	0.04 ± 0.04 a	0.01 ± 0.01 a

Values represent mean ± standard deviation of triplicate measurements.
Values within the same row followed by different lowercase letters indicated significant differences ($P < 0.05$) according to Duncan's multiple comparison tests.
CK, without fertilization; N0, without N fertilization; N375, application of 375 kg/ha N; N563, application of 563 kg/ha N.

functions are affected by various factors, such as soil nutrients, pH, and vegetation. In China, a large area of sugarcane fields was applied with high N fertilization to get higher yields. In our work, a field experiment was conducted to evaluate the impacts of different amounts of N fertilizers on the diversity and community structure in sugarcane soil. Our results showed that higher N fertilization (N563) conversely decreased sugarcane yield than in the N375 treatment, indicating that optimum N application might result in a healthier ecosystem and contribute toward sustainable crop production.

Soil microbial diversity is considered to be critical to integrity, function, and long-term sustainability of soil ecosystems (Kennedy and Smith, 1995). Many studies have shown that greater biodiversity can improve the ecosystem and the stability of microbial functions (Chaer et al., 2009). Therefore, it is critical to maintain and restore the microbial biodiversity in sustainable agriculture systems. Generally, excessive N fertilization decreased the diversity of microbes in bulk and rhizosphere soil (Sun et al., 2019; Wang et al., 2019). In our work, lower ACE, Chao1, and observed species at high N fertilization (N563) compared with those in the N375 and N0 treatments (**Table 2**) indicated that excessive N fertilization decreased the bacterial species richness, which might result from the selection pressure of high concentrated AN and alteration of soil pH on the microbes (Li J. G. et al., 2016). Moreover, some plant physiological characteristics, such as leaf area index and chlorophyll content, could be regulated by the N level, which could change root exudates or signal of the plant and in turn affect the rhizosphere microbes (Pfenning et al., 2009; Basal and Szabó, 2018).

Soil bacterial diversity and community structures were altered in response to different N application amendments, which agreed with previous studies (Zhang et al., 2017). The relative abundance variation at the phylum level and the LEfSe at each taxonomic level (from phylum to genus) (**Figures 3**, **4**) were conducted

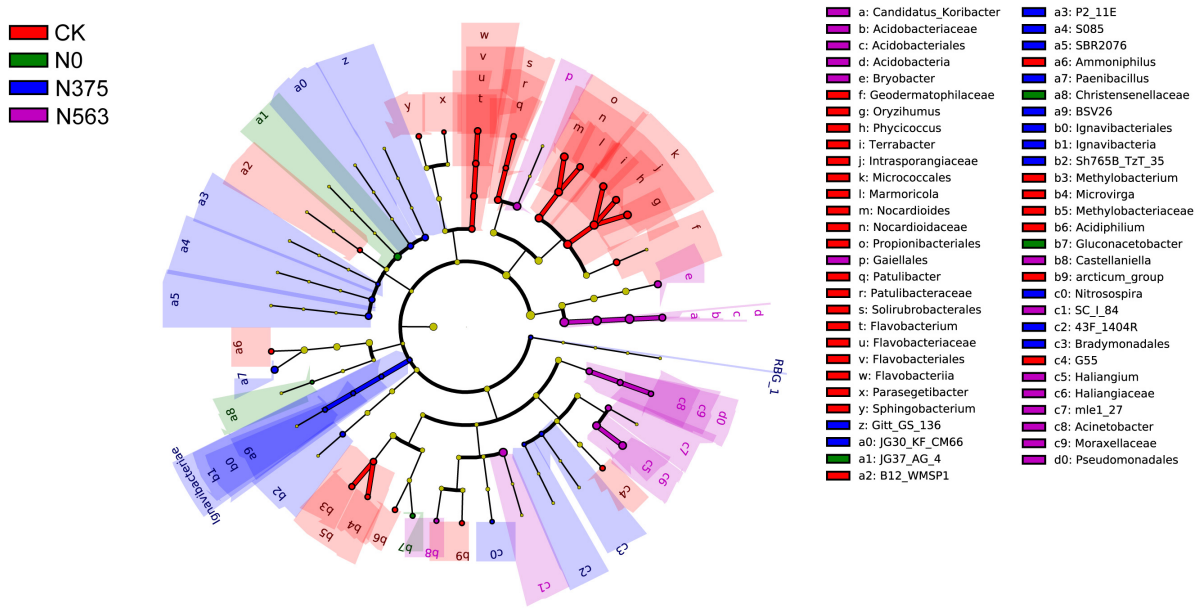

FIGURE 4 | The taxa of bacteria with significantly different abundance in the treatments were identified with the LEfSe method. Colored circles indicate the differentially abundant taxa and the color is corresponding to the different treatments (red for CK, green for N0, blue for N375, and purple for N563). Six rings of the cladogram stand for domain (innermost), phylum, class, order, family, and genus, and lineages with LDA values higher than 2.0 are displayed.

to detect microbial population distribution variations among all the treatments. Firstly, hierarchical cluster analysis of similarity and PCoA analysis of the bacterial communities (**Figure 2**) demonstrated that each treatment formed a unique community structure. *Proteobacteria*, *Acidobacteria*, and *Actinobacteria* were the dominant and responding phyla in all treatments, similar to a previous report in sugarcane soils (Luo et al., 2020). Different *Proteobacteria* have various functions in soil. Generally, *Alphaproteobacteria* and *Gammaproteobacteria* were reported to increase with pH above 4.5 (Rousk et al., 2010), but in our work, N563 treatment with lower pH resulted in a higher abundance of these two subgroups which may be due to a low soil pH below 4.5 (**Table 3**). Therefore, we speculate that there may be some other factors, such as available N reciprocally affecting these organisms in soil. *Bacteroidetes* was associated with decomposition of recalcitrant carbon compounds, showing positive responses to N fertilization (Yuan et al., 2016). Our results indicated that the relative abundances of *Proteobacteria* and *Bacteroidetes* in N563 treatment were significantly higher than those in N375 treatment (**Supplementary Table 1**). Similarly, Fierer et al. (2012) discovered that an improved soil N availability increased the abundance of copiotrophic bacterial taxa including *Proteobacteria* and *Bacteroidetes*, which was consistent with our study. *Actinobacteria* was the second abundant phylum and the relative abundance of the N563 treatment was significantly lower than that of the N375 treatment. Chaudhry et al. (2012) reported that high N input can decrease the relative abundance of *Actinobacteria*. Many studies showed that members of *Actinobacteria* could produce the most known antibiotics, such as *tetracycline*, *oxytetracycline*, *gentamicin*, and *streptomycin* and can survive in the soil environment, which are considered to be beneficial in agricultural soils (Polti et al., 2014). Thus, excessive N fertilizer application is not conducive to *Actinobacteria* so as to be harmful to microorganisms in agricultural systems. *Nitrospirae* was most abundant in the N375 treatment, which has been demonstrated to have a positive effect on enhancing the absorption of trace elements from soil to plants and promoting plant growth. That might be one of the reasons for the higher crop yield in the N375 treatment than in the N563 treatment. A recent study based on meta-analysis indicated that both soil microbial diversity and the relative abundances of *Actinobacteria* and *Nitrospirae* were reduced by N fertilizer application, which confirmed our work (Wang et al., 2018).

The application of a large amount of N fertilizers significantly decreased soil pH. This is well-documented and mainly resulted from soil processes which can produce protons, such as nitrification (Geisseler and Scow, 2014). A survey across China indicated that N fertilization application ranging from 8 to 25 years resulted in a decline of soil pH by 0.45–2.20 (Guo et al., 2010). In this work, pH values of the N563 treatment were significantly lower than those of the N375 treatment resulting from overuse of N fertilizer (Larssen and Carmichael, 2000; Guo et al., 2010). Additionally, N fertilization affects soil microbial community *via* changing the chemical properties of soil indirectly (Fierer et al., 2012). We discovered that N fertilizer application significantly impacted soil pH and available N, which indirectly affected microbial communities. *Acidobacteria*, a ubiquitous and abundant member of the soil bacterial community, have been suggested to be closely associated with pH (Jones et al., 2009). In the present study, the highest *Acidobacteria* abundance was in the N563 treatment, probably due to the relatively acidic soil (pH 4.03). Moreover, the responding microbial

selected by LEfSe analysis further demonstrated that excessive N fertilization altered the bacterial community, which the genus *Candidatus_Koribacter*, belonging to phylum *Acidobacteria*, was a responding bacterium in the N563 treatment (**Figure 4** and **Supplementary Table 2**).

Changes in bacterial communities reflect the corresponding alterations in functional consequences (Dietrich et al., 2017). Fierer et al. (2012) found that catabolic capabilities of bacterial communities shift across the N gradients, which were significantly correlated with the phylogenetic and metagenomic responses, indicating possible linkages between the structure and functioning of soil microbial communities. In our work, N375 treatment significantly increased the relative abundance of *Nitrospira* related to nitrification but showed no significant effect on the other biogeochemical cycles (**Table 4**). Moreover, the beneficial bacteria *Bacillus* and *Paenibacillus* were also found most abundant in the N375 treatment. *Bacillus* isolated from rhizospheric soil of sugarcane has N-fixation and biocontrol property against two sugarcane pathogens (Singh et al., 2020). Our results suggested that optimum N application not only reduces cost and waste but also is good for microbials. Overall, our work indicated that N fertilization may change the predominant microbial life-history strategies, preferring a more active microbial community.

CONCLUSION

In this work, we examined the effects of different N application rates on microbial diversity and community structure by MiSeq high-throughput sequencing of the 16S rRNA gene. We found that the overuse of N fertilizers significantly decreased pH and increased the available N in soils and obtained a lower yield. N fertilizer application indeed changed the bacterial diversity and community structures in sugarcane soils. Excessive N application significantly decreased the bacterial diversity. The optimum amount of N application could be conducive to beneficial microorganisms, such as *Actinobacteria*, *Nitrospira*, and *Bacillus* and resulted in a healthier ecosystem and higher sustainable crop production.

DATA AVAILABILITY STATEMENT

The datasets presented in this study can be found in online repositories. The names of the repository/repositories and accession number(s) can be found below: https://www.ncbi.nlm.nih.gov/, SRP269446.

AUTHOR CONTRIBUTIONS

YG analyzed the data and wrote the manuscript. JW conceived the study. GL, WC, and YM performed the experiment. SY provided the financial support and technical guidance. All authors contributed to the article and approved the submitted version.

FUNDING

This work was financially supported by the National Key Research and Development Program of China (2016YFD0200102) and the State Key Laboratory for Conservation and Utilization of Subtropical Agro-bioresource (SKLCUSA-b201707).

SUPPLEMENTARY MATERIAL

The Supplementary Material for this article can be found online at: https://www.frontiersin.org/articles/10.3389/fmicb.2021.721441/full#supplementary-material

REFERENCES

Bao, S. D. (2000). *Agrochemical Analysis of Soil*. Beijing: China Agriculture Press.

Basal, O., and Szabó, A. (2018). The effects of drought and nitrogen on soybean (Glycine max (L.) Merrill) physiology and yield. *Int. J. Agric. Biosyst. Engin.* 12, 260–265. doi: 10.5281/zenodo.1474431

Belén, M. A., Mary-Rus, M. C., Almudena, B., Francisco, L., and Ana, Q. (2016). Liquid organic fertilizers for sustainable agriculture: nutrient uptake of organic versus mineral fertilizers in citrus trees. *PLoS One* 11:e0161619. doi: 10.1371/journal.pone.0161619

Caporaso, J. G., Kuczynski, J., Stombaugh, J., Bittinger, K., Bushman, F. D., and Costello, E. K. (2010). QIIME allows analysis of high-throughput community sequencing data. *Nat. Methods* 7, 335–336. doi: 10.1038/nmeth.f.303

Chaer, G., Fernandes, M., Myrold, D., and Bottomley, P. (2009). Comparative resistance and resilience of soil microbial communities and enzyme activities in adjacent native forest and agricultural soils. *Microb. Ecol.* 58, 414–424. doi: 10.1007/s00248-009-9508-x

Chaudhry, V., Rehman, A., Mishra, A., Chauhan, P. S., and Nautiyal, C. S. (2012). Changes in bacterial community structure of agricultural land due to long-term organic and chemical amendments. *Microb. Ecol.* 64, 450–460. doi: 10.1007/s00248-012-0025-y

Chen, G., Huang, J., Fang, Y., Zhao, Y., Tian, X., Jin, Y., et al. (2019). Microbial community succession and pollutants removal of a novel carriers enhanced duckweed treatment system for rural wastewater in Dianchi Lake basin. *Bioresour. Technol.* 276, 8–17. doi: 10.1016/j.biortech.2018.12.102

de Souza, R. S., Okura, V. K., Armanhi, J., Jorrín, B., Lozano, N., Silva, M., et al. (2016). Unlocking the bacterial and fungal communities assemblages of sugarcane microbiome. *Sci. Rep.* 6:28774. doi: 10.1038/srep28774

Dietrich, P., Buchmann, T., Cesarz, S., Eisenhauer, N., and Roscher, C. (2017). Fertilization, soil and plant community characteristics determine soil microbial activity in managed temperate grasslands. *Plant Soil* 419, 189–199. doi: 10.1007/s11104-017-3328-4

dos Santos, S. G., da Silva Ribeiro, F., Alves, G. C., Santos, L. A., and Reis, V. M. (2019). Inoculation with five diazotrophs alters nitrogen metabolism during the initial growth of sugarcane varieties with contrasting responses to added nitrogen. *Plant Soil* 44, 363–370. doi: 10.1007/s11104-019-04101-1

Du, Y., Wang, T., Wang, C., Anane, P. S., Liu, S., and Paz-Ferreiro, J. (2019). Nitrogen fertilizer is a key factor affecting the soil chemical and microbial communities in a Mollisol. *Can. J. Microbiol.* 65, 510–521. doi: 10.1139/cjm-2018-0683

Edgar, R. C. (2013). UPARSE: highly accurate OTU sequences from microbial amplicon reads. *Nat. Methods* 10, 996–998. doi: 10.1038/nmeth.2604

Fierer, N., Lauber, C. L., Ramirez, K. S., Zaneveld, J., Bradford, M. A., and Knight, R. (2012). Comparative metagenomic, phylogenetic and physiological analyses of soil microbial communities across nitrogen gradients. *ISME J.* 6, 1007–1017. doi: 10.1038/ismej.2011.159

Geisseler, D., and Scow, K. M. (2014). Long-term effects of mineral fertilizers on soil microorganisms–a review. *Soil Biol. Biochem.* 75, 54–63. doi: 10.1016/j.soilbio.2014.03.023

Gu, Y., Mi, W. H., Xie, Y. N., Ma, Q. X., Wu, L. H., and Hu, Z. P. (2019). Nitrapyrin affects the abundance of ammonia oxidizers rather than community structure in a yellow clay paddy soil. *J. Soil Sediments* 19, 872–882. doi: 10.1007/s11368-018-2075-3

Guo, J. H., Liu, X. J., Zhang, Y., Shen, J. L., Han, W. X., Zhang, W. F., et al. (2010). Significant acidification in major Chinese croplands. *Science* 327, 1008–1010. doi: 10.1126/science.1182570

Guo, Q., Yan, L., Korpelainen, H., Niinemets, Ü, and Li, C. (2018). Plant-plant interactions and n fertilization shape soil bacterial and fungal communities. *Soil Biol. Biochem* 128, 127–138. doi: 10.1016/j.soilbio.2018.10.018

Jones, R. T., Robeson, M. S., Lauber, C. L., Hamady, M., Knight, R., and Fierer, N. (2009). A comprehensive survey of soil acidobacterial diversity using pyrosequencing and clone library analyses. *ISME J.* 3, 442–453. doi: 10.1038/ismej.2008.127

Kennedy, A. C., and Smith, K. L. (1995). Soil microbial diversity and the sustainability of agricultural soils. *Plant Soil* 170, 75–86. doi: 10.1007/BF02183056

Klironomos, J., Zobel, M., Tibbett, M., Stock, W. D., Rillig, M. C., Parrent, J. L., et al. (2011). Forces that structure plant communities: quantifying the importance of the mycorrhizal symbiosis. *New Phytol.* 189, 366–370. doi: 10.1111/j.1469-8137.2010.03550.x

Larssen, T., and Carmichael, G. R. (2000). Acid rain and acidification in China: the importance of base cation deposition. *Environ. Pollut.* 110, 89–102. doi: 10.1016/S0269-7491(99)00279-1

Li, J. G., Shen, M. C., Hou, J. F., Li, L., Wu, J. X., and Dong, Y. H. (2016). Effect of different levels of nitrogen on rhizosphere bacterial community structure in intensive monoculture of greenhouse lettuce. *Sci. Rep.* 6:25305. doi: 10.1038/srep25305

Li, Y. R., Song, X. P., Wu, J. M., Li, C. N., Liang, Q., and Liu, X. H. (2016). Sugar industry and improved sugarcane farming technologies in china. *Sugar Tech.* 18, 603–611. doi: 10.1007/s12355-016-0480-8

Li, Y. R., and Yang, L. T. (2015). Sugarcane agriculture and sugar industry in China. *Sugar Tech*. 17, 1–8. doi: 10.1007/s12355-014-0342-1

Luo, J., Lin, Z. L., Li, S. Y., Que, Y. X., Zhang, C. F., Yang, Z. Q., et al. (2020). Effects of different soil improvement measures on soil physicochemical properties and microbial community structures in mechanically compacted acidified sugarcane field. *Acta Agron. Sin.(China)* 46, 596–613.

Pereira, L. B., Andrade, G. S., Meneghin, S. P., Vicentini, R., and Ottoboni, L. M. M. (2019). Prospecting plant growth-promoting bacteria isolated from the rhizosphere of sugarcane under drought stress. *Curr. Microbiol.* 76, 1345–1354. doi: 10.1007/s00284-019-01749-x

Pfenning, J., Liebig, H. P., Graeff, S., and Claupein, W. (2009). Sensor based fine tuning of nitrogen fertilizer applications using spectral feedback signals from tomato plants (Lycopersicon esculentum Mill.). *Acta Hortic.* 824, 177–182. doi: 10.17660/ActaHortic.2009.824.20

Pisa, G., Magnani, G. S., Weber, H., Souza, E. M., Faoro, H., Monteiro, R. A., et al. (2011). Diversity of 16s Rrna genes from bacteria of sugarcane rhizosphere soil. *Braz. J. Med. Biol. Res.* 44, 1215–1221. doi: 10.1590/S0100-879X2011007500148

Polti, M. A., Aparicio, J. D., Benimeli, C. S., and Amoroso, M. J. (2014). Role of actinobacteria in bioremediation. *Microbiol. Biodegrad. Biorem* 2014, 269–286. doi: 10.1016/B978-0-12-800021-2.00011-X

Robertson, G. P., and Vitousek, P. M. (2009). Nitrogen in agriculture: balancing the cost of an essential resource. *Annu. Rev. Environ. Resour.* 34, 97–125. doi: 10.1146/annurev.environ.032108.105046

Robinson, N., Brackin, R., Vinall, K., Soper, F., Holst, J., Gamage, H., et al. (2011). Nitrate paradigm does not hold up for sugarcane. *PLoS One* 6:e19045. doi: 10.1371/journal.pone.0019045

Rousk, J., Baath, E., Brookes, P. C., and Lauber, C. L. (2010). Soil bacterial and fungal communities across a pH gradient in an arable soil. *ISME J.* 4, 1340–1351. doi: 10.1038/ismej.2010.58

Savario, C. F., and Hoy, J. W. (2011). Microbial communities in sugarcane field soils with and without a sugarcane cropping history. *Plant Soil* 341, 63–73. doi: 10.1007/s11104-010-0622-9

Segata, N., Izard, J., Waldron, L., Gevers, D., Miropolsky, L., Garrett, W. S., et al. (2011). Metagenomic biomarker discovery and explanation. *Genome Biol.* 12:R60. doi: 10.1186/gb-2011-12-6-r60

Singh, R., Singh, P., Haibi, L., Song, Q. Q., Guo, D. J., Solanki, M., et al. (2020). Diversity of nitrogen-fixing rhizobacteria associated with sugarcane: a comprehensive study of plant-microbe interactions for growth enhancement in Saccharum Spp. *BMC Plant Biol.* 20:220. doi: 10.1186/s12870-020-02400-9

Singh, R. K., Singh, P., Li, H. B., Yang, L. T., and Li, Y. R. (2017). "Soil–plant–microbe interactions: use of nitrogen-fixing bacteria for plant growth and development in sugarcane," in *Plant-Microbe Interactions in Agro-Ecological Perspectives*, eds D. Singh, H. Singh, and R. Prabha (Singapore: Springer), 35–39. doi: 10.1007/978-981-10-5813-4_3

Sun, R., Zhang, P., Riggins, C. R., Zabaloy, M. C., Rodríguez-Zas, S., and Villamil, M. B. (2019). Long-term N fertilization decreased diversity and altered the composition of soil bacterial and archaeal communities. *Agronomy* 9:574. doi: 10.3390/agronomy9100574

Val-Moraes, S. P., de Macedo, H. S., Kishi, L. T., Pereira, R. M., Navarrete, A. A., Mendes, L. W., et al. (2016). Liming in the sugarcane burnt system and the green harvest practice affect soil bacterial community in Northeastern Brazil. *Antonie Van Leeuwenhoek* 109, 1643–1654. doi: 10.1007/s10482-016-0764-8

Waclawovsky, A. J., Sato, P. M., Lembke, C. G., Moore, P. H., and Souza, G. M. (2010). Sugarcane for bioenergy production: an assessment of yield and regulation of sucrose content. *Plant Biotechnol. J.* 8, 263–276. doi: 10.1111/j.1467-7652.2009.00491.x

Wang, C., Liu, D., and Bai, E. (2018). Decreasing soil microbial diversity is associated with decreasing microbial biomass under nitrogen addition. *Soil Biol. Biochem.* 120, 126–133. doi: 10.1016/j.soilbio.2018.02.003

Wang, Q., Ma, M., Jiang, X., Guan, D., Wei, D., Zhao, B., et al. (2019). Impact of 36 years of nitrogen fertilization on microbial community composition and soil carbon cycling-related enzyme activities in rhizospheres and bulk soils in northeast China. *Appl. Soil Ecol.* 136, 148–157. doi: 10.1016/j.apsoil.2018.12.019

Yang, W., Li, Z., Wang, J., Wu, P., and Zhang, Y. (2013). Crop yield, nitrogen acquisition and sugarcane quality as affected by interspecific competition and nitrogen application. *Field Crops Res.* 146, 44–50. doi: 10.1016/j.fcr.2013.03.008

Yeoh, Y. K., Paungfoo-Lonhienne, C., Dennis, P. G., Robinson, N., Ragan, M. A., Schmidt, S., et al. (2016). The core root microbiome of sugarcanes cultivated under varying nitrogen fertilizer application. *Environ. Microbiol.* 18, 1338–1351. doi: 10.1111/1462-2920.12925

Yuan, X., Knelman, J. E., Gasarch, E., Wang, D., Nemergut, D. R., and Seastedt, T. R. (2016). Plant community and soil chemistry responses to long-term nitrogen inputs drive changes to alpine bacterial communities. *Ecology* 97, 1543–1554. doi: 10.1890/15-1160.1

Zhang, M., Wang, W., Zhang, Y., Teng, Y., and Xu, Z. (2017). Effects of fungicide iprodione and nitrification inhibitor 3, 4-dimethylpyrazole phosphate on soil enzyme and bacterial properties. *Sci. Total Environ.* 599, 254–263. doi: 10.1016/j.scitotenv.2017.05.011

Zhang, W. F., Dou, Z. X., He, P., Ju, X. T., Powlson, D., Chadwick, D., et al. (2013). New technologies reduce greenhouse gas emissions from nitrogenous fertilizer in China. *Proc. Natl. Acad. Sci. U.S.A.* 110, 8375–8380. doi: 10.1073/pnas.1210447110

Conflict of Interest: The authors declare that the research was conducted in the absence of any commercial or financial relationships that could be construed as a potential conflict of interest.

Publisher's Note: All claims expressed in this article are solely those of the authors and do not necessarily represent those of their affiliated organizations, or those of the publisher, the editors and the reviewers. Any product that may be evaluated in this article, or claim that may be made by its manufacturer, is not guaranteed or endorsed by the publisher.

frontiers in Microbiology

ORIGINAL RESEARCH
published: 13 September 2021
doi: 10.3389/fmicb.2021.729047

Rhizosphere Soil Bacterial Communities of Continuous Cropping-Tolerant and Sensitive Soybean Genotypes Respond Differently to Long-Term Continuous Cropping in Mollisols

Ming Yuan[1], Taobing Yu[2,3], Qihan Shi[2,3], Dongwei Han[1], Kanchao Yu[1], Lianxia Wang[1], Shurong Wang[1], Hao Xiang[4], Ronghui Wen[5], Hai Nian[2,3] and Tengxiang Lian[2,3]**

[1]Qiqihar Branch of Heilongjiang Academy of Agricultural Sciences, Qiqihar, China, [2]The State Key Laboratory for Conservation and Utilization of Subtropical Agro-bioresources, South China Agricultural University, Guangzhou, China, [3]The Key Laboratory of Plant Molecular Breeding of Guangdong Province, College of Agriculture, South China Agricultural University, Guangzhou, China, [4]Institute of Hydrobiology, Chinese Academy of Sciences, Wuhan, China, [5]The State Key Laboratory for Conservation and Utilization of Subtropical Agro-bioresources, College of Life Science and Technology, Guangxi University, Nanning, China

OPEN ACCESS

Edited by:
Hai-Ming Zhao,
Jinan University, China

Reviewed by:
Shuai Zhao,
Chinese Academy of Sciences, China
Xuesong Luo,
Huazhong Agricultural University, China
Weiming Hu,
University of Florida, United States

***Correspondence:**
Tengxiang Lian
liantx@scau.edu.cn
Hai Nian
hnian@scau.edu.cn

Specialty section:
This article was submitted to Terrestrial Microbiology, a section of the journal Frontiers in Microbiology

Received: 22 June 2021
Accepted: 16 August 2021
Published: 13 September 2021

Citation:
Yuan M, Yu T, Shi Q, Han D, Yu K, Wang L, Wang S, Xiang H, Wen R, Nian H and Lian T (2021) Rhizosphere Soil Bacterial Communities of Continuous Cropping-Tolerant and Sensitive Soybean Genotypes Respond Differently to Long-Term Continuous Cropping in Mollisols. Front. Microbiol. 12:729047. doi: 10.3389/fmicb.2021.729047

The continuous planting of soybeans leads to soil acidification, aggravation of soil-borne diseases, reduction in soil enzyme activity, and accumulation of toxins in the soil. Microorganisms in the rhizosphere play a very important role in maintaining the sustainability of the soil ecosystem and plant health. In this study, two soybean genotypes, one bred for continuous cropping and the other not, were grown in a Mollisol in northeast China under continuous cropping for 7 and 36 years in comparison with soybean–maize rotation, and microbial communities in the rhizosphere composition were assessed using high-throughput sequencing technology. The results showed that short- or long-term continuous cropping had no significant effect on the rhizosphere soil bacterial alpha diversity. Short-term continuous planting increased the number of soybean cyst nematode (*Heterodera glycines*), while long-term continuous planting reduced these numbers. There were less soybean cyst nematodes in the rhizosphere of the tolerant genotypes than sensitive genotypes. In addition, continuous cropping significantly increased the potential beneficial bacterial populations, such as *Pseudoxanthomonas*, *Nitrospira*, and *Streptomyces* compared to rotation and short-term continuous cropping, suggesting that long-term continuous cropping of soybean shifts the microbial community toward a healthy crop rotation system. Soybean genotypes that are tolerant to soybean might recruit some microorganisms that enhance the resistance of soybeans to long-term continuous cropping. Moreover, the network of the two genotypes responded differently to continuous cropping. The tolerant genotype responded positively to continuous cropping, while for the sensitive genotype, topology analyses on the instability of microbial community in the rhizosphere suggested that short periods of continuous planting can have a detrimental

effect on microbial community stability, although this effect could be alleviated with increasing periods of continuous planting.

Keywords: continuous cropping, soybean, Mollisol, rhizosphere microorganisms, network

INTRODUCTION

As one of the most important soil resources in China, Mollisols in the northeast play a crucial role in maintaining domestic food demand. Soybean [*Glycine max (L.)* Merrill] is one of the most important food crops in the world, providing a large amount of oil and protein for humans and animals (Chigen et al., 2018; Liu et al., 2020). There is a large demand for soybeans, especially in China (Liu et al., 2020). Due to the limited arable land, climatic conditions, and large proportion of arable land with other crops, soybeans are often continuously planted in this region (Liu et al., 2012). On some farms, soybeans have been planted continuously for 40 years or even longer (Liu et al., 2020). The continuous planting of soybeans leads to soil acidification, aggravation of soil-borne diseases, reduction in soil enzyme activity, and accumulation of toxins in the soil (Zhan et al., 2004; Yan et al., 2012; Pérez-Brandán et al., 2014; Bai et al., 2015). Several studies have clarified that these changes are significantly related to biological factors in the soil (Ji et al., 1996; Dias et al., 2015; Liu et al., 2020).

Rhizosphere microorganisms play a very important role in maintaining the sustainability of the soil ecosystem and plant health (Waldrop et al., 2000; Avidano et al., 2005). Different cropping systems can significantly change the microbial community structure (Meriles et al., 2009; Zhou et al., 2018; Liu et al., 2019). However, these changes depend on the type of cropping system, soil type, and crop species. For instance, both Tang et al. (2009) and Zhu et al. (2014) found that, compared with crop rotation systems, the abundance of Actinobacteria significantly decreased under the continuous cropping of soybean. Xu et al. (1995) found that continuous cropping decreased the abundance of *Penicillium* sp., while it increased the abundance of *Fusarium* sp. However, another study showed that, compared with crop rotation, continuous soybean cropping did not change the microbial community structure (Hu and Wang, 1996). The inconsistencies between these studies are mainly due to the differences in soil types, research methods, crop rotation systems, and years of continuous cropping. At the same time, the mechanisms associated with continuous cropping obstacles are complex and need to be explored in greater depth under different conditions.

Soybean is one of the most sensitive crops to continuous cropping. Studies have shown that continuous cropping of soybean for 3 years could reduce yield by approximately 30% (Liu et al., 2020). In addition, compared to crop rotation, soybean root rot diseases and cyst nematodes in soybean fields increased significantly in a short-term continuously cropped system (Cai et al., 2015). However, root rot and cystic nematode disease in soybean fields might be weakened after long-term continuous cropping (Song et al., 2017). This might be attributed to the fact that long-term continuous cropping could increase the population of beneficial microorganisms, which could help inhibit the colonization and development of pathogens in the soil (Wei et al., 2015; Liu et al., 2020). For example, Liu et al. (2020) found that 13 years of long-term continuously cropped soybean increased beneficial bacteria, such as *Bradyrhizobium* sp., *Gemmatimonas* sp., *Mortierella* sp., and *Paecilomyces* sp. and decreased the pathogenic fungi of *Fusarium* sp. However, some researchers also found that long-term continuous of soybeans may reduce the populations of beneficial microorganisms such as *Trichoderma*, *Colloids*, and *Pseudomonas fluorescens* (Pérez-Brandán et al., 2014). Therefore, the change in the microbial community caused by continuous or rotational cropping is crucial to reveal the mechanisms underlying obstacles to continuous soybean cropping. In addition, the inconsistency of these studies indicates that more research on the soil microbial community needs to be performed.

The rhizosphere microbial community of crops is also affected by genotypes (Kaisermann et al., 2017; Lian et al., 2019). Resistant genotypes can recruit some beneficial microorganisms to help the host resist various stresses (Lebeis et al., 2015; Kwak et al., 2018). For example, tomato genotypes that are resistant to *Fusarium* wilt can recruit a large number of *Flavobacterium* to help alleviate the symptoms of *Fusarium* wilt (Kwak et al., 2018). Our previous studies have also shown that aluminium-resistant soybeans can recruit *Tumebacillus* and *Burkholderia* and alleviate aluminium toxicity (Lian et al., 2019). Regarding the continuous cropping of soybean, although microorganisms are known to play a very important role in alleviating or aggravating continuous cropping obstacles, the comparison of the microbial community in the rhizosphere among different genotypes has not been reported. Understanding the characteristics of the rhizosphere microbial community of continuous-resistant genotype soybeans can help us understanding how those resistant genotypes could better adapt to continuous cropping.

Here, we aimed to characterize the rhizosphere microorganisms of different soybean genotypes, one bred for continuous cropping and one not, grown in a Mollisol in northeast China under continuous cropping for 7 and 36 years with soybean–maize rotation. Based on the higher adaptability of continuous cropping-tolerant (CC-T) soybean genotypes to continuous cropping, we hypothesized that (1) the bacterial diversity in the rhizosphere of CC-T genotypes would be higher than that of continuous cropping-sensitive (CC-S) genotypes and that (2) the response of bacterial community structure to continuous cropping between CC-T and CC-S soybean genotypes would be different. CC-T may recruit beneficial microbial species to alleviate the occurrence of soil-borne diseases.

MATERIALS AND METHODS

Soil Source and Plant Materials

To assess the responses of continuous cropping-tolerant and cropping-sensitive soybean genotypes soil used in this study was a Mollisol, according to USDA soil taxonomy. Soybeans used in the experiment included Qinong1 and Qinong5, which were continuous cropping-tolerant (CCT), and Heihe43 and Henong76, which were continuous cropping-sensitive (CCS).

Experimental Design and Plant and Rhizosphere Soil Collection

Continuous cropping of two soybean genotypes for 7 and 36 years, as well as treatment of soybean-corn rotations for 10 years, were selected for this study. The total area of the experimental field (47°15′N, 123°40′E) was 2 ha, including 1.3 ha of 36-year continuous cropping and 0.3 ha each of 7-year continuous and rotation cropping (**Supplementary Figure S1**). A total of 72 rhizosphere soil samples (six treatments × 12 replicates) were collected at the flowering stage of soybean on July 15, 2020. All rhizosphere soil samples were collected by gently shaking the plant root to remove loosely attached soil, and then the soil adhering to the root system was transported to an aseptic bag. Two grams of rhizosphere soil from each sample was placed in a sterilized microcentrifuge tube and stored at −80°C for DNA extraction. The shoots and roots were separated for biomass measurements. All the soybean cyst nematodes (*Heterodera glycines*) and nodules from the roots were counted after removal from the root system. In brief, after the soybean cyst nematode growth broke through the root surface of soybean (35 days after seedling), 10 soybean plants were randomly selected for the soybean cyst nematodes counting. The yield per square meter was measured after soybean maturity.

Soil DNA Extraction and Next-Generation Sequencing

In total, 72 rhizosphere soil samples were used for sequencing. Soil total DNA was extracted using the Fast DNA SPIN Kit for Soil (MP Biomedicals, Santa Ana, CA). Primer sequences of 341F/805R were used to amplify the V4 (V3–V4) hypervariable regions of the 16S rRNA. The PCR products were purified and then sequenced using the MiSeq Illumina platform (Illumina, United States) at Icongene (Wuhan) Gene Technology Co., Ltd. (Wuhan, China). All sequences were deposited into the GenBank short-read archive PRJNA732989.

After sequencing, the raw FASTQ files were processed using QIIME Pipeline Version 1.19.1. Briefly, all sequence reads were assigned to each sample based on the barcodes. Sequences with low quality (length < 200 bp and average base quality score < 20) were removed before further analysis. The chimera of trimmed sequences was detected and removed using the UCHIME algorithm (Edgar et al., 2011). The sequences were phylogenetically assigned according to their best matches to sequences in the RDP database using the RDP classifier (Cole et al., 2009). Operational taxonomic units (OTUs) were classified at 97% sequence similarity using CD-HIT (Li and Godzik, 2015). Chao1 richness and Shannon's diversity index were calculated in QIIME. Constrained principal coordinate analysis (CPCoA) and significance tests (Adonis test and mantel test) were performed in program R version 3.5.1 for Windows with the "vegan" package. Ternary plots were constructed to show the abundance comparison of OTUs (>5%) for rotation system, and continuous cropping for 7 and 36 years of the two genotypes soybeans, using the "vcd" package (Friendly and Meyer, 2015). One-way analysis of variance (ANOVA) was used in GenStat 13 (VSN International, Hemel Hempstead, United Kingdom) to assess the relative abundances of different taxonomic levels of bacteria. Additionally, a Pearson bivariate correlation analysis was performed to access the correlations between pH, soybean cyst nematode, yield, and the genera with higher relative abundance.

Core Bacteria and Co-occurrence Network Analyses

Core bacteria, which contain a list of OTUs observed in 60% of all rhizosphere samples, were obtained by MicrobiomeAnalyst (Chong et al., 2020). Bacterial co-occurrence networks were analyzed for each cropping system. To study the network structure of OTUs with high abundance, we selected OTUs with more than 0.2% relative abundance to calculate Spearman's rank correlation coefficients. The correlations between OTUs were selected at $p < 0.05$ and Spearman's correlation coefficient of more than 0.8 (Mendes et al., 2018). The nodes and edges represent bacterial OTUs and the correlations between bacterial OTUs, respectively. Statistical analyses were calculated using the "psych" package in R and then visualized in Gephi (Jiang et al., 2017). Keystone species were defined according to high node degree, high betweenness centrality, and high closeness centrality (Berry and Widder, 2014; Agler et al., 2016). The NetShift analysis was performed using the NetShift Software tool[1] to compare the networks of different treatments and find the "driver microbes" between the treatment of soybean-corn rotations and 7, 36 years continuous cropping for the sensitive and tolerant genotypes, respectively (Kuntal et al., 2019).

RESULTS

Soybean Cyst Nematode Numbers and Yield

Both cropping systems and soybean genotypes significantly affected the soybean cyst nematode number and yield (**Table 1**). There was a higher cyst nematode number in the sensitive genotypes than in the tolerant genotypes. In particular, for the sensitive genotypes, the soybean cyst nematode number significantly increased in the 7-year continuous cropping field but markedly decreased in the 36-year continuous cropping field. However, continuous cropping had no significant effect on the tolerant genotypes. In addition, the yield increased in

[1]https://web.rniapps.net/netshift/

TABLE 1 | Soil pH, number of cyst nematode, shoot and root biomass, and yield of different treatments.

	CKT	CKS	7T	7S	36T	36S	Cropping systems	Genotype	Cropping systems*Genotype	LSD
pH	7.08 ± 0.08b	6.91 ± 0.1c	6.91 ± 0.04c	7.29 ± 0.13a	6.69 ± 0.12d	6.66 ± 0.07d	<0.001***	0.075	<0.001***	0.005
Number of cyst nematode	1.5 ± 1.64bc	5.5 ± 1.64b	1.67 ± 1.86bc	15.17 ± 8.84a	0.33 ± 0.52c	4.67 ± 1.63bc	0.002**	<0.001***	0.007**	2.236
Shoot biomass	88.27 ± 32.24ab	59.29 ± 9.9b	81.63 ± 25.51b	79.13 ± 16.13b	115.89 ± 23.18a	88.33 ± 24.65b	0.014*	0.016*	0.301	27.2
Root biomass (g)	10.7 ± 4.29a	10.6 ± 2.29a	11.5 ± 4.35a	10.41 ± 2.33a	11.85 ± 2.99a	11.82 ± 3.85a	0.686	0.72	0.91	1.99
Yield (g/m^2)	353 ± 35.34 cd	293 ± 17.38d	481 ± 45.95a	401 ± 46.82bc	456 ± 35.3ab	351 ± 27.91 cd	<0.001***	<0.001***	0.683	74.1

CKT: crop rotation-tolerance, CKS: crop rotation-sensitive, 7T: 7 year-continuous cropping-tolerant, 7S: 7 year-continuous cropping-sensitive, 36T: 36year-continuous cropping-tolerant, 36S: 36year-continuous cropping-sensitive.
$^{*}p < 0.05$; $^{**}p < 0.01$; $^{***}p < 0.001$.

the 7-year continuous cropping field but decreased in the 36-year continuous cropping field, with a higher yield for the tolerant genotypes than the sensitive genotypes (**Table 1**).

Rhizosphere Soil Bacterial Diversity

Both cropping systems and soybean genotypes had no significant effect on the alpha diversity of rhizobacterial communities (one-way ANOVA, $p > 0.05$; **Figures 1A,B**). Regarding beta diversity, CPCoA and two-way PERMANOVA revealed that cropping systems and soybean genotypes interactively affected the rhizobacterial communities (PERMANOVA, $p < 0.05$; **Figure 2; Supplementary Figure S2**; **Table 2**). In more detail, rhizobacterial community structures differed between tolerant and sensitive soybean genotypes irrespective of cropping systems (**Supplementary Figure S3**; **Table 2**).

Specific Microbiomes of Two Soybean Genotypes in Different Cropping Systems

Proteobacteria, Bacteroidetes, Firmicutes, Acidobacteria, Actinobacteria, and Verrucomicrobia were the most abundant bacterial phyla living in the rhizosphere across all treatments, accounting for 80.57–82.98% of the whole community (**Figure 3; Supplementary Table S1**). Analysis of the phylum abundance with two-way ANOVA (**Supplementary Table S1**) showed that 10, 7, and 10 phyla were significantly ($p < 0.05$) affected by cropping systems. In addition, they were significantly ($p < 0.05$) affected by cropping systems, soybean genotypes, and their interaction (**Supplementary Table S1**). Moreover, the response to continues cropping between the two genotypes was different. For instance, the relative abundances of Acidobacteria were significantly increased in the 7-year continuous cropping field but decreased relative abundances of both soybean genotypes in the 36-year continuous cropping field, and with a higher relative abundance for the sensitive genotypes than the tolerant genotypes. The relative abundances of Proteobacteria significantly decreased and then increased in these cropping systems for the tolerant genotypes, while it continuously decreased for the sensitive genotypes. At the genus level, 16, 20, and 22 genera were significantly ($p < 0.05$) affected by cropping systems, soybean genotypes, and their interaction, respectively (**Table 3**). Among them, some genera in different genotypes respond differently to continuous cropping. For example, *Pseudomonas*, which belong to Proteobacteria, in tolerant genotype rhizosphere increased and then decreased with continuous cropping time, while an opposite trend was observed in the sensitive genotypes. However, there are also some genera that respond to continuous cropping in a consistent trend between the two genotypes. For instance, *Streptomyces* and *Bacillus*, which belong to Actinobacteria and Firmicutes, respectively, decreased in the 7-year continuous cropping field but increased in the 36-year continuous cropping field, with higher relative abundances in the sensitive genotypes. A linear model analysis was used to identify bacterial OTUs significantly enriched in tolerant and sensitive genotypes of rhizosphere soil in the crop rotation system, 7-year continuous

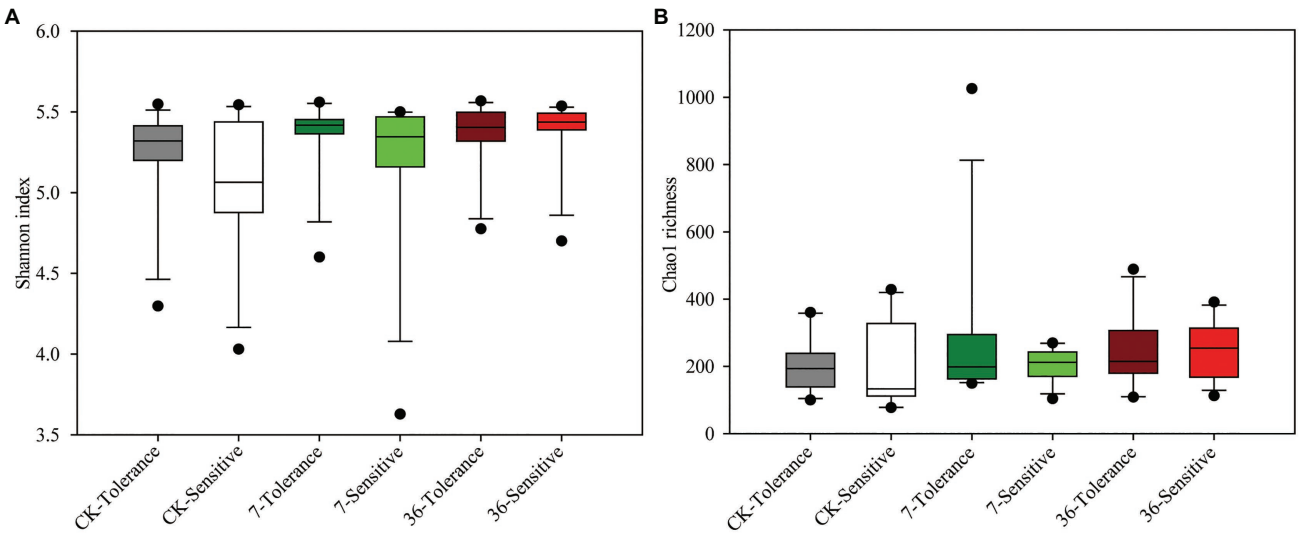

FIGURE 1 | Rhizobacterial community Shannon index **(A)** and Chao1 richness **(B)** of different treatments. One-way ANOVA, $n = 12$, $p < 0.05$.

TABLE 2 | Effects of cropping systems and soybean genotypes on the differentiation of bacterial communities based on PERMANOVA.

Factor	F	R^2	p
Cropping systems	4.3253	0.05819	0.001***
Genotype	2.3132	0.03199	0.024*
Cropping systems: Genotype	4.2608	0.05738	0.002**
36T vs. 36S	1.615	0.06839	0.058
7T vs. 7S	1.9649	0.08199	0.033*
CKT vs. CKS	2.1274	0.08817	0.025*

CKT: crop rotation-tolerance, CKS: crop rotation-sensitive, 7T: 7 year-continuous cropping-tolerant, 7S: 7 year-continuous cropping-sensitive, 36T: 36 year-continuous cropping-tolerant, 36S: 36 year-continuous cropping-sensitive.
$^{*}p<0.05$; $^{**}p<0.01$; $^{***}p<0.001$.

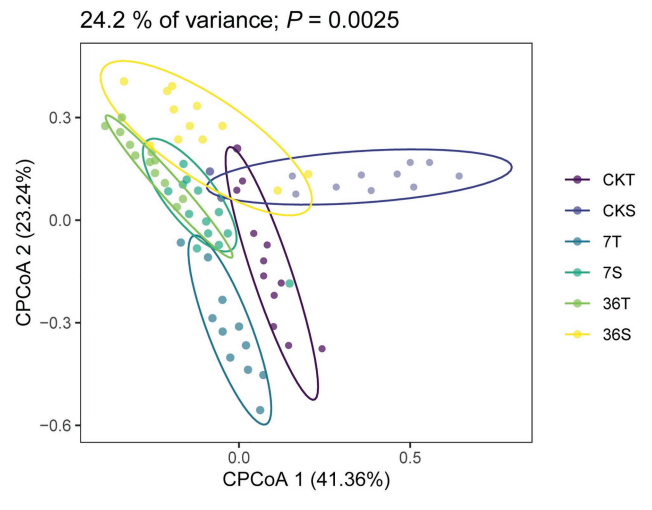

FIGURE 2 | Constrained Principal coordinate analysis (CPCoA) based on Bray-Curtis dissimilarities of 16S rRNA diversity in the rhizosphere.

cropping system and 36-year continuous cropping system. For the tolerant genotypes, OTUs belonging to *Chitinophaga*, *Nitrospira*, and *Saprospirales* dominated in the rhizospheres of the crop rotation system, 7-year continuous cropping system and 36-year continuous cropping system, respectively (**Figure 4A**). For the sensitive genotypes, OTUs belonging to *Phyllobacteriaceae*, *Comamonadaceae*, and *Cytophagaceae* dominated in the rhizospheres of the crop rotation system, 7-year continuous cropping system and 36-year continuous cropping system, respectively (**Figure 4B**). More detailed information is available in Supplemental files (**Supplementary Table S2**).

Correlations between rhizosphere soil microbiota with higher relative abundance and pH, soybean cyst nematode, and yield were obtained *via* Pearson's correlation analysis (**Supplementary Figure S4**). Soil pH was positively correlated with *Acinetobacter* and *Bradyrhizobium*, while it was negatively correlated with other genera. Cyst nematode was negatively correlated with *Thermomonas*, *Flavisolibacter*, and *Opitutus*, while it was positively correlated with Pseudomonas, *Renibacterium*, *Agrobacterium*, *Bacillus*, and Streptomyces. Moreover, the yield was positively correlated with *Sphingobium*, *Flavisolibacter*, and *Opitutus*.

Core Microbiome and Co-occurrence Network

Among the 12,436 OTUs, we found that tolerant and sensitive genotypes shared almost the same core microorganisms, such as OTU3795 (*Thermomonas*), OTU6911 (*norank_Sphingomonadaceae*), OTU8585 (*norank_Sphingomonadaceae*), OTU9044 (norank_*Erythrobacteraceae*), OTU9116 (*norank_Methylophilaceae*), OTU9219 (*Agrobacterium*), OTU4334 (*Nitrospira*), OTU6274 (*norank_Chitinophagaceae*), OTU6533 (*Flavisolibacter*), OTU10447 (*Renibacterium*), OTU4280

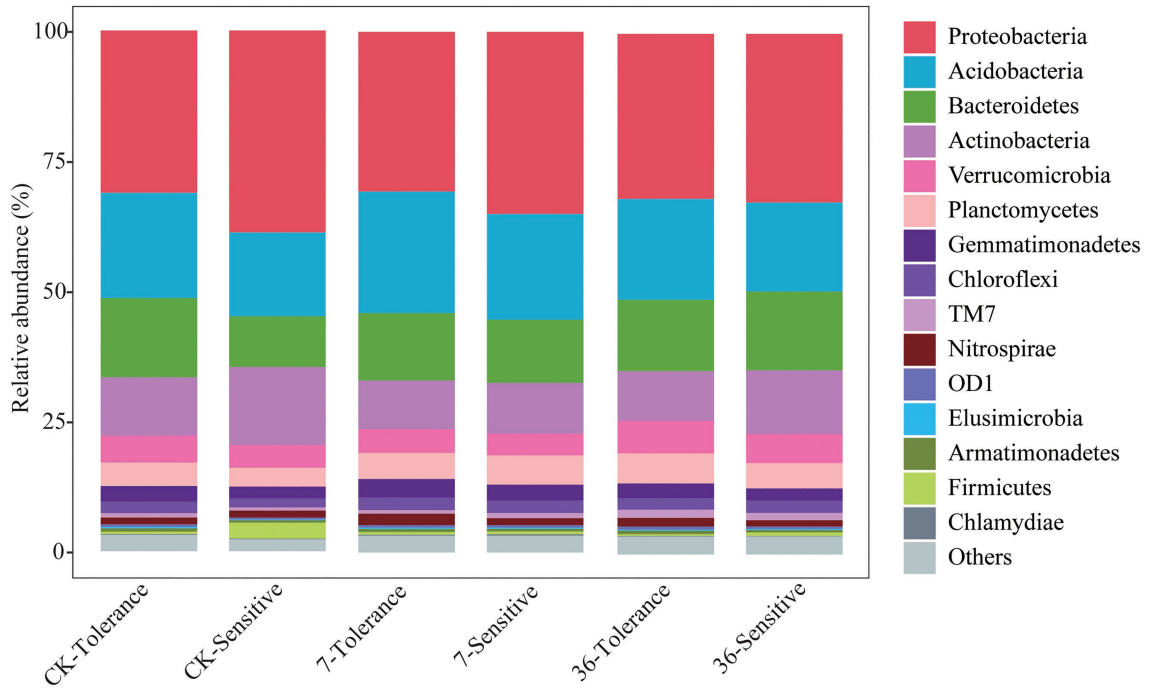

FIGURE 3 | Relative abundance of the phylum of different treatments.

(*norank_ii1-15*), OTU4827 (*norank_Ellin6075*), OTU8697 (*norank_RB41*), and OTU10068 (*norank_ii1-15*; **Figure 5**). Moreover, OTU7122 (*Pseudomonas*) was the core species specific to the sensitive genotypes (**Figure 5B**). The relative abundances of the total core OTUs of tolerant and sensitive Proteobacteria were 7.77% and 11.48, respectively (**Supplementary Table S3**).

Using the combined 16S rRNA data of the two soybean genotypes grown in different cropping systems, the co-occurrence network in the rhizosphere showed marked differences between the treatments (**Figure 6**; **Supplementary Table S4**). For the tolerant genotype, the number of negative correlations and modularity (M) increased with continuous cropping years, suggesting that there were more coupling, cooperation, and exchange events among the dominant bacterial genera. Moreover, there was no significant change in the average clustering coefficient (avgCC) or average degree (avgK). For the sensitive genotype, the modularity (M) increased with continuous cropping years. However, the number of negative correlations, average clustering coefficient (avgCC), and average degree (avgK) increased in the 7-year continuous cropping systems field but decreased in the 36-year continuous cropping systems field. The keystone species of the bacterial network in the rhizosphere were identified by calculating node degree, closeness centrality, and betweenness centrality for all nodes in the network (**Supplementary Table S5**). In general, OTU11321 (*Luteolibacter*), OTU6533 (*Flavisolibacter*), OTU1003 (*Chitinophagaceae*), OTU4362 (*norank_RB41*), OTU881 (*Balneimonas*), and OTU3461 (*norank_Ellin6075*) were identified as keystone species for the two genotypes grown in the different cropping systems. Using NetShift analysis, the common sub-network plot showed the "driver microbes" were OTU2820 (*Unclassified Chitinophagaceae*), OTU881 (*Unclassified oc28*), and OTU3463 (*Unclassified Acidobacteria-6*) for the network between rotations and 7 years continuous cropping system, and OTU881 (*Unclassified oc28*), OTU3487 (*Unclassified Gemm-1*), OTU9219 (*Agrobacterium*), and OTU3461 (*Unclassified Ellin6075*) for the network between rotations and 7 years continuous cropping system. For the sensitive soybean genotype, the "drivers microbes" were OTU2166 (*Unclassified Piscirickettsiaceae*) and OTU9044 (*Unclassified Erythrobacteraceae*) for the network between rotations and 7 years continuous cropping system, and OTU4813 (*Unclassified Saprospiraceae*), OTU3714 (*Unclassified Oxalobacteraceae*), OTU4607 (*Unclassified Cytophagaceae*), OTU3463 (*Unclassified Acidobacteria-6*), and OTU3416 (*Unclassified OPB35*) for the network between rotations and 7 years continuous cropping system (**Figure 7**).

DISCUSSION

Our initial hypotheses were that soybean with a tolerant genotype would have higher rhizosphere bacterial diversity than soybean with a sensitive genotype, and tolerant soybean would recruit microorganisms that benefited continuous cropping tolerance. Our results showed that there was no significant difference in microbial diversity between the two genotypes soybean in all cropping systems. In addition, our second hypothesis was tested: tolerant genotypes recruited specific microorganisms that may help soybean mitigate soil-borne diseases. Short period of continuous cropping is unfavorable for soybean, but long periods of continuous cropping will mitigate this unfavorability.

TABLE 3 | Cropping systems, soybean genotypes, and their interactive effects on the relative abundance of bacteria at genus level.

		Read numbers in each genus						ANOVA (*p*-values)			
Phylum	**Genus**	**CKT**	**CKS**	**7T**	**7S**	**36T**	**36S**	**Year**	**Genotype**	**Year*Genotype**	**LSD**
Bacteroidetes	Chryseobacterium	3.29 ± 7.93	0.03 ± 0.03	0.02 ± 0.01	0.03 ± 0.04	0.81 ± 2.05	0.02 ± 0.02	0.231	0.097	0.118	2.727
Proteobacteria	Acinetobacter	3.78 ± 5.14	3.87 ± 6.67	2.24 ± 6.4	6.45 ± 11.2	3.97 ± 5.4	2.13 ± 5.11	0.811	0.619	0.699	5.692
Proteobacteria	Pseudomonas	0.8 ± 0.55	7.08 ± 6.62	1 ± 0.5	0.8 ± 0.43	0.44 ± 0.41	1.5 ± 1.64	**0.003****	**0.004****	**<0.001*****	2.291
Actinobacteria	Arthrobacter	2.45 ± 0.9	2.23 ± 1.71	1.67 ± 0.9	2.32 ± 0.84	0.71 ± 0.39	2.61 ± 2.93	0.345	**0.04***	**0.034***	1.245
Actinobacteria	Renibacterium	2.71 ± 1.16	5.38 ± 5.23	2.59 ± 1.37	2.7 ± 1.14	1.93 ± 1.83	3.48 ± 2.77	0.148	**0.028***	**0.043***	2.179
Proteobacteria	Agrobacterium	1.13 ± 0.37	2.44 ± 1.54	0.87 ± 0.3	1.15 ± 0.33	1.22 ± 0.98	1.82 ± 1.34	**0.035***	**0.003****	**0.001****	0.778
Actinobacteria	Aeromicrobium	0.33 ± 0.13	0.26 ± 0.18	0.22 ± 0.06	0.28 ± 0.15	0.78 ± 1.03	0.66 ± 0.35	**<0.001*****	0.753	**0.012****	0.3746
Firmicutes	Bacillus	0.27 ± 0.15	2.63 ± 2.58	0.18 ± 0.07	0.31 ± 0.32	0.18 ± 0.12	0.33 ± 0.38	**0.001*****	**0.006****	**<0.001*****	0.876
Actinobacteria	Streptomyces	0.35 ± 0.18	2.15 ± 2.7	0.14 ± 0.06	0.14 ± 0.04	0.34 ± 0.19	0.4 ± 0.2	**0.006****	**0.039***	**<0.001*****	0.905
Proteobacteria	Thermomonas	1.05 ± 0.23	0.99 ± 0.59	1.27 ± 0.23	1.07 ± 0.34	0.75 ± 0.16	1.1 ± 0.41	0.071	0.733	**0.026***	0.2884
Proteobacteria	Sphingobium	0.04 ± 0.02	0.03 ± 0.03	0.02 ± 0.01	0.01 ± 0.01	0.06 ± 0.05	0.53 ± 1.1	0.074	0.174	**0.042***	0.3666
Bacteroidetes	Flavisolibacter	1.14 ± 0.41	0.85 ± 0.41	1.52 ± 0.86	1.03 ± 0.17	1.31 ± 0.32	1.2 ± 0.36	0.102	**0.011***	**0.022***	0.3866
Verrucomicrobia	Opitutus	0.59 ± 0.28	0.44 ± 0.1	0.53 ± 0.22	0.49 ± 0.16	0.8 ± 0.49	0.67 ± 0.41	**0.017***	0.161	0.062	0.2521
Proteobacteria	Bradyrhizobium	0.47 ± 0.24	0.68 ± 0.25	0.31 ± 0.17	0.62 ± 0.51	0.49 ± 0.2	0.4 ± 0.26	0.302	**0.045***	**0.034***	0.2393
Verrucomicrobia	DA101	0.31 ± 0.21	0.45 ± 0.36	0.28 ± 0.19	0.13 ± 0.05	0.51 ± 0.26	0.17 ± 0.09	**0.045***	**0.05***	**<0.001*****	0.18
Nitrospirae	Nitrospira	0.57 ± 0.36	0.75 ± 0.28	1.23 ± 0.68	0.64 ± 0.34	0.96 ± 0.22	0.62 ± 0.36	0.112	**0.017**	**<0.001*****	0.328
Bacteroidetes	Adhaeribacter	0.65 ± 0.29	0.42 ± 0.3	0.76 ± 0.48	0.79 ± 0.32	0.62 ± 0.33	0.7 ± 0.28	0.057	0.633	0.121	0.2773
Proteobacteria	Azohydromonas	0.53 ± 0.17	0.57 ± 0.23	0.71 ± 0.25	0.71 ± 0.18	0.69 ± 0.22	0.67 ± 0.41	0.064	0.98	0.351	0.2074
Proteobacteria	Polaromonas	0.58 ± 0.37	1.28 ± 0.75	0.38 ± 0.18	0.54 ± 0.29	0.44 ± 0.18	0.57 ± 0.34	**<0.001*****	**0.004****	**<0.001*****	0.3264
Actinobacteria	Rubrobacter	0.69 ± 0.26	0.58 ± 0.17	0.73 ± 0.22	0.64 ± 0.23	0.57 ± 0.18	0.4 ± 0.17	**0.005****	**0.018***	**0.004****	0.1701
Proteobacteria	Steroidobacter	0.57 ± 0.17	0.52 ± 0.12	0.55 ± 0.07	0.62 ± 0.18	0.7 ± 0.15	0.63 ± 0.26	0.065	0.664	0.169	0.1378
Bacteroidetes	Flavobacterium	0.29 ± 0.2	0.44 ± 0.6	0.37 ± 0.17	0.56 ± 0.49	0.83 ± 0.89	0.74 ± 0.32	**0.014***	0.518	0.078	0.4155
Proteobacteria	Balneimonas	0.4 ± 0.1	0.46 ± 0.12	0.45 ± 0.2	0.45 ± 0.08	0.38 ± 0.17	0.34 ± 0.22	0.129	0.834	0.391	0.129
Verrucomicrobia	Luteolibacter	0.26 ± 0.12	0.47 ± 0.18	0.26 ± 0.17	0.3 ± 0.09	0.29 ± 0.3	0.47 ± 0.47	0.361	**0.025***	0.128	0.2088
Planctomycetes	Planctomyces	0.34 ± 0.09	0.22 ± 0.1	0.31 ± 0.06	0.36 ± 0.1	0.36 ± 0.2	0.34 ± 0.15	0.175	0.309	0.071	0.1025
Proteobacteria	Pseudoxanthomonas	0.13 ± 0.07	0.09 ± 0.15	0.12 ± 0.09	0.5 ± 0.44	0.64 ± 0.35	0.44 ± 0.3	**<0.001*****	0.57	**<0.001*****	0.2208
Bacteroidetes	Niastella	0.26 ± 0.12	0.37 ± 0.14	0.26 ± 0.11	0.24 ± 0.06	0.25 ± 0.11	0.37 ± 0.14	0.137	**0.013***	**0.009***	0.0944
Bacteroidetes	Dyadobacter	0.2 ± 0.08	0.32 ± 0.19	0.24 ± 0.23	0.3 ± 0.16	0.2 ± 0.08	0.42 ± 0.31	0.691	**0.005***	0.051	0.1583
Bacteroidetes	Pontibacter	0.26 ± 0.11	0.2 ± 0.16	0.26 ± 0.1	0.21 ± 0.07	0.16 ± 0.04	0.31 ± 0.5	0.992	0.839	0.672	0.1837
Proteobacteria	Variovorax	0.23 ± 0.11	0.3 ± 0.16	0.16 ± 0.06	0.19 ± 0.07	0.15 ± 0.05	0.35 ± 0.49	0.364	0.062	0.186	0.1788
Verrucomicrobia	Chthoniobacter	0.2 ± 0.11	0.12 ± 0.06	0.19 ± 0.1	0.23 ± 0.1	0.28 ± 0.16	0.28 ± 0.21	**0.009****	0.685	**0.031***	0.1072
Armatimonadetes	Fimbriimonas	0.21 ± 0.11	0.15 ± 0.08	0.18 ± 0.05	0.17 ± 0.05	0.22 ± 0.1	0.15 ± 0.09	0.957	**0.025***	0.281	0.06785
Bacteroidetes	Pedobacter	0.14 ± 0.15	0.13 ± 0.09	0.15 ± 0.13	0.16 ± 0.11	0.18 ± 0.14	0.27 ± 0.18	0.063	0.357	0.156	0.1117
Bacteroidetes	Chitinophaga	0.16 ± 0.16	0.41 ± 0.41	0.05 ± 0.03	0.05 ± 0.02	0.08 ± 0.04	0.25 ± 0.16	**<0.001*****	**0.008***	**<0.001*****	0.157
Proteobacteria	Nitrosovibrio	0.13 ± 0.11	0.15 ± 0.16	0.19 ± 0.1	0.3 ± 0.38	0.08 ± 0.13	0.12 ± 0.11	**0.028***	0.246	0.104	0.1569
Bacteroidetes	Segetibacter	0.14 ± 0.06	0.11 ± 0.12	0.17 ± 0.16	0.14 ± 0.06	0.23 ± 0.09	0.17 ± 0.09	0.041	0.116	0.095	0.0853
Proteobacteria	Afifella	0.14 ± 0.04	0.12 ± 0.06	0.14 ± 0.03	0.12 ± 0.04	0.15 ± 0.06	0.27 ± 0.51	0.313	0.593	0.536	0.1733
Proteobacteria	Aquicella	0.16 ± 0.07	0.11 ± 0.04	0.17 ± 0.07	0.12 ± 0.04	0.14 ± 0.06	0.17 ± 0.1	0.698	0.116	0.113	0.05423
Proteobacteria	Pedomicrobium	0.15 ± 0.04	0.13 ± 0.05	0.13 ± 0.04	0.12 ± 0.04	0.16 ± 0.04	0.13 ± 0.05	0.271	**0.038***	0.212	0.03692
Actinobacteria	Phycicoccus	0.15 ± 0.05	0.28 ± 0.18	0.08 ± 0.02	0.08 ± 0.03	0.09 ± 0.03	0.11 ± 0.06	**<0.001*****	**0.046***	**<0.001*****	0.06679
Planctomycetes	Gemmata	0.15 ± 0.07	0.12 ± 0.11	0.1 ± 0.05	0.15 ± 0.07	0.17 ± 0.15	0.11 ± 0.07	0.79	0.659	0.368	0.0759
Firmicutes	Paenibacillus	0.06 ± 0.03	0.27 ± 0.18	0.06 ± 0.03	0.12 ± 0.11	0.04 ± 0.01	0.14 ± 0.25	0.15	**<0.001*****	**0.001**	0.1105
Actinobacteria	Kribbella	0.1 ± 0.05	0.22 ± 0.17	0.04 ± 0.02	0.05 ± 0.03	0.12 ± 0.08	0.12 ± 0.05	**<0.001*****	0.082	**<0.001*****	0.0692
Bacteroidetes	Lacibacter	0.1 ± 0.03	0.1 ± 0.08	0.1 ± 0.08	0.1 ± 0.05	0.1 ± 0.05	0.11 ± 0.06	0.959	0.693	0.995	0.0503

CKT: crop rotation-tolerance, CKS: crop rotation-sensitive, 7T: 7 year-continuous cropping-tolerant, 7S: 7 year-continuous cropping-sensitive, 36T: 36 year-continuous cropping-tolerant, 36S: 36 year-continuous cropping-sensitive. P-values less than 0.05 were indicated in bold letters.

$^{*}p < 0.05$; $^{**}p < 0.01$; $^{***}p < 0.001$.

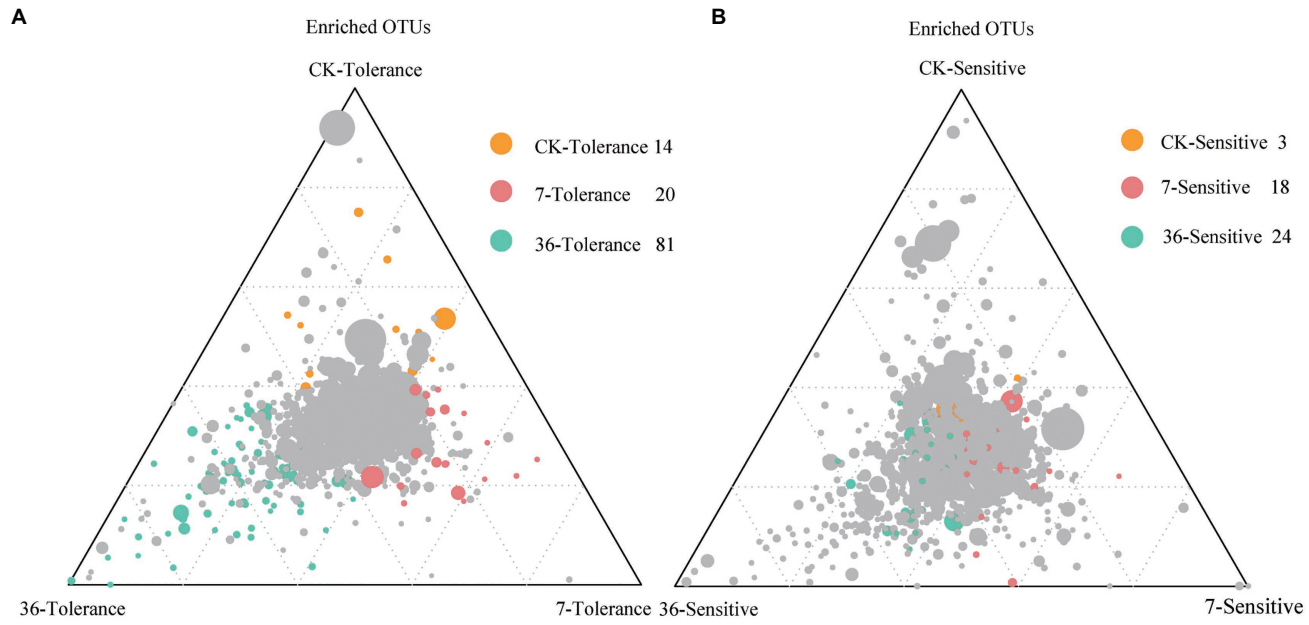

FIGURE 4 | Ternary plots depicting compartments showing the distributions of community differentiation among different cropping systems of tolerant **(A)** and sensitive **(B)** genotypes. The position of each circle depends on its contribution to the total relative abundance. Colored circles represent OTUs that enriched in different cropping systems, which the green for the rotation cropping system; red and green for 7- and 36-year continuous cropping systems, respectively. The gray circles represent the OTUs that are not significantly enriched within a given range.

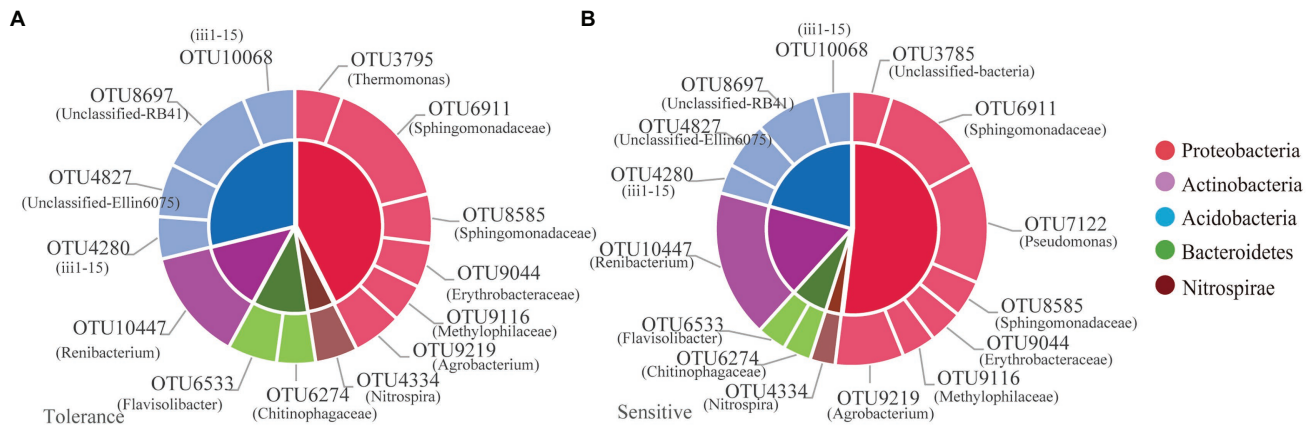

FIGURE 5 | The relative abundance of the core microbiome for tolerant **(A)** and sensitive **(B)** genotypes.

Moreover, different genotypes of soybean respond differently to continuous cropping systems, and microorganisms recruited by tolerant soybeans might play an important role in mitigating the adverse effects of continuous cropping.

In the present study, we found that there was no significant difference in bacterial community diversity among the treatments. Previous studies have shown that an increase in crop type could lead to an increase in soil microbial diversity. Liu et al. (2020) found that rhizosphere bacterial diversity was reduced with continuous cropping of soybean compared to soybean-corn rotation cropping systems. In addition, Zhu et al. (2017) and Liu et al. (2020) found that soil bacterial diversity increased with increasing years of continuous cropping. However, Li et al. (2010) found no significant difference in soil microbial diversity between the soil of continuous soybean and soybean-corn rotations. This might be attributed to the different soil pH in these studies, as Liu et al. conducted their research on acidic soil, while our study was conducted on neutral soil. Changes in soil pH and other physical and chemical properties were significantly associated with microbial diversity, and this variation was related to changes in root secretions, such as organic acids, phenols, and flavonoids, which were significantly affected by the cropping systems (Venter et al., 2016; Liu et al., 2020). For beta diversity, we found that cropping systems and soybean

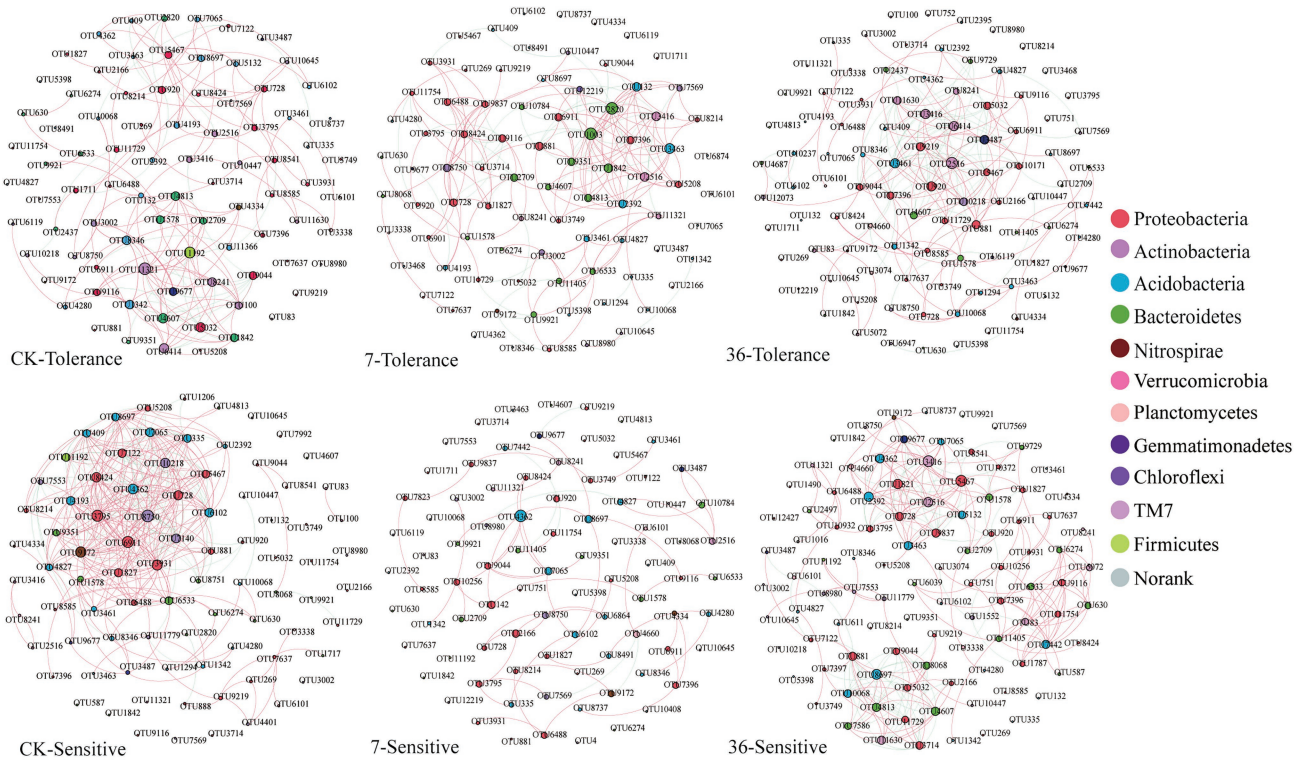

FIGURE 6 | Network analysis of the rhizosphere bacterial community from different treatments. Nodes represent OTUs coded by phyla and are scaled by the number of connections (node degree). Connections are plotted at $r > 0.8$ (positive correlation, red) or $r < -0.8$ (negative correlation, blue) and $p < 0.05$.

genotypes were the main factors that changed the bacterial communities (Adonis tests, $p < 0.05$). This result is consistent with the results reported by Zhu et al. (2017) and Lian et al. (2019), who indicated that there were significant changes in soil bacterial communities in long-term and short-term continuous soybean cropping systems and in different soybean genotypes.

The relative abundance of Proteobacteria was significantly decreased in the rhizospheric soils of the continuous cropping system field compared to those of the rotation system, indicating that those bacteria were decreased with low available nutrients (Fierer et al., 2007; Li et al., 2014). The relative abundances of *Pseudomonas*, *Streptomyces*, and *Bacillus* decreased in the 7-year continuous cropping field but increased in the 36-year continuous cropping field, with a higher relative abundance in the sensitive genotypes. *Pseudomonas* can improve the solubilization of fixed soil phosphorus and applied phosphates, resulting in higher crop yields (Nautiyal, 1999). Moreover, the metabolites of *Pseudomonas* could increase amino acid secretion in alfalfa, maize, and wheat roots (Phillips et al., 2004). *Streptomyces* can help plants resist diseases such as wilt and root rot (Lian et al., 2019; Shi et al., 2020). In addition, some bacteria, such as *Thermomonas*, *Flavisolibacter*, and *Opitutus* were negatively associated with nematodes, which suggested that these bacteria might inhibit the soybean cyst nematode. Thus, based on the functions of the species mentioned above, we speculated that the changed relative abundances of these bacteria might be associated with the antagonistic activity of these taxa against plant pathogens and the improvement of soil nutrients.

We used differential OTU abundance analysis in the treatments and observed a high relative abundance of the OTUs enriched in continuous cropping systems of the tolerant genotypes that belonged to *Chitinophagaceae*, *Pseudoxanthomonas*, *Nitrospira*, and Streptomyces (**Figure 4**; **Table 3**). This finding is consistent with our hypothesis that tolerant genotypes recruited some microorganisms that play an important role in the resistance of soybeans to long-term continuous cropping. OTU4434 (*Nitrospira*), OTU751 (*Pseudoxanthomonas*), and OTU10218 (*Streptomyces*) showed higher relative abundances in the continuous cropping system than in the rotation cropping system in the present study (**Figure 4**; **Table 3**). Many studies have reported that *Nitrospira* can promote the nitrogen cycle and increase the absorption and utilization of nitrogen by plants (Zeng et al., 2014). Therefore, the higher abundances of these bacteria may improve soybean tolerance in the rhizosphere. However, the response of these genera to long-term continuous cropping warrants further investigation of their functional significance in response to different long-term continuous cropping systems.

An association network analysis was performed to gain a more integrated understanding of the bacterial community composition and compare the complexities of the networks operating in the rhizosphere soils of continuous cropping-tolerant and continuous

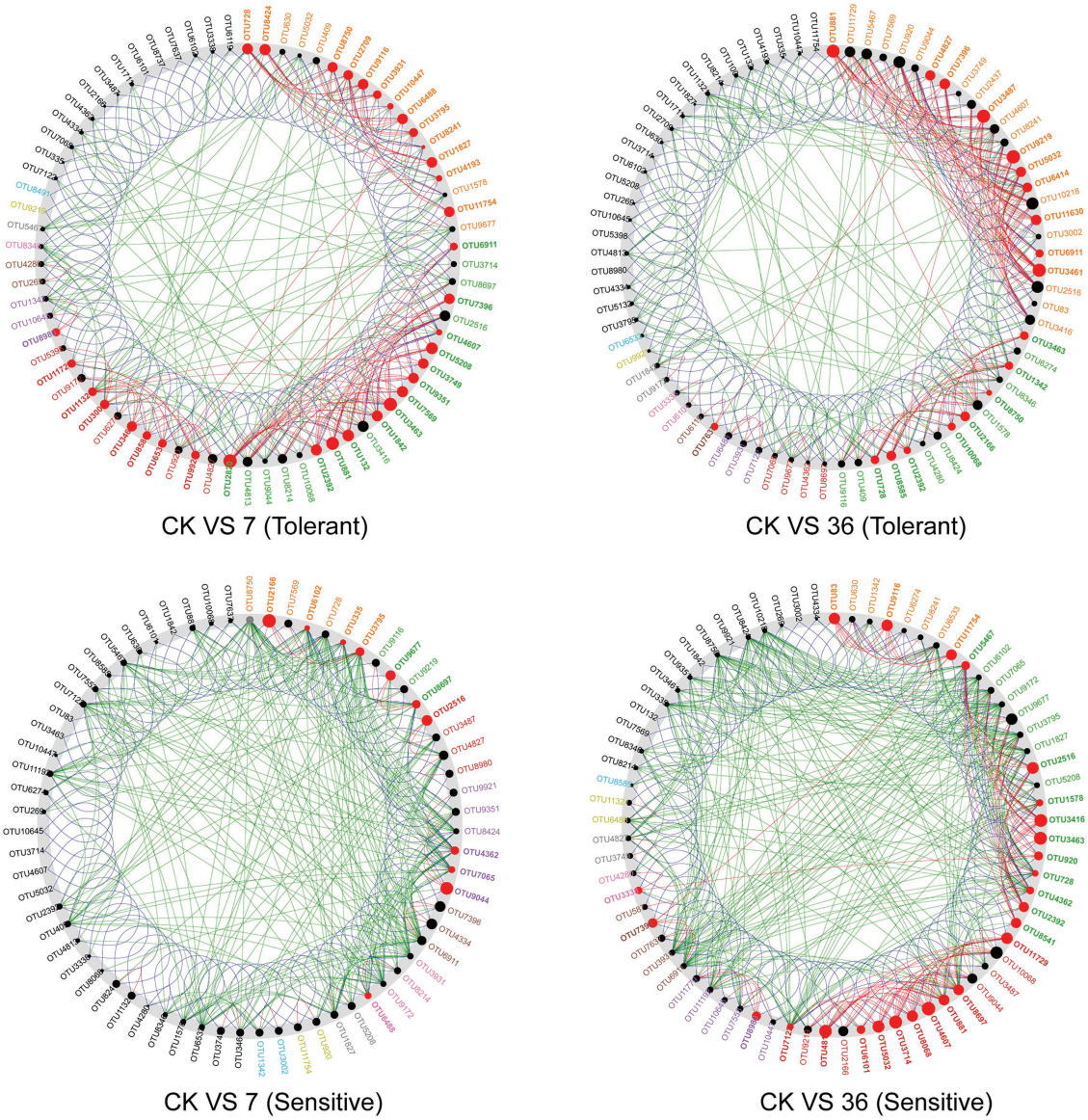

FIGURE 7 | A common sub-network view with the "driver" node highlighted. All nodes belonging to the same community have been randomly assigned a similar color. Gray OTU nodes represent nodes that are present in both cases, but interact directly with the common subnetwork in either the case or control group. The size of the nodes was proportional to their NESH scores, and a node was colored red if its spacing between the control and study groups increased. Large and red nodes are particularly important "drivers." CK VS 7 (36; tolerant or sensitive), network comparison between soybean-corn rotations and 7 (36) years continuous cropping for tolerant or sensitive genotype.

cropping-sensitive soybean genotypes (Jiang et al., 2017). The networks of the two genotypes responded differently to continuous cropping. The modularity and negative correlations in the network of the tolerant genotype responded positively to continuous cropping, suggesting that there were more coupling, cooperation, and exchange events among the dominant bacterial genera (Coyte et al., 2015). For the sensitive genotype, the negative correlations and average degree (avgK) increased in the 7-year continuous cropping system field but decreased in the 36-year continuous cropping system field, suggesting that the instability of the sensitive genotype and short periods of continuous planting can have a detrimental effect on microbial community stability, but this effect could be alleviated with increasing periods of continuous planting. This result was consistent with a previous study, which found that a long-term continuous cropping system has similar microbial interactions to those of a healthy crop rotation system (Liu et al., 2020). Additionally, the important microbial taxa in the networks which serve as "drivers" from the rotations to short or long continue cropping were different between the two soybean genotypes, which indicated that the response of rhizosphere microbial community under different soybean genotypes to short- and long-term continuous cropping was different.

In summary, short- or long-term continuous cropping had no significant effect on the rhizosphere soil bacterial alpha diversity. Short-term continuous planting increased the number of soybean cyst nematodes, while long-term continuous planting reduced these numbers, and tolerant genotypes had lower soybean cyst nematodes than sensitive genotypes. In addition, continuous cropping significantly increased potentially beneficial bacterial populations compared to rotation and short-term continuous cropping, suggesting that long-term continuous cropping of soybean shifts the microbial community into that of a healthy crop rotation system. Soybean genotypes that are tolerant might recruit some microorganisms that play an important role in the resistance of soybeans to long-term continuous cropping. However, further experiment with species isolation and verification is needed to confirm these findings. Moreover, the networks of the two genotypes responded differently to continuous cropping. The tolerant genotype responded positively to continuous cropping, while for the sensitive genotype, topology suggested that the instability of the sensitive genotype and short periods of continuous planting can have a detrimental effect, but this effect could be alleviated with increasing periods of continuous planting.

DATA AVAILABILITY STATEMENT

The datasets presented in this study can be found in online repositories. The names of the repository/repositories and accession number(s) can be found in the article/**Supplementary Material**.

AUTHOR CONTRIBUTIONS

TL, HN, and MY designed the research. MY, KY, LW, DH, and SW performed the research. TY, QS, HX, and RW analyzed the data. MY and TL analyzed the data and wrote the manuscript. All authors contributed to the article and approved the submitted version.

FUNDING

This work was supported by China Agriculture Research System of MOF and MARA (CARS-04), and the Laboratory independent research projects (SKLCUSA-a201913).

ACKNOWLEDGMENTS

We would like to thank Chai Xiaocui and Qiao Zhixian at the Analysis and Testing Center of Institute of Hydrobiology, Chinese Academy of Sciences for their assistance with PCR amplification, sequencing, and data analysis.

SUPPLEMENTARY MATERIAL

The Supplementary Material for this article can be found online at: https://www.frontiersin.org/articles/10.3389/fmicb.2021.729047/full#supplementary-material

REFERENCES

Agler, M. T., Ruhe, J., Kroll, S., Morhenn, C., Kim, S. T., Weigel, D., et al. (2016). Microbial hub taxa link host and abiotic factors to plant microbiome variation. *PLoS Biol.* 14:e1002352. doi: 10.1371/journal.pbio.1002352

Avidano, L., Gamalero, E., Cossa, G. P., and Carraro, E. (2005). Characterization of soil health in an Italian polluted site by using microorganisms as bioindicators. *Appl. Soil Ecol.* 30, 21–33. doi: 10.1016/j.apsoil.2005.01.003

Bai, L., Cui, J. Q., Jie, W. G., and Cai, B. Y. (2015). Analysis of the community compositions of rhizosphere fungi in soybeans continuous cropping fields. *Microbiol. Res.* 180, 49–56. doi: 10.1016/j.micres.2015.07.007

Berry, D., and Widder, S. (2014). Deciphering microbial interactions and detecting keystone species with co-occurrence networks. *Front. Microbiol.* 5:219. doi: 10.3389/fmicb.2014.00219

Cai, B. Y., Wang, L. Y., Hu, W., Jie, W. G., and Ling, H. Z. (2015). Analysis of community structure of root rot pathogenic fungi in seedling stage of soybean continuous cropping. *Chin. Agr. Sci. Bull.* 31, 92–98.

Chigen, T., Muhammad, A. N., Ayaka, K., Bao, L., Jeong, D. L., Eunho, S., et al. (2018). Isoflavone profile diversity in Korean wild soybeans (Glycine soja Sieb. & Zucc.). *Turk. J. Agric. For.* 42, 248–261. doi: 10.3906/tar-1709-119

Chong, J., Liu, P., Zhou, G., and Xia, J. (2020). Using MicrobiomeAnalyst for comprehensive statistical, functional, and meta-analysis of microbiome data. *Nat. Protoc.* 5, 799–821. doi: 10.1038/s41596-019-0264-1

Cole, J. R., Wang, Q., Cardenas, E., Fish, J., Chai, B., Farris, R. J., et al. (2009). The ribosomal database project: improved alignments and new tools for rRNA analysis. *Nucleic Acids Res.* 37, 141–145. doi: 10.1093/nar/gkn879

Coyte, K. Z., Schluter, J., and Foster, K. R. (2015). The ecology of the microbiome: networks, competition, and stability. *Science* 350, 663–666. doi: 10.1126/science.aad2602

Dias, T., Dukes, A., and Antunes, P. M. (2015). Accounting for soil biotic effects on soil health and crop productivity in the design of crop rotations. *J. Sci. Food Agric.* 95, 447–454. doi: 10.1002/jsfa.6565

Edgar, R. C., Haas, B. J., Clemente, J. C., Quince, C., and Knight, R. (2011). UCHIME improves sensitivity and speed of chimera detection. *Bioinformatics* 27, 2194–2200. doi: 10.1093/bioinformatics/btr381

Fierer, N., Bradford, M. A., and Jackson, R. B. (2007). Toward an ecological classification of soil bacteria. *Ecology* 88, 1354–1364. doi: 10.1890/05-1839

Friendly, M., and Meyer, D. (2015). *Discrete Data Analysis With R: Visualization and Modeling Techniques for Categorical and Count Data*. Boca Raton: CRC Press, 63–108.

Hu, J. C., and Wang, S. J. (1996). Study on soil sickness by soybean continuous cropping I. Effect of mycotoxin produced by *Penicillium purpurogenum*. *Chin. J. Appl. Ecol.* 7, 396–400.

Ji, S. N., Xiao, Y. Z., Tian, H. M., and Zhao, F. H. (1996). Effects of sterilized soil from soybean and corn stubble field on the growth development of soybean. *J. Northeast. Agr.* 27, 326–329.

Jiang, Y., Li, S., Li, R., Zhang, J., Liu, Y., Lv, L., et al. (2017). Plant cultivars imprint the rhizosphere bacterial community composition and association networks. *Soil Biol. Biochem.* 109, 145–155. doi: 10.1016/j.soilbio.2017.02.010

Kaisermann, A., Vries, F. T., Grifths, R. I., and Bardget, R. D. (2017). Legacy effects of drought on plant-soil feedbacks and plant-plant interactions. *New Phytol.* 215, 1413–1424. doi: 10.1111/nph.14661

Kuntal, B. K., Chandrakar, P., Sadhu, S., and Mande, S. S. (2019). 'NetShift:' a methodology for understanding 'driver microbes' from healthy and disease microbiome datasets. *ISME J.* 13, 442–454. doi: 10.1038/s41396-018-0291-x

Kwak, M. J., Kong, H. G., Choi, K., Kwon, S., Song, J. Y., Lee, J., et al. (2018). Rhizosphere microbiome structure alters to enable wilt resistance in tomato. *Nat. Biotechnol.* 36, 1100–1109. doi: 10.1038/nbt.4232

Lebeis, S. L., Paredes, S. H., Lundberg, D. S., Breakfield, N., Gehring, J., McDonald, M., et al. (2015). Salicylic acid modulates colonization of the root microbiome by specific bacterial taxa. *Science* 349, 860–864. doi: 10.1126/science.aaa8764

Li, W., and Godzik, A. (2015). Cd-hit: a fast program for clustering and comparing large sets of protein or nucleotide sequences. *Bioinformatics* 22, 1658–1659. doi: 10.1007/978-1-4899-7478-5_221

Li, C. G., Li, X. M., Kong, W. D., Wu, Y., and Wang, J. G. (2010). Effect of monoculture soybean on soil microbial community in the Northeast China. *Plant Soil* 330, 423–433. doi: 10.1007/s11104-009-0216-6

Li, X. Z., Rui, J. P., Mao, Y. J., Yannarell, A., and Mackie, R. (2014). Dynamics of the bacterial community structure in the rhizosphere of a maize cultivar. *Soil Biol. Biochem.* 68, 392–401. doi: 10.1016/j.soilbio.2013.10.017

Lian, T. X., Ma, Q. B., Shi, Q. H., Cai, Z. D., Zhang, Y. F., Cheng, Y. B., et al. (2019). High aluminum stress drives different rhizosphere soil enzyme activities and bacterial community structure between aluminum-tolerant and aluminum-sensitive soybean genotypes. *Plant Soil* 440, 409–425. doi: 10.1007/s11104-019-04089-8

Liu, X. B., Burras, C. L., Kravchenko, Y. S., Duran, A., Huffman, T., Morras, H., et al. (2012). Overview of Mollisols in the world:distribution, land use and management. *Can. J. Soil Sci.* 92, 383–402. doi: 10.4141/cjss2010-058

Liu, Z. X., Liu, J. J., Yua, Z. H., Yao, Q., Li, Y. S., Liang, A. Z., et al. (2020). Long-term continuous cropping of soybean is comparable to crop rotation in mediating microbial abundance, diversity and community composition. *Soil Tillage Res.* 197:104503. doi: 10.1016/j.still.2019.104503

Liu, H., Pan, F. J., Han, X. Z., Song, F. B., Zhang, Z. M., Yan, J., et al. (2019). Response of soil fungal community structure to long-term continuous soybean cropping. *Front. Microbiol.* 9:3316. doi: 10.3389/fmicb.2018.03316

Mendes, L. W., Mendes, R., Raaijmakers, J. M., and Tsai, S. M. (2018). Breeding for soil-borne pathogen resistance impacts active rhizosphere microbiome of common bean. *ISME J.* 12, 3038–3042. doi: 10.1038/s41396-018-0234-6

Meriles, J. M., Gil, S. V., Conforto, C., Figoni, G., Lovera, E., March, G. J., et al. (2009). Soil microbial communities under different soybean cropping systems: characterization of microbial population dynamics, soil microbial activity, microbial biomass, and fatty acid profiles. *Soil Tillage Res.* 103, 271–281. doi: 10.1016/j.still.2008.10.008

Nautiyal, C. S. (1999). An efficient microbiological growth medium for screening phosphate solubilizing microorganisms. *FEMS Microbiol. Lett.* 170, 265–270. doi: 10.1111/j.1574-6968.1999.tb13383.x

Pérez-Brandán, C., Huidobro, J., Grümberg, B., Scandiani, M. M., Luque, A. G., Meriles, J. M., et al. (2014). Soybean fungal soil-borne diseases: a parameter for measuring the effect of agricultural intensification on soil health. *Can. J. Microbiol.* 60, 73–84. doi: 10.1139/cjm-2013-0792

Phillips, D., Fox, T. C., King, M., Bhuvaneswari, T. V., and Teuber, L. R. (2004). Microbial products trigger amino acid exudation from plant roots. *Plant Physiol.* 136, 2887–2894. doi: 10.1104/pp.104.044222

Shi, Q. H., Liu, Y. T., Shi, A. Q., Cai, Z. D., Nian, H., Hartmann, M., et al. (2020). Rhizosphere soil fungal communities of aluminum-tolerant and -sensitive soybean genotypesrespond differently to aluminum stress in an acid soil. *Front. Microbiol.* 11:1177. doi: 10.3389/fmicb.2020.01177

Song, J., Li, S. X., Wei, W., Xu, Y. L., and Yao, Q. (2017). Assessment of parasitic fungi for reducing soybean cyst nematode with suppressive soil in soybean fields of Northeast China. *Acta Agr. Scand. B Soil Plant* 67, 730–736. doi: 10.1080/09064710.2017.1343377

Tang, H., Xiao, C. H., Ma, J. Z., Yu, M., Li, Y. M., Wang, G. L., et al. (2009). Prokaryotic diversity in continuous cropping and rotational cropping soybean soil. *FEMS Microbiol. Lett.* 298, 267–273. doi: 10.1111/j.1574-6968.2009.01730.x

Venter, Z. S., Jacobs, K., and Hawkins, H. J. (2016). The impact of crop rotation on soil microbial diversity: a meta-analysis. *Pedobiologia* 59, 215–223. doi: 10.1016/j.pedobi.2016.04.001

Waldrop, M. P., Balser, T. C., and Firestone, M. K. (2000). Linking microbial community composition to function in a tropical soil. *Soil Biol. Biochem.* 32, 1837–1846. doi: 10.1016/S0038-0717(00)00157-7

Wei, W., Xu, Y. L., Li, S. X., Zhu, L., and Song, J. (2015). Developing suppressive soil for root diseases of soybean with continuous long-term cropping of soybean in black soil of Northeast China. *Acta Agr. Scand. B Soil Plant* 65, 279–285. doi: 10.1080/09064710.2014.992941

Xu, Y. L., Wang, G. H., and Han, X. Z. (1995). Relationship between soil microbial ecological distribution characteristics and soybean root disease in soybean monocropping and rotation. *Syst. Sciemces Compr. Stud. Agr.* 11, 311–314.

Yan, M. C., Xu, T. T., Song, P. H., and Dai, J. J. (2012). Effects of different cropping patterns of soybean and maize seedlings on soil enzyme activities and MBC and MBN. *J. Northeast. Agr. Univ.* 19, 42–47. doi: 10.1016/S1006-8104(13)60049-5

Zeng, W., Bai, X., Zhang, L., Wang, A., and Peng, Y. (2014). Population dynamics of nitrifying bacteria for nitritation achieved in Johannesburg (JHB) process treating municipal wastewater. *Bioresour. Technol.* 162, 30–37. doi: 10.1016/j.biortech.2014.03.102

Zhan, X. M., Han, X. R., Yang, J. F., and Gao, Z. Q. (2004). The effect of succession cropping and soybean stubble on soybean root exudates. *Chin. J. Soil Sci.* 35, 631–635. doi: 10.1300/J064v24n01_09

Zhou, X. G., Wang, Z. L., Jia, H. T., Li, L., and Wu, F. Z. (2018). Continuously monocropped Jerusalem artichoke changed soil bacterial community composition and ammoniaoxidizing and denitrifying bacteria abundances. *Front. Microbiol.* 9:705. doi: 10.3389/fmicb.2018.00705

Zhu, Y. B., Shi, F. Y., Zhang, R. J., and Wu, Y. P. (2014). Comparison of bacterial diversity in rotational and continuous soybean cropping soils in Heilongjiang. *Acta Phytophy. Sin.* 41, 403–409.

Zhu, L., Zeng, C. L., Li, Y. Q., Yu, B. Q., Gao, F., Wei, W., et al. (2017). The characteristic of bacterial community diversity in soybean field with continuous cropping based on the high-throughput sequencing. *Soybean Sci.* 36, 419–424.

Conflict of Interest: The authors declare that the research was conducted in the absence of any commercial or financial relationships that could be construed as a potential conflict of interest.

Publisher's Note: All claims expressed in this article are solely those of the authors and do not necessarily represent those of their affiliated organizations, or those of the publisher, the editors and the reviewers. Any product that may be evaluated in this article, or claim that may be made by its manufacturer, is not guaranteed or endorsed by the publisher.

frontiers in Microbiology

ORIGINAL RESEARCH
published: 15 October 2021
doi: 10.3389/fmicb.2021.745225

Large-Scale Characterization of the Soil Microbiome in Ancient Tea Plantations Using High-Throughput 16S rRNA and Internal Transcribed Spacer Amplicon Sequencing

Ling Kui[1†], Guisheng Xiang[2†], Ya Wang[3†], Zijun Wang[2], Guorong Li[4], Dawei Li[2], Jing Yan[2], Shuang Ye[2], Chunping Wang[2], Ling Yang[2], Shiyu Zhang[2], Shuangyan Zhang[2], Ling Zhou[2,5], Heng Gui[6,7], Jianchu Xu[6,7], Wei Chen[8], Jun Zhang[1], Tingyuan Huang[9], Aasim Majeed[10], Jun Sheng[11,12,13]* and Yang Dong[11,12]**

[1] Shenzhen Qianhai Shekou Free Trade Zone Hospital, Shenzhen, China, [2] Yunnan Agricultural University Applied Genomics Technology Laboratory, School of Biological Big Data, Yunnan Agricultural University, Kunming, China, [3] College of Food Science and Technology, Yunnan Agricultural University, Kunming, China, [4] Lincang Tea Research Institute, Lincang, China, [5] Longrun Pu'er Tea College of Yunnan Agricultural University, Kunming, China, [6] CAS Key Laboratory for Plant Diversity and Biogeography of East Asia, Kunming Institute of Botany, Chinese Academy of Sciences, Kunming, China, [7] Centre for Mountain Futures, Kunming Institute of Botany, Chinese Academy of Sciences, Kunming, China, [8] College of Agronomy and Biotechnology, Yunnan Agricultural University, Kunming, China, [9] Guangzhou Center for Disease Control and Prevention, Guangzhou, China, [10] Molecular Genetics Laboratory, Central University of Punjab, Lahore, India, [11] State Key Laboratory for Conservation and Utilization of Bio-Resources in Yunnan, Yunnan Agricultural University, Kunming, China, [12] Yunnan Research Institute for Local Plateau Agriculture and Industry, Kunming, China, [13] Key Laboratory for Agro-Biodiversity and Pest Control of Ministry of Education, Yunnan Agricultural University, Kunming, China

There is a special interaction between the environment, soil microorganisms, and tea plants, which constitute the ecosystem of tea plantations. Influenced by environmental factors and human management, the changes in soil microbial community affected the growth, quality, and yield of tea plants. However, little is known about the composition and structure of soil bacterial and fungal communities in 100-year-old tea plantations and the mechanisms by which they are affected. In this regard, we characterized the microbiome of tea plantation soils by considering the bacterial and fungal communities in 448 soil samples from 101 ancient tea plantations in eight counties of Lincang city, which is one of the tea domestication centers in the world. 16S and Internal Transcribed Spacer (ITS) rRNA high-throughput amplicon sequencing techniques were applied in this study. The results showed that the abundance, diversity, and composition of the bacterial and fungal communities have different sensitivity with varying pH, altitude, and latitude. pH and altitude affect soil microbial communities, and bacterial communities are more sensitive than fungi in terms of abundance and diversity to pH. The highest α-diversity of bacterial communities is shown in the pH 4.50–5.00 and 2,200-m group, and fungi peaked in the pH 5.00–5.50 and 900-m group. Because of environmental and geographical factors, all microbes are similarly changing, and further correlations showed that the composition and structure of bacterial communities are more sensitive

OPEN ACCESS

Edited by:
Hai-Ming Zhao,
Jinan University, China

Reviewed by:
Wei Sun,
China Academy of Chinese Medical Sciences (CACMS), China
Shruti Choudhary,
Umeå University, Sweden
Hufeng Zhou,
Harvard University, United States

***Correspondence:**
Aasim Majeed
majeedaasim@gmail.com
Jun Sheng
shengjun@dongyang-lab.org
Yang Dong
loyalyang@163.com

[†] These authors have contributed equally to this work and share first authorship

Specialty section:
This article was submitted to Terrestrial Microbiology, a section of the journal Frontiers in Microbiology

Received: *21 July 2021*
Accepted: *31 August 2021*
Published: *15 October 2021*

Citation:
Kui L, Xiang G, Wang Y, Wang Z, Li G, Li D, Yan J, Ye S, Wang C, Yang L, Zhang S, Zhang S, Zhou L, Gui H, Xu J, Chen W, Zhang J, Huang T, Majeed A, Sheng J and Dong Y (2021) Large-Scale Characterization of the Soil Microbiome in Ancient Tea Plantations Using High-Throughput 16S rRNA and Internal Transcribed Spacer Amplicon Sequencing. Front. Microbiol. 12:745225. doi: 10.3389/fmicb.2021.745225

than fungal communities, which were affected by latitude and altitude. In conclusion, the interference of anthropogenic activities plays a more important role in governing fungal community selection than environmental or geographical factors, whereas for the bacterial community, it is more selective to environment adaptation than to adaptation to human activities.

Keywords: *Camellia sinensis* var. *assamica*, microbiome, function, ancient tea plantations, 16S and ITS rRNA

INTRODUCTION

Camellia sinensis L. is an evergreen shrub or small tree belonging to the family Theaceae whose leaves and leaf buds are used to produce tea. It is one of the important crops in the tropical and subtropical regions. It is a common source of tea all over the world and is cultivated widely across 49°N latitude to 33°S latitude (Sharma and Kumudini, 2018). China is the largest tea-producing country and has the largest area under tea cultivation in the world, accounting for 55.83 and 41.32% of the world total, respectively[1,2]. Small-leaf tea and large-leaf tea (*C. sinensis* var. *assamica*) are the two main varieties of today's cultivation[3]. The large-leaf tea cultivation has a long-standing history in China. The Bangwei transition type ancient tea tree that the Yunnan tea planting ancestors Pu'er people cultivated and domesticated represents the experienced cultivation strongly. As an important part of tea industry in China, Pu'er tea (leaf of *C. sinensis* var. *assamica*) is processed as raw materials from Yunnan's large-leaved species of sun-dried green tea, which, as a unique tea in Yunnan province, contains lipid-lowering, antibacterial, and antiviral abilities (Zhang et al., 2012; Pedan et al., 2018).

The soil microbial community plays a dynamic role in the growth and vigor of cultivated plant species. The quality of the soil is determined not only by the physiochemical properties of the soil but also by its microbial profile. Thus, the diversity and structure of the microbial communities within the rhizosphere have a profound impact on the growth and yield of crops. In turn, the type and duration of the cultivated crop species would influence the microbial community. Therefore, soil and crop management are considered the most important factors affecting soil quality (Dang, 2002). The intensity and duration of tea planting have a significant impact on the microbial community structure, biomass, and its function, which is most likely achieved through soil acidification and fertilizer addition (Han et al., 2007). The nitrogen fertilizer application (NH3) significantly enhanced the tea yield but resulted in more soil acidification of the plantation sites (Li S. Y. et al., 2016; Yan et al., 2018; Yang et al., 2018). Tea thrives well in acidic soils, with an optimum pH range of 4.50–5.50. However, rapid acidification is becoming an issue, besides other factors (Yan et al., 2020). Recent evidence suggested that in comparison to the forests, the acidification of the cultivated tea plantations, receiving more fertilizers, has amplified during the past two to three decades. However, no significant change in acidification was experienced in the tea plantations receiving organic manure. Thus, only approximately 43.9% of the tea plantations in China have the optimal pH (4.50–5.50) (Yan et al., 2020). Acidification altered the chemical dynamics of the soil as the cation exchange capacity, the exchangeable Ca, K, and Mg content decreased. The exchangeable Al^{3+} content increased in comparison to the exchangeable H^{+}, which resulted in increased Al extraction, thereby inhibiting tea plants from taking essential nutrients such as P, Fe, K, Ca, and Mg. Furthermore, the biogeochemical cycling of Al in tea leaf litter would accelerate further potential acidification of tea plantation soils. Besides inducing the loss of soil fertility, loss of number of important soil microorganisms, and loss of nitrogen and phosphorus content, the acidification of the tea plantation sites also resulted in the accumulation of organics in the roots and polyphenols plus heavy metals like Pb, Cu, and Cd in the leaves of tea plants. This would even become more intense with the increasing age of tea plants (Oh et al., 2006; Fung et al., 2008; Wang et al., 2010; Alekseeva et al., 2011; Li S. Y. et al., 2016; Li Y. C. et al., 2016; Yan et al., 2018; Yang et al., 2018). The prolonged monoculture of tea plantations leads to the gradual depletion of soil nutrient content, acidification, and deterioration of soil along with suppression of growth in tea plants (Wilson et al., 2004; Yan et al., 2018). This is also true for other annual crops like cucumbers (Zhou and Wu, 2012), potatoes (Liu et al., 2014), soybeans (Bai et al., 2015), and perennial crops such as apples (Mazzola and Manici, 2012), goldthread (Song et al., 2018), and coffee (Zhao et al., 2018). Taken together, these factors critically affected the growth, yield, and quality of the tea due to which the sustainable development of China's tea industry has been constrained, besides economic losses to tea farmers. Therefore, this problem has attracted the attention of many soil ecologists and scientists (Zhao et al., 2012; Li Y. C. et al., 2016; Arafat et al., 2019; Tan et al., 2019).

Due to the large number of microorganisms in tea plantation soils, the complexity of their role, the variability of the soil itself, and the imperfection of research methods, relatively fewer studies are available on the microbial diversity of tea plantation soils. The development and refinement of molecular biology techniques, metagenomics, and high-throughput sequencing have greatly facilitated the study and understanding of the structural profile, diversity, and interactions of the microbiome. The microbiome within the rhizosphere of tea plants plays an important role in enhancing the soil quality, resilience of tea plants, and their resistance against pathogens (Zhao et al., 2012; Li Y. C. et al., 2016; Raaijmakers and Mazzola, 2016; Arafat et al., 2019; Tan et al., 2019). However, certain substances in the rhizosphere of tea plants inhibit microbial activity, with bacteria most sensitive

[1]http://www.fao.org/home/en/

[2]http://www.stats.gov.cn/english/

[3]http://www.efloras.org/

than Actinomycetes and fungi (Pandey and Palni, 1996). In acidic tea plantation soils (pH < 6.0), the growth activity of soil microbes declines with decreasing pH (Koga et al., 2003), but it has also been found that tea plantation soil microbes are generally unaffected by soil pH, and certain research showed that 40- and 90-year-old tea tree soils contain only half the number of bacteria and fungi in contrast to 10-year-old tea tree soils, with bacteria predominating in the microbial community of the root soil (Wilson et al., 2004). Shannon diversity indices and richness were significantly lower in 8-, 50-, and 90-year-old tea plantations than in moorland, but both were significantly higher than in forest, and relatively high community diversity was found in 50-year-old tea plantations (Xue et al., 2006). The order of magnitude of the Shannon Diversity Index for soil microorganisms in tea plantations with four periods of different growth years was as follows: 45-year > 25-year > 7-year > 70-year tea plantations (Zhao et al., 2012). Generally, the application of compost affects the bacterial populations, and interestingly, when the compost is used in combination with nitrogen fertilizer, the soil microbial diversity increases (Qiu et al., 2014; Taha et al., 2016). As tea plants get older, change in composition and structure of the soil microbial communities occurs, and the species richness decreases, which in turn leads to a decrease in beneficial microorganisms along with an increase in soil pathogenic microorganisms (Li Y. C. et al., 2016; Arafat et al., 2019). The relative abundance of Ascomycota, Glomeromycota, and Chytridiomycota was reduced, whereas the relative abundance of Zygomycota and Basidiomycota was increased in the 2-, 15-, and 30-year-old monoculture history of replanted tea plantations. Furthermore, the beneficial fungi like *Mortierella alpina* and *M. elongatula* were gradually reduced along with an increase in pathogenic forms such as *Fusarium oxysporum*, *F. solani*, and *Microidium phyllanthi* in the soil of continuously grown tea plantations (Arafat et al., 2019). The bacterial genetic diversity index of tea plantation soils was lower than that of wasteland soils. The soils of organic tea plantations had higher ecosystem versatility, the soil microbial richness was significantly higher than that of unpolluted tea plantations and conventional tea plantations, and there were significant differences in soil bacterial community structure between the three tea plantations. The analysis of 16S rRNA gene sequences revealed that the dominant bacterial groups in tea plantation soils were Gamma and Alpha and Acidobacteria. The more alike the environmental variables are, the more similar the bacterial community structure in tea plantation soils is. It was found that soil organic carbon (SOC), nitrous nitrogen (NO3-N), and pH were the key soil factors affecting the bacterial community structure in tea plantation soils (Zhao et al., 2012; Qiu et al., 2014; Li Y. C. et al., 2016; Tan et al., 2019).

Lincang city is named for its proximity to the Lancang River, located in the southwestern part of Yunnan province, belonging to the subtropical low-latitude plateau mountain monsoon climate. It is the main stop on the ancient Tea-Horse Road, as well as one of the largest and most representative areas of the ancient tea heritage stock. The vast majority of the current research on tea soil microbes remained focused only on bacterial diversity (16S) and less on fungal diversity (ITS), and there has been less research on altitude drivers. Also, to the best of our knowledge, there are no data available for large samples and cross-regional studies of microbial populations in tea tree soils. With the popularity of high-pass sequencing, 16S and ITS amplicon sequencing have become important tools for studying the composition of microbial communities in environmental samples. In this study, we investigated the soil bacterial and fungal community dynamics of 101 representative ancient tea plantation sites in eight districts and counties of Lincang city. This study aimed to determine the effects of different gradients of pH, altitudes, and geographic locations on the microbial diversity, structure, and taxonomic composition of the tea plantations, and to explore the possible environmental factors that contribute to changes in soil microbial communities. Moreover, microbial classification was used to determine the presence of core microbiomes in tea plantations at different places along with the determination of their relative abundance and their potential role as hub taxa.

MATERIALS AND METHODS

Sample Collection

A total of 448 soil samples from the rhizobiome of 101 ancient tea plantation sites were collected from eight different counties and districts of Lincang city, Yunnan province in October 2019. The geographic coordinates (latitude and longitude) and elevation of the sampling sites were determined through GPS (JIEWEISEN, WS-009). We used real drone visualizations and map surveys for designing an appropriate sampling strategy. The details of the sampling locations are presented in **Figure 1A**. The soil was taken at a depth of approximately 20 cm from the surface. Stones and other impurities were removed. Each sample was collected in triplicate; two in 2-ml sterile tubes and the third in a 50-ml sterile centrifuge tube. The collected samples were snap-frozen in liquid nitrogen and carried to the lab.

Determination of Soil pH

The collected soil samples were air-dried and sieved through a 0.20-mm nylon sieve. The soil and water were then mixed in the ratio of 1:2.5 [4 g of soil and 10 ml of ultrapure water (w/v)] in a 25-ml centrifuge tube. The mixture was vortexed at a maximum frequency for 10 min, left at room temperature for 30 min, followed by determination of pH through a pH meter (METTLER TOLEDO, FiveEasy Plus) using glass electrodes. The reading for each sample was taken five times, and the average was taken as the pH value of the samples (Arafat et al., 2019; Yan et al., 2020).

DNA Extraction, Library Preparation, and Sequencing

Total DNA was extracted from each sample by following the instructions of the Omega Biotek EZNA® Soil DNA Kit. The quality and quantity of the isolated DNA were determined through agarose gel electrophoresis and Nanodrop Photospectrometer, respectively (Thermo Fisher, Nanodrop 2000). A final working concentration of 1 ng/μl was used for downstream analysis. We used the primers

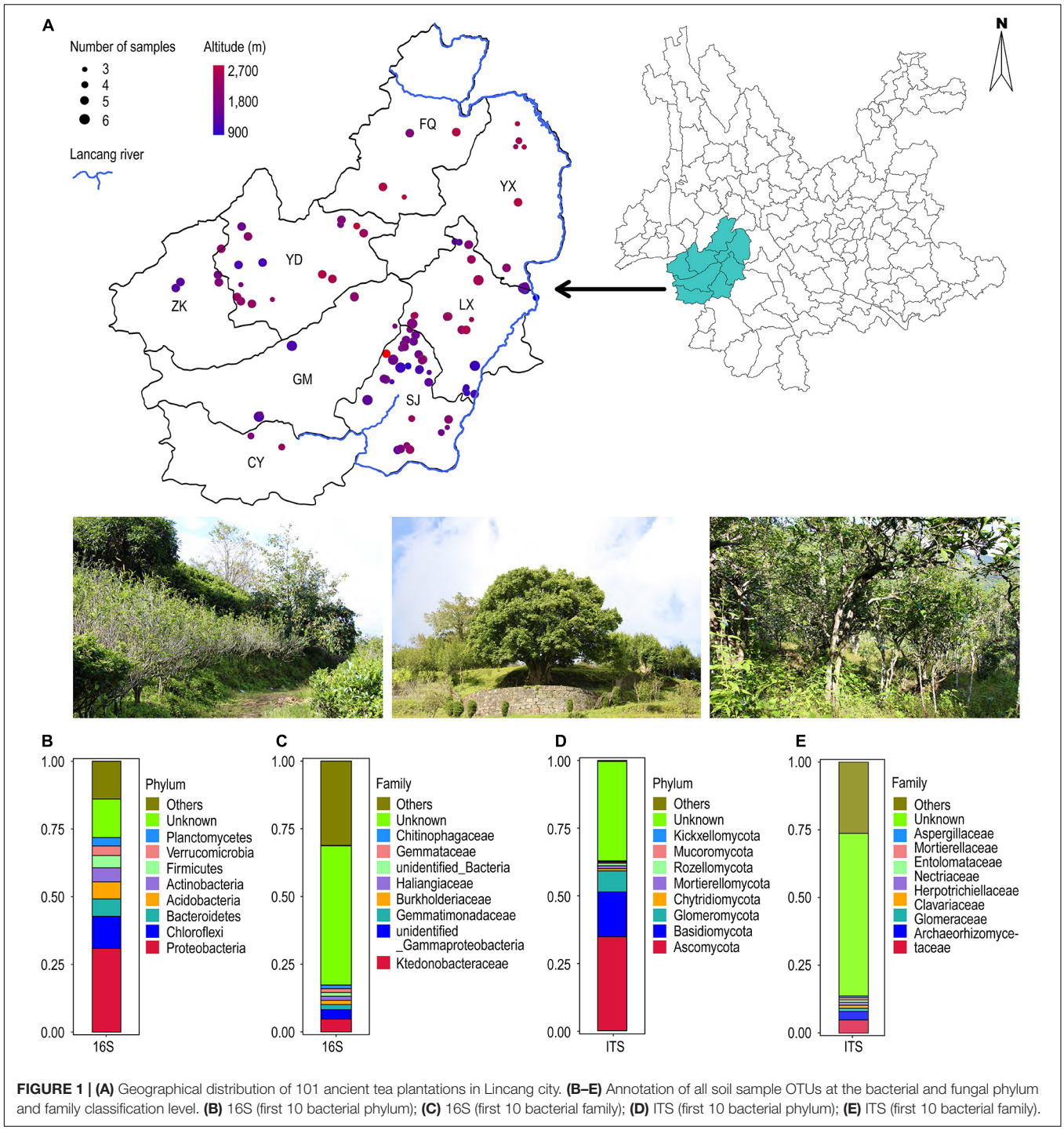

FIGURE 1 | (A) Geographical distribution of 101 ancient tea plantations in Lincang city. **(B–E)** Annotation of all soil sample OTUs at the bacterial and fungal phylum and family classification level. **(B)** 16S (first 10 bacterial phylum); **(C)** 16S (first 10 bacterial family); **(D)** ITS (first 10 bacterial phylum); **(E)** ITS (first 10 bacterial family).

F341 (5′-CCTAYGGGRBGCASCAG-3′) and R806 (5′-GGACTACNNGGGTATCTAAT-3′) (Stephen et al., 2017) for amplifying the V3–V4 region of the 16S rRNA gene. Moreover, the primers ITS-1F (5′-CTTGGTCATTTAGAGGAAGTAA-3′) and ITS-1R (5′-GCTGCGTTCTTCATCGATGC-3′) (Gardes and Bruns, 1993) were used to amplify the ITS1 region. All the primers were barcoded. Amplification of the 16S rRNA and ITS1 regions were performed through PCR reactions using Phusion® High-Fidelity PCR Master Mix, New England Biolabs. Each PCR reaction consisted of Phusion Master Mix (15.0 μl), primers (1.5 μl), genomic DNA (10.0 μl), and dd H2O (2.0 μl). The thermocycler program consisted of an initial denaturation temperature of 98°C for 1 min, followed by 30 cycles each with 98°C for 10 s, 50°C for the 30 s, and 72°C for 30 s, followed by a final 72°C for 5 min. The PCR products were purified with Qiagen Gel Extraction Kit (Qiagen, Germany).

Then, the sequencing library was generated using TruSeq® DNA PCR-Free Sample Preparation Kit (Illumina, United States) following the manufacturer's recommendations. The index codes were added to the library. A total of 448 libraries were generated. The quality of the libraries was assessed through the Qubit@ 2.0 Fluorimeter (Thermo Fisher Scientific, United States) and Agilent Bioanalyzer 2100 system (Agilent Technologies, United States). Subsequently, each library was sequenced on the Illumina NovaSeq 6000 platform and 250-bp paired-end reads were generated.

Sequence Data Processing

The paired-end raw reads were grouped based on their barcode sequences. Then, the paired reads were merged to obtain amplicon sequences using FLASH (version 1.2.7) (Magoč and Salzberg, 2011). The barcode and primer sequences as well as the low-quality amplicon sequences were removed using QIIME2 (v2019.10) (Bolyen et al., 2019). We used UCHIME (Quast et al., 2013) (parameter default) to detect and remove the chimeric sequences. Thus, clean amplicon data were generated, which were used for downstream analysis. The quality amplicons were then clustered into OTUs using Uparse (v10.0.240) (Edgar, 2013), based on a similarity threshold value of ≥97%. A representative sequence of each OTU was selected for further analysis. The representative sequences were aligned against the SILVA 132 database (for 16S rRNA sequences) and the UNITE database (for ITS sequences) (Abarenkov et al., 2010) to determine their taxonomic affiliations. Furthermore, to investigate the phylogenetic relationships among the OTUs, multiple sequence alignments were performed using Muscle (v3.8.31) (Edgar, 2004). QIIME2 (v2019.10) was used to calculate Weighted Unifrac distances and to construct UPGMA clustering trees.

Statistical Analysis and Data Visualization

α-diversity represents the diversity within a sample, including species richness and species evenness measurements. We used QIIME2 (v2019.10) to calculate the sample Chao1 and Shannon indices to evaluate the complexity and diversity of species within the sample. The statistical evaluation of differences in α-diversity between multiple groups was carried out through the Kruskal–Wallis test with a *p*-adjusted cutoff value of 0.05, using agricolae package. β-diversity represents the differences in the microbiome among the samples. We employed non-metric multidimensional scaling (NMDS) test, Anosim, and MRPP analysis using the R vegan package (Philip, 2003; R Core Team, 2020) to calculate β-diversity measurements. We used correlation analysis to identify associations between taxa and environmental factors, such as pH, longitude and latitude, and altitude, using the corr.test function of the psych R package. The correlations were visualized using the pheatmap R package. Moreover, a redundancy analysis (RDA) and Mantel test were performed using the R vegan package to compare the correlations of environmental factors with microbial community composition and structure.

RESULTS

Geographic, Elevation, and pH Range of the Samples

Analysis of geographic locations of the 448 samples from 101 tea plantation sites revealed that they were distributed between 23–25°N latitude and 98–101°E longitude. Their elevation ranged from 900 to 2,700 m (**Figure 1A**). The pH values ranged from 3.90 to 6.30, with an average value of 4.68. We created three pH gradients; pH < 4.50, pH between 4.50 and 5.50, and pH > 5.50. Our analysis revealed 39 sites with pH < 4.50, 58 sites with pH between 4.50 and 5.50, and 4 sites with pH > 5.50 (**Supplementary Figure S1**).

Composition and Structure of Bacterial and Fungal Communities

After merging of paired-end raw reads, their quality control analysis, and filtration of chimeric sequences, a total of 84,691 active amplicon sequences were obtained belonging to the 16S rRNA region. Similarly, a total of 53,228 active sequences were obtained for the ITS region from 448 soil samples. The sequences were clustered to 21,293 OTUs of bacteria belonging to 65 phyla, and 14,978 OTUs of fungi belonging to 17 phyla, at a threshold of 0.97. The sparse curve of the OTUs gradually flattened out (**Supplementary Figure S2**), which indicated that the sequencing depth covered all the species in the sample.

The taxonomic annotation of OTUs was performed from phylum to species level (**Figure 1**). In case of bacteria, Proteobacteria (30.9%) was the most dominant phylum followed by Chloroflexi (11.9%), Bacteroidetes (6.4%), Acidobacteria (6.3%), Actinobacteria (5.2%), and Firmicutes (4.6%). Approximately 14.2% OTUs remained unclassified (**Figure 1B**). Ktedonobacteraceae (4.7%) was the dominant family followed by unidentified Gammaproteobacteria (3.5%) and Gemmatimonadaceae (1.9%). Approximately 53.1% OTUs could not be assigned to any family (**Figure 1C**). Similarly, in the case of fungi, Ascomycota (34.7%) was the most frequent phylum followed by Basidiomycota (16.6%) and Glomeromycota (7.7%). The unclassified OTUs accounted for up to 36.9% (**Figure 1D**). Archaeorhizomycetaceae (4.8%) was the dominant family, followed by Glomeraceae (3.2%) and Clavariaceae (1.2%), with 60.0% remaining unclassified (**Figure 1E**).

Community Structure and Diversity in Response to Variations in pH

We estimated the abundance of bacteria and fungi and analyzed its relationship with variations in pH. Six pH gradients were used during the analysis. We observed that there is no significant trend (ascending or descending) in the relative abundance of bacterial phyla with pH (**Figure 2A**). Acidobacteria, Actinobacteria, and Proteobacteria have relative abundance > 10% at all pH gradients. Actinobacteria and Acidobacteria showed an opposite trend at the lower (pH 3.50–4.00) and upper (pH 6.00–6.50) pH extremes, with the former exhibiting less relative abundance and the latter showing greater relative abundance. However, Spearman's correlation analysis did not show any significant

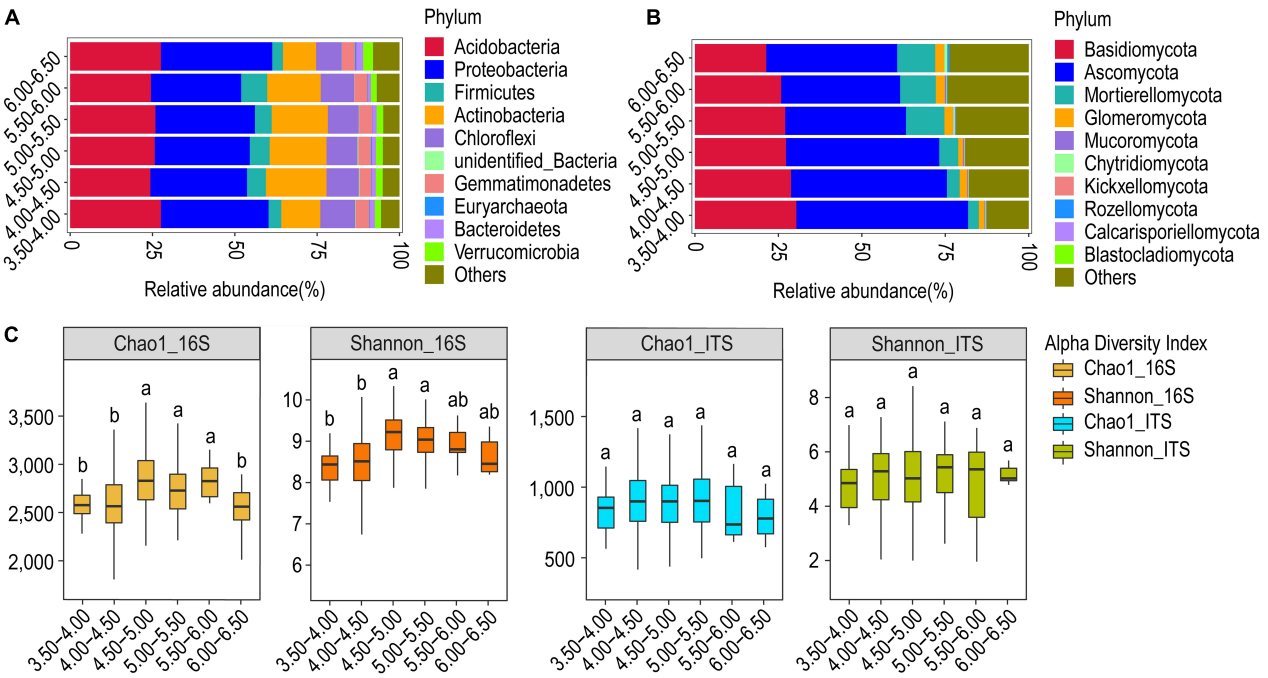

FIGURE 2 | Relative abundance and α-diversity indices of soil bacterial and fungal communities in different pH gradient groups. **(A)** Relative abundance of bacteria at the phylum classification level (first 10 bacterial phylum, same below); **(B)** relative abundance of fungi at the phylum classification level (first 10 fungi phylum, same below); **(C)** Chao1 and Shannon indices of bacteria and fungi. Different lowercase letters indicate significant differences between subgroups ($p < 0.05$) (same below).

relationship of the relative abundance of the bacterial phyla with variations in pH.

The fungal phyla, however, showed a clear relationship of the relative abundance with pH (**Figure 2B**). The relative abundance of Ascomycota and Basidiomycota showed a progressive decline with increasing pH. The trend is more explicit and contrasting in the case of Mortierellomycota, whose abundance increases toward basic pH. At the genus level, the relative abundance and composition of genera in bacteria and fungi were similar in all groups except for the highest pH group. *Arthrobacter* and *Archaeorhizomyces* were the dominant bacterial and fungal genera in all groups, respectively (**Supplementary Figure S3A**). The relative abundance of the genus *Hygrocybe* was substantial in all groups, except the group with pH > 6.0. *Penicillium* and *Russula* were important fungal genera in the low pH group (pH 3.5–4.0) whereas the genus *Mortierella* is important in the high pH group (pH > 6.0) (**Supplementary Figure S3B**).

The α-diversity analysis revealed that both the Chao1 and Shannon's index of the bacterial community were significantly higher for the pH = 4.50–5.00 and 5.00–5.50 than for the pH = 3.50–4.00 and 4.00–4.50 ($p < 0.05$). In contrast, the Chao1 and Shannon's index of the fungal community did not differ between the subgroups (**Figure 2C**). The number of OTUs was found to be highest for both the bacterial and fungal communities at pH = 4.50–5.00. The number of OTUs common to all the groups was observed to be 6,073 and 2,260 for bacterial and fungal communities, respectively (**Supplementary Figure S4**). The β-diversity analysis of microbial communities at different pH gradients through NMDS could not establish any distinctions in both bacterial and fungal communities (**Supplementary Figure S5**). The Anosim and MRPP test also did not reveal any clear trend in between-group or within-group differences. However, the test was statistically significant for some comparisons, although the correlations were weak (**Supplementary Table S1**).

UPGMA clustering revealed that the pH gradients of 4.50–5.00 and 5.00–5.50 formed one sub-cluster, so their community profile tends to be highly similar. Other pH gradients segregated into individual leaves. The gradient 6.00–6.50 was found most distinct from others, followed by the gradient 3.50–4.00, suggesting their distinct community structure as compared to other intermediary gradients (**Supplementary Figure S6A**). The results were slightly different in the case of fungi, with an upper gradient (pH = 6.00–6.50) quite distinct from others. Furthermore, it was revealed that the pH gradients of 5.00–5.50 and 5.5–6.00 host similar fungi, whereas the pH gradients of 3.50–4.00, 4.00–4.50, and 4.50–5.00 have their fungal profile (**Supplementary Figure S6B**).

Community Structure and Diversity in Response to Variations in Elevation

We observed that the overall structural profile of the bacterial and the fungal communities at 14 different altitudinal zones is similar, and no explicit trend is seen in the relative abundance of bacterial phyla along the elevation gradient (**Figure 3A**). Acidobacteria and Proteobacteria were the dominant bacterial phyla in all subgroups and their relative abundance showed

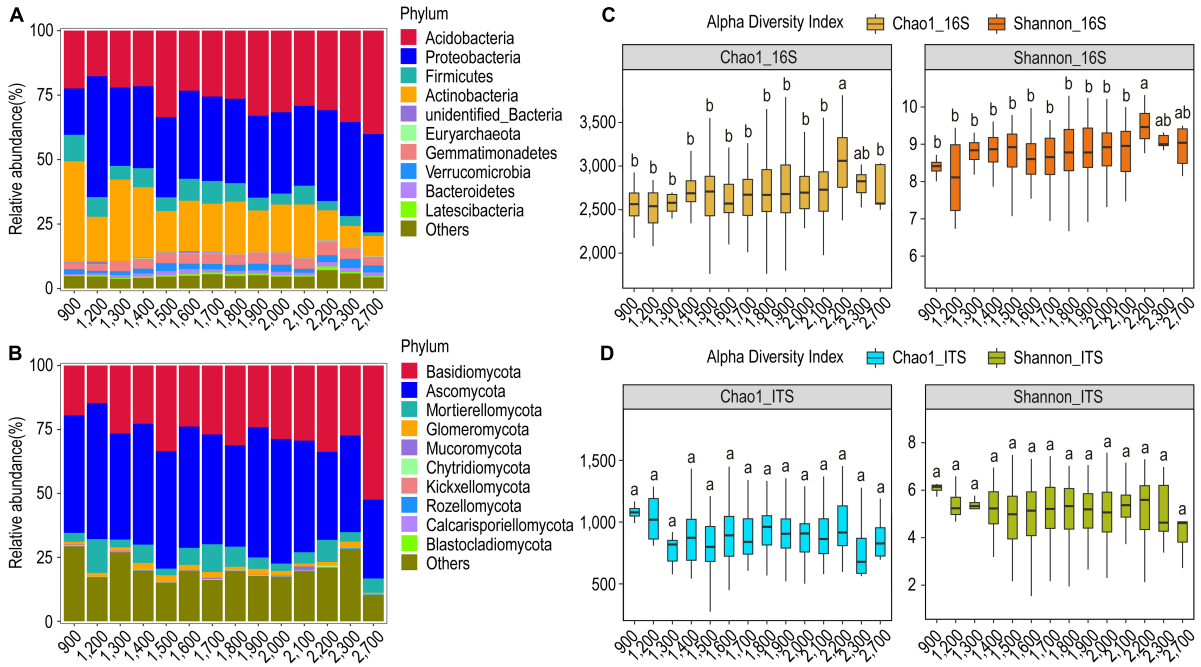

FIGURE 3 | Relative abundance and α-diversity indices of soil bacterial and fungal communities in different altitude groups. **(A)** Relative abundance of bacteria at the phylum classification level; **(B)** relative abundance of fungi at the phylum classification level; **(C)** Chao1 and Shannon indices of bacteria and fungi. **(D)** Different lowercase letters indicate significant differences between subgroups ($p < 0.05$).

an increasing trend with increasing altitude. Actinobacteria in general showed higher abundance toward lower altitude zones. Similarly, Ascomycota and Basidiomycota were the dominant fungal phyla in all subgroups. Basidiomycota showed an absolute dominance (52.4%) at the highest altitude zone (**Figure 3B**).

The relative abundance of the bacterial genera showed a marked difference in the low altitude zones as compared to the high-altitude zones. In general, the relative abundance of the bacterial genera decreased with increasing altitude. The genus *Arthrobacter* showed a remarkable presence in all the altitudinal zones, and it was most dominant in the 900-m zone along with the genus *Tumebacillus*. The genus *Massilia* dominated in the 1,200-m zone (**Supplementary Figure S7A**). In contrast to the bacterial genera, the relative abundance of the fungal genera did not change with the altitude. It seemed that the genus *Archaeorhizomyces* preferred altitude zones > 1,400 m, whereas the genus *Hygrocybe* preferably is more abundant in the altitude zones > 1,500 m. Furthermore, the genus *Saitozyma* favors altitudes < 1,800 m, whereas the genus *Penicillium* dominated the 1,200-m zone followed by the 900-m zone. Moreover, the genera *Russula* and *Coprinellus* dominated the 2,700-m altitude zone (**Supplementary Figure S7B**).

The α-diversity analysis revealed that both the Chao1 and Shannon's index were highest for the altitudinal zone of 2,200 m in the case of bacterial communities. However, these diversity indices were found to be highest in the altitudinal zone of 900 m for fungal communities (**Figure 3C**). The bacterial and the fungal communities had the highest number of OTUs in the 1,400-m and 1,800-m altitudes, respectively, with a total of 2,869 OTUs for bacteria and 453 OTUs for fungi (**Supplementary Figure S8**). Besides, the β-diversity analysis through the NMDS test revealed that both bacterial and fungal communities could not be grouped into distinct clusters based on the altitude variations (**Supplementary Figure S9**). The Anosim test for 16S rRNA showed that the highest difference in the bacterial community structure is exhibited between the 900-m and 1300-m altitude zones ($R = 0.6716$, $p = 0.003$) followed by the 900-m and 2,200-m zones ($R = 0.4056$, $p = 0.003$) (**Supplementary Table S2**). Similar results were shown by the MRPP test. The Anosim test for ITS showed that the highest difference in the fungal community structure is exhibited between altitude zones 1,400 and 2,100 m ($R = 0.3586$, $p = 0.001$) followed by 1,400 and 2,100 m ($R = 0.3315$, $p = 0.001$). Similar results were shown by the MRPP test.

Based on the UPGMA clustering, it was observed that the bacterial community profile at the altitude zone of 900 m is much more distinct as compared to the other altitude zones, followed by the 1,200-m zone. The altitude zones from 1,500 to 2,100 m share a structural similarity in bacterial communities, whereas the altitude zones of 2,300 and 2,700 m looked similar. This indicated that the community profile at the upper extreme (2,300 and 2,700 m) and lower extreme (900 and 1,200 m) altitudinal zones are distinct from the intermediary zones, which tend to be relatively similar (**Supplementary Figure S10A**). Similar results were shown for the fungal community structure in which the 2,700-m zone was most distinct from other zones. The altitude zones of 900, 1,200, and 1300 m formed their sub-cluster, so they tend to be similar, but distinct from others. Likewise, the

altitude zones from 1,400 to 2,300 m formed a single group (**Supplementary Figure S10B**).

Community Structure and Diversity in Response to Variations in Geographical Locations

According to the geographical distribution of the sampling sites, we analyzed ancient tea plantations located in eight counties. At the phylum classification level, the relative abundance of soil bacterial and fungal communities in tea plantations in different regions did not change significantly, but there were some differences in their relative abundance composition. Based on the geographic locations, the bacterial community was dominated by Acidobacteria and Proteobacteria at all sites. The relative abundance of Acidobacteria was highest in Cang Yuan (CY) followed by Geng Ma (GM) and Zhen Kang (ZK), whereas it was least abundant in Lin Xiang (LX) and Shuang Jiang (SJ). Interestingly, LX and SJ host a higher abundance of Actinobacteria and Chloroflexi in comparison to other locations (**Figure 4A**). The fungal community was dominated by Ascomycota and Basidiomycota, with the former being most abundant in CY and the latter being most abundant in ZK (**Figure 4B**).

At the genus level, the LX and SJ were most dominated by the bacterial genera *Arthrobacter, Bacillus*, and *Kitasatospora.* These two sites showed distinct bacterial community profiles in comparison to others. The genus *Tumebacillus* was also more abundant in these sites. However, the fungal community profile showed a distinct pattern across all the sites. CY was occupied mostly by *Amphinema* and *Inocybe. Archaeorhizomyces* formed a substantial proportion of the fungal community in other sites, with the most dominant in ZK. *Hygrocybe* was the least frequent in ZK but formed a substantial part in other sites. Besides, *Mortierella* also formed a substantial proportion in all sites except CY and ZK. *Russula* appeared to be a trademark genus in YK and SJ, whereas *Penicillium* seemed to be a hallmark genus of SJ (**Supplementary Figure S11**).

The bacterial α-diversity analysis revealed the highest average Chao1 value for Yun Xian (YX) and the lowest for LX and SJ; other sites have intermediary values of Chao1. Similar results were obtained for Shannon's diversity index. The fungal α-diversity analysis revealed the highest average Chao1 value for ZK and lowest for CK; others showed intermediary average Chao1 values (**Figure 4C**). The highest number of OTUs for the bacterial (4,389) and fungal (1,564) communities were observed for SJ and LX, respectively (**Supplementary Figure S12**). The β-diversity analysis through the non-metric NMDS test did not cluster the bacterial and fungal communities according to geographical locations (**Supplementary Figure S13**). The Anosim test on bacterial communities revealed that LX was quite distinct from all other sites. It differed most from Feng Qing (FQ) (R = 0.5371, p = 0.001) followed by CY (R = 0.5015, p = 0.001), whereas it showed least difference with YX (R = 0.3685, p = 0.001). The MRPP test also revealed LX distinct from all other sites. In the case of fungal communities, the Anosim test revealed CY to be most distinct from all others, followed by LX (**Supplementary Table S3**).

In the case of bacteria, based on the UPGMA clustering results, LX and SJ formed one cluster, whereas a separate cluster was formed by other locations, with ZK and Yong De (YD) forming their sub-cluster. This indicated that LX and SJ have similar community structures and are quite distinct from other sites. In the case of fungi, two main sub-clusters were formed. GM, LX, and SJ formed one group, whereas YD and YX formed another group. Other sites are segregated into their leaves. This indicated that CY is the most distinct plantation site from others in terms of the fungal community, followed by ZK. The LX, and SJ as well as YD and YX are much similar to each other (**Supplementary Figure S14**).

Correlation Analysis

Redundancy analysis showed that the first two axes explained only 17.11 and 33.95% of the variance. From **Figure 5A**, it is evident that the environmental factors altitude and latitude exhibit highly positively correlated bacterial community profiles, followed by latitude and pH, and altitude and pH. In contrast, the environmental factors pH and longitude exhibit negatively correlated community profiles. The variables latitude and longitude do not correlate. In the case of fungi, the environmental factors pH and latitude have a highly positively correlated community profile, followed by latitude and altitude. In contrast, the environmental factors altitude and longitude exhibit negatively correlated community profiles. The variables pH and latitude and do not correlate (**Figure 5B**). Mantel test revealed very weak correlations between the variables and the bacterial and fungal community composition (**Table 1**). However, altitude and latitude appeared to be relatively more effective. Furthermore, Spearman correlation analysis was used to determine the relationship between the relative abundance of bacterial and fungal communities and environmental and geographic factors. We observed that Proteobacteria did not have any significant correlation with any variable. Furthermore, pH showed a very weak or no correlation with all the variables. Longitude, altitude, and latitude showed a significant positive or negative correlation with all or some phyla (**Figure 5C**). At the genus level, the strongest significant correlations were shown by altitude and latitude (**Figure 5E**). In the case of fungal phyla and genera, significant correlations were lacking (**Figures 5D,F**).

DISCUSSION

In the soil–plant rhizobiome, the most active and decisive soil microorganisms play an active role in the exchange of matter and energy, soil formation and development, plant–soil interactions, etc. (Urbina et al., 2018; Tan et al., 2019). The suitable soil pH for the growth of tea plants is 4.00–6.50, with the most optimum being 4.50–5.50. Recent studies have revealed that in China, the soil is constantly becoming acidic for the tea plantation sites, with pH as low as $<$ 4.50 at many sites (Guo et al., 2010; Yan et al., 2020). Our analysis also revealed an acidic pH (4.68) of ancient tea plantations in Lincang city, which is further corroborated

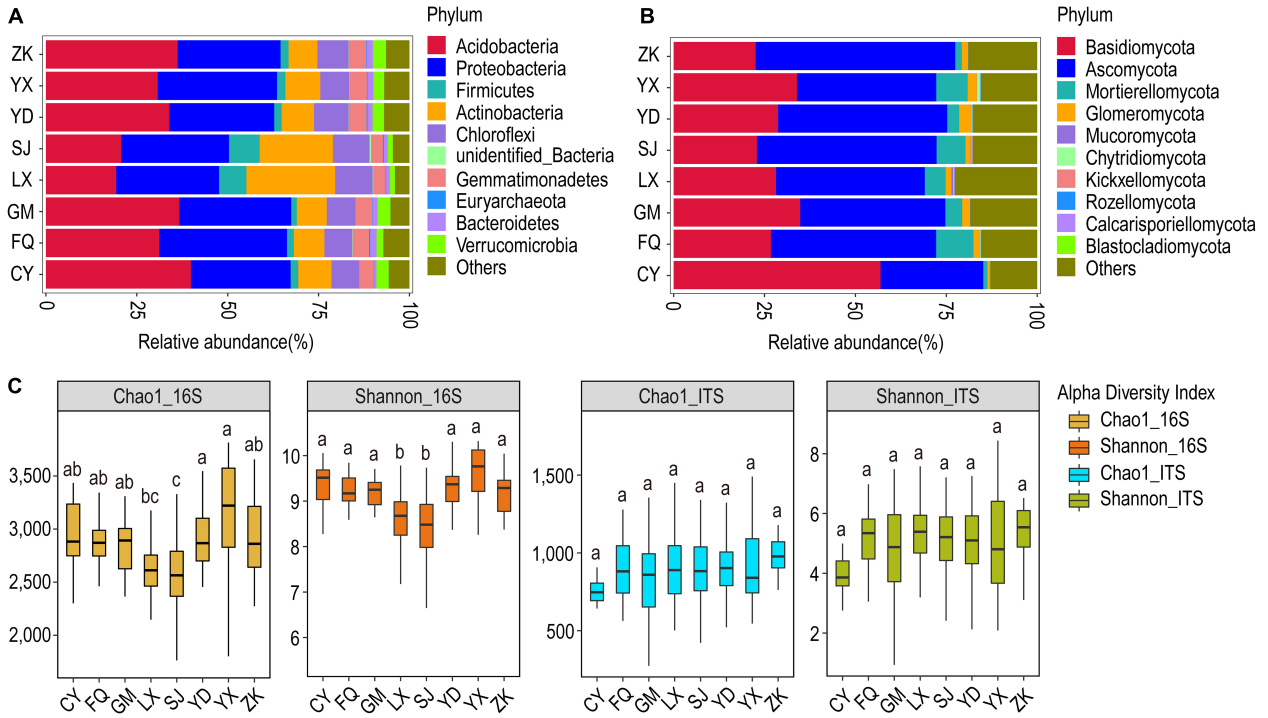

FIGURE 4 | Relative abundance and α-diversity indices of soil bacterial and fungal communities in different region groups. **(A)** Relative abundance of bacteria at the phylum classification level; **(B)** relative abundance of fungi at the phylum classification level. **(C)** Chao1 and Shannon indices of bacteria and fungi. Different lowercase letters indicate significant differences between subgroups ($p < 0.05$). CY, Cang Yuan; GM, Geng Ma; ZK, Zhen Kang; LX, Lin Xiang; SJ, Shuang Jiang; FQ, Feng Qing; YD, Yong De; YX, Yun Xian.

by Yan et al. (2020). Although not more acidic than the lower optimal value (4.00), the situation has reached a critical level for tea plantations in Lincang city, which would lead to a serious reduction in the growth and survival rate of tea plants, thereby affecting the yield.

The microbial diversity of the tea plantation sites not only varies with wastelands and woodlands but also with the age of different tea plantation sites (Xue et al., 2007, 2008). The intensity and duration of tea planting have a significant impact on the microbial community structure, biomass, and its function (Han et al., 2007). Relatively high community diversity was observed in 50-year-old tea plantations (Xue et al., 2006). Thus, tea plantation monoculture, tea plant age, different management patterns, and land use types have a significant impact on soil microbial community diversity, composition, and structure. Our study showed that Acidobacteria and Proteobacteria (Alpha, Delta, and Gamma) were the dominant bacterial phyla in all the tea plantation sites, whereas Ascomycota and Basidiomycota were the dominant fungal phyla (**Supplementary Figure S15**). With some minor differences, our findings were corroborated by several studies (Zhao et al., 2012; Li Y. C. et al., 2016; Arafat et al., 2019; Tan et al., 2019). Acidobacteria are particularly abundant in soils with very low resource utilization (Quaiser et al., 2003; Fierer et al., 2007). Alphaproteobacteria can grow at very low nutrient levels and can induce nitrogen fixation with plants. Gammaproteobacteria are associated with large amounts of available nutrients and control disease inhibitory activity through non-ribosomal peptide synthase (Mendes et al., 2011; Li Y. C. et al., 2016). Deltaproteobacteria are an important contributor to the anaerobic process of the sulfur cycle. Ascomycota promotes the decay of animal and plant remains in the soil (Mendes et al., 2011), whereas basidiomycota forms mycorrhiza with roots of plants. Previous studies have confirmed the presence of *Bacillus* within the rhizobiome of tea plants, with *B. subtilis* and *B. mycoides* forming a major part of the bacterial population, even in unfavorable times. *Bacillus* sp. exhibit antagonistic activity against fungal isolates; they inhibit the growth of fungal mycelium and cause structural abnormalities in the rhizosphere of tea plants (Pandey and Palni, 1997; Singh et al., 2007). The abundance of *Bradyrhizobium*, *Mycobacterium*, and *Sphingomonas* gradually decreases with the increasing age of tea plantation sites, whereas the *Granulicella* shows a reverse trend. Details about their functions are lacking; however, *Bradyrhizobium* is essential in promoting plant growth (Antoun et al., 1998; Li Y. C. et al., 2016). Our study confirmed the presence of the genus *Bacillus* only which occupied a certain percentage of all sampled sites.

Due to the monoculture of tea plants, enhanced use of chemical fertilizers (especially nitrogen fertilizers), and accumulation of organic matter, the soil acidification of tea plantation sites is deepening. This may lead to a significant reduction in microbial species within the soil (Wilson et al., 2004; Abe et al., 2006; Ruan et al., 2007; Li S. Y. et al., 2016;

TABLE 1 | Mantel-test analysis of environmental and geographical factors with bacterial and fungal community composition.

Environmental and geographical factors	Bacterial		Fungal	
	R	*P*	*R*	*P*
pH	– 0.0084	0.6757	– 0.0084	0.6840
Lo	– 0.0013	0.5254	– 0.0013	0.5236
La	0.0354	0.0169*	0.0354	0.0166*
Al	0.0406	0.0047**	0.0406	0.0044**
Lo + La	0.0196	0.1345	0.0196	0.1389
Lo + Al	0.0061	0.3712	0.0061	0.3690
La + Al	0.0441	0.0044**	0.0441	0.0070**
Lo + La + Al	0.0220	0.1074	0.0220	0.1049
pH + Lo + La + Al	0.0113	0.2685	0.0113	0.2825

*Lo, Longitude; La, Latitude; Al, Altitude. *P < 0.05; **P < 0.01.*

Yan et al., 2018). Although the forest and tea plantation soils have similar acidic pH, their microbial community structures are different, suggesting that the differences are not solely due to variations in pH (Yao et al., 2000). Koga et al. (2003) showed that in acidic tea plantation soils, the activity of soil microbes showed a tendency to rise first and then decrease with increasing pH. The application of lime can control the acidification of tea plantation soils. It has a significant effect on the structure and diversity of the microbial community in the soil, as the diversity increases with increasing lime concentration (Xue et al., 2010). However, a study by Wilson et al. (2004) found that soil microorganisms are usually not affected by soil pH. Our study found that the composition and structure of soil bacterial and fungal communities exhibited a mono-peak pattern with pH variation. The relative abundance of the fungi (pH = 4.00–5.50) was more significantly affected by pH than that of the bacteria (pH = 4.50–5.50), whereas the fungal diversity was less correlated with pH than that of the bacteria. Similar results were obtained during soil pH studies on tea plant fitness (Ruan et al., 2007; Guo et al., 2010; Yan et al., 2020). Although the bacterial phyla did not show any significant trend along the pH gradients; however, Actinobacteria were found to be less abundant at low pH, whereas Acidobacteria exhibited higher abundance at higher pH. In contrast, the fungal phyla Ascomycota and Basidiomycota showed a clear declining trend with increasing pH, whereas Mortierellomycota exhibited higher abundance with increasing pH. The α-diversity analysis revealed that the bacterial community composition is more diverse at a pH range of 4.50–5.00, whereas the fungal diversity remained relatively same across different pH gradients. Our study showed that the pH range of 4.50–5.00 seemed more optimal, as the number of OTUs was found to be highest in this range for both bacteria and fungi. Besides, the α-diversity of the rhizosphere bacterial community was positively correlated with pH in perennial shrubs *Caragana* spp., with pH as a significant factor affecting both the α-diversity and richness (Na et al., 2018). Li Y. C. et al. (2016) found that only *Granulicella* in Acidobacteria increased significantly with decreasing pH in tea plantation soil, whereas the relative abundance of Acidobacteria was not significantly correlated with soil pH. Further studies showed that the soil bacterial communities are usually closely related to soil pH and their relative abundance and diversity are positively correlated with pH, a pattern that applies to both the overall bacterial community composition and the composition of individual bacterial communities. However, for fungi, the relative abundance is not affected by pH and the diversity is only weakly correlated with pH, suggesting that tea plantation ecosystems have some similarities and specificities compared to others, such as agroecosystems (Jones et al., 2009; Rousk et al., 2010; Li Y. C. et al., 2016). Besides, our study found that *Archaeorhizomyces* was the dominant fungal genus in all subgroups and had a higher relative abundance in the low pH gradient group. Sequence characteristics indicate that *Archaeorhizomyces* occupy plant root intervals in deep soils with low pH and high nutrient transformation, and their relative abundance is significantly correlated with the fungal plant pathogen *Typhula*, the decaying fungus *Exophiala*, the *Suillus* exophytic root family, and *Tubeufia* and *Omphalotus*, which are all involved in the decay process of vegetation (Carrino-Kyker et al., 2016; Choma et al., 2016; Pinto-Figueroa et al., 2019). When soils become acidic, the soil microorganisms have to elicit a physiological response to cope with decreasing pH like synthesis of protective membrane proteins and fatty acids, production of buffer molecules to maintain internal pH homeostasis, and pumping of H^+ ions to maintain electoral gradient across the membrane. Besides, low pH is associated with low soil inorganic phosphorous (Pi) due to mobilized aluminum (Al). Soil microorganisms overcome this low Pi by acquiring more organic P (Po). Increase in soil pH altered both bacterial and fungal communities in temperate deciduous forests (Carrino-Kyker et al., 2016).

Studies on the relationship between microbial community profile and altitude vary. Some studies establish an inverse relationship between soil microbial diversity and altitude (Tian et al., 2017; Li et al., 2018; Nottingham et al., 2018). Other studies confirm that there is no clear-cut relationship between them and different microbial groups show different patterns along the altitude gradients (Fierer et al., 2011). Our analysis showed an increase in abundance of Acidobacteria and Proteobacteria across the different altitudinal zones, whereas Actinobacteria were abundant at lower altitudes. In case of fungi, Basidiomycota was the most abundant at higher altitudes. In general, the abundance of bacterial genera increased with increasing altitude, whereas the fungal genera did not reveal any recognizable variation. The diversity of the bacterial and the fungal communities was highest at an altitude of 2,200 and 900 m, respectively. Acidobacteria were found to decrease monotonically with increasing altitude (Bryant et al., 2008), whereas a monotonic increase was observed for the bacteria by Wang et al. (2011). Both the single peak pattern (bacteria) and the bimodal pattern (archaebacteria) were observed for the microbial diversity (Singh et al., 2012). The nitrogen-fixing bacteria also showed diverse relationships with altitude (Wang et al., 2019). According to Shen et al. (2015), the composition of the bacterial communities at high altitudes is most complex and diverse among all microbes. In the case of fungi, the abundance

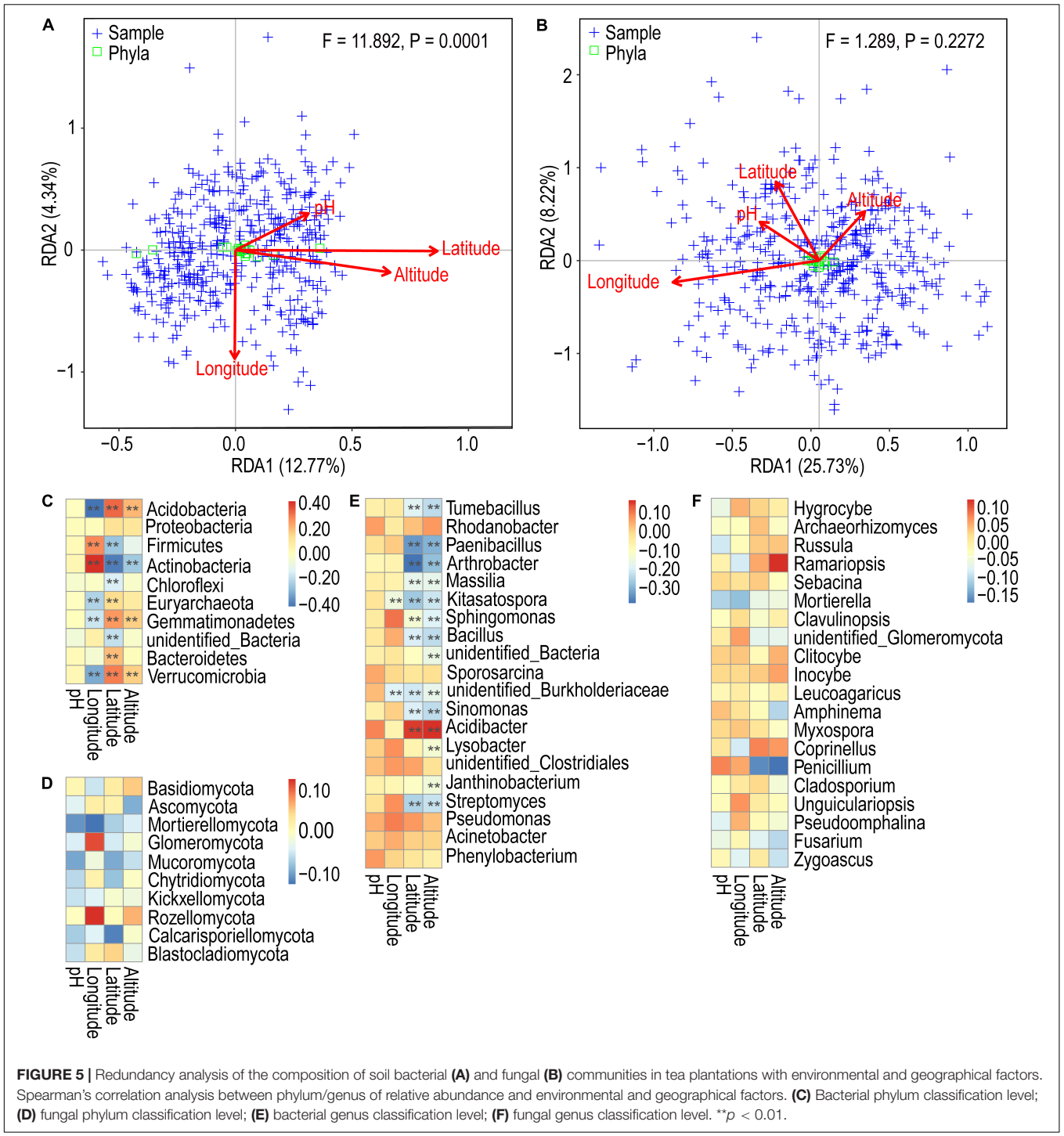

FIGURE 5 | Redundancy analysis of the composition of soil bacterial **(A)** and fungal **(B)** communities in tea plantations with environmental and geographical factors. Spearman's correlation analysis between phylum/genus of relative abundance and environmental and geographical factors. **(C)** Bacterial phylum classification level; **(D)** fungal phylum classification level; **(E)** bacterial genus classification level; **(F)** fungal genus classification level. $^{**}p < 0.01$.

generally decreases with increasing altitude, but there is no significant correlation between its uniformity and altitude. Our study revealed a single peak pattern of bacterial abundance with increasing altitude and a double peak pattern of bacterial diversity with increasing altitude. However, a double peak pattern was observed for both the fungal abundance and fungal diversity with increasing altitude. These results indicate that the diversity, community composition, and structure of bacteria and fungi in tea plantation soil are somewhat different and show different patterns of altitude distribution. Furthermore, *Arthrobacter* showed a higher relative abundance at lower altitudes in comparison to higher altitudes, whereas *Penicillium* showed an absolute predominance at lower altitudes. This is corroborated by several studies (Widden, 2018; Kumar et al., 2019).

With the aim of evaluating the variation in arbuscular mycorrhizal fungi (AMF) along an altitudinal gradient in

rupestrian grasslands in Brazil, Coutinho et al. (2015) found less similarity of AMF species across different altitudinal zones. Altitudinal zone with similar soil characteristics showed overlap in AMF species. The AMF species composition was different at extreme elevations and similar in intermediate zones, suggesting that the distribution of the species along different attitudes may be governed by soil variability (Coutinho et al., 2015). Similarly, altitude had a significant effect on the composition of the soil fungal communities associated with Norway spruce (*Picea abies*), whereas the age of the tree governs community diversity (Schön et al., 2018). Besides, altitude significantly impacts the relative abundances of the dominant phyla and classes of soil fungi and the interface of altitude and season affects the relative abundances of Ascomycota and Basidiomycota (Ji et al., 2021). While evaluating the variations in soil microbial community diversity and structure along five climate zones (from subtropical to cold temperate), with an altitude of 1,600–3,200 m across the eastern slope of Mount Gongga, Yang and Wu (2020) found that the soil bacterial but not fungal diversity changed across the vertical climate zones, with highest bacterial diversity occurring in subtropical and cold temperate zones. The fungal (composed of Ascomycota, Basidiomycota, and Zygomycota) and bacterial (composed of Proteobacteria, Acidobacteria, Actinobacteria, and Bacteroidetes) relative abundance enhanced with increasing altitude. No significant shifts in abundance or community composition were detected for archaeal community with altitude (Siles and Margesin, 2016). Thus, our results of altitudinal impact on tea-associated soil bacterial and fungal communities may be indirectly governed by physiochemical properties of the soil, seasonal effect, age of the tea plants, and interaction between altitude and climate along an altitudinal gradients.

In general, the relative abundance of both bacterial and fungal phyla did not change significantly with geographical locations. Acidobacteria and Proteobacteria were dominant bacterial phyla and Ascomycota and Basidiomycota were dominant fungal phyla at all the eight counties. The locations SJ and LX were peculiar for bacterial communities as they contained highest abundance of Actinobacteria and Chloroflexi, and *Arthrobacter, Bacillus*, and *Kitasatospora*. However, these sites have the lowest bacterial diversity. For fungi, CY and ZK were most peculiar with the former showing dominance of Ascomycota, *Amphinema*, and *Inocybe*, and the latter showing dominance of Basidiomycota and *Archaeorhizomyces.* ZK also showed the highest fungal diversity.

The environmental and geographic factors that sustain the soil microbes in tea plantations are important drivers of the composition and structure of soil microbial communities. Previous studies have found that the soil pH at tea plantation sites is a key factor influencing the bacterial and fungal community structure besides NO3-N, SOC, TOC SOM, and AP (Li Y. C. et al., 2016; Arafat et al., 2019; Tan et al., 2019). Zhao et al. (2012) found that based on limited data, relationships between environmental factors (pH) and tea plantation soil bacterial communities cannot be derived, and observed that the more alike the environmental variables are, the more similar is the bacterial community structure. Based on our results, we obtained somewhat similar patterns of bacterial and fungal communities across the environmental and geographic factors, with only a few phyla and genera showing a significant variation with these factors. Furthermore, Mantel test and Spearman correlation analyses revealed that latitude and altitude were more pronounced for the composition and structure of the bacterial communities (both at the phylum classification level and genus classification level) than those of the fungi, although the correlation was generally weak. Moreover, the analysis of the relative abundance and diversity (**Supplementary Figure S16**) of the bacterial and fungal communities in tea plantations distributed in anthropogenic versus inactive areas did not show any difference (**Supplementary Figure S16**).

The tea plantation sites have been under the management and selection of tea farmers for thousands of years. The composition and structure of the soil microbial community, and the correlation between its abundance and environmental and geographical factors have been artificially domesticated. The interference of anthropogenic activities is the main factor governing the fungal community selection, whereas for the bacterial community, it is more selective to the environmental adaptation, rather than the adaptation to human activities (**Supplementary Figure S16**).

DATA AVAILABILITY STATEMENT

The datasets presented in this study can be found in online repositories. The names of the repository/repositories and accession number(s) can be found in the article/ **Supplementary Material**.

AUTHOR CONTRIBUTIONS

LK, GX, YW, ZW, GL, DL, JY, SY, CW, LY, ShiZ, ShuZ, JZ, and TH collected the soil samples. GX, ZW, and CW performed the DNA extraction and quality control. GX and ZW performed the soil pH measurement. LK, GX, and ZW performed the data analysis and manuscript writing. AM, DL, WC, and JS revised and improved the manuscript. YD, LZ, HG, and JX directed the work. All authors provided ideas, participated in the evaluation of the results and discussion, read and approved the final manuscript.

FUNDING

This work was supported by Digitalization of Biological Resource Project (grant number 202002AA100007), Yunnan; Yunnan provincial key programs of Yunnan Eco-friendly Food International Cooperation Research Center project (grant number 2019ZG00908); and Yunnan Provincial Science and Technology Department Project (Development and Application of Biological Resource Digitalization) (grant number 2019008).

ACKNOWLEDGMENTS

We are grateful to have earnest cooperation from the tea farmers and government authorities in Lincang, Yunnan.

SUPPLEMENTARY MATERIAL

The Supplementary Material for this article can be found online at: https://www.frontiersin.org/articles/10.3389/fmicb.2021.745225/full#supplementary-material

Supplementary Figure S1 | Range of mean pH distribution of tea plantations soil.

Supplementary Figure S2 | Rarefaction curves of bacterial **(A)** and fungal **(B)** communities.

Supplementary Figure S3 | Relative abundance of soil bacterial and fungal communities in different pH groups. **(A)** Relative abundance of bacteria at the genus classification level (first 20 bacterial genus, same below); **(B)** relative abundance of fungi at the genus classification level (first 20 fungi genus, same below).

Supplementary Figure S4 | OTUs petal graph analyses of the soil bacterial **(A)** and fungal **(B)** communities in in different pH groups.

Supplementary Figure S5 | NMDS analysis of soil bacterial **(A)** and fungal **(B)** communities in different pH groups.

Supplementary Figure S6 | UPGMA cluster tree analysis of soil bacterial **(A)** and fungal **(B)** communities in different pH groups.

Supplementary Figure S7 | Relative abundance of soil bacterial and fungal communities in different altitudes groups. **(A)** Relative abundance of bacteria at the genus classification level; **(B)** relative abundance of fungi at the genus classification level.

Supplementary Figure S8 | OTUs petal graph analyses of the soil bacterial **(A)** and fungal **(B)** communities in different altitudes groups.

Supplementary Figure S9 | NMDS analysis of soil bacterial **(A)** and fungal **(B)** communities in different altitudes groups.

Supplementary Figure S10 | UPGMA cluster tree analysis of soil bacterial **(A)** and fungal **(B)** communities in different altitudes groups.

Supplementary Figure S11 | Relative abundance of soil bacterial and fungal communities in different regions groups. **(A)** Relative abundance of bacteria at the genus classification level; **(B)** relative abundance of fungi at the genus classification level.

Supplementary Figure S12 | OTUs petal graph analyses of the soil bacterial **(A)** and fungal **(B)** communities in in different regions groups.

Supplementary Figure S13 | NMDS analysis of soil bacterial **(A)** and fungal **(B)** communities in different regions groups.

Supplementary Figure S14 | UPGMA cluster tree analysis of soil bacterial **(A)** and fungal **(B)** communities in different regions groups.

Supplementary Figure S15 | Relative abundance of soil bacterial and fungal communities in 101 ancient tea plantations. **(A)** Relative abundance of bacteria at the phylum classification level (first 10 bacterial phylum, same below); **(B)** relative abundance of fungi at the phylum classification level (first 10 fungi phylum, same below). (ATP, ancient tea plantation).

Supplementary Figure S16 | Relative abundance and α-diversity indices of soil bacterial and fungal communities in human activity region and human inactive region. **(A)** Relative abundance of bacteria at the phylum classification level; **(B)** relative abundance of fungi at the phylum classification level; **(C)** Chao1 and Shannon indices of bacteria and fungi. Different lowercase letters indicate significant differences between subgroups ($P < 0.05$). (HAR, human activity region; HIR, human inactive region).

Supplementary Table S1 | Significance test by Anosim and MRPP of soil bacterial and fungal community in different pH gradient groups.

Supplementary Table S2 | Significance test by Anosim and MRPP of soil bacterial and fungal community in different altitudes groups.

Supplementary Table S3 | Significance test by Anosim and MRPP of soil bacterial and fungal community in different regions groups.

REFERENCES

Abarenkov, K., Nilsson, R. H., Larsson, K. H., Alexander, I. J., Eberhardt, U., Erland, S., et al. (2010). The UNITE database for molecular identification of fungi-recent updates and future perspectives. *New Phytol.* 186, 281–285. doi: 10.1111/j.1469-8137.2009.03160.x

Abe, S. S., Hashi, I., Masunaga, T., Yamamoto, S., Honna, T., and Wakatsuki, T. (2006). Soil profile alteration in a brown forest soil under high-input tea cultivation. *Plant Prod. Sci.* 9, 457–461. doi: 10.1626/pps.9.457

Alekseeva, T., Alekseev, A., Xu, R. K., Zhao, A. Z., and Kalinin, P. (2011). Effect of soil acidification induced by a tea plantation on chemical and mineralogical properties of Alfisols in eastern China. *Environ. Geochem. Health* 33, 137–148. doi: 10.1007/s10653-010-9327-5

Antoun, H., Beauchamp, C. J., Goussard, N., Chabot, R., and Lalande, R. (1998). Potential of rhizobium and bradyrhizobium species as plant growth promoting rhizobacteria on non-legumes: effect on radishes (*Raphanus sativus* L.). *Plant Soil* 204, 57–67. doi: 10.1023/A:1004326910584

Arafat, Y., Tayyab, M., Khan, M. U., Chen, T., Amjad, H., Awais, S., et al. (2019). Long-term monoculture negatively regulates fungal community composition and abundance of tea orchards. *Agronomy* 9:466. doi: 10.3390/agronomy9080466

Bai, L., Cui, J. Q., Jie, W. G., and Cai, B. Y. (2015). Analysis of the community compositions of rhizosphere fungi in soybeans continuous cropping fields. *Microbiol. Res.* 180, 49–56. doi: 10.1016/j.micres.2015.07.007

Bolyen, E., Rideout, J. R., Dillon, M. R., Bokulich, N. A., Abnet, C. C., Al-Ghalith, G. A., et al. (2019). Reproducible, interactive, scalable and extensible microbiome data science using QIIME 2. *Nat. Biotechnol.* 37, 852–857. doi: 10.1038/s41587-019-0252-6

Bryant, J. A., Lamanna, C., Morlon, H., Kerkhoff, A. J., Enquist, B. J., and Green, J. L. (2008). Microbes on mountainsides: contrasting elevational patterns of bacterial and plant diversity. *Proc. Natl. Acad. Sci. U.S.A.* 105, 1505–11511. doi: 10.1073/pnas.0801920105

Carrino-Kyker, S. R., Kluber, L. A., Petersen, S. M., Coyle, K. P., Hewins, C. R., DeForest, J. L., et al. (2016). Mycorrhizal fungal communities respond to experimental elevation of soil pH and P availability in temperate hardwood forests. *FEMS Microbiol. Ecol.* 92:fiw024. doi: 10.1093/femsec/fiw024

Choma, M., Bárta, J., Šantrůčková, H., and Urich, T. (2016). Low abundance of Archaeorhizomycetes among fungi in soil metatranscriptomes. *Sci. Rep.* 6:38455. doi: 10.1038/srep38455

Coutinho, E. S., Fernandes, G. W., Berbara, R. L., Valério, H. M., and Goto, B. T. (2015). Variation of arbuscular mycorrhizal fungal communities along an altitudinal gradient in rupestrian grasslands in Brazil. *Mycorrhiza* 25, 627–638. doi: 10.1007/s00572-015-0636-5

Dang, M. V. (2002). *Effects of Tea Cultivation on Soil Quality in the Northern Mountainous Zone, Vietnam*. Dissertation: University of Saskatchewan.

Edgar, R. C. (2004). MUSCLE: multiple sequence alignment with high accuracy and high throughput. *Nucleic Acids Res.* 32, 1792–1797. doi: 10.1093/nar/gkh340

Edgar, R. C. (2013). UPARSE: highly accurate OTU sequences from microbial amplicon reads. *Nat. Methods* 10, 996–998. doi: 10.1038/nmeth.2604

Fierer, N., Bradford, M. A., and Jackson, R. B. (2007). Toward an ecological classification of soil bacteria. *Ecology* 88, 1354–1364. doi: 10.1890/05-1839

Fierer, N., McCain, C. M., Meir, P., Zimmermann, M., Rapp, J. M., Silman, M. R., et al. (2011). Microbes do not follow the elevational diversity patterns of plants and animals. *Ecologya* 92, 797–804. doi: 10.1890/10-1170.1

Fung, K. F., Carr, H. P., Zhang, J. H., and Wong, M. H. (2008). Growth and nutrient uptake of tea under different aluminium concentration. *J. Sci. Food Agric.* 88, 1582–1591. doi: 10.1002/jsfa.3254

Gardes, M., and Bruns, T. D. (1993). ITS primers with enhanced specificity for basidiomycetes-application to the identification of mycorrhizae and rusts. *Mol. Ecol.* 2, 113–118. doi: 10.1111/j.1365-294x.1993.tb00005.x

Guo, J. H., Liu, X. J., Zhang, Y., Shen, J. L., Han, W. X., Zhang, W. F., et al. (2010). Significant acidification in major Chinese croplands. *Science* 327, 1008–1010. doi: 10.1126/science.1182570

Han, W., Kemmitt, S. J., and Brookes, P. C. (2007). Soil microbial biomass and activity in Chinese tea plantations of varying stand age and productivity. *Soil. Biol. Biochem.* 39, 1468–1478. doi: 10.1016/j.soilbio.2006.12.029

Ji, L., Yang, Y. C., and Yang, L. X. (2021). Seasonal variations in soil fungal communities and co-o ccurrence networks along an altitudinal gradient in the cold temperate zone of China: a case study on Oakley Mountain. *Catena* 204:105448. doi: 10.1016/j.catena.2021.105448

Jones, R. T., Robeson, M. S., Lauber, C. L., Hamady, M., Knight, R., and Fierer, N. (2009). A comprehensive survey of soil acidobacterial diversity using pyrosequencing and clone library analyses. *ISME J.* 3, 442–453. doi: 10.1038/ismej.2008.127

Koga, K., Suehiro, Y., Matsuoka, S. T., and Takahashi, K. (2003). Evaluation of growth activity of microbes in tea field soil using microbial calorimetry. *J. Biosci. Bioeng.* 954, 429–434. doi: 10.1016/S1389-1723(03)80040-3

Kumar, S., Suyal, D. C., Yadav, A., Shouche, Y., and Goel, R. (2019). Microbial diversity and soil physiochemical characteristic of higher altitude. *PLoS One.* 14:e0213844. doi: 10.1371/journal.pone.0213844

Li, J. B., Shen, Z. H., Li, C. N., Kou, Y. P., Wang, Y. S., Tu, B., et al. (2018). Stair-step pattern of soil bacterial diversity mainly driven by pH and vegetation types along the elevational gradients of gongga mountain, China. *Front. Microbiol.* 9:569. doi: 10.3389/fmicb.2018.00569

Li, S. Y., Li, H. X., Yang, C. L., Wang, Y. D., Xue, H., and Niu, Y. F. (2016). Rates of soil acidification in tea plantations and possible causes. *Agric. Ecosyst. Environ.* 233, 60–66. doi: 10.1016/j.agee.2016.08.036

Li, Y. C., Li, Z., Li, Z. W., Jiang, Y. H., Weng, B. Q., and Lin, W. X. (2016). Variations of rhizosphere bacterial communities in tea (Camellia sinensis L.) continuous cropping soil by high-throughput pyrosequencing approach. *J. Appl. Microbiol.* 1213, 787–799. doi: 10.1111/jam.13225

Liu, X., Zhang, J. L., Gu, T. Y., Zhang, W. M., Shen, Q. R., Yin, S. X., et al. (2014). Microbial community diversities and taxa abundances in soils along a seven-year gradient of potato monoculture using high throughput pyrosequencing approach. *PLoS One* 9:e86610. doi: 10.1371/journal.pone.0086610

Magoč, T., and Salzberg, S. L. (2011). FLASH: fast length adjustment of short reads to improve genome assemblies. *Bioinformatics* 27, 2957–2963. doi: 10.1093/bioinformatics/btr507

Mazzola, M., and Manici, L. M. (2012). Apple replant disease: role of microbial ecology in cause and control. *Annu. Rev. Phytopathol.* 50, 45–65. doi: 10.1146/annurev-phyto-081211-173005

Mendes, R., Kruijt, M., Bruijn, I. D., Dekkers, E., Voort, M. V. D., Schneider, J. H. M., et al. (2011). Deciphering the rhizosphere microbiome for disease-suppressive bacteria. *Science* 332, 1097–1100. doi: 10.1126/science.1203980

Na, X. F., Xu, T. T., Li, M., Zhou, Z. N., Ma, S. L., Wang, J., et al. (2018). Variations of bacterial community diversity within the rhizosphere of three phylogenetically related perennial shrub plant species across environmental gradients. *Front. Microbiol.* 9:709. doi: 10.3389/fmicb.2018.00709

Nottingham, A. T., Fierer, N., Turner, B. L., Whitaker, J., Ostle, N. J., McNamara, N. P., et al. (2018). Microbes follow humboldt: temperature drives plant and soil microbial diversity patterns from the amazon to the andes. *Ecology* 99, 2455–2466. doi: 10.1002/ecy.2482

Oh, K., Kato, T., Li, Z. P., and Li, F. Y. (2006). Environmental problems from tea cultivation in Japan and a control measure using calcium cyanamide. *Pedosphere* 16, 770–777. doi: 10.1016/S1002-0160(06)60113-6

Pandey, A., and Palni, L. M. S. (1996). The rhizosphere effect of tea on soil microbes in a Himalayan monsoonal location. *Biol. Fert. Soils* 21, 131–137. doi: 10.1007/BF00335924

Pandey, A., and Palni, L. M. S. (1997). Bacillus species: the dominant bacteria of the rhizosphere of established tea bushes. *Microbiol. Res.* 152, 359–365. doi: 10.1016/S0944-5013(97)80052-3

Pedan, V., Rohn, S., Holinger, M., Hühn, T., and Chetschik, I. (2018). Bioactive compound fingerprint analysis of aged raw Pu'er tea and young ripened Pu'er tea. *Molecules* 23:19. doi: 10.3390/molecules23081931

Philip, D. (2003). VEGAN, a package of R functions for community ecology. *J. Veg. Sci.* 14, 927–930. doi: 10.1111/j.1654-1103.2003.tb02228.x

Pinto-Figueroa, E. A., Seddon, E., Yashiro, E., Buri, A., Niculita-Hirzel, H., Meer, J. R., et al. (2019). Archaeorhizomycetes spatial distribution in soils along wide elevational and environmental gradients reveal co-abundance patterns with other fungal saprobes and potential weathering capacities. *Front. Microbiol.* 10:656. doi: 10.3389/fmicb.2019.00656

Qiu, S. L., Wang, L. M., Huang, D. F., and Lin, X. J. (2014). Effects of fertilization regimes on tea yields, soil fertility, and soil microbial diversity. *Chil. J. Agr. Res.* 743, 333–339. doi: 10.4067/S0718-58392014000300012

Quaiser, A., Ochsenreiter, T., Lanz, C., Schuster, S. C., Treusch, A. H., Eck, J., et al. (2003). Acidobacteria form a coherent but highly diverse group within the bacterial domain: evidence from environmental genomics. *Mol. Microbiol.* 50, 563–575. doi: 10.1046/j.1365-2958.2003.03707.x

Quast, C., Pruesse, E., Yilmaz, P., Gerken, J., Schweer, T., Yarza, P., et al. (2013). The SILVA ribosomal RNA gene database project: improved data processing and web-based tools. *Nucleic Acids Res.* 41, D590–D596. doi: 10.1093/nar/gks1219

R Core Team. (2020). *R: A Language and Environment for Statistical Computing. R Foundation for Statistical Computing*. Vienna: R Core Team.

Raaijmakers, J. M., and Mazzola, M. (2016). Soil immune responses. *Science* 352, 1392–1393. doi: 10.1126/science.aaf3252

Rousk, J., Bååth, E., Brookes, P. C., Lauber, C. L., Lozupone, C., Caporaso, J. G., et al. (2010). Soil bacterial and fungal communities across a pH gradient in an arable soil. *ISME J.* 4, 1340–1351. doi: 10.1038/ismej.2010.58

Ruan, J. Y., Gerendás, J., Härdter, R., and Sattelmacher, B. (2007). Effect of nitrogen form and root-zone pH on growth and nitrogen uptake of tea (*Camellia sinensis*) plants. *Ann. Bot.* 99, 301–310. doi: 10.1093/aob/mcl258

Schön, M. E., Nieselt, K., and Garnica, S. (2018). Belowground fungal community diversity and composition associated with Norway spruce along an altitudinal gradient. *PLoS One* 13:e0208493. doi: 10.1371/journal.pone.0208493

Sharma, V. S., and Kumudini, M. T. (2018). *Global Tea Science: Current Status and Future Needs*. Cambridge: Burleigh Dodds Science Publishing.

Shen, C. C., Ni, Y. Y., Liang, W. J., Wang, J. J., and Chu, H. Y. (2015). Distinct soil bacterial communities along a small-scale elevational gradient in alpine tundra. *Front. Microbiol.* 6:582. doi: 10.3389/fmicb.2015.00582

Siles, J. A., and Margesin, R. (2016). Abundance and diversity of bacterial, archaeal, and fungal communities along an altitudinal gradient in alpine forest soils: what are the driving factors? *Microb. Ecol.* 72, 207–220. doi: 10.1007/s00248-016-0748-2

Singh, D., Takahashi, K., Kim, M., Chun, J., and Adams, J. M. (2012). A hump-backed trend in bacterial diversity with elevation on mount fuji, Japan. *Microb. Ecol.* 63, 429–437. doi: 10.1007/s00248-011-9900-1

Singh, S., Sood, A., Sharma, S., Kumar, V., Singh, K. D., and Pandey, P. (2007). Studies on rhizospheric mycoflora of tea Camellia sinensis: in vitro antagonism with dominant bacteria. *Chin. J. Appl. Environ. Biol.* 13, 357–360.

Song, X. H., Pan, Y., Li, L. Y., Wu, X. L., and Wang, Y. (2018). Composition and diversity of rhizosphere fungal community in Coptis Chinensis Franch. Continuous cropping fields. *PLoS One* 13:e0193811. doi: 10.1371/journal.pone.0193811

Stephen, W., Ryan, D. P., Lindsay, B., Nicholas, A. P., and Sunil, K. P. (2017). *Kappaphycus alvarezii* as a food supplement prevents diet-induced metabolic syndrome in rats. *Nutrients* 9:1261. doi: 10.3390/nu9111261

Taha, M., Salama, A., El-Seedy, M., and Elakhdar, I. (2016). Potential impact of compost tea on soil microbial properties and performance of radish plant under sandy soil conditions-greenhouse experiments. *Aust. J. Basic. Appl. Sci.* 10, 158–165.

Tan, L., Gu, S. S., Li, S., Ren, Z. H., Deng, Y., Liu, Z. H., et al. (2019). Responses of microbial communities and interaction networks to different management practices in tea plantation soils. *Sustainability* 11:4428. doi: 10.3390/su11164428

Tian, J. Q., Wu, B., Chen, H., Jiang, N., Kang, X. M., and Liu, X. Z. (2017). Patterns and drivers of fungal diversity along an altitudinal gradient on mount gongga, China. *J. Soils Sediments.* 17, 2856–2865. doi: 10.1007/s11368-017-1701-9

Urbina, H., Breed, M. F., Zhao, W. Z., Gurrala, K. L., Andersson, S. G. E., Agren, J., et al. (2018). Specificity in Arabidopsis thaliana recruitment of root fungal

communities from soil and rhizosphere. *Fungal Biol.* 122, 231–240. doi: 10.1016/j.funbio.2017.12.013

Wang, H., Xu, R. K., Wang, N., and Li, X. H. (2010). Soil acidification of Alfisols as influenced by tea cultivation in eastern China. *Pedosphere* 20, 799–806. doi: 10.1016/S1002-0160(10)60070-7

Wang, J. J., Soininen, J., Zhang, Y., Wang, B. X., Yang, X. D., and Shen, J. (2011). Contrasting patterns in elevational diversity between microorganisms and macroorganisms. *J. Biogeogr.* 38, 595–603. doi: 10.1111/j.1365-2699.2010.02423.x

Wang, Y. S., Li, C. N., Shen, Z. H., Rui, J. P., Jin, D. C., Li, J. B., et al. (2019). Community assemblage of free-living diazotrophs along the elevational gradient of mount gongga. *Soil. Ecol. Lett.* 1, 136–146. doi: 10.1007/s42832-019-0013-y

Widden, P. (2018). Fungal communities in soils along an elevation gradient in northern england. *Mycologia* 79, 298–309. doi: 10.1080/00275514.1987.12025708

Wilson, M. J., He, Z. L., and Yang, X. E. (2004). "The red soils of China: their nature, management and utilization," in *Soil Acidification Under Tea Bushes and Its Influence on The Biological Characteristics of a Red Soil*, ed. S. Yu (Berlin: Springer Netherlands), 331–345.

Xue, D., Huang, X. D., Yao, H. Y., and Huang, C. Y. (2010). Effect of lime application on microbial community in acidic tea orchard soils in comparison with those in wasteland and forest soils. *J. Environ. Sci.* 22, 1253–1260. doi: 10.1016/S1001-0742(09)60246-1

Xue, D., Yao, H. Y., and Ge, D. Y. (2008). Soil Microbial community structure in diverse land use systems: a comparative study using biolog, DGGE, and PLFA analyses. *Pedosphere* 18, 653–663. doi: 10.1016/S1002-0160(08)60060-0

Xue, D., Yao, H. Y., and Huang, C. Y. (2006). Microbial biomass, N mineralization and nitrification, enzyme activities, and microbial community diversity in tea orchard soils. *Plant Soil* 288, 319–331. doi: 10.1007/s11104-006-9123-2

Xue, D., Yao, H. Y., and Huang, C. Y. (2007). Genetic diversity of microbial communities in tea orchard soil. *Ying Yong Sheng Tai Xue Bao.* 18, 843–847.

Yan, P., Shen, C., Fan, L. C., Li, X., Zhang, L. P., Zhang, L., et al. (2018). Tea planting affects soil acidification and nitrogen and phosphorus distribution in soil. *Agric. Ecosyst. Environ.* 254, 20–25. doi: 10.1016/j.agee.2017.11.015

Yan, P., Wu, L. Q., Wang, D. H., Fu, J. Y., Shen, C., Li, X., et al. (2020). Soil acidification in Chinese tea plantations. *Sci. Tot. Environ.* 715:136963. doi: 10.1016/j.scitotenv.2020.136963

Yang, X. D., Ni, K., Shi, Y. Z., Yi, X. Y., Zhang, Q. F., Fang, L., et al. (2018). Effects of long-term nitrogen application on soil acidification and solution chemistry of a tea plantation in China. *Agric. Ecosyst. Environ.* 252, 74–82. doi: 10.1016/j.agee.2017.10.004

Yang, Y. J., and Wu, P. F. (2020). Soil bacterial community varies but fungal community stabilizes along five vertical climate zones. *Catena* 195:104841. doi: 10.1016/j.catena.2020.104841

Yao, H., He, Z., Wilson, M. J., and Campbell, C. D. (2000). Microbial biomass and community structure in a sequence of soils with increasing fertility and changing land use. *Microb. Ecol.* 40, 223–237. doi: 10.1007/s002480000053

Zhang, H. M., Wang, C. F., Shen, S. M., Wang, G. L., Liu, P., Liu, Z. M., et al. (2012). Antioxidant phenolic compounds from Pu-erh tea. *Molecules* 17, 14037–14045. doi: 10.3390/molecules171214037

Zhao, J., Wu, X. B., Nie, C. P., Wu, T., Dai, W. H., Liu, H., et al. (2012). Analysis of unculturable bacterial communities in tea orchard soils based on nested PCR-DGGE. *World J. Microbiol. Biotechnol.* 28, 1967–1979. doi: 10.1007/s11274-011-0999-5

Zhao, Q. Y., Xiong, W., Xing, Y. Z., Sun, Y., Lin, X. J., and Dong, Y. P. (2018). Long-term coffee monoculture alters soil chemical properties and microbial communities. *Sci. Rep.* 8:6116. doi: 10.1038/s41598-018-24537-2

Zhou, X. G., and Wu, F. Z. (2012). p-Coumaric acid influenced cucumber rhizosphere soil microbial communities and the growth of *Fusarium oxysporum* f.sp. *cucumerinum* Owen. *PLoS One* 7:e48288. doi: 10.1371/journal.pone.0048288

Conflict of Interest: The authors declare that the research was conducted in the absence of any commercial or financial relationships that could be construed as a potential conflict of interest.

Publisher's Note: All claims expressed in this article are solely those of the authors and do not necessarily represent those of their affiliated organizations, or those of the publisher, the editors and the reviewers. Any product that may be evaluated in this article, or claim that may be made by its manufacturer, is not guaranteed or endorsed by the publisher.

frontiers in Microbiology

ORIGINAL RESEARCH
published: 21 October 2021
doi: 10.3389/fmicb.2021.747541

Modulating Drought Stress Response of Maize by a Synthetic Bacterial Community

*Jaderson Silveira Leite Armanhi[1,2], Rafael Soares Correa de Souza[1,2], Bárbara Bort Biazotti[1,2,3], Juliana Erika de Carvalho Teixeira Yassitepe[2,4] and Paulo Arruda[1,2,3]**

[1] Centro de Biologia Molecular e Engenharia Genética, Universidade Estadual de Campinas (UNICAMP), Campinas, Brazil, [2] Genomics for Climate Change Research Center (GCCRC), Universidade Estadual de Campinas (UNICAMP), Campinas, Brazil, [3] Departamento de Genética e Evolução, Instituto de Biologia, Universidade Estadual de Campinas (UNICAMP), Campinas, Brazil, [4] Embrapa Informática Agropecuária, Campinas, Brazil

Plant perception and responses to environmental stresses are known to encompass a complex set of mechanisms in which the microbiome is involved. Knowledge about plant physiological responses is therefore critical for understanding the contribution of the microbiome to plant resilience. However, as plant growth is a dynamic process, a major hurdle is to find appropriate tools to effectively measure temporal variations of different plant physiological parameters. Here, we used a non-invasive real-time phenotyping platform in a one-to-one (plant–sensors) set up to investigate the impact of a synthetic community (SynCom) harboring plant-beneficial bacteria on the physiology and response of three commercial maize hybrids to drought stress (DS). SynCom inoculation significantly reduced yield loss and modulated vital physiological traits. SynCom-inoculated plants displayed lower leaf temperature, reduced turgor loss under severe DS and a faster recovery upon rehydration, likely as a result of sap flow modulation and better water usage. Microbiome profiling revealed that SynCom bacterial members were able to robustly colonize mature plants and recruit soil/seed-borne beneficial microbes. The high-resolution temporal data allowed us to record instant plant responses to daily environmental fluctuations, thus revealing the impact of the microbiome in modulating maize physiology, resilience to drought, and crop productivity.

Keywords: SynCom, plant microbiome, plant phenotyping, drought stress, maize, plant growth-promoting, PGP, synthetic microbial community

OPEN ACCESS

Edited by:
Hui Li,
Jinan University, China

Reviewed by:
Kai Xue,
University of Chinese Academy of Sciences, China
Anamika Dubey,
Dr. Hari Singh Gour University, India

****Correspondence:***
Paulo Arruda
parruda@unicamp.br

Specialty section:
This article was submitted to Terrestrial Microbiology, a section of the journal Frontiers in Microbiology

Received: *26 July 2021*
Accepted: *20 September 2021*
Published: *21 October 2021*

Citation:
Armanhi JSL, de Souza RSC, Biazotti BB, Yassitepe JEdCT and Arruda P (2021) Modulating Drought Stress Response of Maize by a Synthetic Bacterial Community. Front. Microbiol. 12:747541. doi: 10.3389/fmicb.2021.747541

INTRODUCTION

Crop plants are continuously challenged by adverse environmental conditions that can severely impact their productivity. As sessile organisms, plants have evolved genetically encoded mechanisms to efficiently thrive in adverse circumstances. Breeders have explored the genetic variability associated with tolerance against drought and heat stresses, which are among the most limiting factors for crop production (Lesk et al., 2016). However, genetically encoded water usage traits alone may not be sufficient to make plants better adapt to water restriction and high

temperature conditions. Microbial communities associated with plant roots, stems and leaves have also been shown to play a fundamental role in shaping plant responses to biotic and abiotic stresses and modulating plant phenotypic plasticity (Compant et al., 2019; Vannier et al., 2019; Beirinckx et al., 2020; Chai et al., 2021).

Plants and their associated microbiome have coevolved over a million years under adverse environmental conditions. During this process, evolution may have favored plants recruiting microbial communities that positively affected their fitness by providing or modulating beneficial functions related to phytohormone balance, plant adaptation to drought, nutrition uptake, and disease suppression (Zilber-Rosenberg and Rosenberg, 2008; Lemanceau et al., 2017; Chaudhry et al., 2021). This scenario implies that plants cannot be studied as isolated entities but rather as a unit formed by the plant and its associated microbiome, the holobiont (Vandenkoornhuyse et al., 2015). However, with the exception of few cases, such as nitrogen fixation and phytohormones production (Carvalho et al., 2014), there is little knowledge regarding other modes by which microbes can influence plant phenotypic plasticity.

Investigating how plant–microbe interactions affect plant responses and physiology requires multidisciplinary approaches that allow the integration of different types of data from both the plant and its microbiome (de Souza et al., 2020). The broad concept of plant phenotyping implies the understanding of plant physiological, morphological and biochemical status by methods capable of quantifying relevant plant traits. An increased number of phenotyping platforms have been designed, reducing both time and costs by automating plant cultivation and assessment (Fiorani and Schurr, 2013). However, as plant growth is a dynamic process, common phenotyping strategies lack the ability to monitor plant physiological parameters in real time (Halperin et al., 2017; Rouphael et al., 2018). In most cases, these platforms rely on limited frequency of measures or unsynchronized data points as plants are evaluated individually and during distinct periods. A comprehensive physiological evaluation demands a continuous time series to acquire a detailed physiological profile of each individual plant at the same time points.

We have previously shown that a synthetic community (SynCom) composed of naturally occurring, highly abundant bacteria from the sugarcane root and stalk core microbiomes increased biomass and enhanced root system development of early-stage maize (*Zea mays* L.) plants (de Souza et al., 2016; Armanhi et al., 2018). Here, we investigated the impact of this SynCom on the physiological behavior and yield of mature maize plants under drought conditions. We developed an automated and non-invasive real-time phenotyping platform to evaluate both plant performance and physiological responses in a one-to-one (plant–sensors) set up throughout the entire plant life cycle. The continuous monitoring of individual plants produced high-quality data and images with resolution sufficient to inspect small variations in plant physiological parameters of biological relevance. SynCom was found to modulate plant leaf temperature (T_{leaf}) and water usage with significant differences among plant genotypes. The results were discussed in the context of expanding our comprehension of crop functional trait responses for the mitigation of environmental stresses toward developing microbiome technologies for agricultural sustainability.

MATERIALS AND METHODS

Plant Material, Experimental Conditions and Inoculation

Seeds of the three commercial maize hybrids DKB177 PRO3 (Monsanto, Brazil), SX7341 VIP3 (Syngenta, Brazil), and P3707VYH (DuPont Pioneer, Brazil) were purchased and stored at 4°C prior to sowing. These hybrids were chosen because of their high yield potential and for being locally adopted by farmers when the experiment was set up. The experiments were installed in a 90-m^2 netted greenhouse facility of the School of Agricultural Engineering at the University of Campinas (22°49′11.94″ S 47°3′40.96″ W) under natural environmental conditions from late August to mid-December 2018. The experimental period was counted as days after sowing (DAS) starting on the day seeds were sown (0 DAS) to plant harvesting (117 DAS). From 1 to 65 DAS, the photoperiod was extended until 8:00 pm with halogen bulbs PAR38 100 W (FLC, Brazil) at a density of 1 bulb m^{-2}. Plants were grown in 18-L pots filled with a commercial substrate (Biogrow, Brazil) modified to contain a 7:1 sphagnum:perlite mixture (Agrolink, Brazil). Pots were fertilized with PG MIX 14-16-18 (Yara, Norway) and Osmocote 15-9-12 (ICL Specialty Fertilizers, Summerville, SC, United States) before planting according to suppliers' recommendations for maize. Three seeds were sown per pot, but only the best developed seedling was kept after 9 DAS. A total of 432 pots were distributed along the greenhouse in a twin row experimental design (**Supplementary Figure 1**) and irrigated once a day (at 8:20 am) with ∼430 mL of water by an automated piped system settled at 72 mL min^{-1} from 0 to 56 DAS and three times a day (at 8:20 am, 10:20 am, and 6:20 pm) with the same volume of water each time from 57 to 117 DAS. Plants were subjected to well watering (WW) or drought stress (DS) conditions. WW-treated plants received the full irrigation schedule during all experiments, unless otherwise mentioned. On cloudy days, irrigation was reduced to half the volume to avoid overwatering plants. DS-treated plants received full irrigation until 49 DAS and were then subjected to a 50% WW regime (50–52 DAS), followed by 25% WW (53–80 DAS). Plants were at the V10–V11 stage when exposed to DS. Plants under DS were then rehydrated using the full irrigation regime in the early evening at 80 DAS. Due to occasional rain that increased air relative humidity (RH) to 100%, irrigation was suspended from 61 to 65 DAS and reduced to half from 88 to 108 DAS for all treatments. Plants used for time-lapse imaging were grown under the same abovementioned conditions and exposed to severe drought stress (SDS) (complete water withdrawal from 50 to 84 DAS), with rehydration performed at 84 DAS until full recovery.

In this work, we used a SynCom assembled by mixing naturally occurring, highly abundant bacterial strains from the sugarcane root and stalk core microbiomes that were shown to robustly colonize maize plants (de Souza et al., 2016; Armanhi et al., 2018). As previously described, the SynCom was prepared

by individually growing 17 community-based isolates from the sugarcane Community-Based Culture Collection (CBC) in liquid culture media to late exponential phase and pooled in equal concentration based on optical density (OD) (Armanhi et al., 2018). Bacterial pellets were washed and resuspended in 0.1× Hoagland's solution to reach the final $OD_{620\ nm}$ of 0.6. Seeds of the three commercial maize hybrids were soaked in SynCom solution for 3 h prior to sowing. Uninoculated seeds were soaked in sterile 0.1× Hoagland's solution. After planting, 1 mL of the SynCom solution was pipetted over each seed in each individual pot, while uninoculated seeds received the same volume of sterile 0.1× Hoagland's solution.

The number of emerged seedlings was counted daily in every pot from 3 to 7 DAS. In mature plants, days to anthesis and to silking were considered at the first sign of shedding pollen and extruding silks from the husk, respectively, as observed daily from 70 to 86 DAS. Statistical analyses of seedling emergence timing and reproductive stages of plants were performed by unpaired *t*-test. The flowering time was registered for plants with both anthesis and silking, and plants that lacked pollen shedding (hidden tassel in the whorl or not extruded anthers) or silk extrusion were considered flowerless. The effect of SynCom inoculation on the total number of flowering plants was considered significant when the number of flowering plants was exceeded by 10% the number of flowerless plants.

Plant Sampling, DNA Extraction and 16S rRNA Gene Sequencing for Microbial Profiling

Microbial profiling was performed as previously described (de Souza et al., 2016; Armanhi et al., 2018), with bacterial communities associated with plant roots assessed through 16S profiling using roots sampled from 4 plants (biological replications) per treatment harvested at stages V11–V12 (53 DAS). Plant roots were cleaned of soil excess by hand shaking, then frozen in liquid nitrogen. Cryopreserved samples were ground under cryogenic conditions in a stirred bead mill. DNA of powdered samples was extracted, and V4 16S regions were amplified. Libraries were sequenced in a MiSeq sequencing platform using reagent kit v3 in a 2 × 300 run (Illumina, San Diego, CA, United States). Bacterial taxonomic assignment was performed using the software SYNTAX (Edgar, 2016) and the SILVA v123 database (Quast et al., 2013). Enrichment and depletion of microbial groups were assessed by comparing the differential relative abundance of each operational taxonomic unit (OTU) between microbial profiles of inoculated and uninoculated with a Kruskal–Wallis test with $P < 0.05$. The same test was performed to detect robustness of colonization by comparing the abundance of SynCom OTUs in inoculated and uninoculated plants using a data analysis pipeline previously described (Armanhi et al., 2018).

Harvesting and Assessment of Plant Traits

Apart from plants sampled for microbial profiling, the remaining 10 plants per treatment were harvested at maturity at 117 DAS. For plant biomass estimation, the aerial parts of individual plants and ears were dried at 65°C for 7 days. Kernels were manually removed from the cob, counted and weighed. Yield per plant was considered the weight of grains per plant. The harvest index (HI), in %, was considered as follows:

$$\mathrm{HI} = \frac{\text{mean grain yield}}{\text{mean total aboveground biomass}}$$

where both mean grain yield and mean total aboveground biomass are expressed in grams (Hütsch and Schubert, 2018). All collected data from individual inoculated and uninoculated plants were evaluated for normality by the Shapiro–Wilk test and for homogeneity of variances by Levene's test. The statistical significance of the phenotypic values was determined for all parameters using a three-way ANOVA with the following factors: genotype, irrigation regime, inoculation and all their possible interactions. Mean values were compared when significant factors or interactions were observed using Tukey's test. Statistical analyses were performed using RStudio v4.0.3 (RStudio Team, 2020) and the package "agricolae" (de Mendiburu, 2020).

Monitoring of Environmental Conditions

Environmental conditions were collected by four stations placed along the greenhouse. Air temperature (°C) and RH (%) were measured using DHT22 sensors (Adafruit, New York, NY, United States), while light intensity was captured through BH1750FVI sensors (Adafruit, New York, NY, United States) (**Supplementary Figures 2A,B**). DHT22 was placed on fixed stations 3 m above the ground, while BH1750FVI was placed on moving platforms vertically adjusted at the same level as the plant canopy (**Supplementary Figure 2C**). Light intensity was collected in lux and converted to photosynthetically active radiation (PAR) (μmol m^{-2} s^{-1}) using the correction factor of 0.0185×. Data from environmental sensors were taken by each station every 15 min and stored in a data logger for further analyses. Vapor-pressure deficit (VPD) (kPa) was determined for each data point using the Arden–Buck equation (Buck, 1981), as follows:

$$\mathrm{VPD} = \left(1-\frac{\mathrm{RH}}{100}\right) \times 0.61121 \times \exp\left(\frac{17.502\times \mathrm{T}}{240.97+\mathrm{T}}\right)$$

where T is the air temperature (°C) and RH is the air relative humidity (0–100%). In downstream analyses, data points of all environmental variables were grouped every 30 min, and average values were calculated considering data from all four stations. Outliers were removed based on Tukey's interquartile range (IQR) method.

Monitoring of Plant Physiological Parameters

Forty-eight plants were individually equipped with a set of sensors for T_{leaf}, sap flow and soil water content (SWC). Data were collected for all monitored plants every 5 min and stored in individual data loggers prepared for each plant. T_{leaf} was measured using a 10 K-ohm thermistor placed in the center of a 2×2-cm squared 1-mm-thick cork. The sensor was placed onto the abaxial surface of the 8th leaf of plants 15 cm from

the leaf collar (**Supplementary Figures 2D,E**). Xylem sap flow was measured following the heat dissipation method (Granier, 1987) (**Supplementary Figure 2F**). The water flow upward in plant stalks was considered sap flow. SWC was measured through capacitive soil moisture sensors v1.2 (Adafruit, New York, NY, United States) (**Supplementary Figure 2G**). Data points from each individual sensor type were further rounded every 30 min, in accordance with the environmental data, with averages calculated and outliers removed from the four biological replicates.

Connectivity, Data Retrieval, Automated Image Capture and Time-Lapse Movie

Data from all environmental and physiological parameter sensors were automatically collected by Arduino Uno boards (Arduino, Italy) gathered in a Raspberry Pi 3 model B+ microcontroller (Raspberry Pi Foundation, United Kingdom) using custom scripts written in Python for data communication. Images were automatically captured by custom scripts run in Raspberry Pi. High-resolution RGB images were taken using a 20-MP digital camera Coolpix S3700 (Nikon, Japan) every 10 min during all experiments. The frequency of image capture was increased to every 3 min during DS and every 2 min during plant recovery to maximize the resolution of analysis during these periods. Two cameras were simultaneously allocated to record images for the time-lapse movie and the entire experimental setup. A time-lapse movie was generated using the open-source multimedia software FFmpeg[1].

Data Analysis, Graphs and Figures

All data points collected from sensors were analyzed in a processing pipeline written in Python v3.7.1 run in Jupyter notebook v4.4.0 (Kluyver et al., 2016). Data management and mathematical functions were performed using Pandas v0.23.4 (McKinney and Sheaffer-Jones, 2010), NumPy v1.15.4 (van der Walt et al., 2011), and SciPy v1.1.0 (Jones et al., 2001) libraries. **Figures 3–5**, and **Supplementary Figures 6A**, **7A–C**, **8–10** were prepared using the Matplotlib v3.0.2 (Hunter, 2007) library. **Figures 2**, **6A,B**, and **Supplementary Figures 4**, **5**, **11** were drawn in GraphPad Prism v8.2.0 (GraphPad Software, San Diego, CA, United States)[2]. All figures were prepared with the effective use of colors to help people with low visual acuity or color blindness.

RESULTS

Time-Lapse Imaging Records Differences in Plant Behavior Induced by Synthetic Community Inoculation in Commercial Maize Hybrids Under Severe Drought

A SynCom assembled with bacterial strains highly abundant in sugarcane root and stalk core microbiomes was previously shown to robustly colonize plant organs, improve root architecture and increase the biomass of young maize plants (Armanhi et al., 2018; de Souza et al., 2019). Here, we asked whether this SynCom also elicits drought tolerance in mature maize plants. For this purpose, we set an experiment to evaluate whether there were differences between SynCom-inoculated and uninoculated plants under SDS. Three commercial maize hybrids (DKB177, SX7341, and P3707VYH) were grown under a regular watering regime until 50 DAS, from which they were subjected to complete water withdrawal for 34 days, followed by rehydration. To closely observe the response of each hybrid, plants were monitored by high-resolution RGB imaging every 3 min during SDS and every 2 min during rehydration (**Supplementary Movie 1**).

All plants, inoculated or not, displayed leaf rolling and unrolling in response to daily temperature and RH changes. After 26 days of SDS (76 DAS), leaf rolling movements increased in frequency, and leaves were maintained permanently rolled inward for SX7341 and P3707VYH (**Supplementary Figures 3A,B**). After 28 days of SDS (78 DAS), all hybrids exhibited strong signals of stress characterized by leaf bending, a symptom that intensified over the following days (**Figure 1A** and **Supplementary Figure 3C**).

In general, under SDS, the stalks of uninoculated plants bent before those of inoculated plants. The uninoculated P3707VYH plants displayed the first bending response, starting after 30 days of SDS (80 DAS) and being completely bent at 81 DAS (**Figure 1B** and **Supplementary Figure 3D**). The stalks of the uninoculated DKB177 and SX7341 plants were completely bent by 83 DAS (**Figure 1C** and **Supplementary Figures 3E,F**). SynCom inoculation delayed stalk bending in P3707VYH by 1 day (**Supplementary Figure 3D**). Interestingly, the inoculated SX7341 plants did not show a clear difference in the timing of stalk bending when compared with uninoculated plants, although the effect of SDS was less severe in SynCom-inoculated plants (**Figure 1C** and **Supplementary Figure 3F**). At later stages of SDS treatment (34 days of SDS; 84 DAS), all uninoculated plants bent as a response to turgor loss due to severe water deficit. The inoculated P3707VYH plants completely bent at 34 days of SDS, while the inoculated SX7341 plants partially bent. Interestingly, the inoculated DKB177 plants did not bend even at the most severe stage of water deficit (**Supplementary Figure 3G**).

After rewatering at 84 DAS, the inoculated SX7341 plants immediately recovered and straightened out, an effect only observed 1 day later for their uninoculated counterpart. Similar behavior was found for the P3707VYH plants, although inoculated plants were only completely recovered from bending 2 days after rewatering (86 DAS). Nevertheless, uninoculated SX7341 and P3707VYH plants were unable to completely recover upon rehydration, as their stalks remained partially bent. The hybrid DKB177 was the most responsive to inoculation. Despite the fact that the leaves of both inoculated and uninoculated DKB177 plants remained greener and unrolled, rehydration had no effect on recovering the turgor of the uninoculated plants. In contrast, the inoculated DKB177 plants remained completely straightened during SDS and recovery (**Figure 1D** and **Supplementary Figure 3H**). The effect of SDS and recovery upon rehydration can be seen in the time-lapse video recorded from

[1] http://www.ffmpeg.org

[2] www.graphpad.com

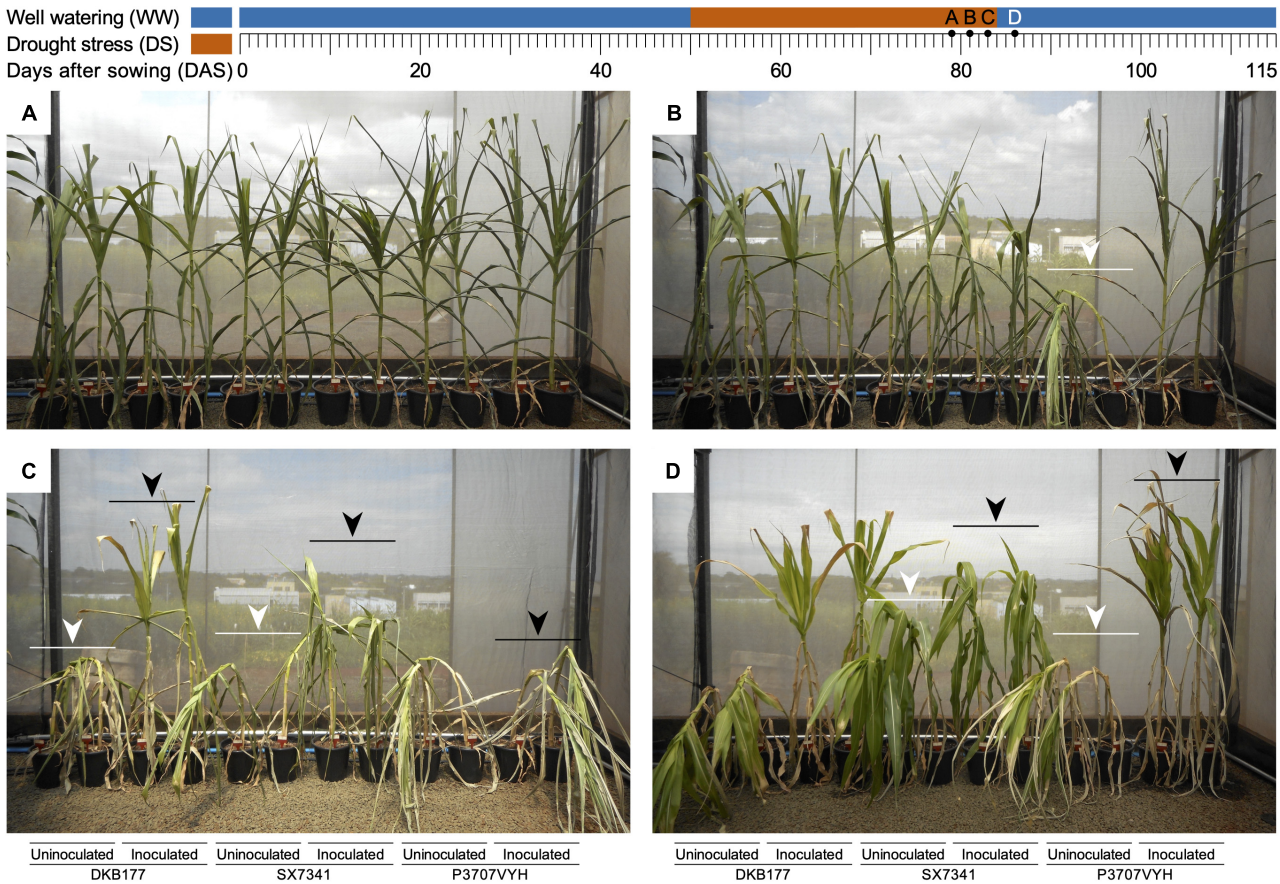

FIGURE 1 | A SynCom containing beneficial microbes induces a physiological response against DS in three commercial maize hybrids. **(A)** Plants kept in SDS for 29 days (79 DAS) had their leaves rolled inward, and older leaves fell for all hybrids, regardless of whether they were inoculated. **(B)** P3707VYH was the less tolerant hybrid in the absence of SynCom, completely bent after 31 days of SDS (81 DAS), in contrast to the inoculated hybrid (white arrow). **(C)** Uninoculated DKB177 and SX7341 were completely bent (83 DAS), as shown by the white arrows. In the presence of SynCom, plants were maintained in a straight position (DKB177) and partially or completely bent (SX7341 and P3707VYH, respectively), as shown by the black arrows. **(D)** Inoculated plants (SX7341 and particularly P3707VYH) straightened 2 days after rewatering (86 DAS; black arrows), while uninoculated plants were not capable of completely recovering their structure (white arrows). Detailed results are shown in **Supplementary Figure 3** and **Supplementary Movie 1**. WW, well watering; DS, drought stress; DAS, days after sowing; SDS, severe drought stress.

the late stage of water restriction until complete recovery after rewatering (**Supplementary Movie 1**).

Synthetic Community Inoculation Reduces the Yield Loss of Commercial Maize Hybrids Under Drought Stress

To better understand the mechanisms underlying plant growth promotion and abiotic stress tolerance induced by SynCom inoculation, we designed a second experiment to dissect the physiological parameters, yield components and colonization patterns of maize hybrids under DS (**Supplementary Figure 1**). The plants subjected to DS were well watered until 50 DAS, from which they were subjected to a reduced irrigation regime until 80 DAS. We intentionally applied DS in early reproductive stages when plants were most susceptible to drought.

Overall, the germination rate was not affected by SynCom inoculation, except for DKB177, which showed a slight reduction in the number of emerged seedlings per pot. Among all three hybrids, only SX7341 presented uniformity in seedling emergence whether inoculated or not. Particularly for P3707VYH, SynCom inoculation delayed seedling emergence without reducing the total number of emerged seedlings (**Supplementary Figures 4A–C**). The anthesis occurred from 70 to 86 DAS. Both anthesis and silking were delayed by DS, with inoculation having no significant effect on synchrony between flowering times. Pollen shedding started at 70–76 DAS under WW and 80–85 DAS under DS conditions, with an average delay of 9 days regardless of inoculation. DS-treated plants also delayed silking by 8 days, on average, with silks extruded from 71 to 78 and 81 to 86 DAS for WW- and DS-treated plants, respectively (**Supplementary Figures 4D,E**). No significant differences in anthesis-silking interval (ASI) between inoculated and uninoculated plants were observed. Although few plants did not shed pollen or did not extrude silks, these characteristics were not influenced by SynCom inoculation under WW conditions.

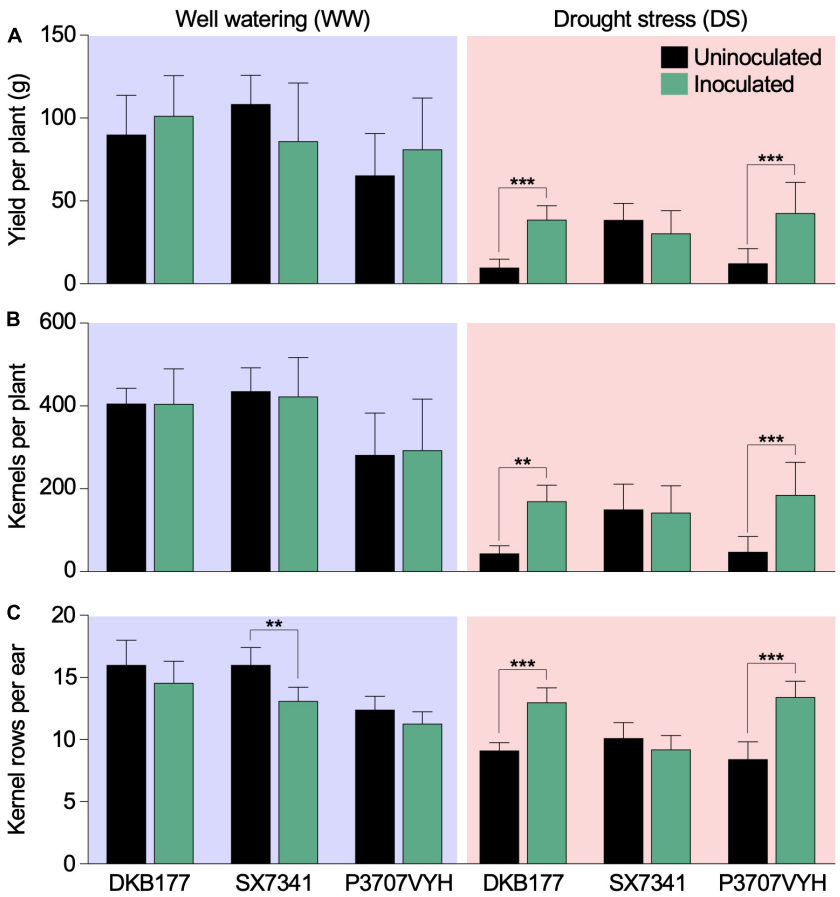

FIGURE 2 | Synthetic community (SynCom) inoculation reduces the yield loss of commercial maize hybrids under DS. During DS, inoculated DKB177 and P3707VYH plants displayed higher **(A)** yield per plant (3.93× and 3.45×, respectively), **(B)** number of kernels per plant (3.87× and 3.85×, in that same order) and **(C)** number of kernel rows per ear (42 and 59%, respectively) under DS. Additional yield results are shown in **Supplementary Figure 5**. Values expressed as the mean ± SD. $n \geq 7$ plants per treatment. WW, well watering; DS, drought stress; SD, standard deviation. $^{**}P \leq 0.01$ and $^{***}P \leq 0.001$.

However, the percentage of plants flowering during DS increased, for inoculated DKB177 at anthesis, which grew from 59 to 80%, and at silking, which grew from 61 to 86%. This behavior was also observed for P3707VYH at silking, which grew from 60 to 75% when inoculated (**Supplementary Figure 4F**).

As expected, DS significantly reduced all yield components and aerial biomass accumulation. Differences in genotypes and in genotype × inoculum were observed for many yield components, showing specific and different responses from hybrids due to SynCom inoculation (**Supplementary Table 1**). SynCom inoculation significantly reduced yield loss caused by DS. Under DS, SynCom-inoculated DKB177 yielded an average of 38.7 g of seeds per plant compared to 9.8 g per plant for the uninoculated counterpart (**Figure 2A**). Similarly, under DS, the inoculated P3707VYH produced 42.7 g per plant compared to 12.4 g of seeds per uninoculated plant (**Figure 2A**). Other yield components, such as the number of kernels per plant and the number of rows per ear, were significantly higher under DS for inoculated DKB177 and P3707VYH plants than uninoculated plants. In contrast, no significant differences in yield parameters between inoculated and uninoculated plants were observed for DS-treated SX7341 (**Figures 2B,C**). DS-treated inoculated DKB177 and P3707VYH plants also showed 64 and 54% increases in ear diameter, respectively, compared with uninoculated plants. A tendency of increase, although not statistically significant, in ear diameter under DS was also observed for inoculated SX7341 (**Supplementary Figure 5A**). We also observed a significant increase of 35 and 36% in the ear length of DS-treated inoculated DKB177 and P3707VYH, respectively (**Supplementary Figure 5B**). Notably, among WW-treated plants, there was no significant impact of SynCom inoculation, except for SX7341, in which SynCom inoculation led to an 18% reduction in the number of kernel rows per ear (**Figure 2C**). Overall, there was no significant difference in the aerial biomass of mature inoculated and uninoculated plants regardless of watering regime, although aerial biomass tended to be higher in WW- and lower in DS-treated inoculated plants (**Supplementary Figure 5C**). The HI was higher in inoculated DKB177 and P3707VYH under both watering regimes. Particularly under DS, the HI was 4 and 3.2 times higher for inoculated DKB177 and P3707VYH, respectively, than for uninoculated plants (**Supplementary Table 2**).

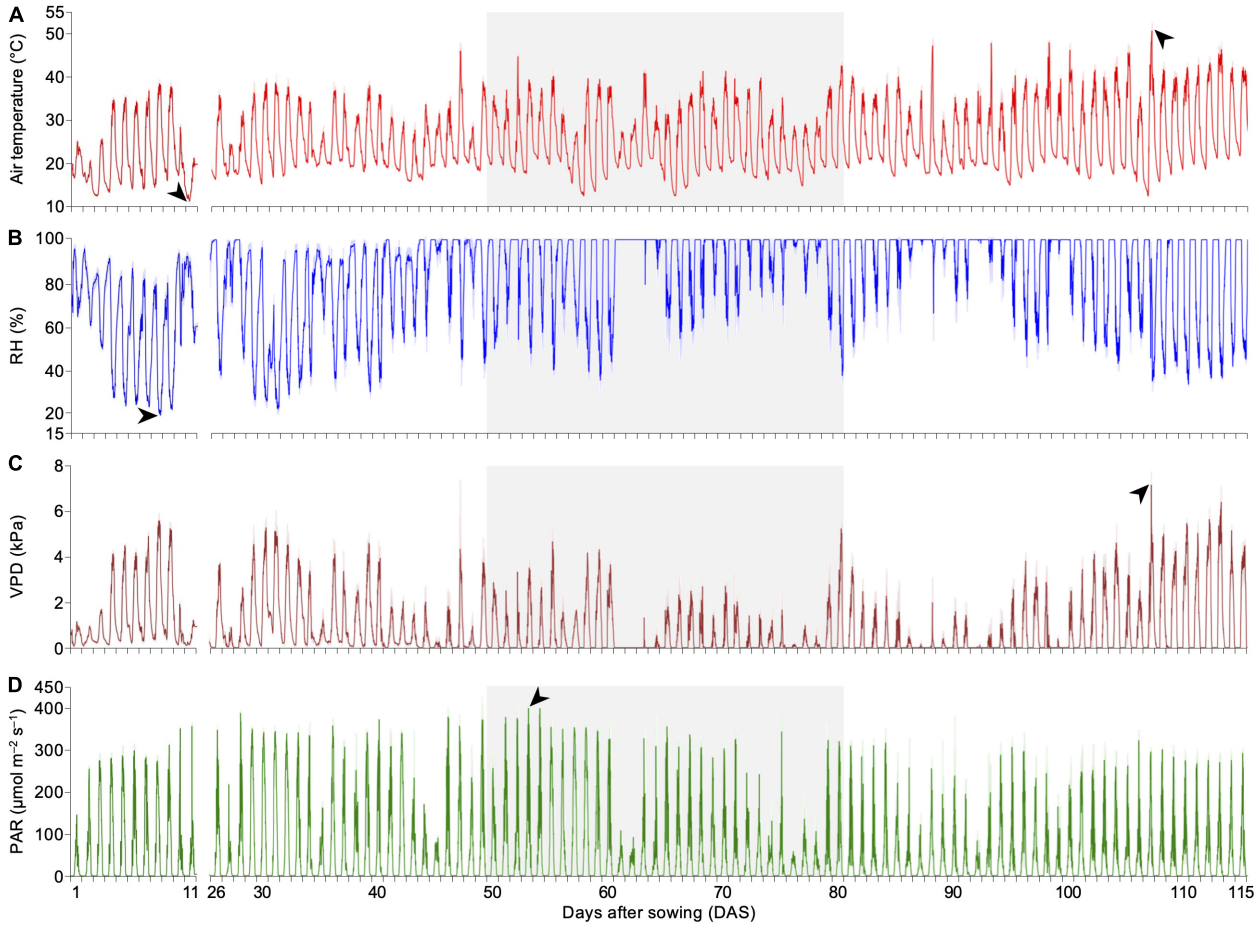

FIGURE 3 | Fluctuation of environmental parameters detected by the non-invasive real-time phenotyping platform. **(A)** Air temperature, with minimum and maximum observed at 11 DAS at 5:30 am (11.35 ± 0.05°C) and 107 DAS at 2:00 pm (51.38 ± 1.93°C), respectively (black arrows). **(B)** RH, with a minimum of 18.85 ± 0.15% at 8 DAS at 4:30 pm (black arrow). **(C)** VPD, found to reach a peak of 7.17 ± 0.60 kPa at 107 DAS at 2:15 pm (black arrow), following the high air temperature variation at that moment. **(D)** PAR, with a maximum peak of 400.53 ± 1.94 µmol m^{-2} s^{-1} observed at 53 DAS at 12:00 pm (black arrow). Gray background highlights period of DS treatment. Data points were missing from 12 to 25 DAS due to an unexpected disruption of the automated measuring routine. DAS, days after sowing; RH, air relative humidity; VPD, vapor-pressure deficit; PAR, photosynthetically active radiation; DS, drought stress.

Daily Changes in Environmental Parameters Directly Impact Plant Physiology

A non-invasive real-time phenotyping platform was developed to investigate parameters affecting the plant physiological response to DS when inoculated with SynCom. To ensure a complete and accurate analysis, the platform also enabled close monitoring of the environmental factors over time. During the experimental period, the average daily air temperature in the greenhouse ranged from 16.4 to 34.5°C. Particularly during the DS treatment, plants faced thermal amplitudes reaching 27.7°C and a maximum air temperature peak of 45.4°C at 52 DAS. During DS, the RH reached a minimum of 35% during the day period (6:00 am to 6:00 pm) (**Figures 3A,B**). Additionally, the VPD was lower during DS, with daily averages of <0.01–2.6 kPa during the day period, which intensified the DS impact (**Figure 3C**). Concerning light intensity, the maximum peak of PAR of 400.5 µmol m^{-2} s^{-1} was observed at 53 DAS at 12:00 pm at the beginning of DS treatment (**Figure 3D**).

Imaging records of plant behavior throughout the experiment revealed a constant response of plants to daily environmental variations. The air temperature, for instance, is directly correlated with the canopy structure. As air temperature increases, leaf rolling becomes proportionally more evident, especially on top leaves, which are generally most affected. At 52 DAS, for example, when plants were at the V11–V12 stage, this effect was observed from 8:00 am until 12:00 pm, when the air temperature increased from 21.4 to 36.2°C. Leaf rolling reached a maximum at 1:00 pm when the air temperature was 45.4°C (**Supplementary Figures 6A–E**). As the air temperature decreased in the afternoon, the leaves started to unroll (**Supplementary Figures 6A,F,G**). We next evaluated whether there was a correlation between air temperature, RH and PAR and the magnitude of the plant response. To this end, we monitored three sequential days (47–49 DAS) that displayed distinct air

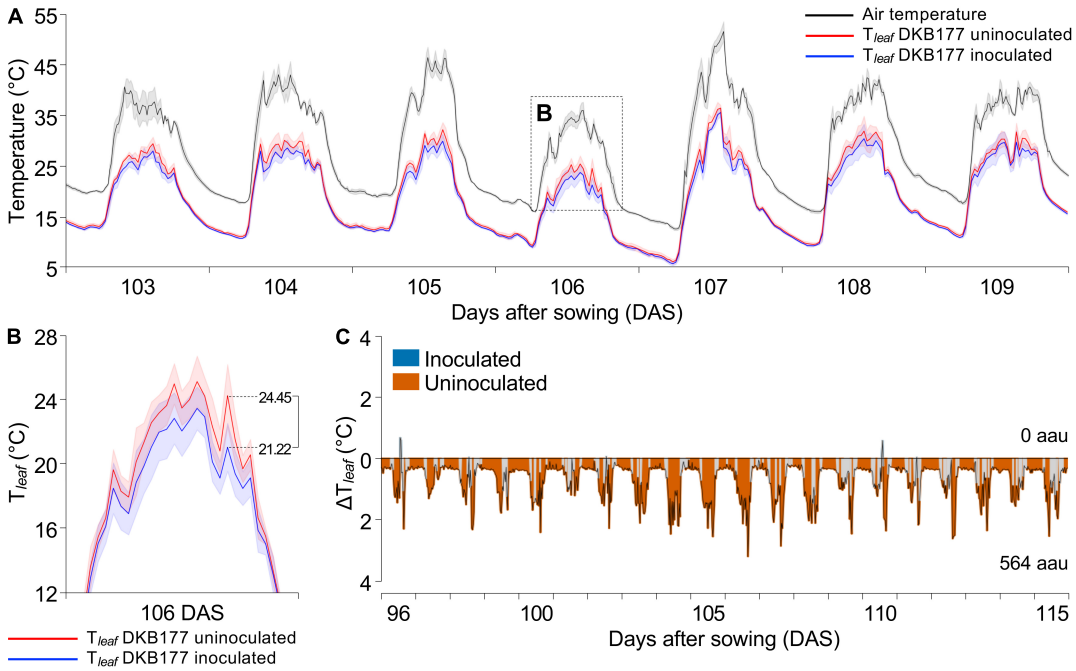

FIGURE 4 | The SynCom-inoculated DKB177 plants displayed lower T_{leaf} than uninoculated plants. **(A)** The hybrid DKB177 showed a low T_{leaf} when inoculated with SynCom, especially in periods when the air temperature was high. The standard deviation is shown as the background for air temperature and both treatments. **(B)** T_{leaf} of uninoculated plants reaches a peak of 3.23°C higher at 106 DAS (inset from panel **A**). **(C)** The difference between T_{leaf} of inoculated and uninoculated plants (ΔT_{leaf}), rounded every 30 min over time, revealed consistency in the high temperature presented by uninoculated DKB177. Values were displayed above the *x*-axis when T_{leaf} of inoculated plants is higher than T_{leaf} of uninoculated plants or below the *x*-axis when T_{leaf} of uninoculated plants is higher than T_{leaf} of inoculated plants, and colored in blue or red, respectively, when significantly different ($P \leq 0.05$). Areas filled with light gray denote not statistically significant differences. The sums of areas in the graph above and below the *x*-axis were considered only for statistically significant differences. See **Supplementary Figure 8** for the entire analyzed period. T_{leaf}, leaf temperature; ΔT_{leaf}, difference of T_{leaf}; aau, arbitrary area units; DAS, days after sowing.

temperature amplitudes, RH and PAR. At 1:45 pm at 47 DAS, when the air temperature peaked at 45°C, RH was 64% and PAR was 321.7 μmol m^{-2} s^{-1}, almost all plants tended to display more leaves rolled inward than unrolled leaves. On that day, the amplitude of air temperature reached 26°C (**Supplementary Figures 7A–E**). In contrast, the leaf surface area was restored for the majority of plants at 48 DAS at 2:00 pm, when the peak air temperature reached 28.6°C, with a smaller thermal amplitude of 9.6°C. At that moment, the RH was 81.1%, and the PAR was 147.9 μmol m^{-2} s^{-1} (**Supplementary Figures 7A–C,F,G**). An intermediate air temperature peak was observed at 12:30 pm at 49 DAS, reaching 39.4°C in a day when the amplitude of the air temperature was 21°C. Combined with a lower RH of 52.1% and reduced PAR of 105.3 μmol m^{-2} s^{-1}, plants had, on average, an intermediate phenotype of leaf rolling (**Supplementary Figures 7A–C,H,I**).

Synthetic Community Inoculation Decreases DKB177 Leaf Temperature During Maximum Daily Air Temperature

Given that SynCom affected plant and canopy behavior under DS, we investigated whether the inoculation could modify plant physiological responses. Plants were monitored throughout the DS period using a set of sensors to capture T_{leaf}, sap flow, and SWC every 5 min, composing a robust data series.

We first evaluated the DKB177 hybrid, which exhibited the most prominent response to SynCom inoculation. The monitoring results shows that the T_{leaf} of DKB177 was significantly lower in SynCom-inoculated plants under WW conditions. For example, during the 103–109 DAS period, the difference in T_{leaf} between uninoculated and inoculated plants (ΔT_{leaf}) reached values of up to 3.2°C (**Figures 4A,B**). This difference was particularly evident in periods where VPD exceeded 2 kPa (**Supplementary Figure 8A**, subpanels i–iv), when high fluctuation of VPD had a strong effect on plant temperature control. During 96–115 DAS, for instance, a total of 763 (79.5%) ΔT_{leaf} peaks, out of 960, were found to be statistically significant. During this period, the integral area of the ΔT_{leaf} peaks in which uninoculated plants displayed higher T_{leaf} accounted for 564 arbitrary area units (aau) versus no area of inoculated plants (**Figure 4C** and **Supplementary Figures 8A,B**). We also analyzed the pattern of T_{leaf} of the other two hybrids (**Supplementary Figures 8C,D**). During the entire experiment, WW-treated inoculated P3707VYH also displayed lower T_{leaf} than uninoculated plants, on average (68 against 195 aau, respectively) (**Supplementary Figure 8D**). Curiously, although the average T_{leaf} of inoculated SX7341, in general, tended to be higher (313 against 234 aau for inoculated and

uninoculated, respectively), during days when VPD was >2 kPa, uninoculated plants displayed higher T_{leaf}, with peaks of ΔT_{leaf} summing to 16, 15, 27, and 171 against 30, 2, 4, and 39 aau for SynCom-inoculated plants (**Supplementary Figures 8A,C**).

An interesting response to SynCom was found for the SX7341 plants. In contrast to that observed for WW-treated DKB177, in which T_{leaf} differences between inoculated and uninoculated plants were observed throughout the whole day, major differences in T_{leaf} for WW-treated inoculated SX7341 plants were observed at the air temperature peaks, suggesting a delayed T_{leaf} increase phenomenon (**Supplementary Figures 9A,B**). For example, from 95 to 114 DAS, at the air temperature peaks, the T_{leaf} of uninoculated plants was, in general, higher than the T_{leaf} of the inoculated plants. The integrated areas of T_{leaf} differences (ΔT_{leaf}) that were statistically significant summed to 164 and 46 aau for uninoculated and inoculated plants, respectively (**Supplementary Figure 9B**). However, inspections into subperiods revealed that the majority of peaks when the T_{leaf} of uninoculated plants were higher than the T_{leaf} of inoculated plants occurred from 9:00 am to 12:00 pm (**Supplementary Figure 9C**), while late peaks when the T_{leaf} of inoculated plants was higher than the T_{leaf} of uninoculated plants were mostly observed from 12:00 pm to 3:00 pm (**Supplementary Figure 9D**).

At the late stages of DS treatment (22–29 days of DS; 72–79 DAS), the integrated ΔT_{leaf} areas among inoculated and uninoculated plants revealed that SynCom increased the T_{leaf} of all hybrids. During an 8-day period immediately before rehydration, the statistically significant differences in T_{leaf} summed to 69 against 3 aau for inoculated and uninoculated DKB177 (**Supplementary Figure 10A**), 53 aau against no area for SX7341 (**Supplementary Figure 10B**) and 48 against 4 aau for P3707VYH (**Supplementary Figure 10C**). The analysis of SWC revealed that plants presented significant differences in soil moisture when comparing WW and DS conditions for each hybrid (**Supplementary Figures 10D–F**).

Synthetic Community Differentially Modulates Sap Flow at Well Watering and Drought Stress Conditions

The effect of SynCom inoculation on T_{leaf} led us to hypothesize whether inoculation treatment influenced plant water usage. We monitored the sap flow of plants 3 days before (late DS stages) and 3 days after rehydration initiation, periods in which variations in water usage should be mostly contrasting between treatments. The analysis of sap flow considered a period between 10:00 am and 4:00 pm, when plant transpiration was maximal due to the high VPD (**Figure 5A**). Under WW, inoculated DKB177 showed a sap flow 1.7–2.2 times higher than that of the uninoculated plants, consistent with the lower T_{leaf} observed for these plants. The most pronounced difference was found at 77 DAS when the sap flow was 2.2 and 5 g H_2O h^{-1} for uninoculated and inoculated plants, respectively (**Figure 5B**). On the other hand, under DS, inoculated DKB177 displayed reduced sap flow compared to the uninoculated plants, which might be related to the fact that these plants did not loss turgor and did not bend under SDS (**Figure 1C** and **Supplementary Figures 3F,G**). In the first 3 days after rehydration (81–83 DAS), the sap flow of inoculated DKB177 was 20.7–25.9% lower (2.3–4 g H_2O h^{-1}) than that of uninoculated plants (3.1–5.3 g H_2O h^{-1}) (**Figure 5C**). During the 6-day window of DS/rehydration, SX7341 presented an undefined pattern of sap flow for inoculated and uninoculated plants under WW conditions (**Figure 5D**). The same lack of pattern was observed under DS and rehydration. At late stages of DS (79 DAS), inoculated SX7341 plants had a significant increase in sap flow compared to uninoculated plants (13 versus 9.6 g H_2O h^{-1}, respectively), a pattern that was also observed on the day immediately after rehydration (81 DAS), with 6.9 versus 4.6 g H_2O h^{-1} sap flow for inoculated and uninoculated plants, respectively (**Figure 5E**). WW-treated inoculated P3707VYH consistently decreased the sap flow by 15–39.7% compared to uninoculated plants. The most pronounced effect of SynCom inoculation was found at 78 DAS, with a sap flow of 3.2 against 5.3 g H_2O h^{-1} for inoculated and uninoculated plants, respectively (**Figure 5F**). Remarkably, a clear shift was found during the 3 days following rehydration (81–83 DAS). The inoculated P3707VYH plants increased sap flow by 2.2–2.6 times compared to the uninoculated plants. On average, the sap flow of the uninoculated plants was 1.8–2.8 g H_2O h^{-1} compared to 4–7.1 g H_2O h^{-1} of the inoculated plants (**Figure 5G**), which is consistent with the observation that inoculated P3707VYH presented a faster recovery than the uninoculated plants (**Figure 1D** and **Supplementary Figure 3H**).

Members of Synthetic Community Robustly Colonize Maize Plants and Reshape Resident Microbiota

We also asked if the impact of inoculation on plant physiology were correlated with colonization by SynCom members. To address this question, we profiled the root microbiome of inoculated and uninoculated plants through 16S rRNA amplicon sequencing. Differences in the bacterial community structure assemblages were first analyzed using principal coordinates analysis (PCoA) of the Bray–Curtis dissimilarity matrix. Inoculated and uninoculated plants clustered separately (ANOSIM; R = 0.135; P = 0.003), indicating that inoculation modified microbial community assemblage in plant roots. No significant difference was observed in community composition between WW- and DS-treated plants (**Figure 6A**). OTUs representative of SynCom members accounted for 9.3, 11.8, and 9.9% of inoculated DKB177, SX7341, and P3707VYH under WW and 11.7, 9, and 9.6% under DS, respectively (**Figure 6B**). SynCom-associated OTUs were then individually evaluated for their relative abundance. In total, 23 OTUs were assigned to 17 SynCom community-based isolates: *Agrobacterium* sp. E09, *Asticcacaulis* sp. F02, *Burkholderia* sp. A10, *Dyella* sp. G12, *Ensifer* sp. B04, *Enterobacter* sp. B02, *Lysobacter* sp. A02, *Microbacterium* sp. C05, *Pantoea* sp. B02/C12, *Pedobacter* sp. A01, *Sphingomonas* sp. D05, *Stenotrophomonas* sp. E09, *Streptomyces* sp. G01, unknown Bradyrhizobiaceae C05, unknown Xanthomonadaceae B08, unknown Xanthomonadaceae G08, and *Variovorax* sp. F04 (**Figure 6C**). From the assigned OTUs, 14 OTUs were considered robust colonizers for at least one hybrid at WW, while 16 OTUs

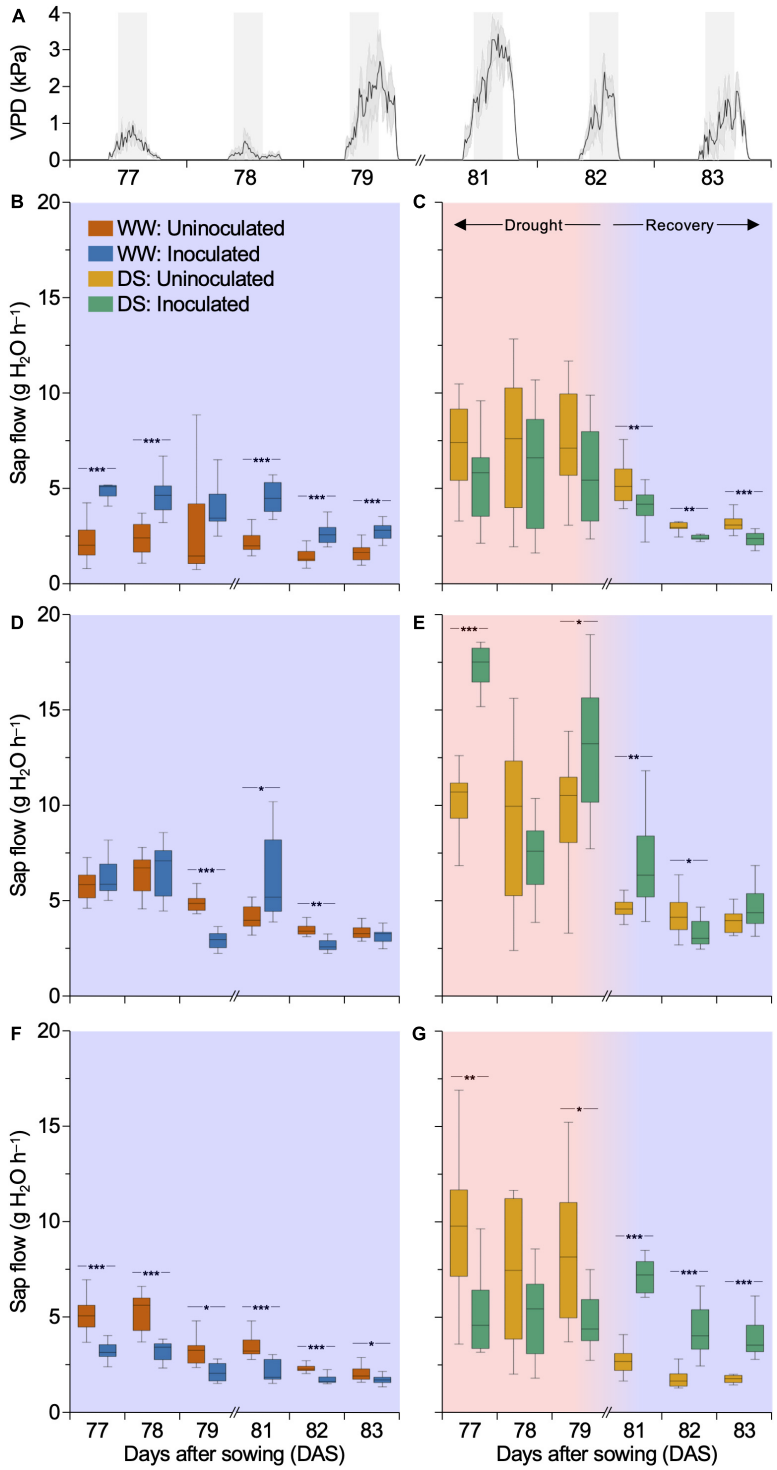

FIGURE 5 | Synthetic community (SynCom) inoculation affects the sap flow of maize hybrids. **(A)** Fluctuation of VPD (kPa) from 77 to 83 DAS. The gray background highlights daily windows from 10:00 am to 4:00 pm, periods considered to measure sap flow of DKB177 **(B,C)**, SX7341 **(D,E)**, and P3707VYH **(F,G)**. Box plots are shown for WW- **(B,D,F)** and DS-treated/rehydrated **(C,E,G)** plants. Rehydration was performed at 80 DAS. **(B)** In WW, SynCom leads to an increase in DKB177 sap flow by up to 2.22×. **(C)** Inoculated DKB177 plants tended to have their sap flow reduced in late stages of DS (77–79 DAS). During recovery (81–83 DAS), this reduction significantly reached up to 25.9%. **(D)** SX7341 presented an undefined pattern of sap flow under WW the regime. **(E)** A lack of pattern was also found during the DS and rehydration periods. **(F)** WW-treated P3707VYH had its sap flow reduced by up to 39.7% when inoculated, the same effect found in DS **(G)**. **(G)** During recovery, SynCom inoculation led to a shift in sap flow of P3707VYH with an increase of up to 2.57× compared to the control. VPD: vapor-pressure deficit; WW, well watering; DS, drought stress; DAS, days after sowing. $^{*}P \leq 0.05$, $^{**}P \leq 0.01$, and $^{***}P \leq 0.001$.

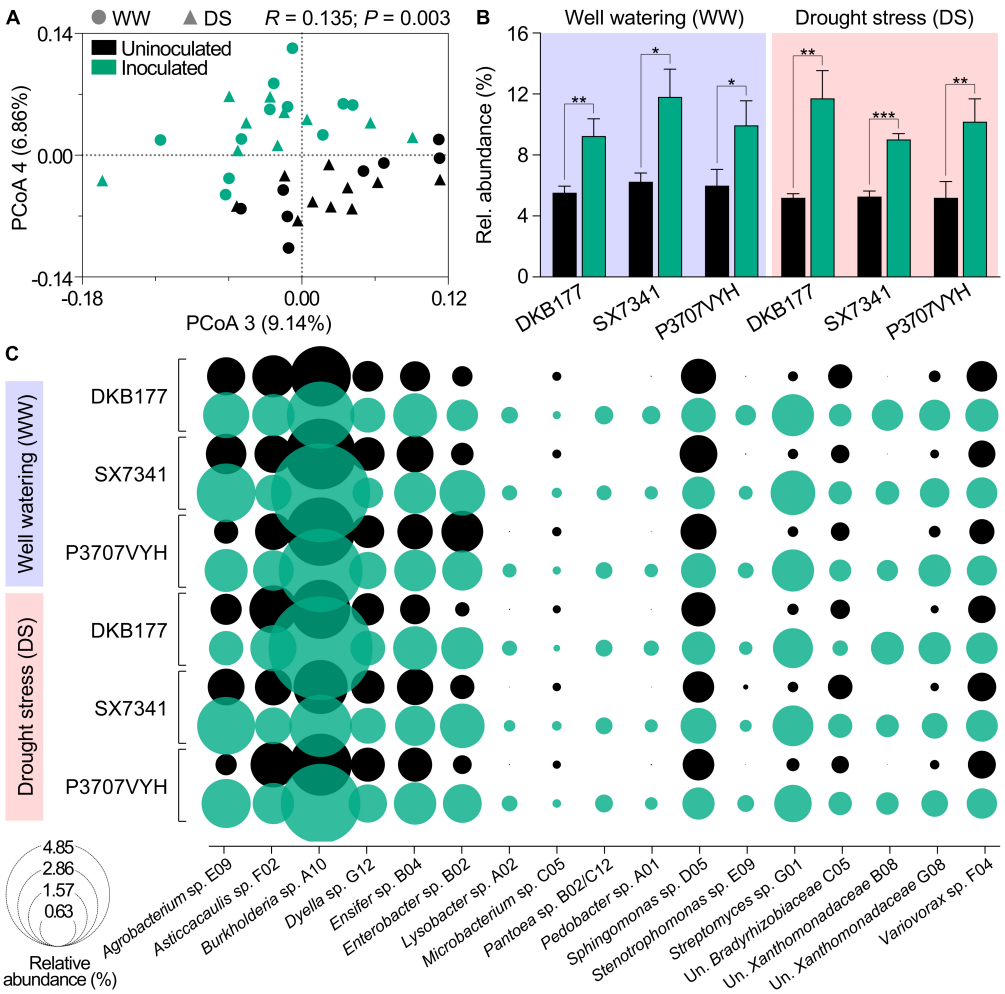

FIGURE 6 | Members of SynCom robustly colonize different maize hybrids. **(A)** PCoA of the Bray–Curtis dissimilarity matrix of inoculated and uninoculated plants. **(B)** Relative abundance of OTUs present in SynCom in WW- and DS-treated inoculated and uninoculated DKB177, SX7341, and P3707VYH hybrids. **(C)** Relative abundance of community-based isolates in SynCom in WW- and DS-treated inoculated and uninoculated maize hybrids. OTUs of community-based isolates identified as robust colonizers are individually highlighted in **Supplementary Table 3**. Values expressed as the mean ± SD. PCoA, principal coordinates analysis; SD, standard deviation; Un., unknown. *$P \leq 0.05$, **$P \leq 0.01$, and ***$P \leq 0.001$.

were found in the same category under DS. Among these, only two, *Agrobacterium* sp. E09 and *Enterobacter* sp. B02, were exclusively found as robust colonizers in at least one hybrid in DS-treated plants but not in plants under WW. Overall, OTUs were classified as non-robust colonizers when considering all hybrids and treatments. Among robust colonizer groups, *Ensifer* sp. B04 was the most efficient colonizer, comprising 0.78−0.86% and 0.72−0.87% of the relative abundance among the three hybrids in WW- and DS-treated plants, respectively. *Variovorax* sp. F04 and *Streptomyces* sp. G01 colonized all hybrids at 0.41–0.49% and 0.37−0.49% (under WW) and 0.42−0.46% and 0.31−0.51% (under DS), respectively (**Figure 6C** and **Supplementary Table 3**). Among 17,437 identified OTUs belonging to resident plant microbiota (apart from those belonging to SynCom), 632 displayed a significant shift in inoculated compared to uninoculated plants for both WW- and DS-treated plants, indicating that members of resident microbiota were enriched or depleted in SynCom-inoculated plants (**Supplementary Figure 11**). Overall, these results indicate that SynCom members efficiently colonize plant root systems, displaced naturally occurring microbes and recruit groups that may help boost the inoculation impact.

DISCUSSION

A Synthetic Community That Mitigates Drought Stress in Maize

Under water restriction, decreased photosynthesis, stomatal conductance and CO_2 assimilation result in reduced yield (Chaves et al., 2003). To cope with DS, plants activate several protective mechanisms, including associations with beneficial microorganisms that help plants survive unfavorable circumstances. However, exploring the benefits and functions

of the plant microbiota is still technically challenging given the diversity and complexity of microbial communities. A promising approach is the use of SynComs, which are consortia of microorganisms that mimic, to some extent, the observed structure of the plant microbiome under natural conditions (Vorholt et al., 2017). Multiple SynComs have been recently investigated for playing important roles in terms of mitigation of different plant stresses, such as protection against pathogens in maize (Niu et al., 2017), more efficient nitrogen fixation in rice (Zhang et al., 2019) and enhanced phosphate starvation responses in *Arabidopsis* (Castrillo et al., 2017). In this work, we evaluated the influence of a SynCom composed of microbes from the sugarcane core microbiome (de Souza et al., 2016, 2019; Armanhi et al., 2018) in three commercial maize hybrids grown to maturity under drought.

Abiotic stresses are known to affect an array of physiological and molecular processes, including stomatal closure, in an attempt to prevent turgor loss (Mahajan and Tuteja, 2005). In this work, leaf rolling, a sensitive indicator of water restriction in maize (Song et al., 2018), was the most premature visual response of all plants subjected to drought. Under SDS, the uninoculated plants of the three maize hybrids were severely affected, resulting in plant bending, a well-known response indicating cell turgor loss. In contrast, SynCom-inoculated maize hybrids retained turgor, either partially or permanently. In DKB177, for instance, SynCom inoculation induced physiological mechanisms that prevented plant bending even in late stages of SDS. Meanwhile, a faster recovery after rehydration, a critical process associated with drought tolerance in maize, was observed for P3707VYH.

The benefit of microbe-inoculated plants subjected to DS has been reported for plant biomass and yield (Rubin et al., 2017). Here, we show that SynCom inoculation reduced the yield loss of maize hybrids under DS, indicating that these microbes play a significant role when plant homeostasis is perturbed, as in regular conditions plants expressed their maximum genetic potential. Under stressful conditions, plants are known to recruit sets of microbes with abilities to mitigate specific detrimental effects (Naylor et al., 2017; Beirinckx et al., 2020). We observed a higher yield of inoculated DKB177 and P3707VYH hybrids under DS, with a tendency toward reduction in aerial biomass and increased HI. This may be due to the remobilization of assimilates from straw to the grains through specific hormonal regulation and enzymatic activities when plants face DS in reproductive stages, as observed for other crops (Plaut et al., 2004), which is supported by increased HI in inoculated plants. Although SynCom inoculation did not mitigate DS impact in terms of flowering time, it reduced the number of plants lacking pollen shed for DKB177 and silk extrusion for both DKB177 and P3707VYH, which is consistent with increased yield in inoculated plants. The higher yield of inoculated plants may indicate carbon mobilization after fertilization by reducing carbon limitation to early kernel development (Oury et al., 2016).

Adverse environmental conditions, plant–microbe interactions and the plant genetic background can collectively contribute to seedling emergence. Upon inoculation, we observed reduced seedling emergence for DKB177 and more uneven seedling emergence for both DKB177 and P3707VYH. Although uneven seedling emergence negatively impacts grain yield and the HI of maize (Liu et al., 2004), we observed no direct correlation with plant yield. The reduced number of seedlings may be explained by the high density of inoculated bacteria at the beginning of seed germination, given that seedlings are a vulnerable stage in plant development (Nelson, 2018). Additionally, at early germination stages, the high density of microbes may compete for the available nutrients in the soil (Kozdrój et al., 2004; Zakeel and Safeena, 2019). Since hybrids were differentially affected by SynCom inoculation, it is more likely that plant genetic background and plant-SynCom crosstalk might have been involved.

Synthetic Community Differentially Impacts Maize Hybrids by Modulating Leaf Temperature Control and Water Usage Optimization

An existing hurdle to plant phenotyping relies on the lack of appropriate instruments capable of non-invasive and real-time plant behavior assessments. Destructive methods for plant phenotyping are often used but may not be operationally desirable, as they require an exponential number of samples. In addition to manual instruments conventionally employed, most platforms for plant phenotyping are mainly based on either sensor-to-plant (De Diego et al., 2017) or plant-to-sensor setups (Fahlgren et al., 2015), in which automated systems harboring cameras/sensors or plants routinely move along a platform. However, as plant growth is a dynamic process, the majority of phenotyping platforms may be restricted to a limited number of data points and specific timepoints (Halperin et al., 2017; Rouphael et al., 2018). In this work, the real-time monitoring of individual plants allowed the establishment of a one-to-one (plant–sensor) setup and assured that even small variations in plant physiology along a single day period were detected. Over time, the environmental and physiological high-resolution data allowed us to record instant plant responses to small daily environmental perturbations in detail.

The results presented in this work revealed that SynCom inoculation directly influenced T_{leaf} under environmental conditions fluctuations. Under DS, the reduction in transpiration typically induces higher canopy temperatures as a consequence of changes in stomatal conductance. The variability in T_{leaf} has been traditionally applied as an indicator of DS symptoms (González-Dugo et al., 2006). We surprisingly observed that SynCom-inoculated plants of the DKB177 hybrid displayed decreased T_{leaf} under WW conditions. This physiological behavior would be advantageous for plants, especially because elevated temperatures cause a reduction in enzyme activities, such as RuBisCO, and impact plant growth (Crafts-Brandner and Salvucci, 2002). We also observed a temporally segmented response of T_{leaf} for the SynCom-inoculated SX7341 hybrid that showed better T_{leaf} control at the beginning of the daily air temperature increase, suggesting that SynCom may contribute to plant primary mechanisms associated with a given environmental disturbance. To our knowledge, this is the first study to describe such plant physiological attributes induced by microbes.

Given that plant transpiration is directly affected by stomatal aperture, sap flow is often used to monitor plant water status. Particularly under DS, xylem sap transports signaling molecules from roots to shoots that signal to reduce plant growth and transpiration (Alvarez et al., 2008). The observation that the sap flow of inoculated DKB177 under WW was significantly higher than that in uninoculated plants correlates with the observed reduced T_{leaf}. However, under DS, the opposite effect is shown, as SynCom inoculation did not reduce T_{leaf}, which is correlated with a significant reduction in sap flow, particularly for DKB177 and P3707VYH plants. Interestingly, the three different maize hybrids presented distinct physiological behavior during recovery from DS, whether maintaining reduced sap flow in stalks (DKB177) or displaying a significant shift in sap flow and recovery capability upon rehydration (P3707VYH). Despite not being evaluated, increased root branching is expected for SynCom-inoculated plants since more developed root systems as a whole were observed for inoculated early stage maize plants (Armanhi et al., 2018). The optimization of water usage and cell turgor maintenance might be associated with osmolyte production induced by SynCom inoculation, a function that should be highly dependent on the genetic background of the three distinct maize hybrids.

In the present study, no significant differences were found between WW and DS concerning the colonization robustness of SynCom members of inoculated plants. Nevertheless, we found that the majority of SynCom members robustly colonized the roots of inoculated plants, consistent with our previous results (Armanhi et al., 2018; de Souza et al., 2019). The SynCom members *Agrobacterium* sp. E09, *Burkholderia* sp. A10, *Ensifer* sp. B04, *Lysobacter* sp. A02, *Pedobacter* sp. A01, *Stenotrophomonas* sp. E09, *Streptomyces* sp. G01 and *Variovorax* sp. F04 were most prevalent and may have been responsible for the beneficial impact on maize hybrids under DS. Curiously, the SynCom members *Enterobacter* sp. B02, *Pantoea* sp. B02/C12, unknown Xanthomonadaceae B08 and unknown Xanthomonadaceae G08, previously found to be non-robust colonizers in early stage maize plants (Armanhi et al., 2018; de Souza et al., 2019), displayed robust colonization in mature plants, suggesting a functional role at the late stages of plant development.

Several bacterial traits associated with DS tolerance in plants have been proposed. For example, the production of exopolysaccharides (EPS) by EPS-producing bacteria was shown to increase the leaf relative water content of maize, thus improving plant fitness under DS (Naseem and Bano, 2014). Bacterial groups present in the SynCom are enriched in genes related to EPS production (de Souza et al., 2019). Many other SynCom-encoded traits related to plant water usage, such as the production of osmolytes that sustain higher tissue water potential, may also contribute to plant DS tolerance. Plant osmolytes are known to increase water influx in cells, thus playing roles in cell turgor maintenance (Bartels and Sunkar, 2005). We hypothesize that members of the SynCom may also stimulate plant osmolyte production for their own benefit, as they are enriched in ABC-type transporters for proline, glycine betaine, sugars, and amino acids, among other compounds (de Souza et al., 2019).

The microbial root profiling of the three hybrids revealed a shift in the soil/seed-borne microbial composition of SynCom-inoculated plants, suggesting reshaping of the natural microbiota. Although the view of a functional plant–microbiome bond is more parsimonious regardless of microbial taxonomic affiliation, taxonomy still may provide preliminary clues for the role of beneficial microbes in plant development and response to environmental perturbations. Microbial groups in the Proteobacteria phylum, for instance, were enriched in all inoculated plants of the three hybrids, particularly families already described as harboring plant beneficial microbes, such as Bradyrhizobiaceae (Shaharoona et al., 2006), Burkholderiaceae (Stoyanova et al., 2007), Caulobacteraceae (Pepe et al., 2013), Comamonadaceae (Belimov et al., 2005), and Phyllobacteriaceae (Wani et al., 2007). Thus, our findings suggest that SynCom inoculation recruits and enriches such beneficial microbial groups naturally found in low abundance in the plant/soil microbiota. This recruitment may have helped to sustain plant homeostasis under stressful DS conditions.

CONCLUSION

The beneficial impact of SynCom inoculation on the plant physiological parameters of commercial maize hybrids subjected to DS was monitored in real time. Detailed information on physiological behavior during the developmental process and in response to DS was made possible by continuous monitoring using a non-invasive phenotyping platform comprised of sensors at the individual plant level and high-quality imaging. Inoculation with SynCom increased drought tolerance and reduced yield loss. The collected dataset provided significant evidence that SynCom inoculation modulates plant T_{leaf} and optimizes water usage. Colonization profiling revealed that members of SynCom robustly colonized plant roots and recruited beneficial soil/seed-borne bacterial members, thus increasing plant resilience to DS. Our findings suggest that although the molecular mechanisms of plant–SynCom interactions remain to be elucidated, a better comprehension of crop functional trait responses to drought can provide evidence of their potential to enhance plant performance.

DATA AVAILABILITY STATEMENT

Sequencing raw data were deposited in the Sequence Read Archive (SRA) database under the accession number PRJNA384812. All physiological and environmental data generated and analyzed during this study can be found in **Supplementary Datasets 1, 2**.

AUTHOR CONTRIBUTIONS

JA and RdS designed the SynCom and the inoculation experiment, prepared sequencing libraries of the 16S rRNA gene for microbe identification, and performed bioinformatics analyses. JA, RdS, and BB prepared the SynCom and

performed the inoculation experiment, plant phenotyping and sampling for microbial profiling. JA designed, built, installed, and analyzed the data from the plant phenotyping platform with significant inputs of RdS, JY, and PA. JY performed statistical analysis of yield components. JA wrote the manuscript with contributions from all authors. RdS and PA critically revised the manuscript. All authors read and approved the final manuscript.

FUNDING

We are grateful to the São Paulo Research Foundation (FAPESP) for supporting this research under the project "The Genomics for Climate Change Research Center (GCCRC)," grant 2016/23218-0, São Paulo Research Foundation (FAPESP). This study was financed in part by the "Coordenação de Aperfeiçoamento de Pessoal de Nível Superior–Brasil (CAPES)"–Finance Code 001. JA received a postdoctoral fellowship, grant 2018/18403-8, São Paulo Research Foundation (FAPESP). RdS received a postdoctoral fellowship, grant 2018/19100-9, São Paulo Research Foundation (FAPESP).

ACKNOWLEDGMENTS

We acknowledge the staff of the Donnelly Sequencing Centre at the University of Toronto for Illumina sequencing and Plantem (Plant Technology and Environmental Monitoring) for supporting the data collection through the plant phenotyping platform.

SUPPLEMENTARY MATERIAL

The Supplementary Material for this article can be found online at: https://www.frontiersin.org/articles/10.3389/fmicb.2021.747541/full#supplementary-material

Supplementary Figure 1 | Experimental design to evaluate the impact of SynCom in three different commercial hybrids of maize under DS.

Supplementary Figure 2 | Sensors and materials used for the non-invasive real-time phenotyping platform.

Supplementary Figure 3 | Differential phenotypic responses of three commercial hybrids of maize (DKB177, SX7341, and P3707VYH) to the presence of SynCom under DS.

Supplementary Figure 4 | SynCom inoculation differentially affects seedling emergence timing and reproductive stages of maize.

Supplementary Figure 5 | SynCom differentially impacts yield-related parameters and plant biomass of commercial hybrids of maize under DS conditions.

Supplementary Figure 6 | Maize canopy structure throughout a day as a function of air temperature detected by the non-invasive real-time phenotyping platform.

Supplementary Figure 7 | Continuous plant monitoring revealed a direct influence of natural environmental variables in canopy aspect.

Supplementary Figure 8 | SynCom differentially affects maize hybrids by dramatically changing T_{leaf} control under WW conditions.

Supplementary Figure 9 | SynCom delays the T_{leaf} increase in SX7341 maize plants under WW conditions.

Supplementary Figure 10 | SynCom induces an increase in the T_{leaf} of maize plants under DS conditions.

Supplementary Figure 11 | Enriched and depleted resident microbial groups in inoculated plants.

Supplementary Table 1 | Three-way ANOVA for phenotypic parameters (yield per plant, kernels per plant, kernel rows per ear, ear diameter, ear length, and aerial biomass) of genotype, irrigation regime, inoculation and all their possible interactions.

Supplementary Table 2 | Harvest index (HI) for inoculated and uninoculated DKB177, SX7341, and P3707VYH under WW and DS conditions.

Supplementary Table 3 | Relative abundance of community-based isolates considered robust colonizers in WW- and DS-treated inoculated DKB177, SX7341, and P3707VYH hybrids.

Supplementary Movie 1 | Time-lapse movie of late stages of severe drought and rehydration of DKB177, SX7341, and P3707VYH maize hybrids inoculated or uninoculated with SynCom.

Supplementary Dataset 1 | Physiological data collected by the plant phenotyping platform.

Supplementary Dataset 2 | Environmental data collected by the plant phenotyping platform.

REFERENCES

Alvarez, S., Marsh, E. L., Schroeder, S. G., and Schachtman, D. P. (2008). Metabolomic and proteomic changes in the xylem sap of maize under drought. *Plant Cell Environ.* 31, 325–340. doi: 10.1111/j.1365-3040.2007.01770.x

Armanhi, J. S. L., de Souza, R. S. C., Damasceno, N. B., de Araújo, L. M., Imperial, J., and Arruda, P. (2018). A community-based culture collection for targeting novel plant growth-promoting bacteria from the sugarcane microbiome. *Front. Plant Sci.* 8:2191. doi: 10.3389/fpls.2017.02191

Bartels, D., and Sunkar, R. (2005). Drought and salt tolerance in plants. *CRC. Crit. Rev. Plant Sci.* 24, 24–58. doi: 10.1080/07352680590910410

Beirinckx, S., Viaene, T., Haegeman, A., Debode, J., Amery, F., Vandenabeele, S., et al. (2020). Tapping into the maize root microbiome to identify bacteria that promote growth under chilling conditions. *Microbiome* 8, 1–13. doi: 10.1186/s40168-020-00833-w

Belimov, A. A., Hontzeas, N., Safronova, V. I., Demchinskaya, S. V., Piluzza, G., Bullitta, S., et al. (2005). Cadmium-tolerant plant growth-promoting bacteria associated with the roots of Indian mustard (*Brassica juncea* L. Czern.). *Soil Biol. Biochem.* 37, 241–250. doi: 10.1016/j.soilbio.2004.07.033

Buck, A. L. (1981). New equations for computing vapor pressure and enhancement factor. *J. Appl. Meteorol.* 20, 1527–1532. doi: 10.1175/1520-0450(1981)020<1527:NEFCVP>2.0.CO;2

Carvalho, T. L. G., Balsemão-Pires, E., Saraiva, R. M., Ferreira, P. C. G., and Hemerly, A. S. (2014). Nitrogen signalling in plant interactions with associative and endophytic diazotrophic bacteria. *J. Exp. Bot.* 65, 5631–5642. doi: 10.1093/jxb/eru319

Castrillo, G., Teixeira, P. J. P. L., Paredes, S. H., Law, T. F., de Lorenzo, L., Feltcher, M. E., et al. (2017). Root microbiota drive direct integration of phosphate stress and immunity. *Nature* 543, 513–518. doi: 10.1038/nature21417

Chai, Y. N., Ge, Y., Stoerger, V., and Schachtman, D. P. (2021). High-resolution phenotyping of sorghum genotypic and phenotypic responses to low nitrogen and synthetic microbial communities. *Plant Cell Environ.* 44, 1611–1626. doi: 10.1111/pce.14004

Chaudhry, V., Runge, P., Sengupta, P., Doehlemann, G., Parker, J. E., and Kemen, E. (2021). Shaping the leaf microbiota: plant-microbe-microbe interactions. *J. Exp. Bot.* 72, 36–56. doi: 10.1093/jxb/eraa417

Chaves, M. M., Maroco, J. P., and Pereira, J. S. (2003). Understanding plant responses to droughtfrom genes to the whole plant. *Funct. Plant Biol.* 30, 239–264. doi: 10.1071/FP02076

Compant, S., Samad, A., Faist, H., and Sessitsch, A. (2019). A review on the plant microbiome: ecology, functions, and emerging trends in microbial application. *J. Adv. Res.* 19, 29–37. doi: 10.1016/j.jare.2019.03.004

Crafts-Brandner, S. J., and Salvucci, M. E. (2002). Sensitivity of photosynthesis in a C4 plant, maize, to heat stress. *Plant Physiol.* 129, 1773–1780. doi: 10.1104/pp.002170

De Diego, N., Fürst, T., Humplík, J. F., Ugena, L., Podlešáková, K., and Spíchal, L. (2017). An automated method for high-throughput screening of *Arabidopsis* rosette growth in multi-well plates and its validation in stress conditions. *Front. Plant Sci.* 8:e01702. doi: 10.3389/fpls.2017.01702

de Mendiburu, F. (2020). *Agricolae: Statistical Procedures for Agricultural Research. R package version 1.3-3* Available online at: https://cran.r-project.org/package=agricolae (accessed November 19, 2020).

de Souza, R. S. C., Armanhi, J. S. L., and Arruda, P. (2020). From microbiome to traits: designing synthetic microbial communities for improved crop resiliency. *Front. Plant Sci.* 11:1179. doi: 10.3389/fpls.2020.01179

de Souza, R. S. C., Armanhi, J. S. L., Damasceno, N. B., Imperial, J., and Arruda, P. (2019). Genome sequences of a plant beneficial synthetic bacterial community reveal genetic features for successful plant colonization. *Front. Microbiol.* 10:17779. doi: 10.3389/fmicb.2019.01779

de Souza, R. S. C., Okura, V. K., Armanhi, J. S. L., Jorrín, B., Lozano, N., da Silva, M. J., et al. (2016). Unlocking the bacterial and fungal communities assemblages of sugarcane microbiome. *Sci. Rep.* 6:28774. doi: 10.1038/srep28774

Edgar, R. (2016). SINTAX: a simple non-bayesian taxonomy classifier for 16S and ITS sequences. *bioRxiv* [Preprint]. 74161. doi: 10.1101/074161

Fahlgren, N., Feldman, M., Gehan, M. A., Wilson, M. S., Shyu, C., Bryant, D. W., et al. (2015). A versatile phenotyping system and analytics platform reveals diverse temporal responses to water availability in Setaria. *Mol. Plant* 8, 1520–1535. doi: 10.1016/j.molp.2015.06.005

Fiorani, F., and Schurr, U. (2013). Future scenarios for plant phenotyping. *Annu. Rev. Plant Biol.* 64, 267–291. doi: 10.1146/annurev-arplant-050312-120137

González-Dugo, M. P., Moran, M. S., Mateos, L., and Bryant, R. (2006). Canopy temperature variability as an indicator of crop water stress severity. *Irrig. Sci.* 24, 233–240. doi: 10.1007/s00271-005-0022-8

Granier, A. (1987). Evaluation of transpiration in a Douglas-fir stand by means of sap flow measurements. *Tree Physiol.* 3, 309–320. doi: 10.1093/treephys/3.4.309

Halperin, O., Gebremedhin, A., Wallach, R., and Moshelion, M. (2017). High-throughput physiological phenotyping and screening system for the characterization of plant–environment interactions. *Plant J.* 89, 839–850. doi: 10.1111/tpj.13425

Hunter, J. D. (2007). Matplotlib: a 2D graphics environment. *Comput. Sci. Eng.* 9, 90–95. doi: 10.1109/MCSE.2007.55

Hütsch, B. W., and Schubert, S. (2018). Maize harvest index and water use efficiency can be improved by inhibition of gibberellin biosynthesis. *J. Agron. Crop Sci.* 204, 209–218. doi: 10.1111/jac.12250

Jones, E., Oliphant, T., and Peterson, P. (2001). *SciPy: Open Source Scientific Tools for Python*. Available online at: http://www.scipy.org/

Kluyver, T., Ragan-Kelley, B., Pérez, F., Granger, B., Bussonnier, M., Frederic, J., et al. (2016). "Jupyter notebook – a publishing format for reproducible computational workflows," in *Positioning and Power in Academic Publishing: Players, Agents and Agendas*, eds L. Fernando and S. Birgit (IOS Press), 87–90. doi: 10.3233/978-1-61499-649-1-87

Kozdrój, J., Trevors, J. T., and van Elsas, J. D. (2004). Influence of introduced potential biocontrol agents on maize seedling growth and bacterial community structure in the rhizosphere. *Soil Biol. Biochem.* 36, 1775–1784. doi: 10.1016/j.soilbio.2004.04.034

Lemanceau, P., Blouin, M., Muller, D., and Moënne-Loccoz, Y. (2017). Let the core microbiota be functional. *Trends Plant Sci.* 22, 583–595. doi: 10.1016/j.tplants.2017.04.008

Lesk, C., Rowhani, P., and Ramankutty, N. (2016). Influence of extreme weather disasters on global crop production. *Nature* 529, 84–87. doi: 10.1038/nature16467

Liu, W., Tollenaar, M., Stewart, G., and Deen, W. (2004). Response of corn grain yield to spatial and temporal variability in emergence. *Crop Sci.* 44, 847–854. doi: 10.2135/cropsci2004.8470

Mahajan, S., and Tuteja, N. (2005). Cold, salinity and drought stresses: an overview. *Arch. Biochem. Biophys.* 444, 139–158. doi: 10.1016/j.abb.2005.10.018

McKinney, W., and Sheaffer-Jones, C. (2010). "Data structures for statistical computing in python," in *Proceedings of the 9th Python in Science Conference*, eds S. van der Walt and J. Millman 51–56. doi: 10.25080/Majora-92bf1922-00a

Naseem, H., and Bano, A. (2014). Role of plant growth-promoting rhizobacteria and their exopolysaccharide in drought tolerance of maize. *J. Plant Interact.* 9, 689–701. doi: 10.1080/17429145.2014.902125

Naylor, D., DeGraaf, S., Purdom, E., and Coleman-Derr, D. (2017). Drought and host selection influence bacterial community dynamics in the grass root microbiome. *ISME J.* 11, 2691–2704. doi: 10.1038/ismej.2017.118

Nelson, E. B. (2018). The seed microbiome: origins, interactions, and impacts. *Plant Soil* 422, 7–34. doi: 10.1007/s11104-017-3289-7

Niu, B., Paulson, J. N., Zheng, X., and Kolter, R. (2017). Simplified and representative bacterial community of maize roots. *Proc. Natl. Acad. Sci. U.S.A.* 114, E2450–E2459. doi: 10.1073/pnas.1616148114

Oury, V., Caldeira, C. F., Prodhomme, D., Pichon, J. P., Gibon, Y., Tardieu, F., et al. (2016). Is change in ovary carbon status a cause or a consequence of maize ovary abortion in water deficit during flowering? *Plant Physiol.* 171, 997–1008. doi: 10.1104/pp.15.01130

Pepe, O., Ventorino, V., and Blaiotta, G. (2013). Dynamic of functional microbial groups during mesophilic composting of agro-industrial wastes and free-living (N_2)-fixing bacteria application. *Waste Manag.* 33, 1616–1625. doi: 10.1016/j.wasman.2013.03.025

Plaut, Z., Butow, B. J., Blumenthal, C. S., and Wrigley, C. W. (2004). Transport of dry matter into developing wheat kernels and its contribution to grain yield under post-anthesis water deficit and elevated temperature. *Field Crop. Res.* 86, 185–198. doi: 10.1016/j.fcr.2003.08.005

Quast, C., Pruesse, E., Yilmaz, P., Gerken, J., Schweer, T., Yarza, P., et al. (2013). The SILVA ribosomal RNA gene database project: improved data processing and web-based tools. *Nucleic Acids Res.* 41, 590–596. doi: 10.1093/nar/gks1219

Rouphael, Y., Spíchal, L., Panzarová, K., Casa, R., and Colla, G. (2018). High-throughput plant phenotyping for developing novel biostimulants: from lab to field or from field to lab? *Front. Plant Sci.* 9:1197. doi: 10.3389/fpls.2018.01197

RStudio Team. (2020). *RStudio: Integrated Development for R*. Boston, MA: RStudio.

Rubin, R. L., van Groenigen, K. J., and Hungate, B. A. (2017). Plant growth promoting rhizobacteria are more effective under drought: a meta-analysis. *Plant Soil* 416, 309–323. doi: 10.1007/s11104-017-3199-8

Shaharoona, B., Arshad, M., and Zahir, Z. A. (2006). Effect of plant growth promoting rhizobacteria containing ACC-deaminase on maize (*Zea mays* L.) growth under axenic conditions and on nodulation in mung bean (*Vigna radiata* L.). *Lett. Appl. Microbiol.* 42, 155–159. doi: 10.1111/j.1472-765X.2005.01827.x

Song, H., Li, Y., Zhou, L., Xu, Z., and Zhou, G. (2018). Maize leaf functional responses to drought episode and rewatering. *Agric. For. Meteorol.* 249, 57–70. doi: 10.1016/j.agrformet.2017.11.023

Stoyanova, M., Pavlina, I., Moncheva, P., and Bogatzevska, N. (2007). Biodiversity and incidence of *Burkholderia* species. *Biotechnol. Biotechnol. Equip.* 21, 306–310. doi: 10.1080/13102818.2007.10817465

van der Walt, S., Colbert, S. C., and Varoquaux, G. (2011). The NumPy array: a structure for efficient numerical computation. *Comput. Sci. Eng.* 13, 22–30. doi: 10.1109/MCSE.2011.37

Vandenkoornhuyse, P., Quaiser, A., Duhamel, M., Le Van, A., and Dufresne, A. (2015). The importance of the microbiome of the plant holobiont. *New Phytol.* 206, 1196–1206.

Vannier, N., Agler, M., and Hacquard, S. (2019). Microbiota-mediated disease resistance in plants. *PLoS Pathog.* 15:e1007740. doi: 10.1371/journal.ppat.1007740

Vorholt, J. A., Vogel, C., Carlström, C. I., and Müller, D. B. (2017). Establishing causality: opportunities of synthetic communities for plant microbiome research. *Cell Host Microbe* 22, 142–155. doi: 10.1016/j.chom.2017.07.004

Wani, P. A., Khan, M. S., and Zaidi, A. (2007). Synergistic effects of the inoculation with nitrogen-fixing and phosphate-solubilizing rhizobacteria on the performance of field-grown chickpea. *J. Plant Nutr. Soil Sci.* 170, 283–287. doi: 10.1002/jpln.200620602

Zakeel, M. C. M., and Safeena, M. I. S. (2019). "Biofilmed biofertilizer for sustainable agriculture," in *Plant Health Under Biotic Stress*, eds R. Ansari and I. Mahmood (Singapore: Springer), 65–82. doi: 10.1007/978-981-13-6040-4

Zhang, J., Liu, Y.-X., Zhang, N., Hu, B., Jin, T., Xu, H., et al. (2019). *NRT1.1B* is associated with root microbiota composition and nitrogen use in field-grown rice. *Nat. Biotechnol.* 37, 676–684. doi: 10.1038/s41587-019-0104-4

Zilber-Rosenberg, I., and Rosenberg, E. (2008). Role of microorganisms in the evolution of animals and plants: the hologenome theory of evolution. *FEMS Microbiol. Rev.* 32, 723–735. doi: 10.1111/j.1574-6976.2008.00123.x

Conflict of Interest: The authors declare that the research was conducted in the absence of any commercial or financial relationships that could be construed as a potential conflict of interest.

Publisher's Note: All claims expressed in this article are solely those of the authors and do not necessarily represent those of their affiliated organizations, or those of the publisher, the editors and the reviewers. Any product that may be evaluated in this article, or claim that may be made by its manufacturer, is not guaranteed or endorsed by the publisher.

frontiers in Microbiology

ORIGINAL RESEARCH
published: 05 November 2021
doi: 10.3389/fmicb.2021.773116

Flooding Causes Dramatic Compositional Shifts and Depletion of Putative Beneficial Bacteria on the Spring Wheat Microbiota

Davide Francioli[1], Geeisy Cid[2], Saranya Kanukollu[1], Andreas Ulrich[1], Mohammad-Reza Hajirezaei[2] and Steffen Kolb[1,3]*

[1] Microbial Biogeochemistry, Research Area Landscape Functioning, Leibniz Center for Agricultural Landscape Research e.V. (ZALF), Müncheberg, Germany, [2] Department of Physiology and Cell Biology, Leibniz Institute of Plant Genetics and Crop Plant Research, Gatersleben, Germany, [3] Faculty of Life Sciences, Thaer Institute, Humboldt University of Berlin, Berlin, Germany

OPEN ACCESS

Edited by:
Hai-Ming Zhao, Jinan University, China

Reviewed by:
Lin Chen, Institute of Soil Science, Chinese Academy of Sciences (CAS), China
Chuntao Yin, Washington State University, United States

***Correspondence:**
Davide Francioli
davide.francioli@zalf.de

Specialty section:
This article was submitted to Terrestrial Microbiology, a section of the journal Frontiers in Microbiology

Received: *09 September 2021*
Accepted: *13 October 2021*
Published: *05 November 2021*

Citation:
Francioli D, Cid G, Kanukollu S, Ulrich A, Hajirezaei M-R and Kolb S (2021) Flooding Causes Dramatic Compositional Shifts and Depletion of Putative Beneficial Bacteria on the Spring Wheat Microbiota. Front. Microbiol. 12:773116. doi: 10.3389/fmicb.2021.773116

Flooding affects both above- and below-ground ecosystem processes, and it represents a substantial threat for crop and cereal productivity under climate change. Plant-associated microbiota play a crucial role in plant growth and fitness, but we still have a limited understanding of the response of the crop-microbiota complex under extreme weather events, such as flooding. Soil microbes are highly sensitive to abiotic disturbance, and shifts in microbial community composition, structure and functions are expected when soil conditions are altered due to flooding events (e.g., anoxia, pH alteration, changes in nutrient concentration). Here, we established a pot experiment to determine the effects of flooding stress on the spring wheat-microbiota complex. Since plant phenology could be an important factor in the response to hydrological stress, flooding was induced only once and at different plant growth stages (PGSs), such as tillering, booting and flowering. After each flooding event, we measured in the control and flooded pots several edaphic and plant properties and characterized the bacterial community associated to the rhizosphere and roots of wheat plant using a metabarcoding approach. In our study, flooding caused a significant reduction in plant development and we observed dramatic shifts in bacterial community composition at each PGS in which the hydrological stress was induced. However, a more pronounced disruption in community assembly was always shown in younger plants. Generally, flooding caused a (i) significant increase of bacterial taxa with anaerobic respiratory capabilities, such as members of Firmicutes and Desulfobacterota, (ii) a significant reduction in Actinobacteria and Proteobacteria, (iii) depletion of several putative plant-beneficial taxa, and (iv) increases of the abundance of potential detrimental bacteria. These significant differences in community composition between flooded and control samples were correlated with changes in soil conditions and plant properties caused by the hydrological stress, with pH and total N as the soil, and S, Na, Mn, and Ca

concentrations as the root properties most influencing microbial assemblage in the wheat mircobiota under flooding stress. Collectively, our findings demonstrated the role of flooding on restructuring the spring wheat microbiota, and highlighted the detrimental effect of this hydrological stress on plant fitness and performance.

Keywords: plant-microbe interactions, flooding, metabarcoding, bacteria, spring wheat, plant traits

INTRODUCTION

Climate change has increased the frequency and magnitude of extreme weather events such as drought, floods, heat waves and wildfires (Cox et al., 2002; Cook et al., 2018; Di Virgilio et al., 2019). These extreme weather events significantly impact on plants and soil biota and, in turn, they affect global biogeochemical cycling and ecosystem services, such as crop plant productivity in farming systems (Schröter et al., 2005; Vanbergen, 2013). It has been predicted that an increased number of incidences of extreme precipitation events will be a result of global warming, which will lead to an increased flooding frequency (Bevacqua et al., 2019; Konapala et al., 2020). Crop fitness and productivity are negatively impacted by water inundation (Bailey-Serres et al., 2012). Under flooding stress, crop yield can be highly reduced (Rhine et al., 2010; Morton et al., 2015; Ding et al., 2020) and even short-term events of few days can significantly affect wheat growth (Malik et al., 2002). Wheat yield losses due to flooding might range from 10 to over 50% (Jincai et al., 2001; Kaur et al., 2020; Tian et al., 2021), which however, depends on waterlogging duration, wheat genotype, growth stage, soil type and agricultural management.

Changes in belowground environments following flooding events are no less important than those that occur aboveground. Plant-associated microbiota plays a key role in fostering the host plant fitness (Turner et al., 2013; Compant et al., 2019), and it is well established that its composition is influenced by many host-associated and environmental factors (Francioli et al., 2016; Eisenhauer and Powell, 2017; Leff et al., 2018; Lewin et al., 2021). Recent research has demonstrated that alteration in soil moisture have significant effects on soil and root-associated microorganisms (Naylor and Coleman-Derr, 2018; Xu et al., 2018; Francioli et al., 2020). Many features of bacterial community, such as biomass, composition, structure and community assembly processes are sensitive to the hydrological regime in soil (Argiroff et al., 2017; Gschwend et al., 2020; Shen et al., 2021). Flooding results in changes of the osmotic activity and promotes oxygen depletion, fostering anoxia and anaerobes able to thrive under such conditions (Schimel et al., 2007). Microbial traits associated with resistance and resilience to hydrological stress may include endospore formation, production of osmoprotectants and specific cell wall structures, as well as different energy metabolisms (e.g., anaerobic and facultative respiration, fermenation, microaerophily; Unger et al., 2009; Bardgett and Caruso, 2020). Such physiological traits might be associated with specific taxa or bacterial clades such as the Gram-positive phylum Firmicutes and its endospore-forming members, e.g., *Bacillus* and *Clostridium*. These traits tend to be conserved at different phylogenetic levels (Martiny et al., 2015). Nonetheless, the response of the soil microbiota on flooding and waterlogging associated with typical crop plant hosts are largely unexplored.

Moreover, indirect effects of hydrological regimes on the plant-associated microbiota can be mediated through plant and soil physicochemical factors. Anoxia resulting from flooding can profoundly influence plant growth and, thus, indirectly altering soil bacterial microbiota through changes in the quality and quantity of rhizodeposits including exudates, competition for nutrients, or other mechanisms (Henry et al., 2007; Hartman and Tringe, 2019). In addition, soil undergoes many physiochemical changes in response to oversaturation by flooding. Several soil physicochemical variables, such as pH, nutrient concentrations, and redox status, are tightly linked to water availability, providing certain possible mechanisms for the association among water regime, edaphic properties and soil bacterial community compositions (Pett-Ridge and Firestone, 2005; Wilson et al., 2011; Moche et al., 2015).

Considering that the frequencies and intensity of extreme precipitation events are predicted to increase over the upcoming years, it is necessary to understand how these environmental changes will affect the composition and biodiversity of the microbiota associated with crop plants in agroecosystems. Thus, we setup a pot experiment to investigate the effect of flooding on the wheat plant-microbiota. Using a metabarcoding approach, we monitored responses of the bacterial community associated with different wheat compartments (rhizosphere and root) to flooding stress. Since plant phenology is an important driver in plant microbiota assembly (Donn et al., 2015; Francioli et al., 2018), and abiotic stress might affect differentially the plant-microbiota complex depending on the specific plant growth stage (PGS) in which it occur (Na et al., 2019; Breitkreuz et al., 2020), we imposed flooding stress only once, either at tillering, booting or flowering. Moreover, several soil and plant traits were measured through the whole experiment to correlate edaphic and physiological plant changes with shifts in bacterial community assemblage. We hypothesized that (1) soil physio-chemistry and plant traits will be strongly influenced by flooding, thus correlated indirectly with shifts in bacterial microbiota structure. (2) The bacterial microbiota will be differentially affected by the timing of flooding events, with early microbiota development being more susceptible to disruption. (3) The general response

of the bacterial microbiota to flooding will show a plant phylogenetic signals together with shifts in abundance of important ecologically taxa.

MATERIALS AND METHODS

Experimental Setup

The response of the wheat microbiota complex to flooding stress was investigated in a pot experiment that was conducted from September to December 2019. The experiment was carried out in a greenhouse at the Leibniz Institute of Plant Genetics and Crop Plant Research IPK-Gatersleben, Germany. Seeds of Chinese spring wheat (*Triticum aestivum* L.) were germinated in sieved soil (2 mm), which was obtained from the experimental station in Dedelow (Germany). The soil was a loamy sandy/medium silty sandy soil (S3/Su3 according to the German texture classification; Ad-hoc-AG-Boden, 2005) and its physiochemical properties are reported in **Supplementary Table 1**.

Seeds were germinated under controlled conditions and optimal watering. After the third leaf had appeared, i.e., 3 weeks after sowing, seedlings were individually transferred to 10L-pots containing 5 kg of the same soil used for germination (one seedling per pot). Tillering stage was initiated under controlled conditions of day/night temperature, i.e., 18/16°C, air humidity 70%, light intensity 250–300 μmol/(m^2·s) and photoperiod of 16 h light/8 h darkness. Pots were placed on tables in the greenhouse in a complete randomize design. Zadoks scale (Zadoks et al., 1974) was considered to monitor the developmental stage of the plants and the application of flooding. Flooding stress was induced only once and for a period of 12 day, at either tillering, booting or flowering and replicates were destructively sampled (**Supplementary Figure 1**). Previous studies on different soil types have reported that complete oxygen depletion in the top soil occurs within 2–8 days of flooding (Cannell et al., 1980; Meyer et al., 1985; Drew, 1992). Since the aim of the experiment was to investigate the response of the soil-wheat-microbe complex to a severe hydrological stress, we applied flooding for 12 days in order to be sure that oxygen was depleted in the flooded treatment. We established six replicates for each combination of PGS and water treatment, for a total of 36 pots. Control and flooding treatments were arranged in parallel considering the water holding capacity (WHC) of the soil used for the experiment. The WHC of the soil used was determined by a pre-experiment prior the set-up of the main experiment. Five individual pots containing the same amount of soil (5 kg) were weighed, over-watered and left draining overnight. The weight of the pots was registered next day and considered as WHC. Control plants were monitored at 50% WHC, which was in correspondence with the field capacity of the soil. Flooding was established by keeping water approximately 5 cm above the soil surface during the 12 days period.

Plant and Soil Sampling

After 12 days under flooding, plants of the control and flooding treatments were harvested, and tillers and spikes number documented. The material of interest (soil rhizosphere and plant tissues) used for further analysis was harvested from the same plants using the following procedure. Shoots and roots were separated, and their fresh weight was immediately measured. Rhizosphere soil, defined as soil which remained attached to the roots after the plant had been uprooted and shaken (Katznelson et al., 1948) was collected in sterile zipbags. Afterward, roots were carefully washed with tap water removing as much as possible of the remaining soil particles. Soil and root samples for molecular analysis were immediately frozen and stored at −80°C. Several macro and micronutrients concentrations in the roots were measured. Nitrogen (N) and carbon (C) concentration were analyzed in 1.5 mg ground powder by a EuroEA3000 (EuroVector SpA, Redavalle, Italy) using software version Callidus 5.1 (Muñoz-Huerta et al., 2013). For calibration the standard 2,5-Bis(5-tert-butyl-benzoxazol-2-yl) thiophene with 72.52% carbon and 6.51% nitrogen from HEKAtech GmbH (Wegberg, Germany) were used. A sector field high-resolution mass spectrometer (HR)-ICP-MS (Element 2, Thermo Fisher Scientific, Germany) was employed to measure P, Mg, S, K Ca, Mn, Zn, and Na concentrations in the root. The following edaphic properties were measured from the soil samples. Total organic carbon (TOC) and total nitrogen (TN) contents were determined in triplicate by dry combustion using a Vario EL III C/H/N analyzer (Elementar, Hanau, Germany). Since the carbonate concentration of the soils was negligible (<2%), the total C concentration measured was considered to represent TOC. Plant available P was extracted from fresh soil with double lactate (1:50 w/v, pH 3.6, 1.5 h; Riehm, 1943). After filtration of the suspension (Whatman Schleicher and Schuell 595 1/5 Ø 270 mm), the extracted P was quantified colorimetrically using the molybdenum blue method (Murphy and Riley, 1962). Mn, Ca, Na, K, Mg, concentration in soil were measured using an inductively coupled plasma-optical emission spectrometry-ICP-OES (ICP-iCAP 6300 DUO, Thermo Fisher Scientific, Germany).

DNA Extraction, Amplicon Library Preparation, and Sequencing

DNA was extracted from the soil and root samples collected using the DNeasy PowerLyzer PowerSoil Kit (Qiagen). Bacterial DNA amplification was performed using the primers 799f (Chelius and Triplett, 2001) and 1193r (Bodenhausen et al., 2013) following the PCR protocol described previously (Francioli et al., 2021a). The amplicons were sequenced on an Illumina MiSeq instrument with 2 × 300 base pair kits by LGC genomics GmbH, Berlin, Germany. Demultiplexing was performed with Illumina bcl2fastq 2.17.1.14 software following clipping of barcode and sequencing adapters. Primer were removed using Cutadapt v3.0 (Martin, 2011) following sequence processing using QIIME 2 v2020. Amplicon sequence variants (ASV; also known as zero-radius operational taxonomic units; Callahan et al., 2017) were determined from raw sequence data using the DADA2 pipeline (Callahan et al., 2016). Only ASVs that were detected in more than two samples were included in the data analyses. Alpha diversity metrics were calculated from the normalized sequence library, which was rarefied to 20,000 reads per sample. For taxonomic assignment of the ASVs, the representative sequences were classified using the

naïve Bayesian classifier for Silva 138. Non-bacterial ASVs were discarded. All sequences have been submitted to the European Nucleotide Archive (study accession number PRJEB47399).

Statistical Analyses

Univariate Analysis of Variance (ANOVA) followed by Tukey's honestly significant difference (HSD) *post hoc* test was used to test for differences in soil and plant properties, among the treatments and PGS. All the variables were tested for normality using Shapiro-Wilk and Jarque-Bera tests and the equality of group variances was examined using Levene's test. A log10 transformation was applied to all variables that did not meet the parametric assumptions. Correlation among the soil and plant traits were determined using Spearman's rank correlation. Environmental variables with a Spearman rank correlation coefficient $p > 0.8$ were removed and excluded from further analysis. Effects of soil-plant compartment, PGS and watering treatment on the bacterial richness were tested by univariate PERMANOVA models (Anderson, 2017). Pairwise differences in bacterial ASV richness between water treatment at the same PGS and compartment were estimated using ANOVA followed by a Tukey's HSD *post hoc* test. All the phylogenetic analyses were performed using the package "picante" (Kembel et al., 2010). First, a phylogenetic distance matrix based on a maximum-likelihood 16S rRNA tree was generated in QIIME2 with FastTree2 (Price et al., 2010). The phylogenetic distance matrix was used to calculated (i) standardized effect size of phylogenetic diversity (ses.PD), (ii) the net relatedness index (NRI), and (iii) the nearest taxa index (NTI). ses.PD was calculated by comparing the observed phylogenetic diversity (PD) value from the mean of the null distribution (999 null iterations) based on random shuffling of ASV labels across the phylogenetic tips. Negative ses.PD values and low quantiles ($p < 0.05$) indicated that co-occurring species are more closely related than expected by chance (clustering), whereas positive values and high quantiles ($p > 0.05$) indicate that the co-occurring species are less closely related than expected by chance (overdispersion) (Webb et al., 2002). NRI was calculated using the "standardized effect size of pairwise distances in communities" function (*ses.mpd*) and the nearest taxa index (NTI) using the "standardized effect size of mean nearest taxon distances" function (*ses.mntd*). NRI is a measure of the mean relatedness between members of microbial communities, and the NTI is a measure of the smallest mean phylogenetic distance between all pairs of n taxa in a community sample. For both NRI and NTI analyses, the null model was randomized 999 times and set to "phylogeny.pool," which randomly draws species from the phylogeny for its null distribution. NRI and NTI were calculated for bacterial microbiota from each soil-plant compartment, PGS and watering treatment. Positive NRI/NTI values indicate a microbiota of which taxa are on average more closely related to one another than they are to members of the randomized (null model) microbial species pool. To statistically compare ses.PD, NRI and NTI values for each type of sample (compartment, PGS, watering treatment), we used one-way ANOVA followed by a Tukey's HSD *post hoc* test. Differences in the bacterial microbiota structure across plant-soil compartment, PGS and flooding treatment, we first calculated Bray-Curtis dissimilarities using square-root transformed relative abundances (Hellinger transformation; Legendre and Gallagher, 2001). Permutational multivariate analysis of variances (PERMANOVA) based on the Bray-Curtis dissimilarity index was performed to analyze the effect of the above mentioned experimental factors on the bacterial community structure, using 999 permutations for each test. Similarities in the bacterial community structure among the control and flooded treatments at each PGS were investigated using Analysis of Similarity (ANOSIM) algorithm. Furthermore, we performed variance partitioning based on redundancy analysis (RDA) to quantify the contribution of soil and root properties, PGS and water treatment to the structure of the bacterial community in each compartment. Following Blanchet et al. (2008) we first tested the significance of the global model using all predictors. Variable selection was then performed using forward selection implemented with function *forward.sel* in the R package "packfor" (Dray et al., 2011). Variance partitioning was conducted using the *varpart* function in the "vegan" R package (Oksanen et al., 2018). Then a model of multivariate analysis of variance was constructed using distance-based redundancy analysis (db-RDA) based on the Bray-Curtis distance to determine the environmental variables that were most influential on the bacterial community structure within each compartment. Ternary plots were performed using the package "microbiomeutilities." Linear discriminant analysis effect size (LEfSe) (Segata et al., 2011) was applied to identify biomarker taxa explaining differences between the bacterial microbiota across PGS in the control treatment, and also between flooded and control samples at each PGS in both plant-soil compartments. All the data were analyzed with R version 3.6 (R Core Team, 2014).

RESULTS

We conducted a pot experiment with the model crop plant spring wheat *Triticum aestivum* cv. *Chinese Spring* to assess the impact of flooding stress on the structure of the bacterial microbiota associated to the rhizo- and endosphere. As plant phenology has been implicated in shaping the plant microbiota and abiotic stress might have a differential impact on the crop microbiota complex depending on the specific PGS, wheat plants were subjected to a period of 12 days of flooding either at tillering, booting and flowering. After such a period, stressed plants were harvested and removed from the experiment. A variety of soil, plant and microbiota related traits were measured to reveal the response of the wheat microbiota complex (**Supplementary Figure 1**).

Plant Performance and Soil-Plant Properties in the Different Watering Treatments and Across Plant Growth Stages

Flooding had a significant effect on plant growth, as well as on soil and plant properties. At tillering, we observed a significant reduction ($p < 0.05$) only in root biomass (55%), but flooding at

booting caused shoot and root dry biomass decreases by 25 and 70%, respectively, compared to control plants (**Supplementary Figure 2**). No change in above- and belowground biomass was observed when the flooding stress occurred at flowering. Wheat plants exposed to flooding stress developed 29% less tillers and a showed a decrease of 18% in the spike to tiller ratio (**Supplementary Figure 2**).

Flooding had a strong influence on edaphic parameters. In general, a significant increase ($p < 0.05$) in soil moisture, pH, Zn, and available P was observed in flooded soil at all developmental stages (**Supplementary Figure 3**). Furthermore, significant increases ($p < 0.05$) of total soil C and S occurred at tillering, whereas a significant increase ($p < 0.05$) of the total N content occurred at flowering in the flooding treatments. At root level, flooding caused a significant decrease ($p < 0.05$) of the concentration of Mg, S, and Ca during tillering (**Supplementary Figure 4**) and booting. We also found a significant increase ($p < 0.05$) of the Mn content under flooding, which was two times higher compared to the control (**Supplementary Figure 4**). In the control plants, we observed shifts in soil and root nutrient concentrations across the different PGS. For example, a significant increase ($p < 0.05$) of soil total C, total S and root S and Na was observed at flowering, while the concentration of soil total N and root P was significantly higher ($p < 0.05$) at tillering and booting.

Bacterial Richness and Biodiversity

A total of 5,318,073 bacterial 16S rRNA gene high quality reads were recovered from all the samples, which clustered in 6241 bacterial ASVs. Overall, bacterial sequences were affiliated to 31 phyla, 89 classes, 194 orders, 325 families, and 630 genera. Proteobacteria was the most abundant phylum, comprising approximately 41% of the reads across all samples (1661 ASVs), followed by Actinobacteriota (30.5% of reads; 1444 ASVs) and Firmicutes (10% of reads; 636 ASVs). A small proportion of members of the Bacteroidota (6.5%, of reads; 496 ASVs), Chloroflexi (2.3% of reads; 425 ASVs), and Myxococcota (2.1% of reads; 315 ASVs) was also detected.

We calculated bacterial richness and several phylogenetic metrics to assess how bacterial alpha-diversity was influenced by soil-plant compartment, PGS and watering treatment. Analysis of variance revealed that the soil-plant compartment had the greatest effect on bacterial richness that significantly ($p < 0.05$) decreased from rhizosphere to the root (**Supplementary Table 2** and **Figure 1A**). Watering treatment had a marginal but significant effect ($p < 0.05$) on bacterial richness, while PGS did not. A significant interaction ($p < 0.05$) between PGS and watering treatment was detected. This latter result was evident when looking at each combination of plant-soil compartment and PGS, since most of the differences in alpha diversity were found at tillering, with significant lower values in the flooded than in the control samples, irrespective of compartment (**Figure 1A**).

Phylogenetic relatedness among the bacterial communities within our samples was evaluated based on the standardized effect size of phylogenetic diversity (ses.PD). Overall, the bacterial communities were relatively phylogenetic clustered, but significantly lower ($p < 0.05$) values in phylogenetic similarity were always found at tillering compared to later PGS (**Figure 1B**). Remarkably, the bacterial communities associated with flooded samples were characterized at tillering by the lowest effect size of phylogenetic diversity. On the contrary, at booting and flowering we observed no significant differences in phylogenetic diversity regardless of watering treatments and PGS. We also calculated NRI and NTI parameters, which measure both alternative aspects of community phylogenetic clustering vs. overdispersion. These results confirmed the findings obtained by the ses.PD analysis (**Supplementary Figure 5**).

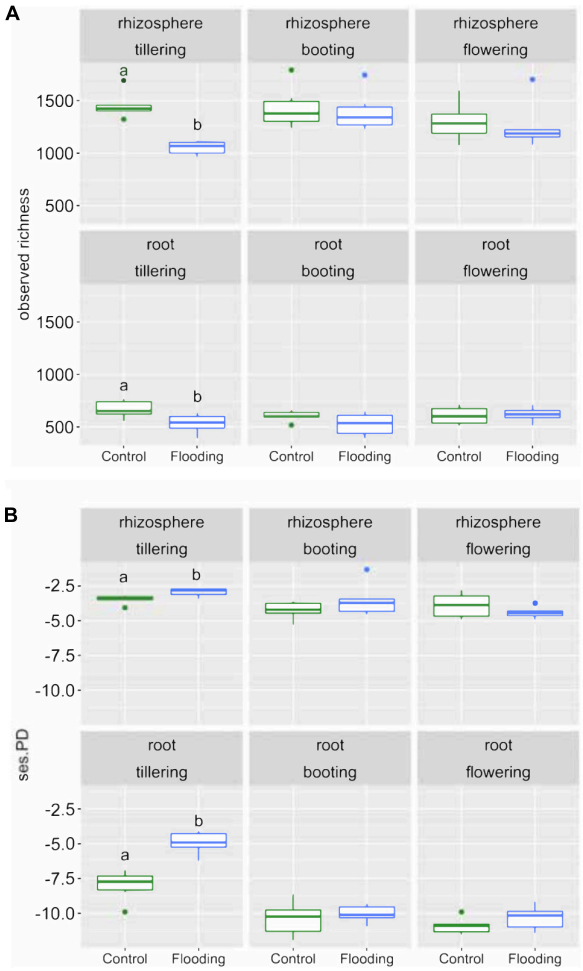

FIGURE 1 | Box plots of the observed richness **(A)** and standardize effect size of phylogenetic diversity (ses.PD) **(B)** of the bacterial communities in the samples studied. Different letters indicate significant differences between water treatments within the same PGS based on Tukey's HSD test $p < 0.05$.

Effect of Compartment, Flooding, and PGS on Bacterial β-Diversity

Factors that were responsible in shaping the microbiota structure between samples were firstly explored by beta-diversity employing a principal coordinate analysis with Bray-Curtis dissimilarities (**Figure 2**). Altogether, the two axes accounted for 55.4% of the variance, with the first coordinate (47.1%) primarily

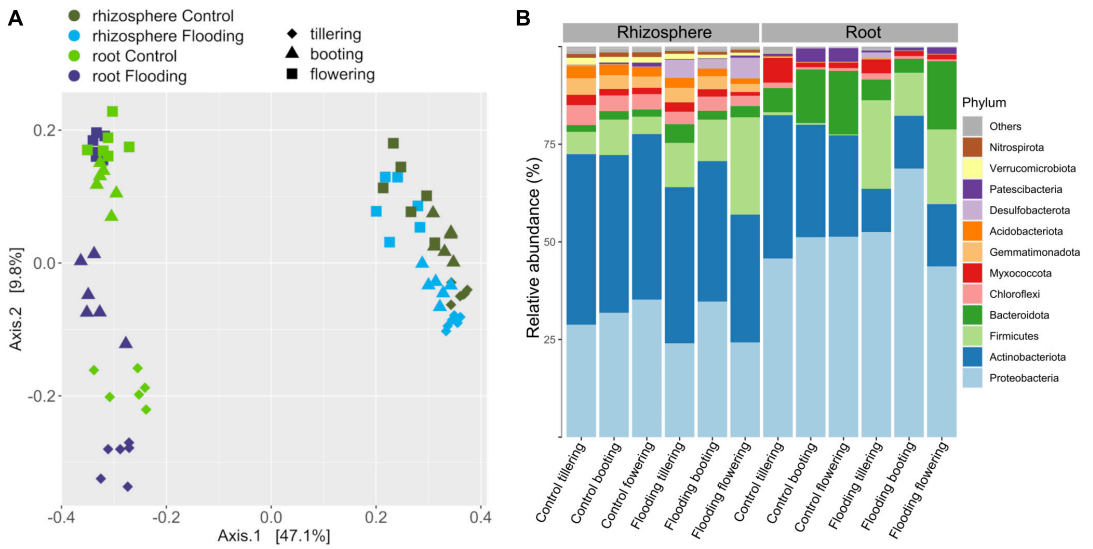

FIGURE 2 | Principal coordinates analysis (PCoA) Bray-Curtis dissimilarity metrics **(A)** and mean relative abundance of the main phyla **(B)** of the bacterial communities detected in this study.

discriminating the samples by compartments, while along the second coordinate (9.8%) a separation by PGS, which was more pronounced in the root samples, was observed. Principal coordinate analysis based on weighted UniFrac distance, which accounts for phylogenetic relationships among microbial taxa, confirmed the discrimination between compartments along the first coordinate, but it also displayed along the second axis a clear separation between the bacterial communities of the flooded and control samples (**Supplementary Figure 6**). This latter result suggested that flooding stress induced a phylogenetic compositional response in the bacterial assemblage dynamics at each PGS it was induced. PERMANOVA analysis on the full bacterial ASV dataset confirmed that rhizosphere and roots were characterized by distinct bacterial microbiota (**Table 1**). The large differences in community structure between the two soil-plant compartments were primarily due to the different composition of their specific microbiota, as more than half of the ASVs that were solely found in the rhizosphere, whereas most of the root-associated bacterial ASVs were also detected in the rhizosphere (**Supplementary Figure 7**). The root microbiota was dominated by Proteobacteria, Patescibacteria, Myxococcota, and Bacteroidota, while the rhizosphere was significantly enriched ($p < 0.05$) in Actinobacteria, Chloroflexi, Desulfobacteriota, Acidobacteria, and Verrucomicrobiota (**Figure 2B** and **Supplementary Figure 7**). Interestingly, bacterial members of the latter two phyla were completely depleted in root samples, further indicating a strong niche compartmentalization effect promoted by the plant host (**Figure 2B** and **Supplementary Figure 7**).

Within each compartment, substantial and significant effects of flooding and plant phenology on the bacterial microbiota structure were found. In the rhizosphere, PERMANOVA analysis revealed that flooding explained 11.4% of variance, PGS 20.5% and the interaction of these two terms accounted for an additional

TABLE 1 | The relative importance of soil-plant compartment, plant growth stage (PGS) and watering treatment (WT) for the total bacterial community structure associated to the samples investigated in this study as revealed by PERMANOVA.

Parameter	df	Pseudo-F	R^2	P−value
Compartment	1	105.279	0.4638	0.001
PGS	2	11.534	0.1016	0.001
WT	1	12.611	0.0690	0.001
Compartment * PGS	2	4.263	0.0375	0.002
Compartment * WT	1	4.365	0.0192	0.007
PGS * WT	2	4.283	0.0377	0.003
Compartment * PGS * WT	2	105.279	0.4638	0.001

9.8% of variation (**Table 2**). However, a higher influence of the experimental treatments on the bacterial microbiota was found in the root compartment, as flooding explained 16.8% of variance, PGS 30% and the interactions of these two factors captured a further 14.5%, for a total of 61% of variation (**Table 2**). Principal coordinates analysis on the bacterial microbiota of the rhizosphere and roots confirmed these results, distinguishing the samples associated with a particular PGS along the first axis, while the flooded samples where clearly separated from the control by the second axis (**Figures 3A,B**). ANOSIM provided further evidence that the bacterial microbiota of the flooded wheat plants were significantly different ($p < 0.05$) compared to the control at each PGS (**Supplementary Tables 3**, **4**).

Variance partitioning was conducted to quantify the contribution of edaphic and root properties, and their interactions with watering treatment and PGS on the structure of the bacterial microbiota. In both compartments, these four experimental factors captured together a large proportion of the variance, accounting for 35 and 54%, in the rhizosphere and root, respectively (**Figures 3C,D**). In general, the pure effect of these

TABLE 2 | The relative importance of plant growth stage (PGS) and watering treatment (WT) for the total bacterial community structure associated to rhizosphere and root compartments in the samples investigated in this study as revealed by PERMANOVA.

	Rhizosphere				Root			
Parameter	**df**	**Pseudo-F**	R^2	***P*–value**	**df**	**Pseudo-F**	R^2	***P*–value**
PGS	2	5.2378	0.2041	0.001	2	11.7182	0.3010	0.001
WT	1	5.8123	0.1132	0.001	1	13.1147	0.1684	0.001
PGS * WT	2	2.5079	0.0977	0.001	2	5.6546	0.1452	0.001

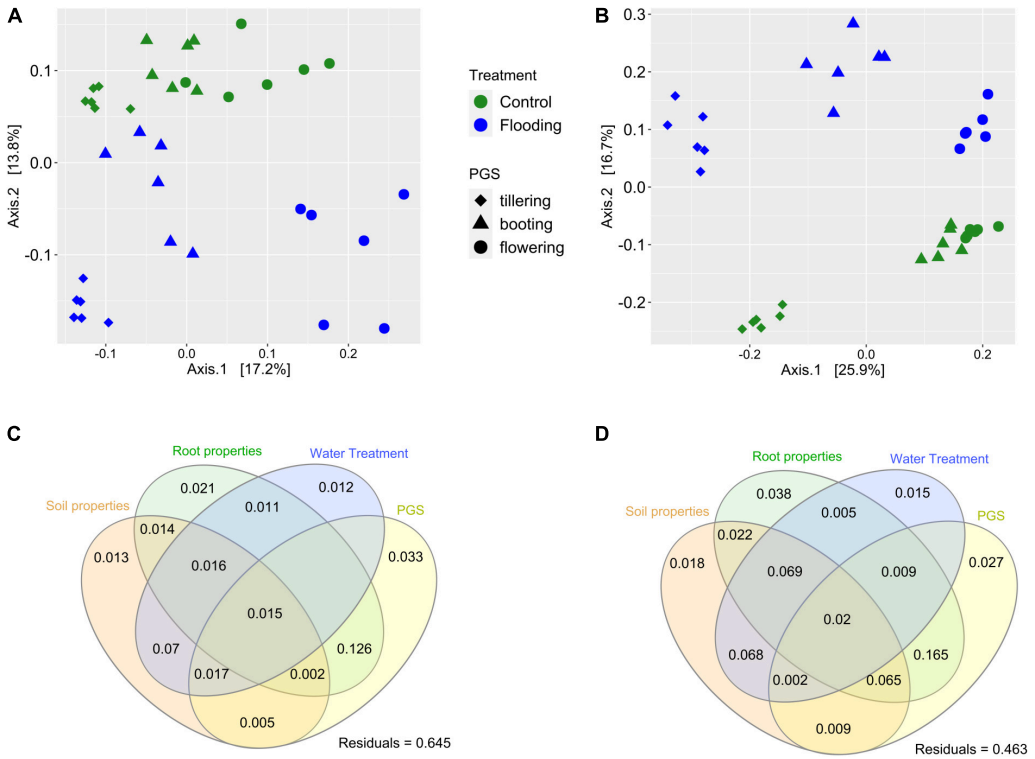

FIGURE 3 | Principal coordinates analysis (PCoA) of the bacterial communities detected in the rhizosphere **(A)** and in the root **(B)** compartment. Variation partitioning analysis, illustrating the effects soil parameters, root traits, watering treatment and plant growth stage (PGS) in the community for the rhizosphere **(C)** and root **(D)** compartment. Each ellipse represents the portion of variation accounted by each factor. Shared variance is represented by the intersecting portions of the ellipses. Values < 0 are not shown. Unexplained variation (residuals) is reported in the plot.

variables on the bacterial community structure was marginal, since most of the variance explained by them was shared, indicating an interactive effect of PGS and watering treatment on the root and soil properties, which in turn significantly affected the bacterial microbiota assemblage. A significant effect ($p < 0.05$) of various soil and root properties on the microbiota was further revealed by partial db-RDA. Soil pH and total N, together with root S content were significant factors affecting the bacterial microbiota structures in both compartments (**Supplementary Table 5**). In addition, the root microbiota was also significantly correlated with root K, Na, Mn, and Ca concentrations (**Supplementary Table 5**).

We compared structural dissimilarities of the bacterial microbiota between flooding and control treatments at each PGS to resolve at which PGS the application of flooding had the largest effect. In the rhizosphere, the largest impact of flooding stress on the bacterial microbiota structure was observed in the earliest (tillering) and latest stage (flowering) of the plant growth. While in the roots, the greatest impact of flooding was found at tillering, followed by booting and flowering (**Figure 4**). It is noteworthy to mention, that dissimilarities between flooding and control samples were always lower in the soil than in the root. This observation confirms that the influence of flooding was more pronounced on the root-associated bacterial microbiota.

Dynamics of the Bacterial Microbiota Over Plant Growth Stages

To better understand the effect of watering treatment in the rhizosphere and root microbiota, we sought to explore the temporal dynamics of the bacterial communities under control condition. β-diversity changes in response to PGS were revealed

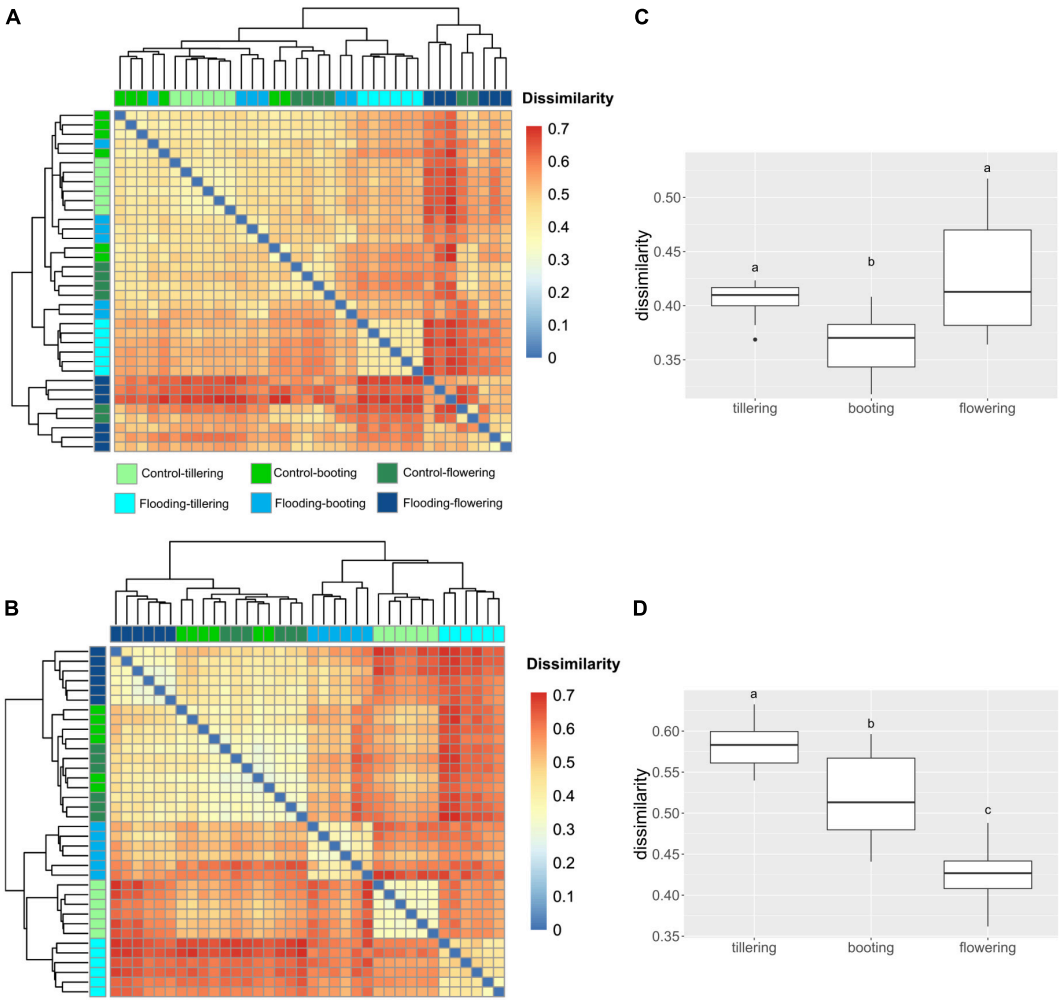

FIGURE 4 | Heatmap representing the Bray-Curtis dissimilarity in bacterial community structure between watering treatment and plant growth stages in the rhizosphere **(A)** and root **(B)**. Box plots of Bray-Curtis dissimilarity index between watering treatment and plant growth stages in the rhizosphere **(C)** and root **(D)**. The different letters indicate significant differences among plant growth stages (Tukey's HSD test $p < 0.05$.).

in both compartments, with the bacterial communities at booting and flowering stages always being more similar among each other than with the one at tillering (**Figures 4**, **5** and **Supplementary Figure 8**). However, higher microbiota dissimilarities between early (tillering) and late PGS (booting, flowering) were found in the root compartment than in the rhizosphere (**Figures 4**, **5** and **Supplementary Tables 3**, **4**). This indicated a stronger plant phenological effect on the endospheric and rhizoplan bacteria. This result was also reflected by variance partitioning analysis, that revealed that the pure and interactive effects captured by PGS and root traits were relatively higher in roots than in the rhizosphere (**Supplementary Figure 9**), suggesting that changes of root traits over time were highly determinant for the root microbiota assembly.

We found that the observed differences in bacterial microbiota over PGS were primarily due to shifts in the abundance of taxa shared across all three PGS. Indeed, PGS-exclusive ASVs accounted for a marginal proportion of sequences (ranging from 1.2 to 5.7%), while more than half of the ASVs detected were found in all PGS and accounted for more than three quarters of the total sequences detected in the control treatment (**Supplementary Figure 10**). Many shared ASVs were affiliated with several representative genera (>1% abundance), most of which showed abundance shifts across PGS (**Supplementary Figure 10**).

Dominant bacterial phylotypes as indicative biomarkers at each PGS were identified by linear discriminant analysis (LDA) effect size (LEfSe) (**Supplementary Figure 11**). In the rhizosphere, members affiliated with the phyla Chloroflexi, Acidobacteria, Gemmatimonadota, and Myxococcota were significant more abundant ($p < 0.05$) at tillering than in other PGS. On the other hand, bacterial taxa within phyla Proteobacteria, Actinobacteria, and Patescibacteria were found significantly more abundant ($p < 0.05$) at flowering, while booting stage showed a significant higher proportion ($p < 0.05$) of Firmicutes. LEfSe analysis identified *Gaiella*, *Streptomycetes*,

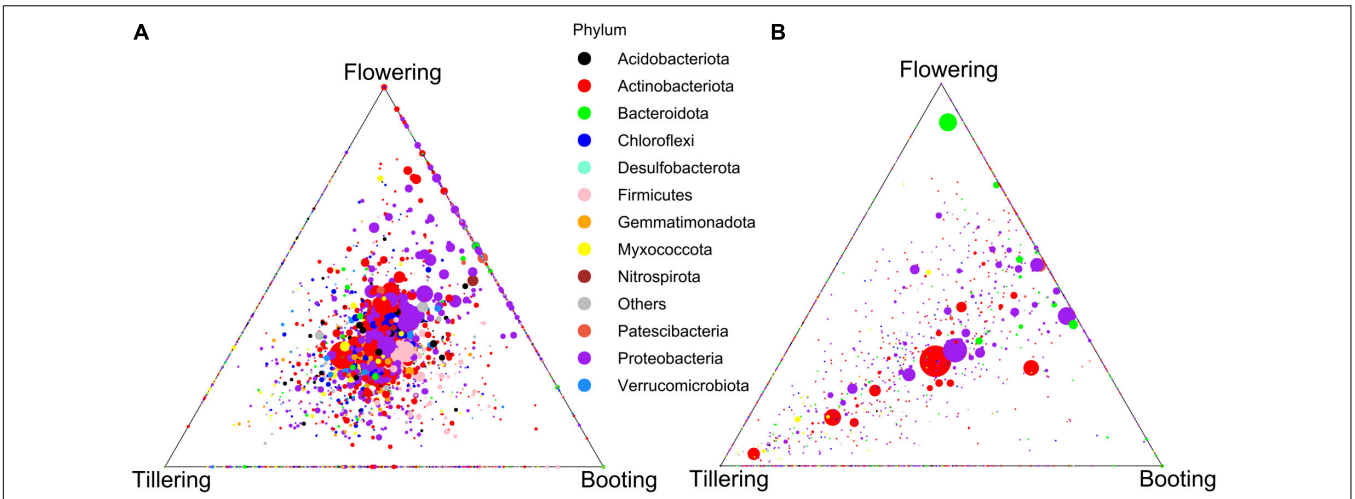

FIGURE 5 | Ternary plot of the ASVs distribution across plant growth stages in the rhizosphere **(A)** and in the roots **(B)** of the control plants.

Mycobacterium, MB-A2_108 at tillering, *Bacillus* and *Penibacillus* (both belonging to the class Bacilli) and *Nitrospira* at booting, and *Sphingomonas*, *Massilia*, *Mesorhizobium,* and *Arthrobacter* at flowering as biomarker genera. In the roots, contrarily to the rhizosphere, Actinobacteria, Firmicutes, Fibrobacterota, and Myxococcota phyla were found as biomarker at tillering stage, Proteobacteria at booting, while Bacteroidota and Patescibacteria were enriched at flowering (**Supplementary Figure 10**). Indeed, the roots of young plants were mainly enriched in several genera affiliated with Actinobacteriota, i.e., *Streptomyces*, *Kribbella* and *Lechevalieria*. The most discriminant biomarker taxa at booting were the Proteobacteria families *Devosiaceae*, *Rhizobiaceae*, *Pseudomonadaceae,* and *Caulobacteraceae,* whereas at flowering they were represented by species of the genus *Flavobacterium* (Bacteroidota phylum) and the family *Saccharimonadaceae* (phylum Patescibacteria).

Compositional Phylogenetic Shifts Characterized the Response of the Bacterial Communities to Flooding Stress

We next investigated the composition and changes in relative abundance patterns of bacterial groups in response to this hydrological stress. The evident differences observed in bacterial beta-diversity between the flooded and control treatments were mainly reflected by substantial shifts in composition of the bacterial microbiota. For example, almost the half of the sequences that were detected in the flooded roots at tillering were not detected in the control treatment. These ASVs were mainly affiliated with the anaerobic or facultative anaerobic bacteria of the genera *Dechloromonas*, *Enterobacter*, *Geobacter* (**Supplementary Figures 12**, **13**). Large proportions of unique ASVs were also only detected in flooding treatments in the roots at booting (38%) and flowering (20%) stages, which belonged mainly to the families *Clostridia, Oxalobacteraceae,* and *Lachnospiraceae.* These findings clearly demonstrated that flooding stress caused a greater disruption to early (tillering) compared to late (booting, flowering) bacterial microbiota, with a significant enrichment ($p < 0.05$) in facultative and strict anaerobes primarily of the class Clostridia (Firmicutes), and the phyla Desulfobacterota and Proteobacteria. LEfSe analysis further corroborated these observations, identifying in the root compartment almost twice of bacterial biomarker taxa at tillering than in the other PGS (**Figure 6**). More importantly, biomarker analysis evidenced that these compositional shifts of the bacterial microbiota due to flooding stress were highly phylogenetically clustered. Indeed, an enrichment of Firmicutes and Desulfobacterota together with a parallel depletion of Actinobacteriota and Proteobacteria, were observed in all the flooded samples. At the genus level, a significant increase ($p < 0.05$) in *Geobacter* and *Clostridium* abundances, with a parallel decrease of *Streptomyces* and *Sphinghomonas* were found.

Compartment-wise depletion and enrichment patterns at particular PGS were also recorded as a response to flooding. For instance, a significant decrease ($p < 0.05$) in the bacterial phyla Myxococcota at tillering, Bacteroidota at booting, Deinococcota at flowering, and Patescibacteria (especially the genus *Saccharimonadia*) in both late PGS was found in the flooded roots (**Figure 6**). On the contrary, a significant increase ($p < 0.05$) of Gammaproteobacteria occurred in all these samples. In particular, ASVs affiliated to Burkholderiales, such as (i) the endophytic non-nodulating diazotroph *Azoarcus*, and (ii) taxa with denitrifying and phosphorous accumulation capabilities of the genera *Dechloromonas* and *Candidatus Accumulibacter* decreased at tillering stage under flooding. In the rhizosphere, a general depletion of Rhizobiales, i.e., *Rhizobiaceae* and *Xanthobacteracee*, occurred due to flooding (**Supplementary Figure 14**). In addition, members of Cloroflexi, Verrucomicrobiota and Acidobacteriota where significantly depleted ($p < 0.05$) at tillering and booting, while an enrichment of Bacteroidota ASVs was detected in both tillering and flowering under flooding.

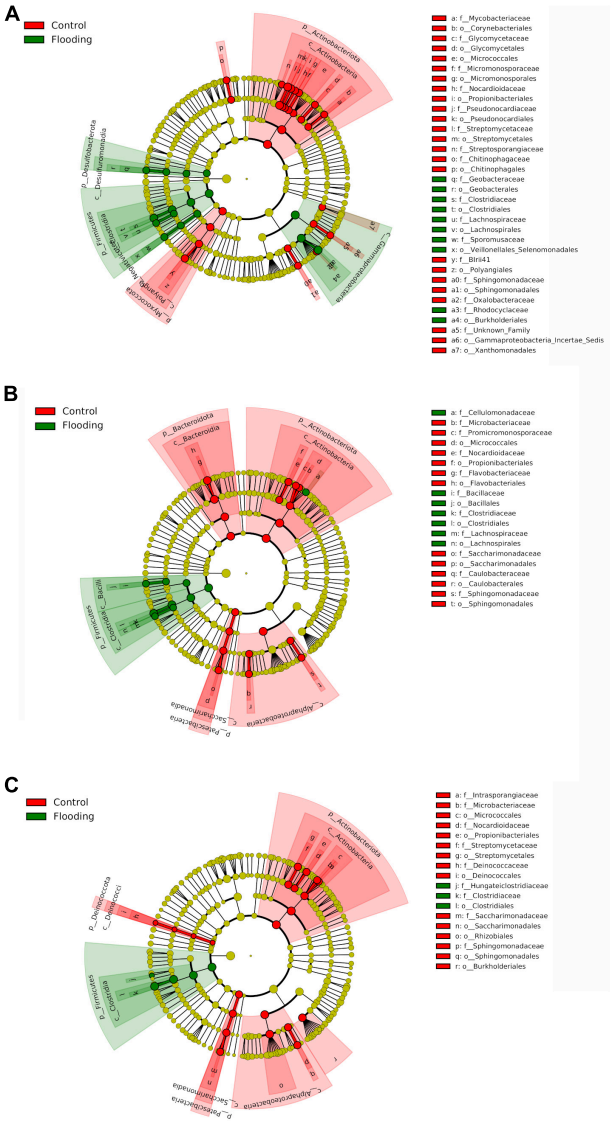

FIGURE 6 | LEfSe analysis at multiple taxonomic levels comparing root bacterial community structure in both control and flooding treatment at tillering **(A)**, booting **(B)** and flowering **(C)**. Cladogram illustrating the taxonomic groups explaining the most variation among root communities. Each ring represents a taxonomic level, with phylum (p_), class (c_), order (o_) and family (f_) emanating from the center to the periphery. Each circle is a taxonomic unit found in the dataset, with circles or nodes shown in colors (other than yellow) indicating where a taxon was significantly more abundant.

DISCUSSION

The plant microbiota is one of the key determinant for plant health and productivity (Turner et al., 2013; Finkel et al., 2017; Compant et al., 2019). Therefore, it is pivotal to unravel the factors influencing its composition and functionality in response to climate change-associated extreme weather events that likely will occur more frequently in the near future (Castro et al., 2010; De Vries and Shade, 2013). Herein, we provide an in-depth characterization of the effects flooding stress on the spring wheat microbiota complex.

Flooding Causes a Joint and Substantial Change in Plant Phenotype and Root Microbiota

In our study, flooding reduced spring wheat performance as revealed by above- and belowground biomass changes, and significantly decreased the number of tillers and spike to tiller ratio, which can negatively affect the final plant productivity (Malik et al., 2002). Our findings are in accordance with previous studies since flooding have been reported to affect negatively plant performance, reducing root and shoot growth (Ghobadi et al., 2017), number of tillers and leaves (Arduini et al., 2016), photosynthesis (Jincai et al., 2001; Wu et al., 2015), kernel weight (Wu et al., 2015), and wheat yield (Pampana et al., 2016; Ding et al., 2020).

The wheat-microbiota was also strongly affected by hydrological stress, since the flooded and control bacterial communities where mainly composed by distinct taxa. These significant differences in community composition were correlated with changes in soil conditions and plant properties caused by flooding. Specifically, we identified pH and total N as the soil, and, S, Na, Mn, and Ca concentrations as the root properties most influencing microbial assemblage in the wheat microbiota under flooding stress (**Supplementary Table 5**). Beside O_2 depletion, flooding strongly altered the soil physicochemical boundary conditions. It increased soil pH, C, and N, and influenced the concentration of several root macro- and micro-nutrients. Changes in soil pH is often reported as a consequence of waterlogging (Sun et al., 2007; Hemati Matin and Jalali, 2017) and it has been recognized as a main factor influencing the structure of bacterial microbiota across a wide range of soils and ecosystems (Fierer and Jackson, 2006; Lauber et al., 2009; Bardelli et al., 2017). Plant traits, such as root architecture and nutrient concentration are also commonly described as important drivers in structuring the root microbiota (Fitzpatrick et al., 2018; Schöps et al., 2018; Francioli et al., 2020), and their alterations might have important consequences in microbiota assembly (Leff et al., 2018; Pervaiz et al., 2020). Overall, these findings validated our first hypothesis, highlighting the fundamental influence of flooding on plant and soil properties, which in turn are firmly correlated with bacterial community assembly.

Our study further revealed that the changing root properties over the various PGS were important determinants for the assembly root-associated bacterial microbiota in both flooded and non-flooded wheat plants confirming previous observations that plant host phenological state plays a pivotal role in microbiota composition and structure (Bulgarelli et al., 2013; Wang et al., 2016; Francioli et al., 2018). In addition, a more severe impact of flooding on the bacterial microbiota occurred in the roots than in the rhizosphere suggesting that the root-associated community is under at a larger degree under host control. We found that the root microbiota showed a higher phylogenetically relatedness than the rhizospheric one, further

highlighting the selective pressure exerted by plant host. It is noteworthy to mention that the two soil-plant compartments were characterized by distinct bacterial microbiota, with the root microbiota being a subset of the rhizospheric one. Collectively, these results proved that (i) niche compartmentalization plays a pivotal role in shaping microbiota in the soil-wheat system (Cordero et al., 2020; Tkacz et al., 2020; Kawasaki et al., 2021), and (ii) the root microbiota is highly controlled by host-factors that change over plant development (Lakshmanan, 2015; Lareen et al., 2016; Francioli et al., 2021b).

The Wheat Microbiota Complex Is Less Resilient at Early Growth Stages to Flooding

Flooding stress caused dramatic shifts in microbiota composition and structure at each PGS in which it was induced, but it has the greatest impact on the bacterial community assembly at tillering stage. Phylogenetic analysis further showed that the bacterial microbiota in all the flooded samples associated with young plants were characterized by the lowest phylogenetic clustering similarities among the other bacterial community investigated in this study. These findings acknowledged our second hypothesis, as they proved that flooding caused a greater disruption to early compared with late PGS bacterial microbiota. Likewise, Xu et al. (2018) found that the juvenile sorghum root microbiota was more affected by drought stress compared to the one associated with late stages of plant development. In summary, all these observations suggest that the microbiota of early growth stages is still in a dynamic process of establishment, in which community assembly is less resilient to external physico-chemical stresses, while during the adult plant phase it is relatively more stable due to prior establishment of a more stable community likely with an higher and tighter degree of interactions (Angel et al., 2016; Edwards et al., 2018). The higher degree of compositional stability of bacterial communities in older wheat plants was also mirrored by the high phylogenetic community relatedness found in both flooding and control treatments at booting and flowering. Considering that flooding significantly affected the bacterial microbiota structure at all PGS, but no substantial differences were found in the phylogenetic alpha diversity metrics among flooded and control samples in older plants, we can deduce a general phylogenetic response of the bacterial microbiota to flooding stress in our wheat microbiota complex investigated, which was further confirmed by phylogenetic beta-diversity analysis using weighted UniFrac metric.

Flooding Caused Shifts in the Phylogenetic Composition of the Bacterial Microbiota

The pattern of compositional shifts that flooding stirs a strong phylogenetic signal, with entire phyla responding roughly in unison, confirmed our third hypothesis. The main features of this pattern were (i) a significant increase of bacterial taxa with anaerobic respiratory capabilities, i.e., within phyla Firmicutes and Desulfobacterota, (ii) a significant reduction in Actinobacteria and the Proteobacteria, (iii) depletion of several putative plant-beneficial bacterial taxa by flooding stress, and (iv) increases of the abundance of potential detrimental taxa. Flooding promoted an enrichment of the genera *Geobacter* and *Clostridium*, that represent strictly anaerobic bacteria that are frequently isolated in waterlogged soils (Gschwend et al., 2020). Recent research showed that several *Clostridium* species might cause soft rot disease in several vegetable crops and their abundance significantly increased with heavy rainfall and flooding (da Silva et al., 2019). On the other hand, a dramatic reduction of the abundance of *Streptomyces* and *Spinghomonas* occurred in all flooding samples, which have been described as beneficial for wheat growth. Members of these two genera, are able to solubilize inorganic phosphorus, to form siderophores and affect phytohormones production and might be involved in biocontrol activity (Correa-Galeote et al., 2018; Kavamura et al., 2021). Specific compartment-wise patterns in enrichment or depletion of plant-health relevant bacteria in response to flooding were also detected. Bacteria affiliated to the genus *Saccharimonadia*, that recently was reported with putative beneficial features such as improving nitrogen uptake efficiency and promoting nutrient conversion, were mainly depleted in flooded roots (Herrmann et al., 2019; Dong et al., 2021). A similar trend was observed in the rhizosphere for families *Rhizobiaceae* and *Xanthobacteraceae* comprising multiple subgroups that might enhance and hinder plant development (Sadowsky and Graham, 1998; Oren, 2014). We also found that plant phenology was a significant and relevant factor shaping the bacterial community structure and differential responses to flooding were observed when such stress was induced at different PGS. Members of different *Massilia* species are considered as putatively plant-beneficial and frequently associated with wheat (Chimwamurombe et al., 2016). They produce proteases, sidephores and the auxin indole-3-acetic acid. *Massilia* ASVs were significantly more abundant in the control roots of young plants, but they were not detected in those of the flooded ones. Likewise, the flooded wheat roots at booting stage revealed a significant reduction of *Flavobacterium* ASVs, which are known for plant growth promoting traits. Bacteria of this genus have the capabilities to solubilize phosphate, use of 1-amino cyclopropan-1-carboxylate as sole nitrogen source and production of auxin, siderophores, salicylic acid, antifungal chitinases and hydrogen cyanide (Soltani et al., 2010; Verma et al., 2015; Gontia-Mishra et al., 2017). In summary, these findings demonstrated that flooding significantly altered negatively the assemblage dynamics of the root microbiota, with a significant depletion of putatively beneficial bacterial taxa associated with the root and rhizosphere of spring wheat plant.

It is important to note that the work undertaken here was limited to one soil type studied under very controlled greenhouse conditions. Further work should therefore investigate a greater range of soil types and flood scenarios, especially under realistic field conditions. Moreover, additional work is needed to fill the knowledge gaps in (i) how root exudation changes when crop species are faced with flooded growth conditions, (ii) how these exudates shape microbial community diversity and composition belowground, and (iii) the consequences for plant growth and functioning.

CONCLUSION

This study illustrated the detrimental effect of flooding stress on the spring wheat-microbiota complex. Our findings demonstrated that such hydrological stress significantly reduced plant growth and fitness, together with dramatic changes in bacterial community assembly. Indeed, flooding significantly restructured spring wheat-microbiota composition and functionality, especially, in early plant development. In particular, flooding promoted an increase in the abundance of potential detrimental taxa, with a parallel reduction of putative plant-beneficial bacterial groups. These compositional shifts were primarily associated with profound alterations of edaphic and root properties, such as oxygen depletion, soil pH variation and changes in the concentration of several macro- and micro-nutrients in the rhizosphere and root compartment. Furthermore, our results revealed the pivotal role of plant phenology on the assemblage dynamics of the wheat root microbiota, since a differential response to flooding was also observed across the three PGSs. This emphasized the importance of temporal sampling when studying plant-associated microbiota, as they provide a more complete and robust picture of community response to environmental threats compared to the investigation of single time points. It is also noteworthy to mention that our study was only a beginning to explore the effect of flooding on wheat-microbiota complex, providing the baseline for future field experiment. Experiments under controlled laboratory conditions represent an essential starting point, but there is an urgent need to confirm insights from controlled study under realistic field conditions.

DATA AVAILABILITY STATEMENT

The datasets presented in this study can be found in online repositories. The names of the repository/repositories and accession number(s) can be found below: European Nucleotide Archive (ENA) under accession PRJEB47399 (ERP131670) https://www.ebi.ac.uk/ena/browser/view/PRJEB47399.

AUTHOR CONTRIBUTIONS

SKo, M-RH, and SKa planned the study. GC collected the samples. DF and GC performed the lab work, analyzed the data, and provided general guidance. DF wrote the manuscript. SKo, AU, M-RH, and GC contributed to reviewing the manuscript. All authors contributed to the article and approved the submitted version.

FUNDING

This study was funded by the Leibniz Competition Program project "Volcorn-Volatilome of a Cereal Crop Microbiota Complex under Drought and Flooding" (K102/2018) (Leibniz Association).

ACKNOWLEDGMENTS

We wish to thank Paul Reim and the workers of the IPK institute for their support during sampling, and Kristina Holz for kindly providing the soil parameters. We thank Prof. Dr. Andreas Börner for providing the seeds of the spring wheat cultivar used in this study.

SUPPLEMENTARY MATERIAL

The Supplementary Material for this article can be found online at: https://www.frontiersin.org/articles/10.3389/fmicb.2021.773116/full#supplementary-material

REFERENCES

Ad-hoc-AG-Boden (2005). *Bodenkundliche Kartieranleitung*. Hannover: Schweizerbart, 438.

Anderson, M. J. (2017). "Permutational multivariate analysis of variance (PERMANOVA)," in *Wiley StatsRef: Statistics Reference Online*, eds N. Balakrishnan, T. Colton, B. Everitt, W. Piegorsch, F. Ruggeri, and J. L. Teugels (Hoboken, NJ: John Wiley & Sons), 1–15. doi: 10.1002/9781118445112.stat07841

Angel, R., Conrad, R., Dvorsky, M., Kopecky, M., Kotilínek, M., Hiiesalu, I., et al. (2016). The root-associated microbial community of the world's highest growing vascular plants. *Microb. Ecol.* 72, 394–406. doi: 10.1007/s00248-016-0779-8

Arduini, I., Orlandi, C., Pampana, S., and Masoni, A. (2016). Waterlogging at tillering affects spike and spikelet formation in wheat. *Crop Pasture Sci.* 67, 703–711. doi: 10.1071/CP15417

Argiroff, W. A., Zak, D. R., Lanser, C. M., and Wiley, M. J. (2017). Microbial community functional potential and composition are shaped by hydrologic connectivity in riverine floodplain soils. *Microb. Ecol.* 73, 630–644. doi: 10.1007/s00248-016-0883-9

Bailey-Serres, J., Lee, S. C., and Brinton, E. (2012). Waterproofing crops: effective flooding survival strategies. *Plant Physiol.* 160, 1698–1709. doi: 10.1104/pp.112.208173

Bardelli, T., Gómez-Brandón, M., Ascher-Jenull, J., Fornasier, F., Arfaioli, P., Francioli, D., et al. (2017). Effects of slope exposure on soil physico-chemical and microbiological properties along an altitudinal climosequence in the Italian Alps. *Sci. Total Environ.* 575, 1041–1055. doi: 10.1016/j.scitotenv.2016.09.176

Bardgett, R. D., and Caruso, T. (2020). Soil microbial community responses to climate extremes: resistance, resilience and transitions to alternative states. *Philos. Trans. R. Soc. Lond. B Biol. Sci.* 375:20190112. doi: 10.1098/rstb.2019.0112

Bevacqua, E., Maraun, D., Vousdoukas, M. I., Voukouvalas, E., Vrac, M., Mentaschi, L., et al. (2019). Higher probability of compound flooding from precipitation and storm surge in Europe under anthropogenic climate change. *Sci. Adv.* 5:eaaw5531. doi: 10.1126/sciadv.aaw5531

Blanchet, F. G., Legendre, P., and Borcard, D. (2008). Forward selection of explanatory variables. *Ecology* 89, 2623–2632. doi: 10.1890/07-0986.1

Bodenhausen, N., Horton, M. W., and Bergelson, J. (2013). Bacterial communities associated with the leaves and the roots of *Arabidopsis thaliana*. *PLoS One* 8:e56329. doi: 10.1371/journal.pone.0056329

Breitkreuz, C., Buscot, F., Tarkka, M., and Reitz, T. (2020). Shifts between and among populations of wheat rhizosphere *Pseudomonas*, *Streptomyces* and *Phyllobacterium* suggest consistent phosphate mobilization at different wheat growth stages under abiotic stress. *Front. Microbiol.* 10:3109. doi: 10.3389/fmicb.2019.03109

Bulgarelli, D., Schlaeppi, K., Spaepen, S., van Themaat, E. V. L., and Schulze-Lefert, P. (2013). Structure and functions of the bacterial microbiota of plants. *Annu. Rev. Plant Biol.* 64, 807–838. doi: 10.1146/annurev-arplant-050312-120106

Callahan, B. J., McMurdie, P. J., and Holmes, S. P. (2017). Exact sequence variants should replace operational taxonomic units in marker-gene data analysis. *ISME J.* 11, 2639–2643. doi: 10.1038/ismej.2017.119

Callahan, B. J., McMurdie, P. J., Rosen, M. J., Han, A. W., Johnson, A. J. A., and Holmes, S. P. (2016). DADA2: high-resolution sample inference from Illumina amplicon data. *Nat. Methods* 13, 581–583. doi: 10.1038/Nmeth.3869

Cannell, R. Q., Belford, R. K., Gales, K., Dennis, C. W., and Prew, R. D. (1980). Effects of waterlogging at different stages of development on the growth and yield of winter wheat. *J. Sci. Food Agric.* 31, 117–132. doi: 10.1002/jsfa.2740310203

Castro, H. F., Classen, A. T., Austin, E. E., Norby, R. J., and Schadt, C. W. (2010). Soil microbial community responses to multiple experimental climate change drivers. *Appl. Environ. Microbiol.* 76, 999–1007. doi: 10.1128/AEM.02874-09

Chelius, M. K., and Triplett, E. W. (2001). The diversity of archaea and bacteria in association with the roots of *Zea mays* L. *Microb. Ecol.* 41, 252–263. doi: 10.1007/s002480000087

Chimwamurombe, P. M., Grönemeyer, J. L., and Reinhold-Hurek, B. (2016). Isolation and characterization of culturable seed-associated bacterial endophytes from gnotobiotically grown marama bean seedlings. *FEMS Microbiol. Ecol.* 92:fiw083. doi: 10.1093/femsec/fiw083

Compant, S., Samad, A., Faist, H., and Sessitsch, A. (2019). A review on the plant microbiome: ecology, functions, and emerging trends in microbial application. *J. Adv. Res.* 19, 29–37. doi: 10.1016/j.jare.2019.03.004

Cook, B. I., Mankin, J. S., and Anchukaitis, K. J. (2018). Climate change and drought: from past to future. *Curr. Clim. Change Rep.* 4, 164–179. doi: 10.1007/s40641-018-0093-2

Cordero, J., de Freitas, J. R., and Germida, J. J. (2020). Bacterial microbiome associated with the rhizosphere and root interior of crops in Saskatchewan, Canada. *Can. J. Microbiol.* 66, 71–85. doi: 10.1139/cjm-2019-0330

Correa-Galeote, D., Bedmar, E. J., and Arone, G. J. (2018). Maize endophytic bacterial diversity as affected by soil cultivation history. *Front. Microbiol.* 9:484. doi: 10.3389/fmicb.2018.00484

Cox, D., Hunt, J., Mason, P., Wheater, H., Wolf, P., and Poff, N. L. (2002). Ecological response to and management of increased flooding caused by climate change. *Philos. Trans. A Math. Phys. Eng. Sci.* 360, 1497–1510. doi: 10.1098/rsta.2002.1012

da Silva, W. L., Yang, K.-T., Pettis, G. S., Soares, N. R., Giorno, R., and Clark, C. A. (2019). Flooding-associated soft rot of sweetpotato storage roots caused by distinct *Clostridium* isolates. *Plant Dis.* 103, 3050–3056. doi: 10.1094/pdis-03-19-0548-re

De Vries, F., and Shade, A. (2013). Controls on soil microbial community stability under climate change. *Front. Microbiol.* 4:265. doi: 10.3389/fmicb.2013.00265

Di Virgilio, G., Evans, J. P., Blake, S. A. P., Armstrong, M., Dowdy, A. J., Sharples, J., et al. (2019). Climate change increases the potential for extreme wildfires. *Geophys. Res. Lett.* 46, 8517–8526. doi: 10.1029/2019GL083699

Ding, J., Liang, P., Wu, P., Zhu, M., Li, C., Zhu, X., et al. (2020). Effects of waterlogging on grain yield and associated traits of historic wheat cultivars in the middle and lower reaches of the Yangtze River, China. *Field Crops Res.* 246:107695. doi: 10.1016/j.fcr.2019.107695

Dong, H., Sun, H., Fan, S., Jiang, L., and Ma, D. (2021). Rhizobacterial communities, enzyme activity, and soil properties affect rice seedling's nitrogen use. *Agron. J.* 113, 633–644. doi: 10.1002/agj2.20538

Donn, S., Kirkegaard, J. A., Perera, G., Richardson, A. E., and Watt, M. (2015). Evolution of bacterial communities in the wheat crop rhizosphere. *Environ. Microbiol.* 17, 610–621. doi: 10.1111/1462-2920.12452

Dray, S., Legendre, P., and Blanchet, G. (2011). *packfor: Forward Selection with Permutation. R Package Version 0.0-8/r100.*

Drew, M. C. (1992). Soil aeration and plant root metabolism. *Soil Sci.* 154, 259–268. doi: 10.1097/00010694-199210000-00002

Edwards, J. A., Santos-Medellín, C. M., Liechty, Z. S., Nguyen, B., Lurie, E., Eason, S., et al. (2018). Compositional shifts in root-associated bacterial and archaeal microbiota track the plant life cycle in field-grown rice. *PLoS Biol.* 16:e2003862. doi: 10.1371/journal.pbio.2003862

Eisenhauer, N., and Powell, J. R. (2017). Plant trait effects on soil organisms and functions. *Pedobiologia* 65, 1–4. doi: 10.1016/j.pedobi.2017.11.001

Fierer, N., and Jackson, R. B. (2006). The diversity and biogeography of soil bacterial communities. *Proc. Natl. Acad. Sci. U.S.A.*103, 626–631. doi: 10.1073/pnas.0507535103

Finkel, O. M., Castrillo, G., Herrera Paredes, S., Salas González, I., and Dangl, J. L. (2017). Understanding and exploiting plant beneficial microbes. *Curr. Opin. Plant Biol.* 38, 155–163. doi: 10.1016/j.pbi.2017.04.018

Fitzpatrick, C. R., Copeland, J., Wang, P. W., Guttman, D. S., Kotanen, P. M., and Johnson, M. T. J. (2018). Assembly and ecological function of the root microbiome across angiosperm plant species. *Proc. Natl. Acad. Sci. U.S.A.* 115, E1157–E1165. doi: 10.1073/pnas.1717617115

Francioli, D., Lentendu, G., Lewin, S., and Kolb, S. (2021a). DNA metabarcoding for the characterization of terrestrial microbiota—pitfalls and solutions. *Microorganisms* 9:361. doi: 10.3390/microorganisms9020361

Francioli, D., van Rijssel, S. Q., van Ruijven, J., Termorshuizen, A. J., Cotton, T. E. A., Dumbrell, A. J., et al. (2021b). Plant functional group drives the community structure of saprophytic fungi in a grassland biodiversity experiment. *Plant Soil* 461, 91–105. doi: 10.1007/s11104-020-04454-y

Francioli, D., Schulz, E., Buscot, F., and Reitz, T. (2018). Dynamics of soil bacterial communities over a vegetation season relate to both soil nutrient status and plant growth phenology. *Microb. Ecol.* 75, 216–227. doi: 10.1007/s00248-017-1012-0

Francioli, D., Schulz, E., Lentendu, G., Wubet, T., Buscot, F., and Reitz, T. (2016). Mineral vs. Organic amendments: microbial community structure, activity and abundance of agriculturally relevant microbes are driven by long-term fertilization strategies. *Front. Microbiol.* 7:1446. doi: 10.3389/fmicb.2016.01446

Francioli, D., van Ruijven, J., Bakker, L., and Mommer, L. (2020). Drivers of total and pathogenic soil-borne fungal communities in grassland plant species. *Fungal Ecol.* 48:100987. doi: 10.1016/j.funeco.2020.100987

Ghobadi, M. E., Ghobadi, M., and Zebarjadi, A. (2017). Effect of waterlogging at different growth stages on some morphological traits of wheat varieties. *Int. J. Biometeorol.* 61, 635–645. doi: 10.1007/s00484-016-1240-x

Gontia-Mishra, I., Sapre, S., Kachare, S., and Tiwari, S. (2017). Molecular diversity of 1-aminocyclopropane-1-carboxylate (ACC) deaminase producing PGPR from wheat (*Triticum aestivum* L.) rhizosphere. *Plant Soil* 414, 213–227. doi: 10.1007/s11104-016-3119-3

Gschwend, F., Aregger, K., Gramlich, A., Walter, T., and Widmer, F. (2020). Periodic waterlogging consistently shapes agricultural soil microbiomes by promoting specific taxa. *Appl. Soil Ecol.* 155:103623. doi: 10.1016/j.apsoil.2020.103623

Hartman, K., and Tringe, S. G. (2019). Interactions between plants and soil shaping the root microbiome under abiotic stress. *Biochem. J.* 476, 2705–2724. doi: 10.1042/BCJ20180615

Hemati Matin, N., and Jalali, M. (2017). The effect of waterlogging on electrochemical properties and soluble nutrients in paddy soils. *Paddy Water Environ.* 15, 443–455. doi: 10.1007/s10333-016-0562-y

Henry, A., Doucette, W., Norton, J., and Bugbee, B. (2007). Changes in crested wheatgrass root exudation caused by flood drought, and nutrient stress. *J. Environ. Qual.* 36, 904–912. doi: 10.2134/jeq2006.0425sc

Herrmann, M., Wegner, C.-E., Taubert, M., Geesink, P., Lehmann, K., Yan, L., et al. (2019). Predominance of *Cand*. Patescibacteria in groundwater is caused by their preferential mobilization from soils and flourishing under oligotrophic conditions. *Front. Microbiol.* 10:1407. doi: 10.3389/fmicb.2019.01407

Jincai, L., Qi, D., and Songlie, Y. (2001). Effect of waterlogging at different growth stages on photosynthesis and yield of different wheat cultivars. *Acta Agron. Sin.* 27, 434–441.

Katznelson, H., Lochhead, A. G., and Timonin, M. I. (1948). Soil microorganisms and the rhizosphere. *Bot. Rev.* 14, 543–587.

Kaur, G., Singh, G., Motavalli, P. P., Nelson, K. A., Orlowski, J. M., and Golden, B. R. (2020). Impacts and management strategies for crop production in waterlogged or flooded soils: a review. *Agron. J.* 112, 1475–1501. doi: 10.1002/agj2.20093

Kavamura, V. N., Mendes, R., Bargaz, A., and Mauchline, T. H. (2021). Defining the wheat microbiome: towards microbiome-facilitated crop production. *Comput. Struct. Biotechnol. J.* 19, 1200–1213. doi: 10.1016/j.csbj.2021.01.045

Kawasaki, A., Dennis, P. G., Forstner, C., Raghavendra, A. K. H., Richardson, A. E., Watt, M., et al. (2021). The microbiomes on the roots of wheat *Triticum aestivum* L.) and rice (*Oryza sativa* L.) exhibit significant differences in structure between root types and along root axes. *J. Funct. Plant Biol.* 48, 871–888. doi: 10.1071/FP20351

Kembel, S. W., Cowan, P. D., Helmus, M. R., Cornwell, W. K., Morlon, H., Ackerly, D. D., et al. (2010). Picante: R tools for integrating phylogenies and ecology. *Bioinformatics* 26, 1463–1464. doi: 10.1093/bioinformatics/btq166

Konapala, G., Mishra, A. K., Wada, Y., and Mann, M. E. (2020). Climate change will affect global water availability through compounding changes in seasonal precipitation and evaporation. *Nat. Commun.* 11:3044. doi: 10.1038/s41467-020-16757-w

Lakshmanan, V. (2015). "Chapter three – Root microbiome assemblage is modulated by plant host factors," in *Advances in Botanical Research*, eds H. Bais, and J. Sherrier (Cambridge, MA: Academic Press), 57–79.

Lareen, A., Burton, F., and Schäfer, P. (2016). Plant root-microbe communication in shaping root microbiomes. *Plant Mol. Biol.* 90, 575–587. doi: 10.1007/s11103-015-0417-8

Lauber, C. L., Hamady, M., Knight, R., and Fierer, N. (2009). Pyrosequencing-based assessment of soil pH as a predictor of soil bacterial community structure at the continental scale. *Appl. Environ. Microbiol.* 75, 5111–5120. doi: 10.1128/AEM.00335-09

Leff, J. W., Bardgett, R. D., Wilkinson, A., Jackson, B. G., Pritchard, W. J., De Long, J. R., et al. (2018). Predicting the structure of soil communities from plant community taxonomy, phylogeny, and traits. *ISME J.* 12, 1794–1805. doi: 10.1038/s41396-018-0089-x

Legendre, P., and Gallagher, E. D. (2001). Ecologically meaningful transformations for ordination of species data. *Oecologia* 129, 271–280. doi: 10.1007/s004420100716

Lewin, S., Francioli, D., Ulrich, A., and Kolb, S. (2021). Crop host signatures reflected by co-association patterns of keystone bacteria in the rhizosphere microbiota. *Environ. Microbiome* 16:18. doi: 10.1186/s40793-021-00387-w

Malik, A. I., Colmer, T. D., Lambers, H., Setter, T. L., and Schortemeyer, M. (2002). Short-term waterlogging has long-term effects on the growth and physiology of wheat. *New Phytol.* 153, 225–236. doi: 10.1046/j.0028-646X.2001.00318.x

Martin, M. (2011). Cutadapt removes adapter sequences from high-throughput sequencing reads. *EMBnet J.* 17:3. doi: 10.14806/ej.17.1.200

Martiny, J. B. H., Jones, S. E., Lennon, J. T., and Martiny, A. C. (2015). Microbiomes in light of traits: a phylogenetic perspective. *Science* 350:aac9323. doi: 10.1126/science.aac9323

Meyer, W., Barrs, H. D., Smith, R. C. G., White, N. S., Heritage, A., and Short, D. L. (1985). Effect of irrigation on soil oxygen status and root and shoot growth of wheat in a clay soil. *Aust. J. Agric. Res.* 36, 171–185. doi: 10.1071/AR9850171

Moche, M., Gutknecht, J., Schulz, E., Langer, U., and Rinklebe, J. (2015). Monthly dynamics of microbial community structure and their controlling factors in three floodplain soils. *Soil Biol. Biochem.* 90, 169–178. doi: 10.1016/j.soilbio.2015.07.006

Morton, L. W., Hobbs, J., Arbuckle, J. G., and Loy, A. (2015). Upper midwest climate variations: farmer responses to excess water risks. *J. Environ. Qual.* 44, 810–822. doi: 10.2134/jeq2014.08.0352

Muñoz-Huerta, R. F., Guevara-Gonzalez, R. G., Contreras-Medina, L. M., Torres-Pacheco, I., Prado-Olivarez, J., and Ocampo-Velazquez, R. V. (2013). A review of methods for sensing the nitrogen status in plants: advantages, disadvantages and recent advances. *Sensors* 13, 10823–10843. doi: 10.3390/s130810823

Murphy, J., and Riley, J. P. (1962). A modified single solution method for the determination of phosphate in natural waters. *Anal. Chim. Acta* 27, 31–36. doi: 10.1016/S0003-2670(00)88444-5

Na, X., Cao, X., Ma, C., Ma, S., Xu, P., Liu, S., et al. (2019). Plant stage, not drought stress, determines the effect of cultivars on bacterial community diversity in the rhizosphere of broomcorn millet (*Panicum miliaceum* L.). *Front. Microbiol.* 10:828. doi: 10.3389/fmicb.2019.00828

Naylor, D., and Coleman-Derr, D. (2018). Drought stress and root-associated bacterial communities. *Front. Plant Sci.* 8:2223. doi: 10.3389/fpls.2017.02223

Oksanen, J., Blanchet, G., Friendly, M., Kindt, R., Legendre, P., McGlinn, D., et al. (2018). *vegan: Community Ecology Package. R Package Version 2.5-2*.

Oren, A. (2014). "The family Xanthobacteraceae," in *The Prokaryotes: Alphaproteobacteria and Betaproteobacteria*, eds E. Rosenberg, E. F. DeLong, S. Lory, E. Stackebrandt, and F. Thompson (Berlin: Springer Berlin Heidelberg), 709–726. doi: 10.1007/978-3-642-30197-1_258

Pampana, S., Masoni, A., and Arduini, I. (2016). Grain yield of durum wheat as affected by waterlogging at tillering. *Cereal Res. Commun.* 44, 706–716. doi: 10.1556/0806.44.2016.026

Pervaiz, Z. H., Contreras, J., Hupp, B. M., Lindenberger, J. H., Chen, D., Zhang, Q., et al. (2020). Root microbiome changes with root branching order and root chemistry in peach rhizosphere soil. *Rhizosphere* 16:100249. doi: 10.1016/j.rhisph.2020.100249

Pett-Ridge, J., and Firestone, M. K. (2005). Redox fluctuation structures microbial communities in a wet tropical soil. *Appl. Environ. Microbiol.* 71, 6998–7007. doi: 10.1128/AEM.71.11.6998-7007.2005

Price, M. N., Dehal, P. S., and Arkin, A. P. (2010). FastTree 2 – approximately maximum-likelihood trees for large alignments. *PLoS One* 5:e9490. doi: 10.1371/journal.pone.0009490

R Core Team (2014). *R: A Language and Environment for Statistical Computing*. Vienna: R Foundation for Statistical Computing.

Rhine, M. D., Stevens, G., Shannon, G., Wrather, A., and Sleper, D. (2010). Yield and nutritional responses to waterlogging of soybean cultivars. *Irrig. Sci.* 28, 135–142. doi: 10.1007/s00271-009-0168-x

Riehm, H. (1943). Bestimmung der laktatlöslichen phosphorsäure in karbonathaltigen Böden. *Phosphorsäure* 1, 167–178. doi: 10.1002/jpln.19420260107

Sadowsky, M. J., and Graham, P. H. (1998). "Soil biology of the rhizobiaceae," in *The Rhizobiaceae: Molecular Biology of Model Plant-Associated Bacteria*, eds H. P. Spaink, A. Kondorosi, and P. J. J. Hooykaas (Dordrecht: Springer Netherlands), 155–172. doi: 10.1007/978-94-011-5060-6_8

Schimel, J., Balser, T. C., and Wallenstein, M. (2007). Microbial stress-response physiology and its implications for ecosystem function. *Ecology* 88, 1386–1394. doi: 10.1890/06-0219

Schöps, R., Goldmann, K., Herz, K., Lentendu, G., Schöning, I., Bruelheide, H., et al. (2018). Land-use intensity rather than plant functional identity shapes bacterial and fungal rhizosphere communities. *Front. Microbiol.* 9:2711. doi: 10.3389/fmicb.2018.02711

Schröter, D., Cramer, W., Leemans, R., Prentice, I. C., Araújo, M. B., Arnell, N. W., et al. (2005). Ecosystem service supply and vulnerability to global change in Europe. *Science* 310, 1333–1337. doi: 10.1126/science.1115233

Segata, N., Izard, J., Waldron, L., Gevers, D., Miropolsky, L., Garrett, W. S., et al. (2011). Metagenomic biomarker discovery and explanation. *Genome Biol.* 12:R60. doi: 10.1186/gb-2011-12-6-r60

Shen, R., Lan, Z., Rinklebe, J., Nie, M., Hu, Q., Yan, Z., et al. (2021). Flooding variations affect soil bacterial communities at the spatial and inter-annual scales. *Sci. Total Environ.* 759, 143471. doi: 10.1016/j.scitotenv.2020.143471

Soltani, A., Khavaz, I. K., Asadi-Rahmani, H., Omidvari, M., Dahaji, P., and Mirhoseyni, H. (2010). Plant growth promoting characteristics in some *Flavobacterium* spp. isolated from soils of Iran. *J. Agric. Sci.* 2, 106–115. doi: 10.5539/jas.v2n4p106

Sun, L., Chen, S., Chao, L., and Sun, T. (2007). Effects of flooding on changes in Eh, pH and speciation of cadmium and lead in contaminated soil. *Bull. Environ. Contam. Toxicol.* 79, 514–518. doi: 10.1007/s00128-007-9274-8

Tian, L.-X., Zhang, Y.-C., Chen, P.-I., Zhang, F.-F., Li, J., Yan, F., et al. (2021). How does the waterlogging regime affect crop yield? A global meta-analysis. *Front. Plant Sci.* 12:634898. doi: 10.3389/fpls.2021.634898

Tkacz, A., Pini, F., Turner, T. R., Bestion, E., Simmonds, J., Howell, P., et al. (2020). Agricultural selection of wheat has been shaped by plant-microbe interactions. *Front. Microbiol.* 11:132. doi: 10.3389/fmicb.2020.00132

Turner, T. R., James, E. K., and Poole, P. S. (2013). The plant microbiome. *Genome Biol.* 14:209. doi: 10.1186/gb-2013-14-6-209

Unger, I. M., Kennedy, A. C., and Muzika, R.-M. (2009). Flooding effects on soil microbial communities. *Appl. Soil Ecol.* 42, 1–8. doi: 10.1016/j.apsoil.2009.01.007

Vanbergen, A. J. (2013). Threats to an ecosystem service: pressures on pollinators. *Front. Ecol. Environ.* 11, 251–259. doi: 10.1890/120126

Verma, P., Yadav, A. N., Khannam, K. S., Panjiar, N., Kumar, S., Saxena, A. K., et al. (2015). Assessment of genetic diversity and plant growth promoting attributes of psychrotolerant bacteria allied with wheat (*Triticum aestivum*)

from the northern hills zone of India. *Ann. Microbiol.* 65, 1885–1899. doi: 10.1007/s13213-014-1027-4

Wang, J., Xue, C., Song, Y., Wang, L., Huang, Q., and Shen, Q. (2016). Wheat and rice growth stages and fertilization regimes alter soil bacterial community structure, but not diversity. *Front. Microbiol.* 7:1207. doi: 10.3389/fmicb.2016.01207

Webb, C. O., Ackerly, D. D., McPeek, M. A., and Donoghue, M. J. (2002). Phylogenies and community ecology. *Annu. Rev. Ecol. Syst.* 33, 475–505. doi: 10.1146/annurev.ecolsys.33.010802.150448

Wilson, J. S., Baldwin, D. S., Rees, G. N., and Wilson, B. P. (2011). The effects of short-term inundation on carbon dynamics, microbial community structure and microbial activity in floodplain soil. *River Res. Appl.* 27, 213–225. doi: 10.1002/rra.1352

Wu, X., Tang, Y., Li, C., Wu, C., and Huang, G. (2015). Chlorophyll fluorescence and yield responses of winter wheat to waterlogging at different growth stages. *Plant Prod. Sci.* 18, 284–294. doi: 10.1626/pps.18.284

Xu, L., Naylor, D., Dong, Z., Simmons, T., Pierroz, G., Hixson, K. K., et al. (2018). Drought delays development of the sorghum root microbiome and enriches for monoderm bacteria. *Proc. Natl. Acad. Sci. U.S.A.* 115, E4284–E4293. doi: 10.1073/pnas.1717308115

Zadoks, J. C., Chang, T. T., and Konzak, C. F. (1974). A decimal code for the growth stages of cereals. *Weed Res.* 14, 415–421. doi: 10.1111/j.1365-3180.1974.tb01084.x

Conflict of Interest: The authors declare that the research was conducted in the absence of any commercial or financial relationships that could be construed as a potential conflict of interest.

Publisher's Note: All claims expressed in this article are solely those of the authors and do not necessarily represent those of their affiliated organizations, or those of the publisher, the editors and the reviewers. Any product that may be evaluated in this article, or claim that may be made by its manufacturer, is not guaranteed or endorsed by the publisher.

frontiers in Microbiology

ORIGINAL RESEARCH
published: 19 November 2021
doi: 10.3389/fmicb.2021.749946

Lime-Phosphorus Fertilizer Efficiently Reduces the Cd Content of Rice: Physicochemical Property and Biological Community Structure in Cd-Polluted Paddy Soil

Xiaolin Kuang[1,2], Kangying Si[1,2], Huijuan Song[1,2], Liang Peng[1,2] and Anwei Chen[1,2]*

[1] Department of Environmental Science and Engineering, Hunan Agricultural University, Changsha, China, [2] Hunan Engineering and Technology Research Center for Irrigation Water Purification, Changsha, China

Due to the biomagnifying effect in the food chains, heavy metals will cause serious harm to the food produced in paddy soil, and then threaten human health. The remediation of soil heavy metals by the addition of amendments is a common method. However, the combination of the two amendments has been less studied and its effect is unknown. In this study, we investigated the effects of different concentrations of a lime and calcium-magnesium phosphate (CMP) amendments metal availability and paddy soil bacteria biodiversity. The experiment proves that the addition of 0.5 and 1.0‰ amendment can effectively reduce cadmium (Cd) availability and the cadmium content in rice to be below 0.2 mg/kg, meeting the national food safety level. The results demonstrate that increasing pH and phosphorous (P) in soil were two important factors decreasing available cadmium. Furthermore, biodiversity analysis of the treated soil showed that the amendment increased biodiversity. Proteobacteria and Chloroflex were the most abundant bacteria at the phylum level, followed by Acidobacterium and Nitrospirae. The abundance of *Bacterodietes-vadinHA17*, *Syntrophaceae*, and *Thiobacillus* increased as phosphorous increased. Cadmium passivation might induce those species.

Keywords: amendment, biodiversity, heavy metals, rice, soil

OPEN ACCESS

Edited by:
Diane Purchase, Middlesex University, United Kingdom

Reviewed by:
Liu Zhongqi, Agro-Environmental Protection Institute, Chinese Academy of Agricultural Sciences (CAAS), China
Patompong Johns Saengwilai, Mahidol University, Thailand

****Correspondence:***
Liang Peng
pengliang2004@126.com;
pengliang@hunau.edu.cn

Specialty section:
This article was submitted to Terrestrial Microbiology, a section of the journal Frontiers in Microbiology

Received: *30 July 2021*
Accepted: *29 September 2021*
Published: *19 November 2021*

Citation:
Kuang X, Si K, Song H, Peng L and Chen A (2021) Lime-Phosphorus Fertilizer Efficiently Reduces the Cd Content of Rice: Physicochemical Property and Biological Community Structure in Cd-Polluted Paddy Soil. Front. Microbiol. 12:749946. doi: 10.3389/fmicb.2021.749946

INTRODUCTION

China's soil safety faces severe challenges. According to reports, more than 82.8% of the soil has been contaminated by heavy metals, with the highest proportion consisting of cadmium (Cd) (7.0%) (Zhao et al., 2015). Cadmium has a strong ability to migrate. Cadmium entering the soil is easily absorbed by crops and enters the human body through the food chain, endangering human health (Singh et al., 2021). Due to various reasons, in recent decades the soil in southern China's paddy fields has become increasingly acidified (Shi et al., 2020). Soil acidification leads to cadmium becoming significantly more soluble in the soil, increasing its availability to plants (Zhen et al., 2019). Rice, one of China's most important food sources, has a strong ability to accumulate cadmium (Mao et al., 2019). Long-term consumption of rice containing high levels of cadmium can harm the human body, for example, by causing "Itai-itai disease" (Li et al., 2019). Consequently, it is imperative to find ways to reduce cadmium concentration in paddy field soil, particularly in southern China.

Currently there are four main strategies for reducing cadmium accumulation in rice: (1) decrease cadmium bioavailability in the soil; (2) reduce cadmium uptake by rice roots; (3) decrease the cadmium transport ratio in rice transport systems; and (4) Screen rice varieties with low cadmium accumulation. The selection of rice varieties is very important; previous studies have found that the response of rice to amendment and Cd uptake depends largely on rice varieties (Saengwilai and Meeinkuirt, 2021; Xu et al., 2021) explored the influence of rice varieties on the cadmium reduction effect of amendment and found that the accumulation of cadmium varies greatly between different rice varieties. Therefore, some efficient technologies have been founded based on these strategies. Treatments with silicone, lime ($CaCO_3$), and calcium-magnesium phosphate (CMP) fertilizers can reduce cadmium activity in the soil, thereby preventing cadmium from moving from the soil to the rice (Li et al., 2018; Rehman et al., 2019). In a high pH environment, cadmium mainly exists in the forms of $CdOH^+$, $Cd_2(OH)^{3+}$, and $Cd(OH)_2$, which reduces its bioavailability (Peng et al., 2016). The PO_4^{3-}, CO_3^{2-}, S^{2-}, and SiO_4^{4-} anions can induce low-resolution minerals after reacting with Cd^{2+}. Other amendment properties such as clay with high adsorption capacity or manure with strong complex ability on the Cd^{2+} were considered as an additional supplement (Sun et al., 2020). Therefore, many normal efficient amendments for cadmium-polluted soil include the alkaline substance (high pH) and some cations (Li et al., 2021; Wang et al., 2021).

The above-mentioned amendments not only reduce the activity of cadmium but also reduce rice's absorption of elements such as iron (Fe), manganese (Mn), zinc (Zn), calcium (Ca), copper (Cu), and magnesium (Mg). Therefore, the formation of Fe/Mn oxide film in rice root is reduced, thus reducing the resistance to cadmium in rice. However, the transport pathway of cadmium in rice is similar to those of some other nutrients. For example, a range of micronutrient transporters from the family of zinc-regulated transporter/iron-regulated transporter-like proteins (ZIP, such as AtIRT1 and TcZNT1/TcZIP4) and natural resistance-associated macrophage protein (NRAMP, such as Nramp5) can also transport cadmium in rice and *Arabidopsis* (Siqi et al., 2019; Guha et al., 2020). Therefore, cadmium can be controlled through the intake of trace elements (Liu et al., 2018). Yang Y. et al. (2018) reported that low concentrations of lime can increase cadmium in rice while high concentrations of lime decrease cadmium. Regrettably, their research did not clearly explain the relationship between amendment amount, essential elements content, and cadmium concentration.

Although soil amendments are widely applied to decrease cadmium content in rice, their effect on the structure of cadmium-contaminated soil's biological communities is rarely reported. Levels of soil metals are highly correlated to bacterial species. Sulfur-reducing bacteria, iron/manganese-oxidizing bacteria, organic matter-degradation bacteria, and lactic acid bacteria can greatly influence cadmium content in the soil. Stroud et al. (2014) reported that manganese bioaccessibility positively correlated to *Acidobacterium* abundance, but negatively correlated to *Holophaga* abundance in the acidic sulfate soil. Cadmium was found to be mineralized by alphaproteobacteria and chloroplast classes in rice crust soil, making it biologically unavailable (Song et al., 2019). Paddy soils contaminated with cadmium usually have low pH and lack phosphorus. Therefore, amending soil with lime and CMP can greatly change environmental parameters and alter biological community structure. However, the relationship of biological composition with metal bioaccessibility after treatment with an amendment remains to be investigated further.

Lime and CMP are two typical amendments for cadmium-polluted soil. In our experiment, an amendment consisting of both lime and CMP was applied to investigate the effect of amendment concentration on essential soil elements and paddy roots. Soil biological community structure after treatment with different concentrations of amendments and the relationship between biological species and metal bioavailability were explored.

MATERIALS AND METHODS

Site, Amendment, and Rice Cultivar

The study began in June 2018 in Chang Feng Village, Liu Yang City, Hunan Province, China. The main source of pollution in paddy fields was wastewater from mining areas. The concentration of cadmium in the soil was 0.3 mg kg^{-1}, a level considered mildly polluted. The basic physical–chemical properties are shown in **Table 1**.

This study used CMP + lime (Fat Baby No.7, FB7) configured in this laboratory as an amendment. **Table 2** shows the detailed components of FB7; all of the materials came from Ma Po Mountains, Changsha City.

The rice cultivar was Zhongzao 39, cultivated by the China Rice Research Institute. Its entire growth period was 112 days.

Experimental Design

The field experiment consisted of four different amounts of FB7 (**Table 2**). Each concentration treatment was repeated three times in parallel; the area of each treatment was 20 m^2. Before transplanting rice, FB7 was applied to the soil, mixed thoroughly, and left alone for a week to reach equilibrium. A concrete enclosure was constructed to separate each plot and to avoid mixing irrigation water and fertilizer. The experimental group and control group were randomly distributed, and rice cultivation and management were consistent with local practices for growing rice. The paddy field was flooded and plowed on July 5, 2018, planted on July 12, 2018, and harvested on November 5, 2018.

Sampling

Five soil samples were randomly selected from each plot for mixing. All experimental samples were air-dried naturally in the laboratory. Biological debris was collected at the ripening stage, and the plant sample in each plot was a mixture of five random samples. First, the rice samples were washed with distilled water. Second, the rice samples were heated at 105°C for 60 min. Finally, the rice samples were dried at 70°C to a constant weight. All samples were ground and sieved before the analysis.

TABLE 1 | Physical-chemical properties of soil in a paddy field.

Total Cd (mg kg^{-1})	Av Cd (mg kg^{-1})	pH	OM (g kg^{-1})	Alkaline-N	Olsen-P(g kg^{-1})	Olsen-K
1.20 ± 0.03	0.21 ± 0.01	6.30 ± 0.08	45.95 ± 2.68	80.50 ± 4.75	22.44 ± 1.49	62.25 ± 3.41

Sample Analysis

The air-dried soil was sieved (pore dimeter < 0.15 mm) and then the 0.500 g soil was put into a digestion tube. Plant samples were soaked overnight in 4.5 mL of concentrated HCl and 1.5 mL of concentrated HNO_3, and then digested. This mixed sample was dissolved at 90°C for 1 h and then up to 150°C until the solution inside boiled, after which the sample was removed and cooled down. After the sample was cool, 5 mL of concentrated $HClO_4$ was added. It was digested again at 190°C for 2 h and then up to 220°C until about 1 mL of sample was left. The digested sample was then diluted to 25 mL with distilled water and filtrated into a plastic bottle. The concentrations of cadmium in the digested solution were measured with ICP-OES (ICPMA 8300, Perkinelmer).

The total concentration of metal in a plant was measured as follows. The 1.0 g (dry weight) rice and 0.5 g (dry weight) root were digested with 15 mL of concentrated HNO_3.The cooled digested solution was diluted to 25 mL. The concentration of cadmium, iron, manganese, copper, and zinc in the filtrate was measured using ICP-OES (ICPMA 8300, Perkinelmer).

The pH value, organic matter, cation exchange capacity, phosphorous, Olsen-K, Alkaline-N, and Total-N of the soil were measured according to Yang's method (Yang et al., 2008). The crystal structures of soil samples were recorded with a diffractometer (TTRIII, Rigaku, Tokyo, Japan), and the surface structure and morphology of the paddy soils were characterized by a scanning electron microscope-energy dispersive spectrometer (SEM-EDS, JEM-1230 HC, JPN).

Bacterial Richness and Diversity

Soil in the rhizosphere area was collected and mixed from five sites at every plot. Detailed measurements of bacterial species richness and diversity is in **Supplementary Material**. Sequencing data generated from this study has been deposited in the National Center for Biotechnology Information (NCBI) with the project accession number PRJNA761207.

Statistical Analyses

Statistical analyses consisted of one-way analysis of variance (ANOVA) using SPSS version 11.5 (SPSS Inc., Chicago, IL). Using the least significant difference (LSD) method, the difference was considered to be statistically significant when $P < 0.05$.

RESULTS AND DISCUSSION

Effects of the Amendment on Soil pH and Conductivity

The pH in the control check (CK) soil treatment ranged from 6.4 to 6.6 during the three stages (transplantation, heading, and harvest) (**Figure 1A**). During the transplantation stage, the soil pH value increased from 7 to 9 after the addition of FB7. In the heading and harvest stages, the soil pH was slightly lower than the transplantation stage, but the overall value was still higher than that of the CK treatment. As the amount of FB7 increased, the pH value of paddy soil increased.

The pH value first increased and then decreased with time. This is because lime can increase the pH of the soil (Bouray et al., 2021), but this effect diminishes over time until it returns to its original pH value (Yin et al., 2021). Some groups have also described reacidification of limed soils in the long term (Wang et al., 2009; Rosa et al., 2020). These reports are similar to the results of this experiment—the pH value decreases to a certain extent during the later stage of rice growth. Specifically, the lower pH was found in the treatment with 0.2‰ amendment. In general, the addition of amendment had a great effect on soil pH.

Soil conductivity (EC) decreased sharply as rice growth increased (**Figure 1B**). Conductivity reflected the ion strength mainly from fertilizer, such as K^+, NO_3^-, and Ca^{2+}. The adsorption and sediment of these ions can decrease conductivity (Lin et al., 2005). Notably, conductivity in the treatment with 0.2‰ FB7 was lowest at the harvest stage. It might correspond to the lowest pH and some special soil microbiological communities.

Effect of FB7 on Cadmium Concentration in the Soil–Root–Rice System

The agronomic information related to rice maturity is shown in **Supplementary Table 1**. After FB7 was applied, the effective tiller number per plant, biomass, yield, and seed setting rate were significantly increased, but there was no significant effect on 1,000-grain weight. The results showed that amendment could increase the yield and biomass of rice by increasing the effective tiller number (Wang et al., 2020). Moreover, the application of amendment also increased the content of calcium and phosphorus in the soil (**Supplementary Table 2**). It not only improves soil fertility, but also reduces the concentration of cadmium in rice roots through the competition between Ca^{2+} and Cd^{2+} (Wang et al., 2021).

TABLE 2 | Material and concentration about amendments.

Marker	Material	Amount
CK	Blank control	
0.2‰	Calcium magnesium phosphate + Lime	315 kg/hm^2 + 105 kg/hm^2
0.5‰	Calcium magnesium phosphate + Lime	787.5 kg/hm^2 + 337.5 kg/hm^2
1.0‰	Calcium magnesium phosphate + Lime	1,575 kg/hm^2 + 675 kg/hm^2

The column of concentration containing 2 concentration values corresponds to the column of material.

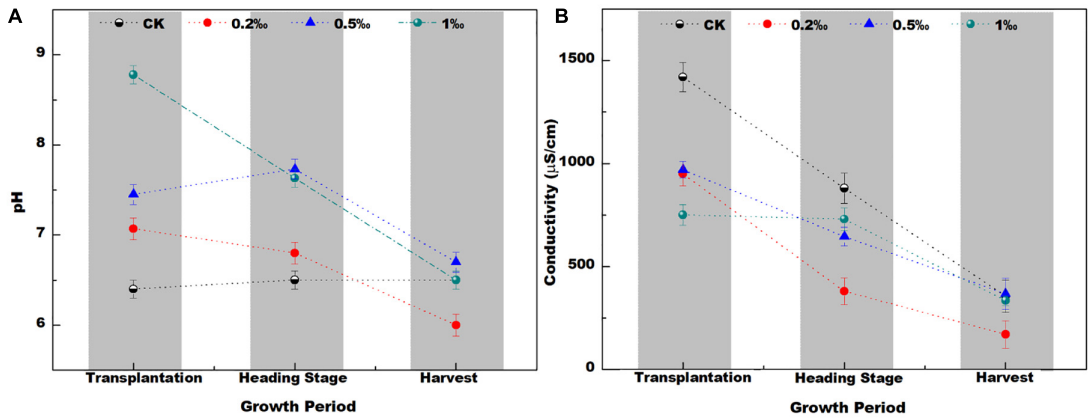

FIGURE 1 | The pH **(A)** conductivity **(B)** in soil with different amendment concentrations at different growth stages of the rice.

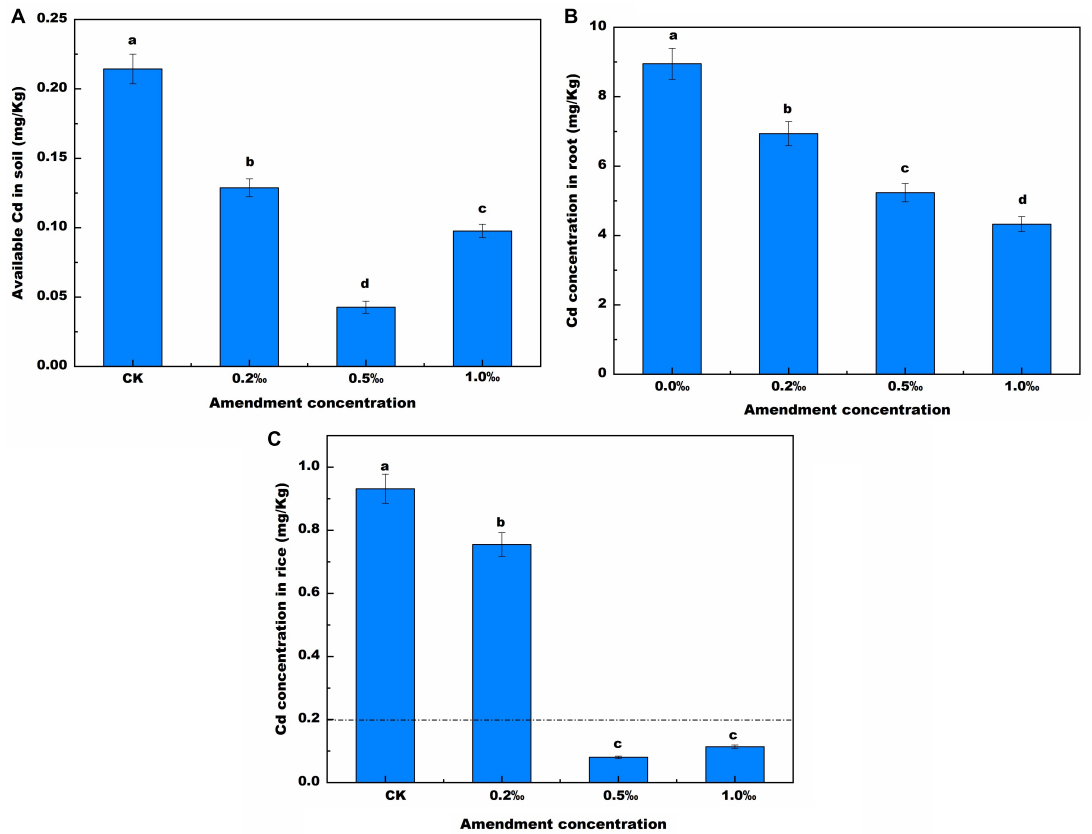

FIGURE 2 | Available Cd in soil **(A)**, Cd concentration **(B)** in root and in the rice **(C)** with different concentration of amendment. Values are means ± SD (n = 3). Different letters above the bars indicate the signifcant differences at $p < 0.05$.

The available cadmium content of treated soil was lower than that of untreated soil. (CK) (**Figure 2A**). The available cadmium concentration was 0.21 mg/kg, and it was only 17.9% of the total cadmium concentration. Compared with the CK soil, the available cadmium concentration decreased by 6.94, 14.33, and 9.74%, after addition of 0.2, 0.5, and 1.0‰ FB7 amendments, respectively. The low available cadmium was attributed to two causes. On the one hand, the solubility of heavy metals decreases as the pH value increases, thereby improving the adsorption capacity of soil particles for heavy metals by increasing the net negative charge of variably charged colloids (Mcbride et al., 2010). On the other hand, the high precipitate effect of CMP for

TABLE 3 | The concentration of metals in the root of rice.

Treatments	Fe/g kg^{-1}	Mn/mg kg^{-1}	Zn/mg kg^{-1}	Cu/mg kg^{-1}	Cd/mg kg^{-1}
CK	319.00 ± 8.75 a	151.35 ± 8.66 d	89.90 ± 4.68 b	77.20 ± 3.75 a	8.95 ± 0.35 a
0.2‰	232.75 ± 9.01 d	233.05 ± 7.68 c	121.70 ± 7.55 a	60.55 ± 2.05 b	6.94 ± 0.48 b
0.5‰	249.20 ± 5.94 bc	364.15 ± 5.71 a	97.20 ± 5.65 b	37.16 ± 1.98 c	5.24 ± 0.24 c
1.0‰	244.05 ± 8.35 cd	273.50 ± 7.36 b	99.05 ± 3.21 b	35.15 ± 2.12 c	4.33 ± 0.18 d

Different lowercase letters indicate significant differences in the content of the same substance between different treatments ($P < 0.05$).

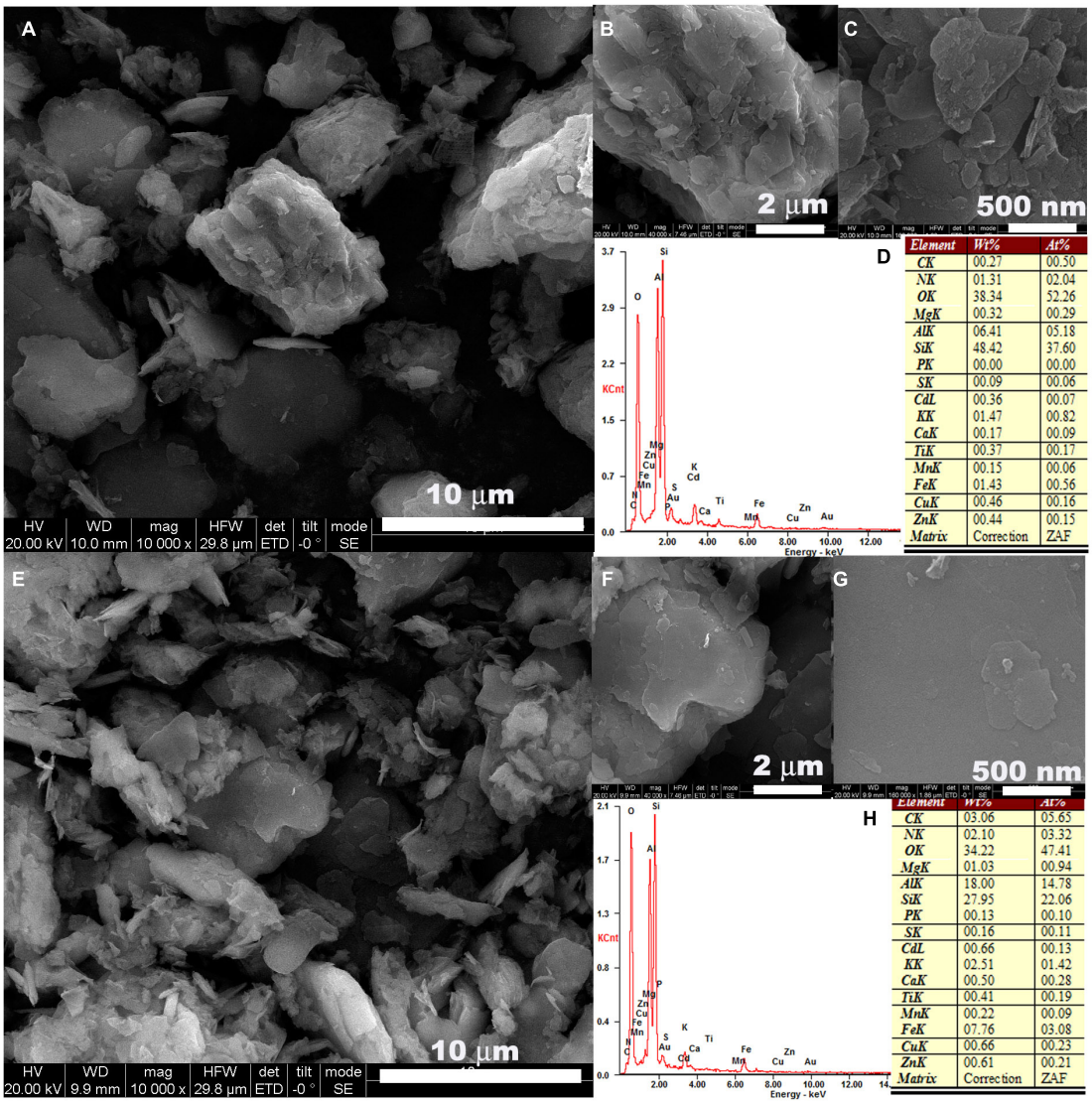

FIGURE 3 | The SEM of soil processed with **(A–C)** 0 and **(E–G)** 1.0‰ amendment, and its corresponding EDS result **(D,H)**.

Cd^{2+} results in low available cadmium. The solubility product (*K*sp) for $Cd_3(PO_4)_2$ was 2.53×10^{-29}, which is far lower than the *K*sp for $Cd(OH)_2$ (6.5×10^{-14}) and the *K*sp for $CdCO_3$ (3×10^{-12}) (Han et al., 2017). Therefore, the available cadmium concentration increases and then decreases greatly as the FB7 amount increases. The available cadmium concentration was very low, only 0.04 mg/kg, in the treatment with 0.5‰ amendment. Furthermore, similar results were found in the available iron, zinc concentration (**Supplementary Table 3**). It was attributed to the highest pH value among the treatments being in the soil from the treatment with 0.5‰ FB7 at the harvest stage.

Cadmium content in roots gradually decreased as the amount of FB7 increased (**Figure 2B**). Cadmium content in roots was 16.68, 11.14, 5.18, and 9.61 mg/kg after addition of 0, 0.2, 0.5,

TABLE 4 | Statistics of the trimmed sequences and alpha-diversity of the bacterial communities.

Sample	Primers	Sequence	Bases (bp)	Mean length (bp)	OUT	Sobs	Shannon	Simpon	Ace	Chao	Coverage
CK	338_806R	43,421	18,103,363	416.990	2,989	3,094	6.858	0.0025	4118.195	4106.610	0.966
0.2‰	338_806R	51,084	21,310,944	417.153	2,943	3,553	6.995	0.0022	4720.416	4691.613	0.964
0.5‰	338_806R	49,104	20,508,293	417.628	2,851	3,747	7.057	0.0023	5157.998	5035.537	0.957
1.0‰	338_806R	49,343	20,636,836	418.207	2,377	3,709	7.044	0.0022	4962.246	4866.319	0.964

and 1.0‰ FB7, respectively. The total iron, manganese, zinc, copper, and cadmium concentration are revealed in **Table 3**. The content of zinc and manganese increased, and the content of iron, copper, and cadmium decreased. Compared with CK, after applying the amendment zinc increased by 7.3–31.8 mg/kg while iron decreased by 69.8–86.25 g/kg and copper was reduced by 16.6–42.05 mg/kg.

Maybe the decrease of metal concentration in the root has relation to the low available metal concentration in soil and the competition effect. Usually, low available metal concentration in the soil induces low concentrations of metals such as iron, copper, and cadmium in the root. Alternatively, the competition effect may be attributed to low cadmium concentration in the root. Cadmium mainly enters the rice root system in the form of ion. Ca^{2+}, Mg^{2+}, Zn^{2+}, and Cd^{2+} are divalent cations with similar physicochemical properties. Therefore, plants often absorb and transport these cations by using the same transport proteins and ion channels, so there is a competition in these ions (Zhang et al., 2019). The large amount of calcium and magnesium in FB7 can occupy the associated ion channels and reduce the root's cadmium uptake. As shown in **Supplementary Figure 1**, the application of amendment significantly reduces translocation factor (TF) and bioconcentration factor (BCF).

An interesting trend was found for manganese and zinc, with these nutrients having lower available concentration in the soil and higher concentration in the root after FB7 treatment. Zinc and manganese are common nutrients in rice and their absorption can be enhanced by the application of calcium-containing fertilizers (Luo et al., 2020). The other mechanism might be attributed to the competition effect between zinc and cadmium. Very low available cadmium concentration induces high zinc uptake (Cai et al., 2019). Similarly, manganese and iron demonstrated a competition effect on each other. Therefore, phosphate fertilizer decreased available iron concentration and then increased manganese uptake. However, Mao et al. (2019) reported that phosphate fertilizer would dramatically reduce the availability of manganese and increase the molar ratio of iron to manganese in iron plaques on root surfaces. The difference might be attributed to soil type and the amount of phosphate fertilizer.

The cadmium content in rice was 0.92, 0.76, 0.08, and 0.11 mg/kg (**Figure 2C**) after addition of 0, 0.2, 0.5, and 1.0‰ FB7, respectively. The cadmium concentration in rice after treatment with 0.5 and 1.0‰ FB7 decreased to less than 0.2 mg/kg, which is the National Food Safety Standard. Specifically, when the FB7 concentration is 0.5‰, the cadmium content in rice is the lowest.

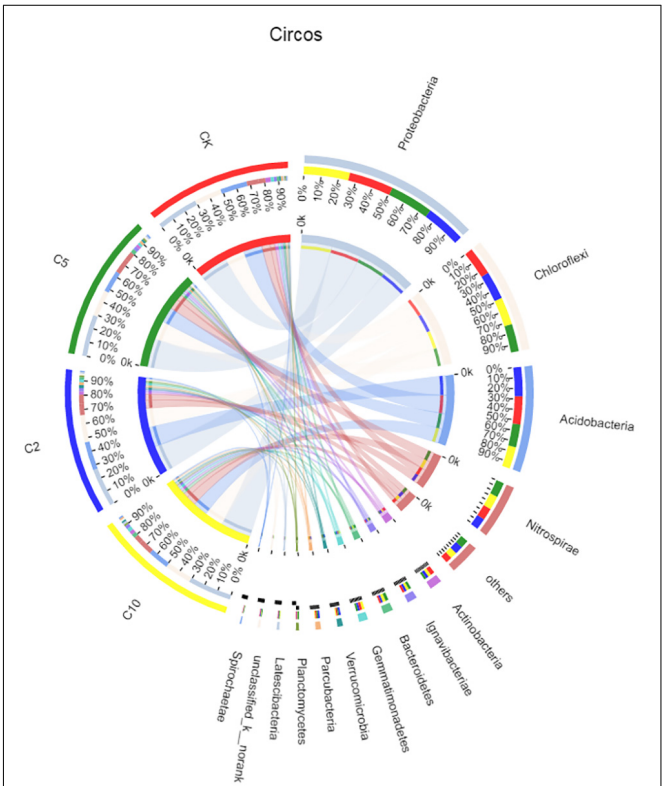

FIGURE 4 | Relationships between samples and phyla are shown in Circos figures. The CK, C2, C5, and C10 is representative of the sample from soil processed with 0, 0.2, 0.5, and 1.0‰ amendment, respectively.

Effects of Amendment on Soil Microstructure

The typical microstructure of the soil from the CK and 1.0‰ treatment are shown in **Figures 3A–H**. Soil samples contained a range of minerals, including quartz, muscovite, and kaolinite, which was determined by the X-ray diffraction (XRD) (**Supplementary Figure 2**). The separated small sheet structure was attributed to the quartz and the aggregated large composites corresponded to the kaolinite and muscovite, as shown in **Supplementary Figures 3**, **4**. There was no obvious variation in the microstructure of soil minerals after treatment with 1.0‰ FB7. However, the surface of the kaolinite became smoother in **Figure 3G** in comparison with that of **Figure 3C**. Furthermore, a small amount of phosphorous was found from the surface of the kaolinite in the CK and its concentration increased to 0.13% after processing with 1.0‰ FB7. Some phosphorous was incorporated

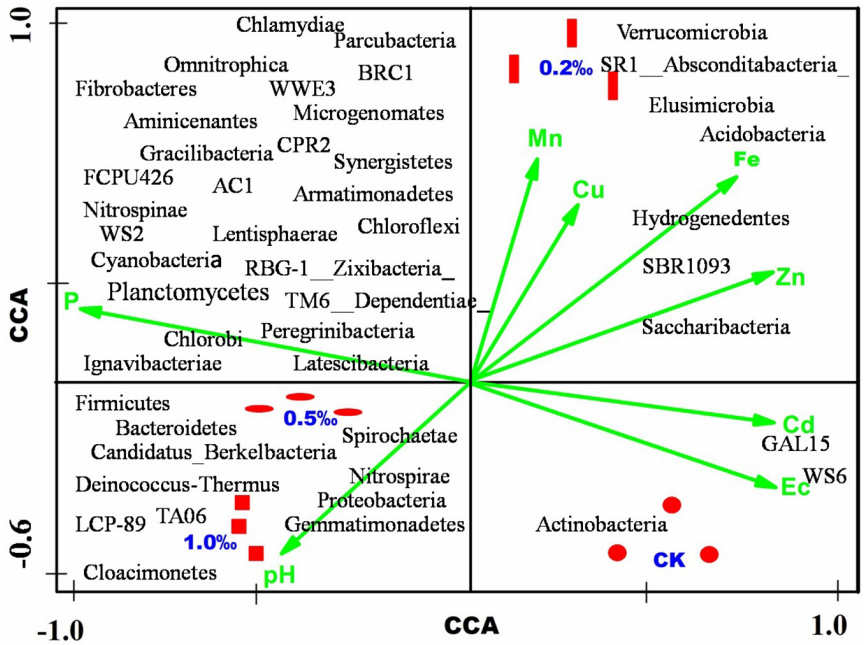

FIGURE 5 | Canonical correspondence analysis (CCA) of the microbial community, environmental parameters, and samples.

into the surface of the mineral. The smooth surface might be attributed to the dissolution-precipitation effect of CMP.

Overview of 16S rRNA Sequencing

In order to study the composition of the microbial community in the paddy soil, we sequenced 16S RNAs. After removing the low-quality readings and trimming the adapters and barcodes, there were 192,952 effective sequences with an average length of 311.85 bp of microbiota generated from the four paddy soil samples: 43,421, 51,084, 49,104, and 49,343 sequences on average for the samples collected from soil treated with 0, 0.2, 0.5, and 1.0‰ FB7 (marked as CK, C2, C5, and C10), respectively. Coverages of 0.966, 0.964, 0.957, and 0.964 were achieved (**Table 4**). The shape of the rarefaction and Shannon–Wiener curves tended to approach the saturation plateau, showing that the bacterial abundance of this sample was relatively complete (data not shown). The sequences were assigned to 11,160 OTUs of bacteria.

Based on the OTUs number, the soil sample from the CK treatment was found to have the richest value, with an OTUs number of 2,989, whereas the samples from 0.2, 0.5, and 1.0‰ FB7 displayed considerably lower richness, with OTUs numbers of 2,943, 2,851, and 2,377. Generally, the Chao1 and Ace indices were used to calculate the OTUs numbers. The experimental results show that the Ace and Chao1 indices of the four samples were negatively correlated with the OTUs numbers. Otherwise, the Shannon indices indicated that the 0.5‰ FB7 treatment showed the greatest diversity (7.057) while the sample of others displayed relatively lower diversity (6.858, 6.995, and 7.044). However, the Simpson index indicated that the CK treatment showed great diversity (0.0025), and the others had relatively lower diversity. Ultimately, the 0.5‰ FB7 treatment was considered to have the highest diversity.

Heavy metals and nutrition are two key parameters affecting biodiversity (Xie et al., 2016). These results indicated that the application of amendment has obvious effects on soil biological community structure. The 0.5‰ FB7 treatment had richer biodiversity than others. This result could be attributed to FB7 optimizing the biological growth environment by increasing fertility and reducing bioavailability of heavy metal, but also destroying its environment to decrease the number of biomes after the addition of too much mineral element.

Karaca et al. (2002) found that when 50 mg/kg of cadmium was added to contaminated soil (sandy loam), the population abundance of bacteria and pseudomonas was significantly increased after also applying sludge and phosphate fertilizer. In addition, their study found that applying red mud, lime, and zeolite to acidic soil contaminated with lead, cadmium, and zinc could effectively improve the number of soil microorganisms. All of these suggest that the addition of amendment leads to an increase in biodiversity.

Gong et al. (2021) found that soil with light heavy metal pollution significantly reduced the diversity of fungi after a large application of amendment. Therefore, excessive amendment would decrease biodiversity. Similarly, the addition of amendment led to the increase and then decrease of biodiversity in this experiment.

Figure 4 shows the distribution of bacterial phyla in the paddy soil samples. Proteobacteria was the most abundant phylum in all the soil, accounting for 31, 30, 28, and 32% of effective bacterial sequences of the CK, C2, C5, and C10 treatments, respectively. The next most dominant phylum in the CK, C5,

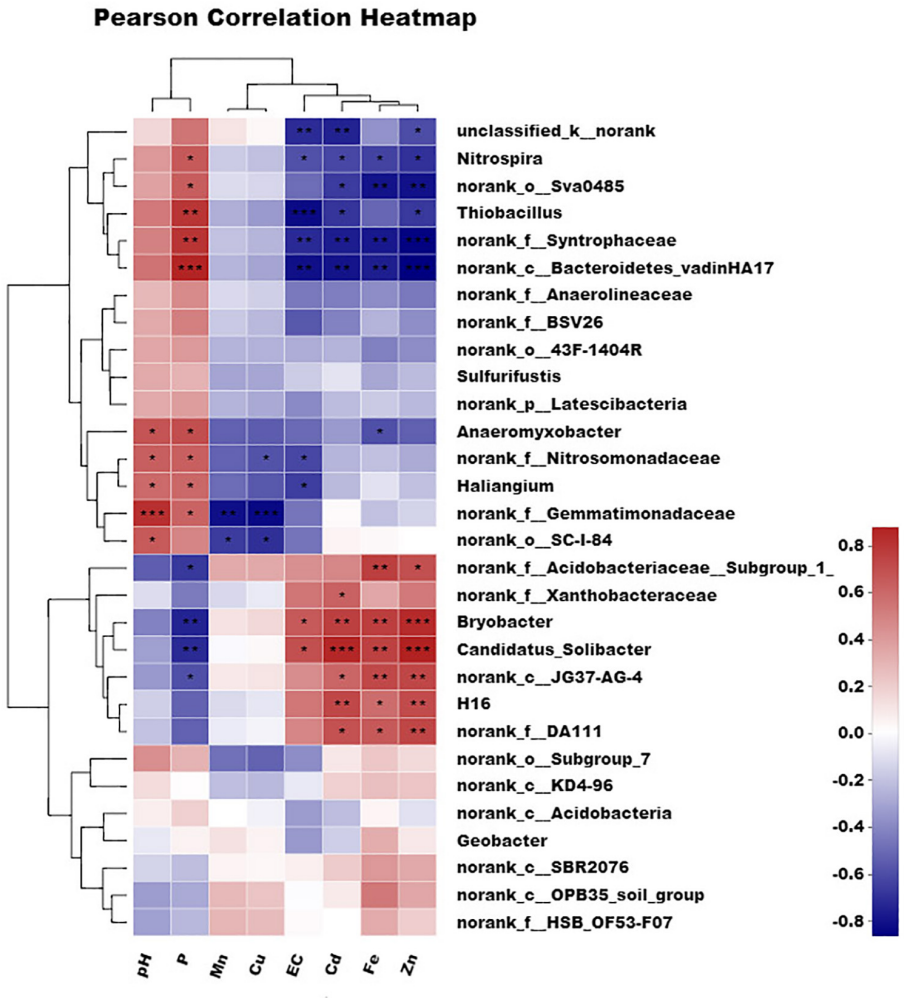

FIGURE 6 | Correlation between different influencing factors and different microorganisms in genus level. Single asterisk (*$P < 0.05$), double asterisk (**$P < 0.01$), and three asterisk (***$P \leq 0.001$) indicate statistically significant differences between values.

and C10 treatments was Chloroflex, with a prevalence of ∼20%. However, in the C2 sample, the second most dominant phylum was Acidobacterium, with a prevalence of 21%. This result might correspond to the strong acidification effect in the soil with 0.2‰ FB7. Consequently, Proteobacteria and Chloroflex were the most abundant phyla, followed by Acidobacterium and Nitrospirae.

Proteobacteria can produce exopolysaccharides, and thus can participate in soil stabilization (Liu et al., 2017). In this study, heavy metals hardly affected the relative abundance of Proteobacteria. The relative abundance of Proteobacteria was only slightly influenced by different levels of heavy metal bioavailability; the main OTUs shared by all samples belonged to the Proteobacteria. Some sequences of Proteobacteria, such as *Halomonas* and *Halovibrio* sp., can also assist carbonate mineral formation (Heijs et al., 2006). Therefore, Proteobacteria have a high detoxifying effect with regard to contamination by heavy metals. Other research has suggested that Proteobacteria offer some resistance to pollution from various heavy metals (Zhu et al., 2013), and this can explain the abundance of this phylum in all samples.

Correlation Between Bacterial Community, Environmental Parameters, and Phyla

In this study, eight physical and chemical indexes (pH, EC, available phosphorus, available iron, manganese, copper, zinc, and cadmium in soil) were analyzed and the relative contribution of the bacterial community at the phylum level was evaluated (**Figure 5**). The available phosphorous and pH were positive corresponded to the C5 and C10 treatments, which were treated with high concentration FB7. The EC and available cadmium were positively related with the CK treatment, and the available manganese and copper were related to the C2 treatment. The environmental parameters results indicated that the high pH and phosphorous effectively decreased the available metal concentration in the soil, such as manganese, copper,

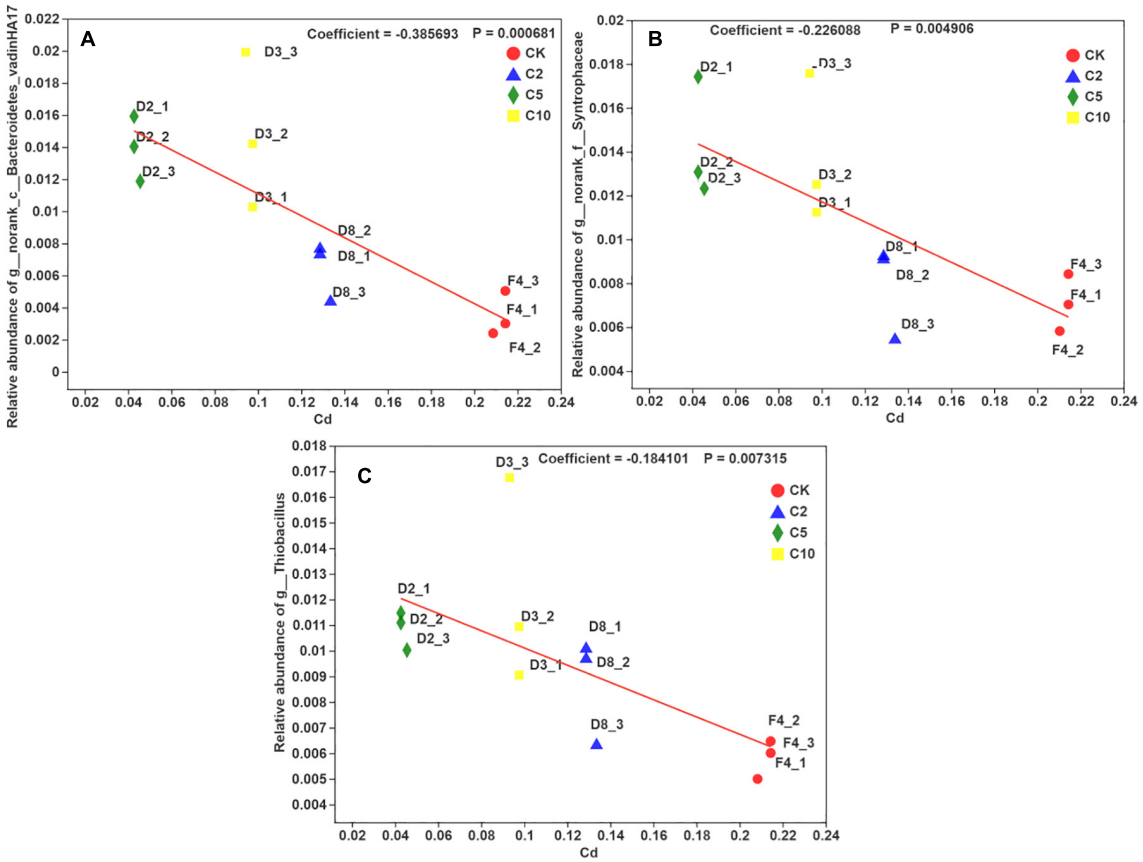

FIGURE 7 | The multivariate association with linear models between the relative abundance of three microorganisms **(A–C)** in the genus level and available Cd concentration in soil with different amendment concentration.

iron, zinc, and cadmium. Environmental parameters regarding phosphorous contributed positively to Peregrinibacteria, RBG-1, Ignavibacteriae, Nitrospinae, Firmicutes, and Latescibacteria. The pH level contributed positively to the Proteobacteria, Cloacimonetes, and Gemmatimonadetes. The available cadmium and EC were positively contributed to the GAL15 and WS6.

The detailed correlation between the organism at the genus level and environmental parameters is shown in **Figure 6** and **Supplementary Table 3**. A genus-level heatmap split the eight parameters into three groups at the first level. One was composed of pH and phosphorous, another was composed of manganese and copper, and the last was composed of EC, cadmium, iron, and zinc. The effect of parameters such as pH and phosphorous on organisms was greatly different from that of EC, cadmium, iron, and zinc. It is corresponded to the results of the canonical correspondence analysis (CCA).

Bacterodietes-vadinHA17, *Syntrophaceae*, and *Thiobacillus* were significantly positively correlated (R = 0.80, $P \leq 0.001$) with phosphorous, while *Bryobacter* and *Candidatus-Solibacter* were significantly negatively correlated with phosphorous (R =–0.70, $P \leq 0.001$). The opposite relationship was present between phosphorous and pH, and cadmium, iron, zinc, and EC. As a result, *Bacterodietes-vadinHA17* and *Syntrophaceae* were negatively correlated with cadmium, iron, zinc, and EC. However, *Bryobacter*, *Candidatus-Solibacter*, and *H16* were positively correlated with these four parameters. Usually, *Thiobacillus thiooxidans* can produce substantial amounts of H^+ and then induce low pH. The treatment with high content FB7 induced the relatively low bioavailable iron, manganese, and zinc for paddy soil. The multivariate association with linear models for three typical microorganisms (*Bacterodietes-vadinHA17*, *Syntrophaceae*, and *Thiobacillus*) and the available cadmium concentration in soil is shown in **Figure 7**. The relationship coefficients in the linear model were –0.38, –0.22, and –0.18 for *Bacterodietes-vadinHA17*, *Syntrophaceae*, and *Thiobacillus,* respectively.

Bacterodietes-vadinHA17 is a typical organic matter-degradation bacterium (Yang J. et al., 2018). Baldwin found the order *Bacteroidetes* environmental group vadinHA17 in environments undergoing complex carbon degradation, especially in samples with relatively high amounts of recalcitrant organic matter (Baldwin et al., 2015). Similarly, *Syntrophaceae* usually play an important part in the methanogenic hexadecane degradation (Lei et al., 2013). Gray et al. (2011) revealed a significant positive correlation between *Syntrophaceae*-affiliated

clones and methane production from a petroleum hydrocarbon-degrading consortium. However, it has not been reported if the resulting high concentration P can increase the abundance of *Bacterodietes-vadinHA17* and *Syntrophaceae*. The present result may imply that adding a higher concentration of phosphorous to the soil can induce more organic matter to degrade into more methane. However, the detailed mechanism on the relationship needs further investigation.

Thiobacillus thiooxidans reduced soil pH and increased the uptake of iron, manganese, and zinc in paddy roots and shoots (Aria et al., 2010). This result may correspond to a lower pH in the C10 than the C5 treatment. It was reported that *Thiobacillus thiooxidans* can be subcultivated in the environment with a high concentration of cadmium, through the formation of a cadmium-complex (Sakamoto et al., 1989). Thus, the low bioavailable cadmium may be attributed to the high abundance of *Thiobacillus* in the soil.

Bacteria in the genus *Bryobacter* and *Candidatus-Solibacter* belong to the Acidobacteria phylum, which is correlated with H^+ production in soil. These two bacteria can decrease with increasing nitrogen fertilizer due to lower soil pH after the application of more nitrogen fertilizer (Wang et al., 2017). However, in our experiment, the addition of a more alkaline substance such as CMP and lime caused higher pH (>7.2) long-term in the soil environment and then decreased these bacteria's abundance. The growth of *Bryobacter* occurs at pH 4.5–7.2 (optimum growth at pH 5.5–6.5) (Kulichevskaya et al., 2010). Therefore, the presence of an appropriate growth pH may be the main effect on the abundance of Acidobacteria. However, *Bryobacter* and *Candidatus-Solibacter* showed a highly positive relationship with available metal ions such as cadmium, iron, and zinc. These bacteria can cause low pH and lots of fatty acid, a type of organic matter with few molecules (Kawai et al., 2012). Therefore, the higher abundance of *Bryobacter* and *Candidatus-Solibacter* induces higher bioavailable metal content.

The bacteria *norank-f-Gemmatimonadaceae* was significantly positively correlated to pH and negatively correlated with manganese and copper. It preferred the high pH environment and can reduce the bioavailability of manganese and copper. The bacteria *norank-f-Gemmatimonadaceae* has a polyphosphate-accumulating function (Takaichi et al., 2010). Therefore, low bioavailable manganese and copper might be attributed to the coprecipitation effect of the phosphate-metal ion (manganese, copper).

CONCLUSION

Application of 0.5‰ CMP + lime amendment could mitigate soil acidity, reduce bioavailable cadmium, and decrease cadmium content in brown rice to the national food safety standard. Enough calcium, magnesium, manganese, and zinc were supplied for rice, although this amendment greatly decreased the iron, copper, and cadmium bioavailable content in soil. There will be a competition between those cations and cadmium ions, but the application of a small amount of amendment can promote the uptake of heavy metals in rice. The amendment can remediate the ecology of the soil and increase biodiversity. Specifically, the abundance of *Bacterodietes-vadinHA17*, *Syntrophaceae*, and *Thiobacillus* was significantly positively correlated with phosphorous, while *Bryobacter* and *Candidatus-Solibacter* were significantly negatively correlated with phosphorous. These microorganisms may potentially affect metal bioavailability and then decrease the cadmium uptake by the rice. Therefore, the CMP + lime amendment is recommended as a highly effective amendment for remediating cadmium-polluted acidic paddy soils in south China.

DATA AVAILABILITY STATEMENT

The original contributions presented in the study are publicly available. This data can be found here: National Center for Biotechnology Information (NCBI) BioProject database under accession number PRJNA761207.

ETHICS STATEMENT

All procedures performed in studies involving human participants were in accordance with the ethical standards of the institutional and/or national research committee.

AUTHOR CONTRIBUTIONS

XK and KS conducted the whole experiment, did the analysis, and wrote the initial draft. HS and AC (ranked in order of their actual contribution) provided necessary facilities for the successful completion of this work. LP provided partial research grants for this study, proofread the manuscript, and also supervised the work. All authors contributed to the article and approved the submitted version.

FUNDING

For financial support, we are grateful to The National Key Research and Development Program of China (2017YFD0801102), Hunan Education Department Projects (No. 20C0948), High-tech Industry Science and Technology Innovation Leading Plan (Science and Technology Tackling) of Hunan Province, China (2020NK200101), and Hunan Provincial Youth Backbone Teacher Plan, Changsha Plan Project of Science and Technology (kq1801025).

SUPPLEMENTARY MATERIAL

The Supplementary Material for this article can be found online at: https://www.frontiersin.org/articles/10.3389/fmicb.2021.749946/full#supplementary-material

REFERENCES

Aria, M. M., Lakzian, A., Haghnia, G. H., Berenji, A. R., Besharati, H., and Fotovat, A. (2010). Effect of *Thiobacillus*, sulfur, and vermicompost on the water-soluble phosphorus of hard rock phosphate. *Bioresour. Technol.* 101, 551–554. doi: 10.1016/j.biortech.2009.07.093

Baldwin, S. A., Khoshnoodi, M., Rezadehbashi, M., Taupp, M., Hallam, S., Mattes, A., et al. (2015). The microbial community of a passive biochemical reactor treating arsenic, zinc, and sulfate-rich seepage. *Front. Bioeng. Biotechnol.* 3:27. doi: 10.3389/fbioe.2015.00027

Bouray, M., Moir, J. L., Condron, L. M., and Lehto, N. J. (2021). Lime-induced ph elevation influences phosphorus biochemical processes and dynamics in the rhizosphere of *Lupinus polyphyllus* and *Lupinus angustifolius*. *J. Soil Sci. Plant Nutr.* 21, 1978–1992. doi: 10.1007/s42729-021-00495-z

Cai, Y., Xu, W., Wang, M., Chen, W., Li, X., Li, Y., et al. (2019). Mechanisms and uncertainties of Zn supply on regulating rice Cd uptake. *Environ. Pollut.* 253, 959–965. doi: 10.1016/j.envpol.2019.07.077

Gong, L., Wang, J., Abbas, T., Zhang, Q., and Di, H. (2021). Immobilization of exchangeable Cd in soil using mixed amendment and its effect on soil microbial communities under Paddy upland rotation system. *Chemosphere* 262:127828. doi: 10.1016/j.chemosphere.2020.127828

Gray, N. D., Sherry, A., Grant, R. J., Rowan, A. K., Hubert, C. R. J., Callbeck, C. M., et al. (2011). The quantitative significance of Syntrophaceae and syntrophic partnerships in methanogenic degradation of crude oil alkanes. *Environ. Microbiol.* 13, 2957–2975. doi: 10.1111/j.1462-2920.2011.02570.x

Guha, T., Barman, S., Mukherjee, A., and Kundu, R. (2020). Nano-scale zero valent iron modulates Fe/Cd transporters and immobilizes soil Cd for production of Cd free rice. *Chemosphere* 260:127533. doi: 10.1016/j.chemosphere.2020.127533

Han, C., Lalley, J., Iyanna, N., and Nadagouda, M. N. (2017). Removal of phosphate using calcium and magnesium-modified iron-based adsorbents. *Mater. Chem. Phys.* 198, 115–124. doi: 10.1016/j.matchemphys.2017.05.038

Heijs, S. K., Aloisi, G., Bouloubassi, I., Pancost, R. D., Pierre, C., Damsté, J. S. S., et al. (2006). Microbial community structure in three deep-sea carbonate crusts. *Microb. Ecol.* 52, 451–462.

Karaca, A., Naseby, D. C., and Lynch, J. M. (2002). Effect of cadmium contamination with sewage sludge and phosphate fertiliser amendments on soil enzyme activities, microbial structure and available cadmium. *Biol. Fertil. Soils* 35, 428–434. doi: 10.1007/s00374-002-0490-4

Kawai, K., Takato, S., Sasaki, T., and Kajiwara, K. (2012). Complex formation, thermal properties, and *in-vitro* digestibility of gelatinized potato starch–fatty acid mixtures. *Food Hydrocoll.* 27, 228–234. doi: 10.1016/j.foodhyd.2011.07.003

Kulichevskaya, I. S., Suzina, N. E., Liesack, W., and Dedysh, S. N. (2010). *Bryobacter aggregatus* gen. nov., sp. nov., a peat-inhabiting, aerobic chemo-organotroph from subdivision 3 of the Acidobacteria. *Int. J. Syst. Evol. Microbiol.* 60, 301–306. doi: 10.1099/ijs.0.013250-0

Lei, C., Chen, D., Qiang, L., Qiao, H., Li-rong, D., Hui, Z., et al. (2013). DNA-SIP reveals that syntrophaceae play an important role in methanogenic hexadecane degradation. *PLoS One* 8:e66784. doi: 10.1371/journal.pone.0066784

Li, H., Abbas, T., Cai, M., Zhang, Q., and Tahir, M. (2021). Cd bioavailability and nitrogen cycling microbes interaction affected by mixed amendments under Paddy-Pak Choi continued planting. *Environ. Pollut.* 275:116542. doi: 10.1016/j.envpol.2021.116542

Li, H., Liu, Y., Zhou, Y., Zhang, J., Mao, Q., Yang, Y., et al. (2018). Effects of red mud based passivator on the transformation of Cd fraction in acidic Cd-polluted paddy soil and Cd absorption in rice. *Sci. Total. Environ.* 640–641, 736–745. doi: 10.1016/j.scitotenv.2018.05.327

Li, Y., Liang, X., Huang, Q., Xu, Y., and Yang, F. (2019). Inhibition of Cd accumulation in grains of wheat and rice under rotation mode using composite silicate amendment. *RSC Adv.* 9, 35539–35548. doi: 10.1039/c9ra07137g

Lin, C., Lu, W., and Wu, Y. (2005). Agricultural soils irrigated with acidic mine water: acidity, heavy metals, and crop contamination. *Soil Res.* 43, 819–826. doi: 10.1071/sr04148

Liu, L., Liu, Y., Peng, Z., Song, G., Rong, H., Wang, Z., et al. (2017). Development of bacterial communities in biological soil crusts along a revegetation chronosequence in the Tengger Desert, northwest China. *Biogeosciences* 14, 1–25.

Liu, Y., Zhang, C., Zhao, Y., Sun, S., and Liu, Z. (2018). Effects of growing seasons and genotypes on the accumulation of cadmium and mineral nutrients in rice grown in cadmium contaminated soil. *Sci. Total. Environ.* 579, 1282–1288. doi: 10.1016/j.scitotenv.2016.11.115

Luo, W., Yang, S., Khan, M. A., Ma, J., and Liu, D. (2020). Mitigation of Cd accumulation in rice with water management and calcium-magnesium phosphate fertilizer in field environment. *Environ. Geochem. Health* 42, 3877–3886.

Mao, P., Zhuang, P., Li, F., McBride, M. B., Ren, W., Li, Y., et al. (2019). Phosphate addition diminishes the efficacy of wollastonite in decreasing Cd uptake by rice (*Oryza sativa* L.) in paddy soil. *Sci. Total Environ.* 687, 441–450. doi: 10.1016/j.scitotenv.2019.05.471

Mcbride, M., Sauve, S., and Hendershot, W. (2010). Solubility control of Cu, Zn, Cd and Pb in contaminated soils. *Eur. J. Soil Sci.* 48, 337–346. doi: 10.1111/j.1365-2389.1997.tb00554.x

Peng, L., Xu, Y., Zhou, F., Sun, B. R., and Tie, B. Q. (2016). Enhanced removal of Cd(II) by poly(acrylamide-co-sodium acrylate) water-retaining agent incorporated nano hydrous manganese oxide. *Mater. Des.* 96, 195–202.

Rehman, M., Rizwan, M., Rauf, A., Ayub, M. A., Ali, S., Qayyum, M. F., et al. (2019). Split application of silicon in cadmium (Cd) spiked alkaline soil plays a vital role in decreasing Cd accumulation in rice (*Oryza sativa* L.) grains. *Chemosphere* 226, 454–462.

Rosa, D. J., Ambrosini, V. G., Kokkoris, V., Brunetto, G., Hart, M., Ricachenevsky, F., et al. (2020). Lime protection for young vines exposed to copper toxicity. *Water Air Soil Pollut.* 231, 1–10.

Saengwilai, P., and Meeinkuirt, W. (2021). Cadmium (Cd) and zinc (Zn) accumulation by Thai rice varieties and health risk assessment in a Cd–Zn co-contaminated paddy field: effect of soil amendments. *Environ. Geochem. Health* 43, 3659–3674. doi: 10.1007/s10653-021-00858-6

Sakamoto, K., Yagasaki, M., Kirimura, K., and Usami, S. (1989). Resistance acquisition of *Thiobacillus thiooxidans* upon cadmium and zinc ion addition and formation of cadmium ion-binding and zinc ion-binding proteins exhibiting metallothionein-like properties. *J. Ferment. Bioeng.* 67, 266–273. doi: 10.1016/0922-338X(89)90230-4

Shi, R. Y., Ni, N., Nkoh, J. N., Dong, Y., Zhao, W. R., Pan, X. Y., et al. (2020). Biochar retards Al toxicity to maize (*Zea mays* L.) during soil acidification: the effects and mechanisms. *Sci. Total Environ.* 719:137448. doi: 10.1016/j.scitotenv.2020.137448

Singh, P., Pokharia, C., and Shah, K. (2021). Exogenous peroxidase mitigates cadmium toxicity, enhances rhizobial population and lowers root knot formation in rice seedlings. *Rice Sci.* 28, 166–177. doi: 10.1016/j.rsci.2021.01.006

Siqi, T., Shuang, L., Kun, Q., Fanhong, W., Yuxiu, Z., and Chai, T. (2019). Co-expression of multiple heavy metal transporters changes the translocation, accumulation, and potential oxidative stress of Cd and Zn in rice (*Oryza sativa*). *J. Hazard. Mater.* 380:120853. doi: 10.1016/j.jhazmat.2019.120853

Song, H., Peng, L., Li, Z., Deng, X., Shao, J., and Gu, J. D. (2019). Metal distribution and biological diversity of crusts in paddy fields polluted with different levels of cadmium. *Ecotoxicol. Environ. Saf.* 184, 1–8.

Stroud, J., Low, A., Collins, R. N., and Manefield, M. (2014). Metal(loid) bioaccessibility dictates microbial community composition in acid sulfate soil horizons and sulfidic drain sediments. *Environ. Sci. Technol.* 48, 8514–8521. doi: 10.1021/es501495s

Sun, G. X., Zhang, L., Chen, P., and Yao, B. M. (2020). Silicon fertilizers mitigate rice cadmium and arsenic uptake in a 4-year field trial. *J. Soils Sediments* 21, 163–171.

Takaichi, S., Maoka, T., Takasaki, K., and Hanada, S. (2010). Carotenoids of *Gemmatimonas aurantiaca* (Gemmatimonadetes): identification of a novel carotenoid, deoxyoscillol 2-rhamnoside, and proposed biosynthetic pathway of oscillol 2,2-dirhamnoside. *Microbiology* 156, 757–763. doi: 10.1099/mic.0.034249-0

Wang, C., Huang, Y., Zhang, C., Zhang, Y., Liu, Y., and Liu, Z. (2021). Inhibition effects of long-term calcium-magnesia phosphate fertilizer application on Cd uptake in rice: regulation of the iron-nitrogen coupling cycle driven by the soil

microbial community. *J. Hazard. Mater.* 416:125916. doi: 10.1016/j.jhazmat.2021.125916

Wang, D. Z., Jiang, X., Rao, W., and He, J. Z. (2009). Kinetics of soil cadmium desorption under simulated acid rain. *Ecol. Complex.* 6, 432–437. doi: 10.1016/j.ecocom.2009.03.010

Wang, L., Ashraf, U., Chang, C., Abrar, M., and Cheng, X. (2020). Effects of silicon and phosphatic fertilization on rice yield and soil fertility. *J. Soil Sci. Plant Nutr.* 20, 557–565.

Wang, R., Xiao, Y., Lv, F., Hu, L., Wei, L., Yuan, Z., et al. (2017). Bacterial community structure and functional potential of rhizosphere soils as influenced by nitrogen addition and bacterial wilt disease under continuous sesame cropping. *Appl. Soil Ecol.* 125, 117–127.

Xie, Y., Wang, J., Wu, Y., Ren, C., Song, C., Yang, J., et al. (2016). Using in situ bacterial communities to monitor contaminants in river sediments. *Environ. Pollut.* 212, 348–357.

Xu, Y., Feng, J., and Li, H. (2021). How intercropping and mixed systems reduce cadmium concentration in rice grains and improve grain yields. *J. Hazard. Mater.* 402:123762.

Yang, Y., Chen, J., Huang, Q., Tang, S., Wang, J., Hu, P., et al. (2018). Can liming reduce cadmium (Cd) accumulation in rice (*Oryza sativa*) in slightly acidic soils? A contradictory dynamic equilibrium between Cd uptake capacity of roots and Cd immobilisation in soils. *Chemosphere* 193, 547–556. doi: 10.1016/j.chemosphere.2017.11.061

Yang, J., Pengfei, L., and Ralf, C. (2018). Response of fermenting bacterial and methanogenic archaeal communities in paddy soil to progressing rice straw degradation. *Soil Biol. Biochem.* 124, 70–80.

Yang, J., Wang, C., and Dai, H. (2008). *Soil Agrochemical Analysis and Environmental Monitoring*. Beijing: China Earth Press.

Yin, H., Yang, C., Yang, P., Kaksonen, A. H., and Douglas, G. B. (2021). Contrasting effects and mode of dredging and *in situ* adsorbent amendment for the control of sediment internal phosphorus loading in eutrophic lakes. *Water Res.* 189, 116644–116654. doi: 10.1016/j.watres.2020.116644

Zhang, Y., Wang, X., Ji, X., Liu, Y., Lin, Z., Lin, Z., et al. (2019). Effect of a novel Ca-Si composite mineral on Cd bioavailability, transport and accumulation in paddy soil-rice system. *J. Environ. Manage.* 233, 802–811. doi: 10.1016/j.jenvman.2018.10.006

Zhao, F. J., Ma, Y., Zhu, Y. G., Tang, Z., and Mcgrath, S. P. (2015). Soil contamination in China: current status and mitigation strategies. *Environ. Sci. Technol.* 49, 750–759. doi: 10.1021/es5047099

Zhen, Z., Wang, S., Luo, S., Ren, L., Liang, Y., Yang, R., et al. (2019). Significant impacts of both total amount and availability of heavy metals on the functions and assembly of soil microbial communities in different land use patterns. *Front. Microbiol.* 10:2293. doi: 10.3389/fmicb.2019.02293

Zhu, J., Zhang, J., Li, Q., Han, T., Xie, J., Hu, Y., et al. (2013). Phylogenetic analysis of bacterial community composition in sediment contaminated with multiple heavy metals from the Xiangjiang River in China. *Mar. Pollut. Bull.* 70, 134–139.

Conflict of Interest: The authors declare that the research was conducted in the absence of any commercial or financial relationships that could be construed as a potential conflict of interest.

Publisher's Note: All claims expressed in this article are solely those of the authors and do not necessarily represent those of their affiliated organizations, or those of the publisher, the editors and the reviewers. Any product that may be evaluated in this article, or claim that may be made by its manufacturer, is not guaranteed or endorsed by the publisher.

frontiers in Microbiology

ORIGINAL RESEARCH
published: 03 December 2021
doi: 10.3389/fmicb.2021.774301

Cadmium Speciation Distribution Responses to Soil Properties and Soil Microbes of Plow Layer and Plow Pan Soils in Cadmium-Contaminated Paddy Fields

Xiaodong Hao[1,2], Lianyang Bai[3], Xueduan Liu[2], Ping Zhu[1,2], Hongwei Liu[2], Yunhua Xiao[4], Jibiao Geng[1], Qianjin Liu[1], Lihua Huang[1] and Huidan Jiang[3]**

[1]Shandong Provincial Key Laboratory of Water and Soil Conservation and Environmental Protection, College of Resources and Environment, Linyi University, Linyi, China, [2]School of Minerals Processing and Bioengineering, Central South University, Changsha, China, [3]Biotechnology Research Institute, Hunan Academy of Agricultural Sciences, Changsha, China, [4]College of Bioscience and Biotechnology, Hunan Agricultural University, Changsha, China

OPEN ACCESS

Edited by:
Hui Li,
Jinan University, China

Reviewed by:
Safdar Bashir,
Ghazi University, Pakistan
Jincai Ma,
College of New Energy and Environment/Jilin University, China

***Correspondence:**
Lihua Huang
huanglihua@lyu.edu.cn
Huidan Jiang
jianghd3961@163.com

Specialty section:
This article was submitted to Terrestrial Microbiology, a section of the journal Frontiers in Microbiology

Received: *11 September 2021*
Accepted: *09 November 2021*
Published: *03 December 2021*

Citation:
Hao X, Bai L, Liu X, Zhu P, Liu H, Xiao Y, Geng J, Liu Q, Huang L and Jiang H (2021) Cadmium Speciation Distribution Responses to Soil Properties and Soil Microbes of Plow Layer and Plow Pan Soils in Cadmium-Contaminated Paddy Fields. Front. Microbiol. 12:774301. doi: 10.3389/fmicb.2021.774301

Cadmium (Cd) speciation ratio in arable land determines the Cd exposure risk and Cd uptake in crops. However, the driving mechanisms of Cd speciation change on the vertical scale of paddy fields remain poorly understood. In this study, the effects of plow layer and plow pan on Cd speciation distribution were investigated in a long-term Cd-contaminated rice ecosystem. The Cd accumulative effect within rice grain was enhanced with high levels of activated Cd speciation ratios in soils. Activated Cd speciation ratios were higher in plow layer soils, while stabilized Cd speciation ratios were elevated in plow pan soils. Soil physicochemical properties and soil microbes synergistically affected the Cd speciation changes in different ways between the two soil layers. Soil pH and organic elements in plow layer environment directly hindered the transformation of stabilized Cd speciation, while in plow pan environment, soil pH and organic elements indirectly decreased activated Cd speciation ratios and resulted in the accumulation of stabilized Cd speciation *via* regulating the predominant bacterial taxa. This study will improve our understanding of how soil environments regulate Cd speciation distributions in rice ecosystems and help to seek effective remediation methods of Cd-contaminated paddy fields to reduce the Cd accumulation in rice.

Keywords: Cd speciation, response characteristic, soil depth, Cd-contaminated paddy, microbial community

INTRODUCTION

Cadmium (Cd), a highly toxic and carcinogenic heavy metal species, has attracted substantial attention from researchers (Aitio and Tritscher, 2004; Hu et al., 2020). The Cd contamination of paddy fields causes soil degeneration and cereal quality degradation, raising serious food supply, and food security concerns (Rafiq et al., 2014; Jiang et al., 2020). Rice (*Oryza sativa* L.), as the main food for more than half the global population, readily assimilates Cd *via*

root uptake (Khan et al., 2017; Shi et al., 2020). Consumption of Cd-contaminated rice enhances the dietary exposure to Cd and threatens human health (Santeramo and Lamonaca, 2021). Consequently, Cd-contaminated paddy soils are in urgent need of remediation to reduce the Cd bioaccumulation of crops and adverse health effects (Huang et al., 2019). This requires a clear understanding of the biogeochemical behavior of Cd and Cd speciation change controlled by various soil environments (Li et al., 2021).

Generally, Cd deposited on soils exists as the complexes precipitated with soil components, such as carbonate, Fe-Mn oxides, organic matter, and primary minerals. Cd speciation can be divided into acid-soluble, reducible, oxidizable, and residual fractions based on sequential extraction procedures developed by the European communities bureau of reference (BCR; Gleyzes et al., 2002). The acid-soluble and reducible fractions are considered to be bioavailable for plants, but the oxidizable and residual fractions of Cd are the recalcitrant chemical forms. The Cd assimilation of crops and remediation efficiency of Cd pollution not only depend on the total Cd content in soils, but also more strongly on the distributional characteristics of Cd speciation, especially on the vertical scale (Chen et al., 2019). The plow layer is the surface soil region of crop growth that is characterized by the rich soil nutrients, loose aggregate structure, and root dense zone. The soil properties in this layer are constantly affected by the agricultural management and natural factors. The plow pan is recognized as the oligotrophic, anoxic, and sparse root soil layer, and is relatively far from the interference of farming practices. However, some soil remediation methods and agricultural production activities like deep tillage, topsoil removal, and soil dilution can alter the soil properties throughout the soil profile, and thereby affect the spatial distribution of Cd and Cd accumulation in plants (Peng et al., 2018). Previous investigations have focused on the spatial distribution and risk assessment of total Cd in a variety of habitats (Li and Ji, 2017; Deng et al., 2019), while Cd speciation differences along the vertical profile and their driving mechanisms are largely ignored.

The changes in soil environmental conditions are associated with the complex and diverse Cd speciation distribution. Soil pH can affect the activity of soil microorganisms and the synthesis of organic matter, changing the equilibrium point of Cd precipitation-dissolution. Soil redox potential can be highly mediated by soil moisture, shaping the sorption/desorption dynamics of Cd bound to Fe-Mn oxides and sulfides (Li et al., 2020a). Soil organic ligand concentration plays an important role in the transformation of different Cd forms in soils (Wu et al., 2018). The Cd speciation can also be transformed through a biogeochemical process, changing the Cd mobility, toxicity, and bioavailability. Chemoautotrophic bacteria, fungi, and the mixture culture of acid-tolerant microorganisms have been used for the biomobilization of Cd compounds through the direct and indirect mechanisms (Li et al., 2020b). The biological methods of Cd bioimmobilization, such as adding microorganism directly, microbial preparation, and biostimulation, can transform toxic Cd compounds into low- or non-toxic states. Although the alterations of soil microbial communities and soil properties in different soil depths are studied extensively (Müller et al., 2016; Anderson et al., 2017; Yu et al., 2021), little has been done to address the significant question concerning the association of Cd speciation change with the diverse soil environments of the plow layer and plow pan soils in Cd-contaminated paddy fields (Zhang et al., 2021). Likewise, the underlying mechanisms of Cd speciation distribution regulated by the composite effects of soil properties and soil microbes remain unclear and need further study. These results will provide a comprehensive understanding of Cd speciation distributions and their driving factors responding to the plow layer and plow pan soils of paddy field systems, and further help to remediate Cd-contaminated paddy fields efficiently (Fonti et al., 2016).

In this study, we analyzed the Cd speciation distribution characteristics between plow layer and plow pan soils in long-term Cd-contaminated paddy fields. The aims of this study were to evaluate the responses of Cd speciation distribution to soil properties and soil microbes, and finally to reveal the transformation mechanisms of Cd speciation regulated by the plow layer and plow pan soil environments.

MATERIALS AND METHODS

Site Description and Sample Collection

The soil sampling site was located in a rice-growing region with a subtropical monsoon humid climate in Xiangtan County, Hunan Province, Southeast China (27°77′ N′112°88′ E; **Supplementary Figure 1A**). The mean annual temperature in this paddy area was 16.7°C–18.3°C, with mean annual precipitation of 1,300 mm. The rice fields were adjacent to a steel smelter factory and had been contaminated by irrigation water mixed with Cd-containing industrial wastewater for about 10 years. For our study, in rice mature period, a total of 15 sampling points covering an approximate area of 1.5 hectares were selected randomly (**Supplementary Figure 1B**) in October 2020. Rice samples of indica rice cultivar (Yuzhenxiang, 15 samples) and paired bulk soil samples (30 samples) including plow layer soils (0–20 cm) and plow pan soils (20–40 cm) were collected using a T-sampler. Plant residues and rocks in each soil sample were removed by a 2-mm nylon mesh. These soil samples were taken back to the laboratory and stored at 4°C or −20°C for the soil physicochemical measurements or microbial community analysis, respectively.

Soil Property Analysis

Rice grain and soil samples were air-dried and milled to power with size of <150 μm using the multi-purpose disintegrator (DE-250, Rhodiola Instrument, Zhejiang, China). Rice grain samples (0.2 g) were digested by an electric heating plate (XJS20-42, Laboratory Instrument, Tianjin, China) using the HNO3 and HClO4 (5:1, vol/vol). Soil samples (0.2 g) were digested with an acid mixture of HNO3, HF, and HClO4 (10:5:2, vol/vol). Total Cd contents in rice grain, soil heavy metals, total P, and total K contents were analyzed by ICP-OES (Optima

5300DV, PerkinElmer, Shelton, United States). Soil pH and oxidation reduction potential values (ORP, vs. Ag/AgCl) were analyzed at a soil-to-water ratio of 1:2.5 (wt/vol) and measured by a pH meter (BPH-220, Bell Instrument, Dalian, China). Soil temperature (Tsoil) was measured immediately during the soil sampling process by a thermometer (TR-6, Shunkeda, Guangzhou, China). Soil moisture was analyzed after drying for 24 h at 80°C using the fresh soil samples. Organic element (organic N, organic C, organic H, and organic S) contents were determined using an Elemental Analyzer (Elementar Vario EL III, Elementar Analysensysteme, Hanau, Germany).

Cd speciation analysis of soil samples was carried out according to the sequential extraction procedure as described previously (Hao et al., 2019). Briefly, (i) the acid-soluble fraction (F-Aci) of Cd in soil samples (0.5 g) was extracted at room temperature for 16 h with 20 ml of 0.1 M acetic acid solution (pH 5.0) with continuous agitation; (ii) the reducible fraction (F-Red) of Cd in residue from (i) was leached with 20 ml of 0.5 M NH2OH·HCl (pH 1.5) at room temperature for 16 h; (iii) the oxidizable fraction (F-Oxi) of Cd was extracted from the residue (ii) through adding 10 ml of 8.8 M H2O2 and was heated to 87 ± 2°C for 1 h with occasional agitation. A second 10 ml aliquot of 8.8 M H2O2 was then added and the sample was heated again to 87 ± 2°C for 1 h with intermittent agitation. After cooling, 20 ml of 1.0 M NH4OAc adjusted to pH 2.0 with HNO3 was added and shaken at room temperature for 16 h; and (iv) the residual fraction (F-Res) of Cd in residue (iii) was digested with a HNO3-HF-HClO4 mixture as described for the total metal analysis. Between successive extractions, the supernatant was collected by centrifugation at 3600 g for 20 min. We used the F-Aci ratio, F-Red ratio, F-Oxi ratio, and F-Res ratio representing the Cd speciation transformation percentages toward the acid-soluble fraction, reducible fraction, oxidizable fraction, and residual fraction of Cd, respectively. The calculation formula is as follows: Cd speciation ratio (%) = C1/C2 × 100, where C1 represents the contents of each Cd speciation, and C2 represents the total Cd contents of soil samples.

Microbial Community Analysis

DNA Extraction, PCR Amplification, High-Throughput Sequencing

Total genomic DNA was extracted from 1.0 g of each soil sample using the E.Z.N.A. Soil DNA kit (Omega Bio-Tek Inc., United States) according to the manufacturer's protocol. DNA concentration and quality were detected by NanoDrop ND-1000 Spectrophotometer (NanoDrop Technologies) using the ratios of absorbance at 260/280 nm and 260/230 nm. Soil microbial biomass was represented by the amount of microbial DNA in soils, which was assessed by the percentage of DNA mass extracted from soils compared to the dried soil weight (Sanaullah et al., 2016).

Paired primers of 515F (5′-GTGCCAGCMGCCGCGGTAA-3′) and 806R (5′-GGACTACHVGGGTWTCTAAT-3′) with unique barcode sequences were used to amplify the V4 hypervariable region of 16S rRNA genes. PCR amplification was performed in 25 μl reactions containing 12.5 μl 2 × Taq PCR Master Mix (Vazyme, Piscataway, United States), 1 μl of template DNA, 1 μl (10 nm) of each primer, and 9.5 μl of ddH_2O water. Thermal cycling procedures were initial denaturation at 94°C for 5 min, followed by 30 cycles of 94°C for 45 s, 62°C for 45 s, and 72°C for 30 s, with final extension at 72°C for 10 min. PCR products were purified by 1.2% (wt/vol) agarose gel and recovered using an E.Z.N.A. TM Gel Extraction Kit (Omega Bio-Tek Inc., United States). PCR amplicons in each sample were pooled in equimolar concentrations, and high-throughput sequencing was performed on the Illumina Miseq platform (Miseq PE250).

Data Processing

Raw 16S rRNA amplicon sequencing data were assigned to each sample according to the unique barcode sequences using the Galaxy Illumina sequencing pipeline.[1] Forward and reverse primers reads were trimmed with up to 1.5 mismatches allowed. The Btrim program was used to remove the unqualified sequences with a threshold of QC > 20 over a 5 bp window size (Kong, 2011), and then, pair-ended sequences were combined and quality filtered by Flash (Magoč and Salzberg, 2011). Operational taxonomic units (OTUs) were clustered by UPARSE with a sequence threshold of 97% similarity (Edgar, 2013). Taxonomic assignment of 16S representative sequences was performed based on the ribosomal database project (RDP) classifier with a minimum of 50% confidence estimates (Wang et al., 2007). The raw 16S rRNA sequencing data were deposited in the NCBI Sequence Read Archive database (SRP291811).

Functional Prediction

The phylogenetic investigation of communities by the reconstruction of unobserved states (PICRTUSt) was used to predict the abundance of gene families in environmental communities using the 16S rRNA sequencing data of plow layer and plow pan soil samples (Langille et al., 2013). The Kyoto encyclopedia of genes and genomes (KEGG) database and closed reference OTUs based on the Greengenes reference taxonomy (Greengenes 13.5) were used to predict the molecular functions of each soil sample. The 16S copy number was normalized, and then, molecular functions were predicted and final data were summarized into KEGG pathways.

Network Construction

Phylogenetic molecular ecological networks (pMENs) were constructed by sequencing of 16S rRNA gene amplicons based on random matrix theory (RMT; Deng et al., 2012). The OTUs detected in at least 12 out of 15 replicates were employed to ensure correlation reliability for network analysis. The pMENs of plow layer and plow pan soil samples were constructed and analyzed on the IEG MENA Pipeline,[2] and the network plots were visualized in Cytoscape 3.6.0 software. The network was split into different modules to represent the modularity property. Sub-networks of plow layer and plow pan soil samples

[1] http://zhoulab5.rccc.ou.edu/
[2] http://ieg2.ou.edu/MENA

were also built separately using the F-Aci ratio, F-Red ratio, F-Oxi ratio, and F-Res ratio as microbial factors to analyze the correlation between the Cd speciation ratio and relevant OTUs.

Statistical Analysis

In this study, the Shannon index was calculated to measure the biodiversity of the microbial community in plow layer and plow pan soils using the resampled 16S OTU subsets (10, 000 sequences per soil sample). A Venn diagram was constructed using "Venny 2.1."[3] Detrended correspondence analysis (DCA) was used to present the bacterial community structure heterogeneity between the two soil layers. Dissimilarity analyses of MRPP, ANOSIM, and Adonis were conducted to test the differences in microbial structure in the plow layer and plow pan soil samples. Redundancy analysis (RDA) and variation partitioning analysis (VPA) were performed to estimate the contributions of environmental variables to the bacterial community using R vegan package. A paired-sample *t*-test was employed to identify the differences in the soil physicochemical properties, relative abundance of dominant microbes and selected pathways, soil DNA concentrations, and Shannon index between the two soil layers using IBM SPSS Statistics 21.0 software. The correlation analysis between Cd accumulation contents of rice grain, soil parameters, soil microbes, and Cd speciation ratios was performed using a Pearson correlation test. A partial least square path model (PLSPM) using the "amap," "shape," "diagram," and "plspm" packages in R was used to show the effects of soil factors and microbial community structures on Cd speciation distribution in plow layer and plow pan soils.

RESULTS

Effects of Soil Properties on Cd Speciation Distribution

Total heavy metal contents showed significant differences between plow layer and plow pan soil samples (**Table 1**). The total Cd, Cr, Cu, Pb, and Zn contents in plow layer soils were significantly ($p < 0.01$) higher than those in plow pan soils, which was mainly attributed to the artificial exogenous introduction and adsorption of heavy metals in plow layer soils. However, only the Cd contents in both plow layer (19.0 mg/kg) and plow pan (0.4 mg/kg) soils exceeded the Environmental Quality Standard for Soils of China (EPM, 2018) for Cd (0.3 mg/kg) in paddy fields. The mean Cd content in rice grain was 2.9 ± 0.8 mg/kg, which was 14.5 times higher than the Cd standard threshold (0.2 mg/kg) of National food safety standards of China. Moreover, the contents of total Mn, total K, and soil pH values decreased, while soil moisture, soil temperature, total P, and organic elements contents (organic N, organic C, and organic H) increased in plow layer soils. Soil ORP and organic S contents showed no significant ($p > 0.05$) differences between these two soil layers.

Similarly, the contents of each Cd species were also significantly higher ($p < 0.001$) in plow layer soils than in plow pan soils, but differences in each Cd speciation ratio in the two soil layers were observed (**Figure 1A**). The acid-soluble fraction (F-Aci) and reducible fraction (F-Red) of Cd with high bioavailability were the dominant fractions of Cd speciation in these two soil layers, but the F-Aci ratio in plow layer soils (61.1%) was significantly higher ($p < 0.05$) than in plow pan soils (38.6%). However, the ratios of the oxidizable fraction (F-Oxi, 11.2%) and residual fraction (F-Res, 23.5%) in plow pan soils were significantly ($p < 0.01$) increased compared to those in plow layer soils (2.9 and 3.7%, respectively). Pearson correlation analysis showed that the Cd accumulation contents of rice grain positively correlated with F-Aci ratio and F-Red ratio in plow layer soils ($p < 0.05$), whereas negatively correlated with F-Res ratio in plow pan soils ($p < 0.01$; **Table 2**), which indicated that activated Cd speciation ratios in soils enhanced the Cd accumulative effect in rice grain. Total Cd content had a significantly positive correlation with organic elements ($p < 0.01$) and total K ($p < 0.05$) in plow layer soils, and a positive correlation with soil moisture, organic N, and organic H ($p < 0.05$) in plow pan soils (**Figure 1B**). For the Cd speciation ratio in the plow layer, soil pH indicated a significantly ($p < 0.01$) positive correlation with the ratios of F-Red, F-Oxi, and F-Res, but a negative correlation with the F-Aci ratio ($p < 0.01$) in the plow pan. Moreover, soil moisture, total K, organic N, and organic H had a significantly positive correlation ($p < 0.01$) with the F-Red ratio of plow pan soils. These results showed that the differences in soil properties, especially soil pH and organic elements, distinctly impacted the Cd speciation distribution between the plow layer and plow pan soils. As a result, more activated Cd species (F-Aci and

[3]http://bioinfogp.cnb.csic.es/tools/venny/index.html

TABLE 1 | Physicochemical properties (means ± standard deviation, $n = 15$) analysis in the plow layer and plow pan soils.

Item	Plow layer	Plow pan	Item	Plow layer	Plow pan
Total Cd, mg/kg	**19.0 ± 11.1**	0.4 ± 0.2	Tsoil,°C	**12.7 ± 1.0**	11.9 ± 0.4
Total Cr, mg/kg	**124.5 ± 21.7**	111.8 ± 16.5	ORP, mV	315.9 ± 17.7	311.6 ± 17.9
Total Cu, mg/kg	**21.2 ± 2.5**	15.1 ± 3.3	Total P, mg/kg	**557.3 ± 119.5**	442.3 ± 89.8
Total Pb, mg/kg	**27.8 ± 12.2**	17.9 ± 8.9	Total K, g/kg	10.0 ± 0.5	**10.7 ± 0.5**
Total Zn, mg/kg	**182.6 ± 63.0**	54.1 ± 6.0	Organic N,%	**0.20 ± 0.04**	0.07 ± 0.02
Total Mn, mg/kg	304.1 ± 110.9	**697.5 ± 595.2**	Organic C,%	**2.2 ± 0.5**	0.6 ± 0.3
pH	6.3 ± 0.4	**7.4 ± 0.3**	Organic H,%	**0.81 ± 0.07**	0.67 ± 0.10
Moisture,%	**50.0 ± 6.9**	24.5 ± 4.8	Organic S,%	0.03 ± 0.01	0.02 ± 0.01

Quantitative values in bold font indicate the significantly higher means in the plow layer or plow pan soils (paired-sample t-test, p < 0.05).

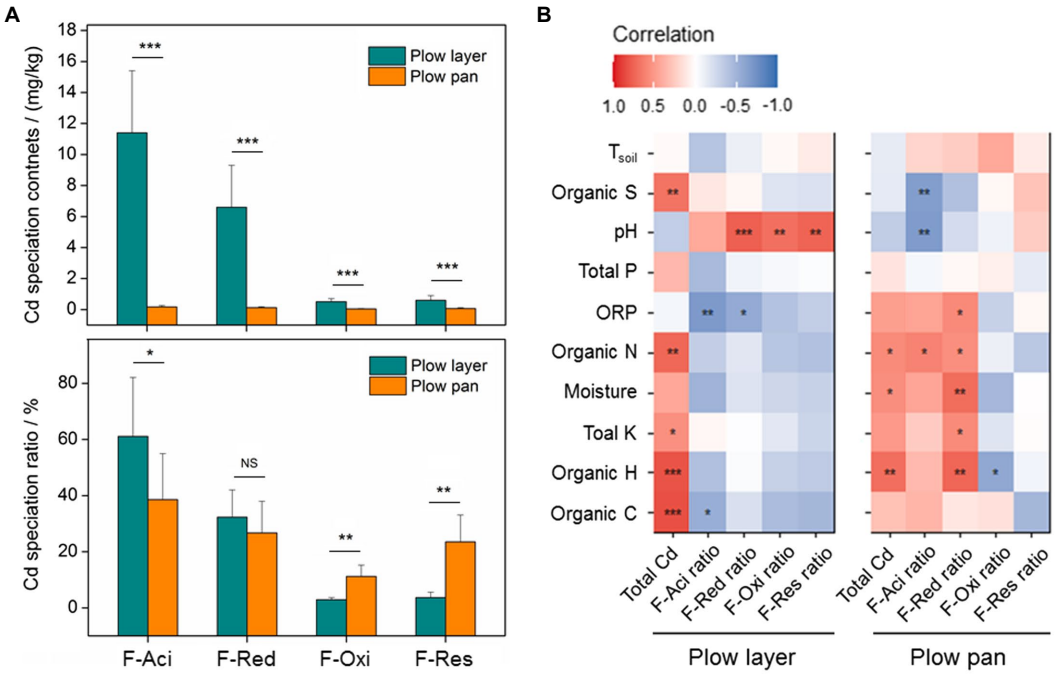

FIGURE 1 | Cd speciation distribution and relationships between the soil variables and Cd speciation ratios in the plow layer and plow pan soils. **(A)** Distributions of Cd speciation contents and ratios between the two soil layers. **(B)** Pearson correlation analysis. F-Aci, F-Red, F-Oxi, and F-Res indicate the acid-soluble fraction, reducible fraction, oxidizable fraction, and residual fraction of Cd, respectively. Asterisks indicate the significant difference or correlation (*$p<0.05$, **$p<0.01$, and ***$p<0.001$).

TABLE 2 | Pearson correlation between Cd accumulation contents in rice grain and Cd speciation ratios in the plow layer and plow pan soils.

Item	Plow layer		Plow pan	
	Coefficient	*P*	Coefficient	*P*
Total Cd, mg/kg	0.225	0.420	0.381	0.161
F-Aci ratio,%	0.573	0.026*	0.136	0.630
F-Red ratio,%	0.569	0.027*	0.171	0.543
F-Oxi ratio,%	0.481	0.070	0.075	0.791
F-Res ratio,%	−0.465	0.081	−0.716	0.003**

*Asterisks indicate the significant correlation *p<0.05; **p<0.01.*

F-Red fractions) were present in plow layer soils, while more stabilized Cd species (F-Oxi and F-Res fractions) were present in plow pan soils.

Phylogenetic Composition and Soil Bacterial Communities

Microbial community differences in plow layer and plow pan soils were detected by 16S rRNA amplicon sequencing. The soil 16S rRNA sequences were assigned to 35 bacterial phyla. The top three dominant phyla, accounting for more than 53% of the relative abundance, were *Proteobacteria* (plow layer 36.0% and plow pan 11.6%), *Chloroflexi* (15.5 and 30.8%, respectively), and *Acidobacteria* (13.1 and 10.6%, respectively), which were significantly different (paired-sample *t*-test, $p<0.05$) between these two soil layers (**Figure 2A**). The relative abundances of *Verrucomicrobia*, *Thaumarchaeota*, *Crenarchaeota*, and *Planctomycetes* in plow layer soils were significantly ($p<0.05$) higher than in plow pan soils, but *Actinobacteria*, *Euryarchaeota*, and *Firmicutes* were significantly ($p<0.05$) lower. Furthermore, the DNA concentration in plow layer soils (50.0 μg/g soil) was much ($p<0.001$) higher than that in plow pan soils (1.2 μg/g soil; **Figure 2B**). Meanwhile, there were more unique OTUs in plow layer soils (1,055, 45.1%) than in plow pan soils (444, 19.0%; **Figure 2C**), indicating the higher microbial mass in plow layer soils.

Shannon index was used to distinguish the variations of α-diversity in plow layer and plow pan soil samples (**Figure 3A**). Shannon indexes from plow layer soils were significantly (paired-sample *t*-test, $p<0.001$) increased compared to those of plow pan soils. Pearson correlation analysis indicated that there were no significant correlations between the Shannon index and Cd speciation ratio in plow layer and plow pan soils (**Supplementary Table 1**). The β-diversity measurements also showed significant divergence between these two soil layers. DCA revealed that the microbial community structure of plow layer soils tended to be more similar, but observably distinct from that of plow pan soils (**Figure 3B**). Dissimilarity tests using MRPP ($p<0.001$), ANOSIM ($p=0.001$), and Adonis ($p=0.001$) further confirmed this differentiation of soil bacterial communities between plow layer and plow pan soils.

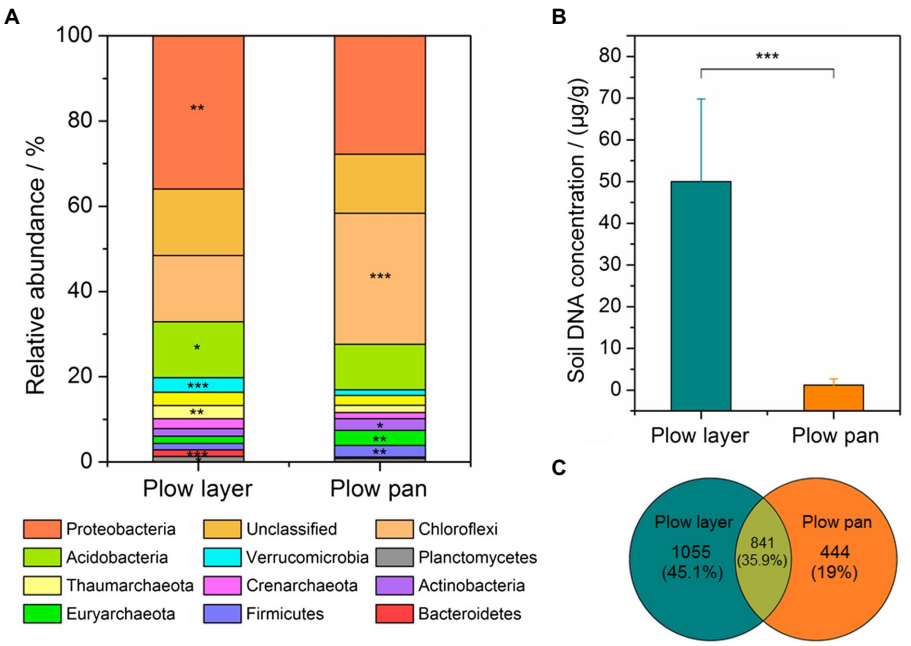

FIGURE 2 | Comparison of the bacterial community composition and microbial mass in the plow layer and plow pan soils. **(A)** Dominant microbes at the phylum level. **(B)** Variations in the soil DNA concentrations. **(C)** Variations in the OTU numbers. Asterisks indicate the significant difference (paired-sample *t*-test, $^{*}p<0.05$, $^{**}p<0.01$, and $^{***}p<0.001$).

Phylogenetic molecular ecology networks (pMENs) were constructed to explore the microbial interactions in plow layer and plow pan soils. The microbial pMEN in plow layer soils (38 modules, 310 nodes, and 551 links) was larger and more complex than that in plow pan soils (16 modules, 160 nodes, and 317 links), indicating that the microbiome in the plow layer had more species interactions (**Figure 3C**). The plow layer group had an average path distance of 8.305, which was higher than that of the plow pan group (4.089), demonstrating closer microbial connectivity in plow layer soils (**Supplementary Table 2**). The molecular functions of each soil sample were predicted using PICRUSt as a predictive exploratory tool. The functional classification and most basic metabolic pathways of level II orthology groups (KOs in KEGG) between plow layer and plow pan soil samples were consistent (**Supplementary Figure 2**). However, several different pathways between these two soil layers were still observed (**Figure 3D**). The cell metabolic functions from plow layer soil samples consistently showed higher relative abundances than those of plow layer soils (paired-sample *t*-test, $p<0.01$), including the protein families: metabolism, amino acid metabolism, carbohydrate metabolism, and energy metabolism. In addition, some xenobiotics biodegradation and metabolism pathways also showed higher abundances in plow layer soils ($p<0.01$).

Relationship Between Soil Microbes and Cd Speciation Distribution

There were great differences in microbial communities between plow layer and plow pan soils (**Figures 2, 3**), and these differences obviously affected the Cd speciation distribution in the two soil layers (**Figure 4**). Redundancy analysis (RDA) showed that the microbial community of plow layer soils had a positive relationship with the F-Aci ratio, F-Red ratio, soil moisture, and organic elements (**Figure 4A**). However, the plow pan soil bacterial community was positively associated with the F-Oxi ratio, F-Res ratio, soil pH, and total Mn. Variation partitioning analysis (VPA) was performed to determine the relative contribution of environmental variables on the bacterial community (**Figure 4B**). The soil Partial least square path modelroperties and Cd speciation ratio could explain 33 and 3% of variation in the soil bacterial communities, respectively. Their interaction explained 20% of variation, leaving 44% of the variation unexplained. These results showed that the soil microbiome might facilitate the Cd speciation transformation process to F-Aci and F-Red fractions in plow layer soils, and to F-Oxi and F-Res fractions in plow pan soils. Moreover, the relative abundance of some heavy metal metabolism-related molecular functions, such as ABC transporters, sulfur metabolism, and cysteine metabolism, was higher ($p<0.05$) in plow layer soils (**Figure 3D**), also indicating the roles of soil microbes in maintaining more activated Cd speciation in plow layer soils compared to plow pan soils.

Pearson correlation analysis revealed the OTU numbers associated with the variations of each Cd speciation ratio between the two soil layers (**Figure 4C**). There were more unique OTUs correlated with the F-Aci ratio and F-Red ratio in plow layer soils (87 and 84, respectively) than plow pan soils (68 and 68, respectively). In contrast, the number of unique OTUs correlated with the F-Oxi ratio and F-Res ratio

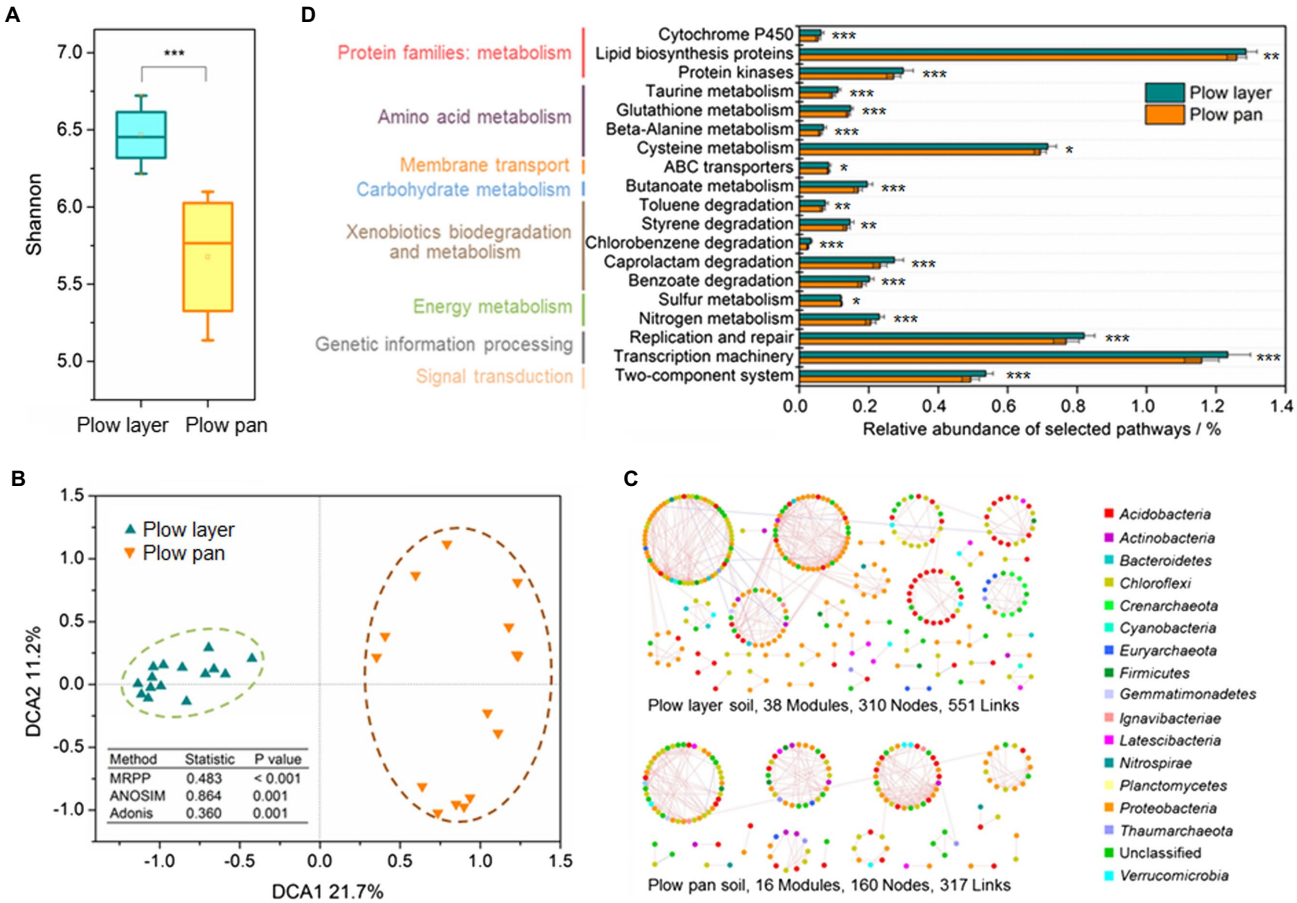

FIGURE 3 | Diversity and structure of bacterial communities in the plow layer and plow pan soils. **(A)** Shannon index. **(B)** DCA analysis. **(C)** Molecular ecological networks. **(D)** Functional predictions. Asterisks indicate the significant difference (paired-sample *t*-test, $^{*}p < 0.05$, $^{**}p < 0.01$, and $^{***}p < 0.001$).

in plow pan soils (92 and 102, respectively) was higher than that in plow layer soils (74 and 69, respectively). Most of the OTUs associated with the F-Aci ratio and F-Red ratio belonged to the dominant phylum-level microbes of *Proteobacteria* and *Acidobacteria* in plow layer soils. However, the major OTUs associated with the F-Oxi ratio and F-Res ratio were the dominant phyla of *Chloroflexi* and *Actinobacteria* in plow pan soils. The sub-networks of plow layer and plow pan soil bacterial communities using each Cd speciation ratio as microbial factors were constructed to detect the interactions between the Cd speciation ratio and related OTUs (**Figure 4D**). A more closely connected sub-network was observed in the plow layer compared with the plow pan. There were 27 OTU nodes linking to four Cd speciation ratios (40 links) in plow layer soils, but only seven OTU nodes linked to F-Aci and F-Oxi ratios (seven links) in plow pan soils. Meanwhile, there were 31 links (77.5%) between the OTU nodes and F-Aci and F-Red ratios in plow layer, while four links (57.1%) associated with the F-Oxi ratio were found in the plow layer. These results indicated that the related OTUs exhibited more cooperation to mediate the activated Cd speciation transformation (F-Aci and F-Red ratios) in plow layer soils, and the soil bacteria of plow pan soils were more inclined to participate in the formation of stabilized Cd speciation (F-Oxi and F-Res ratios).

Linkages Between Soil Factors, Microbial Community Structure, and Cd Speciation Distribution

Partial least square path models (PLSPM) were constructed to investigate the pathways of the impact of soil environments on Cd speciation distribution between plow layer and plow pan soils (**Figure 5**). The goodness-of-fit of the modeling in the plow layer and plow pan soils was 0.6103 and 0.6085, respectively. In plow layer soils, soil pH and organic elements were identified as the most significant factors ($p < 0.05$) with directly positive and negative relationships to the F-Oxi and F-Res ratios, respectively (**Figure 5A**). In plow pan soils, soil pH and organic elements had positive associations with microbial abundance 1 of *Acidobacteria* and *Proteobacteria* and microbial abundance 2 of *Actinobacteria* and *Chloroflexi*, which were positively related to the F-Aci and F-Red ratios, and the F-Oxi and F-Res ratios, respectively (**Figure 5B**). The PLSPM results revealed that the low pH values and high organic element

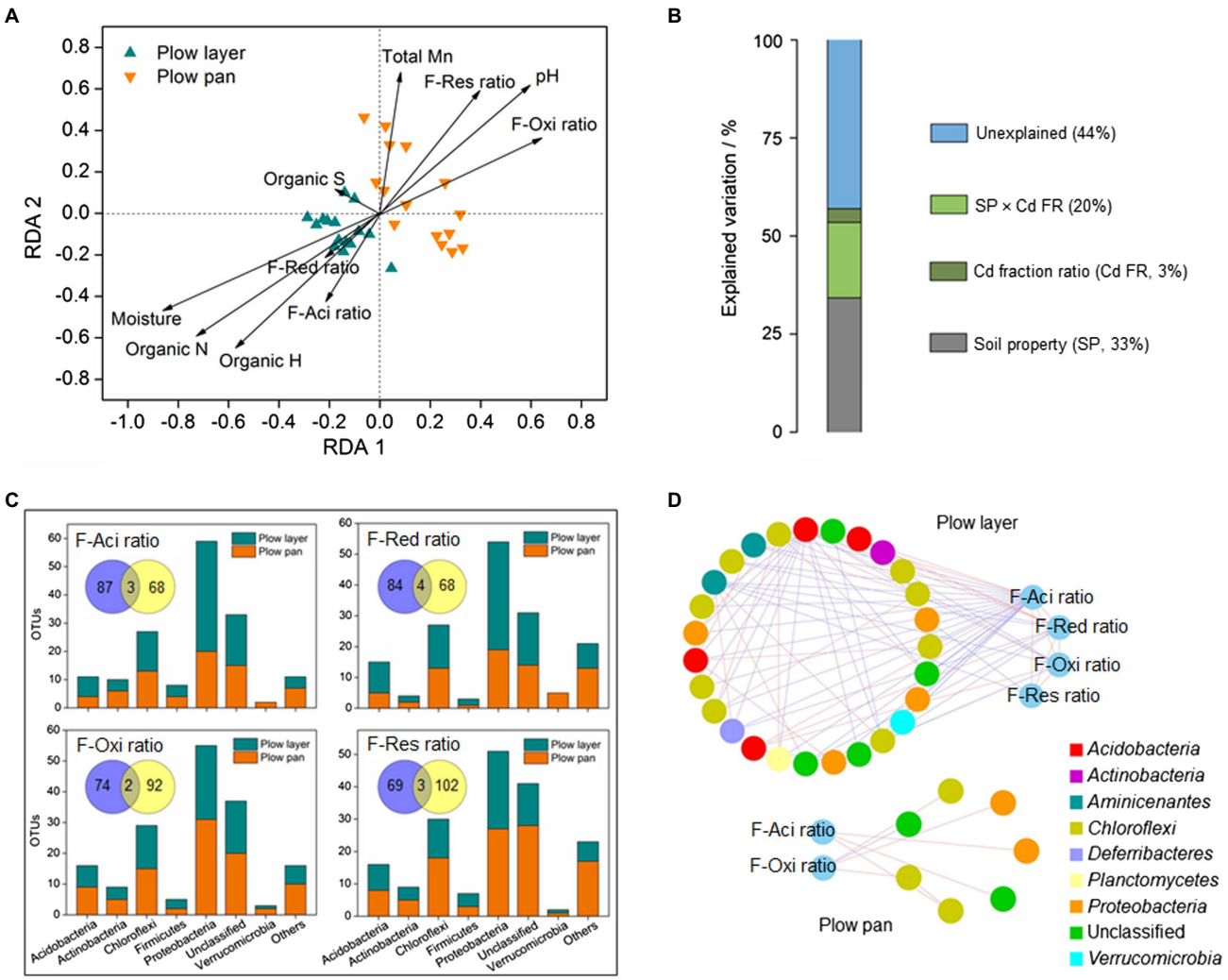

FIGURE 4 | Distinct relationships between the soil microbial community and Cd speciation ratios in the plow layer and plow pan soils. **(A)** Redundancy analysis. **(B)** Variation partitioning analysis. **(C)** Pearson correlation analysis. **(D)** Sub-network analysis. F-Aci, F-Red, F-Oxi, and F-Res indicate the acid-soluble fraction, reducible fraction, oxidizable fraction, and residual fraction of Cd, respectively. Venn diagrams represent the OTU numbers related with the Cd speciation ratio between the plow layer soils (blue) and plow pan soils (yellow).

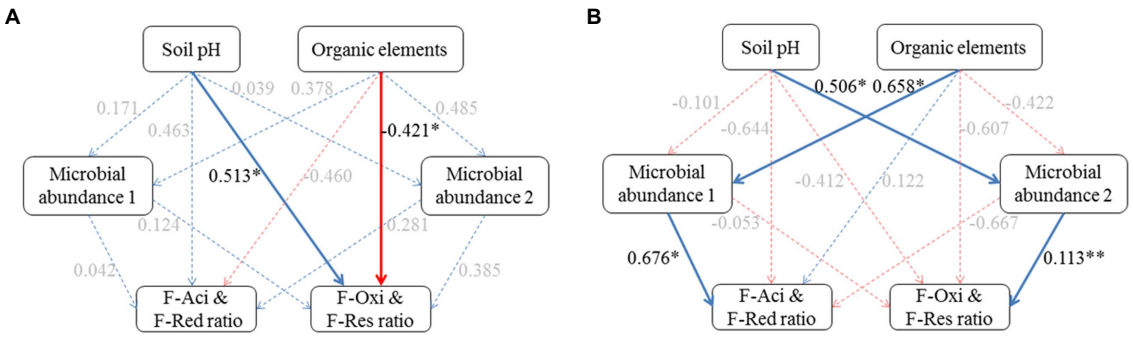

FIGURE 5 | Effects of soil factor and microbial community composition on Cd speciation ratios in the plow layer and plow pan soils. **(A)** Plow layer. **(B)** Plow pan. Blue lines and red lines indicate the positive and negative correlations, respectively, and dashed lines indicate the correlations are not at a significant level. Asterisks indicate the significance level: *p < 0.05, **p < 0.01, and ***p < 0.001.

contents in plow layer soils limited the formation of the F-Oxi and F-Res fractions and thus maintained higher F-Aci and F-Red ratios. In comparison with plow layer soils, the effects of high soil pH and low organic elements in plow pan soils significantly ($p < 0.05$) regulated the relative abundance of dominant phylum-level microbes to mediate the Cd speciation shifts and thereby decrease the F-Aci and F-Red ratios and increase the F-Oxi and F-Res ratios in plow pan soils.

DISCUSSION

In this study, we comparatively investigated the Cd speciation distribution between plow layer and plow pan soils in Cd-contaminated paddy fields and their responses to environmental variables and microbial communities. The results demonstrated that the soil environment of the plow layer maintained higher ratios of activated Cd speciation, while the plow pan soils mediated more stabilized Cd speciation formation. The Cd speciation distribution mechanisms regulated by soil physicochemical properties and soil microbes in two soil layers were different.

Distinct differentiations of total Cd, Cd speciation, and other soil physicochemical properties were observed in plow layer and plow pan soils (**Table 1, Figure 1A**). The changes in soil factors caused by farming practices altered the Cd distributions. Polluted river irrigation, straw turnover, and Cd-bearing fertilizer application resulted in the increased contents of total Cd, total P, and organic elements in plow layer soil. Water-retaining properties and Cd bound to plant residues and oxide minerals restricted the downward migration of Cd to plow pan soils (Matos et al., 2001; Dong et al., 2016), which was in accordance with the findings of significantly higher total Cd contents in plow layer soils and their positive correlation with organic elements ($p < 0.01$; **Table 1B**). Pearson correlation analysis indicated that soil factors, especially soil pH and organic elements, significantly affected the Cd speciation distribution between the two soil layers (**Figure 1B**; Wang et al., 2020). The excessive utilization of chemical fertilizers and rice straw decomposition decreased the soil pH value. A previous study showed that soil pH reduction significantly increased Cd bioavailability while reducing the pH from 7 to 6 (Zhang et al., 2019). In this study, the pH value in plow layer soils (6.3) was significantly decreased ($p < 0.05$) than in plow pan soils (7.4). Under low pH conditions, the produced positive charges could competitively adsorb soil organic substances and metallic oxides with Cd^{2+}. Meanwhile, low pH favored the Cd release associated with soil organic matters, which increased the Cd activity although there were higher organic element contents in plow layer soils (Jia et al., 2021). In addition, soil pH and organic matter were also important soil variables regulating the microbial growth and Cd complexation behaviors in different soil layers, and thereby influenced the microbial roles in the Cd speciation change (Jacob et al., 2018).

After that, 16S rRNA amplicon sequencing was performed to evaluate the alterations of soil microbial communities between plow layer and plow pan soils. The main composition of bacterial taxa was highly conserved, but differentiation in the relative abundance of dominated microbes was recorded between the two soil samples (**Figure 2A**). The bacterial phyla of *Proteobacteria* and *Acidobacteria*, and *Chloroflexi* and *Actinobacteria* were dominant in plow layer and plow pan soils, respectively. Compared with plow pan soil environments, the sufficient nutrients, energy sources, and oxygen-rich conditions in plow layer soils supported the increased microbial mass, Shannon index, and a variety of cellular metabolic functions, dramatically altering the microbial communities of the two soil layers (**Figures 2, 3**). The results of DCA showed that the phylogenetic β-diversities of the two microbial communities were distinctly different, although a large amount of inter-individual variation was found in plow pan soils compared with plow layer soil samples. Agricultural practices, such as fertilization, could serve to homogenize the soil microsites. This might explain why we observed more similar microbial community structures in plow layer soil samples (Liang et al., 2020). Additionally, distinctive network topologies were also observed at two soil sites (**Figure 3C**; **Supplementary Table 2**). The higher modularity and avgK value in the plow layer soil network both indicated that the topsoil bacterial community was more resistant and less influenced by disturbances, such as high heavy metals and toxic pollutants, than plow layer soils based on network theory (Saavedra et al., 2011), which was consistent with the findings that xenobiotic bioremediation-related pathways showed higher abundance in plow layer soils.

The shifts in the soil microbial community mediated the Cd speciation ratio distribution in the two soil layers. VPA showed that the changes between bacterial community and Cd speciation ratio were interrelated (**Figure 4B**). Redundancy analysis demonstrated that the microbial communities of plow layer and plow pan soils were positively associated with the transformations of available Cd speciation (F-Aci and F-Red ratios) and steady Cd speciation (F-Oxi and F-Res ratios), respectively, suggesting that the microbial communities in these two soil samples induced disparate Cd speciation changes (**Figure 4A**). The molecular function prediction analysis further verified the roles of the plow layer soil microbiome in promoting the formation of activated Cd speciation (**Figure 3D**). The plow layer soil bacteria with higher percentages of cysteine metabolism and the ABC transporter system could form Cd-metallothionein complexes and combined ATP-hydrolysis to reduce the microbial immobilization of Cd (Duong et al., 1996; Valls et al., 2000). In addition, the topsoil microbes possessing rich organic matter and the ability to metabolize sulfur could oxidize the Cd fractions bonding to humus and sulfide substrate into soluble Cd fractions, and thereby increase Cd activity in plow layer soils (Cao et al., 2018). Pearson correlation analysis demonstrated that many more unique OTUs mediated the Cd speciation transformation of the F-Aci and F-Red fractions, and these OTUs were mainly the members of *Proteobacteria* and *Acidobacteria* in plow layer soils. In plow pan soils, most of the OTUs participated in the formation of F-Oxi and F-Res fractions, which were the dominant phyla of *Chloroflexi* and *Actinobacteria*. The phylum *Acidobacteria*, with high relative abundance in plow layer soils, was sensitive to changes in pH and preferred relatively acidic soil conditions, which coincided with the low plow layer soil pH values (Mendes et al., 2015). Several members of *Acidobacteria* are able

to degrade complex biopolymers (Conradie and Jacobs, 2021), probably facilitating the transformation of mobile Cd speciation. *Proteobacteria* are regarded as the most stress-tolerant microbes in heavily contaminated soils (Wang et al., 2019). The members belonging to *Proteobacteria* exhibited multiple nutrient classifications and microbial functional diversities. It was reported that multiple heavy metal oxidase genes encoded by *Proteobacteria* were involved in the resistance and transform of heavy metals. The decreasing tendency of *Chloroflexi* along the soil depth was consistent with a previous study (Sagova-Mareckova et al., 2016), which showed the facultative anaerobic members of *Chloroflexi* were widely detected in relatively oxygen poor conditions (Hartmann et al., 2010). They were associated with the degradation of organic compound pollutants, producing more functional group-rich metabolites, and transformed the exchangeable Cd fraction into more stable organic-bound forms. The phylum *Actinobacteria* favored low moisture and alkalescent soil environments, resulting in a higher abundance in plow pan soils. Soil Actinomycetes could generate abundant secondary metabolites and reduce Cd bioavailability through complexation, adsorption, and reduction (Sun et al., 2021).

Although both soil variables and soil microbial communities had apparent effects on Cd fraction changes, different mechanisms regulating Cd speciation change between the two soil layers were observed (**Figure 5**). The results of PLSPM revealed that in plow layer soils the effect of soil variables was higher than that of soil microbial communities, which suggested that soil pH and organic elements were more important than dominant phyla in mediating the Cd speciation transformation in the rice growth layer (Zeng et al., 2011). Anthropogenic management practices seriously altered the soil environments and further affected the Cd speciation variations. In plow layer soils, the decrease of soil pH and organic matter decomposition directly impeded the formation of the F-Oxi and F-Res fractions, and therefore the F-Aci and F-Red fractions accumulated gradually. However, soil pH and organic elements in plow pan soils indirectly influenced Cd speciation ratios through their adversely direct impact on the abundance of predominant bacterial taxa. The plow pan soil environment facilitated the formation of stabilized Cd fractions, which was consistent with the observations that soils with insufficient oxygen content and low ORP values could increase the immobilization of Cd (Khaokaew et al., 2011; Lin et al., 2020).

CONCLUSION

This study investigated the Cd speciation distribution mechanisms regulated by soil properties and microbial communities between the plow layer and plow pan soils of Cd-contaminated paddy fields. The activated Cd speciation ratios were higher in plow layer soils and enhanced the Cd accumulative effect in rice grain, but stabilized Cd speciation ratios were elevated in plow pan soils. Soil physicochemical properties, dominant bacterial taxa, microbial diversities, and metabolic functions showed significantly different between the two soil samples. Differences in the soil environments of the plow layer and plow pan mediated diverse Cd speciation distribution. In plow layer soils, soil pH and organic elements decreased the formation of stabilized Cd speciation directly and resulted in the accumulation of activated Cd speciation, while the soil pH and organic elements indirectly hindered the transformation of activated Cd speciation in plow pan soils, and increased the stabilized Cd speciation *via* regulating the predominant bacteria. This study provides new insight into the effect of soil environments on Cd speciation transformation and will be helpful in bioremediating the Cd pollution of paddy field systems.

DATA AVAILABILITY STATEMENT

The datasets presented in this study can be found in online repositories. The names of the repository/repositories and accession number(s) can be found at: https://www.ncbi.nlm.nih.gov/, SRP291811.

AUTHOR CONTRIBUTIONS

XH, LB, and XL designed the study. PZ and HL conducted the experiment. YX and JG assisted with analysis tools of data. QL and HJ discussed the results and manuscript. XH and LH wrote the manuscript. All authors approved the final manuscript.

FUNDING

This work was supported by the Shandong Provincial Natural Science Foundation (ZR2020QD120), the Project of Introducing and Cultivating Young Talent in the Universities of Shandong Province (Soil Erosion Process and Ecological Regulation; QC2019YY144), and the National Natural Science Foundation of China (41907032).

SUPPLEMENTARY MATERIAL

The Supplementary Material for this article can be found online at: https://www.frontiersin.org/articles/10.3389/fmicb.2021.774301/full#supplementary-material

REFERENCES

Aitio, A., and Tritscher, A. (2004). Effects on health of cadmium-WHO approaches and conclusions. *Biometals* 17:491. doi: 10.1023/B:BIOM.0000045832.13400.02

Anderson, C., Beare, M., Buckley, H. L., and Lear, G. (2017). Bacterial and fungal communities respond differently to varying tillage depth in agricultural soils. *Peer J.* 5:e3930. doi: 10.7717/peerj.3930

Cao, Z. Z., Qin, M. L., Lin, X. Y., Zhu, Z. W., and Chen, M. X. (2018). Sulfur supply reduces cadmium uptake and translocation in rice grains (*Oryza sativa* L.) by enhancing iron plaque formation, cadmium chelation and vacuolar sequestration. *Environ. Pollut.* 238, 76–84. doi: 10.1016/j.envpol.2018.02.083

Chen, X. W., Wu, L., Luo, N., Mo, C. H., Wong, M. H., and Li, H. (2019). Arbuscular mycorrhizal fungi and the associated bacterial community influence

the uptake of cadmium in rice. *Geoderma* 337, 749–757. doi: 10.1016/j.geoderma.2018.10.029

Conradie, T. A., and Jacobs, K. (2021). Distribution patterns of Acidobacteriota in different fynbos soils. *PLoS One* 16:e0248913. doi: 10.1371/journal.pone.0248913

Deng, Y., Jiang, L. H., Xu, L. F., Hao, X. D., Zhang, S. Y., Xu, M. L., et al. (2019). Spatial distribution and risk assessment of heavy metals in contaminated paddy fields–A case study in Xiangtan City, southern China. *Ecotox. Environ. Safe.* 171, 281–289. doi: 10.1016/j.ecoenv.2018.12.060

Deng, Y., Jiang, Y. H., Yang, Y. F., He, Z. L., Luo, F., and Zhou, J. Z. (2012). Molecular ecological network analyses. *BMC Bioinf.* 13, 13–32. doi: 10.1186/1471-2105-13-113

Dong, M. F., Feng, R. W., Wang, R. G., Sun, Y., Ding, Y. Z., Xu, Y. M., et al. (2016). Inoculation of Fe/Mn-oxidizing bacteria enhances Fe/Mn plaque formation and reduces cd and As accumulation in rice plant tissues. *Plant Soil* 404, 75–83. doi: 10.1007/s11104-016-2829-x

Duong, F., Lazdunski, A., and Murgier, M. (1996). Protein secretion by heterologous bacterial ABC-transporters: the C-terminus secretion signal of the secreted protein confers high recognition specificity. *Mol. Microbiol.* 21, 459–470. doi: 10.1111/j.1365-2958.1996.tb02555.x

Edgar, R. C. (2013). UPARSE: highly accurate OTU sequences from microbial amplicon reads. *Nat. Methods* 10, 996–998. doi: 10.1038/nmeth.2604

EPM (2018). Environmental Quality Standard for Soils (In Chinese). GB 15618–2018. Office of Technical Standards, Ministry of Environmental Protection.

Fonti, V., Dell'Anno, A., and Beolchini, F. (2016). Does bioleaching represent a biotechnological strategy for remediation of contaminated sediments? *Sci. Total Environ.* 563-564, 302–319. doi: 10.1016/j.scitotenv.2016.04.094

Gleyzes, C., Tellier, S., and Astruc, M. (2002). Fractionation studies of trace elements in contaminated soils and sediments: a review of sequential extraction procedures. *Trend Anal. Chem.* 21, 451–467. doi: 10.1016/S0165-9936(02)00603-9

Hao, X. D., Zhu, P., Zhang, H. Z., Liang, Y. L., Yin, H. Q., Liu, X. D., et al. (2019). Mixotrophic acidophiles increase cadmium soluble fraction and phytoextraction efficiency from cadmium contaminated soils. *Sci. Total Environ.* 655, 347–355. doi: 10.1016/j.scitotenv.2018.11.221

Hartmann, M., Lee, S., Hallam, S. J., and Mohn, W. W. (2010). Bacterial, archaeal and eukaryal community structures throughout soil horizons of harvested and naturally disturbed forest stands. *Environ. Microbiol.* 11, 3045–3062. doi: 10.1111/j.1462-2920.2009.02008.x

Hu, Y., He, K., Sun, Z., Chen, G., and Cheng, H. (2020). Quantitative source apportionment of heavy metal(loid)s in the agricultural soils of an industrializing region and associated model uncertainty. *J. Hazard. Mater.* 391:122244. doi: 10.1016/j.jhazmat.2020.122244

Huang, Y., Sheng, H., Zhou, P., and Zhang, Y. Z. (2019). Remediation of cd-contaminated acidic paddy fields with four-year consecutive liming. *Ecotoxicol. Environ. Saf.* 188:109903. doi: 10.1016/j.ecoenv.2019.109903

Jacob, J. M., Karthik, C., Saratale, R. G., Kumar, S. S., Prabakar, D., Kadirvelu, K., et al. (2018). Biological approaches to tackle heavy metal pollution: A survey of literature. *J. Environ. Manag.* 217, 56–70. doi: 10.1016/j.jenvman.2018.03.077

Jia, M. Y., Yu, J. P., Li, Z., Wu, L. H., and Christie, P. (2021). Effects of biochar on the migration and transformation of metal species in a highly acid soil contaminated with multiple metals and leached with solutions of different pH. *Chemosphere* 278:130344. doi: 10.1016/j.chemosphere.2021.130344

Jiang, D., Zhou, Y., Tan, M., Zhang, J., and Yan, S. (2020). Cd exposure-induced growth retardation involves in energy metabolism disorder of midgut tissues in the gypsy moth larvae. *Environ. Pollut.* 266:115173. doi: 10.1016/j.envpol.2020.115173

Khan, M. A., Khan, S., Khan, A., and Alam, M. (2017). Soil contamination with cadmium, consequences and remediation using organic amendments. *Sci. Total Environ.* 601, 1591–1605. doi: 10.1016/j.scitotenv.2017.06.030

Khaokaew, S., Chaney, R. L., Landrot, G., Ginder-Vogel, M., and Sparks, D. L. (2011). Speciation and release kinetics of cadmium in an alkaline paddy soil under various flooding periods and draining conditions. *Environ. Sci. Technol.* 45, 4249–4255. doi: 10.1021/es103971y

Kong, Y. (2011). Btrim: A fast, lightweight adapter and quality trimming program for next-generation sequencing technologies. *Genomics* 98, 152–153. doi: 10.1016/j.ygeno.2011.05.009

Langille, M. G. I., Zaneveld, J., Caporaso, J. G., McDonald, D., Knights, D., Reyes, J. A., et al. (2013). Predictive functional profiling of microbial communities using 16S rRNA marker gene sequences. *Nat. Biotechnol.* 31, 814–821. doi: 10.1038/nbt.2676

Li, H., Chen, X. W., Wu, L., Luo, N., Huang, W. X., Mo, C. H., et al. (2020a). Effects of arbuscular mycorrhizal fungi on redox homeostasis of rice under cd stress. *Plant Soil* 455, 121–138. doi: 10.1007/s11104-020-04678-y

Li, H., Huang, W. X., Gao, M. Y., Li, X., Xiang, L., Mo, C. H., et al. (2020b). AM fungi increase uptake of cd and BDE-209 and activities of dismutase and catalase in amaranth (Amaranthus hypochondriacus L.) in two contaminants spiked soil. *Ecotoxicol. Environ. Saf.* 195:110485. doi: 10.1016/j.ecoenv.2020.110485

Li, H. X., and Ji, H. B. (2017). Chemical speciation, vertical profile and human health risk assessment of heavy metals in soils from coal-mine brownfield, Beijing. *China. J. Geochem. Explor.* 183, 22–32. doi: 10.1016/j.gexplo.2017.09.012

Li, Z. M., Liang, Y., Hu, H. W., Shaheen, S. M., Zhong, H., Tack, F. M. G., et al. (2021). Speciation, transportation, and pathways of cadmium in soil-rice systems: A review on the environmental implications and remediation approaches for food safety. *Environ. Int.* 156:106749. doi: 10.1016/j.envint.2021.106749

Liang, Y. T., Ning, D. L., Lu, Z. M., Zhang, N., Hale, L., Wu, L. Y., et al. (2020). Century long fertilization reduces stochasticity controlling grassland microbial community succession. *Soil Biol. Biochem.* 151:108023. doi: 10.1016/j.soilbio.2020.108023

Lin, J. J., He, F. X., Owens, G., and Chen, Z. L. (2020). How do phytogenic iron oxide nanoparticles drive redox reactions to reduce cadmium availability in a flooded paddy soil? *J. Hazard. Mater.* 403:123736. doi: 10.1016/j.jhazmat.2020.123736

Magoč, T., and Salzberg, S. L. (2011). FLASH: fast length adjustment of short reads to improve genome assemblies. *Bioinformatics* 27, 2957–2963. doi: 10.1093/bioinformatics/btr507

Matos, A. T. D., Fontes, M. P. F., Costa, L. M. D., and Martinez, M. A. (2001). Mobility of heavy metals as related to soil chemical and mineralogical characteristics of Brazilian soils. *Environ. Pollut.* 111, 429–435. doi: 10.1016/S0269-7491(00)00088-9

Mendes, L. W., de Lima Brossi, M. J., Kuramae, E. E., and Tsai, S. M. (2015). Land-use system shapes soil bacterial communities in southeastern Amazon region. *Appl. Soil Ecol.* 95, 151–160. doi: 10.1016/j.apsoil.2015.06.005

Müller, K., Kramer, S., Haslwimmer, H., Marhan, S., Scheunemann, N., Butenschön, O., et al. (2016). Carbon transfer from maize roots and litter into bacteria and fungi depends on soil depth and time. *Soil Biol. Biochem.* 93, 79–89. doi: 10.1016/j.soilbio.2015.10.015

Peng, W. H., Li, X. M., Xiao, S. T., and Fan, W. H. (2018). Review of remediation technologies for sediments contaminated by heavy metals. *J. Soils Sediments* 18, 1701–1719. doi: 10.1007/s11368-018-1921-7

Rafiq, M. T., Aziz, R., Yang, X. E., Xiao, W. D., Rafiq, M. K., Ali, B., et al. (2014). Cadmium phytoavailability to rice (*Oryza sativa* L.) grown in representative Chinese soils. A model to improve soil environmental quality guidelines for food safety. *Ecotoxicol. Environ. Saf.* 103, 101–107. doi: 10.1016/j.ecoenv.2013.10.016

Saavedra, S., Stouffer, D. B., Uzzi, B., and Bascompte, J. (2011). Strong contributors to network persistence are the most vulnerable to extinction. *Nature* 478, 233–235. doi: 10.1038/nature10433

Sagova-Mareckova, M., Zadorova, T., Penizek, V., Omelka, M., Tejnecky, V., Pruchova, P., et al. (2016). The structure of bacterial communities along two vertical profiles of a deep colluvial soil. *Soil Biol. Biochem.* 101, 65–73. doi: 10.1016/j.soilbio.2016.06.026

Sanaullah, M., Chabbi, A., Maron, P., Baumann, K., Tardy, V., Blagodatskaya, E., et al. (2016). How do microbial communities in top- and subsoil respond to root litter addition under field conditions? Soil biol. *Biochemist* 103, 28–38. doi: 10.1016/j.soilbio.2016.07.017

Santeramo, F. G., and Lamonaca, E. (2021). Objective risk and subjective risk: The role of information in food supply chains. *Food Res. Int.* 139:109962. doi: 10.1016/j.foodres.2020.109962

Shi, Z. Y., Carey, M., Meharg, C., Williams, P. N., Signes-Pastor, A. J., Triwardhani, E. A., et al. (2020). Rice grain cadmium concentrations in the global supply-chain. *Exp. Health* 12, 869–876. doi: 10.1007/s12403-020-00349-6

Sun, W. J., Cheng, K., Sun, K. Y., and Ma, X. M. (2021). Microbially mediated remediation of contaminated sediments by heavy metals: a critical review. *Curr. Pollut. Rep.* 7, 201–212. doi: 10.1007/s40726-021-00175-7

Valls, M., Atrian, S., De Lorenzo, V., and Fernández, L. A. (2000). Engineering a mouse metallothionein on the cell surface of Ralstonia eutropha CH34 for immobilization of heavy metals in soil. *Nat. Biotechnol.* 18, 661–665. doi: 10.1038/76516

Wang, M., Chen, S. B., Chen, L., and Wang, D. (2019). Responses of soil microbial communities and their network interactions to saline-alkaline stress in cd-contaminated soils. *Environ. Pollut.* 252, 1609–1621. doi: 10.1016/j.envpol.2019.06.082

Wang, Q., Garrity, G. M., Tiedje, J. M., and Cole, J. R. (2007). Naive Bayesian classifier for rapid assignment of rRNA sequences into the new bacterial taxonomy. *Appl. Environ. Microbiol.* 73, 5261–5267. doi: 10.1128/AEM.00062-07

Wang, P. C., Peng, H., Liu, J. L., Zhu, Z. L., Bi, X. Y., Yu, Q. Q., et al. (2020). Effects of exogenous dissolved organic matter on the adsorption-desorption behaviors and bioavailabilities of cd and hg in a plant-soil system. *Sci. Total Environ.* 728:138252. doi: 10.1016/j.scitotenv.2020.138252

Wu, H., Wen, Q., Hu, L., and Gong, M. (2018). Effect of adsorbate concentration to adsorbent dosage ratio on the sorption of heavy metals on soils. *J. Environ. Eng.* 144:4017094. doi: 10.1061/(ASCE)EE.1943-7870.0001306

Yu, H., Deng, Y., He, Z. L., Pendall, E., Carrillo, Y., Wang, S., et al. (2021). Stimulation of soil microbial functioning by elevated CO2 may surpass effects mediated by irrigation in a semiarid grassland. *Geoderma* 401:115162. doi: 10.1016/j.geoderma.2021.115162

Zeng, F. R., Ali, S., Zhang, H. T., Ouyang, Y. N., Qiu, B. Y., Wu, F. B., et al. (2011). The influence of pH and organic matter content in paddy soil on heavy metal availability and their uptake by rice plants. *Environ. Pollut.* 159, 84–91. doi: 10.1016/j.envpol.2010.09.019

Zhang, Q., Chen, H. F., Xu, C., Zhu, H. H., and Zhu, Q. H. (2019). Heavy metal uptake in rice is regulated by pH-dependent iron plaque formation and the expression of the metal transporter genes. *Environ. Exp. Bot.* 162, 392–398. doi: 10.1016/j.envexpbot.2019.03.004

Zhang, J. C., Mu, G. T., Zhang, Z. M., Huang, X. F., and Fang, H. (2021). Speciation variation and bio-activation of soil heavy metals (cd and Cr) in rice-rape rotation lands in karst regions. *Int. J. Environ. Res. Public Health* 18:1364. doi: 10.3390/ijerph18031364

Conflict of Interest: The authors declare that the research was conducted in the absence of any commercial or financial relationships that could be construed as a potential conflict of interest.

Publisher's Note: All claims expressed in this article are solely those of the authors and do not necessarily represent those of their affiliated organizations, or those of the publisher, the editors and the reviewers. Any product that may be evaluated in this article, or claim that may be made by its manufacturer, is not guaranteed or endorsed by the publisher.

frontiers in Microbiology

ORIGINAL RESEARCH
published: 07 December 2021
doi: 10.3389/fmicb.2021.764974

Characteristics of Microbial Community and Function With the Succession of Mangroves

Zhimao Mai[1,2†], Mai Ye[1,3†], Youshao Wang[1,2], Swee Yeok Foong[4], Lin Wang[1,2], Fulin Sun[1,2,5] and Hao Cheng[1,2*]*

[1] State Key Laboratory of Tropical Oceanography, Key Laboratory of Tropical Marine Bio-Resources and Ecology, South China Sea Institute of Oceanology, Chinese Academy of Sciences, Guangzhou, China, [2] Southern Marine Science and Engineering Guangdong Laboratory (Guangzhou), Guangzhou, China, [3] Guangdong Provincial Academy of Environmental Science, Guangzhou, China, [4] School of Biological Sciences, Universiti Sains Malaysia, Penang, Malaysia, [5] Daya Bay Marine Biology Research Station, Chinese Academy of Sciences, Shenzhen, China

OPEN ACCESS

Edited by:
Diane Purchase,
Middlesex University London,
United Kingdom

Reviewed by:
Zhichao Zhou,
University of Wisconsin–Madison,
United States
Alejandra Prieto-Davó,
Universidad Nacional Autónoma
de México, Mexico

***Correspondence:**
Fulin Sun
flsun@scsio.ac.cn
Hao Cheng
chenghao@scsio.ac.cn

[†] These authors have contributed equally to this work

Specialty section:
This article was submitted to Terrestrial Microbiology, a section of the journal Frontiers in Microbiology

Received: 26 August 2021
Accepted: 05 November 2021
Published: 07 December 2021

Citation:
Mai Z, Ye M, Wang Y, Foong SY, Wang L, Sun F and Cheng H (2021) Characteristics of Microbial Community and Function With the Succession of Mangroves. Front. Microbiol. 12:764974. doi: 10.3389/fmicb.2021.764974

In this study, 16S high-throughput and metagenomic sequencing analyses were employed to explore the changes in microbial community and function with the succession of mangroves (*Sonneratia alba*, *Rhizophora apiculata*, and *Bruguiera parviflora*) along the Merbok river estuary in Malaysia. The sediments of the three mangroves harbored their own unique dominant microbial taxa, whereas *R. apiculata* exhibited the highest microbial diversity. In general, Gammaproteobacteria, Actinobacteria, Alphaproteobacteria, Deltaproteobacteria, and Anaerolineae were the dominant microbial classes, but their abundances varied significantly among the three mangroves. Principal coordinates and redundancy analyses revealed that the specificity of the microbial community was highly correlated with mangrove populations and environmental factors. The results further showed that *R. apiculata* exhibited the highest carbon-related metabolism, coinciding with the highest organic carbon and microbial diversity. In addition, specific microbial taxa, such as Desulfobacterales and Rhizobiales, contributed the highest functional activities related to carbon metabolism, prokaryote carbon fixation, and methane metabolism. The present results provide a comprehensive understanding of the adaptations and functions of microbes in relation to environmental transition and mangrove succession in intertidal regions. High microbial diversity and carbon metabolism in *R. apiculata* might in turn facilitate and maintain the formation of climax mangroves in the middle region of the Merbok river estuary.

Keywords: mangrove succession, microbial community and function, carbon metabolism, *Rhizophora apiculata*, Merbok river estuary

INTRODUCTION

Mangroves represent one of the most productive ecosystems in tropical and subtropical estuaries and shorelines. They possess biological resources and play important roles in carbon fixation, erosion mitigation, and water purification (Giri et al., 2011; Brander et al., 2012). They often occur in marine-terrestrial ecotones with obvious geographical and hydrological heterogeneities, leading to interesting sequential species zonation along continuous gradients. The adaptation and

succession of mangroves in intertidal regions are speculated to be closely related to microbes in the sediments. Unfortunately, the potential roles of microbes and their functions in mangrove ecosystems are still poorly understood, although changes in vegetation during mangrove succession and how mangrove plants adapt to intertidal environmental adversities have been well studied (Wang et al., 2019; Cheng et al., 2020).

In recent years, high-throughput sequencing has offered a comprehensive perspective of microbes (Andreote et al., 2012; Alzubaidy et al., 2016; Lin et al., 2019). Benthic microbial community is highly correlated with soil properties (the depth of soil layer, pH, salinity, and nutrient availability) (Abed et al., 2015; Zhou et al., 2017; Tong et al., 2019) and aboveground plants (Bardgett and van der Putten, 2014). Previous findings also showed that microbial diversity and function might vary significantly among different mangrove habitats because of environmental transition and mangrove succession (Bai et al., 2013). Mangrove coverage also regulates the structure and composition of microbial community by altering redox conditions and organic carbon levels in the sediments (Holguin et al., 2001).

Moreover, microbes in sediments also play important biogeochemical roles (e.g., C, N, and S cycles), which can facilitate mangrove survival in intertidal regions (Reis et al., 2017). Owing to the withering and retention of mangrove branches and leaves, mangrove sediments contain a large amount of organic carbon, and most carbon turnover in mangrove ecosystems is carried out by sediment microbes (Alongi, 1988). Benthic microbes may also promote the efficiency of biogeochemical cycles in the sediments, such as C, N, and S cycles (Lin et al., 2019). In addition, anaerobic metabolism can further facilitate the production and consumption of methane and nitrous oxide (Giani et al., 1996; Reis et al., 2017), which can contribute to the emission of greenhouse gases from mangrove wetlands (Rosentreter et al., 2018). However, the responses of microbes to environmental transition and mangrove succession have not been well demonstrated. It is essential to further identify microbial taxa and their metabolic potential in mangrove ecosystems.

Thus, the present study aimed to (i) identify the changes in microbial community and diversity among different mangrove habitats; (ii) explore microbial functions and metabolic potentials in mangrove ecosystems; and (iii) explore the potential correlations among environmental factors, mangrove populations, and benthic microbial communities and functions. The purpose of this study was to evaluate the hypothesis that microbial community and function would respond positively to environmental transitions and might contribute to mangrove survival and succession in intertidal regions. Therefore, surface sediments from three mangrove fields (*Sonneratia alba*, *Rhizophora apiculata*, and *Bruguiera parviflora*) were examined using 16S high-throughput and metagenomic sequencing analyses. The implications of this study should be useful for guiding future research on the roles of the microbial community and their functions in mangrove succession.

MATERIALS AND METHODS

Study Area and Sample Collection

Sediment samples were collected on November 25, 2019, in a mangrove reserve located in the Merbok river estuary, Malaysia (**Figure 1**). In the upper estuary (with lower salinity), the habitats were mainly occupied by *S. alba* and sporadically mixed with *Nypa fruticans*, whereas the lower estuary had groves of *B. parviflora* and sporadic *Avicennia* genera. In the middle region of the Merbok river estuary, the dominant species was *R. apiculata*. According to tidal transition and mangrove succession, surface sediments were collected from three mangrove populations (*S. alba*, *R. apiculata*, and *B. parviflora*), and five parallel samples were collected from each mangrove population. The samples were placed in liquid nitrogen and frozen for nucleic acid extraction. The chemical parameters of the sediments were determined and described as follows.

Determination of the Chemical Parameters of Mangrove Sediments

The sediment properties included salinity, pH, total organic carbon (TOC), total phosphorus (TP), and total nitrogen (TN). Salinity and pH were measured during sampling in the field. The samples were dried naturally and sieved (2 mm). TOC, TP, and TN in the sediments were then analyzed following standard measurements (Huang et al., 2017).

Illumina Sequencing of 16S rRNA Gene and Data Analysis

Sediment samples (1 g) were weighed, and total DNA was extracted using an E.Z.N.A.® Soil DNA Kit (Omega, Norcross, GA, United States). In this study, the V3 and V4 regions of the 16S rRNA gene were sequenced using 338F (5′-ACTCCTACGGGAGGCAGCAG-3′) and 806R (5′-GGACTACHVGGGTWTCTAAT-3′) primers. PCR was performed in a 25 μl reaction containing the following: 5 × *FastPfu* buffer (4 μl), 2.5 mM of dNTPs (2 μl), 5 U/μl of *FastPfu* polymerase (0.5 μl), 5.0 μM of primers (1.0 μl each), and template DNA (10 ng). PCR was performed using the following conditions: pre-denaturation at 95°C for 3 min; 30 cycles of denaturation at 95°C for 30 s, annealing at 55°C for 30 s, and extension at 72°C for 45 s; and a final extension at 72°C for 10 min. After amplification, the PCR products were purified and analyzed by paired-end sequencing (2 × 250) using the Illumina MiSeq platform (Illumina, San Diego, CA, United States) according to standard protocols. All sequences were deposited in the National Center for Biotechnology Information (NCBI) Sequence Read Archive (SRA) Database under accession number PRJNA756333.

For the paired-end reads obtained by MiSeq sequencing, samples were distinguished according to the barcode information and then spliced according to overlap sequences using FLASH (version 1.2.11). After quality control analysis, normalization of clean data was carried out for operational taxonomic unit (OTU) clustering analysis and species taxonomy analysis. CD-HIT tool was used to define tags with sequence similarities >97% as OTU

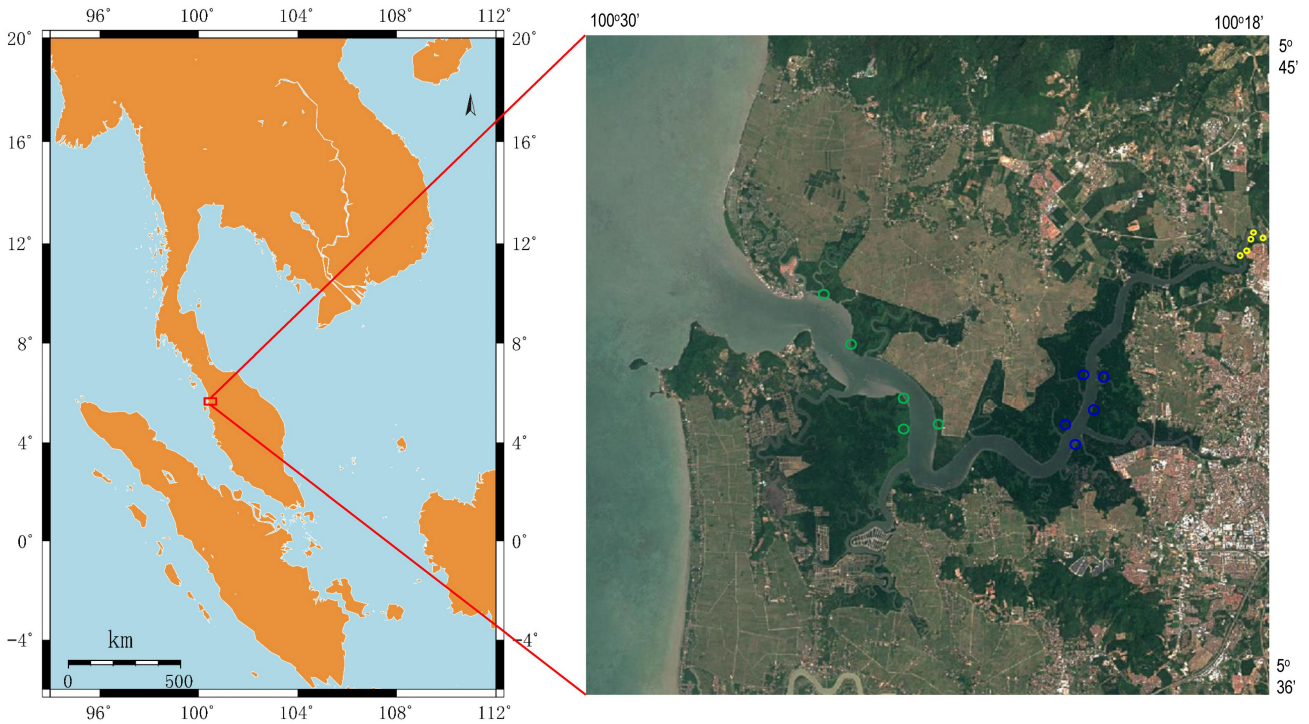

FIGURE 1 | Location of sampling sites in Merbok river estuary, Malaysia. Sediment samples were collected from *Sonneratia alba* (yellow circle), *Rhizophora apiculata* (blue circle) and *Bruguiera parviflora* (green circle).

clusters. QIIME software (version 1.9.1) was used to analyze the alpha diversities of the sequences, based on the Shannon index and ACE index. A representative sequence (showing the highest default abundance) in each OTU was selected for species classification using RDP classifier software (version 2.11) with the default threshold 0.8. Two-sided Welch's *t*-test was used to analyze the statistical significances of microbial community structure in different samples. Beta diversity was calculated using unweighted UniFrac, and principal coordinates analysis (PCoA) was performed with R software (version 3.3.1). Redundancy analysis (RDA) was performed using the R software (version 3.3.1) vegan package, and statistical significances of RDA were judged by performing the PERMUTEST analysis of variance.

Metagenomic Sequencing Analysis

Qualified DNA samples were diluted in fragmentation buffer and randomly disrupted using a Covaris M220 ultrasonicator (Covaris, Inc., Woburn, MA, United States). The DNA fragments obtained after disruption were used for library construction. The qualified library was sequenced using the Illumina HiSeq 2500 high-throughput sequencing platform with 2 × 150 paired-ends. This platform was also used for data configuration and image analysis with HiSeq Control software. Metagenomic data have been deposited in the NCBI SRA Database (PRJNA766709).

Raw sequence data were trimmed with FASTP[1], and low-quality reads, lengths of < 50 base pairs, N-rich reads, and adapter reads were removed. Sequences with different sequencing depths were assembled using Megahit software[2], and contigs were obtained using the succinct de Bruijn graph method. MetaGene (Noguchi et al., 2006) was used to predict open reading frames (ORFs) in contigs, and a statistical table of gene predictions was obtained for each sample. The predicted gene sequences of all samples were clustered by CD-HIT[3], and the longest gene from each cluster was selected as the representative sequence to construct a non-redundant gene set. With the use of SOAPaligner (Li et al., 2009), the high-quality reads of each sample were compared with the non-redundant gene set (95% identity) to determine the abundance information for genes in corresponding samples. BLASTP (version 2.2.28) was used to compare the non-redundant gene set with the NR database (*e*-value: $1e^{-5}$), and species-annotation results were obtained based on the corresponding taxonomy information of the NR database. The analysis of Kyoto Encyclopedia of Genes and Genomes (KEGG) was used for functional annotation according to the BLAST results. Community contributions to functions were determined using the NR database annotation.

RESULTS

Sediment Physicochemical Parameters

The differences in physicochemical properties among the three mangrove populations are shown in **Supplementary Figure 1**.

[1]https://github.com/OpenGene/fastp

[2]https://github.com/voutcn/megahit

[3]http://www.bioinformatics.org/cd-hit

Overall, the highest TOC and TN levels were detected in the sediments of *R. apiculata* among the three mangroves studied ($p < 0.05$). Higher TP and pH, but lower salinity, were observed in the sediments of *S. alba* than *R. apiculata* and *B. parviflora*.

16S rRNA Gene Illumina MiSeq Sequencing

Based on Illumina sequencing, 893,587 sequences were obtained from 15 samples. In total, 4,842 OTUs were observed at a 97% similarity level (**Supplementary Table 1**). In terms of microbial diversity, *R. apiculata* exhibited the highest OTUs number and bacterial richness index among the three mangrove populations ($p < 0.05$; **Figure 2B**). Higher Shannon index values were also represented for *R. apiculata*, although the differences were not significant. The Venn diagram shown in **Figure 2C** revealed a total of 3,532 OTUs in the sediments associated with *R. apiculata*, whereas 640 specific OTUs were observed. In addition, 1,645 common OTUs were observed among the three mangroves. As shown in **Figures 2D–F**, the types and relative abundances of dominant OTUs for *R. apiculata* and *B. parviflora* increased significantly compared with those for *S. alba*. Significant differences were also found in dominant OTUs between *R. apiculata* and *B. parviflora*.

Bacterial Community Composition in Mangrove Sediments

The abundances of bacterial taxa corresponding to the sediments are shown in **Figure 3**. Dominant bacteria (>5% at class level, **Figure 3A**) in mangrove sediments included Actinobacteria, Gammaproteobacteria, Deltaproteobacteria, Alphaproteobacteria, Anaerolineae, Bacilli, and Bacteroidia. However, the abundances of these dominant bacteria varied significantly among the three mangrove populations (**Figure 3B**). The abundances of Alphaproteobacteria, Deltaproteobacteria, and Bacilli were found to be higher for *R. apiculata* and *B. parviflora*, while the highest abundance of Gammaproteobacteria was observed in *S. alba* among the three mangroves.

The dominant bacterial taxa at the order level (**Figure 3C**) were Bacillales, Rhizobiales, Desulfobacterales, Pseudomonadales, Anaerolineales, and Bacteroidales. The highest abundances of Desulfobacterales were observed in the sediments associated with *R. apiculata*, followed by *B. parviflora* and *S. alba* (**Figure 3D**). Relative higher abundances of Bacillales and Rhizobiales were also detected in *R. apiculata* and *B. parviflora* than *S. alba*. In contrast, the highest abundance of Pseudomonadales was observed in *S. alba* among the three mangroves.

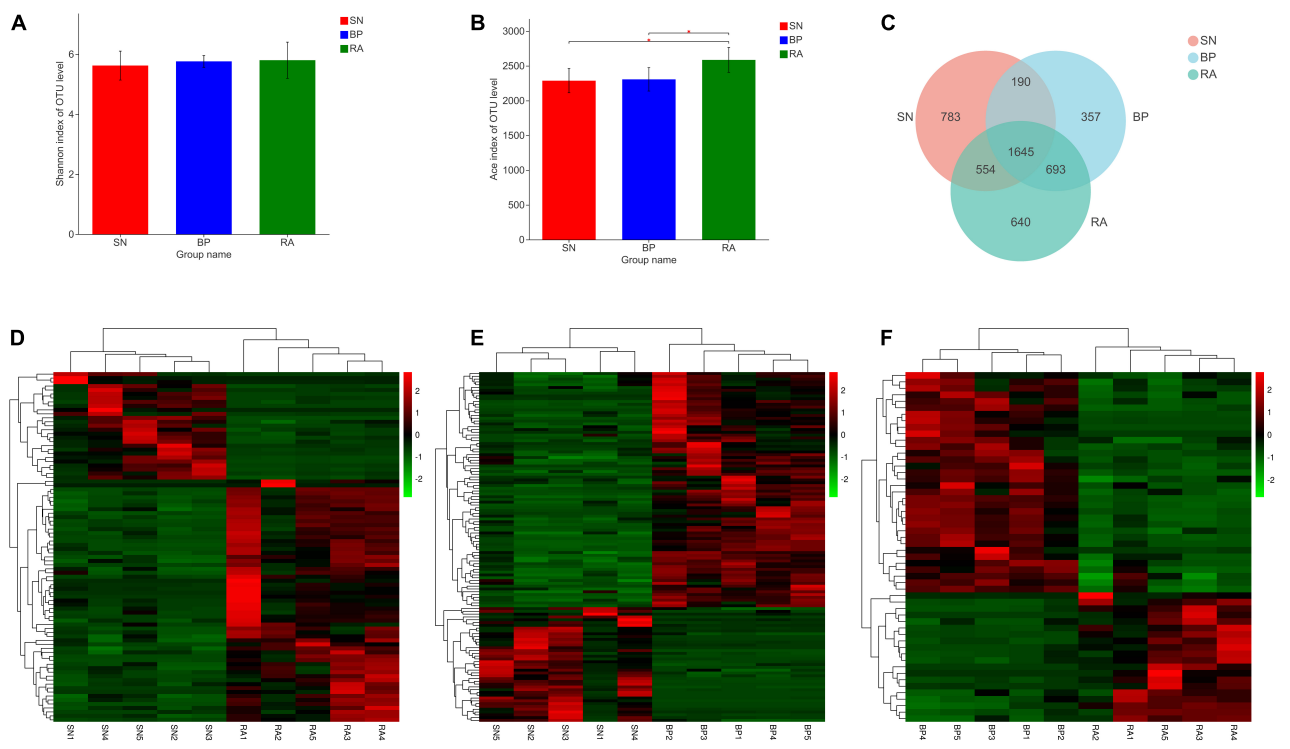

FIGURE 2 | Diversity and significant difference analysis of operational taxonomic units (OTUs). **(A)** Shannon index of OTU level. **(B)** ACE index of OTU level. **(C)** Venn diagram analysis of OTU numbers between samples. **(D)** Significant difference analysis of OTUs between RA and SN. **(E)** Significant difference analysis of OTUs between BP and SN. **(F)** Significant difference analysis of OTUs between RA and BP. SN, *Sonneratia alba*; RA, *Rhizophora apiculata*; BP, *Bruguiera parviflora*.

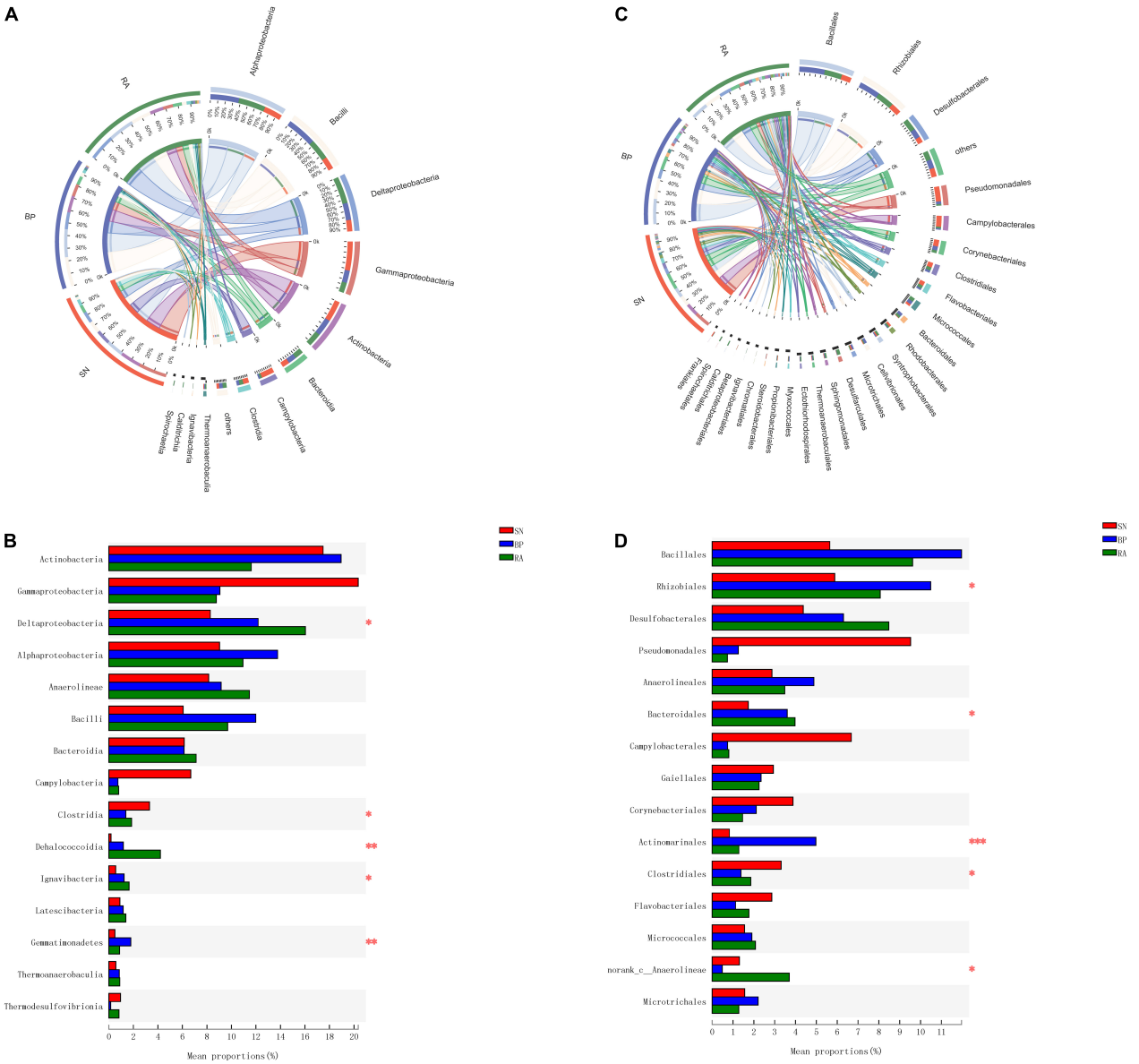

FIGURE 3 | The components of bacterial taxa at class level **(A)** and order level **(B)**. **(C)** Significant difference analysis of dominant taxa at class level. **(D)** Significant difference analysis of dominant taxa at order level. SN, *Sonneratia alba*; RA, *Rhizophora apiculata*; BP, *Bruguiera parviflora*.

Principal Coordinates Analysis and Redundancy Analysis of Microbial Community

The results from PCoA (**Figure 4A**) showed that microbial communities from the same mangrove population clustered together well. RDA was performed to explore the relationships between environmental parameters and microbial community (**Figure 4B**). The microbial communities with *R. apiculata* and *B. parviflora* were highly correlated with TOC, TN, and salinity, whereas bacteria with *S. alba* were highly affected by TP and pH. The results (**Figure 4C**) showed that the dominant microbial taxa were grouped into two clusters. Cluster I, including Chromatiales, Corynebacteriales, Rhodobacterales, and Anaerolineales, showed positive correlations with TP or pH ($p < 0.05$). Cluster II, including Desulfobacterales, Rhizobiales, and Micrococcales, exhibited positive trends for correlations with TOC, TN, and salinity. More detailed information of the dominant bacterial taxa at family level is shown in **Supplementary Figure 2**.

Metagenomic Analysis of Microbial Community Function in Different Mangrove Sediments

Metagenome analysis generated a massive amount of sequence information, ranging from 90,898,652 to 139,622,818 reads among samples. In total, 14,664,335 non-redundant genes were

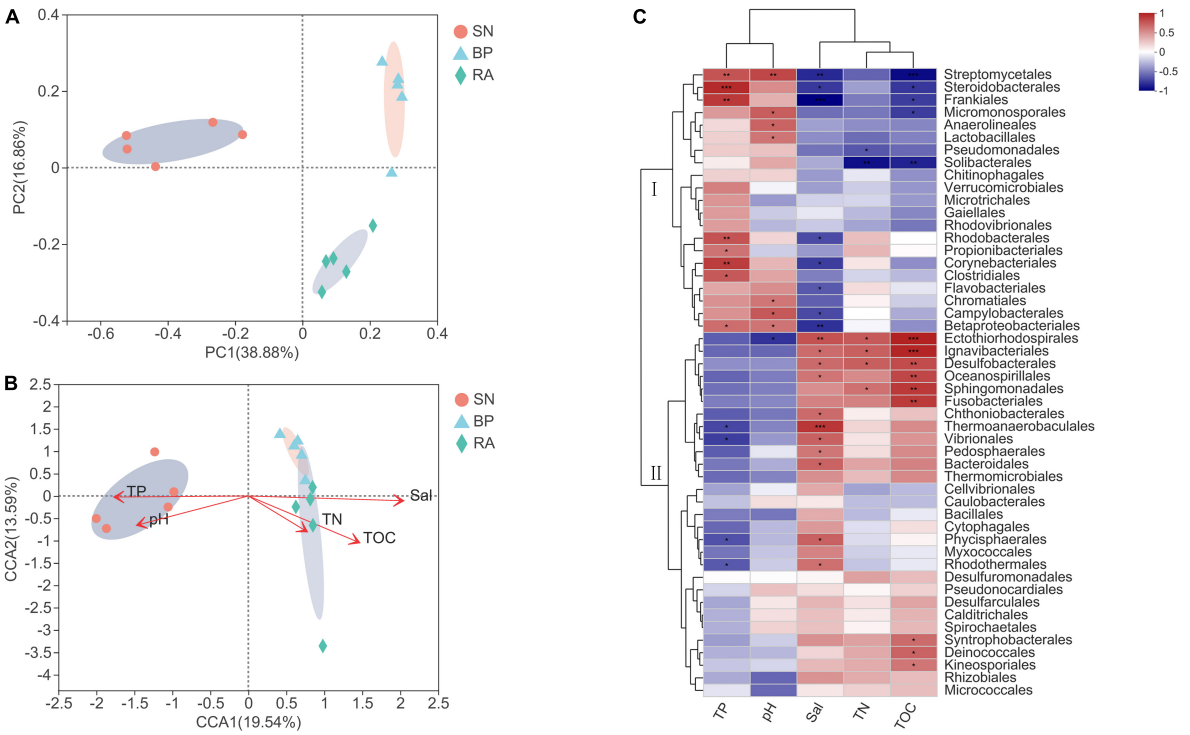

FIGURE 4 | (A) Principal coordinates analysis (PCoA) of bacterial community structure. **(B)** Canonical correlation analysis of environmental factors and bacterial community. **(C)** Correlation analysis of dominant bacterial taxa and environmental factors. SN, *Sonneratia alba*; RA, *Rhizophora apiculata*; BP, *Bruguiera parviflora*.

detected in the metagenomes, and 9,005 KEGG Orthogroups (KOs) were identified. The results from **Supplementary Figure 3** show a high correlation coefficient between the microbial community and functional diversity, with values of 0.84 and 0.87 for α diversity and β diversity, respectively. The data further illustrated the differences in key metabolic pathways (e.g., carbon-related metabolism) among the three mangroves. The sediments associated with *R. apiculata* exhibited the highest carbon metabolism, ABC transporters, prokaryote carbon fixation, and methane metabolism among the three mangroves (**Figure 5** and **Supplementary Figure 4**).

Contribution of Microbial Community to Kyoto Encyclopedia of Genes and Genomes Function

As shown in **Figure 6** and **Supplementary Figure 5**, Desulfobacterales (e.g., Desulfobacteraceae) and Rhizobiales (e.g., Xanthobacteraceae) were two major contributors to metabolic functions. The contribution of microbial taxa to the function varied significantly among the different mangrove species. Desulfobacterales consistently had the highest contributions to carbon-related metabolism (e.g., carbon metabolisms, prokaryote carbon fixation, methane metabolism, and ABC transporters) in the sediments associated with *R. apiculata*. When compared with *S. alba*, Rhizobiales also exhibited higher contributions to carbon-related metabolism in sediments of *R. apiculata* and *B. parviflora*. In addition to Desulfobacterales and Rhizobiales, the highest contributions of Micrococcales and Bacillales to metabolic functions were also observed in sediments associated with *R. apiculata*. In contrast, the lowest contributions of Corynebacteriales, Burkholderiales, and Planctomycetales to the aforementioned metabolic pathways were observed in the sediments associated with *R. apiculata*.

DISCUSSION

Microbial Diversity Was Highly Affected by Tidal Transitions and Mangrove Succession

Significant differences were found in the microbial community among the three mangrove populations along the Merbok river estuary, and specific microbial communities were formed in each mangrove population (**Figures 2**, **3**). Our previous data also indicated that microbial diversity was highly influenced by the structure of mangrove populations (Wu et al., 2016). Root exudates and secondary metabolites, which also could serve as carbon sources and antimicrobial substances, vary significantly among mangrove species (Gao et al., 2003; Koh et al., 2013). Changes in root exudates might not only affect benthic microbial density but also strongly affect the structure and function of microbes (Berendsen et al., 2012; Zhuang et al., 2020). Moreover, the present data showed that sediments associated with *R. apiculata* exhibited

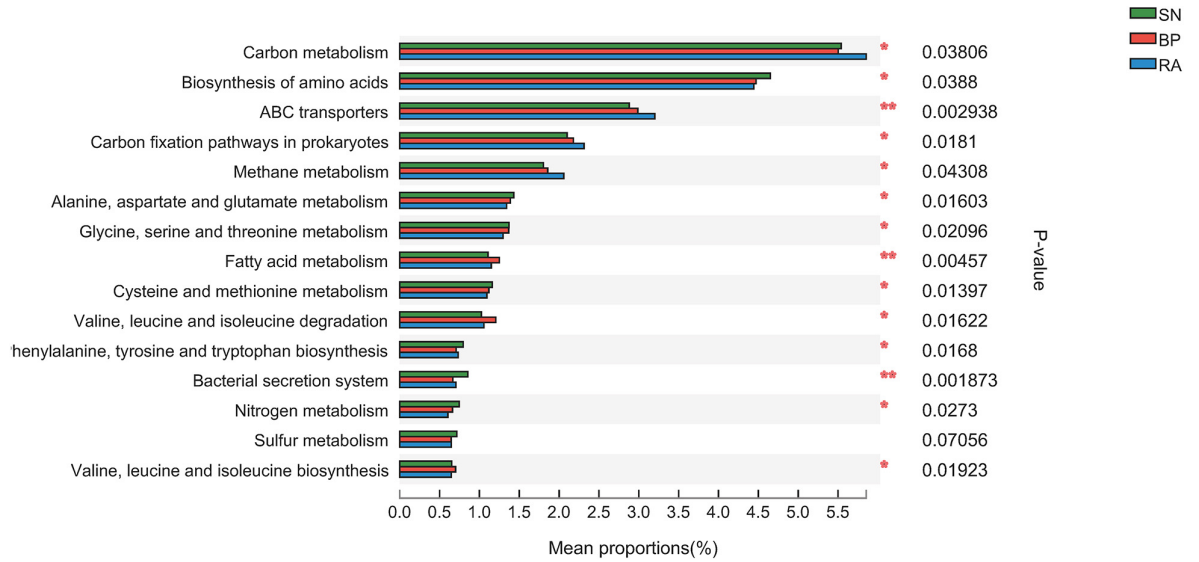

FIGURE 5 | Significant difference analysis of metabolic function based on Kyoto Encyclopedia of Genes and Genomes (KEGG) function annotation. SN, *Sonneratia alba*; RA, *Rhizophora apiculata*; BP, *Bruguiera parviflora*.

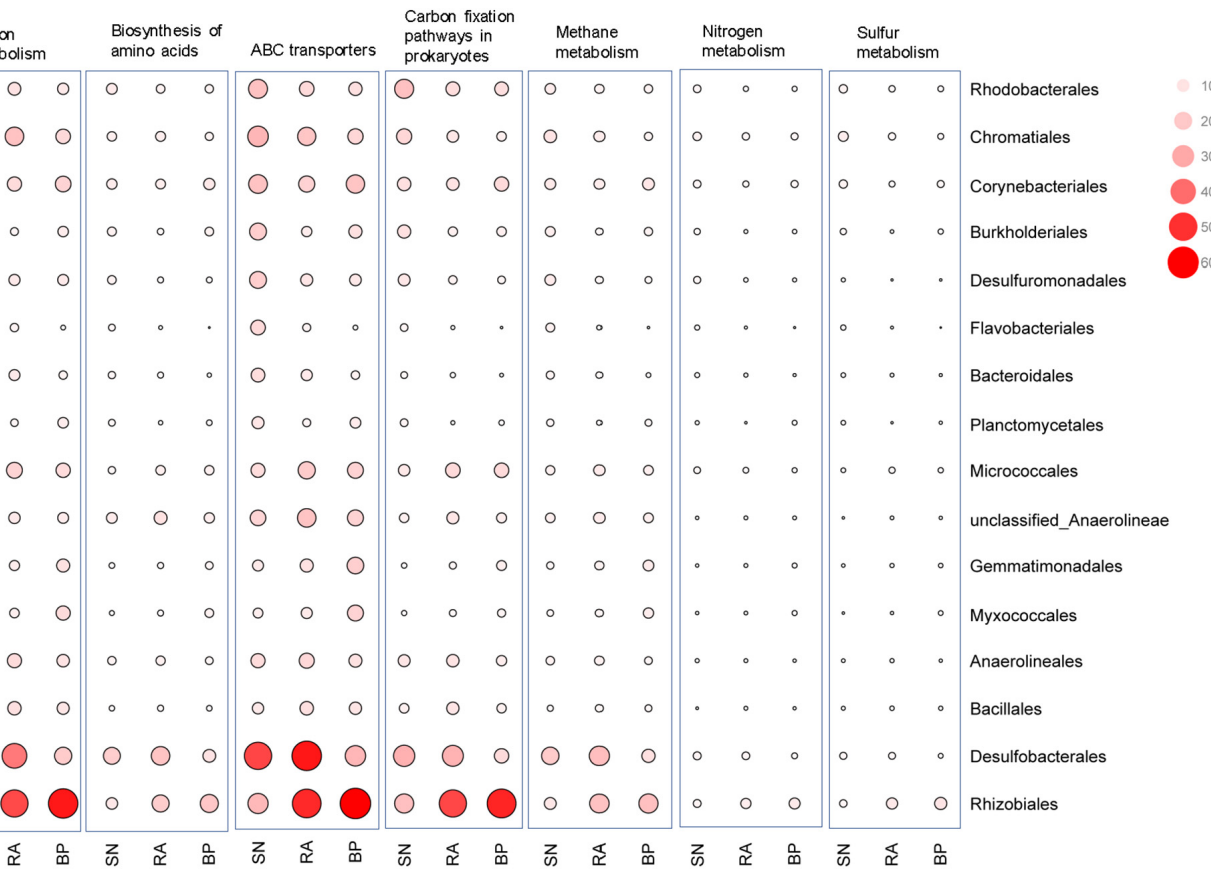

FIGURE 6 | Contribution analysis of dominant microbial taxa to the function at order level. SN, *Sonneratia alba*; RA, *Rhizophora apiculata*; BP, *Bruguiera parviflora*.

the highest microbial diversity. *R. apiculata* is a dominant mangrove species in South Asia and often develops into a stable and fully successional mangrove community. In this study, *R. apiculata* occupied the majority of ecological niches in the central Merbok river estuary, whereas the genera of *Avicennia*, *Bruguiera*, *Sonneratia*, and *Nypa* occupied a smaller habitat in the lower and/or upper estuary. Higher microbial diversity in sediments associated with *R. apiculata* suggested that mangrove succession could enrich benthic microbial community.

Coinciding with high microbial diversity, the sediments associated with *R. apiculata* also exhibited higher TOC than those with *B. parviflora* and *S. alba*, indicating a higher capacity for plant productivity, carbon fixation, and burial. As an important carbon source for microbes, previous investigators also claimed that the accumulation of organic matter in sediments could promote bacterial diversity (Sjöling et al., 2005; Chen et al., 2016). Moreover, the highest TN was also observed in sediments associated with *R. apiculata*. The present results were consistent with previous documents (Zhu et al., 2018), in which the shift in bacterial community structure was partly driven by the increased TOC and total organic nitrogen with the succession of mangrove. Nevertheless, other environmental parameters (salinity, pH, and TP) had significant effects on the microbial community (**Figure 4B**). Salinity and pH have already been reported to have large effects on the microbial communities of mangroves (Ikenaga et al., 2010; Chambers et al., 2016). Moderate salinity was also positively correlated with bacterial abundances and closely linked to community composition and diversity (Morrissey et al., 2014; Crespo-Medina et al., 2016; Tong et al., 2019).

High Carbon-Related Metabolic Potential in Sediments Associated With *Rhizophora apiculata*

In this study, microbial diversity was significantly higher in sediments associated with *R. apiculata*, coinciding with the highest TOC. Enhanced microbial diversity would promote the transformation and utilization of organic carbon (Holguin et al., 2001; Sjöling et al., 2005; Berendsen et al., 2012). Thus, it is not surprising that the sediments associated with *R. apiculata* exhibited a higher carbon metabolic potential (**Figure 5**). Previous data also showed that bacterial diversity and metabolic potential (especially carbon metabolism) appeared to be enhanced during mangrove succession (Zhu et al., 2018).

The findings of this study further showed that sediments associated with *R. apiculata* also exhibited the highest abundances of genes involved in carbon-related pathways (**Supplementary Figure 4**). It is well known that several prokaryotes can assimilate CO_2 into organic carbon (Lynn et al., 2017), although the functions of prokaryotes in carbon fixation have not been fully reported in mangrove ecosystems. In this study, Desulfobacterales and Rhizobiales exhibited high contributions in CO_2 fixation. The enrichment of these bacteria could result in a higher capacity for prokaryotic carbon fixation, which plays an essential role in carbon storage.

It should be noted that the sediments of *R. apiculata* also exhibited the strongest potential for methane metabolism (**Figure 5**). In this study, the high organic carbon contents in *R. apiculata* sediments might promote the growth of methanogens, contributing to the potential production of CH_4. Moreover, CH_4 production and emission are aggravated under anaerobic conditions (Fey et al., 2004; Kutzbach et al., 2004). In addition, ABC transporters were also important indicators of microbial functions that reflected the positive activity of carbon and nutrient transformation. In this study, Desulfobacterales and Rhizobiales were the main contributors to ABC transporters. Higher abundances of ABC transporters in sediments associated with *R. apiculata* indicated that this mangrove had higher carbon and nutrient transportation activities than other mangroves (Wood et al., 2001).

Overall, this study suggested that climax mangroves (e.g., *R. apiculata*) exhibited a faster turnover rate of organic matter between plants and microbes owing to high carbon utilization and transportation. Microbial carbon fixation contributed to carbon sequestration, whereas the degraded small organic molecules could be conducive to the growth and succession of mangroves. The positive feedback of microbial community and function might in turn contribute to the formation of climax mangrove populations with high productivity (Chen et al., 2016). The inherent correlations among carbon metabolism, environmental transition, and mangrove succession need to be further studied.

Specific Microbial Taxa and Functional Potential in Maintaining Mangrove Survival and Succession

Although mangrove sediments are rich in organic matter, they are generally nutrient-deficient. Nutrient limitations were also widely reported in mangrove forests (Feller et al., 2003; Reef et al., 2010; Wang and Gu, 2013; Cheng et al., 2020). Even worse, anaerobic conditions might further aggravate the enrichment of anaerobic microbes and reductive phytotoxins (e.g., CH_4, H_2S, and sulfides). It is worth exploring how mangroves maintain survival and succession in such a terrible habitat in intertidal regions. The present results could partly explain this issue from the perspectives of microbial community and function.

Desulfobacterales, a type of sulfate-reducing bacteria, consistently exhibited the highest contributions to metabolic functions in sediments associated with *R. apiculata* (**Figure 6** and **Supplementary Figure 5**). In this study, Desulfobacterales (e.g., Desulfobacteraceae) was one of the main microbial taxa responsible for the differences among mangroves, whereas *R. apiculata* also exhibited the highest abundances of these bacteria (**Figure 3D** and **Supplementary Figure 2A**). Significantly positive correlations among Desulfobacterales, TOC, and TN were also observed (**Figure 4C** and

Supplementary Figure 2B). Previous investigators also claimed an important role for Desulfobacterales in C, N, and S cycles (Zhu et al., 2018). Increased Desulfobacterales might be beneficial for *R. apiculata* by alleviating the toxicity of sulfides under anaerobic conditions. The high abundances and strong metabolic potential of Desulfobacterales could also accelerate carbon and nutrient transformation and utilization (Lyimo et al., 2002; Meyer and Kuever, 2007), facilitating mangrove survival and succession in intertidal regions.

The important potential of Rhizobiales in C, N, and S metabolisms was also revealed (**Figure 6**). Rhizobiales was a well-studied plant symbiont that widely occurred in the rhizosphere of mangrove plants (Gomes et al., 2010). This taxon played a beneficial role for the host by providing various nutrients, phytohormones, and precursors of essential metabolites (Delmotte et al., 2009; Verginer et al., 2010; Garrido-Oter et al., 2018). The findings of this study also revealed that Rhizobiales (e.g., Xanthobacteraceae) was metabolically versatile, especially in terms of carbon-related metabolism (**Figure 6** and **Supplementary Figure 5**). In this study, relative higher abundances of Rhizobiales (e.g., Xanthobacteraceae) were also detected in the sediments of *R. apiculata* and *B. parviflora* than those of *S. alba* (**Figures 2A**, **3D**). Similarly, positive correlation trends among Rhizobiales, TOC, and TN were also observed in this study (**Figure 4C**).

In addition to Desulfobacterales and Rhizobiales, Micrococcales might also partly contribute to the higher metabolic function in sediments associated with *R. apiculata*. Although little attention has been paid to this taxon, the present data (**Figures 3D**, **4C**, **6**) indicated that Micrococcales might also be important for metabolic functions, which are involved in carbon and nutrient metabolisms. Nevertheless, *Bacillus*, which was often considered a bionematicide, could promote the growth of plants by protecting roots from pathogens (Mendoza et al., 2008; Mendis et al., 2018). Bacillus was also a dominant bacterial component in this study (**Figure 3D**); however, relatively low metabolic potentials of this taxon were observed (**Figure 6**). Multi-omics analyses, such as metagenomics, metatranscriptomics, and metaproteomics, focused on the functions of microbes in mangrove ecosystems should be further conducted.

CONCLUSION

The present findings provided a broader understanding of the relationships among microbes, environmental transition, and mangrove succession from the perspective of microbial community and function. Benthic microbial community was highly correlated with environmental factors and aboveground mangrove species, whereas the highest microbial diversity and metabolic potential (carbon metabolism, prokaryote carbon fixation, methane metabolism, and ABC transporters) were observed in sediments associated with *R. apiculata*. Specific microbial taxa (e.g., Desulfobacterales and Rhizobiales) involved in C, N, and S cycles might facilitate mangrove survival and succession in intertidal regions. The present data indicated that mangrove succession could enrich microbial diversity and carbon metabolism. More detailed multi-omics researches focused on the roles of microbes in mangrove succession should be further conducted.

DATA AVAILABILITY STATEMENT

The original contributions presented in the study are included in the article/**Supplementary Material**, further inquiries can be directed to the corresponding authors.

AUTHOR CONTRIBUTIONS

ZM carried out manuscript writing and revisions. FS and HC designed the research, writing, review, and editing; YW carried out writing – review. SF contributed to the sample collection and data analysis. LW carried out data analysis. All authors contributed to the article and approved the submitted version.

FUNDING

This research was supported by the International Partnership Program of Chinese Academy of Sciences (133244KYSB20180012), Key Special Project for Introduced Talents Team of Southern Marine Science and Engineering Guangdong Laboratory (Guangzhou), China (GML2019ZD0303 and GML2019ZD0305), Science and Technology Basic Resources Investigation Program of China (2017FY100707), Key Research and Development Program of Hainan Province (ZDYF2021XDNY131), National Natural Science Foundation of China (41676086, 41890853, 41906128, and 41406130), and the Project of Guangdong Science and Technology Department (2017A020216008).

SUPPLEMENTARY MATERIAL

The Supplementary Material for this article can be found online at: https://www.frontiersin.org/articles/10.3389/fmicb.2021.764974/full#supplementary-material

REFERENCES

Abed, R. M. M., Al-Kindi, S., and Al-Kharusi, S. (2015). Diversity of bacterial communities along a petroleum contamination gradient in desert soils. *Microb. Ecol.* 69, 95–105. doi: 10.1007/s00248-014-0475-5

Alongi, D. M. (1988). Bacterial productivity and microbial biomass in tropical mangrove sediments. *Microb. Ecol.* 15, 59–79. doi: 10.1007/BF02012952

Alzubaidy, H., Essack, M., Malas, T. B., Bokhari, A., Motwalli, O., Kamanu, F. K., et al. (2016). Rhizosphere microbiome metagenomics of gray mangroves (*Avicennia marina*) in the Red Sea. *Gene* 576(2, Pt 1), 626–636. doi: 10.1016/j.gene.2015.10.032

Andreote, F. D., Jiménez, D. J., Chaves, D., Dias, A. C. F., Luvizotto, D. M., Dini-Andreote, F., et al. (2012). The microbiome of Brazilian mangrove sediments as revealed by metagenomics. *PLoS One* 7:e38600. doi: 10.1371/journal.pone.0038600

Bai, S., Li, J., He, Z., Van Nostrand, J. D., Tian, Y., Lin, G., et al. (2013). GeoChip-based analysis of the functional gene diversity and metabolic potential of soil microbial communities of mangroves. *Appl. Microbiol. Biotechnol.* 97, 7035–7048. doi: 10.1007/s00253-012-4496-z

Bardgett, R. D., and van der Putten, W. H. (2014). Belowground biodiversity and ecosystem functioning. *Nature* 515, 505–511. doi: 10.1038/nature13855

Berendsen, R. L., Pieterse, C. M. J., and Bakker, P. A. H. M. (2012). The rhizosphere microbiome and plant health. *Trends Plant Sci.* 17, 478–486. doi: 10.1016/j.tplants.2012.04.001

Brander, L. M., Wagtendonk, A. J., Hussain, S. S., McVittie, A., Verburg, P. H., de Groot, R. S., et al. (2012). Ecosystem service values for mangroves in Southeast Asia: a meta-analysis and value transfer application. *Ecosyst. Serv.* 1, 62–69. doi: 10.1016/j.ecoser.2012.06.003

Chambers, L. G., Guevara, R., Boyer, J. N., Troxler, T. G., and Davis, S. E. (2016). Effects of salinity and inundation on microbial community structure and function in a mangrove peat soil. *Wetlands* 36, 361–371. doi: 10.1007/s13157-016-0745-8

Chen, Q., Zhao, Q., Li, J., Jian, S., and Ren, H. (2016). Mangrove succession enriches the sediment microbial community in South China. *Sci. Rep.* 6:27468. doi: 10.1038/srep27468

Cheng, H., Liu, Y., Jiang, Z. Y., and Wang, Y. S. (2020). Radial oxygen loss is correlated with nitrogen nutrition in mangroves. *Tree Physiol.* 40, 1548–1560. doi: 10.1093/treephys/tpaa089

Crespo-Medina, M., Bowles, M. W., Samarkin, V. A., Hunter, K. S., and Joye, S. B. (2016). Microbial diversity and activity in seafloor brine lake sediments (Alaminos Canyon block 601, Gulf of Mexico). *Geobiology* 14, 483–498. doi: 10.1111/gbi.12185

Delmotte, N., Knief, C., Chaffron, S., Innerebner, G., Roschitzki, B., Schlapbach, R., et al. (2009). Community proteogenomics reveals insights into the physiology of phyllosphere bacteria. *Proc. Natl. Acad. Sci. U.S.A.* 106, 16428–16433. doi: 10.1073/pnas.0905240106

Feller, I. C., McKee, K. L., Whigham, D. F., and O'Neill, J. P. (2003). Nitrogen vs. phosphorus limitation across an ecotonal gradient in a mangrove forest. *Biogeochemistry* 62, 145–175. doi: 10.1023/A:1021166010892

Fey, A., Claus, P., and Conrad, R. (2004). Temporal change of 13C-isotope signatures and methanogenic pathways in rice field soil incubated anoxically at different temperatures. *Geochim. Cosmochim. Acta.* 68, 293–306. doi: 10.1016/S0016-7037(03)00426-5

Gao, M., Teplitski, M., Robinson, J. B., and Bauer, W. D. (2003). Production of substances by medicago truncatula that affect bacterial quorum sensing. *Mol. Plant Microbe Interact.* 16, 827–834. doi: 10.1094/mpmi.2003.16.9.827

Garrido-Oter, R., Nakano, R. T., Dombrowski, N., Ma, K. W., McHardy, A. C., and Schulze-Lefert, P. (2018). Modular traits of the rhizobiales root microbiota and their evolutionary relationship with symbiotic rhizobia. *Cell Host Microbe* 24, 155–167.e5. doi: 10.1016/j.chom.2018.06.006

Giani, L., Bashan, Y., Holguin, G., and Strangmann, A. (1996). Characteristics and methanogenesis of the Balandra lagoon mangrove soils, Baja California Sur, Mexico. *Geoderma* 72, 149–160. doi: 10.1016/0016-7061(96)00023-7

Giri, C., Ochieng, E., Tieszen, L. L., Zhu, Z., Singh, A., Loveland, T., et al. (2011). Status and distribution of mangrove forests of the world using earth observation satellite data. *Glob. Ecol. Biogeogr.* 20, 154–159. doi: 10.1111/j.1466-8238.2010.00584.x

Gomes, N. C. M., Cleary, D. F. R., Pinto, F. N., Egas, C., Almeida, A., Cunha, A., et al. (2010). Taking root: enduring effect of rhizosphere bacterial colonization in mangroves. *PLoS One* 5:e14065. doi: 10.1371/journal.pone.0014065

Holguin, G., Vazquez, P., and Bashan, Y. (2001). The role of sediment microorganisms in the productivity, conservation, and rehabilitation of mangrove ecosystems: an overview. *Biol. Fertil. Soils* 33, 265–278. doi: 10.1007/s003740000319

Huang, W., Chen, X., Jiang, X., and Zheng, B. (2017). Characterization of sediment bacterial communities in plain lakes with different trophic statuses. *Microbiologyopen* 6:e00503. doi: 10.1002/mbo3.503

Ikenaga, M., Guevara, R., Dean, A. L., Pisani, C., and Boyer, J. N. (2010). Changes in community structure of sediment bacteria along the Florida coastal everglades marsh-mangrove-seagrass salinity gradient. *Microb. Ecol.* 59, 284–295. doi: 10.1007/s00248-009-9572-2

Koh, C. L., Sam, C. K., Yin, W. F., Tan, L. Y., Krishnan, T., Chong, Y. M., et al. (2013). Plant-derived natural products as sources of anti-quorum sensing compounds. *Sensors* 13, 6217–6228.

Kutzbach, L., Wagner, D., and Pfeiffer, E. M. (2004). Effect of microrelief and vegetation on methane emission from wet polygonal tundra, Lena Delta, Northern Siberia. *Biogeochemistry* 69, 341–362. doi: 10.1023/B:BIOG.0000031053.81520.db

Li, R., Yu, C., Li, Y., Lam, T.-W., Yiu, S.-M., Kristiansen, K., et al. (2009). SOAP2: an improved ultrafast tool for short read alignment. *Bioinformatics* 25, 1966–1967. doi: 10.1093/bioinformatics/btp336

Lin, X., Hetharua, B., Lin, L., Xu, H., Zheng, T., He, Z., et al. (2019). Mangrove sediment microbiome: adaptive microbial assemblages and their routed biogeochemical processes in Yunxiao mangrove national nature reserve, China. *Microb. Ecol.* 78, 57–69. doi: 10.1007/s00248-018-1261-6

Lyimo, T. J., Pol, A., and den Camp, H. (2002). Sulfate reduction and methanogenesis in sediments of Mtoni mangrove forest, Tanzania. *Ambio* 31, 614–616.

Lynn, T. M., Ge, T., Yuan, H., Wei, X., Wu, X., Xiao, K., et al. (2017). Soil carbon-fixation rates and associated bacterial diversity and abundance in three natural ecosystems. *Microb. Ecol.* 73, 645–657. doi: 10.1007/s00248-016-0890-x

Mendis, H. C., Thomas, V. P., Schwientek, P., Salamzade, R., Chien, J. T., Waidyarathne, P., et al. (2018). Strain-specific quantification of root colonization by plant growth promoting rhizobacteria *Bacillus firmus* I-1582 and *Bacillus amyloliquefaciens* QST713 in non-sterile soil and field conditions. *PLoS One* 13:e0193119. doi: 10.1371/journal.pone.0193119

Mendoza, A. R., Kiewnick, S., and Sikora, R. A. (2008). In vitro activity of *Bacillus firmus* against the burrowing nematode *Radopholus similis*, the root-knot nematode *Meloidogyne incognita* and the stem nematode *Ditylenchus dipsaci*. *Biocontrol Sci. Technol.* 18, 377–389. doi: 10.1080/09583150801952143

Meyer, B., and Kuever, J. (2007). Molecular analysis of the diversity of sulfate-reducing and sulfur-oxidizing prokaryotes in the environment, using apra as functional marker gene. *Appl. Environ. Microbiol.* 73, 7664–7679. doi: 10.1128/aem.01272-07

Noguchi, H., Park, J., and Takagi, T. (2006). MetaGene: prokaryotic gene finding from environmental genome shotgun sequences. *Nucleic Acids Res.* 34, 5623–5630. doi: 10.1093/nar/gkl723

Morrissey, E. M., Gillespie, J. L., Morina, J. C., and Franklin, R. B. (2014). Salinity affects microbial activity and soil organic matter content in tidal wetlands. *Glob. Chang. Biol.* 20, 1351–1362. doi: 10.1111/gcb.12431

Reef, R., Feller, I. C., and Lovelock, C. E. (2010). Nutrition of mangroves. *Tree Physiol.* 30, 1148–1160. doi: 10.1093/treephys/tpq048

Reis, C. R. G., Nardoto, G. B., and Oliveira, R. S. (2017). Global overview on nitrogen dynamics in mangroves and consequences of increasing nitrogen availability for these systems. *Plant Soil* 410, 1–19. doi: 10.1007/s11104-016-3123-7

Rosentreter, J. A., Maher, D. T., Erler, D. V., Murray, R. H., and Eyre, B. D. (2018). Methane emissions partially offset "blue carbon" burial in mangroves. *Sci. Adv.* 4:eaao4985. doi: 10.1126/sciadv.aao4985

Sjöling, S., Mohammed, S. M., Lyimo, T. J., and Kyaruzi, J. J. (2005). Benthic bacterial diversity and nutrient processes in mangroves: impact of deforestation. *Estuar. Coast Shelf Sci.* 63, 397–406. doi: 10.1016/j.ecss.2004.12.002

Tong, T., Li, R., Wu, S., and Xie, S. (2019). The distribution of sediment bacterial community in mangroves across China was governed by geographic location and eutrophication. *Mar. Pollut. Bull.* 140, 198–203. doi: 10.1016/j.marpolbul.2019.01.046

Verginer, M., Siegmund, B., Cardinale, M., Müller, H., Choi, Y., Míguez, C. B., et al. (2010). Monitoring the plant epiphyte *Methylobacterium extorquens* DSM 21961 by real-time PCR and its influence on the strawberry flavor. *FEMS Microbiol. Ecol.* 74, 136–145. doi: 10.1111/j.1574-6941.2010.00942.x

Wang, W., Li, X., and Wang, M. (2019). Propagule dispersal determines mangrove zonation at intertidal and estuarine scales. *Forests* 10:245.

Wang, Y. F., and Gu, J. D. (2013). Higher diversity of ammonia/ammonium-oxidizing prokaryotes in constructed freshwater wetland than natural coastal marine wetland. *Appl. Microbiol. Biotechnol.* 97, 7015–7033. doi: 10.1007/s00253-012-4430-4

Wood, D. W., Setubal, J. C., Kaul, R., Monks, D. E., Kitajima, J. P., Okura, V. K., et al. (2001). The genome of the natural genetic engineer *Agrobacterium tumefaciens* C58. *Science* 294, 2317–2323. doi: 10.1126/science.1066804

Wu, P., Xiong, X., Xu, Z., Lu, C., Cheng, H., Lyu, X., et al. (2016). Bacterial communities in the rhizospheres of three mangrove tree species from Beilun Estuary, China. *PLoS One* 11:e0164082. doi: 10.1371/journal.pone.0164082

Zhou, Z., Meng, H., Liu, Y., Gu, J. D., and Li, M. (2017). Stratified bacterial and archaeal community in mangrove and intertidal wetland mudflats revealed by high throughput 16S rRNA gene sequencing. *Front. Microbiol.* 8:2148. doi: 10.3389/fmicb.2017.02148

Zhu, P., Wang, Y., Shi, T., Zhang, X., Huang, G., and Gong, J. (2018). Intertidal zonation affects diversity and functional potentials of bacteria in surface sediments: a case study of the Golden Bay mangrove, China. *Appl. Soil. Ecol.* 130, 159–168. doi: 10.1016/j.apsoil.2018.06.003

Zhuang, W., Yu, X., Hu, R., Luo, Z., Liu, X., Zheng, X., et al. (2020). Diversity, function and assembly of mangrove root-associated microbial communities at a continuous fine-scale. *NPJ Biofilms Microbiomes* 6:52. doi: 10.1038/s41522-020-00164-6

Conflict of Interest: The authors declare that the research was conducted in the absence of any commercial or financial relationships that could be construed as a potential conflict of interest.

Publisher's Note: All claims expressed in this article are solely those of the authors and do not necessarily represent those of their affiliated organizations, or those of the publisher, the editors and the reviewers. Any product that may be evaluated in this article, or claim that may be made by its manufacturer, is not guaranteed or endorsed by the publisher.

frontiers in Microbiology

REVIEW
published: 23 December 2021
doi: 10.3389/fmicb.2021.809473

Elucidating the Mechanisms Underlying Enhanced Drought Tolerance in Plants Mediated by Arbuscular Mycorrhizal Fungi

*Shen Cheng[1], Ying-Ning Zou[1], Kamil Kuča[2], Abeer Hashem[3], Elsayed Fathi Abd_Allah[4] and Qiang-Sheng Wu[1,2]**

[1] College of Horticulture and Gardening, Yangtze University, Jingzhou, China, [2] Department of Chemistry, Faculty of Science, University of Hradec Kralove, Hradec Kralove, Czechia, [3] Department of Botany and Microbiology, College of Science, King Saud University, Riyadh, Saudi Arabia, [4] Department of Plant Production, College of Food and Agricultural Sciences, King Saud University, Riyadh, Saudi Arabia

Plants are often subjected to various environmental stresses during their life cycle, among which drought stress is perhaps the most significant abiotic stress limiting plant growth and development. Arbuscular mycorrhizal (AM) fungi, a group of beneficial soil fungi, can enhance the adaptability and tolerance of their host plants to drought stress after infecting plant roots and establishing a symbiotic association with their host plant. Therefore, AM fungi represent an eco-friendly strategy in sustainable agricultural systems. There is still a need, however, to better understand the complex mechanisms underlying AM fungi-mediated enhancement of plant drought tolerance to ensure their effective use. AM fungi establish well-developed, extraradical hyphae on root surfaces, and function in water absorption and the uptake and transfer of nutrients into host cells. Thus, they participate in the physiology of host plants through the function of specific genes encoded in their genome. AM fungi also modulate morphological adaptations and various physiological processes in host plants, that help to mitigate drought-induced injury and enhance drought tolerance. Several AM-specific host genes have been identified and reported to be responsible for conferring enhanced drought tolerance. This review provides an overview of the effect of drought stress on the diversity and activity of AM fungi, the symbiotic relationship that exists between AM fungi and host plants under drought stress conditions, elucidates the morphological, physiological, and molecular mechanisms underlying AM fungi-mediated enhanced drought tolerance in plants, and provides an outlook for future research.

Keywords: drought tolerance, mycorrhizae, plant physiology, symbiosis, water deficit

OPEN ACCESS

Edited by:
Xun Wen Chen, Southern University of Science and Technology, China

Reviewed by:
Raffaella Balestrini, Institute for Sustainable Plant Protection, Consiglio Nazionale delle Ricerche (CNR), Italy
Juan Manuel Ruiz-Lozano, Consejo Superior de Investigaciones Científicas (CSIC), Spain

****Correspondence:***
Qiang-Sheng Wu
wuqiangsh@163.com

Specialty section:
This article was submitted to Terrestrial Microbiology, a section of the journal Frontiers in Microbiology

Received: *05 November 2021*
Accepted: *02 December 2021*
Published: *23 December 2021*

Citation:
Cheng S, Zou Y-N, Kuča K, Hashem A, Abd_Allah EF and Wu Q-S (2021) Elucidating the Mechanisms Underlying Enhanced Drought Tolerance in Plants Mediated by Arbuscular Mycorrhizal Fungi. Front. Microbiol. 12:809473. doi: 10.3389/fmicb.2021.809473

INTRODUCTION

Drought stress (DS) seriously impacts crop growth and productivity (He et al., 2020). Reduced rainfall and global warming are leading to frequent episodes of drought globally. DS decreases photosynthetic efficiency in plants, reduces assimilate production, and impairs cell structure and function (Liang et al., 2019). DS also induces the accumulation of reactive oxygen species (ROS) in

plant cells, causing an oxidative burst, which results in protein denaturation and the degradation of cell membranes (Bahadur et al., 2019). The balance of endogenous hormones in plants is also disturbed by DS, triggering a negative response in plant growth and metabolism (Zhang H. Y. et al., 2018).

The plant rhizosphere is inhabited by numerous, diverse microorganisms including bacteria and fungi. Notably, arbuscular mycorrhizal (AM) fungi have evolved to become symbionts with most terrestrial plants (He et al., 2019). AM fungi infect and reside within and on the surface of plant roots and are involved in the absorption of water and nutrients used by the host plant in exchange for carbohydrates that are provided by their host plant (Jiang et al., 2017). AM fungi dramatically improve the tolerance of host plants to abiotic and biotic stresses (Li et al., 2016). The promotional effect of AM fungi on plant growth is attributed to their developed mycelium network and to glomalin production (Latef et al., 2016). The enhancement of DS by AM fungi is associated with osmotic adjustment, antioxidant defense system, polyamines (PAs), fatty acids (FAs), mineral nutrition acquisition, and induction of gene expression in host plants (Wu et al., 2013; Cheng et al., 2020; Zhang et al., 2020). AM symbiosis alters the physiology of host plants under DS conditions, including adjustments in water potential and gas exchange (Gholamhoseini et al., 2013). This is due to the participation of extraradical hyphae in the absorption of water by mycorrhizal roots, and concomitant increases in the rate of photosynthesis (Zhang F. et al., 2018). The changes in water status of mycorrhizal plants under DS conditions is modulated by hormone signals that result in osmotic adjustments (Wu and Xia, 2006a).

The mechanisms that effectively contribute to enhanced drought tolerance in host plants by AM fungi are complex and involve multiple plant responses (**Table 1**), along with the mechanism of mycorrhizal fungi themselves. Therefore, the present review summarizes the mechanisms by which AMs enhance plant drought tolerance at the morphological, physiological, and molecular levels. Such review would highlight a theoretical basis to understand AM functions on stress tolerance and subsequently potential application of AM fungi in crops of arid areas.

IMPACT OF DROUGHT STRESS ON ARBUSCULAR MYCORRHIZAL FUNGAL DIVERSITY

Arbuscular mycorrhizal fungi are abundant, widely distributed, and adaptable to a variety of ecological environments where they contribute to several ecological processes, including enhancing the stress tolerance of host plants (Chen et al., 2018). The diversity of AM fungi present in a soil environment can vary, depending on the species of host plants present, soil types, and environmental conditions (Lenoir et al., 2016). Over 244 species of Glomeromycota have been identified in a variety of ecosystems (van der Heijden et al., 2015). Low species diversity in AM symbiosis when there is high selectivity by the plant host on their fungal symbiont (Egger and Hibbett, 2004). Functional differences among strains of AM fungi also contribute to low AM fungal diversity by further influencing the network of functional AM fungi and host plants from species to specific AM genotypes (Schüβler et al., 2001). AM fungi play an essential role in improving the productivity of ecosystems and maintaining an ecological balance, especially where AM fungi help host plants to survive in an arid environment (Mathur et al., 2019). Soil water deficits, however, also reduce the colonization ability of AM fungi, hyphal elongation, and spore germination (Wu and Zou, 2017; Zhang F. et al., 2018).

Arbuscular mycorrhizal fungal diversity in water-deficient soils is comparatively lower than it is in water-saturated soils, as water deficit negatively impacts the diversity of AM fungi. However, in watermelon, the 18S rRNA copy numbers of AM fungi were increased in AM versus non-AM roots under DS, indicating that under DS conditions, exogenous AM fungi increase native fungal diversity under water deficit conditions only, resulting in improved colonization and plant responses (Omirou et al., 2013). Although AM fungi are sensitive to droughted soils, individual strains or isolates of AM fungi commonly exist in these environments that are tolerant to DS (Wu et al., 2013). Native strains of AM fungi present in arid environments exhibit a long-term adaptation to dry soils (Sylvia and Williams, 1992). For example, *Glomus* species are commonly present in semi-arid ecosystems, and survive and grow under conditions of low-water availability (Omirou et al., 2013). The AM fungal species *Funneliformis mosseae* can tolerate different environmental conditions, including DS, and is thus considered an early stage colonizer of plants (Lenoir et al., 2016). An antagonistic interaction can exist, however, between host plants and AM fungi diversity under drought conditions. For example, low richness of barley species results in high AM fungal richness under drought (Sendek et al., 2019).

EFFECT OF DROUGHT STRESS ON MYCORRHIZAL SYMBIOSIS

Drought stress strongly inhibits crop growth, although plants have evolved several strategies to enhance DS tolerance and resistance. Plant roots have a high plasticity and have evolved a symbiotic relationship with AM fungi that enhances plant nutrient uptake and water acquisition under DS conditions (Zou et al., 2017). As a result, AM fungi promote crop growth under adverse conditions such as DS (Begum et al., 2019). The growth and development of AM fungi require a certain level of soil moisture, and the level of soil moisture condition strongly affects spore germination, hyphal growth, hyphal branching, and the formation of secondary spores (Omirou et al., 2013; Wu et al., 2013). Therefore, AM fungi must invest more resources in the storage capacity of roots to tolerate a DS environment (Lenoir et al., 2016). AM fungi are an important component of the drought resistance of plants growing in desert ecosystems (Vasar et al., 2021). Water-deficient soils, however, can limit the development of AM fungi in the soil and the rhizosphere, although some AM fungal species can adapt to dry soils and still maintain a relatively high level of root colonization, which

TABLE 1 | Effects of AM fungi inoculation on plant growth and physiological and molecular responses of host plants under drought stress in the selective literatures.

Drought responses	Plant species	AM fungal species	AM fungal variables	Plant variables	References
Plant growth	*Ephedra foliata*	Mixture of *Claroideoglomus etunicatum*, *Funneliformis mosseae*, and *Rhizophagus intraradices*	Total col%$^{\downarrow}$	Shoot fresh and dry weight$^{\uparrow}$; Root length$^{\uparrow}$; Root fresh and dry weight$^{\uparrow}$	Al-Arjani et al., 2020
	Glycine max	No specific AM fungi mentioned	Col%$^{\uparrow}$	LAI$^{\uparrow}$; growth performance$^{\uparrow}$	Pavithra and Yapa, 2018
	Ipomoea batatas	*Glomus* sp. and *Acaulospora* sp.	Col%^{ns}	Plant growth$^{\uparrow}$; tubers per plant$^{\uparrow}$; tuber weight$^{\uparrow}$	Yooyongwech et al., 2016
	Panicum turgidum	Mixture of *C. etunicatum*, *F. mosseae*, and *R. intraradices*	Total col%$^{\downarrow}$	Root morphology (length, surface area and volume)$^{\uparrow}$	Abd_Allah et al., 2019
	Phoenix dactylifera	*G. clarum*, *G. deserticola*, and *G. monosporus*	Col%$^{\uparrow}$	Leaf number$^{\uparrow}$; LAI$^{\uparrow}$	Meddich et al., 2015
	Poncirus trifoliata	*Diversispora versiformis*	Col%$^{\downarrow}$; soil hyphae length$^{\uparrow}$	Plant growth performance$^{\uparrow}$; number of lateral roots$^{\uparrow}$; root morphology$^{\uparrow}$	Zou et al., 2017
	Poncirus trifoliata	*C. etunicatum*, *D. versiformis*, *F. mosseae*, and *Rhizoglomus intraradices*	Col%$^{\downarrow}$	Plant height$^{\uparrow}$; shoot and root biomass$^{\uparrow}$; root hairs density$^{\uparrow}$; leaf number$^{\uparrow}$; stem diameter$^{\uparrow}$	Liu C. Y. et al., 2018
Soil and plant nutrient	*Citrus tangerina*	*G. etunicatum* and *G. mosseae*	Col%$^{\downarrow}$; Hyphal length$^{\downarrow}$	Soil moisture$^{\uparrow}$; soil water potential$^{\uparrow}$	Zou et al., 2013
	Solanum lycopersicum cv.	*F. mosseae*, and *R. intraradices*	Col%^{ns}	leaf P content$^{\uparrow}$; *LePT3*$^{\uparrow}$; *LePT4*$^{\uparrow}$; *LePT5*$^{\uparrow}$;	Volpe et al., 2018
	Ephedra foliata	Mixture of *C. etunicatum*, *F. mosseae*, and *R. intraradices*	Total col%$^{\downarrow}$	Ammonium$^{\uparrow}$; nitrate$^{\uparrow}$; nitrate reductase$^{\uparrow}$; nitrite reductase$^{\uparrow}$	Al-Arjani et al., 2020
	Medicago sativa	*Acaulospora scrobiculata*, *G. intraradices*, and *D. spurcum*	Col%$^{\downarrow}$	Soil structure$^{\uparrow}$; P$^{\uparrow}$	Ye et al., 2013
	Ipomoea aquatica	Unidentified AM fungi	Col%$^{\uparrow}$	Mineral nutrients (P, K, Mg, Na, Fe, Mn, and Zn) uptake$^{\uparrow}$	Halder et al., 2015
	Salsola laricina	*Archaeospora schenckii*, *Scutellospora erythropa*, *Septoglomus deserticola*, and *Septoglomus constrictum*	Col%$^{\downarrow}$	P uptake$^{\uparrow}$	Nouri et al., 2020
	Vaccinium sp.	*G. clarum*, *G. etunicatum*, *Gigaspora margarita*, and *Scutellospora heterogama*	Col%$^{\uparrow}$	Nutrient absorption$^{\uparrow}$	Farias et al., 2014
	Poncirus trifoliata	*G. versiforme*	Col%$^{\downarrow}$	N$^{\uparrow}$; K$^{\uparrow}$; Ca$^{\uparrow}$; Fe$^{\uparrow}$	Wu and Zou, 2009
Photosynthesis	*Ephedra foliata*	Mixture of *C. etunicatum*, *F. mosseae*, and *R. intraradices*	Total col%$^{\downarrow}$	Chlorophyll a$^{\uparrow}$, b$^{\uparrow}$, and a + b$^{\uparrow}$	Al-Arjani et al., 2020
	Ipomoea batatas	*Glomus* sp. and *Acaulospora* sp.	Col%^{ns}	Chlorophyll degradation$^{\downarrow}$; photosynthetic pigments$^{\uparrow}$; maximum quantum yield of PSII (Fv/Fm); photon yield of PSII (ΦPSII) $^{\uparrow}$; Pn$^{\uparrow}$	Yooyongwech et al., 2016
	Leymus chinensis	G. mosseae	Col%$^{\uparrow}$	Gs$^{\uparrow}$; Pn$^{\uparrow}$; chlorophyll$^{\uparrow}$	Lin et al., 2017
	Panicum turgidum	*Mixture of* C. etunicatum, F. mosseae, *and* R. intraradices	Total col%$^{\downarrow}$	Chlorophyll a$^{\uparrow}$, b$^{\uparrow}$, and a + b$^{\uparrow}$; E$^{\uparrow}$; Gs$^{\uparrow}$;	Abd_Allah et al., 2019
	Ricinus communis	F. mosseae *and* Rhizophagus intraradices	Col%^{ns}	Gs$^{\uparrow}$; Pn$^{\uparrow}$; E$^{\uparrow}$; Ci$^{\downarrow}$; Chlorophyll a$^{\uparrow}$, b$^{\uparrow}$, and a + b$^{\uparrow}$	Zhang T. et al., 2018
	Robinia pseudoacacia	*R. irregularis* and *G. versiforme*	Col%$^{\uparrow}$	Chlorophyll$^{\uparrow}$; Pn$^{\uparrow}$; effective quantum yield of PSII(ΦPSII) $^{\uparrow}$; calorific value$^{\uparrow}$; carbon$^{\uparrow}$	Zhu et al., 2014
	Zea mays	*R. irregularis*	Col%^{ns}	Pn$^{\uparrow}$; Gs$^{\uparrow}$; Ci^{ns}	Quiroga et al., 2019
	Sophora davidii	*G. constrictum* and *G. mosseae*	Col%$^{\uparrow}$	Gs$^{\uparrow}$; Pn$^{\uparrow}$; Ci$^{\downarrow}$; maximum quantum yield of PSII (Fv/Fm) $^{\uparrow}$	Gong et al., 2013
Antioxidant responses	*Celtis caucasica*	*F. mosseae* and *R. intraradices*	Col%$^{\uparrow}$	CAT$^{\uparrow}$; SOD$^{\uparrow}$; MDA$^{\downarrow}$; $H_2O_2$$^{\downarrow}$	Sepahvand et al., 2021
	Ephedra foliata	Mixture of *C. etunicatum*, *F. mosseae*, and *R. intraradices*	Total col%$^{\downarrow}$	MDA$^{\downarrow}$; $H_2O_2$$^{\downarrow}$; SOD$^{\uparrow}$; CAT$^{\uparrow}$; APX$^{\uparrow}$; GPX$^{\uparrow}$; glutathione reductase$^{\uparrow}$; reduced glutathione$^{\uparrow}$; ascorbic acid$^{\uparrow}$	Al-Arjani et al., 2020
	Leymus chinensis and *Hemarthria altissima*	*Glomus* sp.	Col%$^{\uparrow}$	CAT$^{\uparrow}$; SOD$^{\uparrow}$; MDA$^{\downarrow}$	Li et al., 2019

(Continued)

TABLE 1 | (Continued)

Drought responses	Plant species	AM fungal species	AM fungal variables	Plant variables	References
Polyamine metabolism	*Poncirus trifoliata*	*F. mosseae*	Col%$^{\uparrow}$	Put and Cad$^{\uparrow}$; Spd and Spm$^{\uparrow}$; PA catabolic enzyme activity$^{\uparrow}$; Put-synthases$^{\uparrow}$	Zhang et al., 2020
	Pelargonium graveolens	*G. intraradices* and *G. mosseae*	Col%$^{\uparrow}$	Essential oil$^{\uparrow}$; total phenol$^{\uparrow}$; flavonoids$^{\uparrow}$; CAT$^{\uparrow}$; SOD$^{\uparrow}$; APX$^{\uparrow}$; GPX$^{\uparrow}$; MDA$^{\downarrow}$; $H_2O_2{}^{\uparrow}$	Amiri et al., 2015
	Poncirus trifoliata	*F. mosseae*	Col%$^{\uparrow}$	$O_2{}^{-\downarrow\downarrow}$; $H_2O_2{}^{\downarrow}$; MDA$^{\uparrow}$	Zou et al., 2021b
Osmotic adjustment	*Poncirus trifoliata*	*F. mosseae* and *Paraglomus occultum*	Col%$^{\downarrow}$	Sucrose, glucose and fructose$^{\uparrow}$; proline$^{\downarrow}$	Wu et al., 2017
	Erythrina variegat	*G. mosseae*	Col%$^{\downarrow}$	Total soluble sugar$^{\downarrow}$; protein$^{\uparrow}$; proline$^{\downarrow}$	Manoharan et al., 2010
	Ephedra foliata	Mixture of *C. etunicatum, F. mosseae*, and *R. intraradices*	Total col%$^{\downarrow}$	Glucose$^{\uparrow}$; proline$^{\uparrow}$; soluble protein$^{\uparrow}$	Al-Arjani et al., 2020
	Populus canadensis	*R. irregularis*	Col%$^{\uparrow}$	Free proline$^{\downarrow}$; soluble protein$^{\uparrow}$	Liu T. et al., 2016
	Ricinus communis	*F. mosseae* and *R. intraradices*	Col%^{ns}	Free proline$^{\uparrow}$; soluble protein$^{\uparrow}$	Zhang T. et al., 2018
	Zenia insignis	*D. versiformis, F. mosseae,* and *R. intraradices*	Col%^{ns}	Proline$^{\uparrow}$; soluble sugars$^{\uparrow}$	Zhang Z. et al., 2018
	Triticum aestivum	*Rhizoglomus irregulare*	Col%$^{\downarrow}$	Proline^{ns}	Pons et al., 2020
	Macadamia tetraphylla	*Acaulospora* sp., *Glomus* sp., *Gigaspora* sp., and *Scutellospora* sp.	Col%$^{\uparrow}$	Proline$^{\uparrow}$; soluble sugars$^{\uparrow}$	Yooyongwech et al., 2013
	Poncirus trifoliata	*F. mosseae*	Col%$^{\uparrow}$	Put$^{\uparrow}$; Cad$^{\uparrow}$; Spd$^{\uparrow}$; ADC$^{\uparrow}$; ODC$^{\uparrow}$; SPMS$^{\downarrow}$; SPDS$^{\uparrow}$; DAO$^{\uparrow}$; PAO$^{\uparrow}$; Precursor of PA$^{\uparrow}$	Zou et al., 2021b
	Poncirus trifoliata	*G. mosseae*	Col%$^{\uparrow}$	Put and Spd$^{\downarrow}$; Spm$^{\uparrow}$; SPMS$^{\uparrow}$	Luo, 2009
	Zea mays	*R. irregularis*	Col%^{ns}	Put^{ns}; ODC and GABA$^{\downarrow}$; DAO$^{\uparrow}$	Hu et al., 2020
	Zea mays	*R. irregularis*	Col%$^{\uparrow}$	Put$^{\downarrow}$; DAO and GABAT$^{\uparrow}$; GABA$^{\uparrow}$	Hu and Chen, 2020
Fatty acids	*Glycine max*	*Claroideoglomus etunicatum, F. mosseae, Gigaspora gigantea, R. clarus,* and *Paraglomus occultum*	Col%$^{\uparrow}$	MUFA$^{\uparrow}$; PUFA$^{\uparrow}$	Igiehon et al., 2021
	Poncirus trifoliata	*F. mosseae*	Col%$^{\downarrow}$	UFA$^{\uparrow}$; SFA$^{\downarrow}$; *PtFAD2*$^{\uparrow}$; *PtFAD6*$^{\uparrow}$; *PtΔ9*$^{\uparrow}$;*PtΔ15*	Wu et al., 2019
	Sesamum indicum	*F. mosseae* and *R. irregularis*	Col%$^{\uparrow}$	UFA$^{\uparrow}$; SFA$^{\downarrow}$	Gholinezhad and Darvishzadeh, 2021
Endogenous hormones	*Poncirus trifoliata*	*D. versiformis*	Col%$^{\downarrow}$	ABA$^{\uparrow}$; GA$^{\uparrow}$; IAA$^{\uparrow}$; MeJA$^{\uparrow}$; ZR$^{\uparrow}$	Zhang et al., 2017
	Solanum lycopersicum	*F. mosseae* and *R. intraradices*	Col%$^{\uparrow}$	ABA$^{\uparrow}$	Chitarra et al., 2016
	S. lycopersicum	*R. irregularis*	Col%^{ns}	ABA$^{\downarrow}$; IAA$^{\uparrow}$; MeJ$^{\uparrow}$; SA$^{\uparrow}$	Sanchez-Romera et al., 2018
	Ephedra foliata	Mixture of *C. etunicatum*, *F. mosseae*, and *R. intraradices*	Total col%$^{\downarrow}$	ABA$^{\uparrow}$; IAA$^{\uparrow}$; IBA$^{\uparrow}$; GA$^{\uparrow}$	Al-Arjani et al., 2020
	Glycyrrhiza uralensis	*R. irregularis*	Col%$^{\downarrow}$	ABA$^{\downarrow}$	Xie et al., 2018
	Panicum turgidum	Mixture of *C. etunicatum, F. mosseae*, and *R. intraradices*	Total col%$^{\downarrow}$	IAA$^{\uparrow}$	Abd_Allah et al., 2019
	Zea mays	*G. manihotis*		ABA$^{\downarrow}$	Kandowangko et al., 2009
Molecular regulation	*Glycine max* and *Lactuca sativa*	*G. mosseae* and *G. intraradices*	Col%^{ns}	*GmPIP2*$^{\downarrow}$; *LsPIP1*$^{\downarrow}$; *LsPIP2*$^{\downarrow}$	Porcel et al., 2006

(Continued)

TABLE 1 | (Continued)

Drought responses	Plant species	AM fungal species	AM fungal variables	Plant variables	References
	Zea mays	*G. intraradices*	Col%↑	*GintAQPF1*↑; *GintAQPF2*↑; AQP activities↑	Li et al., 2013
	Poncirus trifoliata	*F. mosseae*	Col%↓	*PtAHA2*↑; H^+-ATPase activity↑	Cheng H. Q. et al., 2021
	Malus domestica	*R. irregularis*	Col%↑	Strigolactone↑; strigolactone synthesis genes expression↑; *MdIAA24*↑	Huang et al., 2021a
	Zea mays	*R. intraradices*	Col%↑	*ZmPIP1;1*↓; *ZmPIP1;3*↓; *ZmPIP1;4*↓; *ZmPIP1;6*↓; *ZmPIP2;2*↓; *ZmPIP2;4*↓; *ZmTIP1;2*↓; ZmPIP2; 5 protein content↑	Bárzana et al., 2014
	Helianthemum almeriense	*Terfezia claveryi*	Col%↑	*HaPIP1;1*↓	Navarro-Ródenas et al., 2013

↑ *and* ↓ *indicate the significant increasing and decreasing response of the variable to mycorrhizal fungal inoculation. ns, no significant difference; AM, arbuscular mycorrhiza; Col, AM fungal colonization; LAI, leaf area index; Gs, stomatal conductance; Pn, net photosynthetic rate; Ci, intercellular CO_2 concentration; E, transpiration rate; CAT, catalase; SOD superoxide dismutase; MDA, malondialdehyde; H_2O_2, hydrogen peroxide; APX, ascorbate peroxidase; GPX, glutathione peroxidase; O_2^-, superoxide radical; Put, putrescine; Cad, cadaverine; Spd, spermidine; Spm, spermine; ADC, arginine decarboxylase; ODC, ornithine decarboxylase; SPMS, spermine synthase; SPDS, spermidine synthase; DAO, diamine oxidase; PAO, polyamine oxidases; SPDS, spermidine synthetase; GABAT, γ-aminobutyrate aminotransferase; GABA, γ-aminobutyric acid; MUFA, monounsaturated fatty acid; PUFA, polyunsaturated fatty acid; UFA, unsaturated fatty acid; SFA, saturated fatty acid; ABA, abscisic acid; GA, gibberellin; IAA, indoleacetic acid; MeJA, methyl jasmonate; ZR, zeatin nucleoside; SA, salicylic acid.*

is essential for the survival and growth of host plants (Zou et al., 2017). After analyzing the results of a large number of studies, Augé (2001) reported on the diverse effects of drought on AM fungal colonization, manifested as a decrease, undetectable change, or an increase in colonization under DS conditions. Surprisingly, when certain plants experience DS, they secret rhizospheric signaling molecules to attract AM fungi (Oldroyd, 2013). AM fungi also have a certain level of intrinsic drought tolerance, which is imparted to AM host plants under drought conditions. Mycorrhizal spores are resistant to and can survive under drought conditions, thus ensuring a source of AM fungi for continued infection of plant roots (Song, 2005). Notably, soil drought was not a greater determinant of mycorrhizal species or colonization rate than low-temperature, as root growth is more affected by low-temperature than by water-deficient soils (Kilpelainen et al., 2020b). Therefore, poor performance of AM under drought conditions implies an avoidance of DS rather than a tolerance of DS (Kilpelainen et al., 2020b). Importantly, AM fungi isolated from unfavorable environments have been reported to be more effective in enhancing plant stress tolerance (Rivero et al., 2018). Under extreme soil drying, co-adaption of local plants and local soil AM fungi would induce the abundance of mycorrhizal hyphae and arbuscules and fewer vesicles than under moderate soil drying, thus, mitigating DS (Remke et al., 2021). Future studies, however, will need to further analyze how soil moisture levels affect root colonization by mycorrhizal fungi and the acquisition of soil nutrients, such as N and P content, as well as pH.

DROUGHT-STRESS ADAPTIVE MECHANISMS INDUCED IN PLANTS BY ARBUSCULAR MYCORRHIZAL FUNGI

Drought stress has become the major abiotic stress limiting crop growth and productivity (Bárzana and Carvaja, 2020). AM fungi, however, can mitigate the unfavorable effects of DS on plant growth by a series of mechanisms (Pavithra and Yapa, 2018). AM-enhanced drought tolerance of host plants, however, is a complex process, shaped by both the AM fungal species and the plant host. The mechanisms involved in morphological adaptability and physiological and molecular responses had been described by Wu and Zou (2017) and Bahadur et al. (2019). Here, we focused on the recent advances in mycorrhizal regulation of host polyamines and FAs, as well as the expression of stressed genes in arid environments (**Table 1** and **Figure 1**).

Morphological Adaptations in Host Plants and Arbuscular Mycorrhizal Fungi

Arbuscular mycorrhizal symbiosis is associated with morphological adaptations to DS in host plants that improve tolerance to arid environments (Ruiz-Lozano and Aroca, 2010a). AM fungi have been reported to induce DS-tolerant growth phenotypes in response to DS in a variety of plant plants, including trifoliate orange, date palm, and soybean

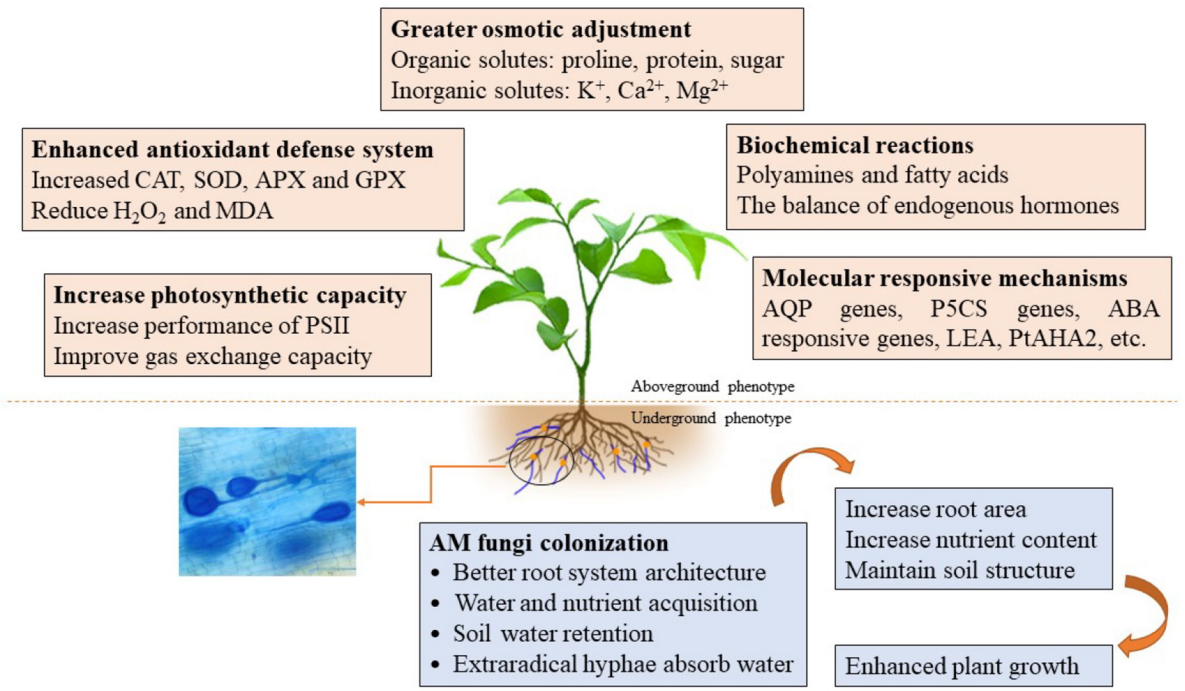

FIGURE 1 | A schematic diagram regarding the underlying mechanisms of AM fungi enhancing plant drought tolerance. AM fungi affect the morphology, physiological activities, and molecular regulation of host plants through direct or indirect interactions in response to drought stress, and thus help host plants regulating and maintaining various processes to deal with the harmful effects of drought on plant.

(Grümberg et al., 2015; Meddich et al., 2015; Zou et al., 2017; **Table 1**). Although DS has a strong inhibitory effect on root system growth and development, inoculation of root systems with AM fungi significantly reduce this negative impact (Wu and Xia, 2006b). AM fungi affect the penetration and distribution of roots in soil by changing root morphology in host plants (Liu J. et al., 2016). Studies have shown significant increases in root traits, such as biomass, length, volume, and surface area, as well as root-hair density, root-hair length, and root branching, occur in trifoliate orange under DS conditions after AM fungal colonization (Zou et al., 2017; Liu C. Y. et al., 2018; Zhang F. et al., 2018; **Table 1**). This implies that increases in water and nutrients occur by optimizing root morphology in response to DS. In addition, mycorrhizal plants maintain their water balance by altering their degree of defoliation (Bryla and Duniway, 2010).

In addition to plant morphology, morphological changes in AM fungi also occur in response to DS conditions. DS negatively affects spore germination and subsequent hyphal development, thus interfering with the formation and further development of mycorrhizal structures, such as arbuscules and vesicles (Giovannetti et al., 2010). Interestingly spores of *Glomus mosseae* and *G. deserticola* had greater colonization ability after storage at a −0.04 MPa soil water potential, while *G. fasciculatum* was most infectious after storage at a −0.8 MPa soil water potential (Wu et al., 2013), indicating that the moisture level in the soil surrounding fungal spores affects the colonization of AM fungi. It also suggests that AM fungi exhibit morphological and ecological adaptability to DS.

Arbuscular Mycorrhizal-Mediated Water and Nutrient Acquisition

A functional aspect of AMs is their ability to increase water and nutrient acquisition in host plants under DS conditions through the production of mycorrhizal extraradical hyphae (Zhao et al., 2015). Mycorrhizae extend from their host plants and form a developed hyphal network in the surrounding soil that partially reduces the flow resistance between the host plant and the surrounding soil (Allen, 2007), thus, improving the water use efficiency of host plants under DS conditions. The size of air spaces between plant roots and the soil particles increase under DS conditions and mycorrhizal hyphae with the diameter of 2–5 μm can bridge the gap between the roots and soil to help maintain the continuity of water transport. Mycorrhizal hyphae absorb water at a higher rate under DS conditions than they do under sufficient water conditions, reflecting their benefit to host plants growing in arid environmental conditions (Zhang F. et al., 2018). Nevertheless, plants obtain less water through AM fungal hyphae, relative to the overall water absorption by roots and the overall water demand of plants (Püschel et al., 2020). In addition, the presence of common mycorrhizal networks among different plants can redistribute interspecific nutrients under DS conditions, thus realizing the enhancement of

drought tolerance of intercropped crops in an arid environment (Mickan et al., 2021).

Mycorrhizal symbionts promote nutrient acquisition in their host plants subjected to drought conditions (**Table 1**). For example, inoculation of trifoliate orange plants with *G. versiforme* increased the level of P, K, Ca, and Fe in leaves and roots under both well-watered and DS conditions (Wu and Zou, 2009). Leaf N, P, and K content also increased in mycorrhizal blueberry plants exposed to DS (Farias et al., 2014). Notably, AM fungi increase both the availability of soil P and the host plant's ability to absorb P, along with increasing the uptake of K, Mg, Fe, Mn, and Zn under DS conditions (Halder et al., 2015). Püschel et al. (2021) further using two-compartment rhizoboxes reported that mycorrhizal P uptake was more effective over relatively short distances (i.e., near plant roots) and less effective over relatively long distances (i.e., exclusively by mycorrhizal hyphal transport) under DS conditions. The long distance mycorrhizal pathway, however, still offered significant advantages in long-distance P transport, especially under medium and low moisture conditions, with a concomitant indirect effect of AM fungi changing substrate hydraulic conductivity (Püschel et al., 2021). Inoculation of plant roots with AM fungi also significantly contributed to P uptake in *Salsola laricina*, a species which is commonly planted for the restoration of degraded grassland (Nouri et al., 2020). The higher P content in AM plants under DS conditions is a primary reason for their greater tolerance to drought stress relative to non-AM plants (Kilpelainen et al., 2020a). The PHOSPHATE TRANSPORTER1 (PHT1) gene family is involved in the uptake and translocation of phosphate (Pi) in the soil, as well as the uptake of Pi from AM (Liu F. et al., 2018). AM fungi induced phosphate transporter (PT) genes expression (*LePT4* and *LePT5*) in tomato plants to enhance tolerance to soil water deficit, dependent on the fungal species (Volpe et al., 2018). Likewise, the expression of certain host *PT* genes (e.g., *PHT1.2* and *PHO9* in *Populus trichocarpa*) was increased under drought conditions, independent of Pi levels, while other *PT* genes may be Pi-dependent (Zhang C. X. et al., 2016). In addition, ammonium transporter protein and potassium (K^+) transporter genes collectively were up-regulated by AM fungal inoculation under DS (Balestrini et al., 2019), which is critical for N and K uptake of host plants in arid environment. Interestingly, drought-adapted AM fungal strains represent better improved nutrient contents of the host plant (i.e., lavender) in arid environments than non-adapted AM fungal strains (Marulanda et al., 2007; Symanczik et al., 2018). In addition, the activities of H^+-ATPase and Ca^{2+}-ATPase of AM extraradical hyphae were induced under DS and caused the acidification of soil environment, which facilitates the absorption of mineral nutrients and the signal exchange between AM fungi and plants to enhance the drought tolerance of plants (Ferrol et al., 2000; Xu et al., 2018a).

Higher water and nutrient uptake of mycorrhizal plants versus non-mycorrhizal plants is also associated with changes in root architecture, including the production of root hairs (Liu C. Y. et al., 2018). Cheng H. Q. et al. (2021) recently reported on the expression of a *PtAHA2* gene, which is involved in H^+-ATPase activity, in trifoliate orange, which was expressed in leaf and root tissues under both well-watered and DS conditions, after plants were inoculated with *F. mosseae*. Such expression patterns in mycorrhizal plants under DS conditions could cause an acidic rhizospheric microenvironment, thus, leading to an increase in NH_4^+ in leaves and roots of AM plants. AM symbiosis also induces the expression of aquaporin (*ZmTIP1;1*) gene expression at high NH_4^+ concentrations, resulting in excessive N storage in vacuoles under DS conditions (Quiroga et al., 2020a). Transcriptomic studies also revealed that under DS, nutrient transporters in AM plants, such as *PT*, ammonium transporter, potassium (K^+) transporter, amino acid transporter, peptide transporter and sulfate transporter, were significantly up-regulated by mycorrhizal fungi (Balestrini et al., 2019). This indicates that the improvement of nutrient absorption by mycorrhizas is closely linked to the regulation of nutrient transporters under DS conditions.

Arbuscular Mycorrhizal-Improved Soil Aggregate Formation

The formation of soil aggregates has a major impact on the saturation status of soils that directly impact plant growth and development (Vergani and Graf, 2016). Notably, AM fungi produce and secrete glomalin through mycelia and spores which adheres to the soil like "super glue" and contributes to the maintenance of good soil structure (Chi et al., 2018). Zou et al. (2014) reported that glomalin-related soil protein (GRSP), more specifically total GRSP but not easily extractable GRSP, contributed to soil water content, suggesting the importance of total GRSP in mediating soil aggregate stability and soil moisture. Mycorrhizal fungi alter the soil water cycle through their network of extraradical mycelia that promotes the formation of soil aggregates and increases soil water holding capacity (Querejeta et al., 2003). Augé et al. (2001) reported that hyphae and exudates of AM fungi improved soil structure by altering soil aggregates, thereby enhancing soil water retention, except for differences caused by root growth in mycorrhizal and non-mycorrhizal soils. In addition, AM soils can influence the growth of non-mycorrhizal plants, and the number of mycorrhizal hyphae in the soil differs significantly between non-AM and AM soils (Augé et al., 2004). Mycorrhizal extraradical hyphae also directly contribute to the dispersive energy in the formation of soil macroaggregates under DS conditions (Ji et al., 2019). Inoculation of *Medicago sativa* plants with AM fungi accelerated the formation of large soil aggregates and the stability of water-stable aggregates under DS conditions, thus, improving soil structure (Ye et al., 2013). Collective studies indicate that the water content of plants increases in mycorrhizal substrates under both water-saturated and DS soil conditions (Bitterlich et al., 2018). AM hyphae in soil may have the function of reducing the air gap at the soil-root interface, and thus better soil-root contact in AM soils promotes the soil-root hydraulic conductance (Augé, 2004). Hydraulic conductivity has been shown to be higher in mycorrhizal soil prior to and during DS conditions (Bitterlich et al., 2018).

Arbuscular Mycorrhizal-Improved Photosynthetic Capacity

Solar radiation is essential for plant growth and development. DS induces stomatal closure, chloroplast structural damage, including the structure and function of the PSII reaction center, and the inhibition of electron transport (Zhang Y. M. et al., 2016). AM fungi have been reported to improve photosynthetic capacity in host plants under DS conditions, as indicated by the increase in net photosynthetic rates, transpiration rates, and stomatal conductance, as well as by a decrease in intercellular CO_2 concentration (**Table 1**; Zhu et al., 2014; Lin et al., 2017; Zhang T. et al., 2018; Abd_Allah et al., 2019). Colonization of plants by AM fungi help the host plant to maintain the integrity and stability of both PSI and PSII under DS conditions (Mathur et al., 2019). This benefit is derived from the AM-enhancement of water absorption and transport and the stimulation of C sinks. AM fungi also directly or indirectly enhance photosynthetic efficiency and chlorophyll concentration under DS conditions (Gong et al., 2013; Zhang T. et al., 2018; Abd_Allah et al., 2019). AM fungi were reported to induce the expression of 14-3-3 genes that reduce the rate of transpiration and modulate stomatal behavior, both of which play a role in the maintenance of water use efficiency (Xu et al., 2018b). A study of AM plants subjected to rewatering of plants after exposure to DS condition demonstrated that AM plants were able to repair damaged photosynthesis-related structures and restore normal levels of photosynthesis faster than non-AM plants (Polcyn et al., 2019). The enhancement of photosynthetic capacity was also reported to be associated with a reduction of specific leaf area in AM plants (Quiroga et al., 2019) and an increase of Rubisco activity and electron transport rates (Valentine et al., 2006).

Arbuscular Mycorrhizal-Enhanced Plant Host Antioxidant Defense Systems

Exposure of plants to DS induces an excessive accumulation of ROS, which results in oxidative damage to proteins, nucleic acids, and lipids (Hussain et al., 2019). Plant exposed to DS conditions activate both enzymatic and non-enzymatic antioxidant defense systems to remove excessive ROS in cells. Antioxidant enzymes include superoxide dismutase (SOD), peroxidase (POD), catalase (CAT), ascorbate peroxidase (APX), glutathione peroxidase (GPX), etc., while antioxidants include ascorbic acid (ASC), glutathione (GSH), flavonoids, carotenoids, etc. (Rapparini and Peñuelas, 2014). Antioxidant compounds directly eliminate ROS and also induce a series of signaling pathways that indirectly regulate ROS production in plant cells. Studies have demonstrated that AM symbiosis helps plants cope with the excessive accumulation of ROS in cells caused by drought stress by enhancing the host plant's antioxidant defense systems, which reduces the oxidative damage that occurs in plant cells under DS conditions (**Table 1**; Rani et al., 2018; Zou et al., 2021a). Plants inoculated with AM fungi and exposed to DS conditions exhibit significantly enhanced levels of CAT, SOD, APX, and GPX activity, along with a reduction in H_2O_2 and malondialdehyde (MDA) content (Amiri et al., 2015; Al-Arjani et al., 2020). AM fungi-inoculated wheat plants were reported to have higher antioxidant enzyme activity and lower superoxide radical, H_2O_2, and MDA levels than non-inoculated plants exposed to DS in both drought-tolerant and drought-susceptible varieties (Rani et al., 2018). Mycorrhizal plants also exhibit higher levels of non-enzymatic antioxidants (GSH, ASC, and flavonoids) under DS conditions than non-mycorrhizal plants, which represents another mechanism to prevent DS-induced oxidative damage in host plants (Al-Arjani et al., 2020; Zou et al., 2021a). AM enhancement of antioxidant defense systems may be due to the accumulation of ROS in AM fungi themselves (Fester and Hause, 2005). In this regard, SOD genes have been identified in AM fungi (Corradi et al., 2009). Native AM fungi have been shown to exhibit higher antioxidant levels and AM development than non-native strains of AM fungi (Marulanda et al., 2007), suggesting that local, native strains of AM fungi should be explored for their potential use in agricultural production systems.

Arbuscular Mycorrhizal-Mediated Osmotic Adjustments

Osmotic adjustments occur in response to drought conditions that involve both inorganic solutes (K^+, Ca^{2+}, Mg^{2+}, etc.) and organic solutes (proline, sugar, proteins, glycine, etc.) (Ozturk et al., 2021). AM symbiosis improves the ability of host plants to make osmotic adjustments under DS conditions due to a greater accumulation of solutes in AM plants (**Figure 1**; Zou et al., 2021b). For example, AM fungi have been reported to improve the water status of sweet potato plants through the accumulation of AM fungi-regulated soluble sugars and free proline (Yooyongwech et al., 2016). Soluble sugars can function as a signal molecule that activates regulatory pathways controlling growth and development in plants and the transport of photosynthetic products (Poór et al., 2019). AM fungi substantially increase sucrose, fructose, and glucose concentrations in trifoliate orange and glucose concentrations in *Ephedra foliata* under DS conditions (Wu et al., 2017; Al-Arjani et al., 2020). These compounds can protect and stabilize macromolecule structures and maintain an appropriate water balance under DS conditions, thus alleviating DS-induced injury. In contrast, AM fungi reduced soluble sugar levels in *Erythrina variegata* under DS conditions (Manoharan et al., 2010), which perhaps could be due to the fact that AM plants exhibit less drought injury without the accumulation of solutes and sugars. In water-deficited plants, proline often functions as an osmoprotectant in DS plants that protects enzymes and proteins from denaturation (AlKahtani et al., 2021). Earlier studies reported lower proline content in mycorrhizal plants under DS conditions than in non-mycorrhizal plants (Manoharan et al., 2010; Liu J. et al., 2016; Wu et al., 2017). This again may be due to the fact that mycorrhizal plants are less affected by DS (Asrar et al., 2012; Pavla et al., 2013; Liu T. et al., 2016). It appears that AM-mediated reduction of proline in plants is caused by the inhibition of the proline synthesis pathway and the promotion of proline degradation (Zou et al., 2013). Other studies, however, have reported that AM plants exhibit a higher accumulation of proline under DS conditions than non-AM plants (Yooyongwech et al., 2013; Zhang T. et al., 2018; Zhang Z. et al., 2018;

Al-Arjani et al., 2020). The accumulation of proline may provide energy and improve osmotic regulation in AM plants under DS conditions which would help to enhance growth (Yooyongwech et al., 2013). In contrast, it has also been shown that AM fungal inoculation of plants did not alter the proline content of wheat plants under DS conditions (Pons et al., 2020), indicating that mycorrhizal regulation of proline is influenced by the species of mycorrhizal fungus, the host plant, and the environment. In other words, AM-mediated changes in proline content are dependent upon host plants, AM fungi, and environmental conditions.

Arbuscular Mycorrhizal-Mediated Polyamine Metabolism

Polyamines are low molecular weight polycationic compounds that are ubiquitous in living organisms (Ali et al., 2020b). Plant PAs mainly include cadaverine (Cad), putrescine (Put), spermine (Spm), and spermidine (Spd), which are associated with various stress responses in plants, but are also involved in many biological processes (Kateřina et al., 2019). PAs are involved in the plant-AM fungi interaction including mycorrhizal fungal colonization of root, mycorrhizal development, plant growth, and stress response (**Table 1**; Salloum et al., 2018). Studies revealed that exogenous application of PAs, especially Put, promotes the growth and development of AM fungi by stimulating AM fungal spore germination and primary hyphal elongation (Wu et al., 2010a; Yao et al., 2010). Endogenous PAs also regulate mycorrhizal development by altering the level of carbohydrates directed to roots (Wu et al., 2010b). In response to a persistent drought stress and 15-day water deficit conditions, trifoliate orange seedlings inoculated with *F. mosseae* had significantly higher levels of Put and Cad but reduced levels of Spd and Spm, relative to non-inoculated plants, in their roots (Zhang et al., 2020; Zou et al., 2021b). In maize, *Rhizophagus irregularis* inoculation also dramatically increased leaf Put concentrations in response to DS, along with more conversion of Put to γ-aminobutyric acid (GABA, a byproduct of PA degradation) (Hu et al., 2020). The activation of the synthesis of GABA by AM fungi may also contribute to enhanced DS tolerance in host plants by means of triggering stomatal closure (Hu and Chen, 2020; Hu et al., 2020). Mycorrhizal plants also had a higher ratio of (Spd + Spm)/Put under drought conditions, which prevented chlorophyll loss and a significant increase in the level of chlorophyll a (Zhang et al., 2020). The increase in PAs in response to DS also protects mycorrhizal plants against oxidative damage by maintaining cell pH and ion homeostasis and enhancing antioxidant defense systems (Zhang et al., 2020). The increment in (Spd + Spm)/Put in drought-stressed AM plants may be higher in sensitive genotype than in tolerant genotype (Sannazzaro et al., 2007). Mycorrhizae-induced increases in Put and Cad and decreases in Spm and Spd brought about by the presence of AM fungi could be attributed to an increase in level of PA precursors, such as arginine, ornithine, agmatine, and *S*-adenosyl methionine (Zou et al., 2021b), along with the down-regulation in the relative expression of PA catabolic enzyme genes (*CuAO* and *PAO*). The reduced levels of Spd and Spm in AM plants under DS conditions could also activate the signal associated with ROS, thus, up-regulating the expression of host antioxidant enzyme genes (e.g., *CAT* and *SOD*) (He et al., 2020; Zhang et al., 2020). Inoculation of plants with AM fungi, however, has also been reported to significantly reduce Put and Spd content in the leaves of host plants but increase Spm content (Luo, 2009; Hu and Chen, 2020). The decrease in Put and Spd levels in AM plants may be a result of the continuous conversion of Put and Spd to Spm in mycorrhizal plants to improve host drought tolerance (Luo, 2009). In addition, AM-induced changes in Put might accelerate trehalose synthesis of host plants, which is involved in improved osmotic adjustment as an organic compatible solute in response to stress (Garg and Saroy, 2020).

Arbuscular Mycorrhizal-Mediated Fatty Acid Metabolism

The saturation level and composition of FAs in organisms are closely related to the lipid fluidity of the cell membrane, and a higher concentration of unsaturated fatty acids (UFAs) is associated with drought tolerance in plants (Mahnaz et al., 2020). FA metabolism has been implicated in AM regulation of plant drought response (**Table 1**). Trifoliate orange plants inoculated with *F. mosseae* had a higher UFA (e.g., C18:1, C18:2, and C18:3N3) level in roots, relative to non-inoculated plants, and a lower level of saturated fatty acids (SFA) (e.g., C18:0) under DS conditions, which resulted in a higher unsaturation index of FAs in AM plants compared to non-AM plants (Wu et al., 2019; Hu et al., 2020). *F. mosseae* and *Rhizophagus intraradices* also increased UFA contents and reduced SFA contents, in sesame plants, as well as increasing the level of non-enzymatic antioxidants under DS conditions (Gholinezhad and Darvishzadeh, 2021). Soybean plants inoculated with AM fungi combined with *Rhizobium cellulosilyticum* strain R3 also exhibited the highest percentage of UFAs, a feature that is beneficial to human health (Igiehon et al., 2021). AM plants also modulate changes in FA unsaturation by inducing the expression level of FA desaturase genes, such as FA desaturase 2 and FA desaturase 6 (Wu et al., 2019). The changes in the composition of FAs induced by AM fungi would help AM plants to maintain the fluidity of cell membranes, thus, mitigating the potential oxidative damage resulting from DS. On the other hand, AM fungi also dramatically increased C14:0 levels of host plants (Meng et al., 2021), which could favor the growth of budding spores and the formation of secondary spores, thus stimulating spore growth and subsequent hyphal colonization event (Sugiura et al., 2020). Such response in AM fungi will enable AM plants to better deal with the drought damage in dry environment than non-AM plants.

Arbuscular Mycorrhizal-Regulation of Endogenous Hormones

Drought stress often induces changes in the level of endogenous hormone in plants (Liu T. et al., 2016). Studies have indicated that the levels of abscisic acid (ABA), indoleacetic acid (IAA), indole butyric acid (IBA), gibberellin (GA), methyl jasmonate (MeJA), and zeatin nucleoside (ZR) were higher in mycorrhizal plants under DS conditions than the levels in non-mycorrhizal

plants (Zhang et al., 2017; Al-Arjani et al., 2020), which promoted both the growth of plants and mycorrhizae. AM fungi dramatically elevated IAA, MeJA, and salicylic acid (SA) content in tomato plants under DS conditions, relative to non-AM plants (**Table 1**; Sanchez-Romera et al., 2018). Recently, Quiroga et al. (2020b) observed that IAA was involved in radial water transport in AM plants under DS through regulating *AQPs* expression. ABA is a key signal molecule in roots and the production of ABA is essential for the colonization of AM fungi (Herrera-Medina et al., 2007). There is evidence that ABA has an impact on the development and function of AM fungi, so the increase in ABA content in AM plants under DS conditions may stimulate AM development, which would be contribute to enhanced drought tolerance of the plants (Herrera-Medina et al., 2007; Pozo et al., 2015). In addition to regulating ABA levels in host plants, fungi, including AM fungi, also produce ABA (Esch et al., 1994)., AM fungi increase ABA biosynthesis under DS conditions, thereby, increasing the ABA content in host plants, which would further promote stomatal closure and reduce water loss caused by transpiration (Chitarra et al., 2016). ABA content in host plants, however, has also been reported to be reduced by AM fungi under DS conditions (Kandowangko et al., 2009; Sanchez-Romera et al., 2018; Xie et al., 2018), indicating that the regulation of ABA levels in host plants by AM fungi can vary. AM inoculation of tomato induced the expression of *9-cis-epoxycarotenoid dioxygenase* (*NCED*) in roots under DS conditions, thus, promoting the synthesis of ABA in roots, which resulted in enhanced drought tolerance (Aroca et al., 2008). Alternatively, the ABA content in the roots of AM plants can be reduced, and the signaling pathway for ABA can be altered (Xie et al., 2018). The reduction in ABA content in AM plants under DS conditions has been associated with the development of AM fungal mycelia (Kandowangko et al., 2009; Goicoechea et al., 2010).

Arbuscular Mycorrhizal-Mediated Gene Expression

Drought stress-induced genes and compounds can be divided into two categories: functional genes, which directly play a role in environmental stress, such as aquaporin (AQP), late embryogenesis abundant (LEA) proteins, sugar, proline, etc., and regulatory genes, which are involved in signal transduction and the regulation of gene expression, including stress-related transcription factors and signal molecules, such as calmodulin-binding protein (Shinozaki and Yamaguchi-Shinozaki, 2007). AM fungi can trigger the expression of host stress-related genes under DS conditions (**Table 1**; Li and Chen, 2012). AM fungi impact the transmembrane transport of water by regulating *AQP* genes that encode aquaporin water-channel proteins located on cell membranes, which may be one of the mechanisms by which mycorrhizal fungi enhance drought tolerance in plants (Rapparini and Peñuelas, 2014; He et al., 2019; Cheng et al., 2020). A total of six fungal AQP proteins including GintAQP1 in *G. intraradices*, GintAQPF1 in *G. intraradices*, GintAQPF2 in *G. intraradices*, RcAQP1 in *Rhizophagus clarus*, RcAQP2 in *R. clarus*, and RcAQP3 in *R. clarus*, were identified (Aroca et al., 2009; Li et al., 2013; Kikuchi et al., 2016). Drought treatment did not alter *GintAQP1* expression, whereas induced *GintAQPF1* and *GintAQPF2* expression; *RcAQP3* expresses in intraradical hyphae to transport water. Studies have demonstrated that the expression of *plasma membrane intrinsic protein* (*PIP*) genes in *Glycine max* and *Lactuca sativa* plants inoculated with AM fungi was down-regulated under adequate soil moisture conditions (Porcel et al., 2006). In contrast, the inoculation of plants with AM fungi have been shown to increase the expression of *PIPs* in host plants under DS conditions (Zézél et al., 2008). Aroca et al. (2007) found that *PIP* gene family was expressed differently in response to various stresses, depending on the presence or absence of AM fungi. The expression of two functional genes encoding *AQPs* in both drought-exposed maize roots and AM fungi have been shown to be elevated in inoculated plants, relative to non-inoculated plants, indicating that AM fungi simultaneously regulate the expression of *AQPs* in both the host plant and endogenously (Li et al., 2013). In addition, AM fungi down-regulated the expression of seven *PIP* genes, four *nodulin-26 like intrinsic protein* (*NIP*) genes, and six *tonoplast intrinsic protein* (*TIP*) genes under DS conditions while maintaining high-water uptake by mycorrhizal extraradical hyphae (Zou et al., 2019). These results suggest that the regulation of host aquaporins by mycorrhizal fungi is supplemental to hyphal water absorption. A further study revealed that the expression of *AQPs* in host plants was also up-regulated by AM fungi in response to salt stress, while expression levels were diversely affected under well-watered conditions, and marginally or not at all affected under waterlogging conditions (Cheng X. F. et al., 2021). Moreover, the regulation of AQP genes in host plants by AM symbiosis depends mainly on irrigation conditions and the severity of soil drought (Bárzana et al., 2014). Therefore, it appears that AM fungi regulate the expression of host *AQPs* in a manner that is dependent on the type of abiotic stress. Quiroga et al. (2017) observed that AM symbiosis in drought-sensitive varieties regulated *AQPs* more extensively and differentially than in drought-tolerant varieties of maize, suggesting that AM-regulated *AQPs* play an important role in water homeostasis or transport of solutes under DS. Inoculation of corn plants with *R. irregularis* increased the phosphorylation status of *PIP2* aquaporins under DS conditions, indicating higher water channel activity in AM plants exposed to DS (Quiroga et al., 2019). Endogenous ABA levels in host plants also affect the impact of AM fungi on *AQP* expression (Ruiz-Lozano and Aroca, 2010b). In addition, SA regulation of plant water conductivity may be related to root *AQP* expression pattern (Quiroga et al., 2018). Two opposing views exist on the mechanism of *AQP* induction in AM plants under DS conditions. The first suggests that an increase in water permeability due to the up-regulation of *AQPs* which would improve the water absorption capacity of plant roots and promote water transport. The second view suggests that the down-regulation of *AQPs* would reduce membrane permeability, thus, preventing cell water loss (Ruiz-Lozano and Aroca, 2010b; Cheng et al., 2020). There is a

certain compensation mechanism between the expression of the aquaporin gene *GintAQP1* of AM fungus (e.g., *G. intraradices*) and the expression of the host root *AQP*s (Aroca et al., 2009). TcAQP1 in mycorrhizal fungus (*Terfezia claveryi*) is a fungal major intrinsic protein with the function of water and CO_2 transport, and TcAQP1 has high water conductivity to adapt to DS (Navarro-Ródenas et al., 2012). The increase in the expression of *LbAQP1* of *Laccaria bicolor* requires the contact between mycorrhizal fungi and roots within a short time, and LbAQP1 promotes the transport of NO, H_2O_2, and CO_2 when it is expressed heterologously in yeast (Navarro-Ródenas et al., 2015). It suggests that the AQPs of the host and mycorrhizal fungus may be involved in the transport of water and solutes after drought induction, thus, contributing to the drought tolerance of AM plants.

LEA and proline synthesis enzyme Δ^1-pyrroline-5-carboxylate synthetase (*P5CS*) gene expression is associated with AM-enhanced drought tolerance in plants (Zheng et al., 2020). LEA proteins play a role in reducing water loss and act as molecular chaperones that increase drought tolerance (Ali et al., 2020a). Studies have shown that AM fungi increase the accumulation of dehydrins, a type of LEA protein, in plants, thereby, playing an important role in improving plant drought tolerance (Ruiz-Lozano et al., 2008). AM fungi also induces the expression of *P5CS* in host plants under abiotic stress conditions (Zheng et al., 2020). Cheng H. Q. et al. (2021) identified and cloned an H^+-ATPase gene, *PtAHA2*, from trifoliate orange and reported that *PtAHA2* expression was up-regulated by both DS and AM fungi inoculation. The up-regulation of *PtAHA2* by mycorrhization further triggered an increase in ammonium nitrogen content in roots and an increase in soil acidification. Huang et al. (2021a) cloned a *MdIAA24* gene from apple and found that overexpression of *MdIAA24* enhanced drought tolerance, as evidenced by a higher level of ROS scavenging, a greater osmotic adjustment ability, improved gas exchange capacity, and increased chlorophyll fluorescence, by regulating AM colonization and arbuscule numbers, as well as an increase in the level of strigolactone. Interestingly, the combination of AM fungi and DS had a synergistic effect on the up-regulation of *malectin-like domain-containing receptor-like kinases* (*MRLKs*) (Luo et al., 2020). A synergistic effect of AM fungi and DS was also observed on the up-regulation of *calcium-dependent protein kinases* (*CDPKs*) in citrus, where 17 *CsCDPK* family members were induced, and *CsCDPK20* and *CsCDPK22* expression was up-regulated in AM plants under DS conditions, relative to well-watered conditions (Shu et al., 2020b). DS and AM fungi colonization collectively induced *calcineurin B-like protein* (*CBL*) *7* and *CBL-interacting protein kinase* (*CIPK*) *4* expression in *Citrus sinensis*. Notably, *CsCBL* and *CsCIPK* exhibited a co-expression pattern in response to DS and AM fungal colonization, as evidenced by the positive correlation of *CsCBL1* expression with *CsCIPK1*, *3*, *6*, and *9* expression (Shu et al., 2020a). Transgenic apple plants overexpressing *MdGH3-2* and *MdGH3-12* and colonized by AM fungi exhibited a greater sensitivity to drought stress than wild type plants, suggesting that *MdGH3-2/12* plays an important role in regulating drought tolerance in apple (Huang et al., 2021b). The regulation of stress-related gene expression and physiology in host plants by AM fungi has been demonstrated to enhance drought tolerance in host plants. The molecular regulatory network associated with mycorrhizal colonization and DS has not been fully elucidated, although the role of several genes has been identified and analyzed.

CONCLUSION AND FUTURE PROSPECTS

Drought stress causes a significant reduction in plant growth and yield. AM symbiosis with host plants has been shown to play a positive role in mitigating drought damage. AM fungi construct some of their own water uptake mechanisms and also rapidly activate the host's physiological, molecular and morphological responses to DS that enhances their ability to cope with the adverse effects of drought (**Figure 1**), increasing the ability of host plants to survive and maintain vigorous growth under drought conditions. Hence, the plant–AM fungi interaction represents a great example of a sustainable agricultural strategy. Notably, the use of biochar amendments further increases AM-mediated drought tolerance in host plants (Hashem et al., 2019). The role of AM fungi in enhancing plant drought tolerance has been extensively demonstrated experimentally, however, the mechanisms involved are very complex and need to be further explored and elucidated. Future work should focus on the following topics:

(1) Studies have demonstrated water absorption by mycorrhizal extraradical hyphae and subsequent transfer to host cells. The mechanism by which extraradical hyphae absorb water and arbuscules unload the water absorbed by the mycorrhizal hyphae, however, is very complex and require further study. Ezawa and Saito (2018) proposed a model on how water and Pi transport may be linked and how fungal aquaporins (AQP3) may participate in the water transport at the intraradical hyphae. How do Pi and water interact in such a complex process? Who is dominant? What specific genes are involved in the offloading of roots from environment to arbuscule-contained root cells?
(2) The benefit of AM fungi is more pronounced under drought conditions than under adequate water conditions. Why does this benefit occur? By what mechanisms does this mycorrhizal benefit occur? Additionally, since AM fungi contribute to enhanced drought tolerance in host plants, they should be utilized in the revegetation of degraded woodlands, farmlands, and pastures in arid and semi-arid areas (Nouri et al., 2020). Further studies in this area are highly warranted.
(3) AM fungi respond to drought by regulating a variety of metabolites, including PAs, FAs, proline, betaine, and osmoregulators in host plants. Studies focusing on a single metabolite cannot fully elucidate its role in drought

tolerance. Additional studies are needed to reveal the impact of AM colonization on metabolomic changes in response to DS conditions. Studies of both the non-targeted metabolome and the targeted metabolome are needed.

(4) Studies of the transcriptome in AM versus non-AM plants under DS conditions will provide further identification of AM fungal-specific gene regulation and how these genes are regulated by AM fungi. Overexpression or silencing of specific identified genes from AM fungi and/or the host plant will help to elucidate the mechanisms by which AM fungi enhance drought tolerance.

(5) Whole genome sequences of individual AM fungal strains (e.g., *R. irregularis*) have been published (Tisserant et al., 2013), and some stress-related genes encoded by AM fungi have been identified. The mechanisms by which these genes regulate stress response should be further explored.

AUTHOR CONTRIBUTIONS

All authors listed have made a substantial, direct, and intellectual contribution to the work, and approved it for publication.

FUNDING

This study was supported by the Plan in Scientific and Technological Innovation Team of Outstanding Young Scientists, Hubei Provincial Department of Education (T201604) and the National Key Research and Development Program of China (2018YFD1000303). The authors would like to extend their sincere appreciation to the Researchers Supporting Project Number (RSP-2021/134), King Saud University, Riyadh, Saudi Arabia.

REFERENCES

Abd_Allah, E. F., Tabassum, B., Alqarawi, A. A., Alshahrani, T. S., Malik, J. A., and Hashem, A. (2019). Physiological markers mitigate drought stress in Panicum turgidum Forssk. By arbuscular mycorrhizal fungi. *Pak. J. Bot.* 51, 2003–2011. doi: 10.30848/PJB2019-6(12

Al-Arjani, A. B. F., Hashem, A., and Abd_Allah, E. F. (2020). Arbuscular mycorrhizal fungi modulates dynamics tolerance expression to mitigate drought stress in *Ephedra faliata* Boiss. *Saudi J. Biol. Sci.* 27, 380–394. doi: 10.1016/j.sjbs.2019.10.008

Ali, M., Gul, A., Hasan, H., Alipour, H., Abbasi, A. A., Khan, F. Z., et al. (2020a). "LEA proteins and drought stress in wheat," in *Climate Change and Food Security with Emphasis on Wheat*, eds M. Ozturk and A. Gul (London: Academic Press), 193–205. doi: 10.1016/B978-0-12-819527-7.00012-1

Ali, R., Hassan, S., Shah, D., Sajjad, N., and Bhat, E. A. (2020b). "Role of polyamines in mitigating abiotic stress," in *Protective Chemical Agents in the Amelioation of Plant Abiotic Stress: Biochemical and Molecular Perspectives*, eds A. Roychoudhury and D. K. Tripathi (Hoboken, USA: John Wiley & Sons Ltd), 291–305. doi: 10.1002/9781119552154.ch13

AlKahtani, M. D. F., Hafez, Y. M., Attia, K., Rashwan, E., Husnain, L. A., AlGwaiz, H. I. M., et al. (2021). Evaluation of silicon and proline application on the oxidative machinery in drought-stressed sugar beet. *Antioxidants* 10:398. doi: 10.3390/antiox10030398

Allen, M. F. (2007). Mycorrhizal fungi: highways for water and nutrients in arid soils. *Vadose Zone J.* 6, 291–297. doi: 10.2136/vzj2006.0068

Amiri, R., Nikbakht, A., and Etemadi, N. (2015). Alleviation of drought stress on rose geranium [*Pelargonium graveolens* (L.) herit.] in terms of antioxidant activity and secondary metabolites by mycorrhizal inoculation. *Sci. Hortic.* 197, 373–380. doi: 10.1016/j.scienta.2015.09.062

Aroca, R., Bago, A., Sutka, M., Paz, J. A., Cano, C., Amodeo, G., et al. (2009). Expression analysis of the first arbuscular mycorrhizal fungi aquaporin described reveals concerted gene expression between salt-stressed and non-stressed mycelium. *Mol. Plant-Microbe Interact.* 22, 1169–1178. doi: 10.1094/MPMI-22-9-1169

Aroca, R., Porcel, R., and Ruiz-Lozano, J. M. (2007). How does arbuscular mycorrhizal symbiosis regulate root hydraulic properties and plasma membrane aquaporin in *Phaseolus vulgaris* under drought, cold or salinity stresses? *New Phytol.* 173, 808–816. doi: 10.1111/j.1469-8137.2006.01961.x

Aroca, R., Vernieri, P., and Ruiz-Lozano, J. M. (2008). Mycorrhizal and non-mycorrhizal *Lactuca sativa* plants exhibit contrasting responses to exogenous ABA during drought stress and recovery. *J. Exp. Bot.* 59, 2029–2041. doi: 10.1093/jxb/ern057

Asrar, A. A., Abdel-Fattah, G. M., and Elhindi, K. M. (2012). Improving growth, flower yield, and water relations of snapdragon (*Antirhinum majus* L.) plants grown under well-watered and water-stress conditions using arbuscular mycorrhizal fungi. *Photosynthetica* 50, 305–316. doi: 10.1007/s11099-012-0024-8

Augé, R. M. (2001). Water relations, drought and vesicular-arbuscular mycorrhizal symbiosis. *Mycorrhiza* 11, 3–42. doi: 10.1007/s005720100097

Augé, R. M. (2004). Arbuscular mycorrhizae and soilant water relations. *Can. J. Soil Sci.* 84, 373–381. doi: 10.4141/S04-002

Augé, R. M., Stodola, A. J. W., Tims, J. E., and Saxton, A. M. (2001). Moisture retention properties of a mycorrhizal soil. *Plant Soil* 230, 87–97. doi: 10.1023/A:1004891210871

Augé, R. M., Sylvia, D. M., Park, S. J., Buttery, B. R., Saxton, A. M., Moore, J. L., et al. (2004). Partitioning mycorrhizal influence on water relations of *Phaseolus vulgaris* into soil and plant components. *Can. J. Bot.* 82, 503–514. doi: 10.1139/B04-020

Bahadur, A., Batool, A., Nasir, F., Jiang, S. J., Qin, M. S., Zhang, Q., et al. (2019). Mechanistic insights into arbuscular mycorrhizal fungi-mediated drought stress tolerance in plants. *Int. J. Mol. Sci.* 20:4199. doi: 10.3390/ijms20174199

Balestrini, R., Rosso, L. C., Veronico, P., Melillo, M. T., De Luca, F., Fanelli, E., et al. (2019). Transcriptomic responses to water deficit and nematode infection in mycorrhizal tomato roots. *Front. Microbiol.* 10:1087. doi: 10.3389/fmicb.2019.01807

Bárzana, G., and Carvaja, M. (2020). Genetic regulation of water and nutrient transport in water stress tolerance in roots. *J. Biotehcnol.* 324, 134–142. doi: 10.1016/j.jbiotec.2020.10.003

Bárzana, G., Aroca, R., Bienert, P., Chaumont, F., and Ruiz-Lozano, J. M. (2014). New insights into the regulation of aquaporins by the arbuscular mycorrhizal symbiosis in maize plants under drought stress and possible implications for plant performance. *Mol. Plant-Microbe Interact.* 27, 349–363. doi: 10.1094/MPMI-09-13-0268-R

Begum, N., Qin, C., Ahanger, M. A., Raza, S., Khan, M. I., Ashraf, M., et al. (2019). Role of arbuscular mycorrhizal fungi in plant growth regulation: implications in abiotic stress tolerance. *Front. Plant Sci.* 10:1068. doi: 10.3389/fpls.2019.01068

Bitterlich, M., Sandmann, M., and Graefe, J. (2018). Arbuscular mycorrhiza alleviates restrictions to substrate water flow and delays transpiration limitation to stronger drought in tomato. *Front. Plant Sci.* 9:154. doi: 10.3389/fpls.2018.00154

Bryla, D. R., and Duniway, J. M. (2010). Growth, phosphorus uptake, and water relations of safflower and wheat infected with an arbuscular mycorrhizal fungus. *New Phytol.* 136, 581–590. doi: 10.1046/j.1469-8137.1997.00780.x

Chen, M., Arato, M., Borghi, L., Nouri, E., and Reinhardt, D. (2018). Beneficial services of arbuscular mycorrhizal fungi – from ecology to application. *Front. Plant Sci.* 9:1270. doi: 10.3389/fpls.2018.01270

Cheng, H. Q., Ding, Y. E., Shu, B., Zou, Y. N., Wu, Q. S., and Kuča, K. (2020). Plant aquaporin responses to mycorrhizal symbiosis under abiotic stress. *Int. J. Agric. Biol.* 23, 786–794. doi: 10.17957/IJAB/15.1353

Cheng, H. Q., Zou, Y. N., Wu, Q. S., and Kuèa, K. (2021). Arbuscular mycorrhizal fungi alleviate drought stress in trifoliate orange by regulating H^+-ATPase activity and gene expression. *Front. Plant Sci.* 12:659694. doi: 10.3389/fpls.2021.659694

Cheng, X. F., Wu, H. H., Zou, Y. N., Wu, Q. S., and Kuča, K. (2021). Mycorrhizal response strategies of trifoliate orange under well-watered, salt stress, and waterlogging stress by regulating leaf aquaporin expression. *Plant Physiol. Biochem.* 162, 27–35. doi: 10.1016/j.plaphy.2021.02.026

Chi, G. G., Srivastava, A. K., and Wu, Q. S. (2018). Exogenous easily extractable glomalin-related soil protein improves drought tolerance of trifoliate orange. *Arch. Agron. Soil Sci.* 64, 1341–1350. doi: 10.1080/03650340.2018.1432854

Chitarra, W., Pagliarani, C., Maserti, B., Lumini, E., Siciliano, I., Cascone, P., et al. (2016). Insights on the impact of arbuscular mycorrhizal symbiosis on tomato tolerance to water stress. *Plant Physiol.* 171, 1009–1023. doi: 10.1104/pp.16.00307

Corradi, N., Ruffner, B., Croll, D., Colard, A., Horak, A., and Sanders, I. R. (2009). High-level molecular diversity of copper-zinc superoxide dismutase genes among and within species of arbuscular mycorrhizal fungi. *App. Environ. Microbiol.* 75, 1970–1978. doi: 10.1128/AEM.01974-08

Egger, K. N., and Hibbett, D. S. (2004). The evolutionary implications of exploitation in mycorrhizas. *Can. J. Bot.* 82, 1110–1121. doi: 10.1139/b04-056

Esch, H., Hundeshagen, B., Schneider-Poetsch, H., and Bothe, H. (1994). Demonstration of abscisic acid in spores and hyphae of the arbuscular-mycorrhizal fungus *Glomus* and in the N_2-fixing cyanobacterium *Anabaena variabilis*. *Plant Sci.* 99, 9–16. doi: 10.1016/0168-9452(94)90115-5

Ezawa, T., and Saito, K. (2018). How do arbuscular mycorrhizal fungi handle phosphate? New insight into fine-tuning of phosphate metabolism. *New Phytol.* 220, 1116–1121. doi: 10.1111/nph.15187

Farias, D. D. H., Pinto, M. A. B., Carra, B., Schuch, M. W., and Souza, P. V. D. D. (2014). Development of seedlings of blueberry inoculated arbuscular mycorrhizal fungi. *Rev. Bras. Frutic.* 36, 655–663. doi: 10.1590/0100-2945-128/13

Ferrol, N., Barea, J. M., and Azcón-Aguilar, C. (2000). The plasma membrane H^+-ATPase gene family in the arbuscular mycorrhizal fungus *Glomus mosseae*. *Curr. Genet.* 37, 112–118. doi: 10.1007/s002940050017

Fester, T., and Hause, G. (2005). Accumulation of reactive oxygen species in arbuscular mycorrhizal roots. *Mycorrhiza* 15, 373–379. doi: 10.1007/s00572-005-0363-4

Garg, N., and Saroy, K. (2020). Interactive effects of polyamines and arbuscular mycorrhiza in modulating plant biomass, N_2 fixation, ureide, and trehalose metabolism in *Cajanus cajan* (L.) Millsp. genotypes under nickel stress. *Environ. Sci. Pollut. Res.* 27, 3043–3064. doi: 10.1007/s11356-019-07300-6

Gholamhoseini, M., Ghalavand, A., Dolatabadian, A., Jamshidi, E., and Khodaei-Joghan, A. (2013). Effects of arbuscular mycorrhizal inoculation on growth, yield, nutrient uptake and irrigation water productivity of sunflowers grown under drought stress. *Agric. Water Manag.* 117, 106–114. doi: 10.1016/j.agwat.2012.11.007

Gholinezhad, E., and Darvishzadeh, R. (2021). Influence of arbusular mycorrhizal fungi and drought stress on fatty acids profile of sesame (*Sesamum indicum* L.). *Field Crop. Res.* 262:108035. doi: 10.1016/j.fcr.2020.108035

Giovannetti, M., Avio, L., and Sbrana, C. (2010). "Fungal spore germination and pre-symbiotic mycelial growth–physiological and genetic aspects," in *Arbuscular Mycorrhizas: Physiology and Function*, eds H. Koltai and Y. Kapulnik (Dordrecht: Springer), 3–32. doi: 10.1007/978-90-481-9489-6_1

Goicoechea, N., Antolin, M. C., and Sanchez-Diaz, M. (2010). Gas exchange is related to the hormone balance in mycorrhizal or nitrogen-fixing alfalfa subjected to drought. *Physiol. Plant.* 100, 989–997. doi: 10.1111/j.1399-3054.1997.tb00027.x

Gong, M., Tang, M., Chen, H., Zhang, Q. M., and Feng, X. X. (2013). Effects of two *Glomus* species on the growth and physiological performance of *Sophora davidii* seedlings under water stress. *New For.* 44, 399–408. doi: 10.1007/s11056-012-9349-1

Grümberg, B. C., Urcelay, C., Shroeder, M. A., Vargas-Gil, S., and Luna, C. M. (2015). The role of inoculum identity in drought stress mitigation by arbuscular mycorrhizal fungi in soybean. *Biol. Fert. Soils* 51, 1–10. doi: 10.1007/s00374-014-0942-7

Halder, M., Dhar, P. P., Mujib, A. S. M., Khan, M. S., and Akhter, S. (2015). Effect of arbuscular mycorrhiza fungi inoculation on growth and up take of mineral nutrition in *Ipomoea aquatica*. *Curr. World Environ.* 10, 67–75. doi: 10.12944/CWE.10.1.08

Hashem, A., Kumar, A., Al-Dbass, A. M., Alqarawi, A. Z., Al-Arjani, A. B. F., Singh, G., et al. (2019). Arbuscular mycorrhizal fungi and biochar improves drought tolerance in chickpea. *Saud. J. Biol. Sci.* 26, 614–624. doi: 10.1016/j.sjbs.2018.11.005

He, J. D., Dong, T., Wu, H. H., Zou, Y. N., Wu, Q. S., and Kuča, K. (2019). Mycorrhizas induce diverse responses of root *TIP* aquaporin gene expression to drought stress in trifoliate orange. *Sci. Hortic.* 243, 64–69. doi: 10.1016/j.scienta.2018.08.010

He, J. D., Zou, Y. N., Wu, Q. S., and Kuča, K. (2020). Mycorrhizas enhance drought tolerance of trifoliate orange by enhancing activities and gene expression of antioxidant enzymes. *Sci. Hortic.* 262:108745. doi: 10.1016/j.scienta.2019.108745

Herrera-Medina, M. J., Steinkellner, S., Vierheilig, H., Bote, J. A. O., and Garrido, J. M. G. (2007). Abscisic acid determines arbuscule development and functionality in tomato arbuscular mycorrhiza. *Proc. Natl. Acad. Sci. U S A.* 104, 14658–14663. doi: 10.1073/pnas.0703594104

Hu, Y. B., and Chen, B. D. (2020). Arbuscular mycorrhiza induced putrescine degradation into γ-aminobutyric acid, malic acid accumulation, and improvement of nitrogen assimilation in roots of water-stressed maize plants. *Mycorrhiza* 30, 329–339. doi: 10.1007/s00572-020-00952-0

Hu, Y. B., Xie, W., and Chen, B. D. (2020). Arbuscular mycorrhiza improved drought tolerance of maize seedlings by altering photosystem II efficiency and the levels of key metabolites. *Chem. Biol. Technol. Agric.* 7:20. doi: 10.1186/s40538-020-00186-4

Huang, D., Wang, Q., Jing, G. Q., Ma, M. N., Li, C., and Ma, F. W. (2021a). Overexpression of *MdIAA24* improves apple drought resistance by positively regulating strigolactone biosynthesis and mycorrhization. *Tree Physiol.* 41, 134–146. doi: 10.1093/treephys/tpaa109

Huang, D., Wang, Q., Zhang, Z. J., Jing, G. Q., Ma, M. N., Ma, F. W., et al. (2021b). Silencing *MdGH3-2/12* in apple reduces drought resistance by regulating AM colonization. *Hortic. Res.* 8:84. doi: 10.1038/s41438-021-00524-z

Hussain, S., Rao, M. J., Anjum, M. A., Ejaz, S., Zakir, I., Ali, M. A., et al. (2019). "Oxidative stress and antioxidant defense in plants under drought conditions," in *Plant Abiotic Stress Tolerance*, eds M. Hasanuzzaman, K. Hakeem, K. Nahar, and H. Alharby (Cham: Springer), 207–219. doi: 10.1007/978-3-030-06118-0_9

Igiehon, N. O., Babalola, O. O., Cheseto, X., and Torto, B. (2021). Effects of rhizobia and arbuscular mycorrhizal fungi on yield, size distribution and fatty acid of soybean seeds grown under drought stress. *Microbiol. Res.* 242:126640. doi: 10.1016/j.micres.2020.126640

Ji, L. L., Tan, W. F., and Chen, X. H. (2019). Arbuscular mycorrhizal mycelial networks and glomalin-related soil protein increase soil aggregation in Calcaric Regosol under well-watered and drought stress conditions. *Soil Till. Res.* 185, 1–8. doi: 10.1016/j.still.2018.08.010

Jiang, Y. N., Wang, W. X., Xie, Q. J., Liu, N., Liu, L. X., Wang, D. P., et al. (2017). Plants transfer lipids to sustain colonization by mutualistic mycorrhizal and parasitic fungi. *Science* 356, 1172–1175. doi: 10.1126/science.aam9970

Kandowangko, N. Y., Suryatmana, G., Nurlaeny, N., and Simanungkalit, R. D. M. (2009). Proline and abscisic acid content in droughted corn plant inoculated with *Azospirillum* sp. and arbuscular mycorrhizae fungi. *Hayati J. Biosci.* 16, 1–42. doi: 10.4308/hjb.16.1.15

Kateřina, P., Ugena, L., Lukáš, S., Karel, D., and Diego, N. D. (2019). Phytohormones and polyamines regulate plant stress responses by altering GABA pathway. *New Biotechnol.* 48, 53–65. doi: 10.1016/j.nbt.2018.07.003

Kikuchi, Y., Hijikata, N., Ohtomo, R., Handa, Y., Kawaguchi, M., Saito, K., et al. (2016). Aquaporin-mediated long-distance polyphosphate translocation directed towards the host in arbuscular mycorrhizal symbiosis: application of virus-induced gene silencing. *New Phytol.* 211, 1202–1208. doi: 10.1111/nph.14016

Kilpelainen, J., Aphalo, P. J., and Lehto, T. (2020b). Temperature affected the formation of arbuscular mycorrhizas and ectomycorrhizas in *Populus angustifolia* seedlings more than a mild drought. *Soil Biol. Biochem.* 146:107798. doi: 10.1016/j.soilbio.2020.107798

Kilpelainen, J., Aphalo, P. J., Barbero-Lopez, A., Adamczyk, B., Nipu, S. A., and Lehto, T. (2020a). Are arbuscular-mycorrhizal *Alnus incana* seedlings more resistance to drought than ectomycorrhizal and nonmycorrhizal ones? *Tree Physiol.* 40, 782–795. doi: 10.1093/treephys/tpaa035

Latef, A. A. H. A., Hashem, A., Rasool, S., Abd-Allah, E. F., Alqarawi, A. A., Egamberdieva, D., et al. (2016). Arbuscular mycorrhizal symbiosis and abiotic stress in plants: a review. *J. Plant Biol.* 59, 407–426. doi: 10.1007/s12374-016-0237-7

Lenoir, I., Fontaine, J., and Lounès-Hadj, S. A. (2016). Arbuscular mycorrhizal fungal responses to abiotic stresses: A review. *Phytochem* 123, 4–15. doi: 10.1016/j.phytochem.2016.01.002

Li, T., and Chen, B. D. (2012). Arbuscular mycorrhizal fungi improving drought tolerance of maize plants by up-regulating of aquaporin gene expressions in roots and the fungi themselves. *Chin. J. Plant Ecol.* 36, 973–981. doi: 10.3724/SP.J.1258.2012.00973

Li, F., Gao, F., and Duan, T. Y. (2016). Response and mechanism of arbuscular mycorrhizal fungi to abiotic stress. *Acta Agrestia Sin.* 24, 491–500. doi: 10.11733/j.issn.1007-0435.2016.03.003

Li, J. Q., Meng, B., Chai, H., Yang, X. C., Song, W. Z., Li, S. X., et al. (2019). Arbuscular mycorrhizal fungi alleviate drought stress in C3 (*Leymus chinensis*) and C4 (*Hemarthria altissima*) grasses via altering antioxidant enzyme activities and photosynthesis. *Front. Plant Sci.* 10:499. doi: 10.3389/fpls.2019.00499

Li, T., Hu, Y. J., Hao, Z. P., Li, H., Wang, Y. S., and Chen, B. D. (2013). First cloning and characterization of two functional aquaporin genes from an arbuscular mycorrhizal fungus *Glomus intraradices*. *New Phytol.* 197, 617–630. doi: 10.1111/nph.12011

Liang, G. T., Bu, J. W., Zhang, S. Y., Jing, G., Zhang, G. G., and Liu, X. B. (2019). Effects of drought stress on the photosynthetic physiological parameters of *Populus*×*euramericana* "Neva". *J. For. Res.* 30, 409–416. doi: 10.1007/s11676-018-0667-9

Lin, J., Wang, Y., Sun, S., Mu, C., and Yan, X. (2017). Effects of arbuscular mycorrhizal fungi on the growth, photosynthesis and photosynthetic pigments of *Leymus chinensis* seedlings under salt-alkali stress and nitrogen deposition. *Sci. Total Environ.* 576, 234–241. doi: 10.1016/j.scitotenv.2016.10.091

Liu, C. Y., Zhang, F., Zhang, D. J., Srivastava, A. K., Wu, Q. S., and Zou, Y. N. (2018). Mycorrhiza stimulates root-hair growth and IAA synthesis and transport in trifoliate orange under drought stress. *Sci. Rep.* 8:1978. doi: 10.1038/s41598-018-20456-4

Liu, F., Xu, Y., Han, G., Wang, W., Li, X., and Cheng, B. (2018). Identification and functional characterization of a maize phosphate transporter induced by mycorrhiza formation. *Plant Cell Physiol.* 59, 1683–1694. doi: 10.1093/pcp/pcy094

Liu, J., Guo, C., Chen, Z. L., He, J. D., and Zou, Y. N. (2016). Mycorrhizal inoculation modulates root morphology and root phytohormone responses in trifoliate orange under drought stress. *Emir. J. Food Agric.* 28, 251–256. doi: 10.9755/ejfa.2015-11-1044

Liu, T., Li, Z., Hui, C., Tang, M., and Zhang, H. (2016). Effect of *Rhizophagus irregularis* on osmotic adjustment, antioxidation and aquaporin pip genes expression of *Populus* × *canadensis* 'neva' under drought stress. *Acta Physiol. Plant.* 38:191. doi: 10.1007/s11738-016-2207-6

Luo, C., Sun, Q. F., Zhang, F., Zhang, D. J., Liu, C. Y., Wu, Q. S., et al. (2020). Genome-wide identification and expression analysis of the Citrus malectin domain-containing receptor-like kinases in response to arbuscular mycorrhizal fungi colonization and drought. *Hortic. Environ. Biotechnol.* 61, 891–901. doi: 10.1007/s13580-020-00273-3

Luo, Y. (2009). *The effects of AMF on cell membrane, endogenous polyamines, and salicylic acid in citrus under drought stress*. Ph. D. thesis. Wuhan: Huazhong Agriculture University.

Mahnaz, Z., Ali, E., Mohammad, S., and Sodabe, J. (2020). Alleviating effect of 24-epibrassinolide on seed oil content and fatty acid composition under drought stress in safflower sciencedirect. *J. Food Compos. Analy.* 92:103544. doi: 10.1016/j.jfca.2020.103544

Manoharan, P. T., Shanmugaiah, V., Balasubramanian, N., Gomathinayagam, S., Sharma, M. P., and Muthuchelian, K. (2010). Influence of am fungi on the growth and physiological status of *Erythrina variegata* linn. grown under different water stress conditions. *Eur. J. Soil Biol.* 46, 151–156. doi: 10.1016/j.ejsobi.2010.01.001

Marulanda, A., Porcel, R., Barea, J. M., and Azcón, R. (2007). Drought tolerance and antioxidant activities in lavender plants colonized by native drought-tolerant or drought-sensitive *Glomus* species. *Microb. Ecol.* 54, 543–552. doi: 10.1007/s00248-007-9237-y

Mathur, S., Tomar, R. S., and Jajoo, A. (2019). Arbuscular mycorrhizal fungi (AMF) protects photosynthetic apparatus of wheat under drought stress. *Photosyn. Res.* 139, 227–238. doi: 10.1007/s11120-018-0538-4

Meddich, A., Jaiti, F., Bourzik, W., Asli, A. E., and Hafidi, M. (2015). Use of mycorrhizal fungi as a strategy for improving the drought tolerance in date palm (*Phoenix dactylifera*). *Sci. Hortic.* 192, 468–474. doi: 10.1016/j.scienta.2015.06.024

Meng, L.-L., Liu, R.-C., Yang, L., Zou, Y.-N., Srivastava, A. K., Kuča, K., et al. (2021). The change in fatty acids and sugars reveals the association between trifoliate orange and endophytic fungi. *J. Fungi* 7:716. doi: 10.3390/jof7090716

Mickan, B. S., Hart, M., Solaiman, Z. M., Renton, M., Siddique, K. H. M., Jenkins, S. N., et al. (2021). Arbuscular mycorrhizal fungus-mediated interspecific nutritional competition of a pasture legume and grass under drought-stress. *Rhizosphere* 18:100349. doi: 10.1016/j.rhisph.2021.100349

Navarro-Ródenas, A., Bárzana, G., Nicolás, E., Carra, A., Schubert, A., and Morte, A. (2013). Expression analysis of aquaporins from desert truffle mycorrhizal symbiosis reveals a fine-tuned regulation under drought. *Mol. Plant-Microbe Interact.* 26, 1068–1078. doi: 10.1094/MPMI-07-12-0178-R

Navarro-Ródenas, A., Ruiz-Lozano, J. M., Kaldenhoff, R., and Morte, A. (2012). The aquaporin *TcAQP1* of the desert truffle *Terfezia claveryi* is a membrane pore water and CO_2 transport. *Mol. Plant-Microbe Interact.* 25, 259–266. doi: 10.1094/MPMI-07-11-0190

Navarro-Ródenas, A., Xu, H., Kemppainen, M., Pardo, A. G., and Zwiazek, J. J. (2015). *Laccaria bicolor* aquaporin *LbAQP1* is required for Harting net development in trembling aspen (*Populus tremuloides*). *Plant Cell Environ.* 38, 2475–2486. doi: 10.1111/pce.12552

Nouri, E., Matinizadeh, M., Moshki, A., Zolfaghari, A., Rajaei, S., and Janouskova, M. (2020). Arbuscular mycorrhizal fungi benefit drought-stressed *Salsola laricina*. *Plant Ecol.* 221, 683–694. doi: 10.1007/s11258-020-01042-z

Oldroyd, G. E. (2013). Speak, friend, and enter: signalling systems that promote beneficial symbiotic associations in plants. *Nat. Rev. Microbiol.* 11, 252–263. doi: 10.1038/nrmicro2990

Omirou, M., Ioannides, I. M., and Ehaliotis, C. (2013). Mycorrhizal inoculation affects arbuscular mycorrhizal diversity in watermelon roots, but leads to improvd colonization and plant response under water stress only. *Appl. Soil Ecol.* 63, 112–119. doi: 10.1016/j.apsoil.2012.09.013

Ozturk, M., Unal, B. T., Garcia-Caparros, P., Khursheed, A., Gul, A., and Hasanuzzaman, M. (2021). Osmoregulation and its actions during the drought stress in plants. *Physiol. Plant.* 172, 1321–1335. doi: 10.1111/ppl.13297

Pavithra, D., and Yapa, N. (2018). Arbuscular mycorrhizal fungi inoculation enhances drought stress tolerance of plants. *Groundwater Sust. Dev.* 7, 490–494. doi: 10.1016/j.gsd.2018.03.005

Pavla, D., Eva, V., and Radka, S. (2013). Arbuscular mycorrhizal symbiosis alleviates drought stress imposed on knautia arvensis plants in serpentine soil. *Plant Soil* 370, 149–161. doi: 10.1007/s11104-013-1610-7

Polcyn, W., Paluch-Lubawa, E., Lehmann, T., and Mikula, R. (2019). Arbuscular mycorrhiza in highly fertilized maize cultures alleviates short-term drougth effects but does not improve fodder yield and quality. *Front. Plant Sci.* 10:496. doi: 10.3389/fpls.2019.00496

Pons, C., Voβ, A. C., Schweiger, R., and Mulle, C. (2020). Effects of drought and mycorrhiza on wheat and aphid infestation. *Ecol. Evol.* 10, 10481–10491. doi: 10.1002/ece3.6703

Poór, P., Czékus, Z., and Ördög, A. (2019). "Role and regulation of glucose as a signal molecule to salt stress," in *Plant Signaling Molecule: Role and Regulation under Stressful Environments*, eds M. Iqbal, R. Khan, P. S. Reddy, A. Ferrante, and N. A. Khan (Cambridge: Woodhead Publishing), 193–205. doi: 10.1016/B978-0-12-816451-8.00012-5

Porcel, R., Aroca, R., Azcón, R., and Ruiz-Lozano, J. M. (2006). *PIP* aquaporin gene expression in arbuscular mycorrhizal *Glycine max* and *Lactuca sativa* plants in relation to drought stress tolerance. *Plant Mol. Biol.* 60, 389–404. doi: 10.1007/s11103-005-4210-y

Pozo, M. J., Lopez-Raez, J. A., Azcon-Aguilar, C., and Garcia-Garrido, J. M. (2015). Phytohormones as integrators of environmental signals in the regulation of mycorrhizal symbioses. *New Phytol.* 205, 1431–1436. doi: 10.1111/nph.13252

Püschel, D., Bitterlich, M., Rydlová, J., and Jansa, J. (2020). Facilitation of plant water uptake by an arbuscular mycorrhizal fungus: a Gordian knot of roots and hyphae. *Mycorrhiza* 30, 299–313. doi: 10.1007/s00572-020-00949-9

Püschel, D., Bitterlich, M., Rydlová, J., and Jansa, J. (2021). Drought accentuates the role of mycorrhiza in phosphorus uptake. *Soil Biol. Biochem.* 157:108243. doi: 10.1016/j.soilbio.2021.108243

Querejeta, J., Egerton-Warburton, L. M., and Allen, M. F. (2003). Direct nocturnal water transfer from oaks to their mycorrhizal symbionts during severe soil drying. *Oecologia* 134, 55–65. doi: 10.1007/s00442-002-1078-2

Quiroga, G., Erice, G., Aroca, R., Chaumont, F., and Ruiz-Lozano, J. M. (2017). Enhanced drought stress tolerance by the arbuscular mycorrhizal symbiosis in a drought-sensitive maize cultivar is related to a broader and differential regulation of host plant aquaporins than in a drought-tolerant cultivar. *Front. Plant Sci.* 8:1056. doi: 10.3389/fpls.2017.01056

Quiroga, G., Erice, G., Aroca, R., Delgado-Huertas, A., and Ruiz-Lozano, J. M. (2020a). Elucidating the possible involvement of maize aquaporins and arbuscular mycorrhizal symbiosis in the plant ammonium and urea transport under drought stress conditions. *Plants* 9:148. doi: 10.3390/plants9020148

Quiroga, G., Erice, G., Aroca, R., Zamarreño, A. M., García-Mina, J. M., and Ruiz-Lozano, J. M. (2018). Arbuscular mycorrhizal symbiosis and salicylic acid regulate aquaporins and root hydraulic properties in maize plants subjected to drought. *Agric. Water Manage.* 202, 271–284. doi: 10.1016/j.agwat.2017.12.012

Quiroga, G., Erice, G., Aroca, R., Zamarreño, A. M., García-Mina, J. M., and Ruiz-Lozano, J. M. (2020b). Radial water transport in arbuscular mycorrhizal maize plants under drought stress conditions is affeced by indole-acetic acid (IAA) application. *J. Plant Physiol.* 246-247:153115. doi: 10.1016/j.jplph.2020.153115

Quiroga, G., Erice, G., Ding, L., Chaumont, F., Aroca, R., and Ruiz-Lozano, J. M. (2019). The arbuscular mycorrhizal symbiosis regulates aquaporins activity and improves root cell water permeability in maize plants subjected to water stress. *Plant Cell Environ.* 42, 2274–2290. doi: 10.1111/pce.13551

Rani, B., Madan, S., Sharma, K. D., Pooja, and Kumar, A. (2018). Influence of arbuscular mycorrhiza on antioxidative system of wheat (*Triticum aestivum*) under drought stress. *Ind. J. Agric. Sci.* 88, 289–295.

Rapparini, F., and Peñuelas, J. (2014). "Mycorrhizal fungi to alleviate drought stress on plant growth," in *Use of Microbes for the Alleviation of Soil Stresses*, ed. M. Miransari (New York, NY: Springer), 165–174. doi: 10.1007/978-1-4614-9466-9_2

Remke, M. J., Johnson, N. C., Wright, J., Williamson, M., and Bowker, M. A. (2021). Sympatric pairings of dryland grass populations, mycorrhizal fungi and associated soil biota enhance mutualism and ameliorate drought stress. *J. Ecol.* 109, 1210–1223. doi: 10.1111/1365-2745.13546

Rivero, J., Alvarez, D., Flors, V., Azcon-Aguilar, C., and Pozo, M. J. (2018). Root metabolic plasticity underlies functional diversity in mycorrhiza-enhanced stress tolerance in tomato. *New Phytol.* 220, 1322–1336. doi: 10.1111/nph.15295

Ruiz-Lozano, J. M., and Aroca, R. (2010a). "Host response to osmotic stresses: stomatal behaviour and water use efficiency of arbuscular mycorrhizal plants," in *Arbuscular Mycorrhizas: Physiology and Function*, eds H. Koltai and Y. Kapulnik (Dordrecht: Springer), 239–256. doi: 10.1007/978-90-481-9489-6_11

Ruiz-Lozano, J. M., and Aroca, R. (2010b). "Modulation of aquaporin genes by the arbuscular mycorrhizal symbiosis in relation to osmotic stress tolerance," in *Symbioses and Stress. Cellular Origin, Life in Extreme Habitats and Astrobiology*, eds J. Seckbach and M. Grube (Dordrecht: Springer), 357–374.

Ruiz-Lozano, J. M., Porcel, R., and Aroca, R. (2008). "Evaluation of the possible participation of drought-induced genes in the enhanced tolerance of arbuscular mycorrhizal plants to water deficit," in *Mycorrhiza: State of the Art, Genetics and Molecular Biology, Eco-Function, Biotechnology, Eco-Physiology, Structure and Systematics,* ed. A. Varma (Berlin: Springer), 185–205. doi: 10.1007/978-3-540-78826-3_10

Salloum, M. S., Menduni, M. F., Benavides, M. P., Larrauri, M., Luna, C. M., and Silvente, S. (2018). Polyamines and flavonoids: key compounds in mycorrhizal colonization of improved and unimproved soybean genotypes. *Symbiosis* 76, 265–275. doi: 10.1007/s13199-018-0558-z

Sanchez-Romera, B., Calvo-Polanco, M., Ruiz-Lozano, J. M., Zamarreno, A. M., Arbona, V., Garcia-Mina, J. M., et al. (2018). Involvement of the *def-1* mutation in the response to tomato plants to arbuscular mycorrhizal symbiosis under well-watered and drought conditions. *Plant Cell Physiol.* 59, 248–261. doi: 10.1093/pcp/pcx178

Sannazzaro, A., Echeverria, M., Olberto, E. O., Ruiz, O. A., and Menendez, A. B. (2007). Modulation of polyamine balance in Lotus glaber by salinity and arbuscular mycorrhiza. *Plant Physiol. Biochem.* 45, 39–46. doi: 10.1016/j.plaphy.2006.12.008

Schüβler, A., Schwarzott, D., and Walker, C. (2001). A new fungal phylum, the Glomeromycota: phylogeny and evolution. *Mycol. Res.* 105, 1413–1421. doi: 10.1017/S0953756201005196

Sendek, A., Karakoc, C., Wagg, C., Dominguez-Begines, J., do Couto, G. M., van der Heijden, M. G. A., et al. (2019). Drought modulates interactions between arbuscular mycorrhizal fungal diversity and barley genotype diversity. *Sci. Rep.* 9:9650. doi: 10.1038/s41598-019-45702-1

Sepahvand, T., Etemad, V., Matinizade, M., and Shirvany, A. (2021). Symbiosis of AMF with growth modulation and antioxidant capacity of Caucasian Hackberry (*Celtis Caucasica* L.) seedlings under drought stress. *Cent. Asian J. Environ. Sci. Technol. Innov.* 2, 20–35. doi: 10.22034/CAJESTI.2021.01.03

Shinozaki, K., and Yamaguchi-Shinozaki, K. (2007). Gene networks involved in drought stress response and tolerance. *J. Exp. Bot.* 58, 221–227. doi: 10.1093/jxb/erl164

Shu, B., Cai, D., Zhang, F., Zhang, D. J., Liu, C. Y., Wu, Q. S., et al. (2020a). Identifying citrus *CBL* and *CIPK* gene families and their expressions in response to drought and arbuscular mycorrhizal fungi colonization. *Biol. Plant.* 64, 773–783. doi: 10.32615/bp.2020.123

Shu, B., Jue, D. W., Zhang, F., Zhang, D. J., Liu, C. Y., Wu, Q. S., et al. (2020b). Genome-wide identification and expression analysis of the citrus calcium-dependent protein kinase (CDPK) genes in response to arbuscular mycorrhizal fungi colonization and drought. *Biotechnol. Biotechnol. Equip.* 34, 1304–1314. doi: 10.1080/13102818.2020.1837011

Song, H. X. (2005). Effects of vam on host plant in the condition of drought stress andits mechanisms. *Genomics* 5, 91–99. doi: 10.1016/0888-7543(89)90091-8

Sugiura, Y., Tanaka, S., Yano, K., Kameoka, H., Marui, S., et al. (2020). Myristate can be used as a carbon and energy source for the asymbiotic growth of arbuscular mycorrhizal fungi. *Proc. Natl. Acad. Sci. U S A.* 117, 25779–25788. doi: 10.1073/pnas.2006948117

Sylvia, D. M., and Williams, S. E. (1992). "Vesicular-arbuscular mycorrhizae and environmental stress," in *Mycorrhizae in Sustainable Agriculture*, eds G. T. Bethlenfalvay and R. D. Linderman (Madison, WI: ASA Special Publication), 101–124. doi: 10.2134/asaspecpub54.c5

Symanczik, S., Lehmann, M. F., Wiemken, A., Boller, T., and Courty, P. E. (2018). Effects of two contrasted arbuscular mycorrhizal fungal isolates on nutrient uptake by *Sorghum bicolor* under drought. *Mycorrhiza* 28, 779–785. doi: 10.1007/s00572-018-0853-9

Tisserant, E., Malbreil, M., Kuo, A., Kohler, A., Symeonidi, A., Balestrini, R., et al. (2013). Genome of an arbuscular mycorrhizal fungus provides insight into the oldest plant symbiosis. *Proc. Natl. Acad. Sci. U S A.* 110, 20117–20122. doi: 10.1073/pnas.1313452110

Valentine, A. J., Mortimer, P. E., Lintnaar, M., and Borgo, R. (2006). Drought responses of arbusuclar mycorrhizal grapevines. *Symbiosis* 41, 127–133. doi: 10.3390/jof7090686

van der Heijden, M. G. A., Martin, F. M., Selosse, M. A., and Sanders, I. R. (2015). Mycorrhizal ecology and evolution: the past, the present, and the future. *New Phytol.* 205, 1406–1423. doi: 10.1111/nph.13288

Vasar, M., Davison, J., Sepp, S. K., Opik, M., Moora, M., Koorem, K., et al. (2021). Arbuscular mycorrhizal fungal communities in the soils of desert habitats. *Microorganims* 9:229. doi: 10.3390/microorganisms9020229

Vergani, C., and Graf, F. (2016). Soil permeability, aggregate stability and root growth: a pot experiment from a soil bioengineering perspective. *Ecohydrology* 9, 830–842. doi: 10.1002/eco.1686

Volpe, V., Chitarra, W., Cascone, P., Volpe, M. G., Bartolini, P., Moneti, G., et al. (2018). The association with two different arbuscular mycorrhizal fungi differently affects water stress tolerance in tomato. *Front. Plant Sci.* 9:1840. doi: 10.3389/fpls.2018.01480

Wu, H. H., Zou, Y. N., Rahman, M. M., Ni, Q. D., and Wu, Q. S. (2017). Mycorrhizas alter sucrose and proline metabolism in trifoliate orange exposed to drought stress. *Sci. Rep.* 7:42389. doi: 10.1038/srep42389

Wu, Q. S., and Xia, R. (2006b). Effects of arbuscular mycorrhizal fungi on leaf solutes and root absorption areas of trifoliate orange seedlings under water stress conditions. *Front. For. Chin.* 1:312–317. doi: 10.1007/s11461-006-0035-3

Wu, Q. S., and Xia, R. X. (2006a). Arbuscular mycorrhizal fungi influence growth, osmotic adjustment and photosynthesis of citrus under well-watered and water stress conditions. *J. Plant Physiol.* 163, 417–425. doi: 10.1016/j.jplph.2005.04.024

Wu, Q. S., and Zou, Y. N. (2009). Mycorrhizal influence on nutrient uptake of citrus exposed to drought stress. *Philipp. Agric.* 92, 33–38. doi: 10.1002/jsfa.3501

Wu, Q. S., and Zou, Y. N. (2017). "Arbuscular mycorrhizal fungi and tolerance of drought stress in plants," in *Arbuscular Mycorrhizas and Stress Tolerance of Plants*, ed. Q. S. Wu (Singapore: Springer), 25–41. doi: 10.1007/978-981-10-4115-0_8

Wu, Q. S., He, J. D., Srivastava, A. K., Zou, Y. N., and Kuča, K. (2019). Mycorrhizas enhance drought tolerance of citrus by altering root fatty acid compositions and their saturation levels. *Tree Physiol.* 39, 1149–1158. doi: 10.1093/treephys/tpz039

Wu, Q. S., Srivastava, A. K., and Zou, Y. N. (2013). AMF-induced tolerance to drought stress in citrus: a review. *Sci. Hortic.* 164, 77–87. doi: 10.1016/j.scienta.2013.09.010

Wu, Q. S., Zou, Y. N., and He, X. H. (2010a). Exogenous putrescine, not spermine or spermidine, enhances root mycorrhizal development and plant growth of trifoliate orange (*Poncirus trifoliata*) seedlings. *Int. J. Agric. Biol.* 12, 576–580. doi: 10.1016/j.compag.2010.03.005

Wu, Q. S., Zou, Y. N., Zhan, T. T., and Liu, C. Y. (2010b). Polyamines participate in mycorrhizal and root development of citrus (*Citrus tangerine*) seedlings. *Not. Bot. Horti Agrobot.* 38, 25–31. doi: 10.1111/J.1364-3703.2010.00617.X

Xie, W., Hao, Z. P., Zhou, X. F., Jiang, X. L., Xu, L. J., Wu, S. L., et al. (2018). Arbuscular mycorrhiza facilitates the accumulation of glycyrrhizin and liquiritin in *Glycyrrhiza uralensis* under drought stress. *Mycorrhiza* 28, 285–300. doi: 10.1007/s00572-018-0827-y

Xu, L. J., Hao, Z. P., Xie, W., Li, F., and Chen, B. D. (2018a). Transmembrane H^+ and Ca^{2+} fluxes through extraradical hyphae of arbuscular mycorrhizal fungi in response to drought stress. *Chin. J. Plant Ecol.* 42, 764–773. doi: 10.17521/cjpe.2018.0089

Xu, L. J., Li, T., Wu, Z. X., Feng, H. Y., Yu, M., Zhang, X., et al. (2018b). Arbuscular mycorrhiza enhances drought tolerance of tomato plants by regulating the 14-3-3 genes in the ABA signaling pathway. *Appl. Soil Ecol.* 125, 213–221. doi: 10.1016/j.apsoil.2018.01.012

Yao, Q., Wang, L. R., Xing, Q. X., Chen, J. Z., and Zhu, H. H. (2010). Exogenous polyamines influence root morphogenesis and arbuscular mycorrhizal development of *Citrus limonia* seedlings. *Plant Growth Regul.* 60, 27–33. doi: 10.1007/s10725-009-9415-7

Ye, J. S., Li, T., Hu, Y. J., Hao, Z. P., Gao, Y. Z., Wang, Y. S., et al. (2013). Influences of AM fungi on plant growth and water-stable soil aggregates under drought stresses. *Acta Ecol. Sin.* 33, 1080–1090. doi: 10.5846/stxb201205140707

Yooyongwech, S., Phaukinsang, N., Cha-Um, S., and Supaibulwatana, K. (2013). Arbuscular mycorrhiza improved growth performance in *Macadamia tetraphylla* L. grown under water deficit stress involves soluble sugar and proline accumulation. *Plant Growth Regul.* 69, 285–293. doi: 10.1007/s10725-012-9771-6

Yooyongwech, S., Samphumphuang, T., Tisarum, R., Theerawitaya, C., and Cha-Um, S. (2016). Arbuscular mycorrhizal fungi (AMF) improved water deficit tolerance in two different sweet potato genotypes involves osmotic adjustments via soluble sugar and free proline. *Sci. Hortic.* 198, 107–117. doi: 10.1016/j.scienta.2015.11.002

Zézél, A., Brou, Y. C., Meddich, A., and Marty, F. (2008). Molecular identification of MIP genes expressed in the roots of an arbuscular mycorrhizal *Trifolium alexandrium* L. under water stress. *Afr. J. Agric. Res.* 3, 78–83. doi: 10.1021/jf072612

Zhang, C. X., Meng, S., Li, M. J., and Zhao, Z. (2016). Genomic identification and expression analysis of the phosphate transporter gene family in poplar. *Front. Plant Sci.* 7:1398. doi: 10.3389/fpls.2016.01398

Zhang, F., Ni, Q. D., Zou, Y. N., Wu, Q. S., and Huang, Y. M. (2017). Preliminary study on the mechanism of AMF in enhancing the drought tolerance of plants. *J. Fungal Res.* 15, 8–13. doi: 10.13341/j.jfr.2014.1702

Zhang, F., Zou, Y. N., and Wu, Q. S. (2018). Quantitative estimation of water uptake by mycorrhizal extraradical hyphae in citrus under drought stress. *Sci. Hortic.* 229, 132–136. doi: 10.1016/j.scienta.2017.10.038

Zhang, F., Zou, Y. N., Wu, Q. S., and Kuča, K. (2020). Arbuscular mycorrhizas modulate root polyamine metabolism to enhance drought tolerance of trifoliate orange. *Environ. Exp. Bot.* 171, 103926. doi: 10.1016/j.envexpbot.2019.103926

Zhang, H. Y., Duan, W. X., Xie, B. T., Dong, S. X., Wang, B. Q., Shi, C. Y., et al. (2018). Effects of drought stress at different growth stages on endogenous hormones and its relationship with storage root yield in sweet potato. *Acta Agron. Sin.* 44, 126–136. doi: 10.3724/SP.J.1006.2018.00126

Zhang, T., Hu, Y. J., Zhang, K., Tian, C. Y., and Guo, J. X. (2018). Arbuscular mycorrhizal fungi improve plant growth of *Ricinus communis* by altering photosynthetic properties and increasing pigments under drought and salt stress. *Indust. Crop. Prod.* 117, 13–19. doi: 10.1016/j.indcrop.2018.02.087

Zhang, Y. M., Ma, K. M., Li, F. L., and Qu, L. Y. (2016). Arbuscular mycorrhizal fungi (AMF) promotes *Bauhinia faberi* var. microphylla seedling growth under drought stress conditions. *Acta Ecol. Sin.* 36, 3329–3337. doi: 10.5846/stxb201506291320

Zhang, Z., Zhang, J., Xu, G., Zhou, L., and Li, Y. (2018). Arbuscular mycorrhizal fungi improve the growth and drought tolerance of *Ze*nia insignis seedlings under drought stress. *New For.* 50, 593–604. doi: 10.1007/s11056-018-9681-1

Zhao, R., Guo, W., Bi, N., Guo, J., and Zhang, J. (2015). Arbuscular mycorrhizal fungi affect the growth, nutrient uptake and water status of maize (*Zea mays* L.) grown in two types of coal mine spoils under drought stress. *Appl. Soil Ecol.* 88, 41–49. doi: 10.1016/j.apsoil.2014.11.016

Zheng, F. L., Liang, S. M., Chu, X. N., Yang, Y. L., and Wu, Q. S. (2020). Mycorrhizal fungi enhance flooding tolerance of peach through inducing proline accumulation and improving root architecture. *Plant Soil Environ.* 66, 624–631. doi: 10.17221/520/2020-PSE

Zhu, X. Q., Wang, C. Y., Chen, H., and Tang, M. (2014). Effects of arbuscular mycorrhizal fungi on photosynthesis, carbon content, and calorific value of black locust seedlings. *Photosynthetica* 52, 247–252. doi: 10.1007/s11099-014-0031-z

Zou, Y. N., Srivastava, A. K., Wu, Q. S., and Huang, Y. M. (2014). Glomalin-related soil protein and water relations in mycorrhizal citrus (*Citrus tangerina*) during soil water deficit. *Arch. Agron. Soil Sci.* 60, 1103–1114. doi: 10.1080/03650340.2013.867950

Zou, Y. N., Wang, P., Liu, C. Y., Ni, Q. D., Zhan, D. J., and Wu, Q. S. (2017). Mycorrhizal trifoliate orange has greater root adaptation of morphology and phytohormones in response to drought stress. *Sci. Rep.* 7:41134. doi: 10.1038/srep41134

Zou, Y. N., Wu, H. H., Giri, B., Wu, Q. S., and Kuča, K. (2019). Mycorrhizal symbiosis down-regulates or does not change root aquaporin expression in trifoliate orange under drought stress. *Plant Physiol. Biochem.* 144, 292–299. doi: 10.1016/j.plaphy.2019.10.001

Zou, Y. N., Wu, Q. S., and Kuča, K. (2021a). Unravelling the role of arbuscular mycorrhizal fungi in mitigating the oxidative burst of plants under drought stress. *Plant Biol.* 23, 50–57. doi: 10.1111/plb.13161

Zou, Y. N., Wu, Q. S., Huang, Y. M., Ni, Q. D., and He, X. H. (2013). Mycorrhizal-mediated lower proline accumulation in *Poncirus trifoliata* under water deficit derives from the integration of inhibition of proline synthesis with increase of proline degradation. *PLoS One* 8:e80568. doi: 10.1371/journal.pone.0080568

Zou, Y. N., Zhang, F., Srivastava, A. K., Wu, Q. S., and Kuèa, K. (2021b). Arbuscular mycorrhizal fungi regulate polyamine homeostasis in roots of trifoliate orange for improved adaptation to soil moisture deficit stress. *Front. Plant Sci.* 11:600792. doi: 10.3389/fpls.2020.600792

Conflict of Interest: The authors declare that the research was conducted in the absence of any commercial or financial relationships that could be construed as a potential conflict of interest.

Publisher's Note: All claims expressed in this article are solely those of the authors and do not necessarily represent those of their affiliated organizations, or those of the publisher, the editors and the reviewers. Any product that may be evaluated in this article, or claim that may be made by its manufacturer, is not guaranteed or endorsed by the publisher.

frontiers in Microbiology

MINI REVIEW
published: 11 January 2022
doi: 10.3389/fmicb.2021.751794

Plant-Soil Feedbacks for the Restoration of Degraded Mine Lands: A Review

Shi-Chen Zhu[1,2,3], Hong-Xiang Zheng[1,2,3], Wen-Shen Liu[1,2,3], Chang Liu[1,2,3,4], Mei-Na Guo[1,2,3,4], Hermine Huot[5], Jean Louis Morel[4], Rong-Liang Qiu[1,6,7], Yuanqing Chao[1,2,3] and Ye-Tao Tang[1,2,3]**

[1] School of Environmental Science and Engineering, Sun Yat-sen University, Guangzhou, China, [2] Guangdong Provincial Key Laboratory of Environmental Pollution Control and Remediation Technology, Guangzhou, China, [3] Guangdong Provincial Engineering Research Center for Heavy Metal Contaminated Soil Remediation, Sun Yat-sen University, Guangzhou, China, [4] Laboratoire Sols et Environnement, INRAE-Universitei de Lorraine, Vandoeuvre-leìs-Nancy, France, [5] CNRS, LIEC, Université de Lorraine, Nancy, France, [6] Guangdong Provincial Key Laboratory of Agricultural and Rural Pollution Abatement and Environmental Safety, College of Natural Resources and Environment, South China Agricultural University, Guangzhou, China, [7] Guangdong Laboratory for Lingnan Modern Agriculture, Guangzhou, China

OPEN ACCESS

Edited by:
Xun Wen Chen, Southern University of Science and Technology, China

Reviewed by:
Luo Xiaobo, Jinan University, China
Xianjin Tang, Zhejiang University, China

***Correspondence:**
Yuanqing Chao
chaoyuanq@mail.sysu.edu.cn
Ye-Tao Tang
eestyt@mail.sysu.edu.cn

Specialty section:
This article was submitted to Terrestrial Microbiology, a section of the journal Frontiers in Microbiology

Received: *02 August 2021*
Accepted: *17 December 2021*
Published: *11 January 2022*

Citation:
Zhu S-C, Zheng H-X, Liu W-S, Liu C, Guo M-N, Huot H, Morel JL, Qiu R-L, Chao Y and Tang Y-T (2022) Plant-Soil Feedbacks for the Restoration of Degraded Mine Lands: A Review. Front. Microbiol. 12:751794. doi: 10.3389/fmicb.2021.751794

Much effort has been made to remediate the degraded mine lands that bring severe impacts to the natural environments. However, it remains unclear what drives the recovery of biodiversity and ecosystem functions, making the restoration of these fragile ecosystems a big challenge. The interactions among plant species, soil communities, and abiotic conditions, i.e., plant-soil feedbacks (PSFs), significantly influence vegetation development, plant community structure, and ultimately regulate the recovery of ecosystem multi-functionality. Here, we present a conceptual framework concerning PSFs patterns and potential mechanisms in degraded mine lands. Different from healthy ecosystems, mine lands are generally featured with harsh physical and chemical properties, which may have different PSFs and should be considered during the restoration. Usually, pioneer plants colonized in the mine lands can adapt to the stressful environment by forming tolerant functional traits and gathering specific soil microbial communities. Understanding the mechanisms of PSFs would enhance our ability to predict and alter both the composition of above- and below-ground communities, and improve the recovery of ecosystem functions in degraded mine lands. Finally, we put forward some challenges of the current PSFs study and discuss avenues for further research in the ecological restoration of degraded mine lands.

Keywords: plant-soil interactions, degraded mine lands, ecological restoration, plant functional traits, ecosystem functions, soil community

INTRODUCTION

In the terrestrial ecosystem, plants alter their surrounding biotic and abiotic soil conditions through root- and litter-induced effects, which in turn influence the growth, productivity, and generation of the coexistent and subsequent plants. This is called plant-soil feedbacks (PSFs) (Wardle et al., 2004; van der Putten et al., 2013). Increasing attention has been paid to PSFs due to their contribution to plant community dynamics and ecosystem functioning regulation. Until now, most of the studies

on plant-soil interactions have focused on uncontaminated natural systems, like tropical forests and temperate grasslands, or agricultural systems (Mariotte et al., 2018). In those ecosystems, most PSFs researches aim to understand the process of plant succession dynamics (Kardol et al., 2006, 2013; van de Voorde et al., 2011), plant expansion and invasion (van Grunsven et al., 2010), plant community composition maintaining (Mangan et al., 2010; Dassen et al., 2017; Teste et al., 2017), and biotic responses toward human-induced global land use and climate changes (Geisen et al., 2017; Fry et al., 2018a; Pugnaire et al., 2019). Even though the degraded mine lands pose obvious threats to the environment, relatively few studies have focused on the PSFs at these sites (Krumins et al., 2015; Jia et al., 2020). According to the facilitating or inhibiting effects toward the adaptive performance and monopolization of conspecifics, PSFs are considered positive, negative, or neutral (van der Putten et al., 2013). Generally, PSFs is considered positive when it improves the growth of contemporaneous or later plants. The PSFs direction may have significant differences during primary and secondary succession. For example, at the beginning of primary succession, positive feedbacks by nursing plants are critical for ameliorating the harsh conditions and motivating the natural colonization of multiple plant species (Reynolds et al., 2003). While in the earlier stages of a secondary succession that starts with a certain soil legacy, negative PSFs caused by rhizosphere pathogen can stimulate species turnover (Kardol et al., 2013; Cortois et al., 2016). However, compared to studies in secondary succession, the knowledge of PSFs patterns and driving factors during the primary succession in mine lands is still in its infancy.

Degraded mine lands are generally provided with a sparse density of vegetation, soil compaction and acidification, heavy metal toxicity, and nutrient deficiency (Boyer and Wratten, 2010; Hu et al., 2012), which may alter the dynamics and outcomes of plant-soil interactions. In order to colonize in mine lands, tolerant plants should be equipped with some species-specific functional traits to adapt to extreme conditions, thus inducing more uncertainties to the performance of PSFs. Soil communities (e.g., bacteria, fungi, protists, and invertebrates) play key roles in influencing the soil environment, buffering plant individuals and harsh soil abiotic conditions, and altering the composition of the above-ground community. To recover biodiversity and ecosystem multifunctionality, we need to explore and follow the laws of nature. A better understanding of the patterns and driving factors of PSFs during the ecological restoration processes would help us to accelerate the recovery of vegetation and soil properties and finally achieve ecosystem multifunctionality.

Here, we address plant-soil feedbacks based on soil properties, plant functional traits, and soil communities in contaminated mine tailings and discuss their consequences for the ecosystem functioning and potential remediation practices. We first describe the current situation and obstacles for ecological restoration of mine lands, then focus on how plant and soil communities interact under harsh conditions. We also review the litter- and rhizosphere-induced PSFs based on multiple plant functional traits and the interactions with associated microorganisms for the tolerant plants established in mine areas. Moreover, we discuss how the understanding of PSFs plays a pivotal role in accelerating the recovery of ecosystem functions including pollutant control, primary productivity, decomposition, nutrient availability, and cycling. In the end, we summarize the challenges and prospects of PSFs study in abandoned mining areas, emphasizing more efforts should be made to fulfill the imperative knowledge and practical gaps.

CURRENT SITUATIONS OF MINE LANDS RESTORATION

Mining activities not only clear above-ground vegetation and damage soil communities but also leave behind large areas of waste, i.e., tailings (Bradshaw, 1997; Hu et al., 2012). These lands are usually featured with compaction, erosion, and desertification of soil, accumulation and pollution of toxic metals, deficiency of nutrient and organic matter, and loss of biodiversity (Boyer and Wratten, 2010; Hu et al., 2012; Wang et al., 2018). Therefore, the development of ecosystems in mine lands can be categorized as a primary succession that commonly needs 50 to 100 years to gain a fundamental vegetation establishment *via* natural processes (Bradshaw, 1997; Li and Liber, 2018). Consequently, different kinds of human interventions (Gastauer et al., 2018) have been developed to accelerate ecological recovery. However, there are still many problems that need to be further considered.

When conducting the restoration of degraded mine lands, it is imperative to improve the physical and chemical environment, eliminate the threats to life health, recover the assemblage of functional species groups, and ultimately achieve the structurally and functionally self-sustaining ecosystems (Society For Ecological Restoration International Science [SER], and Policy Working Group, 2004; Lei et al., 2016). One of the most effective ways to attenuate the soil quality and address ecological restoration is revegetation in such barren lands (Mukhopadhyay et al., 2017; Li and Liber, 2018). However, because of the low level of soil available nutrients and high level of metal toxicity, few plant species can survive in these areas (Li and Liber, 2018; Wang et al., 2018). Additionally, the selection of promising plants is difficult when considering biological invasion risks (Gaertner et al., 2012; Nussbaumer et al., 2016). Some passive or improper managements probably import invasive species at the beginning of restoration (Bauman et al., 2015), while they may hinder the colonization of native species (Davis et al., 2005), resulting in low biodiversity and an unstable ecosystem (Schwenke et al., 2000; Hamman and Hawkes, 2013; Bauman et al., 2015). Furthermore, numerous restoration projects failed to meet the objective of environmental sustainability (Lamb et al., 2015), as the trajectory of succession altered and the diversity of reconstructed plants community declined with time (Schneemann and McElhinny, 2012). For example, the improper combination of species and revegetation management like continual sowing enhanced individual competition and limited the survival of some species (Neldner and Ngugi, 2017).

During the ecological restoration of degraded mine lands, the assistance of the below-ground community cannot be ignored (Grandlic et al., 2009; Rajkumar et al., 2012; Hao et al., 2014; Ullah et al., 2015; Wang, 2017). As an important component of the

ecosystem, soil organisms affect terrestrial ecosystem functions by regulating soil acidity, mediating soil carbon dynamic, stabilizing toxic pollutants, and promoting element cycling (Chen et al., 2016; Fierer, 2017; Sun et al., 2017, 2018b). In a mine land co-contaminated with arsenic (As) and antimony (Sb), the potential tolerant bacteria *Bradyrhizobium*, *Sphingomonas*, *Nocardioides*, *Burkholderia*, and *Streptomyces* induced As and Sb biogeochemical cycling, as well as contributed to the cycling of C (C fixation), N (nitrate/nitrite, N fixation), and S (sulfate reduction) (Li et al., 2021). The rhizospheric microbes serve as an important assistor for plants to survive in harsh environments (Grandlic et al., 2009; Mishra et al., 2017; Sun et al., 2018b). However, the survival and composition of soil microbiome are largely dependent on soil environment factors like soil pH (Lauber et al., 2009), available nitrogen (Cederlund et al., 2014), soil organic carbon (Sul et al., 2013), redox status (Pett-Ridge and Firestone, 2005), and especially heavy metal content and availability (Singh et al., 2019). Technical problems of improper bacteria carriers and poor production of bacteria biomass can lead to insufficient buildup and rapid decline of the plant growth promoting bacteria (PGPB) population during practical inoculation (Bashan et al., 2014). Additionally, it is more efficient to formulate and apply multi-strain inoculants compared to single-strain ones, but the premise is that we have a thorough understanding of the adaptability of microorganisms to the stress environment, the compatibility among microbial populations, and the symbiosis and interaction with plants (Bashan et al., 2014).

Plenty of studies have utilized plant-microbe association in mine lands bioremediation, but few of them have figured out how PSFs influence ecological succession, leading to incomplete and unsustainable remediation. As the intensive interactions and complexity of cooperation among plants and soil biotic and abiotic components (Krumins et al., 2015), it is usually inefficient to execute restoration schemes for degraded mine lands without addressing the underlying processes and mechanisms of above-below ground linkage (Li and Liber, 2018). Only the mechanisms of plant-soil interactions in degraded mine lands are revealed, can we make significant progress on precisely ameliorating stressed conditions in mine areas and facilitating the restoration of the plant community and even the whole ecosystem functioning.

PLANT-SOIL FEEDBACKS IN DEGRADED MINE LANDS

Plant-soil feedbacks can be affected by soil physical, chemical, and biogeochemical properties. As shown in **Figure 1**, the severe soil properties of the degraded mine lands impede the establishment of plant community and alter the composition of the soil biological community. Once the pioneers colonize, the plants and microbes, in turn, ameliorate the soil conditions. Meanwhile, a mutual influence also exists between plants and soil communities (Krumins et al., 2015). Generally, plant-associated soil biota that shapes PSFs can be divided into three categories: enemies like microbial pathogens, symbionts like mycorrhizal fungi and nitrogen-fixing rhizobia, and decomposers like saprophytes (van der Putten et al., 2016). They are the main biotic determinants of the direction (positive, neutral, or negative) and the strength (mild or strong) of PSFs (Wardle, 2013; van der Putten et al., 2016). The pioneer plants equipped with special functional traits are experiencing and modifying the environment with those associated soil biota. The possible responses of the PSFs toward these extreme factors are reviewed as follows.

Responses of Plant-Soil Feedbacks Toward Extreme Conditions

Physical Properties

Due to the scattered or bare vegetation, the soils of the degraded mine lands are always compacted and suffer from either drought or excessive wetness (Bradshaw, 1983). Both too dry and too wet conditions impair plant growth and soil biota survival (Bradshaw, 1997). It has been reported that changes in soil community composition induced by drought can cause negative PSFs to plant species and finally alter plant-plant interactions (Kaisermann et al., 2017). The soil compaction usually produces hardened layers and anaerobic conditions, which is not conducive for plant rooting and brings negative feedbacks to the plant and soil community (Boyer and Wratten, 2010). Besides, the desertification of tailing soil probably causes soil erosion and hinders plant establishment (Zhou et al., 2015). However, some pioneer soil organisms like soil fauna and microorganisms may induce positive PSFs. Among the soil fauna, earthworms are important candidates for attenuating compaction and water retention conditions. They can increase soil macroporosity and soil aggregation by burrowing activity (Boyer and Wratten, 2010). The dry-adapted microorganisms tend to mitigate the drought effects and facilitate seed germination, seedling development, and biomass production (O'Brien et al., 2018). The soil physical stresses tend to be gradually mitigated by plant covering, rooting, and aggregating functions (Li et al., 2013).

Chemical and Biogeochemical Properties

Metal toxicity is one of the most critical factors limiting above- and below-ground lives (Kang et al., 2020). Negative correlations have been found between soil microbial activity and soil extractable heavy metal concentrations (Wang et al., 2007). It is supposed that the capability of plant tolerance to toxic metals and the acceptance of positive feedbacks from soil mutualisms determine the existence and composition of plant communities (Krumins et al., 2015). Tolerant plants may attract and foster oligotrophic and metal-tolerant communities in the rhizosphere through a variety of organic and inorganic exudates (Borymski et al., 2018). Rhizosphere microorganisms would alleviate the detrimental effects of metal toxicity for plants through some biological processes, including complexation by organic acids and siderophores (Schalk et al., 2011), stabilization by secreting extracellular polymeric substances (Ahonen-Jonnarth et al., 2000; Joshi and Juwarkar, 2009), and increasing plant antioxidative defense by producing 1-aminocyclopropane-1-carboxylic acid (ACC) deaminase (Gao et al., 2010). Low pH stress in mine lands can cause negative feedbacks to the biotic community directly

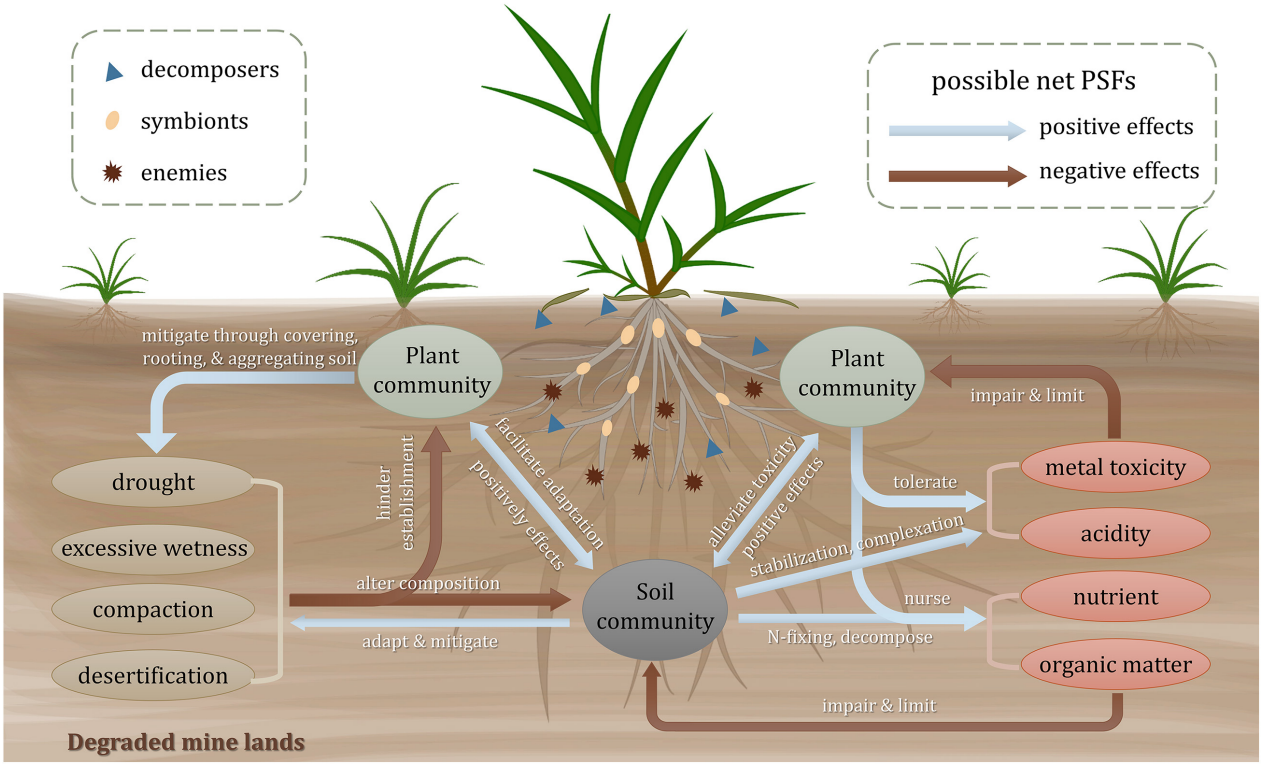

FIGURE 1 | Plant-soil interactions in degraded mine lands. Arrows in the plant-soil systems present the possible net plant-soil feedbacks among soil abiotic properties, plant and soil community, with red arrows for negative feedbacks and blue arrows for positive feedbacks. For ellipses in different colors, green ones represent plant communities, gray ones represent soil community, yellow ones represent physical properties, and red ones represent chemical and biogeochemical properties, respectively. Different graphics in the plant rhizosphere represent three groups of soil biota including enemies, symbionts, and decomposers depending on different shapes.

and indirectly. For one thing, the research on a massive copper mine tailings showed that the increase of acidity arouses the reduction of overall microbiome diversity and relative abundance of dominant assemblages (Liu et al., 2014; Shanmugam and Kingery, 2018). The abundance of soil protozoan taxa is also proved to be regulated by soil pH (Xu et al., 2022). For another, the availability of metals in acid soils is often higher than those in neutral or calcareous soil, which enhances the toxic effect of heavy metals on plant and soil communities. The lack of nutrients and organic matter limits the development of plant communities (Li and Liber, 2018). Some mutualistic symbioses like arbuscular mycorrhizal fungi (AMF) can provide significant assistance for plants to deal with nutrient deficiency *via* AM nutrient uptake pathway (Smith et al., 2010). The nitrogen supplied by diazotrophic communities facilitates the establishment of microbial and the growth of plants in tailings (Sun et al., 2020). The presence of nursing plants like legumes can increase the input of nitrogen through the N-fixing capacity of rhizobia in the rhizosphere, which improves below-ground nitrogen cycling and brings positive feedbacks for later successional plants (del Moral and Rozzell, 2005; Ren et al., 2008). Pioneer plants tend to modify soil fertility conditions beneath their canopy by litter input, which may form vegetated patches and nutrient islands (Navarro-Cano et al., 2018). Additionally, the positive effects between biodiversity and nutrient availability play an important role in ecological succession in degraded mine lands (Wang et al., 2018).

Features of Plant-Soil Feedbacks in Mine Lands

Compared to secondary successional (Kardol et al., 2013) and other multi-species contexts like tropical forest (Mangan et al., 2010) and old-field (van de Voorde et al., 2011), positive PSFs may outweigh the negative ones in the early stage of primary successional ecosystems for further development of plant community and restoration of ecosystem functioning (Reynolds et al., 2003; Ehrenfeld et al., 2005; Krumins et al., 2015). According to the stress gradient hypothesis, the variance between facilitation and competition of plant interactions will change along the environmental stress gradient, with positive feedbacks dominating under high abiotic stress (Travis et al., 2006; He et al., 2013; Song et al., 2019). It is supposed that in a harsh environment, the pioneer plants tend to buffer and modify the biotic and abiotic stresses for adjacent plants (Bertness and Callaway, 1994). Thus, it is legitimate to suppose that positive feedbacks may exist in early successional mine lands and, with the extreme conditions being gradually attenuated,

finally give way to negative feedbacks along the primary successional trajectory (Reynolds et al., 2003; Krumins et al., 2015). However, this supposition is waiting to be confirmed due to the scarcity of relative long-term empirical evidence in these degraded ecosystems.

The harsh physicochemical properties in mine lands determine whether and which plants can survive and make a difference (Ahirwal et al., 2017). So the soil properties act as both important influencing and affected factors in PSFs. From the angle of influencing factors, it is critical to evaluate the dominant soil properties in the PSFs process. From the angle of affected factors, plants produce biotic and abiotic legacy in the soil, which will influence plants for a long period. And the succession of the mine land ecosystem needs to be triggered by the colonization of tolerant lives and their following PSFs. The sum of positive and negative feedbacks i.e., net PSFs, can indicate the direction of succession trajectory, and the strengths of the PSFs can determine the velocity of natural succession. However, the truth and mechanisms about the critical biotic factors altering PSFs direction and strengths in mine lands are still puzzling us out there and waiting to be figured out.

ECOLOGICAL STRATEGIES OF TOLERANT PLANTS

Functional Traits of Tolerant Plants

Plant functional traits, defined as the measurable features that determine plants performance or fitness, include morphological, behavioral, and biochemical attributes (Reich et al., 2003; Cadotte et al., 2011; **Figure 2**). Species that establish in mine lands tend to possess some self-suited resistant traits and functions to conquer the environmental stress (Nirola et al., 2016b; Quintela-Sabaris et al., 2020). Plant functional traits can modify the soil environment and influence the composition of the soil microbial community (Fierer, 2017), thus playing an important role in understanding the PSFs of different plant species when confronting environmental stress and interferences (Colin et al., 2019).

Above-ground functional traits like specific leaf area, leaf dry matter content, nutrient content, and C:N ratio are frequently characterized to reveal the above-ground response of plants to environmental conditions (Schroeder-Georgi et al., 2016; Veen et al., 2019; Quintela-Sabaris et al., 2020). Depending on different leaf traits, the input of plant foliar litter can be beneficial or detrimental to the soil environment and even to the later plant generations (van der Putten, 1997; Veen et al., 2019), which is also regarded as litter-induced PSFs (Kardol et al., 2015). For example, in relatively infertile conditions, the carbon and tissue nutrient concentrations of litter are the key drivers of soil nutrients and organic matter pool (Wardle et al., 2004). The fast-growing or exploitative plants tend to produce high-quality litters relatively rich in nutrients, stimulating a high decomposing rate (Gartner and Cardon, 2004; Parker et al., 2018), from which the later plant species can receive more positive feedbacks (Wardle et al., 2004). However, research on reclamation in an ultramafic degraded area presented opposite results, that is, perennial plant species with a conservative growth strategy are more suitable for the reclamation since they can better adapt to the extremely low available nutrient condition (Quintela-Sabaris et al., 2020). Thus, the economics spectrum patterns of tolerant plants for phytoremediation on different degraded soil still require particular research attention. In heavy metal contaminated mine lands, the enrichment factor of metallic elements in the aerial part is also an important trait (Nirola et al., 2016a). The leaves with high metal concentration may deposit in the soil beneath their canopies and result in the reallocation of available metal toxicity on the upper soil layer (Colin et al., 2019; Reynolds et al., 2020), bringing negative effects to other relatively heavy metal sensitive plants. The accumulation of toxic elements by hyperaccumulator plants also tends to cause harmful effects on decomposing organism community and retard soil carbon and nutrients cycling (Hooda, 2010). It is necessary to consider the balance between the benefit of hyper-accumulating effects and the accompanying ecological influence when applying phytoremediation measures.

The below-ground functional traits we discuss here mainly refer to plenty of root-related traits, including architectural, morphological, and physiological traits. These traits significantly mediate the soil organisms and alter interactions between plant and soil, so-called rhizosphere-induced PSFs (Bardgett et al., 2014; Kardol et al., 2015). For instance, the architectural (e.g., root depth and root branching) and morphological (e.g., root diameter and specific root length) traits determine the life span of roots, the acquisition of water and nutrient (Dunbabin et al., 2004; Colin et al., 2019), and the modification capability toward soil structural stability (Gyssels et al., 2005; Bardgett et al., 2014). A research conducted in abandoned metal mine deposits shows that plant root architecture and morphological structure are among the key factors that condition the diversity and structure of soil bacteria during primary succession (Colin et al., 2019). For adaptation, the trade-offs between source acquisition and environmental stress tolerance, i.e., root economics spectrum, commonly exist among plants (Chave et al., 2009; Lin et al., 2019). Particularly, exploitive species with high specific root length and low tissue density tend to have a higher rate of water and nutrient uptake, however, they are easier to experience negative PSFs due to lower root resistance strength and short life span and *vice versa* (Valenzuela-Estrada et al., 2008; Freschet and Roumet, 2017). The physiological traits (e.g., nutrient content, root respiration, and root exudation) also help plants to accommodate the inhospitable condition, affect soil elemental stoichiometry and drive below-ground food webs (Hines et al., 2006; Zechmeister-Boltenstern et al., 2015; Zhang et al., 2016). For example, the carbon input is capable of stimulating microbial activity and boosting the uptake and immobilization of nutrients by microbes (Zhang et al., 2016). Fine root debris with higher nitrogen content decomposes faster and provides more nutrients for plant and microbial growth (Kardol et al., 2015).

In general, exploitative plant traits (high specific leaf area and leaf N) are more related to a microbial community dominated by bacteria compared with that by fungi (de Vries et al., 2012), leading to more energetic nutrient circulation. Consequently, an increasing number of researchers adopt trait-based approaches

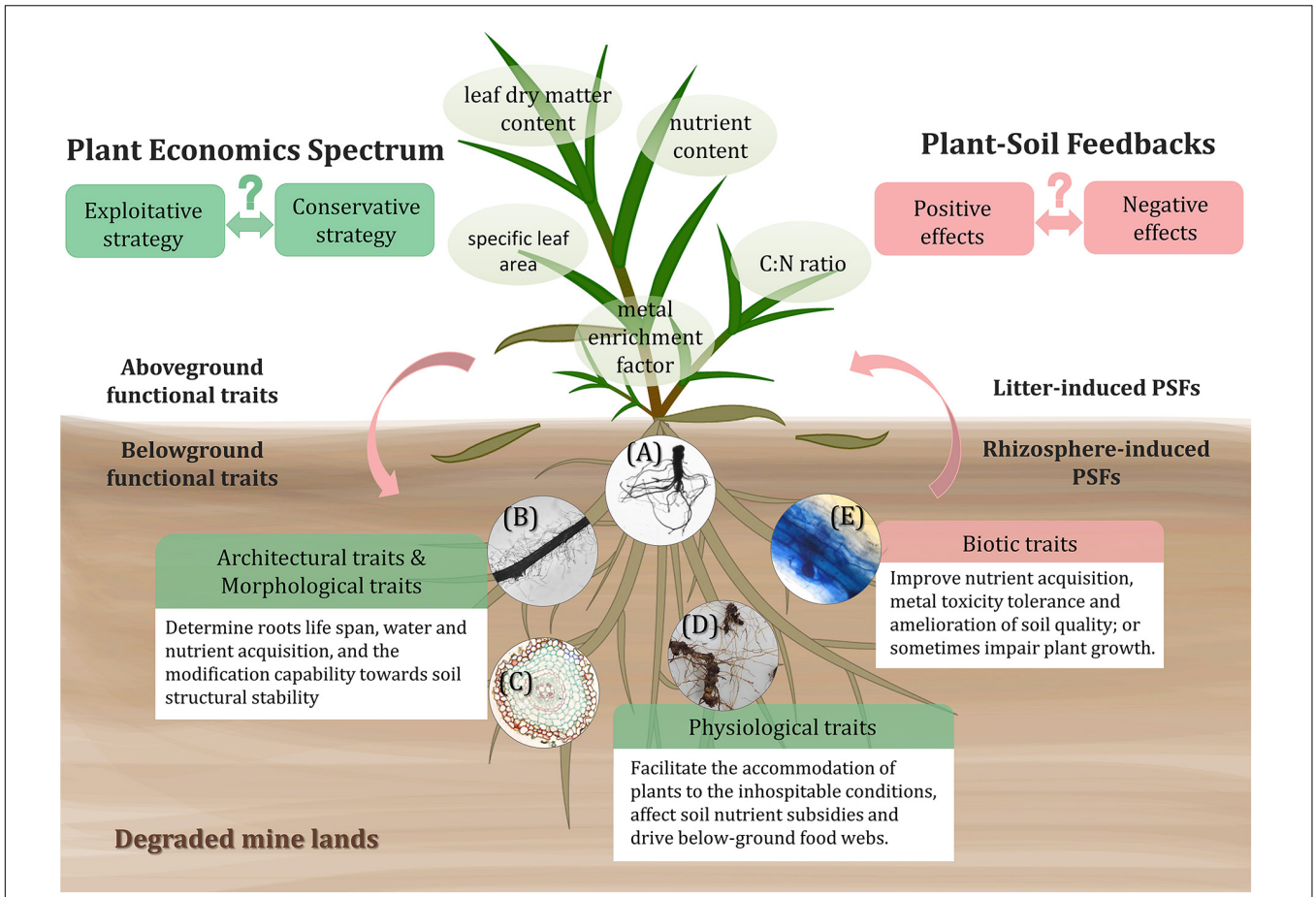

FIGURE 2 | Above- and below-ground functional traits of tolerant plants inducing PSFs in degraded mine lands. The trade-offs of functional traits economics spectrum and the patterns of PSFs of different plants toward severe conditions can alter the ecosystem functioning and are yet to be explored. As for belowground traits, the architectural traits include root depth, root branching; morphological traits contain root diameter, specific root length; physiological traits consist of nutrient content, root respiration, root exudation; and biotic traits refer to the interactions between roots and AMF, rhizobia, PGPB, and pathogens. The shown circular images: **(A)** root system scanning image of *Phytolacca americana*, representing root architectural traits; **(B)** the root segment of *Digitaria sanguinalis* and **(C)** the cross-section of *Dicranopteris linearis* root, both representing morphological traits; **(D)** the rhizome and fine roots of *Miscanthus sinensis*, representing roots nutrient content, i.e., physiological traits; and **(E)** the stained root segment of *Miscanthus sinensis* colonized with AMF, representing biotic traits.

to address plant identity effects on ecosystem developing trajectory based on PSFs (Kardol et al., 2015; Kraft et al., 2015; Cortois et al., 2016; Schroeder-Georgi et al., 2016; Colin et al., 2019). In trait-based ecology, the trade-offs of the plant economics spectrum between resource acquisition and conservation are one of the most important issues (Shen et al., 2019). Within the context of degraded mine lands, the plant functional trait approaches are initially used for the selection of plants for restoration (Ilunga wa Ilunga et al., 2015; Quintela-Sabaris et al., 2020). Take a study in Katangan mine land for instance, with the purpose of revegetation on bare soils in metal-rich lands, annual plants that grow in the wet season and have a deep root system can be chosen as the candidates (Ilunga wa Ilunga et al., 2015). While when considering the vegetation functional biodiversity fulfilling and heavy metal phytostabilization enhancing, it is better to select cespitous grass species with dense rooting mat to avoid long-period bare soil during the dry season (Shutcha et al., 2010). It is of great importance for the restoration of similar situations in mine lands since the appropriate traits category is a more universal criterion than the species pool (Ilunga wa Ilunga et al., 2015).

Roles of Soil Microbial Community in Assisting Plants Performance

The interaction and symbiosis between plants and rhizospheric microbes sometimes are also considered as root biotic traits of plants (**Figure 2**), which act as critical determinants altering PSFs (Bardgett et al., 2014). The associating below-ground microbial community involves AMF, rhizobia, PGPB, and pathogens (Rajkumar et al., 2012; van der Putten et al., 2016). Most plants growing in mine lands are primarily colonized by AMF in the roots, which allow them to receive positive feedbacks (Quoreshi, 2008) *via* improvement of nutrient acquisition (Smith et al., 2003), enhancement of metal toxicity tolerance (Miransari, 2010), and amelioration of soil quality and structure (Madiba, 2014;

Wang, 2017). The large surface area of extraradical hyphae, high affinity and transporting speed toward nutrient elements enable the AMF to assist nutrition acquisition by host plants (Wang, 2017). The AMF could also relieve the heavy metal toxicities to plants through chelating or immobilizing toxic metals by extraradical mycelium (González-Guerrero et al., 2009). Some prokaryotic microorganisms containing nitrogen fixation genes are metal resistant and important for the improvement of N availability in mine lands (Sun et al., 2018a). Rhizobia are also a kind of beneficial microbes that can facilitate the growth of plants by not only fixing nitrogen but also mitigating metal toxicity by increasing metal isolation in root nodules, providing positive PSFs in the rhizosphere of legumes (Hao et al., 2014). Additionally, positive feedbacks are also mediated by rhizosphere PGPB, which excrete multiple metabolites like indole-3-acetic acid (IAA), siderophores, organic acids, and extracellular enzymes, etc (Rajkumar et al., 2012; Mishra et al., 2017). However, except for these beneficial microbes, harmful enemies like pathogens are inevitably dispersed in the plant-soil system, inducing negative feedbacks. For example, during early successional stages, plants with lower specific root lengths are more susceptible to fungal pathogens, and leading to a higher rate of negative inhibition for plant growth (Bergmann et al., 2016).

Together, though relevant researches are increasing, what we know about how plant functional traits and soil microbes facilitate plant growth in degraded mine lands is still far from enough. The integration of shoot and root functional traits and the associated soil communities can help understand the ecological strategy of tolerant plants in driving PSFs in mine lands and select ideal plant functional groups to trigger and accelerate the natural succession process. Digging into the functioning of soil communities on assisting plants performance in mine lands may disentangle the complexity of PSFs and improve the application of bioremediation in the future.

RECOVERY OF ECOSYSTEM FUNCTIONS

To evaluate the consequences of the ecological restoration in degraded lands (Fry et al., 2018b; Jiao et al., 2019), increasing attention has been focused on ecosystem multifunctionality (Sanderson et al., 2004). These ecosystem functions include pollutant control, primary productivity, decomposition, nutrient availability, and cycling, etc (Loreau et al., 2001; Society For Ecological Restoration International Science [SER], and Policy Working Group, 2004; Delgado-Baquerizo et al., 2020). The successfully restored systems can maintain sustainability with minimal need for extra assistance (Society For Ecological Restoration International Science [SER], and Policy Working Group, 2004; Walker and Moral, 2009). Meta-analyses showed that biodiversity is positively correlated with ecosystem functions in most cases (Cardinale et al., 2006; Gross et al., 2014). Thus, achieving more predictable consequences of biodiversity and ecosystem functions recovery turns out to be one of the most important goals in restoration ecology (Matthews and Spyreas, 2010). Up to date, the most practically suitable approaches for mining ecosystem restoration are still under discussion and research.

Functional trait-based approaches play important roles in interpreting the variability of biodiversity and multifunctionality recovery (Zirbel et al., 2017). With a brighter understanding of PSFs outcomes in different types of degraded mine lands, we can apply the mechanisms on selecting the suitable tolerant plant species for revegetation and biodiversity recovery. At the outset of primary succession, nurse plants play an important role in facilitating the colonization and reproduction of later plants (Foronda et al., 2020). In one case, during the restoration of ecosystem functions under extremely stressful mine tailings, some C4 plants with above-ground leaves of lower C:N ratio, acting as potential nurse plants, can improve soil TOC, N, and P content effectively (Navarro-Cano et al., 2018). In another case, the legume community of *Ononis tridentate* L. can form patchy fertility islands beneath its canopy on bare gypsum substrates *via* the symbiosis with below-ground N-fixing rhizobia (Navarro-Cano et al., 2015). Hence, the trait-based selection of nurse plants for remediating degraded mine lands is of great efficiency for long-term recovery. The applications of nurse plants to accelerate post-mining ecological restoration are considered as one of the environmentally friendly and sustainable nature-based solutions.

Soil communities also serve as an important factor driving plant diversity and ecosystem multifunctionality (Wagg et al., 2014; Delgado-Baquerizo et al., 2016). Empirical evidence shows that multiple metabolites like siderophores, IAA, and organic acids excreted by rhizosphere microbes can enhance plant functions of metal detoxification, nutrient uptake, and other biotic and abiotic stress mitigation (Rajkumar et al., 2012). The appropriate application of PGPBs and AMF for enhancing phytoremediation based on PSFs outcomes should be helpful for plant survival and biodiversity increase. Additionally, soil decomposers can ease plant competition by enlarging their habitats chemically (accelerate litter decomposition and improve nutrient uptake) and spatially (deepen plant roots) (Eisenhauer et al., 2012). Regulating the diversity of below-ground decomposers can effectively alter the effect of plant biodiversity on primary production (Eisenhauer et al., 2012). To sum up, by revealing the plant-soil system "black box," it is practicable to use the mechanisms of PSFs to manipulate the trajectory and rate of plant community succession and ecosystem functions recovery. However, cases of applying PSFs mechanisms in natural degraded system recovery are far less than those in other relatively healthy systems (van de Voorde et al., 2011).

CONCLUSION AND PERSPECTIVES

In degraded mine land systems, the terminal objective is to restore a stable and sustainable ecosystem with abundant species and multifunctionality. Figuring out the possible patterns and underlying mechanisms of PSFs in mine lands is significant for understanding and predicting the process of succession under these barren toxic conditions. It is also critical for applying the PSFs mechanisms and functional trait-based approaches in nature-based solutions to accelerate the remediation. Although

ecological researchers gradually focus on plant-soil systems of various environments, a large research gap remains in the restoration of these harsh environments. Here we put forward the perspectives and challenges of PSFs in degraded mine areas that require further research.

Firstly, studies about PSFs in degraded mine lands are necessary. As primary succession sites, degraded mine lands possess few biotic lives and little abiotic material legacy. It is an ideal scene to study the impact of PSFs on the initial formation and interactions of above- and below-ground communities. However, the establishment and regeneration of plant communities and the gathering of multiple species in mine lands are difficult and always take a long time, making the field study difficult. Simultaneously, manipulative experiments in the laboratory are also necessary for precisely understanding the patterns and the influence factors of PSFs. But the problem is that it is hard to fully simulate the condition in the wild. For example, intermittent drought is common in most mine lands, but the lab-grown plant may wither if they are not watered continuously and then we will not even have the biomass for PSFs calculation. Thus, a big challenge for researchers is to think over and make the choice of proper cultivating conditions between better for plant growth and simulating the true field environment.

Secondly, it is important to find out the key environmental factors and mechanisms that determine plant community succession in mine lands. Lots of abiotic stresses impede plant growth, but the critical abiotic factors that determine PSFs remain unknown. Moreover, the response of PSFs is usually context- and time-dependent. Identifying the most important factors that alter or hinder the primary succession can assist restoration efforts in degraded mine lands.

Thirdly, the economic spectrum of tolerant plant functional traits is waiting to be figured out. For one thing, knowing the functional traits that plants are equipped to overcome harsh environments can help to understand the plant economics spectrum along with environmental stresses and provide insights into a trait-based selection of candidate plant species for the restoration of mining sites. For another, plant functional traits are also useful to indicate the relationships between plants and soil community and predict plant effects on succession processing and ecosystem functioning.

Fourthly, it is necessary to combine the structure and functioning of the soil community with the performance of tolerant plants in mine lands to enhance phytoremediation. More emphasis is required on the development of trait-assisted and belowground-derived recovery approaches based on theoretical mechanisms of PSFs. We should surmount the obstacles along the way to revealing PSFs mechanisms and their application on the restoration. This may lead to an important complement to the theory of restoration ecology.

AUTHOR CONTRIBUTIONS

S-CZ and Y-TT conceived the ideas. H-XZ and W-SL provided the figures. S-CZ wrote the first draft of the manuscript. W-SL, Y-TT, YC, and HH reversed the manuscript. All authors contributed to manuscript revision, read, and approved the submitted version.

FUNDING

This work was supported by the National Key Research and Development Program of China (No. 2020YFC1807600), Key Realm Research and Development Program of Guangdong Province (No. 2020B0202080001), National Natural Science Foundation of China (No. 41771343), International Young Scientists Fund of the National Natural Science Foundation of China (No. 21850410450), and Research on Environmental Pollution Control and Ecological Restoration (092018122466v1) funded by Jiangxi Waydiam Environmental Protection Technology Co., Ltd.

ACKNOWLEDGMENTS

We would like to thank all authors listed for their substantial, direct, and intellectual contributions to the work.

REFERENCES

Ahirwal, J., Maiti, S. K., and Satyanarayana Reddy, M. (2017). Development of carbon, nitrogen and phosphate stocks of reclaimed coal mine soil within 8years after forestation with Prosopis juliflora (Sw.) Dc. *Catena* 156, 42–50. doi: 10.1016/j.catena.2017.03.019

Ahonen-Jonnarth, U., Van Hees, P. A. W., Lundström, U. S., and Finlay, R. D. (2000). Organic acids produced by mycorrhizal Pinus sylvestris exposed to elevated aluminium and heavy metal concentrations. *New Phytol.* 146, 557–567. doi: 10.1046/j.1469-8137.2000.00653.x

Bardgett, R. D., Mommer, L., and De Vries, F. T. (2014). Going underground: root traits as drivers of ecosystem processes. *Trends Ecol. Evol.* 29, 692–699. doi: 10.1016/j.tree.2014.10.006

Bashan, Y., de-Bashan, L. E., Prabhu, S. R., and Hernandez, J.-P. (2014). Advances in plant growth-promoting bacterial inoculant technology: formulations and practical perspectives (1998–2013). *Plant Soil* 378, 1–33. doi: 10.1007/s11104-013-1956-x

Bauman, J. M., Cochran, C., Chapman, J., and Gilland, K. (2015). Plant community development following restoration treatments on a legacy reclaimed mine site. *Ecol. Eng.* 83, 521–528. doi: 10.1016/j.ecoleng.2015.06.023

Bergmann, J., Verbruggen, E., Heinze, J., Xiang, D., Chen, B., Joshi, J., et al. (2016). The interplay between soil structure, roots, and microbiota as a determinant of plant-soil feedback. *Ecol. Evol.* 6, 7633–7644. doi: 10.1002/ece3.2456

Bertness, M. D., and Callaway, R. (1994). Positive interactions in communities. *Trends Ecol. Evol.* 9, 191–193. doi: 10.1016/0169-5347(94)90088-4

Borymski, S., Cycoń, M., Beckmann, M., Mur, L. A. J., and Piotrowska-Seget, Z. (2018). Plant species and heavy metals affect biodiversity of microbial communities associated with metal-tolerant plants in metalliferous soils. *Front. Microbiol.* 9:1425. doi: 10.3389/fmicb.2018.01425

Boyer, S., and Wratten, S. D. (2010). The potential of earthworms to restore ecosystem services after opencast mining – A review. *Basic Appl. Ecol.* 11, 196–203. doi: 10.1016/j.baae.2009.12.005

Bradshaw, A. (1997). Restoration of mined lands—using natural processes. *Ecol. Eng.* 8, 255–269. doi: 10.1016/S0925-8574(97)00022-0

Bradshaw, A. D. (1983). The reconstruction of ecosystems. *J. Appl. Ecol.* 20, 1–17. doi: 10.2307/2403372

Cadotte, M. W., Carscadden, K., and Mirotchnick, N. (2011). Beyond species: functional diversity and the maintenance of ecological processes and services. *J. Appl. Ecol.* 48, 1079–1087. doi: 10.1111/j.1365-2664.2011.02048.x

Cardinale, B. J., Srivastava, D. S., Emmett Duffy, J., Wright, J. P., Downing, A. L., Sankaran, M., et al. (2006). Effects of biodiversity on the functioning of trophic groups and ecosystems. *Nature* 443, 989–992. doi: 10.1038/nature05202

Cederlund, H., Wessén, E., Enwall, K., Jones, C. M., Juhanson, J., Pell, M., et al. (2014). Soil carbon quality and nitrogen fertilization structure bacterial communities with predictable responses of major bacterial phyla. *Appl. Soil Ecol.* 84, 62–68. doi: 10.3390/d12060248

Chave, J., Coomes, D., Jansen, S., Lewis, S. L., Swenson, N. G., and Zanne, A. E. (2009). Towards a worldwide wood economics spectrum. *Ecol. Lett.* 12, 351–366. doi: 10.1111/j.1461-0248.2009.01285.x

Chen, L.-X., Huang, L.-N., Méndez-García, C., Kuang, J.-L., Hua, Z.-S., Liu, J., et al. (2016). Microbial communities, processes and functions in acid mine drainage ecosystems. *Curr. Opin. Biotechnol.* 38, 150–158. doi: 10.1016/j.copbio.2016.01.013

Colin, Y., Goberna, M., Verdu, M., and Navarro-Cano, J. A. (2019). Successional trajectories of soil bacterial communities in mine tailings: the role of plant functional traits. *J. Environ. Manage.* 241, 284–292. doi: 10.1016/j.jenvman.2019.04.023

Cortois, R., Schröder-Georgi, T., Weigelt, A., van der Putten, W. H., De Deyn, G. B., and van der Heijden, M. (2016). Plant-soil feedbacks: role of plant functional group and plant traits. *J. Ecol.* 104, 1608–1617. doi: 10.1111/1365-2745.12643

Dassen, S., Cortois, R., Martens, H., de Hollander, M., Kowalchuk, G. A., van der Putten, W. H., et al. (2017). Differential responses of soil bacteria, fungi, archaea and protists to plant species richness and plant functional group identity. *Mol. Ecol.* 26, 4085–4098. doi: 10.1111/mec.14175

Davis, M., Bier, L., Bushelle, E., Diegel, C., Johnson, A., and Kujala, B. (2005). Non-indigenous grasses impede woody succession. *Plant Ecol.* 178, 249–264. doi: 10.1007/s11258-004-4640-7

de Vries, F. T., Manning, P., Tallowin, J. R. B., Mortimer, S. R., Pilgrim, E. S., Harrison, K. A., et al. (2012). Abiotic drivers and plant traits explain landscape-scale patterns in soil microbial communities. *Ecol. Lett.* 15, 1230–1239. doi: 10.1111/j.1461-0248.2012.01844.x

del Moral, R., and Rozzell, L. R. (2005). Long-term effects of *Lupinus lepidus* on vegetation dynamics at Mount St. Helens. *Plant Ecol.* 181, 203–215. doi: 10.1007/s11258-005-6627-4

Delgado-Baquerizo, M., Maestre, F. T., Reich, P. B., Jeffries, T. C., Gaitan, J. J., Encinar, D., et al. (2016). Microbial diversity drives multifunctionality in terrestrial ecosystems. *Nat. Commun.* 7:10541. doi: 10.1038/ncomms10541

Delgado-Baquerizo, M., Reich, P. B., Trivedi, C., Eldridge, D. J., Abades, S., Alfaro, F. D., et al. (2020). Multiple elements of soil biodiversity drive ecosystem functions across biomes. *Nat. Ecol. Evol.* 4, 210–220. doi: 10.1038/s41559-019-1084-y

Dunbabin, V., Rengel, Z., and Diggle, A. J. (2004). Simulating form and function of root systems: efficiency of nitrate uptake is dependent on root system architecture and the spatial and temporal variability of nitrate supply. *Funct. Ecol.* 18, 204–211. doi: 10.1111/j.0269-8463.2004.00827.x

Ehrenfeld, J. G., Ravit, B., and Elgersma, K. J. (2005). Feedback in the plant-soil system. *Annu. Rev. Environ. Resour.* 30, 75–115. doi: 10.1146/annurev.energy.30.050504.144212

Eisenhauer, N., Reich, P. B., and Isbell, F. (2012). Decomposer diversity and identity influence plant diversity effects on ecosystem functioning. *Ecology* 93, 2227–2240. doi: 10.1890/11-2266.1

Fierer, N. (2017). Embracing the unknown: disentangling the complexities of the soil microbiome. *Nat. Rev. Microbiol.* 15, 579–590. doi: 10.1038/nrmicro.2017.87

Foronda, A., Pueyo, Y., Castillejo, J. M., Giner, M. D. L. L., and Alados, C. L. (2020). Substrate-specialist plants for restoring vegetation in post-mining gypsum substrates. *Catena* 186:104308. doi: 10.1016/j.catena.2019.104308

Freschet, G. T., and Roumet, C. (2017). Sampling roots to capture plant and soil functions. *Funct. Ecol.* 31, 1506–1518. doi: 10.1111/1365-2435.12883

Fry, E. L., Johnson, G. N., Hall, A. L., Pritchard, W. J., Bullock, J. M., and Bardgett, R. D. (2018a). Drought neutralises plant-soil feedback of two mesic grassland forbs. *Oecologia* 186, 1113–1125. doi: 10.1007/s00442-018-4082-x

Fry, E. L., Savage, J., Hall, A. L., Oakley, S., Pritchard, W. J., Ostle, N. J., et al. (2018b). Soil multifunctionality and drought resistance are determined by plant structural traits in restoring grassland. *Ecology* 99, 2260–2271. doi: 10.1002/ecy.2437

Gaertner, M., Fisher, J. L., Sharma, G. P., and Esler, K. J. (2012). Insights into invasion and restoration ecology: time to collaborate towards a holistic approach to tackle biological invasions. *NeoBiota* 12, 57–76. doi: 10.3897/neobiota.12.2123

Gao, Y., Miao, C., Mao, L., Zhou, P., Jin, Z., and Shi, W. (2010). Improvement of phytoextraction and antioxidative defense in Solanum nigrum L. under cadmium stress by application of cadmium-resistant strain and citric acid. *J. Hazard. Mater.* 181, 771–777. doi: 10.1016/j.jhazmat.2010.05.080

Gartner, T. B., and Cardon, Z. G. (2004). Decomposition dynamics in mixed-species leaf litter. *Oikos* 104, 230–246. doi: 10.1111/j.0030-1299.2004.12738.x

Gastauer, M., Silva, J. R., Caldeira Junior, C. F., Ramos, S. J., Souza Filho, P. W. M., Furtini Neto, A. E., et al. (2018). Mine land rehabilitation: modern ecological approaches for more sustainable mining. *J. Clean. Prod.* 172, 1409–1422. doi: 10.1016/j.jclepro.2017.10.223

Geisen, S., Kostenko, O., Cnossen, M. C., Ten Hooven, F. C., Vreš, B., and van der Putten, W. H. (2017). Seed and root endophytic fungi in a range expanding and a related plant species. *Front. Microbiol.* 8:1645. doi: 10.3389/fmicb.2017.01645

González-Guerrero, M., Benabdellah, K., Ferrol, N., and Azcón-Aguilar, C. (2009). "Mechanisms Underlying Heavy Metal Tolerance in Arbuscular Mycorrhizas," in *Mycorrhizas - Functional Processes and Ecological Impact*, eds C. Azcón-Aguilar, J. M. Barea, S. Gianinazzi, and V. Gianinazzi-Pearson (Berlin, Heidelberg: Springer Berlin Heidelberg), 107–122.

Grandlic, C. J., Palmer, M. W., and Maier, R. M. (2009). Optimization of plant growth-promoting bacteria-assisted phytostabilization of mine tailings. *Soil Biol. Biochem.* 41, 1734–1740. doi: 10.1016/j.soilbio.2009.05.017

Gross, K., Cardinale, B. J., Fox, J. W., Gonzalez, A., Loreau, M., Polley, H. W., et al. (2014). Species richness and the temporal stability of biomass production: a new analysis of recent biodiversity experiments. *Am. Nat.* 183, 1–12. doi: 10.1086/673915

Gyssels, G., Poesen, J., Bochet, E., and Li, Y. (2005). Impact of plant roots on the resistance of soils to erosion by water: a review. *Prog. Phys. Geogr.* 29, 189–217. doi: 10.1191/0309133305pp443ra

Hamman, S. T., and Hawkes, C. V. (2013). Biogeochemical and microbial legacies of non-native grasses can affect restoration success. *Restor. Ecol.* 21, 58–66. doi: 10.1111/j.1526-100X.2011.00856.x

Hao, X., Taghavi, S., Xie, P., Orbach, M. J., Alwathnani, H. A., Rensing, C., et al. (2014). Phytoremediation of Heavy and Transition Metals Aided by Legume-Rhizobia Symbiosis. *Int. J. Phytoremediation* 16, 179–202. doi: 10.1080/15226514.2013.773273

He, Q., Bertness, M. D., and Altieri, A. H. (2013). Global shifts towards positive species interactions with increasing environmental stress. *Ecol. Lett.* 16, 695–706. doi: 10.1111/ele.12080

Hines, J., Megonigal, J. P., and Denno, R. F. (2006). Nutrient subsidies to belowground microbes impact aboveground food web interactions. *Ecology* 87, 1542–1555.

Hooda, P. (2010). *Trace Elements In Soils*. Chichester, U.K: John Wiley & Sons

Hu, Z., Wang, P., and Li, J. (2012). Ecological restoration of abandoned mine land in China. *J. Resour. Ecol.* 3, 289–296. doi: 10.5814/j.issn.1674-764x.2012.04.001

Ilunga wa Ilunga, E., Mahy, G., Piqueray, J., Séleck, M., Shutcha, M. N., Meerts, P., et al. (2015). Plant functional traits as a promising tool for the ecological restoration of degraded tropical metal-rich habitats and revegetation of metal-rich bare soils: a case study in copper vegetation of Katanga, DRC. *Ecol. Eng.* 82, 214–221. doi: 10.1016/j.ecoleng.2015.04.084

Jia, P., Liang, J.-L., Yang, S.-X., Zhang, S.-C., Liu, J., Liang, Z.-W., et al. (2020). Plant diversity enhances the reclamation of degraded lands by stimulating plant–soil feedbacks. *J. Appl. Ecol.* 57, 1258–1270. doi: 10.1111/1365-2664.13625

Jiao, S., Du, N., Zai, X., Gao, X., Chen, W., and Wei, G. (2019). Temporal dynamics of soil bacterial communities and multifunctionality are more sensitive to introduced plants than to microbial additions in a multicontaminated soil. *Land Degrad. Dev.* 30, 852–865. doi: 10.1002/ldr.3272

Joshi, P. M., and Juwarkar, A. A. (2009). *In vivo* studies to elucidate the role of extracellular polymeric substances from Azotobacter in immobilization of heavy metals. *Environ. Sci. Technol.* 43, 5884–5889. doi: 10.1021/es900063b

Kaisermann, A., de Vries, F. T., Griffiths, R. I., and Bardgett, R. D. (2017). Legacy effects of drought on plant–soil feedbacks and plant–plant interactions. *New Phytol.* 215, 1413–1424. doi: 10.1111/nph.14661

Kang, X., Cui, Y., Shen, T., Yan, M., Tu, W., Shoaib, M., et al. (2020). Changes of root microbial populations of natively grown plants during natural attenuation of V–Ti magnetite tailings. *Ecotoxicol. Environ. Saf.* 201:110816. doi: 10.1016/j.ecoenv.2020.110816

Kardol, P., Bezemer, T. M., and van der Putten, W. H. (2006). Temporal variation in plant-soil feedback controls succession. *Ecol. Lett.* 9, 1080–1088. doi: 10.1111/j.1461-0248.2006.00953.x

Kardol, P., De Deyn, G. B., Laliberté, E., Mariotte, P., and Hawkes, C. V. (2013). Biotic plant-soil feedback across temporal scales. *J. Ecol.* 101, 309–315. doi: 10.1111/1365-2745.12046

Kardol, P., Veen, G. F. C., Teste, F. P., and Perring, M. P. (2015). Peeking into the black box: a trait-based approach to predicting plant-soil feedback. *New Phytol.* 206, 1–4. doi: 10.1111/nph.13283

Kraft, N. J. B., Godoy, O., and Levine, J. M. (2015). Plant functional traits and the multidimensional nature of species coexistence. *Proc. Natl. Acad. Sci. U. S. A.* 112, 797–802. doi: 10.1073/pnas.1413650112

Krumins, J. A., Goodey, N. M., and Gallagher, F. (2015). Plant–soil interactions in metal contaminated soils. *Soil Biol. Biochem.* 80, 224–231. doi: 10.1016/j.soilbio.2014.10.011

Lamb, D., Erskine, P. D., and Fletcher, A. (2015). Widening gap between expectations and practice in Australian minesite rehabilitation. *Ecol. Manag. Restor.* 16, 186–195. doi: 10.1111/emr.12179

Lauber, C. L., Hamady, M., Knight, R., and Fierer, N. (2009). Pyrosequencing-based assessment of soil pH as a predictor of soil bacterial community structure at the continental scale. *Appl. Environ. Microbiol.* 75, 5111–5120. doi: 10.1128/aem.00335-09

Lei, K., Pan, H., and Lin, C. (2016). A landscape approach towards ecological restoration and sustainable development of mining areas. *Ecol. Eng.* 90, 320–325. doi: 10.1016/j.ecoleng.2016.01.080

Li, J.-J., Zheng, Y.-M., Yan, J.-X., Li, H.-J., and He, J.-Z. (2013). Succession of plant and soil microbial communities with restoration of abandoned land in the Loess Plateau. China. *J. Soils Sediments* 13, 760–769. doi: 10.1007/s11368-013-0652-z

Li, S., and Liber, K. (2018). Influence of different revegetation choices on plant community and soil development nine years after initial planting on a reclaimed coal gob pile in the Shanxi mining area, China. *Sci. Total Environ.* 618, 1314–1323. doi: 10.1016/j.scitotenv.2017.09.252

Li, Y., Zhang, M., Xu, R., Lin, H., Sun, X., Xu, F., et al. (2021). Arsenic and antimony co-contamination influences on soil microbial community composition and functions: relevance to arsenic resistance and carbon, nitrogen, and sulfur cycling. *Environ. Int.* 153:106522. doi: 10.1016/j.envint.2021.106522

Lin, D., Yang, S., Dou, P., Wang, H., Wang, F., Qian, S., et al. (2019). A plant economics spectrum of litter decomposition among coexisting fern species in a subtropical forest. *Ann. Bot.* 125, 145–155. doi: 10.1093/aob/mcz166

Liu, J., Hua, Z.-S., Chen, L.-X., Kuang, J.-L., Li, S.-J., Shu, W.-S., et al. (2014). Correlating microbial diversity patterns with geochemistry in an extreme and heterogeneous environment of mine tailings. *Appl. Environ. Microbiol.* 80, 3677–3686. doi: 10.1128/AEM.00294-14

Loreau, M., Naeem, S., Inchausti, P., Bengtsson, J., Grime, J., Hector, A., et al. (2001). Biodiversity and ecosystem functioning: current knowledge and future challenges. *Science* 294, 804–808. doi: 10.1126/science.1064088

Madiba, O. F. (2014). "Alleviation of soil stresses by arbuscular mycorrhizal fungi," in *Mycorrhizal Fungi: use in Sustainable Agriculture and Land Restoration*, eds Z. M. Solaiman, L. K. Abbott, and A. Varma (Berlin, Heidelberg: Springer Berlin Heidelberg), 215–224.

Mangan, S. A., Schnitzer, S. A., Herre, E. A., Mack, K. M., Valencia, M. C., Sanchez, E. I., et al. (2010). Negative plant-soil feedback predicts tree-species relative abundance in a tropical forest. *Nature* 466, 752–755. doi: 10.1038/nature09273

Mariotte, P., Mehrabi, Z., Bezemer, T. M., De Deyn, G. B., Kulmatiski, A., Drigo, B., et al. (2018). Plant-soil feedback: bridging natural and agricultural sciences. *Trends Ecol. Evol.* 33, 129–142. doi: 10.1016/j.tree.2017.11.005

Matthews, J. W., and Spyreas, G. (2010). Convergence and divergence in plant community trajectories as a framework for monitoring wetland restoration progress. *J. Appl. Ecol.* 47, 1128–1136. doi: 10.1111/j.1365-2664.2010.01862.x

Miransari, M. (2010). Contribution of arbuscular mycorrhizal symbiosis to plant growth under different types of soil stress. *Plant Biol.* 12, 563–569. doi: 10.1111/j.1438-8677.2009.00308.x

Mishra, J., Singh, R., and Arora, N. K. (2017). Alleviation of Heavy Metal Stress in Plants and Remediation of Soil by Rhizosphere Microorganisms. *Front. Microbiol.* 8:1706. doi: 10.3389/fmicb.2017.01706

Mukhopadhyay, S., George, J., and Masto, R. E. (2017). Changes in polycyclic aromatic hydrocarbons (PAHs) and soil biological parameters in a revegetated coal mine spoil. *Am. J. Gastroenterol.* 28, 1047–1055. doi: 10.1002/ldr.2593

Navarro-Cano, J. A., Verdú, M., and Goberna, M. (2018). Trait-based selection of nurse plants to restore ecosystem functions in mine tailings. *J. Appl. Ecol.* 55, 1195–1206. doi: 10.1111/1365-2664.13094

Navarro-Cano, J. A., Verdú, M., García, C., and Goberna, M. (2015). What nurse shrubs can do for barren soils: rapid productivity shifts associated with a 40 years ontogenetic gradient. *Plant Soil* 388, 197–209. doi: 10.1007/s11104-014-2323-2

Neldner, V. J., and Ngugi, M. R. (2017). Establishment of woody species across 26 years of revegetation on a Queensland coal mine. *Ecol. Manag. Restor.* 18, 75–78. doi: 10.1111/emr.12243

Nirola, R., Megharaj, M., Beecham, S., Aryal, R., Thavamani, P., Vankateswarlu, K., et al. (2016b). Remediation of metalliferous mines, revegetation challenges and emerging prospects in semi-arid and arid conditions. *Environ. Sci. Pollut. Res.* 23, 20131–20150. doi: 10.1007/s11356-016-7372-z

Nirola, R., Megharaj, M., Aryal, R., and Naidu, R. (2016a). Screening of metal uptake by plant colonizers growing on abandoned copper mine in Kapunda, South Australia. *Int. J. Phytoremediation* 18, 399–405. doi: 10.1080/15226514.2015.1109599

Nussbaumer, Y., Cole, M. A., Offler, C. E., and Patrick, J. W. (2016). Identifying and ameliorating nutrient limitations to reconstructing a forest ecosystem on mined land. *Restor. Ecol.* 24, 202–211. doi: 10.1111/rec.12294

O'Brien, M. J., Pugnaire, F. I., Rodríguez-Echeverría, S., Morillo, J. A., Martín-Usero, F., López-Escoriza, A., et al. (2018). Mimicking a rainfall gradient to test the role of soil microbiota for mediating plant responses to drier conditions. *Oikos* 127, 1776–1786. doi: 10.1111/oik.05443

Parker, T. C., Sanderman, J., Holden, R. D., Blume-Werry, G., Sjögersten, S., Large, D., et al. (2018). Exploring drivers of litter decomposition in a greening Arctic: results from a transplant experiment across a treeline. *Ecology* 99, 2284–2294. doi: 10.1002/ecy.2442

Pett-Ridge, J., and Firestone, M. K. (2005). Redox fluctuation structures microbial communities in a wet tropical soil. *Appl. Environ. Microbiol.* 71, 6998–7007. doi: 10.1128/AEM.71.11.6998-7007.2005

Pugnaire, F. I., Morillo, J. A., Peñuelas, J., Reich, P. B., Bardgett, R. D., Gaxiola, A., et al. (2019). Climate change effects on plant-soil feedbacks and consequences for biodiversity and functioning of terrestrial ecosystems. *Sci. Adv.* 5:eaaz1834. doi: 10.1126/sciadv.aaz1834

Quintela-Sabaris, C., Faucon, M.-P., Repin, R., Sugau, J. B., Nilus, R., Echevarria, G., et al. (2020). Plant functional traits on tropical ultramafic habitats affected by fire and mining: insights for reclamation. *Diversity* 12:248.

Quoreshi, A. M. (2008). "The use of mycorrhizal biotechnology in restoration of disturbed ecosystem," in *Mycorrhizae: sustainable Agriculture and Forestry*, eds Z. A. Siddiqui, M. S. Akhtar, and K. Futai (Dordrecht: Springer Netherlands), 303–320.

Rajkumar, M., Sandhya, S., Prasad, M. N., and Freitas, H. (2012). Perspectives of plant-associated microbes in heavy metal phytoremediation. *Biotechnol. Adv.* 30, 1562–1574. doi: 10.1016/j.biotechadv.2012.04.011

Reich, P. B., Wright, I. J., Cavender−Bares, J., Craine, J. M., Oleksyn, J., Westoby, M., et al. (2003). The evolution of plant functional variation: traits, spectra, and strategies. *Int. J. Plant Sci.* 164, S143–S164. doi: 10.1086/374368

Ren, H., Yang, L., and Liu, N. (2008). Nurse plant theory and its application in ecological restoration in lower subtropics of China. *Prog. Nat. Sci.* 18, 137–142. doi: 10.1016/j.pnsc.2007.07.008

Reynolds, H. L., Packer, A., Bever, J. D., and Clay, K. (2003). Grassroots ecology: plant–microbe–soil interactions as drivers of plant community

structure and dynamics. *Ecology* 84, 2281–2291. doi: 10.1890/02-0298

Reynolds, R. J. B., Jones, R. R., Heiner, J., Crane, K. M., and Pilon-Smits, E. A. H. (2020). Effects of selenium hyperaccumulators on soil selenium distribution and vegetation properties. *Am. J. Bot.* 107, 970–982. doi: 10.1002/ajb2.1500

Sanderson, M. A., Skinner, R. H., Barker, D. J., Edwards, G. R., Tracy, B. F., and Wedin, D. A. (2004). Plant species diversity and management of temperate forage and grazing land ecosystems. *Crop Sci.* 44, 1132–1144. doi: 10.2135/cropsci2004.1132

Schalk, I. J., Hannauer, M., and Braud, A. (2011). New roles for bacterial siderophores in metal transport and tolerance. *Environ. Microbiol.* 13, 2844–2854. doi: 10.1111/j.1462-2920.2011.02556.x

Schneemann, B., and McElhinny, C. (2012). Shrubby today but not tomorrow? Structure, composition and regeneration dynamics of direct seeded revegetation. *Ecol. Manag. Restor.* 13, 282–289. doi: 10.1111/emr.12007

Schroeder-Georgi, T., Wirth, C., Nadrowski, K., Meyer, S. T., Mommer, L., Weigelt, A., et al. (2016). From pots to plots: hierarchical trait-based prediction of plant performance in a mesic grassland. *J. Ecol.* 104, 206–218. doi: 10.1111/1365-2745.12489

Schwenke, G. D., Mulligan, D. R., and Bell, L. C. (2000). Soil stripping and replacement for the rehabilitation of bauxite-mined land at Weipa. III. Simulated long-term soil organic matter development. *Aust. J. Soil Res.* 38, 395–410. doi: 10.1071/SR99045

Shanmugam, S. G., and Kingery, W. L. (2018). Changes in soil microbial community structure in relation to plant succession and soil properties during 4000 years of pedogenesis. *Eur. J. Soil Biol.* 88, 80–88. doi: 10.1016/j.ejsobi.2018.07.003

Shen, Y., Gilbert, G., Li, W., Miao, F., Lu, H., and Yu, S. (2019). Linking aboveground traits to root traits and local environment: implications of the plant economics spectrum. *Front. Plant Sci.* 10:1412. doi: 10.3389/fpls.2019.01412

Shutcha, M. N., Mubemba, M. M., Faucon, M.-P., Luhembwe, M. N., Visser, M., Colinet, G., et al. (2010). Phytostabilisation of Copper-Contaminated Soil in Katanga: an Experiment with Three Native Grasses and Two Amendments. *Int. J. Phytoremediation* 12, 616–632. doi: 10.1080/15226510903390411

Singh, J. P., Vaidya, B. P., Goodey, N. M., and Krumins, J. A. (2019). Soil microbial response to metal contamination in a vegetated and urban brownfield. *J. Environ. Manage.* 244, 313–319. doi: 10.1016/j.jenvman.2019.04.111

Smith, S. E., Facelli, E., Pope, S., and Andrew Smith, F. (2010). Plant performance in stressful environments: interpreting new and established knowledge of the roles of arbuscular mycorrhizas. *Plant Soil* 326, 3–20. doi: 10.1007/s11104-009-9981-5

Smith, S. E., Smith, F. A., and Jakobsen, I. (2003). Mycorrhizal fungi can dominate phosphate supply to plants irrespective of growth responses. *Plant Physiol.* 133, 16–20. doi: 10.1104/pp.103.024380

Society For Ecological Restoration International Science [SER], and Policy Working Group (2004). *The SER international primer on ecological restoration*. Tucson AZ: Society for Ecological Restoration International.

Song, M., Yu, L., Jiang, Y., Korpelainen, H., and Li, C. (2019). Increasing soil age drives shifts in plant-plant interactions from positive to negative and affects primary succession dynamics in a subalpine glacier forefield. *Geoderma* 353, 435–448. doi: 10.1016/j.geoderma.2019.07.029

Sul, W. J., Asuming-Brempong, S., Wang, Q., Tourlousse, D. M., Penton, C. R., Deng, Y., et al. (2013). Tropical agricultural land management influences on soil microbial communities through its effect on soil organic carbon. *Soil Biol. Biochem.* 65, 33–38. doi: 10.1016/j.soilbio.2013.05.007

Sun, W., Xiao, E., Krumins, V., Häggblom, M. M., Dong, Y., Pu, Z., et al. (2018b). Rhizosphere Microbial Response to Multiple Metal(loid)s in Different Contaminated Arable Soils Indicates Crop-Specific Metal-Microbe Interactions. *Appl. Environ. Microbiol.* 84, e00701–18. doi: 10.1128/AEM.00701-18

Sun, W., Xiao, E., Häggblom, M., Krumins, V., Dong, Y., Sun, X., et al. (2018a). Bacterial Survival Strategies in an Alkaline Tailing Site and the Physiological Mechanisms of Dominant Phylotypes As Revealed by Metagenomic Analyses. *Environ. Sci. Technol.* 52, 13370–13380. doi: 10.1021/acs.est.8b03853

Sun, W., Xiao, E., Xiao, T., Krumins, V., Wang, Q., Häggblom, M., et al. (2017). Response of Soil Microbial Communities to Elevated Antimony and Arsenic Contamination Indicates the Relationship between the Innate Microbiota and Contaminant Fractions. *Environ. Sci. Technol.* 51, 9165–9175. doi: 10.1021/acs.est.7b00294

Sun, X., Kong, T., Häggblom, M. M., Kolton, M., Li, F., Dong, Y., et al. (2020). Chemolithoautotropic Diazotrophy Dominates the Nitrogen Fixation Process in Mine Tailings. *Environ. Sci. Technol.* 54, 6082–6093. doi: 10.1021/acs.est.9b07835

Teste, F. P., Kardol, P., Turner, B. L., Wardle, D. A., Zemunik, G., Renton, M., et al. (2017). Plant-soil feedback and the maintenance of diversity in Mediterranean-climate shrublands. *Science* 355, 173–176. doi: 10.1126/science.aai8291

Travis, J. M. J., Brooker, R. W., Clark, E. J., and Dytham, C. (2006). The distribution of positive and negative species interactions across environmental gradients on a dual-lattice model. *J. Theor. Biol.* 241, 896–902. doi: 10.1016/j.jtbi.2006.01.025

Ullah, A., Heng, S., Munis, M. F. H., Fahad, S., and Yang, X. (2015). Phytoremediation of heavy metals assisted by plant growth promoting (PGP) bacteria: a review. *Environ. Exp. Bot.* 117, 28–40. doi: 10.1016/j.envexpbot.2015.05.001

Valenzuela-Estrada, L. R., Vera-Caraballo, V., Ruth, L. E., and Eissenstat, D. M. (2008). Root anatomy, morphology, and longevity among root orders in *Vaccinium corymbosum* (*Ericaceae*). *Am. J. Bot.* 95, 1506–1514. doi: 10.3732/ajb.0800092

van de Voorde, T. F., van der Putten, W. H., and Martijn Bezemer, T. J. (2011). Intra−and interspecific plant–soil interactions, soil legacies and priority effects during old−field succession. *J. Ecol.* 99, 945–953. doi: 10.1111/j.1365-2745.2011.01815.x

van der Putten, W. H. (1997). Plant-soil feedback as a selective force. *Trends Ecol. Evol.* 12, 169–170. doi: 10.1016/s0169-5347(97)01006-9

van der Putten, W. H., Bardgett, R. D., Bever, J. D., Bezemer, T. M., Casper, B. B., Fukami, T., et al. (2013). Plant-soil feedbacks: the past, the present and future challenges. *J. Ecol.* 101, 265–276. doi: 10.1111/1365-2745.12054

van der Putten, W. H., Bradford, M. A., Pernilla Brinkman, E., Voorde, T. F. J., Veen, G. F., and Bailey, J. K. (2016). Where, when and how plant–soil feedback matters in a changing world. *Funct. Ecol.* 30, 1109–1121. doi: 10.1111/1365-2435.12657

van Grunsven, R. H., van der Putten, W. H., Bezemer, T. M., and Veenendaal, E. M. (2010). Plant-soil feedback of native and range-expanding plant species is insensitive to temperature. *Oecologia* 162, 1059–1069. doi: 10.1007/s00442-009-1526-3

Veen, G. F. C., Fry, E. L., ten Hooven, F. C., Kardol, P., Morriën, E., and De Long, J. R. (2019). The role of plant litter in driving plant-soil feedbacks. *Front. Environ. Sci.* 7:168. doi: 10.3389/fenvs.2019.00168

Wagg, C., Bender, S. F., Widmer, F., and van der Heijden, M. G. A. (2014). Soil biodiversity and soil community composition determine ecosystem multifunctionality. *Proc. Natl. Acad. Sci. U. S. A.* 111, 5266–5270. doi: 10.1073/pnas.1320054111

Walker, L. R., and Moral, R. D. (2009). Lessons from primary succession for restoration of severely damaged habitats. *Appl. Veg. Sci.* 12, 55–67. doi: 10.1111/j.1654-109X.2009.01002.x

Wang, D., Zhang, B., Zhu, L., Yang, Y., and Li, M. (2018). Soil and vegetation development along a 10-year restoration chronosequence in tailing dams in the Xiaoqinling gold region of Central China. *Catena* 167, 250–256. doi: 10.1016/j.catena.2018.05.007

Wang, F. (2017). Occurrence of arbuscular mycorrhizal fungi in mining-impacted sites and their contribution to ecological restoration: mechanisms and applications. *Crit. Rev. Environ. Sci. Technol.* 47, 1901–1957. doi: 10.1080/10643389.2017.1400853

Wang, Y., Shi, J., Wang, H., Lin, Q., Chen, X., and Chen, Y. (2007). The influence of soil heavy metals pollution on soil microbial biomass, enzyme activity, and community composition near a copper smelter. *Ecotoxicol. Environ. Saf.* 67, 75–81. doi: 10.1016/j.ecoenv.2006.03.007

Wardle, D. A. (2013). *Communities and ecosystems: linking the aboveground and belowground components (MPB-34)*. Princeton NJ: Princeton University Press.

Wardle, D. A., Bardgett, R. D., Klironomos, J. N., Setala, H., Der Putten, W. H. V., and Wall, D. H. (2004). Ecological linkages between aboveground and belowground biota. *Science* 304, 1629–1633. doi: 10.1126/science.1094875

Xu, R., Zhang, M., Lin, H., Gao, P., Yang, Z., Wang, D., et al. (2022). Response of soil protozoa to acid mine drainage in a contaminated terrace. *J. Hazard. Mater.* 421:126790. doi: 10.1016/j.jhazmat.2021.126790

Zechmeister-Boltenstern, S., Keiblinger, K. M., Mooshammer, M., Peñuelas, J., Richter, A., Sardans, J., et al. (2015). The application of ecological stoichiometry to plant–microbial–soil organic matter transformations. *Ecol. Monogr.* 85, 133–155. doi: 10.1890/14-0777.1

Zhang, N., Van der Putten, W. H., and Veen, G. F. C. (2016). Effects of root decomposition on plant-soil feedback of early- and mid-successional plant species. *New Phytol.* 212, 220–231. doi: 10.1111/nph.14007

Zhou, L., Li, Z., Liu, W., Liu, S., Zhang, L., Zhong, L., et al. (2015). Restoration of rare earth mine areas: organic amendments and phytoremediation. *Environ. Sci. Pollut. Res.* 22, 17151–17160. doi: 10.1007/s11356-015-4875-y

Zirbel, C. R., Bassett, T., Grman, E., and Brudvig, L. A. (2017). Plant functional traits and environmental conditions shape community assembly and ecosystem functioning during restoration. *J. Appl. Ecol.* 54, 1070–1079. doi: 10.1111/1365-2664.12885

Conflict of Interest: The authors declare that the research was conducted in the absence of any commercial or financial relationships that could be construed as a potential conflict of interest.

frontiers in Microbiology

ORIGINAL RESEARCH
published: 12 January 2022
doi: 10.3389/fmicb.2021.781831

Rhizobium Inoculation Enhances the Resistance of Alfalfa and Microbial Characteristics in Copper-Contaminated Soil

*Chengjiao Duan[1,2], Yuxia Mei[3], Qiang Wang[4], Yuhan Wang[4], Qi Li[5], Maojun Hong[6], Sheng Hu[6], Shiqing Li[1] and Linchuan Fang[1,7]**

[1] State Key Laboratory of Soil Erosion and Dryland Farming on the Loess Plateau, Institute of Soil and Water Conservation, Chinese Academy of Sciences & Ministry of Water Resources, Yangling, China, [2] University of Chinese Academy of Sciences, Beijing, China, [3] State Key Laboratory of Agricultural Microbiology, College of Life Science and Technology, Huazhong Agricultural University, Wuhan, China, [4] College of Natural Resources and Environment, Northwest A&F University, Yangling, China, [5] College of Urban and Environmental Sciences, Central China Normal University, Wuhan, China, [6] College of Agronomy, Northwest A&F University, Yangling, China, [7] Chinese Academy of Sciences (CAS), Center for Excellence in Quaternary Science and Global Change, Xi'an, China

Some studies have reported the importance of rhizobium in mitigating heavy metal toxicity, however, the regulatory mechanism of the alfalfa-rhizobium symbiosis to resist copper (Cu) stress in the plant-soil system through biochemical reactions is still unclear. This study assessed the effects of rhizobium (*Sinorhizobium meliloti* CCNWSX0020) inoculation on the growth of alfalfa and soil microbial characteristics under Cu-stress. Further, we determined the regulatory mechanism of rhizobium inoculation to alleviate Cu-stress in alfalfa through plant-soil system. The results showed that rhizobium inoculation markedly alleviated Cu-induced growth inhibition in alfalfa by increasing the chlorophyll content, height, and biomass, in addition to nitrogen and phosphorus contents. Furthermore, rhizobium application alleviated Cu-induced phytotoxicity by increasing the antioxidant enzyme activities and soluble protein content in tissues, and inhibiting the lipid peroxidation levels (i.e., malondialdehyde content). In addition, rhizobium inoculation improved soil nutrient cycling, which increased soil enzyme activities (i.e., β-glucosidase activity and alkaline phosphatase) and microbial biomass nitrogen. Both Pearson correlation coefficient analysis and partial least squares path modeling (PLS-PM) identified that the interactions between soil nutrient content, enzyme activity, microbial biomass, plant antioxidant enzymes, and oxidative damage could jointly regulate plant growth. This study provides comprehensive insights into the mechanism of action of the legume-rhizobium symbiotic system to mitigate Cu stress and provide an efficient strategy for phytoremediation of Cu-contaminated soils.

Keywords: Cu-stress, alfalfa, plant resistance, enzyme activity, symbiosis system

OPEN ACCESS

Edited by:
Hai-Ming Zhao,
Jinan University, China

Reviewed by:
Elisa Bona,
University of Eastern Piedmont, Italy
Hermie J. M. Harmsen,
University Medical Center Groningen, Netherlands

****Correspondence:***
Linchuan Fang
flinc629@hotmail.com

Specialty section:
This article was submitted to Terrestrial Microbiology, a section of the journal Frontiers in Microbiology

Received: *23 September 2021*
Accepted: *17 December 2021*
Published: *12 January 2022*

Citation:
Duan C, Mei Y, Wang Q, Wang Y, Li Q, Hong M, Hu S, Li S and Fang L (2022) Rhizobium Inoculation Enhances the Resistance of Alfalfa and Microbial Characteristics in Copper-Contaminated Soil. Front. Microbiol. 12:781831. doi: 10.3389/fmicb.2021.781831

INTRODUCTION

Heavy metal effluence of the soil is a severe issue that directly interrupts environmental resources, ecosystem, and food safety (Sahito et al., 2021; Wang J. et al., 2021). Of these pollutants, copper (Cu) has become one of the main heavy metal contaminants because of its common use in industry and agriculture such as in mining, metal processing, fertilizers, pesticides, and municipal wastes

(Huang et al., 2018; Saxena et al., 2020). Cu-contaminated soil displays severe phytotoxic effects, for example, plant growth retardation, nutrient disturbances, and interference with several metabolic processes (Chen et al., 2015). Moreover, Cu-contamination not only causes phytotoxicity but also endangers soil enzyme activities, and damages soil environmental health, which is ultimately detrimental to human health (Chen et al., 2019, 2021).

Cu ions, which are readily absorbed by plant roots, compete with each other and are transferred to other organs (Sun et al., 2015; Duan et al., 2018). Excessive Cu concentration can inhibit plant growth, lead to nutrient deficiencies, reduce antioxidant enzyme activity, and cause oxidation stress by producing of reactive oxygen species (ROS) (Liu et al., 2016; Abbas et al., 2017). Malondialdehyde (MDA) is the final product of lipids peroxidation, and its content in plants can be an excellent indicator of plant damage (Beiyuan et al., 2021). Generally, plants directly or indirectly trigger enzymatic antioxidants [comprising of superoxide dismutase (SOD), peroxidase (POD), catalases (CAT), and ascorbate peroxidase (APX)] to balance elevated ROS and MDA levels, thereby alleviating metal-induced oxidative stress and promoting plant growth. Soil enzymes are extremely sensitive to changes in the soil environment, and they are crucial participants in soil nutrient cycles as well as functional sustainability (Duan et al., 2018; Aponte et al., 2020). Excessive metal concentrations have serious detrimental effects on soil enzyme activity and microorganisms, primarily in terms of soil basal respiration, microbial biomass, enzymatic activity, and soil microbial diversity (Molina-Santiago et al., 2019; Xiao et al., 2020). To date, soil enzyme activities have been universally used as an indicator of the ecological health of terrestrial ecosystems under heavy metal contamination (Wang et al., 2019; Hu et al., 2021). Yang et al. (2016) found that catalase is able to decompose H_2O_2 and protect organisms against damage. Moreover, some researchers have reported that phosphatases play an important role in the decomposition of organic phosphorus (P) compounds and have a very important role in improving soil quality (Yang et al., 2019; Wang et al., 2020). Therefore, restoration of soil oxidase and nutrient cycling enzyme activities may be essential for soil health. In this case, plant growth can improve the microbial properties of metal-contaminated soils by root activity their or root secretions. However, the lower nutrient content and higher toxicity of the contaminated soil form two major factors limiting plant growth (Ju et al., 2019; Huang et al., 2020). Therefore, to promote plant growth and reduce potential health risks, there is an urgent need to explore effective strategies that can improve plant resistance and enhance soil quality.

Recently, legumes have attracted interest for their roles in alleviating toxicity to plants in metal-polluted soils (Ju et al., 2020; Basile and Lepek, 2021). The symbiotic relationship between legumes and beneficial rhizobacteria such as plant-growth-promoting-rhizobacteria (PGPRs), can directly or indirectly promote plant growth by increasing nitrogen (N) and P uptake, and by enhancing plant defenses in heavy metal-contaminated soils (He et al., 2020). PGPRs are found in a large group of microorganisms that can interact with plants and promote plant growth, including *Azotobacter*, *Bacillus*, *Pseudomonas*, and *Rhizobium*, etc. (Ferreira et al., 2019). Therefore, as a novel phytobacterial strategy, PGPRs have been used to promote plant growth in heavy metal contaminated soils and enhance soil quality. Ju et al. (2019) showed that inoculation with PGPRs increased the activity of soil enzymes such as urease and β-glucosidase compared to the uninoculated control, which in turn improved soil quality. Moreover, Kong Z. et al. (2015), Kong Z. Y. et al. (2015), and Chen et al. (2018) reported that alfalfa-rhizobium symbiosis can promote plant growth and regulate antioxidant enzyme activity through the synthesis of indoleacetic acid and iron carriers. Allito et al. (2020, 2021) studied the effect of legume-rhizobium symbiosis on the biomass, nodulation, nitrogen fixation and nutrient uptake efficiency of faba bean. However, the soil-plant system is a whole, and the detailed mechanism of legume-rhizobium mediated mitigation of Cu-stress via the biochemical response of the plant-soil system is still limited.

Alfalfa (*Medicago sativa*) is a perennial forage grass that can survive in extreme environments and is widely distributed in the mining areas of northwest China (Wang et al., 2016; Peng et al., 2020). Therefore, it is important to further improve the resistance of alfalfa to heavy metals, reduce their accumulation in plant tissues, and increase the biomass of pastures for safe livestock production. In this study, a Cu-resistant strain (*Sinorhizobium meliloti*) was selected as an exogenous additive to investigate the effects of rhizobium on the growth and physiology of alfalfa in Cu-contaminated soil. We explored the effect of rhizobium inoculation on the microbial properties of Cu-contaminated soil. Further, this study determined the regulatory mechanism of rhizobium inoculation to alleviate Cu-stress in alfalfa through plant-soil system. The results of this study will enhance our understanding of the mechanisms associated with microbial inoculation in promoting plant resistance to Cu stress and providing a new strategy for the phytoremediation of Cu-contaminated soil.

MATERIALS AND METHODS

Experimental Design

Soil samples (obtained from the top 20-cm layer) were collected from a farmland in Yangling District, Shaanxi Province, China. The soil properties were as follows: pH, 8.49; total Cu, 13.2 mg kg^{-1}; soil organic carbon (SOC), 7.65 g kg^{-1}; total nitrogen (TN), 0.20 g kg^{-1}; total phosphorus (TP), 0.36 g kg^{-1}; available phosphorus (AP), 27.5 mg kg^{-1}; cation exchange capacity (CEC), 16.42 cmol kg^{-1}. The collected soil was air-dried, cleared of stones and plant debris, and sieved. Thereafter, $CuSO_4$ solution was added to the soil and mixed thoroughly, and maintained in dark at 25°C for 3 months. Ultimately, the experiment included five Cu-addition levels: 0, 200, 400, 600, and 800 mg kg^{-1}, respectively (denoted as Cu 0, Cu 200, Cu 400, Cu 600, and Cu 800, respectively).

The prepared Cu-contaminated soil was mixed and passed through a 2 mm sieve, and then the soil (600 g) was packed into plastic pots with a diameter of 10 cm. The soil was balanced for 1 week while maintaining at 60% of the water holding capacity. Alfalfa (*M. sativa*) seeds were sterilized with hydrogen peroxide solution (30%, v:v) and washed three times with

distilled water. The seeds were placed in seedling trays containing germination paper and incubated to await seed germination for 72 h, with the germination paper kept moist. Thereafter, 20 seedlings showing the same growth characteristics were selected and transplanted into each pot at a depth of 5 mm. After the alfalfa grew its first leave, the plant roots were injected with a rhizobial bacterial solution; in this study, a metal-resistant rhizobial strain *Sinorhizobium meliloti* CCNWSX0020 was used (Fan et al., 2011). The source and growth of *S. meliloti* has been described in our previous study (Duan et al., 2019). The *S. meliloti* suspensions (20 mL) were added to the plant roots each week (three times in total); in uninoculated controls, same amount of sterile distilled water was used. For the rest of the time, the soil moisture content was maintained at about 60%. Each treatment had three replicates. Finally, a total of 10 treatments: Cu 0, Cu 0 + *S. meliloti*, Cu 200, Cu 200 + *S. meliloti*, Cu 400, Cu 400 + *S. meliloti*, Cu 600, Cu 600 + *S. meliloti*, Cu 800, and Cu 800 + *S. meliloti*. Plants and soils were harvested on day 60 after the first inoculation, and indicators such as plant and soil enzyme activities were measured.

Determination of Plant Growth Indexes and Copper Contents

The chlorophyll content in plant leaves was extracted with 90% acetone, and then quantified using a spectrophotometer (UV3200, Shimador, Japan) (Richardson et al., 2002; Fang et al., 2020). A straightedge was used to measure alfalfa shoot height and root length. The shoots and roots were washed with sterilized deionized water and dried at 60°C to a constant weight. The shoot and root samples digested with H_2SO_4 and H_2O_2 were diluted with distilled water, and analyzed for N and P contents in the tissue using a flow analyzer (AA3, SEAL Company, Germany). Furthermore, approximately 0.3 g alfalfa samples digested with a mixture containing 8 mL HNO_3 and 2 mL $HClO_4$ were diluted to a certain volume (i.e., 100 mL) with distilled water, and the solution was analyzed for Cu concentration using an atomic absorption spectrophotometer (Hitachi, FAAS Z-2000, Japan). The Cu uptake was calculated as follows: Total Cu uptake = shoot/root biomass × shoot/root Cu concentration.

Determination of Malondialdehyde, Soluble Protein Content, and Antioxidant Enzyme Activities

MDA, soluble protein content, and antioxidant enzyme activities in alfalfa were determined using fresh shoots and roots. The MDA content in alfalfa tissues was determined using a kit provided by Suzhou Comin Biotechnology Co., Ltd. (Suzhou, China). The procedure was as follows: alfalfa shoot and root were ground using 1 mL extract. The mixture was centrifuged at 8,000 *g* for 15 min. The supernatant was aspirated and added to the color development solution, and placed in a boiling water bath for 30 min. After cooling and centrifugation, the MDA content in the supernatant was then determined by a microplate reader (Spark, TecanGroup, Ltd.). The soluble protein content was determined according to the manufacturer's instructions.

Plant antioxidant enzyme activities (i.e., SOD, POD, CAT, and APX) were also determined using the purchased kits. Fresh alfalfa tissue samples were ground with 1 mL extract and centrifuged at 8,000 *g* for 15 min. The supernatant was analyzed spectrophotometrically after treating it with the appropriate chromogenic agents corresponding to each enzyme (Chen et al., 2018).

Assays of Soil Physicochemical Properties

Soil pH was determined by conventional methods, and the detailed steps were referred to the previous study (Duan et al., 2018). The cation exchange capacity (CEC) was determined by ammonium acetate (NH_4OAc) method. The SOC and TN were determined using the K_2CrO_7–H_2SO_4 oxidation and Kjeldahl methods, respectively. Air-dried soils were digested with H_2SO_4 and $HClO_4$ were analyzed for TP at 880 nm using an ultraviolet spectrophotometer (UV3200, Shimador, Japan). Soil NH_4^+-N and NO_3^--N were determined using a continuous-flow autoanalyzer. Dissolved organic carbon (DOC) in fresh soil samples was extracted with 50 mL distilled water and then measured using a LiquiTOCII analyzer (Elementar, Germany). Available P (AP) was determined by sodium bicarbonate extraction method. The total soil Cu content was determined using the modified USEPA Method 3051A, with the following procedure: the soil samples (sieved to 0.149 mm) were digested with 15 mL acid mixture (i.e., 8 mL HNO_3, 2 mL $HClO_4$, and 5 mL HCl) and diluted with distilled water. Finally, the Cu concentration was determined using an atomic absorption spectrophotometer.

Assays of Soil Enzyme Activities and Microbial Biomass

Soil enzyme activity, including urease, β-glucosidase, alkaline phosphatase, and catalase was measured as described by Guan (1986) and Duan et al. (2018). The urease, β-glucosidase and alkaline phosphatase activities were determined using a spectrophotometer at 587, 400 and 578 nm, respectively. Among them, urease, was used by the sodium phenolate colorimetric method, β-glucosidase by the *p*-nitrophenol colorimetric method, and alkaline phosphatase by the sodium benzyl phosphate colorimetric method. Moreover, soil catalase activity was determined by titrating with potassium permanganate.

Microbial biomass carbon (MBC) and nitrogen (MBN) were analyzed using a previously described method with slight modifications (Vance et al., 1987; Wang et al., 2020). Fresh soil samples (10 g) were fumigated with ethanol-free chloroform in dark for 24 h and extracted with 0.5 M potassium sulfate solution (40 mL) for 30 min. The supernatant was filtered, and the extractable organic carbon (EOC) and nitrogen (EON) contents were determined simultaneously using a LiquiTOC II analyzer (Elementar, Germany). Similarly, EOC and EON were estimated in 10 g of unfumigated soil samples. MBC and MBN were calculated from the difference in EOC and EON between fumigated and non-fumigated samples, respectively.

Statistical Analyses

A two-way analysis of plant and soil properties between different treatments was performed using IBM SPSS 20.0 software and Duncan's *post-test* ($P < 0.05$) was used for multiple testing. In addition, the difference between non-inoculated and inoculated alfalfa under the same Cu concentration condition was examined by *T*-test. All bar graphs were plotted using Origin Pro 2021. Pearson correlation coefficient analysis and partial least squares path modeling (PLS-PM) analyses were performed using the software packages "ggcorrplot" and "plspm" in R (version 3.6.2). The relationships between different indicators were compared and determined using the correlation heat map, and PLS-PM was used to determine the direct and indirect factors affecting plant growth.

RESULTS

Plant Growth Phenotype and the N and P Content of Alfalfa

As shown in **Figure 1**, the shoot and root length, and biomass of alfalfa decreased with increasing Cu concentration in the control, but rhizobium inoculation alleviated the growth inhibition of alfalfa. In addition, Cu concentration and rhizobium inoculation had significant main and interactive effects on the shoot and root length, and root biomass ($P < 0.01$; **Figure 1**). The total chlorophyll content increased significantly after rhizobium inoculation, and this increase was prominent at a Cu concentration of 800 mg kg^{-1}, which was 1.44 times higher than that of the uninoculated control (**Table 1**). Cu concentration and rhizobium inoculation had significant interactive effects on total chlorophyll and chlorophyll *a* ($P < 0.05$).

The N level in alfalfa shoots and roots was higher in the treatment without Cu, but did not differ significantly with increasing Cu stress (**Table 1**). Rhizobium inoculation increased the shoot N content at the Cu concentrations of 0 and 800 mg kg^{-1}. The root N content increased significantly with rhizobium inoculation. In addition, Cu concentration and rhizobium inoculation had significant main and interactive effects on the P content in the plant shoots and roots ($P < 0.001$; **Table 1**). Compared to the uninoculated control, rhizobium inoculation with significantly increased the P levels in the alfalfa tissues, particularly at Cu 600 and Cu 800 treatments ($P < 0.05$).

Differences in Copper Concentration and Copper Uptake by Alfalfa

Rhizobial effect on Cu concentrations varied in different parts of alfalfa (**Table 2**). Notably, exogenous addition of rhizobium

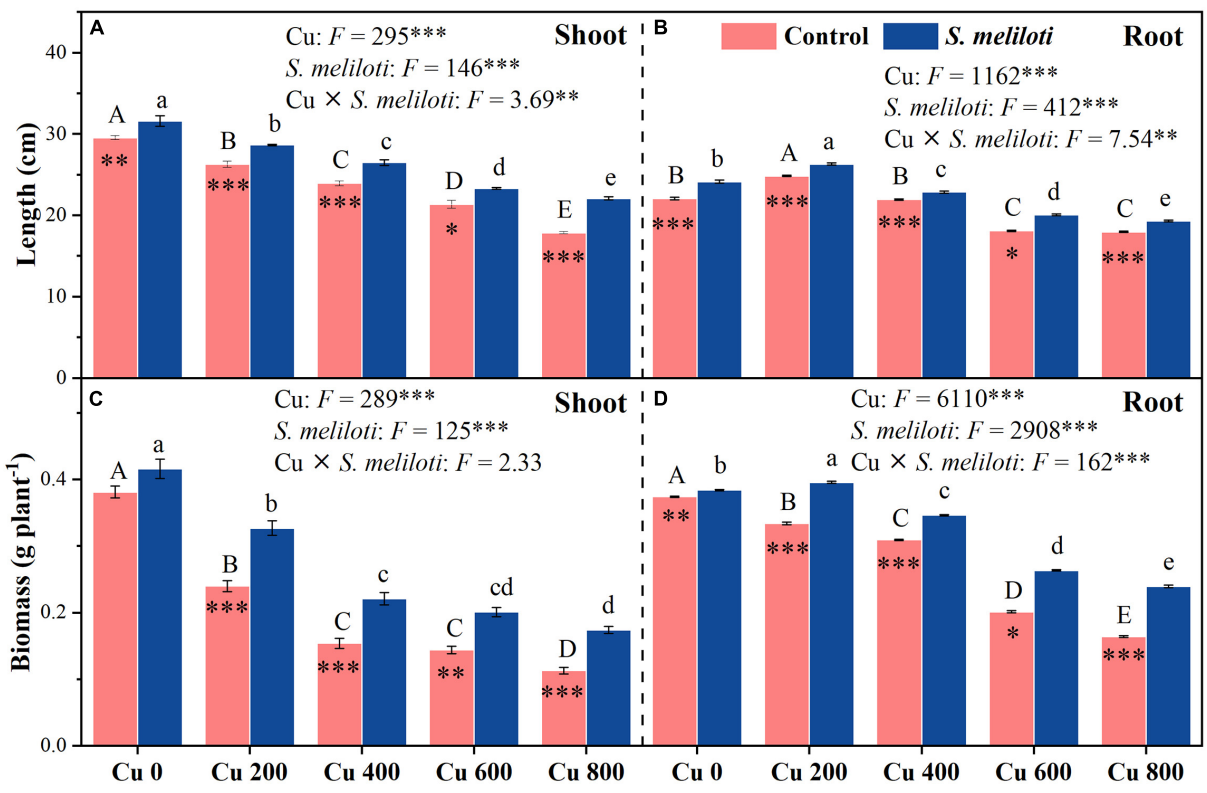

FIGURE 1 | The effect of inoculation with *S. meliloti* on length and biomass in the shoot (left panel) and root (right panel) of alfalfa with different Cu concentration treatments. The capitalized (Cu) and lowercase (*S. meliloti*) letters above the bars indicate significant difference between different Cu concentrations ($P < 0.05$). The asterisks indicate significant differences between non-inoculated and inoculated alfalfa under the same Cu concentration condition. Each value represents the mean ± SE ($n = 3$). ***$P < 0.001$; **$P < 0.01$; *$P < 0.05$.

TABLE 1 | The chlorophyll, nitrogen and phosphorus content in alfalfa tissue.

Treatments		Chlorophyll content (mg g^{-1})			Nitrogen (g kg^{-1})		Phosphorus (g kg^{-1})	
		a	b	Total	Shoot	Root	Shoot	Root
Cu 0	Control	0.62 ± 0.01 Ab	0.42 ± 0.02 Aa	1.04 ± 0.02 ABb	21.1 ± 0.37 Ab	17.5 ± 0.17 Aa	1.25 ± 0.01 Ab	0.81 ± 0.01 Ab
	S. meliloti	0.66 ± 0.02 BCa	0.47 ± 0.03 Aa	1.13 ± 0.03 Ba	23.1 ± 0.41 Aa	17.2 ± 0.18 Aa	1.51 ± 0.03 Aa	1.33 ± 0.02 Aa
Cu 200	Control	0.63 ± 0.01 Ab	0.43 ± 0.01 Aa	1.06 ± 0.01 Ab	20.0 ± 0.39 Ba	15.9 ± 0.29 Bb	1.2 ± 0.01 Ba	0.76 ± 0.01 Ba
	S. meliloti	0.74 ± 0.02 Aa	0.48 ± 0.02 Aa	1.22 ± 0.03 Aa	21.4 ± 0.93 Ba	17.2 ± 0.23 Aa	1.24 ± 0.01 Ba	0.74 ± 0.02 Ba
Cu 400	Control	0.56 ± 0.02 Aa	0.41 ± 0.01 Aa	0.97 ± 0.01 Bb	17.1 ± 0.11 Ca	14.3 ± 0.07 Cb	1.09 ± 0.03 Ca	0.60 ± 0.01 Ca
	S. meliloti	0.62 ± 0.01 Ca	0.42 ± 0.01 ABa	1.04 ± 0.01 Ca	17.8 ± 0.30 Ca	15.2 ± 0.09 Ca	0.97 ± 0.02 Db	0.63 ± 0.01 Ca
Cu 600	Control	0.61 ± 0.03 Aa	0.40 ± 0.02 Aa	1.01 ± 0.04 ABb	17.7 ± 0.32 Ca	14.4 ± 0.12 Cb	0.90 ± 0.01 Db	0.59 ± 0.01 Cb
	S. meliloti	0.71 ± 0.01 ABa	0.45 ± 0.01 Aa	1.16 ± 0.01 ABa	18.4 ± 0.05 Ca	15.6 ± 0.02 Ca	0.97 ± 0.02 Da	0.64 ± 0.02 Ca
Cu 800	Control	0.38 ± 0.04 Bb	0.22 ± 0.01 Bb	0.61 ± 0.02 Cb	17.1 ± 0.18 Cb	14.7 ± 0.15 Cb	0.74 ± 0.01 Eb	0.51 ± 0.01 Db
	S. meliloti	0.52 ± 0.03 Da	0.37 ± 0.01 Ba	0.88 ± 0.02 Da	18.9 ± 0.38 Ca	16.2 ± 0.07 Ba	1.05 ± 0.02 Ca	0.55 ± 0.02 Da
Factor (Df)		*F* *P*	*F* *P*	*F* *P*	*F* *P*	*F* *P*	*F* *P*	*F* *P*
Cu (4)		28.9 ***	37.1 ***	94.3 ***	47.7 ***	94.6 ***	282 ***	788 ***
S. meliloti (1)		32.0 ***	42.1 ***	107 ***	25.2 ***	82.9 ***	106 ***	334 ***
Cu × *S. meliloti* (4)		4.40 *	1.51 NS	6.50 **	1.15 NS	9.27 ***	51.5 ***	221 ***

*The capitalized letters indicate significant differences between different Cu concentrations, whereas the lower-case letters indicate significant differences between non-inoculated and inoculated alfalfa under the same Cu concentration condition ($P < 0.05$). Each value represents the mean ± SE ($n = 3$). ***$P < 0.001$; **$P < 0.01$; *$P < 0.05$; NS, no significant.*

TABLE 2 | Cu concentrations and the total uptake of Cu in alfalfa tissue.

Treatments		Cu concentrations (mg kg^{-1})		Total uptake (μg $plant^{-1}$)		TF
		Shoot	Root	Shoot	Root	
Cu 0	Control	8.54 ± 0.07 Da	24.9 ± 0.56 Ea	3.25 ± 0.03 Ba	9.30 ± 0.21 Da	0.34 ± 0.01 Ab
	S. meliloti	6.45 ± 0.12 Db	3.06 ± 0.22 Eb	2.68 ± 0.05 Bb	1.18 ± 0.08 Eb	2.13 ± 0.19 Aa
Cu 200	Control	12.3 ± 0.90 Ca	42.8 ± 0.92 Da	2.96 ± 0.22 Ba	14.3 ± 0.31 Ca	0.29 ± 0.03 Bb
	S. meliloti	10.4 ± 0.15 Ba	26.1 ± 0.04 Db	3.41 ± 0.05 Aa	10.3 ± 0.02 Db	0.40 ± 0.01 Ba
Cu 400	Control	15.9 ± 0.27 Ba	50.4 ± 0.33 Cb	2.45 ± 0.04 Ca	15.6 ± 0.10 Bb	0.32 ± 0.01 Ba
	S. meliloti	8.54 ± 0.08 Cb	64.6 ± 0.32 Ca	1.89 ± 0.02 Cb	22.4 ± 0.11 Ba	0.13 ± 0.01 Ca
Cu 600	Control	28.7 ± 0.56 Aa	93.3 ± 1.20 Ab	4.13 ± 0.08 Aa	18.8 ± 0.24 Ab	0.31 ± 0.01 Ba
	S. meliloti	15.7 ± 0.70 Ab	119 ± 0.75 Aa	3.16 ± 0.14 Ab	31.5 ± 0.20 Aa	0.13 ± 0.01 Cb
Cu 800	Control	13.2 ± 0.70 Ca	55.2 ± 2.89 Bb	1.49 ± 0.08 Da	9.06 ± 0.47 Db	0.24 ± 0.02 Ca
	S. meliloti	7.50 ± 0.70 CDb	83.1 ± 0.68 Ba	1.31 ± 0.12 Da	19.9 ± 0.16 Ca	0.09 ± 0.01 Cb
Factor (Df)		*F* *P*	*F* *P*	*F* *P*	*F* *P*	*F* *P*
Cu (4)		230 ***	2,025 ***	157 ***	2,145 ***	108 ***
S. meliloti (1)		332 ***	72.3 ***	33.2 ***	642 ***	51.5 ***
Cu × *S. meliloti* (4)		38.2 ***	229 ***	14.2 ***	825 ***	96.6 ***

*The capitalized letters indicate significant differences between different Cu concentrations, whereas the lower-case letters indicate significant differences between non-inoculated and inoculated alfalfa under the same Cu concentration condition ($P < 0.05$). TF (translocation factor: shoot concentration/root concentration). Each value represents the mean ± SE ($n = 3$). ***$P < 0.001$.*

significantly reduced the Cu concentration in the shoots, but noticeably increased it in the roots ($P < 0.05$). In the shoots, the Cu uptake by the inoculated plants was evidently lower than that of the uninoculated plants in the Cu 0, Cu 400, and Cu 600 treatments ($P < 0.05$). Furthermore, rhizobium inoculation decreased the Cu uptake in roots when treated with low Cu concentrations (0 or 200 mg kg^{-1}). However, under high Cu concentrations, Cu uptake in roots increased with rhizobium inoculation. Except for the Cu 0 treatment, the Cu transfer coefficients were considerably less than 1.0. Rhizobium inoculation increased the Cu transfer coefficients in treatments with low Cu concentrations (0 or 200 mg kg^{-1}). However, under high Cu concentrations, the Cu transfer coefficients decreased with rhizobium inoculation.

Plant Oxidative Damage, Soluble Protein, and Antioxidant Enzyme Activity

The effect of heavy metals on lipid peroxidation damage was evaluated by measuring the MDA content (**Figure 2A**), which increased in both shoots and roots as the Cu concentration increased during treatments, but rhizobium inoculation

reduced MDA accumulation in plant tissues. In the same Cu concentration treatment, the reduction of shoot MDA content after inoculation with rhizobium was less than that of the root. Moreover, Cu concentration and rhizobium inoculation had significant interactive effects on the root MDA content ($P < 0.05$). This indicates that rhizobium inoculation had a relatively higher relieving effect on roots than on the aboveground parts. Additionally, MDA content in shoots and roots was negatively correlated with N and P content ($P < 0.001$; **Figure 3**). Cu concentration and rhizobium inoculation had significant main and interactive effects on the soluble protein content in the plant shoots and roots ($P < 0.001$, **Figure 2B**). In addition, soluble protein content in roots was significantly positively correlated with N content ($P < 0.05$; **Figure 3B**).

The SOD activity in the shoots of uninoculated plants showed no obvious change, while the roots of alfalfa showed a downward trend under Cu stress (**Figure 4A**). Compared with the uninoculated alfalfa, plants inoculated with rhizobium exhibited higher SOD activity in the roots ($P < 0.01$; **Figure 4A**); for example, in the Cu 600 and Cu 800 treatments, root SOD was 2.87 and 3.23 times higher after rhizobia inoculation than in the uninoculated treatment, respectively (**Figure 4A**). Under the Cu 600 treatment, there was the highest shoot POD activity but lower in the root, suggesting different response mechanisms in the shoot and root (**Figure 4B**). Cu concentration and rhizobium inoculation had significant main and interactive effects on the POD activity in the plant shoots and roots ($P < 0.001$). Except for Cu 600 treatment, rhizobium inoculation significantly reduced CAT activity in the shoot ($P < 0.01$; **Figure 4C**). Rhizobium inoculation had no obvious effect on CAT activity in alfalfa roots, and no significant interactive effects between Cu and rhizobium inoculation on root CAT. Differences in APX activity in alfalfa tissue between uninoculated and inoculated plants were inconsistent and influenced by specific Cu treatments (**Figure 4D**). In addition, the application of rhizobium increased the alfalfa APX activity at low Cu concentrations (0 or 200 mg kg^{-1}). SOD activity in shoots was significantly and negatively correlated with N and P content ($P < 0.01$). However, the APX activity of alfalfa (shoot and root) was significantly and positively correlated with the content of N and P, respectively ($P < 0.05$; **Figure 3**).

Soil Nutrient, Enzyme Activities, and Microbial Biomass

Soil Cu concentration decreased significantly after rhizobium inoculation ($P < 0.05$; **Supplementary Table 1**). Cu concentration and rhizobium inoculation had significant main and interactive effects on the NO_3^--N and NH_4^+-N contents ($P < 0.001$). The highest AP content was observed in the Cu 600 treatment in both the inoculated and uninoculated treatments. However, rhizobium inoculation did not evidently affect AP. Rhizobium inoculation increased the DOC content at low Cu concentrations (200 or 400 mg kg^{-1}), whereas the DOC was significantly reduced at a Cu concentration of 600 mg kg^{-1} ($P < 0.05$). Soil total N and P contents were only influenced by soil Cu concentration and did not respond significantly to rhizobium inoculation. Cu concentration and rhizobium inoculation had significant main and interactive effects on pH and CEC ($P < 0.01$). Moreover, the pH value decreases with increasing Cu concentration.

The changes in soil enzymes (i.e., catalase, urease, β-glucosidase, and alkaline phosphatase) were shown in **Figure 5**. In the uninoculated control, the catalase activity in Cu 0 was significantly higher than that in the other treatments, and the increase in Cu concentration strongly inhibited catalase activity, whereas rhizobium inoculation remarkably increased catalase activity in the Cu 400 and Cu 600 treatments ($P < 0.05$). Cu concentration and rhizobium inoculation had significant main and interactive effects on β-glucosidase activity ($P < 0.001$). Furthermore, soil phosphatase activity consistently decreased with increasing Cu concentration, rhizobium inoculation notably affected the alkaline phosphatase activity. However, rhizobium inoculation enhanced urease activity only at low Cu concentrations (0 or 200 mg kg^{-1}). Cu concentration and rhizobium inoculation had significant main and interactive effects on MBC and MBN ($P < 0.05$), and rhizobium inoculation significantly increased the MBN content in Cu 200 and Cu 400 treatments ($P < 0.05$; **Figure 6**).

Driving Factors Affecting Plant Growth

The N content in shoots and roots showed the highest positive correlations with SOC, DOC, CEC, pH, and soil enzyme activities ($P < 0.001$), and the highest negative correlations with MBN, NH_4^+-N, TN, AP, and Cu concentrations ($P < 0.05$; **Supplementary Figure 1**). In addition, the plant P showed the strongest positive correlation with MBC, TP, SOC, DOC, CEC, pH, and soil enzyme activities ($P < 0.01$), and the strongest negative correlation with MBN, NH_4^+-N, TN, AP, and Cu concentrations ($P < 0.05$; **Supplementary Figure 1**). We used PLS-PM to further reveal the effects of plant physiological indicators, soil physicochemical properties, and soil biochemical indicators on alfalfa growth (**Figure 7**). The PLS-PM method showed that plant antioxidant enzyme activities, soil nutrient, and soil enzyme activities had a significant positive direct effect (0.35, 0.28, and 0.42, respectively; $P < 0.01$) on plant growth (**Figure 7A**). The application of *S. meliloti* (0.34), soil microbial biomass (0.61), soil enzyme activities (0.82), soil nutrient (0.28), and antioxidant enzyme activities (0.35) had positive total effects on plant growth, whereas the plant oxidative damage (−0.13) induced negative total effects (**Figure 7B**).

DISCUSSION

Plants grown in Cu-contaminated soils may have to endure physiological dysfunction, growth inhibition, reduced biomass, and metal accumulation (Rostami and Azhdarpoor, 2019; Fang et al., 2020). In this study, inoculation of rhizobium (i.e., *S. meliloti*) not only increased the height and biomass of alfalfa, but also increased its chlorophyll content (**Table 1** and **Figure 1**). This indicates that inoculation with rhizobium promoted the photosynthetic reaction rate of plants and alleviated the toxic effects of Cu stress (Chou et al., 2019; Gong et al., 2019).

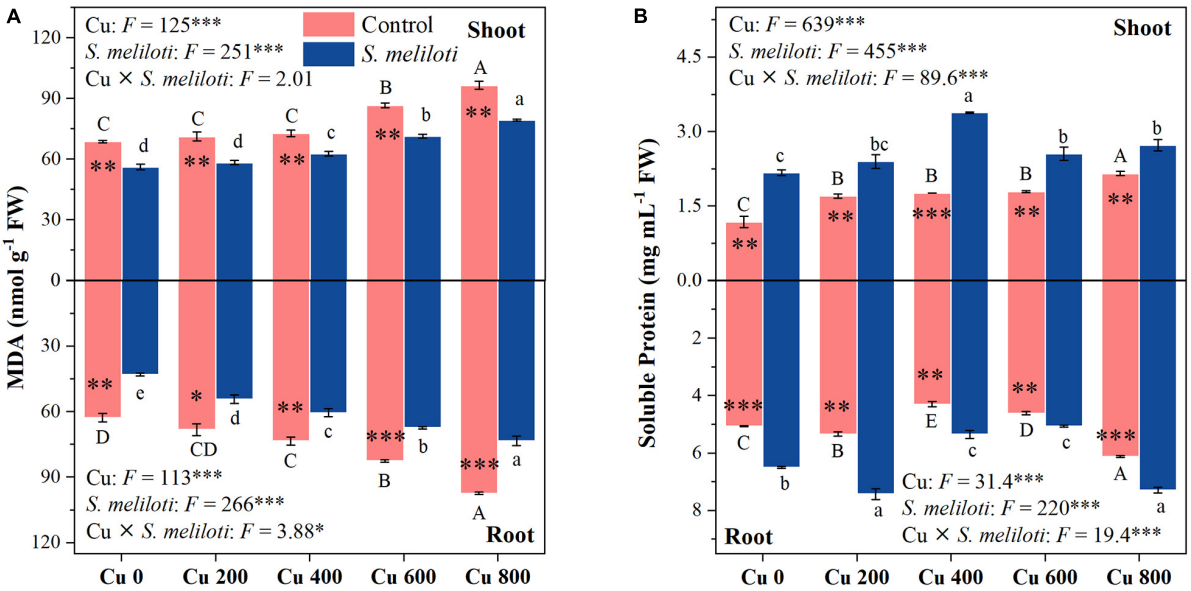

FIGURE 2 | The effect of inoculation with *S. meliloti* on MDA **(A)** and soluble protein **(B)** in shoot (top panel) and root (lower panel) of alfalfa with different Cu concentration treatments. MDA: malondialdehyde. The capitalized (Cu) and lowercase (*S. meliloti*) letters above the bars indicate significant difference between different Cu concentrations ($P < 0.05$). The asterisks indicate significant differences between non-inoculated and inoculated alfalfa under the same Cu concentration condition. Each value represents the mean ± SE ($n = 3$). ***$P < 0.001$; **$P < 0.01$; *$P < 0.05$.

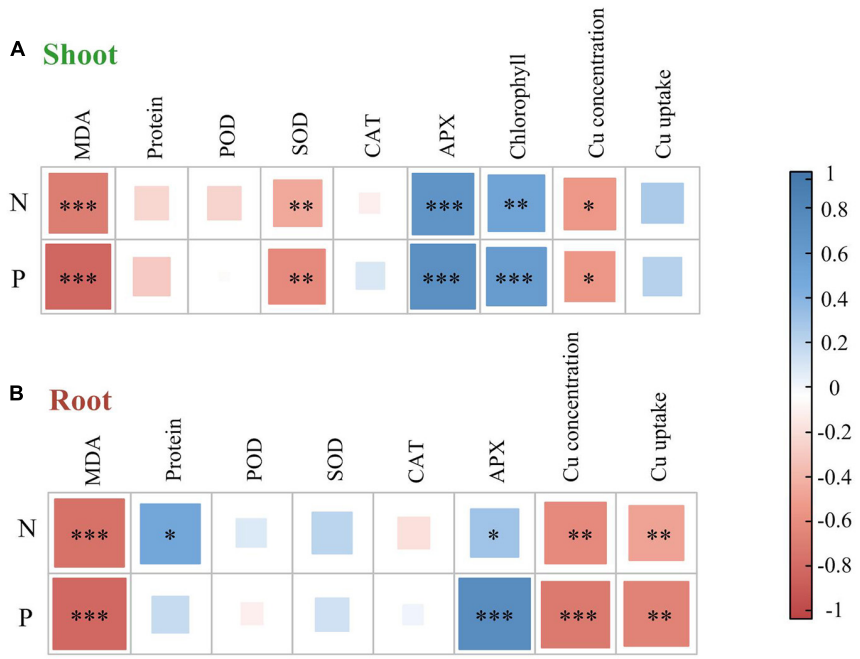

FIGURE 3 | A correlation heat map illustrating pairwise relationships between plant nutrient elements and plant properties in alfalfa shoot **(A)** and root **(B)** based on Pearson correlation coefficient analysis. N, nitrogen concentration; P, phosphorus concentration; MDA, malondialdehyde; Protein, soluble protein; SOD, superoxide dismutase; POD, guaiacol peroxidase; CAT, catalase; APX, ascorbate peroxidase. ***$P < 0.001$; **$P < 0.01$; *$P < 0.05$.

This further confirmed the important role of alfalfa-rhizobium symbiosis in soil Cu bioremediation. Moreover, inoculation with rhizobium significantly reduced the metal transfer coefficient under high Cu-stress (i.e., Cu 600 and Cu 800) (**Table 2**). This suggests that Cu accumulates mainly in the roots, while a very small amount is transferred to the shoots, which not only facilitates the phytostabilization of Cu, but also improves aboveground forage quality. Rhizobium inoculation significantly

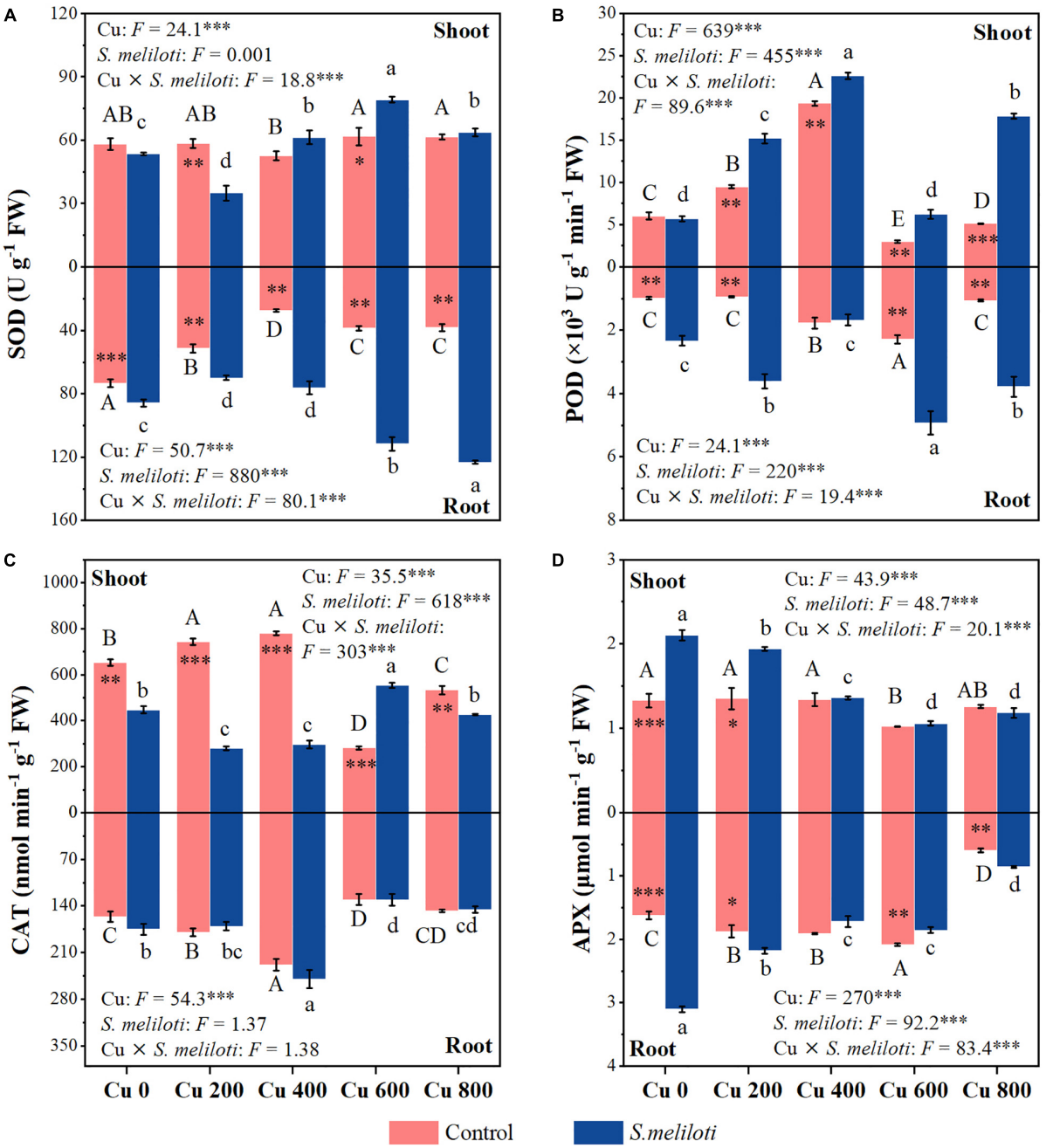

FIGURE 4 | The effect of inoculation with *S. meliloti* on plant antioxidant enzyme activities in alfalfa tissue. SOD, superoxide dismutase; POD, guaiacol peroxidase; CAT, catalase; APX, ascorbate peroxidase. The capitalized (Cu) and lowercase (*S. meliloti*) letters above the bars indicate significant difference between different Cu concentrations ($P < 0.05$). The asterisks indicate significant differences between non-inoculated and inoculated alfalfa under the same Cu concentration condition. Each value represents the mean ± SE ($n = 3$). ***$P < 0.001$; **$P < 0.01$; *$P < 0.05$.

increased the N content in alfalfa roots (**Table 1**), providing a sufficient source of N for plant growth and alleviating alfalfa toxicity. However, the effect of rhizobium inoculation on the N content of the shoots was substantially lower than that of the roots (**Table 1**). The nodules functioning in the root system are probably the main nitrogen-fixing organs (Stambulska and Bayliak, 2019). This also indicates that the Cu-resistant strain (i.e., *S. meliloti*) can survive at 0–800 mg kg^{-1} Cu concentrations and promote alfalfa nitrogen fixation. Heavy metal tolerant rhizobia affect the biological effectiveness of metals in soil by regulating biological nitrogen fixation and promoting plant growth (Duan et al., 2019; Jian et al., 2019; Shen et al., 2020). Furthermore, P plays an important role in plant growth. Our study found that inoculation with rhizobium had a significant main effect on the P content of alfalfa in the shoot and root parts (**Table 1**). This may be due to the fact that the addition

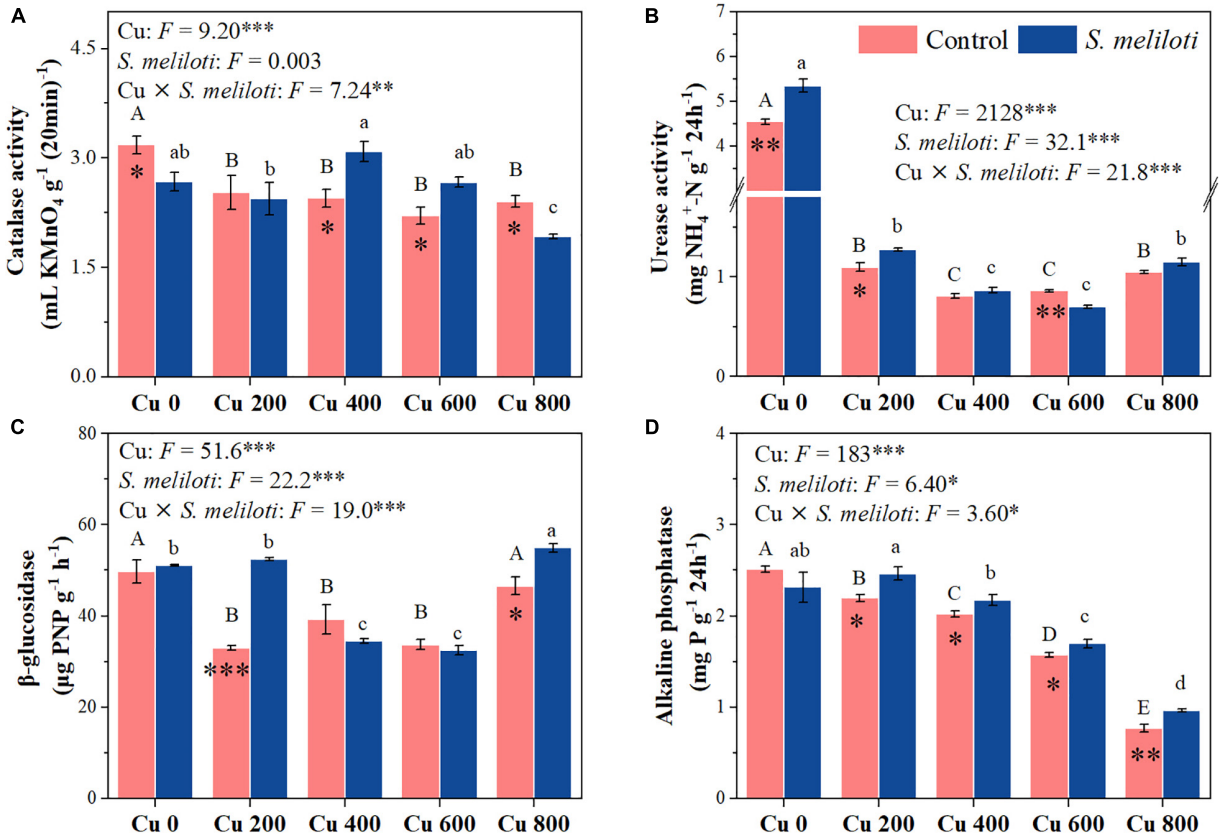

FIGURE 5 | The effect of inoculation with *S. meliloti* on soil enzyme activities under different Cu concentration treatments. The capitalized (Cu) and lowercase (*S. meliloti*) letters above the bars indicate significant difference between different Cu concentrations ($P < 0.05$). The asterisks indicate significant differences between non-inoculated and inoculated alfalfa under the same Cu concentration condition. Each value represents the mean ± SE ($n = 3$). ***$P < 0.001$; **$P < 0.01$; *$P < 0.05$.

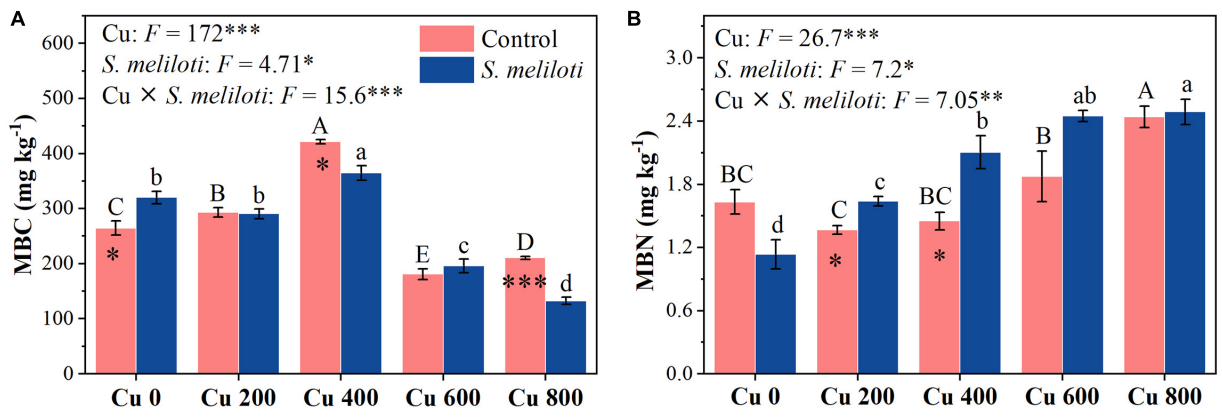

FIGURE 6 | The effect of inoculation with *S. meliloti* on soil microbial biomass carbon and nitrogen under different Cu concentration treatments. MBC, microbial biomass carbon; MBN, microbial biomass nitrogen. The capitalized (Cu) and lowercase (*S. meliloti*) letters above the bars indicate significant difference between different Cu concentrations ($P < 0.05$). The asterisks indicate significant differences between non-inoculated and inoculated alfalfa under the same Cu concentration condition. Each value represents the mean ± SE ($n = 3$). ***$P < 0.001$; **$P < 0.01$; *$P < 0.05$.

of rhizobium induced alfalfa roots to secrete more phosphatase, which increased the effectiveness of soil P for alfalfa uptake (Peng et al., 2020). Rhizobia, as a P-dissolving microorganism, lower soil pH by dissolving various small amounts of insoluble P sources, thus increasing P uptake and plant biomass (Ma et al., 2016; Zhou et al., 2020). These results demonstrate that rhizobium inoculation alleviates metal stress by increasing plant nutrient content (N and P) and reducing Cu transfer to the shoot in alfalfa.

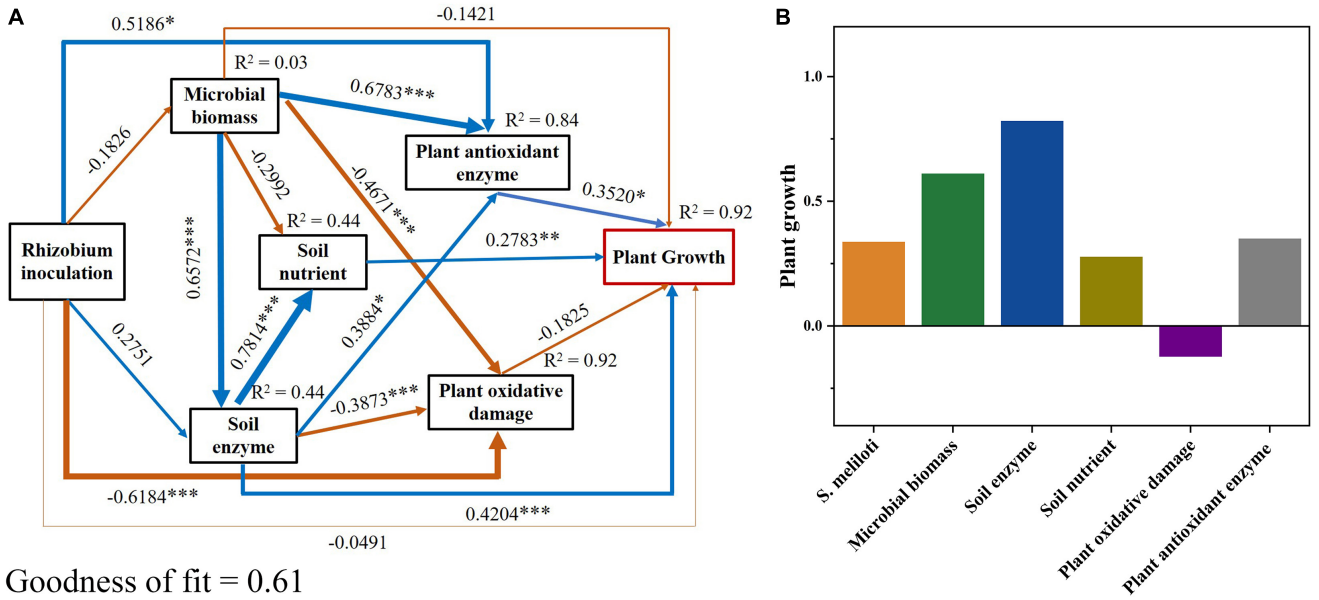

FIGURE 7 | Partial least squares path modeling (PLS-PM) disentangling major pathways of the effects of rhizobium inoculation, soil microbial biomass, enzyme activity, soil nutrient, plant oxidative damage and plant antioxidant enzyme activities on plant growth. Blue and yellow arrows indicate positive and negative flows of causality, respectively. Numbers on the arrow indicate significant standardized path coefficients (***$P < 0.001$; **$P < 0.01$; *$P < 0.05$). R^2 indicates the variance of dependent variable explained by the model. Microbial biomass includes microbial biomass carbon and nitrogen; soil enzyme includes urease, β-glucosidase and phosphatase; soil nutrient includes soil dissolved organic carbon, NO_3^--N and soil available phosphorus; plant oxidative damage includes plant MDA (malondialdehyde); plant antioxidant enzyme includes POD (guaiacol peroxidase), CAT (catalase) and APX (ascorbate peroxidase); plant growth includes the nitrogen and phosphorus contents of tissue.

Inoculation rhizobium can increase alfalfa growth and improve its resistance to Cu stress. A significant increase in the Cu content of roots after inoculation was observed (**Table 2**). However, the increased Cu content in roots did not lead to increased content in shoots nor did it inhibiting alfalfa growth, which further indicated that inoculation could improve alfalfa resistance to Cu stress. Although excessive Cu accumulation produced large amounts of MDA in alfalfa seedlings, exacerbating oxidative stress in the cells (**Figure 2**), inoculation with rhizobium significantly reduced the MDA content in the shoots and roots of the alfalfa. The results of PLS-PM further supported that rhizobium inoculation mitigates oxidative damage caused by Cu toxicity in alfalfa (**Figure 7**). Oxidative damage and antioxidant enzyme activities can effectively reflect the intensity of toxicity endured by plant cells and are important in understanding the metal-specific toxicity mechanisms in plants (Chen et al., 2018; Romero-Puertas et al., 2018). Kong Z. Y. et al. (2015) suggested that the promotion of plant antioxidant defenses by bacteria may improve symbiotic performance, especially under non-optimal conditions. Previous studies have shown that exogenous nitrogen can alleviate oxidative stress induced by heavy metal exposure (Ju et al., 2019; Wang X. et al., 2021), which further demonstrates that rhizobium-legumes can mitigate oxidative stress through symbiotic nitrogen fixation. In summary, this indicates that rhizobium inoculated plants suffered less oxidative damage and exhibited a higher antioxidant capacity under Cu-stress.

The accumulation of soluble proteins in plants is a response to stress caused by toxic elements, either through the reduction of oxidative stress or the regulation of cellular osmotic capacity (Raza et al., 2020). Rhizobium-inoculated plants exhibited higher soluble protein content in alfalfa tissues compared with uninoculated plants (**Figure 2B**). This finding indicates that adding rhizobium improved the symbiotic performance of alfalfa and promoted an increase in soluble protein content, especially under non-optimal conditions. Meanwhile, alfalfa has high antioxidant enzyme activities that protect cells from oxidative damage caused by external environmental stresses (i.e., higher MDA contents) (Morina et al., 2016; Hojati et al., 2017). Cu-stress reduced SOD activity in alfalfa tissues (**Figure 4A**). Cu-contamination-induced destruction of membranes and enzyme systems resulted in reduced SOD activity, especially at high Cu concentrations (600 and 800 mg kg^{-1}). Furthermore, rhizobium inoculation considerably affected the increase in SOD activity in alfalfa roots (**Figure 4A**). This result indicates that rhizobium application enhanced SOD activity in tissues and improved their resistance to stress. Studies have shown that metal resistant beneficial microbes (PGPRs) are often used as bioinoculants to affect metabolic functions and antioxidant enzyme activities of root cells and thus to enhance the establishment, growth and development of remediating plants in metal contaminated soils (Ma et al., 2016; Ju et al., 2020). In comparison with uninoculated alfalfa tissue, the activities of POD and APX in the shoots and roots of inoculated alfalfa increased at different levels of symbiosis (**Figure 4**). The results showed a significant

positive correlation between APX activity, and the N and P contents of alfalfa (**Figure 3**). In addition, the alfalfa-rhizobium symbiotic system can promote plant nitrogen fixation, stimulate the release of phytohormones and antioxidant enzyme activities, and ultimately reduce the toxicity of alfalfa and promote its growth (Hao et al., 2014; Fang et al., 2020). Nonetheless, the addition of rhizobia reduced the Cu-induced CAT activity in the shoots, except for the Cu 600 treatment (**Figure 4C**). This suggests that rhizobium inoculation in the shoots inhibits the damage caused by excess hydrogen peroxide; therefore, more CAT activities are unnecessary in eliminating the hydrogen peroxide produced under Cu− concentration in the alfalfa tissues (Cao et al., 2017; Beiyuan et al., 2021). Overall, the above results indicate that rhizobium inoculation responds to Cu-stress with increasing soluble proteins, POD, and APX activities, which therefore alleviates heavy metals toxicity in alfalfa. The way in which rhizobium inoculation assists in increasing plant resistance is the key to revealing the mechanisms that promote growth in inoculation.

Soil enzymes can be used to evolute the effects of the soil remediation process since they relate to the biogeochemical cycling of elements (Yang et al., 2019). Rhizobium inoculation significantly increased catalase activity in the Cu 400 and Cu 600 treatments (**Figure 5A**). Catalase can participate in the H_2O_2 detoxification process by changing the valence reference of heavy metal ions (Duan et al., 2018), and the addition of beneficial bacteria to the soil can further alleviate soil Cu toxicity and increase catalase activity (Yang et al., 2016; Aponte et al., 2020). In addition, soil carbon (C), N and P cycling activities are also associated with microbial metabolism and reflect the interaction between microorganisms and their associative environment (Cui et al., 2019; Ju et al., 2020). Soil β-glucosidase activity is associated with soluble nutrients, such as DOC, and reflects soil C cycling and fertility (Raiesi and Salek-Gilani, 2018). Rhizobium inoculation increased DOC in this study (**Supplementary Table 1**), and there was a significant positive correlation between DOC and β-glucosidase (**Supplementary Figure 1**), indicating that rhizobium inoculation promotes soil C cycling and provides nutrients for plant growth. Meanwhile, inoculation with rhizobium significantly promoted alkaline phosphatase activity (**Figure 5D**). Phosphatase in soils is mainly produced by microbial activity and is critical for mobilizing the organic forms of P (Wei et al., 2019; Ma et al., 2021). These results demonstrated that rhizobium inoculation can promote soil nutrient cycling by stimulating enzyme activities in metal contaminated soil while subsequently providing higher C, N, and P requirements for microbial activity and plant growth. Moreover, the N and P contents of alfalfa were significantly positively correlated with the soil enzymes activities (**Supplementary Figure 1**), and the PLS-PM results also showed an overall significant positive effect of soil enzymes and microbial biomass on plant growth following *S. meliloti* application (**Figure 7**). The legume-rhizobium symbiosis regulated the rate of enzyme synthesis via Cu or by altering the interference of toxicity in enzyme-producing microbial community, thus reducing metal toxicity in soil (Yu et al., 2019; Fang et al., 2020). Our results show that heavy metal-resistant soil rhizobacteria can significantly reduce the soil Cu concentrations (**Supplementary Table 1**), which was favorable for the survival of microorganisms. Based on the above information, we found that the legume-rhizobium symbiotic system promoted alfalfa growth in Cu-contaminated soil by regulating plant physiological and biochemical properties, soil nutrients, and soil enzyme activities.

CONCLUSION

This study offers comprehensive insight into how symbiotic microbes affect plant physiology and soil microbial properties to assist alfalfa against Cu stress. Excessive accumulation of Cu in alfalfa exhibited varied toxicity symptoms, including decreased biomass, chlorotic leaves, and inhibition of antioxidant enzyme activities. Rhizobium inoculation significantly improved the growth of alfalfa under Cu-stress by effectively improving the detoxification ability. The legume-rhizobium symbiotic system resists Cu-induced oxidative stress in alfalfa tissues by enhancing antioxidant enzyme activities to scavenge superfluous malondialdehyde. Moreover, rhizobium application improved soil microbial parameters, such as soil enzyme activity and microbial biomass, thereby promoting plant growth. These findings are important for further improve plant resistance and ensure forage and crop production.

DATA AVAILABILITY STATEMENT

The original contributions presented in the study are included in the article/**Supplementary Material**, further inquiries can be directed to the corresponding author/s.

AUTHOR CONTRIBUTIONS

CD: writing—original draft, writing—review and editing, and visualization. YM, QW, and YW: methodology and writing—review and editing. QL: investigation and methodology. MH and SH: investigation. SL: writing—review and editing. LF: funding acquisition, methodology, resources, supervision, and writing—review and editing. All authors contributed to the article and approved the submitted version.

FUNDING

This work was financially supported by the National Natural Science Foundation of China (41977031 and 41571314) and National Funds for Distinguished Young Scientists of Shaanxi Province (2020JC-31).

SUPPLEMENTARY MATERIAL

The Supplementary Material for this article can be found online at: https://www.frontiersin.org/articles/10.3389/fmicb.2021.781831/full#supplementary-material

REFERENCES

Abbas, T., Rizwan, M., Ali, S., Zia-ur-Rehman, M., Qayyum, M. F., Abbas, F., et al. (2017). Effect of biochar on cadmium bioavailability and uptake in wheat (*Triticum aestivum* L.) grown in a soil with aged contamination. *Ecotox. Environ. Safe* 140, 37–47. doi: 10.1016/j.ecoenv.2017.02.028

Allito, B. B., Ewusi-Mensah, N., and Logah, V. (2020). Legume-rhizobium strain specificity enhances nutrition and nitrogen fixation in faba bean (*Vicia faba* L.). *Agronomy* 10:826. doi: 10.3390/agronomy10060826

Allito, B. B., Ewusi-Mensah, N., Logah, V., and Hunegnaw, D. K. (2021). Legume-rhizobium specificity effect on nodulation, biomass production and partitioning of faba bean (*Vicia faba* L.). *Sci. Rep.* 11:3678. doi: 10.1038/s41598-021-83235-8

Aponte, H., Meli, P., Butler, B., Paolini, J., Matus, F., Merino, C., et al. (2020). Meta-analysis of heavy metal effects on soil enzyme activities. *Sci. Total Environ.* 737:139744. doi: 10.1016/j.scitotenv.2020.139744

Basile, L. A., and Lepek, V. V. (2021). Legume–rhizobium dance: an agricultural tool that could be improved? *Microb. Biotechnol.* 14, 1897–1917. doi: 10.1111/1751-7915.13906

Beiyuan, J., Fang, L., Chen, H., Li, M., Liu, D., and Wang, Y. (2021). Nitrogen of EDDS enhanced removal of potentially toxic elements and attenuated their oxidative stress in a phytoextraction process. *Environ. Pollut.* 268:115719. doi: 10.1016/j.envpol.2020.115719

Cao, Y., Ma, C., Chen, G., Zhang, J., and Xing, B. (2017). Physiological and biochemical responses of *Salix integra* Thunb. under copper stress as affected by soil flooding. *Environ. Pollut.* 225, 644–653. doi: 10.1016/j.envpol.2017.03.040

Chen, J. R., Shafi, M., Li, S., Wang, Y., Wu, J. S., Ye, Z. Q., et al. (2015). Copper induced oxidative stresses, antioxidant responses and phytoremediation potential of moso bamboo (*Phyllostachys pubescens*). *Sci. Rep.* 5:13554. doi: 10.1038/srep13554

Chen, J., Liu, Y. Q., Yan, X. W., Wei, G. H., Zhang, J. H., and Fang, L. C. (2018). Rhizobium inoculation enhances copper tolerance by affecting copper uptake and regulating the ascorbate-glutathione cycle and phytochelatin biosynthesis-related gene expression in *Medicago sativa* seedlings. *Ecotox. Environ. Safe* 162, 312–323. doi: 10.1016/j.ecoenv.2018.07.001

Chen, L., Wang, J., Beiyuan, J., Guo, X., Wu, H., and Fang, L. (2021). Environmental and health risk assessment of potentially toxic trace elements in soils near uranium (U) mines: a global meta-analysis. *Sci. Total Environ.* 151556. doi: 10.1016/j.scitotenv.2021.151556

Chen, X., Wu, L., Luo, N., Hui, C., Wong, M., and Li, H. (2019). *Arbuscular mycorrhizal* fungi and the associated bacterial community influence the uptake of cadmium in rice. *Geoderma* 337, 749–757. doi: 10.1016/j.geoderma.2018.10.029

Chou, M., Sun, Y., Yang, J., Wang, Y., Li, Y., Yuan, G., et al. (2019). Comprehensive analysis of phenotype, microstructure and global transcriptional profiling to unravel the effect of excess copper on the symbiosis between nitrogen-fixing bacteria and *Medicago lupulina*. *Sci. Total Environ.* 656, 1346–1357. doi: 10.1016/j.scitotenv.2018.12.005

Cui, Y. X., Fang, L. C., Guo, X. B., Han, F., Ju, W. L., Ye, L. P., et al. (2019). Natural grassland as the optimal pattern of vegetation restoration in arid and semi-arid regions: evidence from nutrient limitation of soil microbes. *Sci. Total Environ.* 648, 388–397. doi: 10.1016/j.scitotenv.2018.08.173

Duan, C., Fang, L., Yang, C., Chen, W., Cui, Y., and Li, S. (2018). Reveal the response of enzyme activities to heavy metals through in situ zymography. *Ecotox. Environ. Safe* 156, 106–115. doi: 10.1016/j.ecoenv.2018.03.015

Duan, C., Razavi, B. S., Shen, G., Cui, Y., Ju, W., Li, S., et al. (2019). Deciphering the rhizobium inoculation effect on spatial distribution of phosphatase activity in the rhizosphere of alfalfa under copper stress. *Soil Biol. Biochem.* 137:107574. doi: 10.1016/j.soilbio.2019.107574

Fan, L. M., Ma, Z. Q., Liang, J. Q., Li, H. F., Wang, E. T., and Wei, G. H. (2011). Characterization of a copper-resistant symbiotic bacterium isolated from *Medicago lupulina* growing in mine tailings. *Bioresource Technol.* 102, 703–709. doi: 10.1016/j.biortech.2010.08.046

Fang, L., Ju, W., Yang, C., Jin, X., and Zhang, C. (2020). Exogenous application of signaling molecules to enhance the resistance of legume-rhizobium symbiosis in Pb/Cd-contaminated soils. *Environ. Pollut.* 365:114744. doi: 10.1016/j.envpol.2020.114744

Ferreira, C. M. H., Soares, H., and Soares, E. V. (2019). Promising bacterial genera for agricultural practices: an insight on plant growth-promoting properties and microbial safety aspects. *Sci. Total Environ.* 682, 779–799. doi: 10.1016/j.scitotenv.2019.04.225

Gong, Q., Wang, L., Dai, T., Zhou, J., Kang, Q., Chen, H., et al. (2019). Effects of copper on the growth, antioxidant enzymes and photosynthesis of spinach seedlings. *Ecotoxicol. Environ. Safe* 171, 771–780. doi: 10.1016/j.ecoenv.2019.01.016

Guan, S. Y. (1986). *Soil Enzyme and its Research Approaches*. Beijing: China Agriculture Press.

Hao, X., Taghavi, S., Xie, P., Orbach, M. J., Alwathnani, H. A., and Rensing, C. (2014). Phytoremediation of heavy and transition metals aided by legume-rhizobia symbiosis. *Int. J. Phytoremediat.* 16, 179–202. doi: 10.1080/15226514.2013.773273

He, H. H., Wu, M. M., Guo, L., Fan, C. B., Zhang, Z. K., Sui, R., et al. (2020). Release of tartrate as a major carboxylate by alfalfa (*Medicago sativa* L.) under phosphorus deficiency and the effect of soil nitrogen supply. *Plant Soil* 449, 169–178. doi: 10.1007/s11104-020-04481-9

Hojati, M., Modarres-Sanavy, S. A. M., Enferadi, S. T., Majdi, M., and Pazoki, A. J. (2017). Cadmium and copper induced changes in growth, oxidative metabolism and terpenoids of *Tanacetum parthenium*. *Environ. Sci. Pollut. Res.* 24, 12261–12272. doi: 10.1007/s11356-017-8846-3

Hu, X., Wang, J., Lv, Y., Liu, X., Zhong, J., Cui, X., et al. (2021). Effects of heavy metals/metalloids and soil properties on microbial communities in farmland in the vicinity of a metals smelter. *Front. Microbiol.* 12:707786. doi: 10.3389/fmicb.2021.707786

Huang, G., Rizwan, M. S., Ren, C., Guo, G., Fu, Q., Zhu, J., et al. (2018). Influence of phosphorous fertilization on copper phytoextraction and antioxidant defenses in castor bean (*Ricinus communis* L.). *Environ. Sci. Pollut. Res.* 25, 115–123. doi: 10.1007/s11356-016-8132-9

Huang, G., Zhou, X., Guo, G., Ren, C., Rizwan, M. S., Islam, S., et al. (2020). Variations of dissolved organic matter and Cu fractions in rhizosphere soil induced by the root activities of castor bean. *Chemosphere* 254:126800. doi: 10.1016/j.chemosphere.2020.126800

Jian, L. R., Bai, X. L., Zhang, H., Song, X. Y., and Li, Z. F. (2019). Promotion of growth and metal accumulation of alfalfa by coinoculation with Sinorhizobium and Agrobacterium under copper and zinc stress. *PeerJ* 7:e6875. doi: 10.7717/peerj.6875

Ju, W., Jin, X., Liu, L., Shen, G., Zhao, W., Duan, C., et al. (2020). Rhizobacteria inoculation benefits nutrient availability for phytostabilization in copper contaminated soil: drivers from bacterial community structures in rhizosphere. *Appl. Soil Ecol.* 150:103450. doi: 10.1016/j.apsoil.2019.103450

Ju, W., Liu, L., Fang, L., Cui, Y., Duan, C., and Wu, H. (2019). Impact of co-inoculation with plant-growth-promoting rhizobacteria and rhizobium on the biochemical responses of alfalfa-soil system in copper contaminated soil. *Ecotox. Environ. Safe* 167, 218–226. doi: 10.1016/j.ecoenv.2018.10.016

Kong, Z. Y., Mohamad, O. A., Deng, Z. S., Liu, X. D., Glick, B. R., and Wei, G. H. (2015). Rhizobial symbiosis effect on the growth, metal uptake, and antioxidant responses of *Medicago lupulina* under copper stress. *Environ. Sci. Pollut. Res.* 22, 12479–12489. doi: 10.1007/s11356-015-4530-7

Kong, Z., Glick, B. R., Duan, J., Ding, S., Tian, J., McConkey, B. J., et al. (2015). Effects of 1-aminocyclopropane-1-carboxylate (ACC) deaminase-overproducing *Sinorhizobium meliloti* on plant growth and copper tolerance of *Medicago lupulina*. *Plant Soil* 391, 383–398. doi: 10.1007/s11104-015-2434-4

Liu, X., Wu, F. H., Li, J. X., Chen, J., Wang, G. H., Wang, W. H., et al. (2016). Glutathione homeostasis and Cd tolerance in the *Arabidopsis* sultr1;1-sultr1;2 double mutant with limiting sulfate supply. *Plant Cell Rep.* 35, 397–413. doi: 10.1007/s00299-015-1892-8

Ma, X., Liu, Y., Shen, W., and Kuzyakov, Y. (2021). Phosphatase activity and acidification in lupine and maize rhizosphere depend on phosphorus availability and root properties: coupling zymography with planar optodes. *Appl. Soil Ecol.* 167:104029. doi: 10.1016/j.apsoil.2021.104029

Ma, Y., Oliveira, R. S., Freitas, H., and Zhang, C. (2016). Biochemical and molecular mechanisms of plant-microbe-metal interactions: relevance for phytoremediation. *Front. Plant Sci.* 7:918. doi: 10.3389/fpls.2016.00918

Molina-Santiago, C., Pearson, J. R., Navarro, Y., Berlanga-Clavero, M. V., Caraballo-Rodriguez, A. M., Petras, D., et al. (2019). The extracellular matrix protects *Bacillus subtilis* colonies from *Pseudomonas* invasion and modulates plant co-colonization. *Nat. Comm.* 10:1919. doi: 10.1038/s41467-019-09944-x

Morina, F., Jovanovi, L., Prokić, L., and Veljović-Jovanović, S. (2016). Physiological basis of differential zinc and copper tolerance of *Verbascum* populations from metal-contaminated and uncontaminated areas. *Environ. Sci. Pollut. Res.* 23, 10005–10020. doi: 10.1007/s11356-016-6177-4

Peng, Q., Wu, M., Zhang, Z., Su, R., He, H., and Zhang, X. (2020). The interaction of arbuscular mycorrhizal fungi and phosphorus inputs on selenium uptake by alfalfa (*Medicago sativa* L.) and selenium fraction transformation in soil. *Front. Plant Sci.* 11:966. doi: 10.3389/fpls.2020.00966

Raiesi, F., and Salek-Gilani, S. (2018). The potential activity of soil extracellular enzymes as an indicator for ecological restoration of rangeland soils after agricultural abandonment. *Appl. Soil Ecol.* 126, 140–147. doi: 10.1016/j.apsoil.2018.02.022

Raza, A., Habib, M., Kakavand, S. N., Zahid, Z., Zahra, N., Sharif, R., et al. (2020). Phytoremediation of cadmium: physiological, biochemical, and molecular mechanisms. *Biology* 9:177. doi: 10.3390/biology9070177

Richardson, A. D., Duigan, S. P., and Berlyn, G. P. (2002). An evaluation of noninvasive methods to estimate foliar chlorophyll content. *New Phytol.* 153, 185–194. doi: 10.1046/j.0028-646X.2001.00289.x

Romero-Puertas, M. C., Terrón-Camero, L. C., Peláez-Vico, M., Olmedilla, A., and Sandalio, L. M. (2018). Reactive oxygen and nitrogen species as key indicators of plant responses to Cd stress. *Environ. Exp. Bot.* 161, 107–119. doi: 10.1016/j.envexpbot.2018.10.012

Rostami, S., and Azhdarpoor, A. (2019). The application of plant growth regulators to improve phytoremediation of contaminated soils: a review. *Chemosphere* 220, 818–827. doi: 10.1016/j.chemosphere.2018.12.203

Sahito, Z. A., Zehra, A., Chen, S., Yu, S., Lin, T., Ali, Z., et al. (2021). Rhizobium rhizogenes-mediated root proliferation in Cd/Zn hyperaccumulator *Sedum alfredii* and its effects on plant growth promotion, root exudates and metal uptake efficiency. *J. Hazard. Mater.* 424:127442. doi: 10.1016/j.jhazmat.2021.127442

Saxena, G., Purchase, D., Mulla, S. I., Saratale, G. D., and Bharagava, R. N. (2020). Phytoremediation of heavy metal-contaminated sites: eco-environmental concerns, field studies, sustainability issues, and future prospects. *Rev. Environ. Contamination Toxicol.* 249, 71–131. doi: 10.1007/398_2019_24

Shen, X., Yang, F., Xiao, C., and Zhou, Y. (2020). Increased contribution of root exudates to soil carbon input during grassland degradation. *Soil Biol. Biochem.* 146:107817. doi: 10.1016/j.soilbio.2020.107817

Stambulska, U. Y., and Bayliak, M. M. (2019). "Legume-rhizobium symbiosis: secondary metabolites, free radical processes, and effects of heavy metals," in *Co-Evolution of Secondary Metabolites*, eds J.-M. M'erillon and K. G. Ramawat (Switzerland AG: Springer Nature).

Sun, L., Song, J., Peng, C., Xu, C., Yuan, X., and Shi, J. (2015). Mechanistic study of programmed cell death of root border cells of cucumber (*Cucumber sativus* L.) induced by copper. *Plant Physiol. Biochem.* 97, 412–419. doi: 10.1016/j.plaphy.2015.10.033

Vance, E. D., Brookes, P. C., and Jenkinson, D. (1987). An extraction method for measuring soil microbial biomass C. *Soil Biol. Biochem.* 19, 703–707. doi: 10.1016/0038-0717(87)90052-6

Wang, J., Wang, L. L., Wang, Y. X., Tsang, D. C. W., Yang, X., Beiyuan, J. Z., et al. (2021). Emerging risks of toxic metal(loid)s in soil-vegetables influenced by steel-making activities and isotopic source apportionment. *Environ. Int.* 146:106207. doi: 10.1016/j.envint.2020.106207

Wang, J., Wang, X., Liu, G., Wang, G., Wu, Y., and Zhang, C. (2020). Fencing as an effective approach for restoration of alpine meadows: evidence from nutrient limitation of soil microbes. *Geoderma* 363:114148. doi: 10.1016/j.geoderma.2019.114148

Wang, X., Fang, L., Beiyuan, J., Cui, Y., Peng, Q., Zhu, S., et al. (2021). Improvement of alfalfa resistance against Cd stress through rhizobia and arbuscular mycorrhiza fungi co-inoculation in Cd-contaminated soil. *Environ. Pollut.* 277:116758. doi: . 10.1016/j.envpol.2021.1 16758

Wang, Y., Zhang, Z., Zhang, P., Cao, Y., Hu, T., and Yang, P. (2016). Rhizobium symbiosis contribution to short-term salt stress tolerance in alfalfa (*Medicago sativa* L.). *Plant Soil* 402, 247–261. doi: 10.1007/s11104-016-2792-6

Wang, Z., Tian, H., Tan, X., Wang, F., Jia, H., Megharaj, M., et al. (2019). Long-term as contamination alters soil enzyme functional stability in response to additional heat disturbance. *Chemosphere* 229, 471–480. doi: 10.1016/j.chemosphere.2019.05.055

Wei, X., Hu, Y., Razavi, B. S., Zhou, J., Shen, J., Nannipieri, P., et al. (2019). Rare taxa of alkaline phosphomonoesterase-harboring microorganisms mediate soil phosphorus mineralization. *Soil Biol. Biochem.* 131, 62–70. doi: 10.1016/j.soilbio.2018.12.025

Xiao, L., Zhang, C., Wang, C., Guan, D., Zhang, R., Chen, Y., et al. (2020). Influencing pathways of soil microbial attributes on accumulation of heavy metals in brassica (*Brassica campestris* L. ssp.chinensis var.utilis Tsen et Lee) leaves. *Environ. Pollut.* 262:114215. doi: 10.1016/j.envpol.2020.114215

Yang, J., Yang, F., Yang, Y., Xing, G., Deng, C., Shen, Y., et al. (2016). A proposal of "core enzyme" bioindicator in long-term Pb-Zn ore pollution areas based on topsoil property analysis. *Environ. Pollut.* 213, 760–769. doi: 10.1016/j.envpol.2016.03.030

Yang, W., Li, P., Rensing, C., Ni, W., and Xing, S. (2019). Biomass, activity and structure of rhizosphere soil microbial community under different metallophytes in a mining site. *Plant Soil* 434, 245–262. doi: 10.1007/s11104-017-3546-9

Yu, Y., Zhou, X., Zhu, Z., and Zhou, K. (2019). Sodium hydrosulfide mitigates cadmium toxicity by promoting cadmium retention and inhibiting its translocation from roots to shoots in *Brassica napus*. *J. Agr. Food Chem.* 67, 433–440. doi: 10.1021/acs.jafc.8b04622

Zhou, X., Wang, S., Liu, Y., Huang, G., Yao, S., and Hu, H. (2020). Coupling phytoremediation efficiency and detoxification to assess the role of P in the Cu tolerant *Ricinus communis* L. *Chemosphere* 247:125965. doi: 10.1016/j.chemosphere.2020.125965

Conflict of Interest: The authors declare that the research was conducted in the absence of any commercial or financial relationships that could be construed as a potential conflict of interest.

Publisher's Note: All claims expressed in this article are solely those of the authors and do not necessarily represent those of their affiliated organizations, or those of the publisher, the editors and the reviewers. Any product that may be evaluated in this article, or claim that may be made by its manufacturer, is not guaranteed or endorsed by the publisher.

frontiers in Microbiology

REVIEW
published: 13 January 2022
doi: 10.3389/fmicb.2021.821546

Wheat Microbiome: Structure, Dynamics, and Role in Improving Performance Under Stress Environments

Jian Chen[1†‡], Rouhallah Sharifi[2†‡], Muhammad Saad Shoaib Khan[1†‡], Faisal Islam[3†], Javaid Akhter Bhat[1†], Ling Kui[4*†] and Aasim Majeed[5*†]*

[1] International Genome Center, Jiangsu University, Zhenjiang, China, [2] Department of Plant Protection, College of Agriculture and Natural Resources, Razi University, Kermanshah, Iran, [3] Zhejiang Key Laboratory of Crop Germplasm, Institute of Crop Science, Zhejiang University, Hangzhou, China, [4] Guangxi Key Laboratory of Medicinal Resources Protection and Genetic Improvement, Guangxi Botanical Garden of Medicinal Plants, Nanning, China, [5] Plant Molecular Genetics Laboratory, School of Agricultural Biotechnology, Punjab Agricultural University, Ludhiana, India

Wheat is an important cereal crop species consumed globally. The growing global population demands a rapid and sustainable growth of agricultural systems. The development of genetically efficient wheat varieties has solved the global demand for wheat to a greater extent. The use of chemical substances for pathogen control and chemical fertilizers for enhanced agronomic traits also proved advantageous but at the cost of environmental health. An efficient alternative environment-friendly strategy would be the use of beneficial microorganisms growing on plants, which have the potential of controlling plant pathogens as well as enhancing the host plant's water and mineral availability and absorption along with conferring tolerance to different stresses. Therefore, a thorough understanding of plant-microbe interaction, identification of beneficial microbes and their roles, and finally harnessing their beneficial functions to enhance sustainable agriculture without altering the environmental quality is appealing. The wheat microbiome shows prominent variations with the developmental stage, tissue type, environmental conditions, genotype, and age of the plant. A diverse array of bacterial and fungal classes, genera, and species was found to be associated with stems, leaves, roots, seeds, spikes, and rhizospheres, etc., which play a beneficial role in wheat. Harnessing the beneficial aspect of these microbes is a promising method for enhancing the performance of wheat under different environmental stresses. This review focuses on the microbiomes associated with wheat, their spatio-temporal dynamics, and their involvement in mitigating biotic and abiotic stresses.

Keywords: wheat, microbiome, stress, rhizosphere, phylosphere

OPEN ACCESS

Edited by:
Hai-Ming Zhao,
Jinan University, China

Reviewed by:
Kamlesh Kumar Meena,
National Institute of Abiotic Stress Management (ICAR), India
Shruti Choudhary,
Umeå University, Sweden

***Correspondence:**
Jian Chen
jianchen0722@163.com
Ling Kui
kuiling2008@163.com
Aasim Majeed
majeedaasim@gmail.com

†ORCID:
Jian Chen
orcid.org/0000-0003-1694-8755
Muhammad Saad Shoaib Khan
orcid.org/0000-0002-8925-6285
Faisal Islam
orcid.org/0000-0002-1471-1570
Javaid Akhter Bhat
orcid.org/0000-0001-9136-6275
Rouhallah Sharifi
orcid.org/0000-0001-9013-3445
Ling Kui
orcid.org/0000-0002-1416-1601
Aasim Majeed
orcid.org/0000-0002-8215-6425

‡These authors have contributed equally to this work

Specialty section:
This article was submitted to Terrestrial Microbiology, a section of the journal Frontiers in Microbiology

Received: *24 November 2021*
Accepted: *23 December 2021*
Published: *13 January 2022*

Citation:
Chen J, Sharifi R, Khan MSS, Islam F, Bhat JA, Kui L and Majeed A (2022) Wheat Microbiome: Structure, Dynamics, and Role in Improving Performance Under Stress Environments. Front. Microbiol. 12:821546. doi: 10.3389/fmicb.2021.821546

INTRODUCTION

Modern agriculture is a result of the domestication of wild crops by humans over 1000s of years. The integrated system of agriculture is supporting the ever-growing world population. Wheat is one of the major crops, occupying around 17% of the global cultivated area and providing food for about 35% of the world's population (Laino et al., 2015). To meet the global calorie requirement

by ever-increasing human population, there is a dire need to increase wheat production by 11% till 2026 with only 1.8% increase in cultivated land (Kavamura et al., 2021). Therefore, the agricultural system has to be sustainable, and its sustainability has to be intensified, so as to make productive gains from important crops. The substantiality of the modern agricultural system has kept pace with the ever-increasing global food demands. The development of genetically improved varieties with increased yield, tolerance to biotic and abiotic stresses, improved nutrient use efficiency as well as the development of new bio-fertilizers have ensured the intensification of agricultural sustainability. However, control of biotic pathogens, and weeds, etc., is still dominated by the overuse of environmentally hazardous chemicals, whereas the enhancement of agronomic traits, especially yield, is dominated by the overuse of chemical fertilizers, which alter soil and water properties. One promising way of improving the performance of crops in terms of yield, tolerance to biotic and abiotic factors without altering the environment, is to take advantage of beneficial microorganisms present in the above and below-ground parts of plants. Both above and below-ground parts of plants are colonized with a myriad of microorganisms, many of which interact beneficially with plant to enhance their efficiency.

The ecophysiology of plant-microbe interaction is very complicated and interwoven. Therefore, a thorough understanding of the fine-tuning and integration of multiple signals generated through plant-microbe interactions is required for sustainable crop improvement. Under the natural environment, plants are exposed to a myriad of biotic and abiotic stresses; therefore, the defense responses of plants are very complex. Plant-microbe interactions can result in the prioritization of certain physiological, biochemical, and molecular pathways in plants, the dissection of which requires the application of multi-omics approaches. Using genomic, transcriptomic, proteomic, and metabolomic approaches entwined with bioinformatics have been successful in addressing microbial communities and functions within a given environment at a deeper level (de Castro et al., 2013). The pathogenic fungus, *Rhizoctonia solani* anastomosis group (AG) 8 results in substantial crop losses, including wheat and barley. In the absence of resistant cultivars to this pathogen, biological disease suppression may act as an impressive control mechanism. A thorough investigation of taxonomic and functional characteristics of the soil microbiome is therefore required to decipher the potential biocontrol agents. Through transcriptomic analysis of wheat plants grown in fields with suppressive and non-suppressive capacity against *R. solani*, Hayden et al. (2018) observed *Arthrobacter* spp. and *Pseudomonas* spp. as dominant taxa in the non-suppressive samples and *Stenotrophomonas* spp. and *Buttiauxella* spp. as dominant taxa in the suppressive samples. A higher expression of polyketide cyclase, many cold shock proteins, and a terpenoid biosynthesis backbone gene was observed in the suppressive samples, whereas the non-suppressive samples exhibited relatively greater expression of certain antibiotic genes and genes involved in mitigating oxidative damage (Hayden et al., 2018). Thus, the transcriptomic approaches have the ability to disentangle the molecular interplay of plant-microbe-pathogen interactions, the ultimate goal of which is to identify and promote the beneficial rhizosphere microbes to reduce pathogenic infections. Similarly, the meta-proteomic and metabolomic approaches have the potential to elucidate the important inter-links in plant-microbe interactions.

Recent research has witnessed the potential of microbiome organisms in fulfilling the sustainability goals without harming or altering the physio-chemical and physiological profile of the soil, water, or air. Plant microbiome helps the host species to mitigate both biotic and abiotic stress; therefore, a deeper understanding of how such microbes interact with host plants is required. The chief strategies used by microbes that can help host plants to counter stress include, but not limited to (a) resource competition with potential harmful pathogens to mitigate biotic stress, (b) inhibition of growth and development of pathogens by secretion of certain chemical substances, (c) induction of systemic acquired resistance (SAR) in host species, (d) chelation of salts, toxic and/or heavy metals through secretion of cheating agents to counter salt and heavy metal stress, (e) modulation of several gene expression modules and physiological processes to enable the host species withstand drought and temperature stress, etc. In addition, the host defense response in turn dictates the microbial community structure (Jones et al., 2019). The microbes may produce secondary metabolites, which have suppressive action on host pathogens or exhibit resource competition with the host pathogens to protect the host (Teixeira et al., 2019). A myriad of studies have confirmed the beneficial role of microbiome organisms in mitigation of biotic and abiotic stresses, and enhancement of agronomic traits of many crop species. Therefore, a better understanding of microbial profiles associated with crop species is of fundamental importance to sustainable and eco-friendly agriculture. In addition, much attention is needed to elucidate the molecular and physiological details as well as the regulation involved in such plant-microbe interactions. This review focuses on the wheat microbiome composition, how its structure changes spatially and temporally, and more importantly, the beneficial roles played by the wheat microbiome in enhancing its performance under drought, salinity, temperature, and metal toxicity stress.

OVERVIEW OF THE WHEAT MICROBIOME

The advancement of sequencing technologies has greatly facilitated the profiling of environmental samples through metagenomic and metatranscriptomic approaches. Using amplicon sequencing, both composition and functions of microbes associated with crop species can be evaluated at relative ease now. It is possible to ascertain the effect of different factors affecting microbial communities associated with host plants in both above-ground and below-ground niches (**Figure 1**). The above-ground plant parts include phyllosphere (leaves), caulosphere (stems), inflorescences, and seeds. The term spicosphere was coined by Kavamura et al. (2021) to represent the niche around the spikes, as the later hosts diverse array of pathogenic and beneficial microorganisms. The below-ground niche includes rhizoplane (surface of plant roots) and rhizosphere

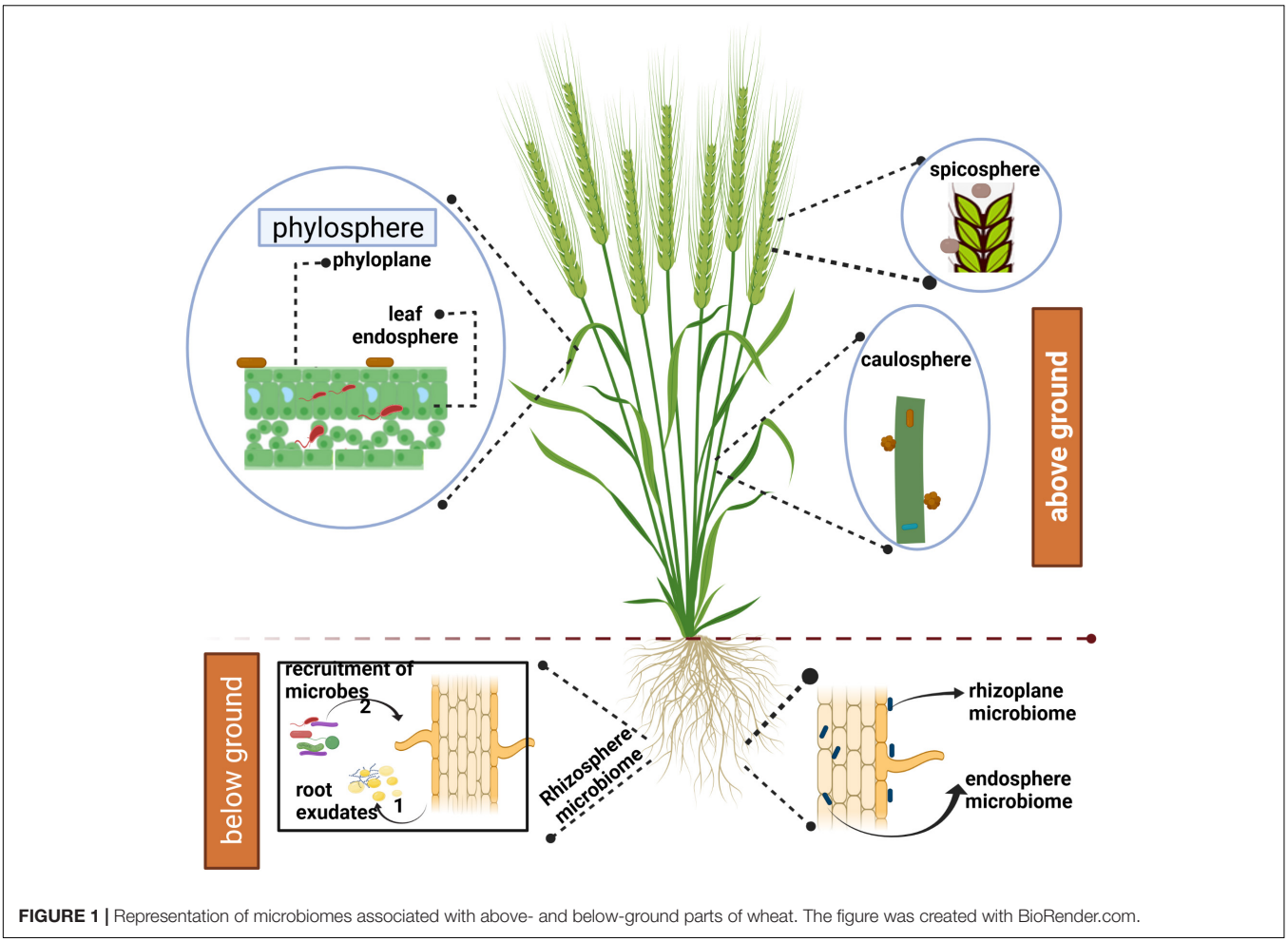

FIGURE 1 | Representation of microbiomes associated with above- and below-ground parts of wheat. The figure was created with BioRender.com.

(the soil in the vicinity of plant roots that is influenced by host plants through root exudation) (Kavamura et al., 2021). Further, microorganisms can live as endophytes in both above and below-ground plant parts. The term spermosphere describes the zone surrounding the germinating seeds (Nelson, 2004).

Although the endophytic microbes remain associated with host species throughout their life cycle, the actual community structure is governed by the tissue type. The underground plant parts harbor higher endophytic species than the above-ground parts. Most often, the endophytes are beneficial to host species as they can stimulate growth, provide protection against environmental stress, enhance nutrient absorption, and inhibit pathogenic microbes. In order to estimate the community structure and diversity of endophytic microbes from aerial and underground parts of wheat, Comby et al. (2016) observed Ascomycota (mostly Sordariomycetes or Dothideomycetes) to be the most dominant fungal phyla followed by Basidiomycota (with dominance by Agaricomycetes in which Polyporales and Russulales were top orders), and Zygomycota. The dominant bacterial classes were Gammaproteobacteia of the Proteobacteria and Bacilli of the Firmicutes. Further, the authors observed three indicator species (*Bacillus megaterium, Microdochium bolleyi,* and *Gaeumannomyces graminis*) characteristic to roots and seven indicator species characteristics to aerial parts (*Alternaria infectoria, Didymella exitialis, Epicoccum nigrum, Erwinia aphidicola, Paenibacillus hordei, Fusarium graminearum*, and *Aureobasidium protae*). Moreover, there were considerable variations in microbiome profiles with developmental stages of wheat plants (Comby et al., 2016). The *Erwinia Paenibacillus* and *Paenibacillus* were the most dominant genera associated with the wheat seeds (Robinson et al., 2016b). Further, Proteobacteria were the most prevalent endophytes in roots and Firmicutes and Actinobacteria in shoots (Robinson et al., 2016a). *Pseudomonas*, *Janthinobacterium*, and *Flavobacterium* were dominant endophytic genera in *T. aestivum* with the dominance of *Pseudomonas* and *Janthinobacterium* increasing from roots, leaves, and coleoptiles. These tissues also hosted six subdominant bacterial genera viz *Variovorax*, *Herbaspirillum*, *Caulobacter*, *Cryobacterium*, *Paenibacillus,* and *Acidovorax*. In addition to the *Pseudomonas*, *Janthinobacterium*, and *Flavobacterium,* the *Triticum spelta* also contains *Pedobacter* as a dominant genus and *Duganella, Ochrobactrum, Taibaiella*, *Rhodococcus*, *Dyadobacter*, *Mucilaginibacter,* and *Staphylococcus* as the subdominant endophytic genera in roots, leaves, and coleoptiles. Therefore, besides the three common core genera, *Pseudomonas*, *Janthinobacterium*, and *Flavobacterium* in both

cultivars, the study established *Paenibacillus* as a core genus specific to *T. aestivum* and *Pedobacter* and *Duganella* as the core genera specific to *T. spelta* (Kuźniar et al., 2020). Most typical wheat endophytic species include *Achromobacter piechaudii, A. xylosoxidans, D. acidovorans, Pseudomonas monteilii, Acinetobacter lwoffii, Staphylococcus epidermis, Delftia lacustris, Ochrobactrum intermedium, Pantoea dispersa, P. eucalypti, Variovorax soli*, and *Serratia* (Mahapatra et al., 2020).

Apart from the endophytes, the microbes grow externally on the caulosphere, phyllosphere, spicosphere, rhizoplane, rhizosphere, and spermosphere of the wheat. There existed a higher fungal community abundance and diversity in wheat tissues, including roots, spikes, first stem under the ear, and stem base as well as wheat rhizosphere. Wheat varieties resistant to *Tilletia controversa*, a wheat dwarf blunt pathogen, showed greater abundance of Sordariomycetes and Mortierellomycetes, whereas the susceptible varieties exhibited higher abundances of Dothideomycetes and Bacteroidia. In contrast to other tissues, the ear and the first stem under the ear revealed greater abundances of Chloroflexi, Verrucomicrobia, Bacteroidetes, Acidobacteria, and Gemmatimonadetes. Further, *Chryseobacterium* and *Massilia,* and *Nocardioides* and *Pseudomonas* were abundant in wheat dwarf blunt infected resistant and susceptible varieties, respectively. *Curtobacterium*, *Planococcus*, *Pantoea,* and *Exiguobacterium* showed dominance in both resistant and susceptible varieties (Xu et al., 2021). The phyllospheric microorganisms can tolerate extreme temperatures as well as substantial UV radiations, so they are a class of extremophiles. The survival and proliferation of the leaf microbes largely is determined by leaf exudates like amino acids, glucose, fructose, and sucrose. Chief phyllospheric microbes include *Achromobacter, Agrobacterium, Lysinibacillus, Corynebacterium, Haemophilus, Pantoea, Alcaligenes, Streptomyces, Paenibacillus, Methylobacterium, Stenotrophomonas, Arthrobacter, Bacillus, Azotobacter, Enterobacter, Micrococcus, Brevundimonas, Micrococcus, Micromonospora, Pseudomonas,* and *Psychrobacter* (Mahapatra et al., 2020). These phyllospheric microbes mediate a variety of physiological and defense responses in wheat. Due to their close association with roots and soil, the rhizospheric microbiomes play an important role in the growth of the plant as they help the plants in nutrient and water uptake, etc. Most typical rhizospheric microbial species include *B. thuringiensis, Serratia marcescens, Azotobacter tropicalis, Rhodobacter capsulatus, Pseudomonas extremorientalis, Rhodobacter sphaeroides, P. rhizosphaerae, Arthrobacter nicotinovorans, Bacillus atrophaeus, B. horikoshii, B. mojavensis, B. siamensis, Enterobacter asburiae, Exiguobacterium acetylicum*, and *Planomicrobium okeanokoites* (Mahapatra et al., 2020).

THE MICROBIOME PROFILE OF WHEAT IS SPATIALLY AND TEMPORALLY DYNAMIC

The microbiome profile associated with host species varies with the plant part, development stage, and environmental conditions. Each stage or condition exhibits dominance of certain microbial groups that confer some positive or negative physiological impact on the host. The growth of one microbial species may alter the microbial profile associated with the host plant significantly.

Spatial and Conditional Variation

Every species has its own peculiar microbial profile associated with its above and below-ground parts. These microbes are affected by diverse factors, thereby influencing the physiology of the host crop species. Several factors cause changes in the microbial profile associated with host species. Most common factors include anthropogenic (fungicides, insecticides, fertilization, landuse, tillage, crop rotation, and irrigation, etc.), edaphic (soil depth, soil type, and soil physiochemical properties, etc.), environmental (biotic and abiotic stress, growing season, etc.), host genotype and growth stage. Anthropogenic factors have a relatively far-most influence on the microbial profile. Use of agrochemicals like fungicides, pesticides, insecticides, and weedicides to control host pathogens and weeds, although promising, has a disadvantage of environmental pollution besides significantly altering the microbes associated with host plant species. To mitigate this problem, one solution is to use environmentally and biologically less harmful agrochemicals. However, only a few such chemicals have been screened till now. The neonicotinoid insecticides and glyphosate herbicides show no or minimal negative impact on wheat rhizosphere microbial communities (Li et al., 2018; Malalgoda et al., 2020). The variations in temperature, humidity, and precipitation significantly affect wheat microbiome composition (Latz et al., 2021). Azarbad et al. (2018) observed that water regime primarily governs the bacterial and fungal community structure in wheat rhizosphere. An increase in soil moisture alters the root exudation and soil properties along with perturbation of interactions within the rhizosphere microbiome, which specifically leads to a decrease in the production of the antibiotic phenazine-1-carboxylic acid (PCA) producers (Phz^+) *Pseudomonas* in the rhizosphere of irrigated plants (Mavrodi et al., 2018). Further, the geographic distance (Fan et al., 2017) and seasonal changes (Schlatter et al., 2019) spatially determine the wheat microbial community structure. The biodegradable plastic mulch films also influence rhizosphere bacterial community composition and structure (Qi et al., 2020). In general, inorganic nitrogen fertilizer application negatively impacts the stability of bacterial community structure along with reduction in richness and diversity and significant depletion of Acidobacteria and Planctomycetes (Kavamura et al., 2018). Tilling also reduces bacterial diversity (Yin et al., 2010). In winter wheat, the rhizoplane and root endosphere bacterial communities were influenced by management practices (conventional vs. organic), whereas tilling affected fungal communities (Hartman et al., 2018). In comparison to monoculture, which reduces the bacterial (Mayer et al., 2019) diversity, rotation of sunflower with wheat or maize showed positive impact on bacterial communities (Wen et al., 2016). In wheat, the soil properties like pH, texture, organic, and inorganic content have also been found to influence microbial community profile (Fan et al., 2017, 2018; Schlatter et al., 2019). Besides, the microbial profile also varies with soil depth with Proteobacteriota enriched in

topsoil and Firmicutes and Bacteroidota enriched in subsoil (Uksa et al., 2017; Schlatter et al., 2020). The microbial load associated with the host may originate from seed-borne microbes, which colonize the developing plant. The host species also affects the overall root microbiome to a greater degree (Cordero et al., 2020). Even the different parts of the host species reveal significant variations in microbial community structure, with Proteobacteriota dominating in the root endosphere, whereas Firmicutes and Actinobacteriota were more frequent in the leaf endosphere (Robinson et al., 2016b). Environmental factors were found to affect the phylosphere microbiome more than that of the rhizosphere in wheat (Latz et al., 2021). Further, host-driven seasonal variations in the rhizosphere microbiome were observed in wheat (Donn et al., 2015). The strong evidence that host species affects the microbial profile comes from the decreased bacterial diversity and complexity across different interaction zones between microbes and host plant (bulk soil > rhizosphere soil > rhizoplane > phylloplane > root endosphere > leaf endosphere) (Xiong et al., 2021).

Temporal Variation

Besides, there occurs a temporal variation in microbial profile associated with host plants species during different stages of development, as the life cycle moves from seed to flowering stage. This effect is more pronounced for bacterial communities than that of fungal communities (Chen et al., 2019). The bacterial rhizosphere diversity increases with age of the host species (Donn et al., 2015; Araujo et al., 2019). Similarly, the bacterial and fungal endosphere communities (Gdanetz and Trail, 2017) and the fungal phylosphere communities (Sapkota et al., 2017) increased with age. However, the relationship between the development stage of the host species and the microbial community structure is not simple and several factors render this relationship more complex. The rhizosphere bacterial richness is reduced by some fertilization regimes. Upon high nitrogen application, the diversity remained stable over time but decreased at sub-optimal nitrogen levels. However, no effect of fertilization was observed on the decreasing root and endosphere bacterial richness with the increasing age of the host (Robinson et al., 2016a). Therefore, more research is needed to disentangle the complex relationship of microbiome and wheat developmental stages.

Variation Due to Selection and Domestication

Modern agriculture evolved as a result of careful selection and breeding of different cultivars and a rapid transition to improved genotypes with desired characters. The wheat cultivars grown today have undergone dramatic genetic, physiological, and morphological changes from their wild relatives. In this course of transition, the root architecture might have significantly changed, which may, in turn, have affected the rhizosphere microbiome. This is evidenced by differential bacterial community structures in tall and semi-dwarf varieties of wheat (Kavamura et al., 2020). Further, during this evolution, there has been a compromise in interaction with plant growth-promoting rhizobacteria (PGPR), with ancient wild wheat varieties having a greater ability to interact with PGPR (Valente et al., 2020). The domestication of crops, especially wheat, has significantly disrupted the associated microbial community. Fungal endophytes exhibit more diversity and richness in wild wheat cultivars than in cultivated ones (Sun et al., 2020). The D genome of hexapoloid wheat strongly favors Glomeromycetes and Nematoda (Tkacz et al., 2020). Root exudation chemistry and susceptibility to pathogens may be the key factors governing the differences in microbiome-based on different wheat genotypes. Further studies are required to explore the deeper insights of the relationship between wheat genotypes and microbial community profiles. The already developed highly efficient wheat cultivars shall be screened for their influence on the microbiome profile and those cultivars with minimal negative influence shall be promoted. Moreover, the breeding programs shall take into consideration the influence of changes in the genetic architecture of a species on the microbiome profile because any negative influence of the newly developed cultivars on the microbiome profile, especially the beneficial elements, would affect its overall performance.

MICROBIOMES MITIGATE STRESS IN WHEAT

Bulk of research involving different crop species revealed that in comparison to un-inoculated plants, the plants inoculated with beneficiary microbes show better performance in terms of root/shoot growth, water and mineral absorption, yield, and resistance to biotic and abiotic stresses (**Figure 2**). The microbes trigger a diverse array of physiological responses in plants, including hormone production, to enhance their performance against stress. The detailed role of the wheat microbiome in ameliorating biotic and abiotic stresses is presented in the following sub-headings.

MICROBIOME ASSISTED RESISTANCE AGAINST BIOTIC STRESS

Biological control is great hope for reducing the overutilization of pesticides in agricultural soils (Köhl et al., 2019). It often involves the use of microorganisms or their metabolites that interact with either a plant or its pathogens to control the growth of the later and restrict its negative influence on the host plant. Infection of wheat plants by the fungal pathogen *Zymoseptoria tritici* resulted in suppression of the host immune system, which facilitated the colonization of other non-adapted *P. syringae* microbes on wheat (Seybold et al., 2020). Several bacterial biocontrol agents inhibit fungal pathogens. For example, they secrete lipopeptide antibiotics, phenazine derivatives, and other antifungal metabolites that negatively influence the fungal pathogen, *Fusarium graminearum* (Legrand et al., 2017). Further, the bacteria *Lysobacter enzymogenes* inhibits ceramide synthase enzyme, thereby causing degradation of the *Aspergillus* cell wall. This inhibitory effect of *L. enzymogenes* is caused due to secretion of a heat-stable antifungal factor (Li et al., 2006). The fungi, in turn, have been observed to trigger a defense response to

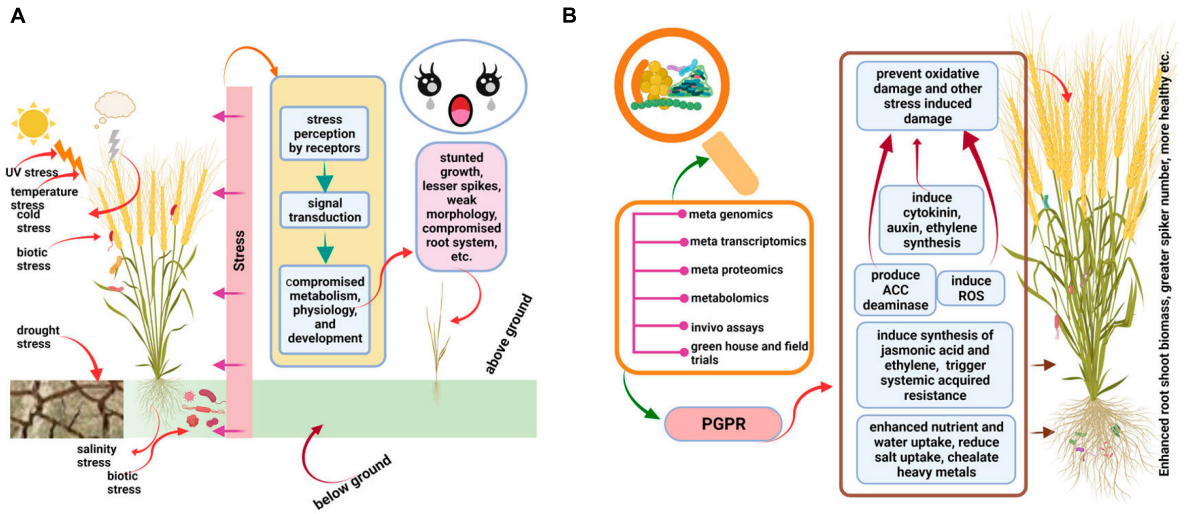

FIGURE 2 | Depiction of how beneficial microbes enhance the performance of wheat under stress. **(A)** Shows that in absence of any beneficial host-microbiome interaction, wheat shows compromised growth and overall performance. **(B)** Shows that after inoculation of wheat by beneficial microbes, its root/shoot biomass and overall performance are enhanced. The figure was created with BioRender.com.

such bacterial antibiotics. For example, *Fusarium oxysporum* produces fusaric acid to inhibit 2,4-diacetylphloroglucinol (2,4-DAPG), a broad-spectrum antibiotic produced by *Pseudomonas fluorescens* (Schouten et al., 2004) and the antifungal metabolite phenazine-1-carboxamide (PCN) by *Pseudomonas chlororaphis* (van Rij et al., 2005). Further, the beneficial bacteria also produce volatile anti-fungal metabolites, degrade the virulence factors of fungi, or even induce systemic resistance in plants against fungal pathogens (Schoonbeek et al., 2002; Effmert et al., 2012; O'Brien, 2017). Fusarium head blight (FHB) is a dangerous cereal disease caused by *Fusarium graminearum* leads to much economic losses over the world. *F. graminearum* seems to be inhibited by the bacterium *Pseudomonas piscium*. The bacteria secretes phenazine-1-carboxamide that affects the fungal histone acetyltransferase (FgGcn5), leading to deregulation of histone acetylation and growth of the fungus. Therefore, *Pseudomonas piscium* could be an important biocontrol agent of fungal wheat diseases (Chen et al., 2018).

The biocontrol agents are generally selected after their successful antagonism with the known plant pathogens *in vitro*, with in-planta screening seldom used. An in-planta study on wheat and its fungal pathogen, *F. graminearum* revealed several microbes, although ineffective in *in vitro* analysis but effective in in-planta screening, along with some novel strains protecting the host against fungal attack. The most important plant protectors found by the authors include *Bacillus* and *Pseudomonas,* and interestingly *Staphylococcus* (Besset-Manzoni et al., 2019). Further, the two bacterial strains, *Lactobacillus plantarum* SLG17 and *Bacillus amyloliquefaciens* FLN13 showed antimicrobial activity against *Fusarium* spp. in durum wheat and are, therefore, promising agents for the reduction of FHB index (Baffoni et al., 2015). In winter wheat, the bacterium *Sphingomonas* showed an antagonistic effect on powdery mildew and FHB. This biocontrol agent significantly reduced the population size of *Fusarium poae* and severity of infection by *Blumeria graminis* f. sp. *tritici* (Wachowska et al., 2013). Moreover, the bacterial inocculents *Paenibacillus jamilae* and *Bacillus amyloliquefaciens* were observed to reduce (82 and 83%, respectively) soil-borne wheat diseases and significantly affect the rhizosphere microbial community structure. The beneficial rhizosphere bacteria like *Sphingomonas*, *Bacillus*, *Nocardioides*, *Rhizobium*, *Streptomyces*, *Pseudomonas*, and *Microbacteriu* and the beneficial fungal genera like *Chaetomium*, *Penicillium*, and *Humicola* were enriched, whereas the pathogenic fungal strains, *Fusarium* and *Gibberella* were restricted upon treatment of *Paenibacillus jamilae* and *Bacillus amyloliquefaciens* (Wang et al., 2021). Likewise, *Stenotrophomonas maltophilia, Bacillus cereus,* and *richoderma harzianum* showed biocontrol activity against *F. graminearum* (Dal Bello et al., 2002). The yeast isolates of the genera *Cryptococcus, Rhodotorula,* and *Saccharomyces* showed an inhibitory effect on the development of *F. sporotrichioides* colonies in wheat. Further, the bacterial isolate *Sphingomonas* inhibited the fungal pathogenic species *F. avenaceum, F. culmorum, F. tricinctum*, and *F. graminearum* (Wachowska et al., 2013).

Tan spot is the most destructive global foliar wheat disease, caused by *Pyrenophora tritici-repentis.* Using both double culture and greenhouse assays to evaluate the effect of wheat endophytes on the growth and sporulation on the tan spot pathogen, Larran et al. (2016) observed significant *in vitro* reduction of the pathogen colony diameter by *Trichoderma hamatum*, *Penicillium* sp., *Bacillus* sp., and *Paecilomyces lilacinus.* Further, *Bacillus* sp. and *Fusarium* sp. reduced the spore germination by 82 and 52%, respectively. Moreover, *T. hamatum, Chaetomium globosum* and *Fusarium* sp. were found to significantly reduce the severity of the disease on wheat leaves in green house assays, with greatest suppression by *T. hamatum* (Larran et al., 2016). The "take all" root disease in wheat, caused by an ascomycete

fungus, *Gaeumannomyces graminis* affects plant growth and yield. Antagonistic assay of the bacterial isolates collected from the rhizosphere of wheat roots on *G. graminis* revealed highest inhibitory action of *Burkholderia* sp., *Pseudomonas* sp., *Bacillus subtilis*, and *Xanthomonas* sp. (Nasraoui et al., 2007). With the aim of characterizing the effect of infection with *Zymoseptoria tritici* fungus on the wheat microbial communities and to identify microorganisms interacting with it, Kerdraon et al. (2019) used meta-barcoding approach and observed significant alteration in microbial communities with some species remaining affected even after the disappearance of the pathogen. Using the pyrosequencing technique, certain microbes were found to suppress *Rhizoctonia* root rot and bare batch disease in wheat, with *Chryseobacterium* and *Pseudomonas* dominating in the rhizosphere over time (Yin et al., 2013). In order to monitor the changes in microbial communities associated with wheat, application of the biocontrol agents, *Paenibacillus fulvissimus* and *Streptomyces* spp. to *Rhizoctonia solani* and *Pythium* sp. infected soils revealed modulation of the endosphere and rhizosphere microbiomes. Further, a low impact on indigenous microbial communities, reduction in root disease, and plant growth enhancement were observed (Araujo et al., 2019, 2020).

MICROBIOME ASSISTED RESISTANCE AGAINST ABIOTIC STRESS

Among the principle factors responsible for declining agricultural produce, abiotic stress stands at the forefront. Around 64% of the land area is affected by drought, 13% by anoxia due to flood submergence, 57% by cold, 15% by acidic soils, 6% by salinity, and 9% by mineral deficiency (Cramer et al., 2011). Around 69.23% of the dryland agriculture is influenced by soil salinity, erosion, and degradation (Riadh et al., 2010). Plants possess internal metabolic re-programming and homeostatic dynamics to cope up with adverse conditions. Following the sensing of stress signal, plants trigger a protective cascade involving synthesis of phytohormones, accumulation of flavonoids and phenolics, onset of antioxidants and osmolytes, and activation of specific genes and their regulation through repression/activation of transcription factors, which ultimately confers timely defense to plants (Meena et al., 2017). The microbes associated with plants form specific interactions with their hosts to evoke local and systemic responses for providing indispensable resistance against abiotic stress. Therefore, plant-microbe interactions are viewed as a key adaptive survival strategy in abiotic stress. The stress response provoked by microbe is termed Induced Systemic Tolerance (IST). The role of microbes in mitigating various biotic stresses has been documented for many crop species (Meena et al., 2017).

Mitigation of Drought Stress

Drought stress is one of the major concerns of agricultural losses worldwide. Maintaining increased crop productivity requires efficient low-cost technologies for abiotic stress management. Drought leads to loss of turgor, an increase in ionic concentration, and cell viscosity. Under drought, plants retain water by decreasing their water potential by making osmotic adjustments (OA) through production of osmolytes like proline, glycine betaine, polyamines, polyols, soluble sugars, and ions especially K^+. Roots are first to sense drought signal. An improved root system in wheat is resistant to drought. In wheat, the soluble sugars contribute most to OA, and starch is degraded to soluble sugars under drought stress. Besides, increase in proline and other amino acids, reactive oxygen species (ROS), antioxidant molecules like catalase, superoxide dismutase (SOD), glutathione peroxidase (GPX), ascorbate peroxidase (APX), and glutathione reductase (GR) are triggered to mitigate drought stress. Hormones, notably abscisic acid (ABA), which causes stomatal closure and expression of ABA-responsive genes to protect the plant from water loss, cytokinin that acts antagonistically to ABA under drought, and ethylene, which at thresh hold levels under acute drought cause senescence, are also involved in drought response. The MYC/MYB, NAC, AREB/ABFs, DREB or CBF, and WRKY transcription factors also regulate drought response through expression/repression of their target genes. Further, volatile organic compounds like isoprenoids are used as a signal to communicate within the plant and with other plants and trigger a stress tolerance in these plants (Camaille et al., 2021).

Several strategies have been proposed to mitigate the adverse effects of drought stress in plants; however, most of these approaches are time-consuming, cost-intensive, and not well accepted in some regions (Wahid et al., 2007). A promising alternative approach is to induce stress tolerance in plants by using beneficial microorganisms. The plant growth-promoting rhizobacteria (PGPR) modulate growth and development to enhance stress tolerance through physiological responses in plants. Besides, PGPR also improves plant performance by causing improved soil structure and increased soil water retention. The application of PGPRs that coevolved with plant roots over millions of years under harsh environments to improve plant fitness under biotic and abiotic stresses has advantages over stress management through genetic modifications. For example the phenazine-producing bacteria grow abundantly in the rhizosphere of dryland-grown wheat. They perform better in rhizospheres with lower moisture content and are particularly abundant in drought-resistant cultivars (Mavrodi et al., 2012, 2018; Mahmoudi, 2017). The wheat seedlings exposed to water deficit but colonized by the phenazine-producing strains of *Pseudomonas* suffered less dehydration and recovered better, thereby conferring better resilience to seedlings. The inoculated seedlings showed higher growth of root system, especially tips. Thus, the phenazine-producing bacteria in the rhizosphere could be harnessed for drought stress management in wheat (Mahmoudi et al., 2019). *Burkholderia phytofirmans* strain PsJN is an extensively studied endophytic bacteria that colonize a wide variety of plants. Significant dilution of adverse effects of drought stress coupled to improvement of the photosynthetic rate, water use efficiency, chlorophyll content, grain yield, and NPK levels in grains was observed in wheat after inoculation with PsJN strain. This revealed that *B. phytofirmans* has the potential to improve the growth, physiology, and quality of wheat under drought conditions (Naveed et al., 2014). In order to determine

the beneficial effect of *Azospirillum brasilense* on wheat suffering from drought during anthesis, relatively higher water content and water potential, apoplastic water fraction, and a lower cell wall modulus of elasticity were observed along with lesser yield loss in trials inoculated with *Azospirillum* than those of non-inoculated ones. Further, the grains obtained from inoculated plants exhibited significantly higher Mg, K, and Ca contents, showing that a higher growth can be promoted under drought stress in wheat through microbial associations (Creus et al., 2004). Further, the priming of wheat seedlings with the rhizosphere bacteria caused enhancement in drought tolerance and resulted in 78% greater biomass and a fivefold higher survival rate. The ROS scavenging enzyme activities increased in response to bacterial priming. Out of the seven volatile compounds emitted from the leaves of the primed seedlings, monitoring of the three viz benzaldehyde, beta-pinene, and geranyl acetone is key to characterize the efficiency of different bacterial strains in priming for drought stress resistance (Timmusk et al., 2014). Besides, inoculation of wheat plants with *Bacillus safensis* or *Ochrobactrum pseudogregnonense* (Chakraborty et al., 2013), *Azospirillum lipoferum* (Arzanesh et al., 2011), *Pantoea alhagi* (Chen et al., 2017), *Bacillus amyloliquefaciens* and *Azospirillum brasilense* (Kasim et al., 2013), *Bacillus thuringiensis* (Timmusk et al., 2014), *Burkholderia phytofirmans* (Naveed et al., 2014), *Klebsiella* sp. (Gontia-Mishra et al., 2016) trigger diverse physiological effects to enhance survival and/or yield under water deficit. Further, to mitigate water stress, *A. brasilense* (Creus et al., 2004), *B. safensis* or *O. pseudogregnonense* (Chakraborty et al., 2013) result in enhancement of osmolytes in wheat, however, inoculation of *Klebsiella* sp., although improved root and shoot growth, lowers the total soluble sugars and proline content in wheat (Gontia-Mishra et al., 2016). Moreover, the PGPRs produce their own volatile compounds like 2,3-butanediol, acetoin, or acetic acid. The acetic acid enhances the formation of biofilm by Exopolysaccharides (EPS) producing bacteria, 2,3-butanediol induces drought tolerance through stomatal closure and reduction of water loss (Camaille et al., 2021). Certain PGPRs have the ability to degrade ethylene precursor ACC into ammonium and α-ketobutyrate through the production of 1-aminocyclopropane-1-carboxylate deaminase (ACCd) enzyme. This reduces the ethylene level in the plant and reduces adverse effects of so-called stress ethylene. ACCd is produced in many PGPR bacterial genera like *Pseudomonas, Bacillus, Rhizobium, Sinorhizobium, Variovorax, Burkholderia* or *Azospirillum* (Camaille et al., 2021). Wheat seedling primed with ACCd producing *Bacillus subtilis* (Barnawal et al., 2017), *Klebsiella* sp. (Gontia-Mishra et al., 2016) exhibited reduced ACC content and better photosynthetic efficiency, root-shoot growth under drought stress. PGPRs can trigger the production of phytohormones, especially auxins in plants, which could modify RSA. Inoculation of wheat seedlings with IAA-producing *Klebsiella* sp. (Gontia-Mishra et al., 2016), *Azospirillum* sp. (Arzanesh et al., 2011), *Bacillus, Enterobacter, Moraxella*, and *Pseudomonas* (Raheem et al., 2018), *B. subtilis* (Barnawal et al., 2017) enhances root number and length, photosynthetic efficiency under drought stress, which allows better assimilation of water and nutrients (Barnawal et al., 2019). Barnawal et al. (2017) observed a 30% reduced ABA level in wheat seedlings primed with PGPRs along with 28% increase in shoot dry weight and 17% increase in root dry weight. Several bacterial attributes which are involved in promoting drought tolerance include the ability to produce 1-aminocyclopropane-1-carboxylate deaminase (ACCd), indole-3-acetic acid (IAA) and siderophores. ACCd acts by preventing ethylene from reaching inhibitory levels to allow proper root growth under water deficit, IAA regulates stomatal aperture and enhances root and shoot growth under drought, siderophores allow proper nutrient cycling under drought (Hone et al., 2021).

The microbial species associated with wheat also enhance drought resistance through the enhancement of antioxidant response. They increase the activity of ROS-scavenging enzymes like GR, SOD, CAT, peroxidase, APX, and GPX, etc (Chakraborty et al., 2013; Timmusk et al., 2014). Kasim et al. (2013), however, obtained decreased activity of ROS-scavenging enzymes APX and dehydroascorbate reductase upon inoculation of wheat seedlings with *Bacillus amyloliquefaciens* and *Azospirillum brasilense*. In this case, the stress mitigation activity of the microbes may be associated with a different mode like the production of ACCd or IAA (Kasim et al., 2013). The EPS is a complex mixture of biomolecules produced by bacterial species. EPS-producing bacterial in the rhizosphere lead to a better soil aggregation around the roots and more efficient water and nutrient flux toward the plant roots. They confer several beneficial properties to the host plant, including tolerance against drought stress. *B. thuringiensis,* when inoculated with wheat, produces biofilm around roots which leads to 2–3 fold more soil aggregation around roots, 63% enhancement in water use effeciency, and higher survival rate under drought stress (Timmusk et al., 2014). Similar results were obtained by inoculation of wheat with *Klebsiella* sp. (Gontia-Mishra et al., 2016). Seed microbes play a vital role in the transmission of microbes between plant generations. Seed microbes are the initial colonizers of plant tissues and are believed to shape the overall plant microbiome composition, therefore have a competitive advantage over microbes recruited from soil and root. The use of metagenomic and culture-based methods for profiling and characterizing the seed microbiome structure in drought-tolerant and susceptible wheat cultivars have shown growth promotion of wheat by *Curtobacterium flaccumfaciens* and *Arthrobacter* sp. under drought conditions. The beneficial seed microbes were line-specific and responsive to environmental stress. The study indicated that seeds collected from stressed plants form an important resource to identify microbes with growth-promoting activity (Hone et al., 2021).

Mitigation of Temperature Stress

Fungal root endophytes are taxonomically, ecologically, and physiologically poorly understood in comparison to their phylosphere counterparts. Fungal endophytes belonging to Ascomycota and Basidiomycota are involved in thermo- and drought tolerance in different plant species (Redman et al., 2002; Márquez et al., 2007; Sherameti et al., 2008; Sun et al., 2010). The endophytic fungi even form symbiotic associations (called mycovitality) with seeds (Vujanovic and Vujanovic,

2007). A close relationship between the endophytic fungal compartmentalization and plant health was observed in wheat (Abdellatif et al., 2009). Endophytic Ascomycetes improve seed germination in wheat under heat and drought stress (Hubbard et al., 2012). Evaluation of the impact of fungal endophytes on the growth, ecophysiological, and reproductive success of heat and drought-stressed wheat revealed that the photosynthetic effeciency, plant height, seed weight showed a general improvement in plants colonized by endophytic fungi as compared to endophyte-free plants. The endophytes promoted heat stress in wheat through the reduction in photosynthetic stress. They enhanced percentage germination and decreased time to 50% germination, proving their capacity to enhance heat and drought stress in parental plants and second-generation seeds via mycovitality (Hubbard et al., 2014). Evaluation of plant-growth-promoting effects and nutrient uptake by PGPR isolated from rhizosphere, phyllosphere and soil in winter wheat showed that both soil type and temperature influence the growth-promoting effects of the bacteria. The root and shoot growth were enhanced under low temperature of 16°C when wheat plants were inoculated by *Pseudomonas fluorescens*, *Pantoea agglomerans,* and *Mycobacterium sp.,* whereas *Mycobacterium phlei* and *Mycoplana bullata* improved the root and shoot growth under nutrient-poor medium. Besides, all the bacteria were found to enhance NPK content of plants (Egamberdiyeva and Höflich, 2003). Using 16S rRNA sequencing, a bacteria collected from Amarnath soils of North-Western Himalayas of India, was identified as *Pseudomonas lurida*, which possessed unique properties, including growth at as low as 4°C. The bacteria have the ability to produce IAA and solubilize phosphate even at 4°C. Inoculation of this bacterium with wheat seeds showed growth-promoting ability. The seed germination percentage, shoot and root lengths were significantly increased in inoculated plants as compared to non-inoculated ones. The strain produced siderophores at mesophilic and cold temperatures, which in low nutrient environments secrete ion-binding ligands, especially iron-binding (siderophores) that bind to ferric iron and make it available to the host microorganisms. All these properties can prove beneficial in wheat breeding in cold environments (Mishra et al., 2009). Based on the evaluation of 23 parameters, investigation of cold response in wheat seedlings inoculated with *Pseudomonas* strains under greenhouse conditions showed that the un-inoculated plants were under cold stress and that eight strains alleviated cold stress in wheat. Inoculation significantly improved chlorophyll, anthocyanin, proline, phenolic, and starch contents along with physiologically available Fe, proteins, and cold tolerance amino acids. Reduced electrolyte leakage and Na^+/K^+ ratio were also observed in inoculated plants, proving the efficacy of Pseudomonas strains in mitigating cold stress, and improving the performance of wheat in cold environments (Mishra et al., 2011).

Mitigation of Salinity Stress

Salinity affects around one-third of the world's arable land resources (Qadir et al., 2000). The important attributes which determine salt tolerance of plants depend on the restricted/controlled uptake of Na^+ and Cl^-, greater intake of K^+ and $NO3^-$, and preferential uptake of K^+ over Na^+ by roots (Jeschke and Wolf, 1988). To adapt to high salt concentrations, plants use following strategies; (a) activation of Na^+ efflux, (b) prevention of Na^+ influx, and (c) Na^+ compartmentalization in vacuoles (Rajendran et al., 2009). The Na^+/H^+ antiporters (SOS1 and NHX1) maintain the optimum ionic concentrations in the cytoplasm to avoid toxicity due to Na^+. Plasma membrane located SOS1 extrudes Na^+ from cytoplasm to apoplast, whereas the tonoplast located NHX1 pumps Na^+ from cytoplasm to vacuoles (Gaxiola et al., 1999; Shi et al., 2000). Both transporters require energy, which is provided through proton motive force generated by H^+-ATPase. In any salt tolerance, the activity and expression of these transporters play a central role in maintaining the optimal concentration of Na^+ in the cytoplasm to avoid salinity-induced damage to the cell. Salinity stress often induces overproduction of ROS like hydroxyl radical ($OH^{\cdot}$), single oxygen ($^1O_2$), superoxide anion ($O_2^{\cdot -}$), and hydrogen peroxide (H_2O_2). These ROS species are very dangerous as they deteriorate membrane structure and alter its permeability. They, therefore, must be immediately scavenged to avoid oxidative damage. Plants exhibit enzymatic and non-enzymatic antioxidant defense systems to neutralize ROS-induced oxidative damage. Chelation of cations or their compartmental sequestration is yet another strategy adapted by plants to counter salt stress. Ethylene is an important plant growth regulator controlling many important developmental processes like seed germination, root hair development and elongation, fruit ripening, leaf abscission, and organ senescence (Ahmad et al., 2011). However, under stress, the ethylene is accumulated in higher detrimental concentrations, which can inhibit plant growth (Erice et al., 2017). Therefore, regulation of ethylene concentration to optimal levels during stress is of utmost importance to avoid ethylene-induced detrimental effects. The level of ethylene can be checked through regulation of ACC deaminase that cleaves ethylene precursor ACC to ammonia and α-ketobutyrate (Kumar et al., 2020). Therefore, role of ACC deaminase in salt and other type of stresses is crucial. Accumulation of compatible solutes such as sugars and proline in root vacuoles, as well as of Ca^{2+} and K^+ also confer salinity tolerance to plants.

Bacterial EPS have the ability to bind cations, including Na^+ (Geddie and Sutherland, 1993). Therefore, the abundance of such bacterial species in the rhizosphere would significantly lock up the Na^+ ions and confer beneficial advantage to plants under salinity stress. Inoculation of wheat seedlings grown in a moderately saline soil by EPS-producing bacteria like *Aeromonas hydrophila/caviae* (strain MAS-765), *Bacillus insolitus* (strain MAS17), and three *Bacillus* sp. strains (MAS617, MAS620, and MAS820) showed an increase in root and shoot dry matter and reduced Na^+ uptake by roots, which indicate that the inoculated plants performed better under salt stress (Ashraf et al., 2004). The utilization of plant root-associated stress-tolerant microbial species has the potential to improve soil fertility and plant resistance toward adverse environmental conditions (Wu et al., 2009). Consequently, the microbial species dwelling in high saline environment can provide salt tolerance to host species. The high

saline habitat-dwelling microbial species like *Bacillus pumilus*, *Pseudomonas mendocina*, *Arthrobacter* sp., *Halomonas* sp., and *Nitrinicola lacisaponensis* have a growth-promoting effect on wheat grown in saline soils. Besides improving certain growth parameters like root/shoot length, root-shoot biomass ratio, chlorophyll, carotenoid, and protein content, the wheat plants inoculated by these species also accumulated higher phenolics, flavonoids, and IAA in the rhizosphere, as well as promoted the overall plant growth in the saline soils (Tiwari et al., 2011). Halotolerant bacterial strains can survive under high salinity, they overcome the adverse effects of high salt by compatible solute accumulation, production of extracellular proteases, and activation of Na^+/H^+ antiporters, etc. Many of the halotolerant microbes possess PGPR properties, therefore can be harnessed to mitigate salt stress in different crop species. In addition to the coating of wheat seeds by phytohormone-rich extract filtered from the bacterial culture, the inoculation of wheat seedlings with a halotolerant methylotrophic *Nocardioides* sp. under saline conditions revealed improved germination in the primed seeds, enhanced growth, protein content, and activity of SOD, CAT, APX, and peroxidase. Further, over-expression of defense-related genes was observed in the seedlings, indicating the potential of the bacterium in salt stress (Meena et al., 2020). Screening of halotolerant bacterial strains from the saline habitats revealed *Hallobacillus* sp. and *Bacillus halodenitrificans* as the potential microbes with PGPR properties under salt stress in wheat (Ramadoss et al., 2013). None of the bacteria, however, had ACC deaminase activity. As IAA may promote root growth by stimulating cell elongation or cell division, evaluation for IAA accumulation revealed that this stress mitigating property on wheat was due to IAA production only in the case of *Hallobacillus* sp. Inoculation of the carotenoid-producing halotolerant bacteria *Dietzia natronolimnaea* improved growth in terms of dry weight and height, photosynthetic pigments, CAT, and peroxidase in wheat under salt stress. Further, modulation of the transcriptional machinery to induce salt tolerance in wheat was observed. The ABA-responsive genes (*ABARE*) and *TaOPR1,* the Salt Overly Sensitive (SOS) genes (*SOS1* and *SOS4*), the transcription factors (*TaWRKY10*, *TaWRKY17,* and *TaMYB33*), the ion transporter genes *TaHKT*, *TaNHX*, *TaHAK*, and the antioxidant genes *POD, CAT, APX, GR, GPX, MnSOD* were over-expressed under salt stress in *D. natronolimnaea* inoculated plants as compared to non-inoculated ones. This indicates that the halotolerant *D. natronolimnaea* induces salinity tolerance through a complex intermingled process involving modulation of ABA-signaling, SOS pathway, ion transporters, and antioxidant machinery (Bharti et al., 2016). The microbial species also mitigate salt stress through up-regulation of antioxidant defense response. Wheat seedlings inoculated with *Piriformospora indica* under salinity stress showed lower lipid peroxidation, relative membrane permeability, and lipoxygenase enzyme (LOX) activity along with the higher accumulation of proline, α-tocopherol, and carotenoids and enhanced activity of SOD, CAT, and APX compared to un-inoculated plants (Singh and Tiwari, 2021).

Besides the production of plant growth regulators like auxins, cytokinins, and gibberellins, PGPRs also have the ability to bring ethylene levels to normal under stress through the production of ACC deaminase that cleaves ethylene precursor ACC to ammonia and α-ketobutyrate (Kumar et al., 2020). Most of the ACC deaminase-producing PGPRs modify root number and area to enhance nutrient uptake from stressed soils. Under salt and drought stress, ABA acts by causing accumulation of the compatible solutes such as sugars and proline in root vacuoles, as well as of Ca^{2+} and K^+, which mitigate the effects of high salinity, and also cause stomatal closure to prevent excessive water loss to mitigate drought effects. The uptake and accumulation of essential nutrients like NPK and H_2O are reduced under salinity stress. Different microbial strains have been shown to enhance the P and K uptake under salt stress (Mayak et al., 2004; Kang et al., 2014). PGPRs also enhance the availability of mineral elements like Cu, Fe, Mn, and Zn, etc., to plants by chelation and acidification of soil (Kumar et al., 2020). The bacterial siderophores have a higher affinity toward Fe than siderophores produced by plants. *Invitro* assessment of the rhizosphere bacteria *Pseudomonas fluorescens*, *Serratia liquefaciens*, *Bacillus subtilis,* and *Bacillus megaterium* revealed their salt tolerance up to 3% salinity levels and ability to produce IAA. *P. fluorescens* and *B. megaterium* also showed ACC deaminase activity. *Invivo* assessment of the salt stress mitigating capacity of the later two revealed improved wheat growth under salinity stress (Fathalla and Abd El-Mageed, 2020).

Mitigation of Metal Toxicity

Heavy metals like lead (Pb), arsenic (As), and Nickel (Ni), etc., especially in soil, pose another stress threat to plants. Once accumulated in soils, they affect the soil dynamics, soil microbial composition and functions,which ultimately leads to loss of soil fertility, thereby crop production. Like other stress types, heavy metal toxicity induces oxidative damage by producing more ROS, alters enzymatic activities and water and mineral transport, impairs growth and developmental processes, decreases the performance of the plant, and causes yield losses. Plantation of species with phytoremediation potential is one of the strategies to manage heavy metal toxicity. An alternative strategy for managing soils polluted by heavy metals is to utilize heavy metal tolerant PGPRs (Liu et al., 2015). As biofertilizers, the heavy metal tolerant microbes detoxify heavy metals by altering/limiting the bioavailability of metals through acidification, chelation, precipitation, exclusion, sequestration or transformation to less toxic forms (Dixit et al., 2015; Mishra et al., 2017). Further, the metal tolerant microbes release metallothioneins (MTs) and phytochelatins (PCs) that chelate metals to confer defense against heavy metals (Jan et al., 2014). *Bacillus subtilis* showed tolerance against Ni and Pb. The oxidative damage and growth inhibition were suppressed when the wheat plants under Ni and Pb stress were inoculated with *B. subtilis*. Shoot length and biomass and grain yield were improved. The growth-promoting effect of *B. subtilis* was due to IAA generation, which accelerates cell division and enlargement, root elongation, and apical dominance in wheat. Further, small amounts of siderophores in liquid medium only were produced by *B. subtilis,* which could confer stress tolerance to wheat. Moreover, the bacteria also

showed ACC deaminase activity, which although was reduced by increasing Ni and Pb concentrations (Rizvi et al., 2019).

HOST-MEDIATED MICROBIOME ENGINEERING

In a generalized fashion, the host-mediated microbiome engineering (HMME) is a technique to selectively pick the rhizosphere microbiome of the most tolerant plants after induced stress, inoculate a fresh sterile medium with the selected rhizomicrobiome followed by planting of new germplasm in the inoculated medium (**Figure 3**). After several cycles with the same host, a microbiome is obtained that confers beneficial interactions to the host. This microbiome, which is now established for its beneficial role under stress, can be characterized in detail using different omics technologies. Therefore, HMME is a host-centric selection process of microbiomes at the community level (Swenson et al., 2000). Both ecological and evolutionary processes are involved in the change in microbiome during HMME process (Mueller and Sachs, 2015). A good amount of evidence has accumulated in recent years acknowledging the potential of HMME in conferring beneficial adaptations to host plants. For example, HMME selected microbiomes provided enhanced growth under less favorable soil pH (Swenson et al., 2000) and altered flowering onset and leaf biomass (Panke-Buisse et al., 2014, 2017) in *Arabidopsis thaliana*. With the aim to improve seedling establishment under extreme drought in wheat, Jochum et al. (2019) used delayed onset of seedling water deficit stress symptoms phenotype to select microbiomes that could provide beneficial interaction to host and enable its better withstand and survival. Following six rounds of artificial selection, the research group obtained a microbial community that not only delayed the stress symptoms in seedlings as long as 5 days but also improved the overall biomass, root length, surface area, and dry weight. This beneficial effect was completely lost upon autoclaving of the medium, indicating the true relationship of the artificially selected microbiome with the host. Taxonomic investigation of the selected microbiome indicated Proteobacteria and Bacteroidetes as the most abundant phyla

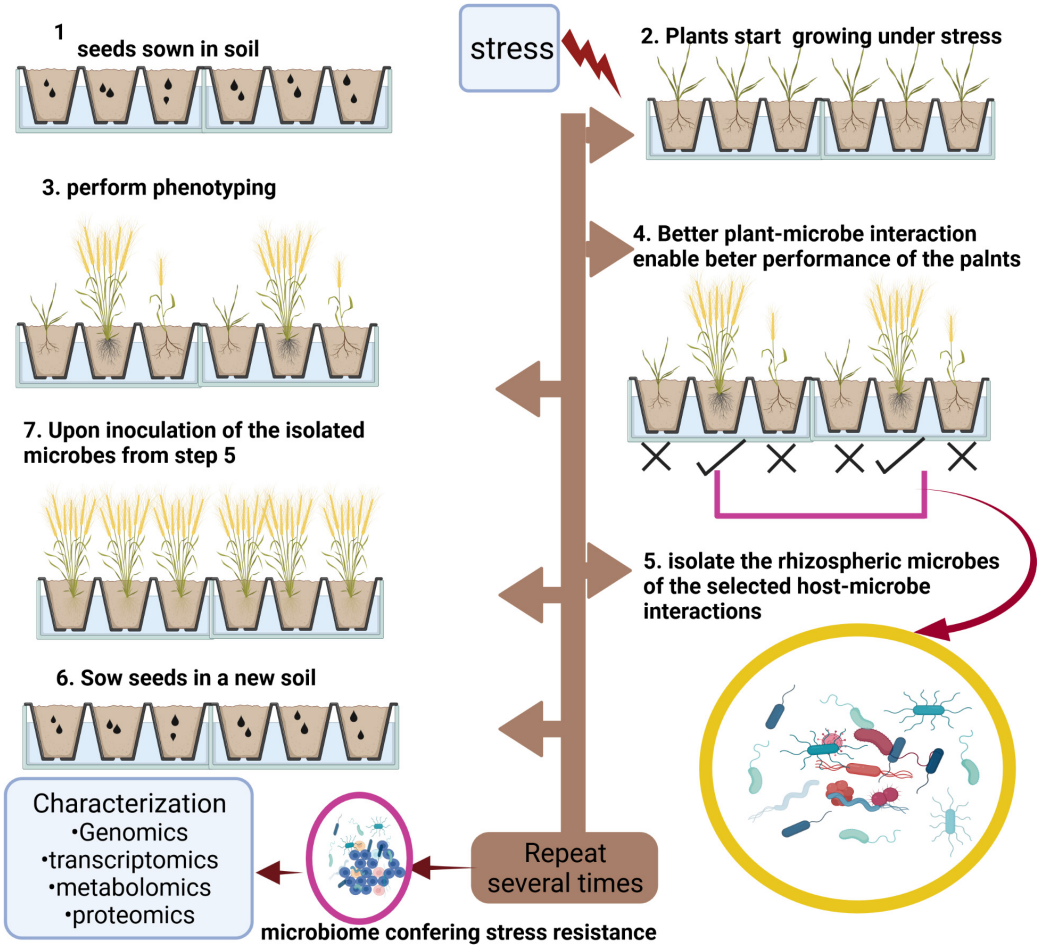

FIGURE 3 | Graphical representation of host-mediated microbiome engineering. The figure shows that under stress, some genotypes perform better than others (step 4), isolation (step 5), and inoculation of the microbes associated with these genotypes (step 6) with new soil result in better performance of plants. Repetition of steps 2–7 would result in a microbiome having the property to confer stress resistance to host species. The figure was created with BioRender.com.

followed by Actinobacteria, and Firmicutes. Gemmatimonadetes was the least abundant phyla followed by Cyanobacteria in the selected microbiome. Among the dominant classes were Betaproteobacteria followed by Gamma-, Delta- and Alphaproteobacteria (Jochum et al., 2019 for image). HMME selected microbiome was also found to provide salt tolerance to *Brachypodium distachyon* (Mueller et al., 2016). Using HMME, specific microbiomes can be engineered to aid wheat and other crop species in mitigating salt, drought, heat, and other types of biotic stresses.

FUTURE PERSPECTIVES

It is now well established that microbiomes mediate diverse beneficial functional roles in the host species. Harnessing these beneficial interactions for sustainable agriculture provides several advantages over other approaches of crop improvement, especially the use of excessive fertilizers, pesticides, and insecticides, etc., for enhancement of yield and crop protection. These chemicals alter the soil microbiome and in certain cases restrict the beneficial microbial species. The details about the effect of these factors on the dynamics of microbial community structure in most crop species are very scarce. Therefore, an ample research shall be focused to dissect how fertilizers, pesticides, and insecticides etc., regulate the beneficial microbes of the host species, especially wheat. Evaluation of trade off between the use of these chemicals and the negative impact of reduction of beneficial microbes by these chemicals on the overall plant performance would provide a useful guide to use these chemicals at optimal quantities, at which there is minimal negative effect on the beneficial microbes. Further, the development of elite cultivars through breeding programmes also influence the host microbiome profile. There is a dire need to generate a robust and elaborate database of cultivar type and associated microbiomes, which would give us an idea about the missing beneficial microbes for each cultivar. Search for alternative microbes providing similar beneficial roles and hosted by the cultivar would suffice for the missing cultivar specific beneficial microbes. The crop improvement programs, during the development of elite cultivars, shall include the assessment of dynamic changes on the microbiome profile as an important parameter in the list of other commonly used screening traits.

AUTHOR CONTRIBUTIONS

AM drew the figures. All authors contributed to writing of the manuscript.

FUNDING

This work was supported by grants from Jiangsu University High-Level Talent Funding (20JDG34), Natural Science Foundation of Jiangsu Province (BK20211319), and National Natural Science Foundation of China (32000201) to JC.

REFERENCES

Abdellatif, L., Bouzid, S., Kaminskyj, S., and Vujanovic, V. (2009). Endophytic hyphal compartmentalization is required for successful symbiotic Ascomycota association with root cells. *Mycol. Res.* 113, 782–791. doi: 10.1016/j.mycres.2009.02.013

Ahmad, M., Zahir, Z. A., Asghar, H. N., and Asghar, M. (2011). Inducing salt tolerance in mung bean through co-inoculation with rhizobia and plant-growth-promoting rhizobacteria containing 1-aminocyclopropane-1-carboxylate deaminase. *Can. J. Microbiol.* 57, 578–589. doi: 10.1139/w11-044

Araujo, R., Dunlap, C., and Franco, C. M. (2020). Analogous wheat root rhizosphere microbial successions in field and greenhouse trials in the presence of biocontrol agents *Paenibacillus peoriae* SP9 and *Streptomyces fulvissimus* FU14. *Mol. Plant Pathol.* 21, 622–635. doi: 10.1111/mpp.12918

Araujo, R., Dunlap, C., Barnett, S., and Franco, C. M. (2019). Decoding wheat endosphere–rhizosphere microbiomes in *Rhizoctonia solani*–infested soils challenged by Streptomyces biocontrol agents. *Front. Plant Sci.* 10:1038. doi: 10.3389/fpls.2019.01038

Arzanesh, M. H., Alikhani, H. A., Khavazi, K., Rahimian, H. A., and Miransari, M. (2011). Wheat (*Triticum aestivum* L.) growth enhancement by *Azospirillum* sp. under drought stress. *World J. Microbiol. Biotechnology* 27, 197–205.

Ashraf, M., Hasnain, S., Berge, O., and Mahmood, T. (2004). Inoculating wheat seedlings with exopolysaccharide-producing bacteria restricts sodium uptake and stimulates plant growth under salt stress. *Biol. Fertil. Soils* 40, 157–162.

Azarbad, H., Constant, P., Giard-Laliberté, C., Bainard, L. D., and Yergeau, E. (2018). Water stress history and wheat genotype modulate rhizosphere microbial response to drought. *Soil Biol. Biochem.* 126, 228–236.

Baffoni, L., Gaggia, F., Dalanaj, N., Prodi, A., Nipoti, P., Pisi, A., et al. (2015). Microbial inoculants for the biocontrol of *Fusarium* spp. in durum wheat. *BMC Microbiol.* 15:242. doi: 10.1186/s12866-015-0573-7

Barnawal, D., Bharti, N., Pandey, S. S., Pandey, A., Chanotiya, C. S., and Kalra, A. (2017). Plant growth-promoting rhizobacteria enhance wheat salt and drought stress tolerance by altering endogenous phytohormone levels and TaCTR1/TaDREB2 expression. *Physiol. Plant.* 161, 502–514. doi: 10.1111/ppl.12614

Barnawal, D., Singh, R., and Singh, R. P. (2019). "Role of plant growth promoting rhizobacteria in drought tolerance: regulating growth hormones and osmolytes," in *PGPR Amelioration in Sustainable Agriculture*, eds A. K. Singh, A. Kumar, and P. K. Singh (Sawston: Woodhead Publishing), 107–128. doi: 10.1016/b978-0-12-815879-1.00006-9

Besset-Manzoni, Y., Joly, P., Brutel, A., Gerin, F., Soudière, O., Langin, T., et al. (2019). Does in vitro selection of biocontrol agents guarantee success in planta? A study case of wheat protection against *Fusarium* seedling blight by soil bacteria. *PLoS One* 14:e0225655. doi: 10.1371/journal.pone.0225655

Bharti, N., Pandey, S. S., Barnawal, D., Patel, V. K., and Kalra, A. (2016). Plant growth promoting rhizobacteria *Dietzia natronolimnaea* modulates the expression of stress responsive genes providing protection of wheat from salinity stress. *Sci. Rep.* 6:34768. doi: 10.1038/srep34768

Camaille, M., Fabre, N., Clément, C., and Ait Barka, E. (2021). Advances in wheat physiology in response to drought and the role of plant growth promoting rhizobacteria to trigger drought tolerance. *Microorganisms* 9:687. doi: 10.3390/microorganisms9040687

Chakraborty, U., Chakraborty, B. N., Chakraborty, A. P., and Dey, P. L. (2013). Water stress amelioration and plant growth promotion in wheat plants by osmotic stress tolerant bacteria. *World J. Microbiol. Biotechnol.* 29, 789–803. doi: 10.1007/s11274-012-1234-8

Chen, C., Xin, K., Liu, H., Cheng, J., Shen, X., Wang, Y., et al. (2017). *Pantoea alhagi*, a novel endophytic bacterium with ability to improve growth and drought tolerance in wheat. *Sci. Rep.* 7:41564. doi: 10.1038/srep41564

Chen, S., Waghmode, T. R., Sun, R., Kuramae, E. E., Hu, C., and Liu, B. (2019). Root-associated microbiomes of wheat under the combined effect of plant

development and nitrogen fertilization. *Microbiome* 7:136. doi: 10.1186/s40168-019-0750-2

Chen, Y., Wang, J., Yang, N., Wen, Z., Sun, X., Chai, Y., et al. (2018). Wheat microbiome bacteria can reduce virulence of a plant pathogenic fungus by altering histone acetylation. *Nat. Commun.* 9:3429. doi: 10.1038/s41467-018-05683-7

Comby, M., Lacoste, S., Baillieul, F., Profizi, C., and Dupont, J. (2016). Spatial and temporal variation of cultivable communities of co-occurring endophytes and pathogens in wheat. *Front. Microbiol.* 7:403. doi: 10.3389/fmicb.2016.00403

Cordero, J., de Freitas, J. R., and Germida, J. J. (2020). Bacterial microbiome associated with the rhizosphere and root interior of crops in Saskatchewan, Canada. *Can. J. Microbiol.* 66, 71–85. doi: 10.1139/cjm-2019-0330

Cramer, G. R., Urano, K., Delrot, S., Pezzotti, M., and Shinozaki, K. (2011). Effects of abiotic stress on plants: a systems biology perspective. *BMC Plant Biol.* 11:163. doi: 10.1186/1471-2229-11-163

Creus, C. M., Sueldo, R. J., and Barassi, C. A. (2004). Water relations and yield in *Azospirillum*-inoculated wheat exposed to drought in the field. *Can. J. Bot.* 82, 273–281.

Dal Bello, G. M., Monaco, C. I., and Simon, M. R. (2002). Biological control of seedling blight of wheat caused by *Fusarium graminearum* with beneficial rhizosphere microorganisms. *World J. Microbiol. Biotechnol.* 18, 627–636. doi: 10.3390/microorganisms8050627

de Castro, A. P., Sartori, A., Silva, M. R., Quirino, B. F., and Kruger, R. H. (2013). Combining "omics" strategies to analyze the biotechnological potential of complex microbial environments. *Curr. Protein Pept. Sci.* 14, 447–458. doi: 10.2174/1389203713149990062

Dixit, R., Wasiullah, D., Malaviya, K., Pandiyan, U. B., Singh, A., Sahu, R., et al. (2015). Bioremediation of heavy metals from soil and aquatic environment: an overview of principles and criteria of fundamental processes. *Sustainability* 7, 2189–2212. doi: 10.3390/su7022189

Donn, S., Kirkegaard, J. A., Perera, G., Richardson, A. E., and Watt, M. (2015). Evolution of bacterial communities in the wheat crop rhizosphere. *Environ. Microbiol.* 17, 610–621. doi: 10.1111/1462-2920.12452

Effmert, U., Kalderas, J., Warnke, R., and Piechulla, B. (2012). Volatile mediated interactions between bacteria and fungi in the soil. *J. Chem. Ecol.* 38, 665–703. doi: 10.1007/s10886-012-0135-5

Egamberdiyeva, D., and Höflich, G. (2003). Influence of growth-promoting bacteria on the growth of wheat in different soils and temperatures. *Soil Biol. Biochem.* 35, 973–978.

Erice, G., Ruíz-Lozano, J. M., Zamarreño, ÁM., García-Mina, J. M., and Aroca, R. (2017). Transcriptomic analysis reveals the importance of JA-Ile turnover in the response of *Arabidopsis* plants to plant growth promoting rhizobacteria and salinity. *Environ. Exp. Bot.* 143, 10–19. doi: 10.1016/j.envexpbot.2017.08.006

Fan, K., Cardona, C., Li, Y., Shi, Y. U., Xiang, X., Shen, C., et al. (2017). Rhizosphere-associated bacterial network structure and spatial distribution differ significantly from bulk soil in wheat crop fields. *Soil Biol. Biochem.* 113, 275–284.

Fan, K., Weisenhorn, P., Gilbert, J. A., and Chu, H. (2018). Wheat rhizosphere harbors a less complex and more stable microbial co-occurrence pattern than bulk soil. *Soil Biol. Biochem.* 125, 251–260. doi: 10.1016/j.soilbio.2018.07.022

Fathalla, A., and Abd El-Mageed, A. (2020). Salt tolerance enhancement Of wheat (*Triticum Asativium* L) genotypes by selected plant growth promoting bacteria. *AIMS Microbiol.* 6:250. doi: 10.3934/microbiol.2020016

Gaxiola, R. A., Rao, R., Sherman, A., Grisafi, P., Alper, S. L., and Fink, G. R. (1999). The *Arabidopsis thaliana* proton transporters, AtNhx1 and Avp1, can function in cation detoxification in yeast. *Proc. Natl. Acad. Sci. U.S.A.* 96, 1480–1485. doi: 10.1073/pnas.96.4.1480

Gdanetz, K., and Trail, F. (2017). The wheat microbiome under four management strategies, and potential for endophytes in disease protection. *Phytobiomes* 1, 158–168. doi: 10.1094/pbiomes-05-17-0023-r

Geddie, J. L., and Sutherland, I. W. (1993). Uptake of metals by bacterial polysaccharides. *J. Appl. Bacteriol.* 74, 467–472. doi: 10.1111/j.1365-2672.1993.tb05155.x

Gontia-Mishra, I., Sapre, S., Sharma, A., and Tiwari, S. (2016). Amelioration of drought tolerance in wheat by the interaction of plant growth-promoting rhizobacteria. *Plant Biol.* 18, 992–1000. doi: 10.1111/plb.12505

Hartman, K., Van Der Heijden, M. G., Wittwer, R. A., Banerjee, S., Walser, J. C., and Schlaeppi, K. (2018). Cropping practices manipulate abundance patterns of root and soil microbiome members paving the way to smart farming. *Microbiome* 6:14.

Hayden, H. L., Savin, K. W., Wadeson, J., Gupta, V. V., and Mele, P. M. (2018). Comparative metatranscriptomics of wheat rhizosphere microbiomes in disease suppressive and non-suppressive soils for Rhizoctonia solani AG8. *Front. Microbiol.* 9:859. doi: 10.3389/fmicb.2018.00859

Hone, H., Mann, R., Yang, G., Kaur, J., Tannenbaum, I., Li, T., et al. (2021). Profiling, isolation and characterisation of beneficial microbes from the seed microbiomes of drought tolerant wheat. *Sci. Rep.* 11:11916. doi: 10.1038/s41598-021-91351-8

Hubbard, M., Germida, J. J., and Vujanovic, V. (2014). Fungal endophytes enhance wheat heat and drought tolerance in terms of grain yield and second-generation seed viability. *J. Appl. Microbiol.* 116, 109–122. doi: 10.1111/jam.12311

Hubbard, M., Germida, J., and Vujanovic, V. (2012). Fungal endophytes improve wheat seed germination under heat and drought stress. *Botany* 90, 137–149.

Jan, A. T., Azam, M., Ali, A., and Haq, Q. M. R. (2014). Prospects for exploiting bacteria for bioremediation of metal pollution. *Crit. Rev. Environ. Sci. Technol* 44, 519–560. doi: 10.1080/10643389.2012.728811

Jeschke, W. D., and Wolf, O. (1988). External potassium is not required for root growth in saline conditions: experiments with *Ricinus communis* L. growth in a reciprocal split-root system. *J. Exp. Bot.* 39, 1149–1167. doi: 10.1093/jxb/39.9.1149

Jochum, M. D., McWilliams, K. L., Pierson, E. A., and Jo, Y. K. (2019). Host-mediated microbiome engineering (HMME) of drought tolerance in the wheat rhizosphere. *PLoS One* 14:e0225933. doi: 10.1371/journal.pone.0225933

Jones, P., Garcia, B. J., Furches, A., Tuskan, G. A., and Jacobson, D. (2019). Plant host-associated mechanisms for microbial selection. *Front. Plant Sci.* 10:862. doi: 10.3389/fpls.2019.00862

Kang, S.-M., Khan, A. L., Waqas, M., You, Y.-H., Kim, J.-H., Kim, J.-G., et al. (2014). Plant growth-promoting rhizobacteria reduce adverse effects of salinity and osmotic stress by regulating phytohormones and antioxidants in *Cucumis sativus*. *J. Plant Interact.* 9, 673–682. doi: 10.1080/17429145.2014.894587

Kasim, W. A., Osman, M. E., Omar, M. N., Abd El-Daim, I. A., Bejai, S., and Meijer, J. (2013). Control of drought stress in wheat using plant-growth-promoting bacteria. *J. Plant Growth Regul.* 32, 122–130.

Kavamura, V. N., Hayat, R., Clark, I. M., Rossmann, M., Mendes, R., Hirsch, P. R., et al. (2018). Inorganic nitrogen application affects both taxonomical and predicted functional structure of wheat rhizosphere bacterial communities. *Front. Microbiol.* 9:1074. doi: 10.3389/fmicb.2018.01074

Kavamura, V. N., Mendes, R., Bargaz, A., and Mauchline, T. H. (2021). Defining the wheat microbiome: towards microbiome-facilitated crop production. *Comput. Struct. Biotechnol. J.* 19:1200. doi: 10.1016/j.csbj.2021.01.045

Kavamura, V. N., Robinson, R. J., Hughes, D., Clark, I., Rossmann, M., de Melo, I. S., et al. (2020). Wheat dwarfing influences selection of the rhizosphere microbiome. *Sci. Rep.* 10:1452. doi: 10.1038/s41598-020-58402-y

Kerdraon, L., Barret, M., Laval, V., and Suffert, F. (2019). Differential dynamics of microbial community networks help identify microorganisms interacting with residue-borne pathogens: the case of *Zymoseptoria tritici* in wheat. *Microbiome* 7:125. doi: 10.1186/s40168-019-0736-0

Köhl, J., Booij, K., Kolnaar, R., and Ravensberg, W. J. (2019). Ecological arguments to reconsider data requirements regarding the environmental fate of microbial biocontrol agents in the registration procedure in the European Union. *BioControl* 64, 469–487. doi: 10.1007/s10526-019-09964-y

Kumar, A., Singh, S., Gaurav, A. K., Srivastava, S., and Verma, J. P. (2020). Plant growth-promoting bacteria: biological tools for the mitigation of salinity stress in plants. *Front. Microbiol.* 11:1216. doi: 10.3389/fmicb.2020.01216

Kuźniar, A., Włodarczyk, K., Grządziel, J., Goraj, W., Gałązka, A., and Wolińska, A. (2020). Culture-independent analysis of an endophytic core microbiome in two species of wheat: *Triticum aestivum* L.(cv.'Hondia') and the first report of microbiota in *Triticum spelta* L.(cv.'Rokosz'). *Syst. Appl. Microbiol.* 43:126025. doi: 10.1016/j.syapm.2019.126025

Laino, P., Limonta, M., Gerna, D., and Vaccino, P. (2015). Morpho-physiolological and qualitative traits of a bread wheat collection spanning a century of breeding in Italy. *Biodiv. Data J.* 3:e4760. doi: 10.3897/BDJ.3.e4760

Larran, S., Simon, M. R., Moreno, M. V., Siurana, M. S., and Perelló, A. (2016). Endophytes from wheat as biocontrol agents against tan spot disease. *Biol. Control* 92, 17–23. doi: 10.1016/j.biocontrol.2015.09.002

Latz, M. A., Kerrn, M. H., Sørensen, H., Collinge, D. B., Jensen, B., Brown, J. K., et al. (2021). Succession of the fungal endophytic microbiome of wheat is dependent on tissue-specific interactions between host genotype and environment. *Sci. Total Environ.* 759:143804. doi: 10.1016/j.scitotenv.2020.143804

Legrand, F., Picot, A., Cobo-Diaz, J. F., Chen, W., and Le Floch, G. (2017). Challenges facing the biological control strategies for the management of *Fusarium* head blight of cereals caused by Fg. *Biol. Control* 113, 26–38. doi: 10.1016/j.biocontrol.2017.06.011

Li, S. J., Du, L. C., Yuen, G., and Harris, S. D. (2006). Distinct ceramide synthases regulate polarized growth in the filamentous fungus *Aspergillus nidulans*. *Mol. Biol. Cell* 17, 1218–1227. doi: 10.1091/mbc.e05-06-0533

Li, Y., An, J., Dang, Z., Lv, H., Pan, W., and Gao, Z. (2018). Treating wheat seeds with neonicotinoid insecticides does not harm the rhizosphere microbial community. *PLoS One* 13:e0205200. doi: 10.1371/journal.pone.0205200

Liu, W., Wang, Q., Wang, B., Hou, J., Luo, Y., Tang, C., et al. (2015). Plant growth-promoting rhizobacteria enhance the growth and Cd uptake of *Sedum plumbizincicola* in a Cd-contaminated soil. *J. Soils Sediments* 15, 1191–1199. doi: 10.1007/s11368-015-1067-9

Mahapatra, S., Rayanoothala, P., Solanki, M. K., and Das, S. (2020). "Wheat microbiome: present status and future perspective," in *Phytobiomes: Current Insights and Future Vistas*, eds M. Solanki, P. Kashyap, and B. Kumari (Singapore: Springer). doi: 10.1007/978-981-15-3151-4_8

Mahmoudi, T. R. (2017). *Bacterially Mediated Water Stress Tolerance in Wheat Conferred by Phenazine-Producing Rhizobacteria*. Master's thesis. College Station, TX: Texas A&M University.

Mahmoudi, T. R., Yu, J. M., Liu, S., Pierson, L. S. III, and Pierson, E. A. (2019). Drought-stress tolerance in wheat seedlings conferred by phenazine-producing rhizobacteria. *Front. Microbiol.* 10:1590. doi: 10.3389/fmicb.2019.01590

Malalgoda, M., Ohm, J. B., Howatt, K. A., and Simsek, S. (2020). Pre-harvest glyphosate application and effects on wheat starch chemistry: analysis from application to harvest. *J. Food Biochem.* 44:e13330. doi: 10.1111/jfbc.13330

Márquez, L. M., Redman, R. S., Rodriguez, R. J., and Roossinck, M. J. (2007). A virus in a fungus in a plant-three way symbiosis required for thermal tolerance. *Science* 315, 513–515. doi: 10.1126/science.1136237

Mavrodi, D. V., Mavrodi, O. V., Elbourne, L. D., Tetu, S., Bonsall, R. F., Parejko, J., et al. (2018). Long-term irrigation affects the dynamics and activity of the wheat rhizosphere microbiome. *Front. Plant Sci.* 9:345. doi: 10.3389/fpls.2018.00345

Mavrodi, O. V., Mavrodi, D. V., Parejko, J. A., Thomashow, L. S., and Weller, D. M. (2012). Irrigation differentially impacts populations of indigenous antibiotic-producing *Pseudomonas* spp. in the rhizosphere of wheat. *Appl. Environ. Microbiol.* 78, 3214–3220. doi: 10.1128/AEM.07968-11

Mayak, S., Tirosh, T., and Glick, B. R. (2004). Plant growth-promoting bacteria confer resistance in tomato plants to salt stress. *Plant Physiol. Biochem.* 42, 565–572. doi: 10.1016/j.plaphy.2004.05.009

Mayer, Z., Sasvári, Z., Szentpéteri, V., Pethőné Rétháti, B., Vajna, B., and Posta, K. (2019). Effect of long-term cropping systems on the diversity of the soil bacterial communities. *Agronomy* 9:878.

Meena, K. K., Bitla, U. M., Sorty, A. M., Singh, D. P., Gupta, V. K., Wakchaure, G. C., et al. (2020). Mitigation of salinity stress in wheat seedlings due to the application of phytohormone-rich culture filtrate extract of methylotrophic actinobacterium Nocardioides sp. NIMMe6. *Front. Microbiol.* 11:2091. doi: 10.3389/fmicb.2020.02091

Meena, K. K., Sorty, A. M., Bitla, U. M., Choudhary, K., Gupta, P., Pareek, A., et al. (2017). Abiotic stress responses and microbe-mediated mitigation in plants: the omics strategies. *Front. Plant. Sci.* 8:172. doi: 10.3389/fpls.2017.00172

Mishra, J., Singh, R., and Arora, N. K. (2017). Alleviation of heavy metal stress in plants and remediation of soil by rhizosphere microorganisms. *Front. Microbiol.* 8:1706. doi: 10.3389/fmicb.2017.01706

Mishra, P. K., Bisht, S. C., Ruwari, P., Selvakumar, G., Joshi, G. K., Bisht, J. K., et al. (2011). Alleviation of cold stress in inoculated wheat (*Triticum aestivum L.*) seedlings with psychrotolerant Pseudomonads from NW Himalayas. *Arch. Microbiol.* 193, 497–513. doi: 10.1007/s00203-011-0693-x

Mishra, P. K., Mishra, S., Bisht, S. C., Selvakumar, G., Kundu, S., Bisht, J. K., et al. (2009). Isolation, molecular characterization and growth-promotion activities of a cold tolerant bacterium *Pseudomonas* sp. NARs9 (MTCC9002) from the Indian Himalayas. *Biol. Res.* 42, 305–313.

Mueller, U. G., and Sachs, J. L. (2015). Engineering microbiomes to improve plant and animal health. *Trends Microbiol.* 23, 606–617. doi: 10.1016/j.tim.2015.07.009

Mueller, U. G., Juenger, T. E., Kardish, M. R., Carlson, A. L., Burns, K., Smith, C. C., et al. (2016). Artificial microbiome-selection to engineer microbiomes that confer salt-tolerance to plants. *bioRxiv* [Preprint]. 081521. doi: 10.1128/mSystems.01125-21

Nasraoui, B., Hajlaoui, M. R., Aïssa, A. D., and Kremer, R. J. (2007). Biological control of wheat take-all disease: I-characterization of antagonistic bacteria from diverse soils toward *Gaeumannomyces graminis* var. tritici. *Tunis J. Plant Prot.* 2, 23–34.

Naveed, M., Hussain, M. B., Zahir, Z. A., Mitter, B., and Sessitsch, A. (2014). Drought stress amelioration in wheat through inoculation with *Burkholderia phytofirmans* strain PsJN. *Plant Growth Regul.* 73, 121–131. doi: 10.1007/s10725-013-9874-8

Nelson, E. B. (2004). Microbial dynamics and interactions in the spermosphere. *Annu. Rev. Phytopathol.* 42, 271–309. doi: 10.1146/annurev.phyto.42.121603.131041

O'Brien, P. A. (2017). Biological control of plant diseases. *Australas. Plant Pathol.* 46, 293–304. doi: 10.1186/s12863-020-00851-5

Panke-Buisse, K., Lee, S., and Kao-Kniffin, J. (2017). Cultivated sub-populations of soil microbiomes retain early flowering plant trait. *Microb. Ecol.* 73, 394–403. doi: 10.1007/s00248-016-0846-1

Panke-Buisse, K., Poole, A. C., Goodrich, J. K., Ley, R. E., and Kao-Kniffin, J. (2014). Selection on soil microbiomes reveals reproducible impacts on plant function. *ISME J.* 9:980. doi: 10.1038/ismej.2014.196

Qadir, M., Ghafoor, A., and Murtaza, G. (2000). Amelioration strategies for saline soils: a review. *Land Degrad. Dev.* 11, 501–521. doi: 10.1002/1099-145x(200011/12)11:6<501::aid-ldr405>3.0.co;2-s

Qi, Y., Ossowicki, A., Yang, X., Lwanga, E. H., Dini-Andreote, F., Geissen, V., et al. (2020). Effects of plastic mulch film residues on wheat rhizosphere and soil properties. *J. Hazard. Mater.* 387:121711. doi: 10.1016/j.jhazmat.2019.121711

Raheem, A., Shaposhnikov, A., Belimov, A. A., Dodd, I. C., and Ali, B. (2018). Auxin production by rhizobacteria was associated with improved yield of wheat (*Triticum aestivum* L.) under drought stress. *Arch. Agron. Soil Sci.* 64, 574–587.

Rajendran, K., Tester, M., and Roy, S. J. (2009). Quantifying the three main components of salinity tolerance in cereals. *Plant Cell Environ.* 32, 237–249. doi: 10.1111/j.1365-3040.2008.01916.x

Ramadoss, D., Lakkineni, V. K., Bose, P., Ali, S., and Annapurna, K. (2013). Mitigation of salt stress in wheat seedlings by halotolerant bacteria isolated from saline habitats. *Springerplus* 2:6. doi: 10.1186/2193-1801-2-6

Redman, R. S., Sheehan, K. B., Stout, R. G., Rodriguez, R. J., and Henson, J. M. (2002). Thermotolerance generated by plant/fungal symbiosis. *Science* 298:1581. doi: 10.1126/science.1072191

Riadh, K., Wided, M., Hans-Werner, K., and Chedly, A. (2010). Responses of halophytes to environmental stresses with special emphasis to salinity. *Adv. Bot. Res.* 53, 117–145. doi: 10.1016/S0065-2296(10)53004-0

Rizvi, A., Ahmed, B., Zaidi, A., and Khan, M. S. (2019). Heavy metal mediated phytotoxic impact on winter wheat: oxidative stress and microbial management of toxicity by Bacillus subtilis BM2. *RSC Adv.* 9, 6125–6142. doi: 10.1039/c9ra00333a

Robinson, R. J., Fraaije, B. A., Clark, I. M., Jackson, R. W., Hirsch, P. R., and Mauchline, T. H. (2016b). Wheat seed embryo excision enables the creation of axenic seedlings and Koch's postulates testing of putative bacterial endophytes. *Sci. Rep.* 6:25581. doi: 10.1038/srep25581

Robinson, R. J., Fraaije, B. A., Clark, I. M., Jackson, R. W., Hirsch, P. R., and Mauchline, T. H. (2016a). Endophytic bacterial community composition in wheat (*Triticum aestivum*) is determined by plant tissue type, developmental stage and soil nutrient availability. *Plant Soil* 405, 381–396. doi: 10.1007/s11104-015-2495-4

Sapkota, R., Jørgensen, L. N., and Nicolaisen, M. (2017). Spatiotemporal variation and networks in the mycobiome of the wheat canopy. *Front. Plant Sci.* 8:1357. doi: 10.3389/fpls.2017.01357

Schlatter, D. C., Hansen, J. C., Schillinger, W. F., Sullivan, T. S., and Paulitz, T. C. (2019). Common and unique rhizosphere microbial communities of wheat and canola in a semiarid Mediterranean environment. *Appl. Soil Ecol.* 144, 170–181. doi: 10.1016/j.apsoil.2019.07.010

Schlatter, D. C., Kahl, K., Carlson, B., Huggins, D. R., and Paulitz, T. (2020). Soil acidification modifies soil depth-microbiome relationships in a no-till wheat cropping system. *Soil Biol. Biochem.* 149:107939.

Schoonbeek, H. J., Raaijmakers, J. M., and De Waard, M. A. (2002). Fungal ABC transporters and microbial interactions in natural environments. *Mol. Plant Microbe Interact.* 15, 1165–1172. doi: 10.1094/MPMI.2002.15.11.1165

Schouten, A., Berg, G. V. D., Steinberg, C., Gautheron, N., Alabouvette, C., Vos, C. H., et al. (2004). Defense responses of *Fusarium oxysporum* to 2,4-diacetylphloroglucinol, a broad-spectrum antibiotic produced by *Pseudomonas fluorescens*. *Mol. Plant Microbe Interact.* 17, 1201–1211. doi: 10.1094/MPMI.2004.17.11.1201

Seybold, H., Demetrowitsch, T. J., Hassani, M. A., Szymczak, S., Reim, E., Haueisen, J., et al. (2020). A fungal pathogen induces systemic susceptibilityand systemic shifts in wheat metabolome and microbiome composition. *Nat. Commun.* 11:1910. doi: 10.1038/s41467-020-15633-x

Sherameti, I., Tripathi, S., Varma, A., and Oelmuller, R. (2008). The root-colonizing endophyte Piriformospora indica confers drought tolerance in *Arabidopsis* by stimulating the expression of drought stress-related genes in leaves. *Mol. Plant Microbe Interact.* 21, 799–807. doi: 10.1094/MPMI-21-6-0799

Shi, H., Ishitani, M., Kim, C., and Zhu, J. K. (2000). The *Arabidopsis thaliana* salt tolerance gene SOS1 encodes a putative Na+/H+ antiporter. *Proc. Natl. Acad. Sci. U.S.A.* 97, 6896–6901. doi: 10.1073/pnas.120170197

Singh, M., and Tiwari, N. (2021). Microbial amelioration of salinity Stress in HD 2967 wheat cultivar by Up-regulating antioxidant defense. *Commun. Integr. Biol.* 14, 136–150. doi: 10.1080/19420889.2021.1937839

Sun, C., Johnson, J. M., Cai, D., Sherameti, I., Oelmuller, R., and Lou, B. (2010). *Piriformospora indica* confers drought tolerance in Chinese cabbage leaves by stimulating antioxidant enzymes, the expression of drought-related genes and the plastid-localized CAS protein. *J. Plant Physiol.* 167, 1009–1017. doi: 10.1016/j.jplph.2010.02.013

Sun, X., Kosman, E., and Sharon, A. (2020). Stem endophytic mycobiota in wild and domesticated wheat: structural differences and hidden resources for wheat improvement. *J. Fungi* 6:180.

Swenson, W., Wilson, D. S., and Elias, R. (2000). Artificial ecosystem selection. *Proc. Natl. Acad. Sci. U.S.A.* 97, 9110–9114.

Teixeira, P. J. P., Colaianni, N. R., Fitzpatrick, C. R., and Dangl, J. L. (2019). Beyond pathogens: microbiota interactions with the plant immune system. *Curr. Opin. Microbiol.* 49, 7–17. doi: 10.1016/j.mib.2019.08.003

Timmusk, S., Abd El-Daim, I. A., Copolovici, L., Tanilas, T., Känneste, A., Behers, L., et al. (2014). Drought-tolerance of wheat improved by rhizosphere bacteria from harsh environments: enhanced biomass production and reduced emissions of stress volatiles. *PLoS One* 9:e96086. doi: 10.1371/journal.pone.0096086

Tiwari, S., Singh, P., Tiwari, R., Meena, K. K., Yandigeri, M., Singh, D. P., et al. (2011). Salt-tolerant rhizobacteria-mediated induced tolerance in wheat (*Triticum aestivum*) and chemical diversity in rhizosphere enhance plant growth. *Biol. Fertil. Soils* 47, 907–916. doi: 10.1007/s00374-011-0598-5

Tkacz, A., Pini, F., Turner, T. R., Bestion, E., Simmonds, J., Howell, P., et al. (2020). Agricultural selection of wheat has been shaped by plant-microbe interactions. *Front. Microbiol.* 11:132. doi: 10.3389/fmicb.2020.00132

Uksa, M., Buegger, F., Gschwendtner, S., Lueders, T., Kublik, S., Kautz, T., et al. (2017). Bacteria utilizing plant-derived carbon in the rhizosphere of *Triticum aestivum* change in different depths of an arable soil. *Environ. Microbiol. Rep.* 9, 729–741. doi: 10.1111/1758-2229.12588

Valente, J., Gerin, F., Le Gouis, J., Moënne-Loccoz, Y., and Prigent-Combaret, C. (2020). Ancient wheat varieties have a higher ability to interact with plant growth-promoting rhizobacteria. *Plant Cell Environ.* 43, 246–260. doi: 10.1111/pce.13652

van Rij, E. T., Girard, G., Lugtenberg, B. J. J., and Bloemberg, G. V. (2005). Influence of fusaric acid on phenazine-1-carboxamide synthesis and gene expression of *Pseudomonas chlororaphis* strain PCL1391. *Microbiology* 151, 2805–2814. doi: 10.1099/mic.0.28063-0

Vujanovic, V., and Vujanovic, J. (2007). Mycovitality and mycoheterotrophy: where lies dormancy in terrestrial orchid and plants with minute seeds? *Symbiosis* 44, 93–99.

Wachowska, U., Kucharska, K., Jędryczka, M., and Łobik, N. (2013). Microorganisms as biological control agents against *Fusarium* pathogens in winter wheat. *Pol. J. Environ. Stud.* 22, 591–597.

Wahid, A., Gelani, S., Ashraf, M., and Foolad, M. R. (2007). Heat tolerance in plants: an overview. *Environ. Exp. Bot.* 61, 199–223. doi: 10.1016/j.envexpbot.2007.05.011

Wang, X., Ji, C., Song, X., Liu, Z., Liu, Y., Li, H., et al. (2021). Biocontrol of two bacterial inoculant strains and their effects on the rhizosphere microbial community of field-grown wheat. *BioMed Res. Int.* 2021:8835275. doi: 10.1155/2021/8835275

Wen, X. Y., Dubinsky, E., Yao, W. U., Rong, Y., and Fu, C. (2016). Wheat, maize and sunflower cropping systems selectively influence bacteria community structure and diversity in their and succeeding crop's rhizosphere. *J. Integr. Agric.* 15, 1892–1902. doi: 10.1016/s2095-3119(15)61147-9

Wu, C. H., Bernard, S. M., Andersen, G. L., and Chen, W. (2009). Developing microbe–plant interactions for applications in plant-growth promotion and disease control, production of useful compounds, remediation and carbon sequestration. *Microb. Biotechnol.* 2, 428–440.

Xiong, C., Zhu, Y. G., Wang, J. T., Singh, B., Han, L. L., Shen, J. P., et al. (2021). Host selection shapes crop microbiome assembly and network complexity. *New Phytol.* 229, 1091–1104. doi: 10.1111/nph.16890

Xu, T., Jiang, W., Qin, D., Liu, T., Zhang, J., Chen, W., et al. (2021). Characterization of the microbial communities in wheat tissues and rhizosphere soil caused by dwarf bunt of wheat. *Sci. Rep.* 11:5773. doi: 10.1038/s41598-021-85281-8

Yin, C., Hulbert, S. H., Schroeder, K. L., Mavrodi, O., Mavrodi, D., Dhingra, A., et al. (2013). Role of bacterial communities in the natural suppression of *Rhizoctonia solani* bare patch disease of wheat (*Triticum aestivum* L.). *Appl. Environ. Microbiol.* 79, 7428–7438. doi: 10.1128/AEM.01610-13

Yin, C., Jones, K. L., Peterson, D. E., Garrett, K. A., Hulbert, S. H., and Paulitz, T. C. (2010). Members of soil bacterial communities sensitive to tillage and crop rotation. *Soil Biol. Biochem.* 42, 2111–2118. doi: 10.1016/j.soilbio.2010.08.006

Conflict of Interest: The authors declare that the research was conducted in the absence of any commercial or financial relationships that could be construed as a potential conflict of interest.

Publisher's Note: All claims expressed in this article are solely those of the authors and do not necessarily represent those of their affiliated organizations, or those of the publisher, the editors and the reviewers. Any product that may be evaluated in this article, or claim that may be made by its manufacturer, is not guaranteed or endorsed by the publisher.

frontiers in Microbiology

ORIGINAL RESEARCH
published: 26 January 2022
doi: 10.3389/fmicb.2021.760512

Field Site-Specific Effects of an *Azospirillum* Seed Inoculant on Key Microbial Functional Groups in the Rhizosphere

*Sébastien Renoud[1†], Jordan Vacheron[1†], Danis Abrouk[1], Claire Prigent-Combaret[1], Laurent Legendre[1,2], Daniel Muller[1] and Yvan Moënne-Loccoz[1]**

[1] Univ Lyon, Université Claude Bernard Lyon 1, CNRS, INRAe, VetAgro Sup, UMR 5557 Ecologie Microbienne, Villeurbanne, France, [2] Univ Lyon, Université de St Etienne, St Etienne, France

OPEN ACCESS

Edited by:
Xun Wen Chen,
Southern University of Science and Technology, China

Reviewed by:
Anelise Beneduzi,
Livestock and Irrigation, Brazil
José David Flores Félix,
Universidade da Beira Interior, Portugal
Entao Wang,
Instituto Politécnico Nacional (IPN), Mexico
Riyazali Zafarali Sayyed,
P.S.G.V.P.M's Arts, Science and Commerce College, India

***Correspondence:**
Yvan Moënne-Loccoz
yvan.moenne-loccoz@univ-lyon1.fr

†Present address:
Sébastien Renoud,
BGene, Grenoble, France
Jordan Vacheron,
Université de Lausanne, Department of Fundamental Microbiology, Lausanne, Switzerland

Specialty section:
This article was submitted to Terrestrial Microbiology, a section of the journal Frontiers in Microbiology

Received: 18 August 2021
Accepted: 03 December 2021
Published: 26 January 2022

Citation:
Renoud S, Vacheron J, Abrouk D, Prigent-Combaret C, Legendre L, Muller D and Moënne-Loccoz Y (2022) Field Site-Specific Effects of an Azospirillum Seed Inoculant on Key Microbial Functional Groups in the Rhizosphere. Front. Microbiol. 12:760512. doi: 10.3389/fmicb.2021.760512

The beneficial effects of plant growth–promoting Rhizobacteria (PGPR) entail several interaction mechanisms with the plant or with other root-associated microorganisms. These microbial functions are carried out by multiple taxa within functional groups and contribute to rhizosphere functioning. It is likely that the inoculation of additional PGPR cells will modify the ecology of these functional groups. We also hypothesized that the inoculation effects on functional groups are site specific, similarly as the PGPR phytostimulation effects themselves. To test this, we assessed in the rhizosphere of field-grown maize the effect of seed inoculation with the phytostimulatory PGPR *Azospirillum lipoferum* CRT1 on the size and/or diversity of selected microbial functional groups important for plant growth, using quantitative polymerase chain reaction and/or Illumina MiSeq metabarcoding. The functional groups included bacteria able to fix nitrogen (a key nutrient for plant growth), producers of 1-aminocyclopropane-1-carboxylate (ACC) deaminase (which modulate ethylene metabolism in plant and stimulate root growth), and producers of 2,4-diacetylphloroglucinol (an auxinic signal enhancing root branching). To test the hypothesis that such ecological effects were site-specific, the functional groups were monitored at three different field sites, with four sampling times over two consecutive years. Despite poor inoculant survival, inoculation enhanced maize growth. It also increased the size of functional groups in the three field sites, at the maize six-leaf and flowering stages for diazotrophs and only at flowering stage for ACC deaminase and 2,4-diacetylphloroglucinol producers. Sequencing done in the second year revealed that inoculation modified the composition of diazotrophs (and of the total bacterial community) and to a lesser extent of ACC deaminase producers. This study revealed an ecological impact that was field specific (even though a few taxa were impacted in all fields) and of unexpected magnitude with the phytostimulatory *Azospirillum* inoculant, when considering microbial functional groups. Further methodological developments are needed to monitor additional functional groups important for soil functioning and plant growth under optimal or stress conditions.

Keywords: microbial functional group, PGPR, inoculation, nitrogen fixers, ACC deaminase producers, 4-diacetylphloroglucinol producers

INTRODUCTION

Plant growth–promoting Rhizobacteria (PGPR) benefit plants mainly by (i) stimulating root system development, thereby allowing seedlings to explore larger soil volumes to gain access to water and mineral nutrients (Vacheron et al., 2013); (ii) enhancing nutrient availability, e.g., via N_2 reduction or P solubilization (Dobbelaere et al., 2003; Basu et al., 2021); (iii) improving root system functioning in terms of ion uptake, by stimulating nutrient transporter expressions and/or activities in roots (Bertrand et al., 2000; Vacheron et al., 2013; Pii et al., 2015); and/or (iv) controlling root parasites via competition or antagonism, which leads to parasite inhibition (Raaijmakers et al., 2009; Basu et al., 2021). Effective PGPR strains have increased crop yields in many (but not all) field trials (Okon and Labandera-Gonzalez, 1994; El Zemrany et al., 2006; García de Salamone et al., 2010). Their use as crop inoculants is promising to reduce chemical inputs and improve farming sustainability, despite plant growth-promotion effects that can fluctuate according to the field, the year, or other farming/environmental parameters (Okon and Labandera-Gonzalez, 1994; Dobbelaere et al., 2003; Castro-Sowinski et al., 2007; Raaijmakers et al., 2009; Rozier et al., 2017; Basu et al., 2021).

Azospirillum is an emblematic PGPR genus and is widely used in certain countries to stimulate maize, wheat, and rice (Castro-Sowinski et al., 2007; Rozier et al., 2017; Schmidt and Gaudin, 2018). The main mode of action is the secretion of phytohormones especially indole acetic acid, involved in stimulation of root branching and growth (Steenhoudt and Vanderleyden, 2000). In certain *Azospirillum* strains, plant hormonal effects may also take place via synthesis of root-branching signal nitric oxide (Creus et al., 2005; Molina-Favero et al., 2008) or deamination of 1-aminocyclopropane-1-carboxylate (ACC), the ethylene precursor in plants (Vacheron et al., 2013; Glick, 2014). Associative nitrogen fixation also occurs in *Azospirillum*, although its contribution is considered minor (Steenhoudt and Vanderleyden, 2000).

The interaction between *Azospirillum* and plant leads to major changes in the physiology of both partners. On the bacterial side, more than 400 genes of *Azospirillum lipoferum* 4B were differentially expressed when the bacterium was in contact with the host plant rather than in the absence of the host (Drogue et al., 2014a). They were involved especially in detoxification of reactive oxygen species and multidrug efflux, which could be important for root colonization. On the plant side, *Azospirillum* resulted in modified expression of thousands of genes, including many involved in plant defense or ethylene/auxin pathways (Drogue et al., 2014b). Therefore, an *Azospirillum* inoculant is likely to change the nature or amount of compounds released by roots (i.e., rhizodeposition patterns), and indeed inoculation resulted in physiological changes in terms of rice content in secondary metabolites (Chamam et al., 2013); metabolite profiles of roots, shoots (Brusamarello-Santos et al., 2017), and xylem sap (Rozier et al., 2016) in maize; protein accumulation in maize seedlings (Cangahuala-Inocente et al., 2013); and production of flavonoids by roots of rice (Chamam et al., 2013) and alfalfa (Volpin et al., 1996). These chemical changes may lead to modified ecological conditions for microorganisms residing in the rhizosphere. Therefore, *Azospirillum* inoculation can be expected to trigger a range of indirect effects on other root-colonizing microorganisms, in addition to direct competition effects with resident rhizosphere populations. However, maize inoculation with *A. lipoferum* CRT1 caused only modest (but statistically significant) changes at the scale of the whole rhizobacterial community (Baudoin et al., 2009), as typically found also for other *Azospirillum* inoculants (Herschkovitz et al., 2005; Lerner et al., 2006; Felici et al., 2008; Naiman et al., 2009; Baudoin et al., 2010; García de Salamone et al., 2012; Bao et al., 2013; da Costa et al., 2018; Di Salvo et al., 2018). This may seem surprising considering the pronounced effects of *Azospirillum* on plant physiology, but perhaps methodological limitations account for these observations. Both direct and indirect microbial interactions between PGPR inoculants and the indigenous microbiota may, in turn, have an impact on rhizosphere functioning (Trabelsi and Mhamdi, 2013; Florio et al., 2017; Di Salvo et al., 2018; Dal Cortivo et al., 2020; Kusstatscher et al., 2020), but this possibility remains poorly documented as microbial functional groups have been neglected. In light of the low reproducibility of plant-beneficial effects of PGPR inoculants in field situations, there is a need to develop our knowledge on the ecological consequences of such inoculations. It is also important because indirect PGPR effects, that is, effects taking place via interactions with indigenous microorganisms, are increasingly considered important for phytostimulation (Trabelsi and Mhamdi, 2013; Vacheron et al., 2013; Ambrosini et al., 2016; Di Salvo et al., 2018; Kusstatscher et al., 2020). In other words, it might be that the low reproducibility of phytostimulation performance in fields could result, in part, from a low reproducibility of the interactions between microbial inoculants and resident microorganisms. To explore this possibility, a prerequisite is to understand the variability of PGPR effects on the indigenous microbiota, as the latter displays spatiotemporal heterogeneity in field conditions (Baudoin et al., 2009; Raaijmakers et al., 2009; García de Salamone et al., 2010; Schmidt and Gaudin, 2018; Kusstatscher et al., 2020; Renoud et al., 2020).

Microbial functioning of the rhizosphere involves a broad range of particular ecological functions carried out by functional groups, for example, nitrogen fixers, phytohormone producers, and so on. Often, each functional group comprised multiple taxa, which may contribute differently to the corresponding ecological function. In addition, the effects of environmental conditions (climate, soil type, plant genotype and phenology, etc.) are likely to differ from one functional group to the other (Fuhrman, 2009; Reed et al., 2011; Schimel and Schaeffer, 2012; Renoud et al., 2020). Therefore, it is not feasible to infer the impact of PGPR inoculation on rhizosphere-relevant microbial functional groups based solely on our knowledge of inoculant impact on the taxonomic composition of the rhizomicrobial community (Trabelsi and Mhamdi, 2013; Ambrosini et al., 2016). Here, we tested the hypotheses that (i) PGPR inoculation can lead to major changes in root-associated functional microbial communities important for plant development/growth, and (ii) these PGPR effects on functional communities may differ in a field site-specific manner.

To address this issue, we assessed the effect of maize seed inoculation with *A. lipoferum* CRT1 on the size (i.e., the number of microbial cells) and/or diversity (i.e., richness, genetic structure, and composition) of three microbial functional groups, that is, nitrogen fixers (using *nifH* marker), ACC deaminase producers (*acdS* marker), and producers of 2,4-diacetylphloroglucinol, a root-branching signal (Brazelton et al., 2008) that may also act as an antimicrobial compound if present at high concentration (Keel et al., 1990) (*phlD* marker). These functional groups were selected based on (i) their importance for phytostimulation (Dobbelaere et al., 2003; Brazelton et al., 2008; Vacheron et al., 2013; Schmidt and Gaudin, 2018); for example, N is a key nutrient for plant, and therefore, N fixation is a key aspect of rhizosphere functioning; (ii) the availability of knowledge on their mode of action and corresponding regulatory processes (Keel et al., 1990; Steenhoudt and Vanderleyden, 2000; Dobbelaere et al., 2003; Brazelton et al., 2008; Vacheron et al., 2013; Glick, 2014; Rozier et al., 2017); (iii) the possibility to monitor them by focusing on a single gene marker shared by all members of the functional group, that is, *nifH*, *acdS*, and *phlD*, respectively (Vacheron et al., 2013; Renoud et al., 2020); (iv) the possibility to infer taxonomic affiliations of individual functional group members from marker gene sequences (for nitrogen fixers and ACC deaminase producers) (Renoud et al., 2020); and (v) the availability of validated polymerase chain reaction (PCR) methodology to enable monitoring in soil systems (Poly et al., 2001; Bouffaud et al., 2016, 2018; Renoud et al., 2020). For instance, auxin synthesis and phosphate solubilization were not considered despite their ecological significance, as they rely on several different pathways, some of them probably not yet documented, which restricts the possibilities of monitoring. It is important to note that the inoculant used here (i.e., *A. lipoferum* CRT1) belongs to nitrogen fixers but not to ACC deaminase producers or 2,4-diacetylphloroglucinol producers.

To this end, the PGPR *A. lipoferum* CRT1 was used as maize seed inoculant in two consecutive years, at three field sites located in the region of Lyon, France, and corresponding to a luvisol (termed L; near Chatonnay), a fluvic cambisol (FC; near Sérézin-de-la-Tour), and a calcisol (C; near Saint Savin), and its impact was investigated by quantitative PCR (qPCR) and/or Illumina MiSeq-based metabarcoding. In addition, maize was grown under optimized or suboptimal conditions of mineral N fertilization to assess the significance of N limitation (nutriment stress) as a factor possibly modulating inoculation effects, based on measurements of the size of the three microbial functional groups. Monitoring was carried out at the six-leaf stage of growth (i.e., six leaves are produced, and maize now relies on its permanent root system rather than the seminal roots) and at flowering time, two key stages to assess maize functioning and performance (Gabriel et al., 2017; Sarabia et al., 2018).

MATERIALS AND METHODS

Field Trials

The field experiments were run in 2014 and 2015 in Chatonnay (L), Sérézin-de-la-Tour (FC), and Saint Savin (C), located near Bourgoin-Jallieu (France). The soils are a luvisol (L), a fluvic cambisol (FC), and a calcisol (C) based on FAO soil classification, and chemical features are given in **Supplementary Table 1**.

These field experiments have been described (Rozier et al., 2017). At each location, the crop rotation includes 1 year of wheat (grown prior to the 2014 trial), 6 years of maize (starting with the 2014 and 2015 trials), and 1 year of rapeseed. Seeds of maize (*Zea mays* cv. Seiddi; provided by the Dauphinoise coop company, France) were sown on April 18 (at FC) and 23 (at C and L) in 2014 and on April 30 (C) and May 11 (FC and L) in 2015. The fields were not irrigated.

Three levels of mineral nitrogen fertilization were considered, that is, X (optimized N fertilization in one application carried out at the six-leaf stage), XS (the same N fertilization level but split into two applications), and 0 (no fertilizer). In 2014, the effect of inoculation with *A. lipoferum* CRT1 was studied at each of the three levels of mineral nitrogen fertilization (X, XS, and 0) for site FC and two levels (X and 0) for sites L and C, using a factorial design with, respectively, six or four combinations of factors (i.e., inoculation or no inoculation × three or two mineral N levels). The optimal dose X for maize (based on local agronomic assessments) was 120 kg mineral N/ha for sites FC and C and 180 kg mineral N/ha for site L. On site FC, the XS nitrogen treatment corresponded to the X fertilizer dose applied half at sowing and half on May 21 (at the six-leaf stage). Individual replicate plots were 12 (FC and C) or 8 (L) maize rows wide and 12 m long. They were organized along a randomized block design with five blocks. Mineral nitrogen fertilizer was applied on May 21 (FC and C) and 22 (L) for fertilized plots.

In 2015, CRT1 inoculation was studied at two N levels (X and 0). Inoculation (or not) and mineral N level were applied to the same plots that had received these applications the year before. In 2015, mineral nitrogen fertilizer was applied on June 5 at C and June 9 at FC and L (at the six-leaf stage).

Inoculum Preparation and Inoculant Monitoring

A. lipoferum CRT1 was isolated in France from the rhizosphere of field-grown maize (Fages and Mulard, 1988) and promoted maize growth when used as inoculant (Fages and Mulard, 1988; Jacoud et al., 1999; Walker et al., 2011; Rozier et al., 2017, 2019). For inoculation, maize seeds were mixed with CRT1 cells included in a sterile peat-based formulation supplied by Agrauxine (Lesaffre Plant care; Angers, France), and the exact same peat-based seed formulation (but without any CRT1 cell added) was used in the non-inoculated control.

Inoculant survival in the rhizosphere was assessed by qPCR, using CRT1-specific primers Q1/Q2 (Couillerot et al., 2010). For quantification on seeds at sowing, inoculum level was also estimated by colony counts on nitrogen-free agar containing 0.2 g/L ammonium chloride and Congo red (Cáceres, 1982). At sowing, the inoculant was recovered in 2014 at 2.0×10^2 colony-forming units (CFUs) (and equivalent to 6.0×10^3 cells by qPCR) per seed, and in 2015 at 3.7×10^2 CFUs (and equivalent to 3.0×10^4 cells) per seed at sites L and FC, and 8.8×10^2 CFUs (and equivalent to 1.5×10^5 cells) per seed at site C.

Sampling of Plants and DNA Extractions

In both years, maize was sampled at six-leaf and flowering stages, as described (Renoud et al., 2020). In 2014, all plots were studied. The six-leaf stage was sampled on May 25 (FC) and 26 (C and L), shortly after fertilizer application. On each plot, six plants were randomly chosen; their entire root system was dug up and shaken vigorously to dislodge loosely adhering soil. At sites FC and C, one pooled sample (i.e., six-root system) was obtained per plot, which made five pooled samples per treatment. At site L, each root system was treated individually to consider variations from one plant to the other, which made 6 root system × 5 plots = 30 samples per treatment. The sampling at flowering stage was done on July 8 (FC and C) and 9 (L), and six plants were sampled per plot and treated individually, which made 30 samples per treatment.

The moderate levels of plant-to-plant variation in 2014 prompted us to reduce samplings to four root systems per plot in 2015. In 2015, six-leaf maize was sampled on May 27 (C), June 5 (FC), and June 8 (L), and only non-fertilized plots were studied because fertilizers had not been applied yet. The flowering stage sampling was done on July 15 (C), 16 (FC), and 17 (L), and all plots were studied. At each sampling, the four root systems sampled per plot were treated individually, which made 20 samples per treatment.

Each root system sample was flash-frozen on the field, using liquid nitrogen, and lyophilized at the laboratory (24 h at −50°C), as described (Renoud et al., 2020). Briefly, roots and their adhering soil (i.e., rhizosphere; approximately 1 mm from root surface) were separated using brushes, and root-adhering soil was stored at −80°C. DNA was extracted from the latter using the FastDNA SPIN kit (BIO 101 Inc., Carlsbad, CA, United States). A total of 500-mg (for the 2014 pooled samples from FC and C) or 300-mg samples (for the other samples) were transferred in Lysing Matrix E tubes, as well as 5 μL of the internal standard APA9 (at 10^9 copies/mL, with primers AV1f/AV1r) in order to normalize the efficiency of DNA extraction between rhizosphere samples (Park and Crowley, 2005; Couillerot et al., 2010). After 1-h incubation at 4°C, DNA was extracted and eluted in 50 mL of sterile ultrapure water, according to the manufacturer's instructions, and DNA concentration assessed using Picogreen (Thermo Fisher Scientific).

Quantitative Polymerase Chain Reaction Analysis of Microbial Functional Groups

The number of genes *nifH*, *acdS*, and *phlD* in the rhizosphere was assessed by qPCR using, respectively, primers polF/polR (Poly et al., 2001; Gaby and Buckley, 2017), acdSF5/acdSR8 (Bouffaud et al., 2018), and B2BF/B2BR3 (Almario et al., 2013). The *nifH* primers polF/polR have been advocated for combined qPCR and diversity analyses (Bouffaud et al., 2016; Gaby and Buckley, 2017), whereas the *acdS* primers acdSF5/acdSR8 have been validated for analysis of true *acdS* genes (i.e., without amplifying related D-cystein desulfhydrase genes coding for other types of PLP-dependent enzymes; Bouffaud et al., 2018). Methods are described in **Supplementary File 1** (see also Renoud et al., 2020 for some of the genes).

Sequencing Analysis of *nifH*, *acdS*, and All Rhizobacteria

Sequencing was carried out using maize at the six-leaf stage (i.e., prior to N fertilizer applications) in 2015, as described (Renoud et al., 2020). Briefly, equimolar composite samples of four rhizosphere DNA extracts (from four plants) were used per plot, that is, 5 plots × 3 fields = 15 samples per treatment. Illumina MiSeq sequencing (paired-end reads; 2 × 300 bp for *nifH* and *rrs*, 2 × 125 bp for *acdS*) was performed by MR DNA laboratory (Shallowater, TX, United States).[1]

nifH, *acdS*, and *rrs* sequencings were done using, respectively, primers polF/polR, acdSF5/acdSR8, and 515/806 targeting the V4 variable region (Yang et al., 2016; Renoud et al., 2020). All forward primers carried a barcode. The 30-cycle PCR (five cycles implemented on PCR products) was performed using the HotStarTaq Plus Master Mix Kit (Qiagen, Valencia, CA, United States) with the following conditions: 94°C for 3 min, followed by 28 cycles of 94°C for 30 s, 53°C for 40 s, and 72°C for 1 min, and a final elongation step at 72°C for 5 min. PCR products were checked in 2% (wt/vol) agarose gel to verify amplification success and relative band intensity. For each gene, the amplicons of the 15 samples were multiplexed (in equal proportions based on their molecular weight and DNA concentrations) and subsequently purified using calibrated Ampure XP beads prior to preparing a DNA library following Illumina TruSeq DNA library preparation protocol. Reads have been deposited in the European Bioinformatics Institute (EBI) database under accession numbers PRJEB14346 (*nifH*), PRJEB14343 (*acdS*), PRJEB14347 (*rrs*).

Sequence data were processed using the analysis pipeline of MR DNA (Renoud et al., 2020). Briefly, sequences were depleted of barcodes, the sequences < 150 bp or with ambiguous base calls were removed, the remaining sequences denoised, operational taxonomic units (OTUs; arbitrarily defined at 3% divergence threshold for the three genes) generated, and chimeras removed. Final OTUs from the *nifH* and *rrs* sequencing were taxonomically classified using BLASTn against a curated database derived from Greengenes (DeSantis et al., 2006), RDPII,[2] and NCBI.[3] Final OTUs of the *acdS* sequencing were classified using an in-house curated *acdS* database (Bouffaud et al., 2018). Datasets without singletons (here, singleton sequences are those found a single time among the 30 sequenced samples from inoculated or control treatments) were used to generate rarefaction curves and diversity indices of Shannon (H) and Simpson (calculated using sequencing subsample data for which each sample had the same number of sequences). Some of the sequences were used previously to describe microbial diversity of non-inoculated maize (Renoud et al., 2020).

Statistical Analyses

Quantitative PCR data were compared by two-factor analysis of variance (i.e., inoculation × fertilizer treatment) and Fisher least significant difference tests, using log-transformed data.

[1] www.mrdnalab.com

[2] http://rdp.cme.msu.edu

[3] www.ncbi.nlm.nih.gov

Comparisons of bacterial diversity were carried out by between-class analysis (BCA) (Dolédec and Chessel, 1987) with the ADE4 (Chessel et al., 2004; Dray et al., 2007) and ggplot2 packages for R. BCA is a robust alternative to linear discriminant analysis (Huberty, 1994) when the number of samples is small compared with the number of predictors. When the number of samples is low, and particularly when it is lower than the number of predictors, discriminant analysis cannot be used. In this case, BCA can be very useful and provides illustrative graphical displays of between-group differences (Thioulouse et al., 2012). The significance of BCA results was assessed using a Monte Carlo test with 10,000 permutations (null hypothesis: absence of difference between groups). Non-metric multidimensional scaling (NMDS) was also performed, using the Bray–Curtis distance and the vegan package for R.

Two analyses were carried out to assess the impact of inoculation on particular genera. First, the genera contributing most to treatment differentiation (independently of their abundance) were identified by BCA; the position in the heatmap indicates the statistical importance of these taxa in positioning samples on the BCA axis with and without inoculation, these taxa being classified according to their importance in contributing to the construction of the BCA axis. As a complementary approach, the genus composition of the bacterial community and functional groups were characterized to consider the relative abundance of the most prevalent taxa. Unless otherwise stated, statistical analyses were performed using R version 3.3.2 at $p < 0.05$.[4]

RESULTS

Effects of Inoculation on Maize Under Field Conditions

The three field trials have been described before (Rozier et al., 2017). The seed inoculant *A. lipoferum* CRT1 was under the detection threshold (of 4.0×10^3 cell equivalents per gram of rhizosphere soil) at the stages sampled in the current work, that is, when maize had produced six leaves and at flowering time, in all three field sites studied and in both years. Previous results from these three fields indicated that seed inoculation had resulted in significant changes in (i) maize morphological properties at the six-leaf stage (which, in 2015, took place mainly at site L; **Table 1**), (ii) plant photosynthetic efficiency except at site L in 2015, (iii) metabolome (studied only in 2015) of maize roots at sites L and C as well as shoots at sites L and FC (i.e., contents of 13 metabolites in roots and 28 metabolites in leaves were significantly affected, with glutamine content modified both in roots and shoot at site FC), and/or (iv) yield at site L (only in 2015, with a significant positive effect), site FC (with a positive effect in 2014 and a negative effect in 2015), and site C (with a significant negative effect in 2014 and a trend for a 16% yield increase in 2015 but that was not statistically significant at $p < 0.05$) (Rozier et al., 2017). Therefore, inoculation effects were statistically significant but fluctuated according to field and year, which provided suitable experimental conditions in this work to assess field-level variability of inoculation impact on the rhizosphere microbiome.

Impact of Inoculation on Numbers of *nifH*, *acdS*, and *phlD* Rhizobacteria in Each Field

At the six-leaf stage in 2014, differences in the size of the *nifH* group between inoculated and non-inoculated maize were not significant at sites FC and C. At site L, however, inoculation resulted in statistically higher number of *nifH* bacteria in non-fertilized plots (nutriment stress) but lower number in fertilized plots (**Table 2**). At the six-leaf stage in 2015, the number of *nifH* bacteria (studied in non-fertilized plots) was statistically lower at site C upon inoculation, but no difference was found at the two other sites. At flowering stage in 2014, the size of the *nifH* group was statistically higher for inoculated than non-inoculated maize

[4]https://www.r-project.org/

TABLE 1 | Effect of *Azospirillum lipoferum* CRT1 on root and shoot parameters of maize at 6 leaves in 2015 (i.e., the sampling date at which metabarcoding was implemented) in field sites L, FC, and C.

	Site L		Site FC		Site C	
	NI	I	NI	I	NI	I
Maximum photochemical yield	0.74 ± 0.05	0.77 ± 0.04	**0.71 ± 0.02**	**0.75 ± 0.04***	**0.72 ± 0.03**	**0.79 ± 0.03***
Shoot weigh (g plant^{-1})	**0.34 ± 0.07**	**0.43 ± 0.11***	0.52 ± 0.14	0.59 ± 0.17	0.34 ± 0.08	0.39 ± 0.07
Leaf length (cm plant^{-1})	13.10 ± 1.63	14.02 ± 1.92	20.74 ± 1.71	19.82 ± 2.13	17.94 ± 2.42	17.18 ± 1.80
Leaf width (cm plant^{-1})	**1.53 ± 0.15**	**1.68 ± 0.12***	1.61 ± 0.11	1.64 ± 0.14	1.71 ± 0.13	1.71 ± 0.17
Stem diameter (mm)	**6.87 ± 0.73**	**7.63 ± 0.78***	7.74 ± 1.07	8.04 ± 0.99	7.24 ± 0.60	7.06 ± 0.84
Root weight (g plant^{-1})	**0.20 ± 0.05**	**0.24 ± 0.05***	**0.28 ± 0.05**	**0.23 ± 0.05***	0.27 ± 0.05	0.25 ± 0.05
Total root length (cm plant^{-1})	**212 ± 56**	**303 ± 86***	418 ± 109	441 ± 90	323 ± 86	321 ± 61
Total root surface (cm^2 plant^{-1})	**51.5 ± 12.0**	**73.3 ± 20.3***	115.4 ± 29.0	116.0 ± 28.2	89.8 ± 23.9	81.7 ± 17.3
Average roots diameter (mm)	0.79 ± 0.13	0.78 ± 0.10	0.88 ± 0.08	0.83 ± 0.08	**0.89 ± 0.07**	**0.81 ± 0.08***
Number of roots	**413 ± 120**	**789 ± 469***	570 ± 88	671 ± 250	804 ± 536	497 ± 139

NI and I correspond respectively to non-inoculated and inoculated conditions. Stem diameter was measured at root collar and foliar morphology parameters on leaf number five. Statistical analyses were carried out using ANOVA ($P < 0.05$), and statistical differences between inoculated and non-inoculated treatments are indicated by stars (*) and bold characters. The data were obtained from Rozier et al. (2017), and they show that inoculation improved 8 of 10 maize parameters at field site L, whereas it increased maximum photochemical yield and decreased root biomass at site FC, and increased maximum photochemical yield and decreased root diameter at site C.

TABLE 2 | Effect of seed inoculation with *Azospirillum lipoferum* CRT1 on the size of the *nifH*, *acdS*, and *phlD* functional groups in the maize rhizosphere at 6-leaf stage and flowering at three field sites L, FC, and C in 2014 and 2015.

	Site L				Site FC				Site C			
	X fertilizer		0 fertilizer		X fertilizer		XS fertilizer		0 fertilizer		X fertilizer		XS fertilizer	
	NI	I	NI	I	NI	I	NI	I	NI	I	NI	I	NI	I
***nifH* rhizobacteria**														
2014-at 6 leaves	**7.60 ± 0.23**	**7.01 ± 0.38** *	**7.02 ± 0.39**	**7.52 ± 0.18** *	7.41 ± 0.42	7.43 ± 0.50	7.36 ± 0.34	7.53 ± 0.27	7.54 ± 0.13	7.44 ± 0.25	7.77 ± 0.59	7.20 ± 0.68	7.81 ± 0.80	8.10 ± 0.86
2014-at flowering	**8.39 ± 0.31**	**8.60 ± 0.21** *	**8.32 ± 0.27**	**8.62 ± 0.20** *	8.77 ± 0.29	8.69 ± 0.44	**8.56 ± 0.23**	**8.87 ± 0.31** *	8.66 ± 0.21	8.59 ± 0.24	9.07 ± 0.34	9.19 ± 0.39	9.17 ± 0.27	9.19 ± 0.17
2015-at 6 leaves			8.40 ± 8.40	8.27 ± 8.27					8.11 ± 8.11	8.42 ± 8.42			**8.97 ± 8.97**	**8.63 ± 8.63** *
2015-at flowering	8.71 ± 0.26	8.78 ± 0.39	8.61 ± 0.28	8.80 ± 0.41	**7.75 ± 0.46**	**8.52 ± 0.21** *			**7.75 ± 0.24**	**8.45 ± 0.31** *	8.29 ± 0.30	8.29 ± 0.24	**7.99 ± 0.26**	**8.45 ± 0.34** *
***acdS* rhizobacteria**														
2014-at 6 leaves	**8.38 ± 0.25**	**8.00 ± 0.29** *	8.09 ± 0.29	8.27 ± 0.16	8.02 ± 0.25	7.83 ± 0.32	8.11 ± 0.20	8.11 ± 0.30	8.24 ± 0.17	7.98 ± 0.27	8.20 ± 0.46	7.63 ± 0.46	7.90 ± 0.55	7.87 ± 0.51
2014-at flowering	**7.80 ± 0.32**	**8.06 ± 0.22** *	**7.71 ± 0.42**	**8.13 ± 0.20** *	7.91 ± 0.23	7.82 ± 0.18	7.82 ± 0.21	8.04 ± 0.28	**7.92 ± 0.19**	**7.71 ± 0.24** *	**8.21 ± 0.20**	**8.48 ± 0.15** *	8.24 ± 0.18	8.22 ± 0.21
2015-at 6 leaves			7.37 ± 7.37	7.40 ± 7.40					7.25 ± 7.25	7.15 ± 7.15			7.45 ± 7.45	7.33 ± 7.33
2015-at flowering	7.70 ± 0.24	7.78 ± 0.32	**7.64 ± 0.20**	**7.88 ± 0.41** *	**6.59 ± 0.25**	**7.50 ± 0.15** *			**6.56 ± 0.12**	**7.39 ± 0.18** *	**7.00 ± 0.21**	**7.12 ± 0.14** *	6.92 ± 0.23	6.97 ± 0.20
***phlD* rhizobacteria**														
2014-at 6 leaves	6.25 ± 0.53	6.03 ± 0.67	5.91 ± 0.47	5.89 ± 0.57	6.05 ± 0.69	5.70 ± 0.59	6.70 ± 0.72	6.07 ± 0.71	6.19 ± 1.06	5.86 ± 0.35	ND	ND	ND	ND
2014-at flowering	5.91 ± 0.70	5.98 ± 0.35	5.62 ± 0.74	6.34 ± 0.44	6.11 ± 0.94	5.94 ± 0.86	6.48 ± 0.55	6.19 ± 0.76	6.01 ± 0.62	6.12 ± 0.74	ND	ND	ND	ND
2015-at 6 leaves			5.82 ± 0.58	5.82 ± 0.49					6.25 ± 0.63	5.82 ± 0.87			ND	ND
2015-at flowering	ND	ND	ND	ND	**5.31 ± 0.58**	**6.24 ± 0.93** *			**4.99 ± 0.76**	**5.85 ± 0.76** *	ND	ND	ND	ND

X and 0 correspond respectively to optimal N fertilizer dose (delivered half at sowing and half at 6 leaves in treatment XS) and no N applied. NI and I correspond respectively to non-inoculated and inoculated conditions. The analysis was done using pooled samples of six roots systems (n = 5) at FC and C and individual root systems (n = 30) at L in 2014, and individual root systems (n = 20) at all three sites in 2015. Data are shown in decimal log units, using means ± standard errors. ND, not detected (under the detection threshold of 3.2 × 10^3 phlD copies per gram of rhizosphere soil). Statistical differences between inoculated and non-inoculated treatments (ANOVA and Fisher's LSD tests, P < 0.05) are indicated by a star (*) and bold characters.

at sites L (with or without X-level fertilization) and FC (with XS-level fertilization) but not at site C. At flowering stage in 2015, a significant increase in the number of *nifH* bacteria following inoculation was found again, at sites FC (this time in both fertilization treatments) and C (in non-fertilized plots) (**Table 2**).

At the six-leaf stage in 2014, the size of the *acdS* group was statistically higher for inoculated than non-inoculated maize at site L in fertilized plots, but not in non-fertilized plots or at the other two sites (**Table 2**). There was no difference at the six-leaf stage in 2015. At flowering stage in 2014, a significant increase in the number of *acdS* bacteria following inoculation was found at sites L (in both fertilization treatments) and FC (with XS-level fertilization), whereas a decrease was observed at site FC (in non-fertilized plots). At flowering stage in 2015, the size of the *acdS* group was statistically higher for inoculated than non-inoculated maize at sites L (in non-fertilized plots), FC (in both fertilization treatments), and C (in fertilized plots).

At the six-leaf stage, there was no difference in the size of the *phlD* group between inoculated and non-inoculated maize, regardless of the site or the year (**Table 2**). At flowering stage in 2014, a significant increase in the number of *phlD* bacteria following inoculation was found at site L in the absence of fertilization, but there was no difference at the other site studied (FC). At flowering stage in 2015, the size of the *phlD* group was statistically higher with inoculated than non-inoculated maize at site FC, in both fertilization treatments.

In summary, when considering the four samplings carried out over the 2 years of the study, statistically significant differences in the size of functional groups resulting from inoculation were found in 8 of 19 comparisons at site L (4 of 7 for *nifH,* 4 of 7 for *acdS*, 0 of 5 for *phlD*), 8 of 27 comparisons at FC (3 of 9 for *nifH*, 3 of 9 for *acdS*, 2 of 9 for *phlD*), and 4 of 14 comparisons at C (2 of 7 for *nifH*, 2 of 7 for *acdS*), depending on year, maize growth stage, and restricted N fertilization level. Within a given field site, some but not all of the differences observed for various functional groups took place for the same comparisons, that is, at the same combinations of sampling date × N fertilization level.

Impact of Inoculation on Diversity of *nifH*, *acdS*, and All Rhizobacteria in Each Field

nifH sequencing of six-leaf maize rhizosphere (prior to N fertilizer applications) in 2015 gave 681,088 sequences, corresponding to 28,475 OTUs. The rarefaction curves reached a plateau (**Supplementary Figure 1A**), indicating that most of the *nifH* diversity had been recovered. Subsampling was done with 10,775 sequences per sample. There was no significant difference when comparing the resulting diversity indices between inoculated and non-inoculated maize, regardless of the index (Shannon or Simpson) and field site (**Figure 1**).

acdS sequencing resulted in 2,883,839 sequences, which gave 31,220 OTUs. Rarefaction analysis showed that the curves reached a plateau (**Supplementary Figure 1B**). Subsampling was implemented with 68,376 sequences per sample. At site FC, inoculated maize gave a significantly higher Shannon index (6.69 vs. 6.32; $p = 0.032$) but a lower Simpson index (3.6 × 10^{-3}

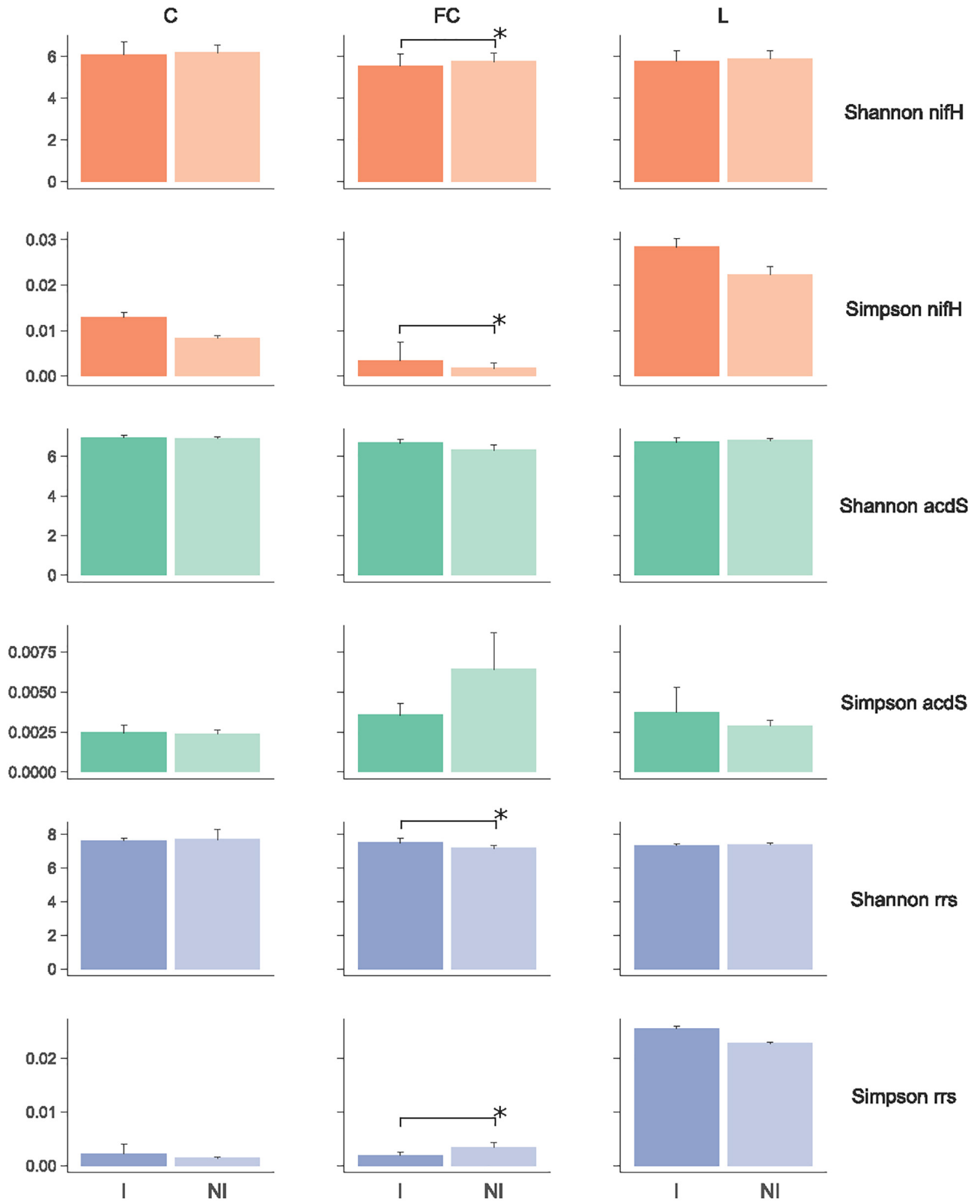

FIGURE 1 | Diversity indices of *nifH* and *acdS* functional groups and the entire (*rrs*) bacterial community at sites L, FC, and C. NI and I correspond, respectively, to non-inoculated and inoculated conditions. Data are shown using means ± standard deviations ($n = 5$). Statistical analyses were carried out by Wilcoxon test between inoculated and non-inoculated conditions, and differences are shown with an asterisk ($p < 0.05$).

vs. 6.4×10^{-3}; $p = 0.032$) in comparison with non-inoculated maize. Inoculation had no effect on diversity level at the other sites (**Figure 1**).

rrs sequencing was also performed to determine whether inoculation effects could also take place at the scale of the whole rhizobacterial community. A total of 3,048,495 reads were obtained, corresponding to 38,419 OTUs. Rarefaction analysis indicated that curves reached a plateau (**Supplementary Figure 1C**). Subsampling was done with 51,696 sequences per sample. As for *acdS*, inoculated maize at site FC led for *rrs* data to a significantly higher Shannon index (7.52 vs. 7.19; $p = 0.032$) but a lower Simpson index (1.9×10^{-3} vs. 3.4×10^{-3}; $p = 0.046$) in comparison with non-inoculated maize. Inoculation had no effect on diversity level at the other sites (**Figure 1**).

In summary, inoculation resulted in statistically significant differences in diversity indices for two of three metabarcoding comparisons at site FC (i.e., for *acdS* and *rrs*) and none of the six other metabarcoding comparisons (at sites L and C).

Impact of Inoculation on Taxa Composition in Each Field

NMDS evidenced that the main differences in the *nifH*, *acdS*, and *rrs* datasets of six-leaf maize were due to field site particularities, with inoculation impact apparent mainly at site FC based on *rrs* data (**Supplementary Figure 2C**). To unmask the overriding effects of field conditions, the impact of inoculation was assessed by BCA. Indeed, BCA of *nifH* sequences from 2015's six-leaf maize indicated that the composition of the diazotroph community differed statistically at site L ($p = 0.008$), at site FC ($p = 0.007$), and at site C ($p = 0.006$) following inoculation with *A. lipoferum* CRT1 (**Figures 2A–C**). Similarly, BCA of *acdS* sequences from 2015's six-leaf maize showed that the composition of ACC-deaminating rhizobacteria differed following inoculation with *A. lipoferum* CRT1, at sites L ($p = 0.012$), FC ($p = 0.005$), and C ($p = 0.013$) (**Figures 3A–C**). Finally, BCA of *rrs* sequences from 2015's six-leaf maize indicated that the composition of rhizobacteria differed following inoculation with *A. lipoferum* CRT1, at sites L ($p = 0.005$), FC ($p = 0.006$), and C ($p = 0.005$) (**Figures 4A–C**).

BCA of *nifH* data showed that the six taxa most often associated with inoculation and the six taxa most commonly associated with the non-inoculated control displayed different rhizosphere levels overall between inoculated and non-inoculated maize. At site L, bacterial genera contributing most to the difference were (by decreasing order of importance) *Treponema*, *Corynebacterium*, *Microbacterium*, *Cyanothece*, *Dehalococcoides*, and *Aeromonas* (genera most commonly associated with inoculated maize), as well as *Hoeflea*, *Cellulosilyticum*, *Serratia*, *Methylocella*, *Rhodanobacter*, and *Cupriavidus* (genera most commonly associated with non-inoculated maize). At site FC, bacterial genera contributing most to the difference were *Raoultella*, *Nitrospirillum*, *Dechloromonas*, *Cellulosimicrobium*, *Microbacterium*, and *Halomonas* (genera most commonly associated with inoculated maize), as well as *Marichromatium*, *Gloeocapsopsis*, *Desulfomaculum*, *Rhizobium*, *Leptothrix*, and *Sideroxydans* (genera most commonly associated with non-inoculated maize). At site C, bacterial genera contributing most to the difference were *Paludibacter*, *Methylococcus*, *Ruminiclostridium*, *Bradyrhizobium*, *Clostridium* and an unclassified genus (genera most commonly associated with inoculated maize), as well as *Ideonella*, *Brucella*, *Methylosinus*, *Pseudacidovorax*, *Pelobacter*, and *Dechloromonas* (genera most commonly associated with non-inoculated maize).

BCA of *acdS* data indicated that the 12 most discriminating taxa displayed different rhizosphere levels overall between inoculated and non-inoculated maize at the sites. At site L, bacterial genera contributing most to the difference were *Gluconobacter*, *Collimonas*, an unclassified genus, *Kutzneria*, *Variovorax*, and *Enterobacter* (genera most commonly associated with inoculated maize); as well as *Hoeflea*, *Micromonospora*, *Meiothermus*, *Bosea*, *Bradyrhizobium*, and *Dickeya* (genera most commonly associated with non-inoculated maize). At site FC, bacterial genera contributing most to the difference were *Tetrasphaera*, *Modestobacter*, *Actinoplanes*, *Roseovarius*, *Mesorhizobium*, and *Saccharothrix* (genera most commonly associated with inoculated maize), as well as *Phycicoccus*, *Hoeflea*, *Gluconobacter*, *Nesterenkonia*, *Collimonas*, and *Burkholderia* (genera most commonly associated with non-inoculated maize). At site C, bacterial genera contributing most to the difference were *Hoeflea*, *Gluconobacter*, *Bosea*, *Meiothermus*, *Ralstonia*, and *Pantoea* (genera most commonly associated with inoculated maize), as well as *Actinoplanes*, *Nakamurella*, *Achromobacter*, *Kribbella*, *Brevibacterium*, and *Micromonospora* (genera most commonly associated with non-inoculated maize).

BCA of *rrs* data revealed that the 12 most discriminating taxa displayed different rhizosphere levels overall between inoculated and non-inoculated maize. At site L, bacterial genera contributing most to the difference were *Desulfopila*, *Methylophilus*, *Azonexus*, *Thiohalophilus*, *Rhodoferax*, and *Flavihumibacter* (genera most commonly associated with inoculated maize), as well as *Candidatus Metachlamydia*, *Oxalicibacterium*, *Jjiangella*, *Desulfuromusa*, *Hydrogenispora*, and *Candidatus Protochlamydia* (genera most commonly associated with non-inoculated maize). At site FC, bacterial genera contributing most to the difference were *Thermosinus*, *Chlorobium*, *Saccharibacter*, *Nevskia*, *Holdemanella*, and *Brucella* (genera most commonly associated with inoculated maize), as well as *Methylosinus*, *Sporomusa*, *Nocardia*, *Candidatus Chloracidobacterium*, *Alkalilimnicola*, and *Zymomonas* (genera most commonly associated with non-inoculated maize). At site C, bacterial genera contributing most to the difference were *Maribius*, *Kangiella*, *Dehalobacterium*, *Rhodobacter*, *Pilimelia*, and *Rhodovastum* (genera most commonly associated with inoculated maize), as well as *Prolixibacter*, *Thermodesulfobium*, *Pyxidicoccus*, *Bellilinea*, *Holospora*, and *Brevinema* (genera most commonly associated with non-inoculated maize).

Despite these rhizomicrobiota modifications, individual comparisons (Wilcoxon test) in the relative abundance of particular genera between inoculated and non-inoculated conditions did not show systematically a statistically significant change, due to low sample number ($n = 5$), high number of variables (e.g., $n = 1{,}111$ genera for the entire community; with the corresponding probability correction effect), and

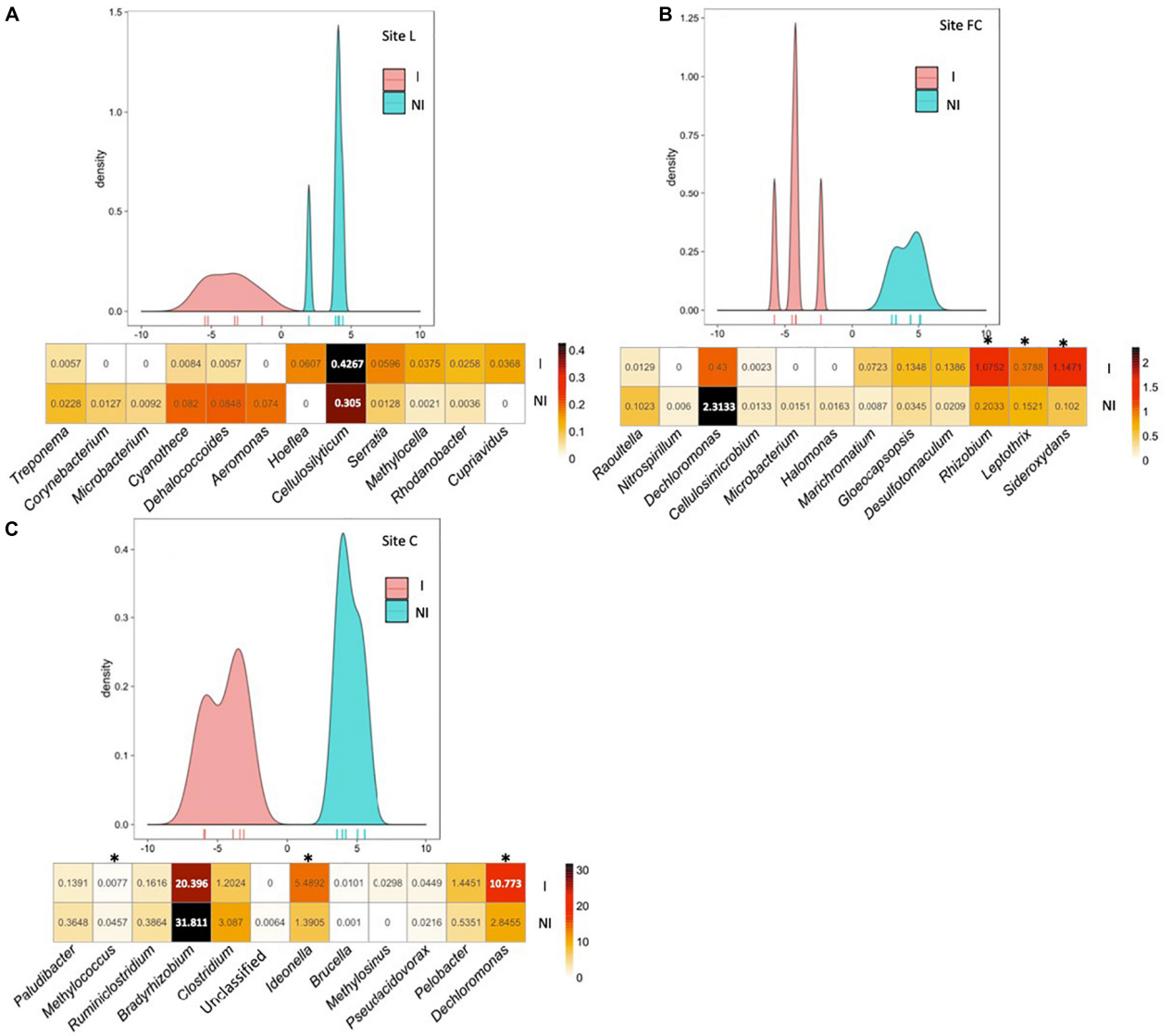

FIGURE 2 | Between-class analysis of the effect of seed inoculation with *A. lipoferum* CRT1 on the composition of the *nifH* functional group in the maize rhizosphere at the six-leaf stage at three field sites L **(A)**, FC **(B)**, and C **(C)**, in 2015. NI and I correspond, respectively, to non-inoculated and inoculated conditions. For each site, the BCA graph is completed (below) by the distribution of the bacterial OTUs according to their contribution to treatment differentiation; BCA is supported statistically by a Monte Carlo test at sites L ($p = 0.008$), FC ($p = 0.007$), and C ($p = 0.006$), and the heatmap below indicates the average relative proportions for the 12 bacterial genera most impacted by inoculation in maize rhizosphere. Six bacterial genera most commonly associated with inoculation are indicated at the left, as well as six bacterial genera most often associated with the non-inoculated control (right). Statistical differences between inoculated and non-inoculated treatments are indicated by stars (*) (Wilcoxon test, $p < 0.05$). Heatmap unit is a percentage of the average relative proportion of taxa.

the fact that taxa found in only one of the two treatments were not necessarily found in all five replicates of that treatment. However, the comparison of genus composition data (**Supplementary Figure 3**) proved useful to emphasize trends among the most prevalent genera in functional groups (but not in the rhizobacterial community as a whole). Among the diazotrophs, there were trends for *Azospirillum*, *Bradyrhizobium*, *Geobacter* (at all three sites), *Desulfovibrio* (at sites L and FC), *Skermanella*, *Clostridium*, and *Rhizobium* (at site L) being more prevalent in inoculated maize, and for *Dechloromonas* (at all three sites), *Ruminiclostridium* (at sites L and FC), *Azoarcus*, *Pseudomonas*, *Leptothrix*, *Cellulosilyticum*, *Ideonella* (at site L), and *Sideroxydans* (at site FC) being less prevalent in inoculated maize. However, contrasted trends were observed for *Paenibacillus* (prevalence in inoculated maize higher at sites FC and C but lower at site L), *Pelosinus* (higher at L and C but lower at FC), and *Clostridium*, *Skermanella*, and *Rhizobium* (all three higher at L but lower at, respectively, FC, C, and both FC and C). Among the ACC deaminase producers, there was a trend for *Variovorax* (at site FC) being more prevalent in inoculated maize, and for *Burkholderia*, *Bradyrhizobium* (at site FC; thus, the trend for *acdS*$^+$ *Bradyrhizobium* at FC was opposite to the

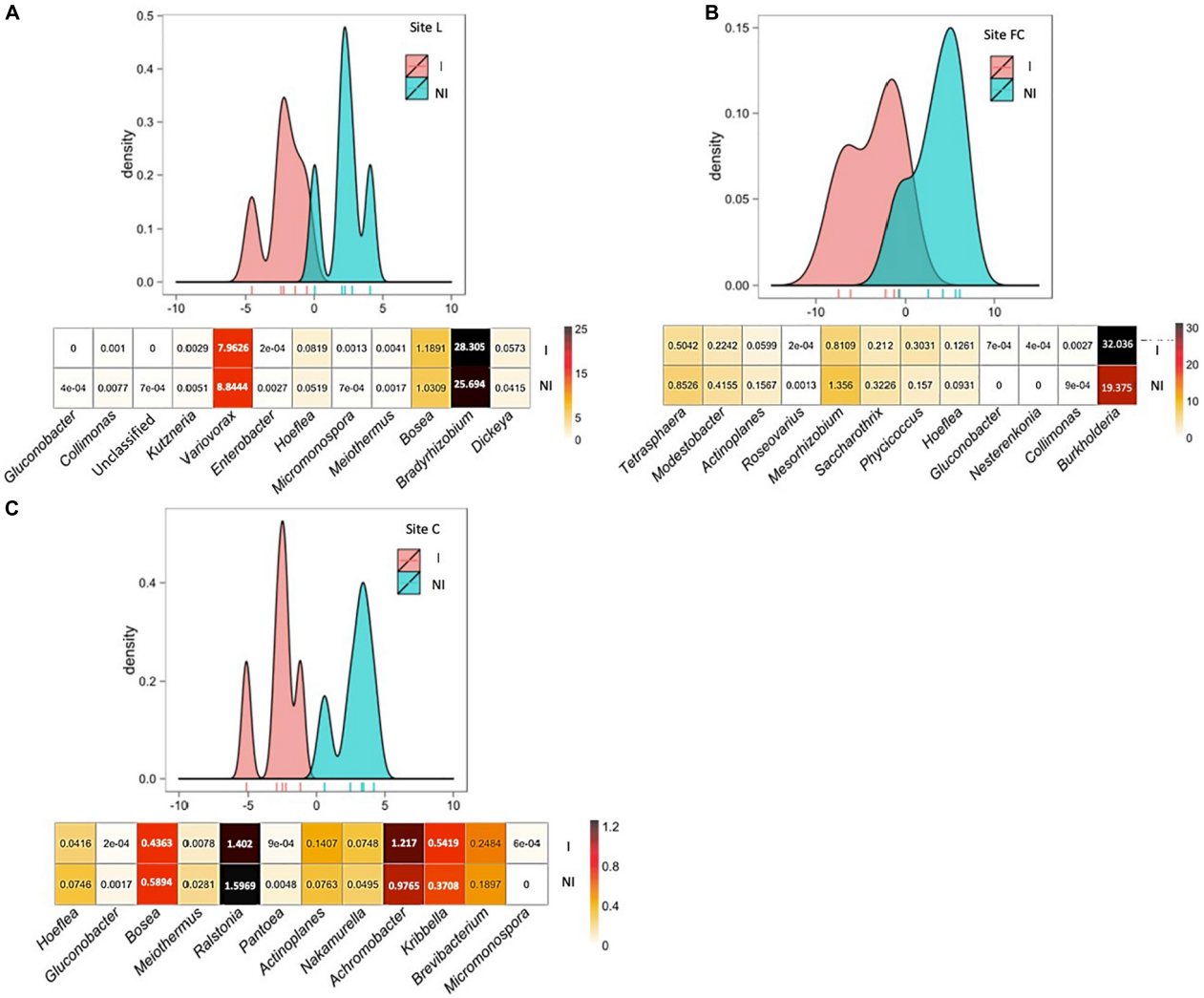

FIGURE 3 | Between-class analysis of the effect of seed inoculation with *A. lipoferum* CRT1 on the composition of the *acdS* functional group in the maize rhizosphere at the six-leaf stage at three field sites L **(A)**, FC **(B)**, and C **(C)**, in 2015. NI and I correspond, respectively, to non-inoculated and inoculated conditions. For each site, the BCA graph is completed (below) by the distribution of the bacterial OTUs according to their contribution to treatment differentiation; BCA is statistically supported by a Monte Carlo test at sites L ($p = 0.012$), FC ($p = 0.005$), and C ($p = 0.013$), and the heatmap below indicates the average relative proportions for the 12 bacterial genera most impacted by inoculation in maize rhizosphere. Six bacterial genera most commonly associated with inoculation are indicated at the left, as well as six bacterial genera most often associated with the non-inoculated control (right). Differences between inoculated and non-inoculated treatments were not statistically significant (Wilcoxon test, $p < 0.05$). Heatmap unit is a percentage of the average relative proportion of taxa.

trend for the entire genus; see above), and *Methylibium* (at site C) being less prevalent in inoculated maize.

In summary, inoculation with *A. lipoferum* CRT1 resulted in significantly different compositions of the diazotroph community, the ACC-deaminating community, and the global bacterial community, at each of the field sites L, FC, and C. For each of the three communities, the bacterial genera contributing most to the distinction between inoculated and non-inoculated maize differed from one field to the other (except that *Microbacterium* was more prevalent among diazotrophs in inoculated maize than the control at both sites L and FC), indicating field-specific inoculation effects on indigenous bacteria.

Taxa Indicative of Inoculation Impact Across the Three Fields

Even though the bacterial genera mainly implicated in functional group (and whole community) differences between inoculated maize and the control mostly differed from one field to the other, an attempt was made to identify differentiating taxa (including taxa with lower contributions) that would contribute to treatment differentiation more reproducibly, that is, across all three sites. To this aim, we pooled bacterial composition data from the maize rhizosphere of the three fields to determine which bacterial genera were the most impacted by *Azospirillum* inoculation at the scale of the three sites studied (**Figures 5A–C**). With this approach, inoculated and non-inoculated maize could be

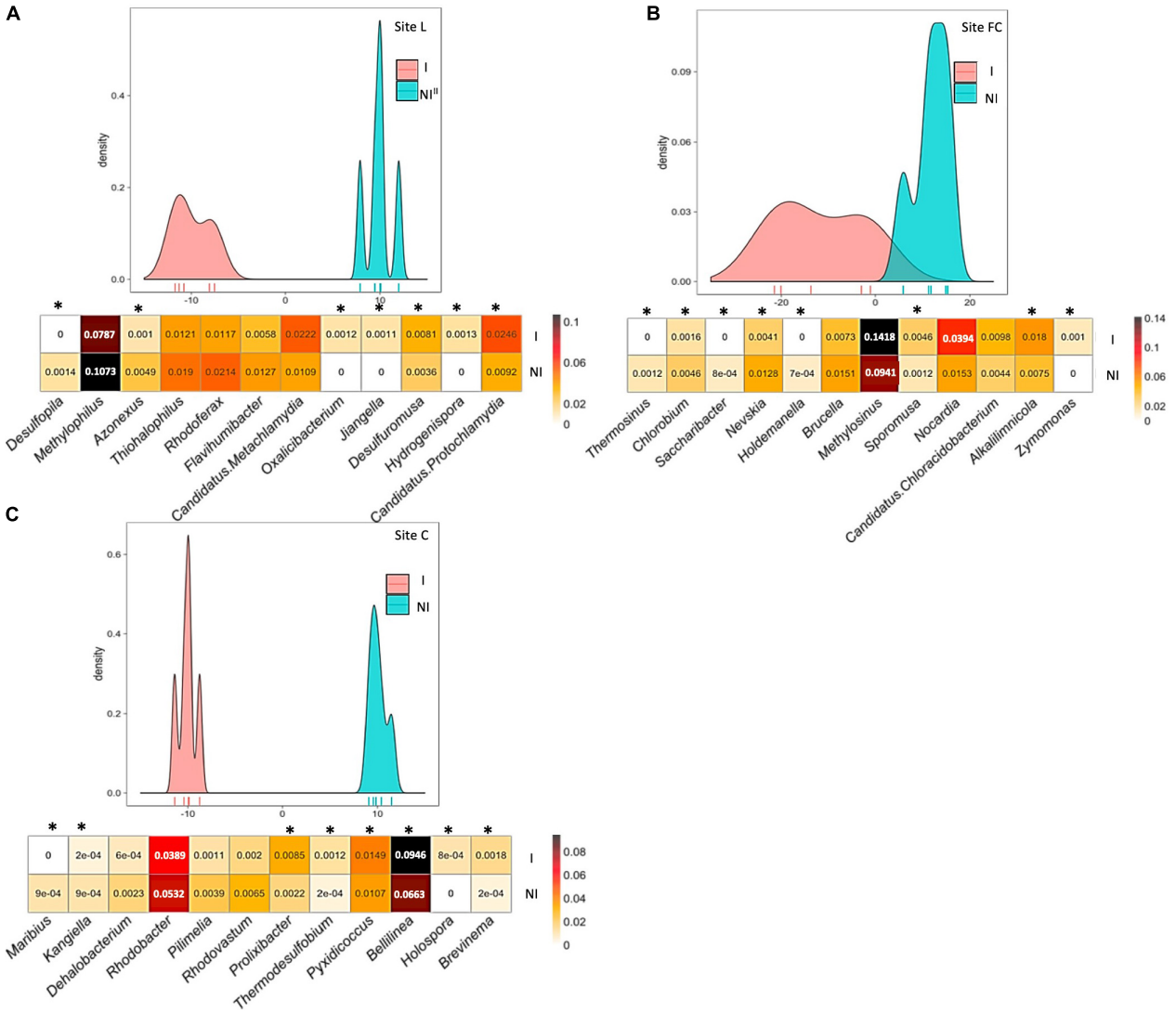

FIGURE 4 | Between-class analysis of the effect of seed inoculation with *A. lipoferum* CRT1 on the composition of the total bacterial community in the maize rhizosphere at the six-leaf stage at three field sites L **(A)**, FC **(B)**, and C **(C)**, in 2015. NI and I correspond, respectively, to non-inoculated and inoculated conditions. For each site, the BCA graph is completed (below) by the distribution of the bacterial OTUs according to their contribution to treatment differentiation; BCA is statistically supported by a Monte Carlo test at sites L (p = 0.005), FC (p = 0.006), and C (p = 0.005), and the heatmap below indicates the relative proportions for the 12 bacterial genera most impacted by inoculation in maize rhizosphere. Six bacterial genera most commonly associated with inoculation are indicated at the left, as well as six bacterial genera most often associated with the non-inoculated control (right). Statistical differences between inoculated and non-inoculated treatments are indicated by stars (*) (Wilcoxon test, $p < 0.05$). Heatmap unit is a percentage of the average relative proportion of taxa.

discriminated by BCA based on *nifH* (p = 0.001) or *rrs* data ($p = 10^{-4}$), but not with *acdS* data (p = 0.19) despite apparent differences in the genus composition profile at two of three sites (**Supplementary Figure 3**).

With *nifH* data, the 12 bacterial genera contributing most to treatment differentiation were an unclassified genus, *Microbacterium*, *Desulfobacca*, *Acinetobacter*, *Pelomonas*, and *Cronobacter* (genera most commonly associated with inoculated maize), as well as *Marichromatium*, *Desulfurivibrio*, *Cupriavidus*, *Hoeflea*, *Ectothiorhodospira*, and *Sideroxydans* (genera most commonly associated with non-inoculated maize). With *rrs* data, the 12 genera contributing most to treatment differentiation were *Roseococcus*, *Leptolinea*, *Gemmata*, *Modestobacter*, *Kangella*, and *Thermoanaerobacterium* (genera most commonly associated with inoculated maize), as well as *Candidatus Phytoplasma*, *Anaerovorax*, *Waddlia*, *Brevinema*, *Hydrogenispora*, and *Nocardiopsis* (genera most commonly associated with non-inoculated maize).

In summary, in our search for more cosmopolitan taxa indicators of inoculation, the artificial pooling of metabarcoding sequences from the three sites did evidence additional taxa (on top of *Microbacterium*) among the 12 taxa contributing most to differentiation of inoculated maize from the non-inoculated control when considering the diazotroph community

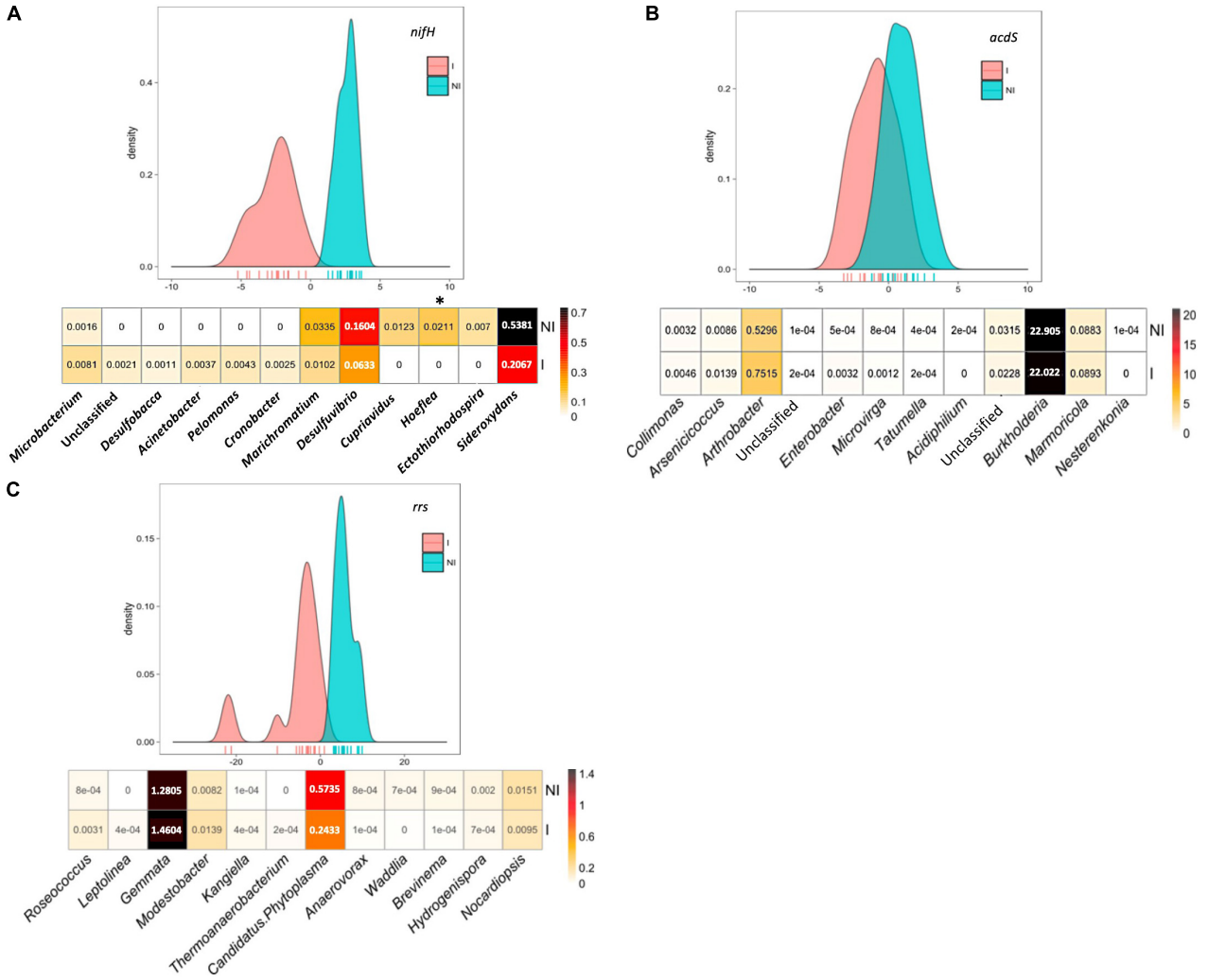

FIGURE 5 | Between-class analysis of the effect of seed inoculation with *A. lipoferum* CRT1 on the composition of **(A)** *nifH* and **(B)** *acdS* functional groups, as well as **(C)** the total bacterial community (*rrs*) over three sites. Analyses were done on pooled data of bacterial composition of maize rhizosphere of the three sites studied. NI and I correspond, respectively, to non-inoculated and inoculated conditions. For each bacterial group, the BCA graph is completed (below) by the distribution of the bacterial OTUs according to their contribution to treatment differentiation. BCA is statistically supported by a Monte Carlo test based on *nifH* ($p = 0.001$) and *rrs* data ($p = 10^{-4}$), but not with *acdS* data ($p = 0.19$), and the heatmap below indicates the relative proportions for the 12 bacterial genera most impacted by inoculation in maize rhizosphere. Six bacterial genera most commonly associated with inoculation are indicated at the left, as well as six bacterial genera most often associated with the non-inoculated control (right). Statistical differences between inoculated and non-inoculated treatments are indicated by stars (*) (Wilcoxon test, $p < 0.05$). Heatmap unit is a percentage of the average relative proportion of taxa.

(and the global bacterial community), but not the ACC-deaminating community.

DISCUSSION

In this work, we tested the hypothesis that PGPR inoculation could result in major changes in root-associated functional microbial communities implicated in phytostimulation, using a range of field trials where the seed inoculant *A. lipoferum* CRT1 had triggered changes in maize metabolome, photosynthetic efficiency, plant development/growth, and/or crop yield (Rozier et al., 2017). Indeed, we observed a modification of strong magnitude in the composition of the diazotroph community and (to a lower degree) of the ACC deaminase community. It is interesting to note that, for both functional groups, these impacts took place irrespective of the morphological or physiological effects evidenced on maize plants at the time of sampling. Rice inoculation with *Azospirillum* (or *Pseudomonas*) in a field had little effect on *nifH* T-RFLP profiles (García de Salamone et al., 2012), whereas maize inoculation with nitrogen-fixing *Pseudomonas* in pots changed diazotroph community composition based on Illumina MiSeq sequencing of *nifH* (Ke et al., 2019). The issue was not investigated so far with the ACC deaminase community, as the methodology needed to do so has not been available for long (Bouffaud et al., 2018). The

impact of inoculation on functional groups needs to receive further research attention, because it may bring additional insight into PGPR modes of action when the latter entail stimulation of indigenous plant-beneficial microorganisms (Trabelsi and Mhamdi, 2013; Vacheron et al., 2013; Ambrosini et al., 2016; da Costa et al., 2018) and also because it is likely to be more informative than taxonomic studies to describe the breadth of inoculant impacts (Ke et al., 2019).

Here, the significant effects of inoculation on the diversity of the *nifH* and *acdS* functional groups were also evidenced with *rrs* data, that is, when considering inoculation effects at the level of the whole rhizobacterial community. Based on *nifH*, *acdS*, and *rrs* analyses, the genera most impacted by inoculation belonged to *Actinobacteria*, *Cyanobacteria*, *Firmicutes*, or *Proteobacteria*, indicating a taxonomic shift larger than what was thought so far. Overall, the effects of inoculation were underpinned by changes in the relative abundance of multiple taxa. Some of these changes were small, but others were of larger magnitude (e.g., a decrease from 32 to 19% for *Burkholderia*; **Figure 3**). These findings contrast with previous studies showing minor and/or transient ecological impact of *Azospirillum* inoculants on the resident bacterial community colonizing the rhizosphere (Ambrosini et al., 2016), by molecular fingerprinting in the case of maize (Herschkovitz et al., 2005; Lerner et al., 2006; Matsumura et al., 2015), wheat (Naiman et al., 2009; Baudoin et al., 2010), rice (Pedraza et al., 2009; García de Salamone et al., 2010, 2012; Bao et al., 2013), or other crops (Correa et al., 2007; Felici et al., 2008), as well as by Illumina MiSeq metabarcoding in the case of maize (da Costa et al., 2018). Modest inoculant impacts on the rhizobacterial community were also found with *Bacillus* on lettuce (by metagenomics; Kröber et al., 2014) and tomato (by pyrosequencing; Qiao et al., 2017), *Pseudomonas* on lettuce (by DGGE and pyrosequencing; Schreiter et al., 2014), *Pseudomonas* or *Achromobacter* on maize (by Illumina MiSeq; da Costa et al., 2018), *Stenotrophomonas* on maize (by Illumina MiSeq; Kusstatscher et al., 2020), multispecies inoculants on tomato (by Illumina MiSeq; Nuzzo et al., 2020) and wheat (by pyrosequencing; Dal Cortivo et al., 2020), or a multispecies organic amendment on sugarcane (by Illumina MiSeq; Berg et al., 2019), whereas a larger impact was observed by Illumina MiSeq with *Pseudomonas* on maize (Ke et al., 2019) and different oilseed crops (Jiménez et al., 2020); *Pseudomonas*, *Paenibacillus*, or *Bacillus* on lettuce (Passera et al., 2020); an organic amendment enriched in microorganisms on strawberry (Deng et al., 2019); or a multispecies inoculant on onion (Pellegrini et al., 2021).

The second hypothesis tested was that the effects of PGPR inoculation on functional communities could be field site-specific, which turned out to be the case. Indeed, the most impacted bacterial genera seldom overlapped between sites, and when they did, modifications did not follow the same trend in all sites. Genus overlap (i.e., the same genera impacted at several sites) was more often found in the *acdS* group, perhaps because there were fewer genera in this group. When we pooled data from all fields, we showed that the *acdS* group did not differ significantly between inoculated and non-inoculated treatments, in contrary to the *nifH* group (and the *rrs* community). This suggests that inoculation effects on *acdS* rhizobacteria were more site-dependent than those on *nifH* rhizobacteria and on all rhizobacteria. These findings are likely to have implications in terms of rhizosphere functioning, phytostimulation implementation, and crop behavior, because they mean that inoculants will stimulate indigenous plant-beneficial microorganisms in a field-specific manner, as the natural soil community, the cropping/agronomic history, the pedoclimatic conditions, and/or crop physiology may differ between fields.

Here, inoculation resulted in 16 increases and 4 decreases in gene copy number (for *nifH*, *acdS*, or *phlD*) of the 60 individual comparisons carried out. These significant differences depended on the gene studied, the field, the year, the crop stage, and nitrogen fertilization (nutriment stress or not). Importantly, they often varied between fields when a given gene × nitrogen fertilization combination was compared across the various sampling dates assessed, pointing again to site-specific effects of inoculation on microbial functional groups important for phytostimulation.

As the *nifH*$^+$ inoculant *A. lipoferum* CRT1 remained under qPCR detection threshold, it suggests that the augmentation in *nifH* copy number in CRT1-inoculated maize in certain comparisons was not due to presence of the *nifH*$^+$ inoculant itself. Lack of inoculant survival does not necessarily mean that inoculation has no effect (Mawarda et al., 2020). Furthermore, inoculation effects on the density of the three functional groups were stronger at flowering stage, even though the inoculant was long below detection limit. Inoculation of *Ensifer* (previously *Sinorhizobium*) *meliloti* resulted also in changes in the number of *nifH*$^+$ bacteria in maize rhizosphere that were plant phenology-dependent (Babić et al., 2008; Gupta et al., 2012). *acdS* gene copies were higher in CRT1-inoculated maize at flowering stage, which could have ecological consequences (Glick, 2014) as ethylene is produced from ACC in higher amount at flowering stage than in early growth stages (Bleecker and Kende, 2000).

Two types of mechanisms could explain the ecological impact of *A. lipoferum* CRT1: first, a direct effect of the inoculant on indigenous rhizobacteria by antagonism, competition, or cooperation (Pandey and Kumar, 1990; Tapia-Hernández et al., 1990; Tortora et al., 2011; Trabelsi and Mhamdi, 2013; Ambrosini et al., 2016), which could modify community composition. So far, *Azospirillum* species are mostly described as plant stimulators (Dobbelaere et al., 2003; Bashan and de-Bashan, 2010) by their capacity to produce phytohormones (Karadeniz et al., 2006; Cohen et al., 2015), but they may interact with other plant-beneficial microorganisms (Russo et al., 2005; Combes-Meynet et al., 2011). Here, the lack of significant inoculant survival (strain CRT1 remaining perhaps at very low levels, as a member of the rare biosphere) means that direct inoculant effects could occur only at the very early stages of maize colonization, where an impact on keystone "hub" microorganisms (Agler et al., 2016; Mawarda et al., 2020) might, in turn, have affected the microbiome network. Second, several studies showed that *A. lipoferum* CRT1 does not need to be well established in the maize rhizosphere to benefit plant growth (Jacoud et al., 1999; Rozier et al., 2017, 2019). In the current work, inoculation had resulted in changes in plant morphology and physiology

(photosynthetic efficiency and metabolome), and at the six-leaf stage in 2015, plant growth modifications were observed at site L and plant metabolome changes at all three sites (Rozier et al., 2017). This starter effect of *A. lipoferum* CRT1 suggests modification of plant physiology from very early development stages of maize (Jacoud et al., 1999; Walker et al., 2011; Rozier et al., 2017, 2019), probably driving root microbiota changes. Indeed, CRT1 inoculation can also result in modification of plant secondary metabolites, especially benzoxazinoids and cinnamic acids (Walker et al., 2011), which are present in root secretions and known to play a major role in plant–microbe interactions (Neal et al., 2012).

CONCLUSION

In conclusion, the seed inoculant *A. lipoferum* CRT1 did not manage to establish itself in the maize rhizosphere. However, it had a significant impact on the diversity of key functional groups important for plant performance and of the whole bacterial community in the rhizosphere, pointing to direct and/or plant-mediated effects of the inoculant on resident rhizobacteria. Importantly, we showed that this impact was field site-specific, thereby validating our hypothesis. This study demonstrated that inoculation has the potential to affect rhizosphere microbial functioning and identified community-based ecological mechanisms by which an inoculant could influence plant performance. It also showed the usefulness of considering microbial functional groups to reveal ecological effects on the plant microbiome, and further research efforts are necessary to develop the molecular toolbox needed to monitor a wider range of plant-beneficial functions under optimized or stress conditions.

DATA AVAILABILITY STATEMENT

The datasets presented in this study can be found in online repositories. The names of the repository/repositories and accession number(s) can be found in the article.

AUTHOR CONTRIBUTIONS

LL, YM-L, CP-C, and DM designed the project. SR, JV, CP-C, LL, YM-L, and DM carried out field work. SR and JV conducted the molecular work. SR and DA implemented bioinformatic analyses. SR, YM-L, and DM analyzed data and prepared the first draft of the manuscript, which was finalized by all authors.

FUNDING

This work was funded through the ANR project Azodure (ANR-12-AGRO-0008) and the IDEX-Lyon project Phytobiome.

ACKNOWLEDGMENTS

We are grateful to Jacqueline Haurat and Hélène Brunet for technical help, farmers for access to fields, Agrauxine for inoculant product, and La Dauphinoise coop for field management.

SUPPLEMENTARY MATERIAL

The Supplementary Material for this article can be found online at: https://www.frontiersin.org/articles/10.3389/fmicb.2021.760512/full#supplementary-material

Supplementary Figure 1 | Rarefaction curves for *nifH* **(A)**, *acdS* **(B)**, and *rrs* **(C)** at field sites L, FC, and C. NI and I correspond, respectively, to non-inoculated and inoculated conditions.

Supplementary Figure 2 | Non-metric multidimensional scaling (NMDS) of *nifH* **(A)**, *acdS* **(B)**, and *rrs* **(C)** data at field sites L, FC, and C. NI and I correspond, respectively, to non-inoculated and inoculated conditions. NMDS of distance matrices was based on the Bray–Curtis distance and was done using the vegan package in R.

Supplementary Figure 3 | Relative abundance of the most prevalent bacterial genera based on analysis of *nifH*, *acdS* and *rrs* data for field sites L, FC, and C (results from the five replicates were pooled). NI and I correspond, respectively, to non-inoculated and inoculated conditions.

REFERENCES

Agler, M. T., Ruhe, J., Kroll, S., Morhenn, C., Kim, S.-T., Weigel, D., et al. (2016). Microbial hub taxa link host and abiotic factors to plant microbiome variation. *PLoS Biol.* 14:e1002352. doi: 10.1371/journal.pbio.1002352

Almario, J., Moënne-Loccoz, Y., and Muller, D. (2013). Monitoring of the relation between 2,4-diacetylphloroglucinol-producing *Pseudomonas* and *Thielaviopsis basicola* populations by real-time PCR in tobacco black root-rot suppressive and conducive soils. *Soil Biol. Biochem.* 57, 144–155. doi: 10.1016/j.soilbio.2012.09.003

Ambrosini, A., de Souza, R., and Passaglia, L. M. (2016). Ecological role of bacterial inoculants and their potential impact on soil microbial diversity. *Plant Soil* 400, 93–207.

Babić, K. H., Schauss, K., Hai, B., Sikora, S., Redžepović, S., Radl, V., et al. (2008). Influence of different *Sinorhizobium meliloti* inocula on abundance of genes involved in nitrogen transformations in the rhizosphere of alfalfa (*Medicago sativa* L.). *Environ. Microbiol.* 10, 2922–2930. doi: 10.1111/j.1462-2920.2008.01762.x

Bao, Z., Sasaki, K., Okubo, T., Ikeda, S., Anda, M., Hanzawa, E., et al. (2013). Impact of *Azospirillum* sp. B510 inoculation on rice-associated bacterial communities in a paddy field. *Microbes Environ.* 28, 487–490. doi: 10.1264/jsme2.me13049

Bashan, Y., and de-Bashan, L. E. (2010). How the plant growth-promoting bacterium *Azospirillum* promotes plant growth - a critical assessment. *Adv. Agron.* 108, 77–136. doi: 10.1016/s0065-2113(10)08002-8

Basu, A., Prasad, P., Das, S. N., Kalam, S., Sayyed, R. Z., Reddy, M. S., et al. (2021). Plant growth promoting rhizobacteria (PGPR) as green bioinoculants: recent developments, constraints, and prospects. *Sustainability* 13:1140. doi: 10.3390/su13031140

Baudoin, E., Lerner, A., Mirza, M. S., El Zemrany, H., Prigent-Combaret, C., Jurkevich, E., et al. (2010). Effects of *Azospirillum brasilense* with genetically modified auxin biosynthesis gene *ipdC* upon the diversity of the indigenous microbiota of the wheat rhizosphere. *Res. Microbiol.* 161, 219–226. doi: 10.1016/j.resmic.2010.01.005

Baudoin, E., Nazaret, S., Mougel, C., Ranjard, L., and Moënne-Loccoz, Y. (2009). Impact of inoculation with the phytostimulatory PGPR *Azospirillum lipoferum* CRT1 on the genetic structure of the rhizobacterial community of field-grown maize. *Soil Biol. Biochem.* 41, 409–413. doi: 10.1016/j.soilbio.2008.10.015

Berg, S., Dennis, P. G., Paungfoo-Lonhienne, C., Anderson, J., Robinson, N., Brackin, R., et al. (2019). Effects of commercial microbial biostimulants on soil and root microbial communities and sugarcane yield. *Biol. Fertil. Soils* 56, 565–580. doi: 10.1007/s00374-019-01412-4

Bertrand, H., Plassard, C., Pinochet, X., Touraine, B., Normand, P., and Cleyet-Marel, J.-C. (2000). Stimulation of the ionic transport system in *Brassica napus* by a plant growth-promoting rhizobacterium (*Achromobacter* sp.). *Can. J. Microbiol.* 46, 229–236. doi: 10.1139/w99-137

Bleecker, A. B., and Kende, H. (2000). Ethylene: a gaseous signal molecule in plants. *Annu. Rev. Cell Dev. Biol.* 16, 1–18. doi: 10.1146/annurev.cellbio.16.1.1

Bouffaud, M.-L., Renoud, S., Dubost, A., Moënne-Loccoz, Y., and Muller, D. (2018). 1-Aminocyclopropane-1-carboxylate deaminase producers associated to maize and other *Poaceae* species. *Microbiome* 6:114. doi: 10.1186/s40168-018-0503-7

Bouffaud, M.-L., Renoud, S., Moënne-Loccoz, Y., and Muller, D. (2016). Is plant evolutionary history impacting recruitment of diazotrophs and *nifH* expression in the rhizosphere? *Sci. Rep.* 6:21690. doi: 10.1038/srep21690

Brazelton, J. N., Pfeufer, E. E., Sweat, T. A., McSpadden Gardener, B. B., and Coenen, C. (2008). 2,4-diacetylphloroglucinol alters plant root development. *Mol. Plant Microbe Interact.* 21, 1349–1358. doi: 10.1094/MPMI-21-10-1349

Brusamarello-Santos, L. C., Gilard, F., Brulé, L., Quilleré, I., Gourion, B., Ratet, P., et al. (2017). Metabolic profiling of two maize (*Zea mays* L.) inbred lines inoculated with the nitrogen fixing plant-interacting bacteria *Herbaspirillum seropedicae* and *Azospirillum brasilense*. *PLoS One* 12:e0174576. doi: 10.1371/journal.pone.0174576

Cáceres, E. A. (1982). Improved medium for isolation of *Azospirillum* spp. *Appl. Environ. Microbiol.* 44, 990–991. doi: 10.1128/aem.44.4.990-991.1982

Cangahuala-Inocente, G. C., Plucani do Amaral, F., Faleiro, A. C., Huergo, L. F., and Maisonnave Arisi, A. C. (2013). Identification of six differentially accumulated proteins of *Zea mays* seedlings (DKB240 variety) inoculated with *Azospirillum brasilense* strain FP2. *Eur. J. Soil Biol.* 58, 45–50. doi: 10.1016/j.ejsobi.2013.06.002

Castro-Sowinski, S., Herschkovitz, Y., Okon, Y., and Jurkevitch, E. (2007). Effects of inoculation with plant growth-promoting rhizobacteria on resident rhizosphere microorganisms. *FEMS Microbiol. Lett.* 276, 1–11. doi: 10.1111/j.1574-6968.2007.00878.x

Chamam, A., Sanguin, H., Bellvert, F., Meiffren, G., Comte, G., Wisniewski-Dyé, F., et al. (2013). Plant secondary metabolite profiling evidences strain-dependent effect in the *Azospirillum–Oryza sativa* association. *Phytochemistry* 87, 65–77. doi: 10.1016/j.phytochem.2012.11.009

Chessel, D., Dufour, A. B., and Thioulouse, J. (2004). The ade4 package - I: one-table methods. *R. News* 4, 5–10.

Cohen, A. C., Bottini, R., Pontin, M., Berli, F. J., Moreno, D., Boccanlandro, H., et al. (2015). *Azospirillum brasilense* ameliorates the response of *Arabidopsis thaliana* to drought mainly via enhancement of ABA levels. *Physiol. Plant.* 153, 79–90. doi: 10.1111/ppl.12221

Combes-Meynet, E., Pothier, J. F., Moënne-Loccoz, Y., and Prigent-Combaret, C. (2011). The *Pseudomonas* secondary metabolite 2,4-diacetylphloroglucinol is a signal inducing rhizoplane expression of *Azospirillum* genes involved in plant-growth promotion. *Mol. Plant Microbe Interact.* 24, 271–284. doi: 10.1094/MPMI-07-10-0148

Correa, O. S., Romero, A. M., Montecchia, M. S., and Soria, M. A. (2007). Tomato genotype and *Azospirillum* inoculation modulate the changes in bacterial communities associated with roots and leaves. *J. Appl. Microbiol.* 102, 781–786. doi: 10.1111/j.1365-2672.2006.03122.x

Couillerot, O., Bouffaud, M.-L., Baudoin, E., Muller, D., Caballero-Mellado, J., and Moënne-Loccoz, Y. (2010). Development of a real-time PCR method to quantify the PGPR strain *Azospirillum lipoferum* CRT1 on maize seedlings. *Soil Biol. Biochem.* 42, 2298–2305. doi: 10.1016/j.soilbio.2010.09.003

Creus, C. M., Graziano, M., Casanovas, E. M., Pereyra, M. A., Simontacchi, M., Puntarulo, S., et al. (2005). Nitric oxide is involved in the *Azospirillum brasilense*-induced lateral root formation in tomato. *Planta* 221, 297–303. doi: 10.1007/s00425-005-1523-7

da Costa, P. B., de Campos, S. B., Albersmeier, A., Dirksen, P., Dresseno, A. L. P., dos Santos, O. J. A. P., et al. (2018). Invasion ecology applied to inoculation of plant growth promoting bacteria through a novel SIMPER-PCA approach. *Plant Soil* 422, 467–478. doi: 10.1007/s11104-017-3492-6

Dal Cortivo, C., Ferrari, M., Visioli, G., Lauro, M., Fornasier, F., Barion, G., et al. (2020). Effects of seed-applied biofertilizers on rhizosphere biodiversity and growth of common wheat (*Triticum aestivum* L.) in the field. *Front. Plant Sci.* 11:72. doi: 10.3389/fpls.2020.00072

Deng, S., Wipf, H. M. L., Pierroz, G., Raab, T. K., Khanna, R., and Coleman-Derr, D. (2019). A plant growth-promoting microbial soil amendment dynamically alters the strawberry root bacterial microbiome. *Sci. Rep.* 9:17677. doi: 10.1038/s41598-019-53623-2

DeSantis, T. Z., Hugenholtz, P., Larsen, N., Rojas, M., Brodie, E. L., Keller, K., et al. (2006). Greengenes, a chimera-checked 16S rRNA gene database and workbench compatible with ARB. *Appl. Environ. Microbiol.* 72, 5069–5072. doi: 10.1128/AEM.03006-05

Di Salvo, L. P., Cellucci, G. C., Carlino, M. E., and García de Salamone, I. E. (2018). Plant growth-promoting rhizobacteria inoculation and nitrogen fertilization increase maize (*Zea mays* L.) grain yield and modified rhizosphere microbial communities. *Appl. Soil Ecol.* 126, 113–120. doi: 10.1016/j.apsoil.2018.02.010

Dobbelaere, S., Vanderleyden, J., and Okon, Y. (2003). Plant growth-promoting effects of diazotrophs in the rhizosphere. *Crit. Rev. Plant Sci.* 22, 107–149.

Dolédec, S., and Chessel, D. (1987). Rythmes saisonniers et composantes stationnelles en milieu aquatique. I- Description d'un plan d'observations complet par projection de variables. Acta oecologica. *Oecol. Generalis* 8, 403–426.

Dray, S., Dufour, A. B., and Chessel, D. (2007). The ade4 package - II: two-table and K-table methods. *R. News* 7, 47–52.

Drogue, B., Sanguin, H., Chamam, A., Mozar, M., Llauro, C., Panaud, O., et al. (2014a). Plant root transcriptome profiling reveals a strain-dependent response during *Azospirillum*-rice cooperation. *Front. Plant Sci.* 5:607. doi: 10.3389/fpls.2014.00607

Drogue, B., Prigent-Combaret, C., Sanguin, H., Borland, S., and Wisniewski-Dyé, F. (2014b). Genome wide profiling of *Azospirillum lipoferum* 4B gene expression during interaction with rice roots. *FEMS Microbiol. Ecol.* 87, 543–555. doi: 10.1111/1574-6941.12244

El Zemrany, H., Cortet, J., Lutz, M. P., Chabert, A., Baudoin, E., Haurat, J., et al. (2006). Field survival of the phytostimulator *Azospirillum lipoferum* CRT1 and functional impact on maize crop, biodegradation of crop residues, and soil faunal indicators in a context of decreasing nitrogen fertilisation. *Soil Biol. Biochem.* 38, 1712–1726. doi: 10.1016/j.soilbio.2005.11.025

Fages, J., and Mulard, D. (1988). Isolement de bactéries rhizosphériques et effet de leur inoculation en pots chez *Zea mays*. *Agronomie* 8, 309–314. doi: 10.1051/agro:19880405

Felici, C., Vettori, L., Giraldi, E., Forino, L. M. C., Toffanin, A., Tagliasacchi, A. M., et al. (2008). Single and co-inoculation of *Bacillus subtilis* and *Azospirillum brasilense* on *Lycopersicon esculentum*: effects on plant growth and rhizosphere microbial community. *Appl. Soil Ecol.* 40, 260–270. doi: 10.1016/j.apsoil.2008.05.002

Florio, A., Pommier, T., Gervaix, J., Bérard, A., and Le Roux, X. (2017). Soil C and N statuses determine the effect of maize inoculation by plant growth-promoting rhizobacteria on nitrifying and denitrifying communities. *Sci. Rep.* 7:8411. doi: 10.1038/s41598-017-08589-4

Fuhrman, J. A. (2009). Microbial community structure and its functional implications. *Nature* 459:193. doi: 10.1038/nature08058

Gabriel, J. L., Zarco-Tejada, P. J., López-Herrera, P. J., Pérez-Martín, E., Alonso-Ayuso, M., and Quemada, M. (2017). Airborne and ground level sensors for monitoring nitrogen status in a maize crop. *Biosyst. Eng.* 160, 124–133.

Gaby, J. C., and Buckley, D. H. (2017). The use of degenerate primers in qPCR analysis of functional genes can cause dramatic quantification bias as revealed by investigation of nifH primer performance. *Microb. Ecol.* 74, 701–708. doi: 10.1007/s00248-017-0968-0

García de Salamone, I. E., Di Salvo, L. P., Escobar Ortega, J. S., Boa Sorte, P. M. F., Urquiaga, S., and Teixeira, K. R. S. (2010). Field response of rice paddy crop to *Azospirillum* inoculation: physiology of rhizosphere bacterial communities and the genetic diversity of endophytic bacteria in different parts of the plants. *Plant Soil* 336, 351–362. doi: 10.1007/s11104-010-0487-y

García de Salamone, I. E., Funes, J. M., Di Salvo, L. P., Escobar-Ortega, J. S., D'Auria, F., Ferrando, L., et al. (2012). Inoculation of paddy rice with *Azospirillum brasilense* and *Pseudomonas fluorescens*: Impact of plant genotypes on rhizosphere microbial communities and field crop production. *Appl. Soil Ecol.* 61, 196–204. doi: 10.1016/j.apsoil.2011.12.012

Glick, B. R. (2014). Bacteria with ACC deaminase can promote plant growth and help to feed the world. *Microbiol. Res.* 69, 30–39. doi: 10.1016/j.micres.2013.09.009

Gupta, R., Bru, D., Bisaria, V. S., Philippot, L., and Sharma, S. (2012). Responses of *Cajanus cajan* and rhizospheric N-cycling communities to bioinoculants. *Plant and Soil* 358, 143–154. doi: 10.1007/s11104-012-1293-5

Herschkovitz, Y., Lerner, A., Davidov, Y., Okon, Y., and Jurkevitch, E. (2005). *Azospirillum brasilense* does not affect population structure of specific rhizobacterial communities of inoculated maize (*Zea mays*). *Environmental Microbiology* 7, 1847–1852. doi: 10.1111/j.1462-2920.2005.00926.x

Huberty, C. J. (1994). *Applied Discriminant Analysis*. New York, NY: Wiley-Interscience.

Jacoud, C., Job, D., Wadoux, P., and Bally, R. (1999). Initiation of root growth stimulation by *Azospirillum lipoferum* CRT1 during maize seed germination. *Can. J. Microbiol.* 45, 339–342. doi: 10.1139/w99-023

Jiménez, J. A., Novinscak, A., and Filion, M. (2020). Inoculation with the plant-growth-promoting rhizobacterium *Pseudomonas fluorescens* LBUM677 impacts the rhizosphere microbiome of three oilseed crops. *Front. Microbiol.* 11:2534. doi: 10.3389/fmicb.2020.569366

Karadeniz, A., Topcuoğlu, Ş, and Inan, S. (2006). Auxin, gibberellin, cytokinin and abscisic acid production in some bacteria. *World J. Microbiol. Biotechnol.* 22, 1061–1064. doi: 10.1007/s11274-005-4561-1

Ke, X., Feng, S., Wang, J., Lu, W., Zhang, W., Chen, M., et al. (2019). Effect of inoculation with nitrogen-fixing bacterium *Pseudomonas stutzeri* A1501 on maize plant growth and the microbiome indigenous to the rhizosphere. *Syst. Appl. Microbiol.* 42, 248–260. doi: 10.1016/j.syapm.2018.10.010

Keel, C., Wirthner, P., Oberhänsli, T., Voisard, C., Haas, D., and Défago, G. (1990). *Pseudomonads* as antagonists of plant pathogens in the rhizosphere: role of the antibiotic 2,4-diacetylphloroglucinol in the suppression of black root rot of tobacco. *Symbiosis (Rehovot)* 9, 327–341.

Kröber, M., Wibberg, D., Grosch, R., Eikmeyer, F., Verwaaijen, B., Chowdhury, S. P., et al. (2014). Effect of the strain *Bacillus amyloliquefaciens* FZB42 on the microbial community in the rhizosphere of lettuce under field conditions analyzed by whole metagenome sequencing. *Front. Microbiol.* 5:252. doi: 10.3389/fmicb.2014.00252

Kusstatscher, P., Wicaksono, W. A., Thenappan, D. P., Adam, E., Müller, H., and Berg, G. (2020). Microbiome management by biological and chemical treatments in maize is linked to plant health. *Microorganisms* 8:1506. doi: 10.3390/microorganisms8101506

Lerner, A., Herschkovitz, Y., Baudoin, E., Nazaret, S., Moënne-Loccoz, Y., Okon, Y., et al. (2006). Effect of *Azospirillum brasilense* inoculation on rhizobacterial communities analyzed by denaturing gradient gel electrophoresis and automated ribosomal intergenic spacer analysis. *Soil Biol. Biochem.* 38, 1212–1218. doi: 10.1016/j.soilbio.2005.10.007

Matsumura, E. E., Secco, V. A., Moreira, R. S., dos Santos, O. J. A. P., Hungria, M., and de Oliveira, A. L. M. (2015). Composition and activity of endophytic bacterial communities in field-grown maize plants inoculated with *Azospirillum brasilense*. *Ann. Microbiol.* 65, 2187–2200. doi: 10.1007/s13213-015-1059-4

Mawarda, P. C., Le Roux, X., van Elsas, J. D., and Salles, J. F. (2020). Deliberate introduction of invisible invaders: a critical appraisal of the impact of microbial inoculants on soil microbial communities. *Soil Biol. Biochem.* 148:107874. doi: 10.1016/j.soilbio.2020.107874

Molina-Favero, C., Creus, C. M., Simontacchi, M., Puntarulo, S., and Lamattina, L. (2008). Aerobic nitric oxide production by *Azospirillum brasilense* Sp245 and its influence on root architecture in tomato. *Mol. Plant Microbe Interact.* 21, 1001–1009. doi: 10.1094/MPMI-21-7-1001

Naiman, A. D., Latrónico, A., and Garcia de Salamone, I. E. (2009). Inoculation of wheat with *Azospirillum brasilense* and *Pseudomonas fluorescens*: impact on the production and culturable rhizosphere microflora. *Eur. J. Soil Biol.* 45, 44–51. doi: 10.1016/j.ejsobi.2008.11.001

Neal, A. L., Ahmad, S., Gordon-Weeks, R., and Ton, J. (2012). Benzoxazinoids in root exudates of maize attract *Pseudomonas putida* to the rhizosphere. *PLoS One* 7:e35498. doi: 10.1371/journal.pone.0035498

Nuzzo, A., Satpute, A., Albrecht, U., and Strauss, S. L. (2020). Impact of soil microbial amendments on tomato rhizosphere microbiome and plant growth in field soil. *Microb. Ecol.* 80, 398–409. doi: 10.1007/s00248-020-01497-7

Okon, Y., and Labandera-Gonzalez, C. A. (1994). Agronomic applications of *Azospirillum*: an evaluation of 20 years worldwide field inoculation. *Soil Biol. Biochem.* 26, 1591–1601. doi: 10.1016/0038-0717(94)90311-5

Pandey, A., and Kumar, S. (1990). Inhibitory effects of *Azotobacter chroococcum* and *Azospirillum brasilense* on a range of rhizosphere fungi. *Indian J. Exp. Biol.* 28, 52–54.

Park, J.-W., and Crowley, D. E. (2005). Normalization of soil DNA extraction for accurate quantification of target genes by real-time PCR and DGGE. *Biotechniques* 38, 579–586. doi: 10.2144/05384ST04

Passera, A., Vacchini, V., Cocetta, G., Arpanahi, A. A., Casati, P., Ferrante, A., et al. (2020). Towards nutrition-sensitive agriculture: an evaluation of biocontrol effects, nutritional value, and ecological impact of bacterial inoculants. *Sci. Total Environ.* 724:138127. doi: 10.1016/j.scitotenv.2020.138127

Pedraza, R. O., Bellone, C. H., de Bellone, S. C., Sorte, P. M. F. B., and dos Santos Teixeira, K. R. (2009). *Azospirillum* inoculation and nitrogen fertilization effect on grain yield and on the diversity of endophytic bacteria in the phyllosphere of rice rainfed crop. *Eur. J. Soil Biol.* 45, 36–43. doi: 10.1016/j.ejsobi.2008.09.007

Pellegrini, M., Spera, D. M., Ercole, C., and Del Gallo, M. (2021). *Allium cepa* L. inoculation with a consortium of plant growth-promoting bacteria: Effects on plants, soil, and the autochthonous microbial community. *Microorganisms* 9:639. doi: 10.3390/microorganisms9030639

Pii, Y., Mimmo, T., Tomasi, N., Terzano, R., Cesco, S., and Crecchio, C. (2015). Microbial interactions in the rhizosphere: beneficial influences of plant growth-promoting rhizobacteria on nutrient acquisition process. A review. *Biol. Fertil. Soils* 51, 403–415. doi: 10.1007/s00374-015-0996-1

Poly, F., Jocteur Monrozier, L., and Bally, R. (2001). Improvement in the RFLP procedure for studying the diversity of *nifH* genes in communities of nitrogen fixers in soil. *Res. Microbiol.* 152, 95–103. doi: 10.1016/s0923-2508(00)01172-4

Qiao, J., Yu, X., Liang, X., Liu, Y., Borriss, R., and Liu, Y. (2017). Addition of plant-growth-promoting *Bacillus subtilis* PTS-394 on tomato rhizosphere has no durable impact on composition of root microbiome. *BMC Microbiol.* 17:131. doi: 10.1186/s12866-017-1039-x

Raaijmakers, J., Paulitz, T. C., Steinberg, C., Alabouvette, C., and Moënne-Loccoz, Y. (2009). The rhizosphere: a playground and battlefield for soilborne pathogens and beneficial microorganisms. *Plant Soil* 321, 341–361. doi: 10.1007/s11104-008-9568-6

Reed, S. C., Cleveland, C. C., and Townsend, A. R. (2011). Functional ecology of free-living nitrogen fixation: a contemporary perspective. *Annu. Rev. Ecol. Evol. Syst.* 42, 489–512. doi: 10.1146/annurev-ecolsys-102710-145034

Renoud, S., Bouffaud, M.-L., Dubost, A., Prigent-Combaret, C., Legendre, L., Moënne-Loccoz, Y., et al. (2020). Co-occurrence of rhizobacteria with nitrogen fixation and/or 1-aminocyclopropane-1-carboxylate deamination abilities in the maize rhizosphere. *FEMS Microbiol. Ecol.* 96:fiaa0622. doi: 10.1093/femsec/fiaa062

Rozier, C., Erban, A., Hamzaoui, J., Prigent-Combaret, C., Comte, G., Kopka, J., et al. (2016). Xylem sap metabolite profile changes during phytostimulation of maize by the plant growth-promoting rhizobacterium, *Azospirillum lipoferum* CRT1. *Metabolomics (Los Angel)* 6, 1–10.

Rozier, C., Gerin, F., Czarnes, S., and Legendre, L. (2019). Biopriming of maize germination by the plant growth-promoting rhizobacterium *Azospirillum lipoferum* CRT1. *J. Plant Physiol.* 237, 111–119. doi: 10.1016/j.jplph.2019.04.011

Rozier, C., Hamzaoui, J., Lemoine, D., Czarnes, S., and Legendre, L. (2017). Field-based assessment of the mechanism of maize yield enhancement by *Azospirillum lipoferum* CRT1. *Sci. Rep.* 7:7416. doi: 10.1038/s41598-017-07929-8

Russo, A., Felici, C., Toffanin, A., Götz, M., Collados, C., Barea, J. M., et al. (2005). Effect of *Azospirillum* inoculants on arbuscular mycorrhiza establishment in wheat and maize plants. *Biol. Fertil. Soils* 41, 301–309. doi: 10.1007/s00374-005-0854-7

Sarabia, M., Cazares, S., González-Rodríguez, A., Mora, F., Carreón-Abud, Y., and Larsen, J. (2018). Plant growth promotion traits of rhizosphere yeasts and their response to soil characteristics and crop cycle in maize agroecosystems. *Rhizosphere* 6:67–73.

Schimel, J., and Schaeffer, S. M. (2012). Microbial control over carbon cycling in soil. *Front. Microbiol.* 3:348. doi: 10.3389/fmicb.2012.00348

Schmidt, J. E., and Gaudin, A. C. M. (2018). What is the agronomic potential of biofertilizers for maize? A meta-analysis. *FEMS Microbiol. Ecol.* 94, fiy094. doi: 10.1093/femsec/fiy094

Schreiter, S., Ding, G. C., Grosch, R., Kropf, S., Antweiler, K., and Smalla, K. (2014). Soil type-dependent effects of a potential biocontrol inoculant on indigenous bacterial communities in the rhizosphere of field-grown lettuce. *FEMS Microbiol. Ecol.* 90, 718–730. doi: 10.1111/1574-6941.12430

Steenhoudt, O., and Vanderleyden, J. (2000). *Azospirillum*, a free-living nitrogen-fixing bacterium closely associated with grasses: genetic, biochemical and ecological aspects. *FEMS Microbiol. Rev.* 24, 487–506. doi: 10.1111/j.1574-6976.2000.tb00552.x

Tapia-Hernández, A., Mascarua-Esparza, M., and Caballero-Mellado, J. (1990). Production of bacteriocins and siderophore-like activity by *Azospirillum brasilense*. *Microbios* 64, 73–83.

Thioulouse, J., Prin, Y., and Duponnois, R. (2012). Multivariate analyses in soil microbial ecology: a new paradigm. *Environ. Ecol. Stat.* 19, 499–520. doi: 10.1007/s10651-012-0198-z

Tortora, M. L., Díaz-Ricci, J. C., and Pedraza, R. O. (2011). *Azospirillum brasilense* siderophores with antifungal activity against *Colletotrichum acutatum*. Arch. Microbiol. 193, 275–286. doi: 10.1007/s00203-010-0672-7

Trabelsi, D., and Mhamdi, R. (2013). Microbial inoculants and their impact on soil microbial communities: a review. *BioMed Res. Int.* 2013:863240. doi: 10.1155/2013/863240

Vacheron, J., Desbrosses, G., Bouffaud, M.-L., Touraine, B., Moënne-Loccoz, Y., Muller, D., et al. (2013). Plant growth-promoting rhizobacteria and root system functioning. *Front. Plant Sci.* 4:356. doi: 10.3389/fpls.2013.00356

Volpin, H., Burdman, S., Castro-Sowinski, S., Kapulnik, Y., and Okon, Y. (1996). Inoculation with *Azospirillum* increased exudation of rhizobial *nod*-gene inducers by alfalfa roots. *Mol. Plant Microbe Interact.* 9, 388–394. doi: 10.1094/mpmi-9-0388

Walker, V., Bertrand, C., Bellvert, F., Moënne-Loccoz, Y., Bally, R., and Comte, G. (2011). Host plant secondary metabolite profiling shows a complex, strain-dependent response of maize to plant growth-promoting rhizobacteria of the genus *Azospirillum*. *New Phytol.* 189, 494–506. doi: 10.1111/j.1469-8137.2010.03484.x

Yang, B., Wang, Y., and Qian, P.-Y. (2016). Sensitivity and correlation of hypervariable regions in 16S rRNA genes in phylogenetic analysis. *BMC Bioinformatics* 17:135. doi: 10.1186/s12859-016-0992-y

Conflict of Interest: The authors declare that the research was conducted in the absence of any commercial or financial relationships that could be construed as a potential conflict of interest.

Publisher's Note: All claims expressed in this article are solely those of the authors and do not necessarily represent those of their affiliated organizations, or those of the publisher, the editors and the reviewers. Any product that may be evaluated in this article, or claim that may be made by its manufacturer, is not guaranteed or endorsed by the publisher.

frontiers in Microbiology

ORIGINAL RESEARCH
published: 03 February 2022
doi: 10.3389/fmicb.2021.785110

Succession Pattern in Soil Micro-Ecology Under Tobacco (*Nicotiana tabacum* L.) Continuous Cropping Circumstances in Yunnan Province of Southwest China

*Dan Chen[1], Yujie Zhou[1], Mei Wang[1], Mehr Ahmed Mujtaba Munir[1], Jiapan Lian[1], Song Yu[1], Kuai Dai[2] and Xiaoe Yang[1]**

[1] *Ministry of Education Key Laboratory of Environment Remediation and Ecological Health, College of Environmental and Resource Sciences, Zhejiang University, Hangzhou, China,* [2] *Yuxi Tobacco Company, Ltd. of Yunnan Province, Yuxi, China*

OPEN ACCESS

Edited by:
Xun Wen Chen, Southern University of Science and Technology, China

Reviewed by:
Giorgia Pertile, Institute of Agrophysics, Polish Academy of Sciences (PAN), Poland
Tengxiang Lian, South China Agricultural University, China

***Correspondence:**
Xiaoe Yang
xeyang@zju.edu.cn

Specialty section:
This article was submitted to Terrestrial Microbiology, a section of the journal Frontiers in Microbiology

Received: *28 September 2021*
Accepted: *08 December 2021*
Published: *03 February 2022*

Citation:
Chen D, Zhou Y, Wang M, Mujtaba Munir MA, Lian J, Yu S, Dai K and Yang X (2022) Succession Pattern in Soil Micro-Ecology Under Tobacco (Nicotiana tabacum L.) Continuous Cropping Circumstances in Yunnan Province of Southwest China. Front. Microbiol. 12:785110. doi: 10.3389/fmicb.2021.785110

Continuous cropping obstacle (CCO) is a common phenomenon in agricultural production and extremely threatens the sustainable development of agriculture. To clarify the potential keystone factors causing tobacco (*Nicotiana tabacum* L.) CCO, tobacco plants, topsoil, and rhizosphere soil were sampled from the fields with no, slight, and severe tobacco disease in Dali and Yuxi of Yunnan province in China. The physicochemical properties of topsoil and rhizosphere soil, the phenolic acids (PAs) contents in rhizosphere soil, and elemental contents in topsoil, rhizosphere soil, and tobacco plants were analyzed. Microbial diversity in rhizosphere soil was determined by the metagenomic sequencing method. The results showed that soil pH, texture, cation exchange capacity, organic matter, TC, TN, and available K contents showed a significant difference ($p < 0.05$) in soil physicochemical properties. There was a deficiency of B, K, Mg, and Mn contents in soil and/or tobacco plants. The contents of PAs, especially syringic acid in rhizosphere soil, varied significantly among the three sampling groups ($p < 0.05$). Meanwhile, microbial communities and functional genes changed from beneficial to harmful, showing an intimate correlation with soil pH and syringic acid content. It can be concluded that tobacco CCO could be allocated to the imbalance of soil micro-ecology, which possessed a regional feature at the two sampling sites.

Keywords: tobacco cultivating, continuous cropping obstacle, soil micro-ecology, succession pattern, metagenomic sequencing

INTRODUCTION

Continuous cropping (CC) in the same field has been widespread in China and even all over the world as the result of the limited soil resources, the driving of economic benefits, and the lack of reasonable cropping concept (Zhang et al., 2013; Yuan et al., 2014). Recently, it has been reported that over 20% of the land in China had displayed severe negative consequences of CC, which is

called continuous cropping obstacle (CCO) (Bai et al., 2019). CCO refers to the phenomenon that constant cultivation of the same plants or closely related plants in the same field can cause stunted plant growth, a favorable environment for plant pests and diseases, and the reduction in plant yield and quality, even under normal cultivating circumstances (Zhang et al., 2013). CCO is listed as one of the major problems and challenges in agricultural production. It has caused enormous economic losses annually and threatened agricultural sustainable development, provoking an increasing concern about the problems associated with it (Bonner and Galson, 1944; Qu and Wang, 2008).

There are three main causes of CCO, namely, deterioration of soil physicochemical properties, accumulation of plant allelopathic substances (primarily phenolic acids), and altered soil microbial diversity, which can be collectively referred to as imbalance of soil micro-ecological environment (Zhou and Wu, 2012; Yin et al., 2016; Chen et al., 2018; Bai et al., 2019). What is noteworthy is that these three parts react close to each other and ultimately cause huge economic and ecological losses. Phenolic acids (PAs), classified as small molecular organic substances and secondary metabolites, can destroy the plant antioxidant system (Hiradate et al., 2005), restrain primary and secondary root growth, and the basal respiration of plant roots under a specific concentration (Gao et al., 2009). PAs can damage the mitochondria, plastids, nuclear membrane, and endoplasmic reticulum membrane to various extents, including membrane structure and function changes in plants (Chen et al., 2005; Wu and Ma, 2006). Meanwhile, PAs have negative influences on seed germination and seedling's normal growth. For instance, Ren et al. (2015) verified that the allelochemicals in tobacco rhizosphere soil played an apparate negative role in seed germination, plant growth, and development of tobacco. Different plant species generate special plant-related types of PAs. The release pathways of PAs into the soil include plant evaporation, leaching, root secretion, and the degradation of litter and residues (Weir et al., 2004). As a result, unique PAs can accumulate in the soil after year's and year's cropping of the same plant. This phenomenon has been demonstrated in the rhizosphere soil of CC plants, such as tobacco (Bai et al., 2019; Chen et al., 2019). When PAs enter the soil, they can change microbial community structure and diversity as C/N sources. Qu and Wang (2008) found that -phenol 2,4-di-tert-butylphenol and vanillic acid influenced microbial biomass, activity, and community composition in an incubation experiment. In a CC field, the microbial communities were changed constantly under exposure to root exudates with crop-specific microorganisms enriched (Chen et al., 2018). Microorganisms in the soil also affect PAs content, persistence, availability, and allelopathy through degradation (Inderjit, 2005). Soil microbes are vital for maintaining soil quality and ecosystem, including the turnover of organic matter (OM), the degradation of toxic substances, the acceleration of nutrient availability, and the improvement of stress tolerance to pathogens to regulate soil-borne diseases (Brussaard et al., 2007a,b). Henceforth, soil microbial communities are crucial to plant establishment and normal growth (Epelde et al., 2010).

Several studies have shown that long-term monocropping leads to changes in the soil microbial community composition, structure, activity, and function in many plants sensitive to CC (Chen et al., 2018; Gao et al., 2019; Liu et al., 2019; Pang et al., 2021). It revealed that the soil bacterial community structure changed significantly under long-term CC of tobacco (*Nicotiana tabacum* L.). The bacterial diversity also reduced with the duration of cropping (Bai et al., 2019). Pang et al. (2021) found that different Kyoto Encyclopedia of Genes and Genomes (KEGG) pathways were accumulated in different CC years of sugarcane. The bacteria in rhizosphere soil related to nitrogen and sulfur cycling decreased, and the pathogenic bacteria enriched (Pang et al., 2021). Tobacco is typical among these plants sensitive to CC. It has been used as a model crop in many fundamental studies, including agriculture, biology, and medicine (Echeverria and Zeitlin, 2012; Nielsen et al., 2012; Sierro et al., 2014). It is well known that nicotine is unique in the components of tobacco. The occurrence of Parkinson's and Alzheimer's diseases can decline under the action of nicotine, which can regulate the central nervous system when entering a human being's body (Echeverria and Zeitlin, 2012; Nielsen et al., 2012). Recently, about one-third of the world's tobacco has been planted in China, and the tobacco industry in China has attributed to approximately 10% of total Chinese revenue as the maximal single revenue source (Zou et al., 2018). Meanwhile, tobacco has been the dominating income source for millions of farmers in China as an economic crop, especially in poor areas, such as in Yunnan and Guizhou province. The tobacco industry plays an essential role in poverty alleviation regions (Hu et al., 2010). However, CCO in tobacco cultivation is also commonly associated with stunted growth, decreased yield, poor quality, and the occurrence of a wide range of destructive soil-borne diseases due to CC (Niu et al., 2017; Chen et al., 2018). It has caused huge economic losses and constrained intensive production.

Although the studies concerning microbial change under CC have widely existed, they usually only focus on the bacterial or/and fungal community composition and diversity, without considering other microorganisms and their functions in soil. Therefore, it is preferable and advised to take the entire microorganisms into consideration under the technology of metagenome sequencing. It can provide us with more information, more accurate results, and maybe new discoveries. Meanwhile, limited studies focus on a soil micro-ecology perspective, and it is unclear that the reasons for CCO in tobacco are coherent or not at different places. The objectives of the present study are the following: (1) to explore the factors that have significant differences and their succession pattern with different levels of tobacco disease under CC circumstances; (2) to further find the key factors contributing to different disease groups; and (3) to elucidate the relationship between the crucial factors and the underlying mechanisms causing tobacco CCO from a soil micro-ecology perspective at the last stage.

MATERIALS AND METHODS

Soil and Tobacco Sampling

Yunnan province is the largest province of tobacco yield and cultivating area in China. We collected two soil and tobacco varieties from Yunnan province with a tropical and subtropical plateau climate, paddy soil cultivating Honghuadajinyuan from Dali city, and red soil cultivating K326 from Yuxi city. Three adjacent fields with the constant natural environment, management methods, and different levels of tobacco disease were chosen in each type of soil, including non-diseased (the disease rate $< 5\%$, named as D1 in Dali and Y1 in Yuxi), slightly diseased (the disease rate approximately 20%, named as D2 in Dali and Y2 in Yuxi), and severely diseased (the disease rate $> 70\%$, named as D3 in Dali and Y3 in Yuxi) groups. The basic information about the sampling groups is listed in **Supplementary Table S1**. The two varieties of tobacco were cultivated according to the local optimal production technology. Twelve tobacco plants of uniformly same size were chosen, and roots were carefully dug up. The non-rhizosphere soil (attached to the root surface loosely) was removed by shaking heavily, and the rhizosphere soil (0–5 mm away from the root) of four tobacco plants was gently collected to form one sample. Immediately, about 50 g of rhizosphere soil per sample was put into an incubator with ice bags, taken back to the laboratory, and put into the -80°C refrigerator for the determination of PAs contents and microbial metagenome. The remaining rhizosphere soil was subjected to analysis of the physicochemical properties and elemental contents. Meanwhile, we collected the four tobacco plants for the measurement of elemental contents. Topsoil (0–20 cm) near the four chosen tobaccos was collected to form a 1-kg mixed topsoil sample. There were three independent repetitions per field for a total of 18 tobacco root, 18 tobacco stem, 18 tobacco leaf, 18 topsoil, and 18 rhizosphere soil samples.

Determination of Soil Physicochemical Properties

The soil was air-dried, ground, and sieved to pass through a 2-mm mesh for the analysis of soil pH, texture, available K, available P, and nitrate-nitrogen (NO_3-N) contents, and through a 0.15-mm sieve for the determination of OM, cation exchange capacity (CEC), and total carbon and nitrogen (TC and TN) contents. The soil pH was analyzed by a pH parameter (soil:water = 1:2.5, Multiparameter SevenExcellence, Shanghai, China) (Bao, 2000). The available K was extracted in ammonium acetate solution and evaluated by an atomic absorption spectrometer (AAS, Analytik Jena novAA 300, Germany) method (Bao, 2000). The available P in acid and alkaline soil was extracted in HCl-H_2SO_4 and $NaHCO_3$ solution, respectively, and then determined by the ultraviolet spectrophotometer (UV-1890, Daojin Instrument Co., Ltd., Jiangsu, China) method (Bao, 2000). The NO_3-N was extracted in potassium chloride solution and determined by the ultraviolet spectrophotometer (UV-1890, Daojin Instrument Co., Ltd., Jiangsu, China) method (Ministry of Agriculture of the People's Republic of China GB/T 32737-2016, 2016). The bulk density of soil was analyzed by cutting rings (Ministry of Agriculture of the People's Republic of China NY/T 1121.4-2006, 2006). Soil texture was measured according to the hydrometer method (Ministry of Agriculture of the People's Republic of China NY/T 1121.3-2006, 2006). The OM was determined through the potassium dichromate-sulfuric acid method (Bao, 2000). The extraction of soil in hexammine cobalt trichloride solution was performed to analyze CEC by the ultraviolet spectrophotometer (UV-1890, Daojin Instrument Co., Ltd., Jiangsu, China) method (Ministry of Environmental Protection of the People's Republic of China HJ 889-2017, 2017). The TC and TN contents in topsoil and rhizosphere soil were determined through an elemental analyzer (Elemental Vario EL Cube, Germany).

Determination of Elemental Contents in Topsoil, Rhizosphere Soil, and Tobacco

Plant and soil samples (0.1–0.2 g) were digested with HNO_3-H_2O_2 (5:1, v/v) and HNO_3-$HClO_4$-HF (5:1:1, v/v/v), respectively (Bao, 2000). The digestion solutions were diluted with ultrapure water, then filtered through 0.45-μm filters. Elemental (K/Ca/Mg/S/Fe/B/Mn/Mo/Zn/Cu) contents in the filtrate were determined by an inductively coupled plasma optical emission spectrometer (ICP-OES, iCAP 6000 series, Thermo Scientific, United States). Certified soil reference sample GBW-07401 (GSS-1) and GBW-07405 (GSS-5, National Standard Detection Research Center, Beijing, China) and plant reference sample GBW-100351 (National Research Center for Certified Reference Materials of China) were included in the digestion procedure.

Determination of Phenolic Acids Contents in Rhizosphere Soil

The method for the determination of phenolic acids contents referred to Tan et al. (2008) with slight modification. Moist rhizosphere soil (15 g) was set overnight with 15 ml 1M NaOH and then was shaken at 210 rpm at 25°C for 30 min the next day. The suspension was centrifuged at 8,000 × *g* for 10 min. Ten milliliters of supernate was acidified with 12M HCl to pH 2.5 and then was set for 2 h for humic acid precipitation. After that, the suspension was centrifuged at 8,000 × *g* for 10 min, and the supernate was passed through a 0.22-μm organic filter subjected to ultra-performance liquid chromatography (UPLC, Agilent 1290, Agilent Technologies Inc., United States). The UPLC analytical conditions for PAs were as follows: chromatographic column, C_{18} (Shimadzu Inert Sustain, 4.6 × 250 mm); column temperature, 40°C; detector wavelength, 280 nm; flow velocity, 1 ml/min; and injection volume, 10 μl. The mobile phase consisted of 0.1% phosphoric acid solution (A-phase) and acetonitrile (B-phase). Seventeen types of standard PAs samples (gallic acid, phthalic acid, *p*-hydroxybenzoic acid, caffeic acid, vanillic acid, vanillin, benzoic acid, coumalic, salicylic acid, ferulic acid, sinapic, benzothiazole, *trans*-cinnamic acid, diethy phthalate, benzyl benzoate, 4-methylphenyl benzoate, and syringic acid) were measured for the retention time and peak size under a certain concentration. The kinds and concentrations of PAs in rhizosphere soil samples were identified by comparing retention time and peak size with respective standards.

Microbial Metagenome Analysis in Rhizosphere Soil

Extraction and Purification of Soil Microbial DNA

The rhizosphere soil in non-diseased and severely diseased groups from Dali and Yuxi was subjected to soil microbial metagenome analysis. There were a total of 12 samples. Rhizosphere soil (0.5 g) was weighted for DNA extraction. According to the manufacturer's protocol, the total DNA of soil was extracted by following the instructions of PowerSoil® DNA Isolation Kit (Qiagen Gmbh, Qiagen Strasse 1, 40724 Hilden, Germany). The purity and concentration of DNA were determined based on the 260/280 and 260/230 nm ratios through a micro-spectrophotometer (Nano-300, Allsheng, Hangzhou, China). DNA integrity was determined by 1.0% agarose gel electrophoresis and visualized. The sufficient qualified DNA was used for the library preparation and metagenomic sequencing on the Illumina novaseq6000 platform (NEB, United States).

Genome Assembly, Non-redundant Gene Catalog Construction, and Gene Function Annotation

We filtered raw tags to get clean tags by using Trimmomatic v0.33, with a quality cutoff of 20. The reads shorter than 100 bp were discarded from the sample. Simultaneously, the reads that were likely to originate from the host were removed using Bowtie2 v2.2.4, referencing the National Center for Biotechnology Information (NCBI) tobacco genome sequences. The remaining high-quality reads of all samples (6.26–7.19 Gb per sample) were taken together and assembled into contigs using MEGAHIT v1.1.2 (Li et al., 2015). We discarded the contigs shorter than 300 bp and assessed the assembly results through QUAST v2.3 (Gurevich et al., 2013). MetaGeneMark v3.26[1] was used for genes prediction from the contigs (Zhu et al., 2010). Predicted genes from all samples were gathered together to form a large gene catalog. The non-redundant gene catalog was constructed by using CD-HIT v4.6.6[2] (Fu et al., 2012). Any two genes with over 95% similarity and 90% coverage of the shorter one were picked out, and subsequently, the shorter one was removed from the large gene catalog. Taxonomic and functional annotations were performed by Diamond v0.9.24 combined with KEGG database (2017-03, blastp, *e*-value $\leq$ 1e-5[3]) (Kanehisa et al., 2004). The KOs were classified into higher KEGG categories and KEGG pathways.

Statistical Analysis

Statistical analysis, except for microbial data, was performed by SPSS 26.0. One-way ANOVA analysis of variance followed by Duncan's test was carried out on the data at the level of significance ($p < 0.05$). For the beta diversity of microbial communities and functional genes, permutational multivariate analysis of variance (PERMANOVA) was used to determine the significance of principal coordinate analysis (PCoA) through the Bray–Curtis dissimilarity. The significance of Bray–Curtis non-metric multidimensional scaling (nMDS) was measured by analysis of similarities (ANOSIM) test. The R package of metagenomeSeq was used to assess the relative abundance of the microbial community at the phyla level and functional genes based on the KEGG metabolic pathways (Segata et al., 2011). The biomarkers among different groups were gained from linear discriminant analysis effect size (LEfSe) and random forest analyses. The correlation between the relative abundance of microbial communities, functional genes, and soil environmental factors was analyzed by correlation heatmap and redundancy analysis (RDA). PCoA, nMDS, metagenomeSeq, LEfSe, random forest, correlation heatmap, and RDA were performed by R 3.1.1. PERMANOVA and ANOSIM tests were achieved by QIIME 1.8.0 (Caporaso et al., 2010).

[1]http://exon.gatech.edu/meta_gmhmmp.cgi

[2]http://www.bioinformatics.org/cd-hit/

[3]http://www.genome.jp/kegg/pathway.html

RESULTS

Soil Physicochemical Properties

The results of soil physicochemical properties are presented in **Table 1**. The pH in the topsoil and rhizosphere soil from Dali increased significantly ($p < 0.01$) with the increase in disease rate. However, the topsoil and rhizosphere soil from Yuxi showed an opposite tendency. The OM content increased with the increase in disease rate, with a more evident phenomenon in the soil from Yuxi, which showed an extremely remarkable difference ($p < 0.01$) among the three groups. For the NO_3-N content, there was no apparent pattern in the topsoil or rhizosphere soil from Dali or Yuxi. The available P content in the topsoil and rhizosphere soil showed a considerable increase ($p < 0.05$) in the severely diseased group from Dali, with no such phenomenon in the soil from Yuxi. The available K content in the topsoil decreased apparently in the severely diseased groups. However, it showed an opposite trend in the rhizosphere soil from Dali and Yuxi. The CEC was higher in the diseased groups than in the non-diseased groups from Dali and Yuxi. There was a negative correlation between bulk density and tobacco disease rate in the topsoil from Yuxi but not in the topsoil from Dali. Simultaneously, the topsoil had more sand and less silt component in the diseased group from Yuxi but owned less sand and more clay in the diseased group from Dali. In general, the contents of TC and TN in the topsoil and rhizosphere soil were higher in the severely diseased groups than in the non-diseased groups from Dali and Yuxi, and the rhizosphere soil showed a more pronounced trend than the topsoil.

Elemental Contents in Topsoil, Rhizosphere Soil, and Tobacco

We detected 10 kinds of elements (K/Ca/Mg/S/Fe/B/Mn/Mo/Zn/Cu) in topsoil, rhizosphere soil, and tobacco. Only the elements whose contents showed a significant difference ($p < 0.05$) among the three groups are presented (**Figures 1**, **2**). For the soil from Dali, only the content of Mn increased evidently ($p < 0.05$) in the topsoil of the diseased group (**Figure 1A**). For the soil from Yuxi, there was a declined trend in the contents of B, Ca, K, Mg, and Mn in the topsoil of the diseased group (**Figure 1B**). The contents of these elements showed a similar tendency in the rhizosphere

TABLE 1 | The physicochemical properties in the topsoil and rhizosphere soil from Dali and Yuxi.

	pH	OM (g/kg)	NO_3-N (mg/kg)	Available P (mg/kg)	Available K (mg/kg)	CEC ($cmol^+$/kg)	TC (%)	TN (%)	Bulk density (g/cm^3)	Sand (%)	Silt (%)	Clay (%)
D1	6.07^b	34.55^a	56.33^{ab}	47.10^b	261.89^a	10.34^c	2.76^b	0.27^b	1.27^a	6.65^a	55.92^a	37.43^c
D2	7.25^a	35.63^a	77.91^a	20.28^c	165.38^b	17.08^a	2.68^b	0.29^a	1.29^a	3.53^c	54.13^b	42.34^a
D3	7.32^a	36.28^a	17.72^b	61.51^a	211.17^{ab}	14.63^b	2.90^a	0.28^{ab}	1.30^a	5.27^b	55.78^a	38.96^b
Y1	7.65^a	26.96^c	8.77^{ab}	54.23^a	165.51^b	13.21^c	2.97^a	0.18^c	1.18^a	5.70^c	59.41^a	34.90^a
Y2	7.33^a	40.22^b	4.23^b	58.06^a	226.41^a	28.13^a	2.97^a	0.22^b	1.13^{ab}	10.54^b	50.29^b	39.16^a
Y3	6.19^b	52.04^a	16.27^a	55.53^a	98.18^c	17.36^b	3.17^a	0.26^a	0.98^b	19.17^a	46.45^c	34.38^a
DR1	5.93^b	36.23^b	4.74^a	46.67^c	182.84^b	9.99^c	2.77^{ab}	0.25^c		/		
DR2	6.94^a	35.92^b	6.67^a	87.46^b	281.81^a	10.14^b	2.75^b	0.29^b				
DR3	6.87^a	40.80^a	14.11^a	111.30^a	277.05^a	15.02^a	3.05^a	0.29^a				
YR1	7.79^a	41.51^b	9.99^a	48.37^a	106.39^b	13.59^c	3.06^b	0.18^c		/		
YR2	7.30^a	46.77^b	6.41^a	42.40^a	200.96^{ab}	22.98^a	2.92^b	0.22^b				
YR3	6.38^b	59.44^a	12.74^a	51.36^a	249.38^a	18.10^b	3.38^a	0.26^a				

D1, D2, and D3 represent the topsoil in non-, slightly, and severely diseased groups from Dali, respectively; those followed by "R" represent the corresponding rhizosphere soil. Y1, Y2, and Y3 represent the corresponding samples from Yuxi. Different letters show a significant difference within a column in the physicochemical properties of topsoil or rhizosphere soil based on the Duncan's method ($p < 0.05$).

soil except for B and Mn (**Figure 1C**). There was an appreciable increase ($p < 0.05$) in the contents of Cu, Fe, S, and Zn in the diseased group's topsoil and rhizosphere soil (**Figures 1B,C**).

For the tobacco collected from Dali, there was an apparent declined trend in B and K contents of tobacco roots in the diseased group ($p < 0.05$) (**Figure 2A**). The Ca and Fe contents of tobacco stems decreased, whereas tobacco leaves increased obviously ($p < 0.05$) in the severely diseased group (**Figures 2B,C**). As for the tobacco collected from Yuxi, the B, K, Mn, and Mg contents of tobacco roots declined evidently in the diseased group ($p < 0.05$) (**Figure 2D**). The B and Mg contents of tobacco stems decreased obviously in the diseased group, but the Mn content increased apparently ($p < 0.05$) (**Figure 2E**). There was an obvious decrease in the Mn and Mg contents in tobacco leaves of the diseased group (**Figure 2F**). The B and K contents in tobacco roots decreased remarkably in the diseased groups both from Dali and Yuxi. There was a marked decrease ($p < 0.05$) in Mg content of tobacco roots, stems, and leaves in the diseased group from Yuxi. Overall, it showed a similar declined trend for B, K, Mn, and Mg contents in the topsoil and roots of the diseased group from Yuxi, without such pattern for Cu, Fe, S, and Zn contents. The differences in the contents of the analyzed elements were more apparent in the soil and tobacco collected from Yuxi than from Dali.

Phenolic Acids Contents in Rhizosphere Soil

Although 17 varieties of standard reference samples of PAs were prepared and determined, only five varieties (syringic acid, vanillic acid, *p*-hydroxybenzoic acid, ferulic acid, and vanillin) could be detected in the rhizosphere soil in our research (**Figure 3**). The vanillin content in the rhizosphere soil was the highest (7.78–26.03 mg/kg dry soil), followed by the ferulic acid (1.12–3.64 mg/kg dry soil), *p*-hydroxybenzoic acid (1.37–2.30 mg/kg dry soil), and vanillic acid (0.81–1.95 mg/kg dry soil). The syringic acid content was the lowest (0.60–1.47 mg/kg dry soil). The syringic acid and vanillic contents in the rhizosphere soil showed a considerable decrease ($p < 0.05$) in the diseased group from Dali. However, they showed an opposite pattern from Yuxi. Overall, there was a significant decreasing trend in the total content of the five PAs in the diseased group from Dali ($p < 0.05$), whereas the rhizosphere soil from Yuxi showed an opposite pattern.

Analysis of Microbial Community in Rhizosphere Soil

After the metagenomic sequencing, we obtained over 15,430,074 clean reads per sample (**Supplementary Table S2**). While in metagenomic assembling, we gained 84,962–193,544 contigs with the mapped ratio ranging from 37.11 to 48.97% per sample after excluding the contigs < 300 bp (**Supplementary Table S3**). Using MetaFeneMark software for gene prediction, over 445,679 genes were obtained per sample (**Supplementary Table S4**). There were a total of 6,596,898 genes with an average length of 360 bp in the non-redundant gene set based on the CD-HIT software (**Supplementary Table S5**).

Composition and Relative Abundance of Microbial Community

There were five kinds of microorganisms at the kingdom level in all rhizosphere soil samples, eukaryote, fungi, viruses, archaea, and bacteria. The bacteria owned the highest relative abundance (81.58–83.78% in all samples), followed by the archaea (0.30–0.39%), viruses (0.18–0.21%), and fungi (0.15–0.47%). The first six highest relative abundance of microorganisms at the phylum level were Proteobacteria (32.88–35.30% in all samples), Acidobacteria (10.18–11.49%), Actinobacteria (8.17–9.04%), Gemmatimonadetes (5.98–7.02%), Chloroflexi (3.48–4.63%), and Bacteroidetes (3.63–5.17%), with the average total relative abundance of 67.69% (**Figure 4A**). The first five highest relative abundance of microorganisms at the species level were *Acidobacteria bacterium* (5.22–6.18% in all samples), *Gemmatimonadetes bacterium* (2.95–3.71%),

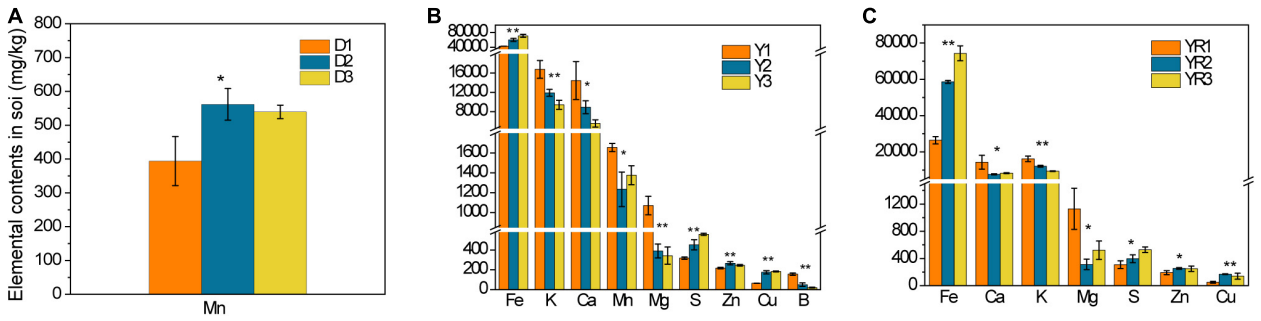

FIGURE 1 | The elemental contents in the topsoil from Dali **(A)** and Yuxi **(B)** and in the rhizosphere soil from Yuxi **(C)**. Values are the average of three replicates with a standard deviation bar. D1, D2, and D3 represent the topsoil in non-, slightly, and severely diseased groups from Dali, respectively. Y1, Y2, and Y3 represent the corresponding samples from Yuxi; those followed by "R" represent the corresponding rhizosphere soil. "**" and "*" represent the contents of the elements showing extremely significant ($p < 0.01$) and significant ($p < 0.05$) difference, respectively.

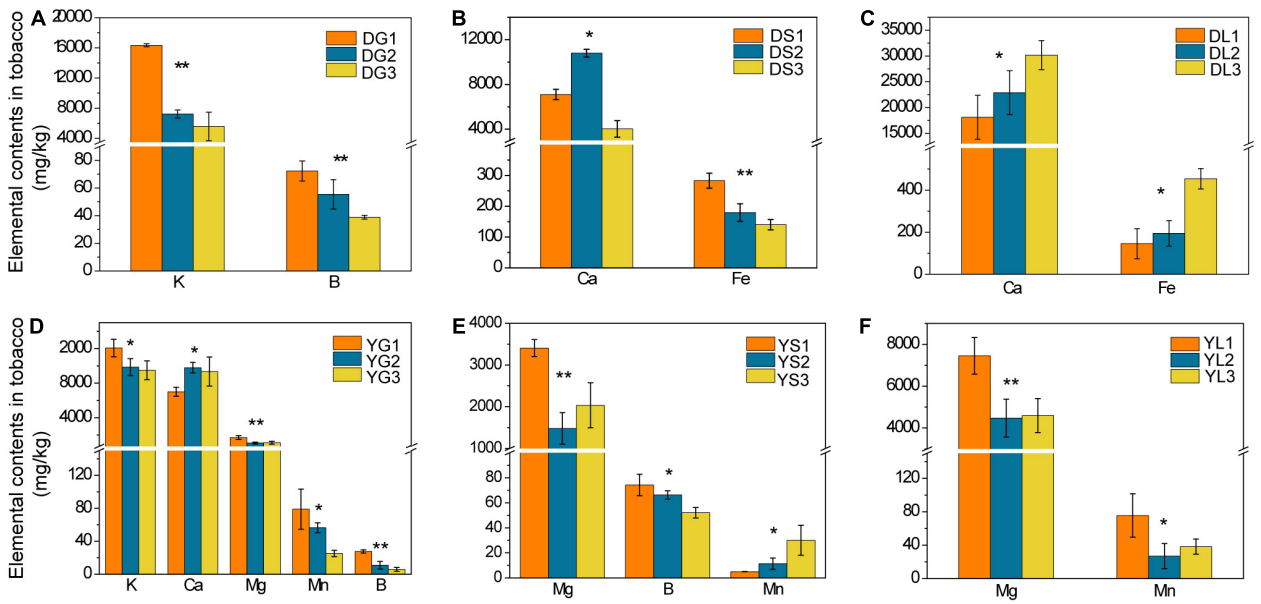

FIGURE 2 | The elemental contents in tobacco roots, stems, and leaves from Dali (**A–C**, respectively) and Yuxi (**D–F**, respectively). Values are the average of three replicates with a standard deviation bar. DG, DS, and DL represent tobacco roots, stems, and leaves from Dali, respectively; those followed by "1," "2," and "3" represent tobacco showing no, slight, and severe disease, respectively. YG, YS, and YL represent the corresponding samples from Yuxi. "**" and "*" represent the contents of the elements showing extremely significant ($p < 0.01$) and significant ($p < 0.05$) difference, respectively.

Chloroflexi bacterium (1.51–2.17%), *Verrucomicrobia bacterium* (1.31–1.73%), and *Candidatus Rokubacteria bacterium* (0.91–1.36%), with the average total relative abundance of 13.45% (**Supplementary Figure S1**).

Beta Diversity and Difference Analysis of Microbial Community

The Bray–Curtis PCoA and PERMANOVA analysis based on species showed that the severely diseased group was remarkably distinct from the non-diseased group, with the first two axes explaining 59.71 and 11.75% variance ($R^2 = 0.631$, $p = 0.002$) (**Figure 4C**). This phenomenon could also be verified from Bray–Curtis nMDS and ANOSIM analysis based on species (**Figure 4D**), which showed remarkable variations between the two groups from Dali and Yuxi (stress = 0.014, $R = 0.559$, $p = 0.002$). The distance between the two groups from Dali was farther than from Yuxi, presenting a more pronounced difference in β-diversity of microbiome from Dali than from Yuxi.

From the metagenomeSeq analysis, the heatmap of the relative abundance of the microbial community at the phylum level was divided into two parts evidently between the two groups from Dali and Yuxi (**Figures 5A,B**). Candidatus Kuenenbacteria, Candidatus Levybacteria, Coprothermobacterota, Candidatus Niyogibacteria, and Candidatus Microgenomates were enriched in the non-diseased group in Dali (**Figure 5A**). Candidatus Verstraetearchaeota, Candidatus Portnoybacteria, Candidatus Tectomicrobia, and Chloroflexi were enriched in the diseased group from Dali ($p < 10^{-4}$) (**Figure 5A**). There was no such

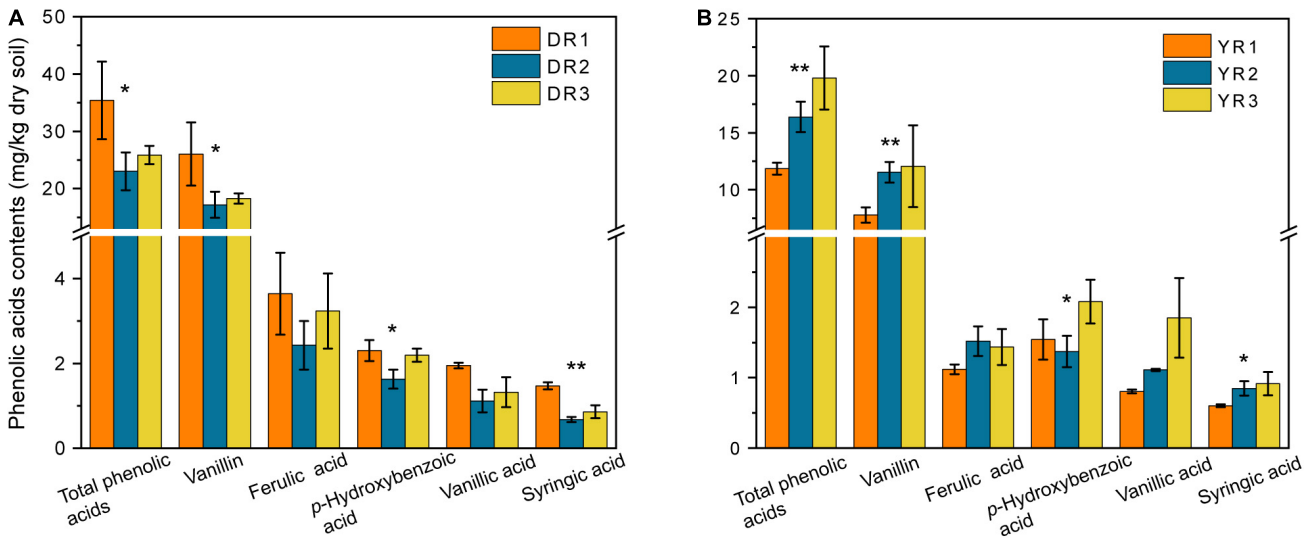

FIGURE 3 | The phenolic acid contents in the rhizosphere soil from Dali **(A)** and Yuxi **(B)**. Values are the average of three replicates with a standard deviation bar. DR1, DR2, and DR3 represent the rhizosphere soil in non-, slightly, and severely diseased groups from Dali, respectively. YR1, YR2, and YR3 represent the corresponding samples from Yuxi. "**" and "*" represent the contents of the phenolic acids showing extremely significant ($p < 0.01$) and significant ($p < 0.05$) difference, respectively.

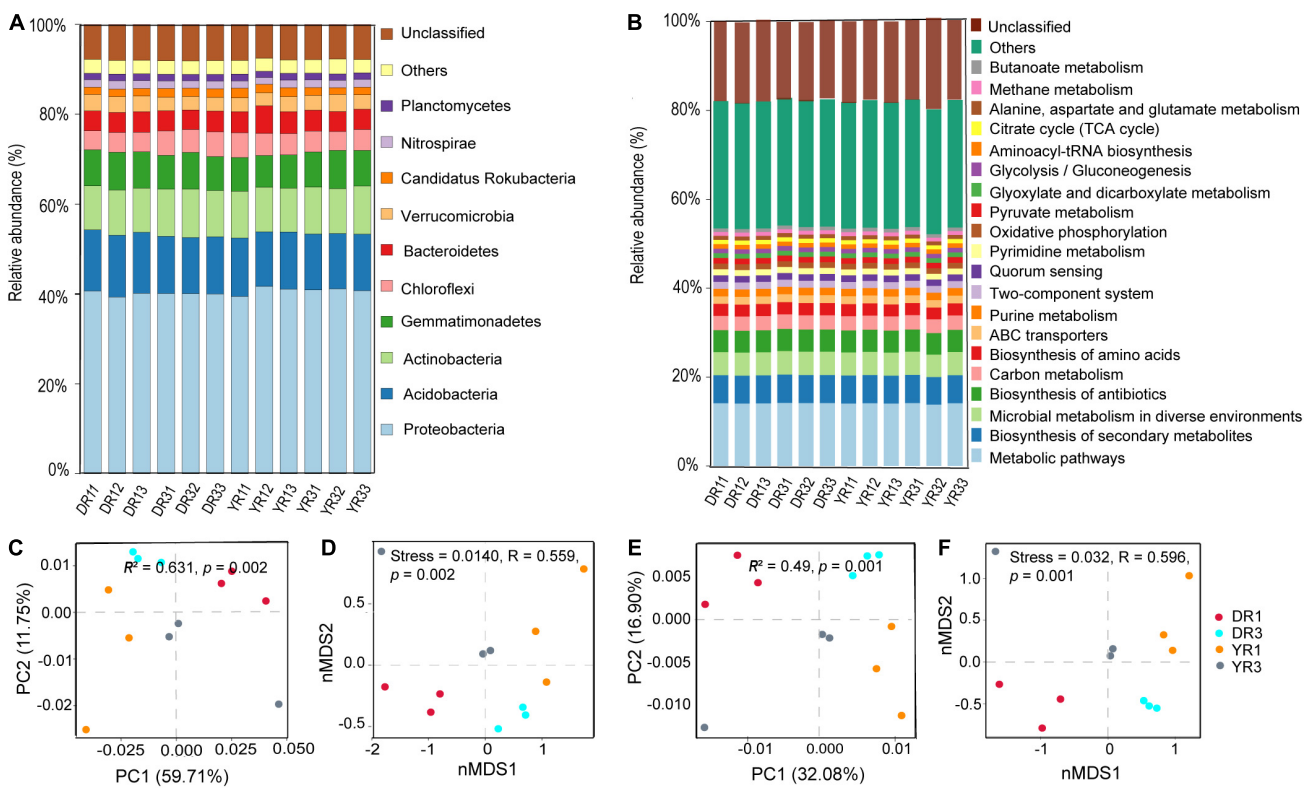

FIGURE 4 | The relative abundance and β-diversity of microbial communities and KEGG pathways. **(A)** The relative abundance of the microbial community at the phylum level. Only the first 10 most dominant microorganisms are presented. **(B)** The relative abundance of KEGG pathways at level 3. Only the first 20 most dominant KEGG pathways are presented. **(C)** Bray–Curtis PCoA and PERMANOVA analysis based on microbial species. **(D)** Bray–Curtis nMDS and ANOSIM analysis based on microbial species. **(E)** Bray–Curtis PCoA and PERMANOVA analysis based on KEGG pathways. **(F)** Bray–Curtis nMDS and ANOSIM analysis based on KEGG pathways. DR1_ and DR3_ (_ = 1, 2, 3) represent the rhizosphere soil in non- and severely diseased groups from Dali, respectively. YR1_ and YR3_ represent the corresponding samples from Yuxi.

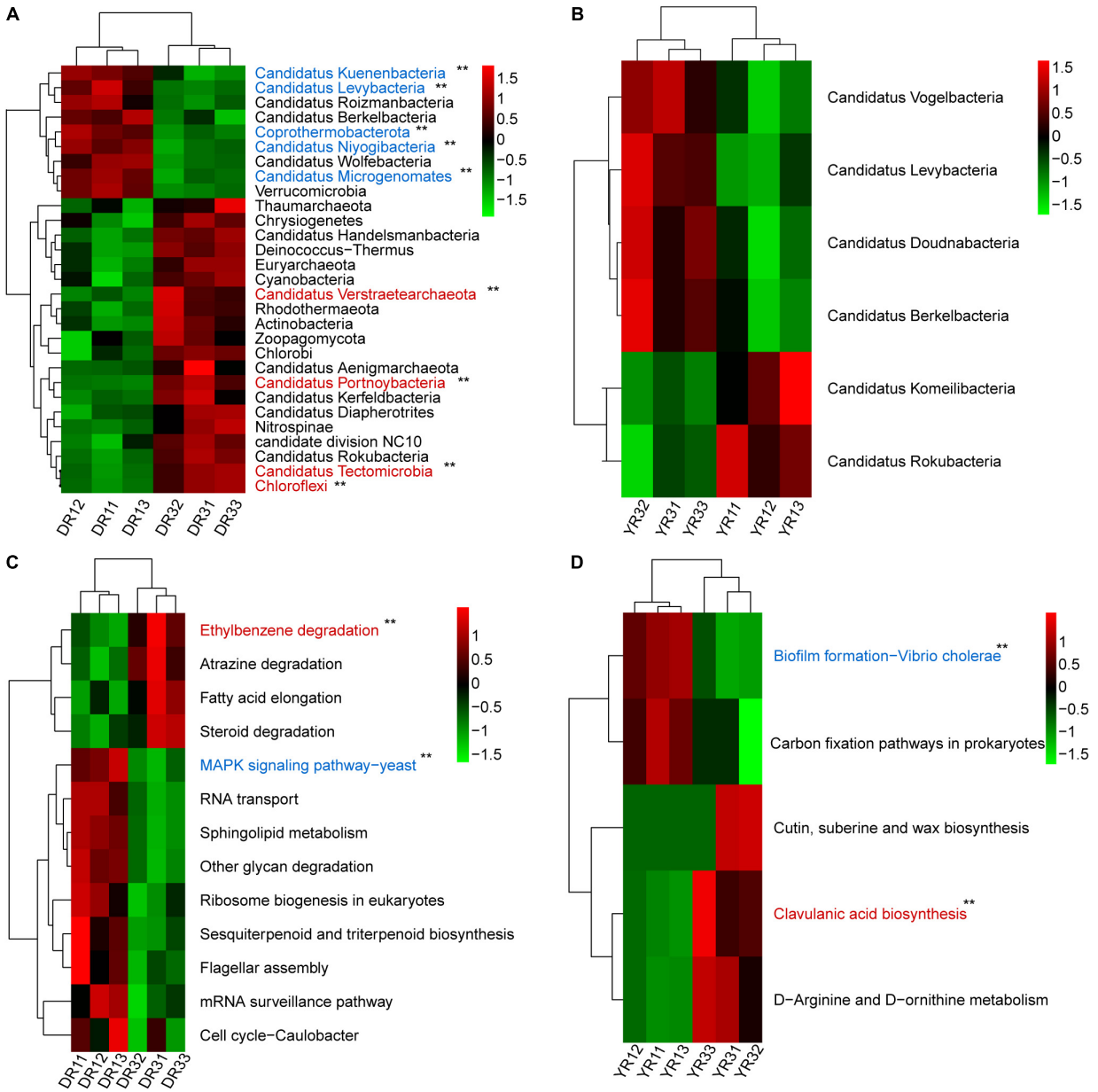

FIGURE 5 | The heatmap of difference analysis of microbial communities and KEGG pathways. **(A,B)** The heatmap of the relative abundance of microorganisms at the phylum level in Dali **(A)** and Yuxi **(B)**. **(C,D)** The heatmap of the relative abundance of KEGG pathways in Dali **(C)** and Yuxi **(D)**. Only the microorganisms and KEGG metabolic pathways are presented whose relative abundance showed a significant difference ($p < 0.05$). The p-value of the microbiome and KEGG pathways marked with "**" was $<10^{-4}$ based on the significance analysis, with the blue one enriched in the non-diseased group and the red one enriched in the severely diseased group. DR1_ and DR3_ (_ = 1, 2, 3) represent the rhizosphere soil in non- and severely diseased groups from Dali, respectively. YR1_ and YR3_ represent the corresponding samples from Yuxi.

phylum existing in the rhizosphere soil from Yuxi ($p > 10^{-4}$) (**Figure 5B**). In every group, except for the diseased group from Yuxi, there existed some biomarkers contributing to group difference based on the LEfSe analysis (**Figure 6A**). It showed that the first two most important biomarkers per group were class Alphaproteobacteria and order Phizobiales in the non-diseased group, and were phylum Chloroflexi and family Xanthomonadaceae in the diseased group from Dali (**Supplementary Figure S2**). Meanwhile, they were class Betaproteobacteria and order Burkholderiales in the non-diseased group from Yuxi (**Supplementary Figure S2**). From the random forest analysis, Candidatus Omnitrophica and Candidatus Levybacteria (enriched in the non-diseased group) and Candidatus Tectomicrobia and Chrysiogenetes (enriched in the diseased group) were the most apparent biomarkers from Dali (**Figure 6B**). They were Synergistetes and Bacteroidetes (enriched

in the non-diseased group) and Candidatus Riflebacteria and Candidatus Saccharibacteria (enriched in the diseased group) from Yuxi (**Figure 6B**).

Correlation Analysis Between Microbial Community and Environmental Factors in Rhizosphere Soil

Based on the correlation heatmap between soil microbial community at the phylum level and environmental factors in rhizosphere soil, soil pH and syringic acid (SA) were the most important factors, showing an obvious correlation ($p < 0.05$) with more microorganisms (**Figure 7A** and **Supplementary Figure S3A**). Noticeably, the relative abundance of Firmicutes and Candidatus Levybacteria had a pronounced positive relationship ($p < 0.05$) with the content of SA. One microbial group showed a positive relationship with soil pH. Simultaneously, it showed a negative interaction with SA or total phenolic acids (TPAs) (**Supplementary Figure S3A**). Based on the RDA analysis between microbial community at the species level and soil environmental factors, the first two components explained 18.56 and 11.55% of the total variance (**Figure 7C**). The three samples in the same group were grouped on a whole view, and different groups were separated primarily on the first component (RDA1). Soil pH, OM, TC, SA, and TPA contents were the most crucial environmental factors influencing the microbial community. For the non-diseased group from Dali, SA, TPA, TN, and AK had a positive effect, whereas soil pH, OM, and TC had a negative influence. Interestingly, there was an opposite phenomenon in the non-diseased group from Yuxi. Meanwhile, OM and TC showed a positive relationship with the diseased group from Yuxi.

Analysis of Microbial Functional Genes in Rhizosphere Soil

Composition and Relative Abundance of Functional Genes

Based on the KEGG analysis of functional genes, the relative abundance of KEGG pathways at level 3 in the samples is listed in **Figure 4B**. The first four dominant KEGG pathways are metabolic pathways (13.8–14.20% in all samples), biosynthesis of secondary metabolites (6.19–6.37%), microbial metabolism in diverse environments (5.05–5.28%), and biosynthesis of antibiotics (4.87–5.01%) (**Figure 4B**).

Beta Diversity and Difference Analysis of Functional Genes

The Bray–Curtis PCoA and PERMANOVA analysis at the KO level showed a distinct functional gene pattern in the non-diseased groups from the diseased groups, with the first two axes depicting 32.08 and 16.90% of the total shift ($R^2 = 0.49$, $p = 0.001$) (**Figure 4E**). The Bray–Curtis nMDS and ANOSIM analysis further confirmed this phenomenon (stress = 0.032, $R = 0.596$, $p = 0.001$) (**Figure 4F**). The difference in the β-diversity of the functional genes was more remarkable between the two groups from Dali than from Yuxi. The metagenomeSeq analysis based on the KEGG metabolic pathways showed that the heatmap of the relative abundance of functional genes was divided into two parts between the non-diseased and the diseased groups in Dali and Yuxi (**Figures 5C,D**). The abundance of genes related to mitogen-activated protein kinase (MAPK) signaling pathway yeast and ethylbenzene degradation showed a

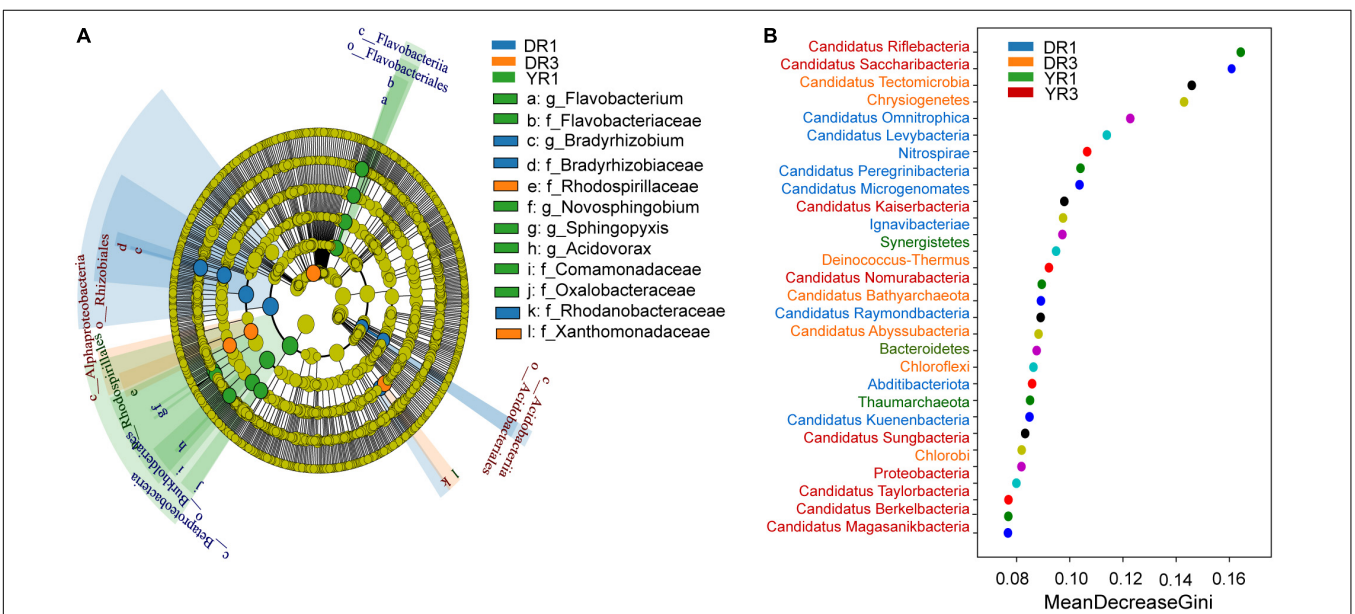

FIGURE 6 | The LEfSe and random forest analyses of microbial communities. **(A)** The cladogram of the microorganisms based on the LEfSe analysis. The threshold value of LDA is 2. The blue, orange, and green taxonomies represent the biomarkers playing an important role in the non- and severely diseased group from Dali and non-diseased group from Yuxi, respectively. No such taxonomy existed in the severely diseased group from Yuxi. The relative abundance of the yellow one showed no significant difference ($p \geq 0.05$). **(B)** The random forest analysis of the microorganisms at the phylum level. DR1 and DR3 represent the rhizosphere soil in the non- and severely diseased group from Dali, respectively. YR1 and YR3 represent the corresponding samples from Yuxi.

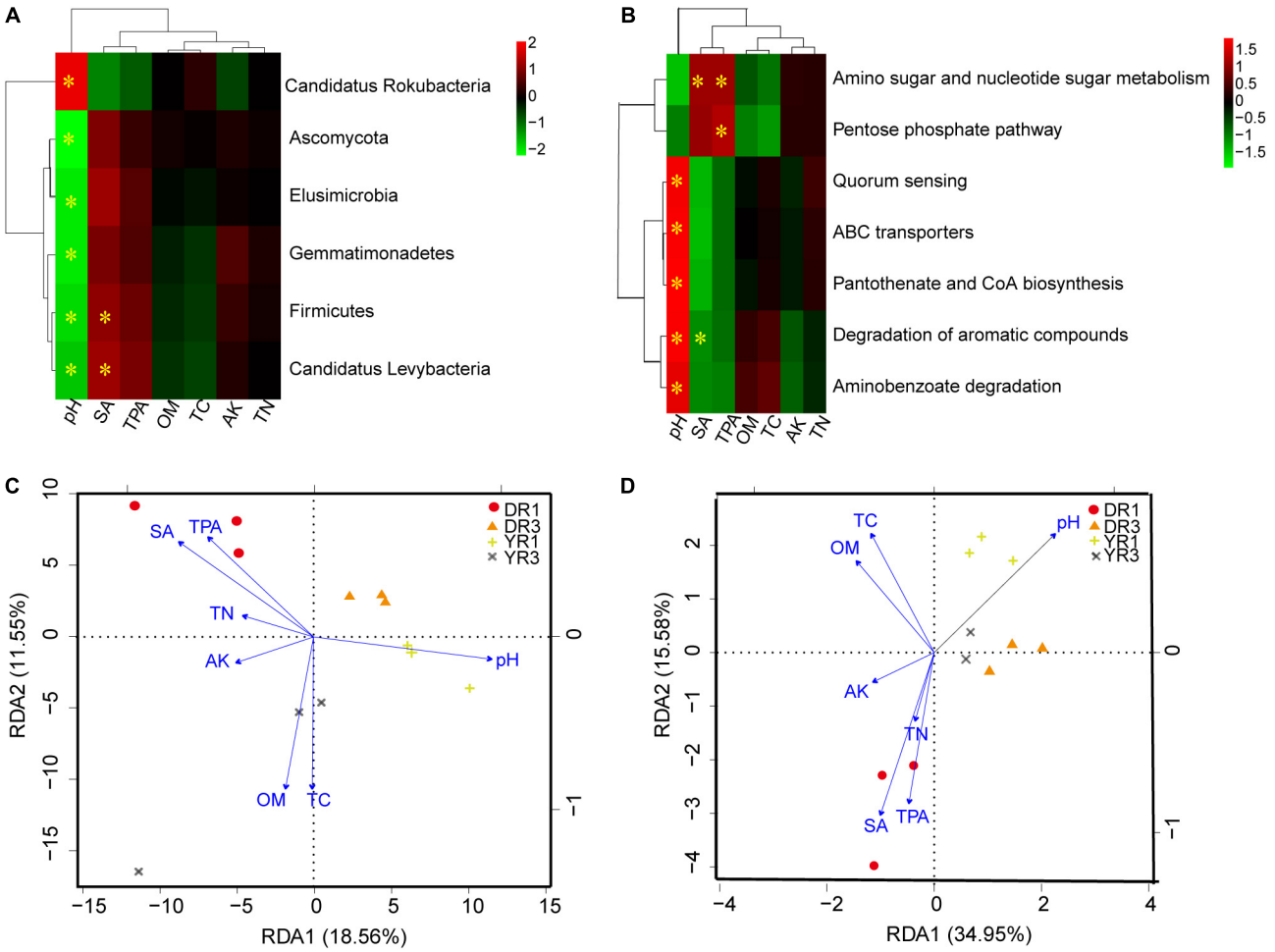

FIGURE 7 | The correlation analysis between microorganisms or KEGG pathways and soil environmental factors. **(A,B)** The correlation heatmap between microorganisms at the phylum level **(A)** or KEGG pathways **(B)** and soil environmental factors. The box marked with "*" showed a significant difference ($p < 0.05$). **(C,D)** The RDA analysis between microorganisms at the species level **(C)** or KEGG pathways **(D)** and soil environmental factors. SA, TPA, OM, TC, AK, and TN represent the contents of syringic acid, total phenolic acids, organic matter, total C, available K, and total N in rhizosphere soil. DR1 and DR3 represent the rhizosphere soil in the non- and severely diseased groups from Dali, respectively. YR1 and YR3 represent the corresponding samples from Yuxi.

significantly higher abundance in the non-diseased and diseased groups in Dali, respectively ($p < 10^{-4}$). In comparison the genes concerning biofilm formation in *Vibrio cholerae* and clavulanic acid biosynthesis were enriched in the non-diseased and diseased groups in Yuxi, respectively ($p < 10^{-4}$).

Correlation Analysis Between Microbial Functional Genes and Environmental Factors in Rhizosphere Soil

From the correlation heatmap between the relative abundance of functional genes and soil environmental factors, soil pH, SA, and TPA owned a more marked correlation with functional genes than OM, TC, AK, and TN (**Figure 7B** and **Supplementary Figure S3B**). The correlation pattern between functional genes and SA was similar to that between functional genes and TPA, which was opposite between functional genes and soil pH (**Supplementary Figure S3B**). Based on the RDA analysis, the first (34.95%) and the second axes (15.58%) explained 50.53% of the total variance (**Figure 7D**). Soil pH, SA, and TPA were the most important environmental factors contributing to the functional gene difference. The three samples from the same group were gathered, and the two diseased groups in Dali and Yuxi were assembled. However, the two non-diseased groups were separated.

DISCUSSION

The deterioration of soil physicochemical properties is a vital cause of CCO (Zhang et al., 2016; Chen et al., 2018; Bai et al., 2019). Plants absorb nutrients directly from the soil to maintain normal life activities. Simultaneously, soil provides microorganisms with nutrient, energy sources, and a suitable living environment. The microbial diversity changes with the variance in soil physicochemical properties (Chen et al., 2018; Bai et al., 2019). Based on the significance analysis, soil pH,

OM, available K, CEC, TC/TN contents, and texture were the main parameters showing differences between the two groups from Dali and Yuxi. Soil acidification is a common phenomenon in long-term CC soil (Zhang et al., 2016; Shen et al., 2018; Bai et al., 2019). Soil pH is closely correlated with tobacco soil-borne diseases, with a lower value in the diseased than non-diseased fields (Li et al., 2017). It is presented in the soil from Yuxi in the present study. However, a reverse result is observed in the soil from Dali, with a higher pH in the diseased group. It has been proposed that cation exchange and mineral weathering are two main ways for proton (H^+) consumption in soil acid-buffering mechanisms (Yang et al., 2013). The two H^+-consumption processes may have played a more dominant role than the H^+-releasing processes in the soil from Dali. The different microbial communities in the soil also contributed to the different change pattern of soil pH at the two sites. Soil organic matter (SOM) plays an important role in maintaining soil ecology as water conservation and providing plants and microbes with nutrients (Obalum et al., 2017). Interestingly, the OM content showed an increasing trend in the diseased groups, which was opposite to the results of other studies. Chen et al. (2018) found that the SOM content and soil fertility decreased in the tobacco CC field. Bai et al. (2019) discovered that soil pH, OM, and available P contents decreased in the CC field of tobacco, whereas the available K content showed an increasing trend over the cropping time. In our study, the available K content in the rhizosphere soil increased with the increase in CC years, which may be ascribed to the accumulation of K fertilizer applied annually, and the destroyed ability of diseased tobacco to absorb K^+ from the rhizosphere soil. We observed a higher CEC in the diseased groups both from Dali and Yuxi, which is coherent with the results of Mareschal et al. (2013). As for the TC and TN contents in the soil, the diseased groups showed an increasing trend in Dali and Yuxi. On the one hand, the nitrogen fertilizers application and the diseased tobacco discarded in the field contributed to the source of C and N. On the other hand, this could be owed to the lower rate of C and N element circle in the diseased groups under the influence of the unbalanced micro-ecology system (Pang et al., 2021). The abundance of genes specific to denitrification like nirK/S, norBC, and nosZ decreased after 30 years of sugarcane continuous cropping (Pang et al., 2021). Although the OM, available K, CEC, and TC/TN contents showed a similar variation trend in the soil from Dali and Yuxi, some parameters still presented an opposite tendency at the two sampling sites, like soil pH, texture, and available P content. This can be owing to the differences in soil types, tobacco varieties, natural conditions, and anthropogenic activities (Bai et al., 2019).

From the analysis of elemental contents in topsoil, rhizosphere soil, and tobacco plants, there was a phenomenon of elemental imbalance in the diseased groups. The Ca and Fe contents declined in tobacco stems but increased in tobacco leaves in the diseased group from Dali. There was a great possibility that Ca and Fe in tobacco stems were transferred to the leaves. The B, K, Mn, and Mg contents decreased consistently in the topsoil and tobacco roots of the diseased group from Yuxi. It was noticed that the deficiency of these elements in tobacco roots could partially originated from the lack of these elements in the soil. Tobacco is favorable in absorbing certain varieties of elements from the soil, and the elemental imbalance will form gradually under long-term CC, improper fertilizer application, and changed processes of soil mineral weathering (Zhang et al., 2016). Elemental imbalance in the soil or/and plants is a common phenomenon under CC circumstances and plays an important role in causing CC problems. For instance, Chen et al. (2018) presented that the content of Fe decreased evidently in the CC tobacco soil. In contrast, B showed an opposite trend, and no significant variance was observed for Ca, Mg, Na, Mn, and Zn. Zhang et al. (2016) found an obvious desilication, weathering of potassium-bearing minerals, and accumulation of Al and Fe under long-term tobacco plantation than under the fallow. Meanwhile, alterations of the mineralogical properties in topsoil is related to change in soil pH (Zhang et al., 2016). In conclusion, B, K, Mg, and Mn played an important role in tobacco disease with a noticeable declining contents in the diseased groups in our study ($p < 0.05$). B is an essential microelement for plants, having an important adjusting function in the formation of cytoderm, cell division, and C and N metabolism (Xiao, 1997; Liu, 2017). B can improve the ability of stress resistance in tobacco by enhancing tobacco root growth. Meanwhile, B influences the yield and quality of tobacco in combination with Ca and K (Xiao, 1997; Liu, 2017). K is a major element that tobacco absorbs most from the soil, and a high content of K in tobacco leaves can promote the quality of tobacco by playing a positive role in the synthesis and accumulation of some aromatic substances (Xiao, 1997; Liu, 2017). It has been verified that K can promote the activation of at least 60 enzymes, therefore can speed up the synthesis of sugar, protein, and photosynthesis by motivating the usage of light energy (Xiao, 1997; Liu, 2017). Potassium fertilizer can improve the stress resistance of tobacco, including drought, salt, disease, and lodging resistance (Xiao, 1997; Liu, 2017). Mg is the component of chlorophylls and is important for the photosynthesis process, which is correlated with many physiological activities as the activator of related enzymes (Xiao, 1997; Liu, 2017). There is a significant possibility that the yield and quality of tobacco decrease for a lack of Mg. Mn is the essential element for plants to form chlorophylls and maintain chlorophylls' normal structure (Xiao, 1997; Liu, 2017). Simultaneously, Mn is the activator of varieties of enzymes, which take part in photosynthesis and respiration (Xiao, 1997; Liu, 2017). Therefore, the scarcity of B, K, Mg, and Mn has an indispensable relationship with the eruption of tobacco disease in recent research. For this reason, appropriate application of B, K, Mg, and Mn fertilizers is suggested in alleviating tobacco CCO.

In our study, there was an increasing trend in the total contents of ferulic acid, vanillin, syringic acid, vanillic acid, and *p*-hydroxybenzoic acid in the rhizosphere soil of the diseased group from Yuxi, indicating that the accumulation of PAs was a vital factor resulting in tobacco disease from Yuxi. This phenomenon was coherent to the results of most recent studies (Qu and Wang, 2008; Bai et al., 2019). Chen et al. (2019) determined 18 PAs in the rhizosphere soil from the CC tobacco field. They found that *p*-hydroxybenzoic acid, *p*-coumaric acid, vanillic acid, ferulic acid, and syringic acid were the predominant PAs, with the total content in the 30-year CC soil higher than that

in the 20-year CC soil. Bai et al. (2019) revealed that the contents of phloroglucinol, coumalic acid, *p*-hydroxybenzoic acid, vanillic acid, and ferulic acid increased with increasing cropping duration of tobacco. In these cases, plant root residues and exudates might provide pathogens with a suitable physical and nutritional environment, thus contributing to the biomass of pathogen fungi. It destroys the balance of bacterial and fungal abundance, with the accumulation of pathogens and the reduction in beneficial microbes (Qu and Wang, 2008; Zhou and Wu, 2012). It should be mentioned that different plants release diverse PAs into the soil. Phlorizin, benzoic acid, and vanillic aldehyde were the predominant phenolic acids in a replanted apple orchard, which maybe causing apple replant diseases (Yin et al., 2016). It was identified that 4-hydroxybenzoic acid, vanillic acid, ferulic acid, benzoic acid, 3-phenylpropionic acid, and cinnamic acid existed in CC cucumber soil (Chen et al., 2011). The impact of PAs on plant growth can be concluded in two aspects: one is to inhibit plants directly by preventing nutrient uptake and causing cell membrane peroxidation *via* allelopathy (Chen et al., 2005; Hiradate et al., 2005; Wu and Ma, 2006), and the other is to suppress plant growth indirectly by changing the soil micro-ecological environment (Wang et al., 2016). However, there was an opposite pattern in the rhizosphere soil from Dali, contrary to the common conclusions. The volatilization and degradation processes in the rhizosphere soil might exert a more dominant effect than that in the plants producing and releasing PAs in Dali. There was a reverse situation in Yuxi.

Our results showed that the microbial composition and structure varied between the non-diseased and diseased groups. The first six dominant phyla in our study were Proteobacteria (32.88–35.30% of all samples), Acidobacteria (10.18–11.49%), Actinobacteria (8.17–9.04%), Gemmatimonadetes (5.98–7.02%), Bacteroidetes (3.63–5.17%), and Chloroflexi (3.48%–4.63%), which was consistent with the results of previous studies (Niu et al., 2016; Bai et al., 2019). We found that the phylum Chloroflexi was enriched in the diseased group from Dali, which was similar to the findings of Chen et al. (2018). Niu et al. (2016) also revealed that Chloroflexi accumulated in the CC tobacco field, and its abundance, was positively related to tobacco disease rate. There is a great possibility that Chloroflexi competes in nitrogen source with tobacco, as Chloroflexi cannot fix nitrogen (Kragelund et al., 2007). Therefore, Chloroflexi is selected under the influence of the deteriorated environment and can be a disease-inducible microorganism. The abundance of Acidobacteria was evidently higher in the non-diseased group in Dali. Other studies also revealed that it was enriched in the non-continuous cropping (NCC) network (Niu et al., 2016; Chen et al., 2018). It was verified that the abundance of Acidobacteria was negatively correlated with the tobacco disease rate. Acidobacteria are listed as potential probiotic bacteria (Niu et al., 2016) and have genes that encode polyketide synthase and non-ribosomal peptide synthase enzymes, which play a typical role in the synthesis of antifungals and antibiotics (Ward et al., 2009). Acidobacteria, Firmicutes, and Proteobacteria might cooperate in providing other microbial species with carbon sources through the degradation function in the microbial network (Chen et al., 2018). There was an apparent change in the microbial β-diversity between the two groups from Dali and Yuxi. Bray–Curtis PCoA combined with PERMANOVA and Bray–Curtis nMDS combined with ANOSIM analysis showed that the microbial composition in the non-diseased groups was distinctly evident from the diseased groups. Bai et al. (2019) found that the bacterial community structure was strongly influenced by tobacco CC based on hierarchical clustering and PCoAs. Correspondingly, the fungal community was strongly affected after 30 years of tea monoculture based on the unweighted pair group method with arithmetic mean (UPGMA) analysis and PCoA (Arafat et al., 2019). Meanwhile, Arafat et al. (2019) found that low tea production could be ascribed to the decrease in beneficial fungal species (*Mortierella alpine* and *Mortierella elongatula*) and the promotion of pathogenic fungal species (*Fusarium oxysporum* and *Fusarium solani*). This is a common phenomenon occurring in other CC crops, such as potato (Lu et al., 2013), soybean (Bai et al., 2015), and coffee (Zhao et al., 2018). Therefore, the change in the microbial community is a key factor associated with tobacco disease.

The first four dominant KEGG pathways were metabolic pathways, biosynthesis of secondary metabolites, microbial metabolism in diverse environments, and biosynthesis of antibiotics. Bray–Curtis PCoA combined with PERMANOVA and Bray–Curtis nMDS combined with ANOSIM analyses at the KO level presented that the functional genes in the non-diseased groups were separated from the diseased groups. The change in the β-diversity of functional genes was a relevant factor causing tobacco disease in our study. The functional genes concerning MAPK signaling pathway in yeast accumulated in the non-diseased group, and the genes related to ethylbenzene degradation accumulated in the diseased group in Dali ($p < 10^{-4}$). MAPK signaling pathway in yeast is listed in the class of environmental information processing, related to the adjustment in nutrient-limiting environment and repair of injuries in the cell wall (KEGG pathway database; Chen and Thorner, 2007). This indicates that the ability of the microorganisms to self-repair and self-adjust has been stimulated and strengthened in the non-diseased group from Dali. Ethylbenzene degradation is in the class of xenobiotics biodegradation and metabolism (KEGG pathway database; Rabus et al., 2002), which means that exotic toxic substances threaten the microbiome in the diseased group from Dali. Simultaneously, the abundance of genes associated with biofilm formation in *V. cholerae* increased significantly in the non-diseased group from Yuxi. The genes related to clavulanic acid biosynthesis accumulated in the diseased group from Yuxi ($p < 10^{-4}$). The pathway of biofilm formation in *V. cholerae* belongs to the class of cellular processes, providing microorganisms with advantages of surface colonization and biofilm formation and development (KEGG pathway database; Teschler et al., 2015). Biofilm formation on the plant rhizoplane plays a vital role in the defense system of the plants through inhibiting pathogens' colonization directly. Therefore, the stronger function of biofilm formation in the microorganisms is an inevitable factor contributing to the non-diseased group in Yuxi. The pathway of clavulanic acid biosynthesis is in the class of biosynthesis of other

secondary metabolites (KEGG pathway database). Clavulanic acid is a strong and broader spectrum of inhibition substance to β-lactamase, and the biosynthesis of β-lactamase is the main mechanism of bacterial drug resistance (McGowan et al., 1998). The strengthening in the biosynthesis of clavulanic acid results in the microorganisms being more sensitive to the environment. The weakening in the microbiome's resilience is a typical feature in the diseased group from Yuxi.

Based on the correlation analysis between the microbial community, functional genes, and soil environmental factors, there was a similar influence pattern of SA and TPA on the microbial community and functional genes, opposite to soil pH. Bai et al. (2019) found that the content of PAs was intimately associated with soil pH. The contents of vanillin, phloroglucinol, *p*-hydroxybenzoic acid, and ferulic acid were negatively related to soil pH. PAs own acidic properties and can accumulate easier under lower pH values. Soil pH is an inevitable crucial factor in soil physicochemical properties influencing microbial composition and diversity in numerous studies (Chen et al., 2018; Bai et al., 2019). It can change microbial osmotic pressure and surface potential directly and PAs contents, the bioavailability of nutrients, and the habitation conditions indirectly (Chen et al., 2018; Bai et al., 2019). The changing pattern of soil pH and SA content between the two groups from Dali was the opposite of that from Yuxi, which was an important reason for the divergent biomarkers of microbiome and functional genes. The different tobacco varieties and natural conditions also contribute to the difference in the two sampling sites. The causes of tobacco CCO are regional from a soil micro-ecology perspective. This phenomenon in other plants and places need to be further studied. Adjusting the soil to the former balanced condition is the basic and crucial concept in alleviating tobacco CCO. Appropriate applications of bio-organic fertilizers, soil conditioners, functional biochar, and tillage regime are suggested according to the specific circumstances.

CONCLUSION

The mechanisms of tobacco disease under CC circumstances can be owed to the imbalance and deterioration of soil micro-ecology, which possesses a remarkable regional feature. There were four aspects of mechanisms in our study: the change in soil physicochemical properties, primarily soil pH, OM, available K, CEC, TC/TN contents, and texture; the variance of PAs contents in rhizosphere soil, especially SA; the deficiency of B, K, Mg, and Mn in soil and/or tobacco; and the transformation in microbial community and functional genes from beneficial to harmful in rhizosphere soil. There was an intimate interaction among these four parts. Soil pH and SA had the most significant influence on the composition and structure of microbial communities and functions in rhizosphere soil.

DATA AVAILABILITY STATEMENT

The datasets presented in this study can be found in online repositories. The names of the repository/repositories and accession number(s) can be found in the article/**Supplementary Material**. Metagenome data were deposited in the SRA database under accession number PRJNA758121.

AUTHOR CONTRIBUTIONS

DC, MW, and XY conceived the original design of the study. KD helped to collect samples. DC, YZ, MW, and SY executed the experiments. DC and JL performed the statistical analysis of the data. DC wrote the manuscript. MM, JL, and XY contributed to the revision of the manuscript.

FUNDING

This study was financially supported by the Science and Technology Key Project from Yunnan branch of China Tobacco Corporation (2020530000241006), the Science and Technology Project from Guizhou Branch of China Tobacco Corporation (201907), and Science and Technology Project from Bijie Branch of Guizhou Province Tobacco Corporation.

SUPPLEMENTARY MATERIAL

The Supplementary Material for this article can be found online at: https://www.frontiersin.org/articles/10.3389/fmicb.2021.785110/full#supplementary-material

REFERENCES

Arafat, Y., Tayyab, M., Khan, M. U., Chen, T., Amjad, H., Awais, S., et al. (2019). Long-term monoculture negatively regulates fungal community composition and abundance of tea orchards. *Agronomy* 9:466. doi: 10.3390/agronomy9080466

Bai, L., Cui, J. Q., Jie, W. G., and Cai, B. Y. (2015). Analysis of the community compositions of rhizosphere fungi in soybeans continuous cropping fields. *Microbiol. Res.* 180, 49–56. doi: 10.1016/j.micres.2015.07.007

Bai, Y. X., Wang, G., Cheng, Y. D., Shi, P. Y., Yang, C. C., Yang, H. W., et al. (2019). Soil acidification in continuously cropped tobacco alters bacterial community structure and diversity via the accumulation of phenolic acids. *Sci. Rep.* 9:12499. doi: 10.1038/s41598-019-48611-5

Bao, S. D. (2000). *Soil and Agricultural Chemical Analysis (3rd version)*. Beijing: China Agriculture Press.

Bonner, J., and Galson, A. W. (1944). Toxic substances from the culture media of guayule which may inhibit growth. *Bot. Gaz.* 106, 185–198.

Brussaard, L., De Ruiter, P. C., and Brown, G. G. (2007a). Soil biodiversity for agricultural sustainability. *Agric. Ecosyst. Environ.* 121, 233–244.

Brussaard, L., Pulleman, M. M., Ouédraogo, É, Mando, A., and Six, J. (2007b). Soil fauna and soil function in the fabric of the food web. *Pedobiologia* 50, 447–462. doi: 10.1016/j.pedobi.2006.10.007

Caporaso, J. G., Kuczynski, J., Stombaugh, J., Bittinger, K., Bushman, F. D., Costello, E. K., et al. (2010). QIIME allows analysis of highthroughput community sequencing data. *Nat. Methods* 7, 335–336. doi: 10.1038/nmeth.f.303

Chen, L. H., Yang, X. M., Raza, W., Li, J. H., Liu, Y. X., Qiu, M. H., et al. (2011). *Trichoderma harzianum* SQR-T037 rapidly degrades allelochemicals in rhizospheres of continuously cropped cucumbers. *Appl. Microbiol. Biotechnol.* 89, 1653–1663. doi: 10.1007/s00253-010-2948-x

Chen, L. X., Wu, F. Z., and Ma, F. M. (2005). Effects of exogenous cinnamic acids on the growth and physiological characteristics of cucumber seedlings. *Agr. Sci. China* 4, 747–751.

Chen, R. E., and Thorner, J. (2007). Function and regulation in MAPK signaling pathways: lessons learned from the yeast Saccharomyces cerevisiae. *Biochim. Biophys. Acta (BBA) Mol. Cell Res.* 1773, 1311–1340. doi: 10.1016/j.bbamcr.2007.05.003

Chen, S., Qi, G. F., Luo, T., Zhang, H. C., Jiang, Q. K., Wang, R., et al. (2018). Continuous-cropping tobacco caused variance of chemical properties and structure of bacterial network in soils. *Land Degrad. Dev.* 29, 4106–4120. doi: 10.1002/ldr.3167

Chen, Y. X., Chen, W., Lan, Y., Wang, K. T., Wu, Y. C., Zhong, X. L., et al. (2019). Determination of 18 phenolic acids in tobacco and rhizosphere soil by ultra high performance liquid chromatography combined with triple quadrupole mass spectrometry. *J. Sep. Sci.* 42, 816–825. doi: 10.1002/jssc.201800819

Echeverria, V., and Zeitlin, R. (2012). Cotinine: a potential new therapeutic agent against Alzheimer's disease. *CNS Neurosci. Ther.* 18, 517–523. doi: 10.1111/j.1755-5949.2012.00317.x

Epelde, L., Becerril, J. M., Barrutia, O., González-Oreja, J. A., and Garbisu, C. (2010). Interactions between plant and rhizosphere microbial communities in a metalliferous soil. *Environ. Pollut.* 158, 1576–1583. doi: 10.1016/j.envpol.2009.12.013

Fu, L. M., Niu, B. F., Zhu, Z. W., Wu, S. T., and Li, W. Z. (2012). CD-HIT: accelerated for clustering the next-generation sequencing data. *Bioinformatic* 28, 3150–3152. doi: 10.1093/bioinformatics/bts565

Gao, X. B., Zhao, F. X., Shen, X., Hu, Y. L., Hao, Y. H., Yang, S. Q., et al. (2009). Effects of cinnamon acid on respiratory rate and its related enzymes activity in roots of seedlings of *Malus hupehensis* Rehd. *Agr. Sci. China* 42, 4308–4314.

Gao, Z. Y., Han, M. K., Hu, Y. Y., Li, Z. Q., Liu, C. F., Wang, X., et al. (2019). Effects of continuous cropping of sweet potato on the fungal community structure in rhizospheric soil. *Front. Microbiol.* 10:2269. doi: 10.3389/fmicb.2019.02269

Gurevich, A., Saveliev, V., Vyahhi, N., and Tesler, G. (2013). QUAST: quality assessment tool for genome assemblies. *Bioinformatic* 29, 1072–1075. doi: 10.1093/bioinformatics/btt086

Hiradate, S., Morita, S., Furubayashi, A., Fujii, Y., and Harada, J. (2005). Plant growth inhibition by cis-cinnamoyl glucosides and cis-cinnamic acid. *J. Chem. Ecol.* 31, 591–601. doi: 10.1007/s10886-005-2047-0

Hu, T. W., Mao, Z. Z., Shi, J., and Chen, W. D. (2010). The role of taxation in tobacco control and its potential economic impact in China. *Tobacco Control* 19, 58–64. doi: 10.1136/tc.2009.031799

Inderjit. (2005). Soil microorganisms: an important determinant of allelopathic activity. *Plant Soil* 274, 227–236. doi: 10.1021/jf0488514

Kanehisa, M., Goto, S., Kawashima, S., Okuno, Y., and Hattori, M. (2004). The KEGG resource for deciphering the genome. *Nucleic Acids Res.* 32 (Suppl_1), D277–D280. doi: 10.1093/nar/gkh063

Kragelund, C., Levantesi, C., Borger, A., Thelen, K., Eikelboom, D., Tandoi, V., et al. (2007). Identity, abundance and ecophysiology of filamentous *Chloroflexi* species present in activated sludge treatment plants. *FEMS Microbiol. Ecol.* 59, 671–682. doi: 10.1111/j.1574-6941.2006.00251.x

Li, D. H., Liu, C. M., Luo, R. B., Sadakane, K., and Lam, T. W. (2015). MEGAHIT: an ultra-fast single-node solution for large and complex metagenomics assembly via succinct de Bruijn graph. *Bioinformatic* 31, 1674–1676. doi: 10.1093/bioinformatics/btv033

Li, S. L., Liu, Y. Q., Wang, J., Yang, L., Zhang, S. T., Xu, C., et al. (2017). Soil acidification aggravates the occurrence of bacterial wilt in South China. *Front. Microbiol.* 8:703. doi: 10.3389/fmicb.2017.00703

Liu, G. S. (2017). *Tobacco Cultivation Science (2nd version)*. Beijing: China Agriculture Press.

Liu, H., Pan, F. J., Han, X. Z., Song, F. B., Zhang, Z. M., Yan, J., et al. (2019). Response of soil fungal community structure to long-term continuous soybean cropping. *Front. Microbiol.* 9:3316. doi: 10.3389/fmicb.2018.03316

Lu, L. H., Yin, S. X., Liu, X., Zhang, W. M., Gu, T. Y., Shen, Q. R., et al. (2013). Fungal networks in yield-invigorating and -debilitating soils induced by prolonged potato monoculture. *Soil Biol. Biochem.* 65, 186–194. doi: 10.1016/j.soilbio.2013.05.025

Mareschal, L., Turpault, M. P., Bonnaud, P., and Ranger, J. (2013). Relationship between the weathering of clay minerals and the nitrification rate: a rapid tree species effect. *Biogeochemistry* 112, 293–309. doi: 10.1007/s10533-012-9725-0

McGowan, S. J., Bycroft, B. W., and Salmond, G. P. (1998). Bacterial production of carbapenems and clavams: evolution of β-lactam antibiotic pathways. *Trends microbial.* 6, 203–208. doi: 10.1016/s0966-842x(98)01251-7

Ministry of Agriculture of the People's Republic of China GB/T 32737-2016 (2016). Soil Determination of Nitrate Nitrogen in Soil-Ultraviolet Spectrophotometry Method. National Standards of the People's Republic of China. Beijing: Ministry of Agriculture of the People's Republic of China.

Ministry of Agriculture of the People's Republic of China NY/T 1121.3-2006 (2006). *Soil Testing Part 3: Method for Determination of Soil Mechanical Composition. Agricultural Industry Standard of the People's Republic of China*. Beijing: Ministry of Agriculture of the People's Republic of China.

Ministry of Agriculture of the People's Republic of China NY/T 1121.4-2006 (2006). *Soil Testing Part 4: Method for Determination of Soil Bulk Density. Agricultural Industry Standard of the People's Republic of China*. Beijing: Ministry of Agriculture of the People's Republic of China.

Ministry of Environmental Protection of the People's Republic of China HJ 889-2017. (2017). *Soil Quality-Determination of Cation Exchange Capacity (CEC)-Hexaminecobalt Trichloride Solution-Spectrophometric Method*. Beijing: Ministry of Environmental Protection of the People's Republic of China.

Nielsen, S. S., Gallagher, L. G., Lundin, J. I., Longstreth, W. T., Smith-Weller, T., Franklin, G. M., et al. (2012). Environmental tobacco smoke and Parkinson's disease. *Mov. Dis.* 27, 293–296. doi: 10.1002/mds.24012

Niu, J. J., Chao, J., Xiao, Y. H., Chen, W., Zhang, C., Liu, X. D., et al. (2017). Insight into the effects of different cropping systems on soil bacterial community and tobacco bacterial wilt rate. *J. Basic Microbiol.* 57, 3–11. doi: 10.1002/jobm.201600222

Niu, J. J., Rang, Z. W., Zhang, C., Chen, W., Tian, F., Yin, H. Q., et al. (2016). The succession pattern of soil microbial communities and its relationship with tobacco bacterial wilt. *BMC Microbiol.* 16:233. doi: 10.1186/s12866-016-0845-x

Obalum, S. E., Chibuike, G. U., Peth, S., and Ouyang, Y. (2017). Soil organic matter as sole indicator of soil degradation. *Environ. Monit. Assess.* 189, 176. doi: 10.1007/s10661-017-5881-y

Pang, Z. Q., Dong, F., Liu, Q., Lin, W. X., Hu, C. H., and Yuan, Z. N. (2021). Soil metagenomics reveals effects of continuous sugarcane cropping on the structure and functional pathway of rhizospheric microbial community. *Front. Microbiol.* 12:627569. doi: 10.3389/fmicb.2021.627569

Qu, X. H., and Wang, J. G. (2008). Effect of amendments with different phenolic acids on soil microbial biomass, activity, and community diversity. *Appl. Soil Ecol.* 39, 172–179. doi: 10.1371/journal.pone.0124096

Rabus, R., Kube, M., Beck, A., Widdel, F., and Reinhardt, R. (2002). Genes involved in the anaerobic degradation of ethylbenzene in a denitrifying bacterium, strain EbN1. *Arch. Microbiol.* 178, 506–516. doi: 10.1007/s00203-002-0487-2

Ren, X., He, X. F., Zhang, Z. F., Yan, Z. Q., Jin, H., Li, X. Z., et al. (2015). Isolation, identification, and autotoxicity effect of allelochemicals from rhizosphere soils of flue-cured tobacco. *J. Agric. Food Chem.* 63, 8975–8980.

Segata, N., Izard, J., Waldron, L., Gevers, D., Miropolsky, L., Garrett, W. S., et al. (2011). Metagenomic biomarker discovery and explanation. *Genome Biol.* 12:R60. doi: 10.1186/gb-2011-12-6-r60

Shen, G. H., Zhang, S. T., Liu, X. J., Jiang, Q. P., and Ding, W. (2018). Soil acidification amendments change the rhizosphere bacterial community of tobacco in a bacterial wilt affected field. *Appl. Microbiol. Biotechnol.* 102, 9781–9791. doi: 10.1007/s00253-018-9347-0

Sierro, N., Battey, J. N. D., Ouadi, S., Bakaher, N., Bovet, L., Willig, A., et al. (2014). The tobacco genome sequence and its comparison with those of tomato and potato. *Nat. Commun.* 5:3833. doi: 10.1038/ncomms4833

Tan, X. M., Wang, H. T., Kong, L. G., and Wang, Y. P. (2008). Accumulation of phenolic acids in soil of a continuous cropping Poplar plantation and their effects on soil microbes. *J. Shandong Univ. (Nat. Sci.)* 43, 14–19.

Teschler, J. K., Zamorano-Sánchez, D., Utada, A. S., Warner, C. J. A., Wong, G. C. L., Linington, R. G., et al. (2015). Living in the matrix: assembly and

control of *Vibrio cholerae* biofilms. *Nat. Rev. Microbiol.* 13, 255–268. doi: 10.1038/nrmicro3433

Wang, Y. P., Li, C. R., Wang, Q. K., Wang, H. T., Duan, B. L., and Zhang, G. C. (2016). Environmental behaviors of phenolic acids dominated their rhizodeposition in boreal poplar plantation forest soils. *J. Soils Sediments* 16, 1858–1870. doi: 10.1007/s11368-016-1375-8

Ward, N. L., Challacombe, J. F., Janssen, P. H., Henrissat, B., Coutinho, P. M., Wu, M., et al. (2009). Three genomes from the phylum Acidobacteria provide insight into the lifestyles of these microorganisms in soils. *Appl. Environ. Microbiol.* 75, 2046–2056. doi: 10.1128/AEM.02294-08

Weir, T. L., Park, S.-W., and Vivanco, J. M. (2004). Biochemical and physiological mechanisms mediated by allelochemicals. *Curr Opin Plant Biol.* 7, 472–479. doi: 10.1016/j.pbi.2004.05.007

Wu, F. Z., and Ma, F. M. (2006). Effect of exogenous cinnamic acid on structure and function of plasmalemma in cucumber seedlings. *Allelopathy J.* 18, 287–298.

Xiao, X. Z. (1997). *Tobacco Chemistry (1st)*. Beijing: China Agricultural Science and Technology Press.

Yang, J. L., Zhang, G. L., Huang, L. M., and Brookes, P. C. (2013). Estimating soil acidification rate at watershed scale based on the stoichiometric relations between silicon and base cations. *Chem Geol.* 337, 30–37. doi: 10.1016/j.chemgeo.2012.11.009

Yin, C. M., Xiang, L., Wang, G. S., Wang, Y. F., Shen, X., Chen, X. S., et al. (2016). How to plant apple trees to reduce replant disease in apple orchard: a study on the phenolic acid of the replanted apple orchard. *PLoS One* 11:e0167347. doi: 10.1371/journal.pone.0167347

Yuan, L., Zhang, Z. C., Cao, X. C., Zhu, S. C., Zhang, X., and Wu, L. H. (2014). Responses of rice production, milled rice quality and soil properties to various nitrogen inputs and rice straw incorporation under continuous plastic film mulching cultivation. *Field Crops Res.* 155, 164–171. doi: 10.1016/j.fcr.2013.09.009

Zhang, X. H., Lang, D. Y., Zhang, E. H., Bai, C. C., and Wang, H. Z. (2013). Diurnal changes in photosynthesis and antioxidants of *Angelica sinensis* as influenced by cropping systems. *Photosynthetica* 51, 252–258. doi: 10.1007/s11099-013-0013-6

Zhang, Y. T., He, X. H., Zhao, J., Zhang, Y. Q., and Shi, X. J. (2016). Soil acidification under long-term tobacco plantation results in alterations of mineralogical properties in an Alisol. *Arch. Agron. Soil Sci.* 62, 1033–1040. doi: 10.1080/03650340.2015.1134252

Zhao, Q. Y., Xiong, W., Xing, Y. Z., Sun, Y., Lin, X. J., and Dong, Y. P. (2018). Long-term coffee monoculture alters soil chemical properties and microbial communities. *Sci. Rep.* 8:6116. doi: 10.1038/s41598-018-24537-2

Zhou, X. G., and Wu, F. Z. (2012). P-Coumaric acid influenced cucumber rhizosphere soil microbial communities and the growth of *Fusarium oxysporum* f.sp. cucumerinum Owen. *PLoS One* 7:e48288. doi: 10.1371/journal.pone.0048288

Zhu, W. H., Lomsadze, A., and Borodovsky, M. (2010). Ab initio gene identification in metagenomic sequences. *Nucleic Acids Res.* 38, 132–132. doi: 10.1093/nar/gkq275

Zou, C. M., Li, Y., Huang, W., Zhao, G. K., Pu, G. R., Su, J. E., et al. (2018). Rotation and manure amendment increase soil macro-aggregates and associated carbon and nitrogen stocks in flue-cured tobacco production. *Geoderma* 325, 49–58. doi: 10.1016/j.geoderma.2018.03.017

Conflict of Interest: KD was employed by the company Yuxi Tobacco Company, Ltd.

The remaining authors declare that the research was conducted in the absence of any commercial or financial relationships that could be construed as a potential conflict of interest.

Publisher's Note: All claims expressed in this article are solely those of the authors and do not necessarily represent those of their affiliated organizations, or those of the publisher, the editors and the reviewers. Any product that may be evaluated in this article, or claim that may be made by its manufacturer, is not guaranteed or endorsed by the publisher.

frontiers in Microbiology

ORIGINAL RESEARCH
published: 21 February 2022
doi: 10.3389/fmicb.2022.794950

Arsenic Transformation in Soil-Rice System Affected by Iron-Oxidizing Strain (*Ochrobactrum* sp.) and Related Soil Metabolomics Analysis

Ziyan Qian[1,2†], Chuan Wu[2,3†], Weisong Pan[1], Xiaoran Xiong[1], Libing Xia[1] and Waichin Li[3]*

[1] College of Bioscience and Biotechnology, Hunan Agricultural University, Changsha, China, [2] School of Metallurgy and Environment, Central South University, Changsha, China, [3] Department of Science and Environmental Studies, The Education University of Hong Kong, Tai Po, Hong Kong SAR, China

Iron-oxidizing bacteria (FeOB) could oxidize Fe(II) and mediate biomineralization, which provides the possibility for its potential application in arsenic (As) remediation. In the present study, a strain named *Ochrobactrum EEELCW01* isolated previously, was inoculated into paddy soils to investigate the effect of FeOB inoculation on the As migration and transformation in paddy soils. The results showed that inoculation of *Ochrobactrum* sp. increased the proportion of As in iron-aluminum oxide binding fraction, which reduced the As bioavailability in paddy soils and effectively reduced the As accumulation in rice tissues. Moreover, the inoculation of iron oxidizing bacteria increased the abundance of KD4-96, *Pedosphaeraceae* and other bacteria in the soils, which could reduce the As toxicity in the soil through biotransformation. The abundance of metabolites such as carnosine, MG (0:0/14:0/0:0) and pantetheine 4'-phosphate increased in rhizosphere soils inoculated with FeOB, which indicated that the defense ability of soil-microorganism-plant system against peroxidation caused by As was enhanced. This study proved that FeOB have the potential application in remediation of As pollution in paddy soil, FeOB promotes the formation of iron oxide in paddy soil, and then adsorbed and coprecipitated with arsenic. On the other hand, the inoculation of *Ochrobactrum* sp. change soil microbial community structure and soil metabolism, increase the abundance of FeOB in soil, promote the biotransformation process of As in soil, and enhance the resistance of soil to peroxide pollution (As pollution).

Keywords: arsenic, iron-oxidizing bacteria, paddy soil, metabolomics, microbial community

OPEN ACCESS

Edited by:
Hai-Ming Zhao,
Jinan University, China

Reviewed by:
Lucia Cavalca,
University of Milan, Italy
Safdar Bashir,
Ghazi University, Pakistan

***Correspondence:**
Weisong Pan
panweisong@hunau.edu.cn

† These authors have contributed equally to this work

Specialty section:
This article was submitted to Terrestrial Microbiology, a section of the journal Frontiers in Microbiology

Received: *14 October 2021*
Accepted: *14 January 2022*
Published: *21 February 2022*

Citation:
Qian ZY, Wu C, Pan WS, Xiong XR, Xia LB and Li WC (2022) Arsenic Transformation in Soil-Rice System Affected by Iron-Oxidizing Strain (Ochrobactrum sp.) and Related Soil Metabolomics Analysis. Front. Microbiol. 13:794950. doi: 10.3389/fmicb.2022.794950

INTRODUCTION

Arsenic (As) is the most widespread toxic non-metallic element in nature, among which inorganic As (iAs) was identified as a class I carcinogen by the International Agency for Research on Cancer (IARC). As mainly exists as a sulfide (FeAsS, As_4S_4, and AsS) or is associated with other metal minerals in the natural environment. As mining and smelting, pesticide production, coal combustion and other human activities are important causes of environmental As pollution, and according to statistics, the global anthropogenic emissions of As in soil are 2.84×10^5–9.4×10^5 t (Clemens and Ma, 2016). According to a survey conducted by the Ministry of Environmental

Protection and the former Ministry of Land and Resources, by 2014, the total exceeding rate of soil pollution in China had reached 16.1%, while the exceeding rate of soil sampling sites on cultivated land was 19.4%, and the exceeding rate of As samples was 2.7%, ranking third among the eight inorganic pollutants after cadmium and nickel. Rice is the staple food for approximately 3 billion people worldwide (Zhao et al., 2015). Pollution in paddy soil not only causes plant poisoning and crop yield loss but also enters the human body through the food chain, posing a serious threat to human health (Saifullah, et al., 2018). Therefore, the remediation of As-contaminated paddy soil is a major ecological and environmental problem, and it is urgent to find a cost-effective and environmentally friendly solution.

Soil microorganisms play an important role in affecting the geochemical cycling of arsenic, regulating its morphological transformation, environmental fate and bioavailability. Sforna et al. (2014) showed that microbial metabolism of As began 2.7 billion years ago, and some specific microorganisms contain active enzymes related to arsenic metabolism, which are able to regulate the redox and methylation processes of As in microbial cells (Sforna et al., 2014). Arsenic-oxidizing bacteria contain the arsenite oxidase gene (aioA), which can mediate arsenic oxidation, and their activities, such as in *Ensifer* sp. and *Acinetobacter* sp., lead to reduced toxicity of arsenic in soil and may help to stimulate the growth/activity of indigenous microorganisms in soil and promote the remediation of arsenic-contaminated soil by hyperaccumulator plants (Wang et al., 2012; Debiec-Andrzejewska et al., 2020). The genetically engineered bacteria *Pseudomonas putida* KT2440, *Bacillus subtilis*, and *Westerdykella aurantiaca* contain the As(III) *S*-adenosylmethionine methyltransferase gene (arsM) in their cells, which can methylate arsenic to methyl arsenate [MAs(V)], dimethyl arsenate [DMAs(V)] and trimethyl arsenic oxide [TMAs(V)O] to promote the production of volatile arsenic compounds, thereby reducing the inorganic arsenic content in soil (Chen et al., 2014; Verma et al., 2016). In addition, some other species of microorganisms have been reported to be involved in the remediation of As contamination. For example, the activity of sulfate-reducing bacteria and their subsequent production of sulfide precipitate As(III) or coprecipitate with iron can sequester As(III) in the mineral phase (Kirk et al., 2004; Alam and McPhedran, 2019). Achal et al. (2012) successfully reduced exchangeable As in soil and sequestered arsenic in carbonate precipitation through a calcite precipitation process induced by *Sporosarcina ginsengisoli*. *In situ* remediation of arsenic in soil by microorganisms has gradually become a popular research topic due to its advantages in regard to environmental disturbance and cost effectiveness (Achal et al., 2012).

The anaerobic oxidation capacity of FeOB offers the possibility for its potential application for effectively removing arsenic in soil and groundwater treatment. It was found that FeOB, including *Acidovorax* sp. strain BoFeN1 and *Rhodobaster ferrooxidans* strain SW2, strain KS has the ability to resist arsenic poisoning, and the oxidation of Fe(II) produces mineral phases such as goethite and nano goethite, which can effectively remove more than 96% of arsenic in solution (Hohmann et al., 2010). The rhizosphere soil environment is influenced by plant root exudates and rhizosphere microorganisms. Physicochemical properties of the soil rhizosphere (pH, Eh, EC, element concentration, etc.) and environmental factors (radial oxidation loss, metabolites secreted by plants, microbial activity, etc.) may affect the bioavailability of arsenic in paddy soil (Bais et al., 2006). Under flooded paddy soil, radial oxidation loss of rice roots induced the formation of iron plaque on the root surface (Wu et al., 2015), which sequestered As by adsorption or coprecipitation with iron oxides, thus affecting the bioavailability of As in the rhizosphere, serving as an important barrier against the uptake of As in rice (Tripathi et al., 2014). The flooding and Fe- and N-rich conditions in the paddy soil provided a suitable living environment for microaerobic nitrate-dependent FeOB (Ratering and Schnell, 2001). The microbial iron oxidation process successfully competes with chemical iron oxidation and occupies a dominant position. Nitrate-dependent FeOB utilizes nitrate as an electron acceptor to oxidize Fe(II) to Fe(III) (Klueglein et al., 2014; Jamieson et al., 2018) and mediates the metabolic pathway of denitrification and the reduction of alien nitrate to ammonia. It is the coupling link of the iron cycle and nitrogen cycle (Li et al., 2016) and plays a role in the biogeochemical cycle of As.

Several studies have proven that artificial inoculation of FeOB could stimulate the formation of iron plaque in rice roots and significantly reduce the concentration of As in rice roots, leaves, glumes and grains (Dong et al., 2016; Xiao et al., 2020). However, most studies focused on the effect of iron-oxidizing bacteria inoculation on arsenic fixation in soil and rice plants but paid little attention to the potential changes of microbial community structure and soil metabolism after iron-oxidizing bacteria inoculation. In this study, a new FeOB isolated in our previously study, *Ochrobactrum* sp. EEELCW01, was inoculated into paddy soil. The main objectives of this study were: (a) to explore the redistribution of arsenic in paddy soil and rice plants by inoculation with FeOB; (b) to investigate the changes of soil microbial community structure after inoculation with FeOB; (c) to understanding the regulatory mechanism of FeOB in soil from the perspective of metabonomics.

MATERIALS AND METHODS

Tested Strain and Growth Conditions

Ochrobactrum EEELCW01, a bacterium that can oxidize ferrous iron under microaerobic conditions, was isolated from a typical arsenic-contaminated paddy soil in Furong District, Changsha city, Hunan Province (Luo et al., 2021). The accession numbers of this bacterium in the NCBI GenBank are CP047598 and CP047599. After activation, *Ochrobactrum* EEELCW01 was cultured in liquid LB medium in a rotary shaker at 28°C and 200 rpm. After 48 h of culture after inoculation, the bacteria grew to the logarithmic phase, and the medium was centrifuged at 8000 rpm to collect the precipitated cells, which were washed with neutral sterile water three times to prepare a resting cell suspension.

Soil Source and Preparation of Pot Experiments

Pot experiment soils were collected from the surface (0–20 cm) of a paddy field near mining areas in Chenzhou, Hunan Province, China. Basic soil physical and chemical properties, including pH, EC, organic matter, available potassium, available nitrogen, total iron, aluminum, manganese and arsenic content, were determined, as shown in **Table 1**. To avoid affecting the composition of the soil microbial community and the abundance of arsenic metabolic genes, soil was immediately collected and used in pot experiments. The soil was packed in PVC pots (height 30 cm, bottom diameter 24 cm, and diameter 28 cm), and each pot contained 10 kg of soil. Fertilizer was applied according to the conventional fertilization ratio of N: P_2O_5:K_2O = 1.5:1:2. In addition, 10 mmol/L sodium nitrate was added to supplement the additional nitrogen source for FeOB growth. The pot soil was irrigated with sterile water to reach field moisture capacity and equilibrated for approximately 1 week.

The rice seeds were soaked in 30% (H_2O_2) hydrogen peroxide solution for 15 min to sterilize the surface and then transferred into petri dishes covered with moist filter paper for germination. When the seedlings (2–3 cm) germinated, they were transferred into seedling raising trays paved with paddy soil for seedling raising. Three uniform 2-week-old seedlings were selected and transplanted into each soil-filled PVC pot (Wu et al., 2014).

Pot Experimental Design

Four treatments were prepared in this study: (1) CK (controls without inoculation of bacteria and cultivation of rice plants), (2) FB (soil with inoculation of FeOB), (3) RP (soil with cultivation of rice plants) and (4) RF (soil with cultivation of rice plants and inoculation of FeOB on rice roots). Each treatment was replicated three times. To simulate actual field operations, rice seedlings were grown under flooded conditions (water surface 2 cm above the soil surface). The prepared bacterial suspension (100 mL/pot) was uniformly injected into rhizosphere soil by syringe.

The rhizosphere and non-rhizosphere soil solutions of rice plants were sampled with a Rhizon soil solution sampling tube (Rhizosphere, Netherlands) on Day 0, Day 15 (rice-tillering stage), Day 30 (rice-jointing stage), Day 45 (rice-heading stage), Day 75 (rice-filling stage) and Day 105 (rice-maturing stage) after seedling growth to analyze their pH, conductivity (EC), total As, available As content, As speciation [As(III) and As(V)] and iron (Fe) content (Wu et al., 2011; Yu et al., 2017). Soil samples were collected to determine the fractionation of As in the soil by sequential extraction procedures (Wenzel et al., 2001), and the available As was extracted by 0.5 mol·L^{-1} $NaHCO_3$ (Woolson et al., 1971). Rice plants were harvested at the mature stage, washed with deionized water and then thoroughly rinsed with deionized water. After the surface moisture was air-dried, the arsenic content and arsenic species in the roots and straw were determined. In addition, at the maturity stage of rice, 50 mg solid soil samples were placed in a 1.5 mL centrifuge tube, quickly frozen in liquid nitrogen and immediately placed in a –80°C refrigerator for subsequent microbial diversity and metabolomics measurements.

Determination of Arsenic Speciation in Rice Plant Parts

The washed rice plants were divided into root and straw parts, dried in a freeze-drying oven, and ground and crushed under liquid nitrogen for later use. A 0.2–0.5 g sample was weighed in a 50 mL centrifuge tube and 20 ml of 0.28 mol/L HNO_3 solution was added and extracted in a 95°C water bath for 1.5 h. The extract was cooled to approximately 25°C and centrifuged at 5000 r/min for 10 min, and the supernatant was filtered through a 0.22 μm membrane for further analysis. The speciation content of arsenic in the samples was determined with hydride generation atomic fluorescence spectrometry (HG-AFS, AFS-8230, Beijing Jitian Instruments Co., Beijing, China).

Microbial DNA Extraction and Illumina Sequencing

Microbial community genomic DNA was extracted from soil samples using the E.Z.N.A.® soil DNA Kit (Omega Bio-tek, Norcross, GA, United States) according to the manufacturer's instructions. The DNA extract was checked on a 1% agarose gel, and DNA concentration and purity were determined with a NanoDrop 2000 UV-vis spectrophotometer (Thermo Scientific, Wilmington, DE, United States). The hypervariable region V3-V4 of the bacterial 16S rRNA gene was amplified with primer pairs 338F (5′-ACTCCTACGGGAGGCAGCAG-3′) and 806R (5′-GGACTACHVGGGTWTCTAAT-3′) by an ABI GeneAmp® 9700 PCR thermocycler (ABI, Los Angeles, CA, United States). PCR amplification of the 16S rRNA gene was performed as follows: initial denaturation at 95°C for 3 min, followed by 27 cycles of denaturing at 95°C for 30 s, annealing at 55°C for 30 s, extension at 72°C for 45 s, a single extension at 72°C for 10 min, and a final extension at 4°C. The PCR mixtures contained 5 × *TransStart* FastPfu buffer 4 μL, 2.5 mM dNTPs 2 μL, forward primer (5 μM) 0.8 μL, reverse primer (5 μM) 0.8 μL, *TransStart* FastPfu DNA Polymerase 0.4 μL, template DNA 10 ng, and ddH_2O up to 20 μL. PCRs were performed in triplicate. The PCR product was extracted from a 2% agarose gel, purified using the AxyPrep DNA Gel Extraction Kit (Axygen Biosciences, Union City, CA, United States) according to the manufacturer's instructions, quantified using a Quantus™ Fluorometer (Promega, Madison, WI, United States), and then sequenced on an Illumina MiSeq PE300 platform (Illumina, San Diego, CA, United States).

Metabolite Extraction and Metabolomics Analysis

Fifty milligrams of soil sample was accurately weighed, and the metabolites were extracted using a 400 μL methanol: water (4:1, v/v) solution. The mixture was allowed to settle at –20°C and treated with a Wonbio-96c high-throughput tissue crusher (Shanghai Wanbo Biotechnology Co., Ltd., Shanghai, China) at 50 Hz for 6 min, followed by vortexing for 30 s and ultrasonication at 40 kHz for 30 min at 5°C. The samples were placed at –20°C for 30 min to precipitate proteins. After centrifugation at 13,000 *g* at 4°C for 15 min, the

TABLE 1 | Basic properties of the soil for pot experiments.

	pH	As (mg/kg)	Al (mg/kg)	Cd (mg/kg)	Cr (mg/kg)	Cu (mg/kg)	Fe (g/kg)	Mn (g/kg)	Pb (g/kg)	Zn (g/kg)
Soil	7.25	142.5	250.4	22.05	168.1	155.1	16.43	9.330	1.460	89.89

supernatant was transferred to sample vials for LC–MS/MS analysis (Wang and Xie, 2020).

A multivariate statistical analysis was performed using ropls (Version 1.6.2[1]) R package. Principal component analysis (PCA) using an unsupervised method was applied to obtain an overview of the metabolic data, and general clustering, trends, or outliers were visualized. All metabolite variables were scaled to unit variances prior to conducting the PCA. Partial least squares discriminate analysis (PLS-DA) was used for statistical analysis. All metabolite variables were scaled to Pareto scaling prior to conducting the PLS-DA. The model validity was evaluated from model parameters R^2 and Q^2, which provide information on interpretability and predictability, respectively, of the model and avoid the risk of overfitting (Wang et al., 2021). Variable importance in the projection (VIP) was calculated in the PLS-DA model, and p values were estimated with paired Student's *t*-test on single-dimensional statistical analysis. The variables with significant differences ($p < 0.05$) and VIP values > 1 were defined as key metabolites.

Univariate Statistical Analysis

Univariate statistical analyses were performed using SPSS 19.0 and summarized as the mean ± standard error (SE). Treatment means were compared using Tukey's ANOVA at the 5% level of significance ($p < 0.05$).

RESULTS

Content of Available Arsenic and Arsenic Fractionation in Soil

Figure 1 shows the changing trend of available arsenic content in soil during the rice growth period. In the flooded paddy soil, the available As content in the soil first increased and then decreased with the growth period of the rice plants. In the CK and RP treatments without inoculation with FeOB, the content of available arsenic in soil increased greatly in the early stage of rice growth because paddy soil was flooded at that time, and the redox potential in the soil decreased, resulting in the reduction and dissolution of arsenic originally adsorbed on iron oxides and their re-release into the soil (Wu et al., 2016). The available arsenic content of soil reached the highest value, 2.228 mg/kg, at the jointing stage in CK, while in the treatments planted with rice (RP), the available As content was lower. In the FB and RF treatments inoculated with FeOB, the available arsenic content in the soil increased slightly with time, but the total content remained at the same low level as the initial value (1.487–1.554 mg/kg). The inoculation of FeOB significantly reduced the available arsenic content in paddy soil from the jointing stage to the maturity stage ($P < 0.05$). In the maturity stage, the available arsenic content of each treatment group was CK > RP > FB > RF, among which the available arsenic contents in the FB and RF treatments were 1.518 mg/kg and 1.516 mg/kg, respectively, which were 6.25–12.31% lower than the 1.731 mg/kg and 1.617 mg/kg of the CK and RP treatments, respectively.

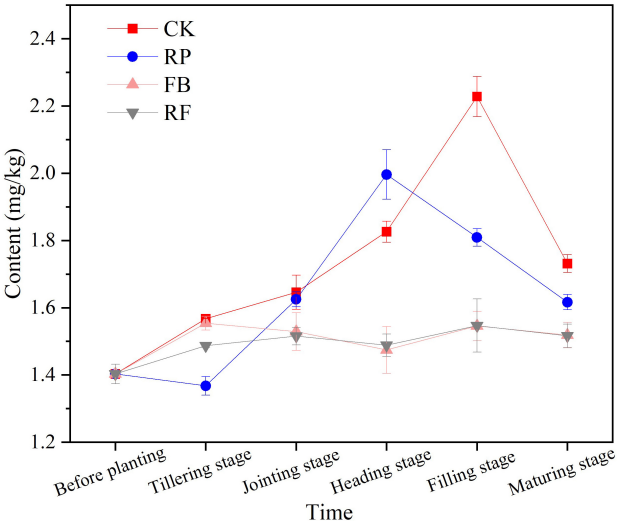

FIGURE 1 | Available arsenic content in soils in different treatments at different growth stages.

Since the total arsenic concentration is insufficient to account for the bioavailability and toxicity of arsenic in soil (Huang et al., 2015), we used different extraction reagents to separate the arsenic components in the soil into the following binding states: (1) non-specific adsorption state, (2) specific adsorption state, (3) amorphous iron-aluminum oxide binding state, (4) crystalline iron-aluminum oxide binding state, and (5) residual state. **Figure 2** shows the different arsenic fractions of soils in the rice maturation stage. In the CK, the As fraction concentration trend was residual state > amorphous iron-aluminum oxide binding state ≥ crystalline iron-aluminum oxide binding state > specific adsorption state > non-specific adsorption state. In other treatments, the As concentration in the residual state was 56.3∼82.0 mg/kg, accounting for 46∼59%; As concentration in the crystalline iron-aluminum oxide binding state was 23.2∼29.8 mg/kg, accounting for 17∼25%; As concentration in the amorphous iron-aluminum oxide binding state was 22.9∼32.7 mg/kg, accounting for 17∼25%; As concentration in the specific adsorption state was 9.55∼10.2 mg/kg, accounting for 7∼8%; and As concentration in the non-specific adsorption state was 0.15∼0.23 mg/kg, accounting for <1%. In unplanted soil, compared with the CK, FeOB inoculation (FB) increased

[1]http://bioconductor.org/packages/release/bioc/html/ropls.html

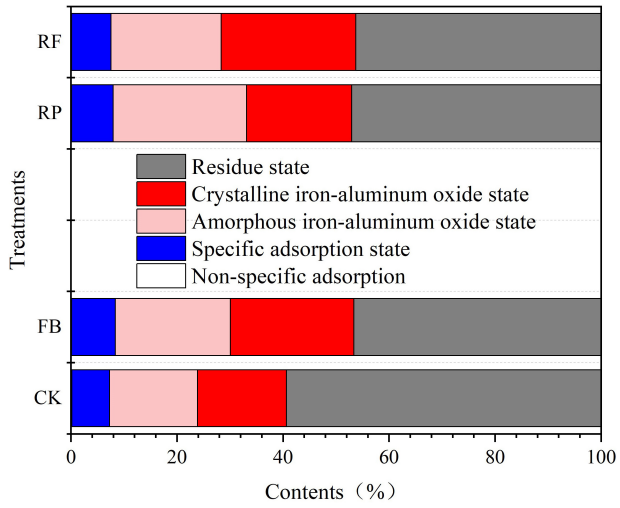

FIGURE 2 | Relative distribution of different arsenic binding states of different treatment groups at the maturing stage in paddy soils.

the As fraction of the amorphous iron-aluminum oxide binding and crystalline iron-aluminum oxide binding states by 5 and 6%, respectively. However, the residual state decreased by 12% in the FB treatment compared with the CK. In rice rhizosphere soil, compared with the RP, FeOB inoculation (RF) increased the As fraction of the crystalline iron-aluminum oxide binding state by 5% but decreased the As fraction of the amorphous iron-aluminum oxide binding state by 4%.

Arsenic Content and Speciation in Rice Plants

In order to explore the effect of inoculation of iron-oxidizing bacteria on the accumulation of As in rice plants, we harvested rice at mature stage and determined the arsenic speciation in the tissues. **Figure 3** shows the As speciation concentrations in roots (A) and stems (B) of rice plants. Most As species in rice plants was inorganic As, while organic As accounted for lower proportions. In rice plants, the different As speciation trend was As(V) > As(III) > DMA ≥ MMA, which was in accordance with Smith (Smith et al., 2008). The contents of As(III) and As(V) in roots with FR treatment were 11.5 and 191 mg·kg^{-1}, respectively, while those with RP treatment were 27.0 and 261 mg·kg^{-1}, which were reduced by 57.4 and 26.8%, respectively. In the stems, with the inoculation of iron oxidizing bacteria, the contents of As(III) and As(V) decreased from 7.74 and 11.3 mg·kg^{-1} to 4.86 and 5.82 mg·kg^{-1}, which were reduced by 37.2 and 48.5%, respectively. Apparently, the inoculation of iron-oxidizing bacteria significantly reduced the contents of As(III), As(V) and DMA in rice tissues.

Microbial Community Diversity

The species diversity index is a function of species richness and evenness and is a statistic used to describe the diversity of a community. As shown in **Table 2**, the evenness (Shannon and Simpson) and abundance (ACE and Chao) of the microbial community decreased in the treatments with FeOB (FB and RF), indicating that the addition of FeOB caused a disturbance to the microbial community structure in the original soil, in which the niches of some kinds of microorganisms were replaced, thus reducing microbial diversity. In addition, the microbial community diversity in the rhizosphere soil under different treatments was higher than that in the unplanted rice soil because the exudates from plant roots could have provided a carbon source for soil microorganisms and could have changed the microenvironmental conditions of the rhizosphere soil. These results were consistent with the results reported by Peiffer et al. (2013), who found that the microbial community diversity in the maize rhizosphere was significantly higher than that in the surrounding soil.

As shown in **Figure 4A**, the number of microbial OTUs in the paddy soil and unplanted soil without FeOB was 5311 and 6182, respectively. The number of microbial OTUs detected in the paddy and unplanted soil inoculated with FeOB was 4643 and 4607, respectively. The number of common OTUs in the four treatment groups was 2691, accounting for 50.67, 43.53, 57.96, and 58.41% of the CK, RP, FB, and RF treatment groups, respectively. **Figure 4B** shows that the CK, RP, FB, and RF treatment groups contained 832, 900, 806, and 794 genera, respectively, and 617 bacterial genera were shared among all treatment groups. Compared with the treatments without inoculation of FeOB, the number of common genera in the soil with inoculation of FeOB decreased relatively, while the number of specific genera increased relatively.

The soil samples collected in this experiment included Proteobacteria, Bacteroidetes, Firmicutes, Acidobacteria, Chloroflexi, Verrucomicrobia, Actinobacteria, Rokubacteria, Planctomycetes, Gemmatimonadetes, and Patescibacteria, accounting for more than 95% of the total phyla (**Figure 5**). Among them, Proteobacteria, Bacteroidetes, Firmicutes, and Acidobacteria were the dominant phyla, and their relative abundances in the CK treatment were 27, 17, 13, and 15%, respectively. In the FB treatment, the relative abundance of Firmicutes increased by 3%, that of Bacteroides increased by 3%, and that of Acidobacteria decreased by 2%. The changing trend of microbial phyla caused by inoculation with FeOB was different in the paddy soil compared with that in the unplanted soil. In the paddy soil, the relative abundances of Proteobacteria and Firmicutes increased by 5 and 2% after inoculation with FeOB, respectively. In genus level, the relative abundance of *Bacteroides*, *Anaerolineaceae*, *Prevotella*, *Faecalibacterium*, *Gemmatimonadaceae*, *Rokubacteriales*, and *Thiobacillus* was higher (**Figure 6**). However, the unclassified KD4-96 (belonging to the phylum Phanerochaete), *Pedosphaeraceae*, *Geobacter* were significantly enriched after inoculation with FeOB, while the abundances of *Gemmatimonadetes* and *Rokubacteriales* etc. were lower in the treatments with FeOB inoculation.

Soil Metabolic Profiling

Soil metabolomics can detect hundreds of chemicals simultaneously and identify metabolic molecular changes that have occurred in the soil. However, current research on the effects of FeOB on soil microbial remediation generally does

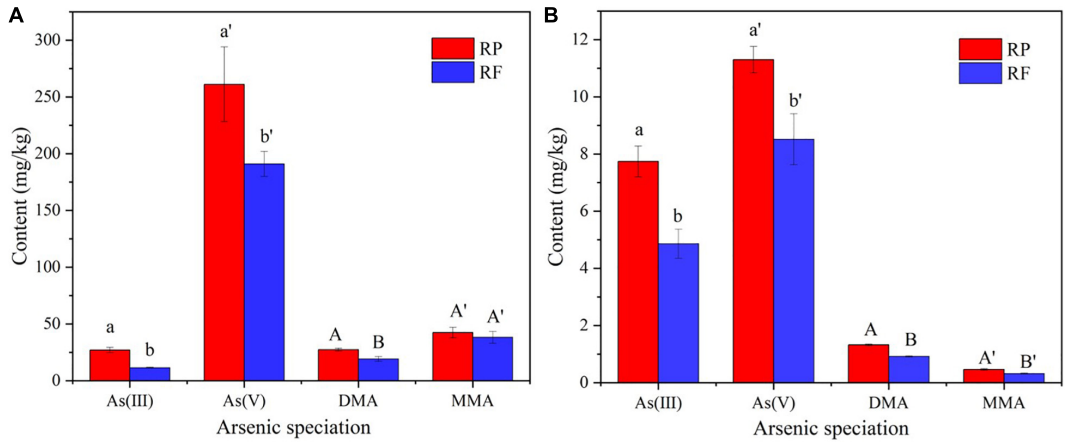

FIGURE 3 | Contents of arsenic in different speciation in roots **(A)** and stems **(B)** of rice plants.

TABLE 2 | α diversity index of microbial communities in the soils.

Sample	Shannon	Simpson	Ace	Chao
RF	6.864	0.003103	5357	5334
FB	6.776	0.003557	5553	5558
RP	7.175	0.002425	7232	7248
CK	6.974	0.002699	6360	6299

not include the analysis of soil metabolites. In this study, FeOB were added to the soil as *in situ* remediation agents to study the long-term effects of FeOB on soil metabolite profiling in the presence and absence of rice plants. To visualize general grouping information as a function of treatment, PCA analysis was performed (**Figure 7**). The results showed that except for the large deviation in the RF4 samples, the remaining samples were within the 95% confidence interval, and there was a significant difference between the two groups. However, the samples in the RP group were not completely separated due to their proximity to each other. The results showed that all samples except RF4 were within the 95% confidence interval. In **Figure 7**, PC1 and PC2 represented 27.20 and 14.40%, respectively, of the overall difference of the samples, and the FeOB inoculated treatments (RP and RF) and the non-inoculated treatments could be completely separated (CK and FB). In addition, whether rice was planted was considered the distinguishing condition, and the samples of the two treatments were also completely separated. And to achieve the maximum separation between soil metabolic samples from different treatment groups, partial least squares analysis (PLS-DA) with a supervised model was used to analyze the difference between two treatments. As shown in **Figure 8**, all 24 samples were in the confidence interval of 95%, and the group of CK, RP and FB, RF were obviously separated, which indicates that components 1 and

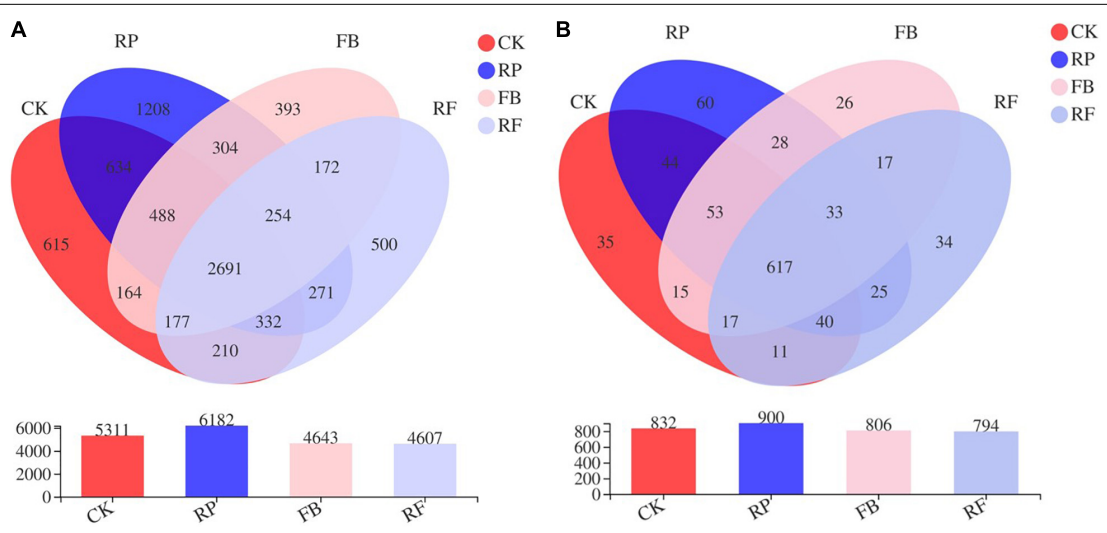

FIGURE 4 | Venn diagram of the microbial community at the OUT **(A)** and genus **(B)** level.

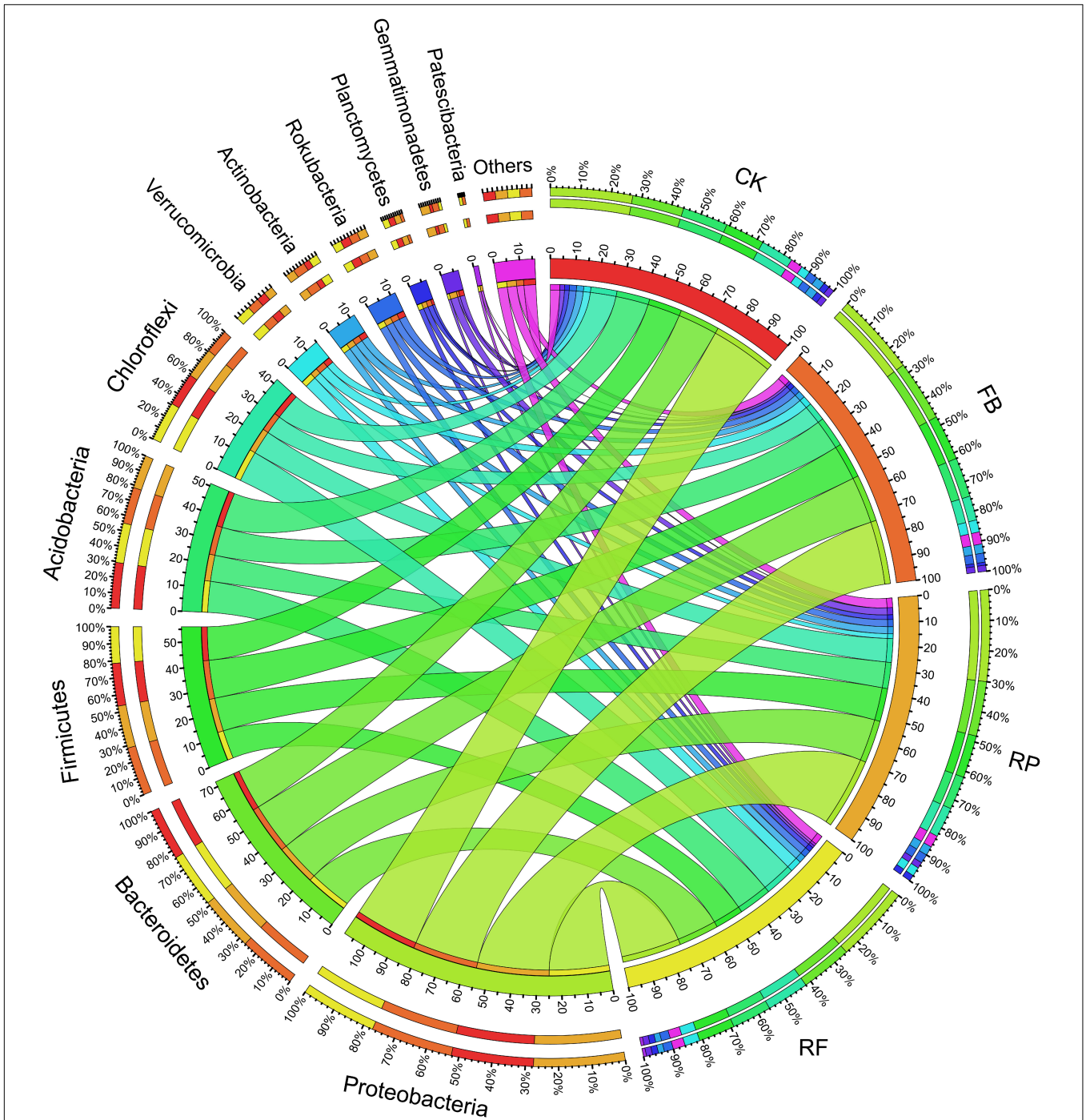

FIGURE 5 | Circos diagram of microbial on phylum levels in different treatments.

2 in this model can better explain the differences between groups, and the metabolite abundance among groups were significantly different. The replacement test of the model (**Table 2**) shows that R2X and R2Y represent the interpretation rate of the x and y matrices, and R2X(cum) and R2Y(cum) represent the cumulative interpretation rate. Q2 indicates the prediction ability of the model. The closer these three indices are to 1, the more stable and reliable the model, and Q2 > 0.5 indicates the better prediction ability of the model. The R2Y(cum) of the two PLS-DA models is close to 1, which indicates that the models agree with the real situation of samples, Q2 is greater than 0.5, and the intercept between q and the longitudinal axis is less than 0, which indicates that the models have good stability.

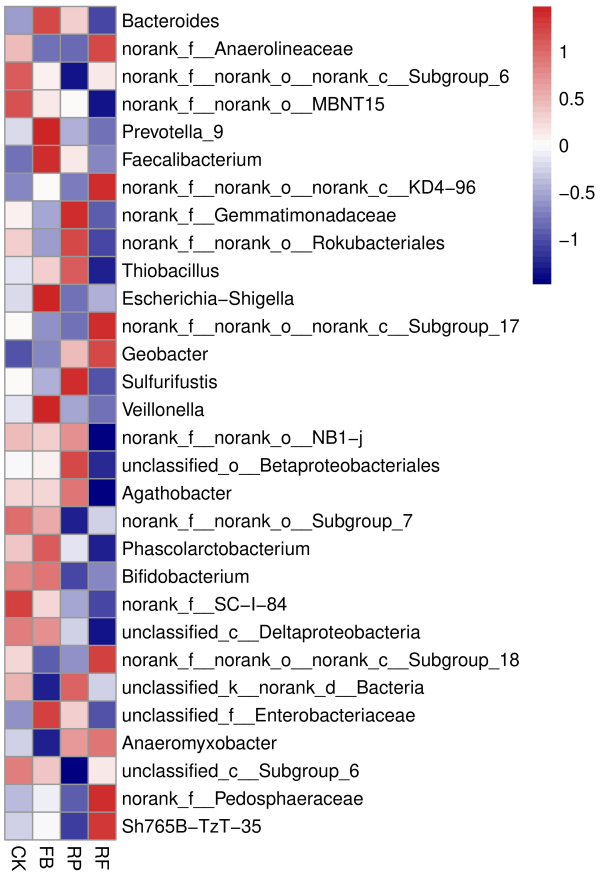

FIGURE 6 | Heat map of microbial communities at the genus level.

A total of 448 metabolites were identified and semiquantified in soil samples by using non-target metabonomics based on liquid chromatography-mass spectrometry (LC–MS). A two-tailed test analysis was performed on all metabolites, and a volcano map of metabolite differences was created (**Figure 9**). **Figure 9A** shows the differential metabolites in the CK and FB, and most differential metabolites were significantly downregulated in the FB, with only a few metabolites were significantly upregulated. Notably, the inoculation of FeOB had different effects on soil metabolites in the rice rhizosphere, more metabolites were significantly upregulated in RF. According to $P < 0.05$ and VIP > 1, the differential metabolites with the top 30 VIP values are shown in **Figure 10**. In the treatment groups without rice planting, except for the increase in two metabolites, the abundance of most differential metabolites was downregulated with the inoculation of FeOB (**Figure 10A**), which indicated that FeOB might affect the metabolism of soil microorganisms, resulting in the inhibition of some metabolite synthesis pathways or the enhancement of decomposition pathways. Notably, the abundance of several lipids and lipid-like compounds was significantly downregulated with inoculation of FeOB, including fatty alcohols (1-acetoxy-2-hydroxy-16-heptadecen-4-one), fatty acid esters (3-hydroxypentadecanoyl carnitine), retinoids (bexarotene), linoleic acids and their derivatives [8(*R*)-hydroperoxylinoleic acid], fatty acyl glycoside (1-octen-3-yl glucoside) and glycerophospholipids [PG (a-13:0/i-12:0)]. In addition, the abundance of carbohydrates and their derivatives, including methyl beta-D-glucopyranoside, D-ribose, 1-octen-3-yl glucoside, sucrose and amino acid derivatives, including rhizonin A, histidinyl-threonine, tryptophyl-aspartate, temocarilat, methionyl-asparagine, aminopentanamide and others, were also downregulated with inoculation with FeOB.

In the presence of rice plants, the soil metabolite pool consists of metabolites secreted by plants and metabolites produced by microbial communities. The results showed that inoculation with FeOB also changed the distribution of soil metabolites in the rhizosphere soil. Part of the key metabolites were consistent with those in the unplanted soil (**Figure 10B**), including some amino acid analogs and some lipid compounds such as *N*-*N*-heptanoyl-homoserine lactone NE and *N*-octanoyl-L-homoserine lactone etc., which were still downregulated after inoculation with FeOB. Furthermore, some other key metabolites not found in the unplanted soil, such as pantetheine 4′-phosphate, etriol-3-glucuronide (not shown in the figure), were also downregulated. Interestingly, in contrast to the unplanted soil, more metabolite abundances were upregulated after inoculation with FeOB in the paddy-planted soil, including carnosine, MG(0:0/18:3(9Z,12Z,15Z)/0:0), MG(0:0/14:0/0:0), todatriol glucoside, avocadyyne 1-acetate, (2,6,6-trimethyl-2-cyclohexen-1-yl)-1,6-heptadien-3-one, and acetoxy-2-hydroxy-16-heptadecyn-4-one.

DISCUSSION

Redistribution of Arsenic in Paddy Soil and Rice Plants by Inoculation With FeOB

The toxicity and mobility of As depend largely on its speciation, the content of total arsenic in soil is of limited significance for measuring the bioavailability of As in soil (Flynn et al., 2002). Therefore, the determination of available As content and the As fractionation in soil is of great significance to the environmental risk assessment of arsenic in soil. The available As content in this study were rank as follow: CK $>$ RP $>$ FB $\geq$ RF (**Figure 1**). The available As content in the treatments planted with rice (RP) was lower than CK, which was due to the oxygen secretion function of the rice root system, promoting the formation of iron plaque on the rice root surface and immobilizing the heavy metals through adsorption or coprecipitation, thus resisting the damage to the plants by the heavy metals in the soil (Wu et al., 2015). The inoculation of FeOB effectively controlled the content of available arsenic in soil and inhibit the desorption and release of adsorbed arsenic in flooded soil. It was because FeOB promoted the aggregation of Fe (II), accelerated the oxidation rate of Fe (II) and promoted the formation of iron (hydroxide) oxides under microaerobic or anaerobic conditions. It was reported that most iron (hydroxide) oxides generated from Fe(II) oxidation mediated by neutral FeOB initially exist

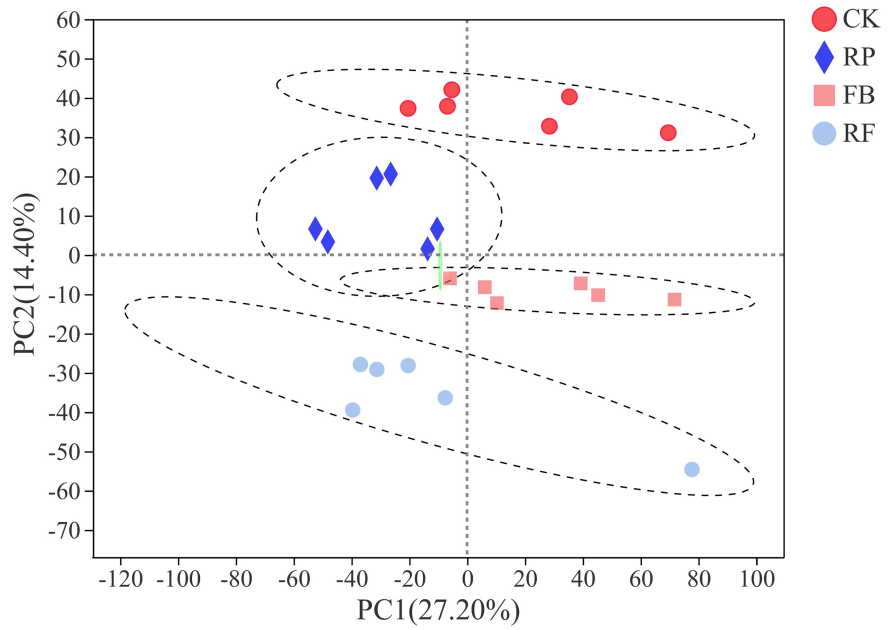

FIGURE 7 | PCA scoring model of different treatments.

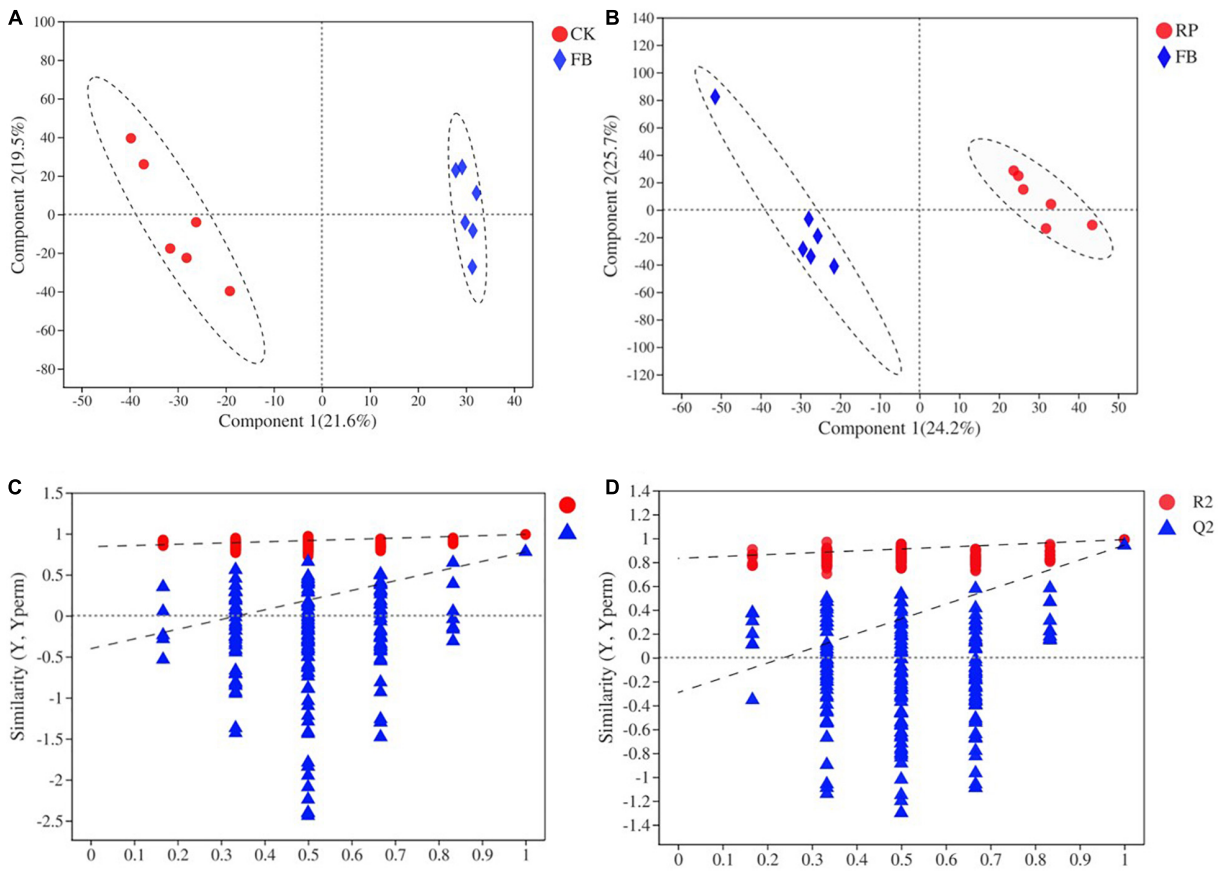

FIGURE 8 | PLS-DA scoring [**(A)** CK and FB and **(B)** RP and RF] models and permutation test [**(C)** CK and FB and **(D)** RP and RF].

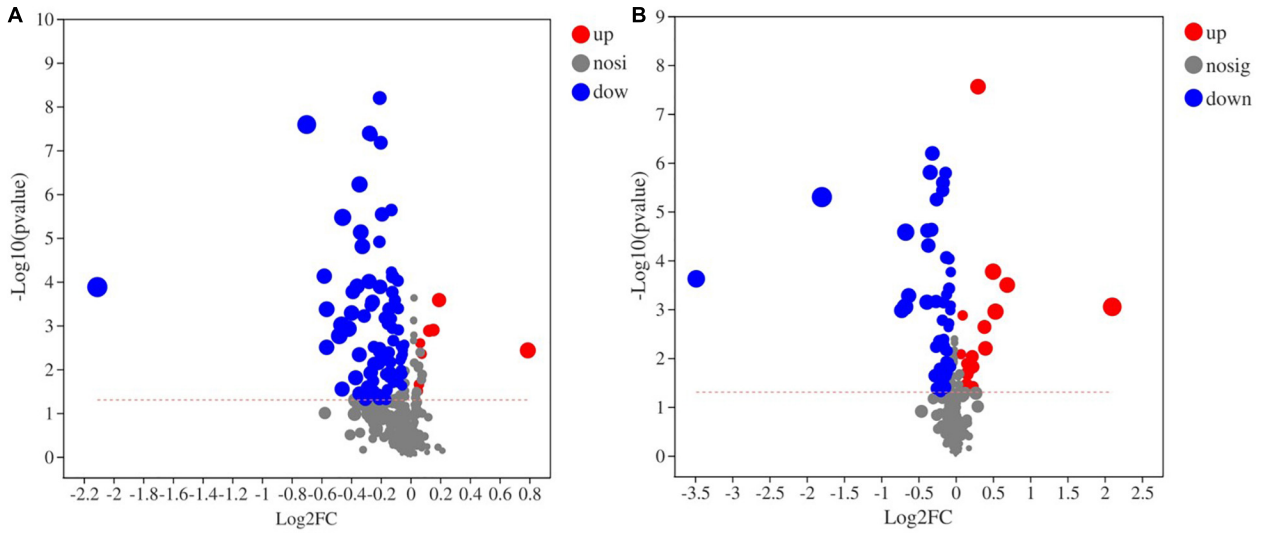

FIGURE 9 | Volcano map of metabolic differences (**A:** CK vs. FB; and **B:** RP vs. RF).

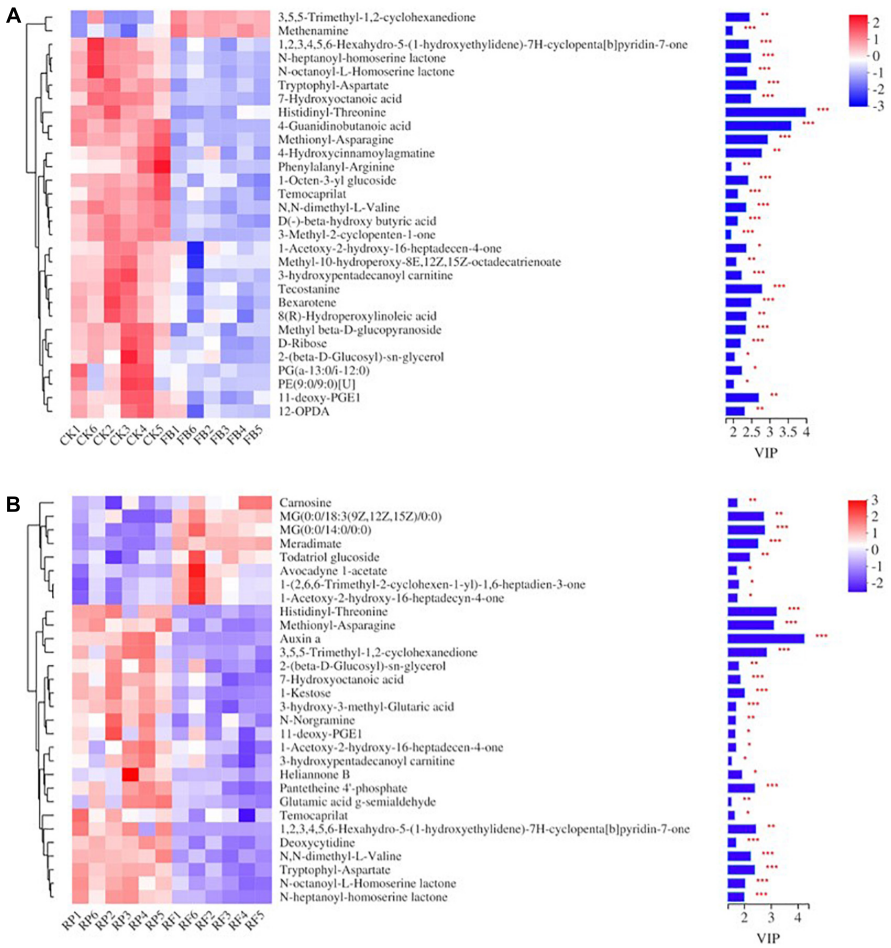

FIGURE 10 | Heat map of metabolic differences of the top 30 metabolites in unplanted **(A)** and rice rhizosphere **(B)** soils.

as second-line ferrihydrite ($Fe_5HO_8{\cdot}4H_2O$) or amorphous iron oxyhydroxide (FeOOH) (Miot et al., 2009). These iron minerals have the characteristics of high surface activity, low crystallinity, amorphous state, and strong adsorption performance for heavy metals. However, second-line ferrihydrite was in a metastable state in the environment and was prone to conversion into mineral phases and morphological structures under the action of chemicals or microorganisms, thus further forming high-crystallinity and more stable iron minerals such as lepidocrocite, hematite, goethite and magnetite. This process was usually accompanied by the migration and release of heavy metals from the mineral surface, followed by secondary adsorption and coprecipitation.

As fractions in the soil could have been affected by the rice rhizosphere environment, including physicochemical properties (such as pH and Eh), radial oxygen loss of rice (ROL) and microbes in the rice rhizosphere. For example, Wu et al. showed that ROL could affect As transfer in soils, leading to the coprecipitation of As and Fe and increasing the As fraction of the amorphous iron-aluminum oxide binding state (Wu et al., 2015). Moreover, the activities of plant roots and microorganisms promote the oxidation of difficult-to-convert substances such as sulfide (FeAsS) and organic matter in soil (Huang et al., 2015). For example, FeOB oxidized Fe(II)to Fe(III), which accelerated the oxidation-dissolution reaction of As-containing minerals such as arsenopyrite, leading to the formation of $FeAsO_4{\cdot}2H_2O$ (Garcia-Sandchez and Alvarez-Ayuso, 2003). This process increased the As content in the iron-aluminum oxide binding state but decreased the As content in the residue state. In addition, the radial oxygen loss of rice might stimulate microbial activities in rhizosphere soil and further affect the behavior of As.

Previous studies (Wenzel et al., 2001; Smith et al., 2008) have shown that As in soil is closely related to amorphous or crystalline iron-aluminum oxides. The As component in the non-specific adsorption state, specific adsorption state, and amorphous iron-aluminum oxide binding state was considered to constitute the main part of bioavailable As (Tang et al., 2007), whereas the crystalline iron-aluminum oxide binding state and residual state were relatively stable. Therefore, the As component associated with the amorphous iron-aluminum oxide binding state was a key part in controlling bioavailability. In these results, the inoculation of FeOB increased the amorphous iron-aluminum oxide binding state and crystalline iron-aluminum oxide binding state of As in the soil without rice planting. In the rhizosphere soil, the inoculation of FeOB promoted the transformation of the amorphous iron-aluminum oxide binding state of As to the crystalline iron-aluminum oxide binding state, which indicated that the application of FeOB in soil resulted in the redistribution of arsenic speciation in soil and effectively reduced the bioavailability of As.

With the inoculation of FeOB, different As speciation, especially As(V), As(III) and DMA, were significantly decreased in both stems and roots. FeOB could have promoted the formation of rhizosphere iron (hydrogen) oxide and the formation of iron plaque, which could have sequestered As on rice roots. This has potential for As remediation in soils and decreasing As accumulation in rice plants. Moreover, other studies also showed that with the addition of FeOB to paddy fields, the As and Cd concentrations in different parts of rice significantly decreased (Dong et al., 2016; Xiao et al., 2020).

Changes of Soil Microbial Community Structure After Inoculation With FeOB

These results of microbial community diversity indicated that inoculation with FeOB changed the microbial composition in the microdomain of paddy soil and could significantly affect the growth of some microorganisms, resulting in significant differences in microbial communities (**Figure 4**). At the phylum level, with the inoculation of iron-oxidizing bacteria, Proteobacteria, Bacteroidetes, and Firmicutes were increased in the unplanted and rice rhizosphere soils (**Figure 5**). The enrichment of Proteobacteria, Bacteroidetes, and Firmicutes was consistent with the previously reported microaerophilic FeOB studies. In the study of enrichment and subculture of micro-aerobic iron-oxidizing bacteria in paddy soil by Chen et al. (2016) and Li et al. (2019), enrichment of some bacteria with iron oxidation function was found, and most of them belong to Proteobacteria, Bacteroides, and Firmicutes, accounting for more than 90% of microbial community, which indicates that the inoculation of *Ochrobactrum* strain promotes the enrichment of iron oxidation-related microorganisms in soil in this study. Moreover, the *Ochrobactrum* strain in our study, belongs to Proteobacteria. Although the abundance increase of Proteobacteria was detected in the results of microbial communities, *Ochrobactrum* sp. was not detected as dominant genus at the genus level, which might be since after a long period of culture, *Ochrobactrum* sp. competed with indigenous microorganisms, and have not developed into the dominant genus or the universal primers used for PCR amplification in this study had no specificity for 16S rRNA genes of Ochrobactrum (Wang et al., 2009).

In the results of the genus level (**Figure 6**), Girardot et al. (2020) reported that KD4-96 was a heavy metal-resistant bacterium, and it may play an important role in the biotransformation of heavy metals. Cao et al. (2020) found that *Pedosphaeraceae* had a significant positive correlation with the accumulation of Pb and Cd in hyperenriched plants, but the behavioral mechanism was not elucidated. The enrichment of *Pedosphaeraceae* might indicate that inoculation with FeOB reduced the toxicity of heavy metals in soil (Cao et al., 2020). The abundances of *Gemmatimonadetes* and *Rokubacteriales* were lower in the FeOB inoculation treatments. *Gemmatimonadetes* is a beneficial bacterium essential for phosphorus dissolution, microbial nitrogen metabolism and soil respiration (Chen et al., 2020) and widely exists in farmland soil. Similarly, studies have shown that Rokubacteriales is a type of bacteria with nitrogen respiratory potential (Becraft et al., 2017). These results indicated that the relevant carbon and nitrogen metabolic pathways were relatively weakened in the treatment with FeOB after 105 days of inoculation. It was speculated that the inoculation of nitrate dependent, FeOB at an early stage stimulated the process of iron oxidation coupled with nitrogen reduction and accelerated the consumption of nitrogen sources in the soil, thus weakening the

nitrogen metabolic pathway at the mature stage. Furthermore, the abundance of *Geobacter*, which is related to iron-reducing bacteria, was higher in the rhizosphere soil than in the unplanted soil, and the abundance was highest in the RF, suggesting that the action of oxygen secretion from the rice rhizosphere and FeOB jointly promoted the iron redox cycle in the soil.

Regulatory Mechanism of FeOB in Soil From the Perspective of Metabonomics

The structure and function of soil ecosystems are very complex, and their key biogeochemical cycles are driven by a variety of factors, including soil animals, microorganisms, extracellular enzymes, and plants. Soil metabolites can be considered phenotypic to changes in soil microbial community activity, as changes at the biological and enzyme levels will ultimately be manifested as changes in the metabolite profiles. In addition, plants can also actively regulate the distribution of rhizosphere secretions. Swenson et al. (2015) first proposed the "soil metabolomics" method to analyze soil organic matter reservoirs, and the changes experienced by organisms and enzyme levels are manifested as changes in metabolic profiling to propose reasonable assumptions for changes in soil biochemistry. In this study, FeOB may directly or indirectly interact with soil organic matter and microorganisms and thus affect biochemical processes and metabolic pathways in soil. The secreted intracellular and extracellular metabolites of soil microorganisms constitute the soil metabolite pool, and monitoring soil metabolites could indirectly reflect the changes in microbial metabolism.

In unplanted soil (**Figure 10A**), (R)-Hydroperoxylinoleic acid is a linoleic acid derivative that can be produced by some fungi through linoleic acid metabolism (Brodowsky et al., 1992; Brodowsky and Oliw, 1993), while PG(a-13:0/i-12:0) is a glycerophospholipid that is not only an important component of biofilms but also involved in protein recognition and signal transduction by the cell membrane. Oxylipins are a type of lipid oxide signal that regulates many physiological processes, such as growth and development, defense responses to pathogens and herbivores, and abiotic stresses (Wang et al., 2020). 12-OPDA, a metabolite of the allene oxide synthase (AOS) pathway, is produced by the oxidation of α-linolenic acid by 13-lipoxygenase, followed by the formation of unstable alkylene oxide through AOS action and subsequent cyclization by alkylene oxide cyclase (Stenzel et al., 2012), which has been reported to arise under stress in response to a variety of environmental changes. Moreover, fatty acids and their derivatives, such as stearidonic acid, 9(S)-HODE, 9-OxoODE, and prostaglandin J2, also showed significant differences between the FB and CK. According to the functional pathway of the KEGG pathway, these unsaturated fatty acid cascades could produce a variety of endogenous signaling molecules to regulate a variety of biological processes (Milne et al., 2005). D-ribose has been reported as the structural skeleton of purine and pyrimidine in genetic material and pentose precursor of some amino acids and is a component of many cofactors (especially adenosine triphosphate), playing a key role in energy metabolism (Croci et al., 2011; Maifiah et al., 2017). The reduction of these carbohydrates and amino acids might affect the normal microbial activities in the soil. The downregulation of carbohydrate abundance in soil might be due to the increase in carbohydrate molecular consumption caused by the addition of FeOB or due to the changes in the composition of microbial communities, which affect the carbon cycle in soil. A series of studies showed that exopolysaccharides and proteins secreted by bacteria are likely to provide nucleation sites for mineralization in the process of metal ion precipitation (Chan et al., 2004, 2009; Miot et al., 2009), inducing the accumulation of metal ions and the formation of different mineral phases. Huang et al. (2015) demonstrated that polysaccharides, such as dextran, chitosan, gelatine, and protein, could serve as nucleation sites and regulate the biomineralization process (Sun and Huang, 2006; Huang and Sun, 2007). The results of this study showed that the abundance of carbohydrates and amino acid analogs was downregulated to a certain extent after inoculation with FeOB. Combined with the results of the increase in the amorphous iron-aluminum oxide binding state and crystalline iron-aluminum oxide binding state of As in paddy soil, it could be speculated that the decrease in the abundance of polysaccharides and protein was due to the sampling time at the maturity stage of rice. A period after inoculation with FeOB promoted the utilization of polysaccharides, amino acids, and other substances in the soil during the growth stage of rice, as well as the occurrence of biomineralization, which in turn led to the downregulation of protein polysaccharide abundance at the maturity stage.

In rice rhizosphere soil (**Figure 10B**), Carnosine was reported as an endogenous dipeptide present in different tissues that inhibits lipid peroxidation and protein carbonylation (Kang et al., 2002; Aldini et al., 2005; Aydin et al., 2010; Kalaz et al., 2014). Carnosine functions as a free radical scavenger, a membrane protector, and a transition metal-chelating agent in organisms and has superoxide dismutase-like activity (Boldyrev et al., 2010) and is capable of neutralizing lipid peroxidation. The increase in carnosine abundance was conducive to resisting the destructive effects of oxidant pollutants. In addition, the abundance of most lipids and their derivatives in soil was upregulated by RP treatment, such as MG(0:0/18:3(9Z,12Z,15Z)/0:0), MG(0:0/14:0/0:0), todatriol glucoside, avocadyyne 1-acetate, (2,6,6-trimethyl-2-cyclohexen-1-yl)-1,6-heptadien-3-one, and acetoxy-2-hydroxy-16-heptadecyn-4-one. The upregulation of lipid compounds indicated that the inoculation of FeOB affected the lipid metabolic pathway in the soil planted with rice, but the abundance of lipid compounds showed the opposite change trend to that in the unplanted soil, which also indicated that the occurrence of lipid peroxidation in the soil was inhibited to a certain extent. Moreover, pantetheine 4'-phosphate was reported to be capable of synthesizing CoA, which is involved in many metabolic pathways, including the citric acid cycle, fatty acid biosynthesis as the coenzyme of acyltransferase (Rath et al., 2018). Some studies have shown that pantothenic acid and its derivatives have a protective effect on cell and tissue damage and are related to resistance to peroxidation damage (Slyshenkov et al., 1995). Besides, the abundances of *N*-*N*-heptanoyl-homoserine lactone NE and *N*-octanoyl-L-homoserine lactone were downregulated. Other studies reported that homoserine internal lipids also affected plant cells. If homoserine lactone

exists around plants, plants might change gene expression, protein levels, and growth status and enhance their defense response (Mathesius et al., 2003; Miao et al., 2012; Zhao et al., 2016).

In summary, FeOB still downregulated the abundance of some metabolites in the rice rhizosphere soil, indicating that inoculation of FeOB caused a disturbance to the microbial community structure in the soil. However, there were a few upregulated metabolites, especially some compounds related to lipid metabolism. It was speculated that the coregulation of plant root exudates and soil microorganisms might enhance the defense ability of the soil-microorganism-plant system against peroxidation damage. However, the potential mechanism of these changes, including the role of plants, and whether such regulation is active or passive are still unclear.

CONCLUSION

The iron-oxidizing strain (*Ochrobactrum* sp. EEELCW01) was inoculated into As polluted paddy soil as a microbial agent, which could effectively reduce As bioavailability. The content of soil available As in the treatments (FB, RF) inoculated with iron oxidizing bacteria was decreased by 6.25–12.31% compared with that in the treatments (CK, RP) not inoculated. The inoculation of iron oxidizing bacteria also increased the proportion of As in the iron-aluminum oxide binding fraction, and significantly reduced As accumulation in rice tissues. The abundances of KD4-96, Pedosphaeraceae and other bacteria in soils increased with the inoculation of iron oxidizing bacteria. These bacteria had heavy metal resistance and could reduce the toxicity of heavy metals in soil through the biotransformation. However, the abundance of Gemmatimonadetes and Rokubacteriales decreased relatively, which was related to the consumption of a large amount of N-derived substances in the early stage. Soil metabolites could reflect the changes in microbial metabolic process. In the unplanted soil, the reduction of most polysaccharides and protein substances might be due to the promotion of iron oxide bacteria to metabolize and decompose polysaccharides, amino acids and other substances in the soils. In the rhizosphere soils, the abundance increases of Carnosine and some lipid substances including MG (0:0/14:0/0:0) and Pantetheine 4′-phosphate indicated that the defense ability of soil-microorganism-plant system against peroxidation damage was improved.

DATA AVAILABILITY STATEMENT

The original contributions presented in the study are included in the article/supplementary material, further inquiries can be directed to the corresponding author/s.

AUTHOR CONTRIBUTIONS

ZQ: experiment, data curation, formal analysis, software, visualization, writing – review and editing. CW: methodology, resources, writing – review and editing. WP: funding, conceptualization, and resources. XX and LX: experiment and data curation. WL: review and editing. All authors contributed to the article and approved the submitted version.

FUNDING

This work was financially supported by the Research Foundation of Education Bureau of Hunan Province, China (No. 20A246), Natural Science Foundation of Hunan Province of China (No. 2021JJ30340), National Natural Science Foundation of China (No. 42177392), and Dean's Research Fund 2020/21 (Project code: 04626) of the Education University of Hong Kong.

REFERENCES

Achal, V., Pan, X., Fu, Q., and Zhang, D. (2012). Biomineralization based remediation of As(III) contaminated soil by *Sporosarcina ginsengisoli*. *J. Hazard. Mater.* 201, 178–184. doi: 10.1016/j.jhazmat.2011.11.067

Alam, R., and McPhedran, K. (2019). Applications of biological sulfate reduction for remediation of arsenic. *Chemosphere* 222, 932–944. doi: 10.1016/j.chemosphere.2019.01.194

Aldini, G., Facino, R. M., Beretta, G., and Carini, M. (2005). Carnosine and related dipeptides as quenchers of reactive carbonyl species: from structural studies to therapeutic perspectives. *Biofactors* 24, 77–87. doi: 10.1002/biof.5520240109

Aydin, A. F., Kucukgergin, C., Ozdemirler-Erata, G., Kocak-Toker, N., and Uysal, M. (2010). The effect of carnosine treatment on prooxidant-antioxidant balance in liver, heart and brain tissues of male aged rats. *Biogerontology* 11, 103–109. doi: 10.1007/s10522-009-9232-4

Bais, H. P., Weir, T. L., Perry, L. G., Gilroy, S., and Vivanco, J. M. (2006). The role of root exudates in rhizosphere interations with plants and other organisms. *Annu. Rev. Plant. Biol.* 57, 233–266. doi: 10.1146/annurev.arplant.57.032905.105159

Becraft, E. D., Woyke, T., Jarett, J., Ivanova, N., Godoy-Vitorino, F., Poulton, N., et al. (2017). Rokubacteria: genomic giants among the uncultured bacterial phyla. *Front. Microbiol.* 8:02264. doi: 10.3389/fmicb.2017.02264

Boldyrev, A. A., Stvolinsky, S. L., Fedorova, T. N., and Suslina, Z. A. (2010). Carnosine as a natural antioxidant and geroprotector: from molecular mechanisms to clinical trials. *Rejuv. Res.* 13, 156–158. doi: 10.1089/rej.2009.0923

Brodowsky, I. D., Hamberg, M., and Oliw, E. H. (1992). A linoleic acid (8R)-dioxygenase and hydroperoxide isomerase of the fungus *Gaeumannomyces graminis*. Biosynthesis of (8R)-hydroxylinoleic acid and (7S,8S)-dihydroxylinoleic acid from (8R)-hydroperoxylinoleic acid. *J. Biol. Chem.* 267, 14738–14745.

Brodowsky, I. D., and Oliw, E. H. (1993). Biosynthesis of 8R-hydroperoxylinoleic acid by the fungus Laetisaria arvalis. *Biochim. Biophys. Acta* 1168, 68–72. doi: 10.1016/0005-2760(93)90267-d

Cao, X., Luo, J., Wang, X., Chen, Z., Liu, G., Khan, M. B., et al. (2020). Responses of soil bacterial community and Cd phytoextraction to a *Sedum alfredii*-oilseed rape (*Brassica napus* L. and *Brassica juncea* L.) intercropping system. *Sci. Total Environ.* 723:138152. doi: 10.1016/j.scitotenv.2020.138152

Chan, C. S., De Stasio, G., Welch, S. A., Girasole, M., Frazer, B. H., Nesterova, M. V., et al. (2004). Microbial polysaccharides template assembly of nanocrystal fibers. *Science* 303, 1656–1658. doi: 10.1126/science.1092098

Chan, C. S., Fakra, S. C., Edwards, D. C., Emerson, D., and Banfield, J. F. (2009). Iron oxyhydroxide mineralization on microbial extracellular polysaccharides. *Geochim. Cosmochim. Acta* 73, 3807–3818. doi: 10.1016/j.gca.2009.02.036

Chen, J., Sun, G. X., Wang, X. X., de Lorenzo, V., Rosen, B. P., and Zhu, Y. G. (2014). Volatilization of arsenic from polluted soil by *Pseudomonas putida* engineered for expression of the arsM Arsenic(III) S-Adenosine

Methyltransferase Gene. *Environ. Sci. Technol.* 48, 10337–10344. doi: 10.1021/es502230b

Chen, L., Hao, Z., Li, K., Sha, Y., Wang, E., Sui, X., et al. (2020). Effects of growth-promoting rhizobacteria on maize growth and rhizosphere microbial community under conservation tillage in Northeast China. *Microb. Biotehchnol.* 14, 535–550. doi: 10.1111/1751-7915.13693

Chen, Y. T., Li, F. B., and Li, X. M. (2016). Diversity and biomineralization of Microaerophilic iron-oxidizing bacteria in paddy soil. *Ecol. Environ. Sci.* 25, 547–554. doi: 10.16258/j.cnki.1674-5906.2016.04.001

Clemens, S., and Ma, J. F. (2016). Toxic heavy metal and metalloid accumulation in crop plants and foods. *Annu. Rev. Plant. Biol.* 67, 489–512. doi: 10.1146/annurev-arplant-043015-112301

Croci, S., Bruni, L., Bussolati, S., Castaldo, M., and Dondi, M. (2011). Potassium bicarbonate and D-ribose effects on A72 canine and HTB-126 human cancer cell line proliferation in vitro. *Cancer Cell Int.* 11, 30. doi: 10.1186/1475-2867-11-30

Debiec-Andrzejewska, K., Krucon, T., Piatkowska, K., and Drewniak, L. (2020). Enhancing the plants growth and arsenic uptake from soil using arsenite-oxidizing bacteria. *Environ. Pollut.* 264:114692. doi: 10.1016/j.envpol.2020.114692

Dong, M. F., Feng, R. W., Wang, R. G., Sun, Y., Ding, Y. Z., Xu, Y. M., et al. (2016). Inoculation of Fe/Mn-oxidizing bacteria enhances Fe/Mn plaque formation and reduces Cd and As accumulation in Rice Plant tissues. *Plant Soil* 404, 75–83. doi: 10.1007/s11104-016-2829-x

Flynn, H. C., McMahon, V., Diaz, G. C., Demergasso, C. S., Corbisier, P., Meharg, A. A., et al. (2002). Assessment of bioavailable arsenic and copper in soils and sediments from the Antofagasta region of northern Chile. *Sci. Total Environ.* 286, 51–59. doi: 10.1016/S0048-9697(01)00962-7

Garcia-Sandchez, A., and Alvarez-Ayuso, E. (2003). Arsenic in soils and waters and its relation to geology and mining activities (Salamanca Province, Spain). *J. Geochem. Explor.* 80, 69–79. doi: 10.1016/s0375-6742(03)00183-3

Girardot, F., Allegra, S., Pfendler, S., Conord, C., Rey, C., Gillet, B., et al. (2020). Bacterial diversity on an abandoned, industrial wasteland contaminated by polychlorinated biphenyls, dioxins, furans and trace metals. *Sci. Total Environ.* 748:142746. doi: 10.1016/j.scitotenv.2020.141242

Hohmann, C., Winkler, E., Morin, G., and Kappler, A. (2010). Anaerobic Fe(II)-oxidizing bacteria show as resistance and immobilize as during Fe(III) mineral precipitation. *Environ. Sci. Technol.* 44, 94–101. doi: 10.1021/es900708s

Huang, G., Chen, Z., Sun, J., Liu, F., Wang, J., and Zhang, Y. (2015). Effect of sample pretreatment on the fractionation of arsenic in anoxic soils. *Environ. Sci. Pollut. Res.* 22, 8367–8374. doi: 10.1007/s11356-014-3958-5

Huang, J. B., and Sun, Z. Y. (2007). An experimental study of the mineralization of iron hydroxide modulated by microbial polysaccharide and dextran. *Acta Ichthyol. Piscat.* 26, 467–473. doi: 10.1631/jzus.2007.B0900

Jamieson, J., Prommer, H., Kaksonen, A. H., Sun, J., Siade, A. J., Yusov, A., et al. (2018). Identifying and quantifying the intermediate processes during nitrate-dependent Iron(II) oxidation. *Environ. Sci. Technol.* 52, 5771–5781. doi: 10.1021/acs.est.8b01122

Kalaz, E. B., Coban, J., Aydin, A. F., Dogan-Ekici, I., Dogru-Abbasoglu, S., Oztezcan, S., et al. (2014). Carnosine and taurine treatments decreased oxidative stress and tissue damage induced by D-galactose in rat liver. *J. Physiol. Biochem.* 70, 15–25. doi: 10.1007/s13105-013-0275-2

Kang, J. H., Kim, K. S., Choi, S. Y., Kwon, H. Y., Won, M. H., and Kang, T. C. (2002). Carnosine and related dipeptides protect human ceruloplasmin against peroxyl radical-mediated modification. *Mol. Cells* 13, 498–502. doi: 10.1002/yea.884

Kirk, M. F., Holm, T. R., Park, J., Jin, Q. S., Sanford, R. A., Fouke, B. W., et al. (2004). Bacterial sulfate reduction limits natural arsenic contamination in groundwater. *Geology* 32, 953–956. doi: 10.1130/g20842.1

Klueglein, N., Zeitvogel, F., Stierhof, Y.-D., Floetenmeyer, M., Konhauser, K. O., Kappler, A., et al. (2014). Potential role of nitrite for Abiotic Fe(II) oxidation and cell encrustation during nitrate reduction by denitrifying bacteria. *Appl. Environ. Microb.* 80, 1051–1061. doi: 10.1128/aem.03277-13

Li, X., Zhang, W., Liu, T., Chen, L., Chen, P., and Li, F. (2016). Changes in the composition and diversity of microbial communities during anaerobic nitrate reduction and Fe(II) oxidation at circumneutral pH in paddy soil. *Soil Biol. Biochem.* 94, 70–79. doi: 10.1016/j.soilbio.2015.11.013

Li, X. M., Mou, S., Chen, Y. T., Liu, T. X., Dong, J., and Li, F. B. (2019). Microaerobic Fe(II) oxidation coupled to carbon assimilation processes driven by microbes from paddy soil. *Sci. China Earth Sci.* 62, 1–11. doi: 10.1007/s11430-018-9329-3

Luo, X. H., Jiang, X. X., Xue, S. G., Tang, X. J., Zhou, C. H., Wu, C., et al. (2021). Arsenic biomineralization by iron oxidizing strain (*Ochrobactrum* sp.) isolated from a paddy soil in Hunan. *China. Land Degrad. Dev.* 32, 2082–2093. doi: 10.1002/ldr.3842

Maifiah, M. H. M., Creek, D. J., Nation, R. L., Forrest, A., Tsuji, B. T., Velkov, T., et al. (2017). Untargeted metabolomics analysis reveals key pathways responsible for the synergistic killing of colistin and doripenem combination against *Acinetobacter baumannii*. *Sci. Rep.* 7:45527. doi: 10.1038/srep45527

Mathesius, U., Mulders, S., Gao, M. S., Teplitski, M., Caetano-Anolles, G., Rolfe, B. G., et al. (2003). Extensive and specific responses of a eukaryote to bacterial quorum-sensing signals. *Proc. Natl. Acad. Sci. U.S.A.* 100, 1444–1449. doi: 10.1073/pnas.262672599

Miao, C., Liu, F., Zhao, Q., Jia, Z., and Song, S. (2012). A proteomic analysis of *Arabidopsis thaliana* seedling responses to 3-oxo-octanoyl-homoserine lactone, a bacterial quorum-sensing signal. *Biochem. Biophys. Res. Commun.* 427, 293–298. doi: 10.1016/j.bbrc.2012.09.044

Milne, G. L., Musiek, E. S., and Morrow, J. D. (2005). The cyclopentenone (A(2)/J(2)) isoprostanes - Unique, highly reactive products of arachidonate peroxidation. *Antioxid. Redox Signal.* 7, 210–220. doi: 10.1089/ars.2005.7.210

Miot, J., Benzerara, K., Obst, M., Kappler, A., Hegler, F., Schaedler, S., et al. (2009). Extracellular iron biomineralization by photoautotrophic iron-oxidizing bacteria. *Appl. Environ. Microb.* 75, 5586–5591. doi: 10.1128/aem.00490-09

Peiffer, J. A., Spor, A., Koren, O., Jin, Z., Tringe, S. G., Dangl, J. L., et al. (2013). Diversity and heritability of the maize rhizosphere microbiome under field conditions. *Proc. Natl. Acad. Sci. U.S.A.* 110, 6548–6553. doi: 10.1073/pnas.1302837110

Ratering, S., and Schnell, S. (2001). Nitrate-dependent iron(II) oxidation in paddy soil. *Environ. Microbiol.* 3, 100–109. doi: 10.1046/j.1462-2920.2001.00163.x

Rath, C. M., Benton, B. M., de Vicente, J., Drumm, J. E., Geng, M., Li, C., et al. (2018). Optimization of CoaD inhibitors against gram-negative organisms through targeted metabolomics. *ACS Infect. Dis.* 4, 391–402. doi: 10.1021/acsinfecdis.7b00214

Saifullah, Dahlawi, S., Naeem, A., Iqbal, M., Farooq, M. A., Bibi, S., et al. (2018). Opportunities and challenges in the use of mineral nutrition for minimizing arsenic toxicity and accumulation in rice: a critical review. *Chemosphere* 194, 171–188. doi: 10.1016/j.chemosphere.2017.11.149

Sforna, M. C., Philippot, P., Somogyi, A., van Zuilen, M. A., Medjoubi, K., Schoepp-Cothenet, B., et al. (2014). Evidence for arsenic metabolism and cycling by microorganisms 2.7 billion years ago. *Nat. Geosci.* 7, 811–815. doi: 10.1038/ngeo2276

Slyshenkov, V. S., Rakowska, M., Moiseenok, A. G., and Wojtczak, L. (1995). Pantothenic acid and its derivatives protect Ehrlich ascites tumor cells against lipid peroxidation. *Free Radic. Biol. Med.* 19, 767–772. doi: 10.1016/0891-5849(95)00084-b

Smith, E., Juhasz, A. L., Weber, J., and Naidu, R. (2008). Arsenic uptake and speciation in rice plants grown under greenhouse conditions with arsenic contaminated irrigation water. *Sci. Total Environ.* 392, 277–283. doi: 10.1016/j.scitotenv.2007.11.023

Stenzel, I., Otto, M., Delker, C., Kirmse, N., Schmidt, D., Miersch, O., et al. (2012). ALLENE OXIDE CYCLASE (AOC) gene family members of *Arabidopsis thaliana*: tissue- and organ-specific promoter activities and in vivo heteromerization. *J. Exp. Bot.* 63, 6125–6138. doi: 10.1093/jxb/ers261

Sun, Z. Y., and Huang, J. B. (2006). Effect of dextran on the crystallization of ferric hydroxide. *Acta Phys. Chim. Sin.* 22, 172–177.

Swenson, T. L., Jenkins, S., Bowen, B. P., and Northen, T. R. (2015). Untargeted soil metabolomics methods for analysis of extractable organic matter. *Soil Biol. Biochem.* 80, 189–198. doi: 10.1016/j.soilbio.2014.10.007

Tang, X. Y., Zhu, Y. G., Shan, X. Q., McLaren, R., and Duan, J. (2007). The ageing effect on the bioaccessibility and fractionation of arsenic in soils from China. *Chemosphere* 66, 1183–1190. doi: 10.1016/j.chemosphere.2006.07.096

Tripathi, R. D., Tripathi, P., Dwivedi, S., Kumar, A., Mishra, A., Chauhan, P. S., et al. (2014). Roles for root iron plaque in sequestration and uptake of heavy

metals and metalloids in aquatic and wetland plants. *Metallomics* 6, 1789–1800. doi: 10.1039/c4mt00111g

Verma, S., Verma, P. K., Meher, A. K., Dwivedi, S., Bansiwal, A. K., Pande, V., et al. (2016). A novel arsenic methyltransferase gene of *Westerdykella aurantiaca* isolated from arsenic contaminated soil: phylogenetic, physiological, and biochemical studies and its role in arsenic bioremediation. *Metallomics* 8, 344–353. doi: 10.1039/c5mt00277j

Wang, J., Muyzer, G., Bodelier, P. L. E., and Laanbroek, H. J. (2009). Diversity of iron oxidizers in wetland soils revealed by novel 16S rRNA primers targeting Gallionella-related bacteria. *ISME J.* 3, 715–725. doi: 10.1038/ismej.2009.7

Wang, J., Wen, X., Zhang, Y., Zou, P., Cheng, L., Gan, R., et al. (2021). Quantitative proteomic and metabolomic analysis of *Dictyophora indusiata* fruiting bodies during post-harvest morphological development. *Food Chem.* 339:127884. doi: 10.1016/j.foodchem.2020.127884

Wang, K. D., Borrego, E. J., Kenerley, C. M., and Kolomiets, M. V. (2020). Oxylipins other than jasmonic acid are xylem-resident signals regulating systemic resistance induced by *Trichoderma virens* in Maize. *Plant Cell* 32, 166–185. doi: 10.1105/tpc.19.00487

Wang, X., Rathinasabapathi, B., de Oliveira, L. M., Guilherme, L. R. G., and Ma, L. Q. (2012). Bacteria-mediated arsenic oxidation and reduction in the growth media of arsenic hyperaccumulator *Pteris vittata*. *Environ. Sci. Technol.* 46, 11259–11266. doi: 10.1021/es300454b

Wang, X. Y., and Xie, J. (2020). Assessment of metabolic changes in *Acinetobacter johnsonii* and *Pseudomonas fluorescens* co-culture from bigeye tuna (*Thunnus obesus*) spoilage by ultra-high-performance liquid chromatography-tandem mass spectrometry. *LWT Food Sci. Technol.* 123:109073. doi: 10.1016/j.lwt.2020.109073

Wenzel, W. W., Kirchbaumer, N., Prohaska, T., Stingeder, G., Lombi, E., and Adriano, D. C. (2001). Arsenic fractionation in soils using an improved sequential extraction procedure. *Anal. Chim. Acta* 436, 309–323. doi: 10.1016/s0003-2670(01)00924-2

Woolson, E. A., Axley, J. H., and Kearney, P. C. (1971). Correlation between available soil arsenic, estimated by six methods, and response of corn. *Soil Sci. Soc. Am. J.* 35, 101. doi: 10.2136/sssaj1971.03615995003500010030x

Wu, C., Ye, Z., Shu, W., Zhu, Y., and Wong, M. (2011). Arsenic accumulation and speciation in rice are affected by root aeration and variation of genotypes. *J. Exp. Bot.* 62, 2889–2898. doi: 10.1093/jxb/erq462

Wu, C., Zou, Q., Xue, S., Mo, J., Pan, W., Lou, L., et al. (2015). Effects of silicon (Si) on arsenic (As) accumulation and speciation in rice (*Oryza sativa* L.) genotypes with different radial oxygen loss (ROL). *Chemosphere* 138, 447–453. doi: 10.1016/j.chemosphere.2015.06.081

Wu, C., Zou, Q., Xue, S.-G., Pan, W.-S., Yue, X., Hartley, W., et al. (2016). Effect of silicate on arsenic fractionation in soils and its accumulation in rice plants. *Chemosphere* 165, 478–486. doi: 10.1016/j.chemosphere.2016.09.061

Wu, W., Swanner, E. D., Hao, L., Zeitvogel, F., Obst, M., Pan, Y., et al. (2014). Characterization of the physiology and cell-mineral interactions of the marine anoxygenic phototrophic Fe(II) oxidizer *Rhodovulum iodosum* - implications for Precambrian Fe(II) oxidation. *FEMS Microbiol. Ecol.* 88, 503–515. doi: 10.1111/1574-6941.12315

Xiao, A., Li, W. C., and Ye, Z. (2020). Effects of Fe-oxidizing bacteria (FeOB) on iron plaque formation, As concentrations and speciation in rice (*Oryza sativa* L.). *Ecotoxicol. Environ. Saf.* 190:110136. doi: 10.1016/j.ecoenv.2019.110136

Yu, H.-Y., Wang, X., Li, F., Li, B., Liu, C., Wang, Q., et al. (2017). Arsenic mobility and bioavailability in paddy soil under iron compound amendments at different growth stages of rice. *Environ. Pollut.* 224, 136–147. doi: 10.1016/j.envpol.2017.01.072

Zhao, F.-J., Ma, Y., Zhu, Y.-G., Tang, Z., and McGrath, S. P. (2015). Soil contamination in China: current status and mitigation strategies. *Environ. Sci. Technol.* 49, 750–759. doi: 10.1021/es5047099

Zhao, Q., Li, M., Jia, Z., Liu, F., Ma, H., Huang, Y., et al. (2016). AtMYB44 positively regulates the enhanced elongation of primary roots induced by N-3-Oxo-hexanoyl-homoserine lactone in *Arabidopsis thaliana*. *Mol. Plant Microb. Interact* 29, 774–785. doi: 10.1094/mpmi-03-16-0063-r

Conflict of Interest: The authors declare that the research was conducted in the absence of any commercial or financial relationships that could be construed as a potential conflict of interest.

Publisher's Note: All claims expressed in this article are solely those of the authors and do not necessarily represent those of their affiliated organizations, or those of the publisher, the editors and the reviewers. Any product that may be evaluated in this article, or claim that may be made by its manufacturer, is not guaranteed or endorsed by the publisher.

frontiers in Microbiology

ORIGINAL RESEARCH
published: 08 March 2022
doi: 10.3389/fmicb.2022.788893

Pseudomonas stutzeri and *Kushneria marisflavi* Alleviate Salinity Stress-Associated Damages in Barley, Lettuce, and Sunflower

Sonia Szymańska[1], Marta Izabela Lis[2], Agnieszka Piernik[2] and Katarzyna Hrynkiewicz[1]**

[1] Department of Microbiology, Faculty of Biological and Veterinary Sciences, Nicolaus Copernicus University, Toruń, Poland, [2] Department of Geobotany and Landscape Planning, Faculty of Biological and Veterinary Sciences, Nicolaus Copernicus University, Toruń, Poland

Soil salinity is one of the most important abiotic factors limiting plant productivity. The aim of this study was to determine the effect of selected halotolerant plant growth-promoting endophytes (PGPEs, *Pseudomonas stutzeri* ISE12 and *Kushneria marisflavi* CSE9) on the growth parameters of barley (*Hordeum vulgare*), lettuce (*Lactuca sativa*), and sunflower (*Helianthus annuus*) cultivated under salt stress conditions. A negative effect of two higher tested salinities (150 and 300 mM NaCl) was observed on the growth parameters of all investigated plants, including germination percentage and index (decreasing compared to the non-saline control variant in the ranges 5.3–91.7 and 13.6–90.9%, respectively), number of leaves (2.2–39.2%), fresh weight (24.2–81.6%); however, differences in salt stress tolerance among the investigated crops were observed (*H. annuus* > *H. vulgare* > *L. sativa*). Our data showed that the most crucial traits affected by endophyte inoculation under salt stress were chlorophyll concentration, leaf development, water storage, root development, and biomass accumulation. Thus, the influence of endophytes was species specific. *K. marisflavi* CSE9 promoted the growth of all tested plant species and could be considered a universal PGPEs for many plant genotypes cultivated under saline conditions (e.g., increasing of fresh weight compared to the non-inoculated control variant of barley, lettuce, and sunflower in the ranges 11.4–246.8, 118.9–201.2, and 16.4–77.7%, respectively). *P. stutzeri* ISE12 stimulated growth and mitigated salinity stress only in the case of barley. Bioaugmentation of crops with halotolerant bacterial strains can alleviate salt stress and promote plant growth; however, the selection of compatible strains and the verification of universal plant stress indicators are the key factors.

Keywords: salinity, growth parameters, crop plants, *Hordeum vulgare*, *Lactuca sativa*, *Heliantus annuus*, endophytes

OPEN ACCESS

Edited by:
Hai-Ming Zhao,
Jinan University, China

Reviewed by:
Philipp Franken,
Friedrich Schiller University Jena, Germany
Sajid Ali,
Yeungnam University, South Korea
Hadi Pirasteh-Anosheh,
National Salinity Research Center, Agricultural Research, Education and Extension Organization, Iran

****Correspondence:***
Sonia Szymańska
soniasz@umk.pl
Katarzyna Hrynkiewicz
hrynk@umk.pl

Specialty section:
This article was submitted to Terrestrial Microbiology, a section of the journal Frontiers in Microbiology

Received: *03 October 2021*
Accepted: *11 January 2022*
Published: *08 March 2022*

Citation:
Szymańska S, Lis MI, Piernik A and Hrynkiewicz K (2022) Pseudomonas stutzeri and Kushneria marisflavi Alleviate Salinity Stress-Associated Damages in Barley, Lettuce, and Sunflower. Front. Microbiol. 13:788893. doi: 10.3389/fmicb.2022.788893

INTRODUCTION

The increasing world population and associated rising demand for agricultural products continually contribute to soil degradation (Adejumobi et al., 2016; Temme et al., 2019) and soil salinization is one of the most critical consequences. Saline areas occur in at least 100 countries and cover 932.2 Mha worldwide (Cuevas et al., 2019). Soil salinization may result from human activities,

such as improper irrigation, deforestation and intensive cropping, and natural factors, e.g., mineral weathering and soil derived from salt-affected rocks (Athar and Ashraf, 2009; Srinivasarao et al., 2021). Due to the level of salinity, soils have been divided into non-saline (ECe 0–2 dS/m), slightly saline (ECe 2–4 dS/m), moderately saline (ECe 4–8 dS/m), strongly saline (ECe 8–16 dS/m), and extremely saline (ECe > 16 dS/m) (Corwin and Scudiero, 2019). Increasing soil salinization decreases seed germination, plant growth and development, water and nutrient uptake, and physiological (e.g., photosynthesis) and biochemical processes of plants (Isayenkov and Maathuis, 2019; Kumar et al., 2020). The tolerance level of plants to salinity may depend on the species, cultivar and growth phase (Munns and Tester, 2008; Rajabi Dehnavi et al., 2020). Only a small group of plants, known as halophytes, have the ability to grow in salt conditions exceeding 200 mM NaCl, while the vast majority of plants are in the group of glycophytes (including most crops) that cannot accumulate salts in plant tissues but are able to survive in saline environments (Carillo et al., 2011; Batool et al., 2014; Guo et al., 2021).

Plant species belonging to the glycophytes can exhibit different levels of tolerance to salt stress (Green et al., 2017). As representatives of the *Asteraceae* family, lettuce (*Lactuca sativa* L.) and sunflower (*Helianthus annuus* L.) are known as moderately salt-sensitive plants (tolerating 50–150 mM NaCl) (Isayenkov and Maathuis, 2019; Temme et al., 2019). Lettuce is a commonly grown vegetable because of its taste and high contents of antioxidants, vitamins (A, C, B9, and K), minerals (calcium, phosphorus, potassium, manganese, and iron) and fiber (Sapkota et al., 2019; Azarmi-Atajan and Sayyari-Zohan, 2020). Sunflower is the third most important source of edible vegetable oil worldwide and an efficient source of biodiesel; it also has other applications, e.g., as medicines, nourishments, feedstocks, fodders, decorations, and phytoremediators (Talia et al., 2011; Fernández-Luqueño et al., 2014; Ittah et al., 2019). Barley (*Hordeum vulgare* L.), representative of the *Poaceae* family, is one of the most salt stress tolerant crops among glycophytes and is considered the most adaptable cereal to salinity (El Madidi et al., 2006; Zhou, 2009; Adjel et al., 2013). Barley is a popular crop and is planted in a wide range of environments worldwide, including the Mediterranean, oceanic and continental climates, as well as in arctic and subarctic zones. The economic importance of this crop is similar to that of wheat and rice, taking fourth place in quantity and area of cultivation (Zhou, 2009; Dawson et al., 2015). This cereal is a great source of food and drink for humans, and it is also used for feeding livestock (FAOSTAT, 2014; Mohammed et al., 2021).

The application of halotolerant plant growth-promoting endophytes (PGPEs) isolated from halophytes, e.g., *Salicornia europaea*, seems to be an appropriate solution in sustainable agriculture (Davy et al., 2001; Furtado et al., 2019a,b; Szymańska et al., 2019; Christakis et al., 2021; El-Tarabily et al., 2021). Endophytes (microorganisms living within plant tissues without causing any negative effect on host plants) associated with crops can directly (e.g., nitrogen fixation and phytohormone and siderophore synthesis) and/or indirectly (e.g., protection against pests and herbivores) stimulate plant growth and protect them against unfavorable environmental conditions (Khan et al., 2016; Rabiey et al., 2019; Eid et al., 2021). In our previous publications, we confirmed the positive effect of the halotolerant bacterium *P. stutzeri* ISE12 isolated from *S. europaea* on beetroot (*Beta vulgaris*) (Piernik et al., 2017; Szymańska et al., 2020) and canola (*Brassica napus* L.) (Szymańska et al., 2019) from the Amaranthaceae and Brassicaceae families, respectively.

In the present work, we hypothesized that the halotolerant endophytic bacterial strains *P. stutzeri* ISE12 and *K. marisflavi* CSE9 isolated from the obligatory halophyte *S. europaea* will alleviate the salt stress of three tested plant species (*H. vulgare*, *L. sativa,* and *H. annuus*). The main objective of the current work was to evaluate: (i) the tolerance of three crops (*H. vulgare*, *L. sativa,* and *H. annuus*) to increasing salinity, (ii) the effect of inoculation with *P. stutzeri* ISE12 or *K. marisflavi* CSE9 on the plant growth parameters of *H. vulgare*, *L. sativa,* and *H. annuus* growing under different salt stress conditions (0, 50, 150, 300 mM NaCl) and (iii) the selection criteria of universal plant growth parameters susceptible to changes caused by salinity and inoculation.

MATERIALS AND METHODS

Experimental Design

In the experiment, we investigated three crops with different salt tolerance properties: sunflower (*H. annuus)*, lettuce (*L. sativa*), and barley (*H. vulgare*). Commercial seeds of sunflower (*H. annuus*) and butterhead lettuce (*L. sativa*) were purchased from Torseed (Toruń, Poland) and Plantico Company (Stare Babice, Poland), while winter barley (*H. vulgare*) seeds were obtained from the Plant Breeding and Acclimatization Institute (IHAR) (National Research Institute, Strzelce, Poland). Healthy and uniformly sized seeds were surface sterilized using a 30% hydrogen peroxide and 70% ethanol mixture (1:1, final concentration 15% hydrogen peroxide and 35% ethanol) for 11 (sunflower), 7 (lettuce), and 3.5 min (barley). Then, seeds were rinsed six times with sterile distilled water. The residual water after the last washing was used for the sterility test for bacteria and fungi, by plating on R2A (Difco^{TM} and BBL^{TM}) and PDA (Difco^{TM} and BBL^{TM}) plates, respectively. Only successfully sterilized seeds were used in the pot experiment. For each investigated plant species, three inoculation variations were used: control (non-inoculated, NI) and inoculated with one of two endophytic bacterial (EB) strains (B1—*P. stutzeri* ISE12 and B2—*K. marisflavi* CSE9). Plants were cultivated in one of 4 salinity treatments: 0, 50, 150, or 300 mM. Substrate (sterile mixture of sand and vermiculite, 1: 1) in plastic tray (each pot: 30 × 46 cm, 0.077 L) was salted by adding to the litter box 2 l of sterile Hoagland's medium enriched with the appropriate concentration of NaCl (**Figure 1**). Seeds were sown into growth substrate and cultivated under controlled conditions (temperature: 24 ± 2°C and light/dark: 16/8 h) and were irrigated with Hoagland medium (once per week) and

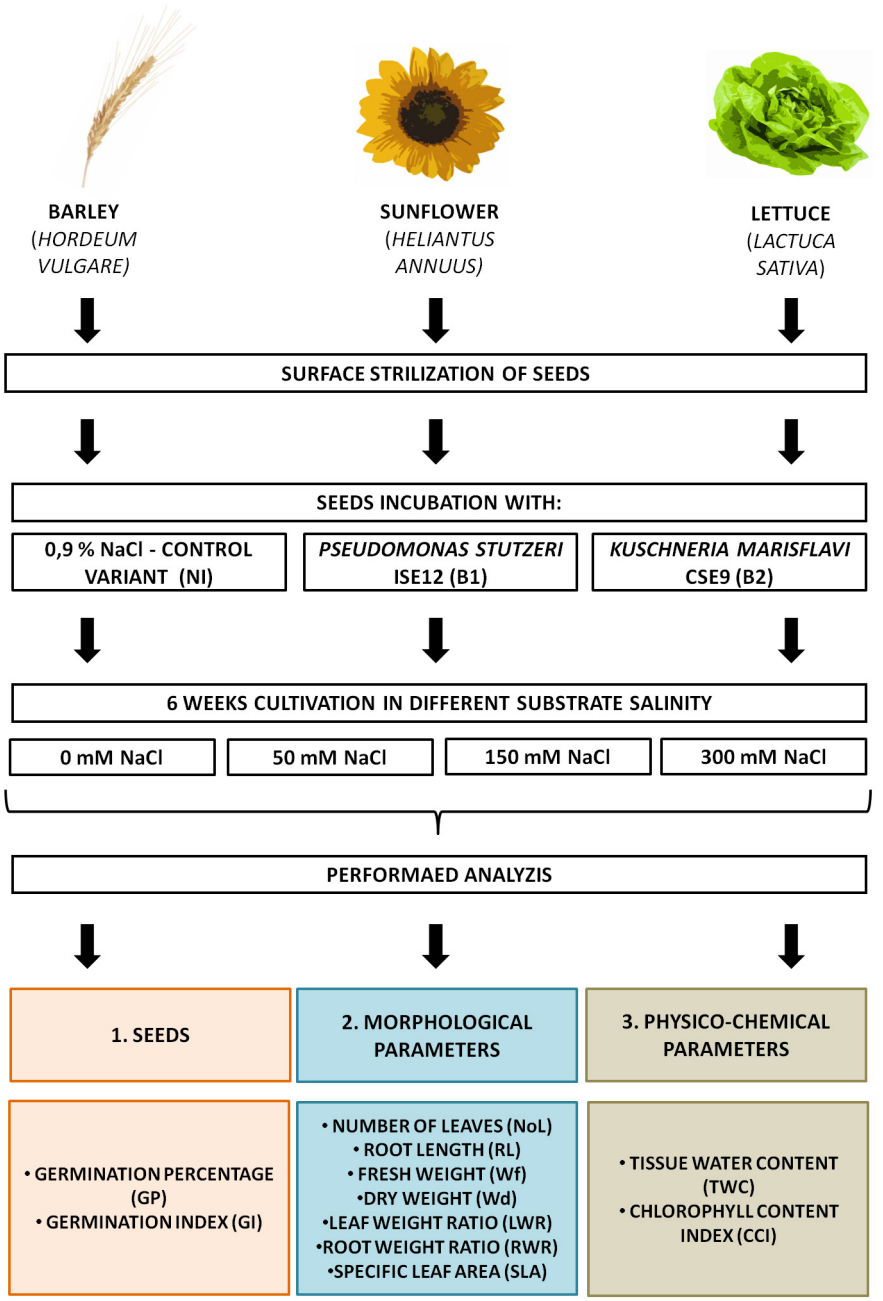

FIGURE 1 | Experimental design.

distilled water (according to plant requirements) (Hoagland and Arnon, 1950). After 6 weeks, plants were collected and analyzed (**Figure 1**).

Characterization of Bacterial Strains and Inoculation Procedure

Two halotolerant endophytic bacterial strains, *P. stutzeri* ISE12 (B1) and *K. marisflavi* CSE9 (B2), were used for the inoculation of plants in the pot experiment. Both bacterial strains were originally isolated from the roots of *S. europaea* and characterized for plant growth promoting (PGP) properties (Szymańska et al., 2016, 2020). *P. stutzeri* ISE12 (NCBI Acc. No. KX686983) was characterized as having a wider range of plant growth-promoting potential (e.g., nitrogen fixation, siderophores, IAA synthesis) and lower tolerance to salinity than *K. marisflavi* CSE9 (NCBI Acc. No. KX027360) (Szymańska et al., 2016, 2020).

Bacterial inocula were prepared using cells suspended in 2% NaCl solution, which was then diluted to OD = 0.5 (OD—optical density, measured at 600 nm, equivalent to 1.5×10^8 cells/ml)

after 72 h of culture incubation on R2A medium (Difco™) supplemented with 2% NaCl at 24°C. Plants cultivated in the pot experiment were inoculated with bacterial strains twice: 1st inoculation—surface sterilized seeds were incubated in bacterial inocula for 45 min at 24°C with shaking (control variant—non-inoculated seeds were incubated in sterile 0.9% NaCl solution); 2nd inoculation—1 ml of bacterial inocula was added to the growth substrate close to the root zone of 2-week-old seedlings (control variant—2% NaCl solution was used).

Growth Assessments

The number of germinated seeds was determined daily (at 10 a.m.) for 10 days.

The germination percentage (GP) was calculated according to the International Seed Testing Association (ISTA) method:

GP = number of normally germinated seeds/total number of seeds sown × 100

The germination index (GI) was calculated using the following formula:

$$GI = \Sigma(Gt/Tt), \quad (1)$$

where Gt is the number of seeds germinated on day t, and Tt is the number of days (Ruan et al., 2002).

Chlorophyll levels in leaves were detected by a hand-held Chl meter CCM-200 (Opti-Sciences, Tyngsboro, Massachusetts, United States) to assess the chlorophyll content index (CCI) after 6 weeks of plant cultivation (Richardson et al., 2002). Then, the plants were carefully removed from the pots, and the roots were washed using tap water to eliminate the residue from the growth substrate. The number of leaves and root and shoot lengths of 42-day-old plants were measured. Leaf area was scanned and measured by digiShape software.

The tissue water content (TWC) was calculated according to the formula of Black and Pritchard (2002):

$$TWC = (W_f - W_d)/W_f^* 100. \quad (2)$$

Biomass accumulation was calculated as fresh (W_f) and dry weight (W_d). The dry weight (W_d) was assessed after 72 h of drying at 85°C. Moreover, the following growth indices were calculated: specific leaf area (SLA), leaf weight ratio (LWR), and root weight ratio (RWR) (Piernik et al., 2017).

Statistical Analysis

Two-way ANOVA was used to check the effect of EB inoculation and NaCl concentration on growth parameters of tested plants. One-way ANOVA was used with Tukey's *post hoc* test to compare differences between treatments. Salt resistance assessments were based on comparisons with NI conditions by one-way ANOVA with Tukey's *post hoc* test. General assessment of the effect of inoculation (*P. stutzeri* ISE12—B1 and *K. marisflavi* CSE9—B2) on the growth of *H. vulgare*, *L. sativa,* and *H. annuus* was performed using multivariate statistical analysis. All above tests were done using the Statistica 10.0 software package (StatSoft, 2006). Discriminant analysis with a forward selection procedure was applied to test which measured features were the most affected in each solution and which discriminated among the NI, B1, and B2 treatments the best (CVA, Canoco 5 package; ter Braak and Šmilauer, 2012).

RESULTS

Differences in the Level of Salt Tolerance of Crops

The analysis of the growth parameters of plants grown in different concentrations of NaCl allowed for the differentiation of the tested crops in terms of tolerance to salinity and indicated their significant species diversity in this respect.

Substrates with increasing salinity (0, 50, 150, 300 mM NaCl) were used for crop cultivation to determine the most significantly affected plant traits (**Table 1** and **Figures 2–4**). *H. vulgare* plants grown under salt condition were smaller than those grown in the control variant (0 mM NaCl): W_f (was lower 25.2% in 50 mM compared to the control to 81.7% in 150 and 300 mM), W_d (from 15.5 to 73.2%, respectively), NoL (16.7–39.2%), and RL (25.7% to above 42.4%). The TWC was 1.7–3.4% lower under each salt treatment than under the control conditions (**Supplementary Tables 1**, **2**). The germination parameters GP and GI decreased only at the highest salinity (300 mM) (**Figure 2**).

In general, the plant genotypes from the family *Asteraceae* (*L. sativa* and *H. annuus*) were similarly affected by salt stress. However, *L. sativa* was more sensitive (non-inoculated plants did not grow in 300 mM NaCl) (**Figure 3**). *L. sativa* cultivated in substrate supplemented with 150 and 300 mM NaCl had a lower germination ability, as expressed by GP and GI (**Figure 3**). The growth parameters were also reduced under salt treatment: W_f (28.7% lower than the control at 50 mM, 72.2% at 150 mM), W_d (25.0 and 68.7%, respectively), and RL (15.1 and 38.8%) (**Figure 3** and **Supplementary Table 3**).

Slightly different strategies to cope with salt stress were demonstrated by *H. annuus*. Similarly, GP and GI decreased under high salinity (150 and 300 mM) (**Figure 4**), along with W_f (24.2% lower compared to the control at 150 mM and 58.4% lower at 300 mM), W_d (56.8% at 300 mM), and NoL (22.1% at 300 mM) (**Supplementary Table 4**). However, RL and RWR first increased significantly at 50 and 150 mM as an adaptation to water deficit and then decreased as a result of salt stress at 300 mM, but only by 34.1% (RL) and 12.6% (RWR). Thus, adaptation to cope with the highest salinity (300 mM NaCl) increased the LWR and CCI (**Supplementary Table 4**).

In summary, the effect of salinity on plant growth revealed the following order of salt tolerance levels in the investigated crops: *H. annuus* > *H. vulgare* > *L. sativa*.

Effect of Bacterial Inoculation on Plant Growth Parameters

The differences between the two tested strains (*P. stutzeri* ISE12—B1 and *K. marisflavi* CSE9—B2) were determined on the basis of their effect on the increase of plant growth parameters and more universal to all investigated crops strain was selected. The results of two-way ANOVA demonstrated

TABLE 1 | Two-way ANOVA results of endophytic bacteria (EB) inoculation (NI, non-inoculated; B1, inoculated with: *P. stutzeri* ISE12; and B2, *K. marisflavi* CSE9) and NaCl effects on growth parameters of *Hordeum vulgare, Lactuca sativa,* and *Helianthus annuus*.

		ANOVA main effects								
	Parameter	**NoL (n)**	**RL (mm)**	**Wf (g·plant^{-1})**	**Wd (g·plant^{-1})**	**SLA (cm^2·g^{-1})**	**LWR (g·g^{-1})**	**RWR (g·g^{-1})**	**TWC (%)**	**CCI**
Hordeum vulgare	EB	$p < 0.0001$	$p < 0.0001$	$p < 0.0001$	$p < 0.0001$	ns	ns	$p < 0.05$	$p < 0.0001$	nc
	NaCl	$p < 0.0001$	$p < 0.0001$	$p < 0.0001$	$p < 0.0001$	$p < 0.01$	$p < 0.0001$	ns	$p < 0.0001$	nc
	EBxNaCl	$p < 0.0001$	$p < 0.0001$	$p < 0.0001$	$p < 0.0001$	ns	$p < 0.0001$	$p < 0.05$	$p < 0.0001$	nc
EB effect	NI	7.8^a	194.8^a	3.64^a	0.422^a	135.9^a	0.515^a	0.098^a	87.25^a	nc
	B1	**10.0^c**	**231.5^b**	**5.01^c**	**0.567^b**	106.3^a	**0.489^b**	**0.113^b**	87.76^a	nc
	B2	**8.5^b**	**259.0^c**	**4.49^b**	0.452^a	116.4^a	**0.481^b**	**0.115^c**	**88.31^b**	nc
Lactuca sativa	EB	$p < 0.001$	$p < 0.0001$	$p < 0.0001$	$p < 0.0001$	$p < 0.01$	$p < 0.001$	$p < 0.0001$	$p < 0.0001$	$p < 0.0001$
	NaCl	$p < 0.001$	$p < 0.0001$	$p < 0.0001$	$p < 0.0001$	ns	$p < 0.001$	$p < 0.01$	$p < 0.0001$	$p < 0.0001$
	EBxNaCl	$p < 0.01$	$p < 0.01$	$p < 0.0001$	$p < 0.01$	$p < 0.001$	$p < 0.001$	ns	$p < 0.0001$	$p < 0.0001$
EB effect	NI	6.6^a	62.45^a	1.51^a	0.087^a	237.2^a	0.606^a	0.051^a	70.4^a	1.74^b
	B1	**9.1^b**	58.36^a	1.34^a	0.081^a	**522.6^b**	**0.819^c**	0.055^a	**93.8^b**	1.48^a
	B2	**10.4^c**	**100.52^b**	**3.25^b**	**0.222^b**	202.2^a	**0.744^b**	**0.128^b**	**91.3^b**	**2.21^c**
Helianthus annuus	EB	$p < 0.0001$	$p < 0.0001$	$p < 0.0001$	$p < 0.0001$	$p < 0.0001$	$p < 0.0001$	$p < 0.0001$	$p < 0.0001$	$p < 0.001$
	NaCl	$p < 0.03$	$p < 0.0001$	$p < 0.0001$	$p < 0.0001$	$p < 0.01$	$p < 0.0001$	$p < 0.001$	$p < 0.0001$	$p < 0.001$
	EBxNaCl	$p < 0.0001$	ns	$p < 0.03$	ns	ns	$p < 0.0001$	ns	$p < 0.001$	$p < 0.001$
EB effect	NI	16.1^a	259.2^b	17.41^a	1.78^a	60.42^b	0.247^a	0.091^b	89.3^a	13.1^a
	B1	15.2^a	206.2^a	17.73^a	1.20^b	**69.20^b**	**0.310^b**	0.070^a	**92.1^b**	12.4^a
	B2	15.6^a	**315.1^c**	**25.12^b**	1.89^a	46.26^a	**0.296^b**	**0.107^c**	89.3^a	**15.4^b**

*Row data for analysis are given in **Supplementary Tables 2–4**. NoL, number of leaves; RL, root length; W_f, fresh weight; W_d, dry weight; SLA, specific leaf area; LWR, leaf weight ratio; RWR, root weight ratio; TWC, tissue water content; CCI, chlorophyll content index; ns, not significant; and nc, not compared. Mean value obtained for all salt concentrations are presented. Significant differences between means in each variant are marked by different letters. Significant positive effects of inoculation are marked in bold.*

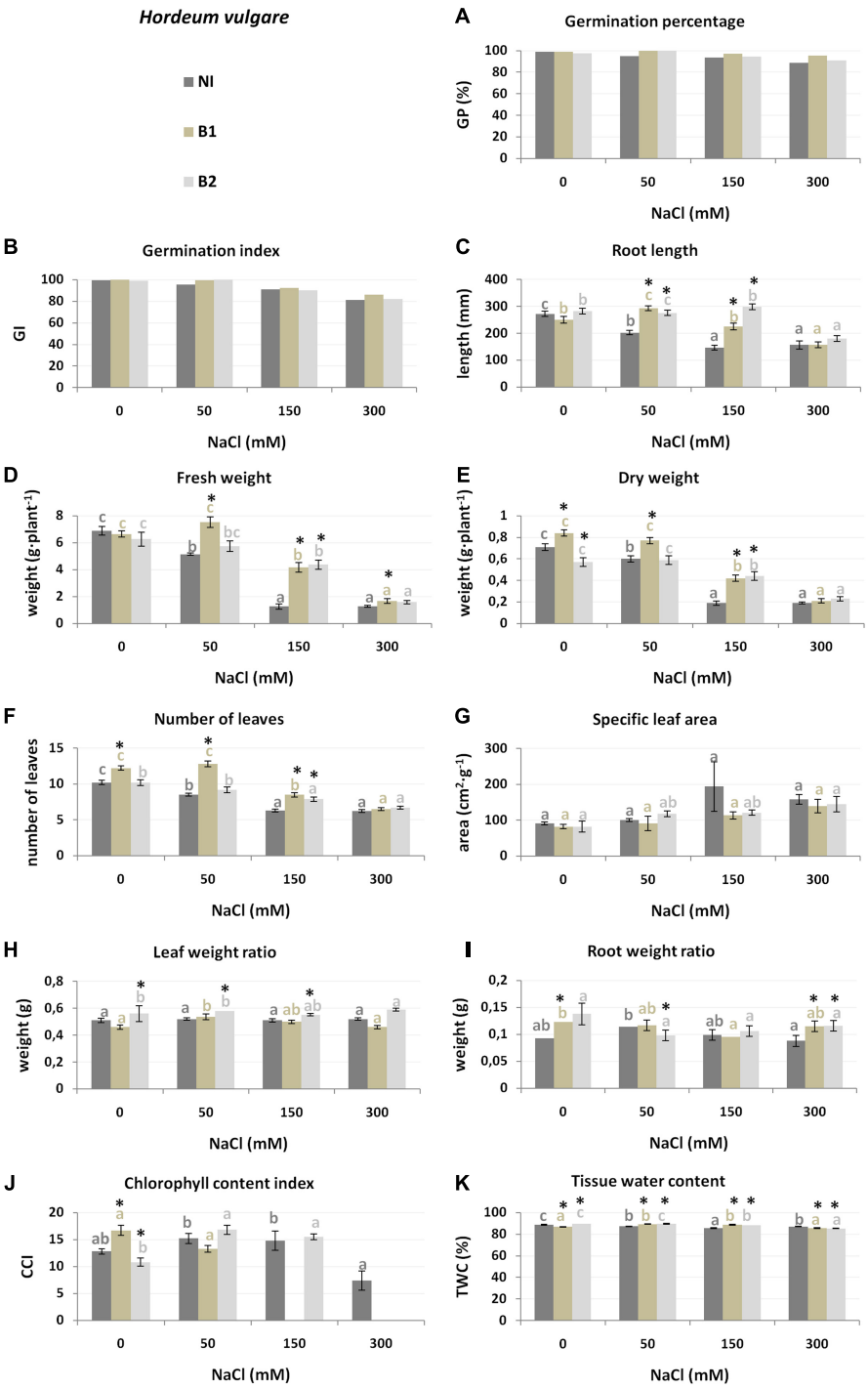

FIGURE 2 | Growth parameters [germination percentage **(A)**, germination index **(B)**, root length **(C)**, fresh weight **(D)**, dry weight **(E)**, number of leaves **(F)**, specific leaf area **(G)**, leaf weight ratio **(H)**, root weight ratio **(I)**, chlorophyll content index **(J)** and tissue water content **(K)** of *H. vulgare* non-inoculated (NI), inoculated with *P. stutzeri* ISE12 (B1) and *K. marisflavi* CSE9 (B2) grown in substrates with different NaCl concentrations (0, 50, 150, and 300 mM NaCl). Significant differences ($p < 0.05$, one-way ANOVA with Tukey's post hoc comparisons) between treatments (NI, control, non-inoculated; B1, inoculated with *P. stutzeri* ISE12; and B2, inoculated with *K. marisflavi* CSE9) at each NaCl concentration are denoted by different marks (*); differences between values for the investigated growth parameters obtained for each treatment at tested NaCl concentrations (0, 50, 150, and 300 mM) are marked with different letters (including a suitable font for each experiment: dark gray for control: non-inoculated; beige for B1; and light gray for B2) one-way ANOVA with Tukey's post hoc comparisons]. The mean ± standard error are presented (n = 10–15). Data for analysis are given in **Supplementary Table 2**.

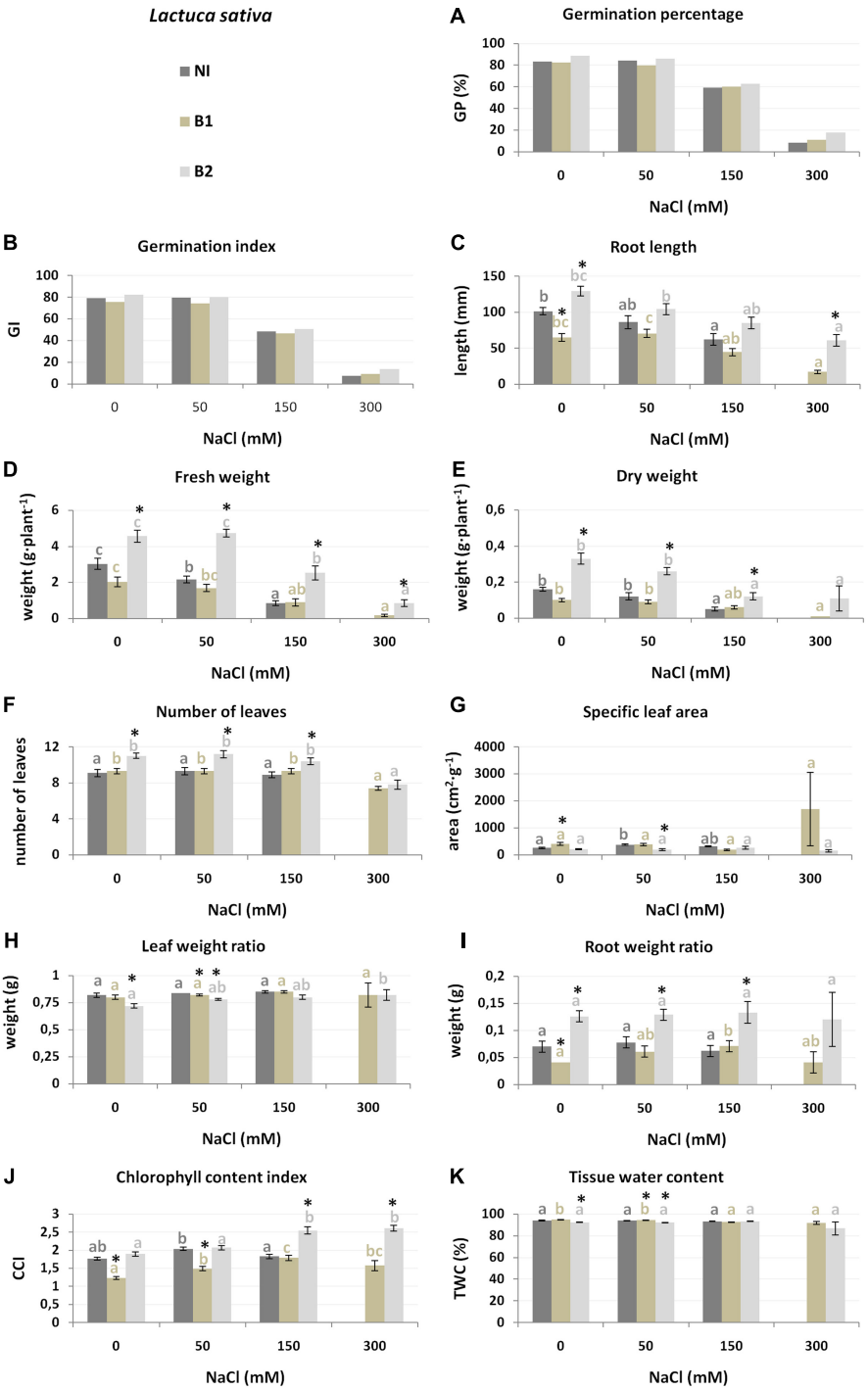

FIGURE 3 | Growth parameters [germination percentage **(A)**, germination index **(B)**, root length **(C)**, fresh weight **(D)**, dry weight **(E)**, number of leaves **(F)**, specific leaf area **(G)**, leaf weight ratio **(H)**, root weight ratio **(I)**, chlorophyll content index **(J)** and tissue water content **(K)** of *L. sativa* non-inoculated (NI), inoculated with *P. stutzeri* ISE-12 (B1) and *K. marisflavi* CSE9 (B2) grown in substrates with different NaCl concentrations (0, 50, 150, and 300 mM NaCl). Significant differences ($p < 0.05$, one-way ANOVA with Tukey's post hoc comparisons) between treatments (NI, control, non-inoculated; B1, inoculated with *P. stutzeri* ISE12; and inoculated with B2, *K. marisflavi* CSE9) at each NaCl concentration are denoted by different marks (*); differences between values for the investigated growth parameters obtained for each treatment at tested NaCl concentrations (0, 50, 150, and 300 mM) are marked with different letters (including a suitable font for each experiment: dark gray for control: non-inoculated; beige for B1; and light gray for B2) one-way ANOVA with Tukey's post hoc comparisons]. The mean ± standard error are presented (n = 10–15). Data for analysis are given in **Supplementary Table 3**.

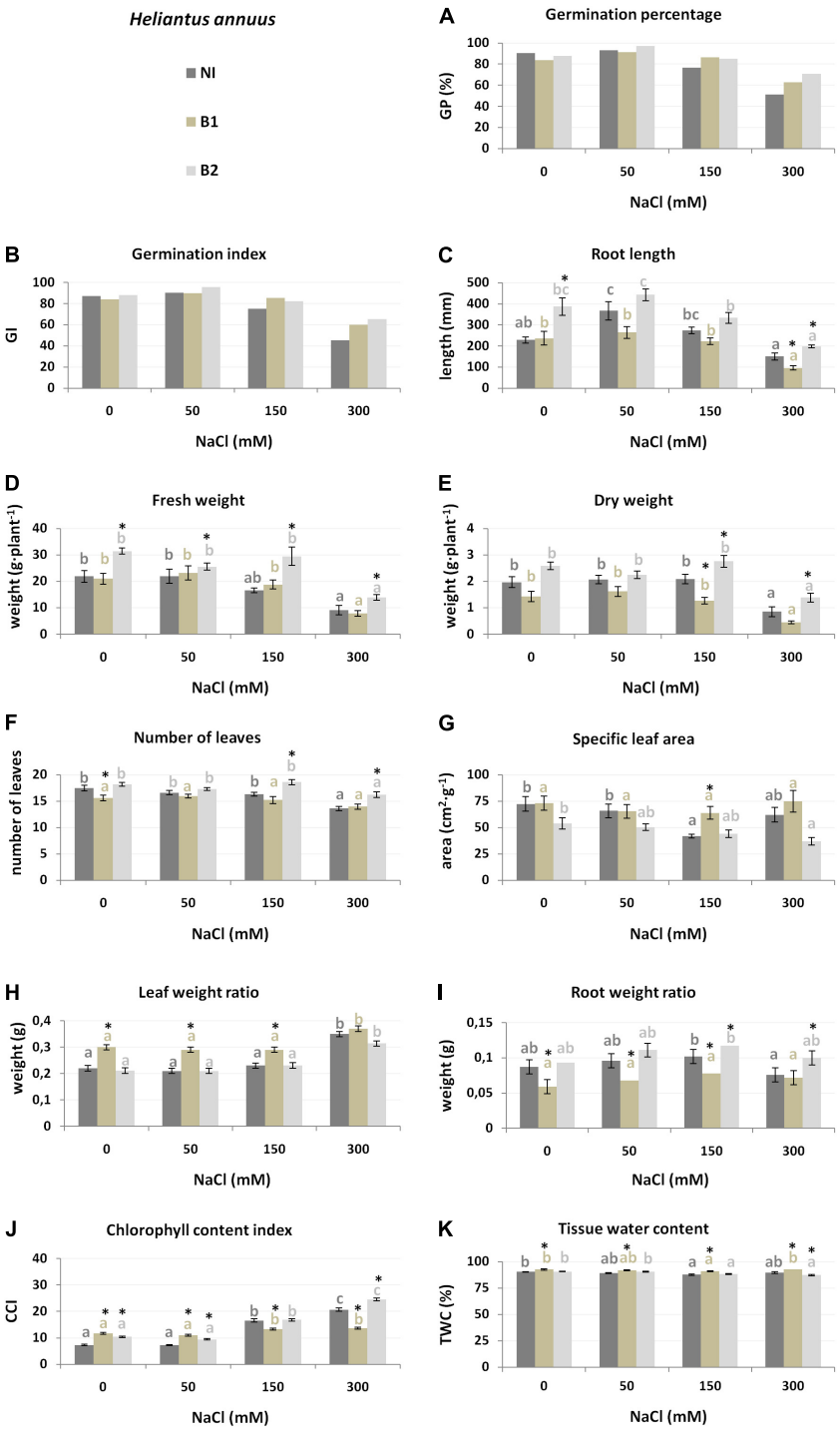

FIGURE 4 | Growth parameters [germination percentage **(A)**, germination index **(B)**, root length **(C)**, fresh weight **(D)**, dry weight **(E)**, number of leaves **(F)**, specific leaf area **(G)**, leaf weight ratio **(H)**, root weight ratio **(I)**, chlorophyll content index **(J)** and tissue water content **(K)** of *H. annuus* non-inoculated (NI), inoculated with *P. stutzeri* ISE-12 (B1) and *K. marisflavi* CSE9 (B2) grown in substrates with different NaCl concentrations (0, 50, 150, and 300 mM NaCl). Significant differences ($p < 0.05$, one-way ANOVA with Tukey's post hoc comparisons) between treatments (NI, control, non-inoculated; B1, inoculated with *P. stutzeri* ISE12; and inoculated with B2, *K. marisflavi* CSE9) at each NaCl concentration are denoted by different marks (*); differences between values for the investigated growth parameters obtained for each treatment at tested NaCl concentrations (0, 50, 150, and 300 mM) are marked with different letters (including a suitable font for each experiment: dark gray for control: non-inoculated; beige for B1; and light gray for B2) one-way ANOVA with Tukey's post hoc comparisons]. The mean ± standard error are presented (n = 10–15). Data for analysis are given in **Supplementary Table 4**.

TABLE 2 | Results of discriminant analysis (CVA) between NI, B1, and B2 treatments under different NaCl concentrations—percentage of the variance explained between groups for each growth parameter.

	***H. vulgare* mM NaCl**				***L. sativa* mM NaCl**				***H. annuus* mM NaCl**			
	0	50	150	300	0	50	150	300*	0	50	150	300
NoL	0.4	**31.4**	1.5	2.7	**9.3**	0.4	1.7	nc	7.7	7.9	2.0	**14.1**
RL	<0.1	3.2	**40.5**	1.9	0.5	<0.1	**15.7**	**62.9**	3.4	0.5	0.3	0.2
Wf	1.1	3.4	0.2	7.8	7.9	2.4	1.7	4.8	**13.4**	0.5	**8.5**	1.3
Wd	0.6	2.1	3.9	3.7	2.2	**44.9**	**27.3**	13.7	0.2	2.1	9.4	0.8
SLA	5.1	2.2	1.0	1.6	<0.1	**39.8**	8.3	0.6	3.7	2.4	<0.1	0.6
LWR	**48.2**	0.8	8.8	0.4	2.2	1.5	3.1	1.8	**24.4**	2.9	5.3	1.0
RWR	1.2	7.8	<0.1	8.5	**37.9**	1.3	3.4	0.6	0.4	**24.0**	**30.7**	6.8
TWC	**28.0**	**25.1**	**14.6**	**17.0**	2.2	0.7	0.7	7.5	1.4	10.6	**18.1**	9.9
CCI	**7.5**	0.8	nc	nc	**15.6**	0.6	1.7	1.1	**22.4**	**9.1**	<0.1	**34.9**

*Figures associated with presented data are given in **Supplementary Figures 1–3**. NoL, number of leaves; RL, root length; W_f, fresh weight; W_d, dry weight; SLA, specific leaf area; LWR, leaf weight ratio; RWR, root weight ratio; TWC, tissue water content; CCI, chlorophyll content index; and nc, not compared. Plants in non-inoculated control at 300 mM did not survive and are denoted by marks *. Significant factors ($p < 0.01$) are underlined in bold.*

that both investigated bacterial strains significantly affected most of the investigated plant traits (**Table 1**). In the case of *H. vulgare,* B1 stimulated NoL development, W_f and W_d, whereas B2 was responsible for better root development (RL and RWR), and water accumulation (TWC). A detailed comparison of salt treatments revealed that bioaugmentation of *H. vulgare* with both investigated strains had a positive effect on plants cultivated in 50 and 150 mM NaCl, as seen for the following parameters: GP, GI, NoL, RL, W_f, W_d, LWR, and TWC (**Figure 2** and **Supplementary Table 2**). Under a lower salinity of 50 mM, inoculation of *H. vulgare* with B1 resulted in higher NoL and biomass accumulation (W_f and W_d) compared to that with B2 (**Figure 2** and **Supplementary Table 2**). At 150 mM, both strains stimulated NoL, Wf, Wd, and TWC, but strain B2 affected root growth more strongly (higher RL).

Both species from the *Asteraceae* family (*L. sativa* and *H. annuus*) were more susceptible to B2 inoculation (**Table 1**). In general, inoculation of *L. sativa* with B2 increased most of the growth parameters. Detailed analysis of the salt treatments demonstrated that under the highest salinity (300 mM), strain B2 stimulated RL, W_f, W_d, and CCI, whereas under lower salinity (50 and 150 mM), NoL and RWR were stimulated (**Figure 3** and **Supplementary Table 3**). The role of B1 in growth stimulation was much smaller than that of B2. Moreover, some traits were negatively affected by this strain, e.g., RL and CCI (**Figure 3** and **Supplementary Table 3**).

The growth of *H. annuus* was also better stimulated by B2 (**Table 1**), resulting in stronger root development (RL and RWR), photosynthesis ability (CCI and LWR), and fresh biomass accumulation (W_f), whereas strain B1 positively affected mainly water accumulation (TWC) and photosynthesis ability (LWR). In general, B2-inoculated plants were characterized by better seed germination (GP and GI) (**Figure 4**). In all salinity treatments, these plants had better developed roots (RL and RWR), higher biomass (W_f and W_d), and a 50 mM higher chlorophyll concentration in the leaves (CCI) (**Figure 4** and **Supplementary Table 4**). Conversely, decreases in growth parameters, e.g., Wd, RWR, and CCI, were observed after inoculation with B1. The results clearly show a lack of compatibility between *H. annuus* and *P. stutzeri* ISE12; moreover, an adverse influence of that strain was observed.

The PCA results presented in **Figure 5** show the percentage differences between plant traits for inoculated and control (NI) treatments, which included three plant species (*H. vulgare*, *L. sativa*, *H. annuus*) and four different levels of salinity (0, 50, 150, 300 mM NaCl). Positive correlations were found between *L. sativa* (all investigated variants: Ls_B2_0, Ls_B2_50, Ls_B2_150) and *H. annuus* (three of the four variants: Ha_B2_0, Ha_B2_150, Ha_B2_300) inoculated with B2 under most salinity treatments among the NoL, W_f, W_d, RL, and RWR traits. Bioaugmentation of plants from this family with B1 was associated only with SLA, TWC, and LWR. Inoculation of all investigated genotypes with B2 stimulated growth parameters according to the following trend: *L. sativa* > *H. annuus* > *H. vulgare* (**Figure 5**). Strain B1 revealed the opposite trend and had no evident effect.

Plant Growth Parameters Were Susceptible to Changes in Response to Salinity and Inoculation

Based on the obtained results, an analysis was carried out, which allowed for the selection of plant growth parameters most sensitive to increasing salinity and bacterial inoculation. The results of the discriminant analysis and forward selection procedure revealed that salinity modified the effect of EB in a quantitative way. In the case of *H. vulgare,* the most critical feature for discrimination between the NI, B1, and B2 groups in all salinity treatments was the water content in plants (TWC), which explained 28–14% of the total variation (**Table 2**). Moreover, under 0 mM NaCl, the most affected plant parameters were LWR (explaining 48.2% of the trait variance between the NI, B1, and B2 groups) and CCI (7.5%) (**Supplementary Figure 1**). At 50 mM, in addition to TWC, significant group separation was found

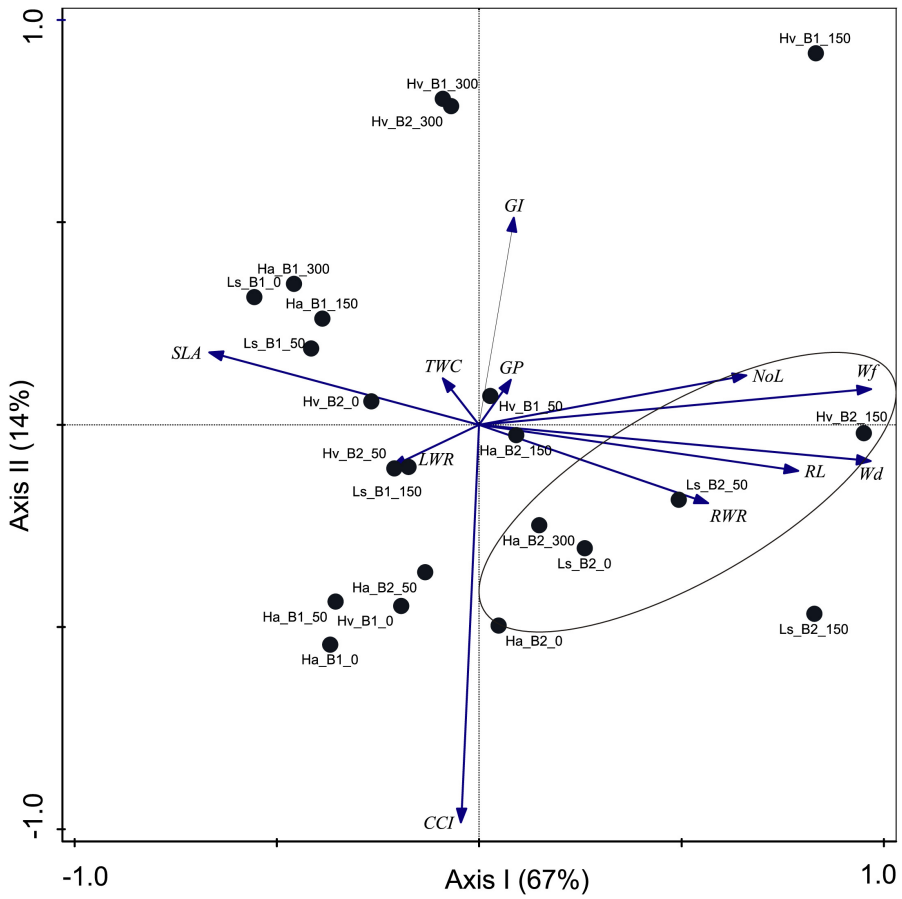

FIGURE 5 | Biplot of the principal component analysis of germination and growth parameters (GP, germination percentage; GI, germination index; NoL, number of leaves; RL, root length; W_f, fresh weight; W_d, dry weight; SLA, specific leaf area; LWR, leaf weight ratio; RWR, root weight ratio; TWC, tissue water content; CCI, chlorophyll content index) obtained for *H. vulgare* (Hv), *L. sativa* (Ls), and *H. annuus* (Ha) inoculated with *P. stutzeri* ISE12 (B1) and K. marisflavi CSE9 (B2) cultivated in substrates enriched with different salinities (0, 50, 150, and 300 mM NaCl). Differences between the values for the parameters obtained for the control (non-inoculated) and inoculated variants were included. B2 treatments with the best relative growth are marked with a circle.

for NoL (31.4%), and in 150 mM, the same was found for RL (40.5%).

The *L. sativa* analysis demonstrated that the most essential features for discrimination between groups were at 0 mM NaCl root development, indicated as RWR (explaining 38% of the variation), chlorophyll index (CCI, 16%), and number of leaves (NoL, 9%) (**Table 2**). At 50 mM NaCl, the most affected traits were W_d (explaining 48.2% of the variance between the NI, B1, and B2 groups) and SLA, whereas under 150 mM, W_d (27%) and RL (16%) were the most affected, and under 300 mM onlyRL was the most affected (63%, NI plants died) (**Supplementary Figure 2**).

The most essential trait for discrimination between the NI, B1, and B2 treatments for *H. annuus* was the chlorophyll index (CCI, explaining 9–35% of trait variance) across all NaCl concentrations, except for 150 mM (**Table 2**). Moreover, under 0 mM NaCl, the critical features for discrimination between the NI, B1, and B2 treatments were LWR (explaining 24% of the variation) and W_f, while under 50 mM, root development, expressed as RWR (24%), under 150 mM, RWR (31%) and TWC (18%) and under 300 mM NaCl, fresh weight (W_f, 8%) and NoL (14%) (**Supplementary Figure 3**).

This analysis allowed us to designate chlorophyll concentration (CCI), the development of leaves (NoL, LWR, SLA), water storage (TWC), root development (RL, RWR), and biomass accumulation (W_f, W_d) as crucial traits affected by salinity and bacterial inoculation. However, the effects reported here are species specific.

DISCUSSION

The adverse effect of salinity on the germination and growth of plants has been confirmed for many crop species, e.g., *Zea mays* (maize), *Lycopersicon esculentum* (tomato), *Oryza sativa* (rice), *Glycine max* (soybean) *Beta vulgaris* (sugar beet), *Brassica oleracea capitata* (cabbage), *Amaranthus paniculatus* (amaranth), and *Brassica campestris* (pak-choi) (Jamil et al., 2006; Doganlar et al., 2010; Turan et al., 2010; Vibhuti et al., 2015); *Brassica napus* and *Beta vulgaris* (Piernik et al., 2017;

Khan et al., 2019a, 2020; Szymańska et al., 2019, 2020; Masmoudi et al., 2021); and *Sorghum bicolor* (Rajabi Dehnavi et al., 2020). Our present research confirmed the negative effect of salinity on *H. vulgare*, *L. sativa*, and *H. annuus* and additionally showed that this effect is conspicuously associated with a reduction in the germination percentage and index, root length, and fresh and dry weights. The assessment of the three-way interaction, saline substrate—crop—endophyte, allowed us to determine the key factors responsible for compatibility between bacterial species and plant genotypes. Since the inoculation of crops with the most efficient plant growth-promoting bacteria (PGPB) is one of the relevant strategies used in sustainable agriculture in salt-affected areas (Kumar et al., 2020), searching for new compatible microorganisms appropriately matched to the plant host and environmental conditions is crucial. *P. stutzeri* is a well-described bacterium and is characterized as a PGPB due to several of its beneficial metabolic properties, e.g., IAA and siderophore synthesis, nitrogen fixation, antifungal activity, and 1-aminocyclopropane-1-carboxylate (ACC) deaminase synthesis (Patel and Patel, 2014; Han et al., 2015; Pham et al., 2017; Lami et al., 2020; Kumar et al., 2021). However, there is a lack of research considering the application potential of *K. marisflavi*. We previously initiated the first studies on the use of this bacteria with two crops (*Beta vulgaris* and *Brassica napus*) (Piernik et al., 2017; Szymańska et al., 2019, 2020) and expanded the range of crops tested in this work.

Salt Stress Tolerance of Plant Species

Determination of plant germination capacity under high salinity conditions is a crucial parameter for assessing plant tolerance to salt stress (Li et al., 2020). Salinity adversely affects the germination stage by limiting water availability and changing stored reserve mobilization and structural protein organization (Demir and Mavi, 2008; Nawaz et al., 2010). The negative effect on germination can be genotype- or cultivar-specific (Al-Ashkar et al., 2020; Li et al., 2020; Kadioğlu, 2021). In the present study, we observed significant differences in salinity between the three investigated crop genotypes. Li et al. (2020) studied the different seed germination stage parameters (such as germination rate, germination index, germination energy, germination vigor index, and water content) of 552 sunflower germplasms with different levels of salt stress tolerance. The authors found that the germination index and the germination vigor index were the most reliable traits and were strongly associated with salt tolerance. In our work, increasing the concentration of NaCl in substrates inhibited seed germination; however, the effect was species-specific. The effect of salinity on the germination of *H. annuus* and *L. sativa* was particularly evident at higher salinities (150 and 300 mM NaCl). However, across all tested plant species, we did not observe decreased germination at 50 mM NaCl. This is because a low concentration of Na^+ has a positive effect on plant growth, since Na^+ participates in osmotic and nutritional mechanisms. This effect was also observed in our studies on red beet and canola (Szymańska et al., 2019, 2020), as well as in experiments with red beet, wheat and *Zygophyllum xanthoxylum* described by Wu et al. (2013). *H. annuus* and *H. vulgare* are crops with the highest levels of salt stress tolerance (Garthwaite et al., 2005; Li et al., 2020; Vasilakoglou et al., 2021), which we confirmed in the experiments presented in this work. In contrast, we observed relatively low tolerance of *L. sativa* to salinity, especially at the highest concentration of NaCl (300 mM), where we observed complete inhibition of germination and plant growth. Moreover, gradual plant death was observed over several weeks during the experiment. Ludwiczak et al. (2021) showed that osmotic stress rather than ionic effects is responsible for this process.

Compatibility Between Plant Growth-Promoting Bacterial Strains and Plant Genotypes

The compatibility between selected strains was plant specific. Both endophytes (*P. stutzeri* ISE12 and *K. marisflavi* CSE9) increased *H. vulgare* adaptation to salt stress, which was confirmed by the growth parameters, especially under supplementation with 50 and 150 mM NaCl. Similarly, a positive effect of the same strains was observed in our earlier studies with *B. napus* and *B. vulgaris* (Szymańska et al., 2019, 2020).

Our results suggest that crops from the same family growing under similar conditions (e.g., substrate, temperature, light) can be compatible with the same microorganisms. Our results show that *H. annuus* and *L. sativa* (family Asteraceae) inoculated with *K. marisflavi* CSE9 showed increases in the same growth parameters (germination percentage and index, number of leaves, fresh weight, root length, root weight ratio, chlorophyll content index). However, the positive effect of inoculation with a specific strain may also be related to the specific metabolic activities of bacteria used for inoculation. *P. stutzeri* ISE12 possesses a wider range of metabolic properties (siderophores and IAA synthesis, cellulolytic activity, and presence of *nif*H) than *K. marisflavi* CSE9 (siderophores and IAA synthesis) (Szymańska et al., 2020). Moreover, although both strains showed high salinity tolerance, we confirmed that *K. marisflavi* CSE9 had higher potential (Szymańska et al., 2020). Both strains had IAA synthesis ability, and multifunctional phytohormones play crucial roles in plant growth and development promotion as well as stress resistance (Numan et al., 2018; Khan et al., 2019b; Saleem et al., 2021). Egamberdieva (2009) observed higher crop productivity after the inoculation of wheat with IAA-producing strains under salinity stress than without salt (2008). Similarly, the mitigation of salt stress and stimulation of plant growth was noted for cotton, and the authors suggested that IAA synthesized by bacteria can be an extremely important factor in the salt stress tolerance of plants (Egamberdieva et al., 2015).

Crucial Traits Affected by Salinity and Inoculation

Based on the results obtained in the study, we also determined universal parameters that are the most affected by inoculation

under salt stress. However, we recognized that the inoculation effect was dependent on the salinity level and was species specific. In the case of *H. vulgare,* we identified TWC as the most affected trait in all salt treatments. In general, bacteria increased the water content in plant tissues at 50 and 150 mM NaCl, but at 300 mM, the water content significantly decreased. This trait was also independently affected by salinity level. TWC decreased together with increased salinity. This result is in line with those by Ludwiczak et al. (2021), who identified the TWC of *H. vulgare* and *A. sativa* as one of the most affected traits under 150 mM NaCl. However, Garthwaite et al. (2005) investigated the salt tolerance of eight wild *Hordeum* species (including *H. bogdanii*, *H. intercedens*, *H. jubatum*, *H. lechleri*, *H. marinum*, *H. murinum*, *H. patagonicum*, and *H. secalinum*) and cultivated barley (*H. vulgare*) and observed the smallest reduction in this parameter for *H. vulgare* compared to the wild *Hordeum* species. On the other hand, stimulation of tissue water storage after inoculation by endophytes was also reported for draught stressed maize by Naveed et al. (2014) and lettuce by Molina-Montenegro et al. (2016). Additional crucial traits of *H. vulgare* were the number of leaves (NoL) under 50 mM NaCl and RL under 150 mM NaCl, which were the most stimulated by B2 bacteria.

The RL trait was also crucial for discriminating between *L. sativa* treatments and was stimulated by B2 bacteria, especially at 150 and 300 mM NaCl. The reduction in root length under salt stress may result from the direct contact of the roots with an unfavorable abiotic factor (Jamil et al., 2006; Vibhuti et al., 2015; Peng-cheng et al., 2021). The stimulation of root growth may be a solution for the improvement of water absorption under salt stress (Piernik et al., 2017).

Interestingly, in the case of lettuce, TWC was not a significant factor for discriminating the investigated treatments. Al-Maskri et al. (2010) noted a negative effect of salinity on several *L. sativa* growth parameters (including the number of leaves, plant fresh weight, shoot fresh and dry weight, shoot dry matter percentage, root fresh and dry weight, root dry weight percentage, leaf area and leaf area index), and similar to our work, they did not observe adverse effects on the root and shoot water content percentages. The opposite results were obtained by Ahmed et al. (2019), who observed a gradual reduction in the water content in *L. sativa* roots and shoots with increasing NaCl concentration (2019). Many differences in the growth parameters of *L. sativa* grown under salt stress have been observed by various researchers (e.g., Bar-Yosef et al., 2005; Ünlükara et al., 2008; Kurunc, 2021). Presumably, the varieties of *L. sativa* are characterized by large differences in salinity tolerance, and plant responses may be related to other morphological and physiological parameters.

Not only the root length but also the root weight ratio (RWR) was crucial for the discrimination between NI, B1, and B2 treatments and was positively stimulated by B2 bacteria, especially in the case of *L. sativa* and *H. annuus*. This result suggests changes in the plant growth strategy and a higher investment in root development with endophyte inoculation (Reynolds and D'Antonio, 1996).

For *L. sativa* and *H. annuus*, biomass accumulation was of crucial importance in the context of salinity and endophytic bacteria interactions. The dry weight (W_d) showed that the best salt levels were 50 and 150 mM NaCl for lettuce. This trait was significantly stimulated by B2 bacteria. The fresh weight (W_f) showed that the best salt levels were 0 and 150 mM for sunflower and was also stimulated by B2 (*K. marisflavi*).

The most interesting result is the impact of the investigated endophytes on the chlorophyll content, expressed here as CCI. Inoculation with B1 (*P. stutzeri*) increased the CCI of *H. vulgare,* whereas inoculation with B2 increased the CCI of *L. sativa* under the 0 mM control conditions. Moreover, the CCI parameter was crucial for discriminating across the investigated treatments of *H. annuus* at 0, 50, and 300 mM, where B2 bacteria were responsible for higher values. An increase in chlorophyll content after inoculation with endophytic bacteria has also been observed by other researchers (e.g., Zhao et al., 2015; Yuan et al., 2018; Tharek et al., 2021). In our previous research, we found the same effect of *P. stutzeri* on beetroot (Piernik et al., 2017; Szymańska et al., 2020). A higher CCI may result in a higher efficiency of photosynthesis under environmental stress (Zhao et al., 2020).

CONCLUSION

In conclusion, our results indicated that salinity reduced crop productivity, but the effect was species specific: *H. annuus* > *H. vulgare* > *L. sativa*. For the most crucial traits affected by endophyte inoculation under salt stress, we found that chlorophyll concentration (CCI), the development of leaves (mostly NoL), water storage (TWC), root development (RL, RWR), and biomass accumulation (W_f, W_d) were the most important. However, all these effects are species specific. We can confidently conclude that *K. marisflavi* is a unique and universal strain that promoted the growth of all tested genotypes, while *P. stutzeri* ISE12 is species specific and requires compatibility testing with a specific host plant before application in the field.

DATA AVAILABILITY STATEMENT

The original contributions presented in the study are included in the article/**Supplementary Material**, further inquiries can be directed to the corresponding author/s.

AUTHOR CONTRIBUTIONS

SS performed the pot experiment, plant growth parameters analysis and part of statistical analysis, and wrote the first version of the manuscript. KH determined the first concept of the experiment and participated in the preparation of the manuscript. AP analyzed the data and wrote part of materials and methods as well as results. ML contributed in the laboratory work and performed statistical analysis. All authors contributed to the final version.

FUNDING

This research was funded by a grant from the National Science Centre (Poland) (DEC-2012/07/B/NZ9/01801).

SUPPLEMENTARY MATERIAL

The Supplementary Material for this article can be found online at: https://www.frontiersin.org/articles/10.3389/fmicb.2022.788893/full#supplementary-material

Supplementary Figure 1 | Results of discriminant analysis (CVA) between *Hordeum vulgare* inoculated with *P. stutzeri* ISE12 (B1) and *K. marisflavi* CSE9 (B2) and non-inoculated (NI) variants in different NaCl solutions. Significant parameters that discriminate the best between groups are denoted by stars ($p < 0.01$).

Supplementary Figure 2 | Results of discriminant analysis (CVA) between *Lactuca sativa* inoculated with *P. stutzeri* ISE12 (B1) and *K. marisflavi* CSE9 (B2) and non-inoculated (NI) variants in different NaCl solutions. Significant parameters that discriminate the best between groups are denoted by stars ($p < 0.01$). In 300 mM NaCl, only B1 and B2 treatments were compared (NI plants died).

Supplementary Figure 3 | Results of discriminant analysis (CVA) between *Helianthus annuus* inoculated with *P. stutzeri* ISE12 (B1) and *K. marisflavi* CSE9 (B2) and non-inoculated (NI) variants in different NaCl solutions. Significant parameters that discriminate the best between groups are denoted by stars ($p < 0.01$).

Supplementary Table 1 | Effect of endophytic bacteria inoculation (NI: non-inoculated, B1: inoculated with *P. stutzeri* ISE12, and B2: inoculated with *K. marisflavi* CSE9) on plant tissue water content (TWC) in different NaCl concentrations (0, 50, 150 and 300 mM NaCl). Means ± SE are presented.

Supplementary Table 2 | Effect of endophytic bacteria inoculation (NI: non-inoculated, B1: inoculated with *P. stutzeri* ISE12, and B2: inoculated with *K. marisflavi* CSE9) on Hordeum vulgare growth parameters in different NaCl concentrations. Means ± SE are presented.

Supplementary Table 3 | Effect of endophytic bacteria inoculation (NI: non-inoculated, B1: inoculated with *P. stutzeri* ISE12, and B2: inoculated with *K. marisflavi* CSE9) on *Lactuca sativa* growth parameters in different NaCl concentrations. Means ± SE are presented.

Supplementary Table 4 | Effect of endophytic bacteria inoculation (NI: non-inoculated, B1: inoculated with *P. stutzeri* ISE12, and B2: inoculated with *K. marisflavi* CSE9) on *Helianthus annuus* growth parameters in different NaCl concentrations. Means ± SE are presented.

REFERENCES

Adejumobi, M. A., Alonge, T. A., and Ojo, O. I. (2016). A review of the techniques for monitoring soil salinity in irrigated fields. *AIMS* 2, 167–170.

Adjel, F., Kadi, Z., Bouzerzour, Z., and Benmahammed, A. (2013). Salt Stress effects on seed germination and seedling growth of barley (*Hordeum vulgare* L.) genotypes. *J. Sustain. Agric.* 3, 223–237.

Ahmed, S., Ahmed, S., Roy, S. K., Woo, S. H., Sonawane, K. D., and Shohael, A. M. (2019). Effect of salinity on the morphological, physiological and biochemical properties of lettuce (*Lactuca sativa* L.) in Bangladesh. *Open Agric.* 4, 361–373. doi: 10.1515/opag-2019-0033

Al-Ashkar, I., Alderfasi, A., Ben Romdhane, W., Seleiman, M. F., El-Said, R. A., and Al-Doss, A. (2020). Morphological and genetic diversity within salt tolerance detection in eighteen wheat genotypes. *Plants* 9:287. doi: 10.3390/plants9030287

Al-Maskri, A., Al-Kharusi, L., and Al-Miqbali, H. (2010). Effects of salinity stress on growth of lettuce (*Lactuca sativa*) under closed-recycle nutrient film technique. *Int. J. Agric. Biol.* 12, 377–380.

Athar, H. R., and Ashraf, M. (2009). "Strategies for crop improvement against salinity and drought stress: an overview," in *Salinity and Water Stress*, eds M. Ashraf, M. Ozturk, and H. R. Athar (Boston: Springer), 1–16. doi: 10.3390/ijms22116119

Azarmi-Atajan, F., and Sayyari-Zohan, M. H. (2020). Alleviation of salt stress in lettuce (*Lactuca sativa* L.) by plant growth-promoting rhizobacteria. *J. Hortic. Postharvest Res.* 3, 67–78.

Bar-Yosef, B., Markovich, T., and Levkovich, I. (2005). Lettuce response to leachate recycling in an arid zone greenhouse. *Acta Hort.* 697, 243–250. doi: 10.17660/ActaHortic.2005.697.29

Batool, N., Shahzad, A., and Ilyas, N. (2014). Plants and salt stress. *Int. J. Agri. Crop Sci.* 7, 582–589.

Black, M., and Pritchard, H. W. (2002). *Desiccation and survival in plants drying without dying*. New York: CABI publishing. doi: 10.1079/9780851995342.0000

Carillo, P., Annunziata, M. G., and Pontecorvo, G. (2011). "Salinity stress and salt tolerance," in *Abiotic stress in plants - mechanisms and adaptations*, eds A. K. Shanker and B. Venkateswarlu (Chorwacja: Intech), 19–38. doi: 10.5772/22331

Christakis, C. A., Daskalogiannis, G., Chatzaki, A., Markakis, E. A., Mermigka, G., Sagia, A., et al. (2021). Endophytic bacterial isolates from halophytes demonstrate phytopathogen biocontrol and plant growth promotion under high salinity. *Front. Microbiol.* 12:681567. doi: 10.3389/fmicb.2021.681567

Corwin, D., and Scudiero, E. (2019). Review of soil salinity assessment for agriculture across multiple scales using proximal and/or remote sensors. *Adv. Agron.* 158, 1–130. doi: 10.1016/bs.agron.2019.07.001

Cuevas, J., Daliakopoulos, I. N., del Moral, F., Hueso, J. J., and Tsanis, I. K. (2019). A review of soil-improving cropping systems for soil salinization. *Agron* 9:295. doi: 10.3390/agronomy9060295

Davy, A. J., Bishop, G. F., and Costa, C. S. B. (2001). Salicornia L. (Salicornia pusilla J. Woods, S. ramosissima J. Woods, S. europaea L., S. obscura P.W. Ball & Tutin, S. nitens P.W. Ball & Tutin, S. fragilis P.W. Ball & Tutin and S. dolichostachya Moss). *J. Ecol.* 89, 681–707. doi: 10.1046/j.0022-0477.2001.00607.x

Dawson, I. K., Russell, J., Powell, W., Steffenson, B., Thomas, W. T., and Waugh, R. (2015). Barley: a translational model for adaptation to climate change. *New Phytol.* 206, 913–931. doi: 10.1111/nph.13266

Demir, I., and Mavi, K. (2008). Effect of salt and osmotic stresses on the germination of pepper seeds of different maturation stages. *Braz. Arch. Biol. Tech.* 51, 897–902. doi: 10.1590/S1516-89132008000500004

Doganlar, Z. B., Demir, K., Basak, H., and Gul, I. (2010). Effects of salt stress on pigment and total soluble protein contents of three different tomato cultivars. *Afr. J. Agric. Res.* 5, 2056–2065.

Egamberdieva, D. (2009). Alleviation of salt stress by plant growth regulators and IAA producing bacteria in wheat. *Acta Physiol. Plant.* 31, 861–864. doi: 10.1007/s11738-009-0297-0

Egamberdieva, D., Jabborova, D., and Hashem, A. (2015). *Pseudomonas induces* salinity tolerance in cotton (*Gossypium hirsutum*) and resistance to *Fusarium* root rot through the modulation of indole-3-acetic acid. *Saudi. J. Biol. Sci.* 22, 773–779. doi: 10.1016/j.sjbs.2015.04.019

Eid, A. M., Fouda, A., Abdel-Rahman, M. A., Salem, S. S., Elsaied, A., Oelmüller, R., et al. (2021). Harnessing bacterial endophytes for promotion of plant growth and biotechnological applications: an overview. *Plants* 10:935. doi: 10.3390/plants10050935

El Madidi, S., El Baroudi, B., and Aameur, F. B. (2006). Genotypic variation for salt tolerance in moroccan barley landraces at seed germination. *Plant Breed. Seeds Sci.* 58, 63–69.

El-Tarabily, K. A., Ramadan, G. A., Elbadawi, A. A., Hassan, A. H., Tariq, S., Ghazal, E. W., et al. (2021). The marine endophytic polyamine-producing *Streptomyces mutabilis* UAE1 isolated from extreme niches in the Arabian Gulf promotes the performance of mangrove (Avicennia marina) seedlings under greenhouse conditions. *Front. Mar. Sci.* 8:710200. doi: 10.3389/fmars.2021.710200

FAOSTAT (2014). *Food and Agriculture Organization of the United Nations Statistics Division Portal.* Rome: Food and Agriculture Organization.

Fernández-Luqueño, F., Lopez-Valdez, F., Miranda-Arambula, M., Rosas-Morales, M., Pariona, N., and Espinoza-Zapata, R. (2014). "An introduction to the sunflower crop," in *Sunflowers*, ed. J. I. Arribas (Valladolid: Nova Science Publishers, Inc), 1–18.

Furtado, B. U., Nagy, I., Asp, T., Skorupa, M., Gołębiewski, M., Tyburski, J., et al. (2019a). Transcriptome profiling and environmental linkage to salinity across *Salicornia europaea* vegetation. *BMC Plant Biol.* 19:427. doi: 10.1186/s12870-019-2032-3

Furtado, B. U., Szymańska, S., and Hrynkiewicz, K. (2019b). A window into fungal endophytism in *Salicornia europaea*: deciphering fungal characteristics as plant growth promoting agents. *Plant Soil* 445, 577–594. doi: 10.1007/s11104-019-04315-3

Garthwaite, A. J., von Bothmeer, R., and Colmer, T. D. (2005). Salt tolerance in wild *Hordeum* species is associated with restricted entry of Na^+ and Cl^- into the shoots. *J. Exp. Bot.* 419, 2365–2378. doi: 10.1093/jxb/eri229

Green, T. G. A., Sancho, L. G., Pintado, A., Saco, D., Martin, S., Arroniz-Crespo, M., et al. (2017). Sodium chloride accumulation in glycophyte plants with cyanobacterial symbionts. *AoB Plants* 9:lx053. doi: 10.1093/aobpla/plx053

Guo, R., Zhao, L., Zhang, K., Lu, H., Bhanbhro, N., and Yang, C. (2021). comparative genomics and transcriptomics of the extreme halophyte *Puccinellia tenuiflora* provides insights into salinity tolerance differentiation between halophytes and glycophytes. *Front. Plant Sci.* 12:649001. doi: 10.3389/fpls.2021.649001

Han, Y., Wang, R., Yang, Z., Zhan, Y., Ma, Y., Ping, S., et al. (2015). 1-aminocyclopropane-1-carboxylate deaminase from *Pseudomonas stutzeri* A1501 facilitates the growth of rice in the presence of salt or heavy metals. *J. Microbiol. Biotechnol.* 25, 1119–1128. doi: 10.4014/jmb.1412.12053

Hoagland, D. R., and Arnon, D. I. (1950). The water-culture method for growing plants without soil. *Calif. Agric. Exp. Stn. Circ.* 347, 36–39.

Isayenkov, S. V., and Maathuis, F. J. M. (2019). Plant salinity stress: many unanswered questions remain. *Front. Plant Sci.* 10:80. doi: 10.3389/fpls.2019.00080

Ittah, M. A., Udo, I. A., and Obok, E. E. (2019). Sunflower (*Helianthaus annuus* L.) seeds germination in saline hydroculture. *J. Plant Sci.* 7, 72–75.

Jamil, M., Lee, D. B., Jung, K. Y., Ashraf, M., Lee, S. C., and Rhal, E. S. (2006). Effect of salt (NaCl) stress on germination and early seedling growth of four vegetables species. *Cent. Eur. Agric.* 7, 273–282.

Kadioğlu, B. (2021). Determination of germination biology of some sage (*Salvia* ssp.) Species under salinity stress. *JOTAF* 18, 359–367.

Khan, A. L., Halo, B. A., Elyassi, A., Ali, S., Al-Hosni, K., Hussain, J., et al. (2016). Indole acetic acid and ACC deaminase from endophytic bacteria improves the growth of *Solanum lycopersicum*. *Elect. J. Biotechnol.* 21, 58–64. doi: 10.1016/j.ejbt.2016.02.001

Khan, M. A., Asaf, S., Khan, A. L., Adhikari, A., Jan, R., Ali, S., et al. (2019a). Halotolerant rhizobacterial strains mitigate the adverse effects of NaCl stress in soybean seedlings. *Biomed. Res. Int.* 2019, 1–15. doi: 10.1155/2019/9530963

Khan, M. A., Asaf, S., Khan, A. L., Adhikari, A., Jan, R., Ali, S., et al. (2020). Plant growth promoting endophytic bacteria augment growth and salinity tolerance in rice plants. *Plant Biol.* 2020, 1–13. doi: 10.1111/plb.13124

Khan, M. A., Asaf, S., Khan, A. L., Ullah, I., Ali, S., Kang, S.-M., et al. (2019b). Alleviation of salt stress response in soybean plants with the endophytic bacterial isolate *Curtobacterium* sp. *SAK1*. *Ann. Microbiol.* 69, 797–808. doi: 10.1007/s13213-019-01470-x

Kumar, A., Kumar, S. P. J., Chintagunta, A. D., Agarwal, D. K., Pal, G., Singh, A. N., et al. (2021). Biocontrol potential of *Pseudomonas stutzeri* endophyte from *Withania somnifera* (Ashwagandha) seed extract against pathogenic *Fusarium oxysporum* and *Rhizoctonia solani*. *Arch. Phytopathol. Plant Prot.* 2021:1983384. doi: 10.1080/03235408.2021.1983384

Kumar, A., Singh, S., Gaurav, A. K., Srivastava, S., and Verma, J. P. (2020). Plant growth-promoting bacteria: biological tools for the mitigation of salinity stress in plants. *Front. Microbiol.* 11:1216. doi: 10.3389/fmicb.2020.01216

Kurunc, A. (2021). Effects of water and salinity stresses on growth, yield, and water use of iceberg lettuce. *J. Sci. Food Agric.* 101, 5688–5696. doi: 10.1002/jsfa.11223

Lami, M. J., Adler, C., Caram-Di Santo, A. M., Zenoff, M. C., de Cristóbal, R. E., Espinosa-Urgel, M., et al. (2020). *Pseudomonas stutzeri* MJL19, a rhizosphere - colonizing bacterium that promotes plant growth under saline stress. *J. Appl. Microbiol.* 129, 1364–5072. doi: 10.1111/jam.14692

Li, W., Zhang, H., Zeng, Y., Xiang, L., Lei, Z., Huang, Q., et al. (2020). A salt tolerance evaluation method for sunflower (*Helianthus annuus* L.) at the seed germination stage. *Sci. Rep.* 10:10626. doi: 10.1038/s41598-020-67210-3

Ludwiczak, A., Osiak, M., Cárdenas-Pérez, S., Lubińska-Mielińska, S., and Piernik, A. (2021). Osmotic stress or ionic composition: which affects the early growth of crop species more? *Agronomy* 11:435. doi: 10.3390/agronomy11030435

Masmoudi, F., Tounsi, S., Dunlap, C. A., and Trigui, M. (2021). Halotolerant *Bacillus spizizenii* FMH45 promoting growth, physiological, and antioxidant parameters of tomato plants expose to salt stress. *Plant Cell Rep.* 40, 1199–1213. doi: 10.1007/s00299-021-02702-8

Mohammed, A. H., Morrison, J. I., and Baldwin, B. S. (2021). Preliminary screening of domestic barley and wild barley genotypes for salt tolerance. *Agrosyst. Geosci. Environ.* 4:e20151. doi: 10.1002/agg2.20151

Molina-Montenegro, M. A., Oses, R., Torres-Díaz, C., Atala, C., Zurita-Silva, A., and Ruiz-Lara, S. (2016). Root-endophytes improve the ecophysiological performance and production of an agricultural species under drought condition. *AoB Plants* 8:lw062. doi: 10.1093/aobpla/plw062

Munns, R., and Tester, M. (2008). Mechanisms of salinity tolerance. *Annu. Rev. Plant Biol.* 59, 651–681. doi: 10.1146/annurev.arplant.59.032607.092911

Naveed, M., Mitter, B., Reichenauer, T. G., Wieczorek, K., and Sessitsch, A. (2014). Increased drought stress resilience of maize through endophytic colonization by *Burkholderia phytofirmans* PsJN and *Enterobacter* sp. FD17. *Environ. Exp. Bot.* 97, 30–39. doi: 10.1016/j.envexpbot.2013.09.014

Nawaz, K., Hussain, K., Majeed, A., Khan, F., Afghan, S., and Ali, K. (2010). Fatality of salt stress to plants: morphological, physiological and biochemical aspects. *Afr. J. Biotechnol.* 9, 5475–5480.

Numan, M., Bashir, S., Khan, Y., Mumtaz, R., Shinwari, Z. K., Khan, A. L., et al. (2018). Plant growth promoting bacteria as an alternative strategy for salt tolerance in plants: a review. *Microbiol. Res.* 209, 21–32. doi: 10.1016/j.micres.2018.02.003

Patel, M. V., and Patel, R. K. (2014). Indole-3-acetic acid (iaa) production by endophytic bacteria isolated from saline dessert, the Little Runn of Kutch. *CJM* 3, 17–28.

Peng-cheng, L., Xiao-yi, L., Hou-miao, W., Ting, P., Ji-yuan, Y., Yun-yun, W., et al. (2021). Metabolic responses to combined water deficit and salt stress in maize primary roots. *J. Integr. Agric.* 20, 109–119. doi: 10.1016/S2095-3119(20)63242-7

Pham, V. T., Rediers, H., Ghequire, M. G., Nguyen, H. H., De Mot, R., Vanderleyden, J., et al. (2017). The plant growth-promoting effect of the nitrogen-fixing endophyte *Pseudomonas stutzeri* A15. *Arch. Microbiol.* 199, 513–517. doi: 10.1007/s00203-016-1332-3

Piernik, A., Hrynkiewicz, K., Wojciechowska, A., Szymańska, S., Lis, M. I., and Muscolo, A. (2017). Effect of halotolerant endophytic bacteria isolated from *Salicornia europaea* L. on the growth of fodder beet (*Beta vulgaris* L.) under salt stress. *Arch. Agron. Soil Sci.* 63, 14004–11418. doi: 10.1080/03650340.2017.1286329

Rabiey, M., Hailey, L. E., Roy, S. R., Grenz, K., Al-Zadjali, M. A. S., Barrett, G. A., et al. (2019). Endophytes vs tree pathogens and pests: can they be used as biological control agents to improve tree health? *Eur. J. Plant Pathol.* 155, 711–729. doi: 10.1007/s10658-019-01814-y

Rajabi Dehnavi, A., Morteza, Z., Ludwiczak, A., Cardenas Perez, S., and Piernik, A. (2020). Effect of salinity on seed germination and seedling development of sorghum (*Sorghum bicolor* (L.) Moench) genotypes. *Agronomy* 10:859. doi: 10.3390/agronomy10060859

Reynolds, H. L., and D'Antonio, C. (1996). The ecological significance of plasticity in root weight ratio in response to nitrogen: opinion. *Plant Soil* 185, 75–97. doi: 10.1007/BF02257566

Richardson, A. D., Duigan, P. S., and Berlyn, G. P. (2002). An evaluation of noninvasive methods to estimate foliar chlorophyll content. *New Phytol.* 153, 185–194. doi: 10.1007/s11120-014-9970-2

Ruan, S., Xue, Q., and Tylkowska, K. (2002). The influence of priming on germination of rice (*Oryza sativa* L.) seeds and seedling emergence and performance in flooded soil. *Seed Sci. Technol.* 30, 61–67.

Saleem, S., Iqbal, A., Ahmed, F., and Ahmad, M. (2021). Phytobeneficial and salt stress mitigating efficacy of IAA producing salt tolerant strains in *Gossypium hirsutum*. *Saudi. J. Biol. Sci.* 28, 5317–5324. doi: 10.1016/j.sjbs.2021.05.056

Sapkota, S., Sapkota, S., and Liu, Z. (2019). Efects of nutrient composition and lettuce cultivar on crop production in hydroponic culture. *Horticulturae* 5:72. doi: 10.3390/horticulturae5040072

Srinivasarao, Ch, Rakesh, S., RanjithKumar, G., Manasa, R., Somashekar, G., SubhaLakshmi, C., et al. (2021). Soil degradation challenges for sustainable agriculture in tropical India. *Curr. Sci.* 120, 492–500. doi: 10.18520/cs/v120/i3/492-500

StatSoft (2006). *Electronic Guide for Statistics*. Kraków: StatSoft.

Szymańska, S., Dąbrowska, G., Tyburski, J., Niedojadlo, K., Piernik, A., and Hrynkiewicz, K. (2019). Boosting the *Brassica napus* L. tolerance to salinity by the halotolerant strain *Pseudomonas stutzeri* ISE12. *Environ. Exp. Bot.* 163, 55–68.

Szymańska, S., Płociniczak, T., Piotrowska-Seget, Z., and Hrynkiewicz, K. (2016). Endophytic and rhizosphere bacteria associated with the roots of the halophyte *Salicornia europaea* L.: community structure and metabolic potential. *Microbiol. Res.* 192, 37–51. doi: 10.1016/j.micres.2016.05.012

Szymańska, S., Tyburski, J., Piernik, A., Sikora, M., Mazur, J., and Hrynkiewicz, K. (2020). Raising beet tolerance to salinity through bioaugmentation with halotolerant endophytes. *Agronomy* 10:1571. doi: 10.3390/agronomy10101571

Talia, P., Greizerstein, E. J., Hopp, H. E., Paniego, N., Poggio, L., and Heinz, R. A. (2011). Detection of single copy sequences using BAC-FISH and C-PRINS techniques in sunflower chromosomes. *Biocell* 35, 19–28. doi: 10.32604/biocell.2011.35.019

Temme, A. A., Kerr, K. L., and Donovan, L. A. (2019). Vigour/tolerance trade-off in cultivated sunflower (*Helianthus annuus*) response to salinity stress is linked to leaf elemental composition. *J. Agron. Crop Sci.* 205, 508–518. doi: 10.1111/jac.12352

ter Braak, C. J. F., and Šmilauer, P. (2012). *CANOCO Reference manual and User's guide: Software ordination (version 5.0)*.

Tharek, M., Khairuddin, D., Najimudin, N., and Ghazali, A. H. (2021). Plant growth promoting potentials of beneficial endophytic *Escherichia coli* USML2 in association with rice seedlings. *Trop. Life Sci. Res.* 32, 119–143. doi: 10.21315/tlsr2021.32.1.8

Turan, M. A., Elkarim, A. H. A., Taban, N., and Taban, S. (2010). Effect of salt stress on growth and ion distribution and accumulation in shoot and root of maize plant. *Afr. J. Agric. Res.* 5, 584–588. doi: 10.1186/s12870-021-03237-6

Ünlükara, A., Cemek, B., Karaman, S., and Erşahin, S. (2008). Response of lettuce (*Lactuca sativa* var. *crispa*) to salinity of irrigation water. *New Zealand J. Crop Hort. Sci.* 36, 265–273. doi: 10.1080/01140670809510243

Vasilakoglou, I., Dhima, K., Giannakoula, A., Dordas, C., Skiada, V., and Papadopoulou, K. (2021). Carbon assimilation, isotope discrimination, proline and lipid peroxidation contribution to barley (*Hordeum vulgare*) salinity tolerance. *Plants* 10:299. doi: 10.3390/plants10020299

Vibhuti, S. C., Bargali, K., and Bargali, S. S. (2015). Assessment of salt stress tolerance in three varieties of rice (*Oryza sativa L.*). *J. Prog. Agric.* 6, 50–56.

Wu, G. Q., Liang, N., Feng, R. J., and Zhang, J. J. (2013). Evaluation of salinity tolerance in seedlings of sugar beet (*Beta vulgaris* L.) cultivars using proline, soluble sugars and cation accumulation criteria. *Acta Physiol. Plant* 35, 2665–2674. doi: 10.1007/s11738-013-1298-6

Yuan, Z.-S., Liu, F., Xie, B.-G., and Zhang, G.-Z. (2018). The growth-promoting effects of endophytic bacteria on *Phyllostachys edulis*. *Arch. Microbiol.* 200, 921–927. doi: 10.1007/s00203-018-1500-8

Zhao, L., Xu, Y., Lai, X. H., Shan, Ch, Deng, Z., and Ji, Y. (2015). Screening and characterization of endophytic *Bacillus* and *Paenibacillus* strains from medicinal plant *Lonicera japonica* for use as potential plant growth promoters. *Braz. J. Microbiol.* 46, 977–989. doi: 10.1590/S1517-838246420140024

Zhao, W., Liu, L., Shen, Q., Yang, J., Han, X., Tian, F., et al. (2020). Effects of water stress on photosynthesis, yield, and water use efficiency in winter wheat. *Water* 12:2127. doi: 10.3390/w12082127

Zhou, M. X. (2009). "Barley production and consumption," in *Genetics and Improvement of Barley Malt Quality*, eds G. Zhang and C. Li (Boston: Springer), 1–17. doi: 10.1007/978-3-642-01279-2_1

Conflict of Interest: The authors declare that the research was conducted in the absence of any commercial or financial relationships that could be construed as a potential conflict of interest.

Publisher's Note: All claims expressed in this article are solely those of the authors and do not necessarily represent those of their affiliated organizations, or those of the publisher, the editors and the reviewers. Any product that may be evaluated in this article, or claim that may be made by its manufacturer, is not guaranteed or endorsed by the publisher.

frontiers in Microbiology

ORIGINAL RESEARCH
published: 29 March 2022
doi: 10.3389/fmicb.2022.824192

Short-Term Grazing Exclusion Alters Soil Bacterial Co-occurrence Patterns Rather Than Community Diversity or Composition in Temperate Grasslands

*Fangfang Wang[1,2], Zongming Li[2,3], Bojie Fu[1,2,4], Yihe Lü[1,2], Guoping Liu[5], Dongbo Wang[6] and Xing Wu[1,2]**

[1] State Key Laboratory of Urban and Regional Ecology, Research Center for Eco-Environmental Sciences, Chinese Academy of Sciences, Beijing, China, [2] College of Resources and Environment, University of Chinese Academy of Sciences, Beijing, China, [3] Key Laboratory of Agro-Ecological Processes in Subtropical Region and Changsha Research Station for Agricultural & Environmental Monitoring, Institute of Subtropical Agriculture, Chinese Academy of Sciences, Changsha, China, [4] State Key Laboratory of Earth Surface Processes and Resource Ecology, Faculty of Geographical Science, Beijing Normal University, Beijing, China, [5] College of Animal Science, Yangtze University, Jingzhou, China, [6] Hulunbuir Eco-environmental Monitoring Center of Inner Mongolia, Hulunbuir, China

OPEN ACCESS

Edited by:
Hai-Ming Zhao,
Jinan University, China

Reviewed by:
Juntao Wang,
Western Sydney University, Australia
Xin Sun,
Yale University, United States
Noelline Tsafack,
Ningxia University, China

***Correspondence:**
Xing Wu
xingwu@rcees.ac.cn

Specialty section:
This article was submitted to Terrestrial Microbiology, a section of the journal Frontiers in Microbiology

Received: *29 November 2021*
Accepted: *31 January 2022*
Published: *29 March 2022*

Citation:
Wang F, Li Z, Fu B, Lü Y, Liu G, Wang D and Wu X (2022) Short-Term Grazing Exclusion Alters Soil Bacterial Co-occurrence Patterns Rather Than Community Diversity or Composition in Temperate Grasslands. Front. Microbiol. 13:824192. doi: 10.3389/fmicb.2022.824192

Grazing exclusion is one of the most common practices for degraded grassland restoration worldwide. Soil microorganisms are critical components in soil and play important roles in maintaining grassland ecosystem functions. However, the changes of soil bacterial community characteristics during grazing exclusion for different types of grassland remain unclear. In this study, the soil bacterial community diversity and composition as well as the co-occurrence patterns were investigated and compared between grazing exclusion (4 years) and the paired adjacent grazing sites for three types of temperate grasslands (desert steppe, typical steppe, and meadow steppe) in the Hulunbuir grassland of Inner Mongolia. Our results showed that short-term grazing exclusion decreased the complexity and connectivity of bacterial co-occurrence patterns while increasing the network modules in three types of temperate grasslands. The effects of grazing exclusion on soil bacterial α-diversity and composition were not significant in typical steppe and meadow steppe. However, short-term grazing exclusion significantly altered the community composition in desert steppe, indicating that the soil bacteria communities in desert steppe could respond faster than those in other two types of steppes. In addition, the composition of bacterial community is predominantly affected by soil chemical properties, such as soil total carbon and pH, instead of spatial distance. These results indicated that short-term grazing exclusion altered the soil bacterial co-occurrence patterns rather than community diversity or composition in three types of temperate grasslands. Moreover, our study suggested that soil bacterial co-occurrence patterns were more sensitive to grazing exclusion, and the restoration of soil bacterial community might need a long term (>4 years) in our study area.

Keywords: grazing exclusion, bacterial diversity, bacterial composition, co-occurrence network, temperate grassland

INTRODUCTION

Grasslands cover nearly 26% of the global land area and play important roles in providing the base of animal husbandry and promoting human sustainable development (Monfreda et al., 2008; Herrero et al., 2013). In recent decades, due to the intensification of human activities and climate change, grassland degradation has become prevalent worldwide (O'Mara, 2012; Jalaludin et al., 2020). The restoration of degraded grasslands has attracted much attention in recent years. Grazing exclusion is an effective and economical strategy for the restoration of degraded grasslands, which is beneficial for restoring vegetation, improving soil physical structure, and restoring soil nutrients (Su et al., 2005; Tang et al., 2016; Yu et al., 2019). However, previous studies predominantly focused on the effect of grazing exclusion on aboveground biomass and soil physical and chemical properties, while less research has been conducted on the restoration of soil bacterial community.

As the critical component in a grassland ecosystem, soil microorganisms play important roles in maintaining the stability and function of grassland ecosystems, including decomposing the organic matter, driving the elements' biogeochemical cycle, and regulating the plant nutrient availability (Yao et al., 2011; Zhao et al., 2020). The structure and function of soil microbial community in degraded grasslands is often disintegrated and limited (Zhou et al., 2011). Thus, the reconstruction of soil microbial community is priority in the process of restoration of degraded grasslands. In addition, soil bacterial community can sensitively reflect the change of soil environment (Hawkes and Keitt, 2015). Therefore, the properties of soil bacterial community have been widely used as important biological indexes of soil quality and ecosystem function in the restoration of degraded grassland, especially diversity, composition, and co-occurrence patterns (Zhou et al., 2010; Gao et al., 2021). Network analysis has been widely used to imply co-occurrence patterns in a bacterial community, which can reflect complex community interactions and ecosystem perturbation (Newman, 2006; Zhou et al., 2010).

The temperate grasslands of Inner Mongolia are representative of the Eurasian grassland belt (Wang et al., 2005). In the 1990s, due to the rapid growth of human population and food demand, nearly 50% degradation of the total grassland area was observed in North China (Zhang et al., 2016; Hu and Nacun, 2018), which predominantly resulted from overgrazing. Since 2003, the nationwide conservation project Returning Grazing Lands to Grasslands has been successively implemented in China to restore degraded grasslands. Plenty of studies have discovered that the diversity and biomass of vegetation have been effectively recovered after grazing exclusion in the temperate grasslands of Inner Mongolia (Chen and Tang, 2016). In addition, soil properties, such as organic matter, improved through the decomposition of litter and root exudate, and the soil bulk density decreased after 6–10 years of grazing exclusion (Wu et al., 2014a; Chen and Tang, 2016; Tang et al., 2016). However, the effect of grazing exclusion on the diversity, composition, or co-occurrence patterns of soil bacterial community is inconsistent in previous studies (Cheng et al., 2016; Zhang et al., 2021). In the temperate grassland in Inner Mongolia, meadow steppe, typical steppe, and desert steppe are the three main grassland types with different types of vegetation and an obvious gradient of water availability. The soil bacterial community may differently respond to different types of grasslands. Therefore, it is valuable to make clear the change of soil bacterial community during grazing exclusion in different types of grasslands in Inner Mongolia.

In this study, we compared the differences in the diversity, composition, and co-occurrence patterns of soil bacterial community between short-term grazing exclusion sites and the paired adjacent grazing sites for three types of temperate grasslands (desert steppe, typical steppe, and meadow steppe) in Inner Mongolia. Our objectives are the following: (1) investigate whether short-term grazing exclusion induces the changes in soil bacterial community and (2) investigate whether the response of soil bacterial community to grazing exclusion differs in three types of temperate grasslands.

MATERIALS AND METHODS

Study Area and Soil Sampling

Hulunbuir grassland (47°05′–53°20′ N, 115°31′–126°04′ E), located in the western part of the Greater Khingan Mountains, is a representative temperate grassland in Inner Mongolia and is selected as the research area. The topography is relatively flat, with an altitude of 650–700 m above sea level. The research area has a temperate continental monsoon climate, with mean annual precipitation of 339 mm and mean annual air temperature of −2.2°C from 1980 to 2010. The main soil types in this region are chernozem and kastanozem (Wu et al., 2014b). The dominant plant species in this area are *Aneurolepidium chinense*, *Stipa baicalensis*, and *Carex korshinskyi*.

In July 2019, nine sites covering the main areas of Hulunbuir grassland were selected, that is, three sites in each of the three grassland types: meadow steppe, typical steppe, and desert steppe (**Figure 1**). At each site, paired plots were sampled, which were a long-term free grazing plot and a nearby grazing exclusion plot (less than 200 m in distance). All the paired plots share the same soil type and similar physiographic conditions, including slope degree, altitude, and topography. Before fencing in 2015, the meadow steppe, typical steppe, and desert steppe sites had been continuously grazed with approximately 9, 7, and 2.7 sheep unit hm^{-1} $year^{-1}$ over the last decades according to local farmers, respectively. The free grazing plots were still grazed when the soil was sampled. The grazing exclusion sites had been fenced without additional management. Besides this, these sites had not been applied with fertilizers. The location, dominant plant species, and main soil characteristics of the sampling sites are shown in **Supplementary Table 1**. In each plot, four replicate subplots were set (1 m × 1 m) at 10-m intervals along a random transect. The surface (10 cm) soils (the litter layer was removed) were collected by a sterile soil sampler. The soil samples were transported to the laboratory on ice. The sample for extracting microbial DNA was freeze-dried and stored at −80°C. The soil samples for measuring chemical properties were air-dried and stored at 4°C until use.

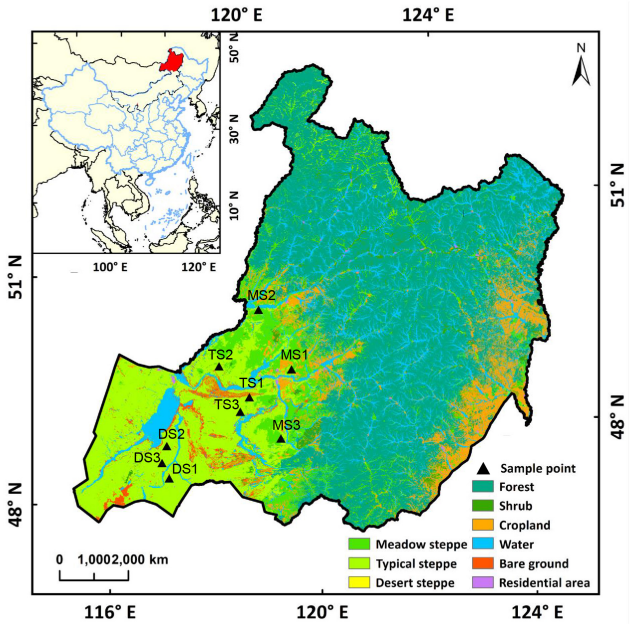

FIGURE 1 | Location of the sampling sites. Each sampling site includes a paired grazing site and grazing exclusion site. MS1, MS2, and MS3 refer to the sampling sites in meadow steppe; TS1, TS2, and TS3 refer to the sampling sites in typical steppe; DS1, DS2, and DS3 refer to the sampling sites in desert steppe.

Soil Chemical Property Analysis

The soil water content was determined gravimetrically by drying the soil samples at 105°C for 24 h. The soil pH was measured at a soil-to-water ratio of 1:5 using a pH meter (Mettler Toledo, Zurich, Switzerland). The soil total carbon (STC) and soil total nitrogen (STN) contents were determined using an automated C and N analyzer (Elementar, Hanau, Germany). Soil organic carbon (SOC) were determined by potassium dichromate oxidation methods using a spectrophotometer (Lambda25 UV–vis spectrometer, United States). Soil total phosphorus (TP) was measured with Mo–Sb colorimetric method using a spectrophotometer (Lambda25 UV–vis spectrometer, United States). Soil ammonium (NH_4^+–N) and nitrate (NO_3^-–N) were extracted from 20 g of fresh soil with 1 M KCl (soil/water = 1:5 w/v) and quantified colorimetrically using a flow injection analyzer (Seal AA3, Norderstedt, Germany).

Bacterial 16S rRNA Gene Sequence Analysis

Soil bacterial community was analyzed using high-throughput sequencing (GeneAmp 9700, ABI, United States). Total microbial DNA was extracted from the soil samples using a FastDNA SPIN Kit for Soil (MP Biochemicals, Solon, OH, United States) following the manufacturer's instruction. The hypervariable V4 region of bacterial 16S rRNA gene was sequenced by PCR with the primers 515F (5′-GTGCCAGCMGCCGCGG-3′) and 907R (5′-CCGTCAATTCMTTTRAGTTT-3′) (Yusoff et al., 2013). The sequencing was performed on an Illumina MiSeq platform (Illumina, San Diego, CA, United States) at Majorbio Bio-Pharm Technology, Shanghai, China. The obtained raw sequences were processed using Quantitative Insights Into Microbial Ecology (QIIME) with the standard operating procedure (Caporaso et al., 2010; Washburne et al., 2018). Operational taxonomic units (OTUs) were classified at 97% similarity. The representative sequences were then aligned to the Silva database in QIIME2 for maximum sequence similarity.

Co-occurrence Network of Bacterial Community

The co-occurrence network among bacterial community based on OTU was conducted to investigate the coexistence and interaction patterns of bacteria. The relative abundance of OTUs lower than 0.1% was deleted to reduce the rare OTUs. The significant ($P < 0.05$) and robust correlations (Pearson's $R > 0.8$) were visualized in the network using Gephi 0.9.2. In the network, the nodes refer to enriched OTUs (relative abundance higher than 0.1%) and edges refer to significant interactive correlations. Four normally used topological properties were calculated in Gephi to describe the complex interaction patterns between OTUs (Newman, 2003). Average degree refers to the average connections of each node with other nodes in the network. Average path length refers to the average distance in shortest paths between two nodes in the network (Faust and Raes, 2012). Average clustering coefficient represents the degree to which the nodes tend to cluster together. Modularity class quantifies the extent to which the network can be divided into different clusters (Rottjers and Faust, 2018). Modularity value >0.4 suggests that the network has a modular structure, and the nodes are highly connected within the cluster but less connected outside the cluster (Newman, 2006). Module in the network is densely

connected clusters of nodes and has been interpreted as ecological niche preferences (Chaffron et al., 2010; Freilich et al., 2010). Average degree and average path length are used to measure the connectivity of the network. Average clustering coefficient and modularity can reflect the cohesion of the network.

Statistical Analysis

All data are presented as mean and standard error. Pearson correlations were performed in SPSS 21 (IBM, Armonk, NY, United States). Statistically significant differences were accepted when $P < 0.05$. Scatter diagram and bar plot were generated in OriginPro 2018 (Origin Lab Corporation, United States). The β-diversity of the bacterial community was estimated based on Bray–Curtis distances in "vegan" package and plotted using "ggplot2" package in R 3.4.3. ANOSIM was performed to test the significance in difference of community composition between groups in "vegan" package in R 3.4.3 (Oksanen et al., 2020). RDA was conducted in "vegan" package in R 3.4.3.

RESULTS

Effect of Grazing Exclusion on Soil Properties

Before grazing exclusion, soil total carbon was significantly higher in meadow steppe than typical steppe and desert steppe soils, while the difference between typical steppe and desert steppe was not significant (**Table 1**). The difference of other soil chemical properties among three grassland types was not significant. After short-term grazing exclusion, the TP of desert steppe significantly decreased while STC and STN were slightly decreased. In typical steppe, grazing exclusion significantly increased the STC by 13%. TP, NH_4^+–N, and NO_3^-–N were slightly decreased. In meadow steppe, grazing exclusion induced a minor increase of the determined soil chemical properties, but the change was not significant. Short-term grazing exclusion increased the difference of STN and TP among the three grassland types.

Effect of Grazing Exclusion on Soil Bacterial Community Diversity and Composition

At the phylum level, Actinobacteria, Proteobacteria, Actinobacteria, and Chloroflexi are the dominant bacteria, which account for 44, 15, 13, and 10% of the total bacteria, respectively (**Supplementary Figure 1**). In grazing sites, only the relative abundance of Proteobacteria was significantly higher in typical steppe than in desert steppe and meadow steppe ($P < 0.01$), and the difference in the relative abundance of the other major phyla was not significant (**Supplementary Table 2**). However, after short-term grazing exclusion, the difference of the relative abundance of bacterial phyla between exclusion and grazing sites was not significant in the three types of grasslands. The α-diversity of the bacterial community based on Shannon index is significantly lower in desert steppe than in typical steppe and meadow steppe in grazing sites ($P = 0.018$,

TABLE 1 | Soil chemical properties between grazing and grazing exclusion treatments.

Grassland type	STC (g C kg^{-1})		STN (g N kg^{-1})		SOC (g C kg^{-1})		TP (g P kg^{-1})		NH_4^+–N (mg N kg^{-1})		NO_3^-–N (mg N kg^{-1})	
	Grazing	Exclusion	Grazing	Exclusion	Grazing	Exclusion	Grazing	Exclusion	Grazing	Exclusion	Grazing	Exclusion
Desert steppe	22.3 ± 1.4 Ba	21.2 ± 1.9 Ba	2.1 ± 0.3 Aa	1.9 ± 0.3 Ba	19.6 ± 0.7 Ba	20.4 ± 2.2 Ba	0.50 ± 0.06 Aa	0.38 ± 0.03 Bb	12.1 ± 0.8 Aa	12.2 ± 0.2 Aa	8.1 ± 1.7 Ab	18.8 ± 6.1 Aa
Typical steppe	25.6 ± 6.6 Bb	29.1 ± 7.1 Ba	2.2 ± 0.5 Aa	2.5 ± 0.5 Ba	23.5 ± 5.6 Bb	25.9 ± 5.6 Ba	0.37 ± 0.08 Aa	0.35 ± 0.05 Ba	14.6 ± 3.4 Aa	12.6 ± 1.7 Aa	10.2 ± 4.0 Aa	6.4 ± 1.3 Aa
Meadow steppe	34.9 ± 4.4 Aa	38.6 ± 4.1 Aa	2.7 ± 0.1 Aa	3.2 ± 0.3 Aa	31.0 ± 4.6 Aa	33.9 ± 3.2 Aa	0.40 ± 0.02 Aa	0.45 ± 0.02 Aa	13.7 ± 2.3 Aa	13.4 ± 1.6 Aa	11.4 ± 8.8 Aa	14.2 ± 11.1 Aa

The means (± SD, N = 4) for each variable followed by different lowercase letters indicate significant differences between grazing and exclusion sites ($P < 0.05$, two-tailed paired t-test). The uppercase letters indicate significant difference among different grassland types ($P < 0.05$, one-way ANOVA, least significant difference).
STC, soil total carbon; STN, soil total nitrogen; SOC, soil organic carbon; TP, total phosphorus.

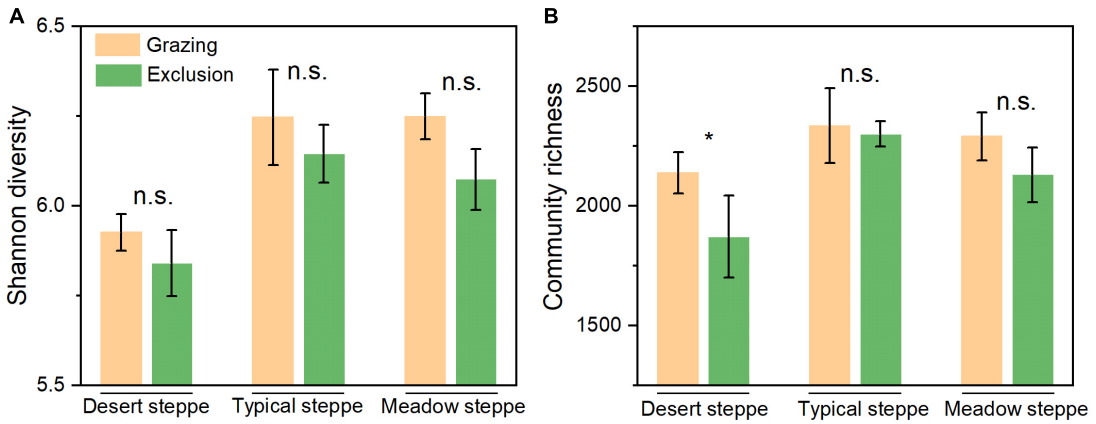

FIGURE 2 | The bacterial α-diversity **(A)** based on Shannon index and community richness **(B)** based on Sobs index between grazing and exclusion sites in three types of grasslands. Error bars indicate standard errors (3 replicate sites). "*" means significant difference ($P < 0.05$) between grazing and exclusion sites. "n.s." means non-significant.

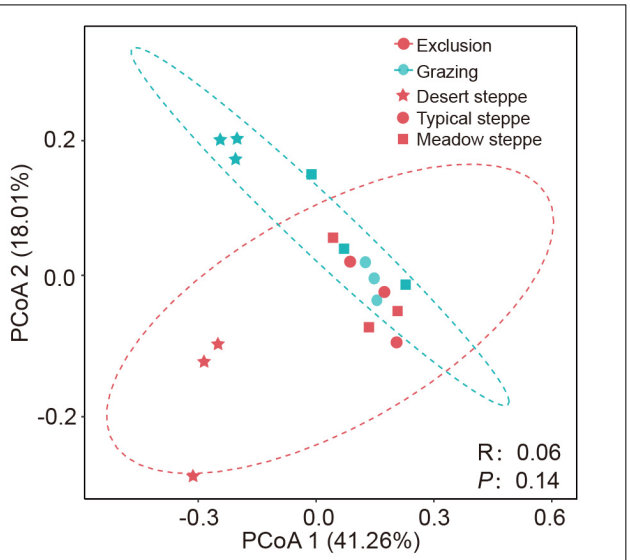

FIGURE 3 | Bacterial community structure assessed by β-diversity patterns using the principal coordinate analysis plots of Bray–Curtis distances. Different color represents exclusion or grazing soils and shape represents grassland types: desert steppe, typical steppe, and meadow steppe. ANOSIM similarity analysis was used to test the significance between groups.

Supplementary Table 2). The difference of community richness based on Sobs index was not significant among the three types of grasslands. After grazing exclusion, α-diversity was decreased in the exclusion treatments, but the difference was not significant (**Figure 2A**). The community richness in the exclusion treatments was significantly lower than in the grazing treatments in desert steppe ($P < 0.05$, **Figure 2B**). However, the difference of community richness between exclusion and grazing was not significant in typical steppe and meadow steppe. The bacterial β-diversity of Bray–Curtis distance among the three grassland types was significant based on ANOSIM analysis ($P < 0.01$). However, the β-diversity between exclusion and grazing treatments was not significant ($P = 0.14$, **Figure 3**).

Effect of Grazing Exclusion on Soil Bacterial Co-occurrence Patterns

The co-occurrence networks were established to investigate bacterial co-existence and interaction for the grazing and exclusion treatments. As shown in **Figures 4A,B**, 184 and 201 enriched OTUs formed 1,413 and 1,465 significant and robust associations in the grazing and exclusion treatments, respectively. The topological properties of the network analysis were calculated (**Figure 4C**). Compared with the exclusion treatments, the grazing treatments exhibited higher average degree, higher average clustering coefficient, and lower average path length, indicating that the grazing treatments have higher connectivity and closer connection in the network. The modularity classes are both higher than 0.4 in the grazing and exclusion treatments, which suggested that the enriched OTUs both exhibited a highly modular structure. In addition, the co-occurrence network in the grazing exclusion treatments exhibited five network modules, while only three network modules were found in the grazing treatments.

Relationships Between Soil Properties and Bacterial Community

The correlations between main soil chemical properties and bacterial α-diversity were not significant in the three types of grasslands of grazing exclusion and grazing soils (**Supplementary Table 3**). The correlations between soil properties and major bacterial phyla are shown in **Figure 5**. The relative abundance of Proteobacteria and *Verrucomicrobia* was significantly positively correlated with the content of STC, STN, and SOC. The relative abundance of Actinobacteria, Choloflexi, Firmicutes, Gemmatimonadota, and Nitrospirota was significantly negatively correlated with STC, STN, and SOC. The pH was significantly correlated with the relative abundance of Chloroflexi. In addition,

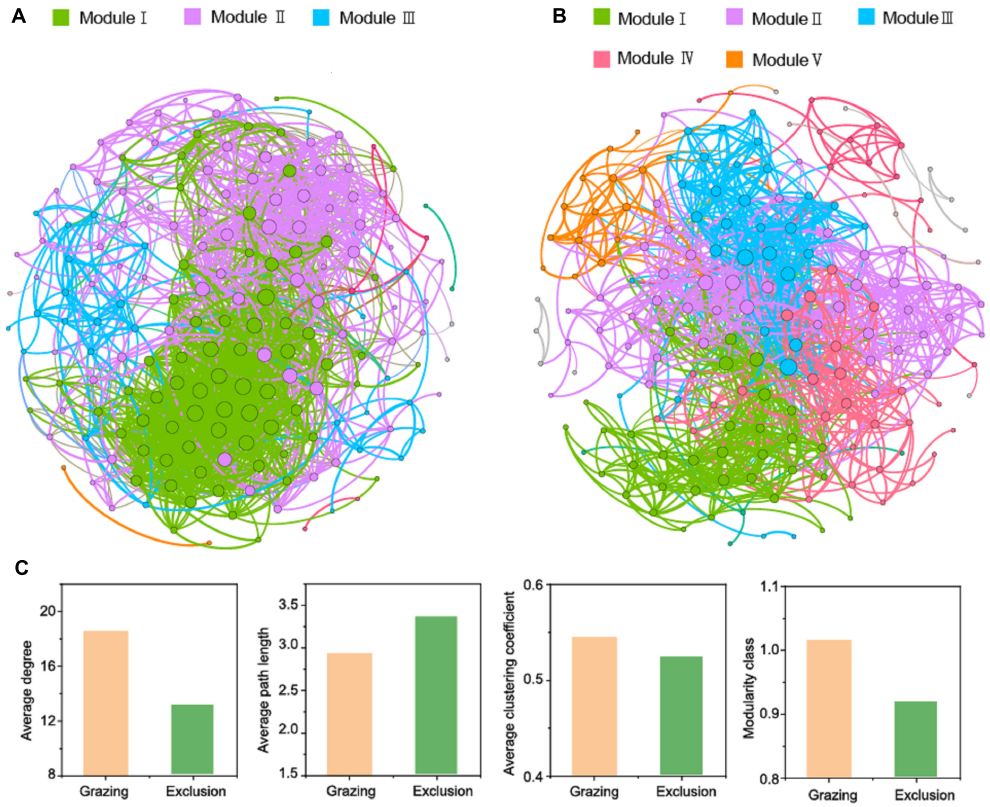

FIGURE 4 | Network analysis depicts the co-occurrence patterns among bacterial community based on operational taxonomic unit (Pearson's $R > 0.8$, $P < 0.05$) for grazing **(A)** and exclusion **(B)** treatments as well as the topological indexes **(C)**. The node size indicates connectivity degree. The colors of the nodes and edges are grouped by modularity class. Different colors refer to different modules.

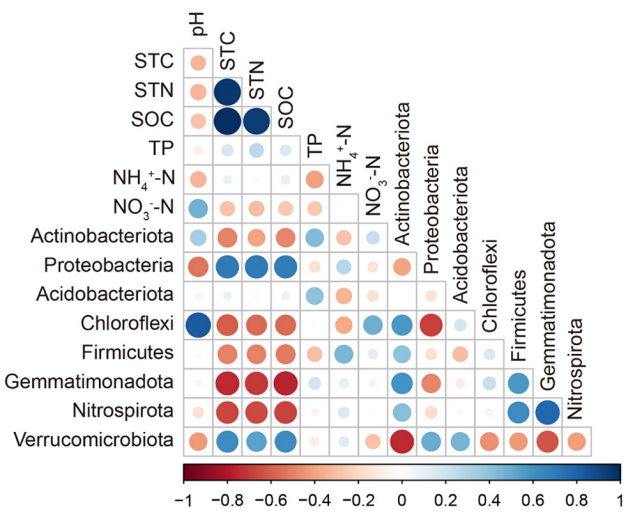

FIGURE 5 | Correlation between soil properties and the major bacterial phyla. Circle size and color represent the Pearson correlation coefficient.

RDA was conducted to investigate the effect of soil chemical properties on the composition of the bacterial community (**Figure 6**). The adjusted R^2 of the RDA model was 0.498, which means that 49.8% of the total variance of the bacterial community can be explained by the selected soil chemical properties in the grazing and exclusion soils. Among them, STC played a leading role in affecting the distribution of the bacterial community, followed by pH, NH_4^+–N, TP, and NO_3^-–N.

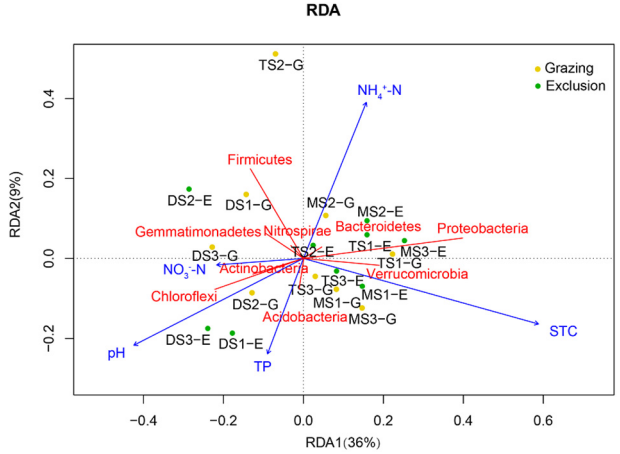

FIGURE 6 | Redundancy analysis of the significant soil chemical properties on the composition of bacterial community on phylum level. Blue arrows refer to soil chemical properties, red solid lines refer to bacterial phyla, and yellow and green dots refer to sampling sites.

DISCUSSION

Effect of Grazing Exclusion on Bacterial Diversity and Composition

In our study, short-term grazing exclusion decreased the α-diversity in the three types of temperate grasslands, but the differences were not significant between the exclusion and grazing treatments. In addition, grazing exclusion did not induce significant changes of the composition and the relative abundance of dominant phyla in typical steppe and meadow steppe. A previous study reported that 7 years of grazing exclusion of upland grassland decreased the soil bacterial diversity as a result of inhibition of soil carbon and nitrogen cycling (Medina-Roldan et al., 2012). Another study also found that the composition of soil bacterial communities was not influenced by 6 years of restoration in a tall-grass prairie in northeastern Kansas (Murphy and Foster, 2014). These results are consistent with our findings. However, other studies had found different results—for example, Yao et al. (2018) found that the composition of soil bacterial community significantly changed after 13 years of fencing in *Leymus chinensis* and *Stipa grandis* steppe. One possible explanation for the different effect of grazing exclusion on community properties is the exclusion duration. Short-term grazing exclusion might not induce significant changes of bacterial diversity and composition in typical steppe and meadow steppe. This may be because the response of soil bacterial community is slow and unresponsive to short-term grazing exclusion (Nunan et al., 2005; Singh et al., 2007). Therefore, the change of soil bacterial diversity and composition through short-term grazing exclusion is not evident or may take a long duration. Grazing exclusion significantly reduced community richness and changed community composition only in desert steppe, which may be attributed to different grazing history and soil property (Huhe et al., 2017; Yao et al., 2018).

Effect of Grazing Exclusion on Soil Bacterial Co-occurrence Patterns

The co-occurrence networks offer insight into the complex interactions between bacteria. These also reflect the associations between bacterial community and environment. Firstly, the co-occurrence patterns of bacterial community can be used as good indicators of grassland ecosystem perturbation (Zhou et al., 2010). As shown in the co-occurrence networks, the bacterial connectivity and interactions are closer and more complex in grazing treatments than in exclusion treatments. The reason may be that grazing soils experience more disturbances from livestock, thus forming more complex linkages to face the challenge of limited resources (Zhang et al., 2018). Although the total amount of soil carbon and nitrogen content did not differ significantly between the grazing and grazing exclusion treatments, the availability of soil carbon and nitrogen content may decrease due to the deterioration of the soil physical conditions in grazing soils (Wang et al., 2021). Therefore, without livestock disturbances, the complexity of a bacterial co-occurrence network decreased in grazing exclusion treatments. A higher value of average path length (AL) has been interpreted to decrease the speed of a bacterial network's response to perturbations (Zhou et al., 2010), which is consistent with the higher AL of the exclusion treatments than the grazing treatments. Secondly, the module is interpreted as a similar environment where microbes share overlapping ecological niches (Barberan et al., 2012). High modularity indicates that the boundary is clear between different modules in the network, and it is also considered as having highly distinguished niches in the community (Chaffron et al., 2010; Freilich et al., 2010; Faust and Raes, 2012), which is exhibited in both grazing and grazing exclusion treatments. Moreover, exclusion soils exhibited more diverse modules than grazing soils, which may be attributed to abundant plant-derived resources and improved soil environments creating more diverse niches for microorganisms (Chen et al., 2020; Lin et al., 2021)—for example, the increased plant root exudates and little decomposition with accumulation of aboveground plant biomass (Cheng et al., 2016). In the same ecological niche, microbes which are sharing resource may form more diverse interactions, including cooperation or competition (Freilich et al., 2010). Therefore, more diverse modules in the grazing exclusion treatments indicate more diverse interactions. In conclusion, short-term grazing exclusion altered the co-occurrence patterns of soil bacterial community, especially increasing the diversity of interactions in the three types of temperate grasslands.

Soil Properties That Affect Bacterial Community Composition

Whether grazing exclusion can change the diversity and composition of soil bacterial community or not, soil chemical properties are the deterministic factors (Zhang et al., 2018; Li et al., 2019; Qin et al., 2021). As shown in RDA, the

main soil chemical properties, especially pH, STC, and TP, are the dominant factors that affect the dissimilarity of soil bacterial community. Previous studies also found that pH (Lauber et al., 2009) and the availability of carbon and nitrogen (Sul et al., 2013; Cederlund et al., 2014) have predominant influences on the abundance and structure of soil microbial community in varied scales. Several mechanisms may explain the deterministic effect of edaphic factors on soil bacterial community. Firstly, pH can directly pose selective pressures on bacteria, as specific species poses different tolerance ability to pH—for example, our study found that the relative abundance of Choloflexi was positively correlated with pH, while the relative abundance of Proteobacteria and Verrucomicrobia showed negative correlations. pH can also indirectly affect the composition of bacterial community as it is normally related with multiple soil factors, including nutrient availability, redox state, and salinity (Lauber et al., 2009; Ren et al., 2020). Secondly, available carbon and nitrogen are the two key resources supporting the survival of most terrestrial heterotrophic microorganisms. Plenty of studies have found that the quality and the quantity of carbon and nitrogen determine the structure of soil bacterial community (Murphy and Foster, 2014; Zhang et al., 2018). Furthermore, soil chemical properties also showed close correlations with some members of the bacterial community. Our study found that the content of carbon and nitrogen exhibited positive correlations with Proteobacteria and Verrucomicrobiota, which is consistent with a previous study indicating that most types of the two phyla are heterotrophic microorganisms (Padhy et al., 2021). In addition, in our study, short-term grazing exclusion did not induce significant changes of the main soil chemical properties, especially pH, STC, and STN, which may explain that the response of bacterial community was not significant.

CONCLUSION

Our results showed that short-term grazing exclusion did not induce significant changes of the diversity and composition of soil bacterial community in typical steppe and meadow steppe but altered the community composition in desert steppe. The complexity and connectivity of bacterial co-occurrence patterns decreased, while the diversity of interactions increased through grazing exclusion management among the three types of temperate grasslands. In addition, soil chemical properties, especially pH, STC, and TP, are the dominant factors that affect the composition of soil bacterial community. These results indicated that the effect of grazing exclusion differs in three main grassland types in Inner Mongolia. Moreover, soil bacterial co-occurrence interactions may be more sensitive to grazing exclusion, and the restoration of soil bacterial community in our study area might need a long term (>4 years).

DATA AVAILABILITY STATEMENT

The 16S rRNA gene sequencing data of all samples were submitted to the NCBI SRA database (https://www.ncbi.nlm.nih.gov/) under accession number PRJNA787389.

AUTHOR CONTRIBUTIONS

FW and XW conceptualized this study and led the writing. ZL, GL, and DW collected and analyzed the data. BF, YL, and XW interpreted the results and revised the text. All authors contributed to this work and approved the final manuscript before submission.

FUNDING

This study was supported by the National Natural Science Foundation of China (42041005 and 41773070), the Second Tibetan Plateau Scientific Expedition and Research Program (2019QZKK0308), and the Youth Innovation Promotion Association of the Chinese Academy of Sciences (2018056).

ACKNOWLEDGMENTS

We acknowledge the data support from the National Earth System Science Data Center, National Science and Technology Infrastructure of China (http://www.geodata.cn). We thank Chaowei Zhou for editing the sampling figure (**Figure 1**). We also would like to thank the editor and the reviewers for valuable suggestions and comments to improve the previous version of the manuscript.

SUPPLEMENTARY MATERIAL

The Supplementary Material for this article can be found online at: https://www.frontiersin.org/articles/10.3389/fmicb.2022.824192/full#supplementary-material

REFERENCES

Barberan, A., Bates, S. T., Casamayor, E. O., and Fierer, N. (2012). Using network analysis to explore co-occurrence patterns in soil microbial communities. *ISME J.* 6, 343–351. doi: 10.1038/ismej.2011.119

Caporaso, J. G., Kuczynski, J., Stombaugh, J., Bittinger, K., Bushman, F. D., Costello, E. K., et al. (2010). QIIME allows analysis of high-throughput community sequencing data. *Nat. Methods* 7, 335–336. doi: 10.1038/nmeth.f.303

Cederlund, H., Wessen, E., Enwall, K., Jones, C. M., Juhanson, J., Pell, M., et al. (2014). Soil carbon quality and nitrogen fertilization structure bacterial communities with predictable responses of major bacterial phyla. *Appl. Soil Ecol.* 84, 62–68. doi: 10.1016/j.apsoil.2014.06.003

Chaffron, S., Rehrauer, H., Pernthaler, J., and Mering, C. V. (2010). A global network of coexisting microbes from environmental and whole-genome sequence data. *Genome Res.* 20, 947–959. doi: 10.1101/gr.104521.109

Chen, J., and Tang, H. P. (2016). Effect of grazing exclusion on vegetation characteristics and soil organic carbon of Leymus chinensis grassland in Northern China. *Sustainability* 8:56.

Chen, L. L., Shi, J. J., Bao, Z. H., and Baoyin, T. (2020). Soil fungal networks are more sensitive to grazing exclusion than bacterial networks. *Peerj* 8:e9986. doi: 10.7717/peerj.9986

Cheng, J. M., Jing, G. H., Wei, L., and Jing, Z. B. (2016). Long-term grazing exclusion effects on vegetation characteristics, soil properties and bacterial communities in the semi-arid grasslands of China. *Ecol. Eng.* 97, 170–178.

Faust, K., and Raes, J. (2012). Microbial interactions: from networks to models. *Nat. Rev. Microbiol.* 10, 538–550. doi: 10.1038/nrmicro2832

Freilich, S., Kreimer, A., Meilijson, I., Gophna, U., Sharan, R., and Ruppin, E. (2010). The large-scale organization of the bacterial network of ecological co-occurrence interactions. *Nucleic Acids Res.* 38, 3857–3868. doi: 10.1093/nar/gkq118

Gao, X. X., Dong, S. K., Xu, Y. D., Li, Y., Li, S., Wu, S. N., et al. (2021). Revegetation significantly increased the bacterial-fungal interactions in different successional stages of alpine grasslands on the qinghai-tibetan plateau. *Catena* 205:105385. doi: 10.1016/j.catena.2021.105385

Hawkes, C. V., and Keitt, T. H. (2015). Resilience vs. Historical contingency in microbial responses to environmental change. *Ecol. Lett.* 18, 612–625. doi: 10.1111/ele.12451

Herrero, M., Havlik, P., Valin, H., Notenbaert, A., Rufino, M. C., Thornton, P. K., et al. (2013). Biomass use, production, feed efficiencies, and greenhouse gas emissions from global livestock systems. *Proc. Natl. Acad. Sci. U S A.* 110, 20888–20893. doi: 10.1073/pnas.1308149110

Hu, Y., and Nacun, B. (2018). An Analysis of Land-Use Change and Grassland Degradation from a Policy Perspective in Inner Mongolia, China, 1990-2015. *Sustainability* 10:4048.

Huhe, Chen, X. J., Hou, F. J., Wu, Y. P., and Cheng, Y. X. (2017). Bacterial and Fungal Community Structures in Loess Plateau Grasslands with Different Grazing Intensities. *Front. Microbiol.* 8:606. doi: 10.3389/fmicb.2017.00606

Jalaludin, B., Johnston, F., Vardoulakis, S., and Morgan, G. (2020). Reflections on the Catastrophic 2019–2020 Australian Bushfires. *Innovation* 1:100010. doi: 10.1016/j.xinn.2020.04.010

Lauber, C. L., Hamady, M., Knight, R., and Fierer, N. (2009). Pyrosequencing-Based Assessment of Soil pH as a Predictor of Soil Bacterial Community Structure at the Continental Scale. *Appl. Environ. Microb.* 75, 5111–5120. doi: 10.1128/AEM.00335-09

Li, Z. G., Qiu, K. Y., Schneider, R. L., Morreale, S. J., and Xie, Y. Z. (2019). Comparison of microbial community structures in soils with woody organic amendments and soils with traditional local organic amendments in Ningxia of Northern China. *PEERJ* 7:e6854. doi: 10.7717/peerj.6854

Lin, Q., Li, L. J., Adams, J. M., Hedenec, P., Tu, B., Li, C. N., et al. (2021). Nutrient resource availability mediates niche differentiation and temporal co-occurrence of soil bacterial communities. *Appl. Soil. Ecol.* 163:103965.

Medina-Roldan, E., Paz-Ferreiro, J., and Bardgett, R. D. (2012). Grazing exclusion affects soil and plant communities, but has no impact on soil carbon storage in an upland grassland. *Agr. Ecosyst. Environ.* 149, 118–123.

Monfreda, C., Ramankutty, N., and Foley, J. A. (2008). Farming the planet: 2. Geographic distribution of crop areas, yields, physiological types, and net primary production in the year 2000. *Glob. Biogeochem.* 22:GB1022.

Murphy, C. A., and Foster, B. L. (2014). Soil Properties and Spatial Processes Influence Bacterial Metacommunities within a Grassland Restoration Experiment. *Restor. Ecol.* 22, 685–691.

Newman, M. E. J. (2003). The structure and function of complex networks. *SIAM. Rev.* 45, 167–256.

Newman, M. E. J. (2006). Modularity and community structure in networks. *Proc. Natl. Acad. Sci. U S A.* 103:8577.

Nunan, N., Daniell, T. J., Singh, B. K., Papert, A., McNicol, J. W., and Prosser, J. I. (2005). Links between plant and rhizoplane bacterial communities in grassland soils, characterized using molecular techniques. *Appl. Environ. Microb.* 71, 6784–6792. doi: 10.1128/AEM.71.11.6784-6792.2005

Oksanen, J., Blanchet, F. G., Kindt, R., Legendre, P., O'Hara, R. G., Simpson, G., et al. (2020). *vegan: community ecology package 2.5-7. Ordination methods, diversity analysis and otherfunctions for community and vegetation ecologists*. Vienna: R Core Team.

O'Mara, F. P. (2012). The role of grasslands in food security and climate change. *Ann. Bot.* 110, 1263–1270. doi: 10.1093/aob/mcs209

Padhy, S. R., Bhatta, Charyya, P., Nayak, S. K., Dash, P. K., and Mohapatra, T. (2021). A unique bacterial and archaeal diversity make mangrove a green production system compared to rice in wetland ecology: A metagenomic approach. *Sci. Total Environ.* 781:146713. doi: 10.1016/j.scitotenv.2021.146713

Qin, Y. Y., Zhang, X. F., Adamowski, J. F., Biswas, A., Holden, N. M., and Hu, Z. Y. (2021). Grassland grazing management altered soil properties and microbial β-diversity but not α-diversity on the Qinghai-Tibetan Plateau. *Appl. Soil Ecol.* 167:104032. doi: 10.1016/j.apsoil.2021.104032

Ren, Z., Niu, D. C., Ma, P. P., Wang, Y., Wang, Z. M., Fu, H., et al. (2020). Bacterial Communities in Stream Biofilms in a Degrading Grassland Watershed on the Qinghai-Tibet Plateau. *Front. Microbiol.* 11:1021. doi: 10.3389/fmicb.2020.01021

Rottjers, L., and Faust, K. (2018). From hairballs to hypotheses-biological insights from microbial networks. *Fems. Microbiol. Rev.* 42, 761–780. doi: 10.1093/femsre/fuy030

Singh, B. K., Munro, S., Potts, J. M., and Millard, P. (2007). Influence of grass species and soil type on rhizosphere microbial community structure in grassland soils. *Appl. Soil Ecol.* 36, 147–155.

Su, Y. Z., Li, Y. L., Cui, H. Y., and Zhao, W. Z. (2005). Influences of continuous grazing and livestock exclusion on soil properties in a degraded sandy grassland, inner mongolia, northern china. *Catena* 59, 267–278.

Sul, W. J., Asuming-Brempong, S., Wang, Q., Tourlousse, D. M., Penton, R., Deng, Y., et al. (2013). Tropical agricultural land management influences on soil microbial communities through its effect on soil organic carbon. *Soil. Biol. Biochem.* 65, 33–38.

Tang, J., Davy, A. J., Jing, D. M., Musa, A., Wu, D. F., Wang, Y. C., et al. (2016). Effects of excluding grazing on the vegetation and soils of degraded sparse-elm grassland in the Horqin Sandy Land. *China Agr. Ecosyst. Environ.* 235, 340–348. doi: 10.1016/j.agee.2016.11.005

Wang, F. F., Chen, Y. Z., Li, T., Wang, C., Wang, D. B., Fu, B. J., et al. (2021). Grazing Reduces the Soil-Atmosphere Exchange of Greenhouse Gases During Freeze-Thaw Cycles in Meadow Steppes in Inner Mongolia. *Front. Ecol. Evol.* 9:795203. doi: 10.3389/fevo.2021.795203

Wang, Y. S., Xue, M., Zheng, X. H., Ji, B. M., Du, R., and Wang, Y. F. (2005). Effects of environmental factors on N_2O emission from and CH_4 uptake by the typical grasslands in the Inner Mongolia. *Chemosphere* 58, 205–215. doi: 10.1016/j.chemosphere.2004.04.043

Washburne, A. D., Morton, J. T., Sanders, J., McDonald, D., Zhu, Q. Y., Oliverio, A., et al. (2018). Methods for phylogenetic analysis of microbiome data. *Nat. Microbiol.* 3, 652–661. doi: 10.1038/s41564-018-0156-0

Wu, X., Brueggemann, N., Butterach-Bahl, K., Fu, B. J., and Liu, G. H. (2014b). Snow cover and soil moisture controls of freeze-thaw-related soil gas fluxes from a typical semi-arid grassland soil: a laboratory experiment. *Biol. Fert. Soils* 50, 295–306.

Wu, X., Li, Z. S., Fu, B. J., Zhou, W. M., Liu, H. F., and Liu, G. H. (2014a). Restoration of ecosystem carbon and nitrogen storage and microbial biomass after grazing exclusion in semi-arid grasslands of Inner Mongolia. *Ecol. Eng.* 73, 395–403.

Yao, H., Bowman, D., and Shi, W. (2011). Seasonal variations of soil microbial biomass and activity in warm- and cool-season turfgrass systems. *Soil Biol. Biochem.* 43, 1536–1543.

Yao, M. J., Rui, J. P., Li, J. B., Wang, J. M., Cao, W. D., and Li, X. Z. (2018). Soil bacterial community shifts driven by restoration time and steppe types in the degraded steppe of Inner Mongolia. *Catena* 165, 228–236.

Yu, L. F., Chen, Y., Sun, W. J., and Huang, Y. (2019). Effects of grazing exclusion on soil carbon dynamics in alpine grasslands of the tibetan plateau. *Geoderma* 353, 133–143. doi: 10.1016/j.geoderma.2019.06.036

Yusoff, M. M., Hu, A., Feng, C., Maeda, T., Shirai, Y., Hassan, M. A., et al. (2013). Influence of pretreated activated sludge for electricity generation in microbial fuel cell application. *Bioresour. Technol.* 145, 90–96. doi: 10.1016/j.biortech.2013.03.003

Zhang, C., Liu, G. B., Song, Z. L., Wang, J., and Guo, L. (2018). Interactions of soil bacteria and fungi with plants during long-term grazing exclusion in semiarid grasslands. *Soil. Biol. Biochem.* 124, 47–58.

Zhang, Q., Liu, K. S., Shao, X. Q., Li, H., He, Y. X., Sirimuji, et al. (2021). Microbes require a relatively long time to recover in natural succession restoration of degraded grassland ecosystems. *Ecol. Indic.* 129:107881. doi: 10.1016/j.ecolind.2021.107881

Zhang, X. F., Niu, J. M., Buyantuev, A., Zhang, Q., Dong, J. J., Kang, S., et al. (2016). Understanding Grassland Degradation and Restoration from the Perspective of Ecosystem Services: A Case Study of the Xilin River Basin in Inner Mongolia, China. *Sustainability* 8:594.

Zhao, C. Z., Zhang, H., Song, C. P., Zhu, J. K., and Shabala, S. (2020). Mechanisms of Plant Responses and Adaptation to Soil Salinity. *Innovation* 1:100017. doi: 10.1016/j.xinn.2020.100017

Zhou, J. Z., Deng, Y., Luo, F., He, Z. L., Tu, Q. C., and Zhi, X. Y. (2010). Functional Molecular Ecological Networks. *Mbio* 1, e169–e110.

Zhou, Z. Y., Li, F. R., Chen, S. K., Zhang, H. R., and Li, G. (2011). Dynamics of vegetation and soil carbon and nitrogen accumulation over 26 years under controlled grazing in a desert shrubland. *Plant Soil* 341, 257–268.

Conflict of Interest: The authors declare that the research was conducted in the absence of any commercial or financial relationships that could be construed as a potential conflict of interest.

Publisher's Note: All claims expressed in this article are solely those of the authors and do not necessarily represent those of their affiliated organizations, or those of the publisher, the editors and the reviewers. Any product that may be evaluated in this article, or claim that may be made by its manufacturer, is not guaranteed or endorsed by the publisher.

frontiers in Microbiology

ORIGINAL RESEARCH
published: 30 March 2022
doi: 10.3389/fmicb.2022.828196

The Cropping Obstacle of Garlic Was Associated With Changes in Soil Physicochemical Properties, Enzymatic Activities and Bacterial and Fungal Communities

Jinyang Yu[1], Yihao Liu[1], Zuyu Wang[1], Xiaohui Huang[1], Dan Chai[2], Yunfu Gu[1], Ke Zhao[1], Xiumei Yu[1], Zhengbin Shuai[2], Hanjun Liu[1,3], Xiaoping Zhang[1], Petri Penttinen[1] and Qiang Chen[1]**

[1] College of Resources, Sichuan Agricultural University, Chengdu, China, [2] Institute of Horticulture, Chengdu Academy of Agriculture and Forestry Sciences, Chengdu, China, [3] Safety and Environmental Protection Quality Supervision and Testing Research Institute, CNPC Chuanqing Drilling Engineering Co., Ltd., Guanghan, China

OPEN ACCESS

Edited by:
Xun Wen Chen, Southern University of Science and Technology, China

Reviewed by:
Xiaomin Li, South China Normal University, China
Yu Shi, Institute of Soil Science (CAS), China

***Correspondence:**
Petri Penttinen
petri.penttinen@helsinki.fi
Qiang Chen
cqiang@sicau.edu.cn

Specialty section:
This article was submitted to Terrestrial Microbiology, a section of the journal Frontiers in Microbiology

Received: *03 December 2021*
Accepted: *28 February 2022*
Published: *30 March 2022*

Citation:
Yu J, Liu Y, Wang Z, Huang X, Chai D, Gu Y, Zhao K, Yu X, Shuai Z, Liu H, Zhang X, Penttinen P and Chen Q (2022) The Cropping Obstacle of Garlic Was Associated With Changes in Soil Physicochemical Properties, Enzymatic Activities and Bacterial and Fungal Communities. Front. Microbiol. 13:828196. doi: 10.3389/fmicb.2022.828196

Aims: In garlic cultivation, long-time monoculture has resulted in continuous-cropping obstacles. However, the cause has not been studied to date.

Methods: We analyzed soils from garlic fields in Pengzhou, China, to determine continuous-cropping obstacle related changes in soil physicochemical properties and enzyme activities, and in the diversity and composition of bacterial and fungal communities. Furthermore, we examined the relationships between soil properties and the bacterial and fungal communities.

Results: The soil pH and the soil catalase, urease, invertase, and polyphenol oxidase activities were lower in the cropping obstacle soil than in the healthy control soil. The richness and diversity of the bacteria were lower in the cropping obstacle soil than in the control. The bacterial and fungal communities in the cropping obstacle soil were clearly different from those in the control soil. The differences in bacterial communities between the cropping obstacle soil and the control soil were associated with differences in pH and available potassium content. The taxa with higher relative abundances in the cropping obstacle soils included potential plant pathogens and the taxa with lower relative abundances included potential plant growth promoters.

Conclusion: The enrichment of plant pathogens and the depletion of plant growth promoting fungi may have contributed to the poor growth of garlic in the cropping obstacle soil. The enzyme activity and microbial community differences were associated with acidification that was likely an important factor in the deterioration of the soil ecological environment and the garlic cropping obstacle. The results provide information to guide agricultural practices in cultivating garlic.

Keywords: garlic, cropping obstacles, soily acidification, soil enzyme activity, soil microbial community

HIGHLIGHTS

- Soil acidification was the primary factor correlating with garlic cropping obstacle.
- The activities of catalase, urease, invertase and polyphenol oxidase were lower in the cropping obstacle soil than in the healthy control soil.
- The enrichment of plant pathogens and the depletion of plant growth promoting fungi may have contributed to the garlic cropping obstacle.
- The assembly of bacterial communities was dominated by stochastic processes in garlic cropping obstacle soil.

INTRODUCTION

Garlic (*Allium sativum* L.) is rich in nutrients and has an appealing flavor and antibacterial properties; thus, it has been used as a seasoning, functional food, and traditional medicine for thousands of years worldwide (Corzo-Martinez et al., 2007; Liu et al., 2020). Currently, Asia, Europe, and Latin America are the main garlic production regions. In China, the garlic cropping area has reached 830 km^2 and the annual yield is approximately 2.3 million tons (FAO, 2019). Growing demand for yields and the limited arable land have resulted in garlic production with high cropping intensity and monocultures over long periods. Generally, long-term monoculture continuous cropping decreased crop yield and quality a phenomenon known as cropping obstacle (Zhu et al., 2018). The cropping obstacle may include numerous biotic and abiotic factors, e.g., changes in microbial communities (Dong et al., 2017), enriched soil-borne plant pathogens (Liu et al., 2014), declines in soil enzyme activity (Fu et al., 2017), changes in soil physicochemical properties (Kaur and Singh, 2014; Perez-Brandan et al., 2014; Li et al., 2016), and autotoxicity of plants (van Wyk et al., 2017).

Soil microorganisms play an important role in agricultural production by maintaining soil quality and affecting nutrient cycling (Blagodatskaya and Kuzyakov, 2013; Sun et al., 2015; Beckers et al., 2017). In some instances, the interactions between soil microbial communities and soil properties modulate plant health through affecting pathogens (Wei et al., 2015). Cropping obstacles have been associated with soil bacterial and fungal communities (Gao et al., 2019, 2021; Xi et al., 2019). For example, decreases in diversity and abundance of beneficial soil microbes and an increase in pathogenic fungi such as *Fusarium* and *Verticillium* were associated with sugarcane cropping obstacle (Pang et al., 2021). However, the relationships between microbial communities and continuous cropping obstacles are not necessarily similar across diverse crops and environmental conditions, thus more studies are called for.

Soil enzymes, i.e., the extracellular enzymes produced by the microorganisms, are considered as indicators of soil fertility (Zeng et al., 2007; Paz-Ferreiro and Fu, 2016). The physicochemical properties of soil affect the composition of soil microbial communities and the enzyme activities (Liu et al., 2021). Among the soil physicochemical properties, soil pH is considered as a master variable in affecting the microbial communities (Fierer and Jackson, 2006). Evidently, the changes brought on by continuous cropping, e.g., the often detected acidification, have resulted in changes in the soil microbial communities and soil enzymatic activities (Gao et al., 2019, 2021; Zheng et al., 2019).

Pengzhou in the Chengdu Plain is one of the five major vegetable cultivation bases in China, with a garlic cultivation history of more than 30 years. In Pengzhou, garlic is commonly grown in rotation with spring rice. In recent years, the long-time monoculture has resulted in continuous-cropping obstacles. The symptoms of the obstacle include yellowing of the leaves starting from the tips and edges, stagnated growth of roots and plant, at its worst, dying of the plants. The continuous-cropping obstacles appear commonly on patches in a field and sometimes on an entire field.

To our knowledge, the continuous-cropping obstacles in garlic cultivation have not been studied to date. We analyzed soils from garlic fields in Pengzhou, with the aim to determine continuous-cropping obstacle related changes in (1) soil physicochemical properties and enzyme activities, and in (2) the diversity and composition of bacterial and fungal communities. Furthermore, we examined (3) the relationships between soil properties and the bacterial and fungal communities. We hypothesized that the continuous cropping obstacle would be associated with soil acidification that would further affect the soil microorganisms and decrease enzyme activities. The results provide information to guide agricultural practices in cultivating garlic.

MATERIALS AND METHODS

Site Description and Field Sampling

The field experiment was performed in a garlic production area in Pengzhou (31°02′31″N-31°05′39″N, 103°50′51″E-103°59′42″E), Chengdu Plain, China, that is in the northern part of the subtropical humid climate zone, with a mean annual temperature of 15.7°C, precipitation of 960 mm and approximately 1,180 h of sunshine. The soil on the site is fertile paddy soil. Garlic was grown in rice-garlic rotation and covered with straw after sowing.

Samples were collected in March 2018 from seven fields with an area of 700–1,000 m^2. In each field, three 60–100 m^2 plots were randomly selected in areas with healthy garlic plants (CK) and in areas with cropping obstacles (D) (**Figure 1**). Five topsoil (0–20 cm) subsamples from a 10 cm circle around the plants were combined into a composite sample, an appropriate amount of homogenized soil was retained by quartering, and placed into sterile plastic bags that were sealed. The bags were kept on ice and transported to the laboratory immediately after sampling. Roots and other debris were removed from the soil samples and the samples were divided into two parts for immediate DNA extraction and physicochemical analyses.

Garlic Growth and Root Activity Analyses

The growth of the plants was assessed by measuring shoot and root lengths and the fresh weight of aboveground and root

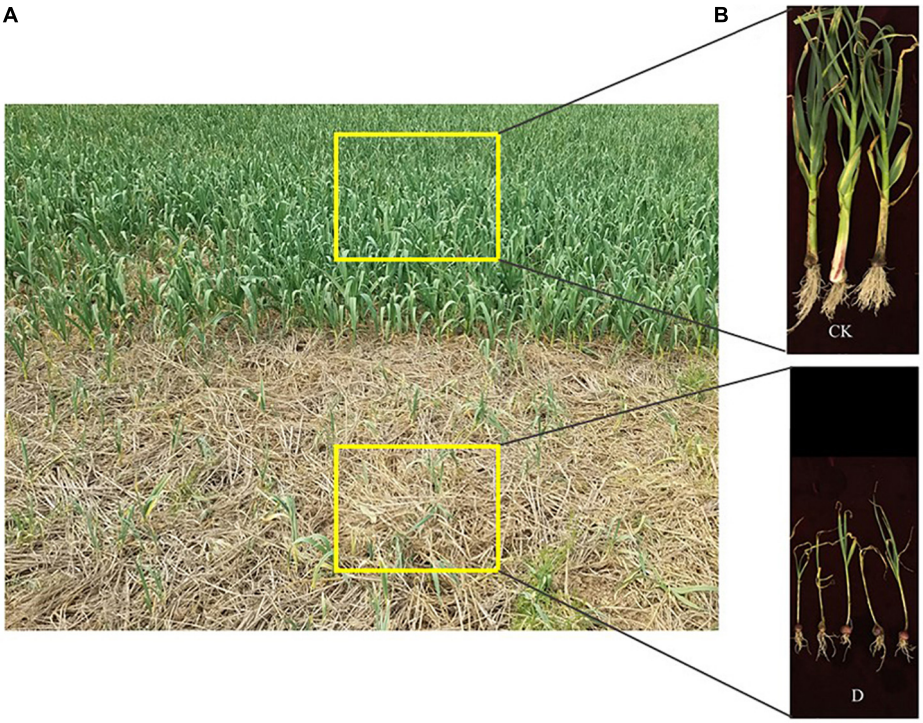

FIGURE 1 | (A) A garlic field with cropping obstacle (foreground) and healthy garlic plants (background). **(B)** Garlic plants grown in the healthy control soil (CK) and in the cropping obstacle soil (D).

biomasses. Root activity was determined using 2,3,5-triphenyl tetrazolium chloride (TTC) staining (Comas et al., 2008).

Soil Physicochemical and Enzyme Activity Analyses

Prior the analyses, the soil samples were air-dried naturally in a cool and ventilated place. Soil pH was measured with a pH meter in a 1:2.5 soil to water slurry. Soil organic carbon content (SOC) was determined using the $K_2Cr_2O_7$ oxidization method. Soil total (TN) and available nitrogen (AN), available phosphorus (AP) and available potassium (AK) contents were determined using Kjeldahl digestion, alkaline hydrolysis diffusion method and molybdenum blue method and flame photometry, respectively.

Soil enzyme activity analyses were performed as described earlier (Guan et al., 1986). Briefly, urease was assayed by colorimetric analysis of sodium phenate-sodium hypochlorite, acid phosphatase was colorimetrically estimated using disodium phenyl phosphate, invertase was colorimetrically determined by DNS based on the decreasing sugar content, phenol oxidase was determined by the pyrogallol colorimetric method, and catalase activity was assayed by potassium permanganate titration.

DNA Extraction, Amplification, and Sequencing

Total genomic DNA was extracted from 0.60 to 0.90 g fresh weight soils (corresponding to 0.50 g dry weight) using Fast DNA® SPIN for Soil Kit (MP BIO Laboratories, California, United States) according to the manufacturer's instructions. The quantity and quality of extracted DNA were estimated using a NanoDrop NC2000 spectrophotometer (Thermo Fisher Scientific, Waltham, MA, United States) and agarose gel electrophoresis, respectively. DNA samples were stored at −20°C.

The V3–V4 region of bacterial 16S rRNA gene was amplified using the primers 338F (5′-ACTCCTACGGGAGGCAGCA-3′) and 806R (5′-GGACTACHVGGGTWTCTAAT-3′). The fungal ITS1 region was amplified using the primers ITS5F (5′-GGAAGTAAAAGTCGTAACAAGG-3′) and ITS1R (5′-GCTGCGTTCTTCATCGATGC-3′) using the Q5 High-Fidelity DNA Polymerase (New England Biolabs, Ipswich, MA). Sample-specific 7-bp barcodes were incorporated into the primers for multiplex sequencing. The reaction mixture of total volume 25 μl comprised the following: 5 μl of 5 × reaction buffer, 5 μl of 5 × GC buffer, 2 μl of 2.5 μM dNTPs, 1 μl of forward primer (10 μM), 1 μl of reverse primer (10 μM), 2 μl of DNA Template, 0.25 μl of Q5 DNA polymerase, and 8.75 μl of ddH_2O. The polymerase chain reaction (PCR) was performed under the following cycling conditions: initial denaturation at 98°C (2 min), denaturation at 98°C (15 s), annealing at 55°C (30 s), extension at 72°C (30 s), and a final extension of 72°C for 5 min, for 25–30 cycles. PCR amplicons were purified with Vazyme VAHTSTM DNA Clean Beads (Vazyme, Nanjing, China) and quantified using the Quant-iT PicoGreen dsDNA Assay Kit (Invitrogen, Carlsbad, CA, United States). Amplicons were pooled in equal amounts, and paired-end 2 × 250 bp sequencing

was performed using the Illumina MiSeq platform with MiSeq Reagent Kit v3 at Shanghai Personal Biotechnology Co., Ltd. (Shanghai, China).

Sequence Analysis

Sequences were processed with QIIME 2 (Bolyen et al., 2019) according to the official tutorial[1] with slight modifications. Briefly, raw sequence data were demultiplexed using the demux plugin followed by removing the primers with cut adapt plugin (Martin, 2011). Quality filtering, denoising, merging and chimera removal were performed using the DADA2 plugin (Callahan et al., 2016). Non-singleton amplicon sequence variants (ASVs) were aligned with mafft (Katoh et al., 2002) and used to construct a phylogeny with fasttree2 (Price et al., 2009). Taxonomy was assigned to ASVs using the classify-sklearn naïve Bayes taxonomy classifier in feature-classifier plugin (Bokulich et al., 2013) against the SILVA Release 132 and UNITE Release 8.0 databases (Koljalg et al., 2013). Taxonomic compositions were visualized using MEGAN and GraPhlAn (Asnicar et al., 2015). Chao1 and Shannon alpha diversity indices were calculated using the ASV table in QIIME2.

Statistical Analyses

Statistical analyses were performed using QIIME2, SPSS 21 (Version 21.0, SPSS Inc., Chicago, IL, United States) and R v.3.6.1.[2] Differences in plant and soil properties were tested using Student's *t*-test. The associations between garlic growth parameters and soil properties were analyzed using Pearson correlation. Differences in alpha diversity indices between treatments were tested using Kruskal-Wallis test and visualized as box plots. Beta diversity was analyzed based on Bray-Curtis dissimilarity and visualized using non-metric multidimensional scaling (NMDS) (Ramette, 2007). The differences in community compositions were tested using permutational multivariate analysis of variance (PERMANOVA) (McArdle and Anderson, 2001). Differential abundance of taxa was tested using linear discriminant analysis effect size (LEfSe) analysis (Segata et al., 2011). The relationships between environmental factors and microbial community structure were analyzed using distance-based redundancy analysis (dbRDA) in the "vegan" package in R v2.5.6 (Oksanen et al., 2020).

[1]https://docs.qiime2.org/2019.4/tutorials/

[2]http://www.r-project.org

The weighted β nearest taxon index (βNTI) and Bray-Curtis-based Raup-Crick (RC_{bray}) values were calculated via a null model methodology to differentiate the ecological processes that regulate microbial community assembly (Stegen et al., 2013, 2015). The βNTI was quantified by determination of the standard deviation between an observed level and the null distribution of the mean nearest taxon distance metric (βMNTD). The βMNTD and RC_{bray} were calculated using the R packages "picante" and "vegan," respectively (Kembel et al., 2010). Specifically, β-NTI > 2 indicated variable selection, and β-NTI < -2 indicated homogeneous selection; at $|\beta\text{-NTI}| < 2$, deterministic processes were associated with dispersal limitation when $RC_{bray} > 0.95$, homogeneous dispersal when $RC_{bray} < -0.95$, and undominated when $|RC_{bray}| < 0.95$ (Stegen et al., 2015; Jiao et al., 2020; Luan et al., 2020).

RESULTS

The Properties of Garlic Plants and Soils

The biomasses, root and shoot lengths and root activities of cropping obstacle plants were lower than those of healthy plants, in which root activities decreased by 61.16% ($P < 0.05$) (**Table 1**). The pH was lower and AK content higher in the cropping obstacle soil than in the control ($P < 0.05$) (**Table 2**). Thus, the soil pH correlated positively and AK content negatively with the garlic growth parameters ($P < 0.01$) (**Supplementary Table 1**).

TABLE 1 | The properties of garlic plants grown in cropping obstacle soil (D) and healthy control soil (CK).

Item tested	D	CK
Shoot length (cm·plant^{-1})	26.34 ± 4.21	71.69 ± 5.14*
Maximum root length (cm·plant^{-1})	4.85 ± 1.03	13.87 ± 1.91*
Aboveground biomass (g·plant^{-1}·FW)	4.65 ± 0.86	40.73 ± 11.04*
Root biomass (g·plant^{-1}·FW)	0.34 ± 0.12	4.11 ± 1.56*
Root activity (μg·g^{-1} ·h^{-1}·FW)	23.54 ± 5.84	60.61 ± 9.83*

*Values are means ± standard deviation. *In a row indicate statistically significant difference at P < 0.05 (Student's t-test).*

TABLE 2 | The properties of cropping obstacle soil (D) and healthy control soil (CK).

	D	CK
pH	5.09 ± 0.19	6.02 ± 0.46*
WC (%)	28.31 ± 1.99	27.02 ± 4.38
AP (mg/kg)	58.81 ± 5.87	55.58 ± 11.13
AK (mg/kg)	250.09 ± 26.49*	194.14 ± 28.35
AN (mg/kg)	65.40 ± 6.26	65.25 ± 8.24
TN (g/kg)	1.86 ± 0.16	1.86 ± 0.25
SOC (g/kg)	34.97 ± 6.61	38.38 ± 9.09

*Values are means ± standard deviation. *In a row indicate statistically significant difference at P < 0.05 (Student's t-test).*
WC, soil water content; AP, available phosphorus content; AK, available potassium content; AN, available nitrogen content; TN, total nitrogen content; SOC, soil organic carbon content.

TABLE 3 | Soil enzyme activities in cropping obstacle soil (D) and healthy control soil (CK).

Enzyme	D	CK
Catalase ($KMnO_4$ ml/g·20 min)	0.54 ± 0.09	0.92 ± 0.23*
Urease (NH_3-N mg/g·24 h)	0.21 ± 0.02	0.31 ± 0.06*
Polyphenol oxidase (Purple gallate mg/g·2 h)	0.88 ± 0.18	1.99 ± 0.49*
Acid phosphatase (Phenol mg/g·24 h)	1.98 ± 0.38*	1.64 ± 0.21
Invertase (Glucose mg/g·24 h)	2.52 ± 0.69	3.57 ± 0.52*

*Values are means ± standard deviation (n = 21). *In a row indicate statistically significant difference at P < 0.05 (Student's t-test).*

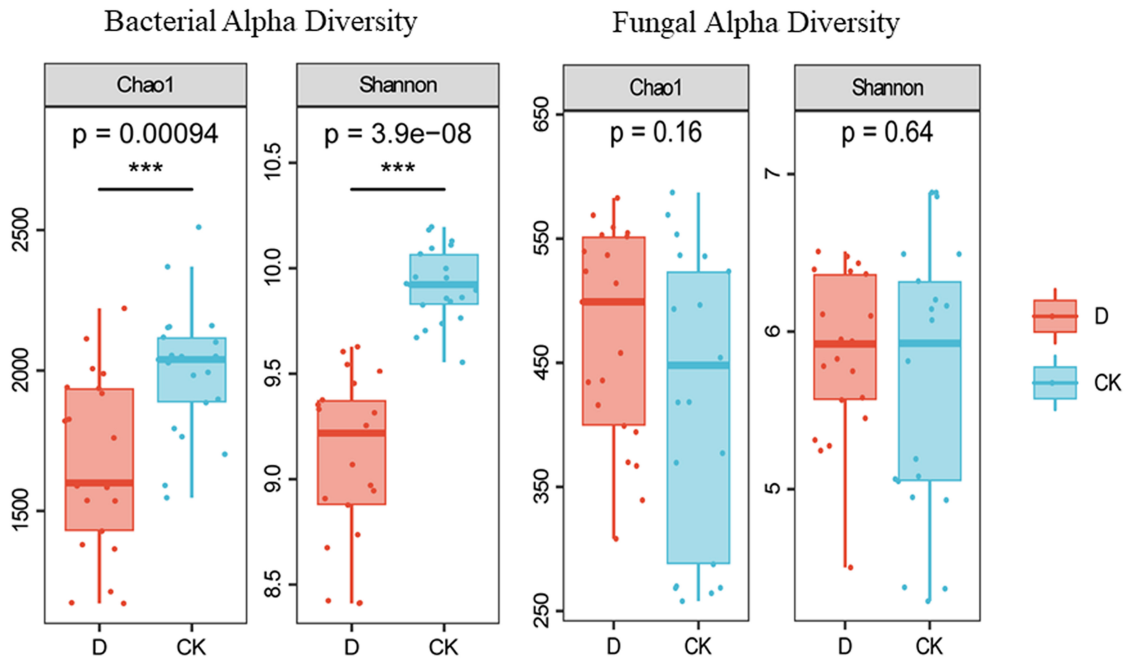

FIGURE 2 | Alpha-diversity of bacterial and fungal communities in the garlic cropping obstacle soil (D) and healthy control soil (CK). *** Indicates statistically significant difference at $P < 0.001$.

The activities of soil catalase, urease, polyphenol oxidase and invertase were lower and the activity of acid phosphatase was higher in the cropping obstacle soil than in the control ($P < 0.05$) (**Table 3**).

Changes in Bacterial and Fungal Communities

The 974,584 16S rRNA gene and 1930,751 ITS sequences were grouped into 67,658 bacterial ASVs and 18,166 fungal ASVs. The richness and diversity indices of the bacteria were lower in the cropping obstacle soil than in the control ($P < 0.05$) (**Figure 2**).

At the phylum level, the bacterial sequences were classified into 36 phyla, out of which the relative abundances of *Proteobacteria*, *Chloroflexi, Acidobacteria,* and *Actinobacteria* were high (**Figure 3A** and **Supplementary Table 2**). Out of the 13 fungal phyla, the relative abundances of *Ascomycota* and *Basidiomycota* were high (**Figure 3B** and **Supplementary Table 3**). The bacterial sequences were classified into 893 genera and the fungal sequences into 453 genera (**Figures 3C,D** and **Supplementary Tables 4, 5**).

Linear discriminant analysis (LDA) effect size (LEfSe) analysis was used to identify differentially abundant taxa. For the bacteria, the taxa with higher relative abundances in the cropping obstacle soil included phylum Chloroflexi, order *Xanthomonadales* and genera *JG30-KF-AS9*, *Chujaibacter* and *Rhodanobacter*; the taxa with lower relative abundances in the cropping obstacle soil included phyla Acidobacteria and Rokubacteria (**Figure 4A**). For the fungi, the taxa with higher relative abundances in the cropping obstacle soil included genera *Stemphylium* and *Aspergillus*; the taxa with lower relative abundances in the cropping obstacle soil included phylum Basidiomycota and genera *Phialophora* and *Oidiodendron* (**Figure 4B**).

The Relationship Between the Microbial Community and Environmental Factors

In the non-metric multidimensional scaling (NMDS) based on the Bray-Curtis dissimilarity, the bacterial and fungal communities in the cropping obstacle soil were separated from those in the control soil (**Figure 5**). In addition, PERMANOVA indicated that the community compositions were different ($P < 0.05$) (**Supplementary Table 6**).

Based on the distance-based redundancy analysis (dbRDA) analysis, the differences in bacterial community composition across samples were related to soil water content, pH, AP, AK, SOC, TN, polyphenol oxidase and acid phosphatase contents ($P < 0.001$) (**Figure 6A** and **Supplementary Table 7**). The differences in community composition between the garlic cropping obstacle soil and the control soil were associated with pH, AK, acid phosphatase, polyphenol oxidase and invertase (**Figure 6A** and **Supplementary Table 7**). The differences in fungal community composition across samples were associated with all the measured soil properties, but no clear treatment related associations were detected (**Figure 6B** and **Supplementary Table 7**).

Assembly Processes of Soil Microbial Communities

In the bacterial communities, $|\beta\text{-NTI}| > 2$ accounted for 32.4% in the cropping obstacle soil and 61.9% in the control (**Figure 7A**),

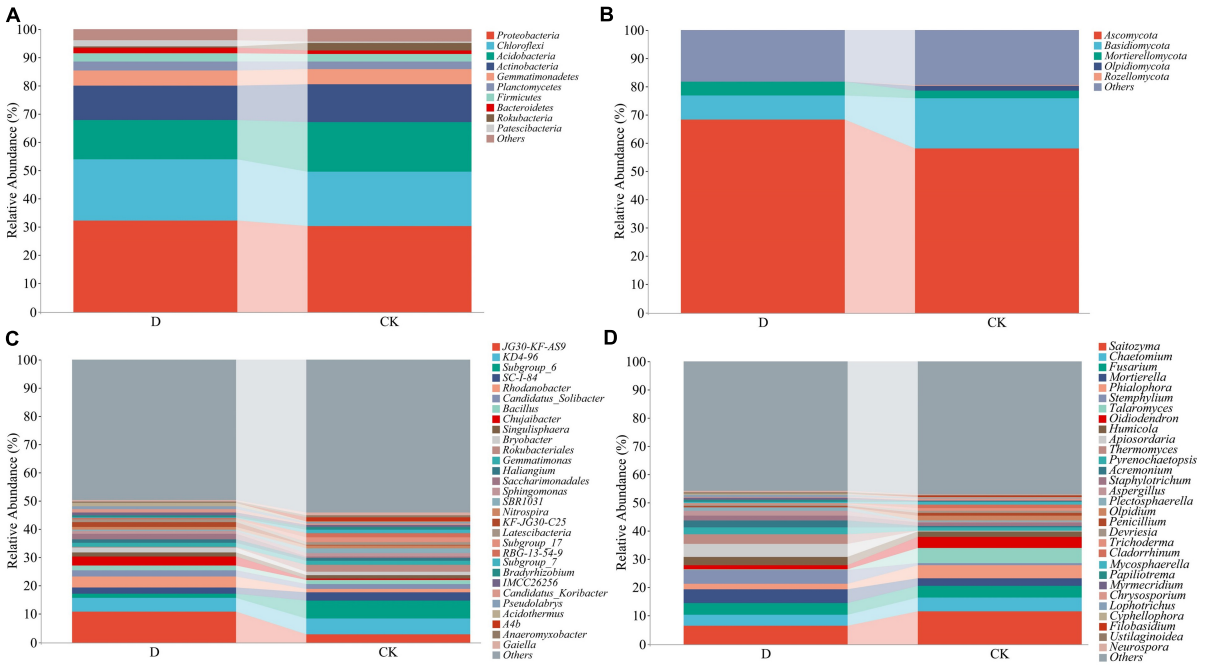

FIGURE 3 | The relative abundances of bacterial and fungal phyla and genera in the garlic cropping obstacle soil (D) and healthy control soil (CK). **(A)** Bacterial phyla, **(B)** fungal phyla, **(C)** bacterial genera, **(D)** fungal genera.

suggesting that the contribution of deterministic processes to community assembly were lower in the cropping obstacle soil. In the cropping obstacle soil, homogeneous dispersal accounted for 65.6% of the community assembly (**Figure 7B**). In the control soil, homogeneous selection accounted for 40.0% of the community assembly and variable selection accounted for 21.9%. In the fungal communities, $|\beta\text{-NTI}| > 2$ accounted for 53.8% in the cropping obstacle soil and 58.6% in the control, suggesting that the assembly processes were primarily deterministic with homogeneous selection as the dominant assembly process (**Figure 7B**).

DISCUSSION

Continuous-cropping obstacle soils have received considerable attention in recent years. For example, the biotic and abiotic factors in cropping obstacle of peanut, strawberry and American ginseng have been determined (Li et al., 2014, 2018; Liu et al., 2021). To our knowledge, whether the conclusions based on other crops can be extrapolated to garlic cropping obstacle problem is still not known. We sampled soil and plants in fields with poorly growing garlic plants and noticed that in addition to the evidently lower aboveground biomass, the root biomass and root activity were also lower in the cropping obstacle soil than in the control soil with healthy garlic plants.

Soil properties can directly affect plant health (Wang et al., 2017). In agreement with previous studies (Li et al., 2018; Liu et al., 2021), compared to the control, the garlic cropping obstacle soil was characterized by lower pH and higher available potassium content. Acid stress in pH below 5.5 triggered sensitivity responses in roots, e.g., arrested root growth and death of root tip cells, and acidic soil limited plant growth and the uptake of nutrients from soil (Agegnehu et al., 2016; Gracas et al., 2021). The application of synthetic fertilizers with high level in rice-vegetable rotation has led to a soil acidification (Li et al., 2020; Shen et al., 2021) that may be an important cause for the garlic cropping obstacle. Although differences in the abiotic and biotic characteristic may exist even within close soil environments that share the same geographies (Fierer, 2017), what causes the patchiness of acidification requires further research.

Soil enzyme activities are employed as one of the important indicators of soil quality and fertility (Bastida et al., 2008). In long-period strawberry cropping, the soil enzyme activities decreased and the probability of diseases increased (Li et al., 2018). Similarly, compared to the control, the activities of soil urease, catalase, sucrase and polyphenol oxidase, i.e., enzymes that release soil nutrients for plants, were lower in the garlic cropping obstacle soil. Since soil enzyme activities and pH correlated strongly (Acosta-Martinez and Tabatabai, 2000), the acidification of the garlic cropping obstacle soil could have affected soil enzyme activity. As the soil enzymes mainly originate from soil microorganisms, changes in microbial metabolic activity, lower microbial abundance or changes in the microbial community composition (Zhao et al., 2009; Nannipieri et al., 2012) may have led to the lower enzyme activities.

Continuous cropping obstacles have been associated with lower microbial diversity, a decrease in beneficial microorganisms, and the enrichment of pathogenic

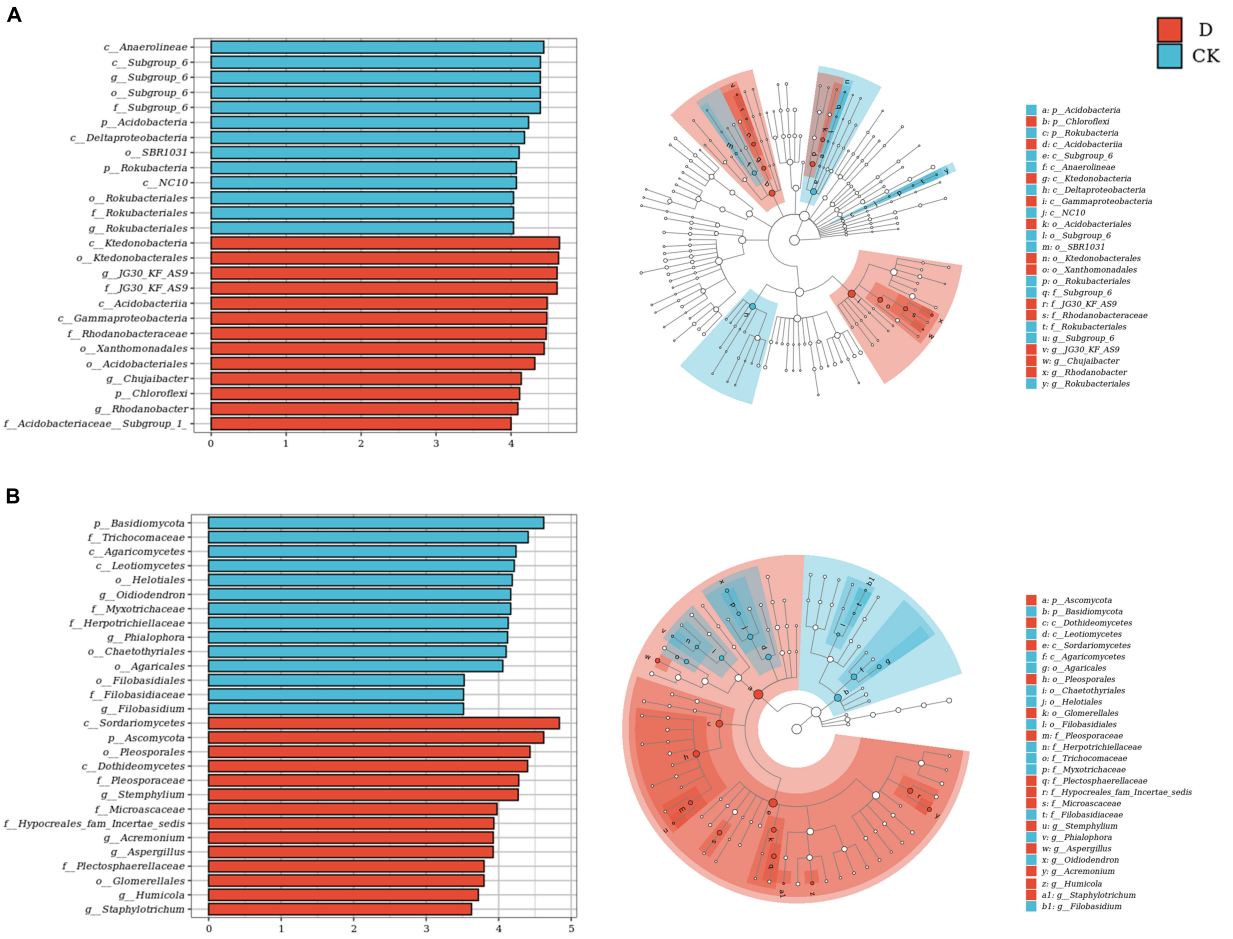

FIGURE 4 | Differential abundances of **(A)** bacterial and **(B)** fungal taxa in the garlic cropping obstacle soil (D) and healthy control soil (CK). The histogram shows taxa with LDA scores ≥ 4.0 for bacterial, and LDA scores ≥ 3.5 for fungal in the linear discriminant (LDA) effect size analysis. The cladogram shows taxonomic differences between D and CK.

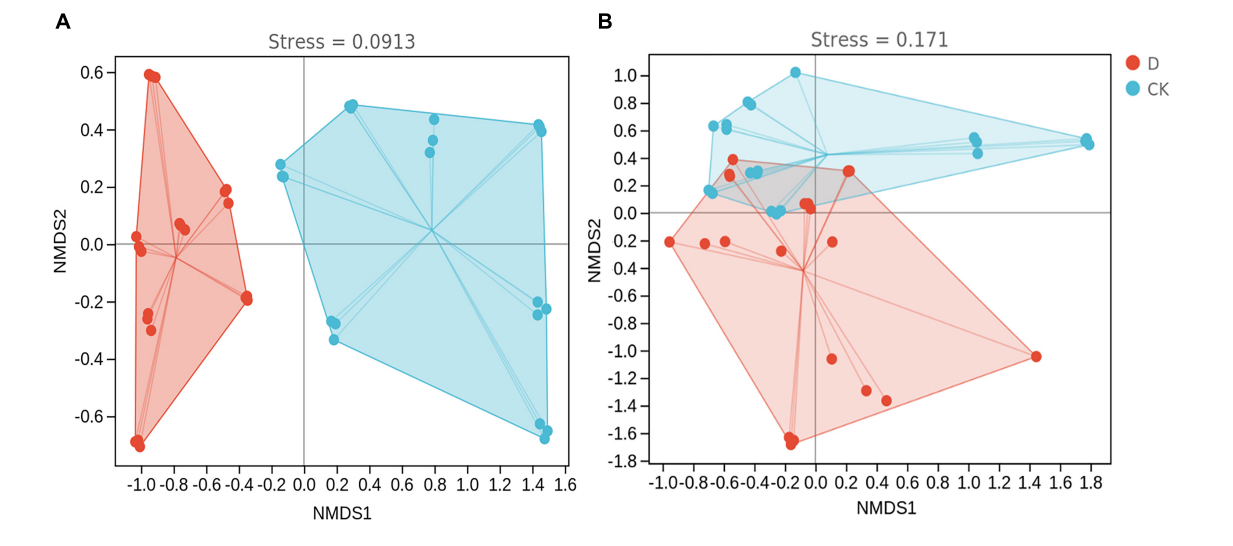

FIGURE 5 | Non-metric multidimensional scaling of **(A)** bacterial and **(B)** fungal communities in the garlic cropping obstacle soil (D) and healthy control soil (CK).

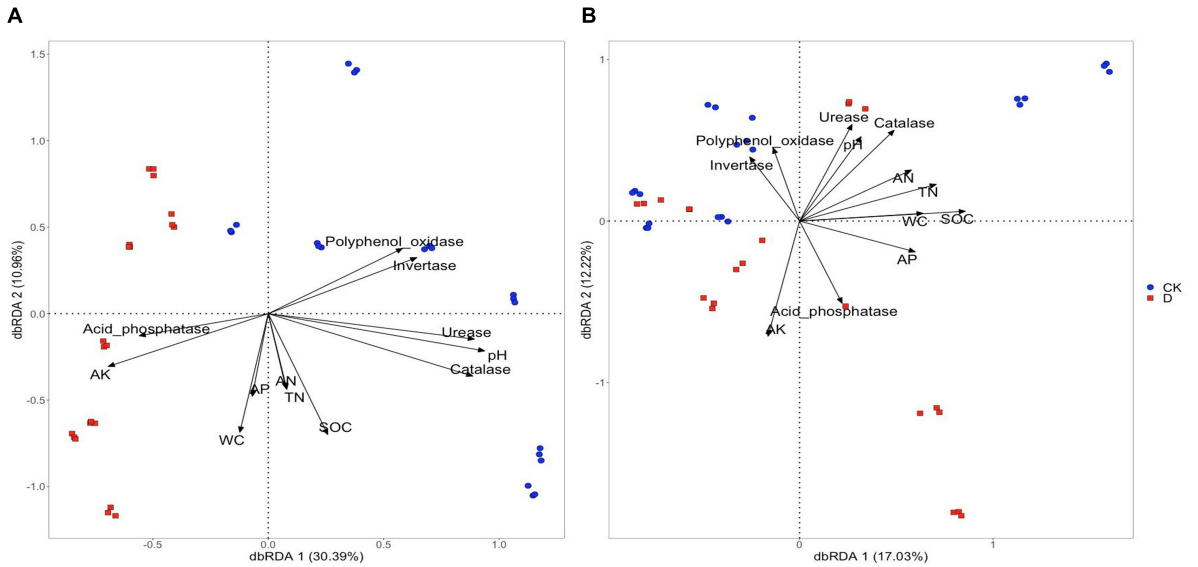

FIGURE 6 | Distance-based redundancy analysis (dbRDA) of environmental factors with **(A)** bacterial and **(B)** fungal taxa in the garlic cropping obstacle soil (D) and healthy control soil (CK).

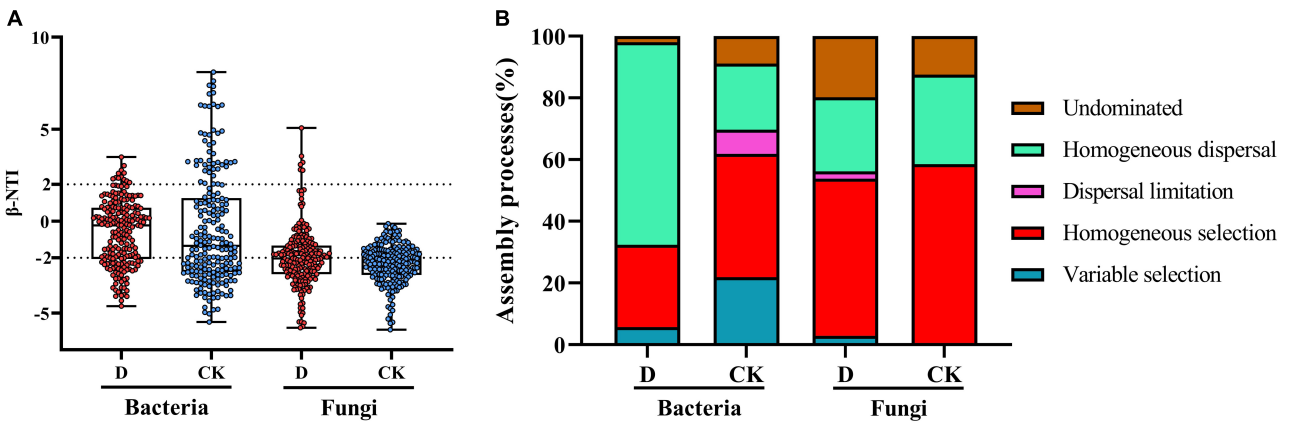

FIGURE 7 | The microbial community assembly processes in the cropping obstacle soil (D) and in the healthy control soil (CK). **(A)** The values of the weighted beta nearest taxon index (βNTI). Horizontal dashed gray lines indicate upper and lower significance thresholds at βNTI = −2 and + 2, respectively. **(B)** The percentages of deterministic processes (homogeneous and variable selection), stochastic processes (dispersal limitation and homogeneous dispersal), and undominated processes.

microorganisms (Gao et al., 2019, 2021; Tan et al., 2021). According to the insurance hypothesis, biodiversity may act as a buffer against disturbances; in a diverse community, some species are likely to withstand disturbance and carry on functions (Yachi and Loreau, 1999). Alarmingly, in our study, both the richness and the diversity of the bacterial communities were lower in the cropping obstacle soil than in the control. Similar with (Shen et al., 2013), the lower bacterial alpha diversity in cropping obstacle soil may have been due to the lower pH.

Beta diversity analyses showed that the compositions of both the bacterial and fungal communities in the cropping obstacle soil were different from those in the control. Environmental factors affect the microbial communities in soil, with soil pH considered as the master variable in affecting bacterial communities (Fierer and Jackson, 2006). In our study, the differences in the bacterial communities between the cropping obstacle soil and the control were associated with differences in soil pH and AK content. Similarly, pH and AK content were among the main factors associated with bacterial community differences in continuously cropped potato fields (Zhao et al., 2020). Even though pH and nutrient contents affect fungal communities as well (Glassman et al., 2017; Li et al., 2022a), we found no clear associations between fungal community composition and soil properties.

Through studies on the community composition of bacteria and fungi, the differentially distributed taxa were identified by LEfSe analysis. The phylum Chloroflexi and the order Xanthomonadales were enriched in the cropping obstacle

soil. Xanthomonadales include plant pathogens of significant economic and agricultural impact (Bayer-Santos et al., 2019). The higher relative abundance of Chloroflexi was mostly due to the uncultured genus JG30-KF-AS9 that can adapt to acidic soil and be detrimental to enzyme activities (Wang et al., 2019). Thus, the enrichment of JG30-KF-AS9 may be connected with the lower enzyme activities in the garlic cropping obstacle soil. *Chujaibacter* and *Rhodanobacter* which were actively developing in the presence of mineral fertilizers were acidophilic microorganisms participating in the nitrogen cycle (Semenov et al., 2020), it is speculated that the increase of these microorganisms may be related to soil acidification. Likewise, the fungal genera *Stemphylium* and *Aspergillus* that were enriched in the cropping obstacle soil include plant pathogens (Syed et al., 2020; Dumin et al., 2021). For example, *Stemphylium* spp. caused garlic leaf spot disease (Dumin et al., 2021). Genus *Oidiodendron*, one of the most widely investigated ericoid mycorrhizal fungi that had plant growth promoting characteristics (Wei et al., 2016; Baba et al., 2021), was depleted in the cropping obstacle soil. Thus, the enrichment of Xanthomonadales, *Stemphylium* and *Aspergillus* and depletion of *Oidiodendron* may have contributed to the poor growth of garlic in the cropping obstacle soil.

Uncovering the microbial community assembly processes is a challenging task (Stegen et al., 2013; Luan et al., 2020). Our results showed that the bacteria assembly processes in garlic cropping obstacle soil was governed by homogeneous dispersal, a stochastic process that homogenizes the bacterial community structure and causes low compositional turnover (Stegen et al., 2013). In the control, the community assembly was characterized by deterministic processes. Root exudates increase available resources that may facilitate the recruitment and selection of bacterial taxa (Li et al., 2022b), which may explain why deterministic processes governed assembly processes in the control soil with vigorously growing garlic plants.

Homogeneous selection was regarded as a factor leading to a stable state after disturbance in progressive succession of communities (Dini-Andreote et al., 2015). Together with the diversity and environmental factor association results, the dominance of homogeneous selection in both the cropping obstacle and control soils suggested that the fungal communities were more resilient than the bacterial communities.

SUMMARY

Cropping obstacle soil was characterized by acidification and lower enzyme activities except for the activity of acid phosphatase. The lower bacterial richness and diversity, and the enrichment of plant pathogens may have contributed to the garlic cropping obstacle. The lower enzyme activity and microbial community differences were associated with lower pH in the cropping obstacle soil. The correlations among plant growth, soil properties and microbial communities cannot reveal cause and effect, thus discovering the exact mechanisms behind the cropping obstacle phenomenon require further controlled experiments.

DATA AVAILABILITY STATEMENT

The data presented in the study are deposited in the National Center for Biotechnology Information (NCBI) with the accession number SRP348212.

AUTHOR CONTRIBUTIONS

JY, QC, and ZS conceived and designed this experiment. JY, ZW, YL, and DC collected samples and carried out experiments. YG, KZ, XY, HL, and PP performed the bioinformatics and statistical analysis. JY, XZ, QC, and PP wrote and revised the manuscript. All authors read and approved the final manuscript.

FUNDING

This work was supported by the Key Research Project of Sichuan Province (No. 2019YFN0149) and the Professional Development Support Program of Sichuan Agricultural University.

ACKNOWLEDGMENTS

We sincerely thank Chaoren Wang, Xiaoyu Zhou, and Die Liu for participating in the experiment. We appreciate technical support for data analysis provided by Shanghai Personalbio Technology Co., Ltd. and Xiangyang Shu.

SUPPLEMENTARY MATERIAL

The Supplementary Material for this article can be found online at: https://www.frontiersin.org/articles/10.3389/fmicb.2022.828196/full#supplementary-material

REFERENCES

Acosta-Martinez, V., and Tabatabai, M. (2000). Enzyme activities in a limed agricultural soil. *Biol. Fertil. Soils* 31, 85–91. doi: 10.1007/s003740050628

Agegnehu, G., Nelson, P. N., and Bird, M. I. (2016). The effects of biochar, compost and their mixture and nitrogen fertilizer on yield and nitrogen use efficiency of barley grown on a Nitisol in the highlands of Ethiopia. *Sci. Total Environ.* 569, 869–879. doi: 10.1016/j.scitotenv.2016.05.033

Asnicar, F., Weingart, G., Tickle, T. L., Huttenhower, C., and Segata, N. (2015). Compact graphical representation of phylogenetic data and metadata with GraPhlAn. *PeerJ* 3:e1029. doi: 10.7717/peerj.1029

Baba, T., Hirose, D., Noma, S., and Ban, T. (2021). Inoculation with two Oidiodendron maius strains differentially alters the morphological

characteristics of fibrous and pioneer roots of Vaccinium virgatum 'Tifblue' cuttings. *Sci. Hortic.* 281:109948. doi: 10.1016/j.scienta.2021.109948

Bastida, F., Zsolnay, A., Hernandez, T., and Garcia, C. (2008). Past, present and future of soil quality indices: a biological perspective. *Geoderma* 147, 159–171. doi: 10.1016/j.geoderma.2008.08.007

Bayer-Santos, E., Ceseti, L. D., Farah, C. S., and Alvarez-Martinez, C. E. (2019). Distribution, function and regulation of type 6 secretion systems of xanthomonadales. *Front. Microbiol.* 10:1635. doi: 10.3389/fmicb.2019.01635

Beckers, B., De Beeck, M. O., Weyens, N., Boerjan, W., and Vangronsveld, J. (2017). Structural variability and niche differentiation in the rhizosphere and endosphere bacterial microbiome of field-grown poplar trees. *Microbiome* 5:25. doi: 10.1186/s40168-017-0241-2

Blagodatskaya, E., and Kuzyakov, Y. (2013). Active microorganisms in soil: critical review of estimation criteria and approaches. *Soil Biol. Biochem.* 67, 192–211. doi: 10.1016/j.soilbio.2013.08.024

Bokulich, N. A., Subramanian, S., Faith, J. J., Gevers, D., Gordon, J. I., Knight, R., et al. (2013). Quality-filtering vastly improves diversity estimates from Illumina amplicon sequencing. *Nat. Methods* 10, 57–59. doi: 10.1038/nmeth.2276

Bolyen, E., Rideout, J. R., Dillon, M. R., Bokulich, N., Abnet, C. C., Al-Ghalith, G. A., et al. (2019). Reproducible, interactive, scalable and extensible microbiome data science using QIIME 2. *Nat. Biotechnol.* 37, 852–857. doi: 10.1038/s41587-019-0209-9

Callahan, B. J., McMurdie, P. J., Rosen, M. J., Han, A. W., Johnson, A. J. A., and Holmes, S. P. (2016). DADA2: high-resolution sample inference from Illumina amplicon data. *Nat. Methods* 13, 581–583. doi: 10.1038/Nmeth.3869

Comas, L., Eissenstat, D., and Lakso, A. (2008). Assesing root death and root system dynamics in a study of grape canopy pruning. *New Phytol.* 147, 171–178. doi: 10.1046/j.1469-8137.2000.00679.x

Corzo-Martinez, M., Corzo, N., and Villamiel, M. (2007). Biological properties of onions and garlic. *Trends Food Sci. Technol.* 18, 609–625. doi: 10.1016/j.tifs.2007.07.011

Dini-Andreote, F., Stegen, J. C., van Elsas, J. D., and Salles, J. F. (2015). Disentangling mechanisms that mediate the balance between stochastic and deterministic processes in microbial succession. *Proc. Natl. Acad. Sci. U.S.A.* 112, 1326–1332. doi: 10.1073/pnas.1414261112

Dong, L. L., Xu, J., Zhang, L. J., Yang, J., Liao, B. S., Li, X. W., et al. (2017). High-throughput sequencing technology reveals that continuous cropping of American ginseng results in changes in the microbial community in arable soil. *Chin. Med.* 12:18. doi: 10.1186/s13020-017-0139-8

Dumin, W., Park, M. J., Han, Y. K., Bae, Y. S., Park, J. H., and Back, C. G. (2021). First report of leaf spot disease caused by *Stemphylium eturmiunum* on garlic in Korea. *Plant Dis.* 106:318. doi: 10.1094/PDIS-03-21-0674-PDN

FAO, (2019). *Food and Agriculture Organization of the United Nations, FAOSTAT Statistics Database*. Available online at: https://www.fao.org/faostat/en/#data

Fierer, N. (2017). Embracing the unknown: disentangling the complexities of the soil microbiome. *Nat. Rev. Microbiol.* 15, 579–590.

Fierer, N., and Jackson, R. B. (2006). The diversity and biogeography of soil bacterial communities. *Proc. Natl. Acad. Sci. U.S.A.* 103, 626–631.

Fu, H. D., Zhang, G. X., Zhang, F., Sun, Z. P., Geng, G. M., and Li, T. L. (2017). Effects of continuous tomato monoculture on soil microbial properties and enzyme activities in a solar greenhouse. *Sustainability* 9:317. doi: 10.3390/su9020317

Gao, Z. Y., Han, M. K., Hu, Y. Y., Li, Z. Q., Liu, C. F., Wang, X., et al. (2019). Effects of continuous cropping of sweet potato on the fungal community structure in rhizospheric soil. *Front. Microbiol.* 10:2269. doi: 10.3389/fmicb.2019.02269

Gao, Z. Y., Hu, Y. Y., Han, M. K., Xu, J. J., Wang, X., Liu, L. F., et al. (2021). Effects of continuous cropping of sweet potatoes on the bacterial community structure in rhizospheric soil. *BMC Microbiol.* 21:2. doi: 10.1186/s12866-021-02194-2

Glassman, S. I., Wang, I. J., and Bruns, T. D. (2017). Environmental filtering by pH and soil nutrients drives community assembly in fungi at fine spatial scales. *Mol. Ecol.* 26, 6960–6973. doi: 10.1111/mec.14414

Gracas, J. P., Belloti, M., Lima, J. E., Peres, L. E. P., Burlat, V., Jamet, E., et al. (2021). Low pH-induced cell wall disturbances in Arabidopsis thaliana roots lead to a pattern-specific programmed cell death in the different root zones and arrested elongation in late elongation zone. *Environ. Exp. Bot.* 190:104596. doi: 10.1016/j.envexpbot.2021.104596

Guan, S. Y., Zhang, D., and Zhang, Z. (1986). *Soil Enzyme and its Research Methods*. Beijing: Agriculture Press, 274–297.

Jiao, S., Yang, Y. F., Xu, Y. Q., Zhang, J., and Lu, Y. H. (2020). Balance between community assembly processes mediates species coexistence in agricultural soil microbiomes across eastern China. *ISME J.* 14, 202–216. doi: 10.1038/s41396-019-0522-9

Katoh, K., Misawa, K., Kuma, K., and Miyata, T. (2002). MAFFT: a novel method for rapid multiple sequence alignment based on fast Fourier transform. *Nucleic Acids Res.* 30, 3059–3066. doi: 10.1093/nar/gkf436

Kaur, J., and Singh, J. P. (2014). Long-term effects of continuous cropping and different nutrient management practices on the distribution of organic nitrogen in soil under rice-wheat system. *Plant Soil Environ.* 60, 63–68. doi: 10.17221/440/2013-Pse

Kembel, S. W., Cowan, P. D., Helmus, M. R., Cornwell, W. K., Morlon, H., Ackerly, D. D., et al. (2010). Picante: R tools for integrating phylogenies and ecology. *Bioinformatics* 26, 1463–1464. doi: 10.1093/bioinformatics/btq166

Koljalg, U., Nilsson, R. H., Abarenkov, K., Tedersoo, L., Taylor, A. F., Bahram, M., et al. (2013). Towards a unified paradigm for sequence-based identification of fungi. *Mol. Ecol.* 22, 5271–5277. doi: 10.1111/mec.12481

Li, Q., Zhang, D., Song, Z., Ren, L., Jin, X., Fang, W., et al. (2022a). Organic fertilizer activates soil beneficial microorganisms to promote strawberry growth and soil health after fumigation. *Environ. Pollut.* 295:118653. doi: 10.1016/j.envpol.2021.118653

Li, T., Li, Y., Wang, S., Wang, Z., Liu, Y., Wen, X., et al. (2022b). Assessing synergistic effects of crop rotation pattern, tillage practice, and rhizosphere effect on soil bacterial community structure and assembly in China's Loess Plateau farmlands. *Appl. Soil Ecol.* 174:104411. doi: 10.1016/j.apsoil.2022.104411

Li, Q. Q., Li, A. W., Yu, X. L., Dai, T. F., Peng, Y. Y., Yuan, D., et al. (2020). Soil acidification of the soil profile across Chengdu Plain of China from the 1980s to 2010s. *Sci. Total Environ.* 698:134320. doi: 10.1016/j.scitotenv.2019.134320

Li, W. H., Liu, Q. Z., and Chen, P. (2018). Effect of long-term continuous cropping of strawberry on soil bacterial community structure and diversity. *J. Integr. Agric.* 17, 2570–2582. doi: 10.1016/S2095-3119(18)61944-6

Li, X. G., Ding, C. F., Zhang, T. L., and Wang, X. X. (2014). Fungal pathogen accumulation at the expense of plant-beneficial fungi as a consequence of consecutive peanut monoculturing. *Soil Biol. Biochem.* 72, 11–18. doi: 10.1016/j.soilbio.2014.01.019

Li, Z. G., Zu, C., Wang, C., Yang, J. F., Yu, H., and Wu, H. S. (2016). Different responses of rhizosphere and non-rhizosphere soil microbial communities to consecutive *Piper nigrum* L. monoculture. *Sci. Rep.* 6:35825. doi: 10.1038/srep35825

Liu, P. X., Weng, R., Sheng, X. J., Wang, X. L., Zhang, W. H., Qian, Y. Z., et al. (2020). Profiling of organosulfur compounds and amino acids in garlic from different regions of China. *Food Chem.* 305:125499. doi: 10.1016/j.foodchem.2019.125499

Liu, S., Wang, Z. Y., Niu, J. F., Dang, K. K., Zhang, S. K., Wang, S. Q., et al. (2021). Changes in physicochemical properties, enzymatic activities, and the microbial community of soil significantly influence the continuous cropping of *Panax quinquefolius* L. (American ginseng). *Plant Soil* 463, 427–446. doi: 10.1007/s11104-021-04911-2

Liu, X., Zhang, J. L., Gu, T. Y., Zhang, W. M., Shen, Q. R., Yin, S. X., et al. (2014). Microbial community diversities and taxa abundances in soils along a seven-year gradient of potato monoculture using high throughput pyrosequencing approach. *PLoS One* 9:86610. doi: 10.1371/journal.pone.0086610

Luan, L., Liang, C., Chen, L. J., Wang, H. T., Xu, Q. S., Jiang, Y. J., et al. (2020). Coupling bacterial community assembly to microbial metabolism across soil profiles. *Msystems* 5:e00298-20. doi: 10.1128/mSystems.00298-20

Martin, M. (2011). CUTADAPT removes adapter sequences from high-throughput sequencing reads. *EMBnet J.* 17, 10–12. doi: 10.14806/ej.17.1.200

McArdle, B., and Anderson, M. (2001). Fitting multivariate models to community data: a comment on distance-based redundancy analysis. *Ecology* 82, 290–297. doi: 10.2307/2680104

Nannipieri, P., Giagnoni, L., Renella, G., Puglisi, E., Ceccanti, B., Masciandaro, G., et al. (2012). Soil enzymology: classical and molecular approaches. *Biol. Fertil. Soils* 48, 743–762. doi: 10.1007/s00374-012-0723-0

Oksanen, J., Blanchet, F. G., Friendly, M., Kindt, R., Legendre, P., McGlinn, D., et al. (2020). *Vegan Community Ecology Package Version 2.5-7 November 2020*.

Pang, Z., Dong, F., Liu, Q., Lin, W., Hu, C., and Yuan, Z. (2021). Soil metagenomics reveals effects of continuous sugarcane cropping on the structure and functional

pathway of rhizospheric microbial community. *Front. Microbiol.* 12:627569. doi: 10.3389/fmicb.2021.627569

Paz-Ferreiro, J., and Fu, S. L. (2016). Biological indices for soil quality evaluation: perspectives and limitations. *Land Degrad. Dev.* 27, 14–25. doi: 10.1002/ldr.2262

Perez-Brandan, C., Huidobro, J., Grumberg, B., Scandiani, M. M., Luque, A. G., Meriles, J. M., et al. (2014). Soybean fungal soil-borne diseases: a parameter for measuring the effect of agricultural intensification on soil health. *Can. J. Microbiol.* 60, 73–84. doi: 10.1139/cjm-2013-0792

Price, M. N., Dehal, P. S., and Arkin, A. P. (2009). FastTree: computing large minimum evolution trees with profiles instead of a distance matrix. *Mol. Biol. Evol.* 26, 1641–1650. doi: 10.1093/molbev/msp077

Ramette, A. (2007). Multivariate analyses in microbial ecology. *FEMS Microbiol. Ecol.* 62, 142–160. doi: 10.1111/j.1574-6941.2007.00375.x

Segata, N., Izard, J., Waldron, L., Gevers, D., Miropolsky, L., Garrett, W. S., et al. (2011). Metagenomic biomarker discovery and explanation. *Genome Biol.* 12:R60. doi: 10.1186/gb-2011-12-6-r60

Semenov, M. V., Krasnov, G. S., Semenov, V. M., and van Bruggen, A. H. C. (2020). Long-term fertilization rather than plant species shapes rhizosphere and bulk soil prokaryotic communities in agroecosystems. *Appl. Soil Ecol.* 154:103641. doi: 10.1016/j.apsoil.2020.103641

Shen, C. C., Xiong, J. B., Zhang, H. Y., Feng, Y. Z., Lin, X. G., Li, X. Y., et al. (2013). Soil pH drives the spatial distribution of bacterial communities along elevation on Changbai Mountain. *Soil Biol. Biochem.* 57, 204–211. doi: 10.1016/j.soilbio.2012.07.013

Shen, J., Tao, Q., Dong, Q., Luo, Y. L., Luo, J. P., He, Y. T., et al. (2021). Long-term conversion from rice-wheat to rice-vegetable rotations drives variation in soil microbial communities and shifts in nitrogen-cycling through soil profiles. *Geoderma* 404:115299. doi: 10.1016/j.geoderma.2021.115299

Stegen, J. C., Lin, X. J., Fredrickson, J. K., Chen, X. Y., Kennedy, D. W., Murray, C. J., et al. (2013). Quantifying community assembly processes and identifying features that impose them. *ISME J.* 7, 2069–2079. doi: 10.1038/ismej.2013.93

Stegen, J. C., Lin, X. J., Fredrickson, J. K., and Konopka, A. E. (2015). Estimating and mapping ecological processes influencing microbial community assembly. *Front. Microbiol.* 6:370. doi: 10.3389/fmicb.2015.00370

Sun, L., Gao, J. S., Huang, T., Kendall, J. R. A., Shen, Q. R., and Zhang, R. F. (2015). Parental material and cultivation determine soil bacterial community structure and fertility. *FEMS Microbiol. Ecol.* 91, 1–10. doi: 10.1093/femsec/fiu010

Syed, S., Tollamadugu, N. V. K. V. P., and Lian, B. (2020). Aspergillus and Fusarium control in the early stages of *Arachis hypogaea* (groundnut crop) by plant growth-promoting rhizobacteria (PGPR) consortium. *Microbiol. Res.* 240:126562. doi: 10.1016/j.micres.2020.126562

Tan, G., Liu, Y., Peng, S., Yin, H., Meng, D., Tao, J., et al. (2021). Soil potentials to resist continuous cropping obstacle: three field cases. *Environ. Res.* 200:111319. doi: 10.1016/j.envres.2021.111319

van Wyk, D. A. B., Adeleke, R., Rhode, O. H. J., Bezuidenhout, C. C., and Mienie, C. (2017). Ecological guild and enzyme activities of rhizosphere soil microbial communities associated with Bt-maize cultivation under field conditions in North West Province of South Africa. *J. Basic Microbiol.* 57, 781–792. doi: 10.1002/jobm.201700043

Wang, R., Zhang, H. C., Sun, L. G., Qi, G. F., Chen, S., and Zhao, X. Y. (2017). Microbial community composition is related to soil biological and chemical properties and bacterial wilt outbreak. *Sci. Rep.* 7:343. doi: 10.1038/s41598-017-00472-6

Wang, Z. B., Yang, Y., Xia, Y. Z., Wu, T., Zhu, J., Yang, J. M., et al. (2019). Time-course relationship between environmental factors and microbial diversity in tobacco soil. *Sci. Rep.* 9:19969. doi: 10.1038/s41598-019-55859-4

Wei, X., Chen, J., Zhang, C., and Pan, D. (2016). A new oidiodendron maius strain isolated from rhododendron fortunei and its effects on nitrogen uptake and plant growth. *Front. Microbiol.* 7:1327. doi: 10.3389/fmicb.2016.01327

Wei, Z., Yang, T., Friman, V. P., Xu, Y., Shen, Q., and Jousset, A. (2015). Trophic network architecture of root-associated bacterial communities determines pathogen invasion and plant health. *Nat. Commun.* 6:8413. doi: 10.1038/ncomms9413

Xi, H., Shen, J., Qu, Z., Yang, D., Liu, S., Nie, X., et al. (2019). Effects of long-term cotton continuous cropping on soil microbiome. *Sci. Rep.* 9:18297. doi: 10.1038/s41598-019-54771-1

Yachi, S., and Loreau, M. (1999). Biodiversity and ecosystem productivity in a fluctuating environment: the insurance hypothesis. *Proc. Natl. Acad. Sci. U.S.A.* 96, 1463–1468. doi: 10.1073/pnas.96.4.1463

Zeng, L. S., Liao, M., Chen, C. L., and Huang, C. Y. (2007). Effects of lead contamination on soil enzymatic activities, microbial biomass, and rice physiological indices in soil-lead-rice (*Oryza sativa* L.) system. *Ecotoxicol. Environ. Safety* 67, 67–74. doi: 10.1016/j.ecoenv.2006.05.001

Zhao, J., Zhang, D., Yang, Y. Q., Pan, Y., Zhao, D. M., Zhu, J. H., et al. (2020). Dissecting the effect of continuous cropping of potato on soil bacterial communities as revealed by high-throughput sequencing. *PLoS One* 15:e0233356. doi: 10.1371/journal.pone.0233356

Zhao, Y., Wang, P., Li, J., Chen, Y., Ying, X., and Liu, S. (2009). The effects of two organic manures on soil properties and crop yields on a temperate calcareous soil under a wheat–maize cropping system. *Eur. J. Agron.* 31, 36–42. doi: 10.1016/j.eja.2009.03.001

Zheng, Q., Hu, Y. T., Zhang, S. S., Noll, L., Bockle, T., Dietrich, M., et al. (2019). Soil multifunctionality is affected by the soil environment and by microbial Choo community composition and diversity. *Soil Biol. Biochem.* 136:107521. doi: 10.1016/j.soilbio.2019.107521

Zhu, S., Wang, Y., Xu, X., Liu, T., Wu, D., Zheng, X., et al. (2018). Potential use of high-throughput sequencing of soil microbial communities for estimating the adverse effects of continuous cropping on ramie (*Boehmeria nivea* L. Gaud). *PLoS One* 13:e0197095. doi: 10.1371/journal.pone.0197095

Conflict of Interest: HL was employed by the CNPC Chuanqing Drilling Engineering Co., Ltd.

The remaining authors declare that the research was conducted in the absence of any commercial or financial relationships that could be construed as a potential conflict of interest.

Publisher's Note: All claims expressed in this article are solely those of the authors and do not necessarily represent those of their affiliated organizations, or those of the publisher, the editors and the reviewers. Any product that may be evaluated in this article, or claim that may be made by its manufacturer, is not guaranteed or endorsed by the publisher.

frontiers in Microbiology

ORIGINAL RESEARCH
published: 31 March 2022
doi: 10.3389/fmicb.2022.794848

Difference of Bacterial Community Structure in the Meadow, Maize, and Continuous Cropped Alfalfa in Northeast China

Zhao Yang†, Yanxia Xu†, Hong Li, Shasha Li, Xiaolong Wang and Hua Chai*

Branch of Animal Husbandry and Veterinary, Heilongjiang Academy of Agricultural Sciences, Qiqihar, China

Maize and alfalfa (*Medicago sativa* L.) have been used extensively in the animal husbandry to compensate for the lack of livestock and fodder yields in the chilly northeast of China. Little is known, however, about the impact on soil characteristics of consecutive plantings in various crops and alfalfa. In this research, the soil characteristics, bacterial community diversity, and structure of the meadow, maize, and alfalfa continuous cropping fields (i.e., 6, 10, 14, 20, and 30 years) were measured. The results showed that maize cropping and continuous cropping of alfalfa increased the soil bacterial alpha diversity compared with meadow cropping, and alpha diversity of alfalfa increased with the continuous planting years. Soil pH, total phosphorus (TP), available P, total potassium (TK), and nitrate nitrogen (NO_3^-) content were soil variables significantly impacting the structure of soil bacterial communities in different plant types and different alfalfa continuous cropping systems. In addition, the relative abundance of some beneficial microbial species, such as *Arthrobacter* and *Gaiellales*, in the cropping maize and continuous cropping of alfalfa was much higher than that in the meadow field. Moreover, the networks differ among different plant types, and also differ among different continuous cropping years of alfalfa, and topologies of the networks suggested that continuous planting of alfalfa promotes cooperation between bacteria, which facilitates the long growth of alfalfa and is beneficial to the soil.

Keywords: meadow, maize, continuous cropping alfalfa, bacterial structure, network

OPEN ACCESS

Edited by:
Hai-Ming Zhao,
Jinan University, China

Reviewed by:
Tengxiang Lian,
ETH Zürich, Switzerland
Shuai Zhao,
Xinjiang Institute of Ecology and Geography (CAS), China

****Correspondence:***
Hong Li
hljlihong@163.com

†These authors share first authorship

Specialty section:
This article was submitted to Terrestrial Microbiology, a section of the journal Frontiers in Microbiology

Received: *14 October 2021*
Accepted: *15 February 2022*
Published: *31 March 2022*

Citation:
Yang Z, Xu Y, Li H, Li S, Wang X and Chai H (2022) Difference of Bacterial Community Structure in the Meadow, Maize, and Continuous Cropped Alfalfa in Northeast China. Front. Microbiol. 13:794848. doi: 10.3389/fmicb.2022.794848

INTRODUCTION

Alfalfa (*Medicago sativa* L.) is one of the most significant perennial herbaceous legume fodder in the world that is widely grown in many countries and contributes significantly to the development of agriculture and livestock (Han et al., 2005; Raiesi, 2007; Li and Huang, 2008). In China, alfalfa grows mainly in the arid and semi-arid soil of northern China and is grown on more than 4,000 ha per year (Zhang et al., 2016). The Northeastern portion of China is an agro-pastoral area with longer winters (Chen et al., 2013). As a result, animal feed in this region is almost entirely dependent on summer pasture and winter silage, and therefore, alfalfa can alleviate forage shortages for cattle in the winter in the Northeast with its more complete nutrition and high yield (Su, 2007; Chen et al., 2013). Thus, alfalfa has been continuously grown on a large scale in northeastern China to meet the winter demand for forage and thus increase livestock productivity (Dong et al., 2003). However, continuous cultivation of alfalfa has led to an increase in pathogenic bacteria and soil acidification, and these changes have been shown to be closely linked to soil microorganisms (Yan et al., 2012; Yao et al., 2019; Liu et al., 2020).

Previous research has shown that the length of the growth stage of alfalfa is related to grass productivity. In the arid regions of northeast China, alfalfa productivity increases for some years after planting, but decreases if planted for too long (Li and Huang, 2008). The ideal duration of the alfalfa growing stage was indicated to be 9 years (Jiang et al., 2007). Moreover, these studies have shown that changes in soil properties with the increasing years of alfalfa cultivation are significantly associated with alfalfa yield (Ren et al., 2011). Soil productivity and environmental safety could be directly or indirectly influenced by soil characteristics (Doran and Parkin, 1994; Yao et al., 2019; Wang et al., 2019; Shi et al., 2020). Luo et al. (2018) showed that growing alfalfa significantly increased nutrient content in the soil, such as SOM, TN, AP, and AK. Dong et al. (2016) observed that the levels of SOM, TN, and TP were considerably enhanced from native sandy grassland when new alfalfa fields were recovered. However, the effect of planting alfalfa on the soil was influenced by the year of successive plantings, with researchers finding a decreasing trend in soil nutrients within 10 years of successive alfalfa plantings, and the opposite trend after 10 years (Jiang et al., 2007).

Soil bacteria play an important role in maintaining plant health and rapidly respond to alterations in soil characteristics, as they can participate in nutrient cycling and influence the immune system of plants (Song et al., 2021). Microbial community structures vary significantly among different cropping systems (Zhou et al., 2018; Liu et al., 2019; Yao et al., 2019; Yuan et al., 2021) and depend on crop species, soil types, and type of cropping system. For instance, soil basal respiration and microbial biomass had progressively fallen from 3 to 9 years of continuous alfalfa cultivation, while it increased between 15 and 25 years (Jiang et al., 2007). Another study showed that continuous cropping of alfalfa considerably improved the microbial diversity and affected the microbial community assembly *via* the changed soil characteristics (Luo et al., 2018). Moreover, Yao et al. (2019) found that the abundance of *Paecilomyces* and *Phaeomycocentrospora* grew significantly with the continuous growth period of the alfalfa. The decreased abundance of *Pencillium* sp. and the increased abundance of *Fusarium* sp. were also found in the continuous copping of alfalfa (Xu et al., 1995). Nevertheless, it has also been shown that continuous cropping did not change the structure of the soil microbial community compared to crop rotation (Hu and Wang, 1996). The inconsistent results of the above studies may be due to differences in soil types, sampling and sequencing methods, crop rotation systems, and duration of continuous cultivation. Therefore, more in-depth studies in different farming systems and environments are needed to explore the mechanisms of barriers to continue cropping.

In view of the changing soil microorganisms to promote sustainable animal feed industry in northeast China, it is meaningful to study the changes among different cropping systems, i.e., meadow, maize, and alfalfa, and to reveal the alfalfa growing responses to long continuous cropping for 6, 10, 14, 20, and 30 years in their soil microorganisms and soil quality. The study examined soil samples from three agricultural systems and different years of continuously crop-grown alfalfa fields in northeast China, and evaluated the soil bacterial structure and soil characteristics. This study aimed to explore the soil microbial community structure of diverse crop systems and alfalfa with continuous cropping time and to assess the complete connection between soil bacterial communities and physical and chemical characteristics.

MATERIALS AND METHODS

Experimental Site and Design

The experimental location is in Furalji District, Qiqihar City, Heilongjiang Province, China (4715′N, 12341′E). Fields that continuously planted alfalfa for 6, 10, 14, 20, and 30 years were selected and coded as C6, C10, C14, C20, and C30, respectively. Moreover, the soils of the meadows and maize field were selected as the controls, which encoded Me and Ma, respectively. Each treatment is over 900 m^2 in size. The sowing density of alfalfa is 4,000,000 seeds ha^{-1}. The chemical compound fertilizer (N 18%, P_2O_5 18%, and K_2O 18%) of 280 kg/ha was applied to each treatment in June each year. The fields of alfalfa are maintained using standard planting and are not greased. The alfalfa was cut to the surface in June and August each year, except for the first year when it is sown.

Soil Sampling and Soil Characteristic Measurement

On June 30, 2019, during the flowering time of alfalfa, soil samples were collected at 0–15 cm ground depth. A combination of over five individual soil nuclei from a total area of 500 m^2 was obtained from each sample. A total of 42 soil samples of meadow, maize, and 5 alfalfa fields were collected. Filtering of stones and plant roots from the soil sample was carried out using a 2-mm sieve. Approximately 2 *g* of soil samples was placed in sterilized centrifuge tubes and stored at −80°C in a refrigerator for soil DNA extraction; fresh soil was used to measure soil Physicochemical properties.

Using a pH meter, the soil pH was determined in a soil water suspension (1:5 w/v). Fifteen grams of fresh soil was dried in an oven at 105°C for 24 h to a constant weight to determine the soil moisture content. An elemental analyzer was used to measure the soil total nitrogen and carbon contents (Jones and Willett, 2006). Using the continuous flow analysis system, 2.0 M KCl was used to extract ammonium (NH_4^+–N) and nitrate (NO_3^{---}N). Moreover, 0.5 M $NaHCO_3$ and H_2SO_4–$HClO_4$ were used to extract the total and available phosphorus, respectively. Additionally, using an inductively coupled plasma emission spectrometry (ICPS-7500), HNO_3–$HClO_4$–HF and 1.0 M CH_3COONH_4 were used to extract soil total and available potassium, respectively (Lu, 1999).

DNA Extraction and High-Throughput Sequencing

Using the Fast DNA Spin Kit (MP Biomedicals, Santa Ana, CA, United States), soil total DNA was extracted from soil samples. Primers of 515F/806R were used to amplify the bacterial

16S rRNA gene (White et al., 1990), and the forward primer being modified at the 5′ end with a unique 6-nt barcode was added. A 20-ml PCR mix with 0.5 ml of each 10 mM primer, 10 ng of DNA template, and 18 ml of Platinum PCR SuperMix were used to produce PCR. The PCR procedure was 95°C for 5 min; 94°C for 35 s, 55°C for 15 s, 72°C for 10 s for 32 cycles, and 75°C extension for 8 min (Liu et al., 2015). All the samples were standardized to equimolar levels and sequenced on the Majorbio Biotechnology Illumina MiSeq platform. All sequences are deposited in GenBank of NCBI with the archive PRJNA760979.

The raw FASTQ data were processed with QIIME Pipeline version 1.19.1 after sequencing. In brief, each barcode-based sample was allocated to all sequence reads. Preliminary analyses were performed to eliminate sequences of low quality (length < 200 bp and average basis quality score < 30). Use the UCHIME algorithm to find and eliminate chimera of the trimmed sequences (Edgar et al., 2011). The RDP classification was used to allocate sequences phylogenetically based on their optimal match to the RDP databases. Operational taxonomic units (OTUs) with a CD-HIT sequence similarity of 97% were categorized (Cole et al., 2009; Li and Godzik, 2015).

For the alpha diversity, Shannon and Chao 1 indices were calculated in QIIME. Additionally, principal coordinate analysis, Adonis test, and canonical correspondence analysis have been carried out in R version 4.1.1 with the "vegan" package. GenStat 13 was used to perform the one-way analysis of variance (ANOVA) to assess differences in soil chemistry and the abundance of bacteria at different taxonomic levels. Bacterial symbiotic networks were analyzed for the Me, Ma, and AC treatments, and AC6-10, AC14-20, and AC30 groups. The raw data were statistically analyzed using the "psych" package in R and then visualized in Gephi (Jiang et al., 2017). The correlation between each of the two OTUs was chosen to be $p < 0.05$, with Spearman correlation coefficients greater than 0.7 (Mendes et al., 2018). Identification of keystone species was based on high nodality, high intermediate centrality, and high compact centrality (Berry and Widder, 2014; Agler et al., 2016).

RESULTS

Soil Physicochemical Characters

Soil pH, NO_3^-, TK, AK, and C/N were significantly higher in the alfalfa soils, compared with the soil of meadow and maize, while NH_4^+, TP, AP, and TN showed the opposite trend. Moreover, soil NO_3^-, AK, TC, and TN contents increased with the extension time in the soil of continuous crop alfalfa, whereas the contents of NH_4^+, TP, and AP decreased with the extension time in continuous cropping alfalfa soils (**Table 1**).

TABLE 1 | Soil physicochemical properties of meadow, maize, and different years of alfalfa continuous cropping.

Treatment	pH	NH4	NO3	TP	TK	AK	AP	TC	TN	C/N
Me	5.66 ± 0.04d	2.24 ± 0.11a	0.48 ± 0.02d	0.66 ± 0.03a	19.97 ± 1.51d	128.5 ± 9.46d	40.5 ± 1.37a	27.75 ± 0.95a	2.72 ± 0.08a	10.22 ± 0.47d
Ma	7.6 ± 0.09c	2.18 ± 0.07a	1.76 ± 0.36a	0.62 ± 0.06a	21.97 ± 1.43c	249.7 ± 10.99a	38.72 ± 1.09b	17.9 ± 0.78d	1.72 ± 0.04c	10.38 ± 0.37d
AC6	7.8 ± 0.02ab	2.29 ± 0.19a	1.39 ± 0.07b	0.63 ± 0.03a	21.25 ± 0.49c	158.9 ± 4.57c	31.66 ± 1.11c	19.91 ± 0.74c	1.55 ± 0.07d	12.87 ± 0.29a
AC10	7.75 ± 0.06b	1.83 ± 0.06c	1.19 ± 0.08c	0.47 ± 0.06b	25.42 ± 0.57a	151.9 ± 8.78c	28.4 ± 1.78d	19.65 ± 0.88c	1.68 ± 0.09c	11.73 ± 0.82c
AC14	7.81 ± 0.04ab	2 ± 0.05b	1.29 ± 0.05bc	0.22 ± 0.01c	24.61 ± 0.75ab	168.8 ± 7.48b	11.71 ± 1.15e	21.34 ± 0.89b	1.77 ± 0.09c	12.05 ± 0.52bc
AC20	7.83 ± 0.06a	1.87 ± 0.03c	1.41 ± 0.08b	0.25 ± 0.02c	24.59 ± 0.51ab	150 ± 5.2c	9.61 ± 0.18f	21.74 ± 0.59b	1.75 ± 0.09c	12.45 ± 0.56ab
AC30	7.76 ± 0.03ab	1.88 ± 0.05c	1.75 ± 0.11a	0.14 ± 0.03d	23.96 ± 0.76b	170.2 ± 9.78b	9.02 ± 0.13f	22.31 ± 0.74b	1.92 ± 0.08b	11.6 ± 0.24c

Soil Bacterial Diversity

According to the Chao index, soil microbial diversity was highest in the AC30 treatment and lowest in the Me treatment ($p > 0.05$; **Figures 1A,B**). Effect of crop type and continuous

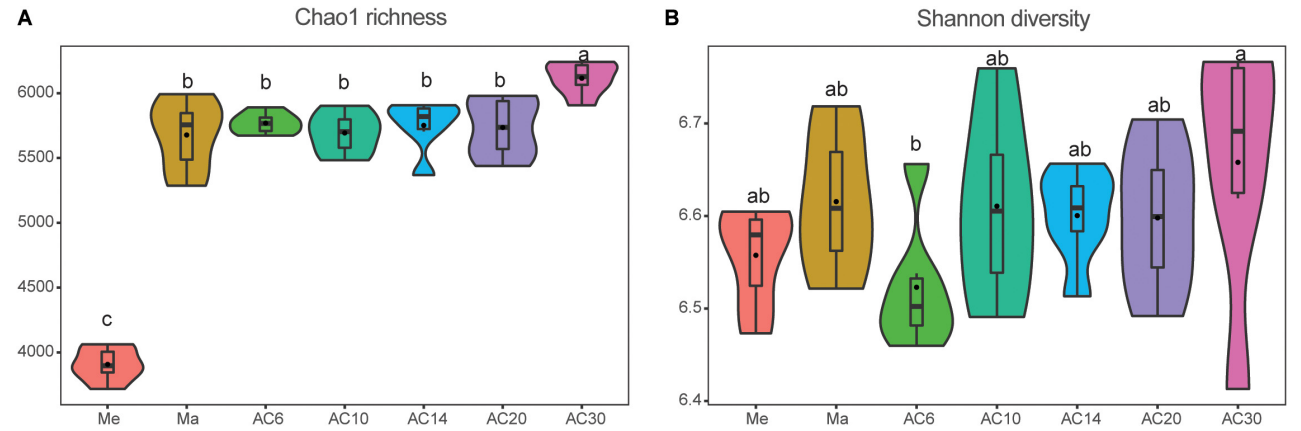

FIGURE 1 | Effect of crop type and continuous cropping years on the bacterial Chao1 richness **(A)** and Shannon diversity **(B)**.

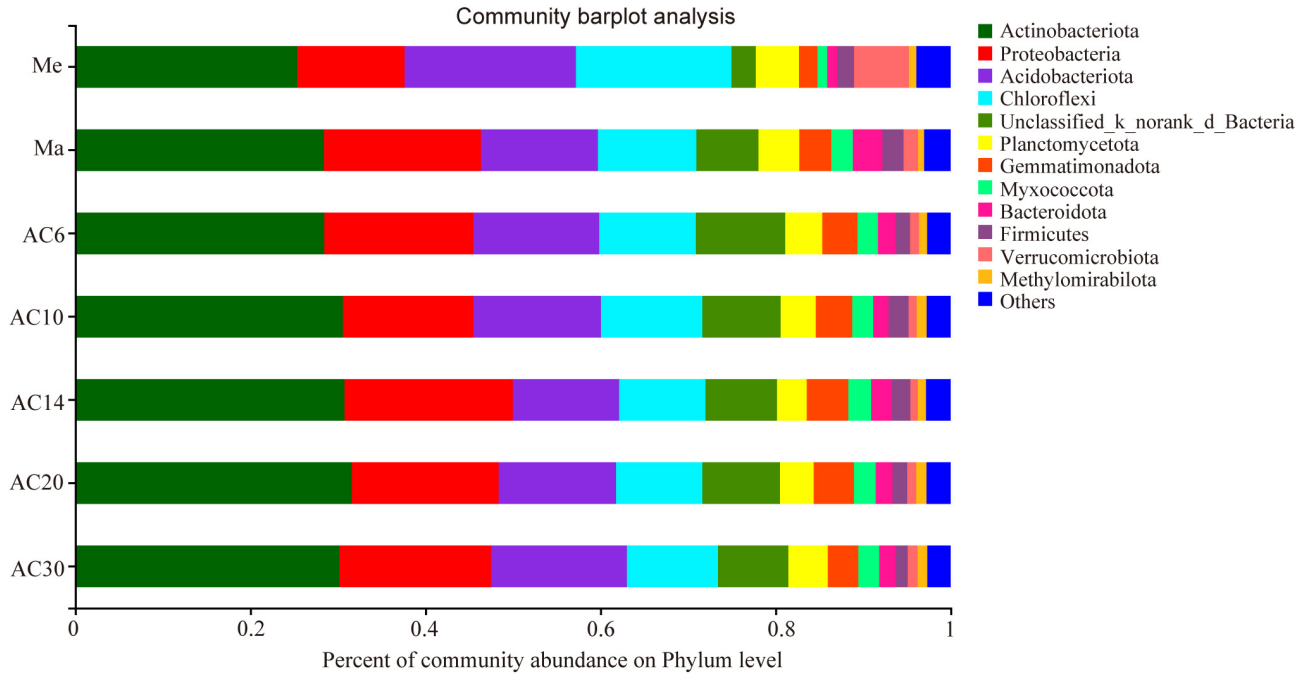

FIGURE 2 | Effect of crop type and continuous cropping years on the bacterial phylum.

cropping years on the bacterial phylum (**Figure 2**). Principal coordinate analysis (PCoA) revealed that cropping systems and alfalfa continuous cropping time significantly affected the soil bacterial communities (PERMANOVA, $p < 0.05$; **Figures 3A–D** and **Table 2**). According to the PCoA result, we divided all treatments into three groups—Me (Meadow), Ma (Maize), and AC (Alfalfa continuous cropping)—and further divided AC into three groups—AC6-10 (alfalfa continuous cropping for 6, 10, and 14 years), AC20 (alfalfa continuous cropping for 20 years), and AC30 (alfalfa continuous cropping for 30 years) (**Figure 3** and **Table 2**). The results of CCA revealed that there was a close relationship between soil physicochemical and soil bacterial community composition (**Figure 4**). Specifically, total C ($r = 0.764$; $p < 0.01$) and N ($r = 0.654$; $p < 0.01$), C/N ($r = 0.876$; $p < 0.01$), TP ($r = 0.732$; $p < 0.05$), AK ($r = 0.732$; $p < 0.01$) and TK ($r = 0.804$; $p < 0.01$), NH_4 ($r = 0.677$; $p < 0.05$), pH ($r = 0.616$; $p < 0.01$), and NO_3 ($r = 0.677$; $p < 0.05$) seemed significantly associated with the microbial community composition.

Specific Microbiomes

Actinobacteria, Acidobacteria, Proteobacteria, and Chloroflexi were the phyla with the highest relative abundance across all the treatments, accounting for 72.14–78.81% of the whole community (**Figure 3**). Overall, the relative abundance of Actinobacteria and Proteobacteria was higher in the

TABLE 2 | Effect of crop type and continuous cropping years on the differences of bacteria communities based on PERMANOVA analysis.

Pairwise comparison	*R*	*p*
Me vs. Ma	0.865	0.001***
Me vs. AC	0.885	0.001***
Me vs. AC	0.839	0.002
AC6,10,14 vs. AC20	0.645	0.017
AC6,10,14 vs. AC30	0.768	0.001***
AC20 vs. AC30	0.654	0.003

****Significant P-value of 0.01.*

Ma and AC treatments compared with the Me treatment, while Acidobacteria showed the opposite trend. On the genera level, the relative abundance with Kruskal–Wallis *H* test showed that some genera, such as *norank_Gaiellales*, *norank_Vicinambacterales*, *Rubrobacter*, and *Arthrobacter*, were significantly ($p < 0.05$) different among the Me, Ma, and AC fields. Moreover, some genera, such as *norank_JG30-KF-CM45, norank_Gaiellales, Arthrobacter, Sphingomonas, Microlunatus,* and *Lysobacter*, were significantly ($p < 0.05$) different among the cropping systems of alfalfa continuous cropping for AC6-10, AC20, and AC30 treatments (**Figure 5**). In more detail, the relative abundance of *Rubrobacter*, *norank_Vicinambacterales*, *norank_JG30-KF-CM45*, *norank_Vicinamibacteraceae*, *Arthrobacter*, and *norank_Gemmatimonadaceae* was significantly higher in the Ma and AC treatments compared with the Me treatment, while the relative abundance of *norank_Acidobacteriales*, *Candidatus_Udaeobacter*, and *norank_TK10* showed the opposite trend (**Figure 5A**). Furthermore, the relative abundance of *norank_Gaiellales*, *norank_67-14*, *norank_Gemmatimonadaceae*, and *Lysobacter* were increased with the alfalfa continuous cropping time, while *norank_JG30-KF-CM45*, *Arthrobacter*, *norank_Geminicoccaceae*, *Sphingomonas*, and *Microlunatus* showed the opposite trend (**Figure 5B**).

Co-occurrence Network

The co-occurrence network based on OTU level shows the relationship between bacteria in different treatments (**Figure 6**). Comparing the Me, Ma, and AC treatments, the ranking of the number of negative correlations and modularity was Me > AC > Ma, while for the average degree (avgK) and clustering coefficient (avgCC), no significant differences were

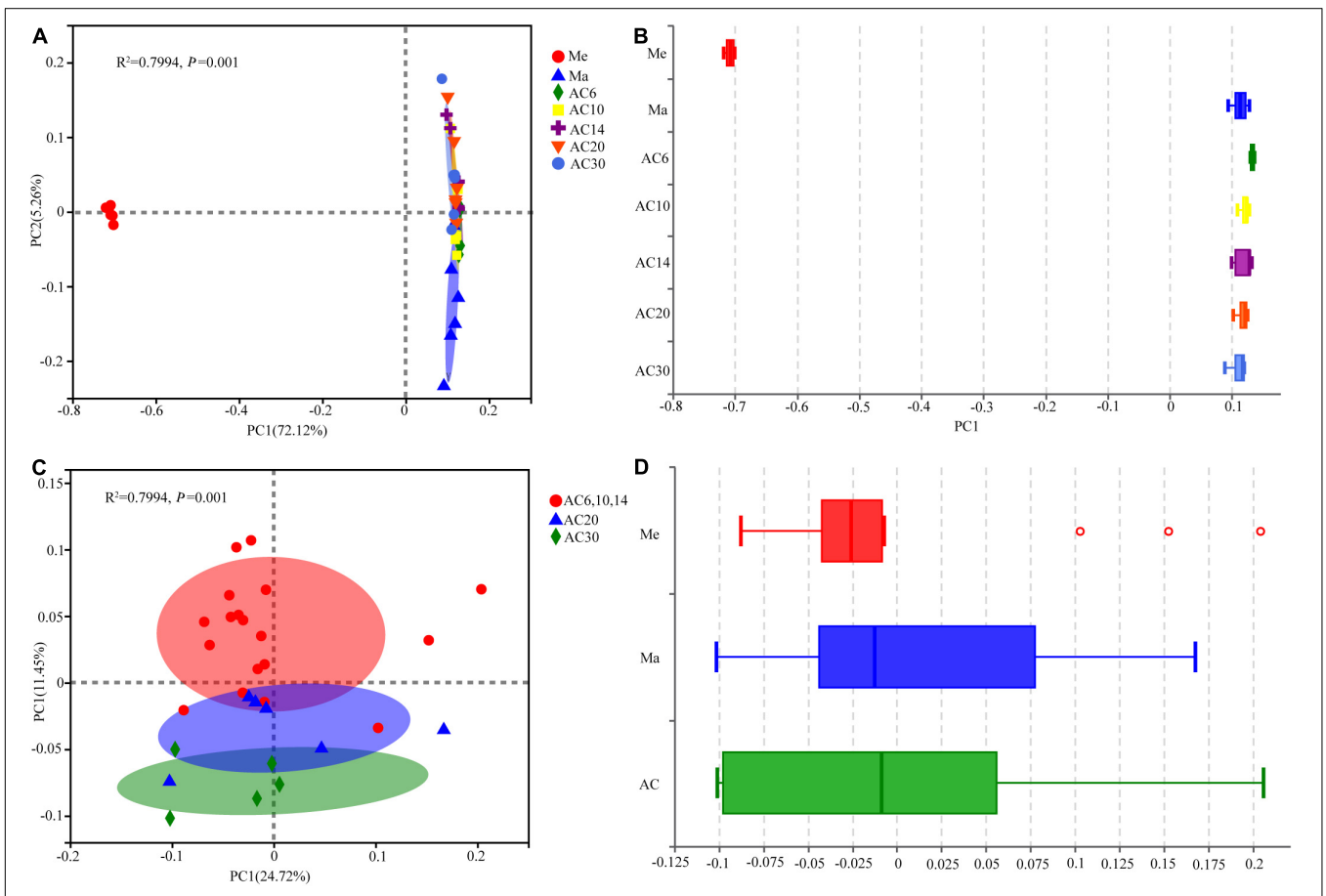

FIGURE 3 | Principal coordinate analysis (PCoA) based on Bray–Curtis dissimilarities in the soil among the seven treatments **(A,B)** and among alfalfa continuous cropping different years **(C,D)**.

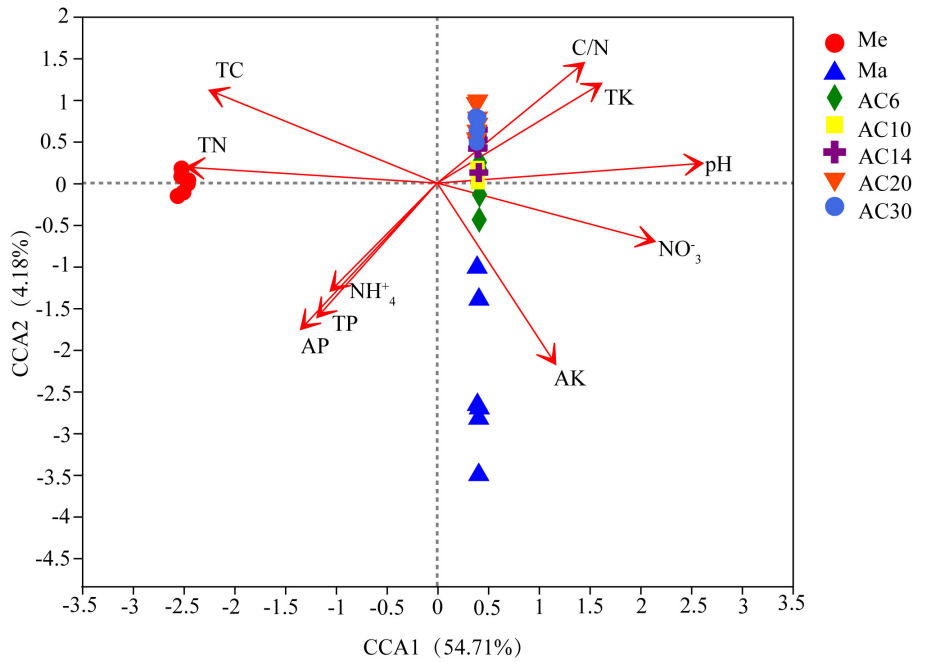

FIGURE 4 | Canonical correspondence analysis (CCA) of bacterial communities changes with the environmental variables.

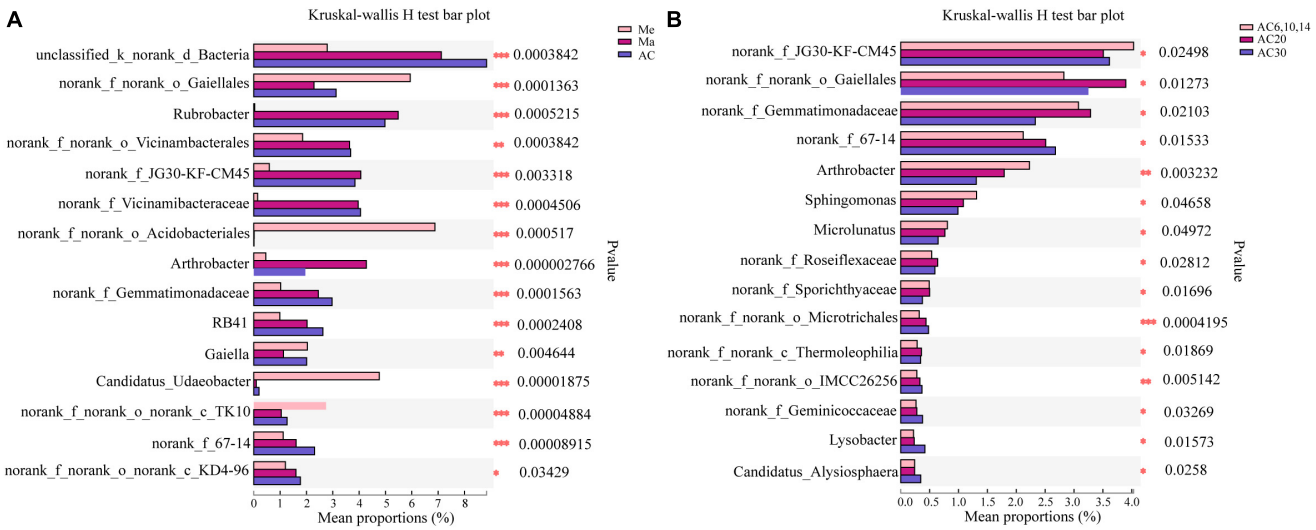

FIGURE 5 | Effect of crop type **(A)** and continuous cropping years **(B)** on the differentiation of bacterial genus.

found among the treatments. When comparing the AC6-10, AC20, and AC30 treatments, the number of negative correlations, modularity, and avgCC increased with the years of continuous cropping. For the keystone species, OTU1210 (*Jatrophihabitans*), OTU10961 (*Blastococcus*), and OTU8174 (*norank_Gemmatimonadaceae*) were identified in the Me, Ma, and AC networks, respectively, while OTU13196 (*Microlunatus*), OTU5705 (*Paenibacillus*), and OTU8419 (*norank_Xanthobacteraceae*) were identified in the AC6-10, AC20, and AC30 networks, respectively (**Table 3**).

DISCUSSION

In the present study, the Ma and AC treatments have higher microbial diversity than the Me treatment, and microbial diversities increased significantly in the long-term continuous (AC30) treatment. These results suggest that maize and alfalfa were enriched with more microbial species and were more conducive to soil conservation and sustainability, at least in terms of microbial diversity. Previous studies have found that, compared with corn–soybean rotation systems, there was less

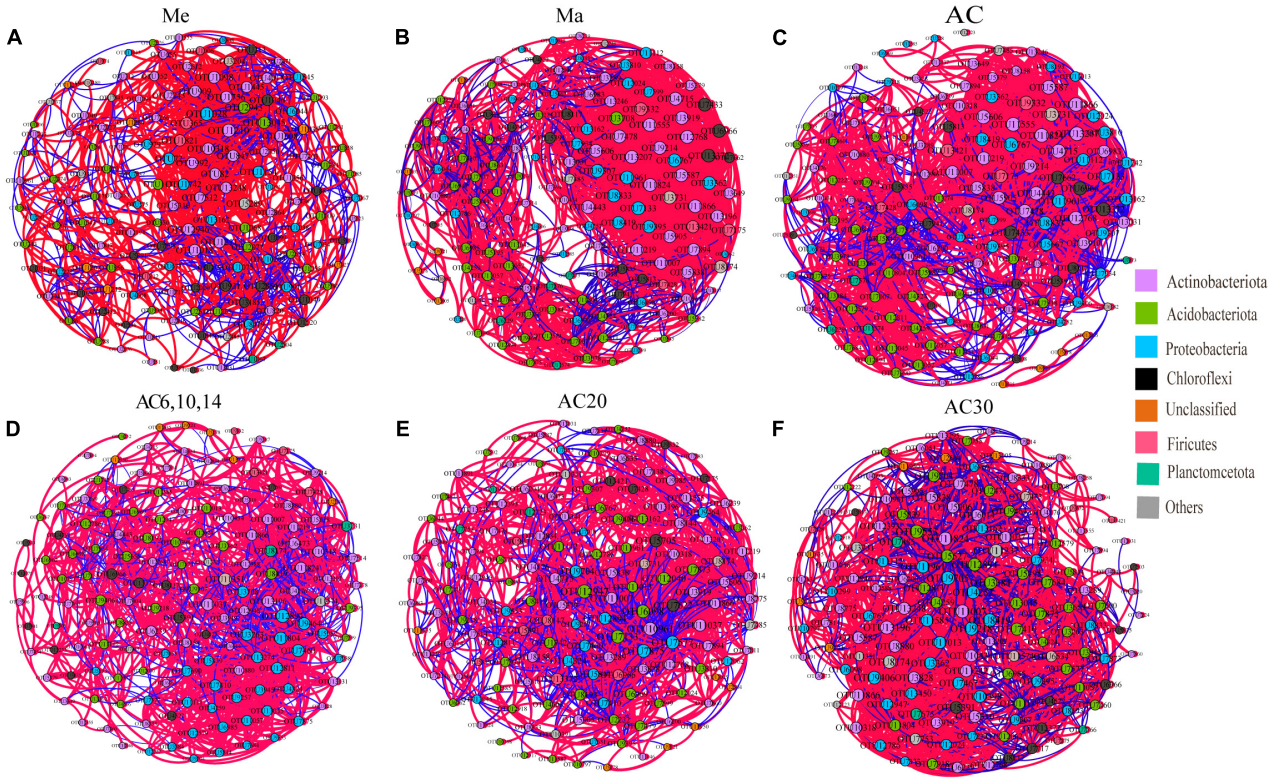

FIGURE 6 | Co-occurrence network of the soil bacterial community for Me **(A)**, Ma **(B)**, AC **(C)**, AC6, 10, 14 **(D)**, AC20 **(E)** and AC30 **(F)** treatment.

TABLE 3 | Topological characteristics of soil bacterial co-occurrence network.

Network metrics	Me	Ma	AC	AC6,10,14	AC20	AC30
Number of nodes	150	150	150	150	150	150
Number of edges	1,338	2,089	1,951	1,416	1,601	2,023
Number of positive correlations	953	1,748	1,582	1,054	1,141	1,348
Number of negative correlations	385	340	369	362	460	675
Average degree (avgK)	17.96	27.853	26.013	18.88	21.347	26.973
Average weighted degree	7.638	23.417	17.018	11.617	8.77	9.339
Network diameter	7	9	8	8	6	7
Graph density	0.121	0.187	0.175	0.127	0.143	0.181
Modularity (M)	1.046	0.587	0.626	1.131	1.099	1.52
Interconnecting piece	1	3	3	2	1	2
Average clustering coefficient (avgCC)	0.615	0.694	0.699	0.591	0.631	0.662
Average path length (APL)	2.855	2.984	2.689	2.63	2.69	2.546

rhizosphere bacterial diversity in continuously grown soybeans (Liu et al., 2020). A positive correlation between continuous cropping years and soil bacterial diversity has also been reported (Liu et al., 2020). Nevertheless, it has also been claimed that soil microbial diversity did not differ between soils grown in continuous soybean and soybean–maize rotations (Li et al., 2010). The different results of these studies might depend on the types of soil utilized and the different years of continuous cropping. Furthermore, differences in crop genotypes may also be responsible for this phenomenon, as microbial diversity has also shown different trends due to successive plantings of resistant and sensitive varieties (Yuan et al., 2021). Changes in soil pH can affect other soil physicochemical properties, and these changes directly or indirectly influence microbial diversity (Tan et al., 2017; Lian et al., 2019). In addition, microbial diversity in different farming systems can be affected by changes in plant root secretions, such as flavonoids and hormones (Tan et al., 2017; Lian et al., 2019; Liu et al., 2020; Shi et al., 2020).

From the results of PCoA and the PERMANOVA analysis, the crop types and years of continuous alfalfa were considered the two most important factors that changed the soil bacterial structure ($p < 0.05$). There is no doubt that different crops

TABLE 4 | Keystone taxa identified in the co-occurrence network.

	OTU ID	Phylum	Class	Order	Family	Genus	Species
Me	OTU1210	Actinobacteriota	Actinobacteria	Frankiales	Frankiaceae	*Jatrophihabitans*	*norank*
	OTU1028	Proteobacteria	Gammaproteobacteria	Burkholderiales	Rhodocyclaceae	*norank*	*norank*
	OTU1098	Actinobacteriota	Actinobacteria	Frankiales	norank	*norank*	*norank*
Ma	OTU10961	Actinobacteriota	Actinobacteria	Frankiales	Geodermatophilaceae	*Blastococcus*	*norank*
	OTU11804	Acidobacteriota	Blastocatellia	Blastocatellales	Blastocatellaceae	*norank*	*norank*
	OTU6973	Proteobacteria	Alphaproteobacteria	Rhizobiales	Rhizobiaceae	*Allorhizobium*	*Pararhizobium*
AC	OTU8174	Gemmatimonadota	Gemmatimonadetes	Gemmatimonadales	Gemmatimonadaceae	*norank*	*norank*
	OTU10318	Actinobacteriota	Thermoleophilia	Gaiellales	norank	*norank*	*norank*
	OTU5813	Chloroflexi	Chloroflexia	Thermomicrobiales	JG30-KF-CM45	*norank*	*norank*
AC6,10,14	OTU13196	Actinobacteriota	Actinobacteria	Propionibacteriales	Propionibacteriaceae	*Microlunatus*	*norank*
	OTU8174	Gemmatimonadota	Gemmatimonadetes	Gemmatimonadales	Gemmatimonadaceae	*norank*	*norank*
	OTU12811	Acidobacteriota	Vicinamibacteria	Vicinamibacterales	Vicinamibacteraceae	*norank*	*norank*
AC20	OTU5705	Firmicutes	Bacilli	Paenibacillales	Paenibacillaceae	*Paenibacillus*	*Paenibacillus*
	OTU12040	Proteobacteria	Gammaproteobacteria	Burkholderiales	Comamonadaceae	*norank*	*norank*
	OTU11037	Actinobacteriota	Actinobacteria	Micrococcales	Microbacteriaceae	*Agromyces*	*Agromyces*
AC30	OTU8419	Proteobacteria	Alphaproteobacteria	Rhizobiales	Xanthobacteraceae	*norank*	*norank*
	OTU11007	Actinobacteriota	Thermoleophilia	norank	norank	*norank*	*norank*
	OTU9218	Proteobacteria	Gammaproteobacteria	Burkholderiales	SC-I-84	*norank*	*norank*

have different microbial community structures (Lian et al., 2019). This was in line with some previous studies that have shown significant variation in soil bacterial communities in short- and long-term alfalfa continuous cropping field (Zhu et al., 2017; Yao et al., 2019). The CCA result demonstrated that the major factors in changing soil bacterial community structure in different treatments in this study were soil pH, NO_3^-, total K, total P, and available P. Similar results were found for the significant effect of soil characteristics, such as soil pH and AP, on the structure of the bacterial community. In our investigation, these soil parameters were impacted significantly by continuous cropping, showing that continuous crops modified their soil characteristics and subsequently changed their bacterial community.

In the Ma and AC soils compared with those of the Me system, the relative abundance of Actinobacteria and Proteobacteria was substantially enhanced, suggesting that the bacteria were increased with high nutrient availability (Li et al., 2014; Yuan et al., 2021). The relative abundances of *Arthrobacter* increased in the Ma and AC cropping field compared with Me, but then decreased in the AC20 and AC30 long continuous cropping field, compared with AC6-14. Hexavalent chromium can cause serious human irritation, while *Arthrobacter* can reduce hexavalent chromium, thus making the soil environment more beneficial. Some specific metabolites of *Arthrobacter* can promote amino acid secretion from plant roots (Romaniuk et al., 2018; Shi et al., 2020). Additionally, some microbial species, such as *norank_Gaiellales* and *Lysobacter,* which play a role in ecological function of ligninolysis and in soil suppression against the fungal root pathogen, were increased with the alfalfa continuous cropping time, suggesting that these bacteria might inhibit soil fungal diseases due to long-term continuous cropping (Gómez Expósito et al., 2015). Therefore, changes in these bacteria across treatments may be related to antagonistic activity of plant pathogens and improved soil nutrition. However, the contribution of these significantly responsive microbial species to the plant is speculative based on their abundance and reported function. Whether they have a definite role in continuous cropping for alfalfa requires further verification.

Association network analysis provides a more detailed understanding of bacterial community composition and associations (Xue et al., 2018; Xiong et al., 2021). The network negative correlations and modularity of the Me were higher than that in Ma and AC treatments, suggesting that continuous planting of alfalfa promotes cooperation between bacteria, which facilitates the long growth of alfalfa and is beneficial to the soil (Yao et al., 2019). This finding corresponds to an earlier research, showing that the soil microbial structure becomes increasingly healthy after a long period of continuous cropping (Yao et al., 2019; Liu et al., 2020).

In summary, maize cropping and continuous cropping of alfalfa increased the soil bacterial alpha diversity, and alpha diversity also increased in the long-term continuous planting system. Soil pH, NO_3^-, total K, and total P content were important factors influencing the structure of soil bacterial community in different plant types and different alfalfa continuous cropping system. Moreover, compared with planting meadow, maize and alfalfa continuous cropping significantly increases a number of beneficial bacterial species, such as *Arthrobacter* and *Gaiellales*, suggesting that the microbial community of maize and long-term alfalfa cropping shifts toward a healthy pattern. However, these microorganisms need to be isolated and formed into synthesized microbial communities to verify their specific benefits to the crop. Furthermore, the networks differ among different plant types and also differ among different continuous cropping years of alfalfa. The topology of the networks suggested that continuous planting of alfalfa promotes cooperation between bacteria, which facilitates the long growth of alfalfa and is beneficial to the soil.

DATA AVAILABILITY STATEMENT

The datasets presented in this study can be found in online repositories. The names of the repository/repositories and accession number(s) can be found in the article/supplementary material.

AUTHOR CONTRIBUTIONS

HL and ZY conceived and designed this study. ZY and YX performed the experiments and wrote the manuscript. SL, XW, and HC analyzed the data. All authors approved the final version of the manuscript.

FUNDING

This work was supported by Outstanding Youth Fund of Heilongjiang Academy of Agricultural Sciences (2020JCQN003), China Agriculture Research System of MOF and MARA (CR34), and the Grass-field Rotation Scientist Studio of Heilongjiang Province (202004).

REFERENCES

Agler, M. T., Ruhe, J., Kroll, S., Morhenn, C., Kim, S. T., Weigel, D., et al. (2016). Microbial hub taxa link host and abiotic factors to plant microbiome variation. *PLoS Biol.* 14:e1002352. doi: 10.1371/journal.pbio.1002352

Berry, D., and Widder, S. (2014). Deciphering microbial interactions and detecting keystone species with co-occurrence networks. *Front. Microbiol.* 5:219. doi: 10.3389/fmicb.2014.00219

Chen, J. S., Gao, C., Di, G. L., Zhu, R. F., and Zhang, Y. X. (2013). Effects of cutting on alfalfa yield and quality in northeast china. *J. Anim. Vet. Adv.* 12, 253–260.

Cole, J. R., Wang, Q., Cardenas, E., Fish, J., Chai, B., Farris, R. J., et al. (2009). The ribosomal database project: improved alignments and new tools for rRNA analysis. *Nucleic Acids Res.* 37, 141–145. doi: 10.1093/nar/gkn879

Dong, S. K., Long, R. J., Hu, Z. Z., Kang, M. Y., and Pu, X. P. (2003). Productivity and nutritive value of some cultivated perennial grasses and mixtures in the alpine region of the Tibetan Plateau. *Grass Forage Sci.* 58, 302–308. doi: 10.1046/j.1365-2494.2003.00382.x

Dong, W. H., Zhang, S., Rao, X., and Liu, C. A. (2016). Newly-reclaimed alfalfa forage land improved soil properties comparison to farmland in wheat–maize cropping systems at the margins of oases. *Ecol. Eng.* 94, 57–64. doi: 10.1016/j.ecoleng.2016.05.056

Doran, J. W., and Parkin, T. B. (1994). Defining and assessing soil quality. *Soil Sci. Soc. Am. J.* 35, 3–21.

Edgar, R. C., Haas, B. J., Clemente, J. C., Quince, C., and Knight, R. (2011). UCHIME improves sensitivity and speed of chimera detection. *Bioinformatics* 27, 2194–2200. doi: 10.1093/bioinformatics/btr381

Gómez Expósito, R., Postma, J., Raaijmakers, J. M., and Bruijin, I. D. (2015). Diversity and activity of Lysobacter species from disease suppressive soils. *Front. Microbiol.* 6:1243. doi: 10.3389/fmicb.2015.01243

Han, Q. F., Jia, Z. K., and Wang, J. P. (2005). The analysis of current situation and development prospect of alfalfa industry at home and abroad. *Pratacultural Sci.* 22, 22–25.

Hu, J. C., and Wang, S. J. (1996). Study on soil sickness by soybean continuous cropping I. Effect of mycotoxin produced by Penicillium purpurogenum. *Chin. J. Appl. Ecol.* 7, 396–400.

Jiang, J. P., Xiong, Y. C., Jia, Y., Li, F. M., Xu, J. Z., and Jiang, H. M. (2007). Soil quality dynamics under successional alfalfa field in the semi-arid loess plateau of northwestern China. *Arid Land Res. Manag.* 21, 287–303. doi: 10.1080/15324980701603524

Jiang, Y., Li, S., Li, R., Zhang, J., Liu, Y., Lv, L., et al. (2017). Plant cultivars imprint the rhizosphere bacterial community composition and association networks. *Soil Biol. Biochem.* 109, 145–155. doi: 10.1016/j.soilbio.2017.02.010

Jones, D. L., and Willett, V. B. (2006). Experimental evaluation of methods to quantify dissolved organic nitrogen (DON) and dissolved organic carbon (DOC) in soil. *Soil Biol. Biochem.* 38, 991–999.

Li, C. G., Li, X. M., Kong, W. D., Wu, Y., and Wang, J. G. (2010). Effect of monoculture soybean on soil microbial community in the northeast China. *Plant Soil* 330, 423–433. doi: 10.1007/s11104-009-0216-6

Li, W., and Godzik, A. (2015). Cd-hit: a fast program for clustering and comparing large sets of protein or nucleotide sequences. *Bioinformatics* 22:1658. doi: 10.1007/978-1-4899-7478-5_221

Li, X. Z., Rui, J. P., Mao, Y. J., Yannarell, A., and Mackie, R. (2014). Dynamics of the bacterial community structure in the rhizosphere of a maize cultivar. *Soil Biol. Biochem.* 68, 392–401. doi: 10.1016/j.soilbio.2013.10.017

Li, Y., and Huang, M. (2008). Pasture yield and soil water depletion of continuous growing alfalfa in the Loess Plateau of China. *Agric. Ecosyst. Environ.* 124, 24–32. doi: 10.1016/j.agee.2007.08.007

Lian, T. X., Ma, Q. B., Shi, Q. H., Cai, Z. D., Zhang, Y. F., Cheng, Y. B., et al. (2019). High aluminum stress drives different rhizosphere soil enzyme activities and bacterial community structure between aluminum-tolerant and aluminum-sensitive soybean genotypes. *Plant Soil* 440, 409–425.

Liu, H., Pan, F. J., Han, X. Z., Song, F. B., Zhang, Z. M., Yan, J., et al. (2019). Response of soil fungal community structure to long-term continuous soybean cropping. *Front. Microbiol.* 9:3316. doi: 10.3389/fmicb.2018.03316

Liu, J., Sui, Y., Yu, Z., Shi, Y., Chu, H., Jin, J., et al. (2015). Soil carbon content drives the biogeographical distribution of fungal communities in the black soil zone of northeast China. *Soil Biol. Biochem.* 83, 29–39. doi: 10.1016/j.soilbio.2015.01.009

Liu, Z. X., Liu, J. J., Yua, Z. H., Yao, Q., Li, Y. S., Liang, A. Z., et al. (2020). Long-term continuous cropping of soybean is comparable to crop rotation in mediating microbial abundance, diversity and community composition. *Soil Tillage Res.* 197:104503. doi: 10.1016/j.still.2019.104503

Lu, R. K. (1999). *Analytical Methods of Soil Agrochemistry*. Beijing: Chinese Agriculture Science and Technology Press.

Luo, C. G., Deng, Y. W., Inubushi, K., Liang, J., Zhu, S. P., Wei, Z. Y., et al. (2018). Sludge biochar amendment and alfalfa revegetation improve soil physicochemical properties and increase diversity of soil microbes in soils from a rare earth element mining wasteland. *Int. J. Environ. Res. Public Health* 15:965. doi: 10.3390/ijerph15050965

Mendes, L. W., Mendes, R., Raaijmakers, J. M., and Tsai, S. M. (2018). Breeding for soil-borne pathogen resistance impacts active rhizosphere microbiome of common bean. *ISME J.* 12, 3038–3042. doi: 10.1038/s41396-018-0234-6

Raiesi, F. (2007). The conversion of overgrazed pastures to almond orchards and alfalfa cropping systems may favor microbial indicators of soil quality in Central Iran. *Agric. Ecosyst. Environ.* 121, 309–318. doi: 10.1016/j.agee.2006.11.002

Ren, X. L., Jia, Z. K., Wan, S. M., Han, Q. F., and Chen, X. L. (2011). The long-term effects of alfalfa on soil water content in the Loess Plateau of northwest China. *Afr. J. Biotechnol.* 10, 4420–4427.

Romaniuk, K., Golec, P., and Dziewit, L. (2018). Insight into the diversity and possible role of plasmids in the adaptation of psychrotolerant and metalotolerant Arthrobacter spp. to extreme Antarctic environments. *Front. Microbiol.* 9:3144. doi: 10.3389/fmicb.2018.03144

Shi, Q. H., Liu, Y. T., Shi, A. Q., Cai, Z. D., Nian, H., Hartmann, M., et al. (2020). Rhizosphere soil fungal communities of aluminum-tolerant and -sensitive soybean genotypesrespond differently to aluminum stress in an acid soil. *Front. Microbiol.* 11:1177. doi: 10.3389/fmicb.2020.01177

Song, C., Jin, K., and Raaijmakers, J. M. (2021). Designing a home for beneficial plant microbiomes. *Curr. Opin. Plant Biol.* 62:102025. doi: 10.1016/j.pbi.2021.102025

Su, Y. Z. (2007). Soil carbon and nitrogen sequestration following the conversion of cropland to alfalfa forage land in northwest China. *Soil Tillage Res.* 92, 181–189. doi: 10.1016/j.still.2006.03.001

Tan, Y., Cui, Y. S., Li, H. Y., Kuang, A. X., Li, X. R., Wei, Y. L., et al. (2017). Rhizospheric soil and root endogenous fungal diversity and composition in response to continuous Panax notoginseng cropping practices. *Microbiol. Res.* 194, 10–19. doi: 10.1016/j.micres.2016.09.009

Wang, C. Y., Zhou, X., Guo, D., Zhao, J. H., and Zhao, L. P. (2019). Soil pH is the primary factor driving the distribution and function of microorganisms in farmland soils in northeastern China. *Ann. Microbiol.* 69, 1461–1473. doi: 10.1007/s13213-019-01529-9

White, T., Bruns, T. D., Lee, S. B., and Taylor, J. W. (1990). "Amplification and direct sequencing of fungal ribosomal RNA genes for phylogenetics," in *PCR Protocols a Guide to Methods and Applications*, eds M. A. Innis, D. H. Gelfand, J. J. Sninsky, and T. J. White (San Diego, CA: Academic Press), 315–322.

Xiong, C., Zhu, Y. G., Wang, J. T., Singh, B., Han, L. L., Shen, J. P., et al. (2021). Host selection shapes crop microbiome assembly and network complexity. *New Phytol.* 229, 1091–1104. doi: 10.1111/nph.16890

Xu, Y. L., Wang, G. H., and Han, X. Z. (1995). Relationship between soil microbial ecological distribution characteristics and soybean root disease in soybean monocropping and rotation. *Syst. Sciemces Compr. Stud. Agr.* 11, 311–314.

Xue, Y., Chen, H., Yang, J. R., Min, L., Huang, B., and Yang, J. (2018). Distinct patterns and processes of abundant and rare eukaryotic plankton communities following a reservoir cyanobacterial bloom. *ISME J.* 12, 2263–2277. doi: 10.1038/s41396-018-0159-0

Yan, M. C., Xu, T. T., Song, P. H., and Dai, J. J. (2012). Effects of different cropping patterns of soybean and maize seedlings on soil enzyme activities and MBC and MBN. *J. Northeast Agric. Univ.* 19, 42–47. doi: 10.1016/S1006-8104(13)60049-5

Yao, Q., Xu, Y., Liu, X., Liu, J., Huang, X., Yang, W., et al. (2019). Dynamics of soil properties and fungal community structure in continuous-cropped alfalfa fields in Northeast China. *PeerJ* 7:e7127. doi: 10.7717/peerj.7127

Yuan, M., Yu, T., Shi, Q., Han, D., Yu, K., Wang, L., et al. (2021). Rhizosphere soil bacterial communities of continuous cropping-tolerant and sensitive soybean genotypes respond differently to long-term continuous cropping in Mollisols. *Front. Micrbiol.* 12:729047. doi: 10.3389/fmicb.2021.729047

Zhang, J., Wang, Q., Xiao, Y., Pang, X. P., Jia, T. T., Song, R., et al. (2016). Effects of alternate furrow irrigation on the biomass allocation and water use efficiency of alfalfa. *Acta Prataculturae Sin.* 25, 164–171.

Zhou, X. G., Wang, Z. L., Jia, H. T., Li, L., and Wu, F. Z. (2018). Continuously monocropped *Jerusalem artichoke* changed soil bacterial community composition and ammonia-oxidizing and denitrifying bacteria abundances. *Front. Microbiol.* 9:705. doi: 10.3389/fmicb.2018.00705

Zhu, L., Zeng, C. L., Li, Y. Q., Yu, B. Q., Gao, F., Wei, W., et al. (2017). The characteristic of bacterial community diversity in soybean field with continuous cropping based on the high-throughput sequencing. *Soybean Sci.* 36, 419–424.

Conflict of Interest: The authors declare that the research was conducted in the absence of any commercial or financial relationships that could be construed as a potential conflict of interest.

Publisher's Note: All claims expressed in this article are solely those of the authors and do not necessarily represent those of their affiliated organizations, or those of the publisher, the editors and the reviewers. Any product that may be evaluated in this article, or claim that may be made by its manufacturer, is not guaranteed or endorsed by the publisher.

frontiers | Frontiers in Microbiology

ORIGINAL RESEARCH
published: 07 April 2022
doi: 10.3389/fmicb.2022.825660

Bio-Matrix Pot Addition Enhanced the Vegetation Process of Iron Tailings by *Pennisetum giganteum*

Yihao Liu[1], Jinyang Yu[1], Zuyu Wang[1], Petri Penttinen[1], Xiumei Yu[1], Ke Zhao[1], Menggen Ma[1], Quanju Xiang[1], Yunfu Gu[1], Hanjun Liu[1,2], Xiaoping Zhang[1] and Qiang Chen[1]**

[1] College of Resources, Sichuan Agricultural University, Chengdu, China, [2] Safety and Environmental Protection Quality Supervision and Testing Research Institute, CNPC Chuanqing Drilling Engineering Co., Ltd., Guanghan, China

The barrenness of large mine tailing sand reservoirs increases the risks for landslides and erosion that may be accompanied with transfer of contaminants into the surrounding environment. The tailing sand is poor in nutrients, which effectively complicates the vegetation process. We investigated direct planting of *Pennisetum giganteum* into tailing sand using two pit planting methods: the plants were transplanted either directly into pits filled with soil or into soil-filled bio-matrix pots made of organic material. After growing *P. giganteum* in iron tailing sand for 360 days, the dry weight of the plants grown in the bio-matrix pot (T2) was approximately twofold higher than that of the plants grown in soil placed directly into the sand (T1). At 360 days, the organic matter (OM) content in the soil below the pit was the lowest in the not-planted treatment (T0) and the highest in T2, the available N (AN) contents were higher in T1 and T2 than in T0, and the available P and K contents were the highest in T2. At 360 days, the Shannon diversity of the soil microbial communities was higher in T1 and T2 than in T0, and the community compositions were clearly separated from each other. The profiles of predicted C cycle catabolism functions and N fixation-related functions in T1 and T2 at 360 days were different from those in the other communities. The results showed that *P. giganteum* grew well in the iron tailing sand, especially in the bio-matrix pot treatment, and the increased nutrient contents and changes in microbial communities indicated that using the bio-matrix pot in planting had potential to improve the vegetation process in iron tailing sands effectively.

Keywords: iron tailing sands, bio-matrix pot, microbial communities, C and N cycle, vegetation

OPEN ACCESS

Edited by:
Hai-Ming Zhao,
Jinan University, China

Reviewed by:
Aleksandr G. Bulaev,
Federal Center Research Fundamentals of Biotechnology (RAS), Russia
Feifei Zhai,
Henan Polytechnic University, China

***Correspondence:**
Xiaoping Zhang
zhangxiaopingphd@126.com
Qiang Chen
cqiang@sicau.edu.cn

Specialty section:
This article was submitted to Terrestrial Microbiology, a section of the journal Frontiers in Microbiology

Received: *30 November 2021*
Accepted: *24 February 2022*
Published: *07 April 2022*

Citation:
Liu Y, Yu J, Wang Z, Penttinen P, Yu X, Zhao K, Ma M, Xiang Q, Gu Y, Liu H, Zhang X and Chen Q (2022) Bio-Matrix Pot Addition Enhanced the Vegetation Process of Iron Tailings by Pennisetum giganteum. Front. Microbiol. 13:825660. doi: 10.3389/fmicb.2022.825660

INTRODUCTION

The waste residue released from ore in mines after refining in the beneficiation plant is referred to as tailing sand (Dudeney et al., 2012; Kossoff et al., 2014; Lei et al., 2016). More than 10 billion tons of tailings are produced each year in the world, and approximately five billion tons of tailing sand are piled in China, with an annual increase of almost 500 million tons (Wang et al., 2017). The large mine tailing sand reservoirs are barren with no plants. The barrenness increases the risks for landslides and erosion that may be accompanied with transfer of contaminants into the

surrounding environment. Tailing sand pond accidents, such as dam breaks and landslides, have been frequent and resulted in serious mudslides and collapses in recent years (Sun et al., 2018).

Several methods have been used to treat tailing sands, including refurbishment and reuse as building or chemical materials. However, the techniques are commonly of high cost and complicated or have resulted in secondary pollution (Alfonso et al., 2018; Galvão et al., 2018; Wu et al., 2018). Alarmingly, the wind-eroded dust from barren tailing sand reservoirs is a potent source of environmental contamination. In Fe-Pb-Zn mining area tailings in Murcia, Spain, the heavy metal concentrations in wind-eroded particulate matter were high, even though the concentrations in tailings were below hazardous levels (Khademi et al., 2018). Thus, the tailings should be stabilized. The tailings may be stabilized using chemical, for example, cementation, or biological methods, i.e., by vegetating the tailings. Tailing sand is poor in nutrients, which effectively complicates the vegetation process. Ensuring the growth of plants may require covering the tailings with soil, making the process laborious.

Pennisetum giganteum is a perennial gramineous plant that grows in the tropical, subtropical, and temperate area, with the merits of easy cultivation, drought and salinity tolerance, and the ability to thrive in barren soils (Hayat et al., 2020; Li et al., 2020). Since *P. giganteum* cultivation increased soil fertility and organic matter (OM) content in barren slopes or sandy decertified soils, it was often chosen as a pioneer plant for comprehensive ecological management in a variety of ecologically fragile areas (Hayat et al., 2020; Li et al., 2020).

In a preliminary study, a corn-based mini bio-matrix pot increased the growth of crop roots, yield, and microbial diversity in rhizosphere (unpublished). Thus, we hypothesized that in vegetating tailing sands, the bio-matrix pot would promote the growth of the plants and increase the OM and nutrient contents and microbial diversity in the sand. To test this, we applied two pit planting methods: the plants were transplanted either directly into pits filled with soil or into soil-filled bio-matrix pots; plant growth was measured, and soil properties and microbial communities as proxies of cultivability were analyzed.

MATERIALS AND METHODS

Materials

Iron tailing sand was kindly provided by Chengdu Leejun Industrial Co., Ltd., Sichuan, China. The pH of the iron tailing sand was 7.90, and the sand contained OM 3.45 g kg^{-1}, total nitrogen 0.12 g kg^{-1}, total phosphorus 8.92 g kg^{-1}, total potassium 7.96 g kg^{-1}, alkaline nitrogen (AN) 16.64 mg kg^{-1}, available phosphorus (AP) 1.78 mg kg^{-1}, and available potassium (AK) 50.13 mg kg^{-1}. The contents of available iron and exchangeable magnesium were 0.19 and 47.20 mg kg^{-1}, respectively. The contents of chromium, copper, cadmium, lead, manganese, and zinc were 12.3, 52.4, 0.12, 4, 807, and 109 mg kg^{-1}, respectively, all below the National Standard for Iron tailing sands in China (GB/T 31288-2014).

Soil for planting was from Jiange County (E105°28′52″, N32°0′52″), Sichuan, China. The soil was dried at room temperature, ground, and sieved through 20 mesh. The soil pH was 7.21; OM content was 11.70 g kg^{-1}; and AN, AP, and AK contents were 35.98, 7.96, and 128.63 mg kg^{-1}, respectively.

Bio-matrix pots were made by mixing corn cob powder (55%) and corn stalk powder (45%), adjusting water content to 55–60%, followed by autoclaving and cooling to room temperature. The mixture was inoculated with *Ganoderma lucidum* SZ-01, placed into a flowerpot mold, and incubated at 25°C for 10 days. During the incubation, the fungal mycelia bound the material firmly. After the incubation, the pots were dried at 80°C. The pots were 30- and 25-cm wide at the top and bottom, respectively, 20-cm high, and 2-cm thick. The OM, AN, AP, and AK contents of the pots were 642, 12.7, 21.7, and 52.8 g kg^{-1}, respectively.

Two-to-three leaved, 15–20-cm high *P. giganteum* seedlings were purchased from the local growers.

Experimental Design and Sampling

The experiment, started in February 2016, was carried out in a greenhouse in 100 × 50 × 45 cm plastic containers. Three treatments were set up: iron tailing sand + soil (T0), iron tailing sand + soil + *P. giganteum* (T1), and iron tailing sand + soil + bio-matrix pot + *P. giganteum* (T2). Approximately 54 kg of iron tailing sand was placed into the container, and a hole the size of the bio-matrix pot was carved in the middle at the top (**Figure 1**). In T0 and T1, 6.5 kg of soil was placed into the hole; in T2, the soil was placed into the bio-matrix pot that was inserted into the hole. In T1 and T2, one *P. giganteum* seedling was transplanted into the soil. The containers were irrigated with distilled water.

Iron tailing sand samples from three containers per treatment were collected at 90, 180, and 360 days (**Figure 1**). The pH and OM, AN, AP, and AK contents were determined as described previously (Siddiqi and Glass, 1981). The plants were harvested at 360 days, and the shoot and root biomasses were measured after drying at 60°C to constant weight.

16S rRNA Gene Amplicon Sequencing

DNA was extracted from 0.5 g of sample using a Fast DNA® SPIN kit for soil (MP Biomedicals, United States) according to the manufacturer's instructions. The DNA concentration and quality were assessed by 0.8% agarose gel electrophoresis and UV spectrophotometer (Thermo Scientific NC2000). DNA extracts were stored at −20°C.

The universal primers 338F (5′-ACTC CTA CGG GAG GCA GCA-3′) and 806R (5′-GGA CTA CHV GGG TWT CTA AT-3′) were used to amplify the V3–V4 region of the 16S rRNA gene of sample DNA (Huse et al., 2008; Göransson et al., 2011). The amplification was done in 25-μl reactions containing 5× reaction buffer 5 μl, 5× GC buffer 5 μl, dNTP (2.5 mM) 2 μl, forward primer (10 mM) 1 μl, reverse primer (10 mM) 1 μl, DNA template 2 μl, ddH_2O 8.75 μl, and Q5 DNA Polymerase 0.25 μl (Magoc and Salzberg, 2011). The thermal program included denaturation at 98°C for 2 min, 26 cycles with denaturation at 98°C for 15 s, annealing at 55°C for 30 s, extension at 72°C for 30 s, and a final extension at 72°C for 5 min. The amplified products were separated by 2% agarose gel electrophoresis, and the target fragments were recovered using AXYGEN's gel

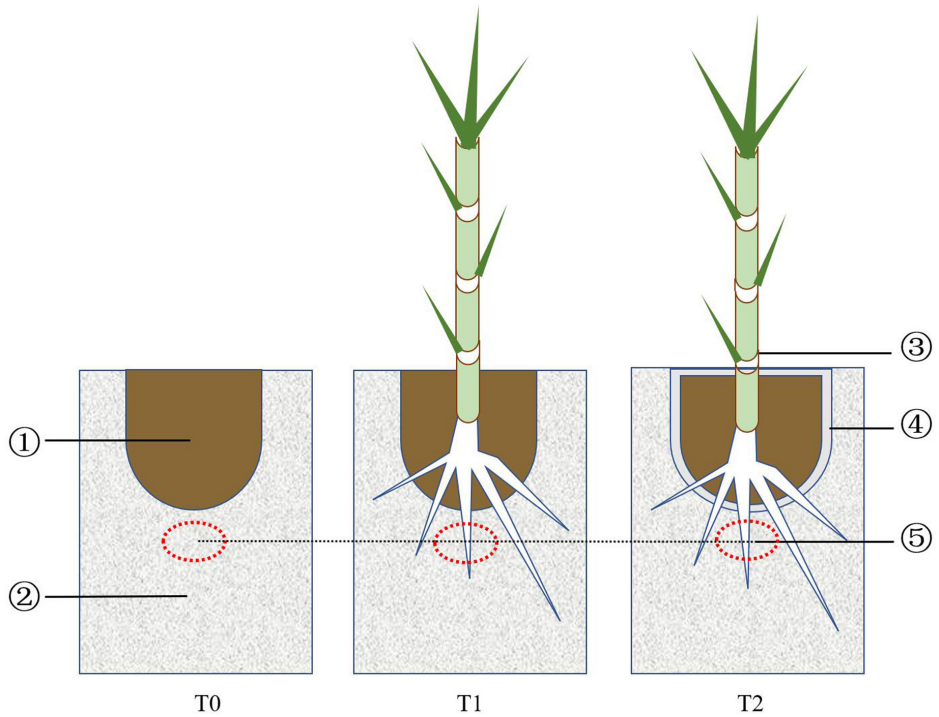

FIGURE 1 | Design of the treatments: (1) soil, (2) iron tailing sand, (3) *Pennisetum giganteum* seedling, (4) bio-matrix pot, and (5) sampling spot.

recovery kit (AXYGEN, United States). PCR products were mixed in equimolar ratios and purified using the GeneJET PCR Purification Kit (Thermo Fisher). Amplicon libraries were prepared using the NEBNext® Ultra™ DNA Library Prep Kit (New England Biolabs) prior to paired-end sequencing on the Illumina Miseq platform (Illumina, San Diego, CA, United States). The PCR products were sequenced at Shanghai Personal Medical Laboratory Co., Ltd. (Shanghai, China).

Bioinformatics and Statistical Analysis

Illumina sequencing reads were paired and quality-filtered using the Quantitative Insights into Microbial Ecology (QIIME, v1.7.0) pipeline with default settings (Caporaso et al., 2010). Chimeric sequences were removed using UCHIME algorithm after alignment with the Gold database[1] (Edgar, 2010). The sequences were assigned into operational taxonomic units (OTUs) at 97% similarity using UPARSE in the USEARCH pipeline v7.0.1090 (Edgar, 2010). The representative sequences of OTUs were assigned into taxa using SILVA rRNA database release 132 (Quast et al., 2013).

Rarefaction curves were created using R package vegan v2.5e2 in R studio (Oksanen et al., 2019). Chao1 and Shannon α-diversity indices at the OTU level were calculated in QIIME pipeline v1.7.0. The microbial communities were visualized at the genus level using cluster heatmaps based on 30 taxa with the highest relative abundances. The relative abundances of taxa were normalized using the *z*-score standardization method. The taxa were hierarchically clustered according to the Pearson correlation distance measure.

Microbial community composition at the genus level was visualized using principal component analysis (PCA) in R package vegan v2.5 in R studio (Oksanen et al., 2019). Partial least squares discriminant analysis (PLS-DA) at the OTU level was done using R packages BiocManager and mixOmics in R studio[2] (Matthew and Rayens, 2003).

Differential abundance at the OTU level was analyzed pairwise at 90, 180, and 360 days using ALDEx2 (Fernandes et al., 2013). In the analysis, the underlying distributions were estimated using 128 Monte Carlo samples, the abundances were transformed using centered log-ratios, differences were tested using *t*-test, and effect sizes were measured as the relative fold difference. OTUs were considered differentially abundant when the effect size is $>|1|$ and $p < 0.1$.

Carbon and nitrogen cycle-related functions were predicted using Functional Annotation of Prokaryotic Taxa (FAPROTAX) analysis in the Python-based FAPROTAX 1.1 package (Louca et al., 2016). Results were visualized as a clustered heatmap with a Pearson correlation dendrogram using the function "pheatmap" v1.0.12 in R studio.

Microsoft Excel 2016 was used to calculate means and standard deviations. Differences in plant and soil characteristics were tested using one-way ANOVA and Tukey's test in IBM SPSS Statistics 20.0 (SPSS Inc., Chicago, IL, United States). Differences were taken as statistically significant at $p < 0.05$.

[1] https://drive5.com/uchime/gold.fa

[2] 10.18129/B9.bioc.mixOmics

RESULTS

Plant and Soil Characteristics

After growing *P. giganteum* in iron tailing sand for 360 days, both the root dry weight (RDW) and shoot dry weight (SDW) of the plants grown in the bio-matrix pot (T2) were approximately twofold higher than those of the plants grown in soil placed directly into the sand (T1) ($p < 0.05$) (**Figure 2**), suggesting that the bio-matrix pot has promoted the growth of the plants.

The OM content of the iron tailing sand in T1 and T2 increased over time (**Table 1**). At 180 days, the OM content was the highest in T2, and at 360 days, the OM content was the lowest in the not-planted treatment (T0) and the highest in T2 ($p < 0.05$). The differences in pH values that ranged from 8.22 to 8.76 showed no clear trend. At 180 and 360 days, the AN contents were higher in T1 and T2 than in T0 ($p < 0.05$) (**Table 1**). The AP contents were the highest in T2 ($p < 0.05$). At 180 and 360 days, the AK contents were the highest in T2, and at 360 days, higher in T1 than in T0 ($p < 0.05$) (**Table 1**).

Bacterial Communities

The 1,399,587 bacterial sequences from the 27 iron tailing sand samples were clustered into 1,436 OTUs at 97% similarity level. At 180 days, Chao1 index was higher in T1 than in T0 ($p < 0.05$) (**Table 2**). At 360 days, Shannon index was higher in T1 and T2 than in T0 ($p < 0.05$). Proteobacteria, Chloroflexi, Acidobacteria, and Actinobacteria were the most dominant phyla. The relative abundances of Proteobacteria accounted for 25.73–51.28% of the total abundance, Actinobacteria for 11.95–38.43%, Chloroflexi for 5.97–14.92%, and Acidobacteria for 4.92–8.76% (**Figure 3** and **Supplementary Table 1**). At the genus level, the relative abundances of *Pseudomonas*, *Sideroxydans*, and *Geobacter* ranged from 0.53 to 9.41, 0.01 to 3.98, and 0.16 to 3.93%, respectively (**Supplementary Table 2**).

The microbial communities in T1 and T2 at 360 days were separated from the other communities in the hierarchical clustering (**Figure 4**). At 90 and 180 days, the communities in T0 and T1 were relatively similar in the PCA (**Figure 5**). The T2 community was separated from those in T0 and T1 at 180 days, and at 360 days, all the communities were clearly separated from each other (**Figure 5**). Based on the PLS-DA, the communities in T0 were different from those in T1 and T2 (**Figure 6**). At 180 days, the relative abundances of Anaerolineaceae (Chloroflexi) OTU7 and MND1 (Proteobacteria) OTU12 were lower in T2 than in T0 (effect size $> |1|$, $p < 0.1$) (**Table 3**). At 360 days, the relative abundances of Xanthobacteraceae (Proteobacteria) OTU24 and Marine Group II (Euryarchaeota) OTU59 were higher in T1 than in T0, and those of Micrococcaceae (Actinobacteria) OTU1, Solirubrobacteraceae (Actinobacteria) OTU30, *Rubellimicrobium* (Proteobacteria) OTU115, and Coleofasciculaceae (Cyanobacteria) OTU187 were lower (effect size $> |1|$, $p < 0.1$). The relative abundances of Sideroxydans (Proteobacteria) OTU31 and Marine Group II OTU59 were higher in T2 than in T0 at 360 days (effect size $> |1|$, $p < 0.1$). In the T1 treatment, the relative abundances of *Aeromicrobium* (Actinobacteria) OTU10 and Uncultured Gitt-GS-136 (Chloroflexi) OTU22 were higher at 180 and 360 days, respectively, than at 90 days (effect size $> |1|$, $p < 0.1$).

Predicted C and N Cycle-Related Functions

We predicted C and N cycle-related functions to estimate the accompanying changes on gene level. In line with the OM

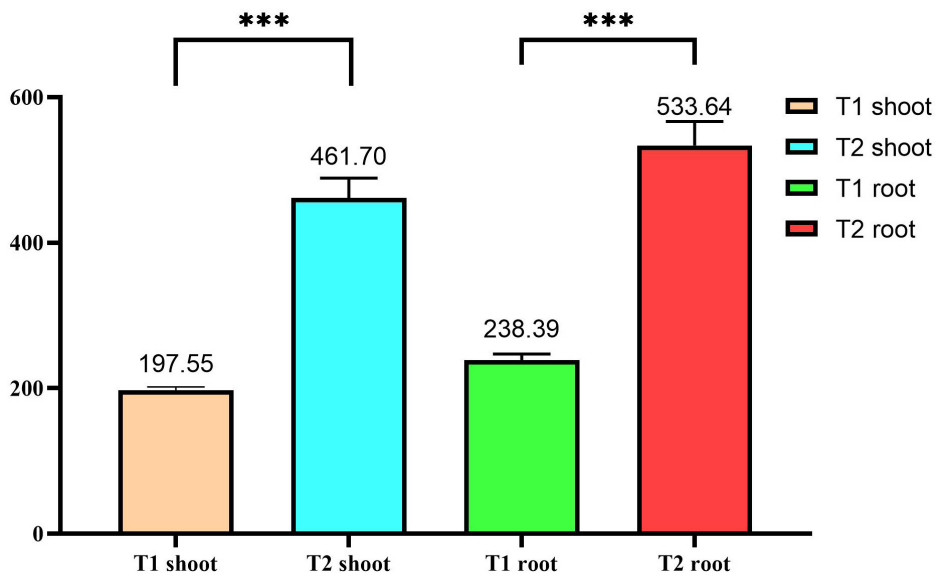

FIGURE 2 | The shoot and root dry weights of *Pennisetum giganteum* grown in tailing sands for 360 days. The error bars indicate standard deviation ($n = 3$). ***Statistically significant difference ($p < 0.05$). T1, iron tailing sand + soil + *Pennisetum giganteum*; T2, iron tailing sand + soil + bio-matrix pot + *Pennisetum giganteum*.

TABLE 1 | The physicochemical properties of the iron tailing sand.

Physicochemical properties	T0[a]			T1			T2		
	90 d	180 d	360 d	90 d	180 d	360 d	90 d	180 d	360 d
OM (g kg^{-1})	3.78ab	3.62ab	3.24a	4.12ab	4.18ab	4.41b	3.72ab	5.33c	5.61c
pH	8.28a	8.59cd	8.53bc	8.75e	8.52bc	8.39ab	8.69de	8.71de	8.76e
Available N (mg kg^{-1})	22.41ab	16.67ab	12.39a	20.67ab	34.21cd	40.80d	26.36bc	35.14cd	43.07d
Available P (mg kg^{-1})	3.07a	3.27a	3.32a	2.80a	2.30a	3.60ab	5.73bc	6.75c	7.14c
Available K (mg kg^{-1})	60.50b	54.67ab	45.93a	59.53b	58.05b	61.75b	58.13b	77.00c	95.00d

T0, iron tailing sand + soil; T1, iron tailing sand + soil + Pennisetum giganteum; T2, iron tailing sand + soil + bio-matrix pot + Pennisetum giganteum. 90 d, 180 d, and 360 d indicate the sampling time in days after the start of the experiment.
Different letters within the same row indicate statistically significant difference between treatments in individual sampling times tested by one-way ANOVA ($p < 0.05$).

TABLE 2 | The α-diversity of the microbial communities in the iron tailing sands.

α-Diversity	T0[a]			T1			T2		
	90 d	180 d	360 d	90 d	180 d	360 d	90 d	180 d	360 d
Simpson	0.9911ab	0.9914ab	0.9863a	0.9949ab	0.9916ab	0.9962b	0.9872ab	0.9963b	0.9967b
Chao1	2,794abcd	2,082ab	2,034a	3,458d	3,172cd	2,921abc	3,108bcd	2,317abcd	2,733abcd
ACE	3,005abc	2,216a	2,157a	3,654c	3,410bc	3,132abc	3,301abc	2,356ab	2,902abc
Shannon	9.68bc	9.29ab	8.73a	10.14c	9.82bc	10.09c	9.62bc	9.97bc	10.01c

T0, iron tailing sand + soil; T1, iron tailing sand + soil + Pennisetum giganteum; T2, iron tailing sand + soil + bio-matrix pot + Pennisetum giganteum. 90 d, 180 d, and 360 d indicate the sampling time in days after the start of the experiment.
Different letters within the same row indicate statistically significant difference between treatments in individual sampling times tested by one-way ANOVA ($p < 0.05$).

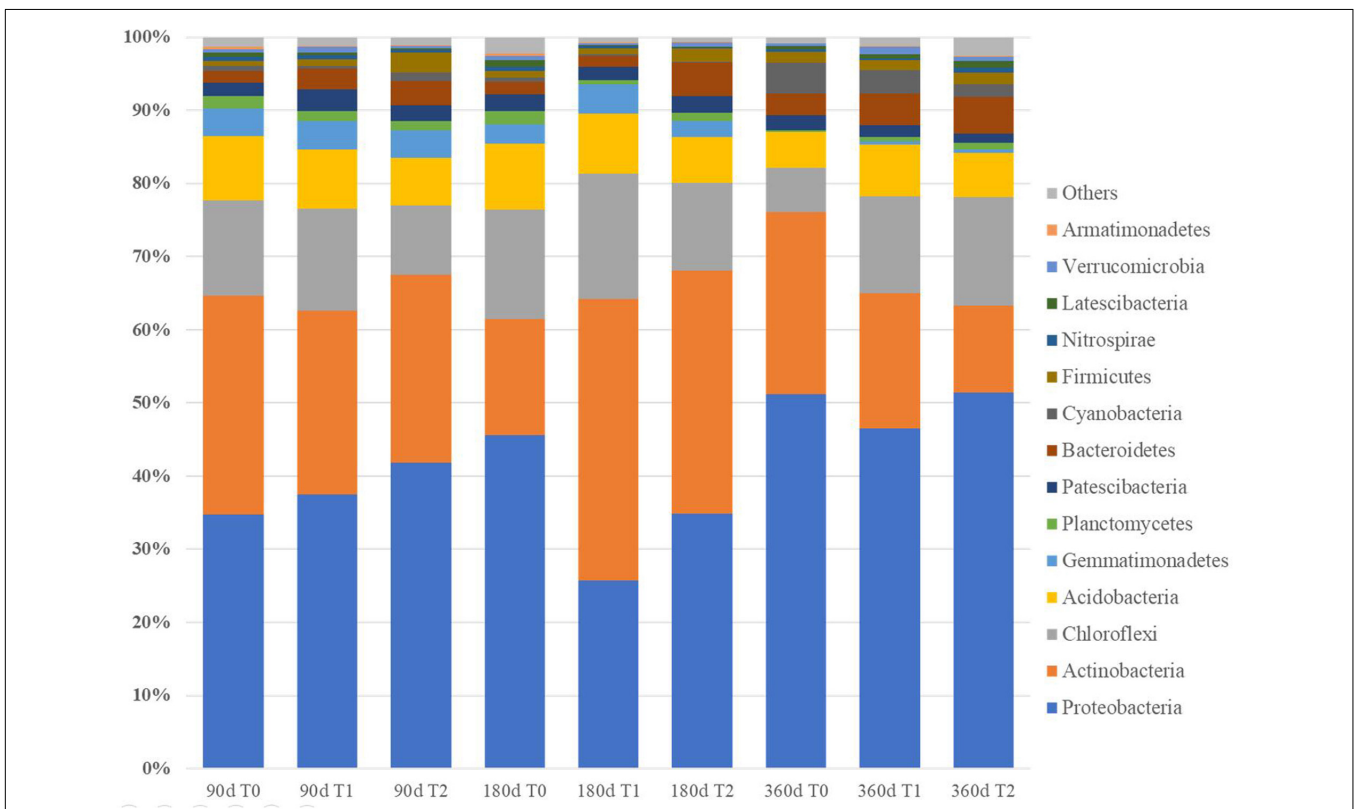

FIGURE 3 | Bacterial community composition in the tailing sand at the phylum level. T0, iron tailing sand + soil; T1, iron tailing sand + soil + *Pennisetum giganteum*; T2, iron tailing sand + soil + bio-matrix pot + *Pennisetum giganteum*; 90 d, 180 d, and 360 d indicate the sampling time in days after the start of the experiment.

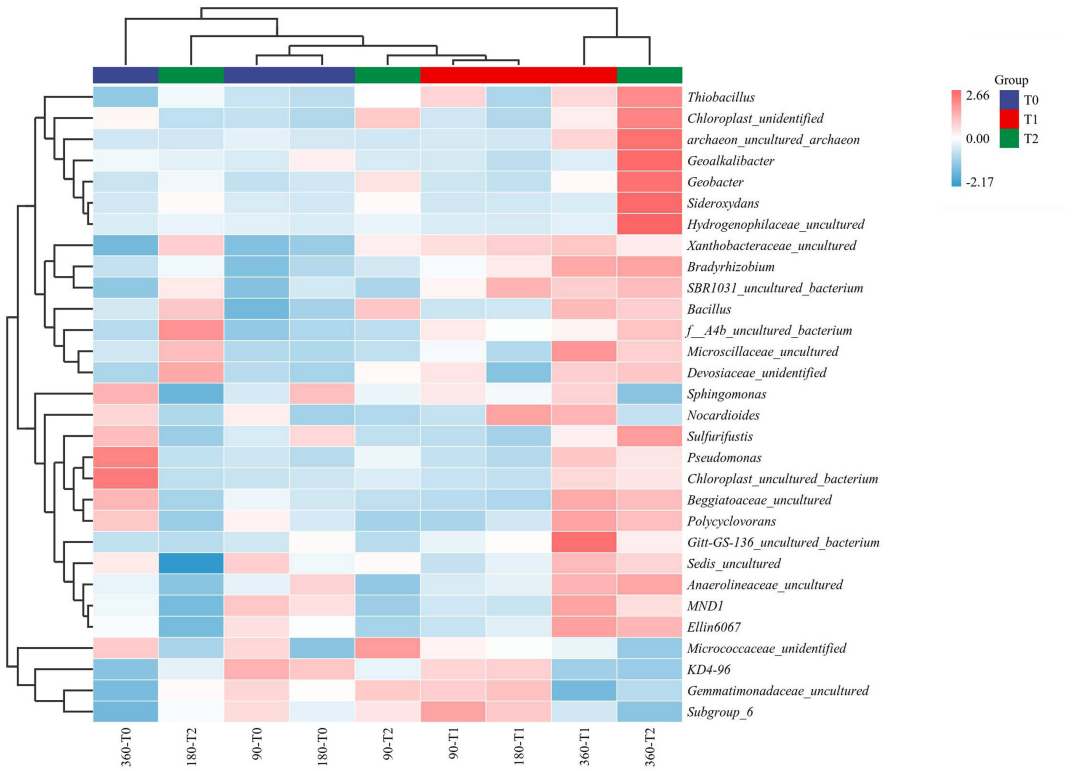

FIGURE 4 | Bacterial community composition and their hierarchical clustering in the tailing sand at the genus level. T0, iron tailing sand + soil; T1, iron tailing sand + soil + *Pennisetum giganteum*; T2, iron tailing sand + soil + bio-matrix pot + *Pennisetum giganteum*; 90 d, 180 d, and 360 d indicate the sampling time in days after the start of the experiment.

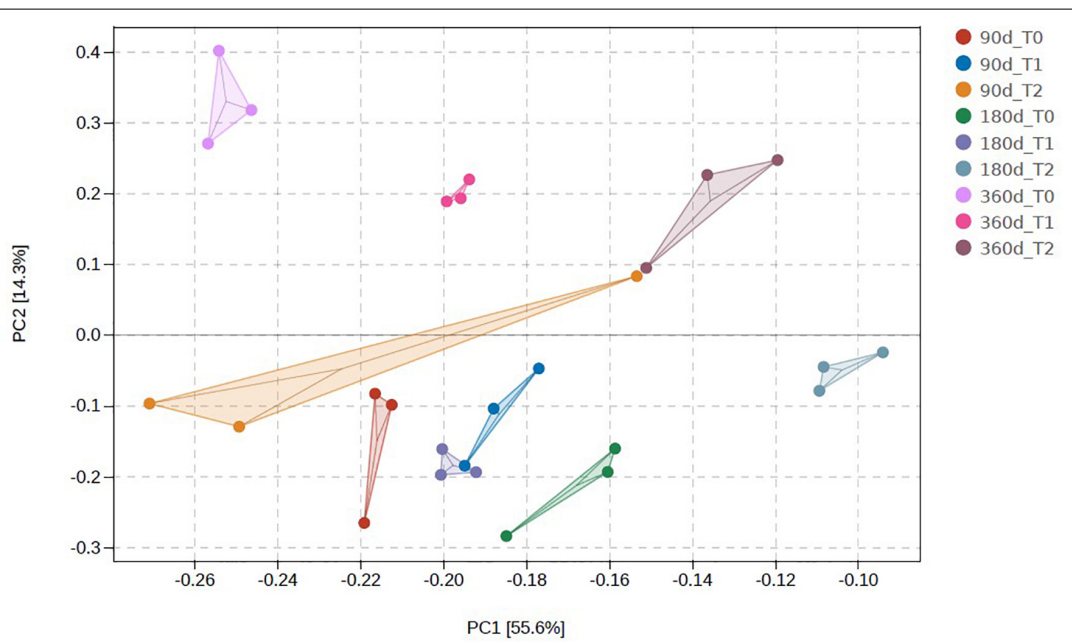

FIGURE 5 | Principal component analysis of the microbial communities in the tailing sand at the operational taxonomic unit (OTU) level. T0, iron tailing sand + soil; T1, iron tailing sand + soil + *Pennisetum giganteum*; T2, iron tailing sand + soil + bio-matrix pot + *Pennisetum giganteum*; 90 d, 180 d, and 360 d indicate the sampling time in days after the start of the experiment.

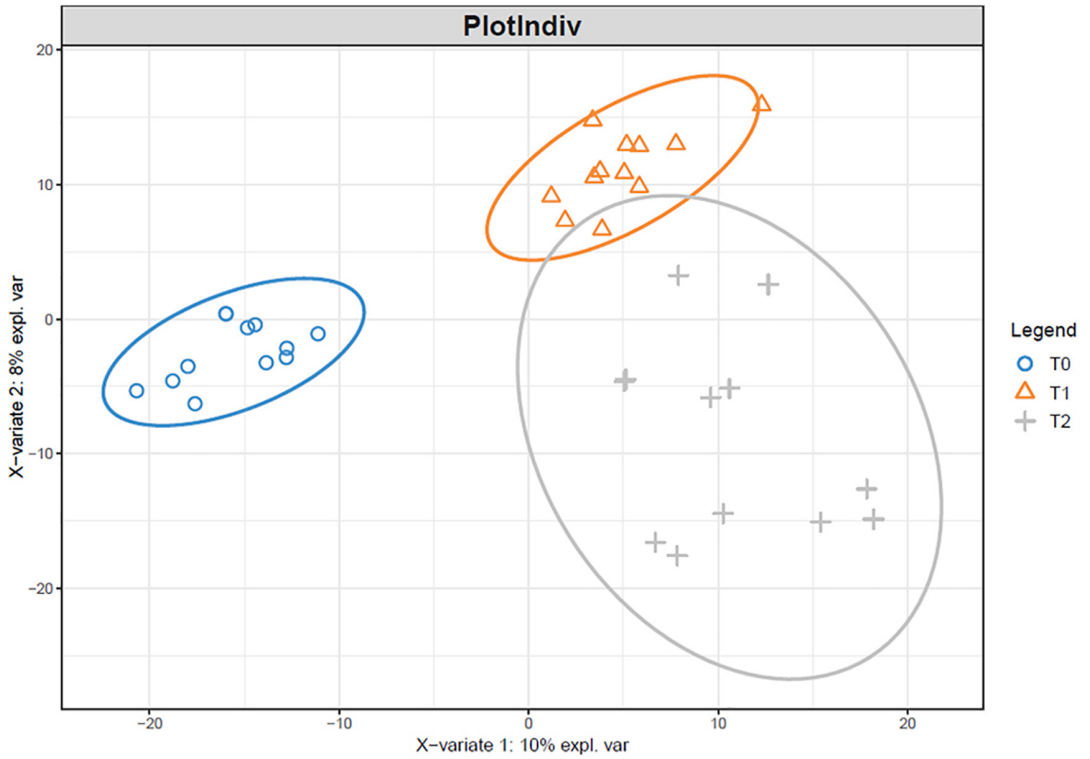

FIGURE 6 | Partial least squares discriminant analysis of the microbial communities in the tailing sand at the OTU level. T0, iron tailing sand + soil; T1, iron tailing sand + soil + *Pennisetum giganteum*; T2, iron tailing sand + soil + bio-matrix pot + *Pennisetum giganteum*.

TABLE 3 | Differentially abundant OTUs in the iron tailing sands.

	OTU	T0	T2	T0	T1	T2	Effect size
		180 d	180 d	360 d	360 d	360 d	
T1 vs T0	Unidentified *Micrococcaceae* (Actinobacteria) OTU1	181 ± 29	283 ± 64	**885 ± 85**	**494 ± 38**	213 ± 83	−5.1
	Uncultured *Xanthobacteraceae* (Proteobacteria) OTU24	49 ± 23	123 ± 22	**34 ± 7**	**126 ± 9**	102 ± 14	4.6
	Uncultured *Solirubrobacteraceae* (Actinobacteria) OTU30	30 ± 5	1 ± 2	**507 ± 247**	**10 ± 3**	7 ± 7	−5.8
	Uncultured Marine Group II (Euryarchaeota) OTU59	6 ± 4	2 ± 3	**4 ± 0**	**106 ± 10**	250 ± 63	6.1
	Rubellimicrobium (Proteobacteria) OTU115	22 ± 4	1 ± 1	**95 ± 17**	**7 ± 1**	2 ± 3	−7.0
	Uncultured *Coleofasciculaceae* (Cyanobacteria) OTU187	4 ± 3	0 ± 0	**100 ± 12**	**5 ± 2**	1 ± 1	−5.7
T2 vs T0	Uncultured *Anaerolineaceae* (Chloroflexi) OTU7	**304 ± 25**	**70 ± 14**	190 ± 27	351 ± 36	369 ± 192	−7.6
	MND1 (Proteobacteria) OTU12	**222 ± 16**	**50 ± 7**	162 ± 7	300 ± 8	214 ± 12	−7.7
	Sideroxydans (Proteobacteria) OTU31	2 ± 3	86 ± 72	**3 ± 1**	16 ± 0	**462 ± 111**	6.4
	Uncultured Marine Group II (Euryarchaeota) OTU59	6 ± 4	2 ± 3	**4 ± 0**	106 ± 10	**250 ± 63**	6.6
			T1 90 d	***T1 180 d***	***T1 360 d***		
180 vs 90 d	*Aeromicrobium* (Actinobacteria) OTU10		**112 ± 94**	**924 ± 81**	142 ± 8		9.0
360 vs 90 d	Uncultured Gitt-GS-136 (Chloroflexi) OTU22		**93 ± 14**	102 ± 59	**191 ± 2**		6.5

The taxonomic identities of the OTUs are shown at the lowest identified taxonomic level; phyla are indicated in brackets. The relative abundances considered as differentially abundant in the ANOVA-like differential expression analysis (ALDEx2) are in bold. Effect sizes were measured as the relative fold difference of the differentially abundant OTUs between treatments.

T0, iron tailing sand + soil; T1, iron tailing sand + soil + Pennisetum giganteum; T2, iron tailing sand + soil + bio-matrix pot + Pennisetum giganteum. 90 d, 180 d, and 360 d indicate the sampling time in days after the start of the experiment. The relative abundances are as mean ± standard deviation (n = 3).

content increase over time in T1 and T2, the predicted functions related to carbohydrate metabolism, C fixation in prokaryotes and photosynthetic organisms, and glycosyltransferases were on the same level at 90 days and high in T1 and T2 at 360 days (**Figure 7A**). The predicted C cycle biosynthesis and catabolism profiles were similar at 90 days (**Figures 7B,C**). The profiles of

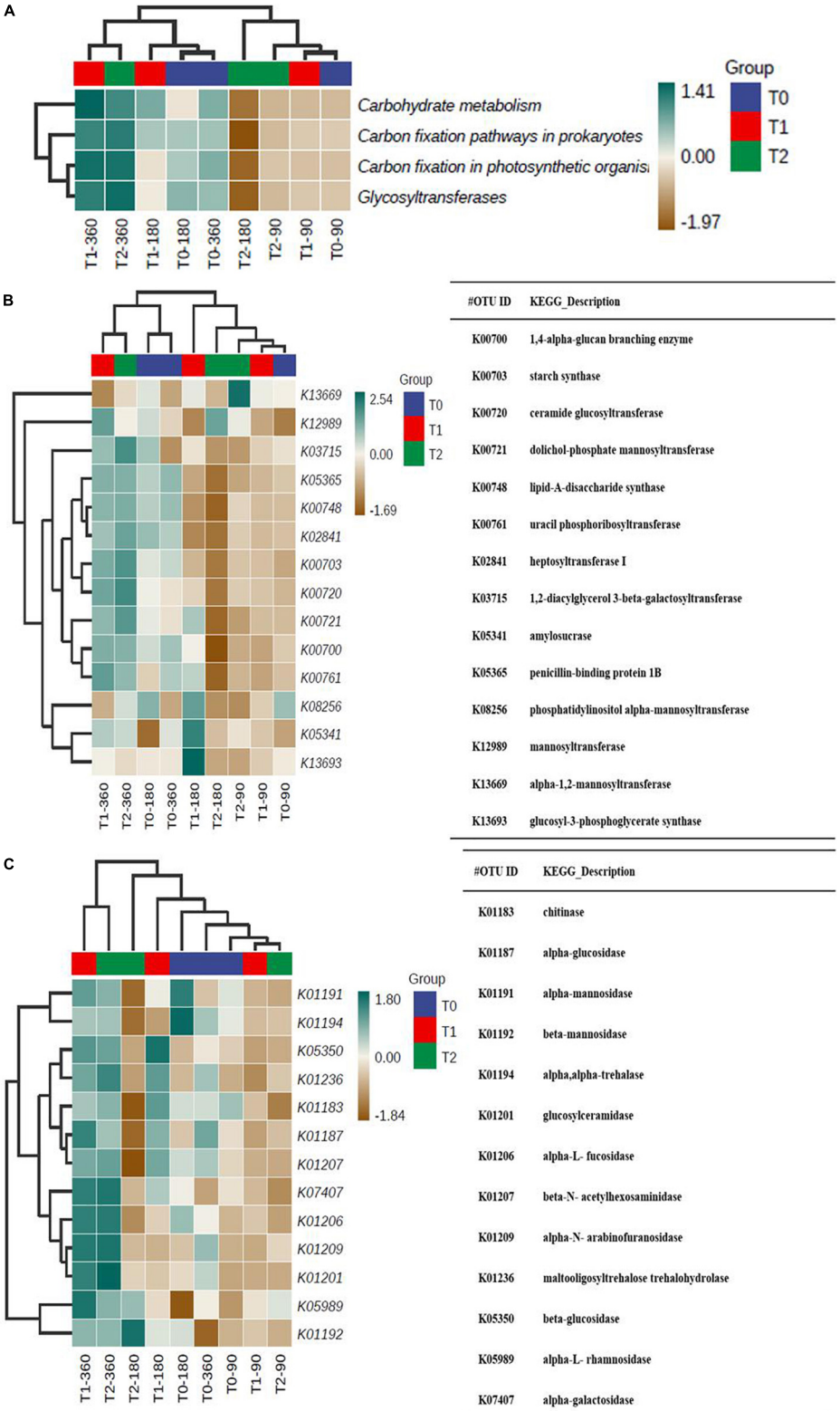

#OTU ID	KEGG_Description
K00700	1,4-alpha-glucan branching enzyme
K00703	starch synthase
K00720	ceramide glucosyltransferase
K00721	dolichol-phosphate mannosyltransferase
K00748	lipid-A-disaccharide synthase
K00761	uracil phosphoribosyltransferase
K02841	heptosyltransferase I
K03715	1,2-diacylglycerol 3-beta-galactosyltransferase
K05341	amylosucrase
K05365	penicillin-binding protein 1B
K08256	phosphatidylinositol alpha-mannosyltransferase
K12989	mannosyltransferase
K13669	alpha-1,2-mannosyltransferase
K13693	glucosyl-3-phosphoglycerate synthase

#OTU ID	KEGG_Description
K01183	chitinase
K01187	alpha-glucosidase
K01191	alpha-mannosidase
K01192	beta-mannosidase
K01194	alpha,alpha-trehalase
K01201	glucosylceramidase
K01206	alpha-L- fucosidase
K01207	beta-N- acetylhexosaminidase
K01209	alpha-N- arabinofuranosidase
K01236	maltooligosyltrehalose trehalohydrolase
K05350	beta-glucosidase
K05989	alpha-L- rhamnosidase
K07407	alpha-galactosidase

FIGURE 7 | (A) The predicted C cycle-related functions in the microbial communities in the tailing sand samples and the predicted C cycle **(B)** biosynthesis and **(C)** catabolism profiles. T0, iron tailing sand + soil; T1, iron tailing sand + soil + *Pennisetum giganteum*; T2, iron tailing sand + soil + bio-matrix pot + *Pennisetum giganteum*. 90 d, 180 d, and 360 d indicate the sampling time in days after the start of the experiment.

predicted biosynthesis functions in T1 and T2 at 360 days were relatively similar to those in T0 at 180 and 360 days (**Figure 7B**). The profiles of predicted C cycle catabolism functions in T1 and T2 at 360 days were different from those in the other communities (**Figure 7C**).

The predicted N fixation-related functions were on approximately the same level at 90 and 180 days and high in T1 and T2 at 360 days (**Figure 8A**). The predicted denitrification-related functions were on approximately the same level at 360 days (**Figure 8B**).

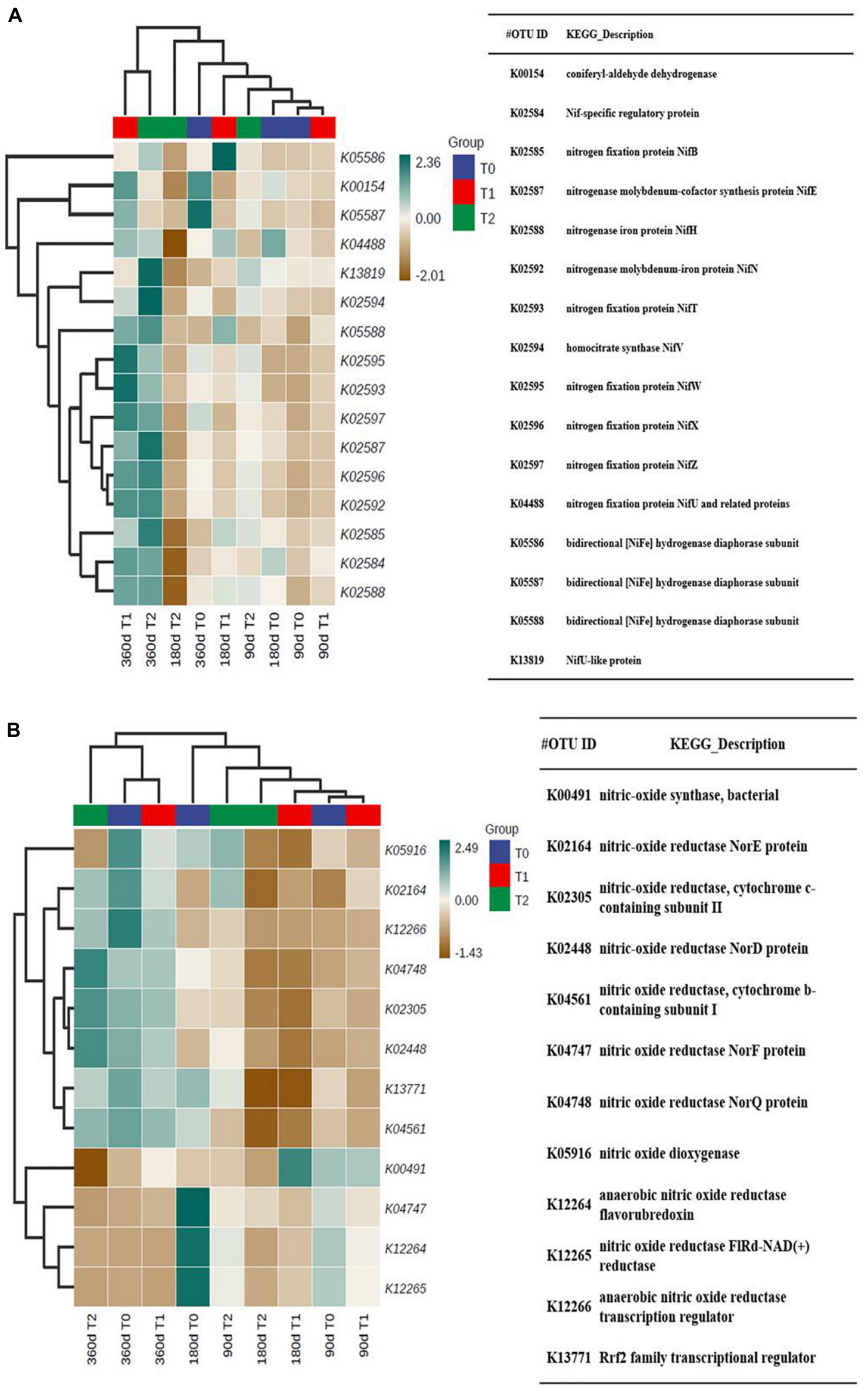

FIGURE 8 | The predicted **(A)** N fixation-related functions and **(B)** denitrification-related functions in the microbial communities in the tailing sand samples. T0, iron tailing sand + soil; T1, iron tailing sand + soil + *Pennisetum giganteum*; T2, iron tailing sand + soil + bio-matrix pot + *Pennisetum giganteum*. 90 d, 180 d, and 360 d indicate the sampling time in days after the start of the experiment.

DISCUSSION

The large mine tailing sand reservoirs are barren with no plants, making them prone to landslides and erosion. Vegetating the tailings is recommended to prevent the transfer of contaminants into surrounding environment (Khademi et al., 2018), yet it is complicated due to the poor nutrient content of the tailing sand. We investigated direct planting into tailing sand using two pit planting methods: the plants were transplanted either directly into pits filled with soil or into soil-filled bio-matrix pots made of corn and *G. lucidum*.

The results showed that *P. giganteum* grew well in the iron tailing sand, especially in the bio-matrix pot treatment (T2). The higher biomass in T2 may have been due to the *G. lucidum* polysaccharides that are known to promote the growth of cotton (Zhang et al., 2019). The OM and AN contents increased in the planted iron tailing sand in the directly-into-soil-planted treatment (T1) and T2, whereas in the not-planted soil-only treatment (T0), the contents remained on the same level, indicating that the increases were due to the roots penetrating into the sand. At the end of the experiment, the AK had increased in the planted treatments and were the highest in T2. This, together with the over two times higher biomass of *P. giganteum* in T2 than in T1, indicated that using the bio-matrix pot in planting had potential to improve the vegetation process in iron tailing sands effectively.

The physicochemical properties of soil affect the diversity and activity of bacterial communities, and in natural tailing restoration, the diversity of soil microbial communities increases along the steps (Colin et al., 2019). In our study, at the end of the experiment, the diversity was higher in the planted treatments than in T0. As for the OM and AN content, the diversity increase was probably due to the plants and not only because of the soil in the pits. The community compositions were relatively similar at 90 days and in T0 and T1 even at 180 days, implying that the community composition changed at a faster rate in T2, possibly due to the quicker build-up of OM in T2. At the end of the experiment at 360 days, all the communities were clearly separated, implying that both the planting and the planting method had contributed to the differences in composition. Consistent with previous studies (Wang et al., 2017), Proteobacteria, Chloroflexi, Acidobacteria, and Actinobacteria were the dominant phyla, indicating the microbial communities have good adaptability. In barren gold mine tailings, Actinobacteria was the dominant phylum (Sibanda et al., 2019). In tailings undergoing restoration, Proteobacteria increased along the restoration process, and the abundance of actinobacteria decreased after remediation (Wu et al., 2018; Xu et al., 2018; Yu et al., 2019). In agreement, the differentially abundant OTUs were mostly assigned into Proteobacteria and Actinobacteria. Despite the community-level differences, the number of differentially abundant OTUs was small due to the large within-treatment variation.

The effect of the treatments on soil C and N cycle-related functions was estimated based on predicted functional profiles of microbial communities. At 360 days, functions related to C cycle catabolism and N fixation were estimated to be more abundant in the planted treatments, whereas the C cycle biosynthesis and denitrification-related functions seemed to change similarly in the treatments over time. Presumably, the increase in OM content with planting explained the increase in C cycle catabolism. In copper mine tailings, the diversity of nitrogen-fixing bacteria increased along natural restoration time together with development of pioneer plant communities (Zhan and Sun, 2012; Xiao et al., 2019). The increase in predicted N fixation functions implied that both planting methods had the potential to promote further development of vegetation, which is often limited by the availability of N (Göransson et al., 2011).

CONCLUSION

The results showed that *P. giganteum* grew well in the iron tailing sand, especially in the bio-matrix pot treatment, and increased the nutrient contents, indicating that using the bio-matrix pot in planting had the potential to improve the vegetation process in iron tailing sands effectively. At the end of the experiment, the diversity of the microbial communities in the tailing sands was higher in the planted treatments. The increase in predicted N fixation functions implied that both planting methods had the potential to promote further development of vegetation.

DATA AVAILABILITY STATEMENT

The original contributions presented in the study are included in the article/**Supplementary Material**, further inquiries can be directed to the corresponding authors.

AUTHOR CONTRIBUTIONS

QC, XZ, and YL designed the research. YL, JY, and ZW performed the research. YL, YG, MM, KZ, QX, and HL analyzed the data. YL, QC, XZ, XY, and PP analyzed the data and wrote the manuscript. All authors contributed to the article and approved the submitted version.

FUNDING

This project was supported by the Key Research Project of Sichuan Province (No. 2019YFN0149) and the Subject Support Program of Sichuan Agricultural University.

ACKNOWLEDGMENTS

We would like to thank Mr. Fu Runqi for his assistance with data analysis and mapping.

SUPPLEMENTARY MATERIAL

The Supplementary Material for this article can be found online at: https://www.frontiersin.org/articles/10.3389/fmicb.2022.825660/full#supplementary-material

REFERENCES

Alfonso, P., Tomasa, O., Garcia-Valles, M., Tarragó, M., Martínez, S., and Esteves, H. (2018). Potential of tungsten tailings as glass raw materials. *Mater. Lett.* 228, 456–458.

Caporaso, J. G., Kuczynski, J., Stombaugh, J., Bittinger, K., Bushman, F. D., Costello, E. K., et al. (2010). QIIME allows analysis of highthroughput community sequencing data. *Nat. Methods* 7, 335–336.

Colin, Y., Goberna, M., Verdu, M., and Navarro-Cano, J. A. (2019). Successional trajectories of soil bacterial communities in mine tailings: The role of plant functional traits. *J. Environ. Manage.* 241, 284–292. doi: 10.1016/j.jenvman.2019.04.023

Dudeney, A. W. L., Chan, B. K. C., Bouzalakos, S., and Huisman, J. L. (2012). Management of waste and wastewater from mineral industry processes, especially leaching of sulphide resources state of the art. *Int. J. Min. Reclam. Environ.* 27, 2–37.

Edgar, R. C. (2010). Search and clustering orders of magnitude faster than BLAST. *Bioinformatics* 26, 2460–2461. doi: 10.1093/bioinformatics/btq461

Fernandes, A. D., Macklaim, J. M., Linn, T. G., Reid, G., and Gloor, G. B. (2013). ANOVA-like differential expression (ALDEx) analysis for mixed population RNA-Seq. *PLoS One* 8:e67019. doi: 10.1371/journal.pone.0067019

Galvão, J. L. B., Andrade, H. D., Brigolini, G. J., Peixoto, R. A. F., and Mendes, J. C. (2018). Reuse of iron ore tailings from tailings dams as pigment for sustainable paints. *J. Clean. Prod.* 200, 412–422.

Göransson, H., Olde Venterink, H., and Bååth, E. (2011). Soil bacterial growth and nutrient limitation along a chronosequence from a glacier forefield. *Soil Biol. Biochem.* 43, 1333–1340.

Hayat, K., Zhou, Y., Menhas, S., Bundschuh, J., Hayat, S., Ullah, A., et al. (2020). *Pennisetum giganteum*: an emerging salt accumulating/tolerant non-conventional crop for sustainable saline agriculture and simultaneous phytoremediation. *Environ. Pollut.* 265:114876. doi: 10.1016/j.envpol.2020.114876

Huse, S. M., Dethlefsen, L., Huber, J. A., Mark Welch, D., Relman, D. A., and Sogin, M. L. (2008). Exploring microbial diversity and taxonomy using SSU rRNA hypervariable tag sequencing. *PLoS Genet.* 4:e1000255. doi: 10.1371/journal.pgen.1000255

Khademi, H., Abbaspour, A., Martinez-Martinez, S., Gabarron, M., Shahrokh, V., Faz, A., et al. (2018). Provenance and environmental risk of windblown materials from mine tailing ponds. Murcia. Spain. *Environ. Pollut.* 241, 432–440. doi: 10.1016/j.envpol.2018.05.084

Kossoff, D., Dubbin, W. E., Alfredsson, M., Edwards, S. J., Macklin, M. G., and Hudson-Edwards, K. A. (2014). Mine tailings dams: Characteristics, failure, environmental impacts, and remediation. *Appl. Geochem.* 51, 229–245.

Lei, H., Peng, Z., Yigang, H., and Yang, Z. (2016). Vegetation and soil restoration in refuse dumps from open pit coal mines. *Ecol. Eng.* 94, 638–646. doi: 10.3390/ijerph17061975

Li, Q., Xiang, C., Xu, L., Cui, J., Fu, S., Chen, B., et al. (2020). SMRT sequencing of a full-length transcriptome reveals transcript variants involved in C18 unsaturated fatty acid biosynthesis and metabolism pathways at chilling temperature in *Pennisetum giganteum*. *BMC Genomics* 21:52. doi: 10.1186/s12864-019-6441-3

Louca, S., Parfrey, L. W., and Doebeli, M. (2016). Decoupling function and taxonomy in the global ocean microbiome. *Science* 353, 1272–1277. doi: 10.1126/science.aaf4507

Magoc, T., and Salzberg, S. L. (2011). FLASH: fast length adjustment of short reads to improve genome assemblies. *Bioinformatics* 27, 2957–2963. doi: 10.1093/bioinformatics/btr507

Matthew, B., and Rayens, W. (2003). Partial least squares for discrimination. *J. Chemom.* 17, 166–173. doi: 10.1016/j.nicl.2015.01.005

Oksanen, J., Blanchet, F. G., Kindt, R., Legendre, P., Minchin, P. R., O'Hara, R. B., et al. (2019). *Vegan: Community Ecology Package.* R package version 2.5-6.

Quast, C., Pruesse, E., Yilmaz, P., Gerken, J., Schweer, T., Yarza, P., et al. (2013). The SILVA ribosomal RNA gene database project: improved data processing and web-based tools. *Nucleic. Acids Res.* 41, D590–D596. doi: 10.1093/nar/gks1219

Sibanda, T., Selvarajan, R., Msagati, T., Venkatachalam, S., and Meddows-Taylor, S. (2019). Defunct gold mine tailings are natural reservoir for unique bacterial communities revealed by high-throughput sequencing analysis. *Sci. Total Environ.* 650, 2199–2209. doi: 10.1016/j.scitotenv.2018.09.380

Siddiqi, M. Y., and Glass, A. D. M. (1981). Utilization index A modified approach to the estimation and comparison of nutrient utilization efficiency in plants. *J. Plant Nutr.* 4, 289–302.

Sun, X., Zhou, Y., Tan, Y., Wu, Z., Lu, P., Zhang, G., et al. (2018). Restoration with pioneer plants changes soil properties and remodels the diversity and structure of bacterial communities in rhizosphere and bulk soil of copper mine tailings in Jiangxi Province. *China. Environ. Sci. Pollut. Res. Int.* 25, 22106–22119. doi: 10.1007/s11356-018-2244-3

Wang, L., Ji, B., Hu, Y., Liu, R., and Sun, W. (2017). A review on in situ phytoremediation of mine tailings. *Chemosphere* 184, 594–600. doi: 10.1016/j.chemosphere.2017.06.025

Wu, Z., Yu, F., Sun, X., Wu, S., Li, X., Liu, T., et al. (2018). Long term effects of Lespedeza bicolor revegetation on soil bacterial communities in Dexing copper mine tailings in Jiangxi Province. *China. Appl. Soil Ecol.* 125, 192–201.

Xiao, E., Ning, Z., Xiao, T., Sun, W., Qiu, Y., Zhang, Y., et al. (2019). Variation in rhizosphere microbiota correlates with edaphic factor in an abandoned antimony tailing dump. *Environ. Pollut.* 253, 141–151. doi: 10.1016/j.envpol.2019.06.097

Xu, L., Naylor, D., Dong, Z., Simmons, T., Pierroz, G., Hixson, K. K., et al. (2018). Drought delays development of the sorghum root microbiome and enriches for monoderm bacteria. *Proc. Natl. Acad. Sci. U.S.A* 115, E4284–E4293.

Yu, X., Kang, X., Li, Y., Cui, Y., Tu, W., Shen, T., et al. (2019). Rhizobia population was favoured during in situ phytoremediation of vanadium-titanium magnetite mine tailings dam using Pongamia *pinnata*. *Environ Pollut* 255:113167. doi: 10.1016/j.envpol.2019.113167

Zhan, J., and Sun, Q. (2012). Diversity of free-living nitrogen-fixing microorganisms in the rhizosphere and non-rhizosphere of pioneer plants growing on wastelands of copper mine tailings. *Microbiol. Res.* 167, 157–165. doi: 10.1016/j.micres.2011.05.006

Zhang, Z., Diao, H., Wang, H., Wang, K., and Zhao, M. (2019). Use of *Ganoderma lucidum* polysaccharide to control cotton *fusarium* wilt, and the mechanism involved. *Pestic. Biochem. Physiol.* 158, 149–155. doi: 10.1016/j.pestbp.2019.05.003

Conflict of Interest: HL was employed by the company CNPC Chuanqing Drilling Engineering Co., Ltd.

The remaining authors declare that the research was conducted in the absence of any commercial or financial relationships that could be construed as a potential conflict of interest.

Publisher's Note: All claims expressed in this article are solely those of the authors and do not necessarily represent those of their affiliated organizations, or those of the publisher, the editors and the reviewers. Any product that may be evaluated in this article, or claim that may be made by its manufacturer, is not guaranteed or endorsed by the publisher.

frontiers | Frontiers in Microbiology

ORIGINAL RESEARCH
published: 02 May 2022
doi: 10.3389/fmicb.2022.826635

Herbivory Protection via Volatile Organic Compounds Is Influenced by Maize Genotype, Not *Bacillus altitudinis*-Enriched Bacterial Communities

*Sierra S. Raglin[1], Angela D. Kent[1] and Esther N. Ngumbi[2]**

[1] Microbial Ecology Laboratory, Department of Natural Resources and Environmental Sciences, University of Illinois, Urbana-Champaign, Urbana, IL, United States, [2] Departments of Entomology, University of Illinois at Urbana-Champaign, Urbana, IL, United States

OPEN ACCESS

Edited by:
Diane Purchase, Middlesex University, United Kingdom

Reviewed by:
Francesco Spinelli, University of Bologna, Italy
Rob Morrison, Center for Grain and Animal Health, Agricultural Research Service (USDA), United States

***Correspondence:**
Esther N. Ngumbi
enn@illinois.edu

Specialty section:
This article was submitted to Terrestrial Microbiology, a section of the journal Frontiers in Microbiology

Received: *01 December 2021*
Accepted: *02 February 2022*
Published: *02 May 2022*

Citation:
Raglin SS, Kent AD and Ngumbi EN (2022) Herbivory Protection via Volatile Organic Compounds Is Influenced by Maize Genotype, Not Bacillus altitudinis-Enriched Bacterial Communities. Front. Microbiol. 13:826635. doi: 10.3389/fmicb.2022.826635

Belowground, plants interact with beneficial soil microbes such as plant growth-promoting rhizobacteria (PGPR). PGPR are rhizosphere bacteria that colonize roots and elicit beneficial effects in plants such as improved plant growth, pathogen resistance, abiotic stress tolerance, and herbivore protection. Treatment of plants with PGPR has been shown to trigger the emission of volatile organic compounds (VOCs). Volatile emissions can also be triggered by herbivory, termed herbivore-induced plant volatiles (HIPV), with important ramifications for chemical-mediated plant and insect interactions. Much of our current understanding of PGPR and herbivore-induced volatiles is based on studies using one plant genotype, yet domestication and modern breeding has led to the development of diverse germplasm with altered phenotypes and chemistry. In this study, we investigated if volatile emissions triggered by PGPR colonization and herbivory varies by maize genotype and microbial community assemblages. Six maize genotypes representing three decades of crop breeding and two heterotic groups were used, with four microbiome treatments: live or sterilized soil, with or without a *Bacillus* inoculant. Soil sterilization was used to delay microbiome establishment, resulting in low-diversity treatments. At planting, maize seeds were inoculated with PGPR *Bacillus altitudinis* AP-283 and grown under greenhouse conditions. Four weeks post planting, plants were subjected to feeding by third instar *Helicoverpa zea* (Lepidoptera: Noctuidae) larvae. Volatiles were collected using solid phase microextraction and analyzed with gas chromatography-mass spectrometry. Illumina NovaSeq 16S rRNA amplicon sequencing was carried out to characterize the rhizosphere microbiome. Maize genotype significantly influenced total volatile emissions, and relative abundance of volatile classes. We did not document a strong influence of microbe treatment on plant VOC emissions. However, inoculating plants with PGPR improved plant growth under sterile conditions. Taken together, our results suggest that genotypic variation

is the dominant driver in HIPV composition and individual HIPV abundances, and any bacterial-mediated benefit is genotype and HIPV-specific. Therefore, understanding the interplay of these factors is necessary to fully harness microbially-mediated benefits and improve agricultural sustainability.

Keywords: herbivore-induced plant volatile (HIPV), plant-growth promoting bacteria (PGPB), volatile organic component (VOC), *Bacillus altitudinis*, maize (*Zea mays* L.)

INTRODUCTION

Plants mount a medley of chemical defenses against insect herbivory, including indirect inducible defenses such as herbivore-induced volatile compounds (Kessler and Baldwin, 2001). Herbivore-induced plant volatile compounds (HIPV) act as chemical beacons to insect predators and parasitoids, allowing them to locate insect pests, promoting plant resilience to insect pests (War et al., 2011). Interest in HIPV utilization for insect pest management has increased in recent years, however, exploiting HIPVs for pest management requires a thorough understanding of the factors that can influence their production, composition, quality and quantity (Turlings and Erb, 2018). Recent evidence has pointed to the role of soil microbiota in HIPV production, depending on agricultural management (Malone et al., 2020). Agricultural manipulation of plant growth promoting rhizobacteria (PGPR), such as *Bacillus* species (Kloepper et al., 2004; Radhakrishnan et al., 2017), has been shown to elicit changes in plant immune response to biotic stressors, like pathogens and insects (Khan et al., 2020). As PGPR are projected to be a fundamental tool in future agricultural sustainability through conferring stress resilience without synthetic chemicals (Kenneth et al., 2019), it is important to assess conditions under which PGPR can promote herbivore resistance. *Bacillus* PGPR may interact with the plant immune system (Choudhary and Johri, 2009; Shafi et al., 2017) to mitigate herbivory, but more research is needed to explore PGPR influence on HIPV production, particularly in major agricultural crops, like maize. Identifying mechanisms of HIPV elicitation, such as the use of *Bacillus* PGPR, can support the sustainable resiliency of maize and other major field crops, reducing the adverse impacts of industrial pesticides and additives.

Numerous biochemical pathways are evoked upon insect herbivory. Leaf herbivory by chewing generalists elicits the production of various intracellular and extracellular metabolites (Ali and Agrawal, 2012). For instance, indole-derived benzoxazinoids are released intracellularly from vacuoles (Oikawa et al., 2001), and extracellularly within root exudates to modulate herbivore growth and recruit PGPR *Pseudomonas putida* to the root zone, assisting in plant defense (Neal et al., 2012). Additionally, herbivore-induced volatile compounds (HIPV) have been recognized as an indirect method of infochemical production (Maffei, 2010), recruiting parasitoids and predators of herbivores, as well as promoting conspecific priming of neighboring plants (Walling, 2000; Scala et al., 2013). Upon leaf damage, plants produce gaseous molecules, volatile organic compounds (VOCs) from numerous biochemical classes, including the oxylipin-derived jasmonates (Borrego and Kolomiets, 2016) and green-leaf volatiles (GLV), terpenoids (Arimura et al., 2009; Block et al., 2019), as well as aromatic amino acid derivates, like indole (Dudareva et al., 2004; D'Alessandro et al., 2006; Maffei, 2010). Ethylene, the first gaseous hormone discovered, is also essential in defense signaling cascades and elicitation of induced systemic resistance post-herbivory (Farag et al., 2013), solidifying the fundamental importance of volatile compounds in plant resiliency to biotic stress. HIPV blends vary by plant genotype (Gouinguené et al., 2001; Block et al., 2018). The blend itself is important for signaling, as well as changes in the abundance of specific HIPVs (Hoballah et al., 2002). As plant biochemical capacity is a function of genotype, as well as resources available for allocation and synthesis of defense metabolites, understanding plant and environmental drivers of HIPV production will reveal the bounds of their potential as novel biological control of insect pests.

Evidence suggests HIPV vary based on maize genotype (Degen et al., 2004). Landrace maize produces the sesquiterpenes (*E*)-β-caryophyllene and β-farnesene in response to oviposition by parasitoid *C. marginventris*, suggesting older varieties may respond to the presence of the parasitoid for HIPV production (Tamiru et al., 2011). Alternatively, American maize produces less (*E*)-β-caryophyllene during herbivory by *Spodoptera littorlis* and *Diabrotica virgifera vergifera* than teosinte (Köllner et al., 2008). (*E*)-β-caryophyllene attracted predators of both herbivores: leaf-chewing *Spodoptera* attracted parasitoid *C. marginventris* by producing (*E*)-β-caryophyllene in the leaves, while root pest *D. virgiferea* induced (*E*)-β-caryophyllene production only in the roots and recruited entomopathogenic nematode predators (Köllner et al., 2008). Interestingly, while the gene encoding *terpene synthase 23* (*tps23*), which produces (*E*)-β-caryophyllene, is maintained via positive selection in maize and teosinte, American maize varieties had significantly reduced transcription of *tp23*, when compared to teosinte and European maize (Köllner et al., 2008), indicating population divergence in HIPV through breeding practices. Moreover, treating maize with commercial resistance elicitors, BTH and Laminarin, reduced the production of numerous HIPV, including (*E*)-β-caryophyllene (Sobhy et al., 2012). However, this reduction was correlated with an increased attractiveness to numerous parasitoids, including *C. marginventris*, *Campoletis sonorensis*, and *Microplitis rufiventris* (Kokuiev) (Sobhy et al., 2012). Indole and aromatic HIPV production also vary significantly by genotype (Gouinguené et al., 2001). Indole has been shown to interfere with parasitoid attraction to herbivore-inflicted plants (D'Alessandro et al., 2006; Sobhy et al., 2012), and the mentioned commercial resistance elicitors reduced expression of maize

indole synthase, implying a tradeoff between indole production and parasitoid attraction (Sobhy et al., 2012). Within teosinte, sesquiterpenes (*E*)-β-caryophyllene, (*E*)-β-farnesene, and (*E*)-bergamotene, were the most significant components of the HIPV blend in *Zea mays* subsp. *parviglumis* and *Zea diploperennis*, yet *Zea mays* subsp. *mexicana* had very low variation in HIPV blends (Gouinguené et al., 2001). These results suggest that genotypic variation is a strong driver of HIPV production, producing distinct inducible volatile profiles.

Bacillus is one of the most well-documented genera of plant-growth promoting rhizobacteria (PGPR) – root-zone inhabiting bacteria which positively influence plant health through various direct (nutrient acquisition, hormone production, etc.) and indirect (pathogen exclusion, antibiosis, etc.) mechanisms (Govindasamy et al., 2010; Bhattacharyya and Jha, 2012). *Bacillus* PGPR have been proposed as sustainable agricultural inoculants to assist in the maintenance of plant growth through one or more of these pathways (Radhakrishnan et al., 2017), making them an attractive solution for highly cultivated crops, like maize (*Zea mays*). However, a major drawback of using inoculants for herbivore resistance is insuring their persistence within the dynamic diversity of the native root microbiome. When combined with genotypic and environmental variation in the root microbiome and soil reservoir, as well as plant defense pathways, the beneficial effect of *Bacillus* on insect defenses may be lost. As insect herbivory results in massive yield losses in maize globally (Miedaner and Juroszek, 2021), research should focus on the efficacy of *Bacillus* in influencing resilience against herbivores. Therefore, a major goal for the utilization of *Bacillus* inoculants in maize agricultural systems is understanding their impact on maize herbivore defense signaling, and the role of the native microbiome and plant genotypic variation in mitigating *Bacillus* plant growth promoting activity.

Bacillus are gram-positive endospore forming bacteria known for their ability to withstand various environmental stressors, such as UV irradiation and desiccation, making them an attractive target for field-scale inoculation for plant growth promotion (Radhakrishnan et al., 2017). Numerous genera of *Bacillus* have been implicated in growth promotion. Plant-growth promoting *Bacillus* inoculants have been reported to confer abiotic stress tolerance, *e.g.,* resistance to salinity, drought, and heavy metals, to various crops species, including maize (*Zea mays*) and wheat (*Triticum aestivum*) (Sun et al., 2017; de Lima et al., 2019; Elfira et al., 2020; Yue et al., 2021). In addition to abiotic stress, *Bacillus* PGPR species can act as biocontrol agents against biotic stress from pathogens and pests (Yan et al., 2002; Lu et al., 2017). *Bacillus* can directly act as biocontrol agents by producing hydrolytic enzymes or antimicrobial agents, suppressing pathogen growth and survival (Hashem et al., 2019). Antagonistic effects against biotic stressors have been reported with numerous *Bacillus* species, such as *Bacillus subtilis*, *B. amyloliquefaciens*, and *B. altitudinis* (Chowdhury et al., 2015; Sunar et al., 2015; Shafi et al., 2017). Indirect methods of biocontrol occur through the production of various plant hormones, like indole-acetic acid, ethylene, and salicylic acid (Patten and Glick, 1996; Ali et al., 2015). Additionally, *Bacillus* species have been recorded modifying the activity of metabolic pathways involved in defense metabolite synthesis. Endophytic *Bacillus altitudinis* modifies transcriptional expression of numerous defense-related genes, like phenylalanine ammonia lyase and phenol oxidase (Hasan et al., 2020). Recent research has also suggested the influence of bacterial volatile compounds (BVCs) in plant response to biotic stressors, the effects of which are due to various mechanisms like direct inhibition of insect or pathogen growth, or modification of plant defense pathways (Cellini et al., 2021). The stimulation of defense-related gene expression by plant growth promoting bacteria is referred to induced systemic resistance (ISR; Kloepper et al., 2004). Interactions between *Bacillus* inoculants and plant immune pathways prime plant defenses for rapid response to herbivore damage.

Modifying microbiomes for plant growth and yield is an attractive solution for maximizing agricultural sustainability but the efficacy of microbial inoculants is under thorough investigation. This is particularly important for complex tri-trophic ecological interactions, such as parasitoid/predator recruitment through HIPV production. Evidence suggests that agricultural management that alters plant-soil feedbacks, such as companion cropping or cover cropping, can alter production or composition of plant defense compounds and herbivore response (Mutyambai et al., 2019; Wang et al., 2019). Pangesti et al. (2015) recorded the release of (E)-α -bergomatene during *Pseudomonas fluorescens* colonization of *Arabidopsis thaliana* roots, which increased recruitment of parasitic wasp *Microplitis mediator* to herbivore-infested leaves (Pangesti et al., 2015). However, the specific contributions of plant-growth promoting *Bacillus* to indirect inducible defense signaling are unknown. *Bacillus altitudinis* has be recorded displaying plant beneficial activity through growth promotion (seed yield and phenology) in maize (Elfira et al., 2020; Zhang et al., 2021). Zhang et al. (2021) reported maize inoculated with *B. altitudinis* showed increased fresh weight (g) and size (Zhang et al., 2021). In *Miscanthus x giganteus* and wheat (*Triticum aestivum*), *B. altitudinis* maintained biomass yield during growth in metal contaminated soils (Pranaw et al., 2020; Yue et al., 2021). *B. altitudinis* application upregulated stress tolerance genes in numerous plant species, like phenylpropanoid and lipoxygenase synthesis genes (Yue et al., 2021; Zhang et al., 2021), and produces indole acetic acid (Sun et al., 2017), indicating it has the capacity to modulate biochemical pathways important for inducible defense metabolite production. However, it is currently unknown if *B. altitudinis* has the capacity to modify herbivore-induced plant volatiles (HIPV), and if its preferred functions are observable within the rhizosphere microbiome. Moreover, as evidence suggests maize genotype is a strong driver of HIPV composition (Gouinguené et al., 2001), it is important to assess the beneficial functions of PGPR across genotypes. Therefore, the purpose of this research is to understand how the rhizosphere microbiome and maize genotype influence the abundance and composition of HIPV, and if the addition of *B. altitudinis* distinctly modifies the induced volatilome.

MATERIALS AND METHODS

Seed Selection and Preparation

Maize (*Zea mays* L. subsp. *mays*) seeds were obtained from the USDA North Central Region Plant Introduction Station (Ames, Iowa). Six inbred maize genotypes (**Table 1**), within two heterotic groups (Stiff Stalk and Non-Stiff Stalk), were chosen for this study. Genotypes were chosen to represent eras which span US pesticide usage during the Green Revolution.

Seeds were rinsed with sterilized deionized (DI) H_2O, washed briefly with 70% ethanol, soaked in 1.5% NaClO solution for 5 minutes, followed by 5 additional DI H_2O rinses. Sterilized seeds were germinated on sterile petri dishes, lined with autoclaved filter paper, within incubation chambers set at 25°C, without supplemental lighting.

Plant Growth Conditions

Seeds were sown in 16.51 cm Azalea pots with steam-sterilized Berger BM7 45% soilless mix (Composted pine bark, coarse peat moss, parboiled rice hulls, dolomitic and calcitic limestone) and grown for 30 days. Three seeds were planted per pot, and thinned to one plant per pot after emergence. The soilless mix was inoculated with a 10% field soil, which was air-dried and sieved (2 mm), prior to incorporation with the planting medium. Field soil was collected from a secondary successional field, to avoid agricultural legacy effects on the microbial community. Soil treatments (sterilization and inoculation) are described below. Plants were grown at 25°C, with 16L:8D photoperiod, and watered via an automatic irrigation system, as needed. Fertilizer was applied as 20-20-20 NPK plus micronutrients fertilizer weekly. The pots were set up in a randomized block design within the greenhouse, with block as a random effect, and transported to an entomology greenhouse for herbivore application and HIPV collection prior to destructive soil sampling.

Plant Growth-Promoting Rhizobacteria Selection and Application

Bacillus altitudinis strain AP-283 was obtained from Auburn University. AP-283 was chosen from a collection of *Bacillus* PGPR selected based on their capacity to promote growth of maize (Calvo et al., 2017), and to induce emission of VOCs in cotton and maize (Kloepper et al., 2013) and confer herbivory protection in maize (Disi et al., 2018a,b).

TABLE 1 | Maize genotypes used during this study.

Genotype	Heterotic Group	Decade
B14*	Iowa Stiff Stalk	1950s
B73	Iowa Stiff Stalk	1970s
PHJ40	Iowa Stiff Stalk	1980s
OH43	Non-Stiff Stalk	1940s
Pa91	Non-Stiff Stalk	1970s
PHG84	Non-Stiff Stalk	1980s

Asterisk denotes genotypes which had insufficient germination and were removed from all analyses.

Bacillus altitudinis strain AP-283 was grown on tryptic soy agar (TSA) plates and diluted in sterile distilled water to achieve a final OD_{600} of 1.0. Each planted seed received aliquots of 1mL AP 283 solution at planting. Following thinning, each plant received 1mL weekly for 4 weeks, to ensure artificial persistence of AP-283.

To explore the synergistic role of the soil microbiome and *Bacillus altitudinis* inoculant in herbivory resistance, four microbial treatments (n = 5) were applied to each maize genotype: *Bacillus* with sterilized soil (BS), *Bacillus* with 10% live microbiome inoculum (BL), live microbiome inoculum without *Bacillus* (L), and sterilized soil without *Bacillus* or live soil inoculum (S). In addition to steam sterilization, the Berger BM7 soil mixture + 10% field soil inoculum (BS and S treatments) was sterilized three times for one hour, each, in the autoclave, for a total of 3h. Sterilization was used to significantly reduce rhizosphere microbial diversity and delay rhizosphere microbiome establishment, as maintaining sterilization in a greenhouse setting is non-plausible.

Herbivory Treatment

Corn earworm (*Heliocoverpa zea*) was selected for the induction of herbivore-induced volatile compounds (HIPV). Third instar larvae were purchased from Benzone Research (Carlisle, PA, United States). Insects were starved for 6 h before feeding on corn plants to induce the emission of volatiles. Four larvae per plant were used. Larvae were gently transferred onto maize plants whorls. Larvae fed for 24 h prior to volatile collection.

Herbivore-Induced Volatile Compound Collection and Analysis

Solid phase micro extraction (SPME) fiber coated with poly dimethyl siloxane-divinyl benzene (PDMS/DVB, 65 μm) purchased from Supelco (Bellefonte, PA, United States) was used to collect herbivore-induced volatile organic compounds following protocols similar to those reported by Ngumbi and Ugarte (2021). One hour prior to headspace volatile collection, maize plants were wrapped with an odor-blocking oven plastic bag (Arcadia INTL, EL Monte, CA), to allow for volatile concentration. One hour later, the SPME was introduced into the sealed plant through an insertion space created with thin forceps. The SPME fiber was exposed and the headspace volatiles (VOCs) were collected for 40 minutes. Immediately after VOCs collection, the fiber was injected into a Hewlett-Packard (HP) 6890 GC (Hewlett-Packard, Sunnyvale, CA, United States) in splitless mode, interfaced to an HP 5973 mass-selective detector (MSD), with helium carrier gas. The column was programmed from 40°C/2 min, with increases by 5°C/min to 200°C. Injector and transfer line temperatures were set at 200°C. Identification of peaks was done by using NIST 98 library (National Institute of Standards and Technology, Gaithersburg, Maryland) and by comparing with published GC profiles of maize head space volatiles (Thompson et al., 1971; Loughrin et al., 1994; McCall et al., 1994; Gouinguené et al., 2001; Pinto-Zevallos et al., 2016; Ngumbi and Ugarte, 2021). The structures of the identified volatile compounds were confirmed using commercially available

synthetic standards with purity > 97% (as indicated on the labels) obtained from Sigma® Chemical Co. (St. Louis, Missouri).

Soil and Plant Sampling

After thirty days of growth, maize plants were destructively sampled by removing the entire root zone from their corresponding pots. Aboveground biomass was removed, weighed, and oven dried. Root systems were stored at 4°C until cleaning, followed by thorough rinsing and oven drying. Root:shoot ratio was quantified using dry root biomass and dry aboveground biomass. Soil adhering to the roots, hereafter rhizosphere soil, was collected in bags and briefly stored at 4°C until processed. The rhizosphere soil was then mechanically mixed, and put into 15 mL centrifuge for lyophilization, then frozen at −20°C while awaiting DNA extractions.

DNA Extractions

Fifty milligrams of freeze-dried soil were weighed into microcentrifuge tubes for DNA extractions on the QiaCUBE HT DNA extraction robot (Qiagen, Germany), using the Qiagen DNAEasy soil extraction kit and protocol. The Qiagen DNAEasy soil kit does not require DNA cleaning with CTAB. Immediately prior extractions, DNA was frozen at −20 °C while awaiting Qubit and NanoDrop quantification. Genomic DNA was submitted to the Roy J. Carver Biotechnology Center at the University of Illinois Urbana-Champaign (Urbana, IL) for 16S rRNA Amplicon Sequencing.

16S rRNA Amplicon Sequencing and Sequence Processing

Illumina NovaSeq was used for 16S rRNA amplicon sequencing, conducted at the Roy J. Carver Biotechnology Center (Urbana, IL) to assess the contributions of microbe treatments on HIPV relative abundance and composition. 16S rRNA gene amplicon sequencing used the 515F (5′-GTGYCAGCMGCCGCGGTAA-3′) and 806R (5′-GGACTACVSGGGTATCTAAT-3′) primers to amplify the V4 region of the prokaryotic 16S rRNA gene (Caporaso et al., 2011). The DNA sequencing and bioinformatics workflow has been previously detailed in Favela et al. (2021). Briefly, forward and reverse paired-end sequences were merged using Fast Length Adjustment of Short reads (FLASH) software (Magoč and Salzberg, 2011). Once merged, reads were filtered using a minimum quality score of 30 for 90% of removed bases via the FASTX-Toolkit (Gordon and Hannon, 2010). FASTQ reads were then converted to FASTA format. Sequences were binned based on 97% similarity into operational taxonomic units (OTUs) using USEARCH version 8.1.1861 (Edgar, 2010). Quantitative Insights into Microbial Ecology (QIIME) was used solely used to generate an OTU table and to assign taxonomy for downstream analyses in R (Kuczynski et al., 2011). After OTU taxonomic assignment, mitochondrial and chloroplast OTUs were removed. The OTU table was rarefied and singleton OTUs were removed prior to statistical analyses. One outlier sample was removed due to low read counts. Results from amplicon sequencing are reported in the supplemental information. Amplicon sequence data for 16S rRNA genes is available for download on the NCBI SRA database at BioProject accession number PRJNA785015.

TABLE 2 | Ranking of Importance of 36 identified herbivore-induced volatile compounds (HIPV) based on maize genotype and rhizosphere microbiome treatment.

Ranking	HIPV	MDA
1	Methyl salicylate	39.084279
2	(E)-4,8-dimethyl-1,3,7-nonatriene*	26.724274
3	Caryophyllene	24.240676
4	trans-Geranylgeraniol	23.811890
5	Linalool	22.880034
6	β-Myrcene	22.070551
7	trans-α-Bergamotene	19.432684
8	epi-Bicyclosesquiphellandrene	16.791102
9	Germacrene D	16.057696
10	D-Limonene	15.561633

*A Random Forest decision tree was used and rankings were determined using Mean Decrease Accuracy (MDA). *Previously identified as (E)-2-Butenoic acid, 2-(methylenecyclopropyl)prop-2-yl ester (Xavier et al., 2011).*

Statistical Analyses

All statistical analyses were performed in R Studio statistical software (Version 4.1.2, 2021) (R Core Team, 2021; Venables et al., 2021). All figures were produced using *ggplot2* v. 3.3.5 (Wickham, 2016). The influence of genotype and microbiome treatment (BS, S, L, BL) on plant growth parameters (root dry biomass, above ground dry and wet biomass, root:shoot), were assessed using two-way mixed effects model, with block as a random effect using the *lme4* package v. 1.1-27 (Bates et al., 2015). B14, a stiff stalk genotype used in this study, had incomplete germination and was excluded from HIPV analyses. Due to this, there is an unbalanced design when comparing heterotic groups, with the Non-Stiff Stalk containing three genotypes, while the Stiff Stalk heterotic group contains only two genotypes. The influence of heterotic group was, therefore, ignored for the remainder of the analyses. Conditional (variance explained by the full model) and marginal (variance explained by fixed effects) coefficients of determination (R^2_c, and R^2_m, respectively) were calculated using the r.squaredGLMM() function of the *MuMIn* package v. 1.43.17 (Barton, 2020).

The interaction of genotype and microbiome treatment on the relative abundance of HIPV compounds classes, as well as individual HIPV compounds, was also assessed using a mixed effects ANOVA. The major compound classes were as follows: sesquiterpenes, monoterpenes, green leaf volatiles, esters, ketones, alkane hydrocarbons, diterpene alcohols, benzoate esters, and other. A Random Forests model using package *randomForest* v 4.6-14 was used to rank individual volatile compounds by importance (Ngumbi and Ugarte, 2021). The top ten compounds are shown in **Table 2** with Mean Decrease Accuracy (MDA) scores, and the top five are visualized in **Figure 1**. Two-way mixed effects ANOVAs were then used to assess influence of genotype and microbe on top HIPV

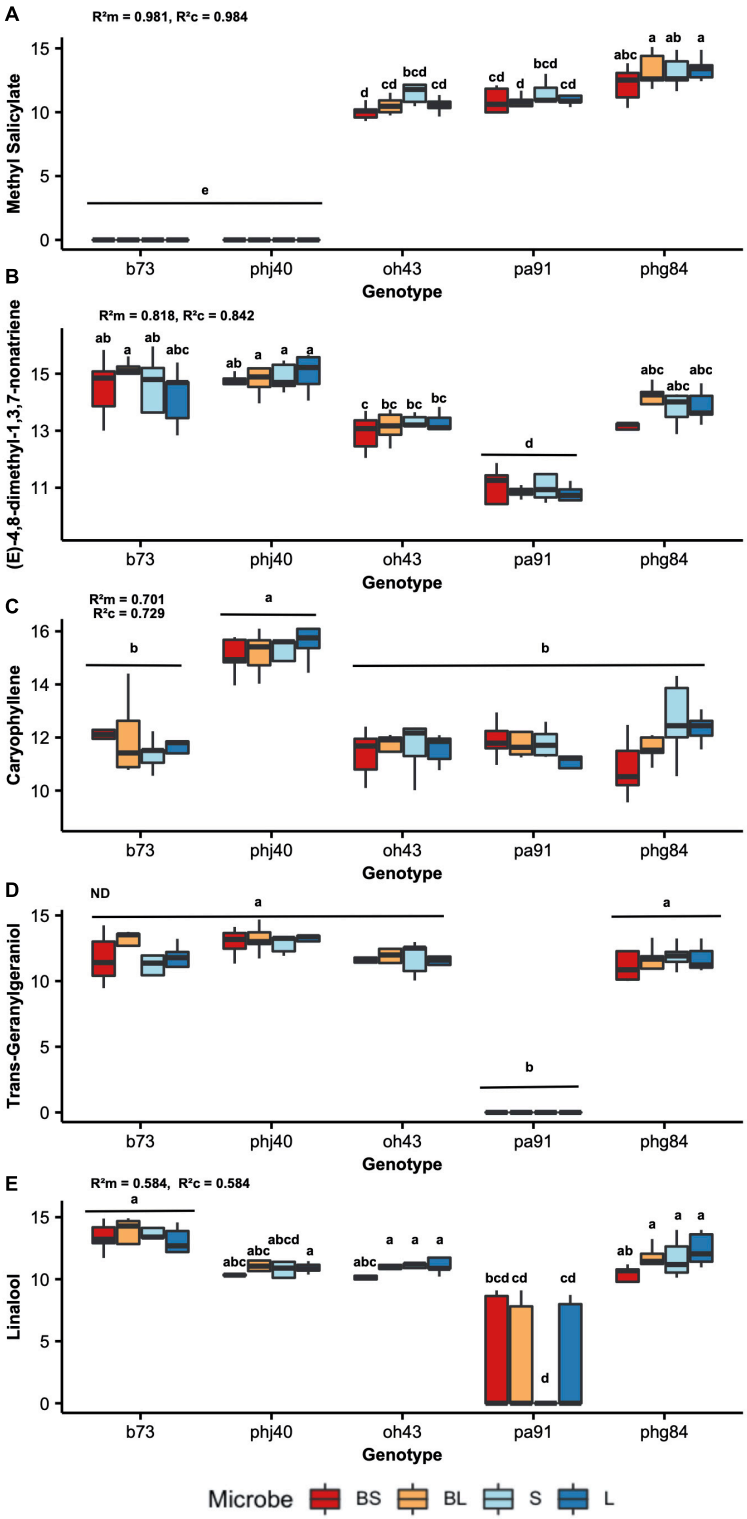

FIGURE 1 | Individual herbivore-induced volatile compound (HIPV) quantities by maize genotype (*x*-axis) and microbe treatment (color, see key on bottom). Random forest model was used to rank individual HIPV based on importance (using MDA score). Peak area quantities were log10 + 1 transformed to assume normality. Tukey's honestly significant difference was used to group means, the results of which are denoted on each boxplot. 2-Way ANOVA coefficients of determination (conditional and marginal, R^2_c, and R^2_m, respectively) are indicated on each graph: **(A)** Methyl salicylate, **(B)** (E)-4,8-dimethyl-1,3,7-nonatriene, **(C)** caryophyllene, **(D)** Trans-Geranylgeraniol, and **(E)** linalool are shown. Coefficient of determination of Trans-Geranylgeraniol is not shown, due to violations of assumptions (denotes with "ns").

compounds. Shapiro-Wilk test was used to identify deviations in residual variances of all models and calculated with the shapiro test function of the *stats* package v. 4.1.1.; $W > 0.9$ was used to indicate normally distributed residual variances. Levene's Test for homogeneity of variances across microbiome and genotype groups was calculated using Levene Test function of the *car* package v. 3.0-11. Type III analysis of variance table with Satterthwaite's method is reported in **Tables 1**, **3** by using the anova function of the *stats* package v. 4.1.1 (R Core Team, 2021). Data was $\log_{10}$ transformed to assume normality, where required. Means were separated using Tukey's honestly significant difference test using the HSD.test function from the *agricolae* package v. 1.3-5 (De Mendiburu, 2021), for plant parameters and total HIPV models.

The composition of HIPV compounds was assessed using a non-metric dimensional analysis (NMDS) on the Bray-Curtis's dissimilarity matrix created from the volatiles profile (Ngumbi and Ugarte, 2021) to understand how the overall blend of HIPV changes with genotype and microbiome treatment, using the metaMDS function of the *vegan* package v. 2.5-7 (Oksanen et al., 2020). PERMANOVA was conducted using the adonis function in *vegan* to identify significant contributions of genotype and microbiome treatment on HIPV blend. The contributions of plant data (root, dry and wet aboveground biomass, and root:shoot ratio), as well as microbial richness (observed, chao1, Shannon diversity index) to HIPV composition was assessed using the envfit function within the *vegan* package v. 2.5-7.

To better understand the influence of the microbiome on HIPV, a Mantel test was used to identify Spearman correlations between the 16S rRNA dissimilarity and HIPV dissimilarity matrices, using Bray-Curtis distances. The bacterial 16S rRNA OTU table was Hellinger transformed, prior to the construction of a Bray-Curtis dissimilarity matrix, and the Mantel test was conducted using the *vegan* package v. 2.5-7 in R, with 9999 permutations.

RESULTS

Treatment Influence on Plant Growth Parameters

Results of two-way mixed effects models are reported in **Tables 3**, **4**. Microbiome treatment (BS, BL, L, S) and genotype impacted plant growth. Dry root biomass and root:shoot (R:S) ratio was significantly influenced by the interaction between genotype and microbiome (**Figure 2**), indicating the genotypic influence on root investment varies based on the available soil microbiota (**Table 3**). Microbe ($P << 0.01$) treatment and genotype ($P < 0.02$) impacted aboveground investment (wet and dry biomass), as well, but independently (**Figure 3**).

Herbivore-Induced Volatile Compounds

A total of 36 volatile compounds were detected following by corn ear worm (*Heliocoverpa zea*) feeding on five maize genotypes (B73, PHJ40, OH43, PHG84, PA91) under four microbiome treatments: live soil (L), sterile soil (S), *Bacillus altitudinis* AP-283 applied to sterile soil (BS), and *B. altitudinis* AP-283 applied to live soil (BL). The detected HIPV were classified as ketone (cyclopentanone, 2-ethylcyclopentanone, [1,1′-bicyclopentyl]-2-one), monoterpenes (β-myrcene, D-limonene, trans-β-ocimene, γ-terpinene, linalool), sesquiterpenes (α-cubebene, α-muurolene, ylangene, α-copaene, β-bourbonene, α-sesquiphellandrene, cis-muurola-3,5-diene, caryophyllene, epi-bicyclosesquiphellandrene, trans-α-bergamotene, humulene, (*E*)-β-farnesene, β-copaene, γ-muurolene, germacrene D, β-guaiene, trans -γ-cadinene, σ-cadinene), alkane hydrocarbons (heptadecane, pentadecane), diterpene alcohol (trans-geranylgeraniol), benzoate ester (methyl salicylate), ester ((*E*)-4,8-dimethyl-1,3,7-nonatriene)), green leaf volatile (3-hexen-1-ol,acetate (*Z*)), and other (bicyclopentyl-1,1′-diene, 4-cyanocyclohexene).

TABLE 3 | Type III analysis of variance table with Satterthwaite's method of treatment (Genotype, Microbe) on plant growth parameters (root biomass, dry aboveground biomass, wet aboveground biomass, and root:shoot ratio).

Fixed Effects	SS	MS	DF	*F*-Value	R^2_m	R^2_c
Root: Shoot					0.4859034	0.5211005
Microbe***	2.9203	0.97343	3	17.3425		
Genotype***	1.3154	0.32885	4	5.8588		
M x G*	1.5532	0.12943	12	2.3060		
Dry Shoot Biomass (g DW)					0.231221	0.3526322
Microbe**	19.736	6.5787	3	4.8403		
Genotype*	16.007	4.0018	4	2.9444		
M x G	11.872	0.9894	12	0.7279		
Wet Shoot Biomass (g)					0.2900259	0.4952666
Microbe**	1766.28	441.57	3	6.6632		
Genotype***	1025.07	341.69	4	5.1560		
M x G	981.68	81.81	12	1.2344		
Root Biomass (g DW)					0.6328723	0.6328723
Microbe***	208.14	69.379	3	26.2236		
Genotype***	123.26	30.814	4	11.6471		
M x G ***	114.21	9.517	12	3.5973		

*Dependent variable is bolded above model fixed effects. Asterisk denote factor significant: P = 0 '***'; 0.001 '**'; 0.01 '*'; 0.05 '.'; Marginal (Fixed Effects) and Conditional (Full Model) coefficients of determination for each model are reported.*

TABLE 4 | Type III analysis of variance table with Satterthwaite's method of treatment (Genotype, Microbe) on HIPV compound classes and total HIPV.

Fixed Effects	SS	MS	DF	*F*-Value	R^2_m	R^2_c
Total HIPV					0.5355116	0.5576677
Microbe·	1.0988e+14	3.6626e+13	3	2.5823		
Genotype***	1.4381e+15	3.5953e+14	4	25.3481		
M x G	1.6484e+14	1.3737e+13	12	0.9685		
Sesquiterpene					0.4697384	0.5417335
Microbe	0.00992	0.00331	3	0.1655		
Genotype***	1.82507	0.45627	4	22.8503		
M x G	0.15548	0.01296	12	0.6489		
Ketone					0.4066252	0.4661853
Microbe	0.01257	0.004188	3	0.2905		
Genotype***	0.93408	0.233521	4	16.1971		
M x G	0.12900	0.010750	12	0.7456		
Alkane Hydrocarbon					–0.3468411	–0.4022934
Microbe	0.0002141	0.00007137	3	0.8857		
Genotype***	0.0038702	0.00096755	4	12.0080		
M x G	0.0004780	0.00003983	12	0.4944		
Monoterpene					0.4440484	0.4837898
Microbe	0.00532	0.001773	3	0.1914		
Genotype ***	0.73526	0.183815	4	19.8433		
M x G	0.03615	0.003013	12	0.3252		
Green Leaf Volatile					0.3861213	0.4044357
Microbe	0.0011729	0.00039098	3	1.4911		
Genotype***	0.0106452	0.00266130	4	10.1494		
M x G	0.0047923	0.00039936	12	1.5230		
Ester					0.535072	0.6271043
Microbe	0.00211	0.000704	3	0.0908		
Genotype***	1.06662	0.266655	4	34.4277		
M x G	0.02088	0.001740	12	0.2246		
Benzoate Ester°						
Diterpene Alcohol§					0.2894044	0.4427281
Microbe	0.0002044	0.00006815	3	0.6577		
Genotype***	0.0047449	0.00118624	4	11.4494		
G x M	0.0003418	0.00002849	12	0.2749		
Other					0.3437729	0.41034
Genotype***	0.0043783	0.0010946	4	11.6835		
Microbe	0.0001560	0.0000520	3	0.5550		
G x M	0.0007644	0.0000637	12	0.6799		

*Dependent variable is bolded above model fixed effects. Asterisk denote factor significant: P = 0 '***'; 0.001 '**'; 0.01 '*'; 0.05 '·'; Marginal (Fixed Effects) and Conditional (Full Model) coefficients of determination for each model are reported.* § *= dependent variable was log10 transformed to assume normality.* ° *= denotes models which violated assumptions after transformations.*

Treatment Influence on Herbivore-Induced Volatile Compounds

Non-metric multidimensional scaling analysis of the HIPV Bray-Curtis dissimilarity matrix revealed strong clustering due to genotype (**Figure 4**). PERMANOVA analyses confirmed that genotype strongly influenced NMDS structure (**Table 5**, $R^2 = 0.47466$, $P = 0.001$). Microbe treatment, via manipulation of the microbial community within the potting mix via sterilization (sterile vs. live) and the addition of *Bacillus altitudinis* strain AP-283, did not significantly influence HIPV composition, determined via PERMANOVA, and did not significantly interact with genotype (**Supplementary Figures 1-3**). This was further supported with non-significant results of the Mantel test ($r = -0.05$, $P = 0.965$), indicating no correlation between HIPV and bacterial 16S rRNA Bray-Curtis distance matrices.

The envfit function in the *vegan* package was used to identify continuous variables that were correlated to NMDS structure (**Figure 4**). Root dry biomass (R = 0.09, $P = 0.011$), shoot wet biomass (R = 0.175, $P = 0.001$), and shoot dry biomass (R = 0.099, $P = 0.011$) significantly influenced NMDS structure. Microbial community richness (Chao1, and Observed) and evenness (Shannon) did not significantly drive NMDS structure. Root:shoot ratio nearly correlated to NMDS structure (R = 0.059, $P = 0.060$).

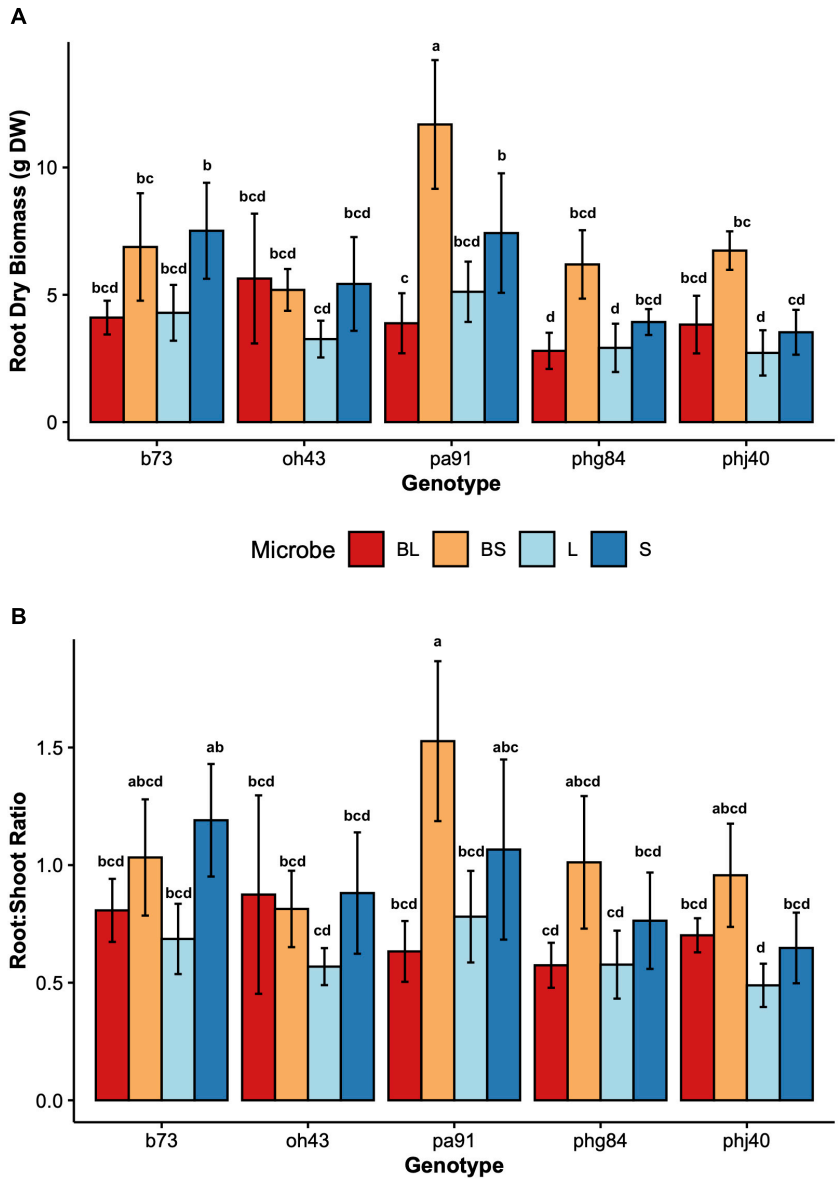

FIGURE 2 | Root growth parameters by maize Genotype (B73, PHJ40, Pa91, OH43, PHG84) and Microbe treatment: Bacillus+Live soil (BL), Bacillus+Sterile soil (BS), Sterile soil (S), Live soil (L). **(A)** Dry root biomass in grams dry weight after washing and oven drying; **(B)** ratio of below to aboveground biomass, root:shoot ratio. Bars represent mean ± 2 SEM. Mean separation groups from Tukey's honestly significant difference test placed above SEM bars.

The total HIPVs produced (**Figure 5A**), and relative abundance of HIPV (**Figure 5B**) compound classes were significantly influenced by maize genotype (**Table 4**). Microbe treatment was significant in influencing total HIPV production (F = 2.5823, P = 0.05). Model summary identified a significant influence of the PHJ40 genotype in live soil (P = 0.01065) on total HIPV produced. All compound classes (monoterpenes, sesquiterpenes, esters, benzoate esters, ketones, green leaf volatiles, diterpene alcohols, alkane hydrocarbons, and other) were significantly influenced by genotypes. Relative abundances were not influenced by microbial treatment (**Table 4**). Benzoate Ester model was inconclusive due to violations of assumptions, even after data transformations.

Results of Random Forest model ranking of importance are reported in **Table 2**. Methyl salicylate was ranked as number one, based on MDA scores. Two-way mixed effects ANOVA results are reported in **Table 6**, for the top 10 ranked individual HIPV. Unfortunately, due to violations of ANOVA assumptions, trans-geranylgeraniol, β-myrcene, trans-α-bergamotene model results are not reported. Plant genotype significantly influenced all ranked individual volatiles ($P < 0.001$, **Table 6**). Only methyl salicylate was weakly influenced by microbe treatment ($P = 0.03$). Interestingly, methyl salicylate was not detected from B73 or

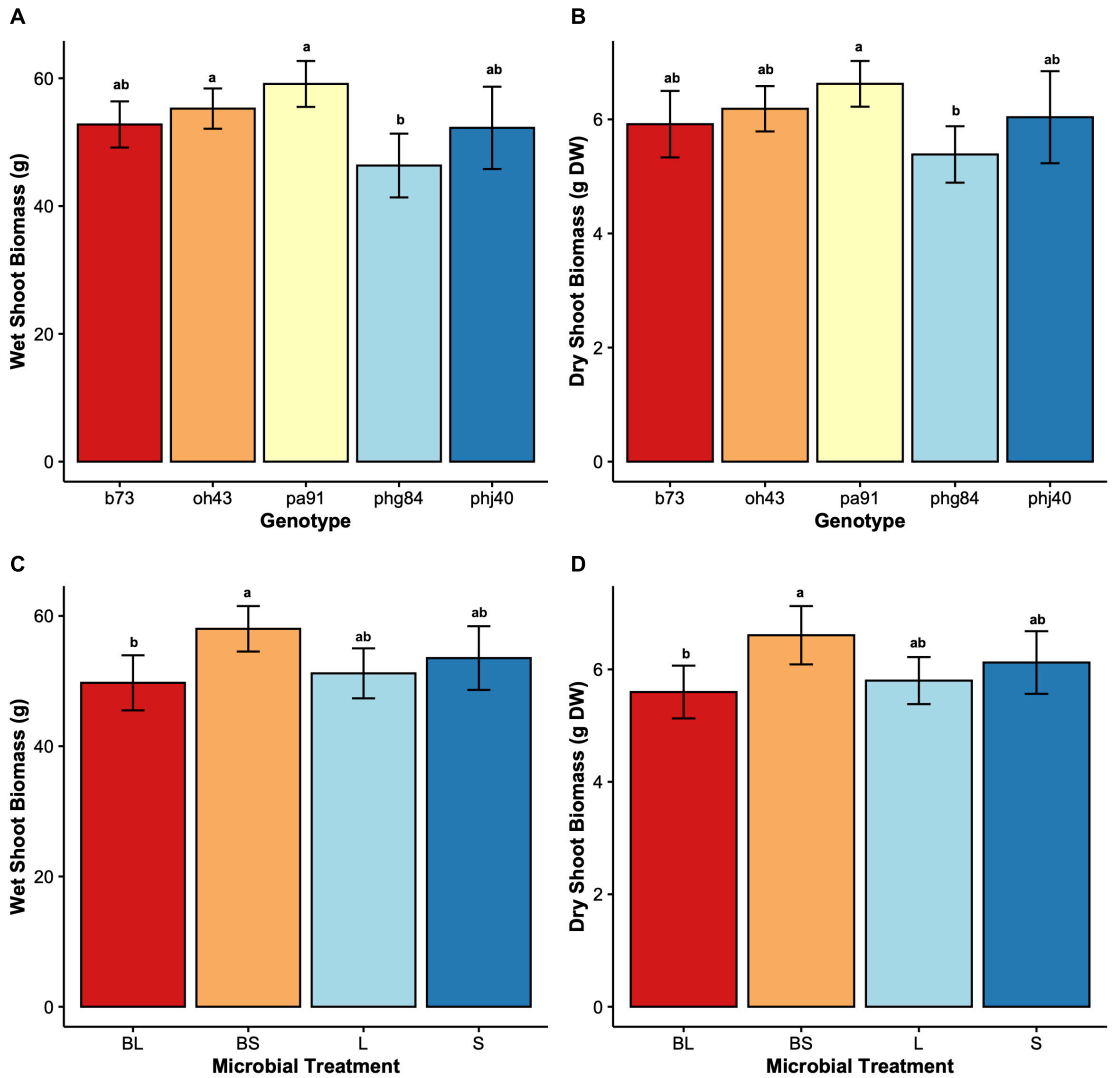

FIGURE 3 | Shoot growth parameters by Genotype (B73, PHJ40, Pa91, OH43, PHG84) and Microbe treatment: Bacillus+Live soil (BL), Bacillus+Sterile soil (BS), Sterile soil (S), Live soil (L). **(A)** wet shoot biomass in g wet weight, displayed by Genotype; **(B)** dry shoot biomass in grams dry weight after oven drying, displayed by Genotype; **(C)** wet shoot biomass in g wet weight, displayed by Microbe treatment; **(D)** dry shoot biomass in g wet weight, displayed by Microbe. Bars represent mean ± 2 SEM. Genotype x Microbe group means were separated using Tukey's honestly significant difference test placed, the results of which are placed above SEM bars.

PHJ40 genotypes in response to *Heliocoverpa zea* feeding, the two stiff-stalk varieties. Due to the lack of B14 germination, however, we are unable to determine if the lack of methyl salicylate production is specific to heterotic groups.

DISCUSSION

This study sought to understand how herbivore-induced plant volatile (HIPV) compounds are modulated by maize genotype and rhizosphere microbiota and if *Bacillus altitudinis* possessed the ability to modify production and composition of HIPV. Results suggest that genotypic variation in HIPV composition overshadowed *Bacillus* or microbiome-mediated HIPV release. Prior research has also recorded maize genotype influencing HIPV production (Gouinguené et al., 2001; Degen et al., 2004). For example, Degen et al. (2004) calculated the broad-sense heritability of total volatile emissions from 31 American and European inbred maize as $H^2 = 0.84$. Specific volatile classes, like terpenes, may have even been maintained throughout maize breeding via stabilizing selection, indicating certain volatile compounds are functionally important for maize and its progenitors across environments (Köllner et al., 2009). This suggests that maize has maintain an impressive degree of HIPV genetic variability, and is a major control point for HIPV total emissions and blend. However, in our study, the Stiff-Stalk inbred variety PHJ40 did influence total volatile emissions within live soil treatments (**Figure 5A**). Recent evidence also

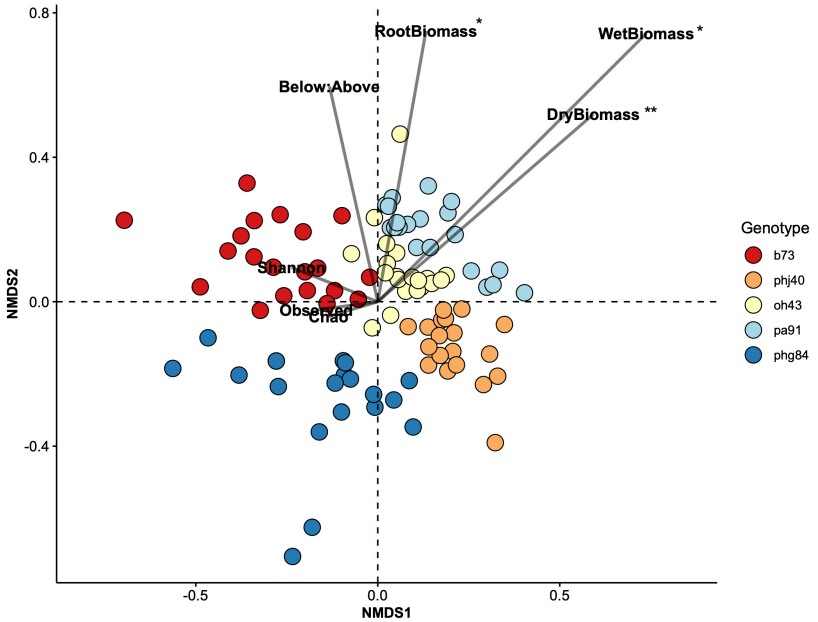

FIGURE 4 | Non-metric multidimensional scaling (NMDS) ordination constructed with a Bray-Curtis dissimilarity matrix of HIPV peak area data. Plant biomass (Shoot dry and weight biomass, dry root biomass, root:shoot ratio) and rhizosphere bacterial community richness parameters (observed richness, Chao1 index, Shannon Evenness) were correlated to NMDS1 and NMDS2 points using the envfit() function of the *vegan* package in R; significance is reported in **Table 7**. Significant vectors displayed with an asterisk: *P* = 0 '***'; 0.001 '**'; 0.01 '*'; 0.05 '.'.

TABLE 5 | Permutational multivariate analysis of variance (PERMANOVA) table.

Factors	Degrees of Freedom	Sums of Squares	Mean Squares	*F*-Value	R^2
Microbe	3	0.3195	0.10650	0.9145	0.01599
Genotype***	4	9.4848	2.37121	20.3629	0.47466
M x G	12	0.8621	0.07184	0.6170	0.04314
Residuals	80	9.3158	0.11645		0.46620
Total	99	19.9822			1.00

*Herbivore-induced plant volatiles (HIPV) Bray's Curtis Dissimilarity matrix was subjected to PERMANOVA to identify significant influence of Microbe treatment (BS, BL, L, S) and Genotype (B73, PHJ40, PHG84, OH43, PA91) on HIPV composition. Bray's dissimilarity matrix was produced using vegdist() function and the PERMANOVA was conducted using the adonis() function, both of the vegan package. Block was used as the constraining strata condition. Asterisk denote factor significance: P = 0 '***'; 0.001 '**'; 0.01 '*'; 0.05 '.'.*

supports a moderate genotypic influence on the diversity of the rhizosphere microbiome (Favela et al., 2021), which is also a heritable phenotype (Walters et al., 2018). This suggests that genotype-specific rhizosphere interactions influence HIPV load. As maize breeding with the goal of controlling insect pest has dominated breeding efforts, like Bt-maize (Horikoshi et al., 2021), the results of this study contribute to the growing body of evidence that HIPV could be genetically manipulated for maize germplasm development (Miedaner and Juroszek, 2021).

Thirty-six individual HIPV were induced upon herbivory by *Heliocoverpa zea*. Methyl salicylate (MeSA) was strongly influenced by maize genotype. Most interestingly, methyl salicylate was not detected in the stiff-stalk varieties, B73 and PHJ40, and was weakly influenced by Microbe treatment ($P = 0.03$). MeSA an aromatic HIPV produced via the shikimic acid pathway (Khan et al., 2020). Salicylic acid is known to coordinate plant defense responses to biotic stressors, such as pathogens, by promoting systemic acquired resistance (SAR) and increased expression of pathogen-related genes (Khan et al., 2020). In *Fusarium verticilliodes*-infected maize B73 silks, MeSA and auxin genes were upregulated, while jasmonic acid (JA) and ethylene (ET) genes were downregulated during induced systemic resistance (ISR) activity (Agostini et al., 2019). This indicates that B73 does possess the capacity for induced MeSA production, but it may be tissue dependent. Moreover, there may be tradeoffs between MeSA- and JA/ET-coordinated defense responses. For example, plant-growth promoting fungi *Trichoderma atroviridae* decreased maize landrace MeSA production by 78%, but increased JA in response to *Spodoptera frugiperda* herbivory, supporting the antagonistic relationship between MeSA and JA during herbivory-defense signaling (Contreras-Cornejo et al., 2018). However, we did not quantify JA in our study, so we are unable to conclude if the lack of MeSA corresponds to high JA concentrations in the

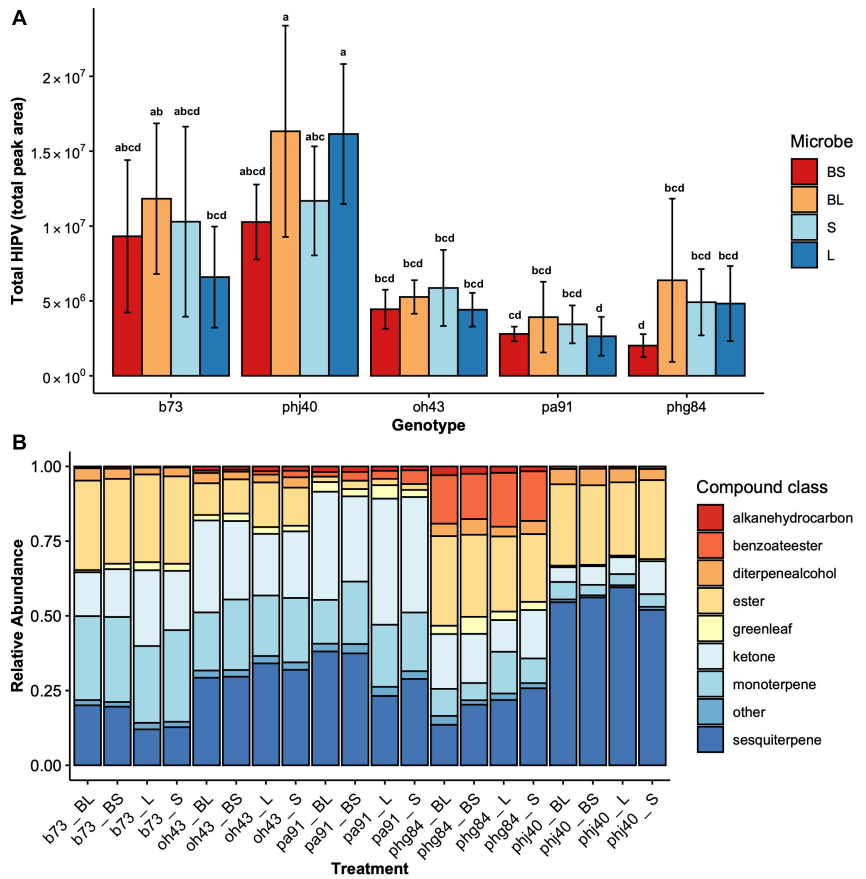

FIGURE 5 | (A) Total HIPV (total peak area) across Genotype (B73, PHJ40, Pa91, OH43, PHG84) and Microbe treatment: Bacillus+Live soil (BL), Bacillus+Sterile soil (BS), Sterile soil (S), Live soil (L). The total peak area for each 36 identified HIPV was summed for each sample. Bars represent mean ± 2 SEM. Mean separation groups from Tukey's honestly significant difference test placed above SEM bars. **(B)** Relative abundance of HIPV compound classes across Genotype and Microbe treatment; they are combined and represented as "Treatment."

TABLE 6 | Two-way analysis of variance table.

Volatile	Genotype			Microbe			Genotype x Microbe		
	df	F	P	df	F	P	df	F	P
A - Methyl Salicylate*	4,76	1600.8900	< 0.001	3, 76	3.0686	0.03287	12, 76	1.3638	0.20213
B - (E)-4,8-dimethyl-1,3,7-nonatriene*	4,76	125.7786	< 0.001	3, 76	1.2386	0.3016	12, 76	0.7606	0.6881
C - Caryophyllene*	4,76	59.5968	< 0.001	3, 76	0.5181	0.6711	12, 76	1.3894	0.1896
D - Trans-Geranylgeraniol*	4,76	–	–	3, 76	–	–	12, 76	–	–
E - Linalool*	4,76	32.8971	< 0.001	3, 76	0.0671	0.9772	12, 76	0.6448	0.7977
F - β-Myrcene*	4,76	–	–	3, 76	–	–	12, 76	–	–
G -trans-α-Bergamotene	4,76	–	–	3, 76	–	–	12, 76	–	–
H - epi-Bicyclosesquiphellandrene*	4,76	48.6385	< 0.001	3, 76	0.7959	0.4999	12, 76	1.5576	0.1227
I - Germacrene D*	4,76	19.7076	< 0.001	3, 76	0.0849	0.9681	12, 76	0.4616	0.9309
J - D-Limonene*	4,76	12.2691	< 0.001	3, 76	0.5719	0.6353	12, 76	0.2722	0.9920

*The top 10 important HIPVs, determined using MDA score via Random Forest Model, were subjected to two-way ANOVA's with Block as a random effect. The HIPV peak area values were $log_{10} + 1$ transformed to assume normality. *Denotes volatiles which were $log_{10} + 1$ transformed. '–' in column indicated models which violated ANOVA assumptions after outlier removal and data transformation*

stiff-stalk varieties. MeSA has been described interacting with parasitoid attraction. Snoeren et al. (2010) used MeSA knock-out *Arabidopsis thaliana* mutants, deficient in MeSA production to show that the mutant *A. thaliana* displayed increased attractiveness to the parasitoid wasp *Diadegma semiclausum* in a dose-dependent manner (Snoeren et al., 2010). Within maize,

TABLE 7 | Significant continuous variables influencing NMDS ordination structure.

Factors	NMDS1	NMDS2	R	P
Root Biomass*	0.1739470	0.9847550	0.09234417	0.011
Wet Shoot Biomass*	0.7045319	0.7096724	0.17473196	0.011
Dry Shoot Biomass**	0.7519955	0.6591682	0.09893165	0.001
Root: Shoot	−0.2171252	0.9761438	0.059398598	0.060
Observed Richness	−0.9910300	−0.1336396	0.004609559	0.810
Chao1 Richness	−0.9569455	−0.2902677	0.003172513	0.860
Shannon Evenness	−0.9281458	0.3722167	0.010365568	0.594

*Plant growth parameters and microbial richness values were fit onto NMDS ordination to identify variables correlating to HIPV composition, using the envfit() function from the vegan package was used and the summary output is reported below. Asterisk denote factor significance: P = 0 '***'; 0.001 '**'; 0.01 '*'; 0.05 '.'.*

Yactayo-Chang et al. (2021) suggested that MeSA acts as a dose-dependent cue for host-selection by female *S. frugiperda*, as it significantly increased oviposition preference for B73 and B104 inbred maize genotypes (Yactayo-Chang et al., 2021). Alternatively, Salamanca et al., 2019 observed MeSA increased attractiveness of European corn borer (*Ostrinia nubilalis*) eggs to numerous predators, including adult lady beetles and predatory mites within cranberry bogs (Salamanca et al., 2019). It is clear that the beneficial presence or absence of MeSA is context dependent (Dicke and Baldwin, 2010), and is reliant an available reservoir of parasitoids and predators and interactions with antagonistic hormone signaling. However, the strong genotypic control of MeSA implies it may be an ideal target for breeding if the context is elucidated.

After MeSA, the top nine HIPV influenced were terpenoids: (e)-4,8-dimethyl-1,3,7-nonatriene, caryophyllene, trans-geranylgeraniol, linalool, β-myrcene, trans-α-bergamotene, epi-bicyclosesquiphellandrene, germacrene D, D-limonene. Terpenoids play a central role in plant-insect interactions and include a wide diversity of compounds (Block et al., 2019). Both non-volatile and volatile terpenoids play pivotal roles in responses to biotic stress. After MeSA, the top HIPVs ranked in this study were all members of the terpenoid family. Pests can physiologically respond to many terpenoids, determined by measured electroantennogram activity of *S. frugiperda* to maize headspace volatiles (Pinto-Zevallos et al., 2016). However, the response of insect pests to maize terpenoids may be genotype- and pest-specific (Yactayo-Chang et al., 2021). In fact, numerous studies support the genotype-specific nature of terpenoid synthesis (Gouinguené et al., 2001; Degen et al., 2004; Block et al., 2018). For example, Degen et al. (2004) showed strong variation in β-caryophyllene production when comparing American inbred and European cultivars (Degen et al., 2004), and it was later shown that American cultivars possessed low activity of *terpene synthase 23*, which produces β-caryophyllene, when compared to European Flint and teosinte varieties (Köllner et al., 2008). However, β-caryophyllene production increased in B73 and B104 post *S. frugiperda* feeding (Yactayo-Chang et al., 2021). Moreover, β-caryophyllene produced in maize roots attract entomopathogenic nematodes upon *Diabrotic virgifera virgifera* belowground herbivory. The production of β-caryophyllene in B73 is catalyzed by *terpene synthase 8*, due to the lack of expression of *terpene synthase 23* (Köllner et al., 2013). The impressive diversity and functional redundancy of terpene synthase enzymes ensures the genotype-specific, and tissue-dependent, nature of terpenoid release. However, this also highlights the necessity for future research regarding the context-dependent response of pest and pest-enemies to terpenoids, across maize genotypes (Michereff et al., 2019).

Microbial Influence on Plant Growth Parameters

The rhizosphere microbiome was experimentally manipulated through sterilization and inoculation with plant growth promoting *Bacillus altitudinis*. While microbe treatments didn't influence HIPV directly, the results of this study suggest an indirect mechanism of HIPV manipulation via changes in biomass allocation. However, the soil sterilization (BS, S) was the major driver of differences in both root and shoot biomass allocation (**Figures 2**, **3**). Moreira et al. (2019) saw similar results when inoculating maize with *Ralstonia eutropha* and *Chryseobacterium humi* PGPR; *Ralstonia* and *Chryseobacterium* promoted root and shoot biomass under sterile conditions (Moreira et al., 2019). In our study, sterilization was used as a control for microbiome effects on plant growth and HIPV production. Yet, the only environment where a microbial inoculant would be added to sterile media is within built environments, such as indoor hydroponics cultivation (Trivedi et al., 2020). Built environments such as indoor agricultural systems are important for specific crops and conditions (Lawson et al., 2019) but using sterilized controls is not ideal, as most research exploring inoculant-driven biotic stress resiliency is aimed at field cultivation in industrial soil agroecosystems (Canfora et al., 2021). When paired with artificial conditions within the greenhouse context, patterns of plant-microbial interactions involved in tri-trophic signaling seen in HIPV elicitation may evade detection. Care should be taken during experimental planning to minimize artificial conditions which prevent accurate observation of ecological phenomena.

When and Where Might Microorganisms Influence Herbivore-Induced Volatile Compounds and Herbivore Response?

There is mounting evidence of single strain *Bacillus* inoculants promoting plant growth and biotic stress resilience

(Vardharajula et al., 2011; Huang et al., 2015; Sun et al., 2017; Saeid et al., 2018; de Lima et al., 2019; Hashem et al., 2019; Pranaw et al., 2020), but research is beginning to emphasize the importance of microbial consortia for PGP functions (Woo and Pepe, 2018; Hindersah et al., 2020). Consortia of PGPR involve two or more beneficial microorganisms, including bacteria and fungi, selected based on growth promoting traits such as nutrient provisioning, hormone production, antibiosis, etc. (Sekar et al., 2016). Trait stacking allows consortia to promote multi-stressor resiliency, amplifying the benefits of PGPR when compared to single-strain inoculums. Bradáčová et al. (2019) identified biomass yield responses of tomato (*Lycopersicum esculentum*) during growth in stressful (drought, P-deficiency, etc.) field conditions when inoculated with microbial consortia which included *Bacillus* species (Bradáčová et al., 2019). That study identified minimal benefits of single strain inoculants on tomato growth in field conditions. Interestingly, when single strain inoculants and consortia were compared in greenhouse cultivated tomatoes, the growth promoting effects were indistinguishable. The lack of PGP effect within the greenhouse was attributed to the absence of stress during greenhouse cultivation, whereby under these optimal conditions the host response to PGPR is determined solely by genetically-controlled mechanisms (Bradáčová et al., 2019). The environmental context for observable PGP traits echoes the importance of experimental design when studying tri-trophic interactions.

Microbiota exist within the remarkably complex soil matrix. Soil structure determines the physiochemical environment in microbial microhabitats, shifting the diversity and function of soil microbiomes. Agricultural manipulation of the biotic and abiotic components of the soil matrix, through crop species and management practices, imprint on soil leading to legacy effects, a term called plant-soil feedback (Pineda et al., 2017). A major limitation to the efficacy of inoculants, whether single strain or consortia, is persistence in rhizosphere of field crops, often because researchers on focus selecting microbial species based on growth promoting traits, ignoring rhizosphere competency requirements (Kaminsky et al., 2019). Manipulation of plant-soil feedbacks can overcome this challenge by enriching the soil matrix with the chemical and physical factors required for promoting microbial diversity and stimulating PGPR abundance (Blundell et al., 2020). Research has only just begun to explore plant-soil feedbacks and how they mediate insect herbivory (reviewed here by Pineda et al., 2017). A recent study with wheat observed greater total emissions of HIPV when grown in a soil inoculum originating from cover crop soil, as opposed to fallow soil (Malone et al., 2020), suggesting wheat grown in fallow rotation has a reduced capacity for recruiting pest predators. However, these effects are dependent on crop species and duration of agricultural management (Howard et al., 2020). In maize, herbivore-induced root exudation of benzoxazinoids recruited PGP *Pseudomonas putida* to the rhizosphere (Neal et al., 2012). But when the benzoxazinoids were metabolically processed by the soil microbiome, the byproduct caused a legacy effect on maize grown in subsequent plantings, conferring insect resiliency through modulating jasmonic acid signaling and defense priming (Hu et al., 2018) and reducing fall army worm (*Spodoptera frugiperda*) growth. Another study saw that maize grown in soil collected from polyculture, as opposed to monoculture, produced more volatile metabolites as well as benzoxazinoids, and had reduced herbivory from *Chilo partellus* larvae (Mutyambai et al., 2019). By inoculating potting mix with 10% live soil in our study, we disconnected the soil microorganisms from their native habitat, potentially altering the mechanisms by which they establish in the rhizosphere and interact with plant root systems for defense metabolite production. Therefore, identifying mechanisms controlling species-specific insect resistance through plant-soil, and plant-insect-soil feedbacks, should be prioritized for feature research endeavors.

Study Limitations

Besides the limitations regarding greenhouse exploration of tri-trophic ecological interactions, this study did not identify changes in herbivore survival, or predator/parasitoid attraction due to genotype and microbiome treatment. Plants have various lines of defense against herbivore generalists (Ali and Agrawal, 2012), such as leaf secondary metabolites, which may directly reduce herbivore growth and survival (Bezemer and Van Dam, 2005). For example, Badri et al. (2013) observed an influence of soil microbiomes on the leaf metabolome which reduced *Trichopulsia ni* leaf feeding behavior, which was hypothesized to be due to variations in amino acid content (Badri et al., 2013). As one of the primary growth-promoting functions of PGPR is nutrient acquisition (Richardson et al., 2009; Nath et al., 2018), assessing variations in tissue nutrient status is important for understanding the multitude of pathways involved in tri-trophic signaling. Moreover, as plant breeding manipulates regulatory elements controlling defense pathways and secondary metabolite synthesis (Maag et al., 2015), assessing breeding-manipulations in direct, and indirect, inducible defenses is of key importance (Swanson-Wagner et al., 2012; Chen et al., 2015; Rowen and Kaplan, 2016).

Additionally, HIPV target organisms are predators and parasitoids which rely on insect pests for survival (Hoballah et al., 2004; Clavijo McCormick et al., 2012). Disentangling which volatile cues recruit predators and parasitoids is fundamental for understanding which HIPV should be targets for anthropogenic manipulation through breeding or plant-soil feedbacks (Degen et al., 2012). Evidence suggests that the difference between basal VOCs and HIPV production upon herbivory is important for parasitoid recruitment (Sobhy et al., 2012). Our study did not disseminate differences in VOC production pre- and post-herbivory, so we cannot conclude if genotype and microbiome alter maize VOC elicitation response to *Heliocoverpa zea.*

CONCLUSION

In conclusion, this study identified limited efficacy of the microbiome in influencing the composition and relative abundances of herbivore-induced volatile compounds (HIPV) in maize. Maize genotype was a strong driver of HIPV abundance and composition, suggesting the capacity to manipulate the maize

volatilome through breeding practices. *Bacillus altitudinis* AP-283 influenced plant growth parameters, pointing to an indirect mechanism of volatilome manipulation. Tri-trophic signaling between herbivores-plant-microorganisms is a complex and highly dynamic process. Future research should ensure inclusion of the relevant environmental contexts if the goal is to explore the contribution of the rhizosphere microbiome to inducible plant defense metabolites.

DATA AVAILABILITY STATEMENT

The datasets presented in this study can be found in online repositories. The names of the repository/repositories and accession number(s) can be found in the article/ **Supplementary Material**.

AUTHOR CONTRIBUTIONS

EN, SR, and AK conceived and designed the project, EN carried out herbivory trial and data collection. SR carried out greenhouse procedures, microbiome, and statistical analyses and wrote the manuscript. EN, SR, and AK provided significant editorial comments. All authors contributed to the article and approved the submitted version.

FUNDING

This work was supported by funding to EN from the Department of Entomology within the School of Integrative Biology and the Department of African American Studies within the College of Liberal Arts and Sciences, at the University of Illinois, Urbana-Champaign.

SUPPLEMENTARY MATERIAL

The Supplementary Material for this article can be found online at: https://www.frontiersin.org/articles/10.3389/fmicb.2022.826635/full#supplementary-material

REFERENCES

Agostini, R. B., Postigo, A., Rius, S. P., Rech, G. E., Campos-Bermudez, V. A., and Vargas, W. A. (2019). Long-lasting primed state in maize plants: salicylic acid and steroid signaling pathways as key players in the early activation of immune responses in silks. *Mol. Plant Microbe Interact.* 32, 90–106. doi: 10.1094/MPMI-07-18-0208-R

Ali, G. S., Norman, D., and El-Sayed, A. S. (2015). Soluble and volatile metabolites of plant growth-promoting rhizobacteria (PGPRs): role and practical applications in inhibiting pathogens and activating induced systemic resistance (ISR). *Adv. Bot. Res.* 75, 241–284. doi: 10.1016/bs.abr.2015.07.004.

Ali, J. G., and Agrawal, A. A. (2012). Specialist versus generalist insect herbivores and plant defense. *Trends Plant Sci.* 17, 293–302. doi: 10.1016/j.tplants.2012.02.006

Arimura, G. I., Matsui, K., and Takabayashi, J. (2009). Chemical and molecular ecology of herbivore-induced plant volatiles: proximate factors and their ultimate functions. *Plant Cell Physiol.* 50, 911–923. doi: 10.1093/pcp/pcp030

Badri, D. V., Zolla, G., Bakker, M. G., Manter, D. K., and Vivanco, J. M. (2013). Potential impact of soil microbiomes on the leaf metabolome and on herbivore feeding behavior. *New Phytol.* 198, 264–273. doi: 10.1111/nph.12124

Barton, K. (2020). *MuMIn: Multi-Model Inference. R package version 1.43.17. 1, 18.* Available online at: https://cran.r-project.org/web/packages/MuMIn/MuMIn.pdf

Bates, D., Mächler, M., Bolker, B. M., and Walker, S. C. (2015). Fitting linear mixed-effects models using lme4. *J. Stat. Softw.* 67, 1–48. doi: 10.18637/jss.v067.i01

Bezemer, T. M., and Van Dam, N. M. (2005). Linking aboveground and belowground interactions via induced plant defenses. *Trends Ecol. Evol.* 20, 617–624. doi: 10.1016/j.tree.2005.08.006

Bhattacharyya, P. N., and Jha, D. K. (2012). Plant growth-promoting rhizobacteria (PGPR): emergence in agriculture. *World J. Microbiol. Biotechnol.* 28, 1327–1350. doi: 10.1007/s11274-011-0979-9

Block, A. K., Hunter, C. T., Rering, C., Christensen, S. A., and Meagher, R. L. (2018). Contrasting insect attraction and herbivore-induced plant volatile production in maize. *Planta* 248, 105–116. doi: 10.1007/s00425-018-2886-x

Block, A. K., Vaughan, M. M., Schmelz, E. A., and Christensen, S. A. (2019). Biosynthesis and function of terpenoid defense compounds in maize (Zea mays). *Planta* 249, 21–30. doi: 10.1007/s00425-018-2999-2

Blundell, R., Schmidt, J. E., Igwe, A., Cheung, A. L., Vannette, R. L., Gaudin, A. C. M., et al. (2020). Organic management promotes natural pest control through altered plant resistance to insects. *Nat. Plants* 6, 483–491. doi: 10.1038/s41477-020-0656-9

Borrego, E. J., and Kolomiets, M. V. (2016). Synthesis and functions of jasmonates in maize. *Plants* 5:41. doi: 10.3390/plants5040041

Bradáčová, K., Florea, A. S., Bar-Tal, A., Minz, D., Yermiyahu, U., Shawahna, R., et al. (2019). Microbial consortia versus single-strain inoculants: an advantage in PGPM-assisted tomato production? *Agronomy* 9:105. doi: 10.3390/agronomy9020105

Calvo, P., Watts, D. B., Kloepper, J. W., and Torbert, H. A. (2017). Effect of microbial-based inoculants on nutrient concentrations and early root morphology of corn (Zea mays)#. *J. Plant Nutr. Soil Sci.* 180, 56–70. doi: 10.1002/jpln.201500616

Canfora, L., Costa, C., Pallottino, F., and Mocali, S. (2021). Trends in soil microbial inoculants research: a science mapping approach to unravel strengths and weaknesses of their application. *Agric.* 11, 1–22. doi: 10.3390/agriculture11020158

Caporaso, J. G., Lauber, C. L., Walters, W. A., Berg-Lyons, D., Lozupone, C. A., Turnbaugh, P. J., et al. (2011). Global patterns of 16S rRNA diversity at a depth of millions of sequences per sample. *Proc. Natl. Acad. Sci. U.S.A.* 108, 4516–4522. doi: 10.1073/pnas.1000080107

Cellini, A., Spinelli, F., Donati, I., Ryu, C. M., and Kloepper, J. W. (2021). Bacterial volatile compound-based tools for crop management and quality. *Trends Plant Sci.* 26, 968–983. doi: 10.1016/j.tplants.2021.05.006

Chen, Y. H., Gols, R., Stratton, C. A., Brevik, K. A., and Benrey, B. (2015). Complex tritrophic interactions in response to crop domestication: predictions from the wild. *Entomol. Exp. Appl.* 157, 40–59. doi: 10.1111/eea.12344

Choudhary, D. K., and Johri, B. N. (2009). Interactions of *Bacillus* spp. and plants - with special reference to induced systemic resistance (ISR). *Microbiol. Res.* 164, 493–513. doi: 10.1016/j.micres.2008.08.007

Chowdhury, S. P., Hartmann, A., Gao, X. W., and Borriss, R. (2015). Biocontrol mechanism by root-associated *Bacillus* amyloliquefaciens FZB42 - A review. *Front. Microbiol.* 6:780. doi: 10.3389/fmicb.2015.00780

Clavijo McCormick, A., Unsicker, S. B., and Gershenzon, J. (2012). The specificity of herbivore-induced plant volatiles in attracting herbivore enemies. *Trends Plant Sci.* 17, 303–310. doi: 10.1016/j.tplants.2012.03.012

Contreras-Cornejo, H. A., Macías-Rodríguez, L., del-Val, E., and Larsen, J. (2018). The root endophytic fungus *Trichoderma atroviride* induces foliar herbivory resistance in maize plants. *Appl. Soil Ecol.* 124, 45–53. doi: 10.1016/j.apsoil.2017.10.004

D'Alessandro, M., Held, M., Triponez, Y., and Turlings, T. C. J. (2006). The role of indole and other shikimic acid derived maize volatiles in the attraction of two parasitic wasps. *J. Chem. Ecol.* 32, 2733–2748. doi: 10.1007/s10886-006-9196-7

de Lima, B. C., Moro, A. L., Santos, A. C. P., Bonifacio, A., Araujo, A. S. F., and de Araujo, F. F. (2019). *Bacillus subtilis* ameliorates water stress tolerance in maize and common bean. *J. Plant Interact.* 14, 432–439. doi: 10.1080/17429145.2019.1645896

De Mendiburu, F., and Simon, R. (2021). Agricolae – ten years of an open source statistical tool for experiments in breeding, agriculture and biology. *PeerJ* 3:e1404v1. doi: 10.7287/peerj.preprints.1404v1

Degen, T., Bakalovic, N., Bergvinson, D., and Turlings, T. C. J. (2012). Differential performance and parasitism of caterpillars on maize inbred lines with distinctly different herbivore-induced volatile emissions. *PLoS One* 7:e47589. doi: 10.1371/journal.pone.0047589

Degen, T., Dillmann, C., Marion-Poll, F., and Turlings, T. C. J. (2004). High genetic variability of herbivore-induced volatile emission within a broad range of maize inbred lines. *Plant Physiol.* 135, 1928–1938. doi: 10.1104/pp.104.039891

Dicke, M., and Baldwin, I. T. (2010). The evolutionary context for herbivore-induced plant volatiles: beyond the "cry for help.". *Trends Plant Sci.* 15, 167–175. doi: 10.1016/j.tplants.2009.12.002

Disi, J. O., Kloepper, J. W., and Fadamiro, H. Y. (2018a). Seed treatment of maize with *Bacillus pumilus* strain INR-7 affects host location and feeding by Western corn rootworm, *Diabrotica virgifera* virgifera. *J. Pest Sci.* 91, 515–522. doi: 10.1007/s10340-017-0927-z

Disi, J. O., Zebelo, S., Kloepper, J. W., and Fadamiro, H. (2018b). Seed inoculation with beneficial rhizobacteria affects European corn borer (Lepidoptera: Pyralidae) oviposition on maize plants. *Entomol. Sci.* 21, 48–58. doi: 10.1111/ens.12280

Dudareva, N., Pichersky, E., and Gershenzon, J. (2004). Biochemistry of plant volatiles. *Plant Physiol.* 135, 1893–1902. doi: 10.1104/pp.104.049981

Edgar, R. C. (2010). Search and clustering orders of magnitude faster than BLAST. *Bioinformatics* 26, 2460–2461. doi: 10.1093/bioinformatics/btq461

Elfira, Y., Kusmiyati, F., and Budiharjo, A. (2020). The effect of *Bacillus altitudinis* P-10 combination treatments on the plant growth and seed quality of corn (Zea mays L). *Bioma* 22, 180–187.

Farag, M. A., Zhang, H., and Ryu, C. M. (2013). Dynamic chemical communication between plants and bacteria through airborne signals: induced resistance by bacterial volatiles. *J. Chem. Ecol.* 39, 1007–1018. doi: 10.1007/s10886-013-0317-9

Favela, A., Bohn, M. O., and Kent, A. D. (2021). Maize germplasm chronosequence shows crop breeding history impacts recruitment of the rhizosphere microbiome. *ISME J.* 15, 2454–2464. doi: 10.1038/s41396-021-00923-z

Gordon, A., and Hannon, G. (2010). *FASTX-Toolkit*. Available online at: http://hannonlab.cshl.edu/fastx_toolkit/index.html

Gouinguené, S., Degen, T., and Turlings, T. C. J. (2001). Variability in herbivore-induced odour emissions among maize cultivars and their wild ancestors (teosinte). *Chemoecology* 11, 9–16. doi: 10.1007/PL00001832

Govindasamy, V., Senthikumar, M., Magheshwaran, V., Kumar, U., Bose, P., Sharma, V., et al. (2010). "Bacillus and Paenibacillus spp.: potential PGPR for sustainable agriculture," in *Plant Growth and Health Promoting Bacteria. Microbiology Monographs*, Vol. 18, ed. D. Maheshwari (Berlin: Springer), doi: 10.1007/978-3-642-13612-2.

Hasan, N., Farzand, A., Heng, Z., Khan, I. U., Moosa, A., Zubair, M., et al. (2020). Antagonistic potential of novel endophytic bacillus strains and mediation of plant defense against verticillium wilt in upland cotton. *Plants* 9, 1–16. doi: 10.3390/plants9111438

Hashem, A., Tabassum, B., and Fathi Abd_Allah, E. (2019). *Bacillus subtilis*: a plant-growth promoting rhizobacterium that also impacts biotic stress. *Saudi J. Biol. Sci.* 26, 1291–1297. doi: 10.1016/j.sjbs.2019.05.004

Hindersah, R., Setiawati, M. R., Asmiran, P., and Fitriatin, B. N. (2020). Formulation of *Bacillus* and *Azotobacter* consortia in liquid cultures: preliminary research on microbes-coated urea. *Int. J. Agric. Syst.* 8:1. doi: 10.20956/ijas.v8i1.2283

Hoballah, M. E. F., Tamò, C., and Turlings, T. C. J. (2002). Differential attractiveness of induced odors emitted by eight maize varieties for the parasitoid Cotesia marginiventris: is quality or quantity important? *J. Chem. Ecol.* 28, 951–968. doi: 10.1023/A:1015253600083

Hoballah, M. E., Degen, T., Bergvinson, D., Savidan, A., Tamò, C., and Turlings, T. C. J. (2004). Occurrence and direct control potential of parasitoids and predators of the fall armyworm (Lepidoptera: Noctuidae) on maize in the subtropical lowlands of Mexico. *Agric. For. Entomol.* 6, 83–88. doi: 10.1111/j.1461-9555.2004.00207.x

Horikoshi, R. J., Vertuan, H., de Castro, A. A., Morrell, K., Griffith, C., Evans, A., et al. (2021). A new generation of Bt maize for control of fall armyworm (Spodoptera frugiperda). *Pest Manag. Sci.* 77, 3727–3736. doi: 10.1002/ps.6334

Howard, M. M., Muñoz, C. A., Kao-Kniffin, J., and Kessler, A. (2020). Soil microbiomes from fallow fields have species-specific effects on crop growth and pest resistance. *Front. Plant Sci.* 11:1171. doi: 10.3389/fpls.2020.01171

Hu, L., Robert, C. A. M., Cadot, S., Zhang, X., Ye, M., Li, B., et al. (2018). Root exudate metabolites drive plant-soil feedbacks on growth and defense by shaping the rhizosphere microbiota. *Nat. Commun.* 9:2738. doi: 10.1038/s41467-018-05122-7

Huang, X. F., Zhou, D., Guo, J., Manter, D. K., Reardon, K. F., and Vivanco, J. M. (2015). Bacillus spp: from rainforest soil promote plant growth under limited nitrogen conditions. *J. Appl. Microbiol.* 118, 672–684. doi: 10.1111/jam.12720

Kaminsky, L. M., Trexler, R. V., Malik, R. J., Hockett, K. L., and Bell, T. H. (2019). The inherent conflicts in developing soil microbial inoculants. *Trends Biotechnol.* 37, 140–151. doi: 10.1016/j.tibtech.2018.11.011

Kenneth, O. C., Nwadibe, E. C., Kalu, A. U., and Unah, U. V. (2019). Plant Growth Promoting Rhizobacteria (PGPR): a novel agent for sustainable food production. *Am. J. Agric. Biol. Sci.* 14, 35–54. doi: 10.3844/ajabssp.2019.35.54

Kessler, A., and Baldwin, I. T. (2001). Defensive function of herbivore-induced plant volatile emissions in nature. *Science* 291, 2141–2144. doi: 10.1126/science.291.5511.2141

Khan, N., Bano, A., Ali, S., and Babar, M. A. (2020). Crosstalk amongst phytohormones from planta and PGPR under biotic and abiotic stresses. *Plant Growth Regul.* 90, 189–203. doi: 10.1007/s10725-020-00571-x

Kloepper, J. W., Fadamiro, H. Y., Ngumbi, E. N., and Nangle, W. (2013). *Inoculants Including Bacillus Simplex for Inducing Production of Volatile Organic Compounds in Plants. 2, 2025–2037*. Available online at: https://www.google.com/patents/US9282745

Kloepper, J. W., Ryu, C. M., and Zhang, S. (2004). Induced systemic resistance and promotion of plant growth by *Bacillus* spp. *Phytopathology* 94, 1259–1266. doi: 10.1094/PHYTO.2004.94.11.1259

Köllner, T. G., Gershenzon, J., and Degenhardt, J. (2009). Molecular and biochemical evolution of maize terpene synthase 10, an enzyme of indirect defense. *Phytochemistry* 70, 1139–1145. doi: 10.1016/j.phytochem.2009.06.011

Köllner, T. G., Held, M., Lenk, C., Hiltpold, I., Turlings, T. C. J., Gershenzon, J., et al. (2008). A maize (E)-β-caryophyllene synthase implicated in indirect defense responses against herbivores is not expressed in most American maize varieties. *Plant Cell* 20, 482–494. doi: 10.1105/tpc.107.051672

Köllner, T. G., Lenk, C., Schnee, C., Köpke, S., Lindemann, P., Gershenzon, J., et al. (2013). Localization of sesquiterpene formation and emission in maize leaves after herbivore damage. *BMC Plant Biol.* 13:15. doi: 10.1186/1471-2229-13-15

Kuczynski, J., Stombaugh, J., Walters, W. A., González, A., Caporaso, J. G., and Knight, R. (2011). Using QIIME to analyze 16S rRna gene sequences from microbial communities. *Curr. Protoc. Bioinforma* 10, 1–20. doi: 10.1002/0471250953.bi1007s36

Lawson, C. E., Harcombe, W. R., Hatzenpichler, R., Lindemann, S. R., Löffler, F. E., O'Malley, M. A., et al. (2019). Common principles and best practices for engineering microbiomes. *Nat. Rev. Microbiol.* 17, 725–741. doi: 10.1038/s41579-019-0255-9

Loughrin, J. H., Manukian, A., Heath, R. R., Turlings, T. C. J., and Tumlinson, J. H. (1994). Diurnal cycle of emission of induced volatile terpenoids by herbivore-injured cotton plants. *Proc. Natl. Acad. Sci. U.S.A.* 91, 11836–11840. doi: 10.1073/pnas.91.25.11836

Lu, X., Zhou, D., Chen, X., Zhang, J., Huang, H., and Wei, L. (2017). Isolation and characterization of *Bacillus altitudinis* JSCX-1 as a new potential biocontrol agent against Phytophthora sojae in soybean [Glycine max (L.) Merr.]. *Plant Soil* 416, 53–66. doi: 10.1007/s11104-017-3195-z

Maag, D., Erb, M., Bernal, J. S., Wolfender, J. L., Turlings, T. C. J., and Glauser, G. (2015). Maize domestication and anti-herbivore defences: leaf-specific dynamics during early ontogeny of maize and its wild ancestors. *PLoS One* 10:e0135722. doi: 10.1371/journal.pone.0135722

Maffei, M. E. (2010). Sites of synthesis, biochemistry and functional role of plant volatiles. *S. Afr. J. Bot.* 76, 612–631. doi: 10.1016/j.sajb.2010.03.003

Magoč, T., and Salzberg, S. L. (2011). FLASH: fast length adjustment of short reads to improve genome assemblies. *Bioinformatics* 27, 2957–2963. doi: 10.1093/bioinformatics/btr507

Malone, S. C., Weaver, D. K., Seipel, T. F., Menalled, F. D., Hofland, M. L., Runyon, J. B., et al. (2020). Herbivore-induced volatile emissions are altered by soil legacy effects in cereal cropping systems. *Plant Soil* 455, 171–186. doi: 10.1007/s11104-020-04674-2

McCall, P. J., Turlings, T. C. J., Loughrin, J., Proveaux, A. T., and Tumlinson, J. H. (1994). Herbivore-induced volatile emissions from cotton (*Gossypium hirsutum* L.) seedlings. *J. Chem. Ecol.* 20, 3039–3050. doi: 10.1007/BF02033709

Michereff, M. F. F., Magalhães, D. M., Hassemer, M. J., Laumann, R. A., Zhou, J. J., Ribeiro, P. E. D. A., et al. (2019). Variability in herbivore-induced defence signalling across different maize genotypes impacts significantly on natural enemy foraging behaviour. *J. Pest Sci.* 92, 723–736. doi: 10.1007/s10340-018-1033-6

Miedaner, T., and Juroszek, P. (2021). Global warming and increasing maize cultivation demand comprehensive efforts in disease and insect resistance breeding in north-western Europe. *Plant Pathol.* 70, 1032–1046. doi: 10.1111/ppa.13365

Moreira, H., Pereira, S. I. A., Marques, A. P. G. C., Rangel, A. O. S. S., and Castro, P. M. L. (2019). Effects of soil sterilization and metal spiking in plant growth promoting rhizobacteria selection for phytotechnology purposes. *Geoderma* 334, 72–81. doi: 10.1016/j.geoderma.2018.07.025

Mutyambai, D. M., Bass, E., Luttermoser, T., Poveda, K., Midega, C. A. O., Khan, Z. R., et al. (2019). More than "push" and "pull"? Plant-soil feedbacks of maize companion cropping increase chemical plant defenses against herbivores. *Front. Ecol. Evol.* 7:217. doi: 10.3389/fevo.2019.00217

Nath, M., Bhatt, D., Bhatt, M. D., Prasad, R., and Tuteja, N. (2018). "Microbe-mediated enhancement of nitrogen and phosphorus content for crop improvement," in *New and Future Developments in Microbial Biotechnology and Bioengineering: Crop Improvement through Microbial Biotechnology*, eds R. Prasad, S. S. Gill, and N. Tuteja (Amsterdam: Elsevier), 293–304. doi: 10.1016/B978-0-444-63987-5.00014-1.

Neal, A. L., Ahmad, S., Gordon-Weeks, R., and Ton, J. (2012). Benzoxazinoids in root exudates of maize attract *pseudomonas* putida to the rhizosphere. *PLoS One* 7:35498. doi: 10.1371/journal.pone.0035498

Ngumbi, E. N., and Ugarte, C. M. (2021). Flooding and herbivory interact to alter volatile organic compound emissions in two maize hybrids. *J. Chem. Ecol.* 47, 707–718. doi: 10.1007/s10886-021-01286-7

Oikawa, A., Ishihara, A., Hasegawa, M., Kodama, O., and Iwamura, H. (2001). Induced accumulation of 2-hydroxy-4,7-dimethoxy-1,4-benzoxazin-3-one glucoside (HDMBOA-Glc) in maize leaves. *Phytochemistry* 56, 669–675. doi: 10.1016/S0031-9422(00)00494-5

Oksanen, A. J., Blanchet, F. G., Friendly, M., Kindt, R., Legendre, P., Mcglinn, D., et al. (2020). *Vegan: Community Ecology Package. R Package version 2.5-7*. doi: 10.1007/978-94-024-1179-9_301576.

Pangesti, N., Weldegergis, B. T., Langendorf, B., van Loon, J. J. A., Dicke, M., and Pineda, A. (2015). Rhizobacterial colonization of roots modulates plant volatile emission and enhances the attraction of a parasitoid wasp to host-infested plants. *Oecologia* 178, 1169–1180. doi: 10.1007/s00442-015-3277-7

Patten, C. L., and Glick, B. R. (1996). Bacterial biosynthesis of indole-3-acetic acid. *Can. J. Microbiol.* 42, 207–220. doi: 10.1139/m96-032

Pineda, A., Kaplan, I., and Bezemer, T. M. (2017). Steering soil microbiomes to suppress aboveground insect pests. *Trends Plant Sci.* 22, 770–778. doi: 10.1016/j.tplants.2017.07.002

Pinto-Zevallos, D. M., Strapasson, P., and Zarbin, P. H. G. (2016). Herbivore-induced volatile organic compounds emitted by maize: electrophysiological responses in *Spodoptera frugiperda* females. *Phytochem. Lett.* 16, 70–74. doi: 10.1016/j.phytol.2016.03.005

Pranaw, K., Pidlisnyuk, V., Trögl, J., and Malinská, H. (2020). Bioprospecting of a novel plant growth-promoting bacterium *Bacillus altitudinis* KP-14 for Enhancing Miscanthus × giganteus growth in metals contaminated soil. *Biology* 9:305. doi: 10.3390/biology9090305

R Core Team (2021). *R: A Language and Environment for Statistical Computing*. Vienna: R Foundation for statistical computing.

Radhakrishnan, R., Hashem, A., Abd Allah, E. F., and Abd_Allah, E. F. (2017). Bacillus: a biological tool for crop improvement through bio-molecular changes in adverse environments. *Front. Physiol.* 8:667. doi: 10.3389/fphys.2017.00667

Richardson, A. E., Barea, J. M., McNeill, A. M., and Prigent-Combaret, C. (2009). Acquisition of phosphorus and nitrogen in the rhizosphere and plant growth promotion by microorganisms. *Plant Soil* 321, 305–339. doi: 10.1007/s11104-009-9895-2

Rowen, E., and Kaplan, I. (2016). Eco-evolutionary factors drive induced plant volatiles: a meta-analysis. *New Phytol.* 210, 284–294. doi: 10.1111/nph.13804

Saeid, A., Prochownik, E., and Dobrowolska-Iwanek, J. (2018). Phosphorus solubilization by Bacillus species. *Molecules* 23, 1–18. doi: 10.3390/molecules23112897

Salamanca, J., Souza, B., Kyryczenko-Roth, V., and Rodriguez-Saona, C. (2019). Methyl salicylate increases attraction and function of beneficial arthropods in cranberries. *Insects* 10:423. doi: 10.3390/insects10120423

Scala, A., Allmann, S., Mirabella, R., Haring, M. A., and Schuurink, R. C. (2013). Green leaf volatiles: a plant's multifunctional weapon against herbivores and pathogens. *Int. J. Mol. Sci.* 14, 17781–17811. doi: 10.3390/ijms140917781

Sekar, J., Raj, R., and Prabavathy, V. R. (2016). "Microbial consortial production for sustainable agriculture: commercializatiton and regulatory issues in India," in *Agriculturally Important Microorganisms*, eds H. B. Singh, B. K. Sarma, and C. Keswani (Berlin: SpringerNature), 108–131.

Shafi, J., Tian, H., and Ji, M. (2017). Bacillus species as versatile weapons for plant pathogens: a review. *Biotechnol. Biotechnol. Equip.* 31, 446–459. doi: 10.1080/13102818.2017.1286950

Snoeren, T. A. L., Mumm, R., Poelman, E. H., Yang, Y., Pichersky, E., and Dicke, M. (2010). The herbivore-induced plant volatile methyl salicylate negatively affects attraction of the parasitoid Diadegma semiclausum. *J. Chem. Ecol.* 36, 479–489. doi: 10.1007/s10886-010-9787-1

Sobhy, I. S., Erb, M., Sarhan, A. A., El-Husseini, M. M., Mandour, N. S., and Turlings, T. C. J. (2012). Less is more: treatment with BTH and laminarin reduces herbivore-induced volatile emissions in maize but increases parasitoid attraction. *J. Chem. Ecol.* 38, 348–360. doi: 10.1007/s10886-012-0098-6

Sun, Z., Liu, K., Zhang, J., Zhang, Y., Xu, K., Yu, D., et al. (2017). IAA producing *Bacillus altitudinis* alleviates iron stress in *Triticum aestivum* L. seedling by both bioleaching of iron and up-regulation of genes encoding ferritins. *Plant Soil* 419, 1–11. doi: 10.1007/s11104-017-3218-9

Sunar, K., Dey, P., Chakraborty, U., and Chakraborty, B. (2015). Biocontrol efficacy and plant growth promoting activity of *Bacillus altitudinis* isolated from Darjeeling hills. *India. J. Basic Microbiol.* 55, 91–104. doi: 10.1002/jobm.201300227

Swanson-Wagner, R., Briskine, R., Schaefer, R., Hufford, M. B., Ross-Ibarra, J., Myers, C. L., et al. (2012). Reshaping of the maize transcriptome by domestication. *Proc. Natl. Acad. Sci. U.S.A.* 109, 11878–11883. doi: 10.1073/pnas.1201961109

Tamiru, A., Bruce, T. J. A., Woodcock, C. M., Caulfield, J. C., Midega, C. A. O., Ogol, C. K. P. O., et al. (2011). Maize landraces recruit egg and larval parasitoids in response to egg deposition by a herbivore. *Ecol. Lett.* 14, 1075–1083. doi: 10.1111/j.1461-0248.2011.01674.x

Thompson, A. C., Baker, D. N., Gueldner, R. C., and Hedin, P. A. (1971). Identification and quantitative analysis of the volatile substances emitted by maturing cotton in the field. *Plant Physiol.* 48, 50–52. doi: 10.1104/pp.48.1.50

Trivedi, P., Leach, J. E., Tringe, S. G., Sa, T., and Singh, B. K. (2020). Plant–microbiome interactions: from community assembly to plant health. *Nat. Rev. Microbiol.* 18, 607–621. doi: 10.1038/s41579-020-0412-1

Turlings, T. C. J., and Erb, M. (2018). Tritrophic interactions mediated by herbivore-induced plant volatiles: mechanisms, ecological relevance, and application potential. *Annu. Rev. Entomol.* 63, 433–452. doi: 10.1146/annurev-ento-020117-043507

Vardharajula, S., Ali, S. Z., Grover, M., Reddy, G., and Bandi, V. (2011). Drought-tolerant plant growth promoting *Bacillus* spp.: effect on growth,osmolytes,and antioxidant status of maize under drought stress. *J. Plant Interact.* 6, 1–14. doi: 10.1080/17429145.2010.535178

Venables, W. N., Smith, D. M., and R Core Team (2021). *An Introduction to R. Notes R A Program. Environ. Data Anal. Graph. Version 4.1.2* 2. doi: 10.4135/9781473920446.n12.

Walling, L. L. (2000). The myriad plant responses to herbivores. *J. Plant Growth Regul.* 19, 195–216. doi: 10.1007/s003440000026

Walters, W. A., Jin, Z., Youngblut, N., Wallace, J. G., Sutter, J., Zhang, W., et al. (2018). Large-scale replicated field study of maize rhizosphere identifies heritable microbes. *Proc. Natl. Acad. Sci. U.S.A.* 115, 7368–7373. doi: 10.1073/pnas.1800918115

Wang, M., Ruan, W., Kostenko, O., Carvalho, S., Hannula, S. E., Mulder, P. P. J., et al. (2019). Removal of soil biota alters soil feedback effects on plant growth and defense chemistry. *New Phytol.* 221, 1478–1491. doi: 10.1111/nph.15485

War, A. R., Sharma, H. C., Paulraj, M. G., War, M. Y., and Ignacimuthu, S. (2011). Herbivore induced plant volatiles:their role in plant defense for pest management. *Plant Signal. Behav.* 6, 1973–1978. doi: 10.4161/psb.6.12.18053

Wickham, H. (2016). *ggplot2: Elegant Graphics for Data Analysis*. Berlin: Springer. doi: 10.1007/978-3-319-24277-4.

Woo, S. L., and Pepe, O. (2018). Microbial consortia: promising probiotics as plant biostimulants for sustainable agriculture. *Front. Plant Sci.* 9:1801. doi: 10.3389/fpls.2018.01801

Xavier, L. M. S., Laumann, R. A., Borges, M., Magalhães, D. M., Vilela, E. F., and Blassioli-Morae, M. C. (2011). Trichogramma pretiosum attraction due to the Elasmopalpus lignosellus damage in maize. *Pesqui. Agropecu. Bras.* 46, 578–585. doi: 10.1590/S0100-204X2011000600002

Yactayo-Chang, J. P., Mendoza, J., Willms, S. D., Rering, C. C., Beck, J. J., and Block, A. K. (2021). Zea mays volatiles that influence oviposition and feeding behaviors of *Spodoptera frugiperda*. *J. Chem. Ecol.* 47, 799–809. doi: 10.1007/s10886-021-01302-w

Yan, Z., Reddy, M. S., Ryu, C. M., McInroy, J. A., Wilson, M., and Kloepper, J. W. (2002). Induced systemic protection against tomato late blight elicited by plant growth-promoting rhizobacteria. *Phytopathology* 92, 1329–1333. doi: 10.1094/PHYTO.2002.92.12.1329

Yue, Z., Chen, Y., Chen, C., Ma, K., Tian, E., Wang, Y., et al. (2021). Endophytic *Bacillus altitudinis* WR10 alleviates Cu toxicity in wheat by augmenting reactive oxygen species scavenging and phenylpropanoid biosynthesis. *J. Hazard. Mater.* 405:124272. doi: 10.1016/j.jhazmat.2020.124272

Zhang, D., Xu, H., Gao, J., Portieles, R., Du, L., Gao, X., et al. (2021). Endophytic *Bacillus altitudinis* strain uses different novelty molecular pathways to enhance plant growth. *Front. Microbiol.* 12:692313. doi: 10.3389/fmicb.2021.692313

Conflict of Interest: The authors declare that the research was conducted in the absence of any commercial or financial relationships that could be construed as a potential conflict of interest.

Publisher's Note: All claims expressed in this article are solely those of the authors and do not necessarily represent those of their affiliated organizations, or those of the publisher, the editors and the reviewers. Any product that may be evaluated in this article, or claim that may be made by its manufacturer, is not guaranteed or endorsed by the publisher.

frontiers | Frontiers in Microbiology

ORIGINAL RESEARCH
published: 06 May 2022
doi: 10.3389/fmicb.2021.809834

Effects of Co-application of Cadmium-Immobilizing Bacteria and Organic Fertilizers on *Houttuynia cordata* and Microbial Communities in a Cadmium-Contaminated Field

Xiumei Yu[1]†, Min Yan[1]†, Yongliang Cui[2]†, Zhongyi Liu[1], Han Liu[1], Jie Zhou[1], Jiahao Liu[1], Lan Zeng[1], Qiang Chen[1], Yunfu Gu[1], Likou Zou[1], Ke Zhao[1], Quanju Xiang[1], Menggen Ma[1] and Shuangcheng Li[1]*

[1] College of Resources, Sichuan Agricultural University, Chengdu, China, [2] Sichuan Provincial Academy of Natural Resource Sciences, Chengdu, China

OPEN ACCESS

Edited by:
Hai-Ming Zhao,
Jinan University, China

Reviewed by:
Yaying Li,
Institute of Urban Environment, Chinese Academy of Sciences (CAS), China
Benjaphorn Prapagdee,
Mahidol University, Thailand

***Correspondence:**
Xiumei Yu
xiumeiyu@sicau.edu.cn

† These authors have contributed equally to this work

Specialty section:
This article was submitted to Terrestrial Microbiology, a section of the journal Frontiers in Microbiology

Received: 05 November 2021
Accepted: 10 December 2021
Published: 06 May 2022

Citation:
Yu X, Yan M, Cui Y, Liu Z, Liu H, Zhou J, Liu J, Zeng L, Chen Q, Gu Y, Zou L, Zhao K, Xiang Q, Ma M and Li S (2022) Effects of Co-application of Cadmium-Immobilizing Bacteria and Organic Fertilizers on Houttuynia cordata and Microbial Communities in a Cadmium-Contaminated Field. Front. Microbiol. 12:809834. doi: 10.3389/fmicb.2021.809834

Cadmium pollution is a serious threat to the soil environment. The application of bio-based fertilizers in combination with beneficial microbial agents is a sustainable approach to solving Cd pollution in farm soil. The present study investigated the effects of co-application of a Cd-immobilizing bacterial agent and two fermented organic fertilizers (fermentative edible fungi residue; fermentative cow dung) on *Houttuynia cordata* and its microbial communities in a Cd-polluted field. It showed that both the application of the Cd-immobilizing bacterial agent alone and the combined application of bio-based soil amendments and the bacterial agent effectively reduced >20% of the uptake of Cd by the plant. Soil nitrogen level was significantly raised after the combined fertilization. The multivariate diversity analysis and co-occurrence network algorithm showed that a significant shift of microbial communities took place, in which the microbial populations tended to be homogeneous with reduced microbial richness and increased diversity after the co-application. The treatment of fermentative cow dung with the addition of the bacterial agent showed a significant increase in the microbial community dissimilarity ($R = 0.996$, $p = 0.001$) compared to that treated with cow dung alone. The co-application of the bacterial agent with both organic fertilizers significantly increased the abundance of *Actinobacteria* and *Bacteroidetes*. The FAPROTAX soil functional analysis revealed that the introduction of the microbial agent could potentially suppress human pathogenic microorganisms in the field fertilized with edible fungi residue. It also showed that the microbial agent can reduce the nitrite oxidation function in the soil when applied alone or with the organic fertilizers. Our study thus highlights the beneficial effects of the Cd-immobilizing bacterial inoculant on *H. cordata* and provides a better understanding of the microbial changes induced by the combined fertilization using the microbial agent and organic soil amendments in a Cd-contaminated field.

Keywords: bacterial community, cadmium-immobilizing bacteria, cadmium, biofertilizer, *Houttuynia cordata*

INTRODUCTION

Metallic elements are a naturally occurring and indispensable component of different soil environments (Kabata-Pendias, 1993). Most of these metals are innocuous and pose no threat to vegetation and soil organisms. However, heavy metals such as arsenic (As), cadmium (Cd), chromium (Cr), mercury (Hg), and lead (Pb) can cause serious hazards to soil ecosystem and health, which could further affect human health and well-being by means of bioaccumulation affects through food chain (Liu X. et al., 2013; Osman et al., 2021). One of the worst health-threatening heavy metal that has been polluting arable land and causing global concerns is cadmium (Cd) (Satarug et al., 2003). Cd in soil often occurs in high concentrations, inevitably posing a risk to the health of humans and animals that reside in the immediate vicinity (Schoeters et al., 2006). Cd is exceedingly bioavailable to both plant and animal cells and the toxicity of Cd can be summarized as interference with essential metal uptake in cells (Martelli et al., 2006). Since Cd is not a naturally-existing metal in organisms, the major sources of Cd pollution are anthropogenic activities (Yuan et al., 2019). These Cd pollution causes include burning of fossil fuels, mining and smelting of ore minerals, and inadequate disposal of electronic wastes (Sun et al., 2010; Li et al., 2011; Gujre et al., 2021). It is estimated that more than 5.6–38 kt of Cd is released into the environment per annum and approximately 20% of China's agricultural soil accounting for 1.3×10^5 ha of the total polluted lands is contaminated with this heavy metal (Rafiq et al., 2014; Liu et al., 2020). Therefore, it is urgent that remediation efforts come into effect for the alleviation of this imminent environmental threat.

Although Cd pollution in soils is known to have a negative impact on the growth and behavior of indigenous plants as well as on the composition and ecological succession of their associated microbial communities (Tiwari and Lata, 2018), beneficial microbial consortia can lead to an improved rhizosphere microenvironment which could help mitigate the negative effects upon plants caused by heavy metal stress (Wenzel, 2009; Kang et al., 2018). There are various ways by which Cd pollution in soils can be alleviated. One classic example is the plant's secretion of root exudates, which mainly contain primary metabolites and can reduce Cd toxicity in the rhizosphere by absorption, chelation, and complexation (Dong et al., 2007; Canarini et al., 2019). Studies showed that these root-secreted phytochemicals were able to ameliorate Cd tolerance in plants under metal-stressed conditions (Bali et al., 2020). However, these chemicals alone can only play a small part in tackling Cd pollution in soil when compared to the approaches using beneficial microorganisms, which are essentially probiotics for plants (Pramanik et al., 2018; Konkolewska et al., 2020). A previous study showed that the application of a plant growth-promoting rhizobia inoculant alleviated stresses to native plants caused by the presence of high levels of toxic heavy metals in multimetallic tailing soil (Kang et al., 2018). Another recent research demonstrated that the application of beneficial *Pseudomonas* strains in the soil mitigated the lethal effects of chromium and significantly improved the growth of *Abelmoschus esculentus* (Mushtaq et al., 2021). In addition, highly soluble metals such as Cd and Cu can be immobilized by plant growth-promoting strains, leading to less metals to be transferred to the above-ground parts of plants (Ke et al., 2021). Recent studies showed that the most important mechanisms of Cd immobilization in soil by microorganisms are microbially induced carbonate precipitation (MICP) and microbially induced phosphate precipitation (MIPP), by which free Cd^{2+} ions in the soil were immobilized after contacting the microbially produced carbonate and various phosphate anions (Fang et al., 2021; Zeng et al., 2021).

Microbial communities are very sensitive to changes in the microenvironments of both rhizosphere and bulk soils in the heavy metal-polluted environment (Yu et al., 2019; Kang et al., 2020; Barra Caracciolo and Terenzi, 2021). Studies indicated that highly toxic metals/metalloids such as As, Cr, Hg, and Pb in the soil can lead to intense changes in the community composition and microbial diversity and cause obstructions to adaptation processes resulting in the decline of microbial populations in metal-polluted ecosystems (Pan et al., 2021; Shuaib et al., 2021). The application of bio-based fertilizers (BBF) in itself is in conformity with circular economy and can mitigate heavy metal pollution in agricultural soil (Huang et al., 2016; Chojnacka et al., 2020; Dhaliwal et al., 2020). In one case, it was reported that the application of metal-immobilizing organic fertilizer led to improved soil quality and more than 50% reduction of extractable Cd, Cu, and Pb (Hu et al., 2021). Other researchers found that bio-based soil amendments decreased soil exchangeable Cd and Cd accumulation in grain, increased soil microbial diversity and species richness, and contributed to faster nutrient turnover (Gong et al., 2021).

However, there is a lack of information on how the microbial communities change with combined application of bio-based fertilizers and beneficial microbial inoculant in a heavy metal-contaminated field with the cultivation of crops. It is also unclear about the *in situ* effects of the combined fertilizers on the growth of plants. Therefore, the present study aims to elucidate the variations in soil microbial communities caused by the field utilization of two bio-based fertilizers and a Cd-immobilizing microbial inoculant, and also to examine the positive resulting effects on *Houttuynia cordata*, which is an important edible and medicinal plant.

MATERIALS AND METHODS

Soil Sampling and Measurements

A cadmium-contaminated field on the Chengdu Plain, Southwest China, was selected for the cultivation of *H. cordata*. The soil type of this field was paddy soil. Soil samples were collected for measurements of cadmium and physicochemical properties and isolation of Cd-immobilizing bacteria.

Soil samples were mixed into slurries with a 2:5 (w/v) soil-water ratio and the pH was then determined using a standard glass/calomel electrode (Shanghai Yoke, China). Air-dried soil samples were digested using a mixture of H_2SO_4, H_2SO_4-$HClO_4$, and HF-$HClO_4$ solutions before the concentrations of soil total nitrogen (TN), phosphorus (TP) and potassium (TK) were measured using the Kjeldahl method (Kjeltec 8400, FOSS, Sweden), the Mo-Sb colorimetric method at OD_{660nm} (WFJ2100, UNICO, China), and flame spectrophotometry

(FP6410, Shanghai Precision & Scientific, China), respectively (Yu et al., 2017; Kang et al., 2020). Soil organic matter (TO) was determined using the Walkley–Black chromic acid wet oxidation method (Storer, 1984). Soil available phosphorus (AP) and potassium (AK) were simultaneously extracted using the ASI soil extracting solution (Bogunovic et al., 2017), and their concentrations were measured with a UV-3300 spectrophotometer (MAPADA, Shanghai, China) and a FP6410 flame spectrophotometer (PRECISION & SCIENTIFIC, Shanghai China), respectively. Available nitrogen (AN) was determined using the Alkali N-proliferation method (Dahnke and Johnson, 1990). Soil samples, fermentative edible fungi residue, and fermentative cow dung were digested using a mixture of HNO_3-HCl-$HClO_4$ in a 1:2:2 (v:v:v) ratio for the determination of total Cd. The bioavailable fraction of Cd was extracted from the soil samples using pentetic acid (DTPA) (Massas et al., 2013). The concentration of Cd was measured using inductively coupled plasma atomic emission spectroscopy (ICP-AES) (IRIS Intrepid II; Thermo Electron Corporation, San Diego, CA, United States) as described before.

Isolation of Cadmium-Immobilizing Bacteria

Bacteria were isolated from the field soil samples by using beef extract-peptone agar medium (Yu et al., 2014). The tolerance of bacteria to Cd was represented by the minimum lethal concentration (MLC) of Cd for these isolates. Then, some bacteria with tolerance against Cd were selected to determine Cd^{2+} immobilization using the previously published method (Li et al., 2019). The bacterial strains with an outstanding immobilizing ability were identified by 16S rRNA gene sequencing and genetic affinity analysis (Yu et al., 2014).

Experimental Design

This research was performed at the *H. cordata* main production field of Chengdu Plain from spring to summer. When *H. cordata* plants emerged as ∼10 cm height seedlings, the field with uniform plant growth was selected to perform six different fertilization treatments. Each treatment had six replications, and each replication of the field had an area of approximately 3 × 5 m^2. A one-meter-width isolation zone was set between each treatment plot. These six treatment groups were composed of non-fertilization (CK), Cd-immobilizing bacteria agent (MB), fermentative edible fungi residue mixed with Cd-immobilizing bacteria agent (FEMB), fermentative edible fungi residue (FE), fermentative cow dung mixed with Cd-immobilizing bacteria agent (FCMB), and fermentative cow dung (FC). For MB treatment, the mixture of Cd-immobilizing bacteria culture medium (approximately 10^9 cells/ml) was applied at 120 l/hm^2 with 400-fold dilution. For the treatments of FEMB and FCMB, the Cd-immobilizing bacteria culture medium was mixed into the fermentative edible fungi and cow dung, with the same application amount of bacteria cells as in MB treatment. The organic fertilizer treatments (FE, FC, FEMB, and FCMB) were applied at 45 t/hm^2 to the field. Then, the experimental field was conformably managed by the conventional field methods, such as watering during drought.

After 6 months of cultivation, *H. cordata* plant samples and rhizosphere soil samples were collected from each treatment area in the field. Plant and soil samples were randomly collected from five points at each treatment area and separately packed into a sterile plastic bags. Afterward, the soil samples were mixed well, transferred into a sterile EP tube, and immediately frozen using liquid nitrogen. The frozen soil samples were then taken to lab in liquid nitrogen and stored at −80°C for extraction of total soil DNA. The remaining soil samples still kept in bags were taken to lab for air-drying, grounding, screening, and measurements of soil physical and chemical properties and heavy metal contents. The plant samples were taken to lab for the measurement of Cd content. As a result, a total of 36 plant and soil samples were collected for the six treatments. Soil samples were used for measurements of cadmium and physicochemical properties by using the above-mentioned method and extraction of soil total DNA for high-throughput sequencing.

Analyses of Plant Cadmium and Nutrient Contents

To remove Cd absorbed on root surface, the roots of the harvested *H. cordata* were washed using tap water and, after being immersed in 10 mM EDTA for 30 min, rinsed thoroughly with deionized water (Luo et al., 2011). The roots and aboveground parts of *H. cordata* plants were separately kept in two envelopes for the deactivation of enzymes at 105°C for 30 min and at 80°C until constant weight in an oven. The oven-dried roots and aboveground parts were triturated and digested with HNO_3/$HClO_4$ solution (4:1, v/v). The Cd contents in roots and aboveground parts were measured with inductively coupled plasma atomic emission spectroscopy (ICP-AES, IRIS Intrepid II; Thermo Electron) (Kang et al., 2018). The contents of nitrogen, phosphorus and potassium in *H. cordata* plant tissues were determined using the commonly used methods (Thomas et al., 1967).

Extraction of Soil Total DNA

A precise amount of 0.5 g of the frozen soil was taken from EP tubes for the extraction of soil total DNA using FastDNA^{TM} SPIN Kit (MP Biomedicals LLC, Santa Ana, CA, United States). A soil sample was put into a sterile EP tube and mixed with phosphate buffer (978 μl) and MTbuffer (122 μl). The tube was shaken for 30 min, and then centrifuged at 14,000 r min^{-1} for 15 min. The supernatant was transferred into another sterile EP tube which was filled with 250 μl 10 × PPS. The mixture was centrifuged at 14,000 r min^{-1} for 5 min to remove the precipitation and the resulting supernatant was transferred into another sterile EP tube. After adding the adsorption suspension (1 ml), the supernatant mixture was precipitated onto the SPIN filter membrane followed by centrifugation at 12,000 r min^{-1} for 1 min to collect total DNA from the membrane. After this, the SPIN filter membrane was washed by adding ethanol liquid and centrifugation at 12,000 r min^{-1} for 1 min. Total DNA on the membrane was dissolved into 50 μl ddH_2O by centrifugation at 14,000 r min^{-1} for 1 min after

being properly air-dried. The quality of the extracted soil total DNA was tested using polyacrylamide gel electrophoresis (PAGE) and a NanoDrop ND1000 spectrophotometer (NanoDrop Technologies, Wilmington, DE, United States) at wavelengths of 260/280 and 260/230 nm. The eligible total DNA was stored at −80 °C.

Amplicon Library Construction and High-Throughput Sequencing

High-quality soil total DNA was used for the high-throughput sequencing of the V3–V4 hyper variable region of prokaryotic 16S rRNA using the universal primers 515F and 806R (Wu X. et al., 2016). PCR reaction was performed in a reaction mixture (30 μl) containing 15 μl Phusion® High-Fidelity PCR Master Mix (New England Biolabs), 0.2 μM primers and 10 ng template DNA. Thermal cycling conditions consisted of initial denaturation at 98°C for 1 min, 30 cycles of denaturation at 98°C for 10 s, annealing at 50°C for 30 s, elongation at 72°C for 30 s, and a final extension step of 72°C for 5 min. The amplicons with a bright main strip between 400 and 450 bp were selected using electrophoresis on 2% agarose gel for sequencing library preparation, which was achieved using NEB Next® Ultra™ DNA Library Prep Kit for Illumina (NEB, Ipswich, MA, United States) following manufacturer's instructions. The quality of the amplicon library was assessed using a Qubit@ 2.0 Fluorometer (Thermo Scientific) and Agilent Bioanalyzer 2100 system. The amplicon library was sequenced on the Illumina HiSeq platform (Illumia, San Diego, CA, United States) (Caporaso et al., 2012).

Bioinformatics and Statistical Analyses

The raw sequences were analyzed using QIIME2 2019.10 workflow. The paired-end reads were first assembled using USEARCH algorithm and those with the Phred quality scores less than 4 or with ambiguous bases were removed before further analysis. The clean sequences were subsequently denoised using deblur algorithm, in which all sequences were trimmed to a length of 350 bp. Given the biases introduced by primers, the first 35 bp of all sequences was trimmed. The amplicon variant sequences (ASVs) produced after denoising were aligned in Silva 132 database using classify-sklearn algorithm to infer their taxonomic classifications. To ensure the accuracy of final results, singletons and sequences classified as mitochondria or chloroplast were filtered before all samples were rarefied to 8,388 sequences. A table containing ASVs were thus created for subsequent diversity analyses. Functional Annotation of Prokaryotic Taxa (FAPROTAX) (Louca et al., 2016) was used to predict the biogeochemical functions of communities, and the functions with significant ($p < 0.05$) differences between treatments were demonstrated on the graphs.

The α diversity indices calculated by QIIME2 workflow were compared using Wilcoxon rank sum test ($p < 0.05$). Bacterial composition in each treatment was visualized using 'ggplot2' in R Studio. To reveal the differences in bacterial composition among six treatments, the Bray–Curtis distance matrices of microbial communities in each treatment were created and subsequently compared through the analysis of similarity (ANOSIM) using 'vegan' package. The 'DESeq2' package (Love et al., 2014) was used to identify differential bacteria among treatments by calculating the enrichment and depletion of ASVs between two treatments (log2 fold changes = 1, FDR < 0.05) (Li F. et al., 2017), and the results generated by this analysis were visualized as volcano diagrams. The LDA effect size (LEfSe) analysis was applied to estimate the differential bacteria at taxonomic levels (LDA score > 4, $p < 0.05$) and the differences in biogeochemical functions (LDA score > 1.5, $p < 0.05$) using 'microeco' package (Liu et al., 2021) hosted on the Microbiome Database[1]. Significant biogeochemical functions were further visualized using 'pheatmap' package. To reveal the relationships between the shifts in bacterial communities and the differences of micro-habitats across six treatments, we performed the redundancy analysis (RDA) based on Bray–Curtis distance using 'vegan' package. To reveal the bacterial relationships in each treatment, six co-occurrence networks at genus level were created using 'igraph' package (Csardi and Nepusz, 2006) (Spearman $\rho = 0.6$, $p < 0.05$) and the results were further visualized using Gephi v0.9.2[2] (Yu et al., 2019; Kang et al., 2020).

RESULTS

Soil Properties and Cd-Immobilizing Bacterial Strains

Soil in the *H. cordata* field contained 0.58 ± 0.04 mg kg^{-1} of total Cd and 0.15 ± 0.01 mg kg^{-1} of bioavailable Cd, which exceeded the standard value stipulated in the Soil Environmental Quality Standard of China. The sample contained a high level of organic matter (10.46% ± 0.13%) with low pH (5.61 ± 0.18). The total contents of nitrogen (N), phosphorus (P), and potassium (K) were 1.87 ± 0.23 g kg^{-1}, 0.93 ± 0.13 g kg^{-1}, and 10.62 ± 0.53 g kg^{-1}, whereas the bioavailable fractions were 185.30 ± 7.93 mg kg^{-1}, 77.63 ± 2.26 mg kg^{-1}, 139.50 ± 3.33 mg kg^{-1}, respectively.

Four bacterial strains with an outstanding immobilizing ability were isolated from the cadmium-contaminated farm field soil. According to 16S rRNA genetic affinity analysis, the Cd-immobilizing bacterial strains GH8-1 and ZJ1-16B were identified as *Bacillus iocasae*, WDGJ-1 as *Bacillus subtilis*, and NQ5-6 as *Bacillus wiedmannii*. Since these four Cd-immobilizing bacterial strains had no antagonism against each other, they were mixed in a ratio of 1:1:1:1 and applied into the treatments of MB, FEMB, and FCMB in the *H. cordata* field experiment.

Cd and Nutrient Contents in *H. cordata*

After a total of 6 months of cultivation, the *H. cordata* showed vigorous growth without significant difference in fertilization treatment groups, but the fertilized plants looked better than the control plants. Cd absorption effect by this plant was observed when grown in Cd-contaminated soil. The enrichment of Cd in roots and aboveground parts of *H. cordata* was significantly different ($p < 0.05$) under different fertilization treatments

[1]http://egcloud.cib.cn/

[2]https://gephi.org/

TABLE 1 | Contents of nitrogen, phosphorus, potassium, and cadmium in roots and shoots of *Houttuynia cordata*.

Measured parameter	Plant tissue	CK	MB	FE	FEMB	FC	FCMB
Cd (mg kg^{-1})	Roots	1.86 ± 0.05b$^{\boldsymbol{a}}$	1.39 ± 0.23c$^{\boldsymbol{b}}$	2.46 ± 0.26a^{a}	1.92 ± 0.14ab^{b}	2.41 ± 0.23a$^{\mathbf{b}}$	1.84 ± 0.16ab$^{\mathbf{a}}$
	Aboveground parts	0.30 ± 0.03c$^{\boldsymbol{a}}$	0.36 ± 0.03bc$^{\boldsymbol{a}}$	0.40 ± 0.01ab^{a}	0.33 ± 0.02bc^{b}	0.46 ± 0.06a$^{\mathbf{a}}$	0.36 ± 0.07bc$^{\mathbf{b}}$
TN (g kg^{-1})	Roots	8.30 ± 0.92ab$^{\boldsymbol{a}}$	8.30 ± 1.44ab$^{\boldsymbol{a}}$	7.20 ± 2.79bc^{a}	4.44 ± 2.30c^{a}	9.85 ± 1.05ab$^{\mathbf{a}}$	10.51 ± 0.49a$^{\mathbf{a}}$
	Aboveground parts	11.95 ± 1.46a$^{\boldsymbol{b}}$	14.97 ± 1.71a$^{\boldsymbol{a}}$	13.63 ± 1.83a^{a}	11.64 ± 2.62a^{a}	13.82 ± 1.89a$^{\mathbf{a}}$	12.41 ± 2.63a$^{\mathbf{a}}$
TP (g kg^{-1})	Roots	24.21 ± 3.29a$^{\boldsymbol{a}}$	11.45 ± 2.68b$^{\boldsymbol{b}}$	11.70 ± 3.52b^{a}	11.03 ± 2.28b^{a}	22.77 ± 4.44a$^{\mathbf{a}}$	11.33 ± 1.78b$^{\mathbf{b}}$
	Aboveground parts	23.48 ± 2.10a$^{\boldsymbol{a}}$	21.73 ± 1.37a$^{\boldsymbol{a}}$	21.27 ± 3.88a^{a}	22.64 ± 2.50a^{a}	13.78 ± 3.96b$^{\mathbf{a}}$	9.83 ± 2.17b$^{\mathbf{a}}$
TK (g kg^{-1})	Roots	34.17 ± 1.50a$^{\boldsymbol{a}}$	33.90 ± 1.69a$^{\boldsymbol{a}}$	33.95 ± 3.65a^{a}	33.35 ± 1.50a^{a}	33.28 ± 1.19a$^{\mathbf{a}}$	30.28 ± 1.95a$^{\mathbf{b}}$
	Aboveground parts	28.93 ± 0.70b$^{\boldsymbol{a}}$	29.47 ± 0.62b$^{\boldsymbol{a}}$	31.38 ± 0.97a^{a}	28.78 ± 1.40b^{b}	31.60 ± 1.07a$^{\mathbf{a}}$	31.60 ± 0.81a$^{\mathbf{a}}$

Different lowercase letters indicate significant differences ($p < 0.05$). Italic bold superscript letters indicate differences between CK and MB; italic superscript letters indicate differences between FE and FEMB; bold superscript letters indicate differences between FC and FCMB. Conventional letters indicate differences of the same measured parameter among all treatments.

(**Table 1**). The Cd content in the roots of *H. cordata* was about four to six times higher than that in the aboveground parts. Compared to the control (CK), both the fermentative edible fungi residue (FE) and fermentative cow (FC) caused approximately 30% and 32% increases of Cd content in roots and 11% and 27% increases of Cd in aboveground parts, respectively. The introduction of the Cd-immobilizing bacteria reduced Cd content in roots by 25% and in aboveground parts by 17%. When the Cd-immobilizing bacterial inoculant was mixed with fermentative edible fungi residue (FEMB) and fermentative cow dung (FCMB), a decrease of Cd content was induced in roots by 22% and in aboveground parts by 24%.

As the three major nutrient elements of plants, the concentrations of nitrogen, phosphorus, and potassium in roots and aboveground parts of *H. cordata* grown in differently treated soils were significantly different (**Table 1**). For nitrogen, the concentration in roots was generally lower than that in aboveground parts. Nitrogen content was highest in the roots of *H. cordata* from the soil treated with FCMB, whereas it was not significantly different ($p < 0.05$) in the aboveground parts of the plant in all treatment groups. The phosphorus content in the roots of *H. cordata* grown in CK and FC were double the amount in other field soil samples. The phosphorus concentration in the aboveground parts of *H. cordata* in the soil treated with FC and FCMB was significantly lower ($p < 0.05$) than that in the other four treatment groups. The potassium concentrations showed no significant difference ($p < 0.05$) among all treatment groups. However, potassium in the aboveground parts of *H. cordata* in the soil treated with FE, FC, and FCMB was significantly higher ($p < 0.05$) than that in other three treatment groups.

Cd Content and Physicochemical Properties in the Substrates

There was no significant change in the soil total Cd content in the field grown with *H. cordata* compared to the background total Cd content after 6 months with different fertilizer regimens (**Table 2**). However, the content of bioavailable Cd in different fertilizer treatment groups was significantly different. Especially, the concentration of bioavailable Cd in FEMB and FCMB-treated soils significantly decreased by 18% compared to CK. We also measured the Cd concentration in the organic fertilizers, which showed that the fermentative fungi residue (FE) contained 0.78 mg kg^{-1} total Cd, while the cow dung (FC) contained 0.56 mg kg^{-1} total Cd. There was 0.15 mg kg^{-1} Cd in FE and 0.14 mg kg^{-1} Cd in FC. Soil pH in CK was not significantly altered after Cd-immobilizing bacteria was added alone, indicating that the addition of Cd-immobilizer on its own could not change soil pH. However, soil pH was significantly increased in the treatments of FE and FC, while it was significantly decreased in FCMB. Although organic fertilizers had been applied in some treatment groups, soil organic matter (TO)

TABLE 2 | Soil cadmium content and physicochemical properties.

Soil property	CK	MB	FE	FEMB	FC	FCMB
ACd (mg kg^{-1})	0.17 ± 0.01ab$^{\boldsymbol{a}}$	0.15 ± 0.01bc$^{\boldsymbol{a}}$	0.18 ± 0.01a^{a}	0.14 ± 0.01c^{b}	0.16 ± 0.01bc$^{\mathbf{a}}$	0.14 ± 0.02c$^{\mathbf{a}}$
TCd (mg kg^{-1})	0.59 ± 0.03a$^{\boldsymbol{a}}$	0.57 ± 0.04a$^{\boldsymbol{a}}$	0.58 ± 0.03a^{a}	0.61 ± 0.03a^{a}	0.59 ± 0.05a$^{\mathbf{a}}$	0.58 ± 0.02a$^{\mathbf{a}}$
pH	5.85 ± 0.08bc$^{\boldsymbol{a}}$	5.88 ± 0.09bc$^{\boldsymbol{a}}$	6.10 ± 0.20a^{a}	5.94 ± 0.09abc^{a}	6.05 ± 0.08ab$^{\mathbf{a}}$	5.78 ± 0.03c$^{\mathbf{b}}$
TO (%)	9.84 ± 0.41ab$^{\boldsymbol{a}}$	10.48 ± 0.68a$^{\boldsymbol{a}}$	10.39 ± 0.22a^{a}	9.73 ± 0.44ab^{b}	10.36 ± 0.42ab$^{\mathbf{a}}$	9.55 ± 0.21b$^{\mathbf{b}}$
AN (mg kg^{-1})	216.83 ± 6.29b$^{\boldsymbol{b}}$	252.47 ± 8.50a$^{\boldsymbol{a}}$	195.73 ± 9.32c^{a}	204.13 ± 4.88bc^{a}	195.73 ± 4.76c$^{\mathbf{b}}$	207.10 ± 7.47bc$^{\mathbf{a}}$
AP (mg kg^{-1})	82.04 ± 3.78d$^{\boldsymbol{a}}$	86.48 ± 6.10cd$^{\boldsymbol{a}}$	95.19 ± 1.66abc^{a}	87.65 ± 4.08bcd^{b}	96.11 ± 6.04ab$^{\mathbf{a}}$	102.04 ± 4.32a$^{\mathbf{a}}$
AK (mg kg^{-1})	210.83 ± 8.81a$^{\boldsymbol{a}}$	101.17 ± 6.87d$^{\boldsymbol{b}}$	132.50 ± 5.44c^{b}	141.33 ± 4.82c^{a}	105.33 ± 5.22d$^{\mathbf{b}}$	184.33 ± 7.91b$^{\mathbf{a}}$
TN (g kg^{-1})	2.21 ± 0.27a$^{\boldsymbol{a}}$	2.52 ± 0.52a$^{\boldsymbol{a}}$	2.65 ± 0.14a^{a}	2.74 ± 0.43a^{a}	2.30 ± 0.20a$^{\mathbf{b}}$	2.94 ± 0.59a$^{\mathbf{a}}$
TP (g kg^{-1})	1.01 ± 0.07b$^{\boldsymbol{a}}$	1.04 ± 0.08b$^{\boldsymbol{a}}$	1.09 ± 0.14ab^{a}	1.26 ± 0.09a^{a}	1.01 ± 0.07b$^{\mathbf{a}}$	1.06 ± 0.16ab$^{\mathbf{a}}$
TK (g kg^{-1})	11.09 ± 0.63a$^{\boldsymbol{a}}$	11.29 ± 0.78a$^{\boldsymbol{a}}$	11.30 ± 0.78a^{a}	11.49 ± 0.58a^{a}	10.94 ± 0.54a$^{\mathbf{a}}$	11.47 ± 0.91a$^{\mathbf{a}}$

Different lowercase letters indicate significant differences ($p < 0.05$). Italic bold superscript letters indicate differences between CK and MB; italic superscript letters indicate differences between FE and FEMB; bold superscript letters indicate differences between FC and FCMB. Conventional letters indicate differences of the same test index among all treatments.

in all the treatment groups did not significantly differ from that in CK after 6 months (**Table 2**). The available nitrogen (AN) in MB was significantly increased ($p < 0.05$) by 16% compared to CK, whereas that in other treatment groups was significantly reduced ($p < 0.05$) (**Table 2**). Available phosphorus (AP) concentration in other fertilizer-treated groups was significantly higher ($p < 0.05$) than that in CK. The concentration of available potassium (AK) in non-fertilized soil was the highest, whereas that in MB was the lowest among all the treatments. The concentrations of total potassium (TK) and total nitrogen (TN) in all treatment groups was not significantly different ($p < 0.05$). Total phosphorus (TP) was the highest in FEMB, followed by FEMB and the other three treatment groups.

Abundance of Bacterial Communities Under Different Fertilization Regimens

A total of 3,304,373 reads of the partial 16S rRNA gene sequences were obtained from the high throughput sequencing for the 42 soil samples. After quality filtering and removal of unique tags, the raw sequences yielded 352,296 of qualified sequences, which were finally clustered into 8388 amplicon sequence variants (ASVs) for the following analyses. The α-diversity indices showed significant changes ($p < 0.05$) in bacterial community richness but no obvious shifts in community diversity among the six treatment groups (**Table 3**).

The abundance analysis revealed that *Proteobacteria* accounted for 42–47% of the entire communities throughout the six groups of fertilizer-treated soils (**Figure 1A**), indicating that *Proteobacteria* was the dominant phylum in the soil grown with *H. cordata*. However, the shift of bacterial communities in different treatment groups was very obvious. The top 12 phyla in CK were *Proteobacteria* (43.92%), *Bacteroidetes* (13.61%), *Acidobacteria* (13.27%), *Actinobacteria* (9.3%), *Gemmatimonadetes* (7.87%), *Chloroflexi* (2.06%), *Nitrospirae* (2.49%), *Thaumarchaeota* (1.66%), *Latescibacteria* (1.18%), *Verrucomicrobia* (1.49%), *Firmicutes* (0.82%), and *Patescibacteria* (0.72%). Compared with the non-fertilization group, Cd-immobilizing bacterial inoculant increased the relative abundance of *Bacteroidetes*, *Actinobacteria*, *Latescibacteria*, *Firmicutes,* and *Patescibacteria* by 7.36, 18.95, 12.25, 78.99, and 18.01%, respectively. When the inoculant was mixed with the fermentative edible fungi residue, the relative abundance of *Bacteroidetes*, *Actinobacteria*, *Chloroflexi*, *Thaumarchaeota*, *Verrucomicrobia, Firmicutes,* and *Patescibacteria* was increased by 39.78, 12.39, 32.44, 8.32, 5.36, 17.61, and 32.35%, respectively, in the soil grown with *H. cordata*. When Cd-immobilizing bacterial agent was applied in combination with the fermentative cow dung, only *Bacteroidetes*, *Actinobacteria*, *Chloroflexi*, and *Patescibacteria* were increased by 27.76, 20.25, 23.49, and 63.22%, respectively. Under the condition that Cd-immobilizing inoculant was applied alone or combined with fermentative edible fungi residue and cow dung, *Bacteroidetes* and *Patescibacteria* were increased, but *Proteobacteria*, *Acidobacteria*, *Gemmatimonadetes*, and *Nitrospirae* were reduced in different degrees.

The pairwise ANOSIM analysis (**Supplementary Table 1**) showed that the bacterial communities of CK were significantly separated ($p < 0.05$) from the other five treatment groups. The bacterial communities in the soil where the Cd-immobilizing bacterial inoculant was applied alone were completely different ($p < 0.05$) from those in the other four treatment groups. The bacterial community dissimilarity between FCMB and FC was significant ($R = 0.996$, $p = 0.001$), whereas no obvious difference was found between FEMB and FE ($R = 0.154$, $p = 0.094$). The dissimilarity distance plot (**Figure 1B**) also showed that the difference in bacterial community structure between FCMB and FC was the highest while that between FEMB and FE was unapparent.

Differences Between Bacterial Communities Under Different Fertilization Regimens

The volcano plots at ASV level indicated that some taxa were enriched but others depleted after fertilization (**Figure 2A**). Compared to CK, only three ASVs were enriched while the other three were depleted after applying the Cd-immobilizing bacterial agent; 159 ASVs were enriched whereas 127 were depleted in FEMB; 118 ASVs were enriched but 119 were depleted in FE; 185 ASVs were enriched while 146 were depleted in FCMB; and only 36 ASVs were enriched whereas 54 ASVs were depleted in FC.

The LDA Effective Size (LEfSe) histogram (**Figure 2B**) demonstrated dramatic changes in these bacterial communities among different fertilized soils. The LDA scores of 34 bacterial taxa in all soil samples (including 4 in CK, 12 in FEMB, 7 in FE, 2 in FCMB, 9 in FC but none in MB) were higher than 3.5. These

TABLE 3 | Alpha-diversity of bacteria communities in the soil grown with *Houttuynia cordata* under different fertilization regimens.

Treatment	CK	MB	FEMB	FE	FCMB	FC
Observed ASVs	2011 ± 65ab^{a}	2001 ± 149ab^{a}	1898 ± 180b^{a}	1885 ± 208b^{a}	2022 ± 150ab^{a}	2193 ± 126a^{a}
Good's coverage	0.92 ± 0.01ab^{a}	0.92 ± 0.01ab^{a}	0.94 ± 0.02a^{a}	0.93 ± 0.02a^{a}	0.93 ± 0.02ab^{b}	0.90 ± 0.01b^{a}
Chao1	2477 ± 162ab^{a}	2474 ± 259ab^{a}	2199 ± 329b^{a}	2200 ± 361b^{a}	2354 ± 312ab^{b}	2824 ± 270a^{a}
ACE	2657 ± 171ab^{a}	2668 ± 283ab^{a}	2318 ± 363b^{a}	2355 ± 410ba^{a}	2509 ± 360ab^{b}	3019 ± 302a^{a}
Shannon	9.82 ± 0.11a^{a}	9.75 ± 0.21a^{a}	9.80 ± 0.24a^{a}	9.72 ± 0.34a^{a}	10.03 ± 0.10a^{a}	10.00 ± 0.13a^{a}
Simpson	0.997 ± 0.001a^{a}	0.996 ± 0.001a^{a}	0.996 ± 0.002a^{a}	0.996 ± 0.002a^{a}	0.998 ± 0.000a^{a}	0.997 ± 0.000a^{a}

Different lowercase letters indicate significant differences ($p < 0.05$); italic bold superscript letters indicate differences between CK and MB; italic superscript letters indicate differences between FE and FEMB; bold superscript letters indicate differences between FC and FCMB. Conventional letters indicate differences of the same index among all treatments.

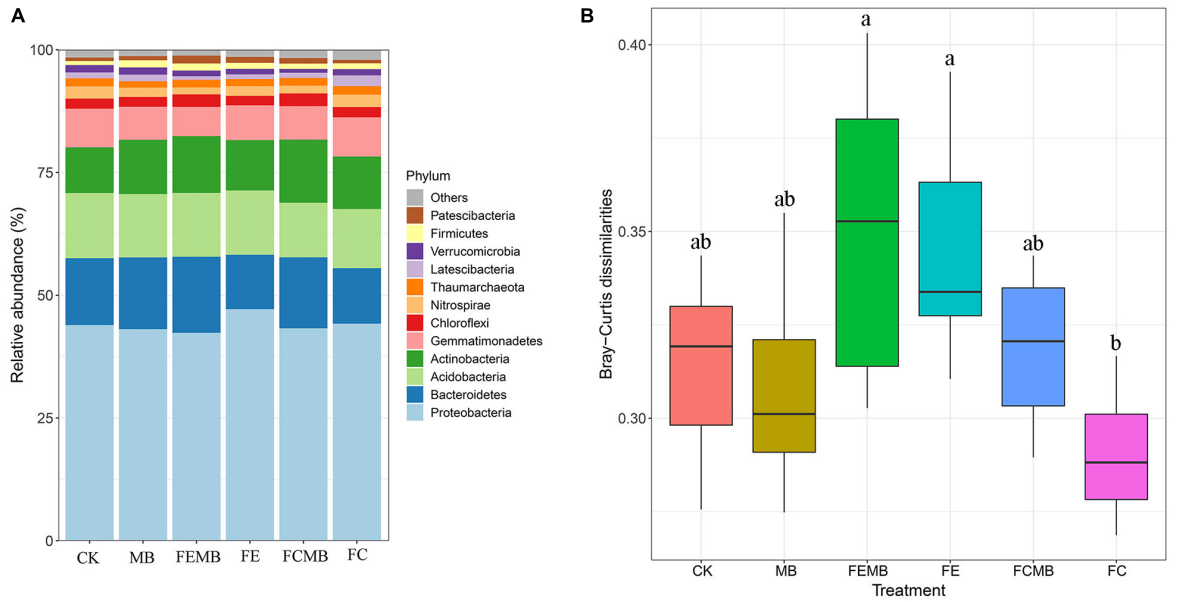

FIGURE 1 | Bacterial community composition in the field grown with *Houttuynia cordata* under different fertilization regimens. **(A)** Relative abundance heatmap of the top 12 phyla. **(B)** Dissimilarity distance of the bacterial community structures; different lowercase letters indicate significant differences ($p < 0.05$).

taxa biomarkers were fully diverse in different fertilized soils, e.g., *Bacteroidetes*, *Nitrosomonadaceae*, *Actinobacteria*, *Nitrospirae*, and *Pseudolabrys* were most prominent in FEMB, FE, FCMB, FC, and CK, respectively.

Community Dissimilarity and Correlations With Environmental Factors

The redundancy analysis (RDA) revealed the roles of the environmental factors in driving the community changes (**Figure 3**). The RDA biplot, with its first and second axis explaining 32.08% and 18.59% of the total variance, showed that there was a significant difference in community composition among the six groups, as indicated by a good separation among them. All the five experimental groups showed distinctive differences from the control group. An obvious community dissimilarity was found between the group applied with Cd-immobilizing inoculant alone (MB) and those with a combination of the inoculant and other fermentative fertilizers (FCMB and FEMB). The combination of the bio-based fertilizers with the bacterial inoculant led to considerable community changes compared to the application of either the inoculant or the fermentative fertilizers. The length of the arrows indicated that the correlations between the environmental factors and the community structure were in the following descending order: available K > available P > available N > TO > pH > available Cd.

Correlations Among Bacterial Communities in the Soil of *H. cordata*

The co-occurrence network (**Figure 4**) showed significant changes in the correlations of bacterial communities under different fertilization regimens. The microbial co-occurrence network of CK included 94 nodes and 219 edges with 98.63% positive correlations, while that of MB contained 102 nodes and 241 edges with 95.44% positive correlations. When the Cd-immobilizing bacterial agent was mixed with the fermentative edible fungi residue, the microbial co-occurrence network in soil had 90 nodes and 423 edges with 99.05% positive correlations, whereas only 85 nodes and 311 edges with 100% positive correlations were found when applied with fermentative edible fungi residue. However, when the Cd-immobilizing bacterial agent was applied in combination with the fermentative cow dung, the microbial metal co-occurrence network in soil contained 78 nodes and 240 edges with 99.58% positive correlations, while 64 nodes and 132 edges with 96.21 positive correlations were observed on the network when applied with fermentative cow dung. For the co-occurrence networks of fertilization treatment without the Cd-immobilizing bacterial agent, the nodes were clustered into 21 modules for CK, 15 modules for FE, and 14 modules for FC. When the Cd-immobilizing bacterial agent was applied, the nodes were clustered into 26, 16, and 15 modules for MB, FEMB, and FCMB, respectively. The average path lengths of the correlation networks of MB (1.32), FEMB (1.22), and FCMB (1.59) were lower than those of the fertilization treatments without the inoculant (CK, 1.84; FE, 1.33; and FC, 1.72). Except for the treatment using fermentative edible fungi residue as organic fertilizer, the network clustering coefficients of other two fertilization treatments with inoculant addition (MB, 0.97 and FCMB, 0.93) were higher than those without the inoculant (CK, 0.91 and FC, 0.90). However, applying the immobilizing inoculant alone (MB, 4.73) yielded higher network average degree than the non-fertilization group (CK, 4.66). The application of the fermentative edible fungi

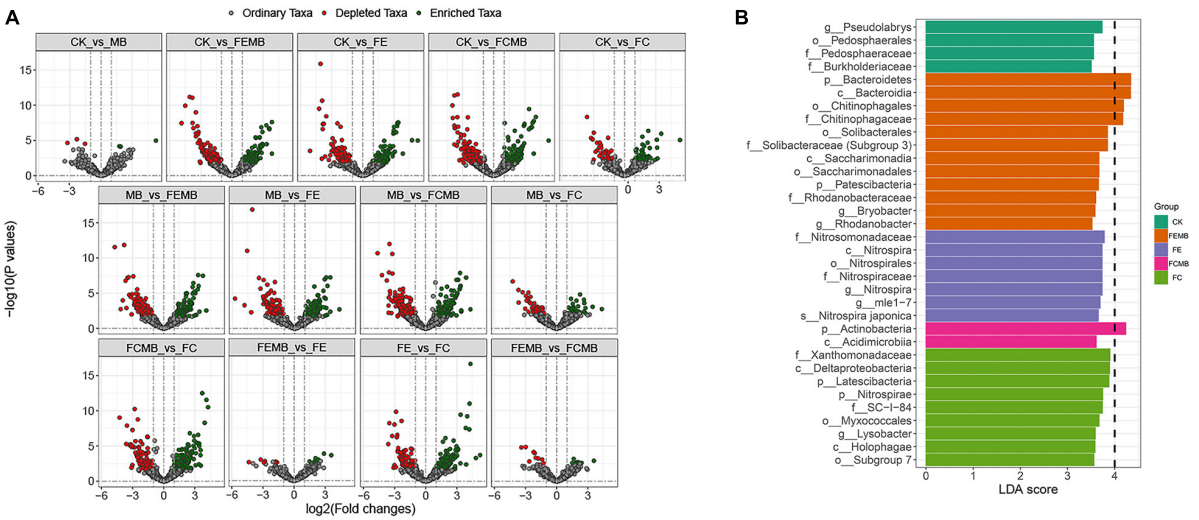

FIGURE 2 | Significance and differential analysis of bacterial communities in the soil grown with *H. cordata* under different fertilization regimens. **(A)** Volcano plots indicating differential ASV changes between different treatments. **(B)** Histogram of linear discriminant analysis (LDA) Effect Size (LEfSe) showing taxa with log10 (LDA scores) ≥ 3.5.

residue with the Cd-immobilizing inoculant (FEMB, 1.22) led to lower average degree than applying fermentative edible fungi residue alone (FE, 1.33). Similarly, the average degree of the application of fermentative cow dung with the inoculant (FCMB, 1.59) was lower than that with only fermentative edible fungi residue (FC, 1.72).

The betweenness centrality value indicated fully different keystone genera among the microbial communities in the field soil of *H. cordata*. According to this parameter, *Sphingobium*, *Herminiimonas*, *Sphingopyxis*, *Clostridium*, *Roseiarcus*, *Sphingobacterium*, *Sorangium*, *Aureimonas*, *Inquilinus*, and *Chryseobacterium* (ranging 50–16) were identified as the top ten keystone bacterial genera in CK. When only the Cd-immobilizing inoculant (MB) was applied into the *H. cordata field*, the top ten keystone genera were changed into *Bradyrhizobium*, *Allorhizobium*, *Mycobacterium*, *Stenotrophomonas*, *Hirschia*, *Paenibacillus*, *Nocardia*, *Luedemannella*, *Aureimonas*, and *Bosea* (ranging 27–1). In the field where only the fermentative edible fungi residue (FE) was applied, the top ten keystone genera consisted of OM27 clade, *Microvirga*, *Aridibacter*, *Geobacter*, *Bifidobacterium*, *Chryseolinea*, *Amycolatopsis*, *Lactobacillus*, *Sphingobacterium*, and *Stenotrophomonas* (ranging 36–1), whereas the top teen keystone genera in the field applied with fermentative edible fungi residue with the bacterial inoculant (FEMB) were changed into *Finegoldia*, *Stenotrophomonas*, *Burkholderia*, *Faecalibacterium*, *Sphingobium*, *Luteitalea*, *Altererythrobacter*, *Geobacter*, *Polyangium*, and *Occallatibacter* (ranging 23–1). When fermentative edible fungi residue was used in the *H. cordata* field (FC), the top ten keystone genera were *Polycyclovorans*, *Rhodanobacter*, *Nordella*, *Ensifer*, *Ruminococcus*, *Caulobacter*, *Sphingobacterium*, *Adhaeribacter*, *Candidatus*, and *Herminiimonas* (ranging 52–7.5), while they were replaced by only the following five genera of *Paracoccus*, *Luteitalea*, *Fictibacillus*, *Sphingobium*, and *Ruminococcus* (ranging 35–5) in the treatment using the combination of fermentative edible fungi residue and Cd-immobilizing inoculant.

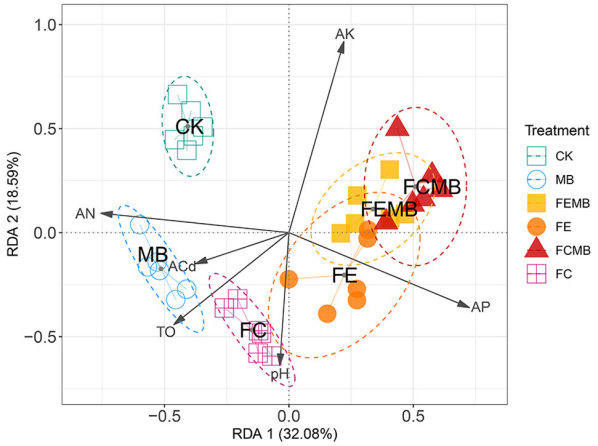

FIGURE 3 | The Bray–Curtis distance-based redundancy analysis (bcRDA) of bacterial ASVs and characteristics of the soil grown with *H. cordata* under different fertilization regimens. Soil variables: pH, AN (available nitrogen), AP (available phosphorus), AK (available potassium), ACd (available Cd), and TO (total organic matter).

Prediction of Bacterial Ecological Functions in *H. cordata* Soil

The FAPROTAX functional prediction revealed that there was a huge difference in microbial functions between CK and other five treatment groups (**Figure 5A**). Only several common functions including interspecies symbiosis (pathogens and parasites), soil nitrogen cycling (nitrite oxidation), biodegradation (chitinolytic

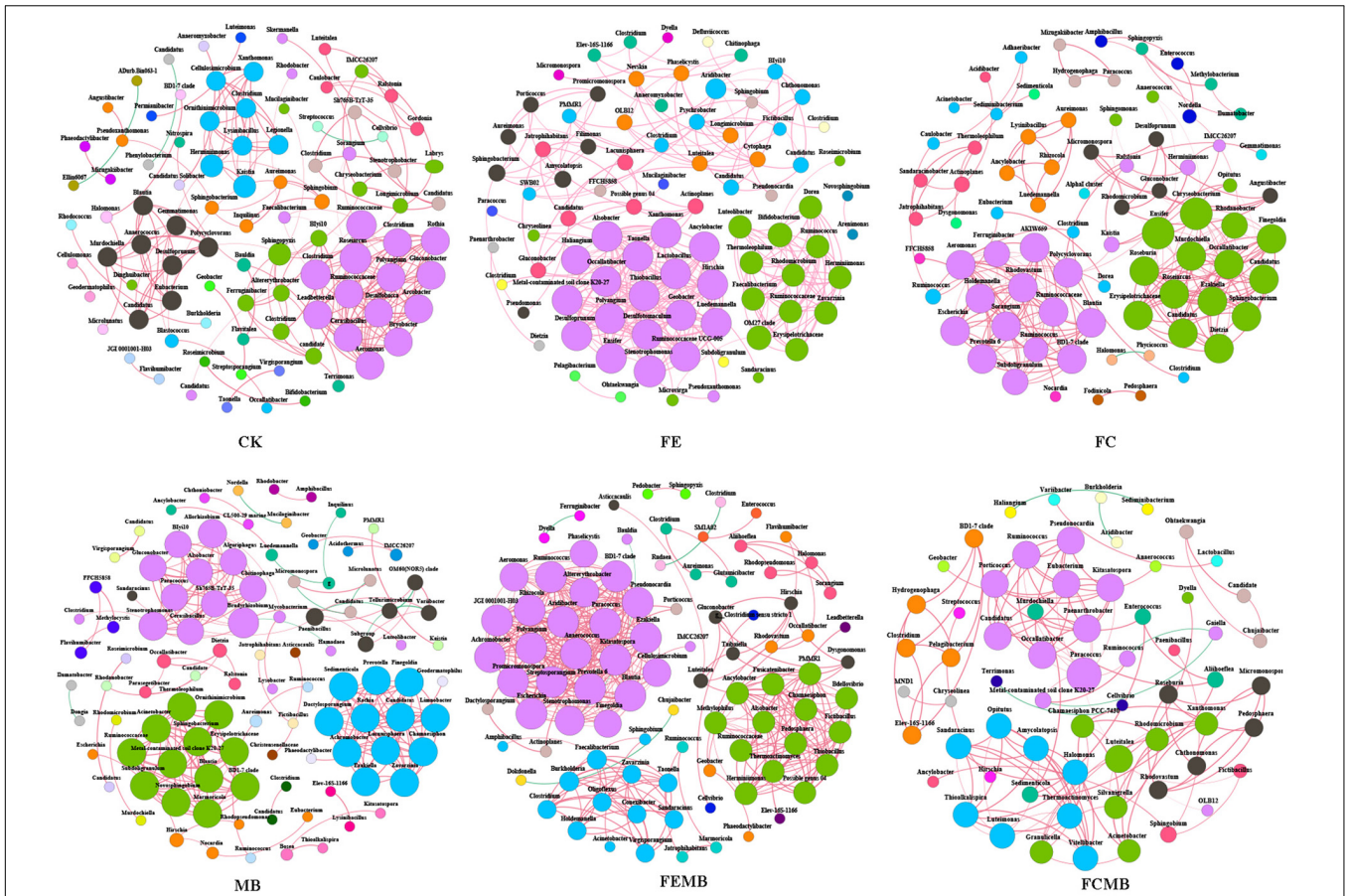

FIGURE 4 | Co-occurrence network of bacterial communities at genus level in the soil grown with *H. cordata* under different fertilization regimens. Different colors of nodes in networks refer to different modularity classes. The size of each node reflects the degree of connection. Red lines represent positive correlations and green lines represent negative correlations.

and cellulolytic processes) and soil sulfur cycling (sulfur/sulfide oxidation) were significantly different ($p < 0.05$) in most soil microorganisms. The control soil was rich in aerobic nitrite oxidation, dark oxidation of sulfur compounds, dark sulfide oxidation, and cellulolysis. Fermentative edible fungi residue-treated soils (FE and FEMB) were rich in human pathogens and animal parasites. The soil with fermentative cow dung mixed with Cd-immobilizing bacterial inoculant (FCMB) contained a high proportion of cellulolysis function, while that with only fermentative cow dung (FC) showed a completely different pattern of the functional profiles, which featured chitinolysis, predatory or exoparasitic, aerobic nitrite oxidation, and sulfur/sulfide oxidation functions. The quantitative analysis visualized by the relative abundance plot showed that the top overall abundance of microbial functions for all the six groups was aerobic nitrite oxidation, followed by predatory or exoparasitic function (**Figure 5B**). Compared to CK, all the other five treatment groups had a lower amount of aerobic nitrite oxidation function. The amounts of sulfur and sulfide-related functions were negligible compared to the other seven functions. Compared to the application of fermentative edible fungi residue alone, the combination of the Cd-immobilizing bacterial inoculant and fermentative edible fungi residue reduced functions including aerobic nitrite oxidation, human pathogens, animal parasites, and predatory or exoparasitic, while slightly increasing chitinolytic function. Compared to the application of fermentative cow dung alone, the inclusion of the Cd-immobilizing inoculant induced a reduction in aerobic nitrite oxidation, predatory or exoparasitic, and chitinolytic functions, but an increase in human pathogens, animal parasites, and cellulolysis. The linear discriminant analysis (LDA) (**Figure 5C**) showed that human pathogen and animal parasite-related functions attained significance in FEMB; aerobic nitrite oxidation and human pathogens were significant in FE; cellulolysis was prominent in FCMB; predatory or parasitic, chitinolytic, sulfur, and sulfide oxidation functions were the significant biomarkers in FC.

DISCUSSION

In our study, it was shown that the Cd-immobilizing bacterial inoculant can effectively prevent the accumulation of Cd in the roots of *H. cordata*, even when this agent was applied alone.

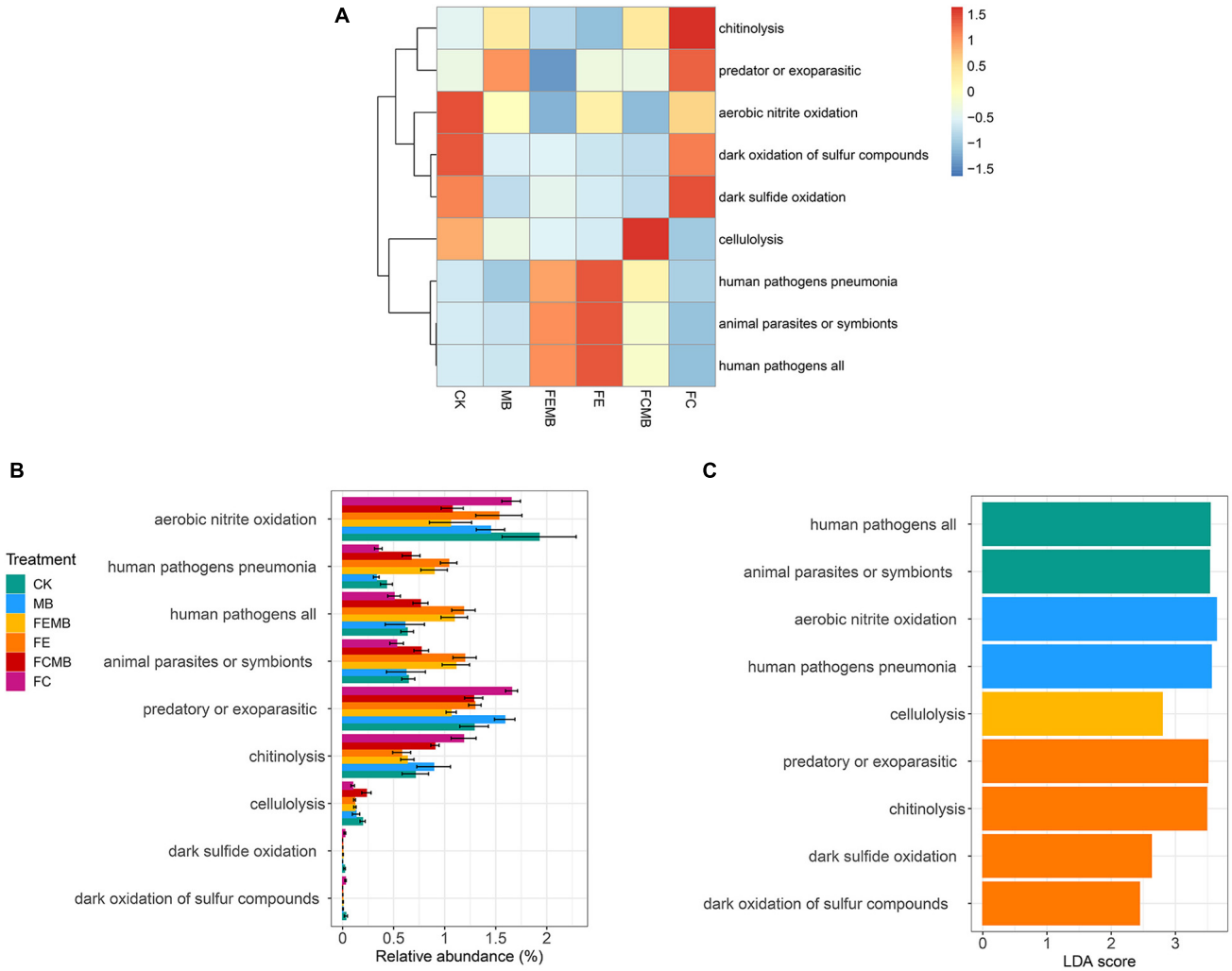

FIGURE 5 | Microbial functional diversity (FAPROTAX) in the field grown with *H. cordata* under different fertilization regimens. **(A)** Relative abundance heatmap of the functions. **(B)** Relative abundance barplot of the functions. **(C)** Linear discriminant analysis (LDA) showing the prominent functions.

This indicated that the microbial agent survived in the Cd-polluted soil and affected the uptake of Cd for the plant. There was very limited information as to the bioaccumulation of Cd and other heavy metals by *H. cordata*. Interestingly, all relevant studies showed that this plant was able to accumulate heavy metals (with or without microbial additives) and could play a role in the phytoremediation of metal-polluted lands. One study showed that *H. cordata* accumulated more than 1,000 ppm Pb in the roots and the inoculation of a *Bacillus* strain facilitated the transportation of Pb from underground to aboveground parts (Liu et al., 2018). Another pot experiment study revealed that the inoculation of a *Serratia marcescens* strain was able to enhance the uptake of Cd by *H. cordata* in both aboveground (by 34.48%) and underground parts (by 59.13%) (Chen et al., 2019). However, our study was performed from a completely different perspective, which featured the prevention of Cd uptake in plants by dint of the immobilizing ability of the bacterial agent. The abovementioned study also found that the growth of this plant was not drastically influenced by the presence of high levels of Cd (5, 50, and 100 mg kg^{-1} Cd in soil), which are way much higher than those in our work (Chen et al., 2019). However, the application of bio-organic fertilizers can promote the growth of *H. cordata* plants in this study. It is known that *in situ* metal immobilization occurs when microbes release inorganic and organic compounds into the soil, causing sorption of metals and metalloids by the reactions of various microbe-produced functional groups such as amine, carboxyl, hydroxyl, and sulfhydryl contained in organic molecules (e.g., chitin, humic, and lignin substances) (Zhou and Haynes, 2010). Other organic composts such as biosolids and animal (livestock and poultry) manure products have been traditionally applied in agriculture and they showed pronounced abilities to reduce the bioavailability of metal(loid)s to plants (Bolan et al., 2014). However, the present study did not corroborate this, as shown by the significant increase of Cd in the roots of the plants. On the contrary, it can be possibly inferred from our results that

since more Cd was absorbed into the roots, the bioavailability of Cd was actually increased after the application of fermentative edible fungi residue (FE) and fermentative cow dung (FC). Studies showed that low bioavailability fractions of heavy metals including Cd, Cu, Ni, Pb, and Zn were increased as a result of composting (Smith, 2009; Shehata et al., 2019), and the mechanisms were closely related to organic acids released during certain stages of the process (Ingelmo et al., 2012; Irshad et al., 2014). Likewise, edible fungi residue was also reported to be able to induce high amounts of humus and organic compounds in soil environment (Li et al., 2020), which could cause the same effects as cow dung on the bioavailability of metals. It should be noted that, in our study, the combined application of the abovementioned bio-based amendments with the Cd-immobilizing agent reduced >20% of the uptake of Cd by the plant. This provided solid evidence to the fact that our beneficial microbial inoculant was able to perform outstanding Cd immobilization in the Cd-contaminated farm soil. In our study, all the four Cd-immobilizing strains were identified as belonging to the *Bacillus* genus. It is widely reported that many *Bacillus* species were very efficient in the immobilization of Cd through the mechanism of MICP and have been used as microbial soil amendments for the remediation of Cd-contaminated soil (Wang et al., 2014; Fang et al., 2021). Although the application of the microbial agent alone and the combination with the bio-based amendments showed no obvious signs of increase of total nitrogen uptake by the plant, they significantly ($p > 0.05$) elevated total and available nitrogen in the Cd-polluted soil. Because nitrogen is an important indicator of soil fertility (Zhong et al., 2010), the increase of N in the Cd-polluted soil implied that the Cd-immobilizing microbial agent was more competent in the improvement of soil quality when combined with organic fertilizers. Our results were in accordance with others where the combined application of different organic fertilizers and microbial agents greatly improved the agronomic traits of crops (e.g., *Elymus dahuricus, Nicotiana tabacum,* and strawberry plants) and soil conditions (Esitken et al., 2010; Liu Y. et al., 2013; Li et al., 2021; Tariq et al., 2021).

The high-throughput Illumina sequencing results indicated that the microbial α-diversity remained almost unchanged when the microbial inoculant was applied alone. The application of fermentative edible fungi residue (FE) apparently reduced while that of fermentative cow dung (FC) increased the microbial α-diversity compared to the non-fertilized control (CK). This may be due to the fact that animal manure itself contains microorganisms and more complicated organic matters compared to spent mushroom substrates (Aira et al., 2015; Xie et al., 2021). Interestingly, the introduction of the Cd-immobilizing bacterial agent to the fermentative cow dung (FCMB) reduced 16.7% of the community richness index (Chao1 estimator), while a slight reduction was found when the inoculant was combined with fermentative edible fungi residue (FEMB). Chao1 index estimates the abundance of microbial communities within the sample and the reduction of it means that the microbial populations in FCMB was reduced in number (Chodak et al., 2013). This phenomenon was probably due to the antagonistic effects of the newly introduced microbial strains on the native microbiome contained in the animal manure. This assumption has been confirmed by numerous studies that microbial soil amendments and bio-organic fertilizers can successfully prevent or reduce bacterial wilt disease in tobacco plants and can have a huge influence on the plant-associated soil microbial populations (Wu et al., 2014; Shen et al., 2015; Wu B. et al., 2016; Li X. et al., 2017; Ma et al., 2018). The combined application of the bacterial agent with both fungi residue and cow dung increased the abundance of *Actinobacteria and Bacteroidetes*. The results that more ASVs were significantly enriched and depleted in FCMB and FEMB than in the control group implied that there were increased microbial turnovers following the combined application of bio-based amendments and the bacterial agent. This may indicate that although the microbial abundance was reduced, the communities were obviously changed. The bcRDA plot clearly showed that there was a marked difference between the treatments with the combined applications (FCMB and FEMB) and those with single fertilization regimen (CK, MB, FC, and FE). This apparently indicated that β-diversity of the plant-associated microbial communities was greatly enhanced after the combined fertilization method was utilized. It also showed that the combination of the bacterial agent with both organic fertilizers (FCMB and FEMB) led to similar microbial composition, whereas the microbial structure between FC and FE showed a marked difference. This may point to the fact that the bacterial agent was competent in the alteration of microbial populations when applied together with organic fertilizers. The increase of diversity and reduction of abundance may be the result of an increase of certain taxa biomarkers (i.e., *Bacteroidetes* in FEMB; *Actinobacteria* in FCMB) discovered using the LDA analysis. The environmental-community structure analysis further identified that available K, P, and N, which are basic soil nutrient parameters, had a greater influence on the community structure dissimilarity compared to total organic matter and available Cd in the soil. Based on the analysis of the angles between environmental factors and sample points, it can be inferred that available nitrogen (AN) was positively correlated with the microbial population in MB but was negatively correlated with that in the co-application groups (FCMB and FEMB). Interestingly, available K and P showed negative correlations with MB but positive correlations with FCMB and FEMB. Although available NPK had a much bigger influence on the overall structure of the microbial population, we cannot directly conclude from the bcRDA plot as to whether they can be increased or reduced as a result of the application of the bacterial agent and organic fertilizers, since they might be the cause of the changes of microbial population.

The co-occurrence network analysis is a very effective tool for the reflection of complexities of the microbial associations under different fertilization regimens (Vendruscolo et al., 2020; Yuan et al., 2021). More edges (indicating co-occurring relationships) and less nodes (indicating taxa abundance) were found in the treatments with combined fertilization compared to the treatments with the bio-based amendments alone, which again implied that the introduction of the Cd-immobilizing inoculant reduced the abundance while at the same time increasing the

complex or diversity of the *in situ* microbial communities. The smaller average path lengths and higher clustering coefficients in the networks of FCMB and FEMB suggested that the bacterial agent enhanced ecological relationships among the microbial populations. The lower average degree values in FCMB and FEMB also implied that the addition of the microbial inoculant led to reduced connections among the individuals as a result of a decrease in abundance. Keystone taxa, which reflect the important roles of certain microbial species play in an ecological network, can be identified using the betweenness centrality value as a measure (Banerjee et al., 2018, 2019; Zeng et al., 2019). Our result showed that the top 10 taxa in the co-occurrence networks varied significantly under different fertilization regimens. This could possibly imply that the microbial agent exercised a prominent influence on the ecological relationships among the communities in the soil.

The FAPROTAX method has been widely used in the prediction of soil microbial functions related to biogeochemical processes (Zhou et al., 2020). Our study revealed that there was a significant increase in the functions pertaining to human pathogen and animal symbiont functions after fermentative edible fungi residue was applied alone (FE), and the cause of this is unknown. However, the addition of the microbial agent slightly reduced the presence of those functions, which could potentially suggest that the microbial agent was able to suppress some harmful microorganisms contained in the fermentative edible fungi residue. On the contrary, the combination of the bacterial agent with the fermentative cow dung could be able to increase those functions, which may be the result of synergism between the microbial agent and the native microorganisms contained in the cow dung. As for other functions, the application of the Cd-immobilizing bacterial agent invariably reduced the aerobic nitrite oxidation function, and this can clearly indicate that there was a reduction of the abundance of nitrite oxidizing bacteria (NOB), which catalyze the second step of nitrification, converting nitrite to nitrate (Daims et al., 2016; Baskaran et al., 2020). NOB species are mainly found in the genera of *Nitrobacter*, *Nitrococcus*, *Nitrospira*, and *Nitrospina*, which play an important role in the process of nitrification after ammonium is firstly oxidized to nitrite by ammonia-oxidizing bacteria (AOB) (Spieck and Lipski, 2011; Yao and Peng, 2017).

CONCLUSION

The present study took a close examination of the effects on the plant *H. cordata* and its microbial communities under different fertilization regimens in a Cd-polluted field. Our research found that both the application of the Cd-immobilizing bacterial agent alone and the combined application of bio-based soil amendments and the bacterial agent can effectively reduce the uptake of Cd by the plant. The combined fertilization can raise soil nitrogen level. After the combined fertilization regimen was introduced, there was a significant shift of microbial communities: the microbial populations tended to be homogeneous with reduced microbial abundance and increased diversity. The combined application of the bacterial agent with fermentative edible fungi residue and cow dung significantly increased the abundances of *Actinobacteria* and *Bacteroidetes*, respectively. The introduction of the microbial agent could potentially suppress human pathogenic microorganisms in the field fertilized with edible fungi residue. The microbial agent can also reduce the nitrite oxidation function in the soil when applied alone or with the bio-based soil amendments. Our study thus highlights the beneficial effects of the Cd-immobilizing bacterial inoculant on *H. cordata* and provides a better understanding of the microbial changes induced by combined fertilization using the microbial agent and natural soil amendments.

DATA AVAILABILITY STATEMENT

The original contributions presented in the study are included in the article/**Supplementary Material**, further inquiries can be directed to the corresponding author.

AUTHOR CONTRIBUTIONS

XY, MY, and YC designed the study and wrote the manuscript. XY, MY, YC, HL, JZ, JL, QX, and LZe performed the experiments. XY, MY, YG, KZ, and LZo analyzed the data. QC, MM, and LZo reviewed and edited the manuscript. XY and YC funded and supervised the experiments. All authors participated in the interpretation and discussion of results and contributed to the article.

FUNDING

This work was supported by the Key Research and Development Program of Sichuan Province (No. 2021YFS0293), the National Natural Science Foundation of China (No. 31872696), Basic Scientific Research Operating Expenses Project of Sichuan Province (2019), and Sichuan Science and Technology planning Project (2020ZHFP0020).

SUPPLEMENTARY MATERIAL

The Supplementary Material for this article can be found online at: https://www.frontiersin.org/articles/10.3389/fmicb.2021.809834/full#supplementary-material

Supplementary Figure 1 | Characteristics of bacterial communities in the soil before and after biofertilizer treatments. **(A)** Volcano plots indicating differential ASV changes before and after different treatments. **(B)** Relative abundance heat map of the top 12 phyla for all treatments. **(C)** Co-occurrence network of bacterial communities at genus level in the soil before biofertilizer treatments.

Supplementary Table 1 | Amplicon sequence variants (ASVs) of 16S rRNA gene for the cadmium-contaminated *Houttuynia cordata* field soil in different biofertilizer treatments.

Supplementary Table 2 | Alpha-diversity of bacterial communities in *Houttuynia cordata* farm soil before the application of bacteria and organic fertilizers.

REFERENCES

Aira, M., Bybee, S., Pérez-Losada, M., and Domínguez, J. (2015). Feeding on microbiomes: effects of detritivory on the taxonomic and phylogenetic bacterial composition of animal manures. *FEMS Microbiol. Ecol.* 91:fiv117. doi: 10.1093/femsec/fiv117

Bali, A. S., Sidhu, G. P. S., and Kumar, V. (2020). Root exudates ameliorate cadmium tolerance in plants: a review. *Environ. Chem. Lett.* 18, 1243–1275. doi: 10.1007/s10311-020-01012-x

Banerjee, S., Schlaeppi, K., and Van Der Heijden, M. G. A. (2018). Keystone taxa as drivers of microbiome structure and functioning. *Nat. Rev. Microbiol.* 16, 567–576. doi: 10.1038/s41579-018-0024-1

Banerjee, S., Walder, F., Buchi, L., Meyer, M., Held, A. Y., Gattinger, A., et al. (2019). Agricultural intensification reduces microbial network complexity and the abundance of keystone taxa in roots. *ISME J.* 13, 1722–1736. doi: 10.1038/s41396-019-0383-2

Barra Caracciolo, A., and Terenzi, V. (2021). Rhizosphere microbial communities and heavy metals. *Microorganisms* 9:1462. doi: 10.3390/microorganisms9071462

Baskaran, V., Patil, P. K., Antony, M. L., Avunje, S., Nagaraju, V. T., Ghate, S. D., et al. (2020). Microbial community profiling of ammonia and nitrite oxidizing bacterial enrichments from brackishwater ecosystems for mitigating nitrogen species. *Sci. Rep.* 10, 1–11. doi: 10.1038/s41598-020-62183-9

Bogunovic, I., Pereira, P., and Brevik, E. C. (2017). Spatial distribution of soil chemical properties in an organic farm in Croatia. *Sci.Total Environ.* 584, 535–545. doi: 10.1016/j.scitotenv.2017.01.062

Bolan, N., Kunhikrishnan, A., Thangarajan, R., Kumpiene, J., Park, J., Makino, T., et al. (2014). Remediation of heavy metal (loid) s contaminated soils–to mobilize or to immobilize? *J. Hazard. Mater.* 266, 141–166. doi: 10.1016/j.jhazmat.2013.12.018

Canarini, A., Kaiser, C., Merchant, A., Richter, A., and Wanek, W. (2019). Root exudation of primary metabolites: mechanisms and their roles in plant responses to environmental stimuli. *Front. Plant Sci.* 10:157. doi: 10.3389/fpls.2019.00157

Caporaso, J. G., Lauber, C. L., Walters, W. A., Berg-Lyons, D., Huntley, J., Fierer, N., et al. (2012). Ultra-high-throughput microbial community analysis on the Illumina HiSeq and MiSeq platforms. *ISME J.* 6, 1621–1624. doi: 10.1038/ismej.2012.8

Chen, Y., Zhu, Q., Dong, X., Huang, W., Du, C., and Lu, D. (2019). How *Serratia marcescens* HB-4 absorbs cadmium and its implication on phytoremediation. *Ecotoxicol. Environ. Saf.* 185:109723. doi: 10.1016/j.ecoenv.2019.109723

Chodak, M., Gołębiewski, M., Morawska-Płoskonka, J., Kuduk, K., and Niklińska, M. (2013). Diversity of microorganisms from forest soils differently polluted with heavy metals. *Appl. Soil Ecol.* 64, 7–14. doi: 10.1016/j.apsoil.2012.11.004

Chojnacka, K., Moustakas, K., and Witek-Krowiak, A. (2020). Bio-based fertilizers: a practical approach towards circular economy. *Bioresour. Technol.* 295:122223. doi: 10.1016/j.biortech.2019.122223

Csardi, G., and Nepusz, T. (2006). The igraph software package for complex network research. *J. InterJournal Complex Syst.* 1695, 1–9. doi: 10.1186/1471-2105-12-455

Dahnke, W., and Johnson, G. V. (1990). Testing soils for available nitrogen. *Soil Testing Plant Anal.* 3, 127–139. doi: 10.2136/sssabookser3.3ed.c6

Daims, H., Lücker, S., and Wagner, M. (2016). A new perspective on microbes formerly known as nitrite-oxidizing bacteria. *Trends Microbiol.* 24, 699–712. doi: 10.1016/j.tim.2016.05.004

Dhaliwal, S. S., Singh, J., Taneja, P. K., and Mandal, A. (2020). Remediation techniques for removal of heavy metals from the soil contaminated through different sources: a review. *Environ. Sci. Pollut. Res.* 27, 1319–1333. doi: 10.1007/s11356-019-06967-1

Dong, J., Mao, W., Zhang, G., Wu, F., and Cai, Y. (2007). Root excretion and plant tolerance to cadmium toxicity-a review. *Plant Soil Environ.* 53:193. doi: 10.1007/s11104-007-9257-x

Esitken, A., Yildiz, H. E., Ercisli, S., Donmez, M. F., Turan, M., and Gunes, A. (2010). Effects of plant growth promoting bacteria (PGPB) on yield, growth and nutrient contents of organically grown strawberry. *Sci. Hortic.* 124, 62–66. doi: 10.1016/j.scienta.2009.12.012

Fang, L., Niu, Q., Cheng, L., Jiang, J., Yu, Y. Y., Chu, J., et al. (2021). Ca-mediated alleviation of Cd2+ induced toxicity and improved Cd2+ biomineralization by Sporosarcina pasteurii. *Sci. Total Environ.* 787:147627. doi: 10.1016/j.scitotenv.2021.147627

Gong, L., Wang, J., Abbas, T., Zhang, Q., Cai, M., Tahir, M., et al. (2021). Immobilization of exchangeable Cd in soil using mixed amendment and its effect on soil microbial communities under paddy upland rotation system. *Chemosphere* 262:127828. doi: 10.1016/j.chemosphere.2020.127828

Gujre, N., Rangan, L., and Mitra, S. (2021). Occurrence, geochemical fraction, ecological and health risk assessment of cadmium, copper and nickel in soils contaminated with municipal solid wastes. *Chemosphere* 271:129573. doi: 10.1016/j.chemosphere.2021.129573

Hu, X., Huang, X., Zhao, H., Liu, F., Wang, L., Zhao, X., et al. (2021). Possibility of using modified fly ash and organic fertilizers for remediation of heavy-metal-contaminated soils. *J. Clean. Prod.* 284:124713. doi: 10.1016/j.jclepro.2020.124713

Huang, M., Zhu, Y., Li, Z., Huang, B., Luo, N., Liu, C., et al. (2016). Compost as a soil amendment to remediate heavy metal-contaminated agricultural soil: mechanisms, efficacy, problems, and strategies. *Water Air Soil Pollut.* 227, 1–18. doi: 10.1007/s11270-016-3068-8

Ingelmo, F., Molina, M. J., Soriano, M. D., Gallardo, A., and Lapeña, L. (2012). Influence of organic matter transformations on the bioavailability of heavy metals in a sludge based compost. *J. Environ. Manage.* 95, S104–S109. doi: 10.1016/j.jenvman.2011.04.015

Irshad, M., Gul, S., Egrinya Eneji, A., Anwar, Z., and Ashraf, M. (2014). Extraction of heavy metals from manure and their bioavailability to spinach (*Spinacia oleracea* L.) after composting. *J. Plant Nutr.* 37, 1661–1675. doi: 10.1080/01904167.2014.888748

Kabata-Pendias, A. (1993). Behavioural properties of trace metals in soils. *Appl. Geochem.* 8, 3–9. doi: 10.1016/S0883-2927(09)80002-4

Kang, X., Cui, Y., Shen, T., Yan, M., Tu, W., Shoaib, M., et al. (2020). Changes of root microbial populations of natively grown plants during natural attenuation of V-Ti magnetite tailings. *Ecotoxicol. Environ. Saf.* 201:110816. doi: 10.1016/j.ecoenv.2020.110816

Kang, X., Yu, X., Zhang, Y., Cui, Y., Tu, W., Wang, Q., et al. (2018). Inoculation of *Sinorhizobium saheli* YH1 leads to reduced metal uptake for *Leucaena leucocephala* grown in mine tailings and metal-polluted soils. *Front. Microbiol.* 9:1853. doi: 10.3389/fmicb.2018.01853

Ke, T., Guo, G., Liu, J., Zhang, C., Tao, Y., Wang, P., et al. (2021). Improvement of the Cu and Cd phytostabilization efficiency of perennial ryegrass through the inoculation of three metal-resistant PGPR strains. *Environ. Pollut.* 271:116314. doi: 10.1016/j.envpol.2020.116314

Konkolewska, A., Piechalak, A., Ciszewska, L., Antos-Krzemińska, N., Skrzypczak, T., Hanć, A., et al. (2020). Combined use of companion planting and PGPR for the assisted phytoextraction of trace metals (Zn, Pb, Cd). *Environ. Sci. Pollut. Res.* 27, 13809–13825. doi: 10.1007/s11356-020-07885-3

Li, F., Chen, L., Zhang, J., Yin, J., and Huang, S. (2017). Bacterial community structure after long-term organic and inorganic fertilization reveals important associations between soil nutrients and specific taxa involved in nutrient transformations. *Front. Microbiol.* 8:187. doi: 10.3389/fmicb.2017.00187

Li, F., Kong, Q., Zhang, Q., Wang, H., Wang, L., and Luo, T. (2020). Spent mushroom substrates affect soil humus composition, microbial biomass and functional diversity in paddy fields. *Appl. Soil Ecol.* 149:103489. doi: 10.1016/j.apsoil.2019.103489

Li, X., Liu, Y., Lu, N., Cai, L., Yuan, Y., and Shi, J. (2017). Integrated bio-control of tobacco bacterial wilt and its effect on soil microbial community structure. *Acta Pedol. Sin.* 54, 216–226.

Li, Y., Huo, X., Liu, J., Peng, L., Li, W., and Xu, X. (2011). Assessment of cadmium exposure for neonates in Guiyu, an electronic waste pollution site of China. *Environ. Monit. Assess.* 177, 343–351. doi: 10.1007/s10661-010-1638-6

Li, Y., Yu, X., Cui, Y., Tu, W., Shen, T., Yan, M., et al. (2019). The potential of cadmium ion-immobilized *Rhizobium pusense* KG 2 to prevent soybean root from absorbing cadmium in cadmium-contaminated soil. *J. Appl. Microbiol.* 126, 919–930. doi: 10.1111/jam.14165

Li, Y., Zhao, Y., Song, Z., Deng, Y., Wang, H., Xu, L., et al. (2021). Effect of microbial combination with organic fertilizer on *Elymus dahuricus*. *Open Geosci.* 13, 233–244. doi: 10.1515/geo-2020-0230

Liu, C., Cui, Y., Li, X., and Yao, M. (2021). microeco: an R package for data mining in microbial community ecology. *FEMS Microbiol. Ecol.* 97:fiaa255. doi: 10.1093/femsec/fiaa255

Liu, X., Song, Q., Tang, Y., Li, W., Xu, J., Wu, J., et al. (2013). Human health risk assessment of heavy metals in soil–vegetable system: a multi-medium analysis. *Sci. Total Environ.* 463, 530–540. doi: 10.1016/j.scitotenv.2013.06.064

Liu, Y., Shi, J., Feng, Y., Yang, X., Li, X., and Shen, Q. (2013). Tobacco bacterial wilt can be biologically controlled by the application of antagonistic strains in combination with organic fertilizer. *Biol. Fertil. Soils* 49, 447–464.

Liu, Z., Cai, J., Wang, T., Wu, L., Chen, C., Jiang, L., et al. (2018). Houttuynia cordata hyperaccumulates lead (Pb) and its combination with *Bacillus subtilis* wb600 improves shoot transportation. *Int. J. Agric. Biol.* 20, 621–627. doi: 10.17957/IJAB/15.0532

Liu, Z.-Q., Li, H.-L., Zeng, X.-J., Lu, C., Fu, J.-Y., Guo, L. J., et al. (2020). Coupling phytoremediation of cadmium-contaminated soil with safe crop production based on a sorghum farming system. *J. Clean. Prod.* 275:123002. doi: 10.1016/j.jclepro.2020.123002

Louca, S., Parfrey, L. W., and Doebeli, M. (2016). Decoupling function and taxonomy in the global ocean microbiome. *Science* 353, 1272–1277. doi: 10.1126/science.aaf4507

Love, M., Anders, S., and Huber, W. J. G. B. (2014). Differential analysis of count data–the DESeq2 package. *Genome Biol.* 15:550. doi: 10.1186/s13059-014-0550-8

Luo, S.-L., Chen, L., Chen, J.-L., Xiao, X., Xu, T.-Y., Wan, Y., et al. (2011). Analysis and characterization of cultivable heavy metal-resistant bacterial endophytes isolated from Cd-hyperaccumulator *Solanum nigrum* L. and their potential use for phytoremediation. *Chemosphere* 85, 1130–1138. doi: 10.1016/j.chemosphere.2011.07.053

Ma, L., Zhang, H.-Y., Zhou, X.-K., Yang, C.-G., Zheng, S.-C., Duo, J.-L., et al. (2018). Biological control tobacco bacterial wilt and black shank and root colonization by bio-organic fertilizer containing bacterium *Pseudomonas aeruginosa* NXHG29. *Appl. Soil Ecol.* 129, 136–144. doi: 10.1016/j.apsoil.2018.05.011

Martelli, A., Rousselet, E., Dycke, C., Bouron, A., and Moulis, J. M. (2006). Cadmium toxicity in animal cells by interference with essential metals. *Biochimie* 88, 1807–1814. doi: 10.1016/j.biochi.2006.05.013

Massas, I., Kalivas, D., Ehaliotis, C., and Gasparatos, D. (2013). Total and available heavy metal concentrations in soils of the *Thriassio plain* (Greece) and assessment of soil pollution indexes. *Environ. Monit. Assess.* 185, 6751–6766. doi: 10.1007/s10661-013-3062-1

Mushtaq, Z., Asghar, H. N., and Zahir, Z. A. (2021). Comparative growth analysis of okra (*Abelmoschus esculentus*) in the presence of PGPR and press mud in chromium contaminated soil. *Chemosphere* 262:127865. doi: 10.1016/j.chemosphere.2020.127865

Osman, H. E. M., Abdel-Hamed, E. M. W., Al-Juhani, W. S. M., Al-Maroai, Y. A. O., and El-Morsy, M. H. E.-M. (2021). Bioaccumulation and human health risk assessment of heavy metals in food crops irrigated with freshwater and treated wastewater: a case study in Southern Cairo, Egypt. *Environ. Sci. Pollut. Res.* 28, 50217–50229. doi: 10.1007/s11356-021-14249-y

Pan, Y., Ye, H., Li, X., Yi, X., Wen, Z., Wang, H., et al. (2021). Spatial distribution characteristics of the microbial community and multi-phase distribution of toxic metals in the geochemical gradients caused by acid mine drainage, South China. *Sci. Total Environ.* 774:145660. doi: 10.1016/j.scitotenv.2021.145660

Pramanik, K., Mitra, S., Sarkar, A., and Maiti, T. K. (2018). Alleviation of phytotoxic effects of cadmium on rice seedlings by cadmium resistant PGPR strain *Enterobacter* aerogenes MCC 3092. *J. Hazard. Mater.* 351, 317–329. doi: 10.1016/j.jhazmat.2018.03.009

Rafiq, M. T., Aziz, R., Yang, X., Xiao, W., Rafiq, M. K., Ali, B., et al. (2014). Cadmium phytoavailability to rice (*Oryza sativa* L.) grown in representative Chinese soils. A model to improve soil environmental quality guidelines for food safety. *Ecotox. Environ. Saf.* 103, 101–107. doi: 10.1016/j.ecoenv.2013.10.016

Satarug, S., Baker, J. R., Urbenjapol, S., Haswell-Elkins, M., Reilly, P. E., Williams, D. J., et al. (2003). A global perspective on cadmium pollution and toxicity in non-occupationally exposed population. *Toxicol. Lett.* 137, 65–83. doi: 10.1016/S0378-4274(02)00381-8

Schoeters, G., Hond, E. D., Zuurbier, M., Naginiene, R., Van Den Hazel, P., Stilianakis, N., et al. (2006). Cadmium and children: exposure and health effects. *Acta Paediatr.* 95, 50–54. doi: 10.1080/08035320600886232

Shehata, E., Liu, Y., Feng, Y., Cheng, D., and Li, Z. (2019). Changes in arsenic and copper bioavailability and oxytetracycline degradation during the composting process. *Molecules* 24:4240. doi: 10.3390/molecules24234240

Shen, Z., Ruan, Y., Chao, X., Zhang, J., Li, R., and Shen, Q. (2015). Rhizosphere microbial community manipulated by 2 years of consecutive biofertilizer application associated with banana *Fusarium* wilt disease suppression. *Biol. Fertil. Soils* 51, 553–562. doi: 10.1007/s00374-015-1002-7

Shuaib, M., Azam, N., Bahadur, S., Romman, M., Yu, Q., and Xuexiu, C. (2021). Variation and succession of microbial communities under the conditions of persistent heavy metal and their survival mechanism. *Microb. Pathog.* 150:104713. doi: 10.1016/j.micpath.2020.104713

Smith, S. R. (2009). A critical review of the bioavailability and impacts of heavy metals in municipal solid waste composts compared to sewage sludge. *Environ. Int.* 35, 142–156. doi: 10.1016/j.envint.2008.06.009

Spieck, E., and Lipski, A. (2011). Cultivation, growth physiology, and chemotaxonomy of nitrite-oxidizing bacteria. *Method. Enzymol.* 486, 109–130. doi: 10.1016/B978-0-12-381294-0.00005-5

Storer, D. A. (1984). A simple high sample volume ashing procedure for determination of soil organic matter. *Commun. Soil Sci. Plant Anal.* 15, 759–772.

Sun, H.-F., Li, Y.-H., Ji, Y.-F., Yang, L.-S., Wang, W.-Y., and Li, H.-R. (2010). Environmental contamination and health hazard of lead and cadmium around Chatian mercury mining deposit in western Hunan Province, China. *T. Nonferr. Metal. Soc.* 20, 308–314. doi: 10.1016/s1003-6326(09)60139-4

Tariq, M., Shah, A. A., Yasin, N. A., Ahmad, A., and Rizwan, M. (2021). Enhanced performance of Bacillus megaterium OSR-3 in combination with putrescine ammeliorated hydrocarbon stress in *Nicotiana tabacum*. *Int. J. Phytoremediat.* 23, 119–129. doi: 10.1080/15226514.2020.1801572

Thomas, R., Sheard, R., and Moyer, J. (1967). Comparison of conventional and automated procedures for nitrogen, phosphorus, and potassium analysis of plant material using a single digestion. *Agron. J.* 59, 240–243. doi: 10.2134/agronj1967.00021962005900030010x

Tiwari, S., and Lata, C. (2018). Heavy metal stress, signaling, and tolerance due to plant-associated microbes: an overview. *Front. Plant Sci.* 9:452. doi: 10.3389/fpls.2018.00452

Vendruscolo, E. C. G., Mesa, D., Rissi, D. V., Meyer, B. H., De Oliveira Pedrosa, F., De Souza, E. M., et al. (2020). Microbial communities network analysis of anaerobic reactors fed with bovine and swine slurry. *Sci. Total Environ.* 742:140314. doi: 10.1016/j.scitotenv.2020.140314

Wang, T., Sun, H., Jiang, C., Mao, H., and Zhang, Y. (2014). Immobilization of Cd in soil and changes of soil microbial community by bioaugmentation of UV-mutated *Bacillus subtilis* 38 assisted by biostimulation. *Eur. J. Soil Biol.* 65, 62–69. doi: 10.1016/j.ejsobi.2014.10.001

Wenzel, W. W. (2009). Rhizosphere processes and management in plant-assisted bioremediation (phytoremediation) of soils. *Plant Soil* 321, 385–408.

Wu, B., Wang, X., Yang, L., Yang, H., Zeng, H., Qiu, Y., et al. (2016). Effects of Bacillus amyloliquefaciens ZM9 on bacterial wilt and rhizosphere microbial communities of tobacco. *Appl. Soil Ecol.* 103, 1–12. doi: 10.1016/j.apsoil.2016.03.002

Wu, K., Yuan, S., Wang, L., Shi, J., Zhao, J., Shen, B., et al. (2014). Effects of bio-organic fertilizer plus soil amendment on the control of tobacco bacterial wilt and composition of soil bacterial communities. *Biol. Fert. Soils* 50, 961–971. doi: 10.1007/s00374-014-0916-9

Wu, X., Zhang, H., Chen, J., Shang, S., Wei, Q., Yan, J., et al. (2016). Comparison of the fecal microbiota of dholes high-throughput Illumina sequencing of the V3–V4 region of the 16S rRNA gene. *Appl. Microbiol. Biot.* 100, 3577–3586. doi: 10.1007/s00253-015-7257-y

Xie, G., Kong, X., Kang, J., Su, N., Fei, J., and Luo, G. (2021). Fungal community succession contributes to product maturity during the co-composting of chicken manure and crop residues. *Bioresour. Technol.* 328:124845. doi: 10.1016/j.biortech.2021.124845

Yao, Q., and Peng, D.-C. (2017). Nitrite oxidizing bacteria (NOB) dominating in nitrifying community in full-scale biological nutrient removal wastewater

treatment plants. *AMB Express* 7, 1–11. doi: 10.1186/s13568-017-0328-y

Yu, X., Kang, X., Li, Y., Cui, Y., Tu, W., Shen, T., et al. (2019). Rhizobia population was favoured during in situ phytoremediation of vanadium-titanium magnetite mine tailings dam using *Pongamia pinnata*. *Environ. Pollut.* 255:113167. doi: 10.1016/j.envpol.2019.113167

Yu, X., Li, Y., Li, Y., Xu, C., Cui, Y., Xiang, Q., et al. (2017). *Pongamia pinnata* inoculated with *Bradyrhizobium liaoningense* PZHK1 shows potential for phytoremediation of mine tailings. *Appl. Microbiol. Biotechnol.* 101, 1739–1751. doi: 10.1007/s00253-016-7996-4

Yu, X., Li, Y., Zhang, C., Liu, H., Liu, J., Zheng, W., et al. (2014). Culturable heavy metal-resistant and plant growth promoting bacteria in V-Ti magnetite mine tailing soil from Panzhihua, China. *PloS One* 9:e106618. doi: 10.1371/journal.pone.0106618

Yuan, Q., Wang, P., Wang, C., Chen, J., Wang, X., and Liu, S. (2021). Indicator species and co-occurrence pattern of sediment bacterial community in relation to alkaline copper mine drainage contamination. *Ecol. Indic.* 120:106884. doi: 10.1016/j.ecolind.2020.106884

Yuan, Z., Luo, T., Liu, X., Hua, H., Zhuang, Y., Zhang, X., et al. (2019). Tracing anthropogenic cadmium emissions: from sources to pollution. *Sci. Total Environ.* 676, 87–96. doi: 10.1016/j.scitotenv.2019.04.250

Zeng, G., Qiao, S., Wang, X., Sheng, M., Wei, M., Chen, Q., et al. (2021). Immobilization of cadmium by *Burkholderia* sp. QY14 through modified microbially induced phosphate precipitation. *J. Hazard. Mater.* 412:125156. doi: 10.1016/j.jhazmat.2021.125156

Zeng, J., Jiao, C., Zhao, D., Xu, H., Huang, R., Cao, X., et al. (2019). Patterns and assembly processes of planktonic and sedimentary bacterial community differ along a trophic gradient in freshwater lakes. *Ecol. Indic.* 106:205491. doi: 10.1016/j.ecolind.2019.105491

Zhong, W., Gu, T., Wang, W., Zhang, B., Lin, X., Huang, Q., et al. (2010). The effects of mineral fertilizer and organic manure on soil microbial community and diversity. *Plant Soil* 326, 511–522. doi: 10.1007/s11104-009-9988-y

Zhou, L., Zhou, Y., Yao, X., Cai, J., Liu, X., Tang, X., et al. (2020). Decreasing diversity of rare bacterial subcommunities relates to dissolved organic matter along permafrost thawing gradients. *Environ. Int.* 134:105330. doi: 10.1016/j.envint.2019.105330

Zhou, Y.-F., and Haynes, R. J. (2010). Sorption of heavy metals by inorganic and organic components of solid wastes: significance to use of wastes as low-cost adsorbents and immobilizing agents. *Crit. Rev. Environ. Sci. Technol.* 40, 909–977. doi: 10.1080/10643380802586857

Conflict of Interest: The authors declare that the research was conducted in the absence of any commercial or financial relationships that could be construed as a potential conflict of interest.

frontiers | Frontiers in Microbiology

ORIGINAL RESEARCH
published: 13 June 2022
doi: 10.3389/fmicb.2022.824437

Water Deficit History Selects Plant Beneficial Soil Bacteria Differently Under Conventional and Organic Farming

Lucie Gebauer[1†], *Claudia Breitkreuz*[1†], *Anna Heintz-Buschart*[1,2,3], *Thomas Reitz*[1,2], *François Buscot*[1,2], *Mika Tarkka*[1] *and Marie-Lara Bouffaud*[1*]

[1] Helmholtz Centre for Environmental Research, Halle, Germany, [2] German Centre for Integrative Biodiversity Research (iDiv) Halle-Jena-Leipzig, Leipzig, Germany, [3] Biosystems Data Analysis Group, Swammerdam Institute for Life Sciences, University of Amsterdam, Amsterdam, Netherlands

OPEN ACCESS

Edited by:
Hai-Ming Zhao,
Jinan University, China

Reviewed by:
Mustafa Saifuddin,
Earthjustice, United States
Vivek Sharma,
Chandigarh University, India
Zhengkun Hu,
Nanjing Agricultural University, China
Xiaoping Xin,
University of Florida, United States
Xiumei Yu,
Sichuan Agricultural University, China

***Correspondence:**
Marie-Lara Bouffaud
marie-lara.bouffaud@ufz.de

[†] These authors share first authorship

Specialty section:
This article was submitted to Terrestrial Microbiology, a section of the journal Frontiers in Microbiology

Received: 29 November 2021
Accepted: 29 April 2022
Published: 13 June 2022

Citation:
Gebauer L, Breitkreuz C, Heintz-Buschart A, Reitz T, Buscot F, Tarkka M and Bouffaud M-L (2022) Water Deficit History Selects Plant Beneficial Soil Bacteria Differently Under Conventional and Organic Farming. Front. Microbiol. 13:824437. doi: 10.3389/fmicb.2022.824437

Water deficit tolerance is critical for plant fitness and survival, especially when successive drought events happen. Specific soil microorganisms are however able to improve plant tolerance to stresses, such as those displaying a 1-aminocyclopropane-1-carboxylate (ACC) deaminase activity. Microorganisms adapted to dry conditions can be selected by plants over time because of properties such as sporulation, substrate preference, or cell-wall thickness. However, the complexity and interconnection between abiotic factors, like drought or soil management, and biotic factors, like plant species identity, make it difficult to elucidate the general selection processes of such microorganisms. Using a pot experiment in which wheat and barley were grown on conventional and organic farming soils, we determined the effect of water deficit history on soil microorganisms by comparing single and successive events of water limitation. The analysis showed that water deficit strongly impacts the composition of both the total microbial community (16S rRNA genes) and one of ACC deaminase-positive (*acdS*$^+$) microorganisms in the rhizosphere. In contrast, successive dry conditions moderately influence the abundance and diversity of both communities compared to a single dry event. We revealed interactive effects of the farming soil type and the water deficit conditioning treatment. Indeed, possibly due to better nutrient status, plants grown on soils from conventional farming showed higher growth and were able to select more adapted microbial taxa. Some of them are already known for their plant-beneficial properties like the Actinobacteria *Streptomyces*, but interestingly, some Proteobacteria were also enriched after a water deficit history under conventional farming. Our approach allowed us to identify key microbial taxa promoting drought adaptation of cereals, thus improving our understanding of drought effects on plant-microbe interactions.

Keywords: drought legacy, ACC deaminase, PGPR, organic and conventional farming, wheat, barley, *acdS* gene, amplicon sequencing

INTRODUCTION

Plants interact with a large diversity of microorganisms in soils, especially in the rhizosphere, the zone directly influenced by the roots. The microbial communities differ between plant species or genotypes and may have various effects on plant health (Raaijmakers et al., 2009; Berendsen et al., 2012). To deal with different stressors, plants recruit beneficial microbes into their rhizospheres (Naylor and Coleman-Derr, 2018), which are summarized as plant growth-promoting rhizobacteria (PGPR). The action spectrum of these PGPR comprises a range of functional traits including biofertilization, root growth stimulation, pathogen suppression, rhizoremediation, and induction of systemic resistance. These processes often are the result of modifications in plant hormone production levels (Lugtenberg and Kamilova, 2009; Vacheron et al., 2013; Backer et al., 2018). Ethylene is a phytohormone that plays a central role in plant development and plant responses to stress conditions, especially at the root level (Tanimoto et al., 1995; Mattoo and Suttle, 2017). Since ethylene biosynthesis increases in response to environmental biotic and abiotic stresses, the production of ethylene can serve as an indicator of the susceptibility of plants to different stressors (Morgan and Drew, 1997; Balota et al., 2004). Lowering ethylene concentrations in stressed plants, the enzyme 1-aminocyclopropane-1-carboxylate (ACC) deaminase encoded by the *acdS* gene in some PGPR, degrades the ethylene precursor ACC to ammonia and α-ketobutyrate (Glick, 2005, 2014). This microbial ACC deaminase-based reduction of plant stress has already been demonstrated for different environmental stressors, such as flooding, drought, heat, cold, pathogen colonization, as well as high concentrations of salt, heavy metals, and organic pollutants (Gamalero and Glick, 2012).

In relation to the present global change, drought events are predicted to increase in frequency and intensity (Spinoni et al., 2018; Hari et al., 2020), which will have significant impacts on plant production as well as on biogeochemically relevant soil processes (Fahad et al., 2017; Canarini et al., 2021). Plants produce increased amounts of ethylene upon imposition of drought stress, and thereby, stress susceptible plants produce higher levels of ethylene than stress-tolerant ones (Balota et al., 2004). The stress releasing action of ACC deaminase containing (*acdS*$^+$) PGPR strains is based on a negative influence on ethylene production on plant growth combined with the support of the antioxidative systems of the plant (Jaemsaeng et al., 2018; Gowtham et al., 2020; Murali et al., 2021). At the functional level, extensive literature exists on the positive effect of the inoculation of *acdS*$^+$ PGPR strains to increase drought tolerance and mitigate drought stress in plants (e.g., Arshad et al., 2008; Shakir et al., 2012; Danish et al., 2020). However, these studies have been performed with a limited set of bacteria, whereas in nature plants are constantly interacting with a multitude of microorganisms with different functional properties. Plant and microbe partners involved in these interactions form the holobiont, which is considered as being the unit of selection in evolution (Zilber-Rosenberg and Rosenberg, 2008) driving acclimation and/or adaptation processes, especially under stress pressure.

Under drought conditions, plants exhibit an altered carbon allocation and root exudate composition (Sanaullah et al., 2012; Gargallo-Garriga et al., 2018), which results in the restructuring of rhizosphere microbial communities (Berg and Smalla, 2009; Santos-Medellín et al., 2017; Zhalnina et al., 2018; Canarini et al., 2021). Members of these restructured plant-associated microbiota can contribute to plant survival by fostering short-term acclimation through the production of phytohormones or exopolysaccharides (direct response) and long-term adaptation (after several plant growth cycles) to drought stress through the selection of an adapted microbial community (Lau and Lennon, 2012; Marasco et al., 2012; Vurukonda et al., 2016). Drought history, i.e., the consequences of recurrent drought events, may affect soil processes or plant performance *via* the impact on the soil microbial community (Canarini et al., 2021; Munoz-Ucros et al., 2022). The impact of drought history has been analyzed in terms of resistance (the ability of the community to tolerate the disturbance) and resilience (the ability of the community to recover from the disturbance after rewetting; Griffiths and Philippot, 2013) after short periods of drought (de Nijs et al., 2019; Veach and Zeglin, 2020; Leizeaga et al., 2021). The processes of resistance and resilience concern rapid responses during or directly following the stress. In contrast, long-term adaptation to stress implies the selection of adapted microbial communities harboring beneficial functions after recurrent stress events in order to better tolerate subsequent stress (Evans et al., 2014; Bastida et al., 2017). In this context, the role of the selection of adapted PGPR to support the plant under stress is unclear.

Plant–soil feedback describes the relative growth of a plant in its own conspecific soil, compared to its growth with heterospecific soil that has been conditioned by another plant species (Bever et al., 1997). Plant–soil feedback (PSF) occurs when plants alter soil properties such as nutrient availability or secondary metabolite spectra, but also modify plant-associated microbial communities (Bennett and Klironomos, 2019). PSF has traditionally been studied in greenhouse experiments and without considering abiotic or biotic drivers, although it has lately become evident that changes in the environment can affect both the strength and the direction of the PSF (De Long et al., 2019). For instance, the previous drought can not only modify PSF, affecting con- and heterospecific plant growth responses and mediating drought legacy effects on microbial communities, but also influence plant and microbial responses to subsequent drought (Kaisermann et al., 2017). By influencing the abundance and composition of plant beneficial microorganisms, for instance, that of the *acdS*$^+$ population, plant-soil feedback and drought history could influence plant growth. Thus, a direct link between water deficit history effect on *acdS*$^+$ plant-beneficial microbial communities and increased plant drought resistance remains to be substantiated (de Vries et al., 2020).

Recently an approach for quantification and characterization of these PGPR was developed by Bouffaud et al. (2018), which uses specific PCR primers to target ACC deaminase-producing microorganisms. The *acdS* gene is highly conserved among microorganisms (bacteria and micro-eukaryotes) and is thus a suitable marker to assess the ACC deaminase functional communities and dynamics in the context of drought. Studies

based on this approach have shown that the abundance and diversity of *acdS*$^+$ microorganisms were modulated by plant species and plant genotype (Bouffaud et al., 2018), by field conditions, and, for maize, by the plant developmental stage (Renoud et al., 2020) as well as by soil depth (Gebauer et al., 2021). What is missing so far, is an analysis of the impact of water deficit on *acdS*$^+$ communities under different farming systems. The α-diversity of microbial communities in organic farming systems is often described to be higher than that in conventional farming systems (Hartmann et al., 2015; Lupatini et al., 2017; Harkes et al., 2019), which increases the potential of the PGPR community to support plant growth in this land-use system (Hole et al., 2005; Jangid et al., 2008; Gomiero et al., 2011). Enriching *acdS*$^+$ microorganisms in the rhizosphere represents an efficient means of stimulating plant growth during abiotic stress (Glick, 2014). Thus, an investigation of how the history of water deficit influences *acdS*$^+$ gene community abundance and composition, and how this is related to agricultural management may provide essential insights into the potential of *acdS*$^+$ soil bacteria to maintain crop production in the context of global change.

With respect to earlier studies on *acdS* gene markers, and since drought history experiments have shown that legacy effects interact with abiotic and biotic drivers (Kaisermann et al., 2017; Bennett and Klironomos, 2019; Canarini et al., 2021), we investigated here how the presence of cereals, cereal species, and farming systems modulate the legacy effect of water deficit on the *acdS*$^+$ microbial community. To this end, we set up a pot experiment using Chernozem soil collected at conventional and organic farming plots of the experimental platform Global Change Experimental Facility (GCEF; Schädler et al., 2019) (**Figure 1**). Wheat (*Triticum aestivum* L.), as the first, and diploid barley (*Hordeum vulgare* L.) as the fifth most extensively cultivated cereal crop worldwide (www.fao.org/faostat), were chosen as model systems. The aim of the current study was to examine the impact of soil water deficit history, i.e., history of water scarcity, on the microbial community composition of wheat and barley grown under water deficit in a second year. For this approach, we analyzed both (i) the total prokaryote community using 16S rRNA gene amplicon sequencing (Illumina MiSeq) as well as (ii) the abundance and community composition of the functional group of *acdS*$^+$ microorganisms (qPCR and Illumina MiSeq).

This work was based on three hypotheses. We first hypothesized that the presence of plants stimulates the selection of microbial communities and was further driven by water deficit history. We expected positive PSF in con-specific soil (wheat in the first and the second year of the experiment), assuming that with the same plant, the microbial community is already selected to dry conditions and niches in the rhizosphere that were present during the first period of water deficit will also be present during the second period of water deficit. Our second hypothesis was raised by the fact that bacterial diversity is expected to be higher under organic farming that represents limited resources but provides more niches (Thakur et al., 2020) and a broader functional pool of soil microorganisms to cope with drought stress. It stated that water deficit history modifies the microbial community assembly and that this effect is stronger in organic farming. Last, the third hypothesis was raised by reports on plant beneficial community selection by the rhizosphere (Mendes et al., 2014; Yuan et al., 2018). We hypothesized that the interaction between the history of water deficit and farming systems particularly impacts the *acdS*$^+$ community composition in the rhizosphere and selects taxa adapted to dry conditions.

MATERIALS AND METHODS

Soil Collection and Experimental Design

The pot experiment was conducted over two complete vegetation periods, a conditioning phase in the first year and an application phase in the second year (**Figure 1**). The experimental setup of the conditioning phase has been published in Breitkreuz et al. (2021). Briefly, the soil was collected from the upper 15 cm of organic (OF) and conventional (CF) farming plots of the Global Change Experimental Facility (GCEF, Schädler et al., 2019) at the UFZ field research station in Bad Lauchstädt, Central Germany [51°2393599N 11°5295599E, 118 m above sea level, average annual temperature: 9.7°C (1993 to 2013)]. The soil type at the research station is a fertile, loamy Haplic Chernozem (Altermann et al., 2005). The organic and conventional farming systems were implemented in autumn 2013. The conventional management comprises a rapeseed-wheat-barley crop rotation and the application of mineral NPK fertilizer, pesticides, and plant growth regulators. In contrast, organic management is conducted according to the EU regulation for organic agriculture (European Union, 2007), i.e., without applying plant protection or growth products. Moreover, mineral N fertilizer is replaced by the inclusion of legumes in the crop rotation (legume-wheat-barley). Besides the biological nitrogen fixation *via* legumes, fertilizers in the organic management are exclusively applied as rock phosphate and patentkali (K-Mg-S). The pre-adapted soils were homogenized and sieved (10 mm). For the pot experiment, 9.3 kg Chernozem was weighed in bags, mixed with fertilizers and water (60% of soil type-specific maximum water holding capacity; WHC), and filled in 7 L Kick–Brauckmann pots (STOMA GmbH, Siegburg, Germany). The applied fertilizers were selected in accordance with the guidelines for conventional and organic farming. Phosphorus (P), potassium (K), and nitrogen (N) sources for conventional farming were triple super phosphate, 60 % K_2O (60er Kali), and ammonium nitrate, while for organic farming they were granulated raw phosphate (Physalg 25), Muriate of potash (patentkali), and urea, respectively. Both conventional and organic farming pots were equally fertilized with 2 g N, 1 g P, and 2 g K. Further addition of 0.5 g Mg ($MgSO_4$), 0.15 g $FeCl_3$, and a mixture of micronutrients (A–Z solution by Hoagland and Snyder, 1933) was exclusive for conventional farming pots.

The pots were first subjected to a conditioning phase, comprising a four-factorial-design (Breitkreuz et al., 2021). Briefly, the pots were filled with soil, which originated from field experiments in Thyrow (Albic Luvisola, sandy soil) and Bad Lauchstädt (Haplic Chernozem, fertile soil) and was long-term adapted to either conventional or organic farming systems. We further decided on two different winter wheat genotypes

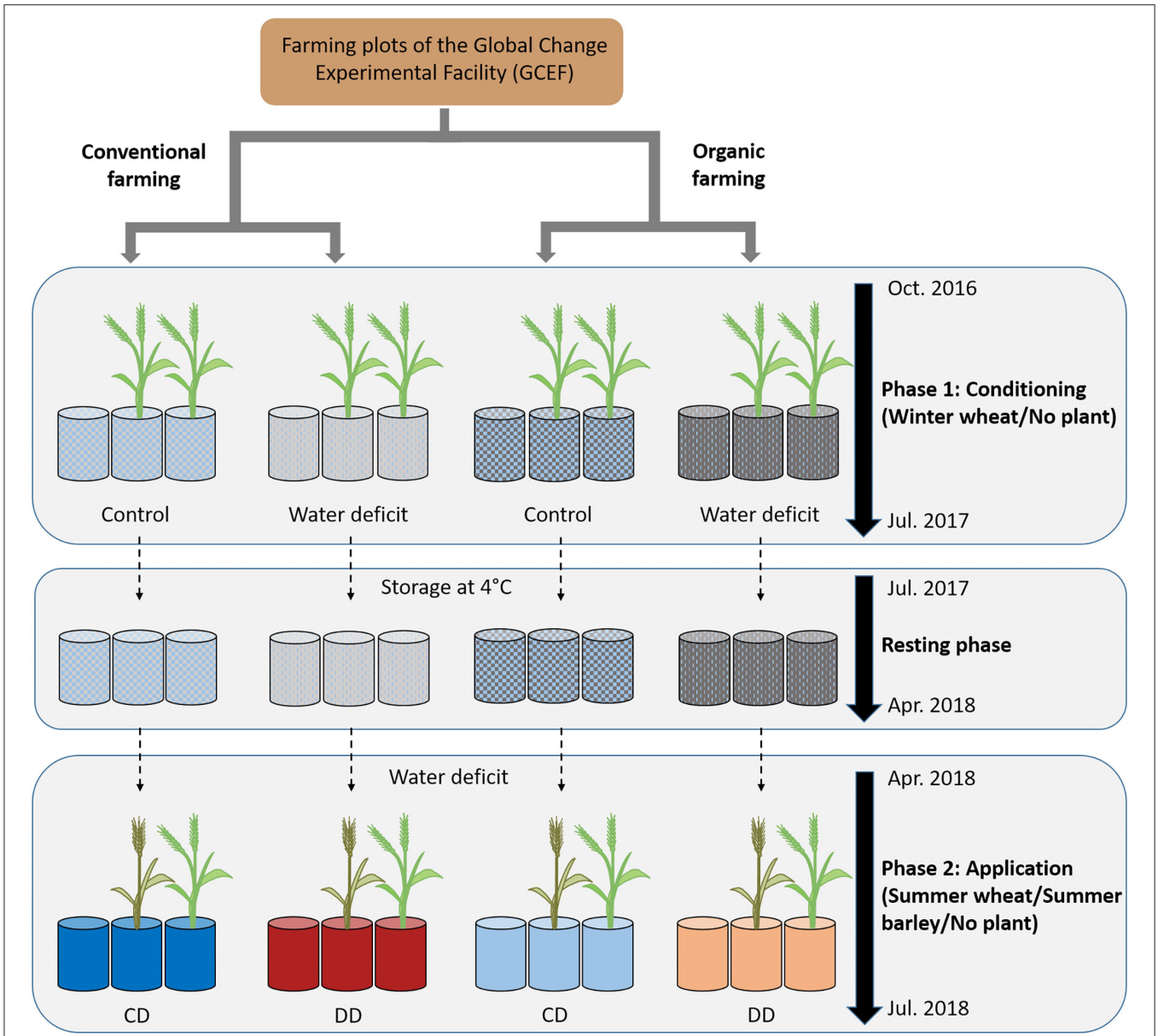

FIGURE 1 | Experimental design. During the conditioning phase (October 2016 to July 2017), pots were filled with soil from the Global Change Experimental Facility (GCEF) managed under conventional or organic farming. Approximately two-thirds of the pots were planted with winter wheat, and one-third remained unplanted. Half of the pots were well-watered (60% maximum soil water content; WHC) while the other half were exposed to water deficit conditions (25% WHC), and appropriate fertilizer was applied for OF and CF (Breitkreuz et al., 2021). Plants were removed in July 2017, and the soil remained in the respective pots till April 2018 at 4°C. The application started in April to July 2018, with a water deficit (25% WHC) applied to all pots, and no further fertilization was applied. The pots planted with winter wheat during the conditioning phase were used to grow summer wheat or summer barley, while the unplanted pots remained with bare soil ($n = 5$ pots). CD: "single water deficit," control and dry conditions, DD: "water deficit history," dry conditions and dry conditions.

with different site specifications to grow (demanding vs. non-demanding) and compared them to unplanted pots as control. Winter wheat was sown with either fungicide-treated seeds per pot for the conventional farming treatment or 16 untreated seeds per pot for the organic farming treatment. The pots were randomly placed on trolleys in a cold greenhouse and kept at 60% WHC over the winter of 2016/17. To guarantee germination, seeds were initially watered from the top until the plants reached the three-leaf stage. In March 2017, plants were equally adjusted to a number of 12 per pot and the watering treatment started. For this purpose, half of the pots were set to 25% WHC. The final design was thus: 2 soil types × 2 farming systems × 3 plant treatments × 2 watering systems x 5 replicates of each treatment = 120 pots. The water content was controlled daily by weighing the pots and adding the lost water. We observed that the prokaryotic communities were comparable between the

two wheat cultivars (Breitkreuz et al., 2021). After the harvest of wheat plants and bare soil in July 2017, the pots were kept at 4°C to preserve the adapted microbial communities. We expected that the microbial communities would remain stable during the storage in the cold room, but we are aware that to be absolutely sure about this, an analysis of pots before and after the storage would have been important to address this issue.

In April 2018, the application phase started. No further fertilization was applied to preserve adapted communities from the conditioning phase. Summer wheat ("Quintus," approved 18th December 2013, W. von Borries-Eckendorf GmbH & Co. KG, Germany) and summer barley ("Avalon," approved 20th December 2012, Saatzucht Josef Breun GmbH & Co. KG, Germany) were sown (12 plants per pot) in the pre-adapted pots from the conditioning phase (**Figure 1**). Both plants species are characterized by broad acceptance of cultivation sites and moderate resistance to drought. The pots were randomly placed on trolleys in a cold greenhouse. To guarantee germination, the seeds were initially watered from the top until the plants reached the three-leaf stage. Thereafter, all pots were subjected to dry conditions (25% WHC), and water loss was compensated daily from the bottom. Shortly before sampling, during the flowering stage in June 2018, above-ground plant heights were determined.

Three plants per pot were harvested to obtain a replicate. Fresh and dried (at 60°C) above-ground biomass was recorded. The soil that was closely attached to the roots, considered the rhizosphere, was carefully collected by brushing, frozen in liquid nitrogen, and stored at −80°C (rhizosphere "wheat" or "barley"). From each pot without plants ("bare soil"), three soil cores were pooled, sieved to 2 mm, frozen in liquid nitrogen, and stored at −80 °C. A total of five replicates (each composed of the three pooled rhizosphere or core soils) were analyzed in this study for each treatment of the application phase. The application phase treatments were termed after watering treatments applied in the first and second year: CD ("single water deficit," control and dry conditions) and DD ("water deficit history," dry conditions and dry conditions).

Construction of 16S rRNA Gene and *acdS* Libraries and Sequencing

To analyze the microbial community composition of the samples, DNA of 400 mg soil was extracted ($n = 5$ for each treatment) with the DNeasy PowerSoil kit (QIAGEN, Hilden, Germany) according to the manufacturer's instructions. DNA purity and quantity were measured with a NanoDrop (ThermoFisher Scientific, Waltham, MA, USA) and extracts stored at −20°C. The amplification of the bacterial 16S rRNA gene V4 region was performed with the universal primer pair 515f and 806r (Caporaso et al., 2011), and the partial *acdS* gene was amplified using the primers *acdS*F5 and *acdS*R8 (Bouffaud et al., 2018), both in duplicate. Primers were equipped with Illumina adapter sequences (Nextera XT Index Kit, Illumina, San Diego, CA, USA). To obtain high-fidelity amplification, PCR was performed using Kapa Hifi HotStart ReadyMix (KAPA-Biosystems, Wilmington, MA, USA). The PCR was performed in a S1000 Thermal Cycler (Bio-Rad Laboratories, Hercules, CA, USA): Initial denaturation at 95°C for 5 min, followed by 25 cycles of 98°C for 20 s, 55°C for 15 s, 72°C for 15 s—16S rRNA gene/30 cycles of 65°C for 10 s, 72 °C for 10 s—*acdS*, and final elongation at 72°C for 5 min. PCR products were purified using AMPure XP beads. To assign the sequences to the respective samples, an index PCR was performed using the Illumina Nextera XT Index Kit and Kapa Hifi HotStart ReadyMix (KAPA Biosystems, Wilmington, MA, USA). The indexed PCR was performed in an S1000 Thermal Cycler (Bio-Rad Laboratories, Hercules, CA, USA): 8 cycles of 95°C for 30 s, 55°C for 30 s, and 72°C for 30 s. PCR products were again purified with AMPure XP beads and quantified with Quant-iT PicoGreen dsDNA Assay Kit (Invitrogen, Life Technologies, Carlsbad, CA, USA) following the manufacturer's instructions. For sequencing, samples were pooled, and the pool's size and quality were checked with an Agilent 2100 Bioanalyzer (Agilent Technologies, Palo Alto, CA, United States). Paired-end sequencing was performed on 16S rRNA and *acd*S libraries using the Illumina MiSeq system. Raw sequences are accessible in the Short Reads Archive under the Bioproject PRJNA783187.

Sequence Data Processing

For both amplicon datasets, only reads with the expected amplification primers were kept, and reads without these primers were removed from further analysis. Primer sequences of the 16S rRNA gene amplicons were removed using cutadapt version 1.18. The obtained sequences were analyzed using dadasnake version.7 (Weißbecker et al., 2020; https://github.com/a-h-b/dadasnake) which depends on the open-source program R's (version 3.6.1; R Core Team 2017) DADA2 package (Callahan et al., 2016). The 16S rRNA gene amplicon reads were truncated to a minimum base quality of 11 and overall maximum expected error of 5, with a minimum length of 150 and 100 nt of the forward and reverse reads. The shorter *acdS* amplicon reads were truncated to 100 and 90 nt for the forward and reverse reads with a minimum base quality of 11 and a maximum expected error of 0.7. For both genes, read pairs were merged with zero mismatches, and exact sequence variants were determined to be used as ASVs (Amplicon Sequence Variants). Chimeric reads were removed using the DADA2 "consensus" algorithm (Callahan et al., 2016). Subsequently, the 16S rRNA gene amplicon sequence variants were taxonomically assigned using the mothur implementation of the 'Bayesian Classifier' (Schloss et al., 2009) against the SILVA database (version 132, non-redundant at 99%; Quast et al., 2013). The *acdS* sequences were aligned against an in-house *acdS* database extracted from FunGene (Fish et al., 2013) using BLASTn (version 2.7.1), according to Bouffaud et al. (2018). The 16S rRNA gene amplicons ASVs that were not assigned to the kingdoms Bacteria or Archaea were removed, and for the *acdS* amplicons, ASVs not assigned taxonomically using BLASTn were also removed.

Real-Time Quantitative PCR

The 16S rRNA and *acdS* genes were quantified in all samples using primers with Illumina linkers for 16S rRNA genes and linker-free *acdSF5/acdSR8* primers for *acdS* genes (Bouffaud et al., 2018). For real-time PCR master mix was prepared to

contain 0.5 μl of each primer with a concentration of 10 μM and ∼20 ng of DNA and made up to a final volume of 15 μl with 2x iQ SYBR Green Supermix. Amplification was run in the iCycler iQ5 (Bio-Rad Laboratories) with the following program: 45 cycles of 94°C for 15 s, 67°C for 15 s, 72°C for 15 s—16S rRNA gene/67°C for 15 s, 72°C for 15 s–*acdS*. The amount of *acdS* genes was normalized by the 16S rRNA gene copy numbers according to the comparative method of Livak and Schmittgen (2001).

Statistics

All statistical analyses and visualizations were performed in R (version 3.6.1; R Core Team, 2017). Fresh and dry plant weights were compared using the Kruskal–Wallis test followed by Dunn's test, as the data were not normally distributed. The effects of the different treatments on plant height as well as on the relative gene expression from qPCR were analyzed using ANOVA followed by Tukey's HSD test. Since the relative gene expression datasets were partly highly skewed, in addition to ANOVA and Tukey tests, the Kruskal–Wallis test followed by *post-hoc* tests were carried out using the Fisher's least significant difference criterion and Benjamini-Hochberg correction in "agricolae" package. Shannon index was calculated for each sample using the "vegan" package and the effect of the treatments on the microbial diversity was tested by the Kruskal–Wallis test followed by Fisher's LSD *post-hoc* test with Benjamini-Hochberg adjustment. ASV patterns were cross-compared with permutational multivariate analysis of variance (PERMANOVA; Anderson, 2001) using the "vegan" package. The effects of the plant, conditioning, and farming on the dominant taxa were tested by PERMANOVA. The effect of water deficit history on differential abundance was tested using DESeq2 for the ASVs representing at least 0.05% of the unrarefied reads (Love et al., 2014), comparing the farming system and the factor plant independently. Correlations between *acdS* and 16S rRNA gene read numbers were analyzed by Spearman's rank correlation test.

RESULTS

Plant Growth

Plant growth was strongly affected by farming management (CF > OF, $P < 0.001$ for both dry weight and height) (**Figure 2**). Thereby, the biomass of both portions of cereal was lower under organic (OF) than under conventional farming (CF), but this difference was only significant in the DD treatment (**Figure 2A**, $P < 0.001$ and $P = 0.003$, for barley and wheat, respectively). In addition, plant height was higher in CF than in OF for both crops in DD and CD (**Figure 2B**). The effect of water deficit conditioning (DD vs. CD) on the plant parameter was limited to a negative impact of water deficit conditioning on the height of the barley plants, in both OF and CF ($P < 0.001$, **Figure 2B**). Interestingly, water deficit conditioning tended to have a positive, but not significant, effect on barley dry weight under CF.

Relative Abundance of *acdS*-Carrying (*acdS*$^+$) Microorganisms

To investigate whether the relative abundance of *acdS*$^+$ microorganisms was affected by the treatments, the amplification levels of *acdS* genes were normalized with the abundances of 16S rRNA genes using the ΔCt method (Livak and Schmittgen, 2001). When all rhizosphere samples (without differentiating by plant species, farming system, or water conditioning) were compared to the bare soil samples, we observed that *acdS* genes were less abundant in bare soil than in rhizosphere soil ($P < 0.001$). More precisely, this difference was significant in CD under CF for barley ($P = 0.03$) and under OF for wheat ($P = 0.006$, **Figure 3**). When the effect of water conditioning on the relative abundance of *acdS* genes was tested for the plant rhizosphere samples, no significant difference was found between CD and DD. However, a significant positive effect of the water conditioning on the relative abundance of the *acdS*$^+$ community was found in the bare soil samples ($P = 0.02$).

Effects of Water Deficit History, Land Use, and Plant Presence on Bacterial Community Composition and Diversity

Barley and wheat rhizospheres, as well as bare soil samples, were subjected to 16S rRNA and *acdS* gene amplicon sequencing. In total, 2,225,931 16S rRNA and 4,406,511 *acdS* sequencing reads formed 1,849 ASVs and 4,945 ASVs, respectively. The rarefaction curves are presented in **Supplementary Figure S1**. The sequences were rarefied to the smallest read numbers per sample (16S rRNA gene 20,058 reads; *acdS* gene 54,660 reads). Altogether, the 16S rRNA gene reads covered a broad phylogenetic range, and the 10 most abundant classes corresponded to Actinobacteria, Alphaproteobacteria, Gammaproteobacteria, Thermoleophilia, Chloroflexi, Gemmatimonadetes, Bacteroidia, Blastocatellia, Nitrososphaeria, and Verrucomicrobiae. By contrast, the *acdS* amplicons were largely associated with only two phyla, Actinobacteria, and Proteobacteria. The majority, 79.6% of the rarefied reads, were affiliated with Actinobacteria, mainly of the families Streptomycetaceae, Intrasporangiaceae, and Nocardioidaceae. Almost a fifth of the *acdS* reads (19.6%) corresponded to Proteobacteria. While 0.8% were unclassified (u.) bacteria, we also gathered 0.0014% corresponding to fungi in the Ascomycota. In order to verify if the changes in the total bacterial community between the treatments were also visible at the *acdS* community level, all genera from the *acdS* and 16S rRNA gene communities were compared with each other. In total, 32 genera were identified in both communities, 18 belonging to the Actinobacteria and 14 to the Proteobacteria. Significant correlations between the distribution patterns of 16S rRNA and *acdS* gene reads were found for five genera identified from the very abundant ones, *Saccharothrix, Amycolatopsis*, *Marmoricola*, *Tetrasphaera,* and *Streptomyces* (**Supplementary Figure S2**), as well as *Achromobacter* ($P = 0.021$, rho 0.3) and u. *Microbacteriaceae* ($P = 0.006$, rho −0.36).

Permutational analysis of variance indicated that plant presence was the main factor driving both 16S rRNA ($R^2 = 0.36$, $P < 0.001$) and *acdS* ($R^2 = 0.22$, $P < 0.001$) community composition (**Table 1**). Moreover, Shannon diversity indices of the bacterial (**Supplementary Figure S3a**) and *acdS* communities (**Supplementary Figure S3b**) were overall higher in bare soil

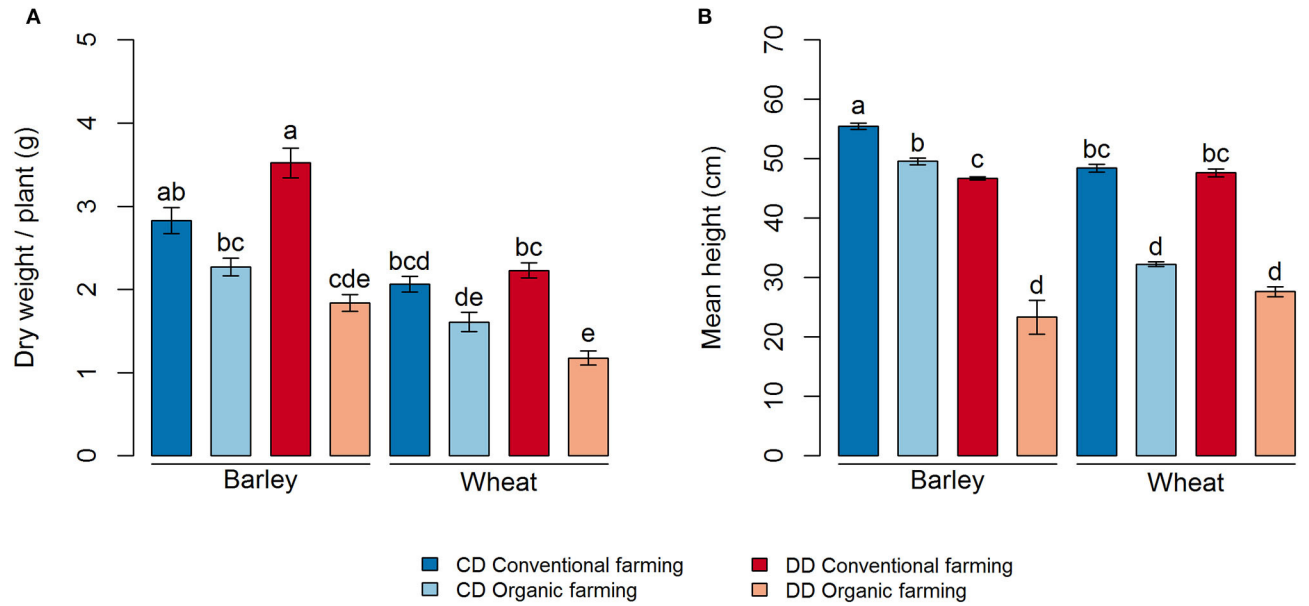

FIGURE 2 | Plant growth measures for each treatment, **(A)** dry weight per plant and **(B)** mean height. Values correspond to the average, and error bars to the respective standard error, of five pot, replicates. Letters show the statistical differences between treatments according to the Kruskal–Wallis test followed by Fisher's LSD *post-hoc* test with Benjamini-Hochberg *P*-value adjustment. CD, no water deficit conditioning; DD, water deficit conditioning.

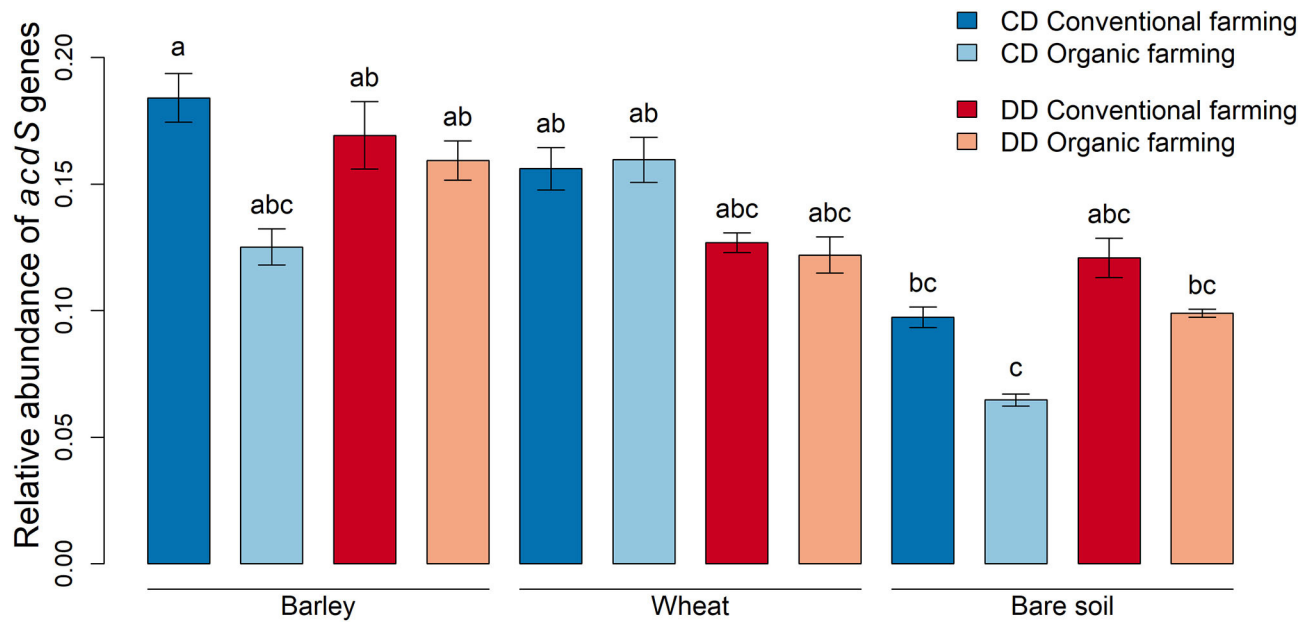

FIGURE 3 | Relative abundances of microorganisms with genes encoding for ACC deaminase. Abundance data obtained by qPCR were normalized with 16S rRNA gene abundances and calculated using the ΔCt method (Livak and Schmittgen, 2001). Values correspond to the average, and error bars to the respective standard error, with five pot, replicates. Letters show the statistical differences between all treatments according to ANOVA followed by Tukey's HSD *post-hoc* test. CD: "single water deficit," control and dry conditions, DD: "water deficit history," dry conditions and dry conditions.

than in rhizosphere samples. This difference was detected for both targeted genes and for all treatments. Although significant, the explanatory values for the effects of conditioning (CD or DD, 16S rRNA: $R^2 = 0.07$, $P < 0.001$; *acdS*: $R^2 = 0.04$, $P = 0.002$) and farming system (16S rRNA: $R^2 = 0.05$, $P < 0.001$; *acdS*: $R^2 = 0.05$, $P < 0.001$) on community composition were comparatively low. In total, 60% of the total variance in the total prokaryotic, and 46% of the variance in the *acdS*$^+$ community composition could

TABLE 1 | PERMANOVA of the 16S rRNA and *acdS* gene composition.

		All treatments (including bare soil)		Wheat and barley treatments	
		R^2	*P*-value	R^2	*P*-value
16S rRNA gene					
	Plant	**0.36**	**<0.001**	0.03	0.067
	Farming	**0.05**	**<0.001**	**0.11**	**<0.001**
	Conditioning	**0.07**	**<0.001**	**0.17**	**<0.001**
	Farming × conditioning	0.01	0.112	**0.04**	**0.044**
	Farming × plant	**0.04**	**0.035**	0.02	0.342
	Conditioning × plant	**0.05**	**0.004**	0.02	0.526
	Farming × conditioning × plant	0.02	0.253	0.02	0.652
	Residual	0.40		0.60	
acdS					
	Plant	**0.22**	**<0.001**	**0.05**	**0.002**
	Farming	**0.05**	**<0.001**	**0.11**	**<0.001**
	Conditioning	**0.04**	**0.002**	**0.07**	**<0.001**
	Farming × conditioning	**0.02**	**0.044**	**0.05**	**0.008**
	Farming × plant	**0.05**	**0.011**	0.03	0.07
	Conditioning × plant	**0.05**	**0.009**	0.03	0.098
	Farming × conditioning × plant	0.03	0.088	0.02	0.405
	Residual	0.54		0.63	

The ASV composition was considered for all treatments, to determine the effect of plant (wheat, barley, and bare soil), farming system (organic and conventional farming), and watering condition during the conditioning phase (CD and DD). The additional analysis of only barley and wheat treatments was used to analyze the effect of the plant species on the 16S rRNA gene base and acdS$^+$ community compositions. Significant factors ($P < 0.05$) are indicated in bold.

be explained by the sole effects of plant presence, water deficit conditioning, and farming alone or by its interaction.

Since the strong difference between the absence and the presence of plants masked the potential effects of plant identity, the rhizosphere samples were again analyzed separately from the bare soil ones. In this subset, the three factors explained 40% of the total variance in the 16S rRNA and 37% of the total variance in the *acdS*$^+$ community composition. Plant species identity (barley or wheat) had no impact on the total bacterial community composition, but a significant effect on *acdS*$^+$ community composition ($R^2 = 0.05$, $P = 0.002$). Furthermore, the farming system ($R^2 = 0.11$, $P < 0.001$) and water conditioning ($R^2 = 0.07$, $P < 0.001$), as well as the interaction between these factors, significantly shaped *acdS* community composition (**Table 1**), in particular for barley (**Figure 4**). A similar pattern was found for 16S rRNA gene composition, whereby conditioning ($R^2 = 0.17$, $P < 0.001$) and farming system ($R^2 = 0.11$, $P < 0.001$) were the main drivers (**Figure 4**). Crop-dependent effects were also found for Shannon indices (**Supplementary Figure S3**). Thus, for barley, the lowest diversity indices comparing all treatments were found for both *acdS* and 16S rRNA genes in OF under DD ($P = 0.004$ and $P = 0.032$ for *acdS* and 16S rRNA genes, respectively). For wheat, only the Shannon index of 16S rRNA genes was negatively impacted by the history of water deficit under OF, with a lower index in DD than in CD ($P = 0.015$). In contrast, the Shannon index of the *acdS* community in the rhizosphere of wheat was positively influenced by water deficit history under CF (DD > CD, $P = 0.02$) and further by farming soil type in DD (CF > OF, $P < 0.001$).

Distribution of Dominant Bacterial Genera Across Treatments

The 20 most abundant genera identified in the wheat and barley rhizospheres, as well as in the bare soil samples contributed on average 52.1 % to the total 16S rRNA gene amplicon reads (**Supplementary Figure S4**). Out of these, one genus was assigned to Archaea and 19 genera to Bacteria. Within the bacteria, the phylum of Actinobacteria was represented by six genera and Proteobacteria by five genera. Other phyla comprised each of two genera of Gemmatimonadetes (*Gemmatimonas* and u. Gemmatimonadaceae), Acidobacteria (*Acidobacteria SG6* and *RB41*), and *Chloroflexi* (*JG30 KF CM45* and *KD4 96*), and one genus of *Verrucomicrobia* (*C. Udeobacter*) and *Bacteroidetes* (u. Chitinophagaceae), respectively. The relative abundances of the 20 most abundant 16S rRNA gene-based genera varied among treatments (**Supplementary Table S1**). As for the whole community, three-way ANOVA performed on each of the 20 most abundant 16S rRNA gene-based genera showed that the presence/identity of the plant and then the farming and conditioning significantly shaped their distribution (**Supplementary Table S1**, **Supplementary Figure S4**). Genera from u. Chitinophagaceae, *Gemmatimonas,* and *Acidobacteria subgroup 6* were only affected by the plant presence but not by the farming system or the conditioning. For both plant rhizosphere samples, a farming effect was found for *Rhodanobacter* (OF > CF) and *Glycomyces* (CF > OF), and a conditioning effect for C. *udeobacter* and Chloroflexi *JG30-KF-CM45* (CD > DD) as well as for *Dyella* and *Nocardioides* (DD > CD). Finally, a farming and a conditioning effect were present for both plant rhizospheres, with a prevalence of u. Nitrososphaeraceae, KD4 96 and u. Solirubrobacterales in the CF and CD treatments and *Sphingomonas* and *Streptomyces* in the OF and DD treatments (**Supplementary Table S1**).

The *acdS* sequences from the 20 most abundant genera in the rhizosphere and bare soil represented on average 92% of the total number of reads (**Figure 5**). The sequences were either affiliated with the Actinobacteria (79.6 % of total reads) or the Proteobacteria (19.6 % of total reads). Actinobacteria were represented by 13 genera distributed among five different orders: one genus from the Streptomycetales, five genera from the Micrococcales, two from the Propionibacteriales, two from the Pseudonocardiales, one from the Geodermatophilales and from the Micromonosporales and the group of u. Actinobacteria. The seven genera belonging to the Proteobacteria corresponded to six genera of the order Burkholderiales and one of u. Bacteria.

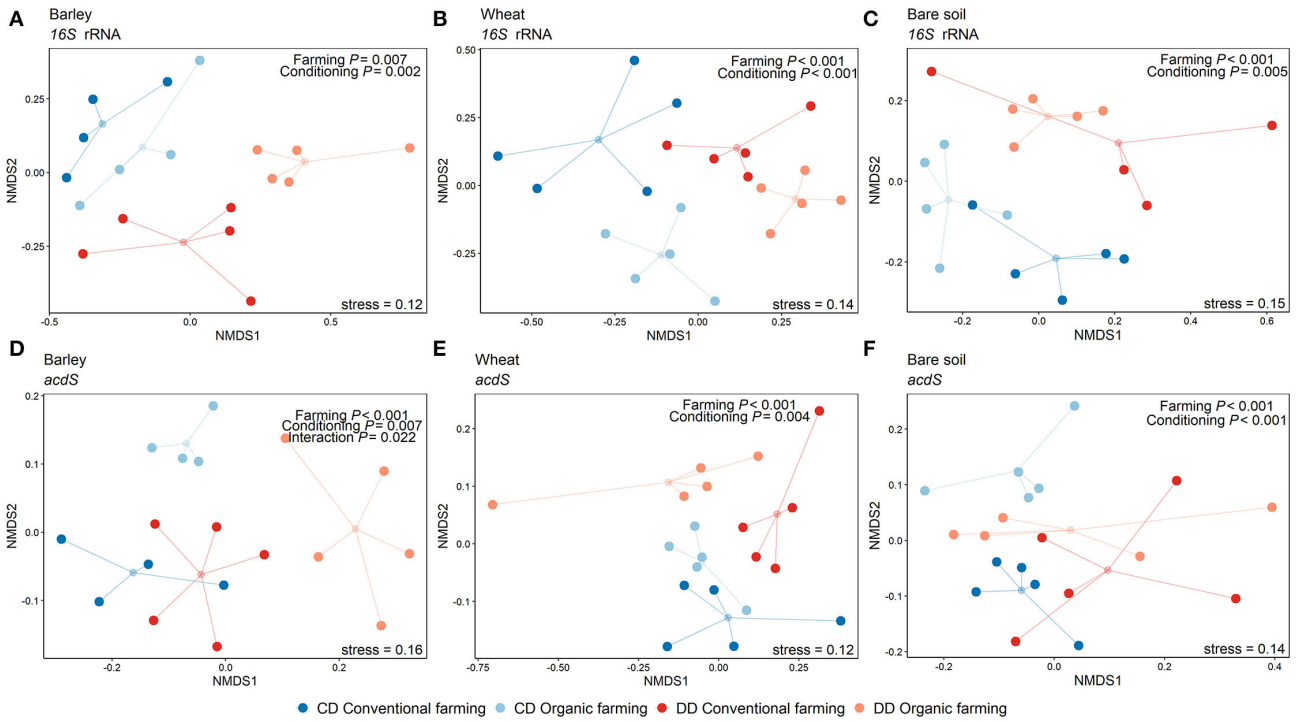

FIGURE 4 | Non-metric multidimensional scaling showing the effects of the farming system and watering during the conditioning phase per plant treatment. NMDS was performed on Amplicon Sequence Variants (ASV) using the Bray-Curtis dissimilarity matrix. The small circles correspond to the geometric center (centroid) of each treatment, and the lines indicate the distance of the samples to the centroid. Data from the 16S rRNA gene-based analysis are shown in subfigures a-c and *acdS* gene analyses are presented in subfigures d-f, for barley **(A,D)**, wheat **(B,E)**, and the pots without plants **(C,F)**. Results of the PERMANOVA are indicated in each plot ($n = 5$ pots). CF: conventional farming, OF: organic farming, CD: "single water deficit," control and dry conditions, DD: "water deficit history," dry conditions and dry conditions.

Three-way ANOVA analyses showed that 19 out of the 20 most abundant *acdS* genera were significantly affected by at least one factor (**Figure 5** and **Supplementary Table S1**), with the exception of the *Burkholderia* (Proteobacteria). These abundant genera were strongly affected by the plant presence, but also by the farming system and the conditioning, or their combined effects. In contrast to the 16S rRNA gene-based analysis, only two genera were only impacted by the plant presence without the direct effect of farming or conditioning. The other 18 genera were impacted in the plant rhizosphere by the effect of the farming system (five genera), conditioning (four genera), or by both (eight genera) (**Supplementary Table S1**).

Water Deficit History Responsive Genera of the *acdS*+ Community in the Rhizosphere

Due to the higher effect of water conditioning on the *acdS*+ bacteria in the rhizosphere (**Table 1**), their higher relative abundance in the rhizosphere compared to the bulk soil ($P < 0.001$) and the hypothesis that this functional group of bacteria helps the plant to face stress conditions, the bare soil was not analyzed to determine the effect of water deficit conditioning. The abundances of the unrarefied rhizosphere ASVs representing at least 0.05% of the $acdS^+$ reads corresponding to 377 ASVs with at least 1,400 reads were determined, and the $\log_2$ fold changes between CD and DD were calculated (**Supplementary Table S2**).

For both plants and under both farming systems, 122 conditioning-responsive ASVs were detected (**Supplementary Table S2**), including 87 with a fold change higher than two (**Figure 6**). The results showed that the effect of conditioning on the abundance of $acdS^+$ ASVs was often planting species- and farming system-specific (**Figure 6**). Much higher abundances of ASVs under water deficit conditioning (DD) treatment (log2 fold change < -12) were highly associated with samples from CF, especially ASVs associated with Actinobacteria. Interestingly, a significantly higher abundance of several ASVs corresponding to *Marmoricola* sp. were only found under OF. In addition, some Actinobacteria ASVs were only detected under DD (log2 fold change < -20) and this pattern was found independently of the farming condition. In contrast, the ASVs detected only in the treatments without drought conditioning (CD, log2 fold change > 20) were exclusively found in the wheat treatments, independently of the farming condition.

DISCUSSION

Climate predictions suggest an increased probability of summer drought in Central Europe (Spinoni et al., 2018; Hari et al.,

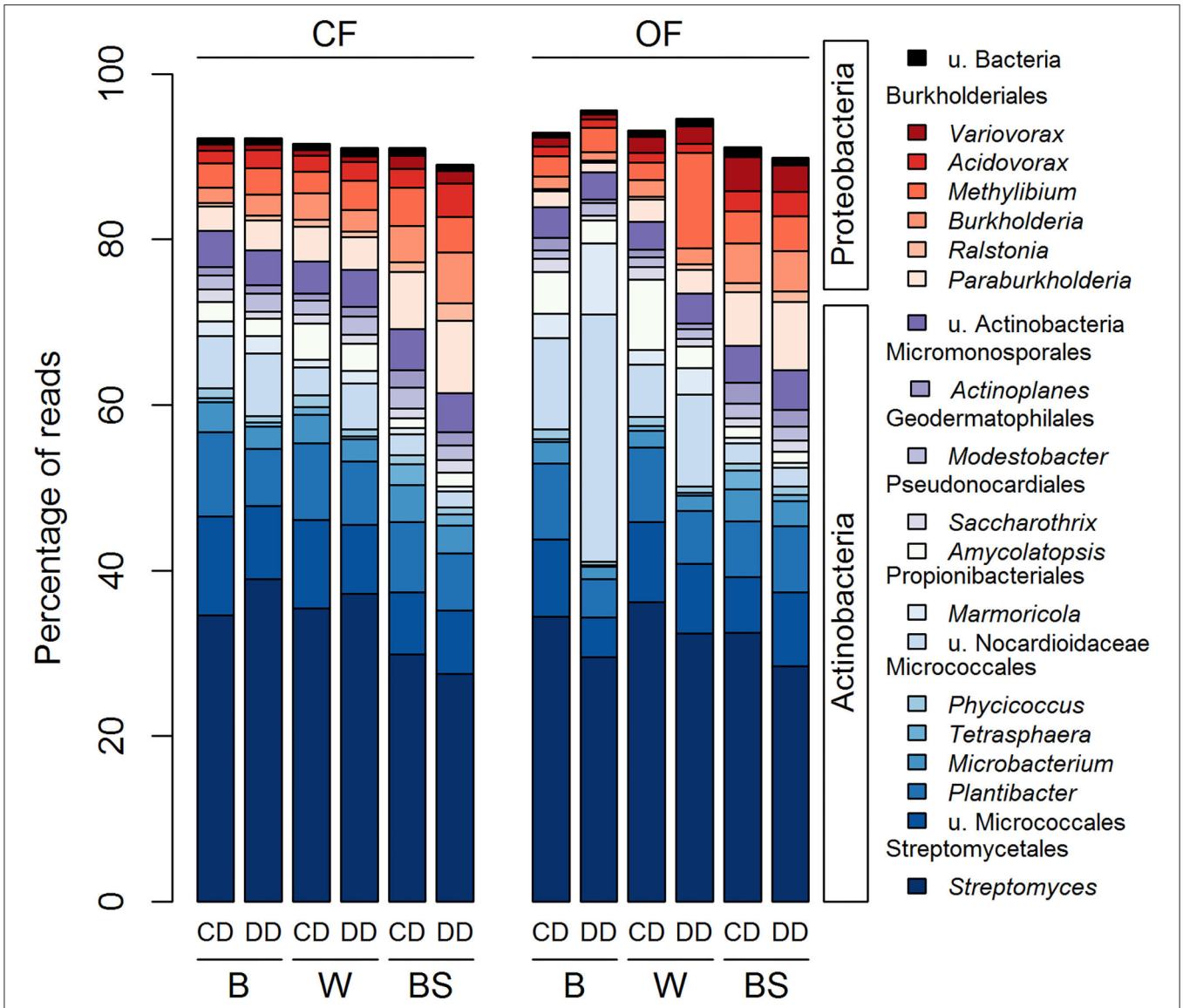

FIGURE 5 | Distribution of the 20 most abundant genera across all treatments based on the *acdS* dataset. CF, conventional farming; OF, organic farming; B, barley; W, wheat; BS, bare soil; CD, "single water deficit," control and dry conditions; DD, "water deficit history," dry conditions and dry conditions; $n = 5$ pots.

2020), which represents a threat to plant water and nutrient uptake. This threat is supposed to be mitigated by plant-beneficial rhizobacteria (de Vries et al., 2020). Drought legacy effects may have a strong effect on soil functioning, by long-term adaptations in the microbial community composition and microbial-mediated plant functioning. For the first time, this study analyzed the impact of successive dry conditions on the diversity and community composition of the $acdS^+$ functional group of microbes potentially contributing to plant stress tolerance. We show that the rhizosphere prokaryotes and especially the $acdS^+$ community are adaptable to water limitations. The impact of the watering regime during the application phase on the microbial communities indicates a legacy of water deficit.

Water Deficit Conditioning Structures the Microbial Community, Especially in the Rhizosphere

We expected in our first hypothesis that the response to water deficit conditioning by the microbial communities would be specific for planted and non-planted pots due to the selection of specific microbes by the roots. Our results show that this proved to be the case. We observed that plant presence was the main factor influencing both 16S rRNA and *acdS* gene diversity, and this was reflected by distinct community compositions in bare soil and in the rhizosphere of both barley and wheat. We would like to point out that we did not perform an analysis of the soil outside the rhizosphere in the planted pots, which would have been an important supplementary control treatment. Due to the

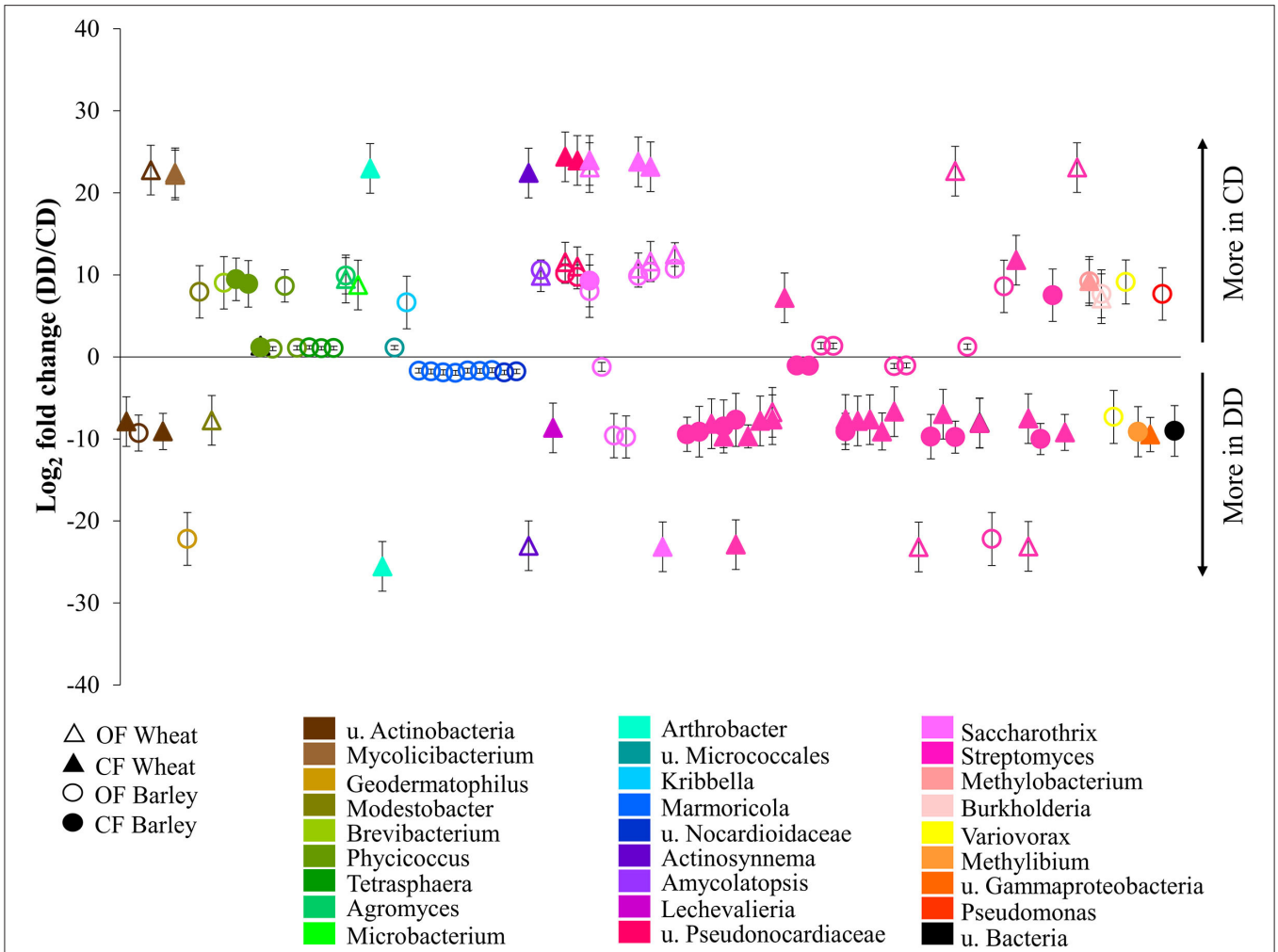

FIGURE 6 | Relative abundances of the *acdS*$^+$ ASVs significantly impacted by drought conditioning. Taxa were identified using DESeq2 and *P*-value < 0.05, and log2-fold changes between respective treatments are represented. CF, conventional farming; OF, organic farming; CD, "single water deficit," control and dry conditions; DD, "water deficit history," dry conditions and dry conditions; $n = 5$ pots.

strong selection effect of plants in combination with adaptation to water stress conditions, the microbial community is supposed to be less complex in the rhizosphere soil (Mendes et al., 2014), which was confirmed by the lower diversity (Shannon index) of the total bacterial as well as the ACC deaminase microbial communities in the rhizosphere treatments compared to the bare soils. However, despite this reduced diversity, water deficit conditioning-induced community shifts were more obvious in the rhizosphere than in the bare soil. As root exudation changes under drought conditions (Preece and Peñuelas, 2016), these results suggest specialization of the taxa recruited in the rhizosphere in order to help the plant to face the stress.

Farming Systems Select Taxa After Recurrent Drought Events

Soils under organic farming are often a reservoir of higher microbial diversity and activity than soils under conventional farming due to higher soil organic carbon levels (Lori et al., 2017; Harkes et al., 2019), which may lead to a stronger plant-beneficial response to stress. However, contrary to our second hypothesis, we found that several taxa were enriched in the plant rhizosphere under conventional farming after the water deficit conditioning. Similarly, while the diversity of the *acdS*$^+$ community decreased in the rhizosphere under organic farming in DD, it increased in DD under conventional farming. Noteworthy, this higher diversity of plant-beneficial, *acdS*+ taxa under conventional farming was not visible at the level of the entire bacterial community, suggesting that plants under water deficit specifically selected plant beneficial organisms to counteract the stress.

These farming type-specific effects on microbial communities are in line with the indicator species that were identified from agricultural soils after short drought stress by Kundel et al. (2020). Under moderate drought, plants release more organic acids in their root exudates, especially the drought-tolerant ones (Song et al., 2012). Organic acids stimulate microbial activity in the rhizosphere (Macias-Benitez et al., 2020). In our samples under conventional farming, plants had a better fitness due to the fertilization amendments in CF, which may lead

to higher exudation rates of these organic acids, and to the selection of the plant-beneficial ACC deaminase bacteria after a successive period of water deficit. Consequently, the *acdS*$^+$ taxa specifically enriched in the rhizosphere after water deficit conditioning potentially represent good indicators of drought-adapted microbes.

History of Water Deficit and Farming Systems Affect Strongly the *acdS*+ Community in the Rhizosphere

The majority of the dominant microbial taxa were influenced by water deficit conditioning, which may be surprising, as not all microbial individuals within a genus have similar functions, and the effect of a particular treatment might be diluted at a certain phylogenetic level. During the conditioning phase, the predicted abundance of ACC deaminase-related genes was higher in organic farming communities of well-watered soils compared to drought treatment (Breitkreuz et al., 2021). This difference in abundance was not observed in the DD samples of organic farming of barley or wheat in the present study. However, and presumably, as a result of this, the Shannon index was lower in organic farming DD, especially in the barley rhizosphere. This suggests that the *acdS*+ community was already under selection during the conditioning phase, especially by water limitation in organic farming, and some less abundant taxa might have been already selected and their proportions increased. Consequently, the selection during the conditioning phase may have led to a decrease in Shannon index at the application phase that was further enhanced by hetero-specific plant-soil feedback which means changing the plant from wheat in the conditioning phase to barley in the application phase.

In this study, we found several ASVs from *acdS*$^+$ Proteobacteria and Actinobacteria enriched by water deficit conditioning in the conventionally managed soils. Proteobacteria are generally described to be less abundant after drought stress. Indeed, after the conditioning phase, abundances of species belonging to phyla Acidobacteria, Chloroflexi, Firmicutes, and Latescibacteria were significantly increased under drought, while Proteobacteria decreased (Breitkreuz et al., 2021). This negative trend may be balanced by the plant-growth-promoting properties Proteobacteria often possess, like ACC deaminase. For that reason, Proteobacteria are commonly inoculated on plants to improve drought stress tolerance. In line with our results, the enrichment of the *acdS*$^+$ *Variovorax paradoxus* under drought as well as its beneficial effect on plant growth under drought was already shown (Belimov et al., 2009; Teijeiro et al., 2019). Several Actinobacteria were also more abundant after water deficit conditioning. Bouffaud et al. (2018) already described the dominance of *acdS*$^+$ Actinobacteria in the rhizosphere, and their consistent enrichment in soil by drought is established (Hartman and Tringe, 2019), as they are mostly known to be drought-tolerant, due to their strong cell wall and drought avoidance by spore formation (Pérez Castro et al., 2019). The genus *Streptomyces* was the most abundant *acdS*$^+$ genus and its abundance was enhanced by conditioning with limited water. Members of this Gram-positive genus are characterized as drought tolerant and plant-beneficial (Schrey and Tarkka, 2008; Breitkreuz et al., 2020), which we could also confirm within our study. We particularly identified ASVs corresponding to several *Streptomyces* species enriched by water limitation conditioning, including *S. mutabilis*, *S. resistomycificus*, *S. scabiei*, and *S. viridochromogenes*. These *Streptomyces* species have a strong potential to affect the growth of wheat and barley. *S. viridochromogenes* has been characterized as the producer of the herbicide phosphinothricin tripeptide (Schwartz et al., 2004), whereas *S. mutabilis* promotes wheat growth and disease resistance (Toumatia et al., 2016). And finally, the biology of *S. scabiei* is complex and isolate specific; whereas pathogenic *S. scabiei* strains produce thaxtomins and suppress plant defense responses causing growth reduction and scab formation in potatoes (Bignell et al., 2010), other strains of the same species produce staurosporine and control effectively wheat take-all disease (Wen et al., 2012). However, their positive impact on the plant under drought has not yet been described.

Effect of Plant Identity

While the effect of plant identity on the overall community was comparably low, it had a strong effect on the *acdS*$^+$ community, as it was suggested in our third hypothesis. This indicates a strong selection by plant species, likely caused by differential rhizodeposition. Wheat root exudates have been described to differ considerably from those of barley, most notably by the abundance and composition of dominant mugineic acids, and also by differences in the relative quantities of amino acids (Fan et al., 2001). Wheat plants seemed to be less impacted by water deficit conditioning, as reflected by their similar plant heights in the two treatments. The associated microbial communities displayed even higher diversity indices under conventional farming. One explanation may come from the use of winter wheat as a model plant during the first year of the experiment, i.e., the conditioning phase. The close relationship between winter and summer wheat, probably selecting specifically adapted taxa, may have favored the growth of summer wheat plants more than barley in the application phase. This implies that by changing the crop, the positive effect of water deficit history decreased. Similarly, Kaisermann et al. (2017) found that drought legacy effects on plant growth were at their strongest in soils that were conditioned with the same plant species.

Does Niche Selection Explain the History of Water Deficit?

Differences in the water supply were applied during the conditioning, 25 vs. 60% WHC, and a constant water deficit, 25% WHC, during the application phase. Drought legacy effects on bacterial communities have been reported both after consecutive drought periods (Evans et al., 2014; Bastida et al., 2017) like in our experiment, but also after the drought was terminated (de Vries et al., 2018). A well-supported explanation for changes in microbial composition in response to chronic low soil moisture is niche selection (Evans et al., 2014) leading to an enrichment of taxa that are drought tolerant compared to those that are sensitive to drought. As a result, entire soil microbial communities could develop drought tolerance through time (Bastida et al., 2017),

which could lead to increased rates of microbial activity at low soil moistures. When the changes are introduced in the context of plant community and plant-soil feedback, the changes may ultimately sustain the beneficial impact of rhizosphere organisms on plant growth (Canarini et al., 2021). In line with the holobiome concept of the extended plant phenotype, these consequent stages of selection may contribute to overall plant fitness upon drought stress (Liu et al., 2020). Our data support the idea of niche selection by two consecutive drought periods and suggests that resistance of the *acdS*$^+$ community is sustained by a highly dynamic community structure. These high dynamics is in line with our observations on the maize rhizosphere *acdS*$^+$ community; they were strongly modulated by soil type, but also by soil depth (Gebauer et al., 2021) and the developmental stage of maize (Renoud et al., 2020).

CONCLUSIONS AND PERSPECTIVES

We demonstrated that water deficit can induce a modification of the community of the specialized plant beneficial prokaryotes that remains detectable during a successive period of low soil moisture in the following year. This result adds to the information on rhizosphere microbial selection by drought and emphasizes that plant growth-promoting bacteria can be especially responsive to abiotic stress. Future work should target how long the difference between the conditioned and unconditioned communities holds up, and whether it vanishes after a period of optimal watering. Members of the *acdS*$^+$ community were mainly selected from proteobacterial and actinobacterial species pools, which in the overall community made up the majority of rhizosphere-associated microorganisms. Members of many of the identified taxa can be readily isolated by cultivation, and experiments with synthetic communities would reveal their functional potential. That the responses are distinct in bare soils and rhizospheres, and further modulated by the farming conditions, underlines the context-dependency of the community responses, but hints also that a change in community structure might buffer the negative impacts of water deficit. Future work should thus investigate how these drought-adapted rhizosphere *acdS*$^+$ communities represent ACC deaminase activity and support plant performance. This can be used to identify tipping points, thresholds of water deficit severity, or length where even the stress-adapted community cannot sustain plant growth.

DATA AVAILABILITY STATEMENT

The datasets presented in this study can be found in online repositories. The names of the repository/repositories and accession number(s) can be found below: https://www.ncbi.nlm.nih.gov/, PRJNA783187.

AUTHOR CONTRIBUTIONS

CB, TR, and MT conceived and designed the experiment. LG, CB, and M-LB performed the laboratory work. LG, AH-B, and M-LB analyzed the data. M-LB, MT, and CB wrote the manuscript with input from all authors. All authors interpreted the results, contributed to revisions, and approved the submission of the manuscript.

FUNDING

This work was done with the support of the Helmholtz Centre for Environmental Research-UFZ. AH-B received funding from the German Centre for Integrative Biodiversity Research (iDiv) Halle-Jena- Leipzig of the German Research Foundation (FZT118, 202548816). CB received funding from the Deutsche Bundesstiftung Umwelt (DBU) in the form of a scholarship (AZ: 20015/391).

ACKNOWLEDGMENTS

We appreciate the Helmholtz Association, the Federal Ministry of Education and Research, the State Ministry of Science and Economy of Saxony-Anhalt, and the State Ministry for Higher Education, Research, and the Arts Saxony to fund the Global Change Experimental Facility (GCEF) project. We thank the staff of the Bad Lauchstädt Experimental Research Station (especially Ines Merbach and Konrad Kirsch) and Martin Schädler for their work in maintaining the plots and infrastructures of the Global Change Experimental Facility (GCEF), and Harald Auge, François Buscot, Stefan Klotz and Martin Schädler for their role in setting up the GCEF. We also want to thank all helpers participating in the sampling. We further want to thank Beatrix Schnabel for her support in Illumina sequencing. The sequencing data were computed using the High-Performance Computing (HPC) Cluster EVE, a joint effort of both the Helmholtz Center for Environmental Research-UFZ and the German Center for Integrative Biodiversity Research (iDiv) Halle-Jena-Leipzig, whose administrators are thanked.

SUPPLEMENTARY MATERIAL

The Supplementary Material for this article can be found online at: https://www.frontiersin.org/articles/10.3389/fmicb.2022.824437/full#supplementary-material

REFERENCES

Altermann, M., Rinklebe, J., Merbach, I., Körschens, M., Langer, U., and Hofmann, B. (2005). Chernozem-soil of the year 2005. *J. Plant Nutr. Soil Sci.* 168, 725–740. doi: 10.1002/jpln.200521814

Anderson, M. J. (2001). A new method for non-parametric multivariate analysis of variance. *Austral Ecol.* 26, 32–46 doi: 10.1111/j.1442-9993.2001.01070.pp.x

Arshad, M., Shaharoona, B., and Mahmood, T. (2008). Inoculation with *Pseudomonas* spp. containing ACC-deaminase partially eliminates the effects of drought stress on growth, yield, and ripening of pea (*Pisum*

sativum L.). *Pedosphere* 18, 611–620. doi: 10.1016/S1002-0160(08)60055-7

Backer, R., Rokem, J. S., Ilangumaran, G., Lamont, J., Praslickova, D., Ricci, E., et al. (2018). Plant growth-promoting rhizobacteria: Context, mechanisms of action, and roadmap to commercialization of biostimulants for sustainable agriculture. *Front. Plant Sci.* 9, 1473. doi: 10.3389/fpls.2018.01473

Balota, M., Cristescu, S., Payne, W. A., te Lintel Hekkert, S., Laarhoven, L. J., and Harren, F. J. (2004). Ethylene production of two wheat cultivars exposed to desiccation, heat, and paraquat-induced oxidation. *Crop Sci.* 44, 812–818. doi: 10.2135/cropsci2004.8120

Bastida, F., Torres, I. F., Andrés-Abellán, M., Baldrian, P., López-Mondéjar, R., Větrovský, T., et al. (2017). Differential sensitivity of total and active soil microbial communities to drought and forest management. *Glob. Chang. Biol.* 23, 4185–4203. doi: 10.1111/gcb.13790

Belimov, A. A., Dodd, I. C., Hontzeas, N., Theobald, J. C., Safronova, V. I., and Davies, W. J. (2009). Rhizosphere bacteria containing 1-aminocyclopropane-1-carboxylate deaminase increase yield of plants grown in drying soil via both local and systemic hormone signaling. *New Phytol.* 181, 413–423. doi: 10.1111/j.1469-8137.2008.02657.x

Bennett, J. A., and Klironomos, J. (2019). Mechanisms of plant–soil feedback: interactions among biotic and abiotic drivers. *New Phytol.* 222, 91–96. doi: 10.1111/nph.15603

Berendsen, R. L., Pieterse, C. M. J., and Bakker, P. A. H. M. (2012). The rhizosphere microbiome and plant health. *Trends Plant Sci.* 17, 478–486. doi: 10.1016/j.tplants.2012.04.001

Berg, G., and Smalla, K. (2009). Plant species and soil type cooperatively shape the structure and function of microbial communities in the rhizosphere. *FEMS Microbiol. Ecol.* 68, 1–13. doi: 10.1111/j.1574-6941.2009.00654.x

Bever, J. D., Westover, K. M., and Antonovics, J. (1997). Incorporating the soil community into plant population dynamics: the utility of the feedback approach. *J. Ecol.* 85, 561–573. doi: 10.2307/2960528

Bignell, D. R., Huguet-Tapia, J. C., Joshi, M. V., Pettis, G. S., and Loria, R. (2010). What does it take to be a plant pathogen: genomic insights from *Streptomyces* species. *Antonie Van Leeuwenhoek* 98, 179–194. doi: 10.1007/s10482-010-9429-1

Bouffaud, M.-L., Renoud, S., Dubost, A., Moënne-Loccoz, Y., and Muller, D. (2018). 1-Aminocyclopropane-1-carboxylate deaminase producers associated to maize and other Poaceae species. *Microbiome* 6, 114. doi: 10.1186/s40168-018-0503-7

Breitkreuz, C., Buscot, F., Tarkka, M., and Reitz, T. (2020). Shifts between and among populations of wheat rhizosphere *Pseudomonas*, *Streptomyces* and *Phyllobacterium* suggest consistent phosphate mobilization at different wheat growth stages under abiotic stress. *Front. Microbiol.* 10, 3109. doi: 10.3389/fmicb.2019.03109

Breitkreuz, C., Herzig, L., Buscot, F., Reitz, T., and Tarkka, M. (2021). Interactions between soil properties, agricultural management and cultivar type drive structural and functional adaptations of the wheat rhizosphere microbiome to drought. *Environ. Microbiol.* 23, 5866–5882. doi: 10.1111/1462-2920.15607

Callahan, B. J., McMurdie, P. J., Rosen, M. J., Han, A. W., Johnson, A. J. A., and Holmes, S. P. (2016). DADA2: high-resolution sample inference from Illumina amplicon data. *Nat. Methods* 13, 581–583. doi: 10.1038/nmeth.3869

Canarini, A., Schmidt, H., Fuchslueger, L., Martin, V., Herbold, C. W., Zezula, D., et al. (2021). Ecological memory of recurrent drought modifies soil processes via changes in soil microbial community. *Nat. Commun.* 12, 5308. doi: 10.1038/s41467-021-25675-4

Caporaso, J. G., Lauber, C. L., Walters, W. A., Berg-Lyons, D., Lozupone, C. A., Turnbaugh, P. J., et al. (2011). Global patterns of 16S rRNA diversity at a depth of millions of sequences per sample. *Proc. Natl. Acad. Sci. U. S. A.* 108, 4516–4522. doi: 10.1073/pnas.1000080107

Danish, S., Zafar-ul-Hye, M., Mohsin, F., and Hussain, M. (2020). ACC-deaminase producing plant growth promoting rhizobacteria and biochar mitigate adverse effects of drought stress on maize growth. *PLoS ONE* 15, e0230615. doi: 10.1371/journal.pone.0230615

De Long, J. R., Fry, E. L., Veen, G. F., and Kardol, P. (2019). Why are plant–soil feedbacks so unpredictable, and what to do about it? *Funct. Ecol.* 33, 118–128. doi: 10.1111/1365-2435.13232

de Nijs, E. A., Hicks, L. C., Leizeaga, A., Tietema, A., and Rousk, J. (2019). Soil microbial moisture dependences and responses to drying–rewetting: the legacy of 18 years drought. *Glob. Chang. Biol.* 25, 1005–1015. doi: 10.1111/gcb.14508

de Vries, F. T., Griffiths, R. I., Bailey, M., Craig, H., Girlanda, M., Gweon, H. S., et al. (2018). Soil bacterial networks are less stable under drought than fungal networks. *Nat. Commun.* 9, 1–12. doi: 10.1038/s41467-018-05516-7

de Vries, F. T., Griffiths, R. I., Knight, C. G., Nicolitch, O., and Williams, A. (2020). Harnessing rhizosphere microbiomes for drought-resilient crop production. *Science* 368, 270–274. doi: 10.1126/science.aaz5192

European Union (2007). *Council regulation (EC) No 834/2007 of 28 June 2007 on organic production and labelling of organic products and repealing regulation (EEC) No 2092/91*. Official Journal of the European Union L189/1-23, Luxembourg.

Evans, S. E., Matthew, D., Wallenstein, and Ingrid, C., Burke. (2014). Is bacterial moisture niche a good predictor of shifts in community composition under long term drought? *Ecology* 95, 110–122. doi: 10.1890/13-0500.1

Fahad, S., Bajwa, A. A., Nazir, U., Anjum, S. A., Farooq, A., Zohaib, A., et al. (2017). Crop production under drought and heat stress: plant responses and management options. *Front. Plant Sci.* 8, 1147. doi: 10.3389/fpls.2017.01147

Fan, T. W.-M., Lane, A. N., Shenker, M., Bartley, J. P., Crowley, D., and Higashi, R. M. (2001). Comprehensive chemical profiling of gramineous plant root exudates using high-resolution NMR and MS. *Phytochemistry* 57, 209–221. doi: 10.1016/S0031-9422(01)00007-3

Fish, J., Chai, B., Wang, Q., Sun, Y., Brown, C. T., Tiedje, J., et al. (2013). FunGene: the functional gene pipeline and repository. *Front. Microbiol.* 4, 291. doi: 10.3389/fmicb.2013.00291

Gamalero, E., and Glick, B. R. (2012). "Ethylene and abiotic stress tolerance in plants," in *Environmental Adaptations and Stress Tolerance of Plants in the Era of Climate Change*, eds P. Ahmad and M. N. V. Prasad (New York, NY: Springer), 395–412. doi: 10.1007/978-1-4614-0815-4_18

Gargallo-Garriga, A., Preece, C., Sardans, J., Oravec, M., Urban, O., and Peñuelas, J. (2018). Root exudate metabolomes change under drought and show limited capacity for recovery. *Sci. Rep.* 8, 12696. doi: 10.1038/s41598-018-30150-0

Gebauer, L., Bouffaud, M.-L., Ganther, M., Yim, B., Vetterlein, D., Smalla, K., et al. (2021). Soil texture, sampling depth and root hairs shape the structure of ACC deaminase bacterial community composition in maize rhizosphere. *Front. Microbiol.* 12:616828. doi: 10.3389/fmicb.2021.616828

Glick, B. R. (2005). Modulation of plant ethylene levels by the bacterial enzyme ACC deaminase. *FEMS Microbiol. Lett.* 251, 1–7. doi: 10.1016/j.femsle.2005.07.030

Glick, B. R. (2014). Bacteria with ACC deaminase can promote plant growth and help to feed the world. *Microbiol. Res.* 169, 30–39. doi: 10.1016/j.micres.2013.09.009

Gomiero, T., Pimentel, D., and Paoletti, M. G. (2011). Environmental impact of different agricultural management practices: conventional vs. organic agriculture. *Crit. Rev. Plant Sci.* 30, 95–124. doi: 10.1080/07352689.2011.554355

Gowtham, H. G., Singh, B., Murali, M., Shilpa, N., Prasad, M., Aiyaz, M., et al. (2020). Induction of drought tolerance in tomato upon the application of ACC deaminase producing plant growth promoting rhizobacterium *Bacillus subtilis* Rhizo SF 48. *Microbiol. Res.* 234, 126422. doi: 10.1016/j.micres.2020.126422

Griffiths, B. S., and Philippot, L. (2013). Insights into the resistance and resilience of the soil microbial community. *FEMS Microbiol. Rev.* 37, 112–129. doi: 10.1111/j.1574-6976.2012.00343.x

Hari, V., Rakovec, O., Markonis, Y., Hanel, M., and Kumar, R. (2020). Increased future occurrences of the exceptional 2018–2019 Central European drought under global warming. *Sci. Rep.* 10, 12207. doi: 10.1038/s41598-020-68872-9

Harkes, P., Suleiman, A. K. A., van den Elsen, S. J. J., de Haan, J. J., Holterman, M., Kuramae, E. E., et al. (2019). Conventional and organic soil management as divergent drivers of resident and active fractions of major soil food web constituents. *Sci. Rep.* 9, 13521. doi: 10.1038/s41598-019-49854-y

Hartman, K., and Tringe, S. G. (2019). Interactions between plants and soil shaping the root microbiome under abiotic stress. *Biochem. J.* 476, 2705–2724. doi: 10.1042/BCJ20180615

Hartmann, M., Frey, B., Mayer, J., Mäder, P., and Widmer, F. (2015). Distinct soil microbial diversity under long-term organic and conventional farming. *ISME J.* 9, 1177–1194. doi: 10.1038/ismej.2014.210

Hoagland, D. R., and Snyder, W. C. (1933). Nutrition of strawberry plant under controlled conditions. (a) Effects of deficiencies of boron and certain other elements, (b) susceptibility to injury from sodium salts. *Proc. Am. Soc. Horticult. Sci.* 30, 288–294.

Hole, D. G., Perkins, A. J., Wilson, J. D., Alexander, I. H., Grice, P. V., and Evans, A. D. (2005). Does organic farming benefit biodiversity? *Biol. Conserv.* 122, 113–130. doi: 10.1016/j.biocon.2004.07.018

Jaemsaeng, R., Jantasuriyarat, C., and Thamchaipenet, A. (2018). Molecular interaction of 1-aminocyclopropane-1-carboxylate deaminase (ACCD)-producing endophytic *Streptomyces* sp. GMKU towards salt-stress resistance of *Oryza sativa* L. cv. KDML105. *Sci. Rep.* 8, 1–15. doi: 10.1038/s41598-018-19799-9

Jangid, K., Williams, M. A., Franzluebbers, A. J., Sanderlin, J. S., Reeves, J. H., Jenkins, M. B., et al. (2008). Relative impacts of land-use, management intensity and fertilization upon soil microbial community structure in agricultural systems. *Soil Biol. Biochem.* 40, 2843–2853. doi: 10.1016/j.soilbio.2008.07.030

Kaisermann, A., de Vries, F. T., Griffiths, R. I., and Bardgett, R. D. (2017). Legacy effects of drought on plant–soil feedbacks and plant–plant interactions. *New Phytol.* 215, 1413–1424. doi: 10.1111/nph.14661

Kundel, D., Bodenhausen, N., Jørgensen, H. B., Truu, J., Birkhofer, K., Hedlund, K., et al. (2020). Effects of simulated drought on biological soil quality, microbial diversity and yields under long-term conventional and organic agriculture. *FEMS Microbiol. Ecol.* 96, fiaa205. doi: 10.1093/femsec/fiaa205

Lau, J. A., and Lennon, J. T. (2012). Rapid responses of soil microorganisms improve plant fitness in novel environments. *Proc. Nat. Acad. Sci. U. S. A.* 109, 14058–14062. doi: 10.1073/pnas.1202319109

Leizeaga, A., Hicks, L. C., Manoharan, L., Hawkes, C. V., and Rousk, J. (2021). Drought legacy affects microbial community trait distributions related to moisture along a savannah grassland precipitation gradient. *J. Ecol.* 109, 3195–3210. doi: 10.1111/1365-2745.13550

Liu, H., Brettell, L. E., Qiu, Z., and Singh, B. K. (2020). Microbiome-mediated stress resistance in plants. *Trends Plant Sci.* 25:733–743. doi: 10.1016/j.tplants.2020.03.014

Livak, K. J., and Schmittgen, T. D. (2001). Analysis of relative gene expression data using real-time quantitative PCR and the 2−ΔΔCT method. *Methods* 25, 402–408. doi: 10.1006/meth.2001.1262

Lori, M., Symnaczik, S., Mäder, P., Deyn, G. D., and Gattinger, A. (2017). Organic farming enhances soil microbial abundance and activity—a meta-analysis and meta-regression. *PLoS ONE* 12, e0180442. doi: 10.1371/journal.pone.0180442

Love, M. I., Huber, W., and Anders, S. (2014). Moderated estimation of fold change and dispersion for RNA-seq data with DESeq2. *Genome Biol.* 15, 550. doi: 10.1186/s13059-014-0550-8

Lugtenberg, B., and Kamilova, F. (2009). Plant-growth-promoting rhizobacteria. *Annu. Rev. Microbiol.* 63, 541–556. doi: 10.1146/annurev.micro.62.081307.162918

Lupatini, M., Korthals, G. W., de Hollander, M., Janssens, T. K. S., and Kuramae, E. E. (2017). Soil microbiome is more heterogeneous in organic than in conventional farming system. *Front. Microbiol.* 7, 2064. doi: 10.3389/fmicb.2016.02064

Macias-Benitez, S., Garcia-Martinez, A. M., Caballero Jimenez, P., Gonzalez, J. M., Tejada Moral, M., and Parrado Rubio, J. (2020). Rhizospheric organic acids as biostimulants: monitoring feedbacks on soil microorganisms and biochemical properties. *Front. Plant Sci.* 11, 633. doi: 10.3389/fpls.2020.00633

Marasco, R., Rolli, E., Ettoumi, B., Vigani, G., Mapelli, F., Borin, S., et al. (2012). A drought resistance-promoting microbiome is selected by root system under desert farming. *PLoS ONE* 7, e48479. doi: 10.1371/journal.pone.0048479

Mattoo, A. K., and Suttle, J. C. (2017). *The Plant Hormone Ethylene*. Boca Raton, FL: CRC press. doi: 10.1201/9781351075763

Mendes, L. W., Kuramae, E. E., Navarrete, A. A., van Veen, J. A., and Tsai, S. M. (2014). Taxonomical and functional microbial community selection in soybean rhizosphere. *ISME J.* 8, 1577–1587. doi: 10.1038/ismej.2014.17

Morgan, P. W., and Drew, M. C. (1997). Ethylene and plant responses to stress. *Physiol. Plant.* 100, 620–630. doi: 10.1111/j.1399-3054.1997.tb03068.x

Munoz-Ucros, J., Wilhelm, R. C., Buckley, D. H., and Bauerle, T. L. (2022). Drought legacy in rhizosphere bacterial communities alters subsequent plant performance. *Plant Soil.* 471, 443–461. doi: 10.1007/s11104-021-05227-x

Murali, M., Singh, S. B., Gowtham, H. G., Shilpa, N., Prasad, M., Aiyaz, M., et al. (2021). Induction of drought tolerance in *Pennisetum glaucum* by ACC deaminase producing PGPR-*Bacillus amyloliquefaciens* through Antioxidant defense system. *Microbiol. Res.* 253, 126891. doi: 10.1016/j.micres.2021.126891

Naylor, D., and Coleman-Derr, D. (2018). Drought stress and root-associated bacterial communities. *Frontiers in Plant Science* 8. doi: 10.3389/fpls.2017.02223

Pérez Castro, S., Cleland, E. E., Wagner, R., Sawad, R. A., and Lipson, D. A. (2019). Soil microbial responses to drought and exotic plants shift carbon metabolism. *ISME J.* 13, 1776–1787. doi: 10.1038/s41396-019-0389-9

Preece, C., and Peñuelas, J. (2016). Rhizodeposition under drought and consequences for soil communities and ecosystem resilience. *Plant Soil* 409, 1–17. doi: 10.1007/s11104-016-3090-z

Quast, C., Pruesse, E., Yilmaz, P., Gerken, J., Schweer, T., Yarza, P., et al. (2013). The SILVA ribosomal RNA gene database project: improved data processing and web-based tools. *Nucleic Acids Res.* 41, D590–D596. doi: 10.1093/nar/gks1219

Raaijmakers, J. M., Paulitz, T. C., Steinberg, C., Alabouvette, C., and Moënne-Loccoz, Y. (2009). The rhizosphere: a playground and battlefield for soilborne pathogens and beneficial microorganisms. *Plant Soil* 321, 341–361. doi: 10.1007/s11104-008-9568-6

Renoud, S., Bouffaud, M.-L., Dubost, A., Prigent-Combaret, C., Legendre, L., Moënne-Loccoz, Y., et al. (2020). Co-occurrence of rhizobacteria with nitrogen fixation and/or 1-aminocyclopropane-1-carboxylate deamination abilities in the maize rhizosphere. *FEMS Microbiol. Ecol.* 96, fiaa062. doi: 10.1093/femsec/fiaa062

Sanaullah, M., Chabbi, A., Rumpel, C., and Kuzyakov, Y. (2012). Carbon allocation in grassland communities under drought stress followed by 14C pulse labeling. *Soil Biol. Biochem.* 55, 132–139. doi: 10.1016/j.soilbio.2012.06.004

Santos-Medellín, C., Edwards, J., Liechty, Z., Nguyen, B., and Sundaresan, V. (2017). Drought stress results in a compartment-specific restructuring of the rice root-associated microbiomes. *MBio* 8, e00764–e00717. doi: 10.1128/mBio.00764-17

Schädler, M., Buscot, F., Klotz, S., Reitz, T., Durka, W., Bumberger, J., et al. (2019). Investigating the consequences of climate change under different land-use regimes: a novel experimental infrastructure. *Ecosphere* 10, e02635. doi: 10.1002/ecs2.2635

Schloss, P. D., Westcott, S. L., Ryabin, T., Hall, J. R., Hartmann, M., Hollister, E. B., et al. (2009). Introducing mothur: open-source, platform-independent, community-supported software for describing and comparing microbial communities. *Appl. Environ. Microbiol.* 75, 7537–7541. doi: 10.1128/AEM.01541-09

Schrey, S. D., and Tarkka, M. T. (2008). Friends and foes: streptomycetes as modulators of plant disease and symbiosis. *Antonie Van Leeuwenhoek* 94, 11–19. doi: 10.1007/s10482-008-9241-3

Schwartz, D., Berger, S., Heinzelmann, E., Muschko, K., Welzel, K., and Wohlleben, W. (2004). Biosynthetic gene cluster of the herbicide phosphinothricin tripeptide from *Streptomyces viridochromogenes* Tu494. *Appl. Environ. Microbiol.* 70, 7093–7102. doi: 10.1128/AEM.70.12.7093-7102.2004

Shakir, M. A., Bano, A., and Arshad, M. (2012). Rhizosphere bacteria containing ACC-deaminase conferred drought tolerance in wheat grown under semi-arid climate. *Soil Environ.* 31, 108–112.

Song, F., Han, X., Zhu, X., and Herbert, S. J. (2012). Response to water stress of soil enzymes and root exudates from drought and non-drought tolerant corn hybrids at different growth stages. *Can. J. Soil Sci.* 92, 501–507. doi: 10.4141/cjss2010-057

Spinoni, J., Vogt, J. V., Naumann, G., Barbosa, P., and Dosio, A. (2018). Will drought events become more frequent and severe in Europe? *Int. J. Climatol.* 38, 1718–1736. doi: 10.1002/joc.5291

Tanimoto, M., Roberts, K., and Dolan, L. (1995). Ethylene is a positive regulator of root hair development in *Arabidopsis thaliana*. *Plant J.* 8, 943–948. doi: 10.1046/j.1365-313X.1995.8060943.x

Teijeiro, R. G., Belimov, A. A., and Dodd, I. C. (2019). Microbial inoculum development for ameliorating crop drought stress: a case study of *Variovorax paradoxus* 5C-2. *N. Biotechnol.* 56, 103–113. doi: 10.1016/j.nbt.2019.12.006

Thakur, M. P., Phillips, H. R. P., Brose, U., De Vries, F. T., Lavelle, P., Loreau, M., et al. (2020). Towards an integrative understanding of soil biodiversity. *Biol. Rev.* 95, 350–364. doi: 10.1111/brv.12567

Toumatia, O., Compant, S., Yekkour, A., Goudjal, Y., Sabaou, N., Mathieu, F., et al. (2016). Biocontrol and plant growth promoting properties of *Streptomyces*

mutabilis strain IA1 isolated from a Saharan soil on wheat seedlings and visualization of its niches of colonization. *South Afr. J. Bot.* 105, 234–239. doi: 10.1016/j.sajb.2016.03.020

Vacheron, J., Desbrosses, G., Bouffaud, M.-L., Touraine, B., Moënne-Loccoz, Y., Muller, D., et al. (2013). Plant growth-promoting rhizobacteria and root system functioning. *Front. Plant Sci.* 4, 356. doi: 10.3389/fpls.2013.00356

Veach, A. M., and Zeglin, L. H. (2020). Historical drought affects microbial population dynamics and activity during soil drying and re-wet. *Microb. Ecol.* 79, 662–674. doi: 10.1007/s00248-019-01432-5

Vurukonda, S. S. K. P., Vardharajula, S., Shrivastava, M., and Sk, Z. A. (2016). Enhancement of drought stress tolerance in crops by plant growth promoting rhizobacteria. *Microbiol. Res.* 184, 13–24. doi: 10.1016/j.micres.2015.12.003

Weißbecker, C., Schnabel, B., and Heintz-Buschart, A. (2020). Dadasnake, a Snakemake implementation of DADA2 to process amplicon sequencing data for microbial ecology. *Gigascience* 9, giaa135. doi: 10.1093/gigascience/giaa135

Wen, C., Zheng, D., Shen, S., Chen, J., Liu, W., and Liu, T. (2012). *Streptomyces scabiei* subsp. xuchangensis, a novel Streptomycete isolate for staurosporine production and a wheat take-all control agent. *Int. J. Microbiol. Res.* 4, 282–289. doi: 10.9735/0975-5276.4.7.282-289

Yuan, J., Zhao, J., Wen, T., Zhao, M., Li, R., Goossens, P., et al. (2018). Root exudates drive the soil-borne legacy of aboveground pathogen infection. *Microbiome* 6, 156. doi: 10.1186/s40168-018-0537-x

Zhalnina, K., Louie, K. B., Hao, Z., Mansoori, N., da Rocha, U. N., Shi, S., et al. (2018). Dynamic root exudate chemistry and microbial substrate preferences drive patterns in rhizosphere microbial community assembly. *Nat. Microbiol.* 3, 470–480. doi: 10.1038/s41564-018-0129-3

Zilber-Rosenberg, I., and Rosenberg, E. (2008). Role of microorganisms in the evolution of animals and plants: the hologenome theory of evolution. *FEMS Microbiol. Rev.* 32, 723–735. doi: 10.1111/j.1574-6976.2008.00123.x

Conflict of Interest: The authors declare that the research was conducted in the absence of any commercial or financial relationships that could be construed as a potential conflict of interest.

Publisher's Note: All claims expressed in this article are solely those of the authors and do not necessarily represent those of their affiliated organizations, or those of the publisher, the editors and the reviewers. Any product that may be evaluated in this article, or claim that may be made by its manufacturer, is not guaranteed or endorsed by the publisher.

Advantages of publishing in Frontiers

OPEN ACCESS
Articles are free to read for greatest visibility and readership

FAST PUBLICATION
Around 90 days from submission to decision

HIGH QUALITY PEER-REVIEW
Rigorous, collaborative, and constructive peer-review

TRANSPARENT PEER-REVIEW
Editors and reviewers acknowledged by name on published articles

Frontiers
Avenue du Tribunal-Fédéral 34
1005 Lausanne | Switzerland

Visit us: www.frontiersin.org
Contact us: frontiersin.org/about/contact

REPRODUCIBILITY OF RESEARCH
Support open data and methods to enhance research reproducibility

DIGITAL PUBLISHING
Articles designed for optimal readership across devices

FOLLOW US
@frontiersin

IMPACT METRICS
Advanced article metrics track visibility across digital media

EXTENSIVE PROMOTION
Marketing and promotion of impactful research

LOOP RESEARCH NETWORK
Our network increases your article's readership